N 69 26572

NASA CR 101109

NATIONAL AERONAUTICS AND SPACE ADMINISTRATION

Technical Report 32-1203

Mariner Venus 67 Final Project Report: Volume II. Midcourse Maneuver Through End of Mission

CASE FILE COPY

JET PROPULSION LABORATORY
CALIFORNIA INSTITUTE OF TECHNOLOGY
PASADENA, CALIFORNIA

May 1, 1969

NATIONAL AERONAUTICS AND SPACE ADMINISTRATION

Technical Report 32-1203

Mariner Venus 67 Final Project Report: Volume II. Midcourse Maneuver Through End of Mission

JET PROPULSION LABORATORY
CALIFORNIA INSTITUTE OF TECHNOLOGY
PASADENA, CALIFORNIA

May 1, 1969

TECHNICAL REPORT 32-1203

Copyright © 1969
Jet Propulsion Laboratory
California Institute of Technology

Prepared Under Contract No. NAS 7-100
National Aeronautics and Space Administration

Preface

The work described in this report was performed by the *Mariner* Venus 67 project of the Jet Propulsion Laboratory.

Mariner V was successfully launched from the Air Force Eastern Test Range at 02:01 EDT on June 14, 1967. On October 19, the spacecraft encountered the planet Venus; the closest approach distance during the encounter phase was 2543 miles. All systems functioned as planned.

The primary objective of the *Mariner* Venus 67 project was to conduct a flyby mission to Venus to obtain scientific information that would complement and extend the results obtained by *Mariner II* relevant to determining the origin and nature of Venus and its environment. Secondary objectives were to acquire engineering experience in converting (and operating) a spacecraft designed for a flight to Mars into one flown to Venus, and to obtain information on the interplanetary environment during a period of increasing solar activity.

The single spacecraft, prepared by converting the *Mariner IV* spacecraft, carried seven scientific experiments. Of these, two experiments (S-band radio occultation and celestial mechanics) used tracking and telecommunications facilities, but no special flight instruments; the dual-frequency radio propagation experiment required a new instrument package; the remaining instruments were essentially as developed for the *Mariner* Mars 1964 mission.

All *Mariner* Venus 67 project objectives were fully achieved, attesting to the high degree of technical skill exercised on the part of the participating project personnel.

This volume (Vol. II) and its companion (Vol. I) comprise the *Mariner* Venus 67 Final Project Report describing the formation and organization of the project, mission planning, spacecraft design and development, mission operations, and tracking and data acquisition from project inception until termination of tracking activities after encounter and data playback.

The data returned by *Mariner V* have greatly expanded the store of information about the veiled planet, and will significantly deepen our insight into the history of its evolution. It is also hoped that the operations and results documented in this report will be a useful reference to those planning future space missions.

Contents

I. Introduction 1

A. *Mariner* Venus 67 Mission Objectives 1

B. Acquisition of Science Data 1

C. Mission Operations 3

II. Science Measurements and Data 5

A. Science Experiments and Overall Results 5

1. Interaction of interplanetary medium with Venus 7

2. Ultraviolet photometer experiment 8

3. Occultation experiments 8

4. Celestial mechanics experiment 9

B. Solar Plasma Probe Experiment 9

1. Description of instrumentation 9

2. Plasma and magnetic field data 10

3. Schematic model 14

C. Helium Magnetometer Experiment 15

D. Trapped Radiation Detector Experiment 15

E. Ultraviolet Photometer Experiment 18

1. Description and operation of photometer 18

2. Discussion of results 18

3. Conclusions 20

F. S-Band Radio Occultation Experiment 21

1. Comparison of Venus and Mars experiments 21

2. Data acquisition 22

3. Data analysis 23

4. Results of experiment 23

G. Dual-Frequency Radio Occultation Experiment 26

1. Data acquisition 29

2. Analysis of data 29

3. Interaction definition 34

4. Conclusion 35

H. Celestial Mechanics Experiment 36

Contents (contd)

III. Trajectory and Orbit Determination 39

A. Trajectory 39

1. Launch to maneuver phase 39

2. Maneuver analysis 40

3. Postmidcourse maneuver cruise phase 47

4. Encounter phase 47

5. Postencounter phase 49

B. Orbit Determination 49

1. Tracking data coverage 49

2. Premaneuver orbit determination results 51

3. Midcourse-maneuver analysis from radio tracking data . . . 54

4. Cruise orbit-determination results 55

5. Real-time encounter orbit-determination results 63

IV. Space Flight Operations 69

A. Mission-Independent Support 69

1. Facilities and support 69

2. Schedule and control of interfaces 91

3. DSN coverage 94

4. Interaction with other missions 96

5. Mark I and Mark II ranging ground equipment configuration and utilization 103

B. Organization and Functions 104

1. Flight-path analysis and command 104

2. Space science analysis and command 116

C. Data Recovery and Processing 117

1. Tracking data 117

2. Science and engineering telemetry data 118

3. Cruise and encounter 118

4. Program refinements 119

5. Occultation 120

6. Master data library production 120

D. Mission Operations 121

Contents (contd)

1. Readiness testing 121
2. Flight chronology 123
3. Spacecraft command criteria 123
4. Critical operations 124

V. Organization and Function of SPAC 139

A. Organization of SPAC. 139
B. SPAC Operations 139
1. SPAC responsibility and function 139
2. Organization 140
3. Operations philosophy. 142
4. SPAC interfaces 144
5. SPAC data output 148
C. Performance Evaluation 149
1. Performance parameters 149
2. Facilities 150
3. Organization 151
4. Preparation and planning 153
5. Operations. 154
6. SPAC testing 155
D. Planning Philosophy 173
E. Launch Planning 176
1. Countdown and liftoff. 177
2. Nose-fairing ejection 177
3. Spacecraft injection 177
4. Spacecraft–*Agena* separation 177
5. Sun acquisition. 179
6. Magnetometer roll calibration 180
7. Canopus acquisition 180
F. Trajectory-Correction Maneuver Planning. 180
1. Midcourse maneuver planning phase 181
2. Midcourse maneuver execution phase. 182
3. Maneuver-inhibit planning. 183

Contents (contd)

G. Encounter Planning 185

1. Description 185

2. Encounter sequence development 188

3. Operational considerations 198

4. Contingency plans 199

H. Postencounter Planning 206

1. Description 206

2. Operations 206

VI. Spacecraft Performance 213

A. *Mariner V* Description 213

B. *Mariner* Spacecraft Conversion From Mars to Venus 214

C. *Mariner V* Performance 217

1. Launch to Canopus acquisition 217

2. Pretrajectory-correction cruise 227

3. Trajectory-correction maneuver 227

4. Interplanetary cruise 228

5. Planetary encounter 236

6. Playback 243

7. Postencounter cruise 244

D. Science Instrument Performance 249

1. Data automation subsystem 249

2. Helium-magnetometer performance 250

3. Trapped radiation detector performance 250

4. Plasma-probe performance 256

5. Ultraviolet-photometer performance 256

6. Dual-frequency receiver flight performance 258

E. Telecommunications System Performance 258

1. Description 258

2. Mission-related hardware 263

3. Radio subsystem performance 265

4. Interferometer performance 267

5. Flight command subsystem performance 269

Contents (contd)

6. Data encoder performance 269
7. Tape-recorder subsystem performance 269
8. Dual-frequency receiver antenna subsystem performance. . . 275

F. Guidance and Control Subsystem Performance 278
1. Introduction 278
2. Description. 278
3. Flight performance. 281
4. Recommendations 300
5. Power subsystem flight performance 302
6. Solar-panel flight performance 303
7. Power-conditioning equipment flight performance 304
8. Battery flight performance. 304
9. Central computer and sequencer flight performance 304

G. Engineering Mechanics 305
1. Structure subsystem 305
2. Mechanical-devices subsystem. 306
3. Cabling subsystem. 308
4. Temperature-control subsystem 310

H. Propulsion Subsystem Performance 324
1. Propulsion subsystem 324
2. Pyrotechnics subsystem 325

I. Reliability Spacecraft Program Results 325
1. Basic areas of reliability concern 325
2. Electronic piece parts 325
3. Environmental and system test constraints 326
4. New development hardware 327
5. Problem failure report summary 327

VII. Flight Support Testing 331

A. Postlaunch Test Operations 331
1. Support at Air Force Eastern Test Range 331
2. Return of the spare spacecraft to JPL 332
3. Spacecraft performance analysis and command encounter tests and special tests 332

Contents (contd)

4. Standby during flight spacecraft encounter 332

5. Preparation for storage of the spare spacecraft 332

B. *Occultation Ground Equipment Description and Configuration* 332

C. Trajectory-Correction Maneuver Anomaly. 333

1. Introduction 333

2. Propulsion subsystem 333

3. Pyrotechnics subsystem 336

4. Autopilot analysis 336

5. Conclusions and recommendations 344

Appendix A. Project Organization and Management . . . 347

Appendix B. *Encounter Sequence and Command Descriptions* . . 353

Appendix C. Telemetry Data Curves . . 397

Glossary . 437

References . . 441

Tables

I-1. *Mariner* Venus 67 mission scientific experiments . . . 3

II-1. Chronology of significant events during Venus encounter. . . . 6

II-2. Mean residuals for encounter solutions 36

II-3. Mean residuals for cruise solution (AU known) 37

III-1. Geocentric characteristics of *Mariner V* trajectory. . . . 42

III-2. Midcourse-maneuver sequence 43

III-3. Midcourse-maneuver parameter sensitivity to time 43

III-4. Desired-vs-achieved injection and maneuver results 43

III-5. Computed- and commanded-vs-achieved midcourse maneuver performance 44

III-6. Heliocentric orbital elements of *Mariner V* spacecraft trajectory 44

III-7. Venus-centered orbital elements of *Mariner V* spacecraft trajectory 47

Contents (contd)

Tables (contd)

III-8. Preliminary *Mariner* Venus 67 solutions for solar-radiation pressure, station locations, and geocentric equatorial state vector 53

III-9. Comparison of nominal and achieved maneuver velocity increments for *Mariner V* 54

III-10. Commanded-vs-achieved attitude-control performance . . . 55

III-11. Nominal-vs-achieved attitude-control performance . 55

III-12. Mark IA ranging data obtained during *Mariner* Venus 67 mission. 56

III-13. Summary of ranging data noise increases . 57

III-14. Sample of cruise doppler residual statistics . . . 58

IV-1. Deep Space Instrumentation Facility capabilities for the *Mariner* Venus 67 project 71

IV-2. Requested and actual Class I tracking coverage, liftoff to L+5178 s 94

IV-3. Requested and actual Class I tracking coverage, *Agena*/spacecraft separation to end of mission . 94

IV-4. Total *Mariner V* tracking coverage by the Deep Space Network 97

IV-5. Mark I ranging data summary . 104

IV-6. Mark II ranging data summary 104

IV-7. Mark I ranging (DSS post-track reports) . . . 107

IV-8. Mark II ranging (DSS post-track reports). 112

IV-9. Test schedule 124

IV-10. *Mariner V* flight chronology 128

V-1. Direct and quantitative commands . . . 160

V-2. SPAC testing summary 164

V-3. Spacecraft–*Agena* separation functions 178

V-4. *Mariner V* planned midcourse sequence of events, including UV-photometer rolls 183

V-5. SPAC midcourse maneuver turn constraints 183

V-6. SPAC criteria for use of DC-V13 184

V-7. Ground commands related to the encounter sequence 185

V-8. Spacecraft configuration before DC-V25 186

V-9. Receive via high-gain antenna 186

Contents (contd)

Tables (contd)

V-10. Roll-control modes for encounter 187

V-11. Effects of DC-V25 188

V-12. Effects of DC-V24 191

V-13. Outputs from DAS encounter clocks 191

V-14. Predicted occultation times 194

V-15. Planned encounter sequence chronology 197

V-16. Emergency action summary 200

V-17. Proposed sequence for UV-photometer MT-6 exercise. 209

V-18. Phase I–conditioning for long-term cruise plan 211

VI-1. Flight sequence adopted before launch 218

VI-2. Major deviations from nominal flight sequence 223

VI-3. *Mariner V* sequence of events. 223

VI-4. Spacecraft problems and minor anomalies during mission . . . 225

VI-5. Data automation subsystem real-time word description . . . 254

VI-6. Mission-related hardware ECRs (RWV) 263

VI-7. Mission-related hardware ECRs (GTS) 264

VI-8. Ground telemetry system ECRs to incorporate **DDT** 265

VI-9. Log of *Mariner* Venus 67 mission tape recorder subsystem operations. 273

VI-10. *Mariner V* launch events 281

VI-11. Spacecraft–*Agena* separation data 281

VI-12. Attitude-control subsystem cruise operating parameters 285

VI-13. Midcourse maneuver performance sequence 288

VI-14. Postmaneuver analysis, midcourse maneuver performance . . . 288

VI-15. *Mariner V* CC&S sequenced events 305

VI-16. *Mariner V* CC&S cyclic events 305

VI-17. Locations of temperature transducers 312

VI-18. Telemetered flight temperatures 313

VI-19. Summary of *Mariner V* parts count by subsystem 329

VII-1. *Mariner V* (M67-1) Spacecraft Assembly Facility electrical operations 331

VII-2. Midcourse maneuver performance parameters 334

Contents (contd)

Tables (contd)

VII-3. Jet-vane interaction test summary 338

A-1. Major review sessions 351

B-1. *Mariner V* command list 353

B-2. Sequence of events for *Mariner* Venus 67 encounter 355

Figures

I-1. *Mariner V* spacecraft 2

II-1. Isometric projection of Venus encounter orbit 6

II-2. Venus encounter orbit shown in the orbit plane 7

II-3. Venus encounter orbit projected on the terminator plane . . . 7

II-4. *Mariner V* magnetic field data near earth 10

II-5. Plasma and magnetic field data near Venus 11

II-6. *Mariner V* orbit relative to sun–Venus axis 12

II-7. *Mariner V* trajectory and magnetic field vectors 13

II-8. Schematic representation of the solar wind interaction with Venus 15

II-9. Counting rate of the electron detector $E_e > 45$ keV . . . 16

II-10. Polar plot of encounter trajectory 17

II-11. Signal obtained from lithium-fluoride/Lyman-alpha channel during Venus encounter 19

II-12. Signals obtained from photometer channels during critical periods of Venus encounter 20

II-13. Received signal strength during entry into occultation . . . 22

II-14. Frequency residuals from data taken during entry into occultation 23

II-15. Entry residuals with theoretical models 23

II-16. Exit residuals with theoretical models 24

II-17. Refractivity of Venus atmosphere 24

II-18. Pressure of Venus atmosphere (pseudo inversion) 24

II-19. Pressure of Venus atmosphere (direct inversion) 25

II-20. Temperature of Venus atmosphere (pseudo inversion) 25

II-21. Temperature of Venus atmosphere (direct inversion) 25

Contents (contd)

Figures (contd)

II-22. Number density in lower atmosphere of Venus 25

II-23. Electron density in Venus daytime ionosphere 26

II-24. Venus atmospheric temperatures for F_1 and E ionosphere models 27

II-25. Venus atmospheric number density for F_1 and E ionosphere models 28

II-26. Signal amplitudes at two frequencies during entry (nightside) and exit (dayside) occultation 30

II-27. Dispersive phase due to the ionosphere at entry and exit . . . 31

II-28. Electron concentrations in night and day ionospheres of Venus 32

II-29. Possible constituents and plasma temperatures for nighttime upper atmosphere 33

III-1. Ascent trajectory profile 40

III-2. Sequence of events to Canopus acquisition 41

III-3. Midcourse-maneuver results 44

III-4. Spacecraft distance from earth, launch through 1971 . . . 45

III-5. Spacecraft celestial latitude, launch through 1971 45

III-6. Spacecraft celestial longitude, launch through 1971 46

III-7. Spacecraft distance from sun, launch through 1971 46

III-8. Spacecraft distance from Venus, launch through 1971 . . . 47

III-9. Clock and cone angles of earth, launch through 1971 . . . 48

III-10. Encounter velocities and altitude 49

III-11. Heliocentric plan view of *Mariner IV* and *Mariner V* spacecraft 50

III-12. Cone angle of Canopus, launch through 1971 51

III-13. Block diagram of S-band two-way doppler system 52

III-14. *Doppler residual during controlled roll* 53

III-15. *Mariner V* cruise solution for solar-pressure coefficient 59

III-16. Cruise-data estimate of station location, distance off spin axis 61

III-17. Cruise-data estimate of station location, geocentric longitude 62

III-18. Lunar gravitational constant $GM_{\mathbb{C}}$ estimate from combined *Ranger* and *Mariner II, IV,* and *V* data 63

Contents (contd)

Figures (contd)

III-19. Lunar gravitational constant GM estimate from *Mariner V* postcruise analysis 63

III-20. Cruise orbit estimates of time of closest approach to Venus . . 64

III-21. Elliptic **B**-plane aiming point from cruise orbit determination 64

III-22. Tracking data distribution from E−5 to E+5 days . . . 65

III-23. Real-time *Mariner* Venus 67 encounter **B**-plane estimates . 66

III-24. Encounter solution for station location, distance off spin axis 67

III-25. Encounter solution for station location, geocentric longitude . . 68

IV-1. Telemetry system configuration for the *Mariner* Venus 67 mission 70

IV-2. Deep Space Instrumentation Facility/ground communication system configuration for *Mariner V* encounter 72

IV-3. Ground communications, deep-space phase . . 73

IV-4. Deep Space Network/ground communication system teletype circuits 74

IV-5. Mission control network (MI-CON) . . 75

IV-6. Operations control network (VAL-PRIME) . . 76

IV-7. Facilities operations control network (FAC-PRIME) . 77

IV-8. FPAC analysis control network (FPAC 3) . 78

IV-9. SPAC analysis control network (BUSS) . 79

IV-10. SSAC analysis control network (SPACE) . 80

IV-11. Command network (MAR-COMMAND) . . . 81

IV-12. Data-coordination network (DA-COR) . . 82

IV-13. Data processing functions performed by the Deep Space Network elements 83

IV-14. Telemetry and command processing at the Deep Space Instrumentation Facility 84

IV-15. Tracking data handling and orbit determination . . . 84

IV-16. Trajectory computation 86

IV-17. Predicts computation 86

IV-18. Midocurse maneuver program 87

IV-19. SPAC user programs 87

IV-20. Mode 3 operation 88

Contents (contd)

Figures (contd)

IV-21. Mode 4 operation 89
IV-22. Master data library programs 90
IV-23. Dual-frequency receiver data handling 91
IV-24. *Mariner* Venus 67 mission support area layout 92
IV-25. Mark I ranging configuration 103
IV-26. Mark II ranging configuration 105
IV-27. Functions performed by the FPAC team 105
IV-28. FPAC organization 106
IV-29. Data processing system to support the *Mariner* Venus 67 mission 118
IV-30. 7094 user program environment 119
IV-31. High-speed tracking data configuration 120
IV-32. Occultation experiment data recovery, station block diagram . . 121
IV-33. Occultation experiment predetection recording 122
IV-34. Validation processing telemetry 123
IV-35. 7094 master data library processing telemetry 125
IV-36. Test configuration 127
V-1. SPAC line organization 141
V-2. SPAC–SPAC JR interface 143
V-3. SPAC layout 145
V-4. Spacecraft to SPAC real-time data transmission 156
V-5. Internal SPAC organization and communications 158
V-6. SPAC testing summary 162
V-7. Science-experiment value function vs aiming-plane coordinates . . 181
V-8. Midcourse maneuver final aiming point 182
V-9. Sun constraint regions 184
V-10. Earth constraint regions 184
V-11. Occultation time dispersions 192
V-12. Nominal *Mariner V* record pattern 193
V-13. Nominal *Mariner V* playback times 196
V-14. Expected doppler shift at encounter 198
V-15. Receiver configuration during Goldstone encounter pass 199

Contents (contd)

Figures (contd)

V-16. Encounter decision diagram 201

V-17. Data storage relative to encounter 203

V-18. Early planet sensor output timing diagram 204

V-19. Number of tape passes for early planet sensor output 204

VI-1. *Mariner V* spacecraft configuration (top view) 214

VI-2. *Mariner V* spacecraft configuration (bottom view) 215

VI-3. Nominal *Mariner* Venus 67 encounter sequence matrix 237

VI-4. *Mariner* Venus 67 encounter logic diagram 251

VI-5. Data automation subsystem real-time data format 253

VI-6. Data automation subsystem stored-data format 254

VI-7. *Mariner* Venus 67 encounter sequence and data automation subsystem events 255

VI-8. Pointing directions of UV-photometer tubes A, B, and C (apparent position of Tau-Scorpii as seen by each tube) 257

VI-9. Dual-frequency receiver antenna gain, day 311 258

VI-10. Telecommunications performance analysis, downlink, 85-ft antenna 259

VI-11. Telecommunications performance analysis, uplink, 85-ft antenna 260

VI-12. Interferometer antenna pattern, high-gain antenna in position No. 1 268

VI-13. Interferometer antenna pattern, high-gain antenna in position No. 2 270

VI-14. Uplink received signal strength in interferometer region 271

VI-15. Uplink received signal strength in interferometer region (low-gain antenna used) 272

VI-16. *Mariner V* playback times 274

VI-17. How a bit is dropped during loss of lock 274

VI-18. Tape position after playback-motor rundown 274

VI-19. Tape position after record-motor rundown 274

VI-20. DFR 49.8-MHz antenna patterns from flight data and predicted performance 276

VI-21. DFR 423.3-MHz antenna patterns from flight data and predicted performance 277

VI-22. Flight spacecraft (M67-2) gyro headings (AFETR) 281

Contents (contd)

Figures (contd)

VI-23. *Mariner V* gyro activity (launch to start of sun acquisition) . . . 282

VI-24. *Mariner V* spacecraft–*Agena* separation, June 14, 1967 283

VI-25. Geometry of false null at initial sun acquisition 284

VI-26. Spacecraft spin rate from earth-sensor data 285

VI-27. Attitude-control gas weight from launch through midcourse maneuver 286

VI-28. "Best-estimate" temperatures in vacuum after GCA turn-on . . . 286

VI-29. *Mariner V* gyro-commanded turn rates 287

VI-30. Representative *Mariner V* roll transients 290

VI-31. Roll transient, June 23, 1967 291

VI-32. *Mariner V* attitude data 292

VI-33. Venus-lighted limb geometry at planet sensor output . . . 293

VI-34. Contours of constant luminance for Venus encounter . . 294

VI-35. Planet sensor—approximate encounter orientation . . . 295

VI-36. Terminator sensor—approximate encounter geometry . . 296

VI-37. Venus-lighted limb geometry at terminator sensor output . . . 297

VI-38. *A priori* and telemetered star maps (roll search start to earth acquisition) 298

VI-39. *A priori* and telemetered star maps (earth acquisition to Canopus acquisition) 299

VI-40. Stars near UV-photometer field of view 300

VI-41. Postencounter roll transients 301

VI-42. *Gas-weight history, June 14–November 21, 1967* 302

VI-43. Case 7 temperature and CC&S clock error 306

VI-44. Daily CC&S clock error 307

VI-45. Separation-initiated timer temperature 309

VI-46. Solar intensity 310

VI-47. Battery-charger temperature 315

VI-48. Increase in solar absorptance 316

VI-49. Temperature vs time, midcourse maneuver (high- and low-gain antennas and magnetometer) 317

VI-50. Temperature vs time, midcourse maneuver (bay 2, propellant tank, and PIPS N_2 tank) 318

VI-51. Temperature vs time, midcourse maneuver (bays 1 and 3) . . . 319

Contents (contd)

Figures (contd)

VI-52. Temperature vs time, midcourse maneuver (primary sun sensor) 319

VI-53. Temperature vs time, midcourse maneuver (UV photometer) . . 320

VI-54. In-flight temperatures of S-13 and S-13M white coatings . . 321

VI-55. Predicted and actual temperatures of black coating . . 322

VI-56. Degradation of S-13 and S-13M white coatings 323

VI-57. Change in apparent absorptance/emittance during mission . . . 323

VI-58. Histogram of problem failure report activity vs time . . 328

VII-1. Occultation simulator block diagram 333

VII-2. Maneuver telemetry sequence of events from 23:08:10 ±0.1 GMT on day 170 334

VII-3. Chamber pressure telemetry data points . . . 335

VII-4. Propellant tank pressure telemetry data points . . . 335

VII-5. Jet vane positions during midcourse maneuver No. 1 . 337

VII-6. Jet vane drag 338

VII-7. Six-component test stand 339

VII-8. Six-component test stand, top view . . 340

VII-9. Six-component test stand, side view . . 341

VII-10. Jet vanes (full scale) 342

VII-11. Sign conventions for vane-produced forces . . . 342

VII-12. Autopilot interaction test of *Ranger* jet vanes . . 343

VII-13. Transfer characteristics of *Ranger* jet vanes . . 343

VII-14. *Mariner V* thrust vector control assembly 344

VII-15. Modified *Mariner V* thrust vector control assembly (only two actuators mounted) 344

VII-16. Modified *Mariner V* thrust vector control assembly (view looking up engine noggle) 344

A-1. Key elements of the *Mariner V* Space Flight Operations organization (conventional structure) 347

A-2. Space Flight Operations functional arrangement . . . 348

A-3. *Mariner* Venus 67 project—Mission Operations System schedule 349

A-4. *Mariner* Venus 67 project—tracking and data system schedule 350

Contents (contd)

Figures (contd)

B-1. Two-way transmission time vs flight time 354

C-1. Solar intensity 397

C-2. Canopus sensor intensity, channel 108 . . . 398

C-3. Canopus sensor cone angle, channel 303 398

C-4. Nitrogen gas (+X/−Y) pressure, channel 208 . . . 399

C-5. Nitrogen gas (−X/+Y) pressure, channel 209 . . . 399

C-6. Propellant tank pressure (posmaneuver), channel 119 . . 400

C-7. Nitrogen tank pressure (postmaneuver), channel 228 . . . 400

C-8. Tape recorder pressure, channel 304 401

C-9. Oxidizer pressure, channel 305 401

C-10. Solar panel 4A5 V_{OC} cell output, channel 417 402

C-11. Exciter No. 1 (−25) voltage (data number), channel 301 . . 402

C-12. Exciter No. 2 (−15) voltage (data number), channel 302 . . 403

C-13. Power switching and logic voltage, channel 109 . . . 403

C-14. 2400-Hz inverter output voltage, channel 207 . . . 404

C-15. Battery voltage, channel 206 405

C-16. Spacecraft receiver low-drive (data number), channel 210 . . . 405

C-17. High-gain antenna drive (data number), channel 213 406

C-18. Low-gain antenna drive (data number), channel 214 407

C-19. Central computer and sequencer 28-V monitor, channel 309 . . . 408

C-20. Solar panel 4A5 I_{SC} cell output, channel 415 408

C-21. Solar panel 4A5 I_{SCR} cell output, channel 416 409

C-22. Solar panel 4A1 current, channel 222 409

C-23. Solar panel 4A3 current, channel 224 410

C-24. Solar panel 4A5 current, channel 223 410

C-25. Solar panel 4A7 current, channel 225 411

C-26. Total current of solar panels 4A1, 4A3, 4A5, and 4A7, channels 222, 223, 224, and 225, respectively 411

C-27. Dual booster-regulator input current, channel 203 411

C-28. Communications converter and magnetic heater current, channel 204 412

C-29. Battery charger current, channel 216 412

C-30. Maneuver booster-regulator output current, channel 221 413

Contents (contd)

Figures (contd)

C-31. Main booster-regulator output current, channel 205 413

C-32. 2400-Hz inverter output current, channel 227 414

C-33. External RF power output (data number), channel 229 414

C-34. Traveling-wave tube cathode/helix current (data number), channel 300 415

C-35. Terminator sensor excitation (data number), channel 306 . . . 415

C-36. Bay 1 temperature, channel 401 416

C-37. Bay 2 temperature, channel 421 416

C-38. Bay 3 temperature, channel 402 417

C-39. Bay 4 temperature, channel 423 417

C-40. Bay 5 temperature, channel 404 418

C-41. Bay 6 temperature, channel 405 418

C-42. Bay 7 temperature, channel 426 419

C-43. Bay 8 temperature, channel 407 419

C-44. High-gain antenna temperature, channel 419 . . . 420

C-45. Low-gain antenna temperature, channel 432 420

C-46. Solar panel 4A1 and 4A5 substrate temperature, channels 409 and 429 421

C-47. Solar cell (I_{SC}—V_{OC}) temperature, channel 403 421

C-48. Solar panel temperature, channels 409 and 429 422

C-49. Solar panel spar temperature, channel 427 423

C-50. Solar panel 4A5 spar zener temperature, channel 427 423

C-51. Postinjection propulsion system nitrogen temperature, channel 408 424

C-52. Canopus tracking temperature, channel 410 424

C-53. Black temperature control reference temperature, channel 413 . . 425

C-54. Auxiliary oscillator No. 1 temperature, channel 414 425

C-55. Auxiliary oscillator No. 2 temperature, channel 418 426

C-56. Plasma probe temperature, channel 422 426

C-57. Voltage-controlled oscillator temperature, channel 424 427

C-58. Roll and yaw (+X) jet temperature, channel 406 427

C-59. Roll and yaw (−X) jet temperature, channel 433 428

Contents (contd)

Figures (contd)

C-60. Attitude control (−Y) jet temperature, channel 425 429
C-61. Battery temperature, channel 428 429
C-62. Primary sun sensor temperature, channel 430 430
C-63. Omni-antenna mast temperature (data number), channel 431 . . 431
C-64. Upper shield temperature, channel 434 431
C-65. Lower shield temperature, channel 435 432
C-66. Tape recorder temperature, channel 436 433
C-67. Ultraviolet photometer temperature, channel 437 433
C-68. Trapped radiation detector temperature, channel 438 . 434
C-69. Magnetometer temperature, channel 439 434
C-70. Propulsion fuel temperature, channel 217 435
C-71. Nitrogen tank (+X/−Y) temperature, channel 218 . . . 435
C-72. Nitrogen tank (−X/+Y) temperature, channel 219 . . . 436

Abstract

Volume I of this Report described the *Mariner* Venus 67 mission from launch to the midcourse maneuver; in this Volume II, mission planning, operations, and performance are discussed from the midcourse maneuver, which was commanded at 03:00 GMT on June 19, 1967, to the project-defined end of mission (Phase I) on December 1, 1967. The *Mariner V* spacecraft performed as planned, and data were telemetered to earth from all seven scientific experiments carried aboard the spacecraft. The telemetry system functioned in accordance with expectations, and coverage exceeded requirements. Spacecraft performance was excellent, with very few anomalies, and those of a minor nature. Recommendations for modifications affecting organization, software, etc., are included for possible use on future space missions of a similar type.

I. Introduction

The flight of the *Mariner V* spacecraft from the midcourse maneuver through the end of the mission is described in this Volume II of the *Mariner* Venus 67 Final Project Report. The formation of the project, mission planning, and the events from launch to the midcourse maneuver are described in Volume I.

The *Mariner* Venus 67 mission was primarily of a scientific nature, its objective being the gathering of data regarding the planet Venus and the area of space circumambient to that planet. The operation of the science instruments carried aboard the spacecraft, and the quantity and quality of the data telemetered from *Mariner V* to earth are, therefore, of paramount concern in the present volume.

In addition to these science measurements and data, the present volume covers trajectory and orbit determination, space flight operations, spacecraft performance analysis and command (SPAC) organization and function, spacecraft performance, and flight support testing. Project organization and management, encounter sequence and command descriptions, and telemetry data curves are contained in appendixes.

A. *Mariner* Venus 67 Mission Objectives

The primary objective of the *Mariner* Venus 67 mission was to conduct a flyby mission to Venus in 1967 to obtain scientific information that would complement and extend the results obtained by *Mariner II* relative to determining the origin and nature of Venus and its environment.

The secondary objectives of this mission were twofold: (1) to acquire engineering experience in the conversion of a spacecraft designed for a mission to Mars (the spare flight spacecraft from the *Mariner* Mars 1964 project) into one designed for a mission to Venus, and in the operation of this spacecraft (Fig. I-1); and (2) to obtain information on the interplanetary environment during a period of increasing solar activity.

All of the *Mariner* Venus 67 mission objectives were fully achieved.

B. Acquisition of Science Data

The primary scientific objective of the *Mariner* Venus 67 mission was to obtain information about the atmosphere, ionosphere, and plasma environment of Venus.

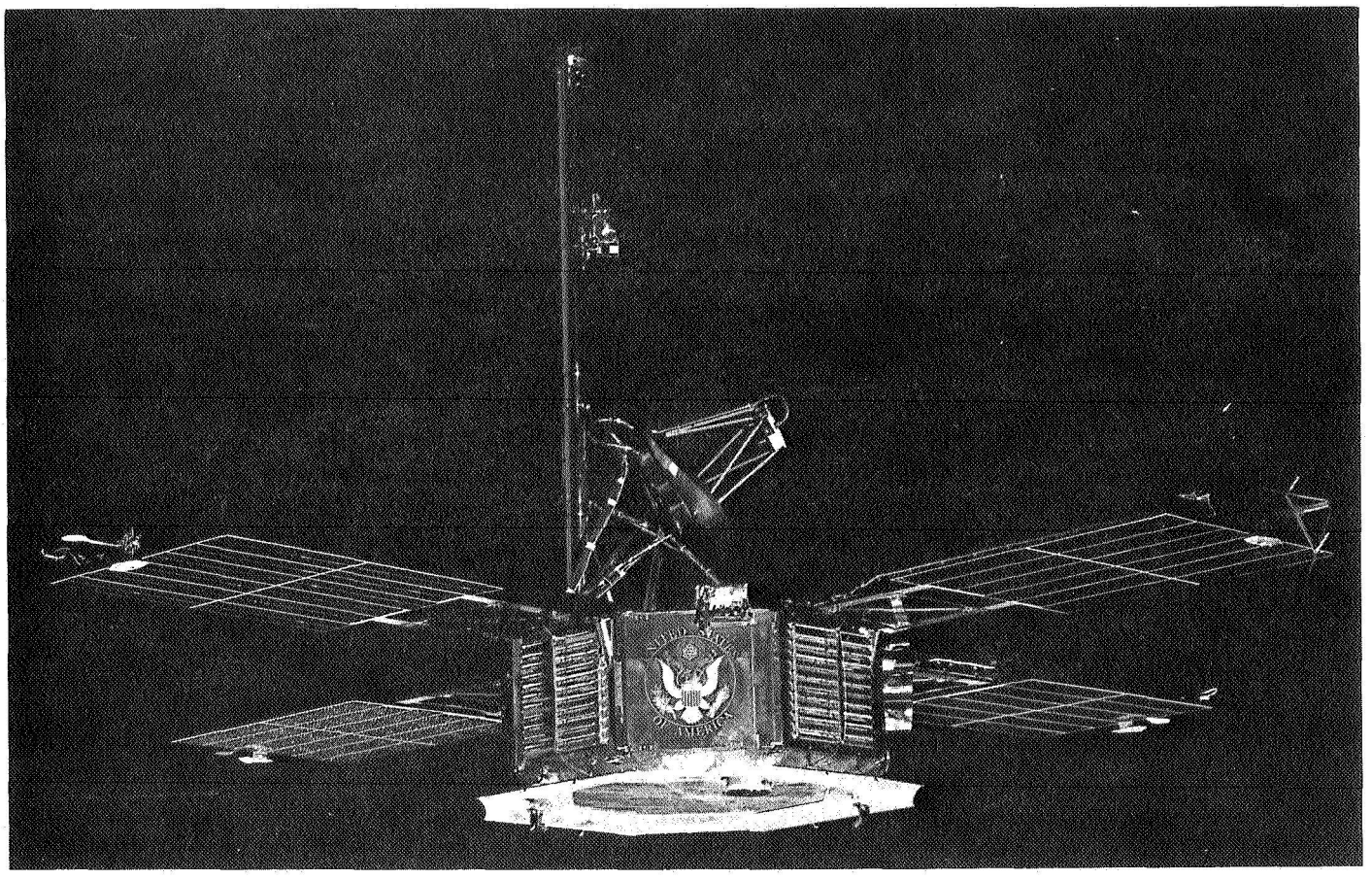


Fig. I-1. *Mariner V spacecraft*

Table I-1. *Mariner* Venus 67 mission scientific experiments

Experiment	*Principal scientific* investigator	Affiliation
S-band radio occultation	A. J. Kliore	JPL
Ultraviolet photometer	C. A. Barth	University of Colorado
Dual-frequency radio propagation	V. R. Eshleman	Stanford University
Helium magnetometer	E. J. Smith	JPL
Solar plasma probe	H. S. Bridge	Massachusetts Institute of Technology
Trapped radiation detector	J. A. Van Allen	University of Iowa
Celestial mechanics	J. D. Anderson	JPL

Table I-1 lists the seven science experiments carried aboard *Mariner V*, along with the names and affiliations of the principal scientific investigators. Most of these experiments evolved from previous projects. The S-band radio occultation experiment required the use of only the RF transmission subsystem on the spacecraft. The celestial mechanics experiment used only the tracking doppler data derived from the RF carrier. The UV photometer, helium magnetometer, solar plasma probe, and trapped radiation detector (TRD) were slightly modified to make them more suitable for a mission to Venus. Only the dual-frequency radio propagation experiment required the incorporation of a new science instrument, the dual-frequency receiver (DFR), into the payload.

Data were received from all seven instruments, which operated as planned. The experiments can be conveniently divided into the following four groups:

(1) Solar plasma probe, helium magnetometer, and TRD.

(2) UV photometer.

(3) S-band radio occultation and dual-frequency radio propagation.

(4) Celestial mechanics.

The solar plasma probe, helium magnetometer, and TRD experiments were designed to measure the interrelated phenomena concerned with the interaction between the planet and the interplanetary medium (the environment of Venus).

The objective of the UV-photometer experiment was to measure the properties of the topmost layers of the Venusian atmosphere.

In the S-band radio occultation and dual-frequency radio propagation experiments, radio waves were sent through the atmosphere of the planet to probe its properties.

The planet-related objectives of the celestial mechanics experiment were the very precise measurements of the mass of Venus and the shape of its gravitational field.

C. Mission Operations

In addition to the acquisition and telemetering of science measurements and data, operations for the *Mariner* Venus 67 mission from the midcourse maneuver through the end of the mission include the various phases of the *Mariner V* trajectory and information on orbit determination. Space flight operations cover support, organization and functions of the flight-path and space science analysis and command groups (FPAC and SSAC), as well as SPAC; data recovery and processing; and mission operations. A general description of the *Mariner V* spacecraft is included, along with the performance of onboard subsystems and instrumentation, and flight-support testing.

II. Science Measurements and Data

A. Science Experiments and Overall Results

The primary scientific objective of the *Mariner* Venus 67 mission was to obtain information about the atmosphere, the ionosphere, and the plasma environment of the planet. The following discussions present detailed and technical (although in all cases preliminary) accounts of the results.

Seven scientific experiments were planned, and all were conducted successfully. The seven experiments can be classified into four groups:

(1) The plasma probe, the magnetometer, and the energetic particle detectors were designed to measure the interrelated phenomena concerned with the interaction between the planet and the interplanetary medium — the environment of Venus.

(2) The UV photometer was designed to measure the properties of the topmost layers of the atmosphere.

(3) In the two occultation experiments, radio waves were sent through the atmosphere to probe its properties, from the highest level at which there was any perceptible effect on the propagation of a radio wave to the surface (if possible).

(4) The very precise measurement of the mass of Venus and the shape of its gravitational field was the planet-related objective of the celestial mechanics experiment.

An abbreviated chronology of significant events during the Venus encounter is shown in Table II-1, which also lists the codes used to represent the events on the orbit plots.

Of the specifically scientific instruments aboard, four were slightly modified versions of instruments originally built for the *Mariner* Mars 1964 mission: the magnetometer, the plasma probe, the charged-particle detectors, and the UV photometers. The fifth scientific instrument was the radio dual-frequency receiver (DFR).

The spacecraft science-data subsystem provided the sequencing command pulses to operate all of these instruments, and transferred their data outputs to the telemetry subsystem. The DFR provided scientific data whenever it was receiving signals from the Stanford University transmitter. The other instruments produced data continuously throughout the flight. The spacecraft transponder received commands from the earth and

Table II-1. Chronology of significant events during Venus encounter

Code	Time from encounter E, min	Event
P1	−156	Initial passage through a boundary in solar plasma
SHA	−22	Closest approach to shadow of Venus
IONI	−13.1	Initial detection of ionosphere by DFR
DL	−7.9	Dark limb of planet observed by UV photometer
ATMI	−3.18	Initial detection of atmosphere by S-band occultation experiment
GO	−2.0	"Geometrical occultation" — earth–spacecraft line of sight intersects dark limb of planet
LOS	−0.23	Loss of spacecraft radio signal resulting from occultation
E	0	Periapsis (encounter)
TER	+3.4	Terminator crossing observed by UV photometer
QUAD	+3.55	Quadrature; sun–Venus–*Mariner V* angle 90 deg
CO	+10.0	Center of geometrical occultation
BL	+16.7	Bright-limb crossing observed by UV photometer
P5	+18	Final passage through a boundary in the solar plasma
ROS	+20.6	Reacquisition of signal by Goldstone tracking station
XGO	+22.8	Exit from geometrical occultation at bright limb
ATMF	+23.0	Final observation of atmospheric effect on S-band signal
IONF	+24.0	Final detection of ionosphere by DFR

transmitted data to the earth. In addition, it provided the capability for the range data and the doppler range-rate data required for the celestial mechanics experiment and the radio signal required for the S-band occultation experiment.

The output of the science-data subsystem was in binary digital form, arranged into a frame 420 bits in length, repeated every 50.4 s during the latter portion of the flight. During the Venus encounter, this "real-time data format" was recorded on the magnetic tape and simultaneously sent to the telemetry transmitter. In addition, the data from certain instruments (DFR, UV photometers, and one of the charged-particle detectors) were sampled more frequently and recorded on the tape; the data storage rate was 133.33 bits/s.

At the time that *Mariner* V flew by Venus, it was 79,764,370 km from the earth, so that the transit time for radio signals was 266 s. Shown in Fig. II-1 is an isometric view of the orbit from E−210 to E+30 min, a period that includes all planet-related observations except that of the outermost edges of the hydrogen corona. The

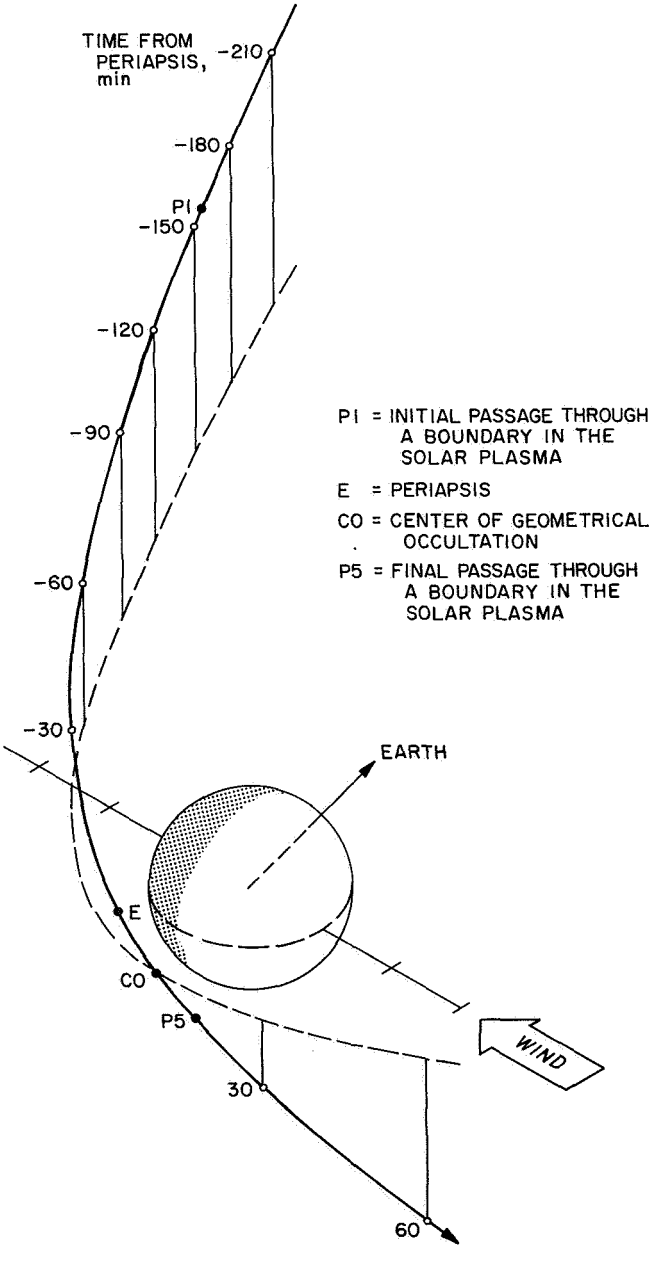


Fig. II-1. Isometric projection of Venus encounter orbit

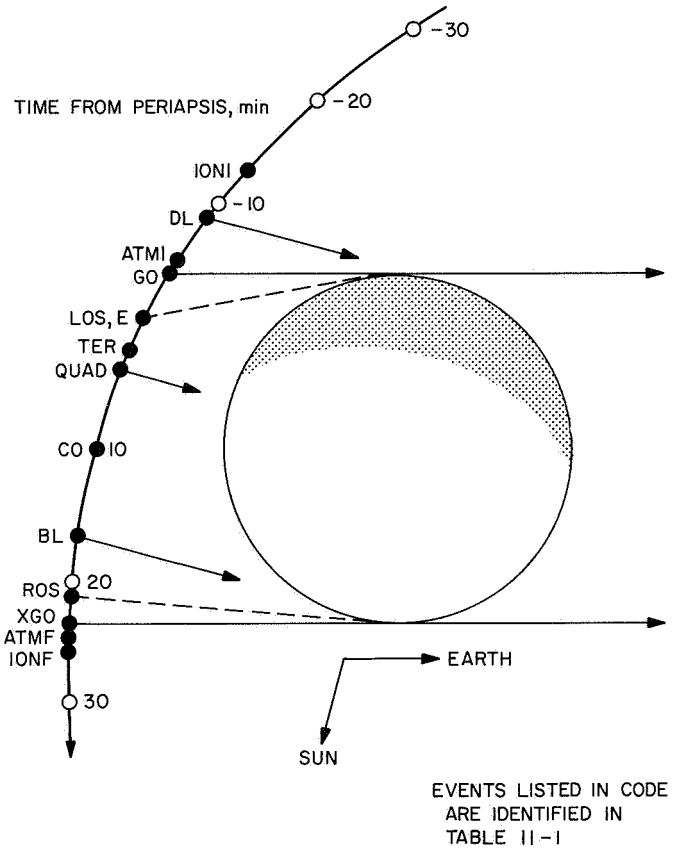


Fig. II-2. Venus encounter orbit shown in the orbit plane

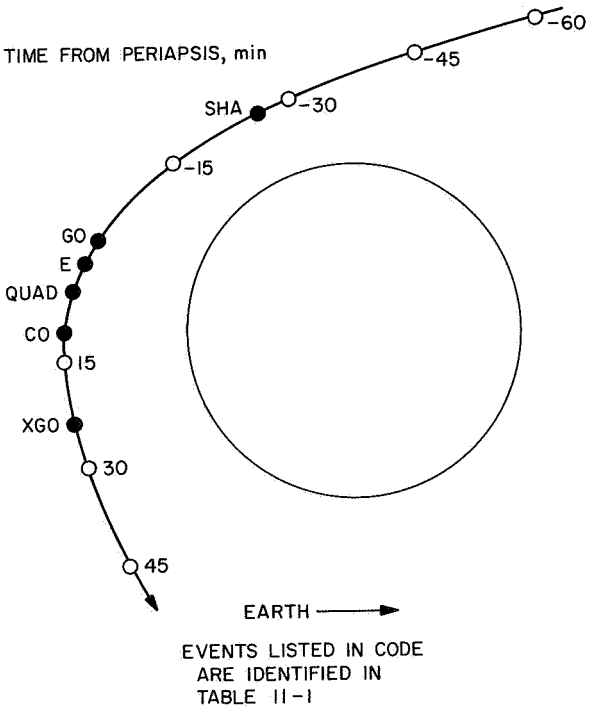


Fig. II-3. Venus encounter orbit projected on the terminator plane

spacecraft approached the dark side of Venus from north of the planetary orbit, crossed the plane of the terminator shortly after passing periapsis, and was deflected sharply (101.5 deg) toward the sun by the gravitational field.

The motion of the spacecraft in its actual orbital plane is shown in Fig. II-2. This view is the appropriate one for most purposes, as the center of the earth lies only 1.5 deg off this plane, and the line of sight for the UV photometers makes an angle of only 3.2 deg with the plane. Events pertinent to the ultraviolet experiment and the two occultation experiments are also shown in Fig. II-2.

A projection onto the plane of the terminator (Fig. II-3) depicts the orbit as seen from the sun. This view demonstrates that the spacecraft did not pass into the optical shadow of the planet; if this had occurred, orientation control would have been lost. The minimum distance to the shadow was more than 2400 km (at E−22 min).

The neutral atmosphere first became observable in the S-band signal by a change in frequency at 6140-km range (or 85-km altitude),[1] where the pressure is about 1 mbar (0.001 atm). As the spacecraft moved behind Venus, the shift in the signal frequency increased steadily to a maximum value of 16,000 Hz at the moment of occultation. In the *Mariner IV* occultation of Mars, the total shift had been only 5 Hz. Thus, the very great density of the Venus atmosphere is immediately apparent.

The signal frequency shift is related directly to the refractivity of the atmosphere. The derivation of more interesting atmospheric properties (composition, temperature, density, and pressure) requires the comparison of the refractivity data with other information; from these, a consistent model of the atmosphere can eventually be derived. Details of the preliminary model generated from the *Mariner V* data and the assumptions involved in the model are contained in the S-band discussion (Subsection E).

The results of the four groups of scientific requirements are summarized in the following paragraphs.

1. Interaction of interplanetary medium with Venus. The interplanetary medium is a very hot, tenuous, ionized

[1]For convenience, altitudes relative to the assumed 6056-km radius are quoted, although their validity is questionable.

gas (a plasma) that is an extension of the atmosphere of the sun. It is called the "solar wind." It flows outward from the sun at a velocity averaging about 400 km/s essentially because one layer in the atmosphere of the sun (the corona) is so hot and energetic that the gravitational field cannot confine it. This plasma carries with it a magnetic field that originates in the sun.

The *Mariner* Venus 1962 mission, which first established the presence and the properties of the solar wind, included a study of its interaction with Venus; but the encounter orbit, which was chosen to optimize the overall scientific mission, did not pass through the region where this interaction occurs. Consequently, the plasma environment of Venus has been completely unknown until now.

The interaction of the solar wind with the earth has been studied extensively by satellites for almost a decade. The plasma is deflected by the geomagnetic field and flows around the earth, approaching no closer than about 50,000 km. Upstream from the cavity (the magnetosphere) that the solar wind does not penetrate, there is a detached bow shock in the plasma because the solar wind is, in a sense, "supersonic."

The lunar satellite *Explorer XXXV* has explored the environment of the moon, and found a completely different kind of interaction. The plasma appears to strike the surface of the moon (and be absorbed), and the magnetic field passes through the moon with little, if any, interference.

Mariner V spent 2 h within the interaction region around Venus, observing an interface that is similar to the bow shock near earth and some additional structure inside of the interface. Two very significant inferences can be made from the mission data:

(1) The magnetic dipole moment of Venus is much smaller than that of earth (roughly at least a thousand times smaller), as proved by the small extent of the interaction region.

(2) The solar wind flows around the planet without striking it, in contrast to the case of the moon.

The obstacle that deflects the plasma appears to be the dense ionosphere on the sunlit side of Venus. Its high electrical conductivity prevents the passage of the incoming magnetic field (essentially an eddy-current effect), and the pile-up of the field alters the flow of the plasma. The most persuasive evidence supporting this conclusion is the observation by the Stanford occultation experiment that the upper boundary of the daylight ionosphere is exceedingly sharp and is pushed down very close to the planet (about 500-km altitude) by the momentum of the solar wind. No such phenomenon has previously been observed in space.

At the shock, and elsewhere in the interaction region near the earth, energetic particles accelerated by electric fields are observed. None was observed near Venus, probably because the region is too small.

2. Ultraviolet photometer experiment. The UV photometer aboard *Mariner V* sought to detect atomic hydrogen and atomic oxygen, which have strong lines in the far-ultraviolet region of the spectrum, at 1216 and 1304 Å, respectively. In the upper atmosphere of a planet, a gravitational fractionation process separates the constituents according to molecular weight (hydrogen on top, helium below it, and atomic oxygen next). By designing the UV photometer so that the scattered light was observed only in a very narrow cone, and by causing the spacecraft motion to sweep the cone across the planet, a record of light intensity as a function of altitude was obtained; this record can be interpreted as a density-vs-altitude profile for each species. The spatial rate of change of density is a measure of temperature.

Precise quantitative results are not yet available because the analysis of the ultraviolet data is a very complex problem in radiative transfer. However, three very significant and mutually consistent observations were made:

(1) The light scattered from hydrogen on the sunlit side was intense, indicating a total quantity of hydrogen comparable to or greater than that in upper atmosphere of the earth.

(2) The scale height, and hence the temperature of the hydrogen, is much lower than terrestrial exosphere; therefore, the escape rate of neutral hydrogen, which is determined by this temperature, is very much slower.

(3) The quantity of oxygen in the upper atmosphere of Venus is so small that it was not detected.

3. Occultation experiments. To probe the atmosphere, radio signals of three frequencies were sent through the atmosphere as the spacecraft passed behind Venus. The Stanford University transmitter sent two signals, at 49.8

and 423.3 MHz, which were received and analyzed aboard the spacecraft. Slightly more than half of the data storage was allotted to these data. The spacecraft telemetry signal at S-band (near 2298 MHz), traveling in the opposite direction, was received on earth, where vastly more data could be recorded. In both cases, the measured effects on the radio waves consisted of reduction of signal strength (because of absorption and defocusing) and shift in frequency (because of the refraction effect). In both experiments, data were obtained on the neutral atmosphere and on the ionized atmosphere. The use of two harmonically related frequencies in the Stanford experiment provided extremely high sensitivity for the ionized component. Consequently, the weak nighttime ionosphere was clearly observed in this experiment; whereas, in both experiments, altitude profiles of the strong daytime ionosphere were obtained. The S-band experiment, because of its enormous quantity of data, provided more precise information on the neutral atmosphere.

The altitude in the atmosphere at which data were obtained at any given time was calculated from the spacecraft orbit, which was very precisely known (to within less than 1 km relative to Venus) from the measurements of range and range rate relative to the earth. Accordingly, spacecraft position was determined relative to the gravitational center of Venus. To convert this distance to altitude required a knowledge of the local Venus radius. The then currently accepted value of the mean radius near the equator was 6056 km, but it was not known how accurately this represented the radius at the point of interest. This uncertainty became troublesome when attempting to relate the *Mariner V* measurements to those of the *Venera-4* spacecraft where the data were related to the local planet surface by means of a radio-altimeter.

The nighttime ionosphere was first observable several thousand kilometers from the surface of Venus. A fairly complex layered structure was observed, with a peak in density near 200-km altitude. On the daylight side, a peak density about 50 times greater was observed near an altitude of 130 km, and the density declined with altitude, terminating abruptly near 500 km, as previously discussed.

4. Celestial mechanics experiment. *Mariner V* ranging and doppler radio tracking data were fit to obtain, along with other measurements, the mass of Venus. In terms of the universal gravitational constant, this value is 324,859.61 ± 0.49 km^3/s^2.

B. Solar Plasma Probe Experiment

The first attempt to observe a disturbance in the interplanetary medium caused by the planet Venus was made with *Mariner II* on December 14, 1962. No effect was observed (Ref. 1) partly because the spacecraft passed on the sunward side of the planet and approached no closer than 40,000 km or 6.6 Venus radii (r_V). Thus, it was shown that an upper limit to the magnetic dipole moment of Venus is approximately 20 times less than that of the earth.

The trajectory of *Mariner V* was more favorable for this type of observation because the spacecraft approached to within 0.4 r_V of the optical shadow of the planet and to within 0.7 r_v of the surface. The data from the magnetometer and plasma probe show unmistakable evidence of the existence of a bow shock around Venus similar to (but much smaller than) that near the earth, as well as additional structure inside the shock.

1. Description of instrumentation. The low-field-vector helium magnetometer was first flown on *Mariner IV* (Ref. 2). This instrument has an intrinsic noise level of 0.1 γ (rms) and a digitization uncertainty of 0.2 γ. (1 $\gamma = 10^{-5}$ G). Five triaxial field samples were obtained each 50.4 s.

The magnetometer sensor was located about 2 m from the main body of the spacecraft. To minimize the spacecraft field, magnetic constraints were imposed on the spacecraft, which was also demagnetized before launch. The magnitude of the spacecraft field at the sensor was determined in flight to be 10 γ. First, the rolling of the spacecraft about the sun direction for 17 h immediately after launch and for several hours after the midcourse orbit correction established the values of the two components perpendicular to the axis of rotation. Second, all three components were computed using a new technique (Ref. 3) based upon the frequently occurring changes in the interplanetary field that conserve the field magnitude. Such changes are associated with contact surfaces traveling outward in the solar wind (Ref. 4). This procedure allows continual checking of the spacecraft fields in flight, which is an important consideration because *Mariner V* was attitude-stabilized. It was estimated that the components of the spacecraft field were determined to within 0.5 γ.

The plasma detector, a modulated-grid Faraday cup (Ref. 5) was essentially identical to that flown aboard *Mariner IV*. Positive ion currents were measured in 32 energy intervals covering the range 40–9400 eV. The detector, which points at the sun, had a sensitivity that

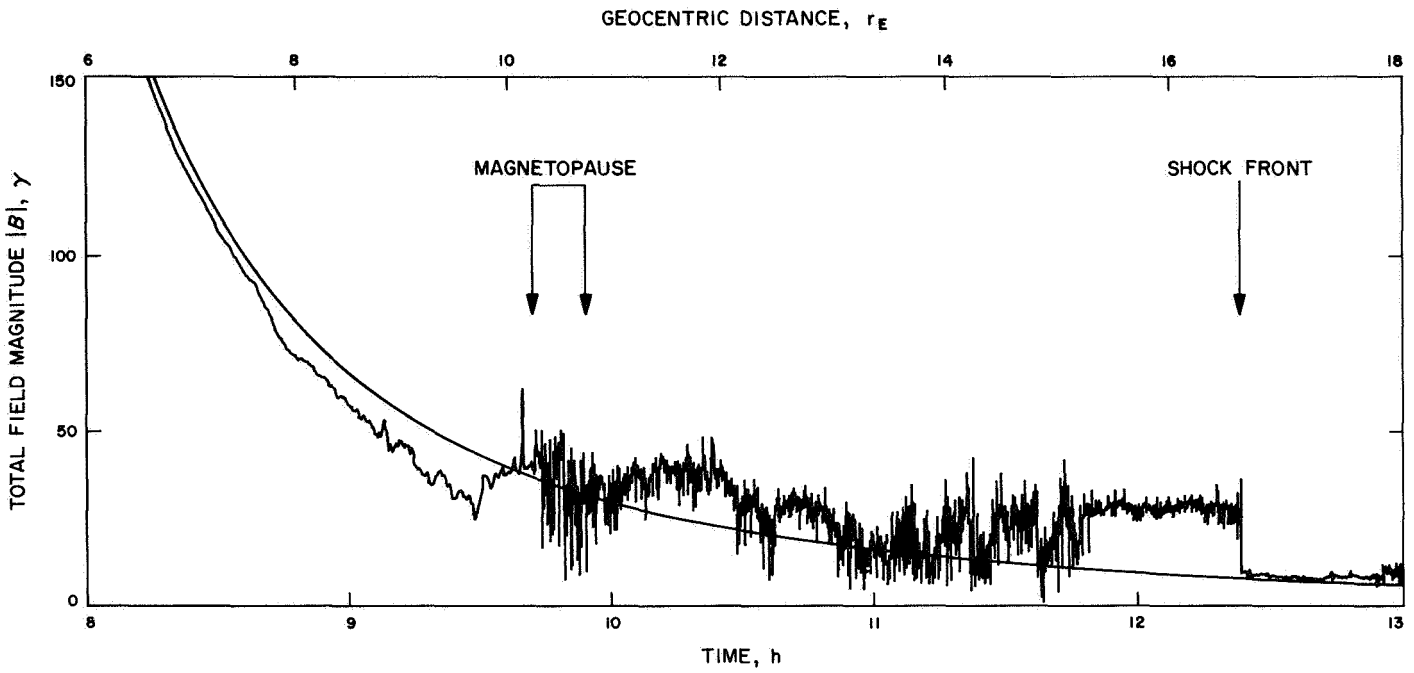


Fig. II-4. *Mariner V* magnetic field data near earth

was fairly constant up to 30 deg off the sun–spacecraft line, and then decreased rapidly to zero at 65 deg. A current measurement at one energy level had an integration time of ~5 ms, and the sampling rate was such that a plasma energy spectrum was determined every 5 min. However, all the significant measurements in a spectrum required less time, and were completed in 3.8 min or less.

2. Plasma and magnetic field data. For comparison with the near-Venus data, Fig. II-4 shows the total field magnitude $|B|$ as observed by *Mariner V* in the vicinity of the earth. These data clearly show the characteristic field changes at the magnetopause (the surface separating magnetic lines of force connected to the earth from the heated, compressed, and semi-turbulent region called the magnetosheath) and the bow shock (the usually sharp boundary outside of which lies the free-streaming interplanetary medium). The presence of two or more regimes in the magnetosheath, characterized by different amplitudes of fluctuation and different values of average field strength, is a common occurrence. It is probably the effect of the convection into the magnetosheath of filamentary structures in the solar wind, which often shows abrupt changes in properties.

The plasma and magnetic field data near Venus are shown in Fig. II-5. The two uppermost curves, the positive ion number density n and the bulk velocity V, are plasma parameters computed from the observed energy spectra. The middle trace is the ambient field magnitude $|B|$ computed from the three measured components after subtracting the spacecraft field. The two bottom curves give the field direction in spherical coordinates. The angle α is the longitude or azimuth measured in the $\mathbf{R} \cdot \mathbf{T}$ plane, where $\mathbf{R}$ is a unit vector in the anti-solar direction and $\mathbf{T}$ is an orthogonal vector that is parallel to the equatorial plane of the sun, and points in the direction of the orbital motion of the planet. For most purposes, the $\mathbf{R} \cdot \mathbf{T}$ plane may be regarded as parallel to the ecliptic plane with which it makes an angle of only 7 deg. The angle β is the latitude measured from the $\mathbf{R} \cdot \mathbf{T}$ plane; positive values indicate that the field has a northward component. The direction toward the sun corresponds to $\alpha = \pm 180$ deg, and the ideal spiral field direction near the orbit of Venus to $\alpha = 145$ deg when the sense of β is toward the sun.

The data are plotted as a function of time (in minutes), zero being taken at the instant of periapsis. Five features (events) in the plasma and field data are identified by circled numbers.[2] The positions of these events on the *Mariner V* orbit are indicated in Figs. II-6 and II-7.

[2]To avoid possible confusion, the symbols ① through ⑤ in Figs. II-6 through II-8 are referred to as events whether they are descriptive of time of location; the symbols ① through ⑤ in Fig. II-26 (Subsection G) relate to other parameters for purposes of the Subsection G discussion only.

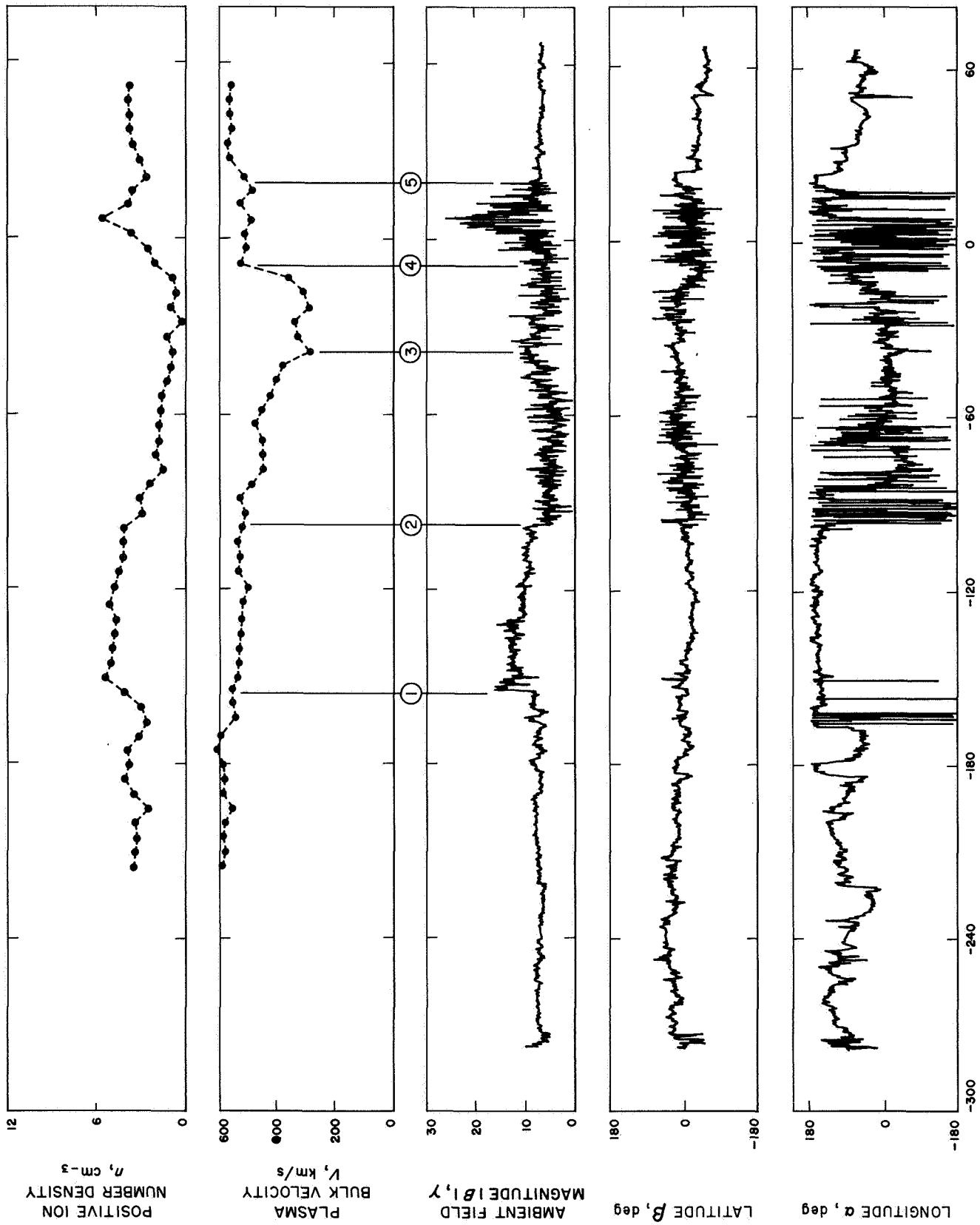


Fig. II-5. Plasma and magnetic field data near Venus

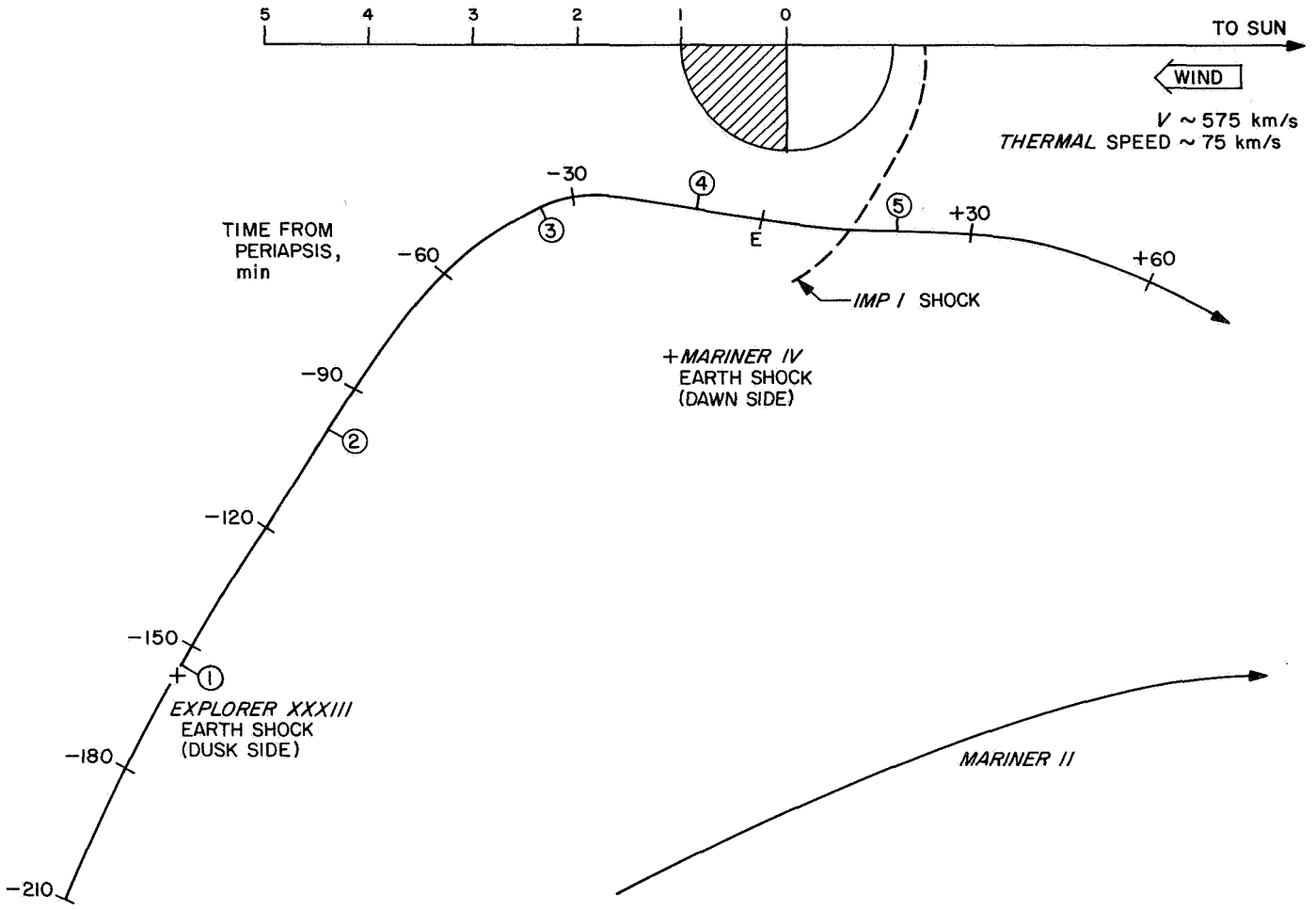


Fig. II-6. *Mariner V* orbit relative to sun–Venus axis

Figure II-6 shows a polar plot using the planet–spacecraft separation and the sun–planet–spacecraft angle as coordinates. It is equivalent to tracing the path of the spacecraft in a plane that rotates about the Venus–sun line with the spacecraft. To the extent that the phenomena have cylindrical symmetry about this line, these are the pertinent parameters.

The three parts of Fig. II-7 show the usual orthographic projections of both the *Mariner V* trajectory and the measured fields. The aphrodiocentric–solar–ecliptic (ASE) coordinates are defined by a plane parallel to the ecliptic passing through the center of Venus and by X_{ASE} (the projection in this plane of the direction to the sun). The axis Z_{ASE} points toward the north ecliptic pole, and Y_{ASE} completes the orthogonal, right-handed set. The field vectors are not shown at equally spaced intervals, but at times that best illustrate the character of the average magnetic field within the various regions.

The observations are most easily described in terms of a specific model, which will be developed in the course of the discussion. This model should be regarded only as a phenomenological description; its dynamical validity has not been substantiated.

The interplanetary conditions prior to and after encounter were only moderately disturbed. The plasma properties were quite steady, but the velocity (~590 km/s) and temperature [$\sim 3 \times 10^5$ (°K)] were unusually high. The direction of the magnetic field showed substantial fluctuations, but its magnitude was nearly constant at ~8 γ, a value close to that expected at the orbit of Venus. Apparently, a series of solar-wind structures (perhaps filaments) were convected past the spacecraft at intervals of a few minutes to 30 min. The solar-wind structures would require 1.3 min to sweep over the region between events 1 and 5 (Fig. II-7).

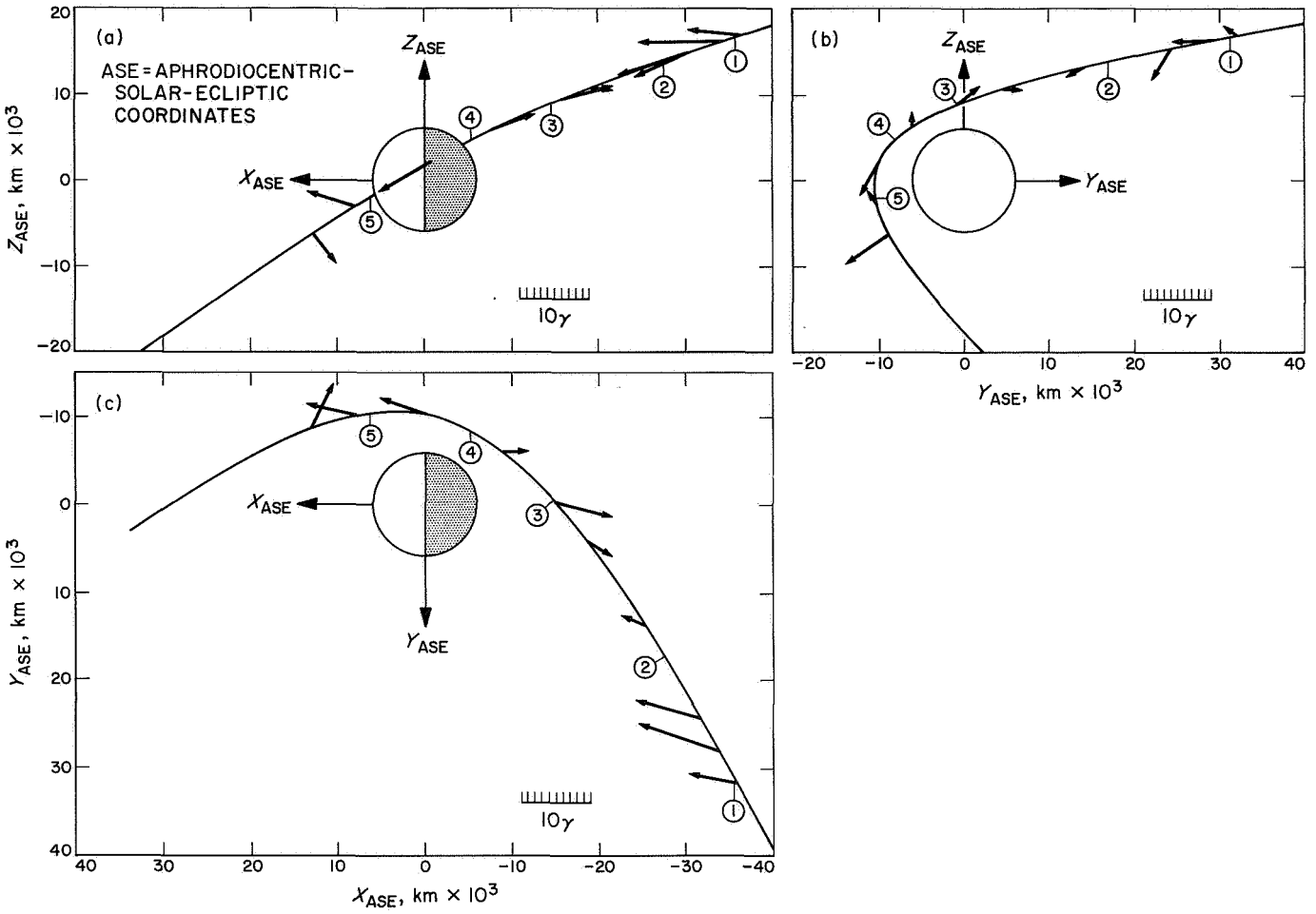


Fig. II-7. *Mariner V* trajectory and magnetic field vectors

The influence of Venus on the solar-wind flow first became apparent at event 1. The magnetic field strength increased abruptly from 8 to 15 γ and the fluctuations increased markedly, although the average direction remained nearly along the line from the sun. The plasma velocity dropped slightly (~10%), and the density decreased markedly (~40%). Such changes are commonly seen across a shock; the identification of event 1 as a bow shock is almost inescapable in view of this and later observations.

For a few minutes just before event 1 and again just after event 5 (identified below as a shock crossing), the field had a characteristic direction and strength. It would be possible to identify these regions as part of the shock structure and to ascribe a previous occurrence at −180 min to a motion of the shock front of the kind often seen near earth. However, in the absence of a corresponding magnitude change, this identification is rejected and the field at these times is considered interplanetary in origin.

During the hour after event 1, the plasma velocity and density dropped slightly, and there was a marked broadening of the velocity distribution. The field characteristics were unchanged except for one abrupt decrease in magnitude and in the amplitude of the fluctuations. Because similar changes are often observed in the magnetosheath of the earth (see Fig. II-4), this decrease is interpreted as a response to changes in the interplanetary medium.

At event 2, there was a second abrupt change: the field strength dropped from 9 to 6 γ (less than the average magnitude in interplanetary space), with little change in average direction, and the fluctuations increased substantially. The plasma density and velocity began to decrease steadily, reached their minimum values near event 3, and returned to high values by event 4. Fifteen minutes after event 2, the direction of the field made the first of three reversals that are not associated with other significant changes; presumably, the field direction in the

undisturbed solar wind was reversing (much as it did during the 2 h before event 1). The change at event 2 does not appear to be a magnetopause crossing, both because of these reversals, and because the plasma characteristics resemble those of a magnetosheath, not a magnetosphere or magnetospheric tail.

The most natural interpretation of these results is that the electrically conducting ionosphere of Venus cannot be penetrated quickly by the solar-wind field; therefore, most of the plasma is prevented from reaching the atmosphere. As a result, a standing shock is formed ahead of the planet. The compressed solar plasma behind the shock flows around the sides of the planet, becomes supersonic, and tends to leave a cavity behind the planet. The magnetic and gas-kinetic pressures should produce an expansion into the partially empty cavity; the edge of the expansion wave may approximate a cone running through event 2, near event 4, and about 500 km above the surface of the planet. Within 45 deg of the subsolar point, the interface between the atmosphere and the solar wind, the anemopause (Ref. 6), appears to be at about this level, where the Stanford group observed an abrupt decrease in the ion density from 10^4 cm^{-3} to an interplanetary value.[3] This interpretation is compatible with the argument given below, which is based upon the conservation of interplanetary magnetic flux.

The total flux contributed by the weak field inside a cone through events 2 and 4, and the strong field crossing the cone connecting events 1 and 2, is roughly equal to the flux of undisturbed interplanetary field that would occupy this area if Venus were absent. If the edge of an expansion wave is typically much less sharp than event 2, a possible explanation is that, as occurs near the earth, all boundaries move rapidly from time to time, and that event 2 is a rapid shift of the expansion region across the position of the spacecraft.

At event 3, the total plasma flux was reduced to $\sim 10^7$ $(cm^2\ s)^{-1}$ (about a factor of 20 below the interplanetary value) and, primarily because of the low density, the Alfvén velocity rose to several hundred kilometers/second. Thus, the plasma had little inertia, and the field should have adjusted rapidly to a vacuum configuration. The field direction, nearly radially outward from the sun, and the slight increase in magnitude near event 3, which could compensate for the decreased plasma pressure, are consistent with this model. However, the very low plasma density near event 3 and the accompanying increase in $|B|$ cannot both be explained as caused by an expansion wave. Perhaps the plasma flow along these tubes of flux, which must pass very close to the planet, was partially obstructed by an interaction with the atmosphere. As to whether the unobserved region in the shadow of Venus was occupied by an interplanetary field that passed through the planet, by a magnetosheath field carried in by the expansion wave, or by an intrinsic planetary field, any comments would be pure speculation at this preliminary stage in the data analysis.

Conditions in the region between events 4 and 5 were comparable to those observed in the magnetosheath of the earth at about the same local time. The high values of $|B|$ may have been caused by the compression of the plasma as it passed through the shock or, in part, by the very irregular structure of the magnetic field generated at the shock. No feature characteristic of a magnetopause was present. On the basis of the abrupt decrease in the magnetic fluctuations and the return of the plasma velocity to its interplanetary value, event 5 is identified as the bow shock. The unaccountable absence of any sudden change in the average value of $|B|$ or in the plasma density (as there was at event 1) illustrates the incompleteness of current experimental and theoretical knowledge of the structure of collisionless hydromagnetic shocks.

3. Schematic model. Most of the features seen in the data appear to fit a schematic model (Fig. II-8) in which the solar wind is deflected, but not absorbed, by the ionosphere and upper atmosphere of Venus. According to Lees (Ref. 7) the major deficiency of this model is that a laboratory gas-dynamic shock with appropriate scaling would be expected to pass more nearly through event 2 than through event 1. Several factors, in combination, might explain this:

(1) The normal aberration caused by the motion of Venus and the observed average azimuthal velocity of the solar wind could rotate the axis through about 5 deg toward event 1.

(2) The solar-wind direction is known to fluctuate and, at times, to be as much as 5 deg from its average position (Ref. 8).

[3]The differences that are apparent between the interactions of the solar wind with Venus and with the earth make the term "magnetopause" inappropriate in the former case. It is convenient to have a more general name for the surface that separates the solar-wind plasma from the region occupied by a planetary atmosphere, magnetic field, or wake. For this surface, where the "wind stops," the name "anemopause" seems agreeably descriptive, euphonious, and proper Greek.

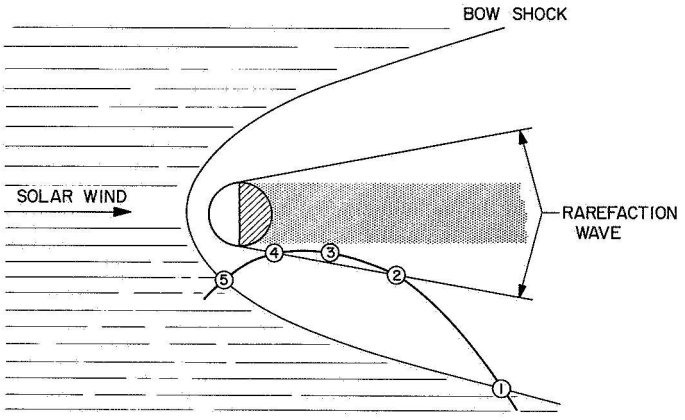


Fig. II-8. Schematic representation of the solar wind interaction with Venus

(3) The magneto-acoustic velocity deduced from the plasma and field observations in the undisturbed solar wind is ~120 km/s, corresponding to a Mach number of ~5, which is somewhat low for the hypersonic limit and may give a shock that is farther from the axis.

(4) The highly irregular magnetic field in the magnetosheath region contributes an additional pressure that is not included in the usual gas-dynamic analysis.

Until further analyses (and perhaps further observations) have been made, these suggestions must be regarded as speculation, and the dynamic soundness of this model must be regarded as uncertain.

Other models are possible, but are unattractive. Most of the features seen near Venus could be regarded individually as features of the interplanetary medium, although some of them are very unusual. However, it seems extremely unlikely that all of these features would have been observed during the short period in which *Mariner V* was near the planet, and that they would have been organized purely by coincidence into the observed pattern.

The magnetopause and bow shock observed around the earth can be scaled so that the shock passes through event 1 and very near to event 5. The scaled magnetopause is then in the upper atmosphere at the subsolar point, and the trajectory would be inside the magnetosphere between events 2 and 4. The corresponding scaling of the dipole moment gives a value for Venus about 1/700 that of the earth. Although the presence and position of the shock is an attractive feature of this model, the presence of solar wind inside the scaled magnetopause and the very low value of $|B|$ near event 3 seem to rule out the model completely.

An upper boundary can be placed on the magnetic moment of Venus, but it depends for its precise value upon the details of the model used. The unsuitability of the scaled geomagnetic analog summarized above requires that the actual ratio of dipole moments be significantly smaller than that derived from the model. A reasonable limit is estimated to be within a factor of two of 10^{-3} times that of the earth. Obviously, there is no way to tell from such analyses whether Venus has an intrinsic field smaller than the upper boundary. Nothing reported here is inconsistent with the available information on the recent Russian observations, which appear to give an even lower limit.

The interaction of the solar wind with Venus differs from its interaction with either the earth or the moon. In the case of the moon, the plasma ions are absorbed by the lunar surface, and no shock develops (Ref. 9). Moreover, the moon appears to provide sufficient insulation to enable the interplanetary field to be convected through it nearly unchanged (Ref. 10). Except for a region close to or inside the lunar shadow, the plasma flow near the moon is unaffected by its presence. In contrast, the plasma flow near Venus is bounded by an anemopause. The shock around Venus resembles that around earth except in scale, but conditions inside are quite different because the anemopause around Venus is probably supported by the ionosphere, whereas that around the earth is supported by the geomagnetic field. The plasma appears to expand into the cavity on the downwind side of Venus, whereas behind the earth, inward expansion is prevented by the magnetic field in the geomagnetic tail.

C. Helium Magnetometer Experiment

The helium magnetometer experiment is discussed in Subsection B, above, as part of the solar plasma probe experiment.

D. Trapped Radiation Detector Experiment

The University of Iowa apparatus aboard *Mariner V* comprises three Geiger tubes and a 32-μm-thick, totally depleted, silicon surface barrier detector, with four electronic discrimination levels. The data obtained during the

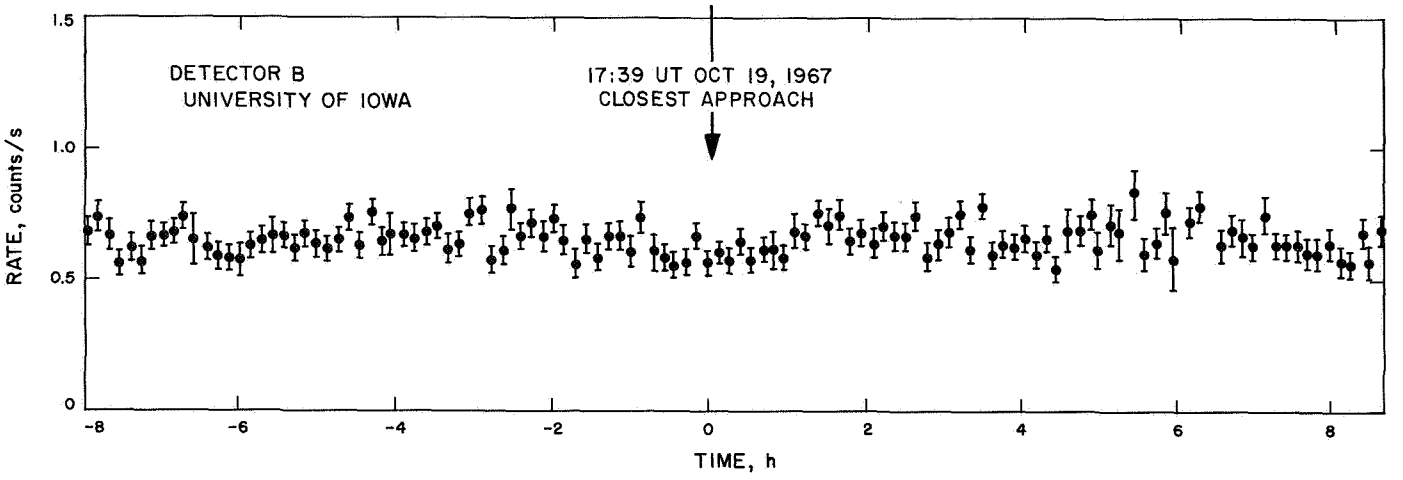


Fig. II-9. Counting rate of the electron detector $E_e > 45$ keV

encounter with Venus on October 19, 1967, shows a complete (or nearly complete) absence of energetic electrons and protons associated with the planet in to the minimum radial distance of approach of 10,150 km. These results are consistent with results from the 41,000-km approach of *Mariner II* to Venus in 1962, but are much more definitive by virtue of the closer approach.

Specific upper limits on the average unidirectional intensities of planet-associated particles during any 216-s interval of the encounter period are 3.0 $(cm^2\ s\ sr)^{-1}$ for electrons $E_e > 45$ keV, and 1.0 $(cm^2\ s\ sr)^{-1}$ for protons $0.32 < E_p < 12$ MeV.

Figure II-9 shows a plot of the 216-s averaged counting rate of the most sensitive of the electron detectors ($E_e > 45$ keV) for a 16-h period centered on the time of closest approach. The counting rate at points remote from the planet was caused principally by galactic cosmic rays that penetrated the sidewalls of the detector. There was also a small contribution from solar particles.

By contrast, the same apparatus observed maximum unidirectional intensities of 1×10^6 $(cm^2\ s\ sr)^{-1}$ for electrons $E_e > 45$ keV, and of 3.5×10^6 $(cm^2\ s\ sr)^{-1}$ for protons $E_p > 320$ keV during its outbound traversal of the magnetosphere of the earth on June 14, 1967. The spacecraft passed through the outer portion of the magnetosphere of the earth on its sunward side. A major, precipitous decline of the intensities of geomagnetically trapped particles occurred during the period 09:35–09:43 UT on June 14 at a geocentric radial distance of about 10 r_E and a sun–earth–spacecraft angle of 59 deg.

However, rapid increases of electron and proton intensity were observed in the "transition region" for several hours thereafter. The last such sharp rise occurred at 12:25–12:27 UT at a radial distance of 16.8 r_E and a sun–earth–spacecraft angle of 62 deg, in almost exact coincidence with the last magnetometer indication of the presence of the earth—a discontinuous drop from 25×10^5 to 8×10^{-5} G.

The flow of the solar wind is arrested on the sunward side of a planet at such a radial distance R that the dynamic pressure of the wind is equal to the opposing pressure of the (compressed) magnetic field B of the planet:

$$knmv^2 = \frac{B^2}{8\pi} \tag{1}$$

Where n is the number density of protons each of mass m and directed velocity v in the solar wind, and k is a numerical factor between 1 and 2.

A necessary condition for the existence of a radiation belt of trapped particles is that the "stagnation point" be far enough above the surface so that the atmospheric density is adequately small. For Venus, it appears safe to take an altitude of several thousand kilometers or a radial distance of $\sim 2\ r_V$ as a generous value. Assuming that n is inversely proportional to the square of the distance from the sun and v is independent of this distance, and noting that $B \propto M/R^3$, physical similitude with the known properties of the magnetosphere of the earth yields a scaling law from Eq. (1), namely

$$\frac{R_\varphi}{R_\oplus} = 0.9 \left(\frac{M_\varphi}{M_\oplus}\right)^{1/3} \tag{2}$$

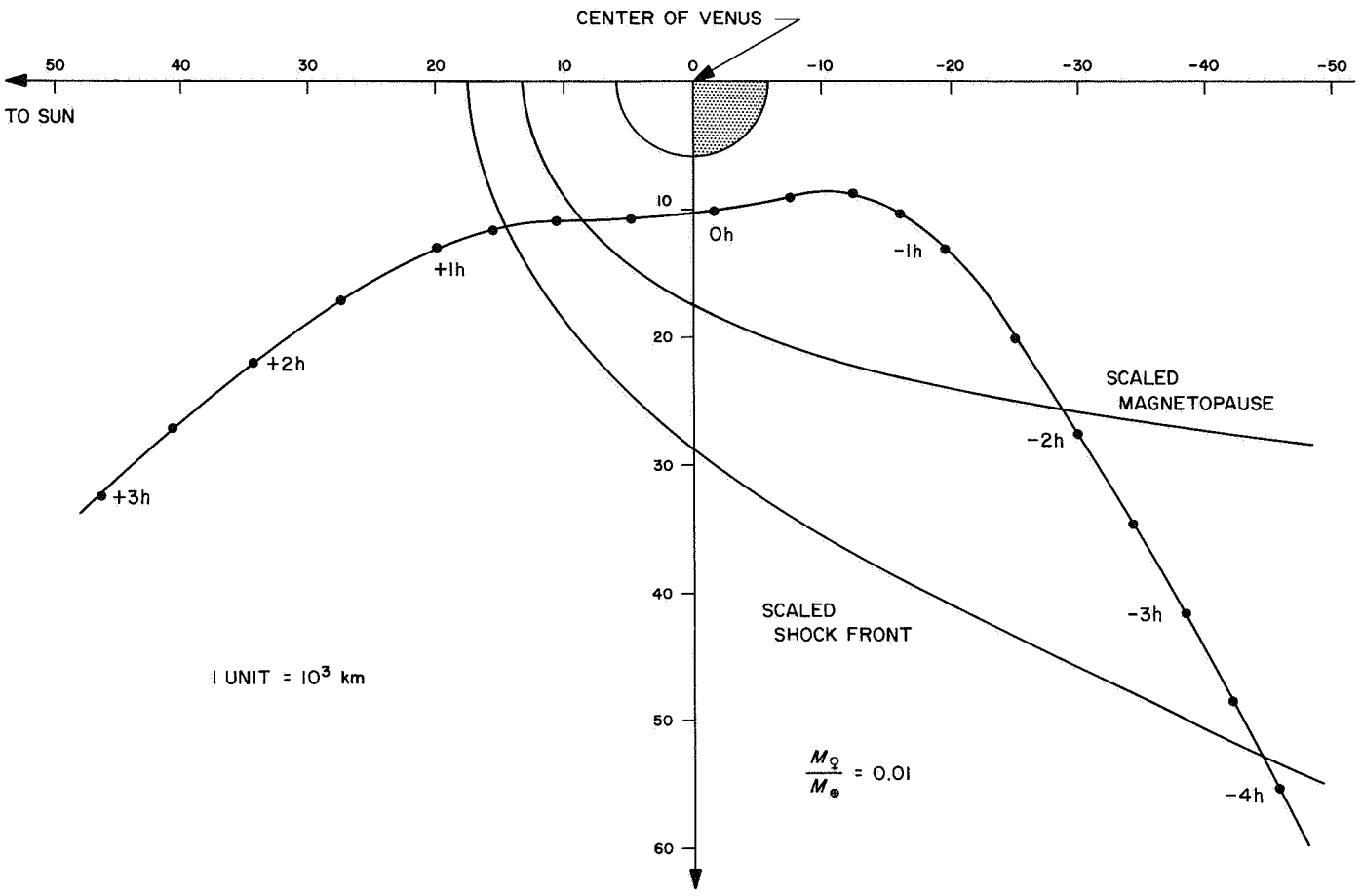


Fig. II-10. Polar plot of encounter trajectory

where R_φ and $R_\oplus$ are the radial distance from the centers of Venus and the earth to corresponding points on their respective magnetospheric boundaries, and M_φ and $M_\oplus$ are their respective magnetic dipole moments.

In Fig. II-10 is shown a sketch of the magnetopause and shock front to be expected for $M_\varphi/M_\oplus = 0.01$, as scaled from the observed boundaries for the earth using Eq. (2). Also shown is a portion of the encounter trajectory of *Mariner V* plotted in polar coordinates in the (rotating) plane that passes through the sun, the center of the planet, and the spacecraft. The interpretative use of such a plot includes the assumption of approximate axial symmetry about the sun–planet line, as is established adequately for the present purpose by both theory and experiment. It is clear that *Mariner V* penetrated deeply into such a scaled magnetosphere.

Although the foregoing discussion is believed to be reliable in establishing a necessary condition for the existence of a radiation belt of durably trapped particles, it is less clear that such a condition is sufficient to assure the existence of a trapped particle population that would be detectable by the *Mariner V* apparatus. Sufficiency is argued on the following grounds:

(1) The magnetic and magneto-fluid dynamical conditions at the shock front and between the shock front and the magnetopause would be essentially identical to those of the physical system of the earth.

(2) The existence of easily observable patches or "spikes" of electrons $E_e > 45$ keV is characteristic of these regions around the earth (as confirmed by the *Mariner V* apparatus), as well as to distances as great as 500,000 km "downstream" from the earth.

(3) The frictional interaction between the solar wind and the magnetic field and ionized gas of the exosphere of Venus would result in a system of polarization electric fields (or magnetic convection) that would accelerate particles and deliver them into the inner magnetosphere with an average increase of energy of some tens of kilovolts.

It is concluded, therefore, that the absence of a detectable population of electrons $E_e > 45$ keV (Fig. II-9) near Venus establishes $M_♀/M_⊕ = 0.01$ as a generous upper limit.

A diagram similar to that in Fig. II-10 for $M_♀/M_⊕ = 0.001$ shows that the sunward magnetopause would then lie at the surface of the planet, and that durable trapping of charged particles would be impossible. Even in this case, however, shock-generated energetic electrons and/or protons might be expected. No such indications are present in the data.

Nonetheless, both the magnetometer and the solar-wind detector aboard *Mariner V* observed clear and significant (though weak) "signatures" of the planet. These effects have been attributed to the magneto-fluid dynamical interaction of the solar wind with the conducting ionosphere of the planet; the latter was clearly established by other experiments aboard *Mariner V*.

Because Venus has about the same size and average density as the earth, and probably has a metallic core and an internal temperature similar to or greater than those of the earth, the very small (or perhaps zero) value of the intrinsic magnetic dipole moment of Venus is presumably attributable to its very slow rotation—a sidereal period of 245.1 ±2 days—and the consequent weakness of dynamic electromotive forces.

E. Ultraviolet Photometer Experiment

The *Mariner V* flyby mission to Venus presented an opportunity to measure ultraviolet emissions from the upper atmosphere of the planet with a small instrument. The atmospheric species of atomic hydrogen and atomic oxygen have resonance lines at 1216 and 1304 Å that may be measured with a simple UV photometer. The measurement of the ultraviolet emissions that result from resonance scattering of solar radiation by these atoms is a method of determining their density. The variation of the density as a function of height above the surface is a measure of the temperature of the outermost region of the atmosphere. This experiment provided one part of a systematic study of the structure of the atmosphere of Venus. This is a report of the first preliminary results from the UV-photometer experiment.

1. Description and operation of photometer. The UV photometer consisted of three photomultiplier tubes, each with a different filter to isolate different regions of the vacuum ultraviolet spectrum. These photomultipliers, which have cesium-iodide photocathodes and lithium-fluoride windows, respond to ultraviolet radiation between 1050 and 2200 Å, and have greatly decreased sensitivity at longer wavelengths. The three filters are the lithium-fluoride window of the first tube and additional filters of calcium fluoride and barium fluoride for the other two tubes.

The effective pass bands for the three channels are: 1050–2200, 1250–2200, and 1350–2200 Å. The difference between the signals observed by the first two channels is caused by the 1216-Å Lyman-alpha line of atomic hydrogen, and the difference between the second and third channels is caused by the 1304-Å triplet of atomic oxygen. The third channel also measures any ultraviolet radiation at wavelengths greater than 1350 Å. The field of view (FOV) of the lithium-fluoride/Lyman-alpha channel is 3.0 deg; the other two channels have FOVs of 1.2 deg. The three channels of the UV photometer are aligned to look in the same direction. The photomultiplier tubes operate with a variable high voltage that is so controlled by the anode output current that each tube may operate with a dynamic range of 10^3 and may be protected from potential damage caused by the albedo of Venus. Similar photometers have been carried by some *Aerobee* rockets since 1963.

The UV photometer was mounted rigidly on the *Mariner V* spacecraft with its FOV perpendicular to the spacecraft–sun line, and was pointed approximately toward the center of the planet at the time of closest approach. The FOV of the instrument was approximately in the plane of the trajectory. The sun lay 32 deg above this plane. As the spacecraft approached the planet, the instrument viewed the galactic background. Moving past Venus, the UV photometer observed successively its outer atmosphere on the night side, the dark planet, the terminator, and finally the day side. The FOV then passed off the bright limb and measured the outer atmosphere, which dropped off until only the galactic background was again observed. The arrows along the flight path (see Fig. II-2) indicate the viewing direction at the times of the dark-limb, terminator, and bright-limb crossings.

2. Discussion of results. The measurements made by the lithium-fluoride/Lyman-alpha channel of the UV photometer from 60 min before until 60 min after encounter are shown in Fig. II-11. The signals are given as apparent emission rates of the source in units of kilorayleighs [10^9 photons $(cm^2\ s)^{-1}$] for 1216-Å photons. The horizontal arrows on the left and right give the background level measured 2½ h before and after encounter.

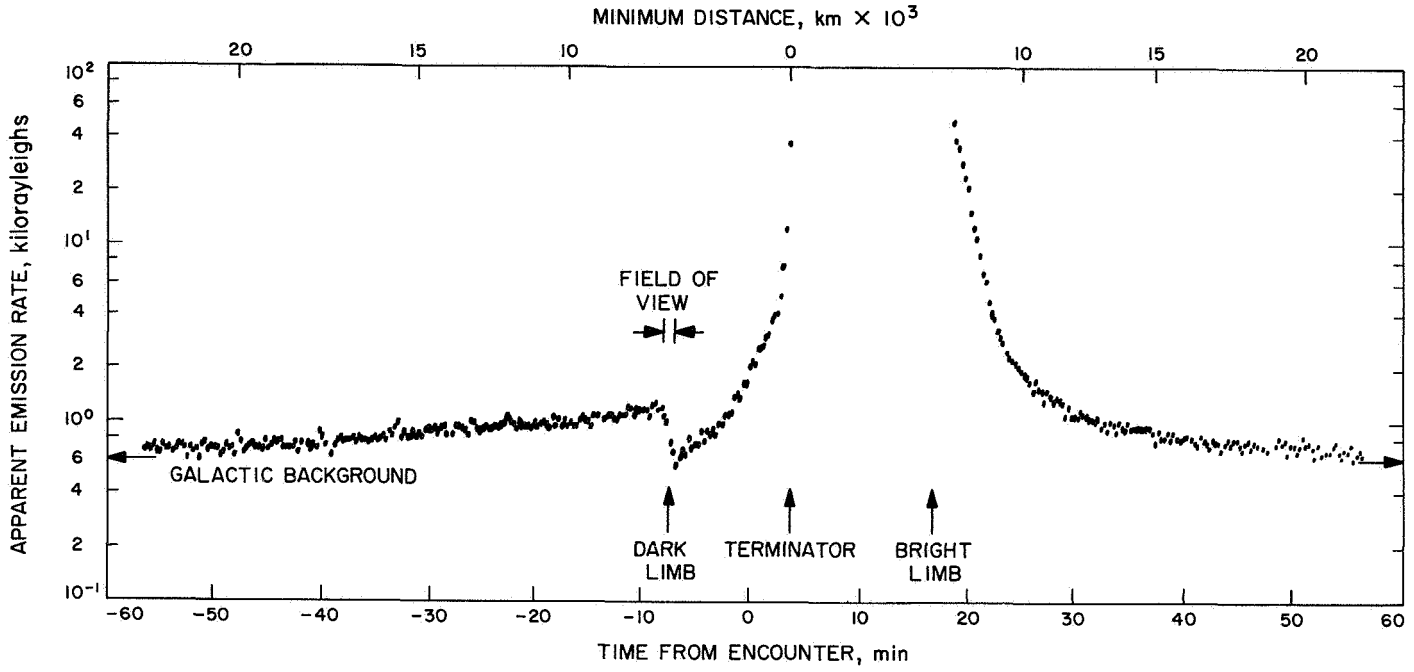


Fig. II-11. Signal obtained from lithium-fluoride/Lyman-alpha channel during Venus encounter

This level is interpreted as principally caused by atomic-hydrogen/Lyman-alpha photons that originate in the galaxy. As the spacecraft approached the planet, the signal increased. This additional intensity was caused by the presence of hydrogen atoms in the outer atmosphere of Venus that absorb solar Lyman-alpha photons, re-radiate them, and produce an ultraviolet airglow. As the viewing direction of the UV photometer approached the dark side of the planet, the Lyman-alpha signal reached a nightglow level of several hundred rayleighs above the galactic background. As the FOV crossed the dark limb, the ultraviolet signal from the galaxy was cut off by an absorbing gas or cloud layer. The signal level dropped by an amount equal to the galactic background. The sharp cut-off occurred during the time when the projected FOV moved past the absorbing edge of the planet (Fig. II-11).

The spacecraft continued along its trajectory with the UV photometer looking at the night side of Venus. The Lyman-alpha signal level (a measurement of the Lyman-alpha twilight glow) increased as the FOV moved towards the terminator. The decreasing shadow height allowed progressively more of the hydrogen atoms to be illuminated by sunlight. As the FOV reached the terminator, and the lower atmosphere became fully illuminated by sunlight, the lithium-fluoride channel of the UV photometer read off scale in response to ultraviolet daylight at longer wavelengths. Because of the long-wavelength response, all three channels were adjusted to emphasize the terminator and bright-limb measurements, and were allowed to go off scale during the traversal of the bright disk.

The lithium-fluoride/Lyman-alpha channel signal indication remained off scale as the FOV of the UV photometer moved across the daylight side of Venus. As the viewing direction passed off the bright limb, the lithium-fluoride channel again measured Lyman-alpha radiation scattered by hydrogen atoms in the outer atmosphere of Venus. When the bright limb passed completely out of the FOV of the lithium-fluoride channel, a strong signal was measured. The emission rate of the Lyman-alpha dayglow decreased rapidly as the viewing direction of the photometer moved away from the planet. The hydrogen atoms observed were in the upper atmosphere of the planet.

The observations of planetary Lyman-alpha radiation continued as the spacecraft moved in front of and away from the planet. The Lyman-alpha signal level decreased until it again approached the intensity of the galactic background (the right edge of Fig. II-11).

The measurements made by all three channels of the UV photometer for particular phases of encounter are shown in Fig. II-12. The signals from the lithium-fluoride, calcium-fluoride, and barium-fluoride channels are plotted

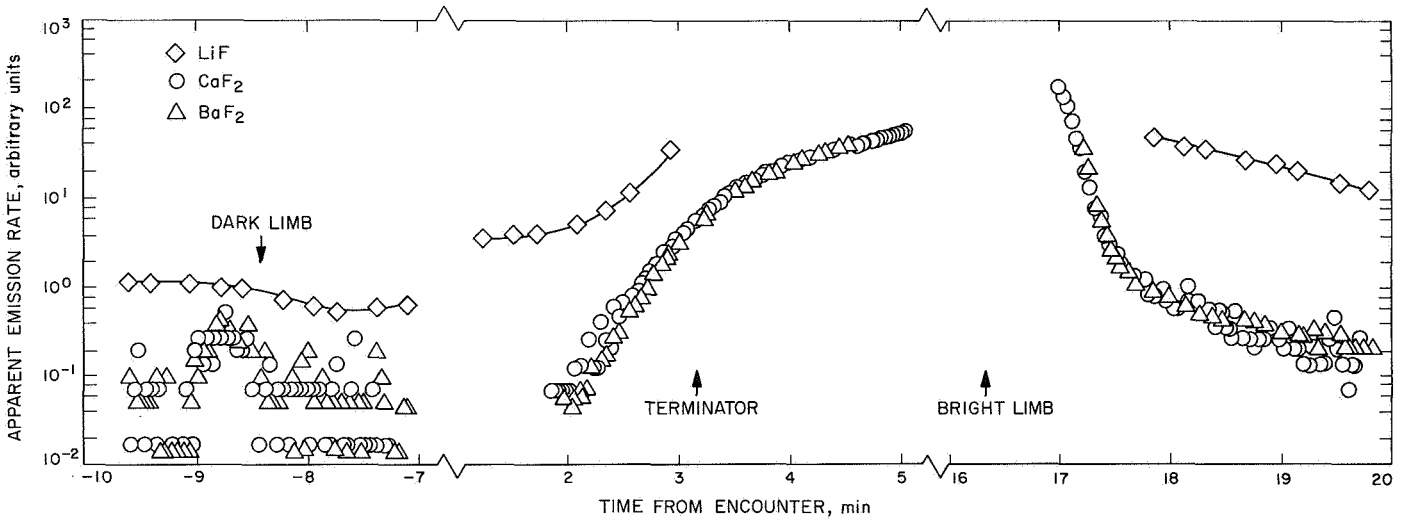


Fig. II-12. Signals obtained from photometer channels during critical periods of Venus encounter

(in arbitrary units) against the time (in minutes) from encounter. Compared with that of Fig. II-11, the time scale is greatly expanded.

Measurements from 9½ to 7 min before encounter at the time of the dark-limb crossing are shown in the left third of Fig. II-11. Measurements by the lithium-fluoride channel (the same as those in Fig. II-11) show the position of the crossing of the absorbing edge of the planet at the time when the galactic signal dropped to half of its value. Immediately before the dark-limb crossing, both the calcium-fluoride and barium-fluoride channels measured an increase in signal level followed by a decrease. These measurements were interpreted as a night airglow that was enhanced because of the instrument looking through the layer edge-on. The airglow layer was narrower than the projected FOV of the instrument because the width of the maximum (Fig. II-12) was equal to the time required for the FOV to pass over a narrow source. Both the calcium-fluoride and barium-fluoride channels measured the same variation in intensity, indicating that the wavelength of this airglow must be longer than 1350 Å.

Data obtained from 1–5 min after encounter, including the time of terminator crossing, are shown in the middle part of Fig. II-12. The relative intensities of the signals from the calcium-fluoride and barium-fluoride channels have been adjusted to apply to an equivalent wavelength of 2200 Å. These two channels substantially tracked each other in the twilight and daylight observations on both sides of the terminator. These data suggest that the two channels measured the ultraviolet daylight, possibly the result of rayleigh and particle scattering in the lower atmosphere of Venus. Perhaps the calcium-fluoride channel also measured a weak airglow emission before reaching the terminator. The lithium-fluoride channel, which had been measuring only Lyman-alpha radiation, increased in signal level rapidly when it approached the terminator because of the contribution of longer-wavelength ultraviolet daylight to its signal. The calcium-fluoride and barium-fluoride channel levels were both off scale after they crossed the terminator.

Data obtained 16–20 min after encounter, including the bright-limb crossing, are shown in the right third of Fig. II-12. The calcium-fluoride and barium-fluoride channels again have their relative intensities adjusted for an equivalent 2200-Å signal. The signals from these two channels coincided when they were again on scale as a result of the ultraviolet daylight at the edge of the planet, which gradually moved out of the FOV. The lithium-fluoride channel level remained off scale for almost 1 min longer than those of the other two channels because of its greater sensitivity and larger FOV; when the channel returned to scale, the indicated signal was principally caused by Lyman-alpha radiation.

3. Conclusions. The results from the lithium-fluoride/Lyman-alpha channel show that the amount of atomic hydrogen in the upper atmosphere of Venus is comparable to the amount in the upper atmosphere of the earth. The atomic-hydrogen atmosphere of Venus is much less extended than that of the earth. This implies that the temperature in the upper atmosphere of Venus, several hundred kilometers above the surface, is much lower than the temperature at comparable altitudes in the atmosphere of the earth. The lower temperature means

that the escape rate of atomic hydrogen from Venus is much less than that for the earth.

The signals obtained from the calcium-fluoride and barium-fluoride channels just beyond the bright-limb crossing show no evidence of atomic-oxygen emission. These signals are consistent with the low temperature determined from the atomic-hydrogen density measurements.

On the dark side of Venus, there is a weak ultraviolet airglow above the ultraviolet-absorbing atmosphere. This emission may result from chemical reactions between atmospheric species that have previously been photodissociated or from charged-particle bombardment.

F. S-Band Radio Occultation Experiment

On October 19, 1967, *Mariner V* passed within 4100 km of the surface of Venus. Its trajectory had been designed in a manner such that, as observed from the earth, it appeared to pass almost diametrically behind the planet.

About 3 min before the closest approach time, the S-band radio beam emanating from the parabolic high-gain antenna of the spacecraft began to enter the sensible neutral atmosphere on the dark side of Venus with a relative velocity of about 7.3 km/s at a radial distance of about 6140 km from the center. At the point of tangency, the latitude was about 37 deg N and the solar zenith angle was 142.3 deg. As the beam penetrated into the atmosphere, refraction caused the path of propagation to deviate from a straight line and the velocity of propagation to vary from the speed of light in free space. In addition, the lenslike effect of the gradient of refractivity caused defocusing, which spread the power in the beam over a greater angular width, causing the signal power received on earth to decrease. These effects were observed as changes in the frequency, phase, and signal strength received during this period at the tracking stations on earth.

As the beam penetrated deeper into the dense atmosphere of Venus, these effects became more pronounced until, at about 2 min 40 s past the closest approach time, the received signal strength gradually descended below the threshold of the receiver apparatus. This indicated that, rather than being physically interrupted by the limb of the planet, the signal was gradually extinguished by rapidly increasing refractive defocusing as the critical refraction level was approached.

Approximately 15 min later, the signal again began to be discernible as the radio beam emerged from behind the sunlit side of the planet and began to rise through the atmosphere. The latitude at this point was about 32.4 deg S and the solar zenith angle was 33.3 deg. Effects similar to those that occurred during the entry into occultation were again observed, except that a very strong effect of an ionosphere was observed during the exit on the daytime side. About 23 min after closest approach, the radio beam left the atmosphere of Venus, and the frequency, phase, and amplitude characteristics of the signal returned to those observed in free space.

1. Comparison of Venus and Mars experiments. The experiment described above is very similar to the one performed at Mars with *Mariner IV* in 1965 (Ref. 11); however, certain significant differences were caused by the nature of the Venus atmosphere as compared with that of Mars.

In the case of Mars, the experiment was performed in the so-called two-way mode, in which a frequency referenced by a rubidium-frequency standard (stable to about 1 part in 10^{12}) was transmitted to the spacecraft, where it was coherently retransmitted by a transponder. The signal received on the ground had thus completed two traversals of the atmosphere of Mars, and the effects of these traversals could be measured very precisely by comparison to the highly stable frequency reference. In preparing for the Venus experiment, however, it was felt that, because of the high frequency rates and massive defocusing attenuation, it would be unwise to risk loss of lock in the spacecraft receiver during a critical data period. For this reason, it was decided to carry out all of the entry portion of the experiment and most of the exit portion in the one-way mode. In this mode, the frequency transmitted by the spacecraft is referenced to an onboard crystal oscillator, which is inherently less stable. However, as borne out in the data, the stability of the oscillator was quite sufficient for the Venus experiment. An attempt was made to establish two-way lock after the spacecraft left the neutral atmosphere on exit to probe the ionosphere more precisely, but, because of rapid changes in frequency rate and uncertainties in the predicted time of leaving the neutral atmosphere, two-way lock was not reestablished until later.

Another significant change involved the high-gain antenna of the spacecraft (Ref. 12). If this antenna had pointed directly at the earth in free space, it would have performed poorly during occultation because the refracted radar beam would have emanated from a position on the antenna differing from the boresight position by

the amount of the refractive bending angle; in addition, the gain of the antenna would have been reduced at a time when maximum gain was needed to overcome increasing refractive defocusing.

To counteract this problem, a movable high-gain antenna was used. This antenna was initially positioned to point about 8.2 deg away from the earth in the direction of the expected bending. While the spacecraft was behind the planet, a signal from a terminator sensor initiated a positioning change that moved the antenna axis to a position offset by 9.7 deg in the opposite direction to improve the gain during the exit portion of the data. In addition to increasing the amount of data collected by the S-band experiment, this pointing angle change also improved tracking coverage.

Data for the *Mariner V* experiment were received at all four of the Deep Space Stations (DSSs) at Goldstone, Calif. The basic instrumentation and type of data are adequately described elsewhere. The major differences between the ground station equipment used for the *Mariner IV* occultation experiment (Refs. 12, 13, 14) and that used for *Mariner V* were caused by the availability of more sensitive receiving equipment and the differences in the expected rate of frequency change.

2. Data acquisition. The 210-ft advanced antenna system (AAS) was used as the prime station for both open- and closed-loop data. The system temperature of this station was 28°K at the encounter elevation angle. The closed-loop receiver was in the normal station configuration, in which the doppler extractor and resolver were used to obtain frequency in a digital form, and automatic gain control voltage was used to indicate received signal level (both in real time).

The closed-loop data were then processed through the JPL Orbit Determination Program, which removed all effects except those caused by the atmosphere of Venus. Because these data were based upon a nondestructive cycle count, the summing of the frequency residuals yielded a precise measurement of the total phase-path change in cycles. These data were then used to obtain the results described later in this report.

The open-loop data were obtained in the form of a wide-band predetection analog magnetic tape recording from a fixed-tuned receiver. This recording had a bandwidth in excess of 100 kHz, which was required because of the high rate of frequency change caused by the orbit as well as the effects of the planetary atmosphere.

The analog magnetic tape was digitized by slowing the original 60-in./s tape to 3¾ in./s so that the 320-kHz synchronizing tone was reduced to 20 kHz, which was used to trigger the digitizer. The data were first reduced by narrow-band filtering of the signal, which permitted a great reduction in the amount of data to be processed. A digital spectral-anaysis program was used to determine the time–frequency function. This time–frequency function was then used to run a digital local oscillator to minimize the rate of frequency change.

A digital phase-lock-loop program was then used to obtain the remaining frequency changes. These were compared to predictions based upon the orbit, and the residuals caused only by the atmosphere were computed. The received signal level as a function of time was also obtained from the phase-lock-loop program, and is shown in Fig. II-13. The undulations that appear in the received signal level are apparently caused by phenomena in the atmosphere of Venus, such as focusing and defocusing by changing gradients. The closed-loop receiver at the AAS site lost lock at about 17:39:07 GMT, but the open-loop data extend to about 17:42:05 GMT. The combined open- and closed-loop data obtained during entry are shown in Fig. II-14. Similar data were obtained during exit, except that a smaller percentage was obtained by the closed-loop receivers.

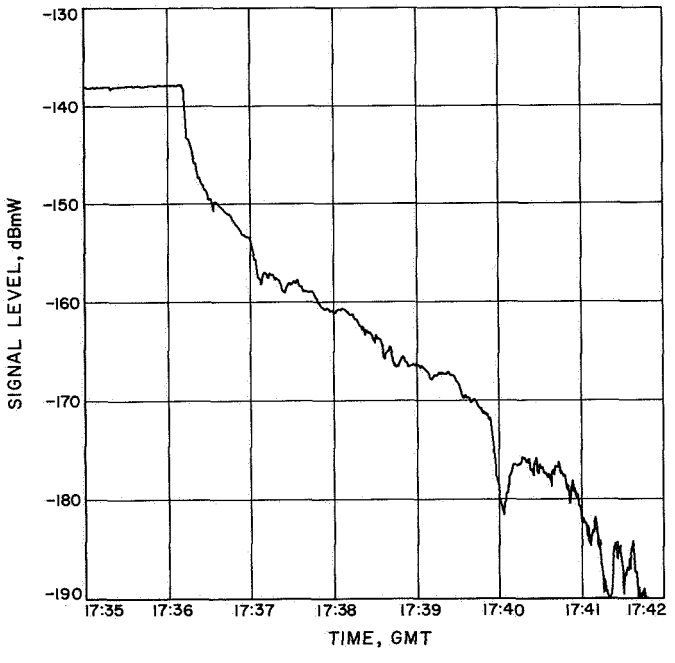


Fig. II-13. Received signal strength during entry into occultation

In addition to the AAS, two operational DSSs at Goldstone with 85-ft antennas provided backup capability for closed-loop operation. The Venus site 85-ft antenna at DSS 13 had a new low-noise system with 16.5°K system temperature that provided an open-loop backup capability.

3. Data analysis. The data were analyzed using two basically different approaches, both having the same objective: to find the profile of index of refraction (or refractivity) as a function of height in the atmosphere from data that basically consist of measurements of frequency or phase residuals at certain specified times.

The most direct method makes use of the trajectory of the spacecraft to establish the connection between time and geometry, and then uses direct inversion of the integral equation describing the ray-optical refraction effects to obtain directly the profile of refractivity in the atmosphere (Ref. 14). This method is completely general, since no *a priori* assumptions regarding the analytical form of the refractive index profile have to be made.

The other method, referred to as "pseudo inversion," is based upon a step-by-step "construction" of a profile of refractivity to match the observed phase-delay data. This method makes use of certain properties of planetary atmospheres that can be expected to apply also in the atmosphere of Venus. In the upper levels of the atmosphere, the temperature is assumed to be constant above some predetermined altitude; the refractivity function is, therefore, exponential with constant scale height. Once the refractivity at this reference altitude (which can be chosen arbitrarily) is determined by adjusting until the computed and observed data match, the refractivity in each succeeding interval of height of arbitrary thickness is represented by an expression valid for a linearly changing scale height. The rate of change of scale height is adjusted until convergence is achieved.

4. Results of experiment. Figures II-15 and II-16 show frequency residuals obtained at the very top of the atmosphere during entry and exit, respectively. Theoretical predictions based upon constant scale-height (isothermal) models are superimposed as dashed curves on the observed data (represented by the dots). Figure II-15 shows the actual data to be quite consistent with a constant scale height of about 5.4 km for the first 20–30 km of the sensible upper atmosphere. The exit data appear to be similar; however, they include the effects of a rather intense daytime ionosphere, which must be removed before the neutral atmosphere itself can be investigated.

Because of uncertainties in timing, a probable error of ±0.2 km can be assigned to the measurement of scale height in the upper atmosphere. This yields a range of ratio of temperature to mean molecular weight of about 5.49–5.9. On the basis of the solar constant at the orbit of Venus and of the observed albedo of the planet, the effective temperature is computed to be about 230°K.

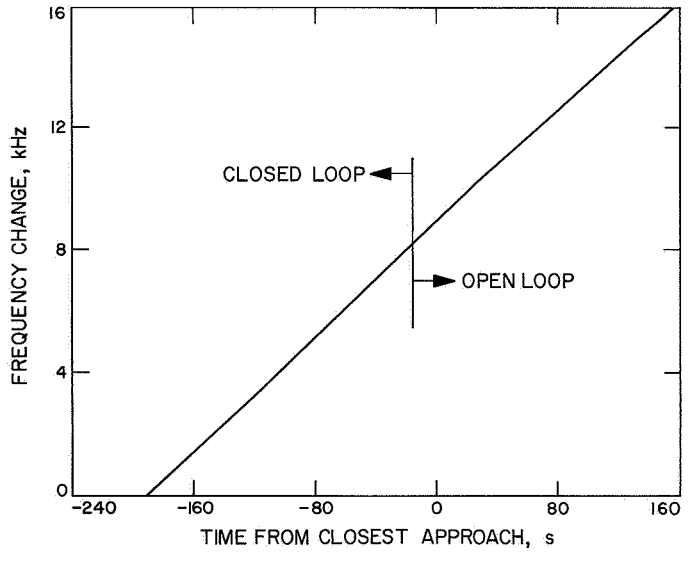


Fig. II-14. Frequency residuals from data taken during entry into occultation

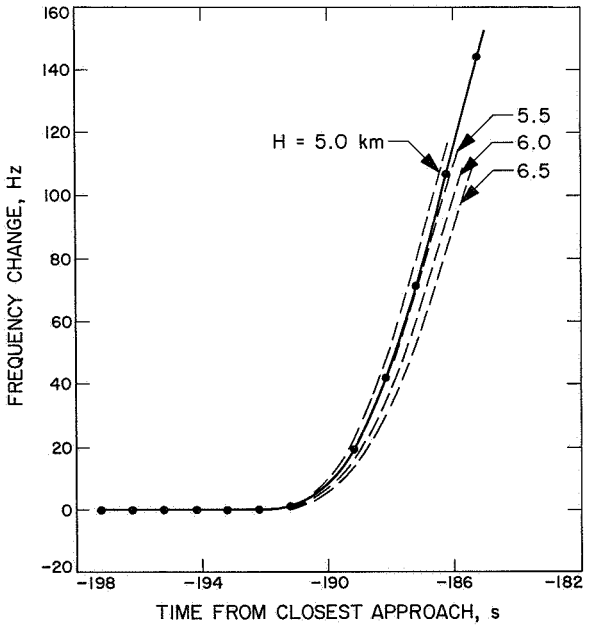


Fig. II-15. Entry residuals with theoretical models

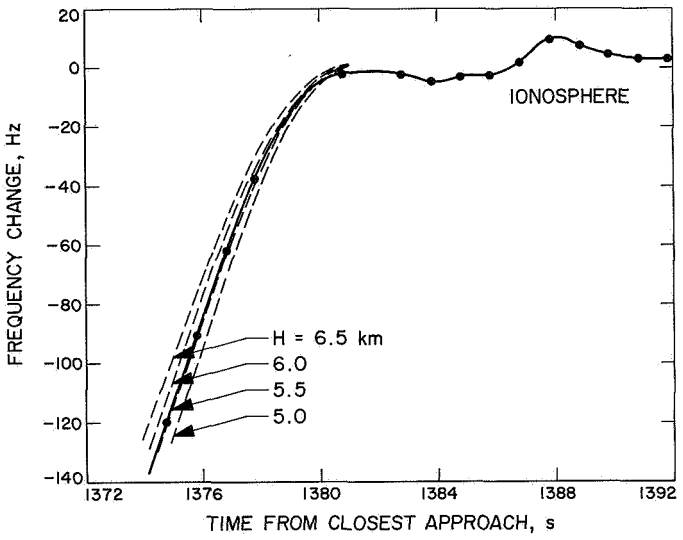


Fig. II-16. Exit residuals with theoretical models

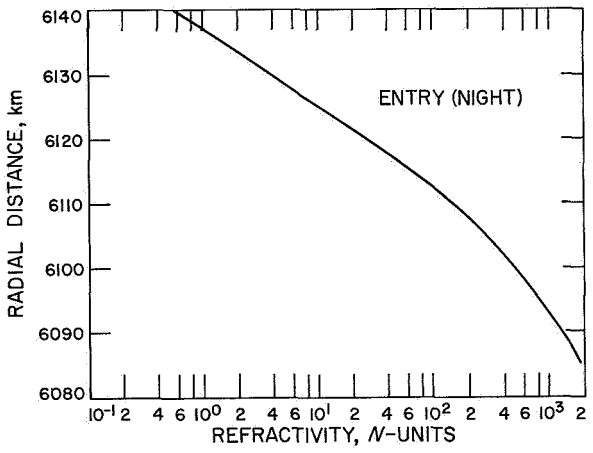


Fig. II-17. Refractivity of Venus atmosphere

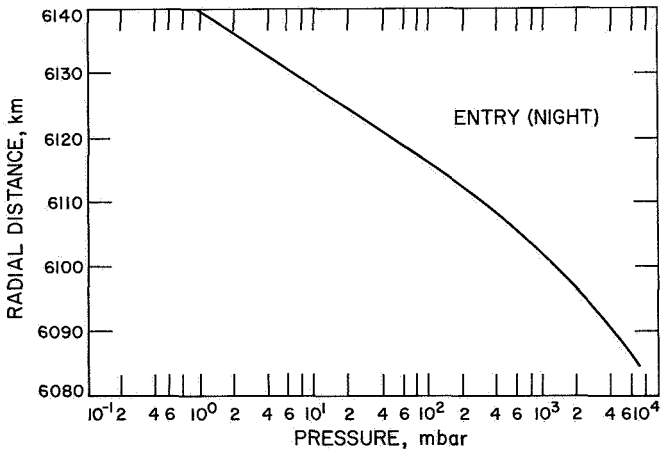


Fig. II-18 Pressure of Venus atmosphere (pseudo inversion)

Because this temperature would correspond to some level above the visible tops of the clouds, it can be argued that, at the altitude at which occultation measurements begin (about 6140 km from the planet center), the actual temperature would be less than the effective temperature. If one assumes, then, that 230°K is the upper limit of temperature in the region in which the scale height of 5.4 ±0.2 km is measured, the range of mean molecular weight is 39.0–42.0. This corresponds to percentages of carbon dioxide of about 69–87%, provided that the balance of the atmosphere is composed of nitrogen. If heavier gases are present, the amount of CO_2 may be lower; if lighter gases are present, the amount of CO_2 would have to be correspondingly higher. The measurement of scale height in the upper neutral atmosphere has thus provided an estimate of composition.

A profile of refractivity as a function of radial distance is shown in Fig. II-17.

To compute pressure and temperature from refractivity, it is necessary to specify the composition. On the basis of the preceding discussion, it was decided to restrict the range of CO_2 abundance to 75–90%. Because the ratio of refractivity and molecular weight for CO_2 and N_2 are very similar, the computed pressure profiles for the two extreme compositions are coincident to the accuracy of illustration, as shown in Figs. II-18 and II-19. Figure II-18 shows a profile obtained from the results of the pseudo-inversion program, and Fig. II-19 is based upon the direct inversion. The resulting profiles are quite similar, and the pressure at the present limiting minimum radial distance of 6085 km is about 7 atm.

The variation of temperature in the lower atmosphere is presented in Figs. II-20 and II-21. Figure II-20 shows the temperature profiles computed from the results of the pseudo-inversion program for CO_2 abundance of 75 and 90%; the balance is assumed to be nitrogen. Figure II-21 shows the same result computed by the method of direct inversion. Again, the results of the two very different reduction methods are essentially similar, showing a constant temperature above the tropopause at about 6114 km radial distance, and a rapid increase in temperature with decreasing altitude below that level. In the case of 90% CO_2, the temperature is about 241°K above the tropopause, and the maximum is about 477°K at 6085 km. For 75% CO_2, the temperatures are correspondingly lower, starting at about 228°K above the tropopause and increasing to about 400°K at 6085 km.

These temperatures are considered good upper and lower limits for the actual temperatures in the regions

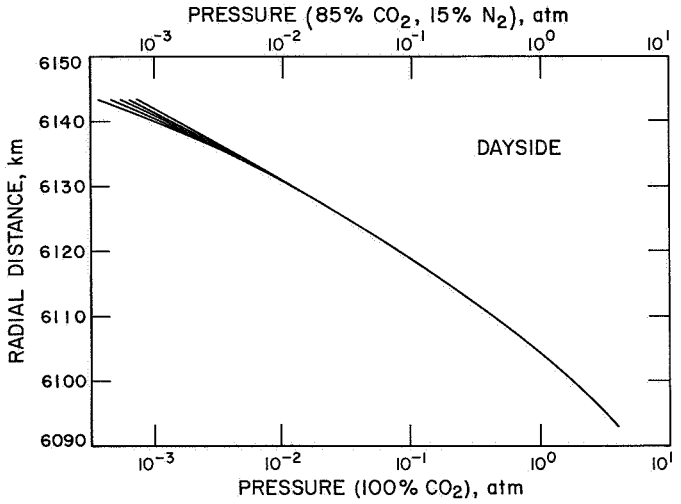


Fig. II-19. Pressure of Venus atmosphere (direct inversion)

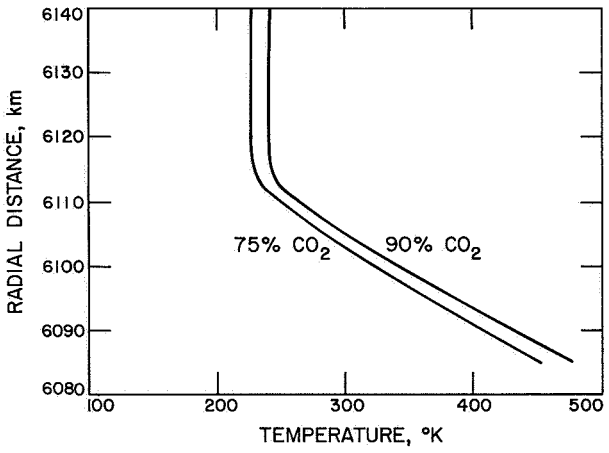


Fig. II-20. Temperature of Venus atmosphere (pseudo inversion)

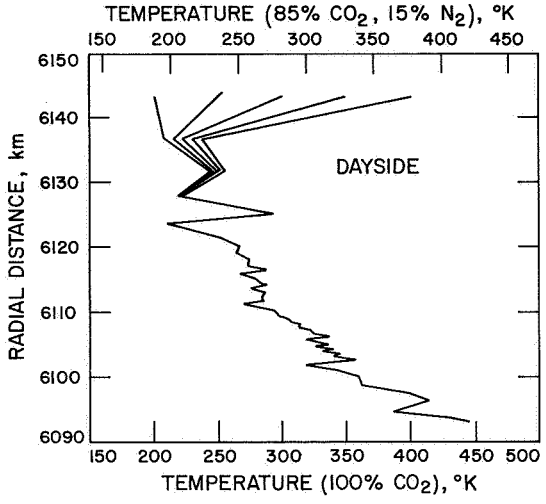


Fig. II-21. Temperature of Venus atmosphere (direct inversion)

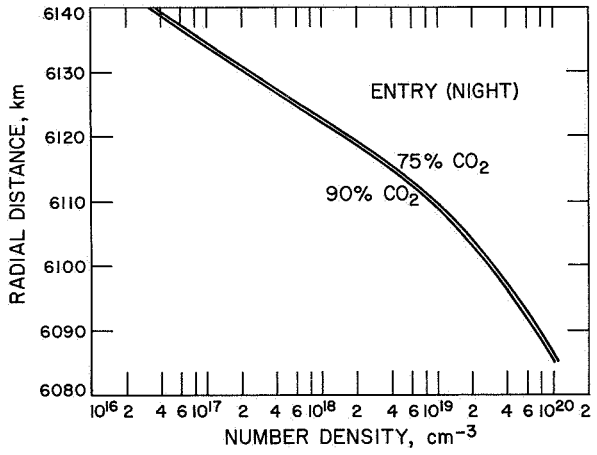


Fig. II-22. Number density in lower atmosphere of Venus

of the dark side atmosphere that were probed by the S-band occultation experiment. The number density was also computed for the two limiting abundances of CO_2, and the results are shown in Fig. II-22.

Although the profiles of temperature and pressure do not extend to the surface of Venus, one is tempted to extend them to the region apparently measured by the Soviet *Venera-4* spacecraft. If these profiles are extended to the region of 15–22 atm of pressure and about 550°K in temperature, as reported in *Izvestia,* the resulting radial distance is found to be about 6078 ±10 km. If this is truly the surface radius, it differs quite markedly from the surface radius of 6056 ±1.5 km established from analysis of planetary radar data (Ref. 15).

The dayside ionization profile shows a distinct layer, with a peak density between 5×10^5 and 6×10^5 electrons/cm³ near 6195 km (Ref. 16). Clear evidence also exists of a minor layer approximately 15 km below the ionization maximum. The electron density profile is shown in Fig. II-23.

Just above the ionization peak, the plasma scale height is about 13 km. This value for the scale height corresponds to a plasma temperature of about 300°K if temperature gradients are negligible and if CO_2^+ is the principal ion. The plasma scale height on the ionospheric topside increases as a function of altitude, indicating a higher plasma temperature and/or a change to a lighter ion at greater altitude.

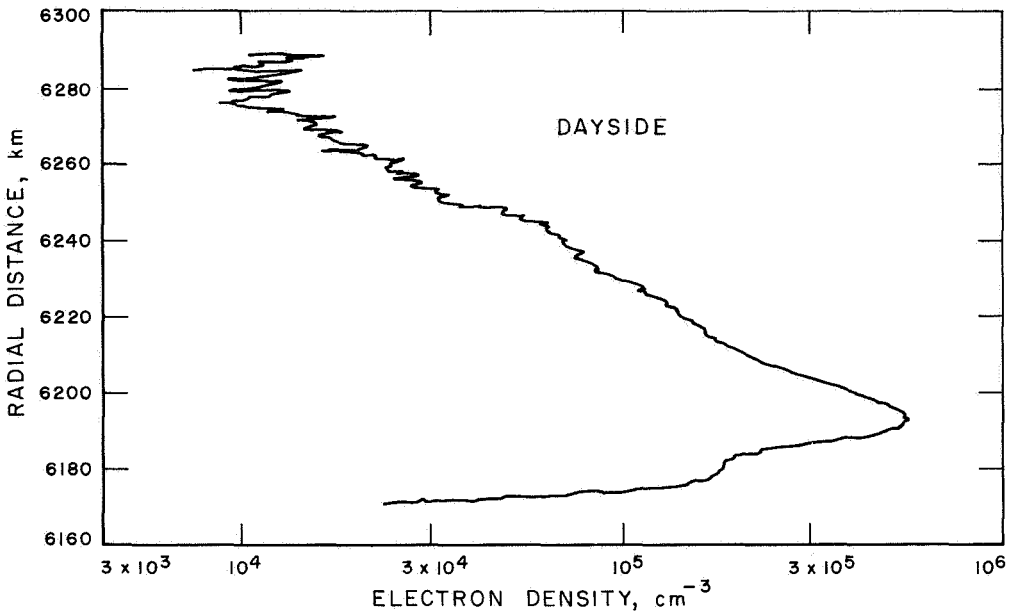


Fig. II-23. Electron density in Venus daytime ionosphere

By analogy with the formation of ionization layers in the terrestrial atmosphere, one can interpret the dayside ionization peak in terms of three types of models. For this discussion, these three classes of models are designated F_2, F_1, and E.

The F_2, or Bradbury, models rest upon the assumption that the observed ionization peak results from a rapid upward decrease of the ion recombination loss coefficients together with downward diffusion of plasma. In the F_2 models, the electron density peak is above the region where most of the electron production and recombination occurs. The F_1 and E models are based upon the assumption that the observed ionization profile is a Chapman-type layer, in which the peak coincides with the electron-production peak caused by extreme solar ultraviolet and X-rays, respectively.

In the UV-photometer experiment (Ref. 17), no atomic oxygen was found on Venus. Thus, it appears that one can rule out F_2 models that are based on atomic oxygen as the principal constituent at the ionization peak. Examples of F_1 and E models are illustrated in Figs. II-24 and II-25. The solid temperature and electron density profiles below 6130 km were obtained from the refractivity measurements in the lower neutral atmosphere for the case of 100% CO_2. The dashed and dotted curves above 6130 km represent an extrapolation of the measurements in the lower atmosphere up to the level of the ionization peak. The minor layer may have been produced by X-rays and solar protons in the F_1 and E models, respectively.

These results are based upon preliminary analysis, using data available as of May 1968. The results will be improved and refined in the future as more of the open-loop data become available and reduction methods become more efficient. Among the results that will be available in the near future are complete profiles of refractivity, pressure, temperature, and number density on both the entry (nighttime) and exit (daytime) sides, using both the closed- and open-loop data. In addition, further study of these results will enable conclusions to be drawn regarding the evolution of the lower atmosphere and the processes at work in the ionosphere.

G. Dual-Frequency Radio Occultation Experiment

As *Mariner V* passed behind Venus on October 19, dual-frequency radio transmissions from earth reached the spacecraft after passing through the ionosphere and atmosphere of Venus. Signal characteristics were measured and stored on magnetic tape for later transmission to earth via the telemetry channel. From these characteristics, preliminary profiles of electron concentration as a function of radius have been derived by techniques described previously (Refs. 16 and 18), for both the

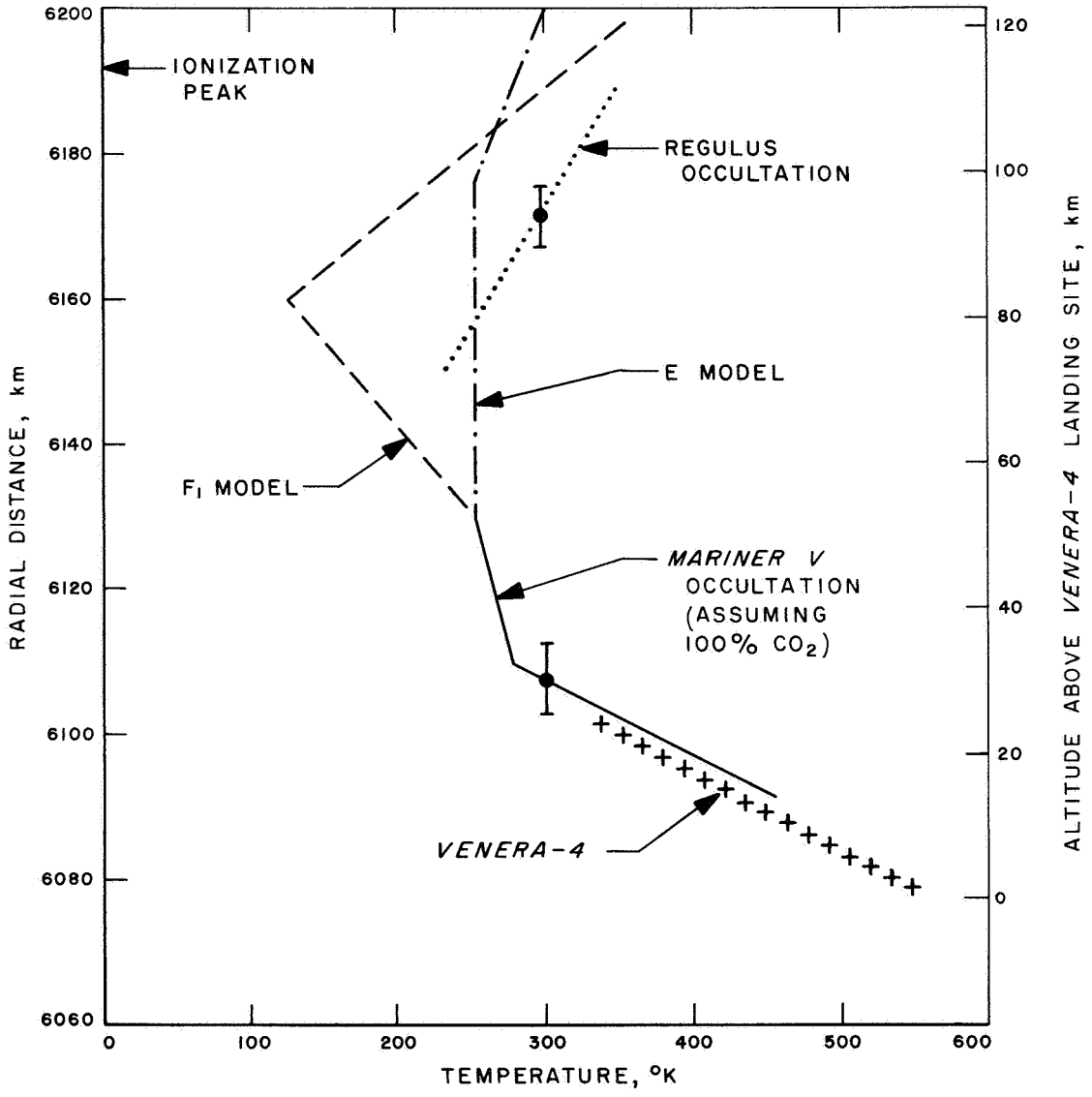


Fig. II-24. Venus atmospheric temperatures for F_1 and E ionosphere models

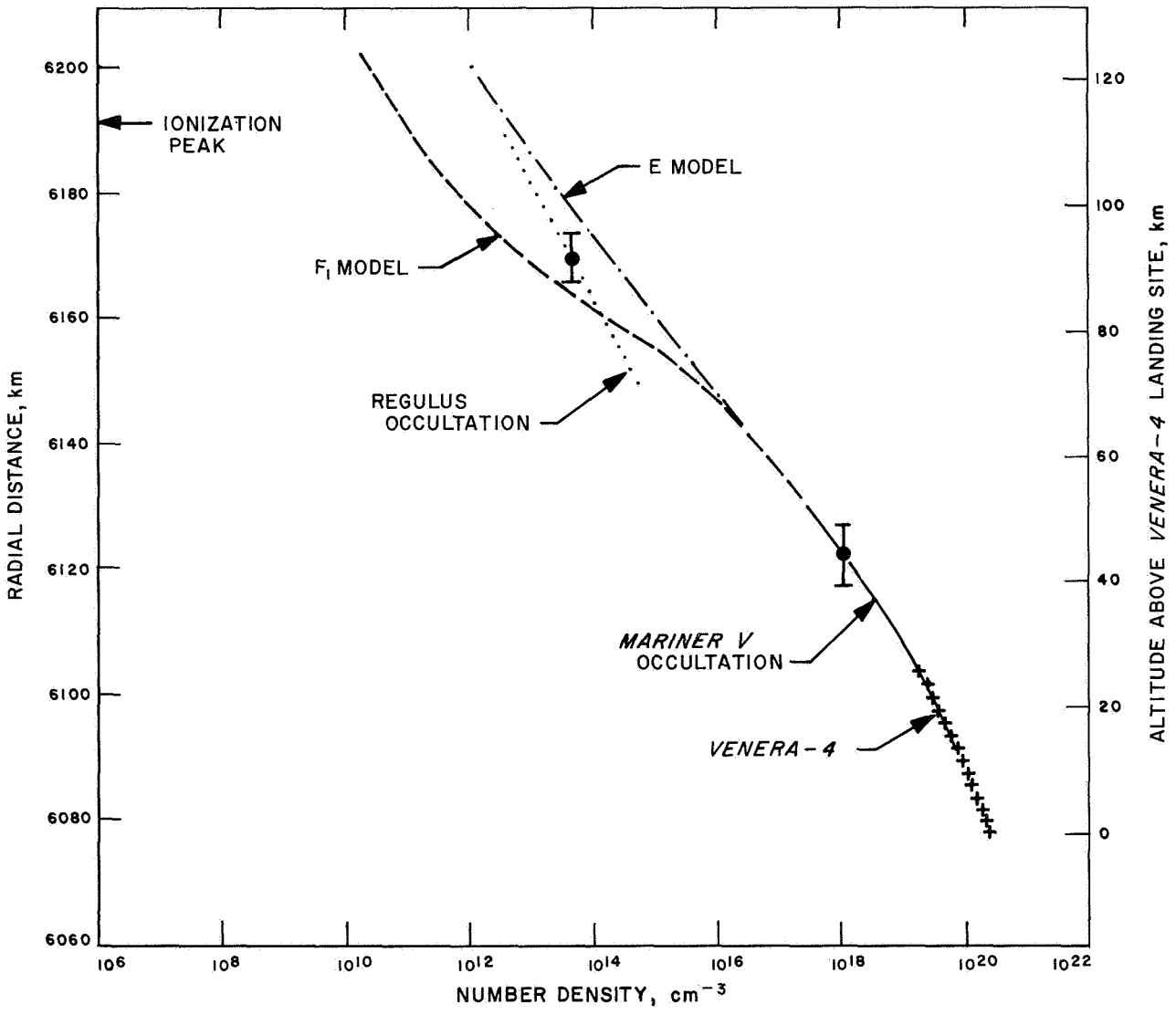


Fig. II-25. *Venus atmospheric number density for F_1 and E ionosphere models*

nighttime and daytime ionospheres probed by the signals. In addition, effects of the dense neutral atmosphere were measured over the same two regions on Venus, but very little analysis has been attempted thus far because the principal effects of the lower atmosphere were more accurately determined in the S-band experiment. During the cruise portion of the mission, the dual frequency experiment measured characteristics of the interplanetary plasma.

This subsection is primarily a report on the planetary data obtained from the dual-frequency experiment. However, some very preliminary discussion and interpretation relative to physical and chemical properties of the upper atmosphere are included with the initial data analysis. In addition, there is a brief discussion of how the results may help to define a third type of interaction of a planetary body with the solar wind; those of earth and the moon represent the other two types.

1. Data acquisition. Harmonic, continuous-wave signals at 49.8 and 423.3 MHz were transmitted from a 150-ft, steerable, parabolic antenna at Stanford University. Transmitter power was about 350 kW and 30 kW at the lower and higher frequencies, respectively. The signals were received by fixed, low-gain antennas aboard the spacecraft. These were provided by feeding two of the solar panels for the lower frequency, and by adding a dipole with reflectors at the end of one of the panels for the higher frequency. The design of a phase-locked DFR for interplanetary plasma measurements aboard *Pioneer* spacecraft was modified for the *Mariner V* instrument.

At the spacecraft, the 2/17 subharmonic of the higher frequency was compared with the lower frequency to provide a beat note whose frequency was measured by counting positive and negative zero crossings. These counts provided a dispersive doppler measurement of the change in the amount of plasma along the path, with one count representing a change of about 2×10^{14} electrons. The sign of the change could also be determined because the two frequencies actually differed from the 2/17 ratio by a precisely determined bias of 50 Hz. Thus, the count was 60 in the 0.6-s sampling period if no change of ionization occurred along the changing path in that interval; values larger or smaller than 60 indicated the amount and sign of the change.

The amplitudes of each of the two signals were measured every 0.6 s during encounter. Changes in amplitude caused by Venus were expected because of the following: (1) focusing and defocusing in the Venusian ionosphere; (2) defocusing in its neutral atmosphere; (3) possible absorption in its ionosphere or atmosphere; and (4) possible diffractive cutoff of signals by the limb of the solid planet. It appears that (1) and (2) were seen and (4) was not seen, whereas it has not yet been determined whether there was any measurable absorption.

2. Analysis of data. The dispersive doppler and two sets of amplitude measurements constitute the results of the experiment that are to be discussed further. Although the frequencies of the two signals were also measured, and several differential group-path measurements were made near encounter, they are not sufficiently precise to aid in the preliminary analysis. The frequency measurements were included in the original DFR design for engineering and operational use; the group-path measurement is of particular value for the interplanetary studies.

The regions probed at Venus by the radio signals are shown in Fig. II-2. During entry, the ionosphere and atmosphere at about 35-deg N lat were measured. The solar zenith angle was 140 deg, and this area had been out of direct sunlight for about 15 earth days. At exit, the latitude was 30 deg S, the solar zenith angle 40 deg, and the region studied had been in sunlight for about 30 earth days. Assuming that the solar wind arrives at about 5 deg from the sun–Venus line because of aberration, the angle between the subsolar-wind point and the daytime region of the atmosphere probed by the radio waves was about 45 deg.

a. Amplitude measurements. The amplitude measurements are shown in Fig. II-26. In the absence of the planet, all amplitude curves shown would ideally stay at the level indicated as 0 dB. The most obvious effect of Venus is the general reduction of signal strength upon entry and the rise upon exit, showing the defocusing effects of the neutral atmosphere. However, for purposes of this discussion, the ionospheric effects indicated by numbers *1–5* in this figure are of prime interest.

The number *1* in Fig. II-26 indicates the focusing and defocusing at 423.3 MHz caused by the dense part of the nighttime ionosphere. These effects should be magnified at the lower frequency because the angle of ray bending is proportional to f^{-2}, where f is the radio frequency (see Ref. 15). At 49.8 MHz, the number 2 shows 16 dB of signal loss caused by ionospheric defocusing.

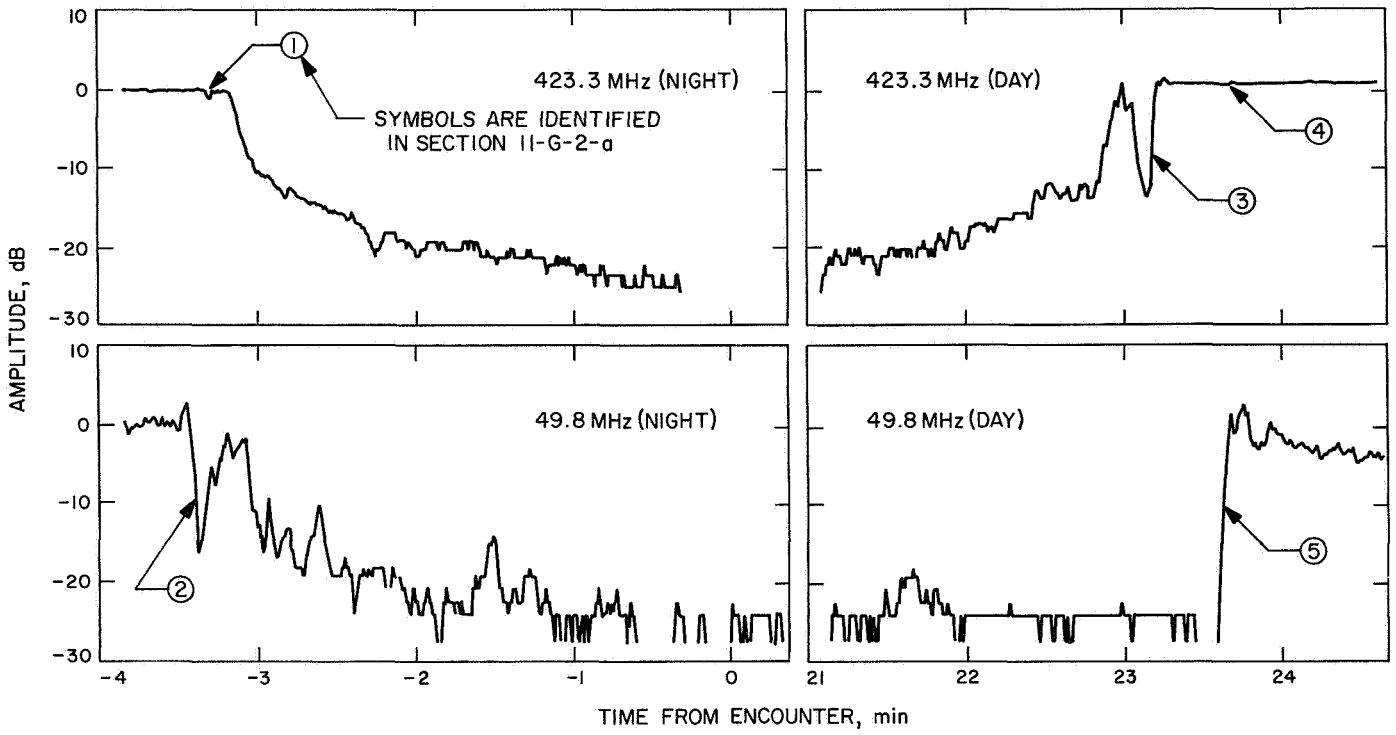


Fig. II-26. Signal amplitudes at two frequencies during entry (nightside) and exit (dayside) occultation

Upon exit over the daytime side of the planet, the main ionospheric effect at 423.3 MHz is indicated by the number 3. This feature is rather similar to 2 for the nighttime ionosphere measured at 49.8 MHz. If 2 and 3 were the same, it would follow that the shapes of the two layers near their peaks would be approximately the same, but the peak electron concentration would be related as

$$\frac{(N_{\max})_{\text{day}}}{(N_{\max})_{\text{night}}} = \left(\frac{17}{2}\right)^2 \frac{z_{\text{night}}}{z_{\text{day}}}$$

where z_{night} and z_{day} are the distances from the limb of the planet to the spacecraft upon entry and exit occultation, respectively, and $N_{\max}$ is the peak electron concentration (Ref. 18). Thus, to the extent that 2 and 3 are similar, $(N_{\max})_{\text{day}} \cong 50\,(N_{\max})_{\text{night}}$.

The more detailed amplitude features of 2 and 3, in particular the cusps on the right side of 2 and on the left side of 3, are similar to what would be expected if caustics were formed before the rays reached the spacecraft. That is, it appears that certain of the adjacent rays that were parallel (having come from earth) as they entered the ionosphere were refracted differentially to the extent that they crossed over (formed caustics) in the region between the planetary limb and the spacecraft. This results from high values of the second derivative of electron concentration with altitude (Ref. 18). Because of the caustics, special precautions and procedures are required in the analysis.

It appears from the number 5 (Fig. II-26) that the effects of the daytime ionosphere were so intense that they may have prevented reliable measurement of the 49.8-MHz signal for most of the time until the rays had passed several hundreds of kilometers above the peak of the layer. Indicated signal strength between E+22 min, 0 s and E+23 min, 30 s is so low that the receiver may actually have been out of lock at this time. However, such inospheric interference would be quite incompatible with the low densities and gradients expected at these altitudes if the main layer decays with altitude, as would be expected. It is possible that 5 is caused by the receiver not locking to a strong signal in the expected way. An alternative possibility is that this high region of the atmosphere has unsuspected characteristics. The latter possibility is strengthened by the small amplitude fluctuation noticed at 4 in the strength of the 423.3-MHz signal. This point will be further discussed after the dispersive doppler results are presented.

b. Doppler measurements. Figure II-27 shows the main results of the dispersive doppler measurements.

Curves of integrated doppler frequency, or cycles of dispersive doppler phase, are shown as a function of time relative to encounter, with the time scales for entry and exit positioned so that the two curves can be compared in terms of altitude. The distance scale is not quite linear with time, but several positions of interest are indicated for ρ (the distance from the center of the planet to the nearest point on a straight-line path between earth and the spacecraft).

Before encounter, the very sensitive doppler system was measuring a dispersive frequency of about +0.06 Hz, corresponding to an increase in the integrated electron content between earth and *Mariner V* of about 2.4×10^{13} electrons $(m^2\ s)^{-1}$. This is almost entirely because of changes with time of the content of the ionosphere of the earth. In fact, measurements between the Stanford University station and the *ATS* (*Applications Technology Satellite*) taken during the time of entry and exit, showed effects caused by the terrestrial ionosphere corresponding to a nearly constant frequency of about 0.07 Hz when analyzed for the *Mariner V* path.

At about E−13 min, the *Mariner V* doppler frequency changed to approximately 0.11 Hz, and stayed near this value until about E−5 min when it started to increase more dramatically. Because the earth measurements remained about the same, the change starting at E−13 min must be caused either by a changing interplanetary content or by ionization extending nearly 10,000 km from the center of Venus on the night side.

The measured effect of the terrestrial ionosphere was subtracted for both curves of Fig. II-27, and it was assumed that the remainder, in terms of changing electron content along the path, was caused by the nighttime and daytime ionospheres of Venus. It is possible that changes in interplanetary conditions could have caused the slow build-up of phase indicated between E−13 and E−5 min. This does not seem likely, however, because the *Mariner V* and *Applications Technology Satellite* measurements of changing content along their paths correspond very closely before E−13 and after E+24 min. In addition, the interplanetary content appeared to remain relatively steady throughout the day, indicating an average electron concentration of about 4.3 cm^{-3} along the earth–*Mariner V* path.

After E−5 min, the dense part of the nighttime ionospheric layer caused the rapid changes in phase that are shown in Fig. II-27.

The effect of the daytime ionosphere is dramatically different. There does not appear to be any effect of the planet above about $\rho = 6570$ km; i.e., above an altitude of about 500 km. Even more surprising is the sudden transition from interplanetary conditions to the very sharp, large increase of dispersive phase with decreasing altitude. Unfortunately, the dispersive doppler apparently was not accurately measured farther down into the ionosphere because of the near or complete absence of signal at 49.8 MHz, as indicated before the rise at 5 in Fig. II-26.

c. Electron concentration. A combination of the doppler and amplitude results has been used to deduce preliminary profiles of electron concentration as a function of distance from the center of Venus. Integral inversion was used to derive profiles directly from the measured doppler data (Ref. 18), whereas very preliminary model-fitting computations have been used to obtain approximate characteristics of profiles from the measured amplitude data. The results are illustrated in

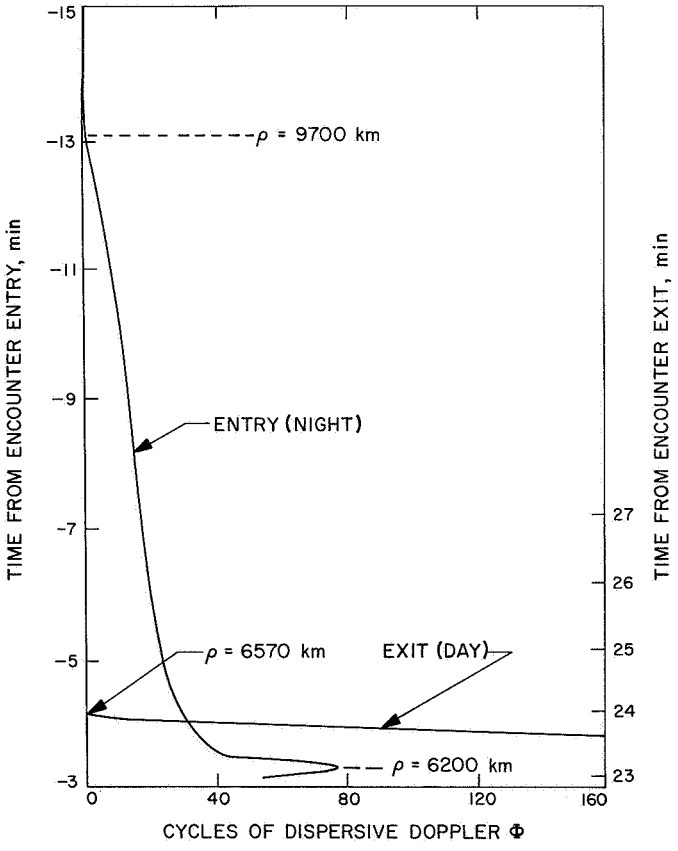


Fig. II-27. Dispersive phase due to the ionosphere at entry and exit

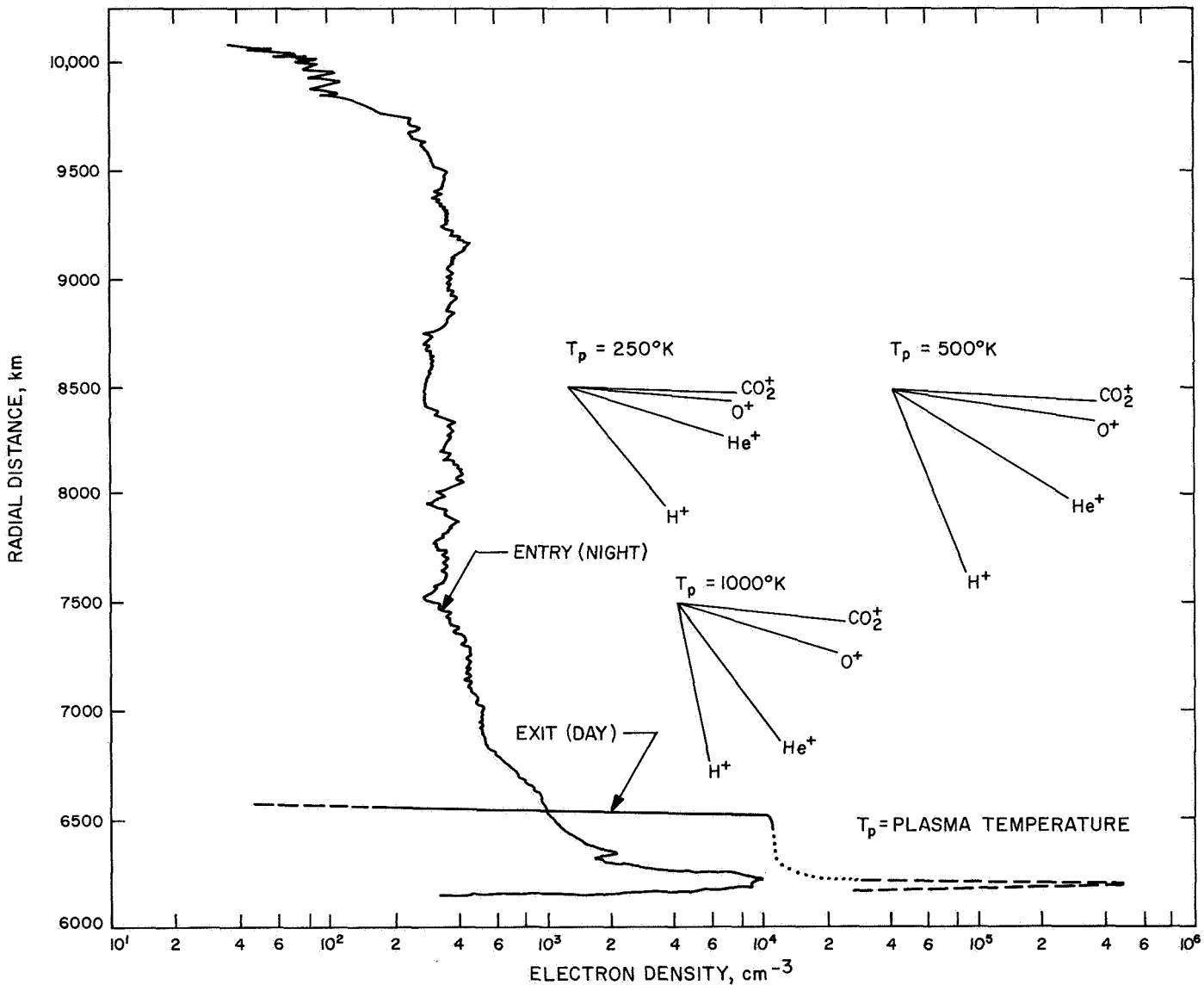


Fig. II-28. Electron concentrations in night and day ionospheres of Venus

Fig. II-28. Because of the wide range of electron concentrations that were measured, a logarithmic scale is used. This also permits comparisons of slopes with plasma scale heights computed for various possible constituents and temperatures.

The total nighttime profile that is illustrated in Fig. II-28 was obtained by inversion of the doppler data, assuming straight-line propagation. When ray bending was included in the analysis, a profile was obtained with practically no change from Fig. II-27 down to a radius of about 6250 km, but this analysis could not proceed farther down because of cross-over of the computed ray-paths. This could be caused either by noise in the data or by the formation of a real caustic, and it is believed that a real caustic formed (as discussed above). Thus, the profile shown below this altitude cannot be said to be a true representation of the layer. On the other hand, the error in peak concentration may not be very large because model fitting, using a limited number of Chapman layers, shows reasonable agreement (including the cusp) with 2 of Fig. II-26 for $N_{max} = 10^4$ cm^{-3} and a plasma scale height of 10 km near the peak.

Above 6250 km, there appear to be several regimes on the night side characterized by different scale heights. The almost constant density shelf with $N = 300$ cm^{-3} between radii of 7500 and 9500 km is difficult to explain. The method of data analysis was discussed in some detail to indicate the problems involved in measuring such extremely low densities. If the constant doppler bias used in setting the zero of the phase curve in Fig. II-27 were changed, the magnitude of N in the shelf would change, but not its near constancy with radius. From the shape of the phase curve, it appears that the electron density is probably fairly constant up to a relatively sudden plasmapause near 9700-km radius. However, it could well be that a very small, nonconstant frequency term caused by the interplanetary medium or a lack of spherical symmetry could tilt this portion of the profile sufficiently to correspond to a diffusive equilibrium distribution of H^+ at a reasonable temperature on the order of 1000°K.

There is not much latitude in interpreting the slope between 6800 and 7500 km. Hydrogen ions and a plasma temperature (mean electron and ion temperature) between 625 and 1100°K seem to be the only likely explanation for this feature in the data. The region below 6800 km, and down to 6300 km, is most probably composed of He^+ with a plasma temperature of 620–970°K. At lower altitudes, the presence of a number of heavier ions could explain the observed scale heights, as illustrated in Fig. II-29.

The ionization peak observed on the night side of Venus is probably analogous to the E and D regions found in the nighttime atmosphere of the earth. This would require a neutral density of 10^{13}–10^{15} molecules cm^{-3} at the ionization peak. Possible energy sources include galactic cosmic rays, solar Lyman radiation backscattered from hydrogen, and meteoric bombardment. It also seems possible that the peak may have been produced by horizontal transport of plasma from the day side of the planet. In this case, the peak may be located at a neutral density level that is several orders of magnitude lower. The dayside peak may be of the F_1, E, or D type. An F_2 layer with the principal ion O^+ can probably be ruled out because no oxygen was detected with the UV-photometer experiment.

It is not possible to limit the number of possibilities before the neutral density at the observed peaks can be determined by extrapolation from the lower atmosphere.

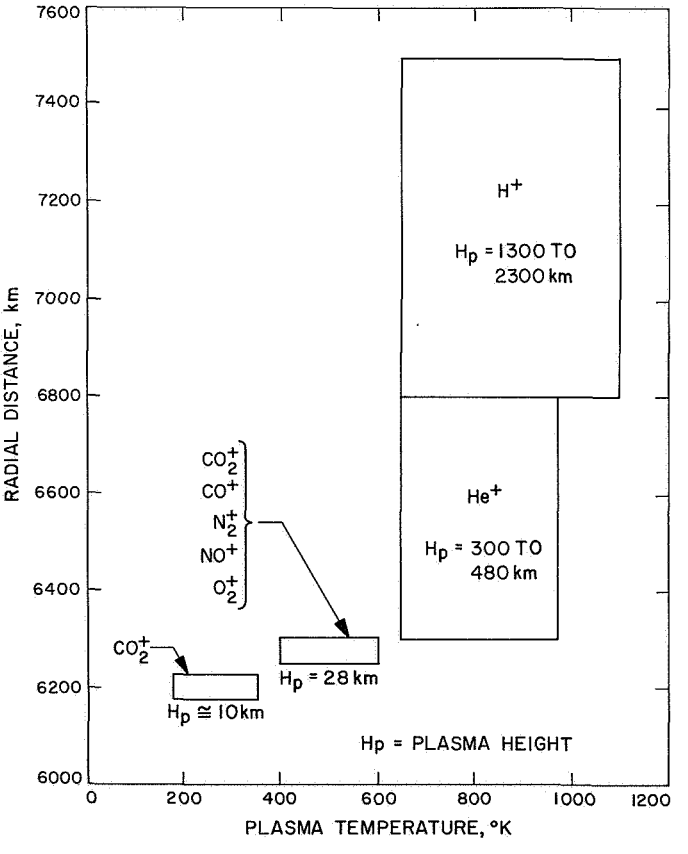


Fig. II-29. Possible constituents and plasma temperatures for nighttime upper atmosphere

As discussed below, it is expected that current systems are set up in the ionosphere, and these might have an effect on the distribution of ionization on both sides of the planet.

Integral inversion of the dispersive doppler measurements near the daytime plasmapause provides the profile indicated by the solid curve in Fig. II-28. As discussed above with regard to scaling between 2 and 3 of Fig. II-26 and the fit obtained for the nighttime peak, it follows that a Chapman layer of $N_{max} = 5 \times 10^5$ cm^{-3} and a plasma scale height of 10 km provide a first-order approximation to the features of 3. These values were used to show the dashed-line daytime peak of Fig. II-28. Neither the amplitude nor doppler measurements provide direct information about the ionization lying between the main peak and the higher plasmapause. The dotted line shown in Fig. II-28 is meant only to illustrate the transition.

Because of the unusual and unpredicted nature of the daytime plasmapause, a possible alternative explanation of the measurements was attempted. It was hypothesized that the indicated high values of N do not exist in these regions, which are several hundred kilometers above the main ionization peak. This condition would seem to require both an unusual raypath geometry (because of complex lower layers that focus refracted rays up towards the spacecraft) and unexpected behavior of the 49.8-MHz receiver in not locking onto the strong direct signal to explain both 5 and the measured doppler. Even this combination of events would not account for the amplitude ripple in the 423.3-MHz signal at 4. Although this ripple is small, it represents a change of two data levels in a region where it stands out as being unusual, and its shape, position, and magnitude correspond approximately to the derived plasmapause features. Consequently, the preliminary conclusions are that the indicated daytime plasmapause (ending at 6570-km radius) is most likely real, and the complete or very nearly complete absence of planetary plasma above this radius is also real.

3. Interaction definition. The daytime plasmapause may be of great significance for understanding the interaction of the solar wind with Venus. Although this ionospheric feature was described above as unusual and unpredicted, in retrospect it is now beginning to appear to be a natural extension of previous work on the interaction of the magnetized plasma of the solar wind with a planetary body having little or no intrinsic magnetic field, but having relatively high conductivity. The interplanetary magnetic field lines cannot pass rapidly through the conducting body; therefore, a stagnation field builds up that deflects subsequent lines and particles, and a bow shock forms.

The simplest case of a solid, nonmagnetic, conducting body in the solar wind has been treated by Gold (Ref. 19). He discussed the problem in terms of the moon, where the concept is probably inapplicable because the conductivity is not sufficiently high (see Ref. 10). The presence of an atmosphere complicates the problem, but can provide the needed high conductivity caused by the formation of an ionosphere. Dessler (Ref. 20) has treated this case in the context of nonmagnetic Mars, where the concept is probably applicable, although no measurements have been made that relate directly to the predictions. Dessler considers the potential flow of the solar wind around Mars, which would have a standing bow-shock wave at a radius of about 1.4 times the radius of Mars on the day side. The shock, in turn, results from the pile-up of interplanetary magnetic field against the nearly impervious (to motion of magnetic field lines) conducting ionosphere. [In the absence of both body magnetism and body (including the atmosphere and ionosphere) conductivity, the interplanetary magnetic field would pass through the body, and the solar-wind particles would be undeviated until they struck the atmosphere or surface.] In his treatment, Dessler was primarily concerned with the ionizing effect of the shocked solar plasma inside the bow shock as it interacts with the upper atmosphere of Mars. This mechanism may be the cause of the high level of ionization seen in comets (Ref. 21), and may help to explain the relatively high plasma density just inside the plasmapause.

After the possible existence of a sharp plasmapause in the upper atmosphere of Venus was announced as a preliminary result of the *Mariner* Venus 67 mission, Johnson extended the concepts introduced by Dessler. He made a preliminary consideration of the transition region between the region where the currents flow (the main ionospheric layer) and the level where the shocked solar wind can flow past the planet without being impeded by the atmosphere. In his description, the plasmapause would also be the magnetopause of an induced magnetosphere. Above this level, any planetary atmosphere particle that is or becomes ionized is quickly carried away by the shocked solar wind that flows by the planet between the bow shock and the magnetopause. The induced magnetosphere consists of a compressed interplanetary magnetic field having sufficient magnetic pressure to deflect both the particles and the field of the solar wind. The pressure is transferred to the

level of the ionosphere where currents sufficient to nearly terminate the magnetic field can flow, and where the pressure can, in turn, be transferred from the ionospheric plasma to the neutral atmosphere through collisions.

Although the dual-frequency measurements of the neutral atmosphere have not been analyzed in detail, a few points of interest are apparent from the data shown in Fig. II-26. There is no evidence of a diffractive cutoff of the signal by the limb of the solid planet, as would be expected from the results of the *Venera-4* spacecraft, which indicate that the atmosphere should be super-refractive. Thus, horizontal radio and light rays at the critical level are bent completely around the planet. From the duration of the 423.3-MHz signals upon entry, for example, it follows that the atmosphere was probed down to within a few kilometers of the level of critical refraction.

The 423.3-MHz signal shows more fluctuation in amplitude when it is going through the atmosphere E−3 min, 10 s to E−20 s and E+21 min, 10 s to E+23 min, 0 s than when there are no planetary effects. This has implications with regard to atmospheric irregularities and possible layering. The average values of defocusing at the higher frequency could be used to find average refractivity as a function of height; from this, temperature and number-density profiles could be derived assuming CO_2 as the principal constituent, and assuming no absorption. Although the principal atmospheric properties are better defined from the S-band frequency measurements, it is still important to conduct a detailed analysis of the dual-frequency results as a check, in a search for possible differential absorption with frequency, and for study of the fluctuations.

At 49.8 MHz, the amplitude fluctuations are much larger; therefore, the differential effect relative to the higher frequency may help to determine characteristics of ionospheric irregularities. The up-fades between E−1 min, 40 s and E−1 min, 10 s reach a strength about 7 dB greater than the relative strength of the signal at 423.3 MHz. This would have been attributed to the generally irregular atmospheric–ionospheric effects except for a similar up-fade in the 49.8-MHz signal at E+21 min, 30 s to E+21 min, 50 s. It appears to be possible that these are reflections from the solid surface of Venus.

The expected signal characteristics for surface reflections from a planetary body with a super-refractive atmosphere had been studied earlier; it was concluded that atmospheric defocusing on the direct signal could, under certain conditions, be markedly greater than for a near-grazing reflection path that would be bent around the planet by the same amount. This effect can more than compensate for the loss at reflection; it was predicted, for example, that the reflected signal would become stronger than the direct signal in the vicinity of these up-fades. If they do represent reflections, the dispersive doppler should show differences caused by the different paths for the direct ray at 423.3 MHz and the bounce ray at 49.8 MHz.

Although dispersive doppler measurements in this region are not completely reliable, they do show effects upon both entry and exit that are of the right sign, and are reasonably close to the predicted magnitude, to correspond to surface reflections. The ability of the phase-locked systems to respond to such reflections is critically dependent upon their spectral width. Only at the lower frequency would the predicted bandwidth of reflected signals be small enough for most of the energy to lie within the receiver bandwidth. Raypaths can, of course, reach the surface through a super-refractive atmosphere because they pass through the critical level at angles of incidence less than 90 deg, whereas direct occultation rays would be at 90 deg when they reach the critical refraction level.

4. Conclusion. Considerably more work needs to be done in the analysis and study of the dual-frequency measurements, particularly as regards the amplitude measurements and the neutral atmosphere; model fitting to the daytime ionization peak; constituents, number densities, and temperatures above the nighttime ionization peak; characteristics and theories of both peaks; characteristics of the daytime plasmapause; and comparisons with the results of the S-band and other *Mariner V* experiments.

The dynamic range of the dual-frequency experiment in terms of electron concentration at Venus (see Fig. II-28) is more than three orders of magnitude. The precision is variable, depending upon whether dispersive doppler or amplitude measurements are used in the analysis. Caustics cause particularly difficult problems, and were certainly encountered on the day side and probably on the night side near the main ionization peak. For a future flight, it would be valuable to have a second dispersive doppler comparison (e.g., between 423.3 MHz and S-band) so that all of the levels of ionization could be measured with the high precision of this type of measurement.

Perhaps the most important single result of the dual-frequency experiment was the discovery of the day-side plasmapause. It seems very likely that Mars also has an induced magnetosphere, magnetopause, and plasmapause caused by the solar wind. Mars appears to be without appreciable self-magnetism, and it has a conducting daytime ionosphere comparable to that of Venus (Ref. 22). The sensitivity of a dispersive doppler experiment may be required for its detection (see Ref. 18). There appear to be three different types of interaction of planetary bodies with the magnetoplasma of the solar wind; the earth is one, the moon a second, and Venus and Mars a third class. These differ because of planetary magnetism (earth); high ionospheric conductivity and an atmosphere, but no magnetism (Venus and Mars); and no magnetism, no atmosphere, and low conductivity (moon).

H. Celestial Mechanics Experiment

The ranging and doppler radio tracking data from *Mariner V* have been fit by the method of weighted least squares to obtain, along with other measurements, the masses of Venus and the moon.

The direct determination of the mass of Venus from the encounter orbit is expressed fundamentally in terms of the universal gravitational constant G times the mass M and is given by $GM_\varphi = 324{,}859.61 \pm 0.49$ km^3/s^2. If the radar value of the astronomical unit (AU = 149,597,890 km) is assumed, the corresponding sun–Venus mass ratio from *Mariner V* is 408,522.6 ±0.6.

The monthly periodic motion of the earth about the center of mass or barycenter of the earth–moon system is appreciable in both range and doppler data. Therefore, the amplitude of this motion can be determined from the 4 mo of cruise data between the end of the midcourse maneuver and planetary encounter; from this, a value of the earth–moon mass ratio μ^{-1} can be deduced. Because of the ranging data, which have not been available from other spacecraft in interplanetary space, the determination of μ^{-1} from *Mariner V* is potentially the most accurate of any value reported to date. Indeed, the expected uncertainty in μ^{-1} is on the order of ±0.0002. However, various fits to the ranging and doppler data have produced values ranging from a low of 81.2999 to a high of 81.3009. Systematic errors are evidently entering into current solutions. Until these error sources can be removed, the best that can now be done is to set $\mu^{-1} = 81.3004$, and to increase the uncertainty figure to ±0.0007.

To obtain some measure of the accuracy of fit of the encounter and cruise solutions, the rms and mean residuals are respectively listed in Tables II-2 and II-3 for each tracking station and for the total of data from all stations. If there are N residuals (δz_i; $i = 1, 2, \cdots, N$) for which mean residuals are to be computed, then the rms residual is defined by

$$\left[\sum_{i=1}^{N} \frac{(\delta z_i)^2}{N}\right]^{1/2}$$

and the mean residual is simply

$$\sum_{i=1}^{N} \frac{\delta z_i}{N}$$

The rms residual does not account for the distribution of residuals with respect to sign, whereas the mean residual indicates whether or not the residuals are distributed about a zero mean.

In all solutions, the rms doppler residual is less than 1 mm/s, an indication of the accuracy of the data. Two encounter solutions are represented in Table II-2. The first is a fit to doppler data only in an interval from 5 days before to 5 days after encounter. The second is a fit to doppler and range data over the same interval. Moreover, the doppler-only solution includes corrections to the six orbital elements of the spacecraft and the mass of Venus, whereas the doppler-and-ranging solution also includes corrections to the position vector of Venus at encounter, a solar-radiation pressure constant, and the locations of the tracking stations.

Table II-2. Mean residuals for encounter solutions[a]

Deep Space Station	No. of points[b]	rms residual (no range), mm/s[c]	Mean residual (no range), mm/s	rms residual (with range), mm/s[d]	Mean residual (with range), mm/s
Cebreros	354	0.691	−0.131	0.686	−0.063
Tidbinbilla	18	0.502	0.021	0.504	−0.029
Woomera	344	0.653	0.042	0.568	−0.127
Johannesburg	31	—	—	0.424	0.008
Echo	177	0.558	0.025	0.737	−0.040
Mars	181	0.932	0.209	0.966	0.258
Total	1105	0.704	0.010	0.709	−0.020

[a]10-min sample interval.
[b]Doppler error weight = 1.67 mm/s.
[c]Total rms residual error weight = 0.422 (no range).
[d]Total rms residual error weight = 0.425 (with range).

Table II-3. Mean residuals for cruise solution (AU known)[a]

Deep Space Station	Number of doppler points[b]	rms doppler residual, mm/s[c]	Mean doppler residual mm/s	Number of range points[d]	rms range residual, m[e]	Mean range residual, m
Cebreros	410	0.567	0.235	6	72.6	20.2
Tidbinbilla	971	0.424	0.066	298	51.5	−5.3
Woomera	553	0.408	0.137	74	50.1	42.8
Robledo	1074	0.377	0.155	285	52.6	10.1
Echo	457	0.671	0.093	65	41.2	−3.3
Mars	249	0.555	0.121	140	2027	450
Total doppler	3714	0.474	0.128			
Total range less Mars				728	51.2	6.0

[a]10-min sample interval.
[b]Doppler error weight = 0.791 mm/s.
[c]Total rms doppler residual/error weight = 0.599.
[d]Range error weight = 162 m.
[e]Total rms range residual/error weight = 0.316.

Table II-2 shows that the fit is good in both solutions. The mass of Venus that best fits the data is the same in both; the only difference is about one-third the standard deviation of ± 0.49 km^3/s^2 on GM_φ. In computing standard deviations, an error of ± 1.67 mm/s has been assumed for each encounter doppler measurement, as indicated in the table. When the total rms residual is divided by this assumed error, a dimensionless overall goodness-of-fit measure of about 0.425 is obtained for both solutions.

The cruise solution that gives a value for the earth–moon mass ratio (Table II-3) shows similar mean residuals in the doppler data; in addition, the range residuals reveal an rms residual of about 50 m. This value is the result of numerical round-off error arising when the range data are computed to only eight significant figures (single precision on the 7094 computer), and does not represent the measurement error of about 10–20 m.

The range residuals from DSS 14, the 210-ft-antenna Mars station, are much greater than from the 85-ft sites, which track to a distance of approximately 6×10^6 km. By contrast, the 210-ft antenna can track to planetary encounter (about 80×10^6 km) and beyond, and the round-off error is proportionately larger.

Solutions by the weighted-least-squares method depend, of course, upon the relative weighting of the range and doppler data. The total rms residual divided by the assumed error weight is about the same for both types of data (Table II-3), which indicates that the relative weighting is reasonably correct.

In the future, the computation of ranging data will be accomplished in extended precision, and the error weight will be reduced to the level of the measurement error. Also, the cruise and encounter data will be combined in a single solution to obtain important information on the AU and certain elements of the orbit of the earth. At present, the best that can be said is that the radar value of the AU (149,597,890 km) is consistent with the *Mariner V* data, and that the cruise solutions accomplished to date (those which include corrections to the orbital elements of the earth) indicate that significant corrections on the order of ⅒ s of arc are needed to fit the data. For example, one correction requires that the instantaneous axis of revolution of the earth about the sun be moved by at least ½ s of arc toward the axis of rotation of the earth to produce residuals as small as those indicated by Table II-3.

III. Trajectory and Orbit Determination

The various phases of the *Mariner V* trajectory, launch to maneuver, maneuver analysis, postmaneuver cruise, encounter, and postencounter, are described in this section. Also, orbit-determination information on tracking data coverage, premaneuver results, midcourse-maneuver analysis from radio tracking data, cruise results, and real-time encounter results are included.

A. Trajectory

1. Launch to maneuver phase. The *Mariner V* spacecraft was launched from launch complex 13 at the Air Force Eastern Test Range (AFETR), Cape Kennedy, Fla., on Wednesday, June 14, 1967. The launch vehicle consisted of an *Atlas/Agena* combination. The ascent is shown in Fig. III-1; Fig. III-2 depicts the sequence of events from launch to Canopus acquisition. Liftoff occurred at 06:01:00.176 GMT, with an inertial launch azimuth of 101.1 deg east of north. After liftoff, the booster rolled to an azimuth of 102.3 deg and performed a programmed pitch maneuver until booster cutoff. During the sustainer and vernier stages, adjustments in vehicle attitude and engine cutoff times were commanded, as required, to adjust the altitude and velocity at *Atlas* vernier cutoff. Vernier engine cutoff occurred as anticipated at 317.75 s into the mission. Following *Atlas* cutoff, the shroud protecting the spacecraft during the ascent through the atmosphere was jettisoned and the *Atlas* booster separated from the *Agena* stage. The *Agena* engine was then burned for 142.5 s, injecting itself and the spacecraft into a near-circular parking orbit at 06:09:45.360 GMT at an altitude of 185.04 km.

After a parking orbit coast time of 13.28 min, determined by the ground guidance computer and transmitted to the *Agena* during the *Atlas* vernier stage, a second ignition of the *Agena* engines occurred. After the burn duration of 94.40 s, the *Agena* and the spacecraft were traveling in a geocentric escape hyperbola at 11.40 km/s. The *Agena* and the spacecraft then separated, and the *Agena* performed a maneuver to place it in a separate orbit from that of the spacecraft. This maneuver reduced the probability of the *Agena* impacting Venus and contaminating the surface of the planet.

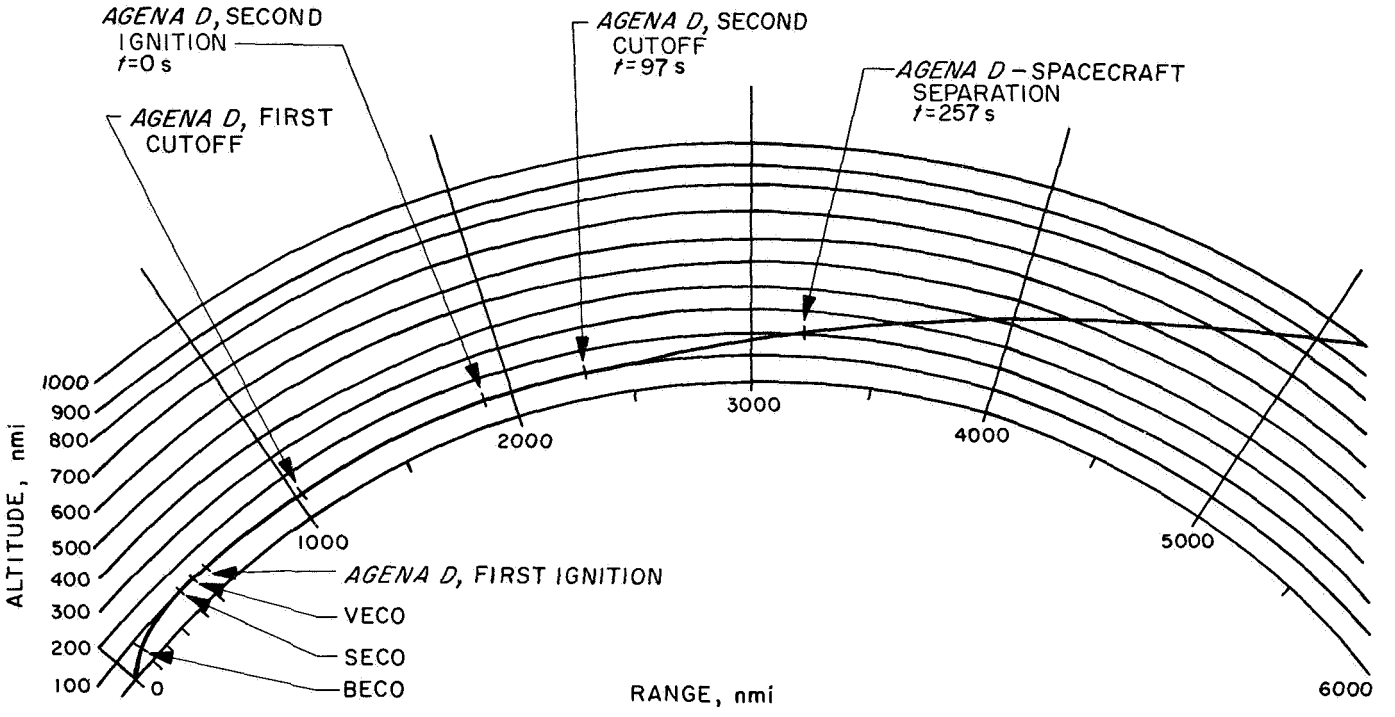


Fig. III-1. Ascent trajectory profile

Injection (second *Agena* cutoff) occurred at 06:24:35.500 GMT over the Atlantic ocean at a geocentric latitude of −4.67 deg and longitude of 351.54 deg. At that time, the *Agena*–spacecraft combination was at an altitude of 192.65 km and traveling at an inertial speed of 11.40 km/s. The geocentric characteristics of the *Mariner* V trajectory are listed in Table III-1.

The *Agena*–spacecraft combination was in the shadow of the earth from launch to 19.27 min after launch. *Agena*–spacecraft separation occurred 161.3 s after transfer-orbit injection. Within 1 h after injection, the spacecraft was receding from the earth in an almost radial direction, with decreasing speed. This reduced the geocentric angular rate of the spacecraft (in inertial coordinates) until the angular rate of the rotation of the earth exceeded that of the spacecraft.

Because of the low sensitivities of the transfer orbits of both the spacecraft and the *Agena* to changes in the injection (second *Agena* cutoff) conditions, it was necessary to bias the targeted aiming point away from the target, Venus. The bias was done to ensure a probability of less than 3×10^{-5} of either the *Agena* or the spacecraft impacting and contaminating Venus. After several days of continuous tracking without a midcourse correction, an estimate showed the spacecraft to be on a nominal biased trajectory that would pass the leading edge of Venus at a closest approach altitude of 69,693 km. The closest approach would have occurred at 03:52:45.155 GMT on October 19, 1967.

To alter the trajectory so that the spacecraft would pass at the closest approach through a selected aiming region located at approximately 10,200 km from the center of Venus (4000 km from the surface), a midcourse maneuver, using a 17.40-m/s velocity increment (80-m/s capability), was required. In addition to altering the miss distance at Venus, this correction changed the arrival time to 17:35:00 GMT on October 19, 1967, permitting the central computer and sequencer (CC&S) of the spacecraft to activate various subsystems at the correct times near encounter and for the closest approach to occur over the prime tracking stations at Goldstone, Calif. The midcourse motor was ignited at 23:08:06 GMT on June 19, 1967. At this time, the spacecraft was at a geocentric range of 1,581,570.3 km and traveling at an inertial velocity of 2.9915344 km/s relative to the earth.

2. Maneuver analysis. The control of the encounter parameters on an interplanetary trajectory is accomplished by means of midcourse maneuvers that are changes in the velocity of the spacecraft and are implemented by means of a small rocket motor on board the spacecraft. The capability to make two midcourse maneuvers was necessary for the *Mariner* Venus 67 mission

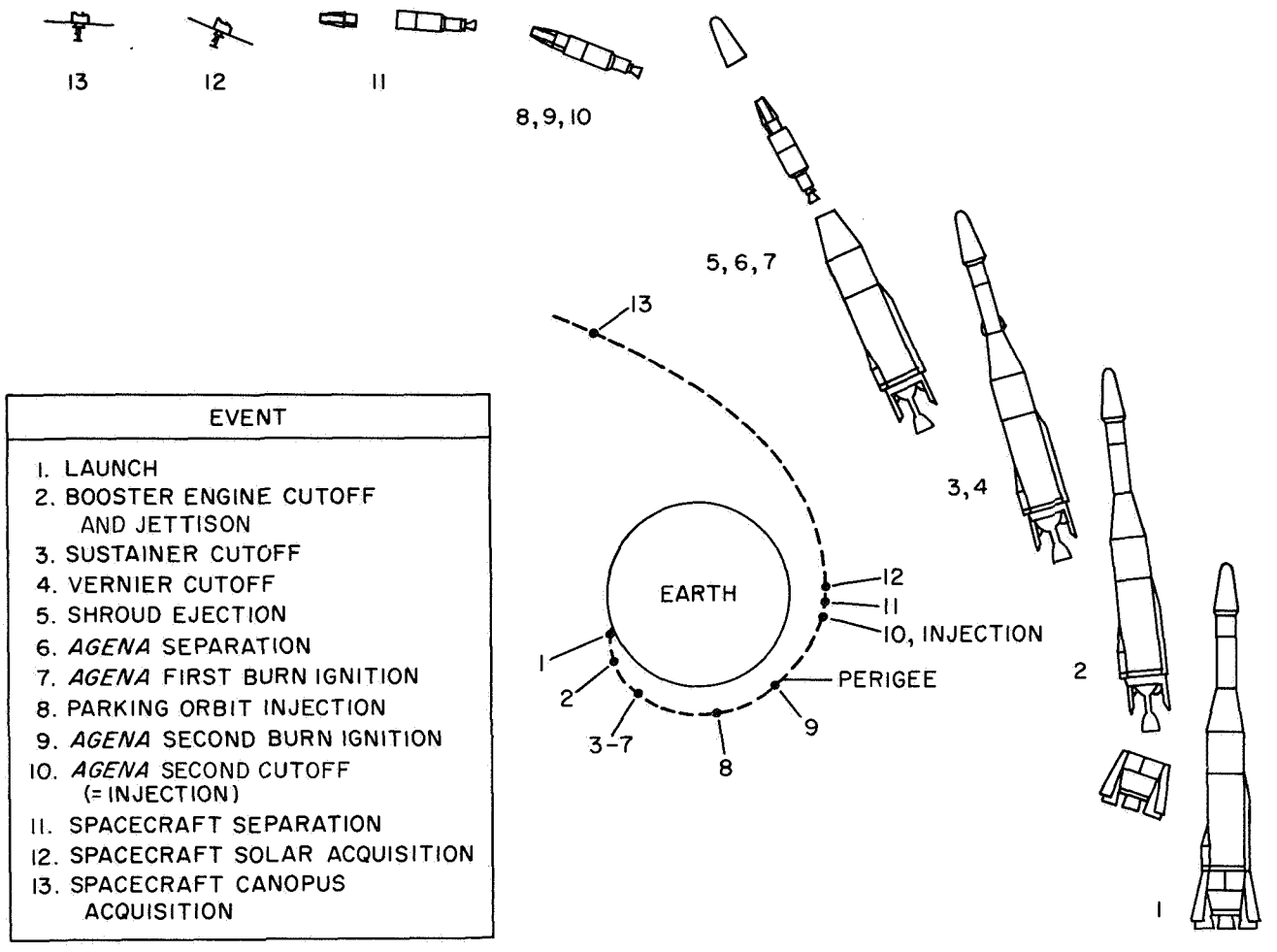


Fig. III-2. Sequence of events to Canopus acquisition

to ensure an acceptable *a priori* probability of achieving a satisfactory set of encounter parameters. The allowable variations in the encounter parameters were quite limited because the spacecraft was designed for a specific encounter geometry and arrival time. The prelaunch probability of achieving a satisfactory encounter with no maneuvers was essentially zero for two reasons. First, because of normally occurring in-tolerance injection dispersions, the resulting encounter dispersions are much larger than the acceptable encounter zone. Second, the planetary quarantine constraint required targeting the spacecraft at injection to a biased aiming point with a closest approach distance of approximately 55,000 km greater than needed. Similarly, the expected in-tolerance dispersions of the first maneuver implied a significant probability of requiring a second maneuver.

The maneuver implementation for the *Mariner* V spacecraft was accomplished by storing the maneuver command in the appropriate registers of the CC&S; and, at the proper time, the signal was sent to execute these commands. Upon receipt of this signal, a gyro-warmup period started, followed by the pitch turn, roll turn, and motor burn. Table III-2 shows the relative timing of each of these events.

The pitch and roll turn registers were counted down by a 1-pulse/s wave train. (Although the nominal turning rate was 0.18 deg/s, the latest telemetry measurements made it possible to compute the turn duration from a best estimate of turning rates.) The burn register was counted down by a 25-pulse/s wave train with every fifth pulse deleted. This mechanization permitted efficient use of circuits elsewhere in the spacecraft. Although the nominal acceleration was approximately 1 m/s^2, computation of the burn duration from a best estimate of motor performance was based upon the latest telemetry measurements.

Table III-1. Geocentric characteristics of *Mariner V* trajectory

Characteristics	Pre-encounter, injection	Pre-encounter, postmidcourse	Encounter
Parameter	June 14, 1967	June 19, 1967	Oct 19, 1967
Radial distance R, km	6569.6304	1,581,614.7	79,764,369
Inertial velocity V, km/s	11.400128	2.9906291	25.350066
Earth-fixed velocity v, km/s	10.989368	112.96141	5767.1726
Geocentric latitude ϕ, deg	−4.6930562	−11.661170	6.0399302
Longitude θ, deg	351.53082	245.89289	230.61465
Right ascension Θ, deg	349.55227	140.46105	161.85034
Path angle of inertial velocity Γ, deg	1.8980037	89.329033	40.868340
Azimuth of inertial velocity Σ, deg	119.97742	61.817187	117.01311
Path angle of earth-fixed velocity γ, deg	1.9689745	1.5169653	0.16479112
Azimuth of earth-fixed velocity σ, deg	121.22208	270.00839	269.91349
Time of event T, GMT	06:24:37.100	23:08:20.650	17:34:55.841
Hyperbolic orbital element	June 14, 1967	June 14, 1967	
Semimajor axis a, km	−46,261.501	−47,228.659	
Eccentricity e	1.1418646	1.0783954	
Inclination to earth's equator i, deg	30.308785	30.315918	
Longitude of ascending node Ω, deg	161.47921	161.12906	
Argument of perigee ω, deg	185.77009	179.05761	
Perigee distance p, km	6562.8713	3702.5079	
Time of perigee passage T, GMT	06:24:01.322	06:14:55.037	

a. Constraints. A number of essential constraints were considered in the design of a maneuver for the *Mariner V* spacecraft. The constraints were divided into two categories: (1) Hard constraints that were physically impossible to violate without serious mission degradation; and (2) soft constraints that could have been violated when necessary at the risk of possible mission degradation. Volume I of this report contains a brief discussion of how the constraints were considered by the midcourse maneuver operations program and the operational personnel.

The hard constraints were:

(1) The required velocity must not exceed the capability of the propulsion system.

(2) The spacecraft must not be pointed within a cone half angle of 1.5 deg that exists about the initial pitch axis. This constraint is discussed in greater detail in another report (Ref. 23).

(3) Because of the CC&S logic design, each turn must be less than 237.6 deg.

(4) In the late maneuvers, the pitch turn must be limited to avoid overheating parts of the spacecraft that are normally shadowed because of the proximity of the sun.

A problem arising as a result of any of these constraints would be solved by either modifying the maneuver slightly, with a resulting change in the encounter parameters, or by changing the date when the maneuver would be performed.

The soft constraints were:

(1) The earth–spacecraft, low-gain antenna angle shall not exceed 90 deg at any time during the turns. This is to maintain telemetry and command capability throughout the maneuver.

Table III-2. Midcourse maneuver sequence

Time	Event description
t_a	Time at which maneuver execute was enabled. Gyro-warmup period began.
$t_b = t_a + 59.5 \pm 0.5$ min[a]	Time at which sun and Canopus sensors relinquished AC and pitch turn started with polarity and for duration as commanded. After pitch turn was completed, spacecraft was inertially stabilized until CC&S register was counted out completely.
$t_a = t_b + 22.0$ min	Time at which roll turn started with polarity and for duration as commanded. After roll turn was completed, spacecraft was inertially stabilized until CC&S register was counted out completely.
$t_d = t_c + 22.0$ min	Time at which motor was ignited to burn for length of time commanded. After burn was completed, spacecraft was inertially stabilized until CC&S register was counted out completely.
$t_c = t_a + 102.36$ s	Sun- and Canopus-acquisition phase (began as at injection). Spacecraft was in cruise-phase orientation after acquisition.

[a]This ±0.5 min is the *a priori* uncertainty in the gyro-warmup period. When the commands are sent, the phasing between the controlling pulse train and transmission time is known to the order of tenths of seconds.

(2) Neither turn may end within the region of the low-gain antenna pattern where the interferometer effect is present.

(3) The roll turn shall not exceed 180 deg to allow time to ascertain that the turns are correct before it is too late to inhibit motor ignition.

(4) The maneuver will be performed during a Goldstone pass while a high-rate telemetry is still possible.

(5) The turns shall be limited to avoid having the sun come close to the field of view of the various sensitive instruments, such as the UV photometer, the terminator sensor, and the Canopus sensor.

When possible, each of these constraints is honored. However, the constraints may be violated when necessary. Under normal conditions, the soft constraints are not expected to degrade the mission.

b. In-flight results. A number of possible maneuvers were studied to find variations that would lead to a "best" maneuver. One important result of this study was the observation that the maneuver parameters showed very little sensitivity to the time when the maneuver was performed, as indicated in Table III-3.

Table III-3. Midcourse-maneuver parameter sensitivity to time

Parameter	Days from injection					
	5.8	7.8	9.8	11.8	13.8	15.8
V, m/s	16.556	16.447	16.441	16.515	16.657	16.859
Pitch turn, deg	54.38	57.01	59.48	61.81	64.01	66.08
Roll turn, deg	71.94	71.10	70.30	69.53	68.80	68.13

Table III-4. Desired-vs-achieved injection and maneuver results

Event	Aiming point		
	B • **R**, km	**B** • **T**, km	T_f, days
Injection			
Achieved	−65,343	81,483	126.2451
Desired	−54,275	87,414	127.1911
Maneuver			
Achieved	−14,855	24,278	126.8152
Desired	−12,761	21,738	126.8333

These results are based on an aiming point of $\mathbf{B} = 24{,}250$ km, $\theta = -29$ deg, and an arrival time of 18:00 GMT on October 19, 1967.

Only one maneuver was performed on the *Mariner* Venus 67 mission. Although the execution errors associated with this maneuver were larger than expected, the achieved postmaneuver encounter parameters were considered acceptable, and the second maneuver was not used. Table III-4 indicates the results of the injection and maneuver.

The final-maneuver calculation was performed on June 18, 1967, based on the best estimate of the orbit at that time. It was determined that a maneuver existed that satisfied all constraints. The commands were transmitted to the spacecraft at 21:23:57 GMT on June 19, 1967. Motor ignition occurred at 23:08:03 GMT. Table III-5 shows the computed and commanded maneuver parameters, and the best estimate of the values actually achieved. The difference between the computed and commanded values is a result of the quantizing of the commands. The difference between the commanded and achieved values is because of maneuver execution errors.

Table III-5. Computed- and commanded-vs-achieved midcourse maneuver performance

Parameter	Pitch turn, deg	Roll turn, deg	Velocity, m/s
Computed	55.35	71.02	16.127
Commanded	55.267	70.946	16.135
Best estimate of achieved value	55.12	70.63	15.412
Estimated error	0.15	0.32	0.723
A priori standard deviation	0.7	0.7	0.121 (0.75%)
Error in *a priori* standard deviations	0.21	0.46	5.96

Table III-6. Heliocentric orbital elements of *Mariner V* spacecraft trajectory

Elliptical orbital element	Pre-encounter orbit	Postencounter orbit
	Oct 28, 1967	Jan 4, 1968
Semimajor axis *a*, km	129,733,170	98,313,649
Eccentricity *e*	0.17436497	0.11849217
Inclination to ecliptic *i*, deg	2.6968311	1.3733747
Longitude of ascending node ☊, deg	81.968201	114.58310
Argument of perihelion ω, deg	350.65626	91.603240
Perihelion distance *p*, km	107,112,250	86,664,251
Time of perihelion passage *T*, GMT	10:45:37.572	08:59:27.189
Period *P*, days	294.97604	194.59467

Even though the spacecraft limit-cycle position is not predicted for maneuver calculations, the telemetered values were used for the performance error analysis.

The estimates of the achieved values were obtained by using the postmidcourse orbit, as determined by the orbit-determination program after about 1 mo of post-maneuver tracking, and by running the midcourse maneuver program to compute the maneuver parameters required to achieve that orbit. These computations showed the turns to be very accurate, but a significant error existed in the velocity magnitude. The $\mathbf{B} \cdot \mathbf{R}$ and $\mathbf{B} \cdot \mathbf{T}$ values achieved by the maneuver lie very near to

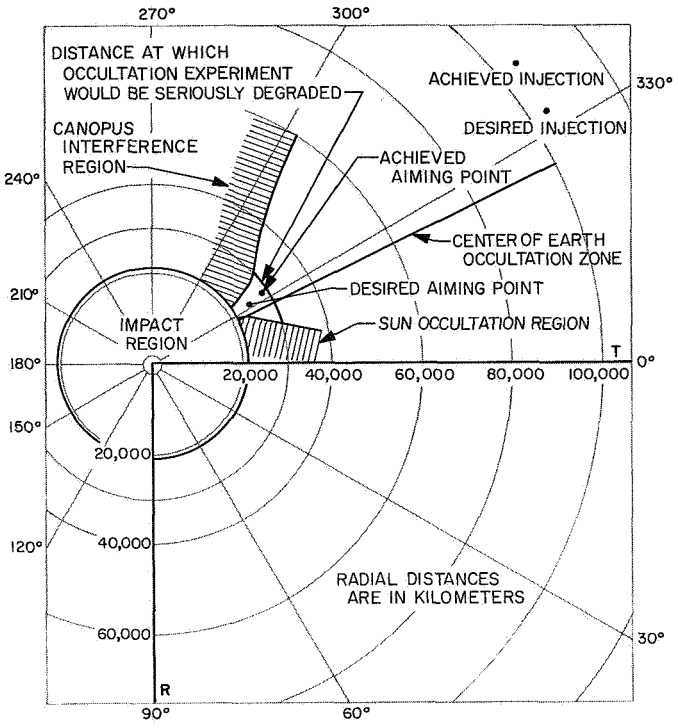


Fig. III-3. Midcourse-maneuver results

the straight line connecting the achieved injection aiming point and the desired maneuver aiming point as shown in Fig. III-3. The result was an acceptable encounter geometry. If a miss of the same magnitude had been aligned perpendicular to the radial direction, the spacecraft would have been either at the edge of the sun occultation or the Canopus interference regions, and a second maneuver would have been performed.

Figures III-4 through III-9 present curves of earth–spacecraft distance, celestial latitude, celestial longitude, heliocentric distance, Venus–spacecraft distance, and cone and clock angles of earth as functions of time from launch to the end of 1971. The heliocentric characteristics of the *Mariner V* orbit are shown in Table III-6.

During the interplanetary phase of the flight, several orbital computations were made covering the period from June 19, 1967, when the midcourse maneuver was performed, to October 19, 1967, when the encounter with Venus occurred. These computations stabilized very early in the flight of the *Mariner V* spacecraft, and the predicted near-Venus orbit did not change by any considerable amount. The Venus-centered orbital characteristics of the *Mariner V* trajectory, as predicted during the interplanetary portion of the flight, are listed in Table III-7.

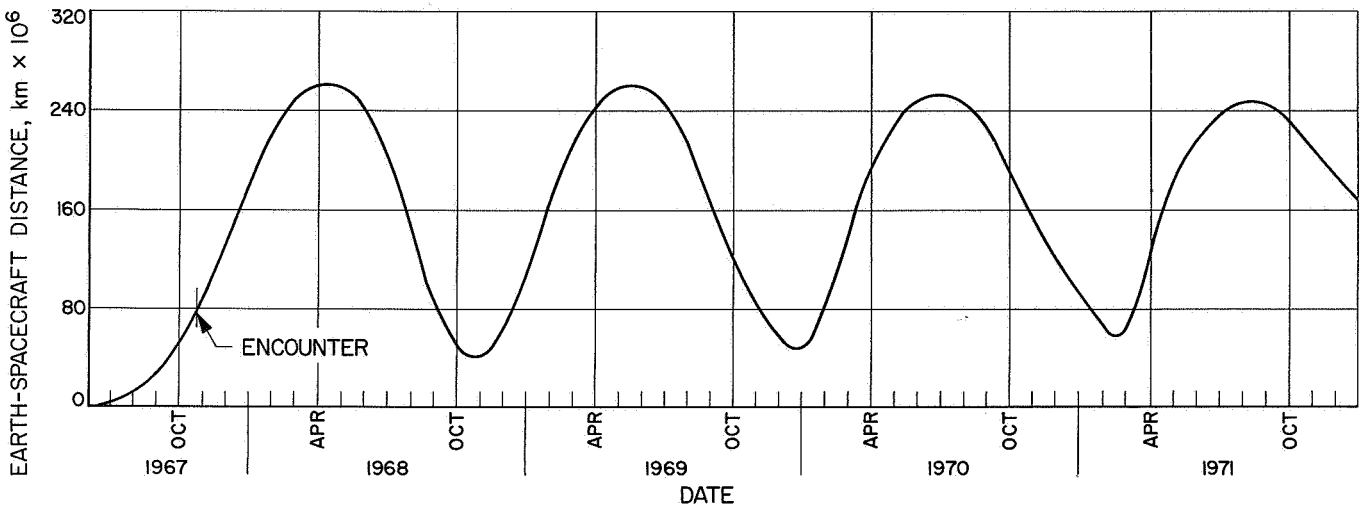


Fig. III-4. Spacecraft distance from earth, launch through 1971

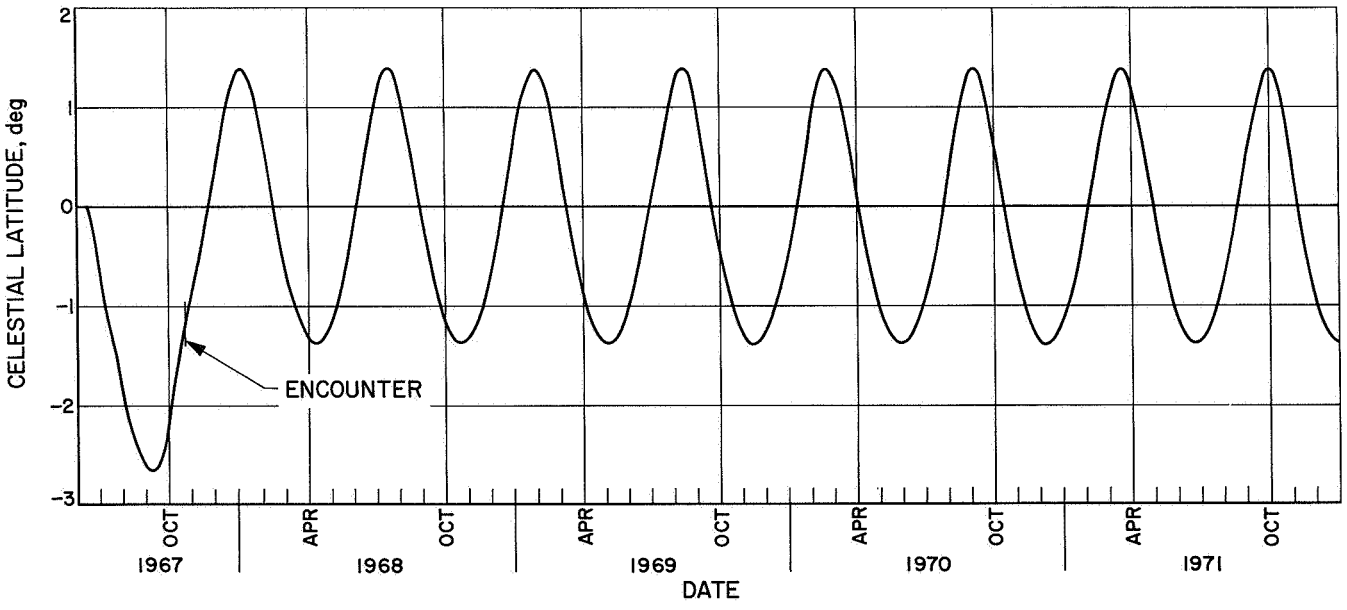


Fig. III-5. Spacecraft celestial latitude, launch through 1971

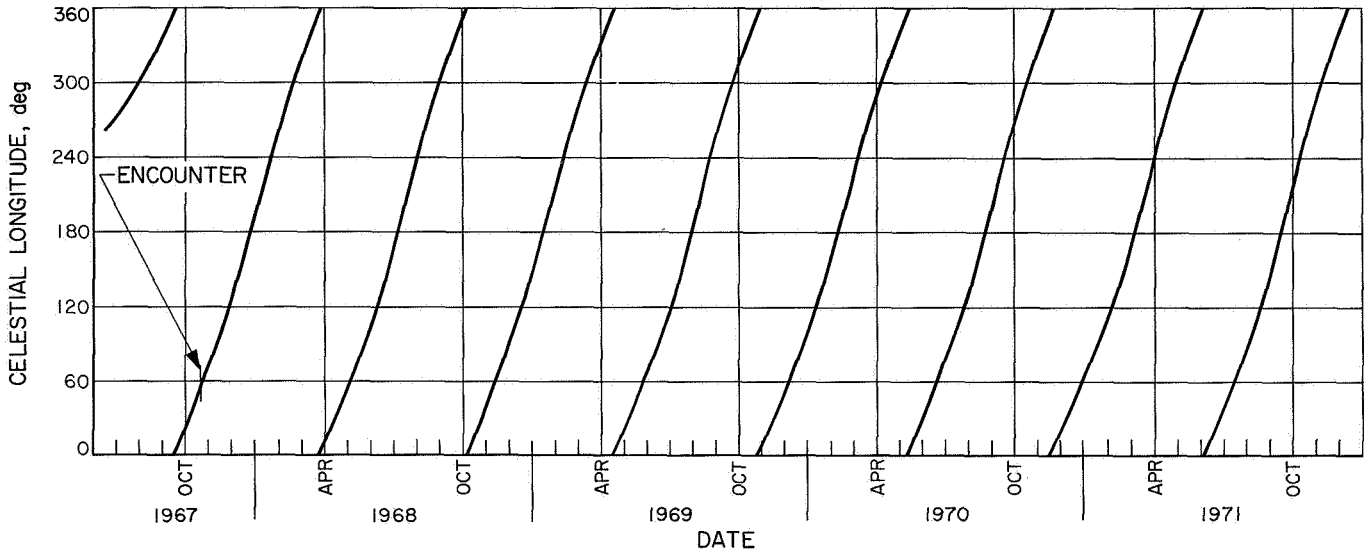


Fig. III-6. Spacecraft celestial longitude, launch through 1971

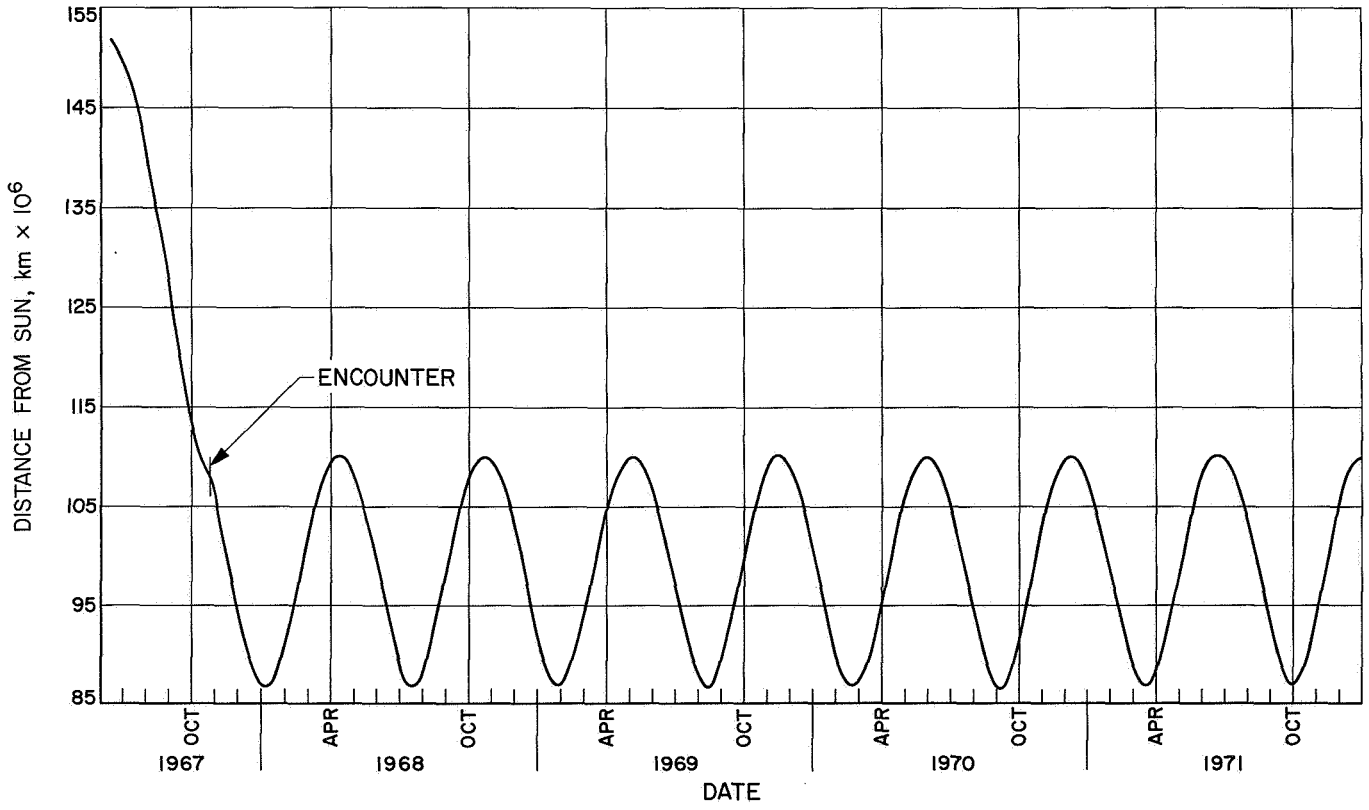


Fig. III-7. Spacecraft distance from sun, launch through 1971

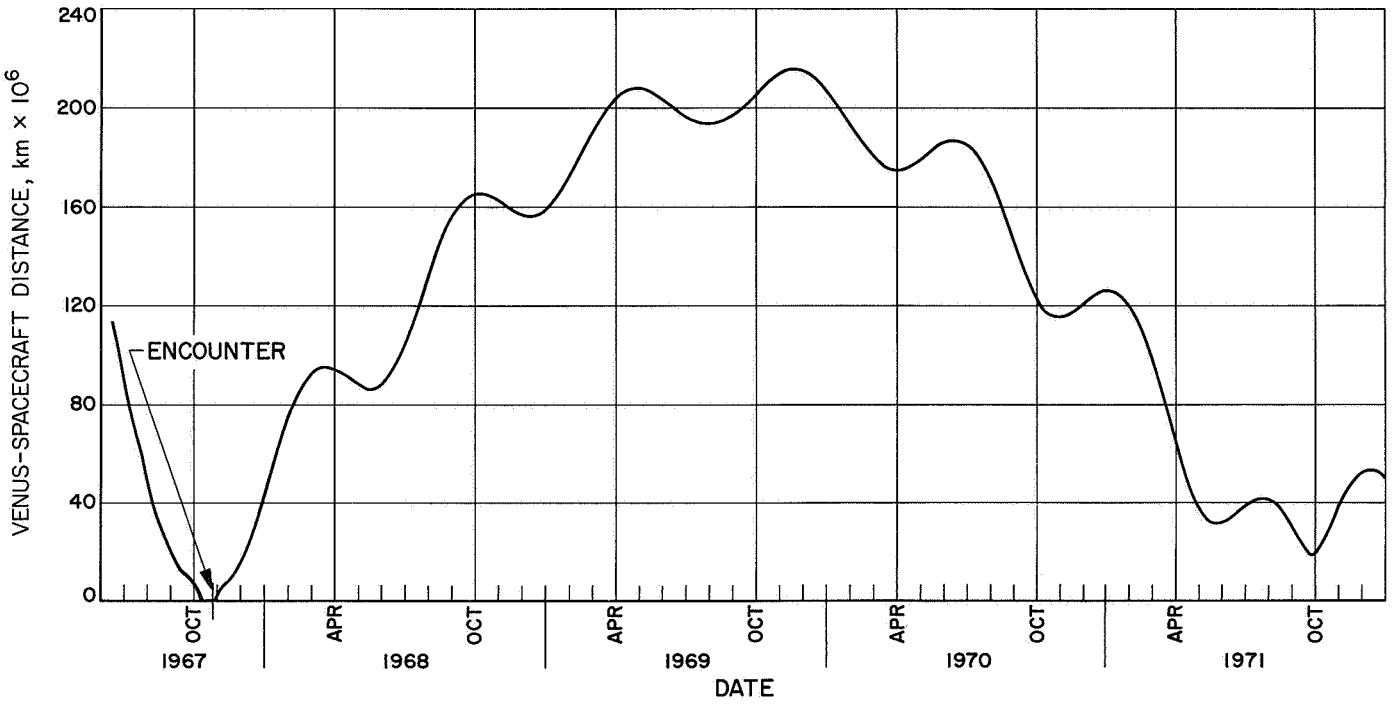


Fig. III-8. Spacecraft distance from Venus, launch through 1971

3. ***Postmidcourse maneuver cruise phase.*** Following the midcourse maneuver, the spacecraft reacquired the sun and Canopus, and returned to the cruise mode. At this time, the spacecraft was moving primarily under the gravitational influence of the sun in an ellipse with the sun at the focus. During the early portion of the cruise phase, the heliocentric velocity of the spacecraft was less than that of the earth, causing the spacecraft to trail the earth for several days around the sun. However, as the *Mariner V* spacecraft began moving closer to the sun, the spacecraft accelerated and eventually caught up with the earth and passed it.

4. ***Encounter phase.*** The *Mariner V* spacecraft approached Venus along the leading edge and from outside the orbit of the planet. At approximately 3.3 min before the closest approach, the radio signal was lost as the spacecraft was occulted behind Venus. While the spacecraft was behind the planet, the antenna position was switched automatically from its original position by a sensor that triggered the mechanism when it saw the planet terminator approximately halfway through the occultation. The new antenna position compensated for the trajectory bending near the planet. Otherwise, the antenna beam would have been displaced from its ideal position during emergence from occultation. As a result, the chances of a rapid reacquisition of the signal as it passed through the atmosphere of Venus coming out of occultation were enhanced.

Tracking data gathered and analyzed during the encounter sequence indicated that the Venus encounter

Table III-7. Venus-centered orbital elements of *Mariner V* spacecraft trajectory

Hyperbolic orbital element	Pre-encounter prediction	Actual Venus encounter orbit
	Oct 19, 1967	Oct 19, 1967
Semimajor axis a, km	−34,825.175	−34,824.285
Eccentricity e	1.2917091	1.2914715
Inclination to ecliptic i, deg	32.001963	31.700211
Longitude of ascending node Ω, deg	341.30976	341.19472
Argument of periapsis ω, deg	152.82175	152.92873
Periapsis distance p, km	10,158.819	10,150.288
Time of periapsis passage T, GMT	17:34:22.823	17:34:55.841

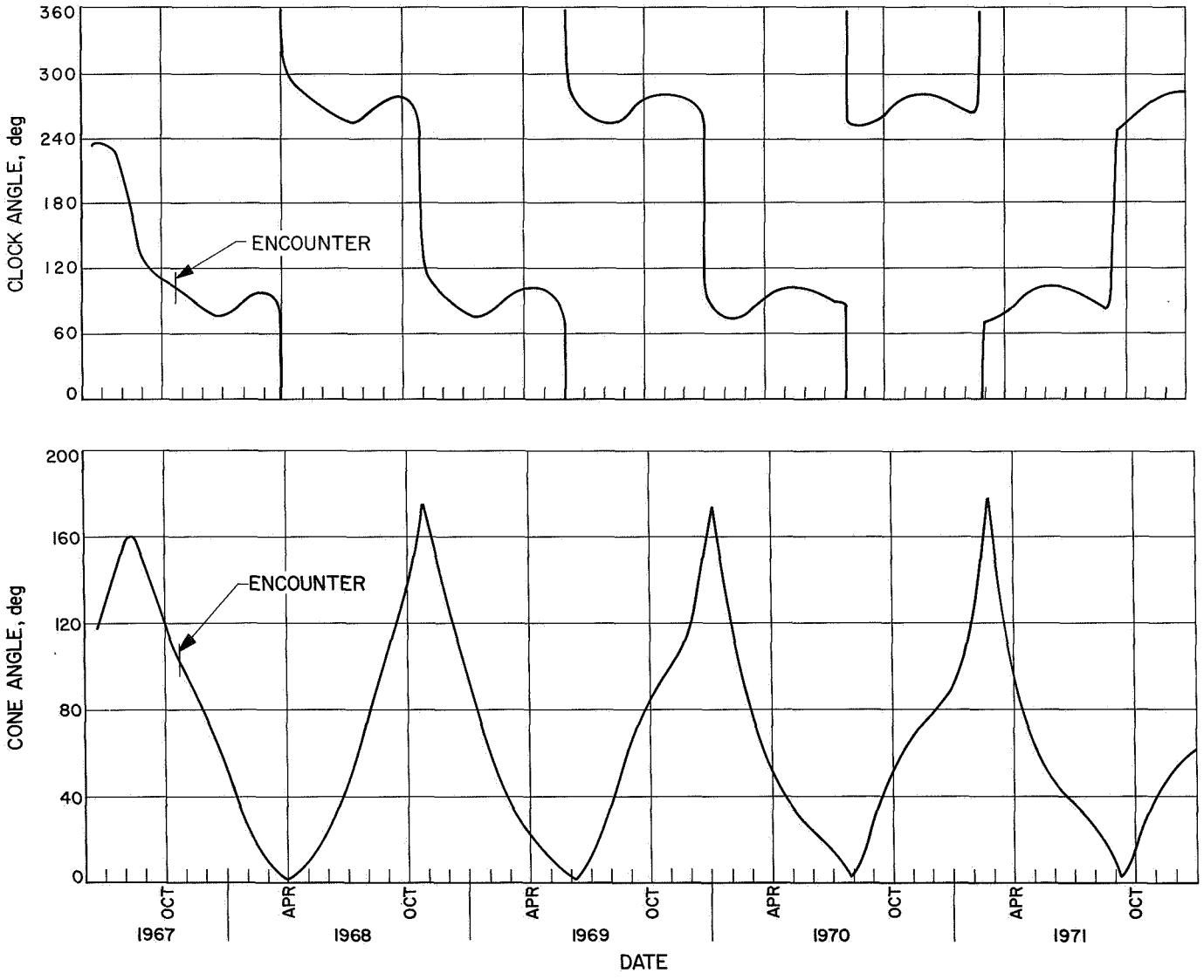


Fig. III-9. Clock and cone angles of earth, launch through 1971

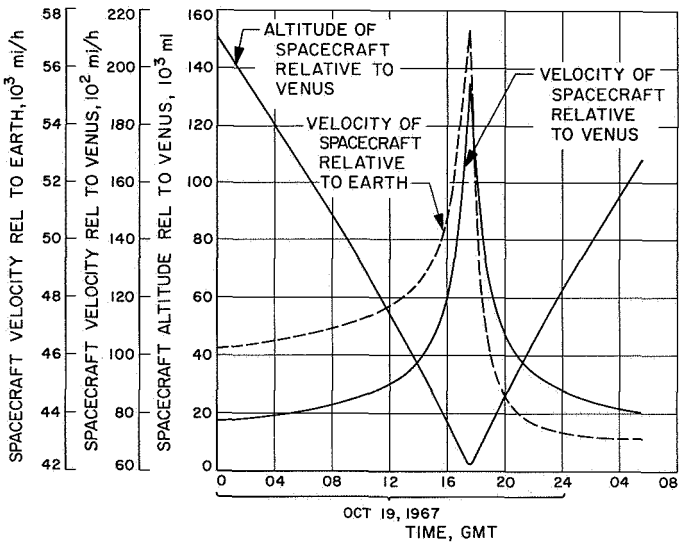


Fig. III-10. Encounter velocities and altitude

trajectory predicted during the cruise portion of the flight did not differ significantly from the observed encounter trajectory. The Venus-centered characteristics of the *Mariner V* spacecraft trajectory determined from encounter data are given in Table III-7. A plot of the encounter velocities and altitude is shown in Fig. III-10 with respect to the closest approach epoch of 17:34:55.8 GMT on October 19, 1967.

5. Postencounter phase. When the spacecraft left the vicinity of Venus, the gravitational pull of the planet altered the heliocentric orbit of the spacecraft, changing the perihelion distance from 107,112,250 to 86,664,251 km. The changes in other elements of the trajectory are shown in Table III-6.

The *Mariner V* spacecraft returned for a close pass at earth on October 27, 1968, when it approached within 38,995,000 km. The spacecraft will return to the vicinity of earth approximately every 14 mo. The next time the *Mariner V* spacecraft will return close to Venus will be at the end of October 1975. The closest approach distance to Venus will be 4,300,000 km. The heliocentric characteristics of the *Mariner V* spacecraft postencounter trajectory are shown in Table III-6. The trajectories of the *Mariner IV* and the *Mariner V* spacecraft are illustrated in a heliocentric plan view of the ecliptic in Fig. III-11 (see Figs. III-4 through III-9 for plots of the postencounter celestial latitude, celestial longitude, heliocentric distance, earth–spacecraft distance, Venus–spacecraft distance, cone angle of earth, and clock angle of earth). Figure III-12 shows the plots of the cone angle of Canopus from launch through 1971.

B. Orbit Determination

1. Tracking data coverage. The primary Deep Space Instrumentation Facility (DSIF) tracking data type is two-way, phase-coherent doppler data. A functional block diagram of the standard DSIF doppler system is shown in Fig. III-13. During the mission, the doppler digital resolver became fully operational throughout most of the network with the exception of Deep Space Station (DSS) 51. This subsystem provided a means of correcting the doppler count for the non-integer number of cycles between sampling times. The doppler digital resolver demonstrated its effectiveness by reducing either the high-frequency noise or the doppler data by more than an order of magnitude.

The *Mariner* Venus 67 mission provided the first opportunity to employ the Mark IA ranging system at ranges substantially greater than the distance of the moon. Mark IA ranging data were taken from just after the midcourse maneuver on June 19, 1967, until system threshold was reached on July 6, at a distance of 5.8×10^6 km. A total of 10,400 ranging points were taken. The Mark IA ranging system was used to provide time correlations between DSIF stations via both the *Mariner V* and the operational *Lunar Orbiter* spacecraft.

During the latter part of the mission, the planetary ranging subsystem (PRS) became operative at DSS 14. PRS data were taken during the approach phase to the planet and in close proximity to Venus on either side of the closest approach time. After encounter, PRS measurements were made to distances in excess of 110×10^6 km.

Another innovation introduced during the *Mariner* Venus 67 mission was the use of the pseudo-residual program for real-time tracking data monitoring. This is a 7044 program that compares any of the various tracking data types with their corresponding computed values from the Deep Space Network predict program (**PRDX**), and outputs observed-minus-predicted quantities and noise estimates. Although a number of problems invalidated much of the noise computations, the program proved a valuable aid in detecting and diagnosing DSIF hardware problems quickly. A modification of the program was used to provide real-time plots of the atmospheric effects for the occultation experiment.

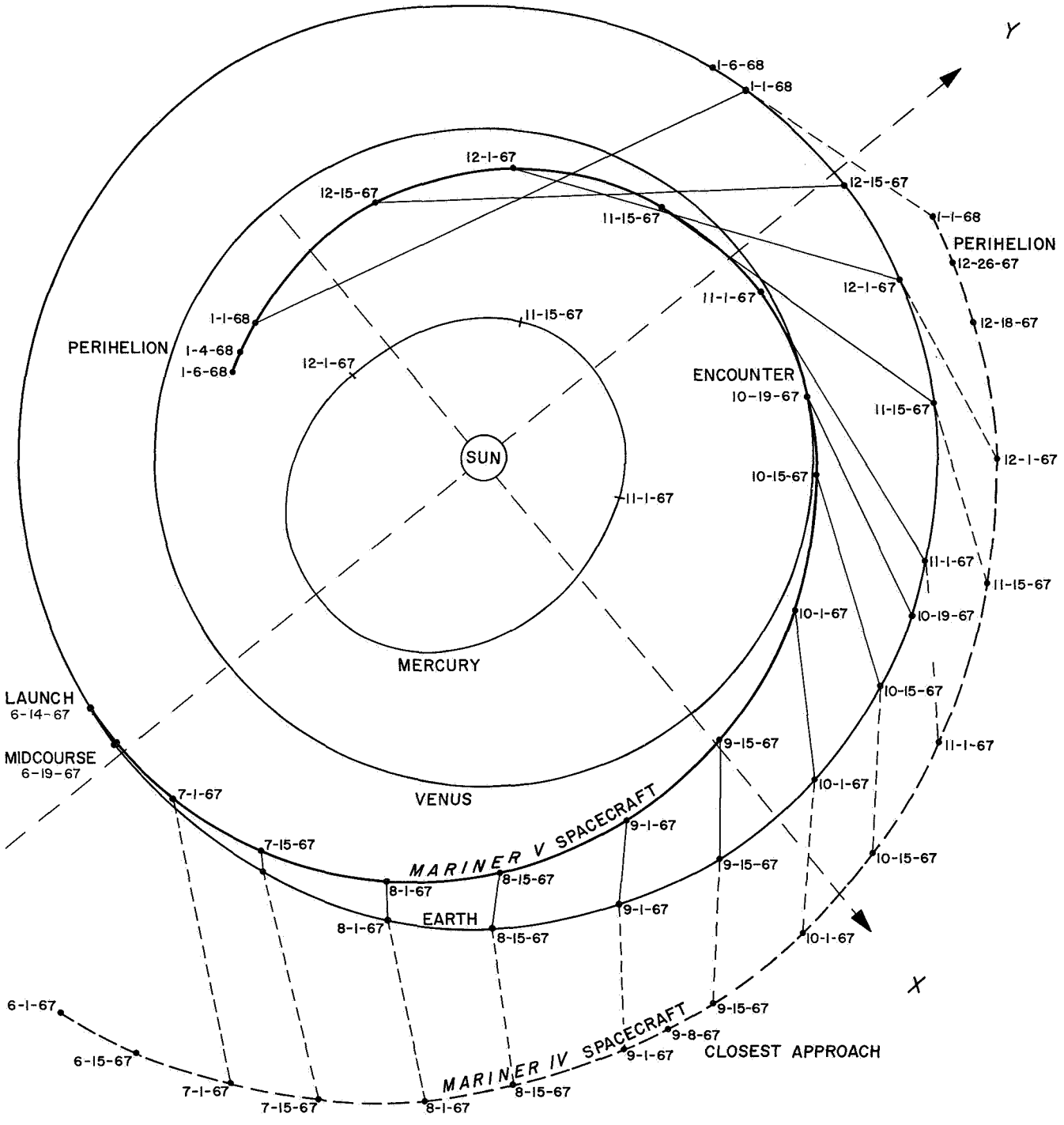


Fig. III-11. Heliocentric plan view of *Mariner IV* and *Mariner V* spacecraft

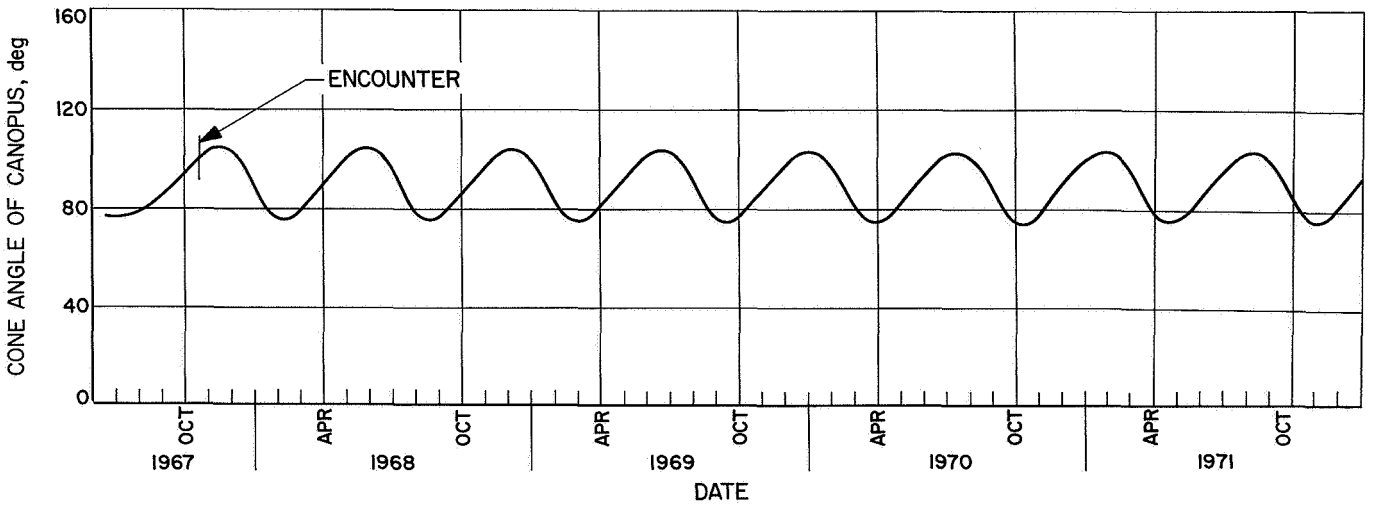


Fig. III-12. Cone angle of Canopus, launch through 1971

a. Description. During the nonpowered transfer flight period between 06:29 GMT on June 14, and 23:07 GMT on June 19, essentially continuous tracking coverage was obtained by DSSs 11 (Goldstone Pioneer), 41 (Woomera), 42 (Canberra), 51 (Johannesburg), and 61 (Madrid). Deep Space Stations 41 and 51 participated only briefly in the early phase of the period. The data types used in determining the orbit of the spacecraft were:

(1) Hour angle, declination (HA-dec). This data type is the pointing angle of the tracking antenna in degrees, and was used only in the very early orbits.

(2) S-band phase-coherent counted (two-way) doppler (CC3). This is a measure of the topocentric radial velocity of the spacecraft, and is the prime orbit data type. Units: 1 m/s $\simeq$ 15.3 Hz.

b. Summaries. Angle data were obtained only until 07:03:57 GMT, approximately 40 min after injection into transfer orbit. The angles from DSS 51 were biased until this time, when it was discovered that the antenna had been tracking on a side lobe. Consequently, several orbits were corrupted by these biased angles. The DSS 42 angles in two early real-time orbits were effectively biased by an incorrect DSS latitude used in the computations of these orbits.

c. Controlled roll data. The spacecraft was in a controlled roll until approximately 22:50 GMT on June 14. Because the antenna is offset from the center of gravity at the spacecraft, a sine curve resulted in the observed computer-doppler residuals with the amplitude of approximately 0.02 Hz. This may be seen in the DSS 11 residual curve of Fig. III-14.

d. Time resolver doppler. Normally, doppler cycles are counted to the nearest cycle at a fixed sample rate under control of the station clock. However, for this mission, DSS 11 used a special device for incrementing the sample time to the exact time of zero phase delay between transmitter and receiver. This operation has the advantage of eliminating counter-truncation error. As an example, DSS 11 doppler achieved a standard deviation of 0.00234 Hz for six 600-s points and two hundred thirty-three 60-s points. This compares favorably with a similar pass of DSS 42 doppler in the same orbit, with the standard deviation of 0.00460 Hz for two hundred twenty-two 60-s samples. Only DSS 11 used a time-resolver device in the premaneuver phase of the mission.

2. *Premaneuver orbit determination results.*

a. Orbit state vector. The JPL orbit determination program (**ODPM**) used a weighted least-squares technique for estimating up to 20 parameters and forming up to a 20 $\times$ 20 covariance matrix. The first 12 premaneuver orbits, through 19:38 GMT, June 15, 1967, estimated geocentric equatorial position and velocity of the spacecraft only, with a corresponding 6 $\times$ 6 covariance matrix. Of these early orbits, the first three were degraded by biased angles, as previously mentioned. These orbits were based on one-way data. If two-way lockup had been achieved during the first hour after liftoff, the angle data biases would not have distorted these orbits. Two-way doppler data, as well as ranging data, are most valuable when taken while the spacecraft is near the earth. Two epochs were used for starting the trajectory integration. Orbits using an epoch of $06^h24^m37^s.000$

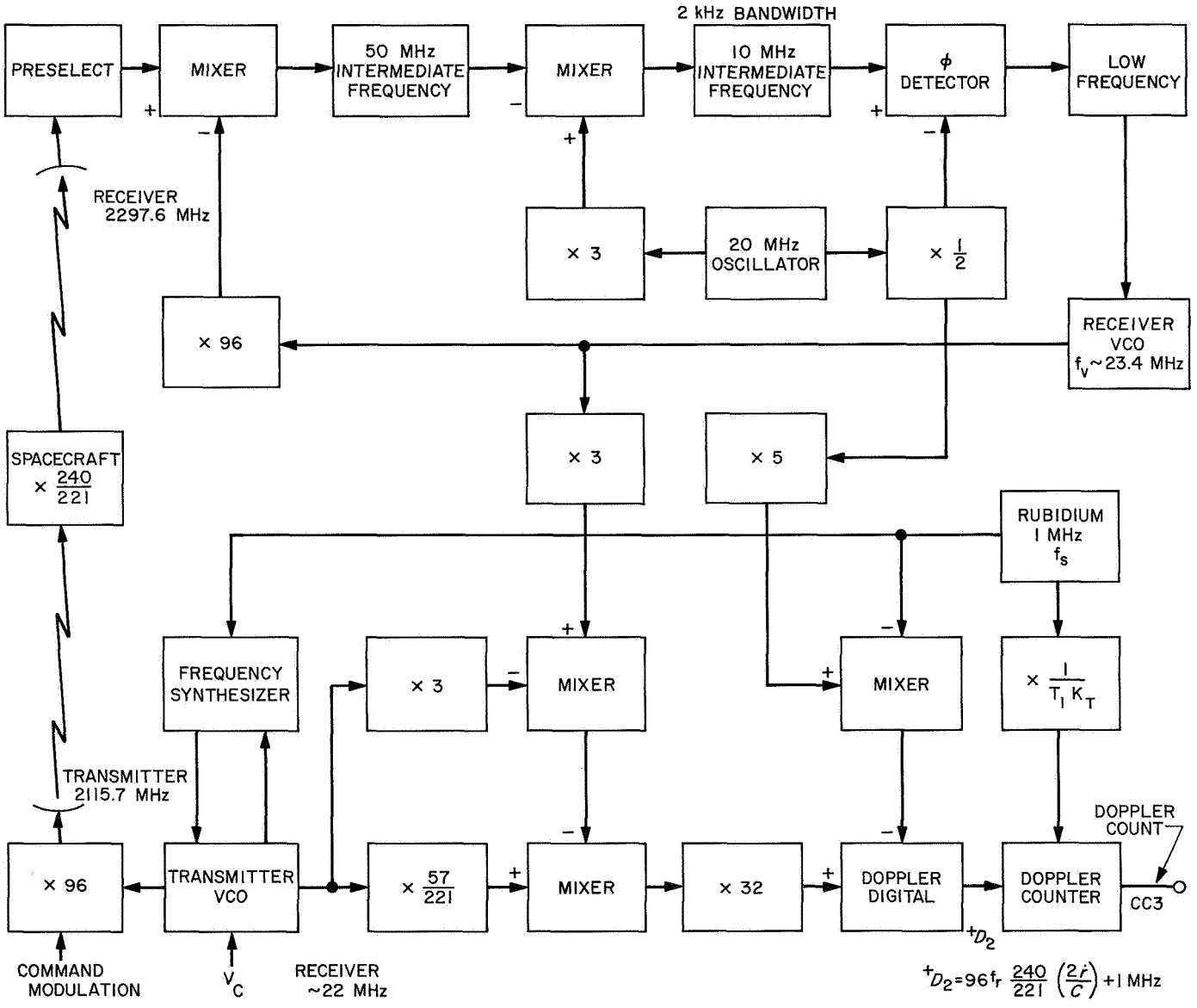


Fig. III-13. Block diagram of S-band two-way doppler system

included data during the controlled-roll period, whereas orbits with an epoch of $22^h00^m00^s.000$ did not include these data in the least-squares fit.

b. Target point. The **ODPM** has the capability of mapping the covariant matrix from epoch to the target planet at time of closest approach. These target parameters are expressed in the **B** plane system (see Section III of Volume I of this report for definitions).

c. Solar-radiation pressure. The perturbable spacecraft acceleration, resulting from solar-radiation pressure, is modeled by

$$\Delta\mathbf{R} = \frac{kA}{m\mathbf{R}^2}(1 + \gamma_B)$$

where

$\mathbf{R}$ = the spacecraft–sun vector in km

$k = 1.031 \times 10^8$, a solar-radiation constant

A = spacecraft effective area normal to $\mathbf{R}$ (nominally 6.60519 m^2)

m = spacecraft mass (nominally 245.71 kg)

γ_B = reflectivity coefficient of the spacecraft (nominally 0.40123054)

Table III-8 compares the premaneuver and postmaneuver solutions for γ_B. It is apparent that the span of tracking data available in the premaneuver solution is not adequate for a strong solution, as the standard deviation has not significantly improved over the *a priori* standard deviation assigned to the nominal value. By contrast, the postmaneuver solution contains nearly a month of tracking data, including ranging data. As a result, the ranging data are particularly effective in this type of solution.

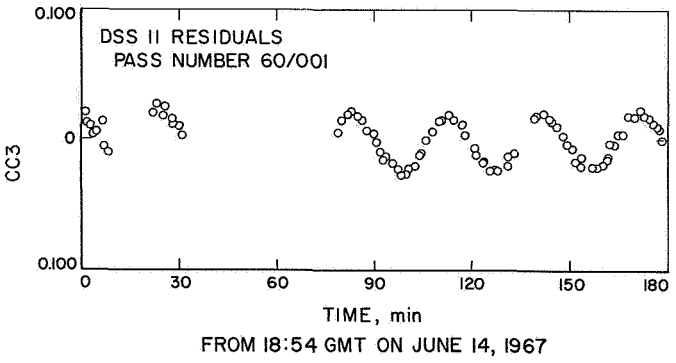


Fig. III-14. Doppler residual during controlled roll

d. Station locations. The **ODPM** is capable of estimating tracking station locations to a high degree of precision where sufficient doppler tracking data have been obtained. In the premaneuver phase of the mission, solutions were obtained for the locations of DSSs 11, 42, and 61. These are tabulated and compared with nominal values and postmaneuver solutions in Table III-8. (γ is the geocentric radius vector to the station, ϕ is the geocentric latitude, and λ is the longitude). The systematic

Table III-8. Preliminary *Mariner* Venus 67 solutions for solar-radiation pressure, station locations, and geocentric equatorial state vector[a]

Parameter	Nominal postmaneuver, σ	ODPM 15 estimated postmaneuver, σ	Estimated premaneuver, σ	Difference of postmaneuver − premaneuver
γ_B	0.40123054 ±0.0400	0.37740661 ±0.0112	0.40864007 ±0.0288	−0.03123346
$r_{11}\cos\phi_{11}$, m	5,206,353.3 ±20.0	5,206,327.1 ±3.5	5,206,331.4 ±6.3	−4.3
λ_{11}, deg	243.15091 ±0.00050	243.15070 ±0.00018	243.15101 ±0.00015	−0.00031
$r_{12}\cos\phi_{12}$, m	5,205,341.6 ±20.0	5,205,347.3 ±2.7	5,205,353.5 ±6.0	−6.2
λ_{42}, deg	148.98148 ±0.00050	1489.98141 ±0.00018	148.98174 ±0.00015	−0.00033
$r_{61}\cos\phi_{61}$, m	4,862,604.5 ±18.7	4,862,597.6 ±4.3	4,862,606.4 ±6.0	−8.8
λ_{61}, deg	355.75113 ±0.00050	355.75114 ±0.00018	355.75146 ±0.00015	−0.00032
x, km	−1,194,559 ±3.2	−1,194,553.1 ±3.2	−1,194,557.7 ±3.2	4.6
y, km	986,069.1 ±3.3	986,080.15 ±3.3	986,069.08 ±3.3	11.07
z, km	−319,692.7 ±8.5	−319,678.29 ±8.5	−319,692.25 ±8.5	13.96
$\dot{x}$, m/s	−2,280.931 ±0.13	−2,280.8194 ±0.0067	−2,280.1899 ±0.0065	−0.6295
$\dot{y}$, m/s	1,842.512 ±0.13	1,842.7422 ±0.0071	1,849.3605 ±0.0067	−6.6183
$\dot{z}$, m/s	−588.9205 ±0.13	−588.24114 ±0.00567	−574.33642 ±0.01668	−13.90472

[a]At 23:08:20.650 GMT on June 19, 1967.

differences in longitude of about 0.0003 deg between the premaneuver and postmaneuver solutions are probably caused by the manner in which WWV–UT time differences are represented in the orbits. However, the differences produce only an insignificant error at target. The cause of the systematic differences in $r \cos \phi$, the distance from the spin axis of the earth, is unknown. Also, these differences are very small (4.3–8.8 m).

3. Midcourse-maneuver analysis from radio tracking data. The *Mariner V* spacecraft was injected into its earth–Venus trajectory at 6:24:19.2 UT on June 14, 1967. The nominal aiming point was designed to place the spacecraft 8165 km from the center of Venus on October 19, 1967. However, at injection, this aiming point was deliberately biased out to 75,000 km from the center of Venus to avoid any chance of impacting the planet. As a result, a midcourse maneuver was planned at the outset to achieve the nominal aiming point. The spacecraft had the capability for two maneuvers, but the second maneuver capability was considered to be in the category of a backup procedure, which would be used only in case primary mission objectives were not achieved by the first maneuver. The second maneuver capability was not exercised during the *Mariner* Venus 67 mission.

Subsequent orbit determination after injection showed that the spacecraft would fly just within 76,000 km of the center of Venus in the absence of a maneuver. Accordingly, a midcourse maneuver was planned and executed at 23:08:06 UT, June 19, 1967. The planned motor burn duration was 17.66 s and an additional velocity of 16.1272 m/s was imparted to the spacecraft. The maneuver was to have put the spacecraft within 8200 km of Venus center at the closest approach on October 19. Telemetry and tracking data showed that the duration of the motor burn was approximately nominal, and the direction of the impulse was within 0.5 deg of the nominal pointing angle. However, orbit determination soon indicated that the spacecraft would fly by Venus at a closest approach distance of not less than 10,000 km from the planet center, and that the velocity imparted to the spacecraft by the motor burn was 15.4123 ±0.0163 m/s rather than the planned 16.1272 ±0.13 m/s. Because primary mission objectives were not jeopardized by the new arrival point, it was decided not to execute a second midcourse maneuver. The following analysis shows how orbit determination can be used to analyze the magnitude and direction of the midcourse maneuver.

Table III-9. Comparison of nominal and achieved maneuver velocity increments for *Mariner V*[a]

Velocity component	Nominal[b] post-premaneuver, σ	Achieved post-premaneuver, σ
$\Delta\dot{x}$, m/s	−0.73797 ±0.13	−0.6295 ±0.0093
$\Delta\dot{y}$, m/s	−6.84993 ±0.13	−6.6183 ±0.0098
$\Delta\dot{z}$, m/s	−14.5815 ±0.13	−13.90472 ±0.0176
Δv, m/s	16.1272 ±0.13	15.4123 ±0.0163

[a]At 23:03:20.650 UT on June 19, 1967.
[b]Based on earlier premaneuver orbit.

The orbit-determination procedure involved a weighted-least-squares fit of approximately 1200 points of 600-s count-interval, two-way coherent doppler tracking data in the 5 days from injection to midcourse maneuver. In the 28-day period from midcourse to July 17, approximately 2000 points of 600-s doppler data and 900 points of ranging data were included in the least-squares fit. The premidcourse least-squares solution was tabulated for the spacecraft velocity at 23:08:20.650 UT on June 19 (without a maneuver). Actually, this time occurred during the motor-burn interval, but only premidcourse tracking data were used in the solution, and were designated "estimated premidcourse." The next tabulation indicated "nominal postmidcourse"; i.e., the velocity that would have been achieved at this time had a nominal maneuver been executed. Lastly, the "estimated postmidcourse" tabulated the least-squares solution for velocity based on postmidcourse tracking data to July 17. It was then possible to compare the nominal maneuver with that actually achieved. Table III-9 compares the velocity components and magnitudes of the nominal and achieved maneuvers.

The comparison indicates that an error of 0.715 ±0.016 m/s was committed in the magnitude of the maneuver velocity increment. If a pointing error was not made, this may account for the achieved closest-approach distance of 10,151 km, compared to the nominal value of 8165 km radial distance. Furthermore, the pointing error of the maneuver thrust axis is easily calculated. The pitch and roll turns may be calculated as follows:

$$\text{pitch turn} = \arctan\left(\frac{\mathbf{V}\cdot\mathbf{j}}{\mathbf{V}\cdot\mathbf{k}}\right) + \arccos\left\{\frac{-\cos\xi}{\left[1-\left(\frac{\mathbf{V}\cdot\mathbf{i}}{\mathbf{V}}\right)^2\right]^{1/2}}\right\} = 55.453 \pm 0.062 \text{ deg}$$

$$\text{roll turn} = -\gamma - \arccos\left(\frac{\mathbf{V}\cdot\mathbf{i}}{\mathbf{V}\sin\xi}\right)$$

$$= 70.660 \pm 0.004 \text{ deg}$$

where

$\mathbf{V}$ = maneuver velocity

$\mathbf{i,j,k}$ = unit vectors of premaneuver pitch, yaw, and roll axes

ξ = orientation of maneuver thrust axis to roll axis = 88.5 deg

γ = orientation of projection of maneuver thrust axis on pitch-yaw plane from pitch axis = 45 deg

The pitch and roll uncertainties were obtained from a computer program that makes use of the 3×3 velocity covariant matrix of $\Delta\dot{x}$, $\Delta\dot{y}$, $\Delta\dot{z}$. The unit vectors used in the above calculations assume the AC error to be zero. Table III-10 shows the corrections indicated by limit-cycle telemetry and the commanded values of the turns.

Thus, errors of about 0.3 deg were made in execution of the turns. However, the actual errors must include the effects of AC displacement. It is obvious that the execution and displacement errors partially cancel. An additional limitation on the system is imposed by the command-pulse system used to fire the gas jets. This system limits the turn duration to an integral number of seconds. As a result, the commanded turns differed from the nominal turns. Table III-11 shows the nominal turns and the total achieved minus nominal pointing error, including AC contribution. This result is directly measured to a high degree of accuracy by orbit determination.

If subscripts denote achieved and nominal velocities, and ψ is the total angle of the achieved thrust axis from the nominal thrust axis, then

$$\sin\psi = \frac{|\mathbf{V}_A \times \mathbf{V}_N|}{\mathbf{V}_A\,\mathbf{V}_N\,\hat{\psi}} = 0.007062989$$

$$\psi = 0.405 \text{ deg}$$

This pointing error can contribute only about 300 km in closest approach distance. The remaining 1700-km error is caused entirely by the magnitude of the velocity being in error by 0.714 ± 0.016 m/s.

Table III-10. Commanded-vs-achieved attitude-control performance

Command	Premaneuver telemetry corrections, deg	Corrected (achieved) turns, deg	Commanded turns, deg	Achieved − commanded turns, deg
Pitch	0.333 ± 0.020	55.120 ± 0.065	55.267	-0.147 ± 0.065
Roll	0.028 ± 0.014	70.632 ± 0.015	70.946	-0.314 ± 0.015

Table III-11. Nominal-vs-achieved attitude-control performance

Command	Nominal, deg	Achieved, deg	Duration, s		Total achieved − nominal pointing error, deg
			Commanded	Measured	
Pitch	55.350	55.453 ± 0.062	304.0	304.46	0.103 ± 0.062
Roll	71.025	70.660 ± 0.004	380.0	380.43	-0.365 ± 0.004

4. Cruise orbit-determination results.

a. Tracking data types. The types of tracking data used are described in the paragraphs that follow.

Ranging data. In addition to the angular and doppler data described earlier, two types of ranging measurements were performed during cruise. These were performed with the Mark IA system at the DSS sites shown in Table III-12 and with the Mark II ranging system at DSS 14 (Goldstone Mars). Mark IA range units (RU) are defined as follows:

$$\rho_{\text{DSIF}} = \left[\frac{15(\Delta t + \epsilon)}{221}\, 96 f_q\right] \bmod 785762208$$

where

ρ_{DSIF} = measured round-trip interval in RU

Δt = round-trip light time in seconds

f_q = transmitter reference frequency $\simeq 22$ MHz

ϵ = time delay in seconds from station equipment, spacecraft transponder, and intervening space plasma–ionospheric medium

785762208 RU = code length of system

Table III-12. Mark IA ranging data obtained during *Mariner Venus 67 mission*

DSS	Location	Start date (1967)	Stop date (1967)	No. of points, sampling interval 60 s
62	Cebreros	7/06	7/06	48
11	Goldstone Pioneer	6/20	6/29	2390
42	Tidbinbilla	6/24	7/06	3031
41	Woomera	6/21	6/22	714
12	Goldstone Echo	6/30	7/02	1503
61	Robledo	6/20	6/29	2720

The Mark IA ranging system is limited to an effective one-way range of about 5.8×10^6 km, attained on July 6, 1967, as shown in Table III-12.

The Mark II (planetary) ranging system at DSS 14 (Goldstone-Mars) measures the round-trip delay directly in nanoseconds. The code length of the equipment is 1.00947/1.0002 s, hence

$$\rho_{\text{planetary}} = [10^{-9}(\Delta t + \epsilon)] \bmod \frac{1.00947 \times 10^{-9}}{1.0002}$$

With the use of the Mark II equipment and the 210-ft antenna at the Mars site, Mark II ranging measurements may be made to planetary distances, as the name of the data type implies. During the *Mariner* Venus 67 mission, approximately 7000 points of 60-s sampled planetary ranging data were obtained between July 21 and November 20, 1967.

Tracking data statistics. Table III-13 shows the manner in which ranging data noise increases as a function of range when processed by the single precision orbit determination program (**SPODP**).

Statistics are given for individual passes of tracking data on the days shown, where ρ is the one-way spacecraft range in meters, and standard deviations on planetary RU and RU have been converted to $\sigma\rho$. The last column shows that eight-place accuracy is being retained in the computations, which is all that may be expected of a single precision program with a floating-point word length of 27 bits.

Doppler residuals do not display large numerical truncation and round-off as a function of range, but are limited by single precision and by the stability of the reference frequency standard over the light-time interval. Table III-14 shows a sample of cruise doppler residual statistics reduced by **SPODP**. These data have been averaged over 10-min intervals to reduce the total number of points to a manageable level. These statistics reflect the precision of the least-squares fit over a long arc (3 mo). Also, Table III-14 gives combined ranging statistics through July 28, 1967. The degradation from fitting a long arc is more apparent here than in the individual-pass statistics of Table III-13. As a result, individual passes are biased differently, partly from single precision truncation and partly from the nature of the least-squares fitting process.

b. Cruise solutions for physical constants. The cruise solutions for physical constants are described in the paragraphs that follow.

Solar-radiation pressure. During cruise, continuous least-squares estimates were made of γ_B, the solar-radiation pressure coefficient defined in the first paragraph under the subtitle *Cruise solutions for mass of moon*, below. Figure III-15 shows the time history of these solutions. The solutions are consecutively identified by orbit number. There appears to be a distinct trend towards lower pressure with increasing time. The physical interpretation of this phenomenon could be that an actual degradation of the total reflectance of the spacecraft took place during cruise. For instance, temperature monitoring of the bus indicates that the absorptance of the bus radiation shield may have increased approximately 30% through UV darkening.

This would cause a corresponding decrease in reflectivity of the shield that could account for a decrease in γ_B of up to 0.007. In addition, there is the possibility of a decrease in specularity of the shield that could cause a decrease in γ_B of as much as 0.028. As seen in Fig. III-15, the observed change in γ_B is on the order of 0.06, which is nearly twice as much as the maximum combined effect of the explanations noted above. Because the standard deviations on the orbit solutions for γ_B are typically less than 0.01, it is likely that the effect is real. The use of ranging data, in particular, add great strength to the cruise solutions. However, the possibility remains that the observed effect is at least partially caused by a small force other than solar-radiation pressure. This

Table III-13. Summary of ranging data noise increases

Day		Date 1967	$\sigma_{\text{planetary RU}}$	$\sigma_{\rho,m}$	ρ^m	$\sigma_{\rho,\rho}$
DSS 14 planetary RU residuals (standard deviation)						
172		6/21	103	15	0.18E10	0.83E-8
191		7/10	492	74	0.68E10	1.09E-8
203		7/22	628	94	1.00E10	0.94E-8
204		7/23	654	98	1.03E10	0.95E-8
209		7/28	730	110	1.19E10	0.92E-8
279		10/06	3580	537	6.25E10	0.86E-8
283		10/10	5600	840	6.78E10	1.23E-8
DSS 11 and 12 RU residuals (standard deviation)						
11	172	6/21		20	0.18E10	1.11E-8
	173	6/22		26	0.21E10	1.24E-8
	174	6/23		30	0.24E10	1.25E-8
	175	6/24		36	0.27E10	1.33E-8
	177	6/26		37	0.30E10	1.23E-8
	178	6/27		40	0.33E10	1.21E-8
	179	6/28		41	0.36E10	1.14E-8
	180	6/29		62	0.39E10	1.59E-8
12	182	7/1		43	0.42E10	1.02E-8
	183	7/2		45	0.45E10	1.00E-8
DSS 42 last RU data						
187		7/6		53	0.58E10	0.91E-8
DSS 62 last RU data						
187		7/6		61	0.58E10	1.05E-8

Table III-14. Sample of cruise doppler residual statistics

Coherent-counted two-way doppler residuals by station (cruise data, $T_c = 600$ s)[a]							
DSS	No. of points	rms, Hz	First moment, Hz	σ, Hz	rms, mm/s	μ, mm/s	σ, mm/s
11	422	0.00348	−0.000395	0.00346	0.227	−0.0258	0.226
12	255	0.00400	−0.000356	0.00398	0.261	−0.0233	0.260
14	165	0.00433	−0.000976	0.00421	0.283	−0.0638	0.275
41	311	0.00368	−0.000452	0.00365	0.241	−0.0295	0.239
42	770	0.00312	−0.000762	0.00302	0.204	−0.0498	0.197
61	831	0.00411	−0.000682	0.00405	0.269	−0.0446	0.265
62	172	0.00473	−0.000158	0.00473	0.309	−0.0103	0.309
Totals	2926	0.00378	−0.000595	0.00373	0.247	−0.0389	0.244
Planetary RU residuals[b]							
DSS	No. of points	rms, ns	μ, ns	σ, ns	rms, m	μ, m	σ, m
14	847	868.9	−433.4	753.1	130	−65	113
RU residuals							
DSS	No. of points	rms, cycles	μ, cycles	σ, cycles	rms, m	μ, m	σ, m
11	240	45.4	0.251	45.4	47	0.3	47
12	65	52.6	−30.1	43.1	55	−31.0	45
41	74	59.4	54.1	24.4	62	57.0	26
42	298	55.3	−17.5	52.4	58	−18.0	55
61	285	49.9	0.255	49.9	52	0.3	52
62	6	59.5	−10.5	58.6	62	−11.0	61
Total RU	968	51.6	−3.2	51.5	54	−3.0	54

[a]Data span is June 19–Sept. 16, 1967.
[b]Through July 29, 1967.

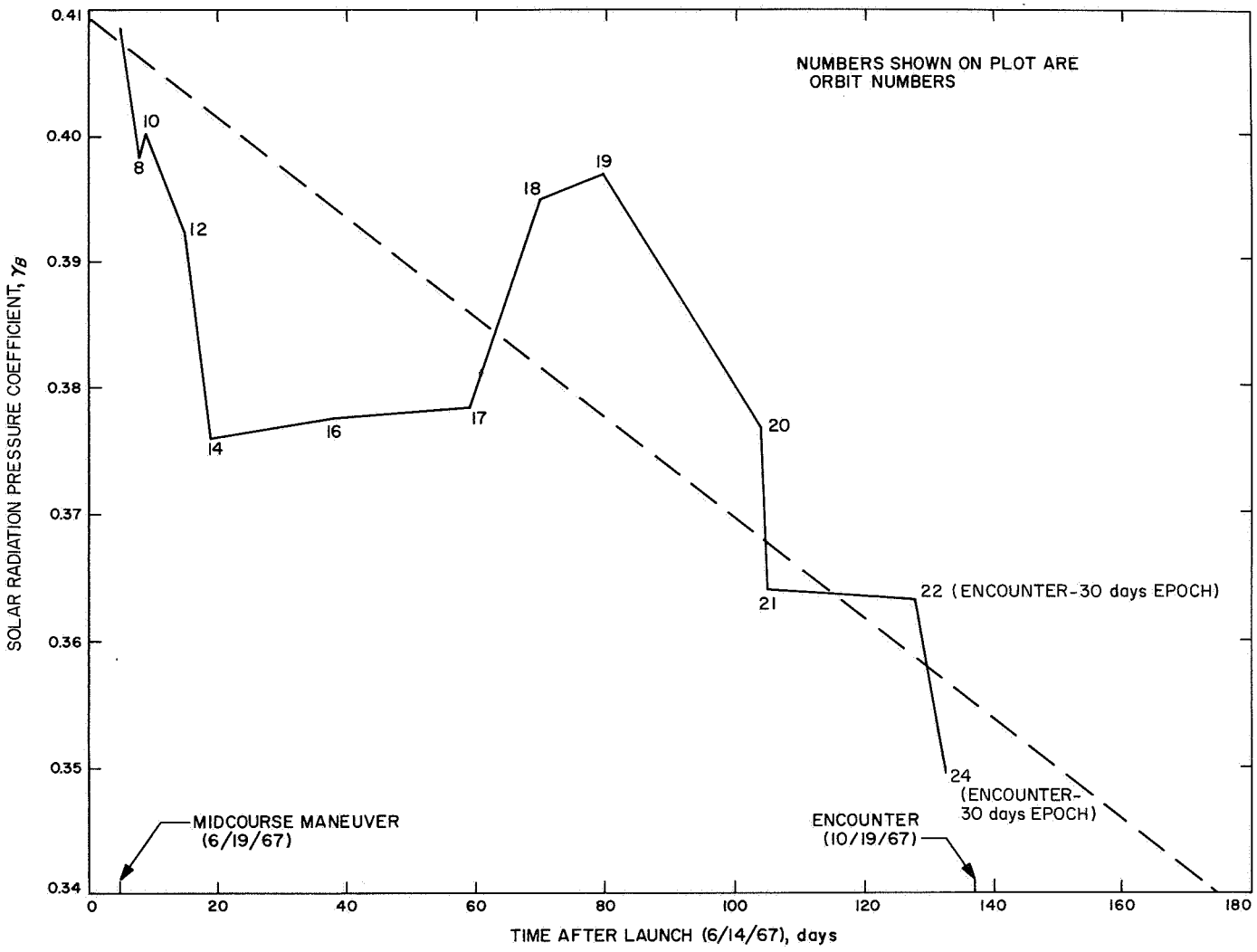


Fig. III-15. *Mariner V* cruise solution for solar-pressure coefficient

could result from a systematic decoupling of the AC gas-jet torques, which could, in turn, result from such problems as temperature differential between the sunlit jets and the shaded jets. A discussion of the AC telemetry measurements is contained in Subsection VI-F of this report.

Station locations. Least-squares estimates of station locations based on postmidcourse maneuver tracking data are shown in Figs. III-16 and III-17. The *a priori* standard deviation for spin axis distance r_s and longitude λ are $\widetilde{\sigma r_s} = 24$ m, $\widetilde{\sigma\lambda} = 50$ m. These were reduced to the mean pole of 1900–1905. Figure III-16 shows the solutions for perpendicular distance off the spin axis of the earth, and the associated standard deviations (plotted as vertical bars). In general, the solutions are consistent to ± 5 m.

Figure III-17 plots the *Mariner V* spacecraft cruise longitude solutions reduced to the pole of 1900–1905. The salient feature of these solutions is the 25- to 30-m difference between early and late cruise solutions. The high values obtained shortly after the midcourse maneuver tend to be in good agreement with the longitude obtained before the maneuver, whereas the late cruise solutions tend to be close to those obtained during encounter. Runs up to post 14 did not represent WWV–UT timing differences, whereas later runs used a polynomial representation of these differences. The timing error caused by making WWV–UT = 0 was about -10 ms on June 19, or 4 m in longitude. The remaining differences are probably because of earth–sun ephemeris errors.

Cruise solutions for mass of moon. Figure III-18 shows the lunar gravitational constant solutions based upon the combined *Ranger* missions (Ref. 24), *Mariner II* (Ref. 25) and *IV* (Ref. 26), and *Mariner V* in real time. The low *Ranger* result, $GM_☾ = 4902.6493$ km^3/s^2, was obtained by measuring the effect of the lunar gravity field on spacecraft acceleration. The *Mariner* results, by contrast, measured the barycentric motion of the tracking station over the long cruise interval and determined the earth/moon mass ratio, assuming a known value for the earth–moon distance from optical and radar observations. The *Mariner II* result of $GM_☾ = 4902.8442$ km^3/s^2 is based upon the *Ranger* earth-gravitational constant, $GM_⊕ = 398601.27$ km^3/s^2, yielding a mass ratio $\mu^{-1} = 81.3000 \pm 0.0011$. The *Mariner IV* value also uses the *Ranger* $GM_⊕$ to obtain $\mu^{-1} = 81.30147 \pm 0.0016$ from $GM_☾ = 4902.756 \pm 0.1$ km^3/s^2. The real-time *Mariner V* solutions shown in Fig. III-18 display a sharp break between data spans respectively incorporating 2 and 3 mo of data. Although this phenomenon has not been explained, it is probably related to ephemeris errors of the earth–moon barycenter. Over the cruise interval, three relatively uncorrelated parameters, solar-radiation pressure, tracking station longitudes, and the moon/earth mass ratio show a marked decrease. If a representative value were to be given for the real-time cruise solutions for $GM_☾$, it would have to be between the two extremes of 4902.86 and 4902.68 km^3/s^2. A realistic evaluation of the real-time results yields $GM_☾ = 4902.77 \pm 0.1$ km^3/s^2. Because all *Mariner V* solutions assume a value $GM_☾ = 398601.33$ km^3/s^2, the corresponding real-time estimate of μ^{-1} is 81.30125 ± 0.00166.

The gravitational-constant values given in Fig. III-19 reflect the result of an effort to estimate physical constants, including $GM_☾$, by careful post-processing of the cruise data for the *Mariner* celestial mechanics experiment. These results seem to indicate a value of $GM_☾ = 4902.81 \pm 0.5$ km^3/s^2, yielding $\mu^{-1} = 81.30059 \pm 0.00083$. This value is remarkably close to the *Mariner II* mass ratio, and is in good agreement with the *Mariner IV* value.

c. Target parameters from cruise solutions. Target parameters in terms of time from closest approach and **B**-plane target point are discussed below.

Time of closest approach. Figure III-20 shows the cruise orbit estimates of time of closest approach to Venus. As in Fig. III-15, these are labeled by orbit number in order of increasing time. The solutions cluster around 17:35 UT on October 19, 1967. The actual encounter time was 17:34:55 UT, which demonstrates that the cruise solutions were free from detectable systematic errors in the flight-time parameter.

B-*plane target point.* A standard measurement of trajectory aiming point is the position of the incoming asymptote in the **B**-plane; i.e., in the plane normal to the asymptote and passing through the center of the target planet. Figure III-21 shows the predicted aiming points from cruise orbit determination in planet-centered **B**-plane components $\mathbf{B}\cdot\mathbf{R}$ and $\mathbf{B}\cdot\mathbf{T}$, where **T** is in the ecliptic plane and **R** is normal to **T**. The solutions appear to cluster randomly about $\mathbf{B}\cdot\mathbf{R} = -14{,}830$ km and $\mathbf{B}\cdot\mathbf{T} = 24{,}270$ km. They are noticeably offset on the plot from the current postencounter solution of $\mathbf{B}\cdot\mathbf{R} = 14{,}761.9 \pm 1$ km, $\mathbf{B}\cdot\mathbf{T} = 24{,}334.3 \pm 1$ km. Probably, the offset of about 100 km is mainly attributable to earth–Venus ephemeris errors, station-location, and timing errors.

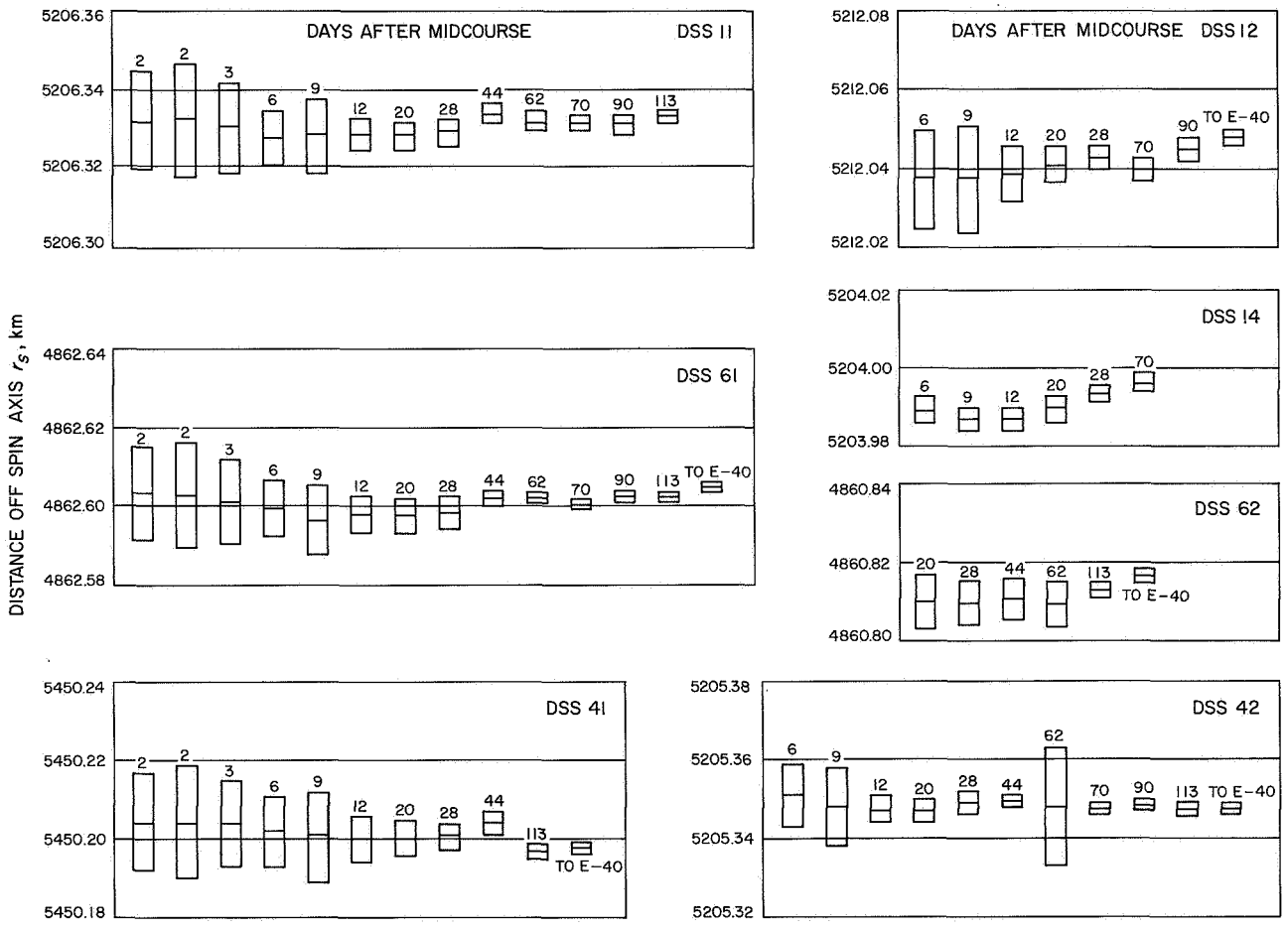


Fig. III-16. Cruise-data estimate of station location, distance off spin axis

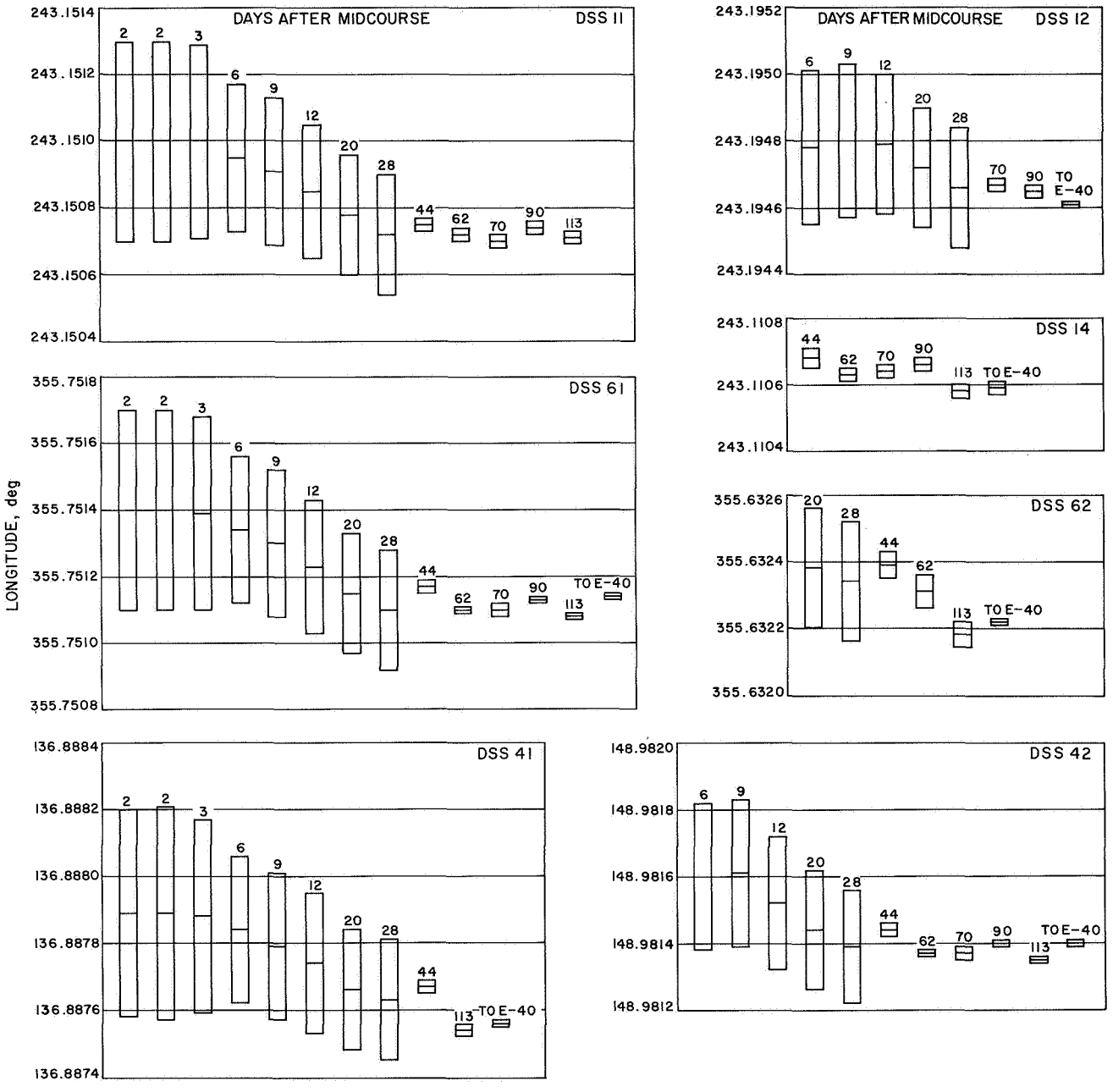


Fig. III-17. Cruise-data estimate of station location, geocentric longitude

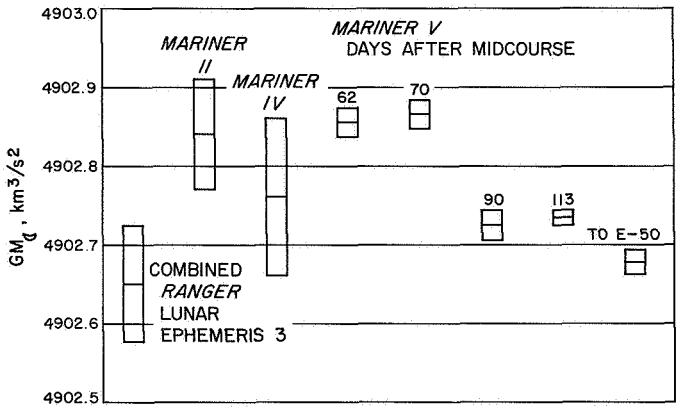


Fig. III-18. Lunar gravitational constant $GM_{\mathbb{C}}$ estimate from combined *Ranger* and *Mariner II, IV,* and *V* data

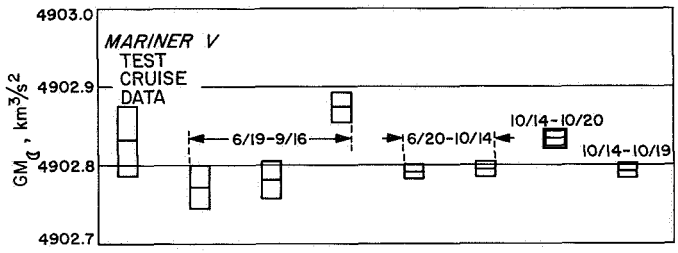


Fig. III-19. Lunar gravitational constant $GM_{\mathbb{C}}$ estimate from *Mariner V* postcruise analysis

5. Real-time encounter orbit-determination results.

a. Tracking data acquisition. During the period E−12 to E+3h, eleven orbits were run on two 7044–7094 computer strings as tracking data were acquired in real time by the DSN. Figure III-22 shows the tracking data distribution from E−5 to E+5 days. The real-time encounter orbits used data from E−5 days to E+1h, the postencounter analyses made use of the full 10 days.

b. Orbit-estimation procedure. Orbits run on the prime computer string were labeled with a *10* prefix, whereas those run as backup support were given a *20* prefix. The prime runs estimated spacecraft trajectory, the astronomical unit (AU), and station locations. The backup runs estimated various combinations of parameters, including Venus ephemeris elements.

c. Real-time encounter aiming point estimates. The primary excursions noted in the real-time encounter orbits were in the direction normal to the **B** vector. Thus, the solutions line up very nearly along a line normal to **B** in the **R** • **T** planes shown in Fig. III-23. The total variation amounts to either 900 km or 1.8 deg, measured from planet center. This is in good agreement with uncertainties predicted by prelaunch studies. The major error source seems to be numerical instability in the station-location and Venus-ephemeris solutions. Some of the numerical difficulties are discussed in more detail in Subsection B-5-e. The current best estimate based upon 10 days of encounter tracking data is shown in Fig. III-23. The systematic offset of the solutions from the current value is approximately 100 km, which is much smaller than the total scatter. The systematic offset is in the opposite direction from the cruise solutions. The current values of $\mathbf{B} \cdot \mathbf{R} = -14{,}761.9$ km, $\mathbf{B} \cdot \mathbf{T} = 24{,}334.3$ km are known to ±1 km.

d. Solution for astronomical unit. The radar value of 149,597,900 ±100 km was adopted as an *a priori* starting value in the encounter runs. The solutions showed no tendency to significantly deviate from this value within the limitations of single precision, indicating three possibilities:

(1) The radar value is correct within ±100 km.

(2) Ephemeris errors in the range direction are within ±100 km.

(3) The strength of the single-precision solution is not great enough to detect errors of the order of 100 km.

The latter possibility may be ruled out, as the ranging data are sufficiently powerful to establish the earth–Venus distance to better than ±10 km even in single precision, although the program cannot separate Venus ephemeris error in the range direction from error in the AU. The current best *Mariner V* AU solution yields 149,597,904 ±44 km.

e. Ephemeris error. Pre-encounter estimates of ephemeris errors were hampered by low numerical stability and unfavorable partial derivatives. As a result, these solutions were not accurate to the requisite of 100 km as needed to define ephemeris errors. The planetary ephemeris used successfully for the mission was the very accurate JPL development ephemeris No. 24 using radar corrections to the older optical ephemeris. The current *Mariner V* solution for corrections to the development ephemeris No. 24 position of Venus at 17:35:33.138 UT on

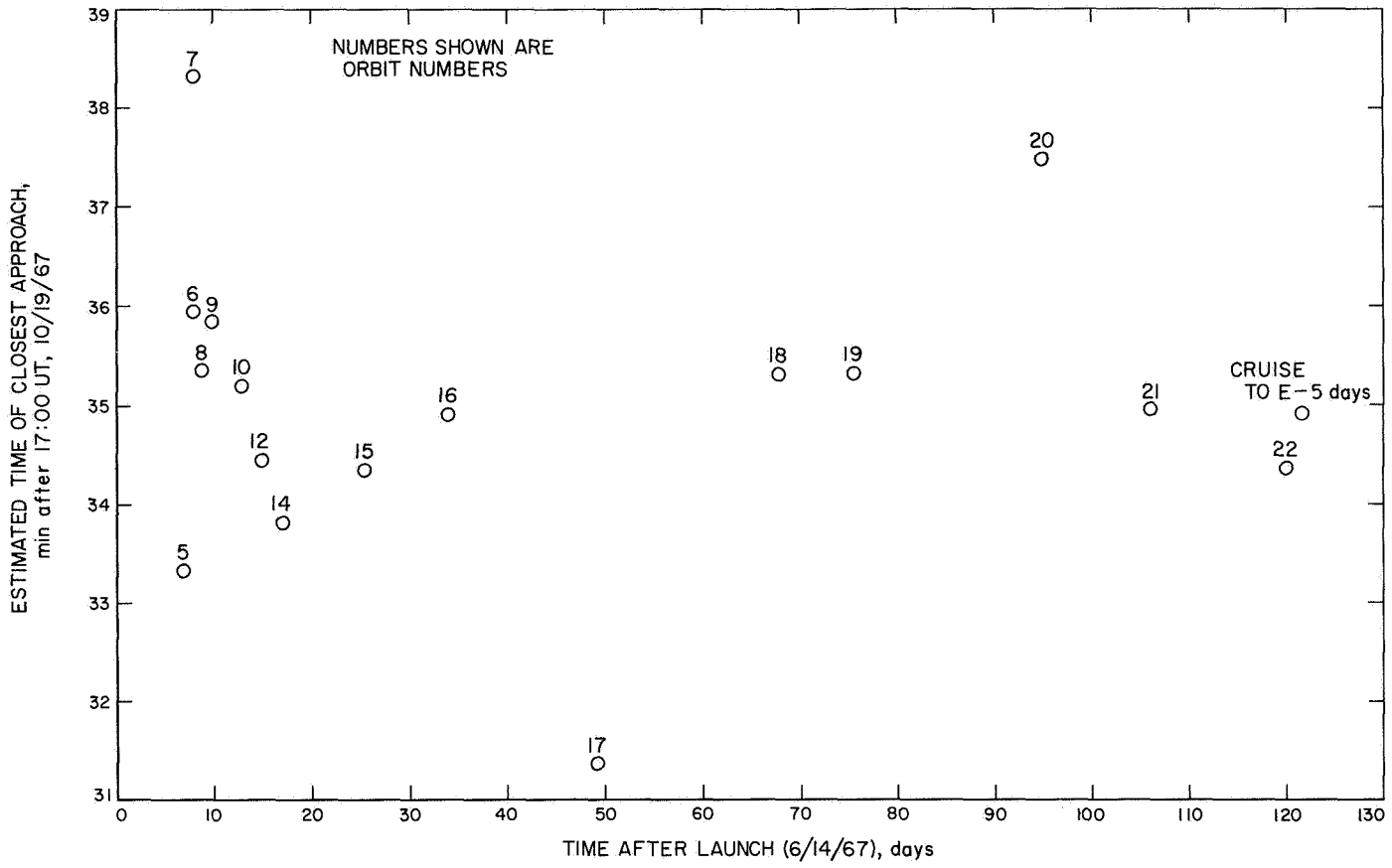


Fig. III-20. Cruise orbit estimates of time of closest approach to Venus

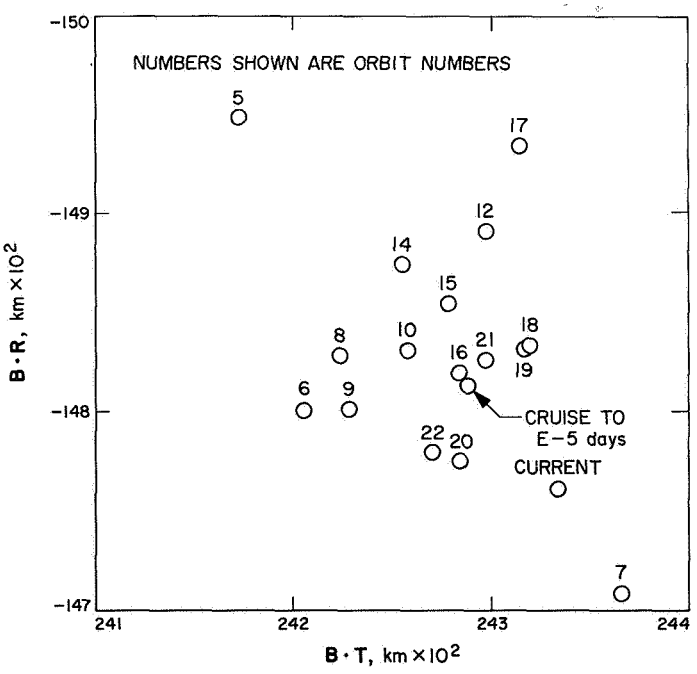


Fig. III-21. Elliptic B-plane aiming point from cruise orbit determination

October 19 is in earth-equatorial coordinates, $x = -0.76 \pm 23$ km, $y = -29.23 \pm 12$ km, $z = 11.95 \pm 34$ km. The ability to measure relatively small corrections to the AU and planetary ephemeris was primarily a result of the planetary ranging system used with the *Mariner V* spacecraft.

f. Encounter station-location solutions. Figures III-24 and III-25 show the *Mariner V* encounter solutions for station locations reduced to the pole of 1903.0. Solutions for distance off the spin axis of the earth r_s are plotted by station number with associated standard deviations in Fig. III-24, whereas station longitudes λ are plotted with their standard deviations in Fig. III-25. Assumed *a priori* standard deviations were the same as for cruise, $\tilde{\sigma}r_s = 24$ m, $\tilde{\sigma}\lambda = 50$ m. The r_s solutions exhibit very few systematic trends except for orbit 1026. the AU and ranging data were not included in the least- This orbit, run with an earlier data span, did not estimate squares fit. Comparison of the other solutions with the data shown in Fig. III-16 shows that the cruise, and encounter spin-axis distance solutions are in good agreement.

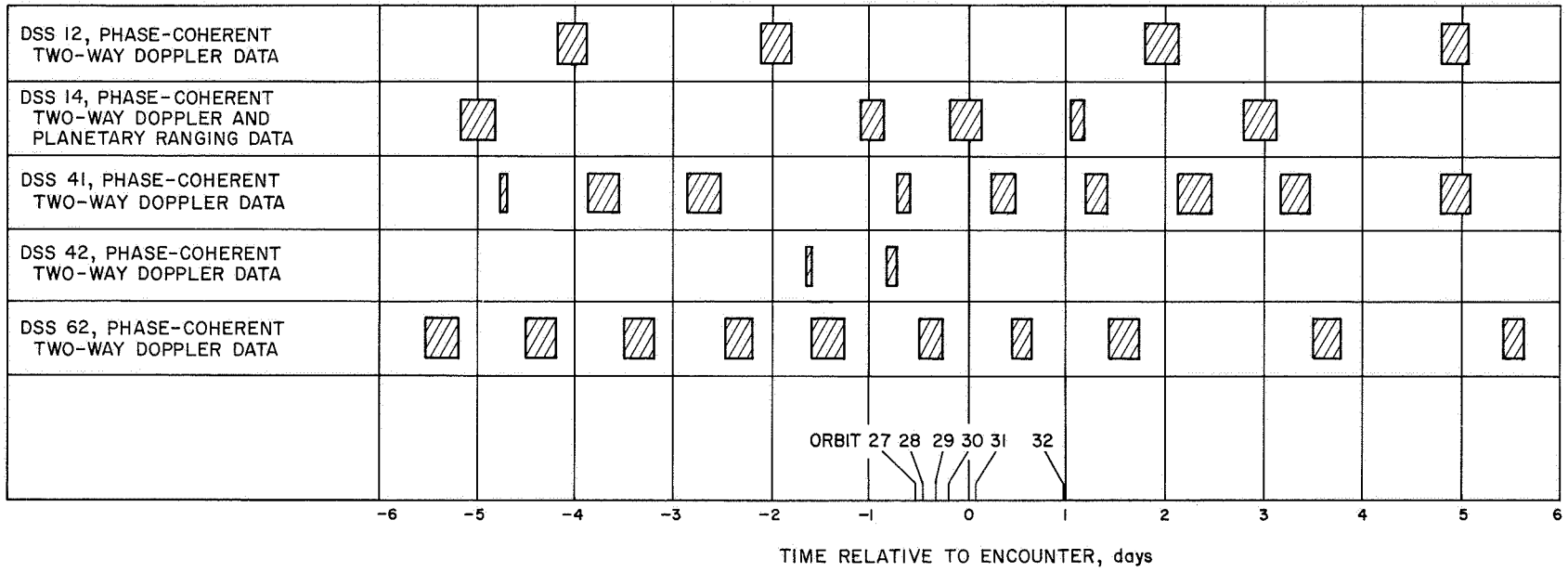


Fig. III-22. Tracking data distribution from E − 5 to E + 5 days

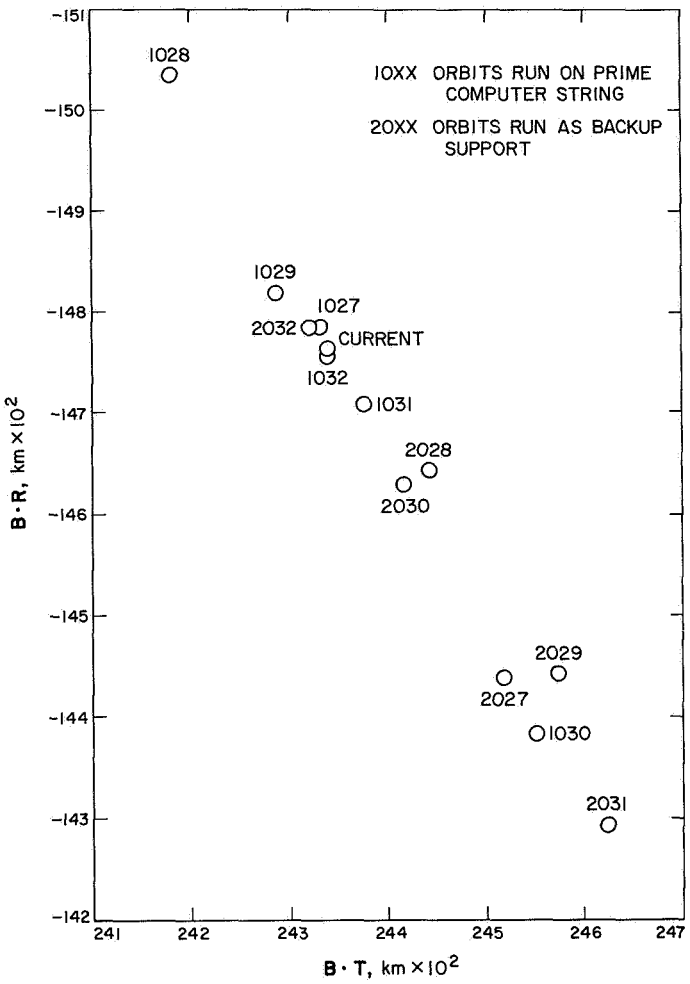


Fig. III-23. Real-time *Mariner* Venus 67 encounter B-plane estimates

Although considerably noisier than the spin-axis estimates, the encounter solutions for station longitude shown in Fig. III-25 are in good agreement with the cruise longitude solutions of Fig. III-17. The high random noise is caused by numerical instability in the **SPODP**. The trend towards increasing longitude with increasing data, in contrast to the opposite trend in the cruise solutions, should be noted. The longitudes deduced from tracking data from E−5 to E+5 days are, in general, even higher than the early cruise longitudes. The longitude determinations in deep space, under the gravitational influence of the sun, are systematically lower by about 25 m than those in the gravitational presence of the earth and Venus. This difference indicates the existence of significant earth–sun ephemeris errors of 300 km.

The total spread in mean station locations during encounter operations on the prime computer string amounts to $\Delta\dot{r}_s = 4$ m, $\Delta\lambda = 12$ m. These are important quantities, as theory predicts the uncertainty in station location to be a predominant error source.

Deep Space Station 51 was used for only a brief period after encounter. Insufficient data were accumulated to allow a good solution for station-location parameters. As a result, the need was indicated to use the stations that had been calibrated during the cruise phase to cover critical periods, such as the encounter phase.

g. Mass of Venus. The mass of Venus is the astrodynamical quantity most precisely determined by *Mariner V* encounter tracking data because the Venus-centered hyperbolic encounter trajectory is curved nearly 90 deg by the gravitational influence of the planet; also, the trajectory bending is very accurately measured by doppler tracking data. The *Mariner II* spacecraft, using L-band doppler data, yielded a sun–Venus mass ratio of 408,505 ±6 (see Ref. 25). This value was used as *a priori* information in the *Mariner V* encounter solutions, but the *a priori* standard deviation was enlarged to 150 to avoid possible biasing of the solution towards the *Mariner II* result. The current *Mariner V* estimate of the sun–Venus mass ratio is 408,522.66 ±3. This is based upon doppler and ranging tracking data from E−5 to E+5 days, assuming $GM_\odot = 13{,}271{,}251 \times 10^4$ km³/s² and an AU of 145,957,904 km, so that $GM_\varphi = 324{,}859.6$ ±3 km³/s².

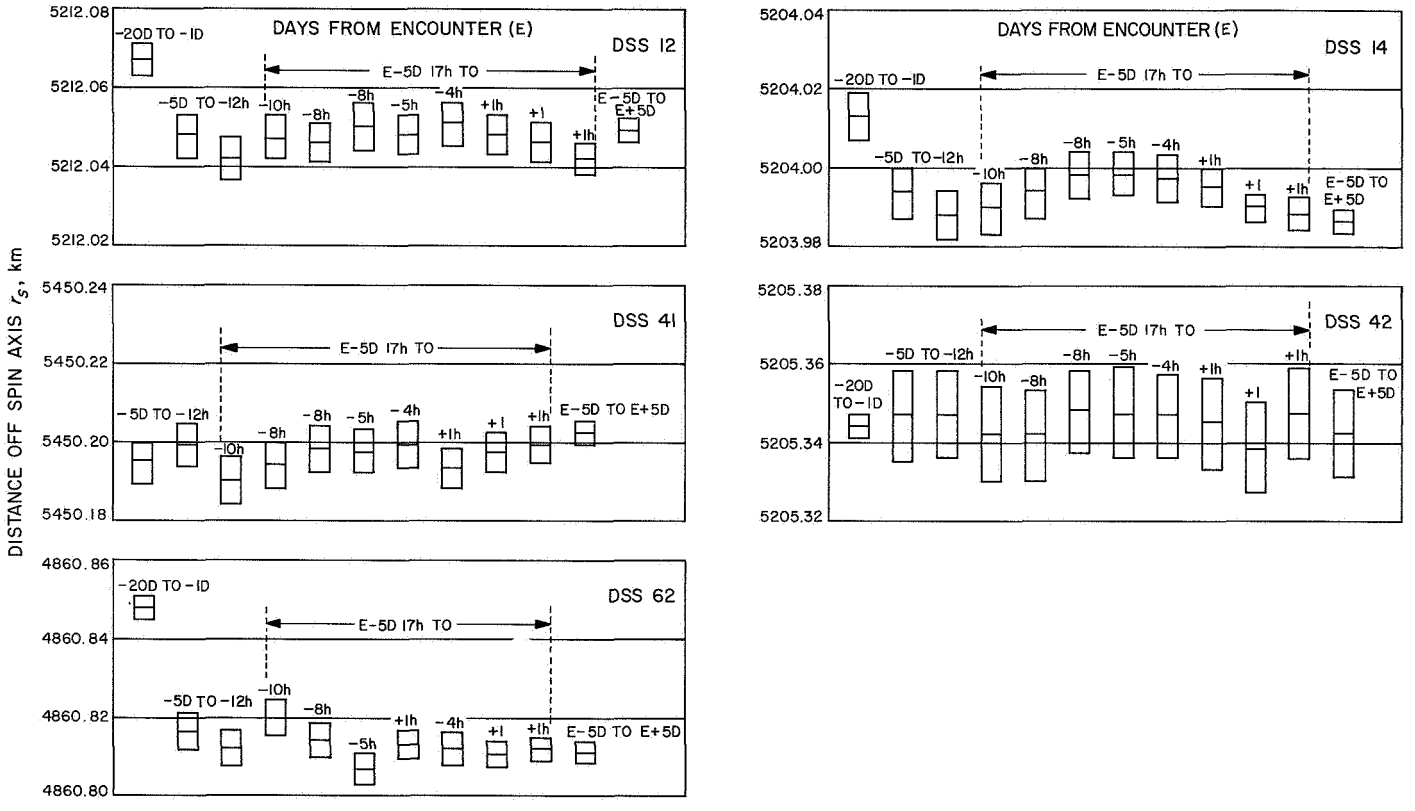


Fig. III-24. Encounter solutions for station location, distance off spin axis

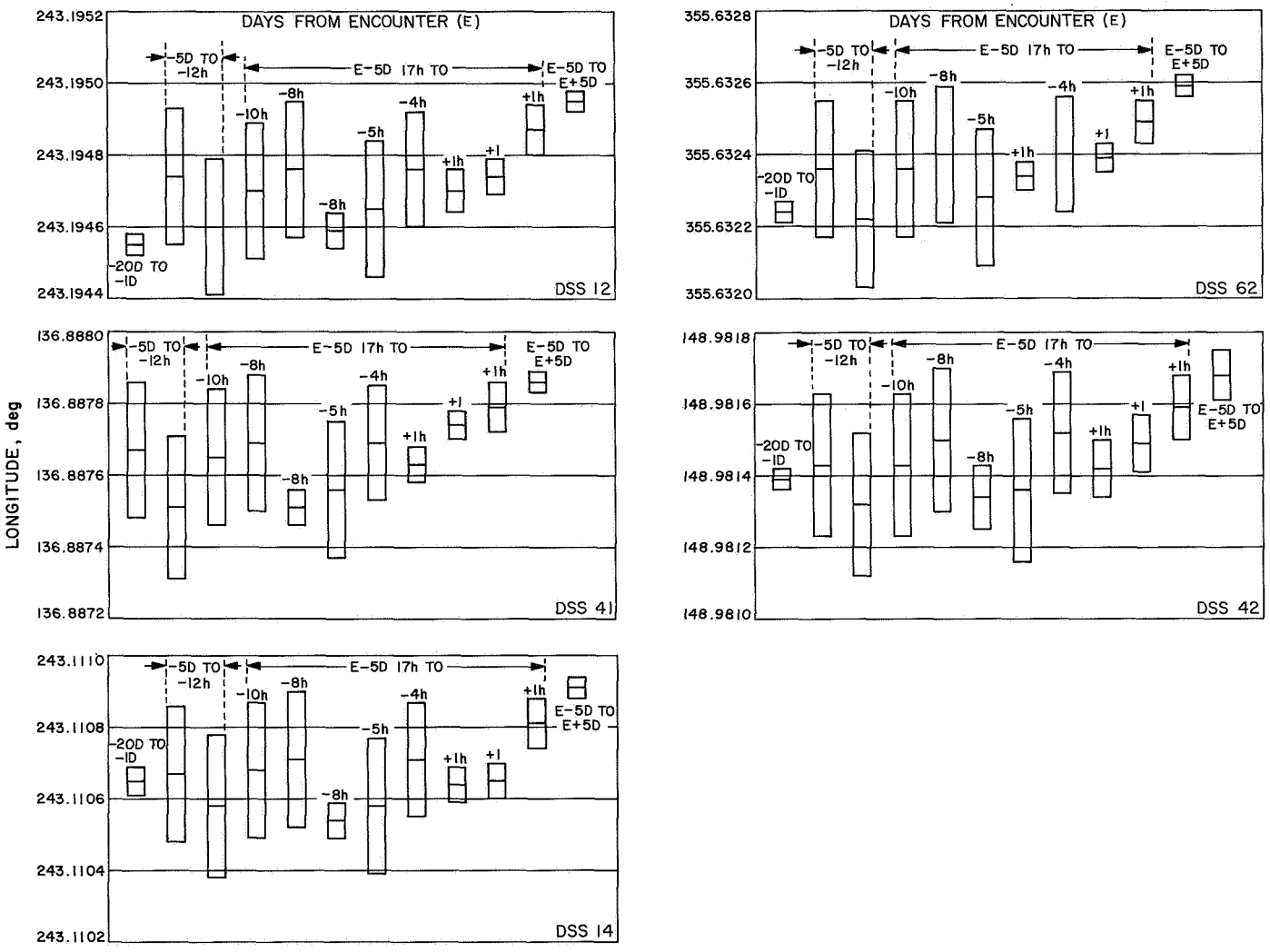


Fig. III-25. Encounter solution for station location, geocentric longitude

IV. Space Flight Operations

A. Mission-Independent Support

For the *Mariner* Venus 67 mission, mission-independent support of Space Flight Operations (SFO) was provided by various support facilities, through schedule and control of interfaces, Deep Space Network (DSN) coverage, interaction with other missions, and Mark I and Mark II ranging ground equipment configuration and utilization. These are described in the paragraphs that follow.

1. Facilities and support.

a. Deep Space Instrumentation Facility. The Deep Space Instrumentation Facility (DSIF) telemetry configuration (Fig. IV-1) for the *Mariner* Venus 67 mission consisted of an 85-ft parabolic antenna providing receiving gain of approximately 53 dB (Table IV-1). The 210-ft parabolic antenna at the Goldstone Mars Deep Space Station (DSS 14) provided a gain of approximately 61 dB (Table IV-1). Two receivers at each station provided backup capability during the *Mariner* Venus 67 mission.

A predemodulation/postdemodulation analog recording was provided by DSS 14. A digital recording of the telemetry and command processor (TCP) output was also provided as a DSS function.

The TCP digital output tape was used as the prime data source for constructing the master data library (MDL). When the TCP digital tape did not meet MDL requirements, the analog tape was requested and used as the data source. The analog tape was used exclusively when the telemetry threshold was exceeded.

During the encounter phase, which occurred during the Goldstone pass, four Goldstone stations (DSS 11, DSS 12, DSS 13, and DSS 14) provided prime and backup coverage (Fig. IV-2).

b. Communications. The teletype, voice, and high-speed data lines (HSDLs) required for data acquisition at the Space Flight Operations Facility (SFOF), in Pasadena, and for voice communications with all of the DSSs are shown in Fig. IV-3. This configuration covers both the cruise and encounter periods of the mission. Figure IV-4 shows a more detailed routing of the TTY circuits

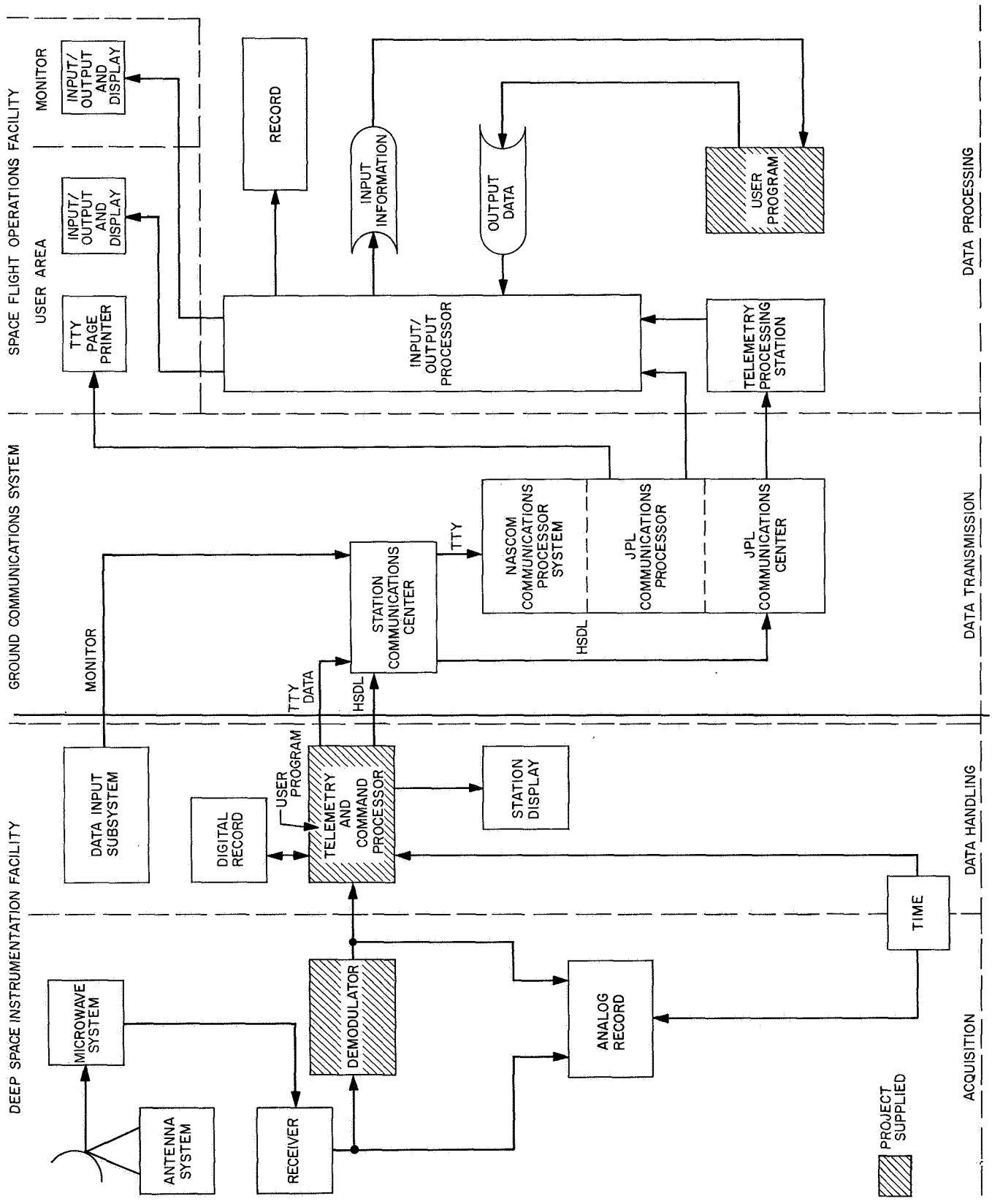


Fig. IV-1. Telemetry system configuration for the *Mariner* Venus 67 mission

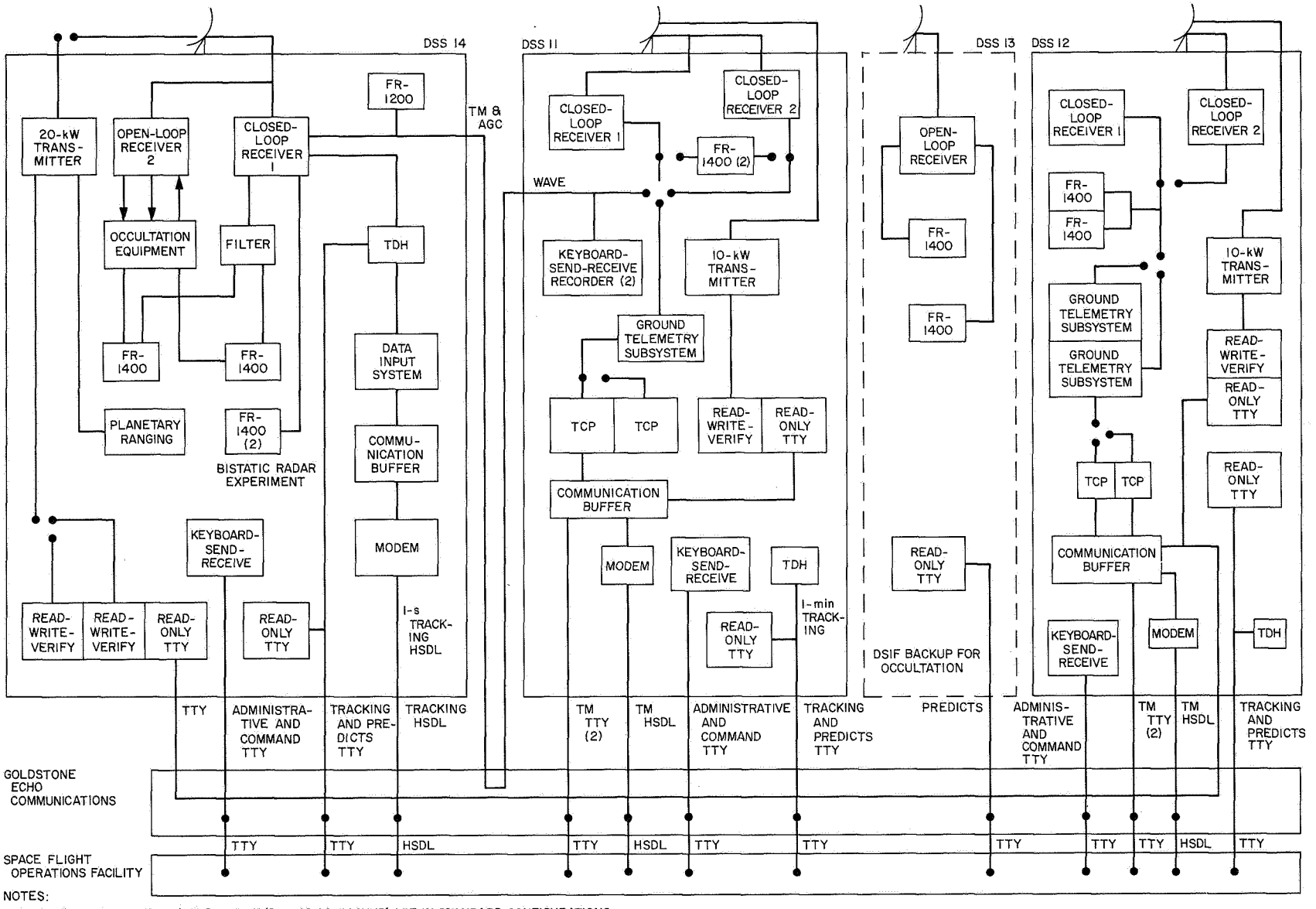
Table IV-1. Deep Space Instrumentation Facility capabilities for the *Mariner* Venus 67 project

Capability	Station name[a]						
	Pioneer Deep Space Station (GSDS[b] S-band)	Echo Deep Space Station (GSDS S-band)	Mars Deep Space Station	Woomera Deep Space Station (GSDS S-band)	Tidbinbilla Deep Space Station (GSDS S-band)	Johannesburg Deep Space Station (GSDS S-band)	Robledo Deep Space Station (GSDS S-band)
Station identification	DSS 11	DSS 12	DSS 14	DSS 41	DSS 42	DSS 51	DSS 61
Receiver capability	Two	Two	Two	Two	Two	One	Two
Antenna	85-ft parabolic	85-ft parabolic	210-ft	85-ft parabolic	85-ft parabolic	85-ft parabolic	85-ft parabolic
Mount	Polar (HA-dec)	Polar (HA-dec)	Az-el	Polar (HA-dec)	Polar (HA-dec)	Polar (HA-dec)	Polar (HA-dec)
Maximum angular rate (both axes), deg/s	0.7	0.7	0.5	0.7	0.7	0.7	0.7
Antenna gain, dB							
Receiving	$53.0\ ^{+1}_{-0.5}$	$53.0\ ^{+1}_{-0.5}$	−61.0	$53.0\ ^{+1}_{-0.5}$	$53.0\ ^{+1}_{-0.5}$	$53.0\ ^{+1}_{-0.5}$	$53.0\ ^{+1}_{-0.5}$
Transmitting	51.0 ±1	51.0 ±1	−59.0	51.0 ±1	51.0 ±1	51.0 ±1	51.0 ±1
Antenna beamwidth, deg	−0.4	−0.4	0.1	−0.4	−0.4	−0.4	−0.4
Typical system temperature, °K	55 ±10	55 ±10	—	55 ±10	55 ±10	55 ±10	55 ±10
Transmitter power, kW	10	10	20	10	10	10	10
Data transmission (TTY)							
Angles	Real time	Real time	Real time	Real time	Real time	Real time	Real time
Doppler	Real time	Real time	Real time	Real time	Real time	Real time	Real time
Ranging (to 800,000 km)[c]	Real time	Real time	Real time	Real time	Real time	NA	Real time
Telemetry	Real and near-real time	Real and near-real time	Real and near-real time	Real and near-real time	Real and near-real time	Real and near-real time	Real and near-real time
Demodulated telemetry	Dual channel	Dual channel	Dual channel	Dual channel	Dual channel	One	Dual channel
Command capability	Yes	Yes	Yes	Yes	Yes	Yes	Yes
Data pack air shipment time to JPL	1 day	1 day	1 day	2 wk	2 wk	2 wk	10 days

[a]The following stations have acquisition aid: DSS 11, DSS 41, DSS 42, and DSS 51. The Cebreros Deep Space Station, DSS 62 (GSDS S-band), had no data available except data pack air shipment time to JPL (10 days).

[b]GSDS = Goldstone duplicate standard.

[c]Mars site ranged beyond the 800,000-km range (encounter).



NOTES:
DSS 62 (DSS 51 AS BACKUP) AND DSS 41 (DSS 42 AS BACKUP) ARE IN STANDARD CONFIGURATIONS.
TM = TELEMETRY

Fig. IV-2. Deep Space Instrumentation Facility/ground communication system configuration for *Mariner V* encounter

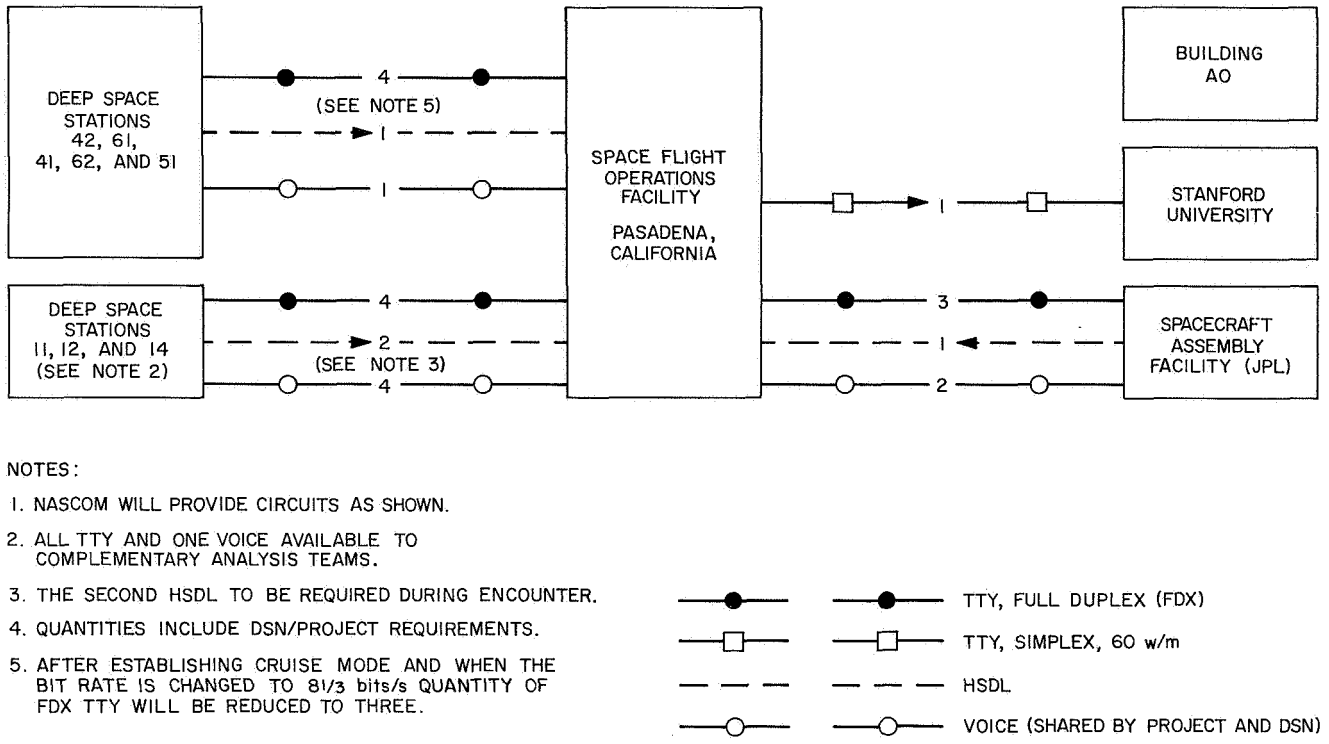


Fig. IV-3. Ground communications, deep-space phase

for the handling of *Mariner V* telemetry data. Special microwave coverage, communication engineering support, and communication prediction information were made available for encounter.

With the exception of test activity and command operations, the Venus operations controllers coordinated the operations effort for the project during the cruise phase on a 24-h/day basis during periods when the spacecraft was being tracked continually. All voice communications from supporting agencies were channeled through the Venus operations controller position. This included telephone communications between Stanford and the SFOF.

Use of the networks and their configurations (excluding the DSIF, communication control, and SFOF networks) during encounter and other high-activity phases are described in the paragraphs that follow. (Dotted lines in the figures indicate listen-only capability.)

The mission control network (MI-CON) was used by the project manager, the Space Flight Operations Director (SFOD), and the area directors for discussing mission direction. Positions assigned to this network are shown in Fig. IV-5.

The operations control network (VAL-PRIME) was controlled by an assistant SFOD (ACE-5 position). The ACE-5 position conducted the sequence of events, requested reports, and obtained reports from all area directors on this network. Positions assigned to this network are shown in Fig. IV-6.

The facilities operations control network (FAC-PRIME) was controlled by an assistant SFOD (PRIME-5 position) and used in conjunction with the VAL-PRIME network for conducting the sequence of events. The PRIME-5 position requested and obtained reports from the DSN on matters relating to the sequence of events. Positions assigned to this network are shown in Fig. IV-7. This network was also used by the Venus operations controllers for cruise-phase coordination.

The flight-path analysis and command (FPAC) analysis control network (FPAC 3) was controlled by the FPAC director. The stations assigned to the FPAC 3 network are shown in Fig. IV-8. All internal FPAC coordination was conducted over this network.

The spacecraft performance analysis and command (SPAC) analysis control network (BUSS) was controlled by the SPAC director. The stations assigned to this network are shown in Fig. IV-9. This was an analysis network used for conference discussions, moderated by the SPAC director or his authorized representative, and for periodic status reporting on spacecraft subsystems to the SPAC director.

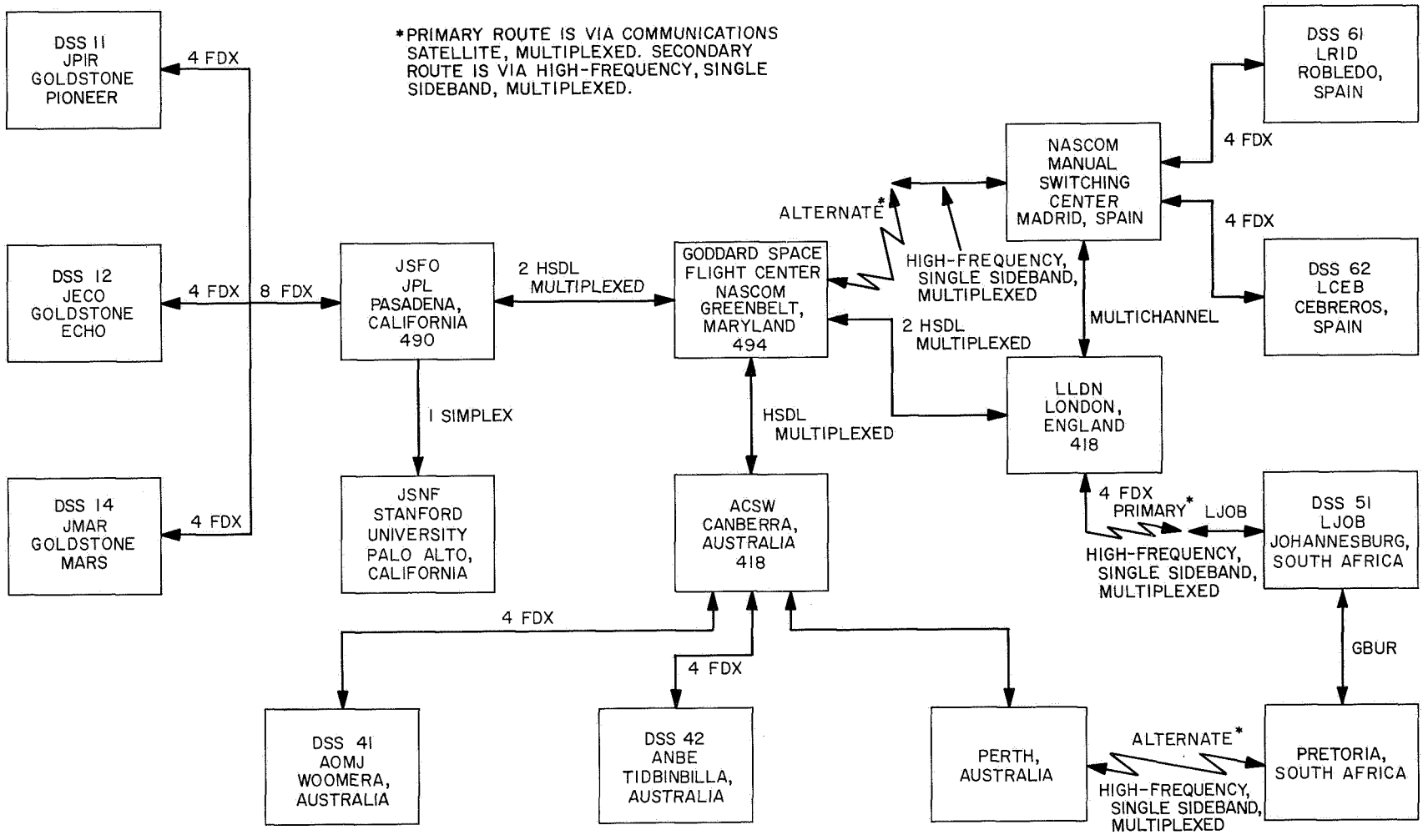


Fig. IV-4. Deep Space Network/ground communication system teletype circuits

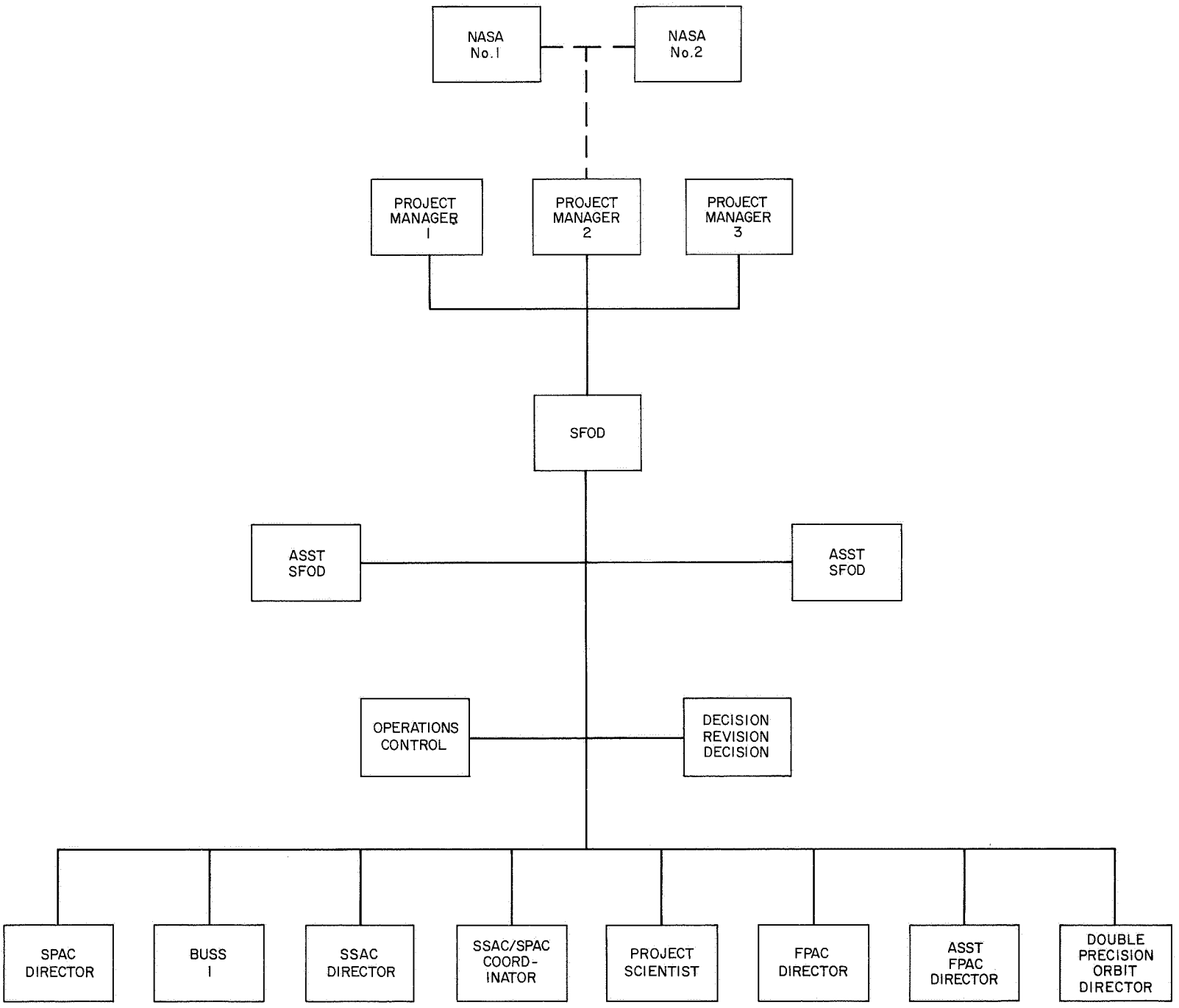


Fig. IV-5. Mission control network (MI-CON)

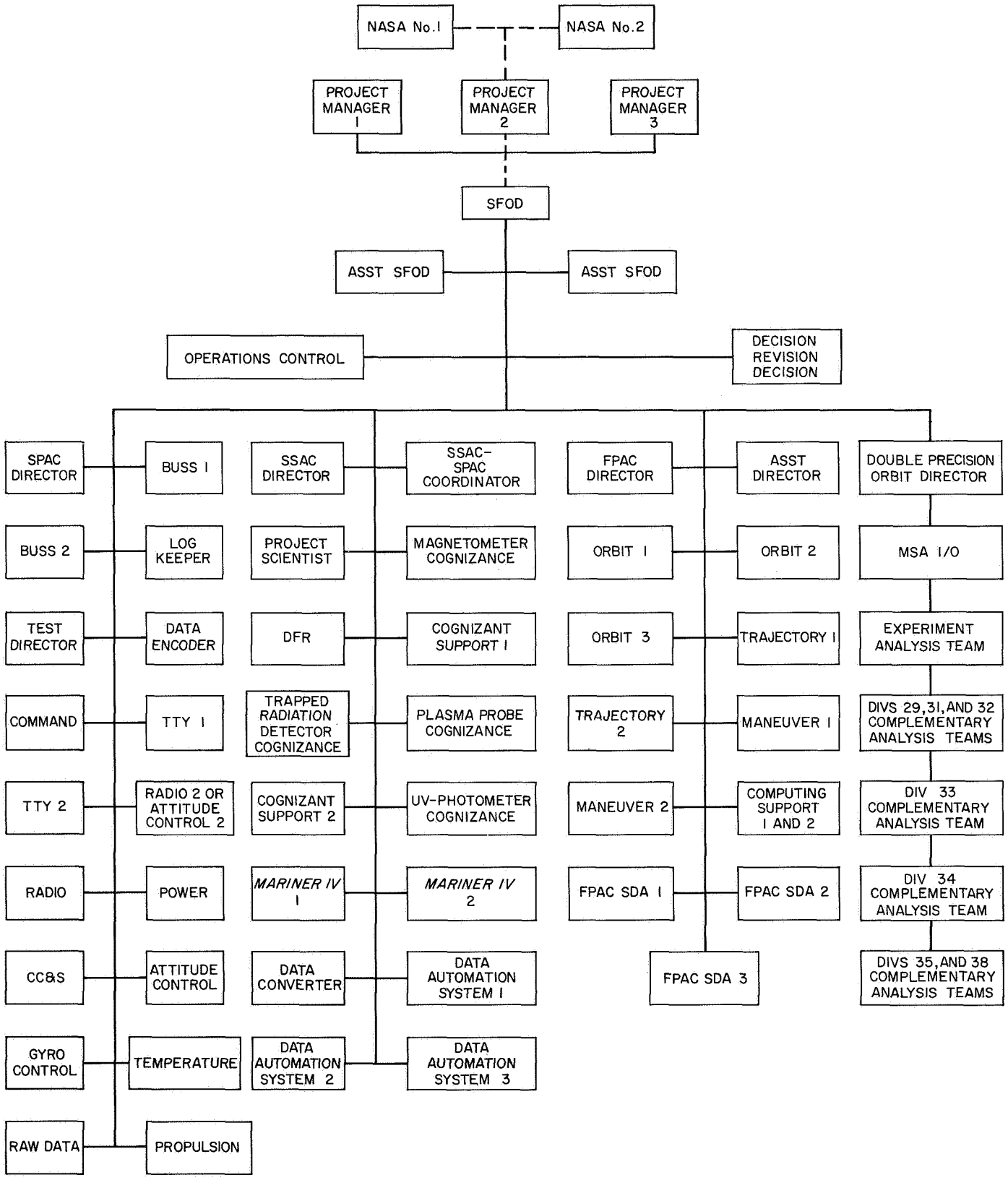


Fig. IV-6. Operations control network (VAL-PRIME)

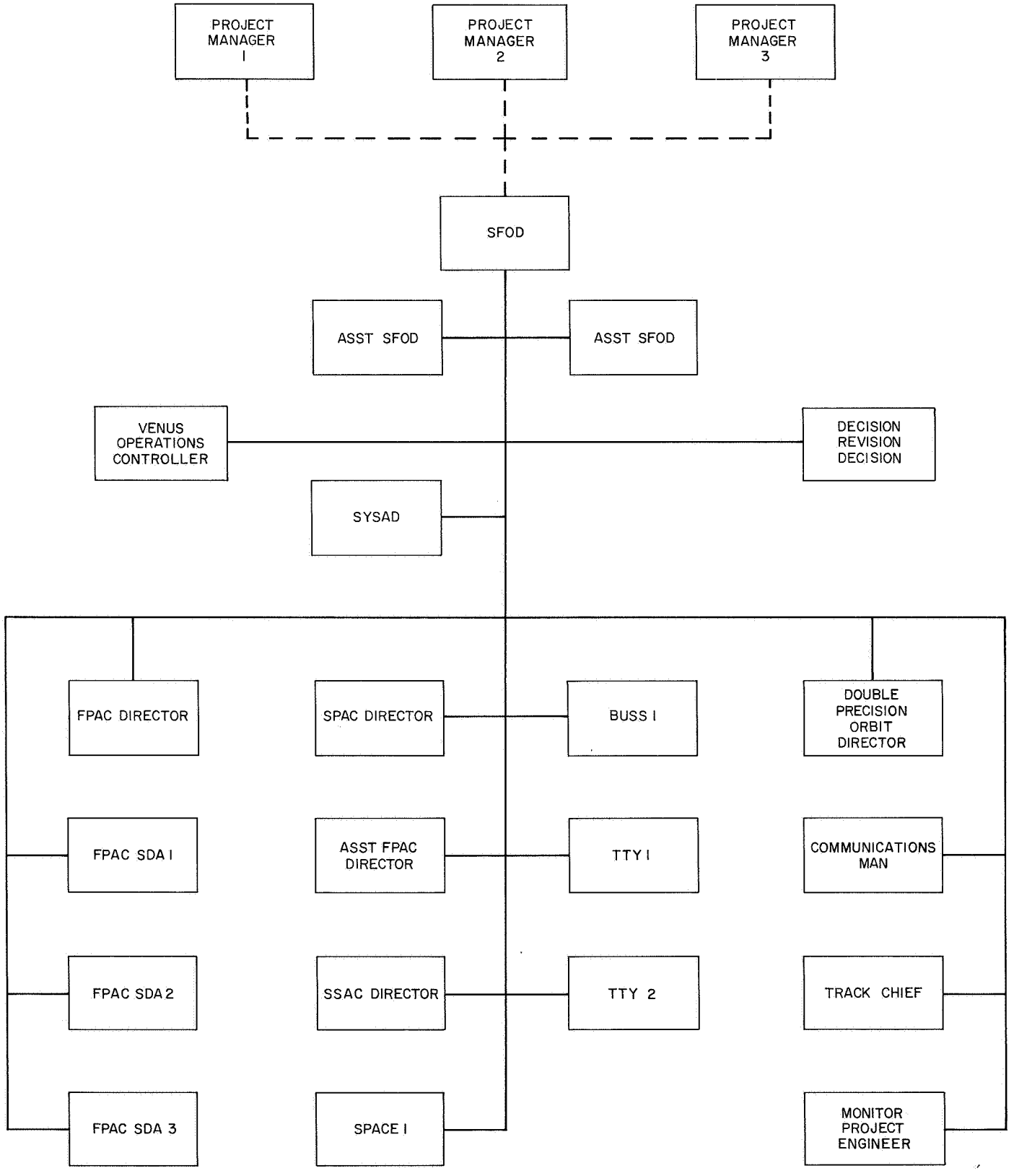


Fig. IV-7. Facilities operations control network (FAC-PRIME)

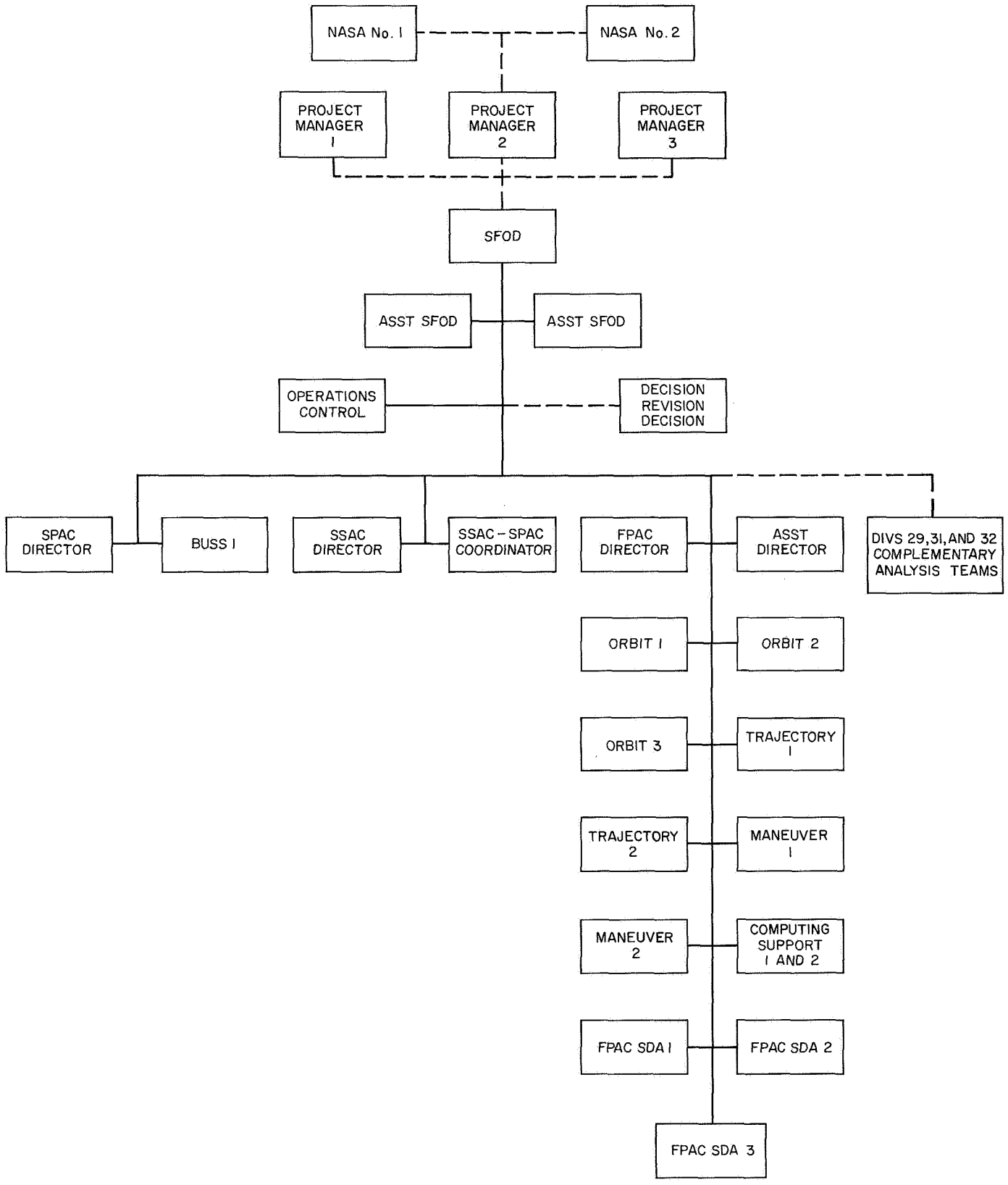


Fig. IV-8. FPAC analysis control network (FPAC 3)

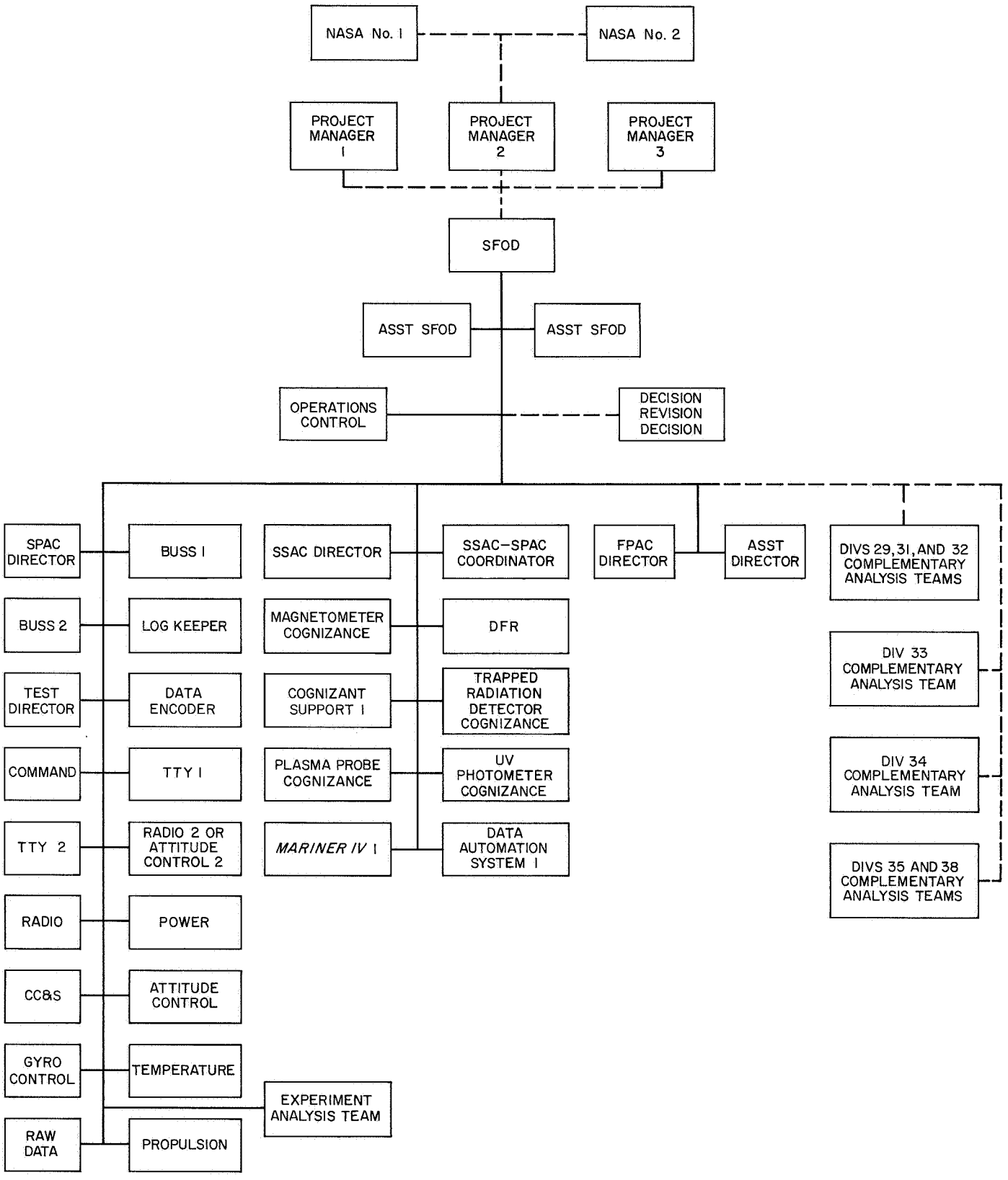


Fig. IV-9. SPAC analysis control network (BUSS)

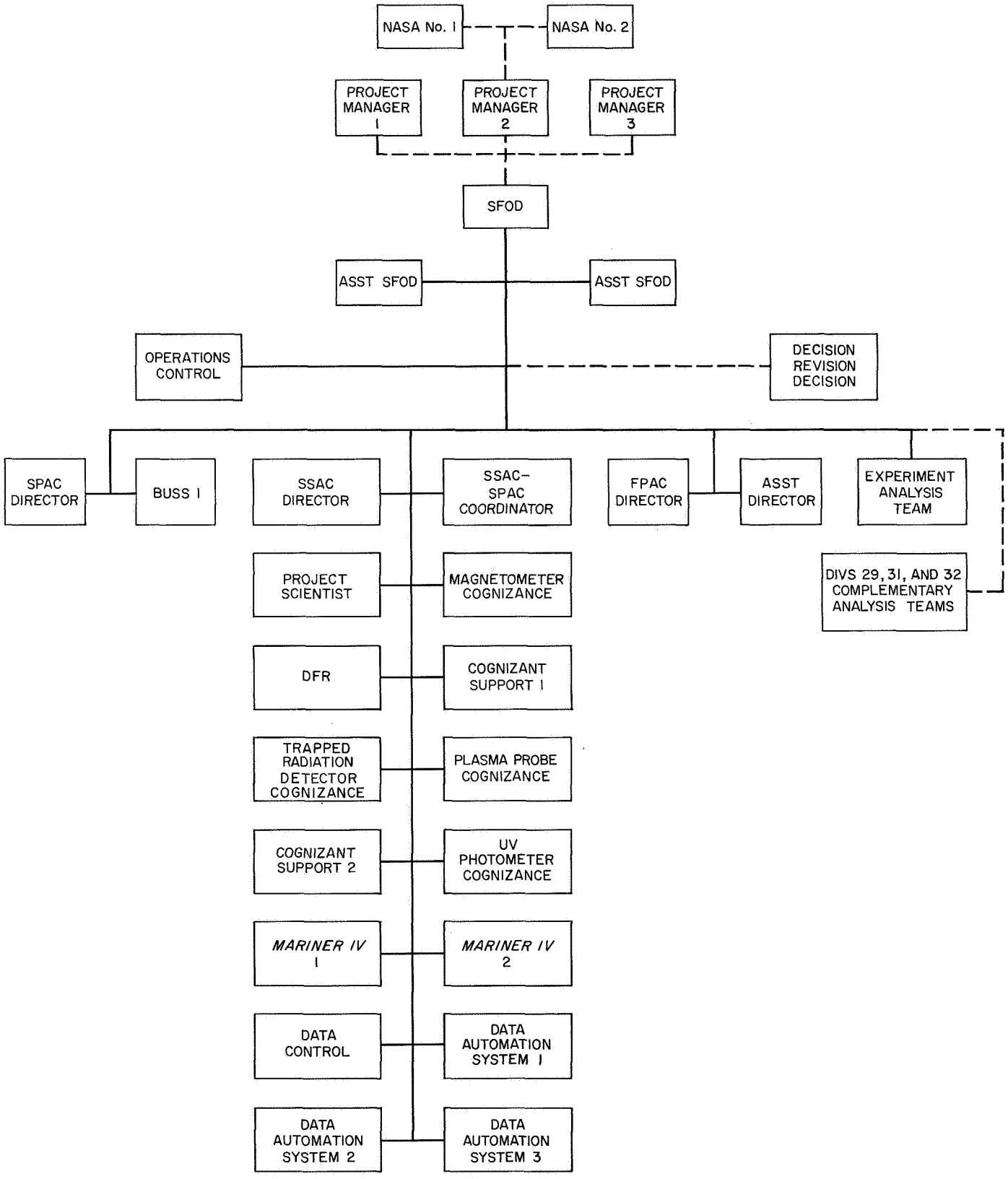


Fig. IV-10. SSAC analysis control network (SPACE)

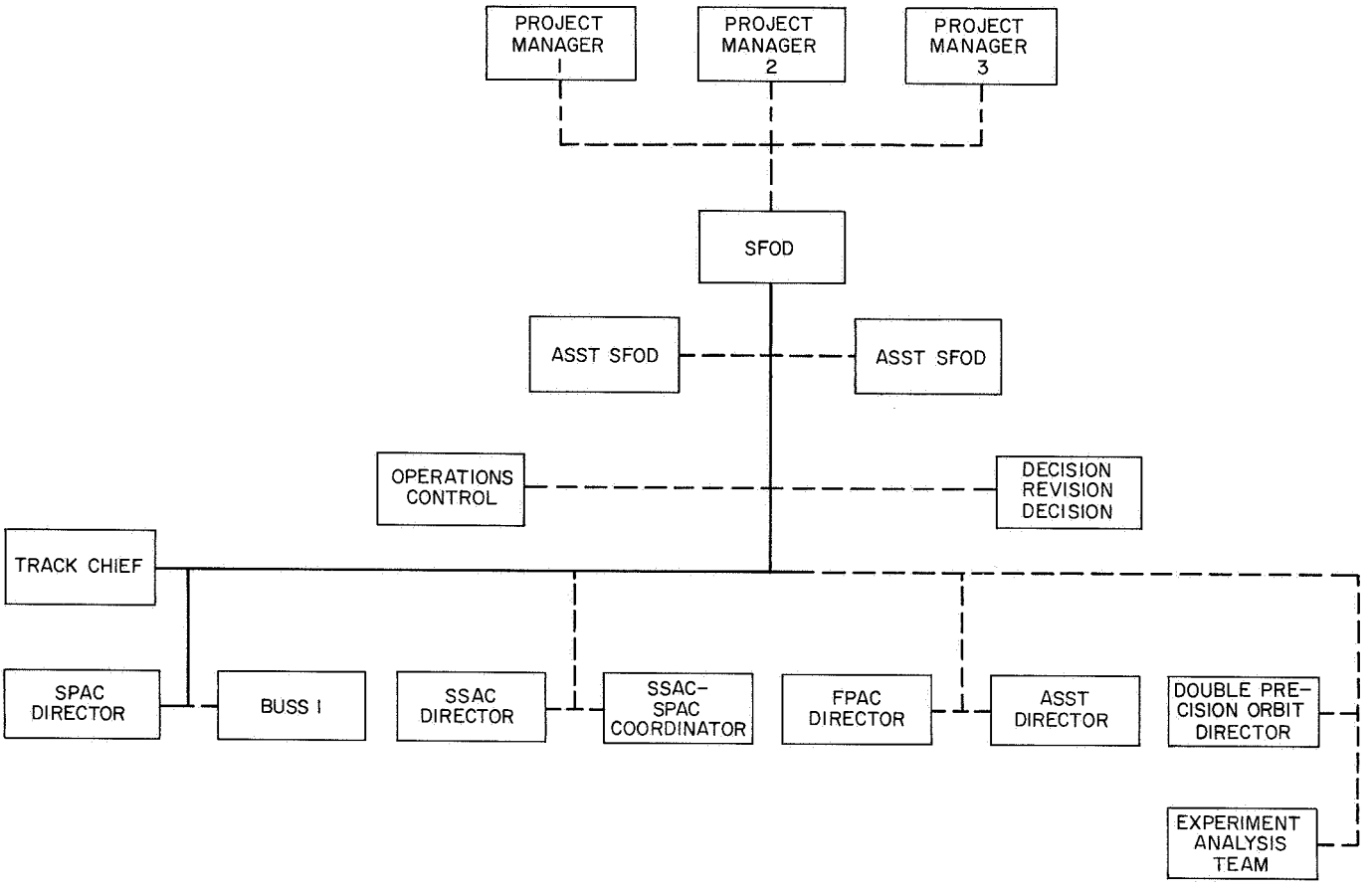


Fig. IV-11. Command network (MAR-COMMAND)

The space science analysis and command (SSAC) analysis control network (SPACE) was controlled by the SSAC director. The stations assigned to this network are shown in Fig. IV-10. This was an analysis network used for conference discussions and reporting on the status of the science instruments.

The command network (MAR-COMMAND) was used and controlled by the SFOD for conducting all command activities. Access to this network was limited to the SFOD, the SPAC director, and the track chief. Command execution and verification by the DSIF were reported on this network. Positions assigned to this network are shown in Fig. IV-11.

The data-coordination network (DA-COR) was under control of the data processing operations director, and was used as a coordination network between him and computer-support personnel. Assignments to this network are shown in Fig. IV-12. This network was also used by the Venus operations controllers during the cruise phase for data processing coordination.

A special network was established during the encounter phase for coordination between the occultation personnel at Goldstone and those at the SFOF in Pasadena.

c. Data Processing. This section outlines the data processing requirements of the *Mariner* Venus 67 mission with respect to each of the supporting facilities (the DSIF and the SFOF).

The prime concern of the data processing system was the expeditious manipulation and display of the data required to monitor and control the performance of the spacecraft.

To ensure the ability of the mission operations team adequately to support the *Mariner* Venus 67 mission, certain tasks had to be performed by the facilities supporting the mission. These tasks are discussed below, and are shown in Fig. IV-13.

The Deep Space Stations performed on-site data processing in support of the *Mariner* Venus 67 and *Mariner* Mars 1964 missions. The following tasks were

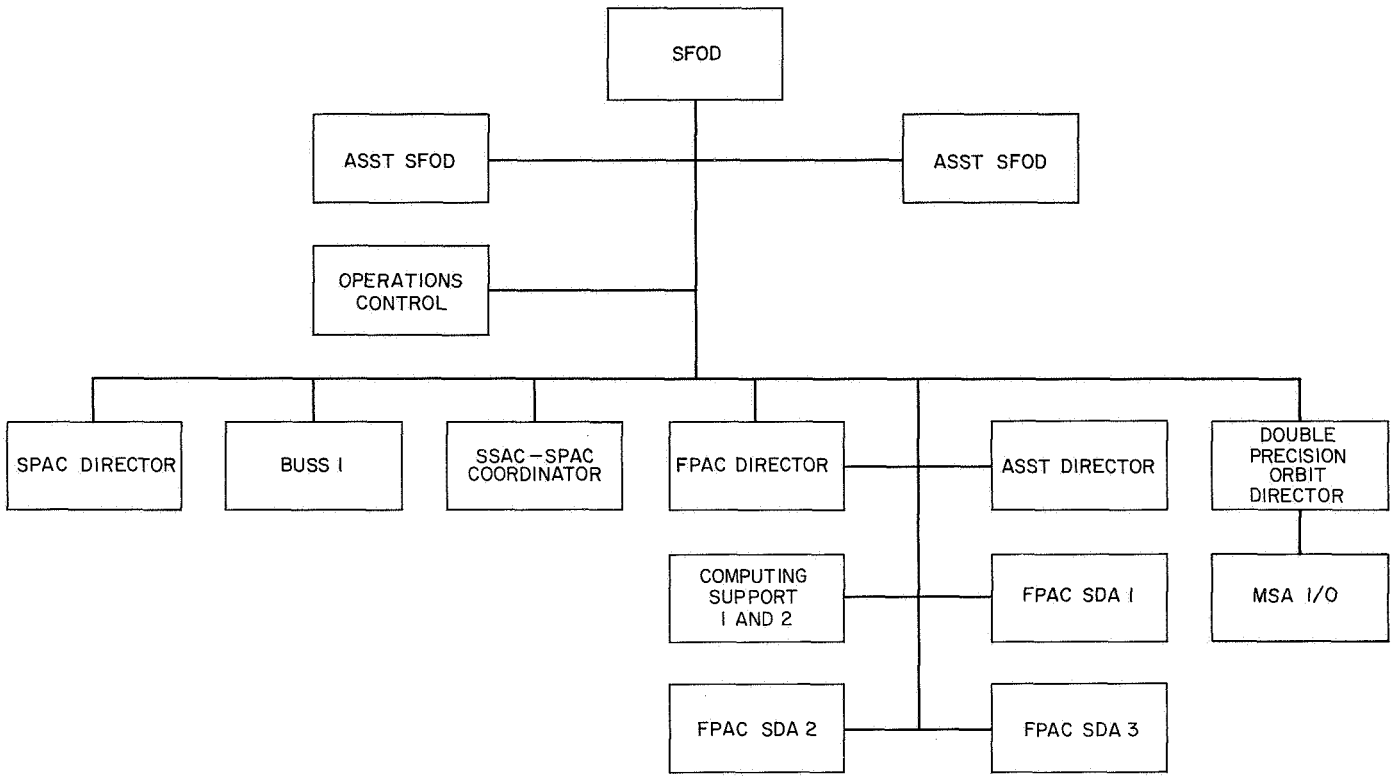


Fig. IV-12. *Data-coordination network* (DA-COR)

performed by the subsystems that compose the DSIF data processing system:

(1) Telemetry and command processor (Fig. IV-14):
  (a) Format telemetry data received from *Mariner V* mission-related hardware for transmission to SFOF in real time.
  (b) Provide selected station functions to SFOF (receiver in-out lock, demodulator in-out lock, and receiver automatic gain control).
  (c) Assign DSIF time to telemetry data.

(2) Tracking data handling equipment:
  (a) Format tracking data (angle, doppler, ranging and/or transmitter frequency) for transmission to SFOF.
  (b) Assign DSIF time to tracking data.

(3) Recording subsystem:
  (a) Record telemetry data (composite and mission-related hardware output).
  (b) Record selected station functions.
  (c) Record DSIF time.

The major data-handling effort within the SFOF was the processing and display of incoming tracking and telemetry data. The type of data (tracking or telemetry) and the ultimate users' requirements determined the required computation. The following services were provided by the SFOF data processing subsystems:

(1) Input/output (I/O) processor (7044R):
  (a) Format, convert to engineering units, and output in real time to display devices the telemetry and tracking data received from DSIF and spacecraft testing areas.
  (b) Alarm-monitor engineering and science telemetry data from spacecraft.
  (c) Record all incoming DSIF data on digital magnetic tape.
  (d) Transmit tracking predictions and commands to DSIF.

(2) Main processor (7094):
  (a) Perform detailed analysis of spacecraft engineering and science data in nonreal time when required by sequence of events or upon request from SFOD.
  (b) Perform spacecraft positioning analysis.
  (c) Determine spacecraft orbit and generate tracking predictions.
  (d) Generate maneuver commands.
  (e) Generate an MDL consisting of all spacecraft data forwarded from DSIF.

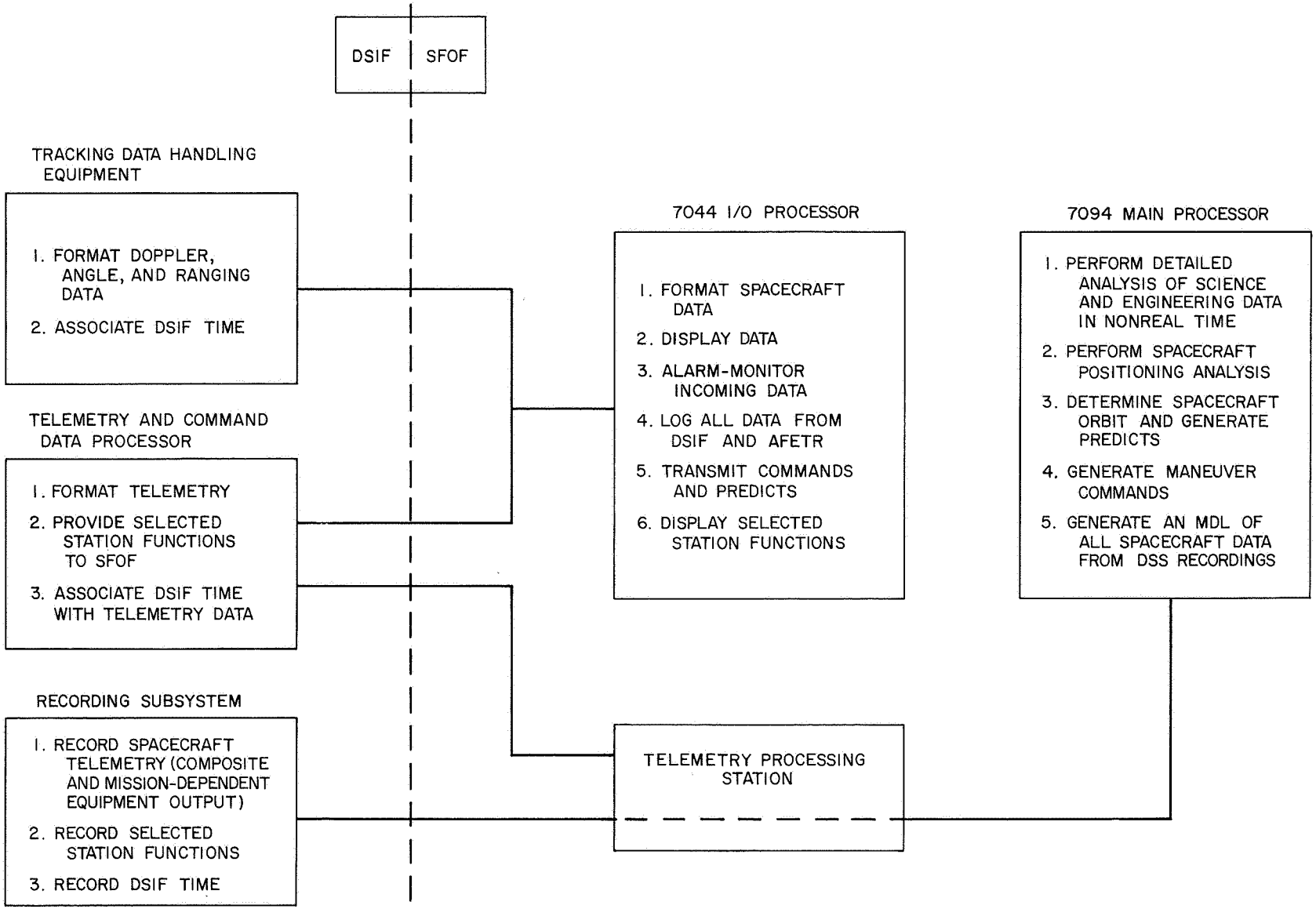


Fig. IV-13. Data processing functions performed by the Deep Space Network elements

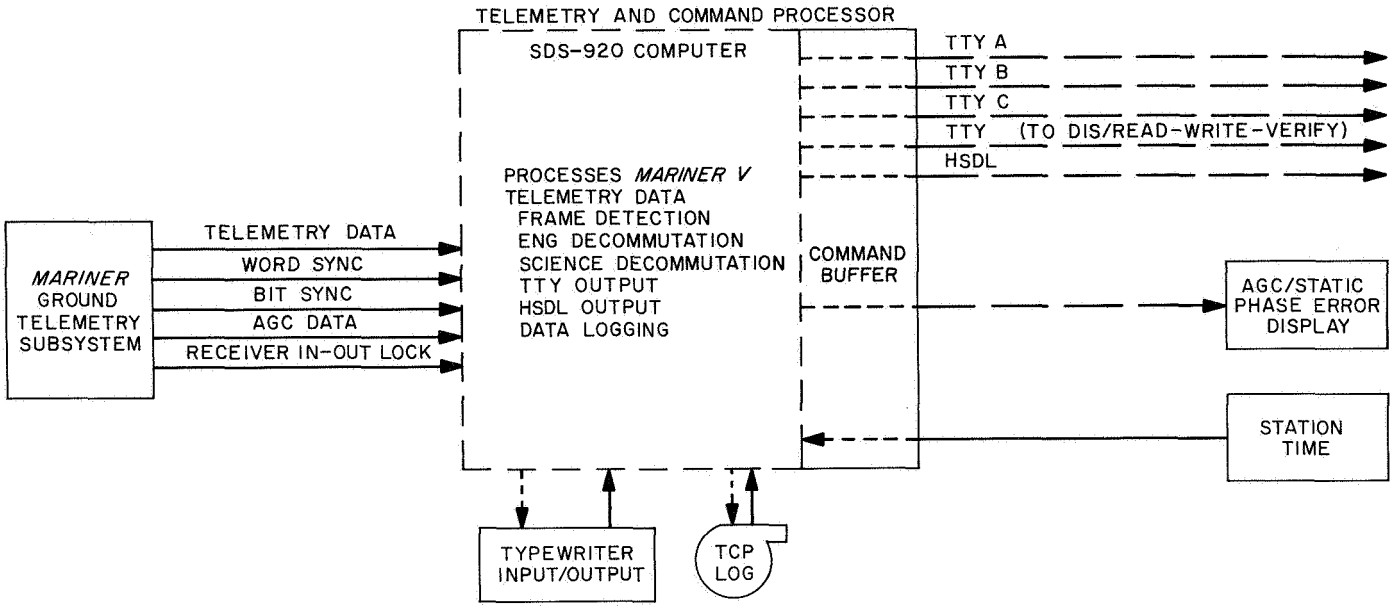


Fig. IV-14. Telemetry and command processing at the Deep Space Instrumentation Facility

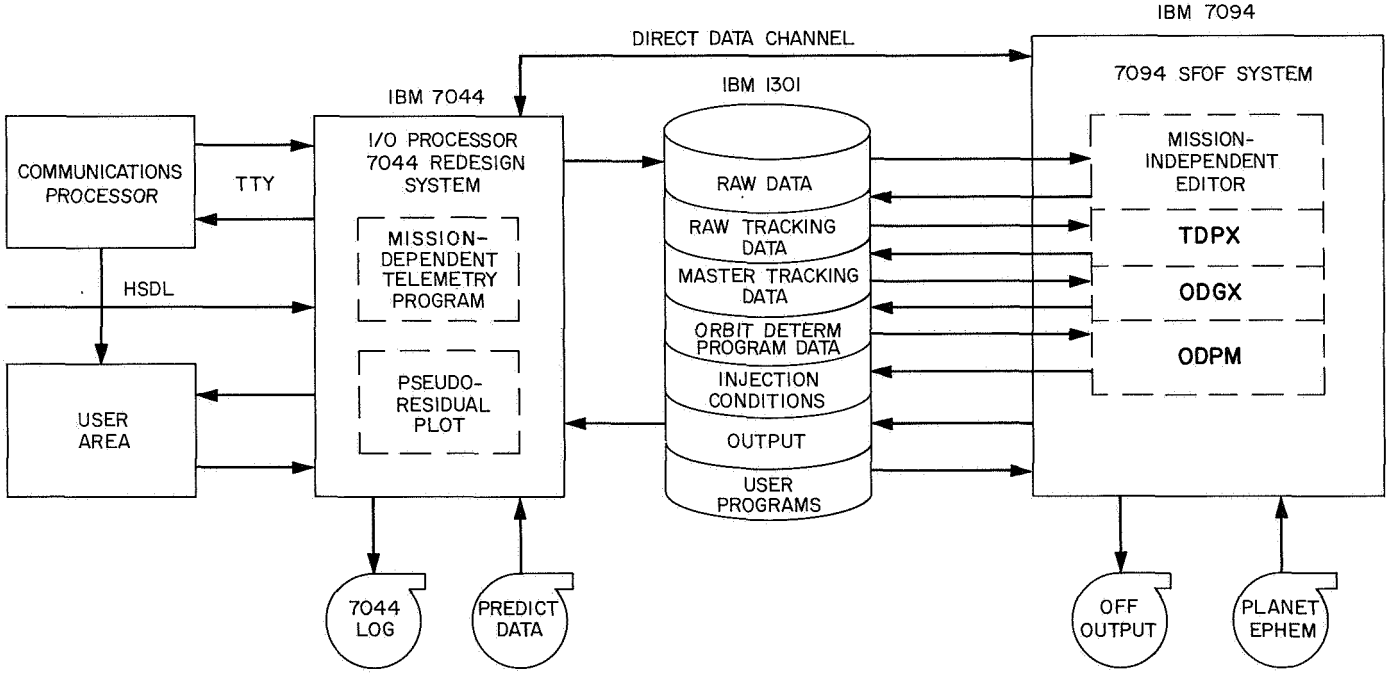


Fig. IV-15. Tracking data handling and orbit determination

The operating modes and format-selection capability of the DSIF–TCP were controlled by the SFOD or his designated representative through instructions to the DSIF track chief.

The selection of SFOF data processing system operations was primarily controlled by the standard sequence of events. The mission was, in most cases, provided full data processing capabilities within 30 min after a request

had been made by the SFOD or his designated representative.

Briefly to summarize the data processing system for the *Mariner* Venus 67 mission, teletype data were received from the NASA Communications Network (NASCOM) system by the communications processor, and provided to the 7044. In addition, information generated by the 7044 or 7094 was routed to the communications processor for distribution to SFOF user areas or overseas sites. In the 7044 redesign system, the mission-dependent telemetry program performed data processing functions similar to those of the TCP. It performed frame detection, decommutation, identification, and time tagging of spacecraft telemetry data. These data could then be transmitted by the 7044 to user areas or anywhere in NASCOM. The pseudo-residual plot program compared tracking data to prediction data obtained from the predict data tape. Residuals were computed, based upon incoming tracking data and predicted tracking observables, and then displayed as plots in the user areas. All data entering the 7044 system were logged on magnetic tapes.

The user programs illustrated in Figs. IV-15 through IV-19 are shown operating in SFOF mode 2. A 7044, a 1301 disk, and a 7094 were operating together and communicating with one another. Control inputs, usually from punched cards or switches, could be entered at the user areas, received by the 7044, and sent to the 7094 via the direct data channel. Modes 3 and 4 are described below (see Figs. IV-20 and IV-21), as are the MDL programs (see Fig. IV-22).

As raw tracking data were received, these data were placed on the disk (see Fig. IV-15) by the 7044 system, and were then accessible to the 7094 user programs.

Four tracking data handling and orbit-determination programs are illustrated, but only one program operated within the 7094 SFOF system at a time. The mission-independent editor acquired the raw teletype data from the disk that contained mixed tracking and telemetry data, and separated the data, extracting and storing the tracking data on the disk in the raw tracking data file.

The tracking data processor program (**TDPX**) retrieved these data, edited and reformatted them, and then placed the data back on the disk in the master tracking data file.

The orbit data generator program (**ODGX**) used this file to prepare a block of data for the orbit determination program. Essentially, the **ODGX** program extracted a subset of the master tracking data and formatted it, using control inputs that had been provided to the program.

The orbit-determination program (**ODPM**) retrieved the block of **ODPM** data that had been compiled by the **ODGX** program, and, employing a least-squares curve fit and an iterative technique, determined the orbit of the spacecraft. The injection conditions were placed on the disk, and were then available for use by other programs.

The area on the disk labeled USER PROGRAMS contained the actual programs called up by the system and brought into the 7094 for operation. The normal output of these programs could be accessed by the 7044 from the "output" area on the disk, and sent to the user areas for display.

Trajectory computations were performed by the programs **TJIM** (**I** = 1, 2, 3) and **POWM** (see Fig. IV-16). The injection conditions and the planetary ephemeris were used by **TJIM** to compute the spacecraft ephemeris and to generate a trajectory "save" tape. This tape consisted of tabulated information that had been computed at specified points along the trajectory. These values included earth–sun–spacecraft angles, clock angles, and velocities. The **POWM** program was essentially a trajectory program that prepared input for the **PRDX** program, which generated tracking predictions. These predictions were used for early acquisition, and were based upon predicted or actual liftoff time. Various outputs of these programs were displayed in the user areas or were recorded on magnetic tape for subsequent off-line processing. With reference to Fig. IV-17, the **PRDX** program computed:

(1) Predict data for up to 15 stations.

(2) Station view periods.

(3) Transmitter voltage-controlled oscillator frequencies.

This information was formatted for teletype, and subsequently transmitted to the DSIF stations to aid in spacecraft acquisition.

In addition, **PRDX** produced a predict data tape that was used as an input to the 7044 for computation of pseudo-residual plots. The **PRDX** program used the injection conditions and the planetary ephemeris as inputs. Selected outputs were displayed in the user areas or were recorded on magnetic tape for subsequent off-line processing.

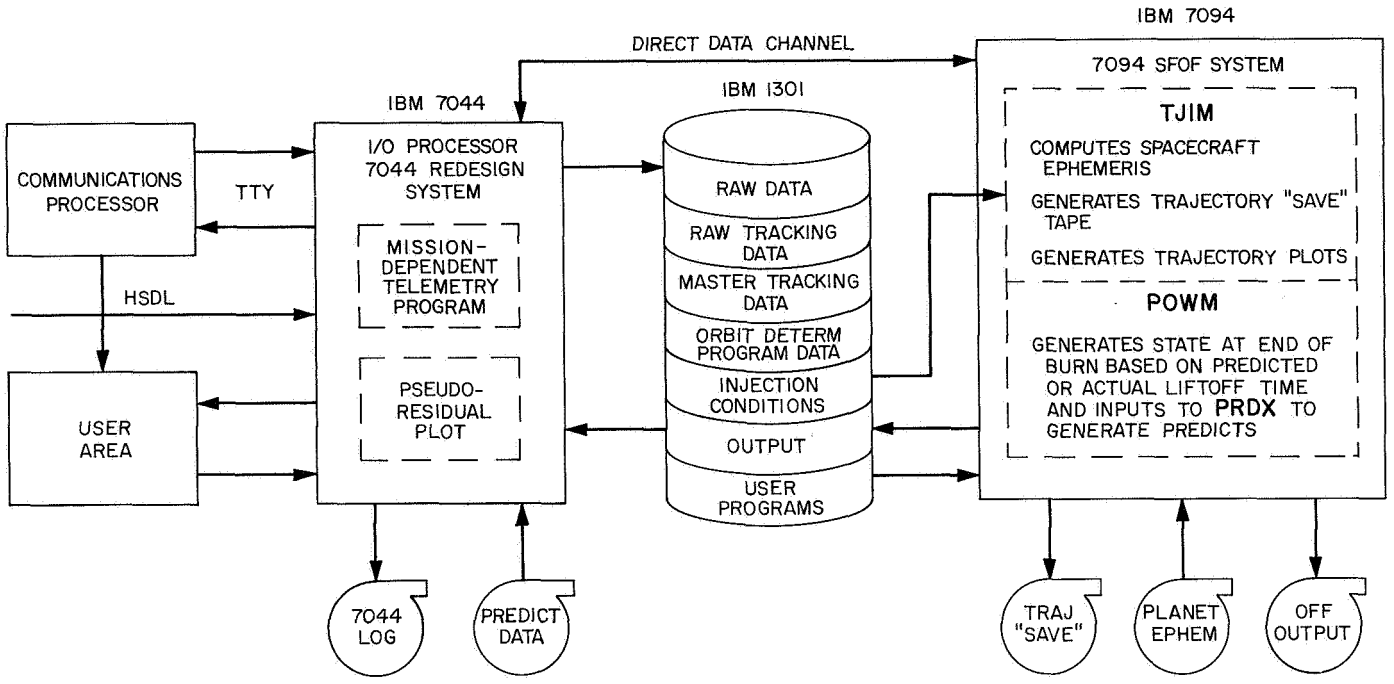


Fig. IV-16. *Trajectory computation*

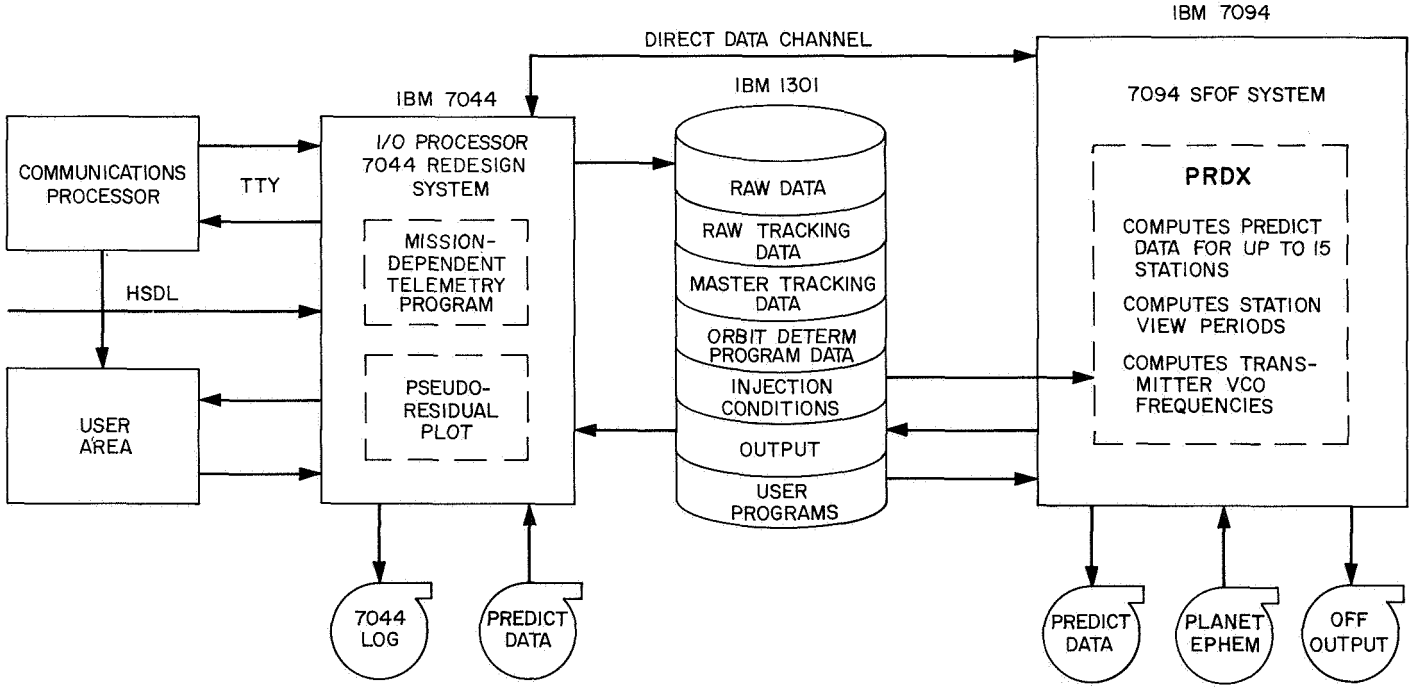


Fig. IV-17. Predicts computation

The midcourse maneuver (**MC1M**) program, as shown in Fig. IV-18, performed the following:

(1) Provided necessary information to select a midcourse maneuver that satisfied all spacecraft constraints.

(2) Generated capability ellipse plots.

(3) Generated maneuver commands.

Again, the inputs were the injection conditions and planetary ephemeris, and the outputs were recorded for off-line processing.

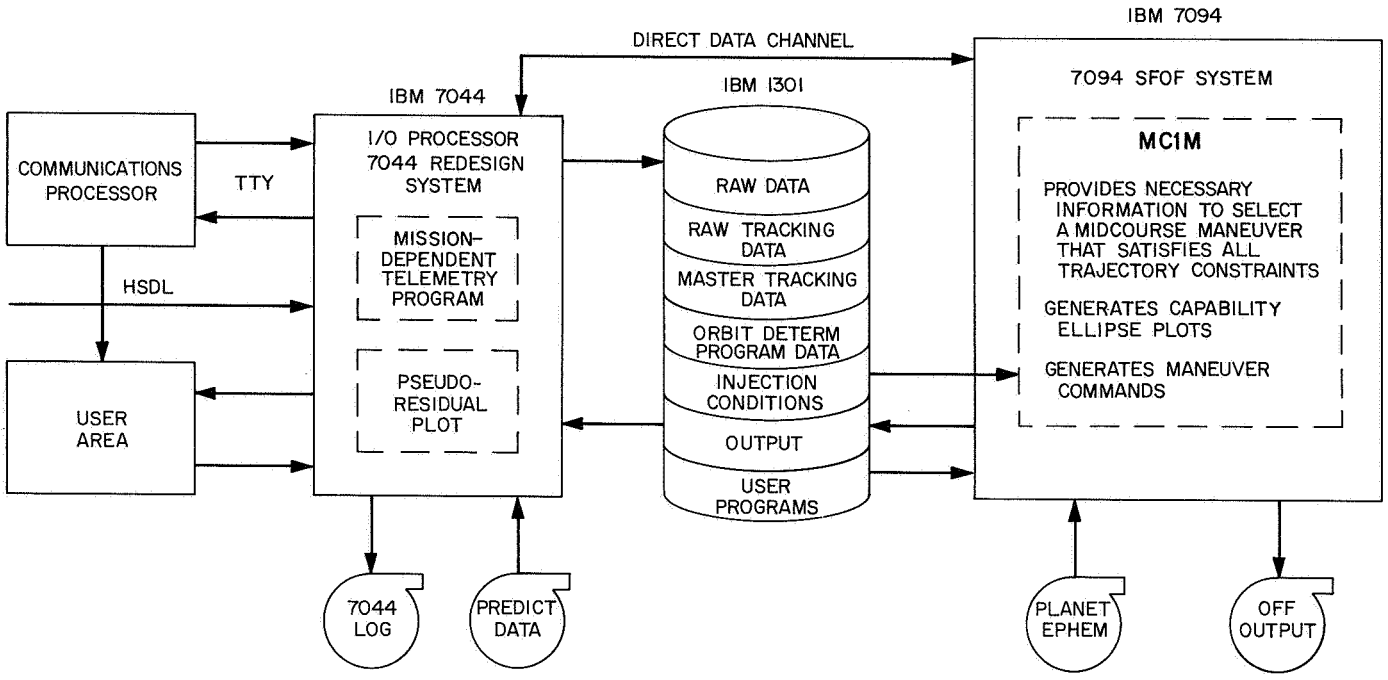


Fig. IV-18. Midcourse maneuver program

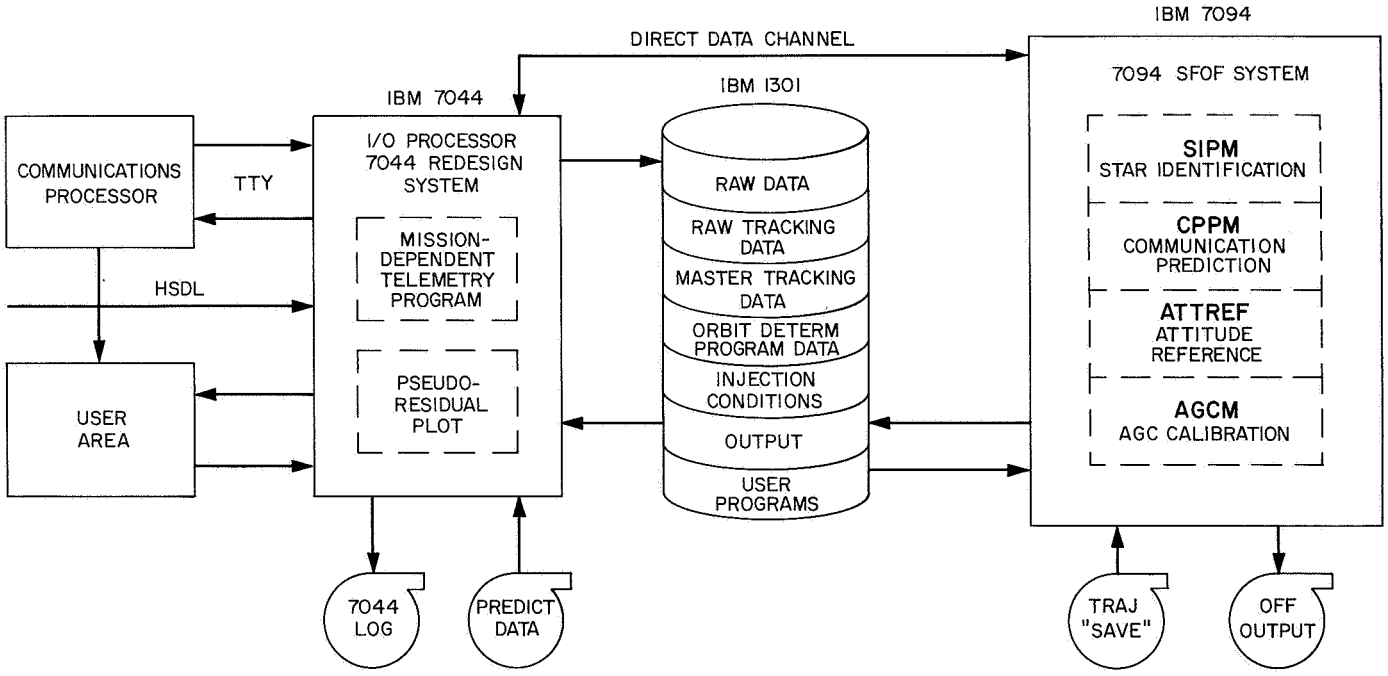


Fig. IV-19. SPAC user programs

The SFOF contained three technical areas: FPAC, SPAC, and SSAC. The user programs discussed above were primarily FPAC-oriented, but there were also a few SPAC programs (see Fig. IV-19). These programs were the star identification program (**SIPM**), the communication prediction program (**CPPM**), the attitude reference program (**ATTREF**), and the automatic gain control calibration program (**AGCM**).

The SPAC programs received telemetry data information from the 7044 via a direct data channel, not from the disk. (There was also the system capability of the

mission-independent editor to extract the telemetry data and to store these data on the disk, as was done with the tracking data; this capability was not used by the *Mariner* Venus 67 project.) Another input for three of the SPAC programs (**SIPM**, **CPPM**, and **ATTREF**) was the trajectory "save" tape. The need for this tape is obvious because these programs required an exact knowledge of the location of the spacecraft in space to accomplish their individual tasks.

The results of the SPAC programs were available to the user area via the 7044 and the output portion of the disk. Selected results were recorded on magnetic tape for subsequent off-line processing.

The user programs illustrated above were shown operating in mode 2. Mode 3 (Fig. IV-20) did not use the 7094 computational capabilities, but retained all real-time display and processing capabilities. All incoming data were still recorded on the 7044 log for subsequent processing.

Mode 4 (Fig. IV-21) was essentially the postprocessing mode. The 7044 was replaced by a previously recorded 7044 log tape, and control inputs from the user area were replaced by direct card inputs to the 7094. All 7094 programs, previously discussed as operating in mode 2, could also operate in mode 4.

The MDL programs (Fig. IV-22) for the *Mariner* Venus 67 mission were identical to those used for the

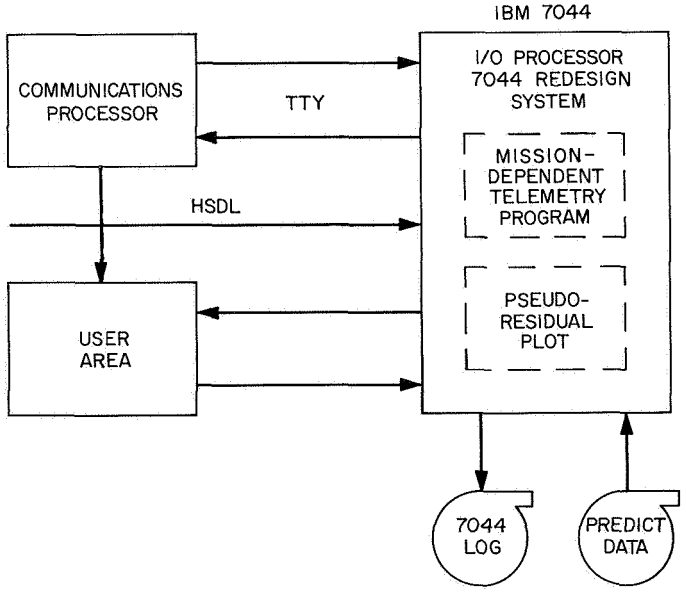


Fig. IV-20. Mode 3 operation

Mariner Mars 1964 mission except for two additional input processors and the MDL interface user program. The MDL programs did not operate in the SFOF software system, but in the standard International Business Machines System (IBSYS).

The purpose of the MDL programs was to generate, in nonreal time, a tape containing the most accurate stream of telemetry data possible. This tape then became the basis for analysis by experimenters and spacecraft engineers. This processing of various input source tapes into a final tape was done by the three basic software portions of the MDL chain: the **EDIT** program, the **REEDIT** program, and the **MERGE** program. These programs are discussed in some detail in the paragraphs that follow.

Data were recorded in various places and in various formats in the total data processing system. The tapes containing these data were the inputs to the MDL programs. The telemetry processing station and TTY paper-tape inputs were used for the *Mariner* Mars 1964 project. Their input capabilities were retained, but for the *Mariner* Venus 67 project they were replaced by two new sources: the TCP log tape, recorded at the TCP, and the 7044 log tape, recorded at the 7044.

Each tape input had an associated input processor specifically designed to handle a particular format. The input processors performed a translation function from the varied input tape formats to a standard format recognizable by the **EDIT** program.

The **EDIT** program performed frame detection and evaluated the quality of each frame.

Included in the telemetry data stream was status information regarding the processing, recording, and receiving equipment; e.g., receiver in and out of lock and demodulator in and out of sync. The **EDIT** program recognized this information, and used it in evaluating data quality during the frame-detection process.

A spacecraft data frame consisted of a certain number of words, or data bits, between science pseudo-noise sequences. The **EDIT** program, while performing frame detection, was able to draw some conclusions regarding the quality of the data stream based upon the proper or improper locations of these science pseudo-noise sequences. The standard MDL tape generated by the **EDIT** program contained not only the time-tagged data, but information regarding the worth of the data. This judgment was based on conclusions drawn from the

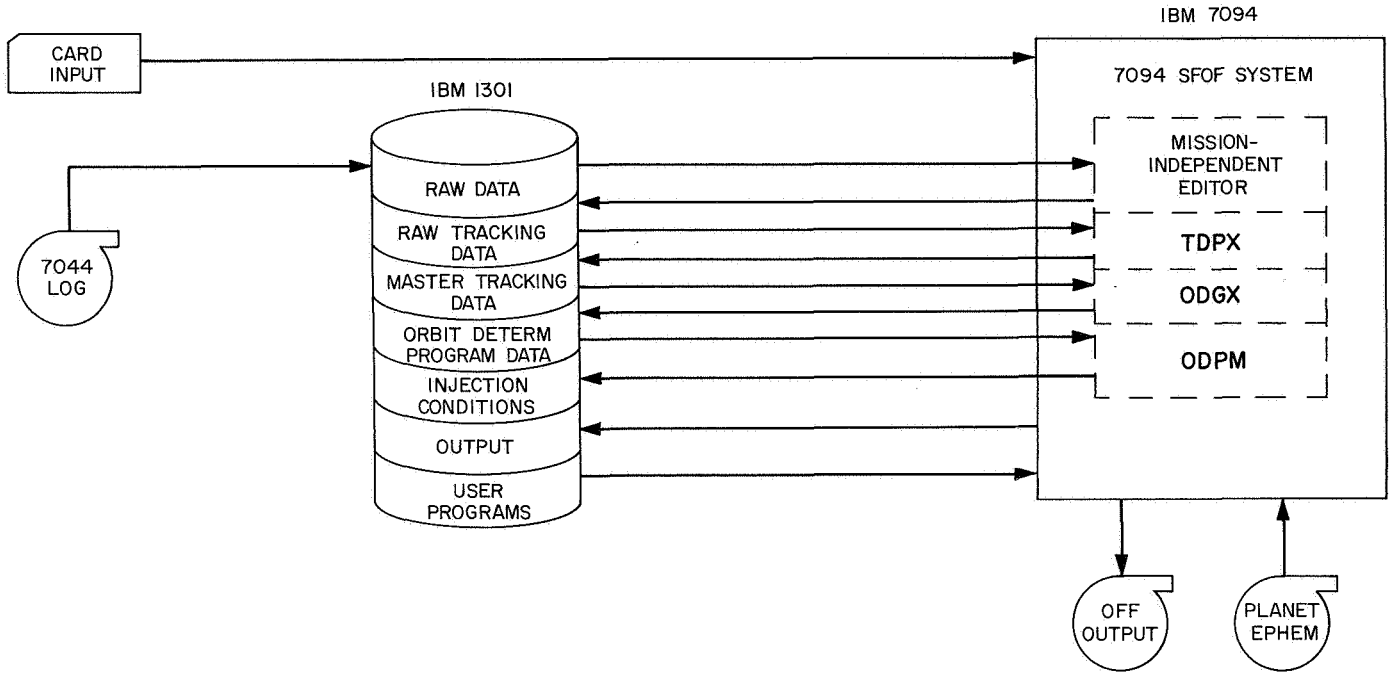


Fig. IV-21. Mode 4 operation

accurate location of the science pseudo-noise sequences and the previously discussed incoming status information contained in the original telemetry stream.

In addition to the standard MDL tape, a bad-data listing was recorded on magnetic tape. This listing was formatted for subsequent off-line printout. The printout containing bad or questionable data could then be examined visually to resolve such matters as the following:

(1) Whether the data required reprocessing farther upstream.

(2) Whether a pattern existed that would allow correction of the data by making certain inputs to the program.

(3) Whether the data were good enough to accept as they were.

The bad-data listing was thus essentially an evaluation tool for determining the additional processing required to improve the MDL tape.

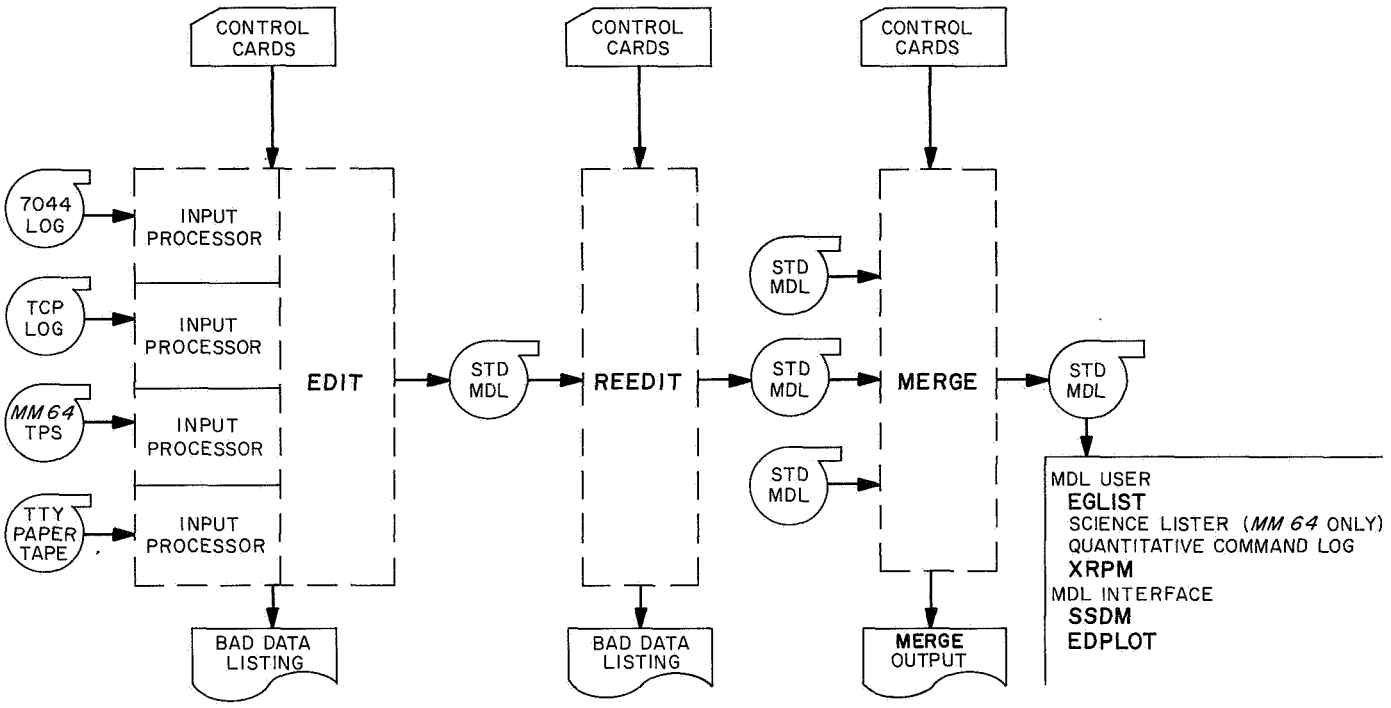
The **REEDIT** program provided a means of correcting the MDL tape by supplying appropriate control cards based upon the investigation of the bad-data listing generated by the **EDIT** program.

One of the main problems encountered in generating the MDL was that of inconsistent times. There were many potential sources for these "bad" times. At the DSIF station, the recorders were often turned on before the spacecraft had been acquired. Recording of time on the time track would begin later; finally, recording of the spacecraft analog signals would begin. The telemetry processing station then put the station analog tape through a demodulator, and digitized it. An attempt was made to begin this process at the inception of data recording, but often a "no-data" section of the tape would be digitized, and occasionally digitizing would begin before the time-track signals were encountered. Consequently, there would be "bad-data" periods and meaningless times in the resulting digital tape.

Inconsistent times would also result from bit errors in the time track. These bit errors could occur in any of the time units (days, hours, minutes, or seconds).

The **EDIT** program checked for consistency of time, but had no means of correcting the errors thus discovered. The errors appeared on the bad-data listing of the **EDIT** program, along with other bad-data frames. An examination and analysis of this listing, with intelligent selection of control cards, allowed the **REEDIT** program to correct much of the bad data flagged by the **EDIT** program.

The **REEDIT** program also produced a bad-data listing, which, if the correction process had been done



MM 64 *MARINER* MARS 1964
STD STANDARD

Fig. IV-22. Master data library programs

properly, would have been appreciably smaller than the one produced by the **EDIT** program.

The **MERGE** program processed a number of tapes (up to six) from various sources, covering the same period of transmission, and merged them into one "best possible" standard MDL tape. The tapes processed by the **EDIT** and **REEDIT** programs were also from a variety of sources. Consequently, many tapes contained telemetry data for identical tracking periods. This occurred during station overlaps; i.e., when more than one station was tracking the spacecraft at a time. It also occurred during in-station overlaps; i.e., when, in switching from one tape to another during a pass, the second recorder was started before the first had finished. (Approximately three analog tapes were required for a station pass.)

The **MERGE** program evaluated each data frame based upon quantitative command information, data condition information, and control inputs that instructed it to place more weight on one data source than another, etc. The best data frame was selected for each time step, and recorded on the MDL output tape. The "**MERGE** output" was a magnetic tape recording similar to the previously discussed bad-data listings, except that it simply indicated data gaps in the final standard MDL output tape.

The user programs were used as tools in the evaluation process of the standard MDL tapes generated at any stage (i.e., **EDIT**, **REEDIT**, or **MERGE**).

The standard MDL tapes, regardless of the stage of processing, were in an identical format. The **REEDIT** and **MERGE** programs refined the data stream, but did not alter this format. As a result, any of the MDL user programs could use any MDL tape as an input.

The engineering lister extracted all of the engineering data from an MDL tape, and organized these data into a "quick-look" format. The science lister did essentially the same with science data. (This capability was for the *Mariner* Mars 1964 mission only.) The quality control log program was still in the developmental stage. Its purpose was to compute qualitative statistics about a tape by scanning the tape for data gaps, poor data frames, etc. The **XRPM** program was a selective extract program with various uses; e.g., a magnetometer experimenter, by providing certain control inputs to the **XRPM** program, could extract all magnetometer data from a given MDL tape.

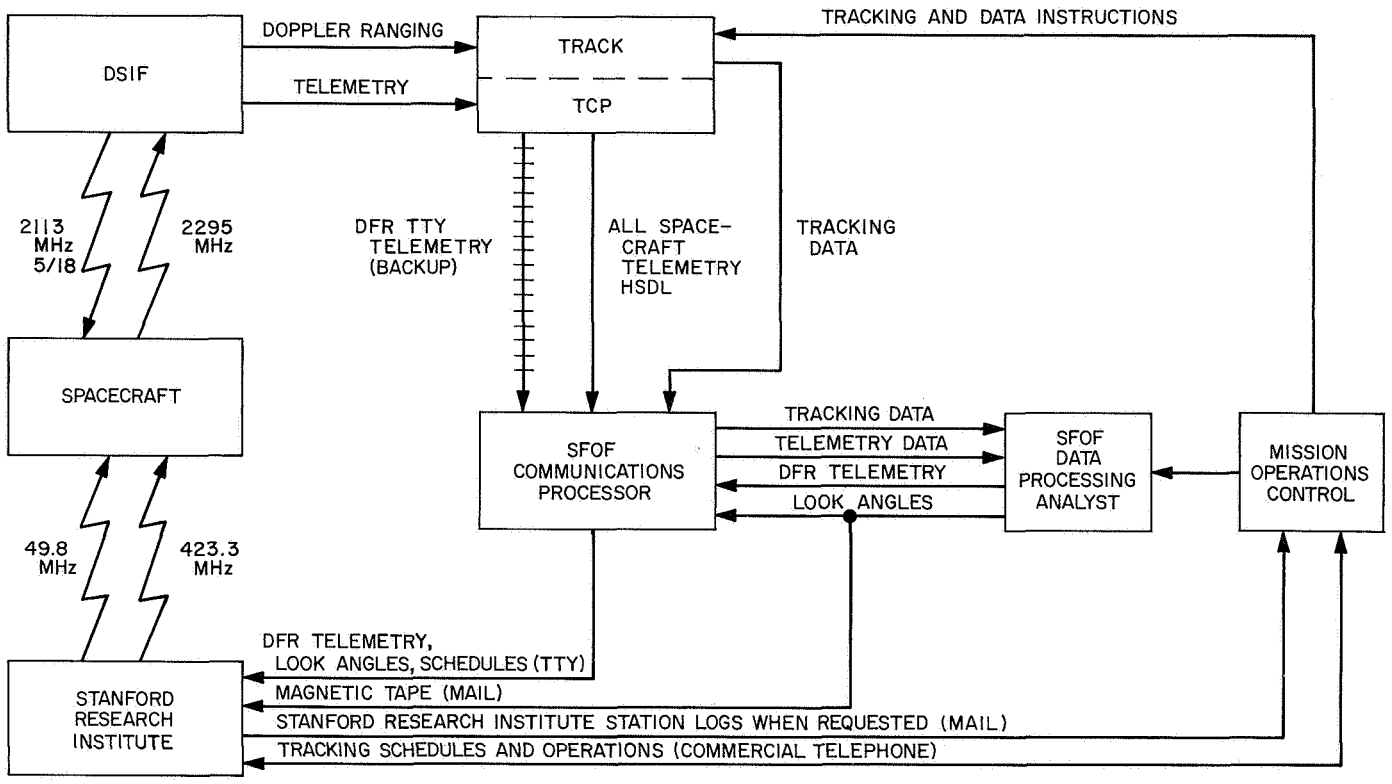


Fig. IV-23. Dual-frequency receiver data handling

The MDL interface program acted as an interface between the MDL tape and two programs carried over from the *Mariner* Mars 1964 project. In the discussion of SPAC user programs, above, it was pointed out that telemetry data were not stored on the 1301 disk as were tracking data. The *Mariner* Mars 1964 project, on the other hand, stored telemetry data on the disk, and two very useful programs (**SSDM** and **EDPLOT**) made use of this feature. The MDL interface program allowed these programs to operate from the standard MDL tapes. The **EDPLOT** program provided a plot of the engineering values recorded. The **SSDM** program was a suppressed data printout; i.e., only values that violate certain constraints were printed out, and repetitive values were ignored.

Prior to encounter, a residual program (**RSID**) was generated for the purpose of making available real-time, pseudo-residual plots.

Tracking data (1-s sample rate) were transmitted from Goldstone over an HSDL to the 7044 at the SFOF. The **RSID** program compared these data with predicts and output residuals, which were plotted on a 30×30 Milgo plotter in the FPAC area.

Figure IV-23 illustrates operational dual-frequency radio propagation experiment data flow.

d. Mission support area. The *Mariner* Venus 67 mission support area (MSA), located in the SFOF at Pasadena, housed the SPAC team, the SSAC team, and the operations team. All mission-control functions originated from this central control point.

The equipment layout provided for the analysis of spacecraft and science instrument performance, and for the mission-control function, is shown in Fig. IV-24. The FPAC team was housed in flight-path analysis area (FPAA) No. 2, adjacent to the MSA. This area was provided with similar equipment for performing trajectory analysis, orbit determination, and predict-generation functions.

2. Schedule and control of interfaces. Scheduling for the *Mariner* Venus 67 mission encounter and pre-encounter testing was conducted exactly as it was during the entire mission. Users of DSN facilities submitted requirements to three types of DSN scheduling techniques: (1) the 16-mo loading schedule, which was an attempt to predict DSN loading 16 mo in the future;

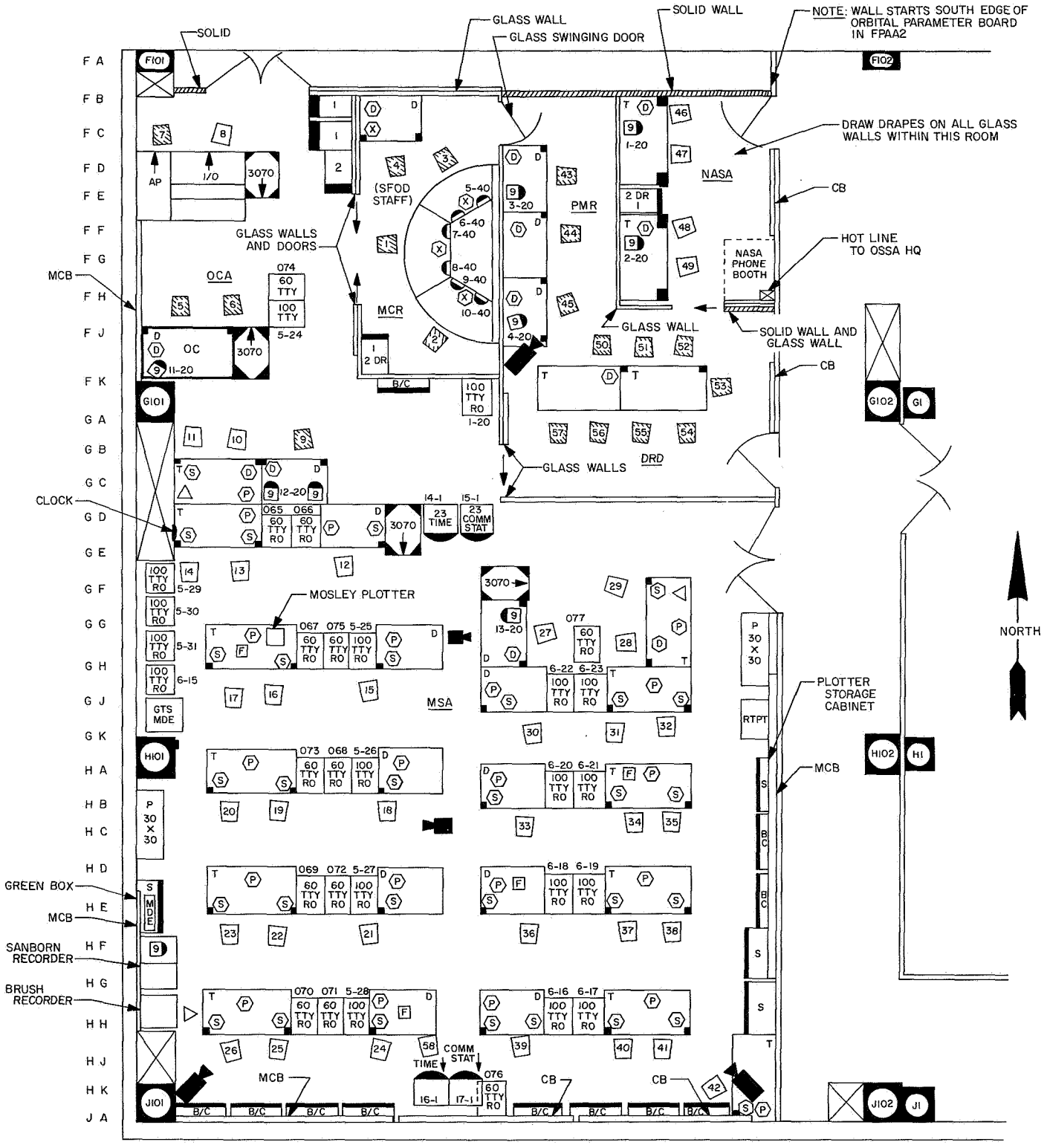
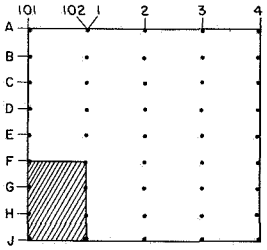


Fig. IV-24. *Mariner* Venus 67 mission support area layout

LEGEND-NOT TO SCALE

- (D) OVCS PHONE STATIONS
  - D - CALL DIRECTOR
  - P - 1500
  - S - 6040 KEY SET AND JACK
- [F] FRIDEN CALCULATOR
- ■ OVCS EXTENSION JACK
- ▽ H/C TV CAMERA
- [9] DESK TV MONITOR
- CCTV CAMERA
- [23] CEILING MOUNTED TV MONITOR
- [AP] ADMINISTRATIVE PRINTER
- [RO] TTY RECEIVE ONLY SET
- [P] 30 × 30 MILGO PLOTTER
- CHAIR
- GREEN CHAIR
- [2] 1 FILE
  2 BURROUGHS CARD READER
- BOOKCASE-STORAGE CABINET (BC OR S)
- SPACECRAFT 3070
- [I/O] I/O CONSOLE
- [D] DESK
- [T] TABLE
- MCB MAGNETIC CHALK BOARD



SEATING ARRANGEMENT

MCR-MISSION CONTROL ROOM

1- SFOD-OPERATIONS CONTROL
2- ASST SFOD-ACE 5
3- ASST SFOD-PRIME 5
4- COORDINATOR-DEUCE 5

OCA-OPERATIONS CONTROL ROOM

5- MOS OPERATIONS CONTROL-"V-OPS"
6-
7- MSA I/O No. 1
8- MSA I/O No. 2

MSA-MISSION SUPPORT AREA

SPAC-SPACECRAFT PERFORMANCE ANALYSIS AND COMMAND

9- SPAC DIRECTOR-BUS CHIEF
10- BUS I
11- BUS II
12- DATA ENCODER
13- TEST DIRECTOR
14- LOGKEEPER
15- TTY 1
16- TTY 2
17- COMMUNICATIONS
18- POWER
19- RADIO
20- RADIO OR ATTITUDE CONTROL
21- GYRO CONTROL
22- ATTITUDE CONTROL
23- CC&S
24- PROPULSION
25- RAW DATA CHIEF
26- TEMPERATURE

SSAC-SPACE SCIENCE ANALYSIS AND COMMAND

27- SSAC DIRECTOR-SPACE CHIEF
28- SPAC/SSAC COORDINATOR-SPACE I
29- PROJECT SCIENTIST-SPACE II
30- DATA AUTOMATION SYSTEM I
31- DATA AUTOMATION SYSTEM 2
32- DATA AUTOMATION SYSTEM 3
33- MAGNETOMETER COGNIZANCE
34- DUAL FREQUENCY RECEIVER COGNIZANCE
35- COGNIZANT SUPPORT I
36- TRAPPED RADIATION DETECTOR COGNIZANCE
37- PLASMA PROBE COGNIZANCE
38- COGNIZANT SUPPORT 2
39- UV PHOTOMETER COGNIZANCE
40- *MARINER IV* 1
41- *MARINER IV* 2
42- DATA CONTROL

PMR-PROJECT MANAGERS ROOM

43 THROUGH 45

NASA-PROGRAM MANAGERS ROOM

46 THROUGH 49

DRD-CONFERENCE ROOM

50 THROUGH 57

Fig. IV-24 (contd)

(2) the DSN 12-wk schedule, which allocated DSN resources to project requirements on an hours/week basis; and (3) the DSN 7-day operations schedule, which defined project requirements and was used to conduct DSN activities on a day-by-day, hour-by-hour basis. Changes to the DSN 7-day schedule were conducted through the DSN operations control group. The *Mariner* Venus 67 project DSN scheduling requirements followed the prescribed routes indicated above, whether the time was for testing or flight support. All interfacing with respect to scheduling was conducted through the *Mariner* Venus 67 mission DSN project engineer. It was his responsibility to collect and review all inputs to eliminate all possible internal project conflicts and redundancy in requests for DSN resources. His approval was required on all inputs to the DSN scheduling systems.

3. DSN coverage.

a. Class I tracking requirements. Table IV-2 shows a comparison between the Class I tracking requirements requested in the support instrumentation requirements document (SIRD) and the actual coverage obtained from the Air Force Eastern Test Range and Manned Space Flight Network C-band radar stations. All of the requested Class I coverage was provided.

Post-Agena/spacecraft separation tracking requirements. Table IV-3 shows a comparison between the Class I tracking requirements requested in the SIRD and the actual coverage provided by the DSN. The time interval covered in Table IV-3 is from *Agena*/spacecraft separation (L+1575.8 s) to end of mission (day 325 at 20:00:00 GMT). Launch occurred on day 165 at 06:01:00 GMT.

Table IV-2. Requested and actual Class I tracking coverage, liftoff to L+5178 s

Coverage requested	Actual coverage	Coverage requested	Actual coverage
Liftoff to parking orbit insertion plus 85 s (from L = 0 to L+610.2 s)	Cape Kennedy (1.16) L+10 to L+265 s Kennedy Space Center (19.18) L+12 to L+365 s Patrick Air Force Base (0.18) L+15 to L+480 s Grand Bahama Island (3.18) L+48 to L+450 s Grand Bahama Island (3.16) L+69 to L+467 s Grand Turk (7.18) L+199 to L+610 s Bermuda (FPQ-6) L+282 to L+642 s		Antigua (91.18) L+368 to L+768 s
		Any continuous 60 s of coverage between *Agena* second burn cutoff (L+1415.324 s) and *Agena*/spacecraft separation (L+1576.724 s)	Ascension (12.18) L+1232 to L+1515 s Ascension (12.16) L+1245 to L+1474 s RIS[a] *Twin Falls* (FPS-16) L+1414 to L+1912 s
		Any continuous 60 s of coverage after *Agena* retro burnout	Pretoria (13.16) L+1667 to L+3046 s L+3078 to L+4967 s Carnarvon (FPQ-6) L+2343 to L+5178 s

[a]RIS = *Range Instrumentation Ship.*

Table IV-3. Requested and actual Class I tracking coverage, *Agena*/spacecraft separation to end of mission

Coverage requested	Actual coverage	Coverage requested	Actual coverage
Continuous coverage from Agena/spacecraft separation (L+1575.8 s) to first maneuver (day 170 at 21:23:59 GMT—DC-V27 transmit time) minus 1 h. 60-s sample rate required, with the following exception: 5-s sample rate required from initial DSIF acquisition to L+60 min (day 165 at 07:01:00 GMT)	C-band radar RIS *Twin Falls* (FPS-16) L+1414 to L+1912 s. Included *Agena*/spacecraft separation at L+1575.8 s (day 165 at 06:27:16 GMT) Pretoria (13.16) L+1667 to L+3046 s L+3078 to L+4967 s Carnarvon (FPQ-6) L+2342 to L+5178 s		DSIF coverage DSS 51 acquired spacecraft at L+1675 s (day 165 at 06:28:55 GMT). TDH[a] to 5-s sample rate at 07:06:45 GMT (L+3900 s). TDH went to 60-s sample rate at 07:19:00 GMT, day 165 DSIF tracking coverage was continuous from initial acquisition to M_1−60 min (M_1 being the transmission of DC-V27)

[a]TDH = tracking data handling.

Table IV-3 (contd)

Coverage requested	Actual coverage
Continuous coverage from M_1—60 min (day 170 at 20:23:59 GMT) to sun reacquisition (day 170 at 23:21:19 GMT). 10-s sample rate	Continuous coverage DSS 14, day 170 TDH to 10-s sample rate at 22:20 GMT TDH to 1- and 10-s sample rates at 23:05 GMT TDH to 60-s sample rate at 23:30 GMT DSS 11, day 170 TDH to 10-s sample rate at 18:21 GMT TDH to 1- and 10-s sample rates at 23:05 GMT TDH to 60-s sample rate at 23:50 GMT
Start of pitch turn (22:24:10.9 GMT, day 170) minus 1 min to completion of pitch turn (22:29:13.9 GMT) plus 1 min. 1-s sample rate Start of roll turn (22:46:11 GMT, day 170) minus 1 min to completion of roll turn (22:52:31 GMT) plus 1 min. 1-s sample rate Start of motor burn (23:08:11 GMT, day 170) minus 5 min to completion of motor burn (23:08:29.4 GMT) plus 5 min. 1-s sample rate	DSS 14, day 170 TDH to 1- and 10-s sample rates at 23:05 GMT TDH to 60-s sample rate at 23:30 GMT DSS 11, day 170 TDH to 1- and 10-s sample rates at 23:05 GMT TDH to 60-s sample rate at 23:50 GMT
Continuous coverage Motor burn completion (23:08:29.4 GMT, day 170) plus 5 min to sun reacquisition (23:21:19 GMT, day 170). 10-s sample rate	Continuous coverage DSS 14 TDH to 1- and 10-s sample rates at 23:05 GMT TDH to 60-s sample rate at 23:30 GMT DSS 11 TDH to 1- and 10-s sample rates at 23:05 GMT TDH to 60-s sample rate at 23:50 GMT
Continuous coverage from sun reacquisition (day 170 at 23:21:19 GMT) to sun reacquisition plus 2 days (day 172 at 23:21:19 GMT). 60-s sample rate	Continuous coverage from sun reacquisition to sun reacquisition plus 2 days at 60-s sample rate

Coverage requested	Actual coverage
One pass/day coverage from maneuver plus 3 days (day 173) through maneuver plus 53 days (day 223). 60-s sample rate	An average of 2.46 passes/day coverage was provided during this period. 60-s sample rate
One pass/day coverage from maneuver plus 54 days (day 224) through E—10 days (day 282). 60-s sample rate	An average of 2.28 passes/day coverage was provided from maneuver plus 54 days through E—10 days. 60-s sample rate
One pass/day from E—9 days (day 283) through E—2 days (day 290). 60-s sample rate	Continuous coverage provided from E—9 through E—2 days. 60-s sample rate
Continuous coverage from E—1 day (day 291 at 17:34:54 GMT) to E—60 min (day 292 at 16:34:54 GMT). 30-s sample rate	Continuous coverage provided from E—1 day to E—60 min. 30-s sample rate
Continuous coverage from E—60 min (day 292 at 16:34:54 GMT) to E+30 min (day 292 at 18:04:54 GMT). 1- and 10-s sample rates	Continuous coverage provided from E—60 to E+60 min. Encounter planning changed this SIRD requirement, and initialized the 1- and 10-s sample rates to start at approximately E—40 min and continue until E+60 min
Continuous coverage from E+100 min (day 292 at 19:14:54 GMT) to E+12 h (day 293 at 05:34:54 GMT). 30-s sample rate	Continuous coverage provided from E+100 min to E+12 h. 1- and 60-s sample rates
Continuous coverage from E+12 to E+24 h. 60-s sample rate	Continuous coverage provided from E+12 to E+24 h. 60-s sample rate
Continuous coverage from E+24 to E+72 h. 60-s sample rate	Continuous coverage provided from E+24 to E+72 h. 1-, 10-, and 60-s sample rates
Two passes/day coverage from E+3 to E+10 days. 60-s sample rate	Continuous coverage provided from E+3 to E+10 days. 1-, 10-, and 60-s sample rates
Two passes/5 days or 1 pass/2.5 days from E+10 days to end of mission. 60-s sample rate	An average of 1.8 passes/day coverage provided from E+10 days to end of mission. 60-s sample rate

b. Class I telemetry requirements. Table IV-4 presents the total tracking coverage of *Mariner V* by the DSN. It also compares the actual telemetry coverage with the Class I telemetry coverage requested in the SIRD. In observing the comparisons for the various periods indicated, it can be seen that the total coverage provided was approximately twice the total coverage requested. This figure is based upon total passes requested vs total passes provided.

During the flight of *Mariner V*, a total of 2.03×10^8 bits of data were transmitted by the spacecraft, of which 1.78×10^8 bits were received. In arriving at the latter figure, no consideration was given to any receiver out-of-lock times, as the number of lost bits represented would be insignificant to the total.

The total bits received represent 86.7% of the total bits transmitted by the spacecraft.

4. Interaction with other missions.

a. Established guidelines for priorities. Guidelines were established for the determination of priorities to be accorded to a project. The following paragraphs state the contents of *Guidelines for Scheduling of DSN Support for Lunar and Planetary Flight Missions*:

> I. Purpose and Intent
>
> The purpose of this document is to form the guidelines to be used (1) by Lunar and Planetary Project Management in determining the priority to be accorded a project in the utilization of DSN facilities and (2) by DSN Management in establishing schedules for the use of DSN facilities and for resolving conflicts that may arise in the scheduling of near-term[1] DSN support for flight missions having equal priorities. It is intended that these guidelines be utilized at the lowest appropriate operational levels within the project and DSN organizational elements in order to permit decisions being made which will minimize conflicts in the scheduling of DSN resources. Where conflicts may arise which cannot be resolved by the application of these guidelines at the Project Manager and DSN Manager levels, the conflicts will be referred to the cognizant Program Manager at NASA Headquarters, who will arrange to establish relative priorities for the use of DSN resources on a mission-to-mission basis.
>
> II. Responsibilities
>
> Each Project Manager shall examine the project objectives and mission plans to determine what data must be obtained, what elements of the mission are mandatory for data acquisition and what the time requirements are in order to derive a specific set of DSN support requirements. The Project Office shall list the approved mission objectives and within this framework categorize each phase of each mission into priority classifications listed below. These mission classification lists shall be submitted to the appropriate Program Manager at NASA Headquarters for concurrence. The lists are then to be included in the SIRD for use by the DSN Managers in preparation of the NASA Support Plan. Existing or predicted limitations involving the scheduling of DSN facilities should not constrain project management in the categorization of mission phases into appropriate priority classifications. DSN management will publish an allocation of DSN resources on the basis of approved project priorities. The DSN management shall also have the responsibility for indicating to the concerned project management those portions of the mission which it cannot support or which will conflict with other project requirements.
>
> III. Definitions
>
> A. Critical Phase—The period during which certain events are expected to occur which are mandatory for attaining primary mission objectives.
>
> B. Semi-Critical Phase—The period during which certain events are expected to occur which are not mandatory for attaining primary mission objectives but which are required to obtain other mission objectives.
>
> C. Non-Critical Phase—The period during which near real-time data acquisition is not required to meet the mission objectives.
>
> IV. Priority Classifications/Category
>
> Priorities are established in the following order:
>
> 1. In-Flight Critical—The period during flight when certain events are expected to occur which are mandatory to attaining the primary mission objectives.
> 2. In-Flight Semi-Critical—The periods during flight when certain events are expected to occur which are either mandatory for achieveing other mission objectives or which are required to maximize achievement of mission objectives.
> 3. Pre-Flight Critical—The periods preceding flight when certain activities must occur at specifically set times in the Pre-Flight Schedule to permit meeting the mission objectives.
> 4. DSN Routine Maintenance—The period during which the maintenance activity, necessary to assure that the DSN is operational and can meet its project commitments, must occur.
> 5. Pre-Flight Semi-Critical—The periods preceding flight when certain activities must occur to permit meeting the mission objectives but which can be carried out at conveniently scheduled times in the Pre-Flight Schedule.

[1]Near-term is defined as a 12-week period.

Table IV-4. Total *Mariner V* tracking coverage by the Deep Space Network

Actual coverage provided										Requested vs actual coverage
MV-5	STA-51/	/	PASS-0001	ACQ-	165	062855	EOT-	165	194151	
MV-5	STA-41/	/	PASS-0001	ACQ-	165	064854	EOT-	165	121152	
MV-5	STA-42/	/	PASS-0001	ACQ-	165	065305	EOT-	165	112057	
MV-5	STA-61/	/	PASS-0001	ACQ-	165	111055	EOT-	165	202349	
MV-5	STA-11/	/	PASS-0001	ACQ-	165	183336	EOT-	166	044000	
MV-5	STA-42/	/	PASS-0002	ACQ-	165	235001	EOT-	166	115507	
MV-5	STA-61/	/	PASS-0002	ACQ-	166	110753	EOT-	166	203829	
MV-5	STA-11/	/	PASS-0002	ACQ-	166	183129	EOT-	167	045000	
MV-5	STA-42/	/	PASS-0003	ACQ-	166	235753	EOT-	167	115635	
MV-5	STA-61/	/	PASS-0003	ACQ-	167	110308	EOT-	167	204627	
MV-5	STA-11/	/	PASS-0003	ACQ-	167	182850	EOT-	168	044756	
MV-5	STA-42/	/	PASS-0004	ACQ-	167	235500	EOT-	168	115400	
MV-5	STA-61/	/	PASS-0004	ACQ-	168	105749	EOT-	168	204159	
MV-5	STA-11/	/	PASS-0004	ACQ-	168	182553	EOT-	169	044800	
MV-5	STA-42/	/	PASS-0005	ACQ-	168	235116	EOT-	169	115152	Launch through first maneuver plus 2 days (day 165 through day 172)
MV-5	STA-61/	/	PASS-0005	ACQ-	169	105513	EOT-	169	203805	Requested Class I coverage per SIRD — Continuous
MV-5	STA-11/	/	PASS-0005	ACQ-	169	182215	EOT-	170	044700	Actual coverage — Continuous
MV-5	STA-42/	/	PASS-0006	ACQ-	169	235122	EOT-	170	114800	
MV-5	STA-62/	/	PASS-0006	ACQ-	170	105128	EOT-	170	204914	
MV-5	STA-61/	/	PASS-0006	ACQ-	170	105745	EOT-	170	203500	
MV-5	STA-11/	/	PASS-0006	ACQ-	170	182034	EOT-	171	044300	
MV-5	STA-14/	/	PASS-0006	ACQ-	170	182350	EOT-	171	030000	
MV-5	STA-41/	/	PASS-0007	ACQ-	170	002240	EOT-	171	111505	
MV-5	STA-42/	/	PASS-0007	ACQ-	170	234755	EOT-	171	012800	
MV-5	STA-61/	/	PASS-0007	ACQ-	171	104814	EOT-	171	203127	
MV-5	STA-11/	/	PASS-0007	ACQ-	171	195615	EOT-	172	043600	
MV-5	STA-41/	/	PASS-0008	ACQ-	172	032755	EOT-	172	112845	
MV-5	STA-61/	/	PASS-0008	ACQ-	172	104430	EOT-	172	202842	
MV-5	STA-11/	/	PASS-0008	ACQ-	172	183000	EOT-	173	033915	
MV-5	STA-14/	/	PASS-0008	ACQ-	172	190716	EOT-	172	225500	
MV-5	STA-41/	/	PASS-0009	ACQ-	173	022603	EOT-	173	110100	
MV-5	STA-61/	/	PASS-0009	ACQ-	173	104000	EOT-	173	200000	
MV-5	STA-11/	/	PASS-0009	ACQ-	173	181500	EOT-	174	040400	
MV-5	STA-42/	/	PASS-0010	ACQ-	174	025502	EOT-	174	113200	
MV-5	STA-61/	/	PASS-0010	ACQ-	174	103540	EOT-	174	202003	
MV-5	STA-11/	/	PASS-0010	ACQ-	174	180606	EOT-	175	021800	
MV-5	STA-42/	/	PASS-0011	ACQ-	175	002542	EOT-	175	112730	
MV-5	STA-61/	/	PASS-0011	ACQ-	175	103208	EOT-	175	183500	
MV-5	STA-12/	/	PASS-0011	ACQ-	175	180500	EOT-	176	013000	
MV-5	STA-42/	/	PASS-0012	ACQ-	176	010217	EOT-	176	110000	
MV-5	STA-61/	/	PASS-0012	ACQ-	176	102311	EOT-	176	183000	
MV-5	STA-11/	/	PASS-0012	ACQ-	176	175500	EOT-	176	020000	
MV-5	STA-42/	/	PASS-0013	ACQ-	176	235428	EOT-	177	110500	
MV-5	STA-61/	/	PASS-0013	ACQ-	177	102207	EOT-	177	192807	
MV-5	STA-11/	/	PASS-0013	ACQ-	177	175338	EOT-	178	030000	
MV-5	STA-42/	/	PASS-0014	ACQ-	178	015246	EOT-	178	111425	
MV-5	STA-61/	/	PASS-0014	ACQ-	178	101644	EOT-	178	190000	
MV-5	STA-11/	/	PASS-0014	ACQ-	178	174638	EOT-	179	031800	
MV-5	STA-42/	/	PASS-0015	ACQ-	179	015405	EOT-	179	111008	
MV-5	STA-61/	/	PASS-0015	ACQ-	179	101110	EOT-	179	191500	
MV-5	STA-11/	/	PASS-0015	ACQ-	179	175315	EOT-	180	031530	
MV-5	STA-42/	/	PASS-0016	ACQ-	180	015830	EOT-	180	110615	
MV-5	STA-61/	/	PASS-0016	ACQ-	180	100637	EOT-	180	195711	
MV-5	STA-11/	/	PASS-0016	ACQ-	180	173802	EOT-	181	024500	
MV-5	STA-42/	/	PASS-0017	ACQ-	181	020000	EOT-	181	110200	
MV-5	STA-51/	/	PASS-0017	ACQ-	181	094654	EOT-	181	185926	
MV-5	STA-12/	/	PASS-0017	ACQ-	181	184215	EOT-	182	030000	
MV-5	STA-42/	/	PASS-0018	ACQ-	182	010000	EOT-	182	105800	
MV-5	STA-61/	/	PASS-0018	ACQ-	182	100023	EOT-	182	190616	
MV-5	STA-12/	/	PASS-0018	ACQ-	182	180138	EOT-	183	030500	
MV-5	STA-42/	/	PASS-0019	ACQ-	183	020000	EOT-	183	105400	
MV-5	STA-61/	/	PASS-0019	ACQ-	183	095305	EOT-	183	190048	
MV-5	STA-42/	/	PASS-0020	ACQ-	184	015000	EOT-	184	104800	
MV-5	STA-62/61/		PASS-0020	ACQ-	184	093948	EOT-	184	194400	
MV-5	STA-62/		PASS-0021	ACQ-	185	093800	EOT-	185	194000	
MV-5	STA-41/	/	PASS-0022	ACQ-	185	232045	EOT-	186	112000	
MV-5	STA-42/	/	PASS-0023	ACQ-	186	224315	EOT-	187	101700	
MV-5	STA-62/	/	PASS-0023	ACQ-	187	092939	EOT-	187	193200	
MV-5	STA-12/	/	PASS-0023	ACQ-	187	163900	EOT-	188	032130	
MV-5	STA-41/	/	PASS-0024	ACQ-	187	231149	EOT-	188	111208	
MV-5	STA-41/	/	PASS-0025	ACQ-	188	230732	EOT-	189	110700	
MV-5	STA-62/	/	PASS-0025	ACQ-	189	091900	EOT-	189	192400	
MV-5	STA-12/	/	PASS-0025	ACQ-	189	163017	EOT-	189	234000	
MV-5	STA-41/	/	PASS-0026	ACQ-	189	230252	EOT-	190	110300	
MV-5	STA-12/	/	PASS-0026	ACQ-	190	162614	EOT-	191	030716	
MV-5	STA-14/11/		PASS-0027	ACQ-	191	173350	EOT-	191	220007	
MV-5	STA-62/61/		PASS-0028	ACQ-	192	090600	EOT-	192	191200	
MV-5	STA-12/	/	PASS-0028	ACQ-	192	161427	EOT-	192	234000	
MV-5	STA-41/	/	PASS-0029	ACQ-	192	225014	EOT-	193	104900	
MV-5	STA-62/61/		PASS-0029	ACQ-	193	090000	EOT-	193	190800	
MV-5	STA-12/	/	PASS-0029	ACQ-	193	160938	EOT-	194	025356	

Table IV-4 (contd)

Actual coverage provided										Requested vs actual coverage
MV-5	STA-41/	/	PASS-0030	ACQ-	193	224512	EOT-	194	104525	
MV-5	STA-62/	/	PASS-0030	ACQ-	194	085400	EOT-	194	190400	
MV-5	STA-12/	/	PASS-0030	ACQ-	194	160830	EOT-	195	024910	
MV-5	STA-41/	/	PASS-0031	ACQ-	194	224018	EOT-	195	104000	
MV-5	STA-62/	/	PASS-0031	ACQ-	195	084900	EOT-	195	190000	
MV-5	STA-62/	/	PASS-0032	ACQ-	196	090000	EOT-	196	163000	
MV-5	STA-12/	/	PASS-0032	ACQ-	196	155640	EOT-	197	024010	
MV-5	STA-41/	/	PASS-0033	ACQ-	196	223132	EOT-	197	103000	First maneuver plus 2 days through cruise and transition to radial *Mariner V*–earth–*Mariner IV* position (day 173 through day 223) Requested Class I coverage per SIRD — 1 pass/day Actual coverage — Average of 2.46 passes/day
MV-5	STA-62/	/	PASS-0034	ACQ-	198	083440	EOT-	198	184800	
MV-5	STA-12/	/	PASS-0034	ACQ-	198	154535	EOT-	199	023100	
MV-5	STA-41/	/	PASS-0035	ACQ-	198	222013	EOT-	199	102100	
MV-5	STA-62/	/	PASS-0035	ACQ-	199	082911	EOT-	199	184400	
MV-5	STA-12/	/	PASS-0035	ACQ-	199	154140	EOT-	200	022600	
MV-5	STA-42/	/	PASS-0036	ACQ-	200	021230	EOT-	200	092610	
MV-5	STA-62/	/	PASS-0036	ACQ-	200	082334	EOT-	200	184000	
MV-5	STA-11/	/	PASS-0036	ACQ-	200	172530	EOT-	200	231500	
MV-5	STA-42/	/	PASS-0037	ACQ-	200	215100	EOT-	201	092056	
MV-5	STA-61/	/	PASS-0037	ACQ-	201	082030	EOT-	201	171400	
MV-5	STA-11/	/	PASS-0037	ACQ-	201	155927	EOT-	201	230130	
MV-5	STA-42/	/	PASS-0038	ACQ-	201	214310	EOT-	202	091540	
MV-5	STA-51/	/	PASS-0038	ACQ-	202	133307	EOT-	202	172320	
MV-5	STA-14/12/		PASS-0038	ACQ-	202	185440	EOT-	203	020002	
MV-5	STA-42/	/	PASS-0039	ACQ-	203	012513	EOT-	203	091007	
MV-5	STA-61/	/	PASS-0039	ACQ-	203	080850	EOT-	203	182331	
MV-5	STA-14/	/	PASS-0039	ACQ-	203	185200	EOT-	204	020000	
MV-5	STA-42/	/	PASS-0040	ACQ-	204	003118	EOT-	204	090447	
MV-5	STA-51/	/	PASS-0040	ACQ-	204	134022	EOT-	204	171410	
MV-5	STA-14/	/	PASS-0040	ACQ-	204	184603	EOT-	205	020038	
MV-5	STA-42/	/	PASS-0041	ACQ-	205	010000	EOT-	205	085934	
MV-5	STA-61/	/	PASS-0041	ACQ-	205	075717	EOT-	205	170500	
MV-5	STA-14/11/		PASS-0041	ACQ-	205	153555	EOT-	205	233023	
MV-5	STA-11/	/	PASS-0041	ACQ-	205	161100	EOT-	205	220500	
MV-5	STA-42/	/	PASS-0042	ACQ-	205	225753	EOT-	206	085404	
MV-5	STA-61/	/	PASS-0042	ACQ-	206	083000	EOT-	206	170517	
MV-5	STA-11/	/	PASS-0042	ACQ-	206	160000	EOT-	206	220242	
MV-5	STA-42/	/	PASS-0043	ACQ-	206	212400	EOT-	207	084800	
MV-5	STA-61/	/	PASS-0043	ACQ-	207	074735	EOT-	207	170000	
MV-5	STA-11/	/	PASS-0043	ACQ-	207	160000	EOT-	207	240000	
MV-5	STA-42/	/	PASS-0044	ACQ-	207	211800	EOT-	208	084230	
MV-5	STA-61/	/	PASS-0044	ACQ-	208	074039	EOT-	208	162000	
MV-5	STA-11/	/	PASS-0044	ACQ-	208	152540	EOT-	208	232200	
MV-5	STA-42/	/	PASS-0045	ACQ-	208	222000	EOT-	209	083700	
MV-5	STA-61/	/	PASS-0045	ACQ-	209	073613	EOT-	209	180400	
MV-5	STA-14/11/		PASS-0045	ACQ-	209	174700	EOT-	210	014128	
MV-5	STA-42/	/	PASS-0046	ACQ-	210	010000	EOT-	210	083300	
MV-5	STA-61/	/	PASS-0046	ACQ-	210	073024	EOT-	210	180054	
MV-5	STA-11/	/	PASS-0046	ACQ-	210	170610	EOT-	211	015722	
MV-5	STA-42/	/	PASS-0047	ACQ-	211	010000	EOT-	211	082700	
MV-5	STA-61/	/	PASS-0047	ACQ-	211	072455	EOT-	211	163000	
MV-5	STA-11/	/	PASS-0047	ACQ-	211	160400	EOT-	212	003200	
MV-5	STA-42/	/	PASS-0048	ACQ-	211	223000	EOT-	212	082230	
MV-5	STA-61/	/	PASS-0048	ACQ-	212	081500	EOT-	212	161500	
MV-5	STA-42/	/	PASS-0049	ACQ-	213	000000	EOT-	213	081636	
MV-5	STA-61/	/	PASS-0049	ACQ-	213	071258	EOT-	213	150900	
MV-5	STA-14/11/		PASS-0049	ACQ-	213	145224	EOT-	214	010500	
MV-5	STA-42/	/	PASS-0050	ACQ-	214	000000	EOT-	214	080100	
MV-5	STA-61/	/	PASS-0050	ACQ-	214	070650	EOT-	214	150400	
MV-5	STA-42/	/	PASS-0051	ACQ-	214	230000	EOT-	215	070000	
MV-5	STA-61/	/	PASS-0051	ACQ-	215	070300	EOT-	215	150000	
MV-5	STA-42/	/	PASS-0052	ACQ-	215	225100	EOT-	216	065200	
MV-5	STA-61/	/	PASS-0052	ACQ-	216	065808	EOT-	216	145200	
MV-5	STA-42/	/	PASS-0053	ACQ-	216	223718	EOT-	217	075500	
MV-5	STA-61/	/	PASS-0053	ACQ-	217	065103	EOT-	217	144700	
MV-5	STA-42/	/	PASS-0054	ACQ-	217	223309	EOT-	218	064100	
MV-5	STA-61/	/	PASS-0054	ACQ-	218	064630	EOT-	218	144100	
MV-5	STA-42/	/	PASS-0055	ACQ-	218	233315	EOT-	219	074400	
MV-5	STA-61/	/	PASS-0055	ACQ-	219	064032	EOT-	219	173103	
MV-5	STA-11/	/	PASS-0055	ACQ-	219	170150	EOT-	219	210000	
MV-5	STA-42/	/	PASS-0056	ACQ-	219	203042	EOT-	220	074000	
MV-5	STA-61/	/	PASS-0056	ACQ-	220	063438	EOT-	220	172755	
MV-5	STA-61/	/	PASS-0057	ACQ-	221	063220	EOT-	220	172448	
MV-5	STA-61/	/	PASS-0058	ACQ-	222	062328	EOT-	222	172143	
MV-5	STA-11/	/	PASS-0058	ACQ-	222	172013	EOT-	223	011500	
MV-5	STA-61/	/	PASS-0059	ACQ-	223	061815	EOT-	223	171902	
MV-5	STA-42/	/	PASS-0060	ACQ-	223	201642	EOT-	224	072000	
MV-5	STA-61/	/	PASS-0060	ACQ-	224	061245	EOT-	224	171556	
MV-5	STA-11/	/	PASS-0060	ACQ-	224	163000	EOT-	225	003300	
MV-5	STA-42/	/	PASS-0061	ACQ-	224	232500	EOT-	225	071500	
MV-5	STA-61/	/	PASS-0061	ACQ-	225	060940	EOT-	225	171202	
MV-5	STA-42/	/	PASS-0062	ACQ-	225	201217	EOT-	226	071000	
MV-5	STA-61/	/	PASS-0062	ACQ-	226	060300	EOT-	226	170903	

Table IV-4 (contd)

Actual coverage provided									Requested vs actual coverage
MV-5	STA-14/12/	PASS-0062	ACQ-	226	153000	EOT-	226	220100	
MV-5	STA-42/ /	PASS-0063	ACQ-	226	213246	EOT-	227	060100	
MV-5	STA-61/ /	PASS-0063	ACQ-	227	055700	EOT-	227	170508	
MV-5	STA-42/ /	PASS-0064	ACQ-	227	213454	EOT-	228	055500	
MV-5	STA-61/ /	PASS-0064	ACQ-	228	055340	EOT-	228	170201	*Mariner V*—earth—*Mariner IV* radial solar position period (day 224 through day 233)
MV-5	STA-14/11/	PASS-0064	ACQ-	228	162200	EOT-	228	220000	
MV-5	STA-42/ /	PASS-0065	ACQ-	228	214056	EOT-	229	054500	
MV-5	STA-61/ /	PASS-0065	ACQ-	229	054655	EOT-	229	165844	Requested Class I coverage per SIRD — 2 passes/day
MV-5	STA-42/ /	PASS-0066	ACQ-	229	212735	EOT-	230	054000	
MV-5	STA-61/ /	PASS-0066	ACQ-	230	054224	EOT-	230	165530	Actual coverage — Average of 2.3 passes/day
MV-5	STA-42/ /	PASS-0067	ACQ-	230	213009	EOT-	231	053728	
MV-5	STA-61/ /	PASS-0067	ACQ-	231	053919	EOT-	231	165205	
MV-5	STA-14/11/	PASS-0067	ACQ-	231	165600	EOT-	232	000234	
MV-5	STA-42/ /	PASS-0068	ACQ-	231	212811	EOT-	232	053000	
MV-5	STA-61/ /	PASS-0068	ACQ-	232	053300	EOT-	232	164846	
MV-5	STA-42/ /	PASS-0069	ACQ-	232	211729	EOT-	233	052500	
MV-5	STA-61/ /	PASS-0069	ACQ-	233	052850	EOT-	233	164548	
MV-5	STA-42/ /	PASS-0070	ACQ-	233	212820	EOT-	234	052000	
MV-5	STA-61/ /	PASS-0070	ACQ-	234	052630	EOT-	234	164306	
MV-5	STA-14/11/	PASS-0070	ACQ-	234	152700	EOT-	234	220000	
MV-5	STA-42/ /	PASS-0071	ACQ-	234	211200	EOT-	235	052345	
MV-5	STA-61/ /	PASS-0071	ACQ-	235	052100	EOT-	235	154540	
MV-5	STA-11/ /	PASS-0071	ACQ-	235	154117	EOT-	235	221500	
MV-5	STA-42/ /	PASS-0072	ACQ-	235	210920	EOT-	236	051100	
MV-5	STA-61/ /	PASS-0072	ACQ-	236	051500	EOT-	236	163607	
MV-5	STA-11/ /	PASS-0072	ACQ-	236	152921	EOT-	236	220000	
MV-5	STA-42/ /	PASS-0073	ACQ-	236	210817	EOT-	237	051100	
MV-5	STA-61/ /	PASS-0073	ACQ-	237	050922	EOT-	237	163411	
MV-5	STA-42/ /	PASS-0074	ACQ-	237	205810	EOT-	238	0510	
MV-5	STA-61/ /	PASS-0074	ACQ-	238	050548	EOT-	238	163127	
MV-5	STA-42/ /	PASS-0075	ACQ-	238	205340	EOT-	239	050400	
MV-5	STA-61/ /	PASS-0075	ACQ-	239	050200	EOT-	239	162913	
MV-5	STA-42/ /	PASS-0076	ACQ-	239	205706	EOT-	240	045800	
MV-5	STA-61/ /	PASS-0076	ACQ-	240	050000	EOT-	240	162644	
MV-5	STA-42/ /	PASS-0077	ACQ-	240	204748	EOT-	241	052100	
MV-5	STA-61/ /	PASS-0077	ACQ-	241	051710	EOT-	241	162346	
MV-5	STA-14/ /	PASS-0077	ACQ-	241	163530	EOT-	241	220100	
MV-5	STA-42/ /	PASS-0078	ACQ-	241	204020	EOT-	242	044600	
MV-5	STA-61/ /	PASS-0078	ACQ-	242	045033	EOT-	242	162211	
MV-5	STA-11/ /	PASS-0078	ACQ-	242	164750	EOT-	242	204500	Transition period from radial to spiral position (day 234 through day 252)
MV-5	STA-42/ /	PASS-0079	ACQ-	242	203955	EOT-	243	045000	
MV-5	STA-61/ /	PASS-0079	ACQ-	243	044612	EOT-	243	162016	Requested Class I coverage per SIRD — 1 pass/day
MV-5	STA-42/ /	PASS-0080	ACQ-	243	203554	EOT-	244	054000	
MV-5	STA-61/ /	PASS-0080	ACQ-	244	052316	EOT-	244	151025	Actual coverage — Average of 2.13 passes/day
MV-5	STA-12/ /	PASS-0080	ACQ-	244	150000	EOT-	244	235513	
MV-5	STA-61/ /	PASS-0081	ACQ-	245	043722	EOT-	245	161513	
MV-5	STA-12/ /	PASS-0081	ACQ-	245	151041	EOT-	246	000300	
MV-5	STA-61/ /	PASS-0082	ACQ-	246	043303	EOT-	246	131647	
MV-5	STA-12/ /	PASS-0082	ACQ-	246	122650	EOT-	246	222833	
MV-5	STA-62/ /	PASS-0083	ACQ-	247	052900	EOT-	247	161500	
MV-5	STA-12/ /	PASS-0083	ACQ-	247	160000	EOT-	247	223000	
MV-5	STA-41/ /	PASS-0084	ACQ-	247	192130	EOT-	248	052500	
MV-5	STA-62/ /	PASS-0084	ACQ-	248	042500	EOT-	248	103000	
MV-5	STA-41/ /	PASS-0085	ACQ-	248	191402	EOT-	249	052300	
MV-5	STA-62/ /	PASS-0085	ACQ-	249	042100	EOT-	249	161200	
MV-5	STA-41/ /	PASS-0086	ACQ-	249	191200	EOT-	250	050000	
MV-5	STA-62/ /	PASS-0086	ACQ-	250	041800	EOT-	250	103000	
MV-5	STA-41/ /	PASS-0087	ACQ-	250	191025	EOT-	251	051500	
MV-5	STA-62/ /	PASS-0087	ACQ-	251	041000	EOT-	251	160800	
MV-5	STA-41/ /	PASS-0088	ACQ-	251	190806	EOT-	252	051200	
MV-5	STA-62/ /	PASS-0088	ACQ-	252	041000	EOT-	252	160600	
MV-5	STA-12/ /	PASS-0089	ACQ-	253	120930	EOT-	253	233000	
MV-5	STA-41/ /	PASS-0089	ACQ-	253	225400	EOT-	254	011000	
MV-5	STA-62/ /	PASS-0090	ACQ-	254	040000	EOT-	254	100600	
MV-5	STA-41/ /	PASS-0091	ACQ-	254	190303	EOT-	254	240000	
MV-5	STA-62/ /	PASS-0091	ACQ-	255	040453	EOT-	255	130000	Spiral *Mariner V*—earth—*Mariner IV* magnetic force line solar position period (day 253 through day 257)
MV-5	STA-14/12/	PASS-0091	ACQ-	255	115100	EOT-	255	220100	
MV-5	STA-62/ /	PASS-0092	ACQ-	256	040000	EOT-	256	120000	
MV-5	STA-12/ /	PASS-0092	ACQ-	256	130000	EOT-	256	200000	Requested Class I coverage — 2 passes/day
MV-5	STA-41/ /	PASS-0093	ACQ-	256	185855	EOT-	257	050000	
MV-5	STA-12/ /	PASS-0093	ACQ-	257	113715	EOT-	257	210000	Actual coverage — Average of 2 passes/day
MV-5	STA-41/ /	PASS-0094	ACQ-	257	185930	EOT-	258	050000	
MV-5	STA-62/ /	PASS-0094	ACQ-	258	035948	EOT-	258	125500	
MV-5	STA-12/ /	PASS-0094	ACQ-	258	113900	EOT-	258	231753	
MV-5	STA-62/ /	PASS-0095	ACQ-	259	035000	EOT-	259	125300	
MV-5	STA-14/12/	PASS-0095	ACQ-	259	113550	EOT-	259	220000	
MV-5	STA-62/ /	PASS-0096	ACQ-	260	035040	EOT-	260	125000	
MV-5	STA-12/ /	PASS-0096	ACQ-	260	113500	EOT-	260	220000	
MV-5	STA-62/ /	PASS-0097	ACQ-	261	040000	EOT-	261	130000	
MV-5	STA-14/12/	PASS-0097	ACQ-	261	113835	EOT-	261	220000	
MV-5	STA-41/ /	PASS-0098	ACQ-	261	225931	EOT-	262	060230	

Table IV-4 (contd)

Actual coverage provided									Requested vs actual coverage
MV-5	STA-62/	/	PASS-0098	ACQ-	262	050000	EOT-	262 130000	Spiral *Mariner V*–earth–*Mariner IV* magnetic force line solar position period during *Mariner V* 85-ft antenna grayout region (day 258 through day 268) Requested Class I coverage — 1 pass/day from DSS 14 Actual coverage — Average of 2.36 passes/day
MV-5	STA-14/12/		PASS-0098	ACQ-	262	114511	EOT-	262 220000	
MV-5	STA-41/	/	PASS-0099	ACQ-	262	210141	EOT-	263 060530	
MV-5	STA-62/	/	PASS-0099	ACQ-	263	050000	EOT-	263 130000	
MV-5	STA-12/	/	PASS-0099	ACQ-	263	120042	EOT-	263 220000	
MV-5	STA-41/	/	PASS-0100	ACQ-	263	210225	EOT-	264 055700	
MV-5	STA-14/12/		PASS-0100	ACQ-	264	115505	EOT-	264 220000	
MV-5	STA-12/	/	PASS-0101	ACQ-	265	120000	EOT-	265 220014	
MV-5	STA-62/	/	PASS-0102	ACQ-	266	033700	EOT-	266 130000	
MV-5	STA-12/	/	PASS-0102	ACQ-	266	124632	EOT-	266 220500	
MV-5	STA-41/	/	PASS-0103	ACQ-	266	221428	EOT-	267 055620	
MV-5	STA-62/	/	PASS-0103	ACQ-	267	050000	EOT-	267 130000	
MV-5	STA-12/	/	PASS-0103	ACQ-	267	122122	EOT-	267 220000	
MV-5	STA-41/	/	PASS-0104	ACQ-	267	220811	EOT-	268 055450	
MV-5	STA-62/	/	PASS-0104	ACQ-	268	050000	EOT-	268 124500	
MV-5	STA-12/	/	PASS-0104	ACQ-	268	114200	EOT-	268 194200	
MV-5	STA-41/	/	PASS-0105	ACQ-	268	184205	EOT-	269 040100	
MV-5	STA-62/	/	PASS-0105	ACQ-	269	032600	EOT-	269 123000	
MV-5	STA-12/	/	PASS-0105	ACQ-	269	113000	EOT-	269 193000	
MV-5	STA-41/	/	PASS-0106	ACQ-	269	183948	EOT-	270 040100	
MV-5	STA-62/	/	PASS-0106	ACQ-	270	032500	EOT-	270 154800	
MV-5	STA-62/	/	PASS-0107	ACQ-	271	032400	EOT-	271 123000	
MV-5	STA-12/	/	PASS-0107	ACQ-	271	113000	EOT-	271 193000	
MV-5	STA-41/	/	PASS-0108	ACQ-	271	184423	EOT-	272 040000	
MV-5	STA-11/	/	PASS-0108	ACQ-	272	121200	EOT-	272 225905	
MV-5	STA-42	/	PASS-0109	ACQ-	272	202300	EOT-	273 043100	
MV-5	STA-61/62/		PASS-0109	ACQ-	273	033000	EOT-	273 123000	
MV-5	STA-11/	/	PASS-0109	ACQ-	273	113300	EOT-	273 225900	Spiral *Mariner V*–earth–*Mariner IV* magnetic force line solar position period (day 269 through day 278) Requested Class I coverage — 2 passes/day Actual coverage — Average of 2.7 passes/day
MV-5	STA-41	/	PASS-0110	ACQ-	273	215717	EOT-	274 023001	
MV-5	STA-61	/	PASS-0110	ACQ-	274	083000	EOT-	274 123000	
MV-5	STA-11/	/	PASS-0110	ACQ-	274	112830	EOT-	274 225825	
MV-5	STA-42/	/	PASS-0111	ACQ-	274	202114	EOT-	275 043700	
MV-5	STA-61/	/	PASS-0111	ACQ-	275	033938	EOT-	275 123700	
MV-5	STA-11/	/	PASS-0111	ACQ-	275	113500	EOT-	275 203700	
MV-5	STA-42/	/	PASS-0112	ACQ-	275	200600	EOT-	276 043600	
MV-5	STA-61/	/	PASS-0112	ACQ-	276	040532	EOT-	276 124059	
MV-5	STA-11/	/	PASS-0112	ACQ-	276	120900	EOT-	276 203600	
MV-5	STA-42/	/	PASS-0113	ACQ-	276	200500	EOT-	277 043500	
MV-5	STA-61/	/	PASS-0113	ACQ-	277	035003	EOT-	277 124919	
MV-5	STA-12/	/	PASS-0113	ACQ-	277	120630	EOT-	277 173500	
MV-5	STA-41/	/	PASS-0114	ACQ-	277	184827	EOT-	278 032001	
MV-5	STA-61/	/	PASS-0114	ACQ-	278	034410	EOT-	278 120102	
MV-5	STA-11/	/	PASS-0114	ACQ-	278	112020	EOT-	278 195151	
MV-5	STA-42/	/	PASS-0115	ACQ-	278	185000	EOT-	279 032200	
MV-5	STA-62/	/	PASS-0115	ACQ-	279	031000	EOT-	279 112002	
MV-5	STA-11/	/	PASS-0115	ACQ-	279	111716	EOT-	279 194500	
MV-5	STA-14/	/	PASS-0115	ACQ-	279	114500	EOT-	279 145900	
MV-5	STA-41/	/	PASS-0116	ACQ-	279	191636	EOT-	280 041139	
MV-5	STA-62/	/	PASS-0116	ACQ-	280	031500	EOT-	280 114500	
MV-5	STA-41/	/	PASS-0117	ACQ-	280	191633	EOT-	281 035052	
MV-5	STA-62/	/	PASS-0117	ACQ-	281	031500	EOT-	281 114500	
MV-5	STA-12/	/	PASS-0117	ACQ-	281	111500	EOT-	281 164500	
MV-5	STA-42/	/	PASS-0118	ACQ-	281	183000	EOT-	282 024900	
MV-5	STA-61/	/	PASS-0118	ACQ-	282	040000	EOT-	282 130000	
MV-5	STA-11/	/	PASS-0118	ACQ-	282	114346	EOT-	282 210000	
MV-5	STA-42/	/	PASS-0119	ACQ-	282	195907	EOT-	283 043000	
MV-5	STA-61/	/	PASS-0119	ACQ-	283	031829	EOT-	283 130000	
MV-5	STA-14/	/	PASS-0119	ACQ-	283	110400	EOT-	283 163500	
MV-5	STA-11/	/	PASS-0119	ACQ-	283	120023	EOT-	283 210000	
MV-5	STA-42/	/	PASS-0120	ACQ-	283	201210	EOT-	284 043000	
MV-5	STA-61/	/	PASS-0120	ACQ-	284	031712	EOT-	284 130000	
MV-5	STA-12/	/	PASS-0120	ACQ-	284	120130	EOT-	284 210000	
MV-5	STA-41/	/	PASS-0121	ACQ-	284	195535	EOT-	285 050020	
MV-5	STA-61/	/	PASS-0121	ACQ-	285	031614	EOT-	285 100000	Period of *Mariner V* encounter testing using *Mariner IV* (day 279 through day 290) Requested Class I coverage — 1 pass/day Actual coverage — Continuous
MV-5	STA-12/	/	PASS-0121	ACQ-	285	120000	EOT-	285 210000	
MV-5	STA-62/	/	PASS-0122	ACQ-	285	040450	EOT-	286 130000	
MV-5	STA-41/	/	PASS-0122	ACQ-	285	195547	EOT-	286 050000	
MV-5	STA-14/11/		PASS-0122	ACQ-	286	105848	EOT-	286 224138	
MV-5	STA-11/	/	PASS-0122	ACQ-	286	111108	EOT-	286 181300	
MV-5	STA-12/	/	PASS-0122	ACQ-	286	114900	EOT-	286 180000	
MV-5	STA-41/	/	PASS-0123	ACQ-	286	195401	EOT-	287 050000	
MV-5	STA-62/	/	PASS-0123	ACQ-	287	040000	EOT-	287 130000	
MV-5	STA-14/	/	PASS-0123	ACQ-	287	105829	EOT-	287 224020	
MV-5	STA-11/	/	PASS-0123	ACQ-	287	111049	EOT-	287 224120	
MV-5	STA-12/	/	PASS-0123	ACQ-	287	120825	EOT-	287 190000	
MV-5	STA-41/	/	PASS-0124	ACQ-	287	195819	EOT-	288 050030	
MV-5	STA-62/	/	PASS-0124	ACQ-	288	040000	EOT-	288 130000	
MV-5	STA-14/	/	PASS-0124	ACQ-	288	105750	EOT-	288 205000	
MV-5	STA-12/	/	PASS-0124	ACQ-	288	115800	EOT-	288 210000	
MV-5	STA-41/	/	PASS-0125	ACQ-	288	200050	EOT-	289 050010	
MV-5	STA-62/	/	PASS-0125	ACQ-	289	040000	EOT-	289 130000	

Table IV-4 (contd)

Actual coverage provided	Requested vs actual coverage
MV-5 STA-14/ / PASS-0125 ACQ- 289 105700 EOT- 289 210000	
MV-5 STA-12/ / PASS-0125 ACQ- 289 120000 EOT- 289 210000	
MV-5 STA-41/ / PASS-0126 ACQ- 289 195908 EOT- 290 053000	
MV-5 STA-62/ / PASS-0126 ACQ- 290 040000 EOT- 290 140000	
MV-5 STA-14/ / PASS-0126 ACQ- 290 110034 EOT- 290 201855	
MV-5 STA-12/ / PASS-0126 ACQ- 290 120000 EOT- 290 223000	
MV-5 STA-42/ / PASS-0127 ACQ- 290 225320 EOT- 291 033000	
MV-5 STA-51/ / PASS-0127 ACQ- 291 015220 EOT- 291 112200	
MV-5 STA-62/ / PASS-0127 ACQ- 291 030248 EOT- 291 130000	
MV-5 STA-14/12/ PASS-0127 ACQ- 291 105718 EOT- 291 223500	
MV-5 STA-41/ / PASS-0128 ACQ- 291 235331 EOT- 292 053334	
MV-5 STA-42/ / PASS-0128 ACQ- 291 180700 EOT- 292 042602	
MV-5 STA-51/ / PASS-0128 ACQ- 292 014837 EOT- 292 125025	
MV-5 STA-62/ / PASS-0128 ACQ- 292 025941 EOT- 292 151826	
MV-5 STA-12/ / PASS-0128 ACQ- 292 104800 EOT- 292 224600	
MV-5 STA-14/ / PASS-0128 ACQ- 292 105630 EOT- 292 223404	
MV-5 STA-11/ / PASS-0128 ACQ- 292 111309 EOT- 292 224110	
MV-5 STA-41/ / PASS-0129 ACQ- 292 180808 EOT- 293 053447	
MV-5 STA-42/ / PASS-0129 ACQ- 292 180420 EOT- 293 042741	
MV-5 STA-51/ / PASS-0129 ACQ- 293 014905 EOT- 293 125250	
MV-5 STA-62/ / PASS-0129 ACQ- 293 030223 EOT- 293 151624	
MV-5 STA-12/ / PASS-0129 ACQ- 293 104830 EOT- 293 224500	
MV-5 STA-14/ / PASS-0129 ACQ- 293 110022 EOT- 293 223249	
MV-5 STA-11/ / PASS-0129 ACQ- 293 111510 EOT- 293 224050	
MV-5 STA-42/ / PASS-0130 ACQ- 293 180132 EOT- 294 042730	
MV-5 STA-41/ / PASS-0130 ACQ- 293 180246 EOT- 294 053540	
MV-5 STA-51/ / PASS-0130 ACQ- 294 014545 EOT- 294 125100	*Mariner V* encounter and tape playback period (day 291 through day 302)
MV-5 STA-62/ / PASS-0130 ACQ- 294 030420 EOT- 294 151444	
MV-5 STA-12/ / PASS-0130 ACQ- 294 104751 EOT- 294 223250	Requested Class I coverage — Continuous (plus DSS 13 and DSS 14 on encounter pass)
MV-5 STA-11/ / PASS-0130 ACQ- 294 165554 EOT- 294 224200	
MV-5 STA-41/ / PASS-0131 ACQ- 294 205652 EOT- 295 053400	Actual coverage — Continuous (plus DSS 13 and DSS 14 on encounter pass)
MV-5 STA-51/ / PASS-0131 ACQ- 295 042855 EOT- 295 120000	
MV-5 STA-14/12/ PASS-0131 ACQ- 295 105730 EOT- 295 222956	
MV-5 STA-41/ / PASS-0132 ACQ- 295 202833 EOT- 296 053600	
MV-5 STA-62/ / PASS-0132 ACQ- 296 040000 EOT- 296 120000	
MV-5 STA-12/ / PASS-0132 ACQ- 296 104800 EOT- 296 214500	
MV-5 STA-41/ / PASS-0133 ACQ- 296 212535 EOT- 297 053700	
MV-5 STA-62/ / PASS-0133 ACQ- 297 043000 EOT- 297 120000	
MV-5 STA-12/ / PASS-0133 ACQ- 297 120000 EOT- 297 195500	
MV-5 STA-41/ / PASS-0134 ACQ- 297 191215 EOT- 298 043030	
MV-5 STA-62/ / PASS-0134 ACQ- 298 031315 EOT- 298 123000	
MV-5 STA-12/ / PASS-0134 ACQ- 298 120000 EOT- 298 211500	
MV-5 STA-41/ / PASS-0135 ACQ- 298 193740 EOT- 299 043000	
MV-5 STA-62/ / PASS-0135 ACQ- 299 031630 EOT- 299 123000	
MV-5 STA-12/ / PASS-0135 ACQ- 299 123000 EOT- 299 173000	
MV-5 STA-41/ / PASS-0136 ACQ- 299 192104 EOT- 299 235500	
MV-5 STA-51/ / PASS-0136 ACQ- 300 015216 EOT- 300 125400	
MV-5 STA-62/ / PASS-0137 ACQ- 301 031421 EOT- 301 123000	
MV-5 STA-12/ / PASS-0137 ACQ- 301 123000 EOT- 301 203000	
MV-5 STA-41/ / PASS-0138 ACQ- 301 192718 EOT- 302 043500	
MV-5 STA-61/ / PASS-0138 ACQ- 302 032329 EOT- 302 112400	
MV-5 STA-12/ / PASS-0138 ACQ- 302 110000 EOT- 302 203000	
MV-5 STA-41/ / PASS-0139 ACQ- 302 192217 EOT- 303 043000	
MV-5 STA-41/ / PASS-0140 ACQ- 303 192447 EOT- 304 043000	
MV-5 STA-62/ / PASS-0140 ACQ- 304 032200 EOT- 304 123000	
MV-5 STA-12/ / PASS-0140 ACQ- 304 113000 EOT- 304 203100	
MV-5 STA-41/ / PASS-0141 ACQ- 304 192242 EOT- 305 035002	
MV-5 STA-62/ / PASS-0141 ACQ- 305 032300 EOT- 305 123000	
MV-5 STA-12/ / PASS-0141 ACQ- 305 115010 EOT- 305 180000	
MV-5 STA-12/ / PASS-0142 ACQ- 306 114000 EOT- 306 180000	
MV-5 STA-62/ / PASS-0143 ACQ- 307 032500 EOT- 307 123000	
MV-5 STA-12/ / PASS-0143 ACQ- 307 113100 EOT- 307 180000	
MV-5 STA-62/ / PASS-0144 ACQ- 308 033010 EOT- 308 123000	
MV-5 STA-12/ / PASS-0144 ACQ- 308 113000 EOT- 308 203000	
MV-5 STA-14/12/ PASS-0145 ACQ- 309 112112 EOT- 309 190500	
MV-5 STA-41/ / PASS-0146 ACQ- 309 192700 EOT- 310 043000	
MV-5 STA-62/ / PASS-0146 ACQ- 310 033000 EOT- 310 123000	
MV-5 STA-12/ / PASS-0146 ACQ- 310 113000 EOT- 310 203000	*Mariner IV* engineering test period (day 303 through day 319)
MV-5 STA-62/ / PASS-0147 ACQ- 311 033254 EOT- 311 123000	Requested Class I coverage — 1 pass/day
MV-5 STA-14/12/11 PASS-0147 ACQ- 311 111533 EOT- 311 160000	Actual coverage — Average of 1.8 passes/day
MV-5 STA-12/ / PASS-0148 ACQ- 312 113000 EOT- 312 160000	
MV-5 STA-41/ / PASS-0149 ACQ- 312 192011 EOT- 313 043000	
MV-5 STA-62/ / PASS-0149 ACQ- 313 033240 EOT- 313 121500	
MV-5 STA-12/ / PASS-0149 ACQ- 313 113000 EOT- 313 203000	
MV-5 STA-62/ / PASS-0150 ACQ- 314 033435 EOT- 314 123000	
MV-5 STA-12/ / PASS-0150 ACQ- 314 113000 EOT- 314 203000	
MV-5 STA-51/ / PASS-0151 ACQ- 315 052900 EOT- 315 113000	
MV-5 STA-12/ / PASS-0151 ACQ- 315 112930 EOT- 315 203000	
MV-5 STA-62/ / PASS-0152 ACQ- 316 033951 EOT- 316 123000	
MV-5 STA-14/12/ PASS-0152 ACQ- 316 113730 EOT- 316 210000	
MV-5 STA-62/ / PASS-0153 ACQ- 317 043000 EOT- 317 130000	
MV-5 STA-12/ / PASS-0153 ACQ- 317 120000 EOT- 317 220500	

Table IV-4 (contd)

Actual coverage provided	Requested vs actual coverage
MV-5 STA-51/ / PASS-0154 ACQ- 318 043200 EOT- 318 130000 MV-5 STA-62/ / PASS-0155 ACQ- 319 043000 EOT- 319 124500 MV-5 STA-12/ / PASS-0155 ACQ- 319 120000 EOT- 317 210000 MV-5 STA-62/ / PASS-0156 ACQ- 320 043000 EOT- 320 130000 MV-5 STA-12/ / PASS-0156 ACQ- 320 120000 EOT- 320 210000 MV-5 STA-51/ / PASS-0157 ACQ- 321 042500 EOT- 321 130000 MV-5 STA-62/ / PASS-0158 ACQ- 322 043000 EOT- 322 130000 MV-5 STA-41/ / PASS-0159 ACQ- 322 202826 EOT- 323 050010 MV-5 STA-62/ / PASS-0159 ACQ- 323 041826 EOT- 323 130000 MV-5 STA-14/12/ PASS-0159 ACQ- 323 115346 EOT- 323 210000 MV-5 STA-41/ / PASS-0160 ACQ- 323 202728 EOT- 324 050000 MV-5 STA-62/ / PASS-0160 ACQ- 324 035812 EOT- 324 130000 MV-5 STA-12/ / PASS-0160 ACQ- 324 123000 EOT- 324 222000 MV-5 STA-41/ / PASS-0161 ACQ- 324 235858 EOT- 325 050010 MV-5 STA-14/12/ PASS-0161 ACQ- 325 152154 EOT- 325 200000	*Mariner IV* engineering test period (day 320 through day 325) Requested Class I coverage — None Actual coverage — Average of 1.83 passes/day
MV-5 STA-14/ / PASS-0174 ACQ- 338 160200 EOT- 338 200000	*Mariner IV* engineering test period (day 338) Requested Class I coverage — None Actual coverage — 1 pass/4 hr

6. In-Flight Non-Critical—The periods during which primary or secondary objectives would not be adversely affected by loss of data or by non-completion of certain events.
7. Pre-Flight Non-Critical—The periods during which certain desirable but not mandatory activities should occur to enhance the attainment of mission objectives.
8. DSN Development—(Exclusive of critical flight support development or maintenance.)
9. Post-Flight Data Processing.

V. Priority Conflict Guidelines

In the case where two or more projects have an activity carrying equal priorities for DSN support beyond that expected to be available, the following guidelines shall be observed to resolve the conflict:

A. A planetary mission which has a fixed opportunity shall have priority over other missions with frequent or regular recurring opportunities.

B. During training and mission simulation tests, those projects with no prior flight experience shall have priority over those with previously successful missions.

C. The occurrence of unusual scientific opportunities, such as solar flare events, will be considered as in-flight semi-critical activity.

b. Exceptions to guidelines. The *Mariner* Venus 67 project reviewed *Guidelines for Scheduling of DSN Support for Lunar and Planetary Flight Missions.* The guidelines were acceptable with the following exceptions:

The priority classifications for the *Mariner* Venus 67 project will not be approved by the NASA Program Manager because of time limitations.

Existing and predicted limitations of DSN support were used in determining the requirements outlined in the *Mariner* Venus 67 project SIRD, dated February 3, 1967. The requirements outlined in previous editions of the *Mariner* Venus 67 project SIRD recognized no limitations.

Because of the nature of a planetary mission, many encounter tests are performed after launch. These tests fall into the same category as preflight critical and semi-critical tests. Dynamic tests involving the actual in-flight spacecraft are categorized as in-flight critical or semi-critical, but do not necessarily require critical scheduling.

All *Mariner V* tests prior to launch were considered as preflight critical and semi-critical tests. All pre-encounter tests were also classified in the same categories.

The classification of flight-coverage requirements for *Mariner V* were as follows:

(1) SIRD Class I requirements are in-flight critical.

(2) SIRD Class II requirements are in-flight semi-critical.

(3) SIRD Class III requirements are in-flight non-critical.

c. Priority conflicts with other missions. During preflight testing, in-flight testing, and in-flight operations of *Mariner V*, all priority conflicts were adequately resolved. All preflight critical and semi-critical test requirements were met. In-flight critical and in-flight semi-critical requirements established in the SIRD as Class I and Class II requirements, respectively, were satisfied.

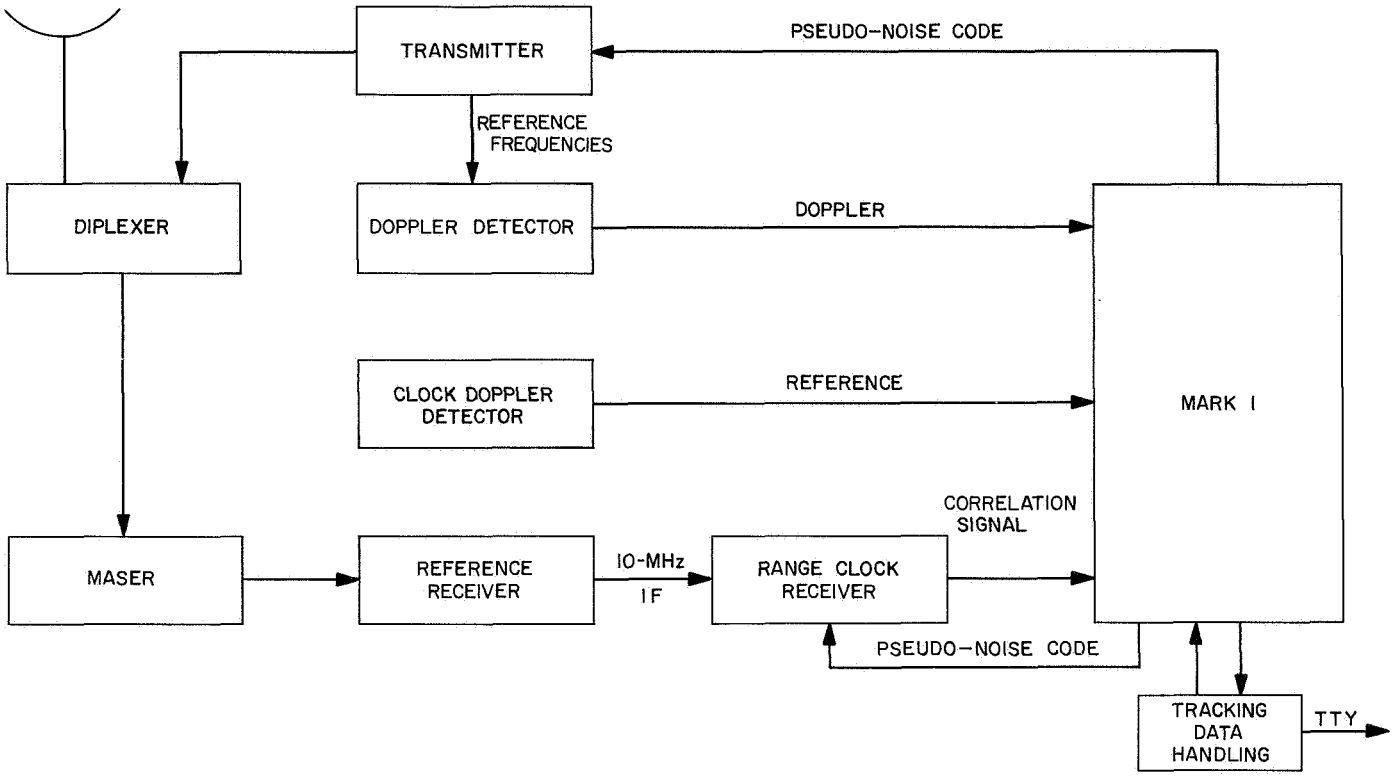


Fig. IV-25. Mark I ranging configuration

5. Mark I and Mark II ranging ground equipment configuration and utilization.

a. Mark I ranging. The *Mariner* Venus 67 mission was the first in-house mission to use the JPL-developed Mark IA pseudo-random code-ranging system. This was also the first time that the Mark IA system had been used to range a spacecraft beyond lunar distances.

The first DC-V9 (turn ranging on) command was transmitted by DSS 11 on day 171 at 02:39:00 GMT. The Mark IA ranging system first became active on day 171 during the DSS 61 pass. Ranging modulation was applied at 11:32:58 GMT, and the ranging receiver was in lock at 11:33:34 GMT. The first range code was acquired at 12:11:00 GMT.

The Mark IA ranging system was used through L+22 days. At L+23 days, an unsuccessful attempt to range on the spacecraft occurred. On July 10, 1967 (L+25 days), a decision was made to attempt no further ranging with the Mark IA system. All ranging accomplished after this date would employ the Mark II research and development (R&D) ranging subsystem.

The Mark IA system ranged to a distance of 6×10^6 km from earth to an accuracy of approximately 45 m.

Figure IV-25 is a block diagram of the Mark IA ranging system. Table IV-5 gives a summary of the ranging data.

b. Mark II ranging. The Mark II ranging subsystem was designed and developed as one of the *Mariner* Venus 67 mission experiments. The purpose of this experiment was to range on the *Mariner V* spacecraft in the vicinity of Venus and thus to refine the astronomical unit. The R&D ranging subsystem was installed at DSS 14 in May 1967. Figure IV-26 is a block diagram of the Mark II ranging subsystem. One of the major interfaces between Mark II ranging and the GSDS receiver was to replace the 20-MHz free-running oscillator in the receiver with a 10-MHz signal and the required multipliers, which were coherently related to the station rubidium standard and developed in the Mark II ranging subsystem. This coherent reference signal was also required and used for the occultation experiment.

The first ranging operation on the *Mariner V* spacecraft took place on June 21, 1967. Valid range numbers were observed, except for a 3-μs difference between engineering predicts and range numbers. This was attributed to two factors: (1) predicts did not include spacecraft delay (933 ns) and (2) the station delay was unknown. The R&D

Table IV-5. Mark I ranging data summary

Start time		End time		Standard deviation, m	DSS No.	Start time		End time		Standard deviation, m	DSS No.
Day	Time, GMT	Day	Time, GMT			Day	Time, GMT	Day	Time, GMT		
171	19:41:02	171	20:02:02	17.4	61	177	20:22:02	178	02:33:02	44.9	11
171	21:29:02	172	03:49:02	31.5	11	178	07:36:02	178	10:52:02	22.1	42
172	04:10:02	172	08:50:02	17.5	41	178	11:36:02	178	18:24:02	30.9	61
172	19:46:02	173	02:05:02	21.6	11	178	19:17:02	179	02:52:12	32.8	11
173	03:24:02	173	10:44:02	23.3	41	179	04:13:02	179	10:53:12	39.9	42
173	11:33:02	173	18:45:02	20.8	61	179	12:15:02	179	18:51:02	31.9	61
173	19:18:02	174	03:19:02	32.9	11	179	19:59:02	180	01:49:02	39.6	11
174	11:19:02	174	19:01:02	41.4	61	180	02:33:42	180	08:53:02	37.4	42
174	19:30:02	175	00:59:02	39.2	11	180	10:44:42	180	17:35:02	39.4	61
175	01:35:02	175	05:46:02	31.1	42	181	20:27:01	182	00:50:02	38.1	12
176	03:34:02	176	10:46:02	30.2	42	182	02:10:42	182	09:44:02	41.6	42
176	11:31:02	176	18:00:02	27.8	61	182	19:54:02	183	02:45:02	41.4	12
176	19:01:02	177	01:33:02	36.7	11	183	03:52:02	183	10:24:02	46.8	42
177	02:21:02	177	09:07:02	32.5	42	187	03:22:02	187	09:32:02	39.5	42
177	11:08:02	177	18:55:02	45.2	61	187	12:42:02	187	15:00:02	45.3	62

ranging operations continued routinely until about mid-August, when range data and predicts were in gross disagreement. This prompted redesigning of the subsystem range coders. It was subsequently discovered that the predicts were in error; however, the redesign resulted in a system that was less susceptible to noise. Because of code-acquisition time (a function of signal level), ranging was not attempted on *Mariner V* until after the spacecraft had switched to its high-gain antenna. Ranging on the *Mariner V* spacecraft was next accomplished on October 4, 1967 (day 277).

The value of the Mark II ranging experiment data was greatly enhanced as the spacecraft approached the planet Venus. The encounter sequence was initially planned to stop ranging some 4 h before encounter to allow the command loop to be locked up. To obtain maximum value from the ranging data, a test was proposed to ascertain whether the station uplink could be modulated by command and ranging modulation signals simultaneously, and to determine whether there was any interaction between the two. On October 6, 1967, DSS 14 locked up the spacecraft command loop and ranged the spacecraft. No interaction was observed. Later analysis showed that there was no significant difference between range data with and without command modulation. During the mission, no commands were transmitted with ranging modulation applied. Ranging on the *Mariner V* spacecraft was performed up to 1 h before encounter. Ranging on the spacecraft was accomplished to a distance of 98 million km, with an accuracy of approximately 10 m.

Table IV-6 gives a summary of the Mark II ranging data.

Tables IV-7 and IV-8 give a summary of Mark I and Mark II DSS activities as taken from station post-track reports.

B. Organization and Functions

1. Flight-path analysis and command. The FPAC team was responsible for determining the best estimate of the orbit of the spacecraft based upon tracking and appropriate telemetry data. This orbit was then supplied, in proper formats, to various users. It was also used to generate other data, as described below. Figure IV-27 indicates the functions performed during the mission.

The organization of the FPAC team and its interfaces with other functional groups are shown in Fig. IV-28. Each organizational group had a specific set of tasks.

Table IV-6. Mark II ranging data summary

Start time		End time		Standard deviation, m	DSS No.
Day	Time, GMT	Day	Time, GMT		
172	20:40:02	172	21:12:02	7.98	14
191	18:46:02	191	21:50:02	84.15	14
203	19:56:02	204	01:56:02	84.00	14
204	19:39:02	205	02:00:02	88.65	14
209	22:55:02	209	23:40:02	117.30	14
279	12:38:02	279	14:53:02	537.00	14
286	12:04:00	286	21:50:02	840.00	14
287	13:40:22	287	22:17:02	1192.50	14
291	15:06:32	291	21:13:42	880.50	14
292	13:06:02	292	21:37:52	1359.00	14
293	18:45:52	293	21:31:02	769.50	14
295	12:31:02	295	21:08:02	961.50	14
309	13:11:02	309	17:51:03	1087.50	14

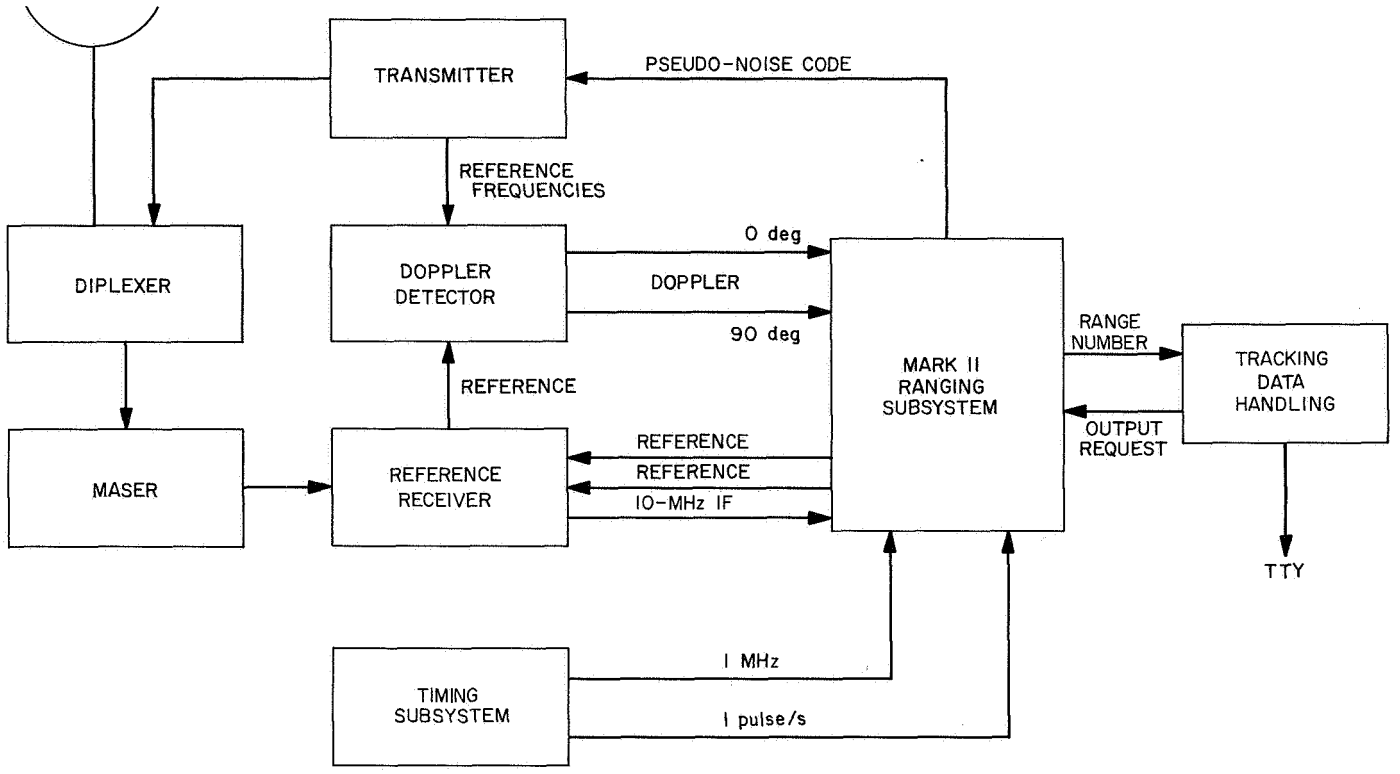


Fig. IV-26. Mark II ranging configuration

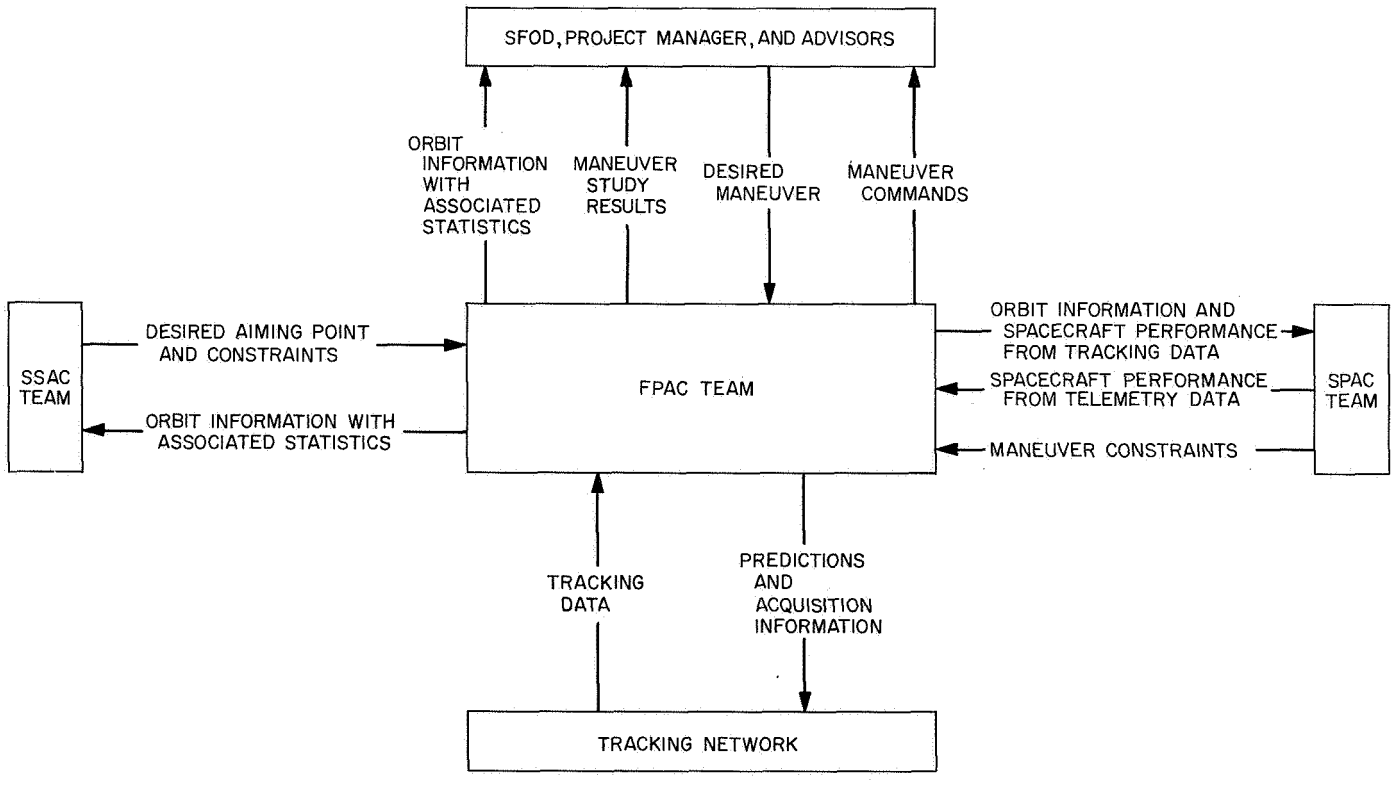


Fig. IV-27. Functions performed by the FPAC team

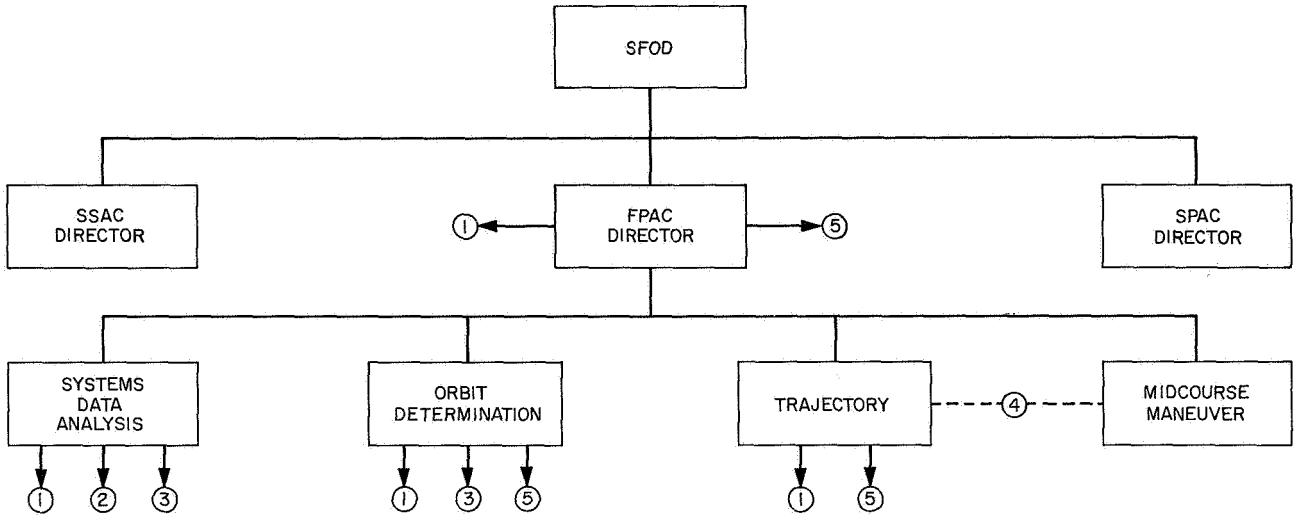


Fig. IV-28. FPAC organization

a. Systems data analysis group. The responsibilities of the systems data analysis (SDA) group are described in the paragraphs that follow.

Before launch, spacecraft transponder characteristics have been calibrated, and tracking predictions are sent to the station for a large set of nominal trajectories.

Just before liftoff, final measurements are made at the Cape Kennedy Deep Space Station (DSS 71). These measurements are used by the SDA group, in conjunction with the radio system analyst on the SPAC team, to predict the spacecraft frequency as a function of time after launch. This frequency is then used to generate predicted frequencies for the tracking stations to aid in signal acquisition. Subsequently, these predictions are updated whenever new information becomes available (e.g., after launch, after a maneuver, etc.).

A printed display of the incoming data is monitored in real time to evaluate the degree to which the actual signal characteristics conform to the predicted values. Pseudo-residuals (defined as the difference between observed and predicted measurements) are automatically plotted in real time to aid in this monitoring effort.

b. Orbit determination group. The responsibilities of the orbit determination group are described below.

Tracking data are accumulated and used to estimate the orbital parameters. As soon as possible after launch, data-consistency checks are performed by fitting to various subsets of the tracking data (e.g., all data are used except those from DSS 41; another orbit is then fitted with all data except those from DSS 51). If any systematic differences are detected, remedial action is recommended.

As late as possible before the maneuver (so as to use the most up-to-date tracking data), a final orbit is estimated and used to compute the actual maneuver that is performed. After the maneuver has been performed, and sufficient tracking data are accumulated, a postmaneuver orbit is estimated. A comparison of these two orbits makes an accurate estimate of the maneuver performance possible (real-time telemetry gives the first indication; the comparison of orbits is generally more precise).

Before encounter, orbits are estimated in rapid succession to observe the spacecraft acceleration, which is very sensitive to the exact encounter geometry. Approximately 4 h before encounter, the latest orbit is used to determine the times at which backup commands should be sent to the spacecraft to ensure that the desired encounter sequence will be carried out.

Table IV-7. Mark I ranging (DSS post-track reports)

Pass	Day	Time, GMT	Station	Comments
07	171	11:32:58	DSS 61	Ranging modulation on.
		11:33:34		Ranging receiver in lock.
		12:11:00		Ranging code acquired.
		12:25:00		Ranging modulation off.
		12:25:18		Ranging receiver out of lock.
		12:35:00		Ranging modulation on.
		12:35:19		Ranging receiver in lock.
		16:05:00		Ranging code acquired.
		16:50:40		Ranging code acquired.
		20:10:00		Ranging modulation off. Time-correlation test complete.
		20:10:19		Ranging receiver out of lock.
		20:25:14		Ranging receiver in lock.
		20:26:17		Ranging modulation on.
		20:27:21		Ranging modulation off.
08	172	04:04:23	DSS 41	Ranging modulation on.
		04:09:57		Ranging acquired.
		04:20:00		Time-correlation commenced.
		04:25:00		Time-correlation completed.
		09:00:00		Ranging modulation off.
08	172	15:17:50	DSS 61	Ranging modulation on.
		15:30:35		Ranging to test mode.
		15:31:50		Ranging to normal.
		15:35:25		Ranging modulation off.
		19:48:00		Ranging receiver in lock.
		19:54:00		Ranging modulation on.
		20:14:43		Ranging modulation off.
09	173	03:11:09	DSS 41	Ranging modulation on.
		03:15:20		Ranging acquired.
		03:33:00		Time-correlation commenced.
		03:38:00		Time correlation completed.
09	173	11:06:00	DSS 61	Ranging modulation on.
		11:16:07		Ranging receiver in lock.
		11:32:35		Acquired ranging code.
		11:39:00		Good ranging number acquired.
		15:24:27		Ranging receiver in lock.
		15:29:27		Acquired ranging code; bad number.
		15:34:10		Acquired ranging code; good number.
		15:39:10		Acquired ranging code; bad number.
		15:44:15		Acquired ranging code; good number.
		15:49:20		Acquired ranging code; good number.
		18:50:00		Ranging modulation off.
		18:50:26		Ranging receiver out of lock.
		19:00:05		Ranging modulation on.
		19:08:04		Ranging receiver in lock.
		19:08:08		Ranging receiver out of lock.
		19:14:30		Ranging receiver in lock.
		19:18:40		Acquired ranging code.
		19:23:10		Acquired ranging code; bad number.
		19:28:05		Acquired ranging code; bad number.
		19:30:00		Acquired ranging code; bad number.
		19:33:00		Acquired ranging code; bad number.
		19:40:30		Ranging receiver out of lock.
		19:43:21		Ranging receiver in lock.
		19:47:00		Acquired ranging code; bad number.
		19:55:00		Acquired ranging code; bad number.

Table IV-7 (contd)

Pass	Day	Time, GMT	Station	Comments
10	174	03:07:00	DSS 42	DSS 11 ranging receiver locked.
				DSS 42 no ranging receiver lock.
		03:18:00		No ranging signal into DSS 42. Time correlation put off until after DSS 42 acquires two-way.
		03:38:00		Ranging modulation on.
		03:40:00		Ranging receiver not in lock.
		03:42:00		DSS 11 ranging receiver in lock. DSS 42 still unable to acquire ranging.
		05:53:00		Still investigating ranging fault.
		08:15:40		Ranging modulation off for testing.
		08:16:38		Ranging modulation on.
		08:20:20		Ranging modulation off.
		08:23:20		Ranging modulation on.
		08:51:37		Ranging modulation off.
		09:02:45		Ranging modulation on.
		09:40:00		Ranging code acquired.
		10:45:00		Ranging modulation to clock only.
		10:50:00		Ranging modulation off.
		10:50:21		Ranging receiver out of lock.
		11:10:38		Ranging receiver in lock with 61 code.
10	174	10:41:44	DSS 61	Ranging receiver in lock.
		10:50:26		Ranging receiver out of lock.
		11:10:00		Ranging modulation on.
		11:10:56		Ranging receiver in lock.
		18:51:00		Started time correlation test with DSS 11.
		18:56:00		Completed time correlation test with DSS 11.
		19:00:00		Started time-correlation test with DSS 11.
		19:03:00		Completed time-correlation test with DSS 11.
		19:06:09		Ranging modulation off.
		19:06:30		Ranging receiver out of lock.
		19:16:22		Ranging modulation on.
		19:21:01		Ranging receiver in lock.
		19:53:00		Started time-correlation test with DSS-11.
		19:58:00		Completed time-correlation test with DSS-11.
		20:02:00		Started time-correlation test with DSS 11.
		20:05:00		Completed time-correlation test with DSS 11.
11	175	00:43:46	DSS 42	Ranging modulation on.
		01:02:00		Time correlation with DSS 11.
		01:09:00		Ranging modulation off.
		01:25:00		Ranging modulation on.
		01:25:50		Ranging receiver in lock.
		01:35:09		Acquired ranging code; good ranging number.
		01:46:00		Acquired ranging code; good number.
		01:49:00		Time correlation for 5 min.
		05:50:00		Ranging modulation off.
		05:58:20		Cyclic event ranging off on spacecraft.
12	176	03:17:12	DSS 42	Ranging modulation on.
		03:24:00		Ranging receiver in lock.
		03:34:00		Good ranging number.
		03:35:00		Ranging number bad. Lost clock lock.
		03:46:02		Good ranging number.
		04:22:00		Good ranging number.
		04:34:00		Dropped clock lock.
		04:44:00		Dropped clock lock.
		05:39:15		Ranging code off. Radiating ranging clock only.
		09:40:50		Ranging receiver out of lock.

Table IV-7 (contd)

Pass	Day	Time, GMT	Station	Comments
12	176	09:45:40	DSS 42	Ranging code on.
		09:45:50		Reset ranging.
		09:46:59		Ranging receiver in lock.
		09:48:00		Started to acquire ranging code.
		09:56:00		Acquired ranging code.
		10:48:25		Ranging modulation off.
12	176	10:33:55	DSS 61	Ranging receiver in lock.
		18:05:25		Ranging receiver out of lock.
13	177	00:10:20	DSS 42	Acquired ranging code. Interrogation switch 14.
		00:43:29		Acquired ranging code.
		00:43:50		Started second ranging code acquisition.
		00:53:00		Acquired ranging code.
		00:54:00		Starting third acquisition. Interrogation switch 15.
		01:28:00		Ranging code acquisition unsuccessful.
		01:51:18		Ranging modulation on.
		03:42:00		Ranging code out of lock.
		04:57:00		Ranging modulation off.
		05:05:00		Ranging modulation on. Commence code acquisition.
		05:24:02		Ranging code acquisition; good number. Ranging code off. On clock.
		05:57:00		Lost ranging clock lock. Acquiring ranging code.
		06:11:02		Ranging code acquired; good number. Ranging code off. On clock.
		06:21:00		Ranging code lost.
		06:34:14		Ranging code acquired.
		08:24:00		Clock lock lost.
		08:37:00		Ranging code acquired. Back to clock only radiated.
		09:21:00		Dropped clock lock; reacquiring.
		09:49:30		Ranging code acquired. False acquisition; reacquiring.
		10:44:00		Ranging modulation off.
13	177	10:58:37	DSS 61	Ranging modulation on.
		10:59:10		Ranging receiver in lock.
		18:53:00		Started time correlation.
		19:02:00		Completed time correlation.
		19:05:00		Ranging modulation off.
		19:05:31		Ranging receiver out of lock.
14	178	02:00:00	DSS 42	Ranging receiver in lock.
		02:10:00		Started ranging code acquisition; switch position 14.
		02:20:20		Acquired ranging code. Ready for time correlation.
		02:23:00		Start time correlation for 5 min.
		02:38:00		Start time correlation for 3 min.
		02:39:29		Ranging receiver out of lock. DSS 11 ranging modulation off at 20:39.
		07:08:00		Ranging modulation on.
		08:22:30		Code acquired. Interrogation No. 14.
		08:32:00		Clock modulation only.
		10:19:30		Ranging code on.
		10:48:00		Time correlation with DSS 61.
		10:53:56		Ranging receiver out of lock.
14	178	10:18:10	DSS 61	Ranging modulation on.
		10:48:00		Time-correlation test started with DSS 42.
		10:53:00		Time-correlation test completed with DSS 42.
		10:53:30		Ranging modulation off.
		11:19:00		Ranging modulation on.
		11:19:25		Ranging receiver in lock.
		12:13:04		Ranging modulation off.

Table IV-7 (contd)

Pass	Day	Time, GMT	Station	Comments
14	178	13:41:10	DSS 61	Ranging modulation on.
		13:41:45		Ranging receiver in lock.
		18:20:00		Time-correlation test started with DSS 11.
		18:28:00		Time-correlation test completed with DSS 11.
		18:30:00		Ranging modulation off.
		18:30:29		Ranging receiver out of lock.
15	179	02:12:40	DSS 42	Ranging receiver in lock.
		02:23:00		Code acquired ranging No. 1781.
		02:32:00		Code acquired ranging No. 1576.
		02:55:00		Ranging modulation off.
		03:20:00		Ranging modulation on.
		03:21:00		Ranging receiver in lock.
		03:55:00		Ranging receiver lock broken as ranging numbers wrong.
		04:04:00		Ranging receiver in lock.
		04:14:00		Ranging numbers as per predicts.
		05:00:00		Ranging modulation on.
		05:03:00		Ranging receiver in lock.
		05:14:00		Ranging number good as per predict.
		05:23:30		Ranging number good as per predict.
		10:00:00		Ranging interrogation setting 15.
		10:53:00		Start time correlation check with DSS 61.
		11:00:00		Complete time correlation.
		11:01:00		Ranging modulation off.
		11:09:08		Ranging receiver out of lock.
15	179	10:11:35	DSS 61	Ranging modulation on.
		10:17:23		Ranging receiver in lock.
		11:01:00		Ranging modulation off.
		11:01:33		Ranging receiver out of lock.
		11:23:50		Ranging modulation on.
		11:24:29		Ranging receiver in lock.
		18:50:00		Started time-correlation test with DSS 11.
		18:55:00		Completed time-correlation test with DSS 11.
		18:55:20		Ranging modulation off.
		18:55:58		Ranging receiver out of lock.
16	180	02:22:00	DSS 42	Ranging modulation on.
		02:28:00		Ranging VCO reads 498.606.4 Hz.
		02:34:00		Ranging code acquired; good number.
		02:54:00		Ranging code acquired; good number.
		03:03:00		Start time correlation with DSS 11.
		03:09:00		End time correlation.
		03:17:00		Time-correlation numbers look wrong. Counter probably triggering incorrectly.
		10:00:00		Ranging modulation off.
		10:28:27		Ranging modulation on. Interrogation switch 14.
		10:40:30		Code acquired.
		10:44:00		Reset and reacquired code.
		10:52:00		Code acquisition.
		10:53:00		Start time correlation with DSS 61.
		10:54:00		Two codes do not agree.
		10:59:00		Time correlation complete.
		11:05:02		Ranging receiver out of lock.
16	180	10:28:00	DSS 61	Ranging modulation on.
		10:53:00		Started time-correlation test with DSS 42.
		10:59:00		Completed time-correlation test with DSS 42.
		17:40:00		Ranging modulation off.
		17:40:35		Ranging receiver out of lock.

Table IV-7 (contd)

Pass	Day	Time, GMT	Station	Comments
16	180	18:27:57	DSS 61	Ranging modulation on.
		18:30:24		Ranging receiver in lock.
		18:30:25		Ranging receiver out of lock.
		18:31:00		Ranging receiver in lock.
		19:05:00		Ranging modulation off.
		19:05:31		Ranging receiver out of lock.
17	181/182	20:00:00	DSS 12	Ranging modulation on.
		20:15:30		Ranging receiver in lock.
		20:27:01		Acquired ranging code.
		00:55:00		Ranging modulation off.
		01:22:30		Ranging modulation on.
		01:39:38		Acquired ranging code.
		02:17:00		Started time-correlation test with DSS 42.
		02:22:00		Completed time-correlation test with DSS 42.
		02:44:59		Acquired ranging code.
		02:49:00		Started time-correlation with DSS 42.
		02:54:00		Completed time-correlation check.
18	182	01:22:02	DSS 42	Ranging modulation on.
		01:32:20		Ranging receiver in lock. VCO 498.606.8 Hz.
		01:53:00		Ranging receiver malfunctioning.
		02:22:15		Time correlation completed with DSS 12. Started reacquisition code.
		02:27:00		Ranging receiver malfunctioning.
		02:44:55		Ranging code acquired.
		02:54:00		Time correlation with DSS 12.
		09:51:00		Ranging modulation off.
		10:33:00		Ranging modulation on. Ranging receiver in lock.
		10:35:00		Ranging receiver malfunctioning.
		10:57:10		Ranging receiver malfunctioning.
		10:57:45		Ranging modulation off.
18	182	10:16:00	DSS 61	Ranging modulation on.
		15:00:30		Ranging receiver in lock.
		15:33:56		Ranging receiver malfunctioning.
		15:38:44		Ranging receiver malfunctioning.
		15:41:44		Ranging receiver malfunctioning.
		15:52:06		Ranging receiver malfunctioning.
		15:53:52		Ranging receiver malfunctioning.
		15:57:11		Ranging receiver malfunctioning.
		16:49:15		Ranging receiver malfunctioning.
		16:50:15		Ranging receiver malfunctioning.
		16:52:48		Ranging receiver malfunctioning.
		16:53:08		Ranging receiver malfunctioning.
		16:54:19		Ranging receiver malfunctioning.
		16:57:00		Ranging to clock mode.
		17:13:00		Ranging clock acquisition.
		17:17:00		Back to code mode.
		17:18:38		Ranging receiver malfunctioning.
		17:21:12		Ranging receiver malfunctioning.
		17:31:14		Ranging receiver malfunctioning.
		18:04:50		Ranging receiver malfunctioning.
		18:24:00		Ranging modulation off.
		18:24:34		Ranging receiver out of lock.
18	182/183	18:06:29	DSS 12	Ranging modulaton on.
		18:24:00		Ranging modulation off.
		18:36:50		Ranging modulation on.
		18:40:55		Ranging receiver in lock.
		18:54:00		Acquired ranging code; interrogation setting 16.

Table IV-7 (contd)

Pass	Day	Time, GMT	Station	Comments
18	182/183	02:53:00	DSS 12	Ranging modulation off.
		02:53:38		Ranging receiver out of lock.
19	183	02:30:00	DSS 42	Ranging code acquired.
		02:31:50		Reset and reacquisition code.
		02:49:00		*Ranging code acquired; not same first 3 digits as before.*
		02:53:00		Time correlation complete with DSS 12.
		02:53:39		Ranging receiver out of lock.
		03:15:00		Ranging modulation on.
		03:51:15		Ranging code acquired; interrogation switch 15.
		10:33:00		*Ranging modulation off.*
23	187	00:50:00	DSS 42	Ranging modulation on.
		01:04:30		Ranging receiver in lock.
		03:22:00		Acquisition ranging code; good number.
		03:22:10		Ranging code only radiated.
		09:42:00		Ranging modulation off.
		10:01:00		Ranging modulation on.
		10:07:20		Ranging modulation off.
24	188	23:26:00	DSS 41	Ranging modulation on. Several ranging acquisitions made, but no good acquisitions obtained.
26	190/191	03:20:00	DSS 41	Ranging modulation on.
		09:44:47		Ranging modulation off.

Table IV-8. Mark II ranging (DSS post-track reports)

Pass	Day	Time, GMT	Station	Comments
08	172	20:32:00	DSS 14	Ranging modulation on.
		20:37:00		Ranging first acquisition completed.
		20:39:28		Ranging second acquisition completed.
		21:02:00		Ranging third acquisition completed.
		21:20:00		Ranging modulation off.
		22:20:00		Ranging modulation on.
		22:22:34		Ranging first acquisition completed.
		22:24:28		Ranging second acquisition completed.
25	189	20:25:31	DSS 12	Ranging modulation on.
		21:35:42		Ranging modulation off.
27	191	17:33:50	DSS 14	Ranging loop in lock; test completed.
		18:08:02		Ranging modulation on.
		18:14:20		Acquired ranging modulation.
		18:17:00		Reacquired ranging modulation.
		18:28:10		Reacquired ranging modulation.
		18:30:00		Reacquired ranging modulation.
		19:30:25		Ranging in lock.
		19:40:00		Ranging out of lock.
		19:43:40		Ranging in lock.
		20:00:00		Ranging out of lock.
		20:03:00		Ranging in lock.
		21:53:00		Ranging modulation off.
39	203/204	19:47:00	DSS 14	Ranging modulation on.
		19:55:00		Ranging in lock.
		20:10:50		Ranging out of lock.
		20:22:18		Ranging in lock.
		22:54:59		Ranging out of lock due to power surge.

Table IV-8 (contd)

Pass	Day	Time, GMT	Station	Comments
39	203/204	23:15:35	DSS 14	Ranging in lock; data condition 4.
		01:59:00		Ranging modulation off.
40	204	19:25:00	DSS 14	Ranging modulation on.
		19:28:37		Ranging in lock; data condition 6.
45	209	18:54:30	DSS 14	Ranging modulation on.
		20:21:00		Ranging modulation on.
		20:30:00		Ranging modulation on.
		20:39:10		Ranging modulation off.
		21:19:20		Ranging modulation on.
		22:34:30		Ranging modulation on.
		23:48:00		Ranging indicating false lock.
		23:50:00		Ranging modulation off. Ranging terminated.
115	279	12:25:00	DSS 14	Ranging modulation on.
		12:40:00		Ranging in lock.
		13:03:00		Ranging modulation off.
		13:27:00		Ranging modulation on.
		13:51:45		Ranging in lock.
		14:16:00		Ranging modulation off.
		14:18:00		Ranging modulation on.
		14:20:00		Ranging modulation off.
		14:22:00		Ranging modulation on.
		14:24:00		Ranging modulation off.
		14:26:00		Ranging modulation on.
		14:28:00		Ranging modulation off.
		14:30:00		Ranging modulation on.
		14:43:00		Ranging in lock.
119	283	11:46:00	DSS 14	Ranging modulation on.
		12:17:00		Ranging modulation off.
		13:07:00		Ranging modulation on.
		13:20:00		Ranging acquired.
119	283	13:40:00	DSS 14	Ranging modulation off.
		15:50:00		Ranging modulation on.
		16:12:00		Ranging modulation off.
122	286	13:04:00	DSS 14	Ranging modulation on.
		13:19:00		TDH patched wrong in last range digit—TFR 101703.
		13:30:56		Reacquired ranging.
		13:41:00		Ranging modulation off.
		14:05:00		Ranging modulation on.
		14:17:01		Ranging acquisition.
		14:43:00		Ranging computer failed—reprogrammed.
		14:47:00		Ranging modulation off.
		16:49:00		Ranging modulation on.
		17:00:46		Ranging in lock.
		18:12:07		Ranging out of lock.
		18:15:51		Ranging in lock.
		19:01:06		Ranging out of lock for reacquisition.
		19:05:28		Ranging acquired.
		20:00:00		Ranging out of lock for reacquisition.
		20:03:15		Ranging acquired.
		21:00:00		Ranging out of lock for reacquisition.
		21:03:37		Ranging acquired.
		21:56:00		Ranging modulation off.
		22:01:15		Ranging out of lock.
125	289	10:34:00	DSS 14	Ranging precals complete.
		13:45:00		Ranging modulation on.
		16:37:00		Ranging modulation on.
		16:48:20		Ranging acquired.

Table IV-8 (contd)

Pass	Day	Time, GMT	Station	Comments
125	289	17:05:00	DSS 14	Ranging out of lock for reacquisition.
		17:07:25		Ranging acquired.
		17:24:00		Ranging modulation off.
		19:00:00		Ranging modulation on.
		19:13:17		Ranging acquired.
		19:48:21		Ranging modulation off.
126	290	15:05:00	DSS 14	Ranging modulation on.
		15:23:38		Ranging acquired.
		16:24:00		Ranging modulation off.
		17:32:00		Ranging modulation on.
		17:48:51		Ranging acquired.
127	291	12:00:00	DSS 14	Ranging modulation on.
		12:14:47		Acquired ranging lock.
		12:26:41		Reacquired ranging lock.
		13:30:00		Started ranging reacquisition.
		13:34:08		Reacquired ranging lock.
		14:30:00		Started ranging reacquisition.
		14:34:08		Acquired ranging code; good data.
		15:30:00		Started ranging reacquisition.
		15:34:08		Ranging acquired.
		16:30:00		Started ranging reacquisition.
		16:35:08		Ranging acquired.
		17:29:00		Ranging modulation off.
		18:04:00		Ranging modulation on.
		18:17:06		Ranging acquired.
		20:14:00		Ranging modulation off.
		20:59:03		Ranging modulation on.
		21:13:27		Ranging acquired.
		21:24:00		Ranging modulation off.
128	292	12:35:00	DSS 14	Ranging modulation on.
		12:48:35		Ranging acquired.
		12:53:55		Ranging out of lock for reacquisition.
		14:20:00		Ranging modulation off.
		15:47:22		Ranging modulation on.
		16:00:24		Ranging acquired.
		16:04:00		Started ranging reacquisition.
		16:09:27		Ranging reacquisition completed.
		16:30:00		Ranging modulation off.
		19:13:00		Ranging modulation on.
		19:33:15		Ranging acquired.
		20:23:00		Started ranging reacquisition.
		20:37:43		Ranging acquisition completed.
		20:48:00		Ranging modulation off.
129	293	12:23:24	DSS 14	Ranging acquired.
		16:03:00		Ranging out of lock for reacquisition.
		16:07:32		Ranging acquired.
		17:03:00		Ranging out of lock for reacquisition.
		17:04:34		Ranging acquired.
		18:03:00		Ranging out of lock for reacquisition.
		18:07:25		Ranging acquired.
		19:01:39		Ranging out of lock for reacquisition.
		19:04:24		Ranging acquired.
		20:00:00		Ranging out of lock for reacquisition.
		20:07:24		Ranging acquired.
		21:00:00		Ranging out of lock for reacquisition.
		21:10:56		Ranging acquired.
		21:39:00		Ranging modulation off.

Table IV-8 (contd)

Pass	Day	Time, GMT	Station	Comments
131	295	12:15:00	DSS 14	Ranging modulation on.
		12:29:59		Ranging acquired.
		13:40:23		Ranging out of lock.
		13:40:25		Ranging reacquired.
		14:26:04		Ranging acquisition completed.
		17:04:00		Started ranging acquisition.
		17:08:48		Ranging acquisition completed .
		18:05:00		Started ranging acquisition.
		18:10:18		Ranging acquisition completed.
		19:01:00		Started ranging acquisition.
		19:06:18		Ranging acquisition completed.
		21:15:00		Ranging modulation off.
145	309	12:25:00	DSS 14	Ranging modulation on.
		12:41:43		Ranging acquired.
		19:03:15		Ranging modulation off.
147	311	15:35:00	DSS 14	Ranging modulation on.
		15:59:00		Ranging modulation off.
152	316	12:40:00	DSS 14	Ranging modulation on.
		12:57:00		Acquired ranging code.
		13:06:04		Malfunction in primary power ranging code dropped out.
		13:19:00		Cannot reacquire ranging code; reprogramming computer.
		13:35:00		Ranging computer will not accept program. Working on computer.
		20:59:00		Ranging modulation off.
161	325	15:57:53	DSS 14	Ranging modulation on.
		16:20:00		Started ranging acquisition.
		16:50:00		Ranging acquisition incomplete.
		16:53:00		Started new range acquisition.
		17:36:00		Started new range acquisition.
		18:14:00		Ranging modulation off.

After encounter, the orbit can be estimated very accurately because of the sensitivity of the tracking data to the near-planet geometry. This final orbit is used by the experimenters to evaluate their data.

c. Trajectory group. The responsibilities of the trajectory group are outlined below.

Typical trajectories are generated before launch so that all project elements can prepare for the expected spacecraft behavior.

During the launch countdown, the nominal trajectory based upon expected liftoff time is generated. This is repeated immediately after launch if the liftoff time is different from that anticipated.

Whenever an updated orbit determination is made, a new trajectory is computed with the required printout intervals and associated trajectory quantities (e.g., angles between earth, sun, and spacecraft) so that spacecraft performance and science data can be adequately evaluated. A special format containing quantities of interest to the Public Information Office is also generated.

d. Midcourse maneuver group. The duties of the midcourse maneuver group are described below.

Maneuver capabilities are computed before launch, and plotted in a convenient format so that a rough evaluation of the midcourse-maneuver requirements can be made as soon as the first orbit estimate is available.

After a definitive orbit has been determined (usually about 25–30 h after launch), a maneuver study is initiated to investigate alternate possible maneuvers that may be performed.

Based upon the desired maneuver chosen as a result of the maneuver study, and upon an updated orbit using the latest tracking data, the desired maneuver is computed. A command message is generated, including a

punched-paper tape that can be transmitted via teletype to the proper tracking station for transmission to the spacecraft.

e. Planning and performance. Prior to the launch phase, detailed studies were carried out to evaluate the effectiveness of all possible tracking patterns. A minimum acceptable pattern was defined and requested. The actual coverage was augmented by additional coverage, as available. The in-flight results showed that it was possible to compute orbits with the necessary accuracy in a near-optimum schedule.

Operational interruptions to the flow of tracking data impeded the semi-automatic logging of this large volume of data. As a result, a considerable effort was made to ensure that all of the available data were used in the orbit computations. Additional efforts were necessary to coordinate station transmitter on and off times with the data, and with the proper transmitter frequency. These conditions should logically be transmitted to the SFOF, along with the raw data (rather than in separate reports). Future mission plans will include these procedural changes.

Elaborate sequences were developed for critical mission phases. These sequences contained both nominal and nonstandard branches. In practice, it was shown that misunderstandings of operational requirements resulted in unexpected deviations from these sequences (none of catastrophic nature). Future mission sequences will have to clearly indicate tolerances associated with all events to clarify the actual requirements to operational personnel.

2. Space science analysis and command. The SSAC group was the active arm of the space sciences division during the flight of *Mariner V*. Its members were drawn from the cognizant personnel for each of the scientific instruments and for the data automation system. The SSAC included such ancillaries as a logging function and ground data handling. The performance of the various instruments and of the data automation system, as well as the intricacies of ground data handling, are discussed elsewhere. The functions and responsibilities of the SSAC were as follows:

(1) Monitoring of data from the scientific instruments (this was done in real time during crucial phases of the mission, and on a daily basis at other times).

(2) Reporting of data anomalies that might suggest instrument or spacecraft malfunction.

(3) Reporting periods for which the data are of particular scientific interest.

(4) Reporting results that might aid the SPAC team in evaluating the condition and performance of the spacecraft.

(5) Providing the spacecraft manager with information regarding the relative scientific merit of various proposals during the mission.

(6) Rendering assistance to the principal investigators and the members of their teams in the interpretation of data.

(7) Establishing standards for the MDL, and ensuring that these standards are met.

The ground data handling section describes the treatment accorded the data stream from the spacecraft before it was presented to the members of the SSAC. In general, each member was presented with that portion of the data of interest to him, in a form best calculated to reveal the condition of the instrument and the quality of the measurements. All members of the SSAC had telephones and headsets that gave them access to appropriate networks for communication of results to the SSAC director and to others for whom this information could be of immediate value.

The SSAC was located in the MSA. In an area physically removed from the MSA, the same data were presented to the principal investigators and their teams. Direct communication was also maintained with the SSAC director. This minimized confusion in the MSA, and provided for the principal investigators.

To provide for failure of some elements in the ground communication system, two backup modes were available in the SSAC area. The first of these consisted of two 60-w/m TTY machines, which presented the raw data stream in octal form. The second was a real-time data translator. Both of these were useful at times, but their primary value lay in providing assurance that the data were not being lost.

Throughout the greater part of the mission, the *Mariner V* spacecraft was accorded 2 passes/day (16–18 h) by the DSN. From launch through the midcourse maneuver, and throughout encounter, 24-h coverage was provided. Arrangements were also made that, in case of spacecraft difficulties or a period of major scientific interest, full (24-h) coverage would be given.

The members of the SSAC were trained in their duties using data from the flight spacecraft while it was at JPL and before launch from Cape Kennedy. Simulated data were also prepared for use in the training exercises. Numerous forms of electrical interference, as well as difficulties in exercising some of the instruments properly, made training difficult at times when the live spacecraft was used. The simulated data were rejected *in toto* by the computer system. The first really clean data came from the spacecraft when it was in the environment for which it was designed—in flight.

One of the weakest units in the data-handling system was the NASCOM communications processor. It frequently became necessary to hardwire around this device to obtain meaningful data for the SSAC. Inasmuch as this was the first mission to make use of the communications processor, however, some difficulty was expected.

During critical phases of the mission, when 24-h coverage was necessary, the SSAC was seriously limited by a shortage of manpower. In most cases, there were available only one cognizant scientist and one cognizant engineer for each instrument. The SSAC director had adequate backup for his position, but some of the instruments did not. This shortage was not serious during the cruise phase of the mission because there were only 2 passes/day, and a daily review of the data by cognizant personnel sufficed.

The spacecraft manager granted two unscheduled changes of spacecraft attitude to increase the reliability of the data from the UV photometer.

As the mission progressed, the desirability of having a data automation system man, who reported directly to the SPAC director, became obvious. This was largely because the format chosen presented items of engineering interest to the data automation system man that were not available to the SPAC director from any other source. It should not be construed from this that the SSAC should be a subsidiary of SPAC, but it indicates that there was indeed a strong dependence between the two. They shared a common interest in the success of the mission, but from somewhat different points of view.

On the basis of instrument performance and preliminary scientific results, the mission was immensely successful. The choice of the assistant project scientist as SSAC director was sound, but it pointed out the necessity of having available personnel with an equal overview of the mission to back him up. If 24-h SSAC coverage had been required throughout this mission, it would have been extremely difficult for all concerned.

C. Data Recovery and Processing

1. Tracking data. Figure IV-29 shows the hardware and software system used to support the *Mariner* Venus 67 mission. In high-activity periods, tracking data followed a completely automated route from the DSIF to the project users in FPAC.

As raw tracking data were received in the SFOF, they were placed on the disk by the 7044 system. The raw data on the disk were then accessible by the 7094 user programs.

Four tracking data handling programs are illustrated (Fig. IV-30), but only one program operated within the 7094 SFOF system at a time. The mission-independent editor acquired the raw TTY data from the disk that contained mixed tracking and telemetry data. This editor separated the data, extracting the tracking data and storing these data on the disk in the raw tracking data file.

The **TDPX** program retrieved these data, edited and reformatted them, and then placed these data back on the disk in the master tracking data file.

The **ODGX** program used this file to prepare a block of data for the **ODPX** program. Essentially, the **ODGX** program extracted a subset of the master tracking data and formatted it, using control inputs that had been provided to the program.

The **ODPM** program retrieved the block of **ODPM** data that had been compiled by the **ODGX** program, and, employing a least-squares curve fit and an iterative technique, determined the orbit of the spacecraft. The injection conditions were placed on the disk, and were then available for use by other programs.

In low-activity cruise periods, tracking data were recorded by the 7044 on a special log tape. This tape was batch-processed in nonreal time by the 7094 tracking data handling programs.

The tracking data master file produced by the **TDPX** program was part of the MDL. The DSN monitor group assisted in the generation of this file to assure that the project was getting its committed percentage of possible data points.

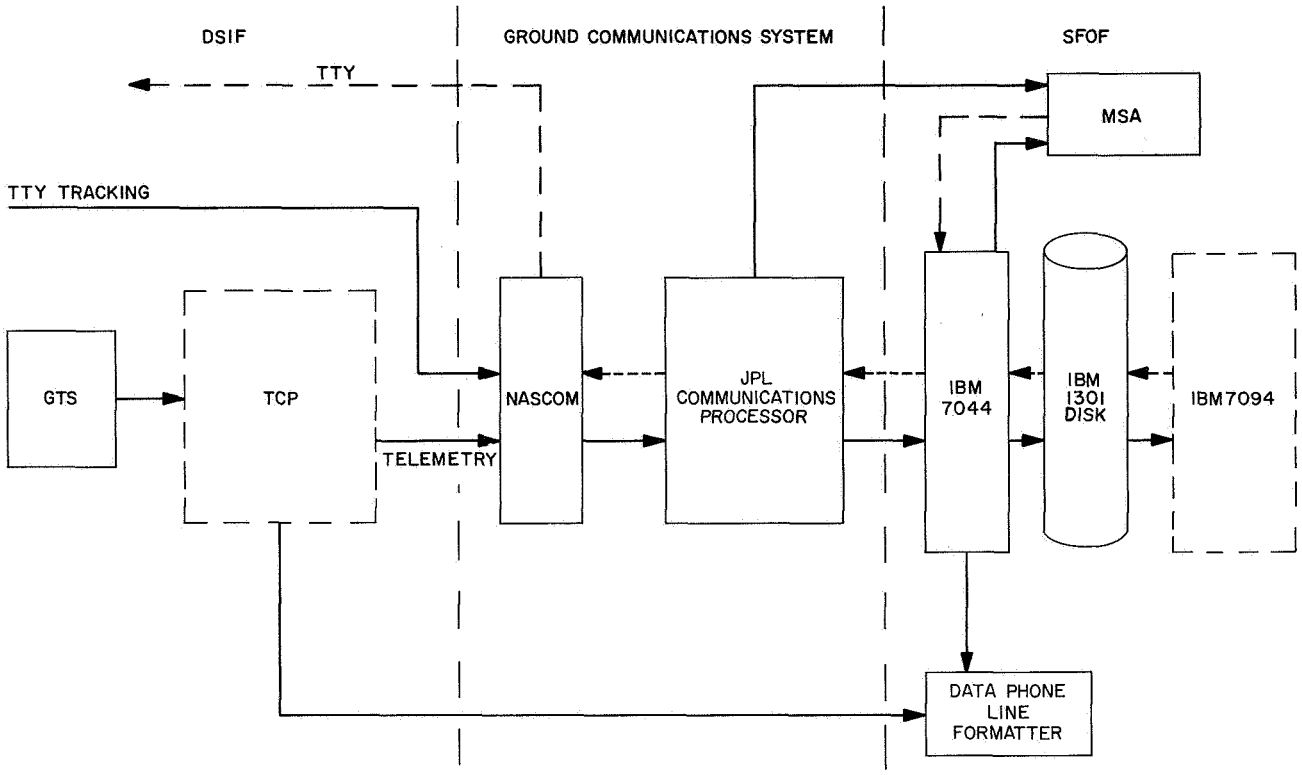


Fig. IV-29. Data processing system to support the *Mariner* Venus 67 mission

2. Science and engineering telemetry data. The system at the DSIF stations included the ground telemetry system and the TCP consisting of an SDS-920 computer and a communication buffer. The communication buffer is the external (or output) interface. The primary function of the TCP program was to process *Mariner V* spacecraft telemetry data. This included frame detection, engineering decommutation, science decommutation, TTY output, HSDL output, and data logging.

Data received from the ground telemetry system were in the form of digital telemetry data, word sync, bit sync, ground receiver automatic gain control data, and receiver in- and out-of-lock status. In addition, the station time input was used in time-tagging the data.

The output data were formatted for transmission through the communication buffer on various TTY lines and HSDLs, and for visual display of the spacecraft automatic gain control and static phase error at the DSIF station.

Except for automatic gain control data, all data received by the TCP were formatted and stored on a log tape. This tape was one of the prime inputs to the MDL.

Received telemetry data were processed in real time by the 7044 in the SFOF. The mission-dependent processors in the 7044 performed frame sync, decommutation, scaling, and alarm checking on the data. The output from the 7044 consisted of print, plot, and TTY displays of the processed data.

All telemetry data received by the 7044 were placed on a log tape. This tape was the primary source for nonreal-time telemetry processing. The daily processing of telemetry data used the same set of programs as was used for MDL production. The purpose, however, was to produce quick-look prints and plots for SPAC rather than to compile the MDL.

3. Cruise and encounter. The *Mariner V* cruise operations consisted of supporting tests and real-time operations with the telemetry software. The configuration was similar to that shown in Fig. IV-29, but without the 7094 and disk attached. Whenever the spacecraft was being tracked by the DSIF, the TCP and 7044 were used to display real-time data in the SFOF. The 7094 software was used regularly in nonreal time by FPAC personnel to process tracking data and to update the orbit of the spacecraft. The 7094 was also used on a daily basis to

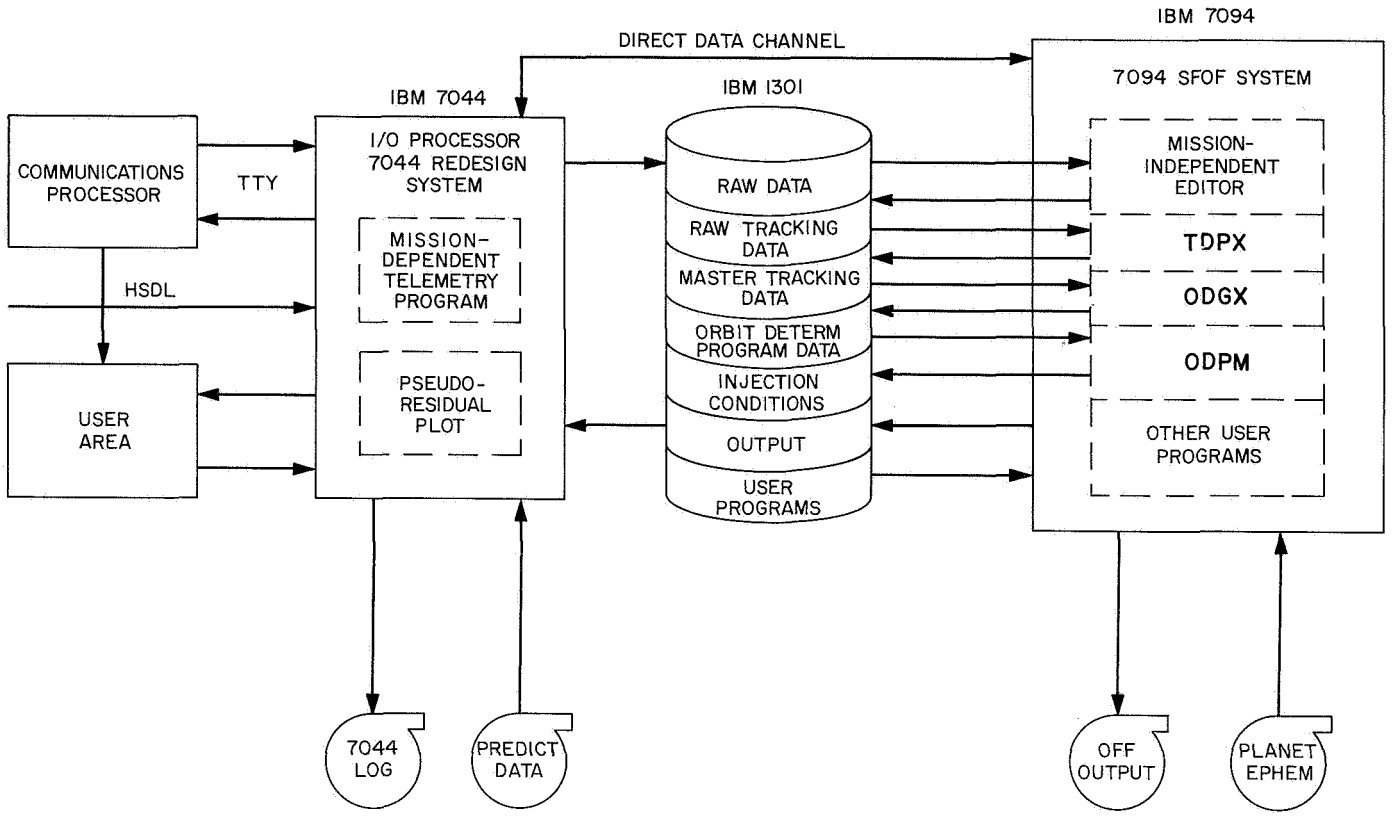


Fig. IV-30. 7094 user program environment

produce prints and plots of telemetry data for use by SPAC personnel.

During *Mariner V* encounter operations, the data processing system was operated in a maximum-redundancy mode. Telemetry and tracking data were processed in parallel by two sets of computers. Any hardware failures on one computer string would interrupt data only momentarily.

Because of the great amount of interest in the encounter, the 7044s were asked to display real-time data on over 40 devices throughout the SFOF. These included displays for the experimenters and for Public Information Office purposes, as well as for SPAC, SSAC, and FPAC personnel.

A new capability, developed for use by the S-band occultation experiment, was used in the encounter sequence. This capability was the display in real time of doppler residuals from high-speed tracking data. Figure IV-31 shows the system used to generate and display these data.

A special program was written for the digital instrumentation system at DSS 14 to take tracking data from the TDH at 1-s intervals and transmit these data to the 7044 over HSDLs. The 7044 then computed a residual by subtracting a predicted doppler value from the observed doppler. This pseudo-residual was then displayed on print and plot devices.

This display showed the effects of the atmosphere of Venus on the returning signal from the spacecraft.

4. Program refinements. Very few modifications were made to the software between launch and encounter. Gradual updating of the 7044 software started after the midcourse maneuver, and continued until a software freeze was applied on September 1, 1967. The TCP program was updated to correct several known errors. This new program was in use at all DSIF stations several months before encounter.

New versions of the 7094 programs **ODGX** and **PRDX** were certified and used for encounter.

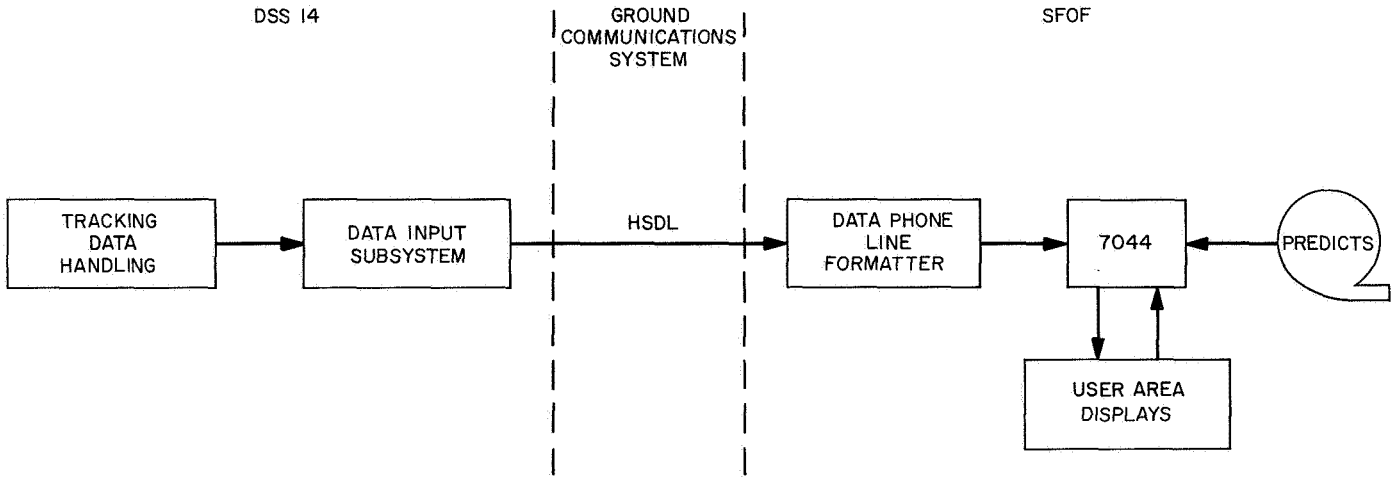


Fig. IV-31. High-speed tracking data configuration

The high-speed tracking data system, involving changes to the 7044 and the writing of a new data input subsystem program, was delivered to the project for testing on August 15, 1967.

All software modifications were used during the Mission Operations System pre-encounter tests and the encounter readiness tests.

In general, the performance of the data processing system during cruise and through encounter was excellent. All user programs worked well, and, except for a problem with the 7044 pseudo-residuals near occultation, the sequence of events was executed successfully.

5. Occultation. The occultation experiment used the spacecraft radio signal to measure atmospheric parameters. By measuring frequency changes, a refractive index profile was obtained from which atmospheric parameters could be inferred.

a. Data recovery. The data for this experiment were gathered by two methods: (1) the normal doppler readout of the tracking data subsystem, and (2) predetection recording of the entire spacecraft radio signal and rather complex postprocessing to obtain as much data as possible. The station block diagram is shown in Fig. IV-32.

To obtain data for predetection recording, one receiver at DSS 14 was converted from its normal phase-locked operation to an open-loop, triple-conversion configuration. The block diagram is shown in Fig. IV-33. The first local oscillator was tuned to a frequency that resulted in the spacecraft signal being translated to an ultrasonic frequency between 20 and 100 kHz. This signal was recorded on two FR-1400 tape recorders, at 60 in./s, simultaneously with a 320-kHz tone from a stable oscillator.

b. Data processing. The tapes were played back at 3.75 in./s, and the 20-kHz tone (320k/16) was used as a clock to trigger a digitizer. The interesting portions of time were digitized and recorded on magnetic tape. Spectral analysis was then used to locate the signal, and to determine its rate of change ($\dot{f}$) and acceleration ($\ddot{f}$). Once these had been determined, the data were processed through a digital-filter program to improve the signal-to-noise ratio, using the rate and rate-rate terms in a digital local oscillator to keep the signal centered in the filter passband. Because the sample rate was higher than needed, it was possible to throw away (decimate) some data while filtering. This effectively reduced the frequency of the data by a known amount. The decimated data were then processed in a digital, phase-locked-loop computer program, which tracked any remaining frequency variations and gave both frequency and amplitude vs time as outputs.

6. Master data library production. The production of the *Mariner* Venus 67 MDL was performed by the use of modified *Mariner* Mars 1964 MDL programs. Two new programs were written to analyze and make minor corrections to the final MDL output. The *Mariner* Mars 1964 MDL editor was modified to enable it to accept the telemetry and command data (TCD) recordings and the SFOF 7044 log tape recording. The modified MDL editor was used to furnish near-real-time, quick-look data to the experimenters.

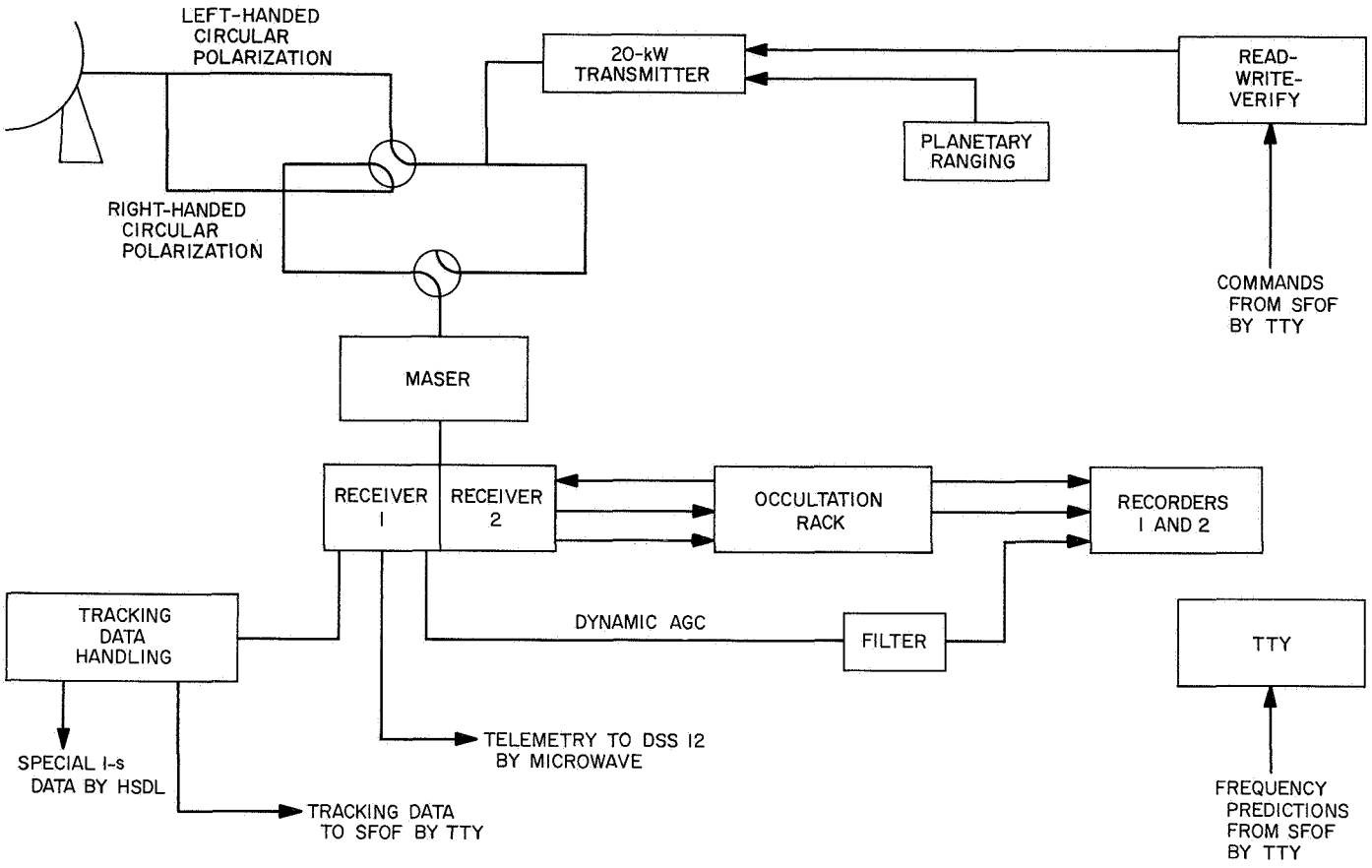


Fig. IV-32. Occultation experiment data recovery, station block diagram

a. Telemetry. The prime source of data for the *Mariner* Venus 67 MDL was digital recordings made by the TCD processor at the DSIF stations. Data outages on the TCD recordings were filled by processing the analog recordings of the DSIF receiver output.

Validation programs were written to analyze the TCD digital recordings in respect to data quality and quantity. This validation, which was performed at JPL, served the purpose of expediting requests for DSIF analog recordings that might be required to fill data outages on the TCD recordings.

For a period of 3 wk, *Mariner V* spacecraft data were below analog demodulator threshold. An experimental digital demodulation program was written in an attempt to recover these data. The digital demodulation program recovered data that were approximately 1 dB above receiver threshold. The analog demodulator was only capable of recovering data that were approximately 3 dB above receiver threshold. A significant amount of data was added to the MDL by the use of the digital demodulation program.

The quantity of telemetry data recovered was in excess of 99% of the spacecraft data received by the DSIF.

Figures IV-34 and IV-35 schematically illustrate the flow of telemetry data through the MDL system.

b. Tracking data. Production of the MDL tracking data was performed by the use of the tracking data processor (**TDPA**) program. A validation program was written to statistically evaluate the master files generated by **TDPA**. Outages in the master files were filled by using the tracking-data paper tapes shipped to JPL from the DSIF stations.

The **TDPA** master files were updated to satisfy the orbit determination and celestial mechanics criteria established before launch.

D. Mission Operations

1. Readiness testing. The Mission Operations System conducted five tests in preparation for the Venus encounter by the *Mariner V* spacecraft. These tests were

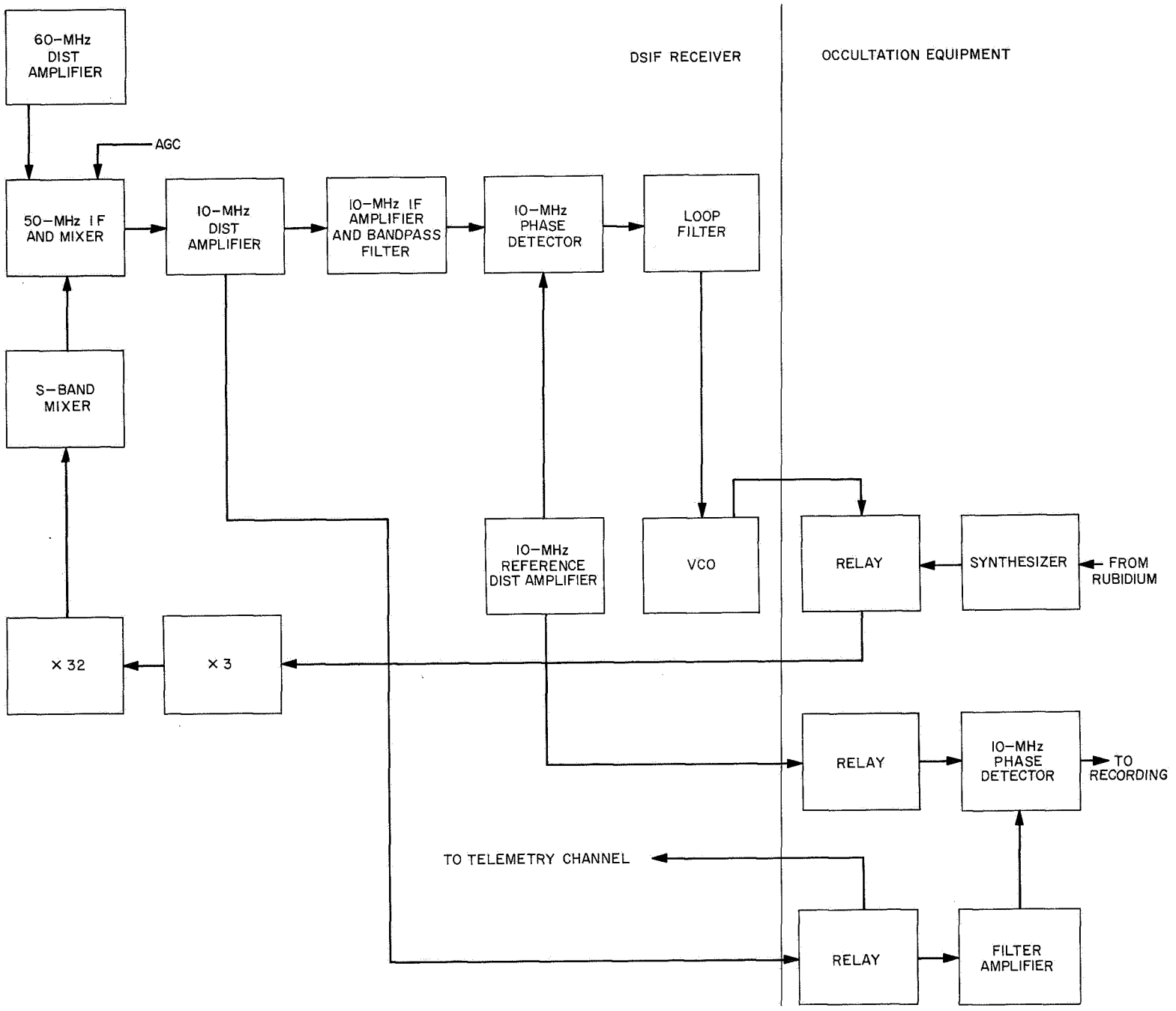


Fig. IV-33. Occulation experiment predetection recording

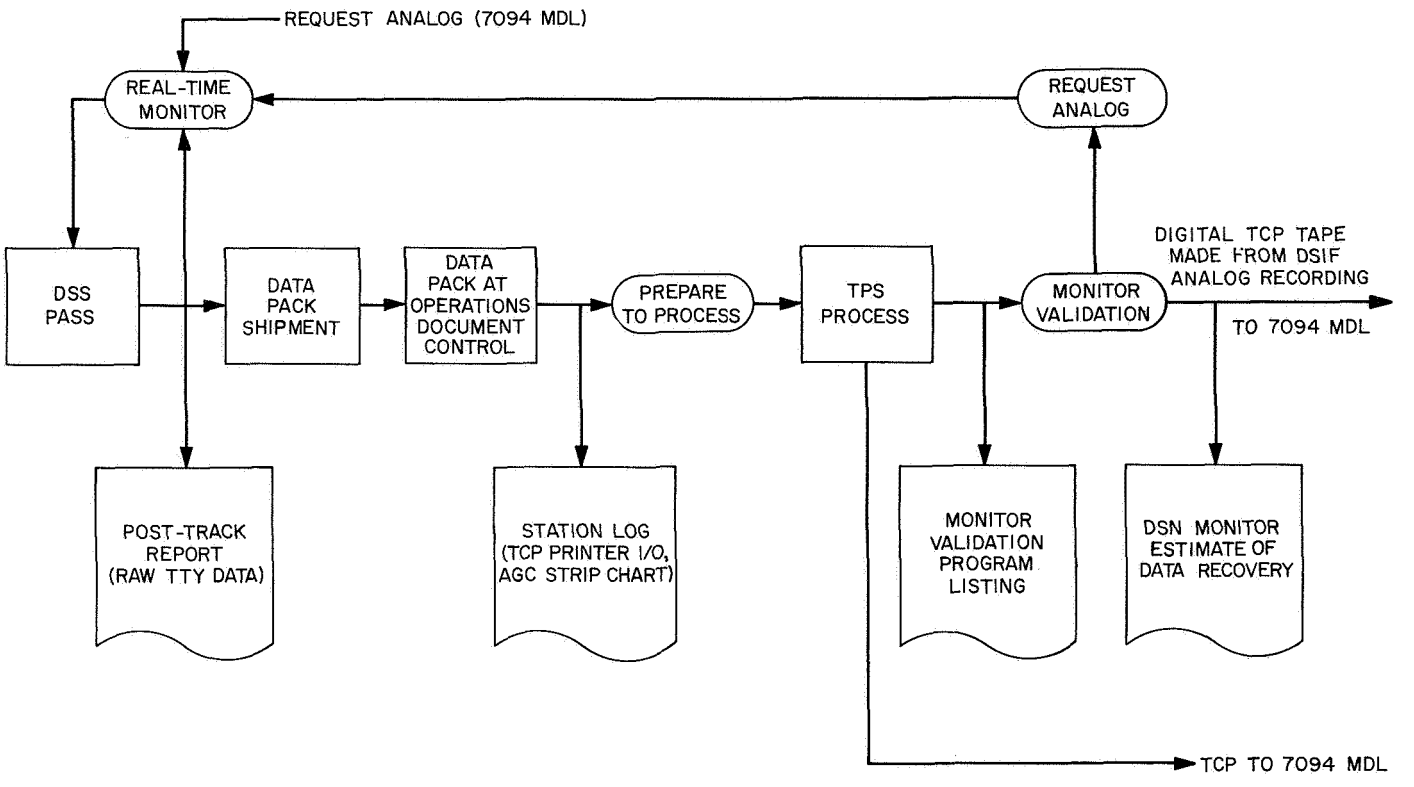


Fig. IV-34. Validation processing telemetry

primarily designed to familiarize and train personnel in the analysis and response required for real-time operations during encounter.

The M67-1 spacecraft, located in the Spacecraft Assembly Facility at JPL, provided real-time spacecraft telemetry data to analysis teams in the *Mariner* MSA for all tests. Known spacecraft anomalies were introduced by the spacecraft test team.

Tracking data for all tests were provided by the ASI-6050 and/or the 7094 computer, and were controlled from the simulated data conversion center located in the SFOF. The operational readiness tests were supplemented by real-time tracking data (simulated) transmitted over the HSDL from DSS 14 at Goldstone. The tracking data transmitted over the HSDL consisted of 1-s samples containing doppler and resolver information.

The SPAC and SSAC teams participated in all tests involving analysis of spacecraft (M67-1) telemetry data. Spacecraft anomalies introduced by the test team in the Spacecraft Assembly Facility were recognized, and corrective measures were recommended. The spacecraft telemetry data were processed by the 7044 real-time processor, located in the SFOF, for display to the analysis teams in the *Mariner* MSA.

The FPAC team computed orbital, trajectory, residual, and prediction data with the 7094 computer, using the incoming simulated data as their source. The FPAC team operated from the FPAA located adjacent to the *Mariner* MSA.

The first three tests used a 7044/7094 combination for rapid data movement within the facility. The final two tests used two such combinations (7044/7094 X and 7044/7094 W) to exercise personnel in the operation of the two computer strings required during critical mission phases. This configuration provided additional insurance that one computer system (7044/7094) would be available during critical periods. The testing achieved the desired results.

Table IV-9 and Fig. IV-36 define the days, times, and configuration used to test the *Mariner V* Mission Operations System for encounter preparation.

2. Flight chronology. Table IV-10 presents a complete flight chronology as excerpted from mission operations logs.

3. Spacecraft command criteria. The basic guiding philosophy regarding ground commands and the control to be exercised over them is as follows:

Table IV-9. Test schedule

Date (1967)	Local time, PDT	Day/time, GMT
Sep 15	7:30 a.m. to 6:00 p.m.	258/14:30 to 259/01:00
Sep 28	7:30 a.m. to 6:00 p.m.	271/14:30 to 272/01:00
Oct 3	7:30 a.m. to 6:00 p.m.	276/14:30 to 277/01:00
Oct 10	7:00 a.m. to 2:00 a.m. (10/11)	283/14:00 to 284/09:00
Oct 12	7:30 a.m. to 6:00 p.m.	285/14:30 to 286/01:00

(1) Any command or commands considered necessary for corrective action or for achieving standard space-flight operation must be approved by the SFOD. Upon concurrence of the project manager, the command or commands will be transmitted to the appropriate DSS for execution.

(2) Command requests will be made only by the technical and operations teams within the SFOF, using approved command-decision procedures.

(3) Two trajectory-correction maneuvers are available to achieve a nominal space-flight operation; the second maneuver will be used only if the first maneuver does not supply an adequate trajectory correction.

(4) Approved procedures will be used to transmit command instructions from the SFOF to the DSIF.

General guidelines for the approval and transmission of commands to the *Mariner V* spacecraft were published on July 5, 1967, by the project manager. These guidelines are as follows:

(1) No command shall be sent that may be determined to have a potential failure mode that may be catastrophic to the mission.

(2) No command is to be sent that substantially degrades the probability of achieving the primary mission objectives.

(3) The spacecraft design embodies commands as backup. The midcourse maneuver is a special case. Actual command operations seem to result in more commands and in sequences that were not comprehended early and were probably not tested during the qualification of the spacecraft for flight. Therefore, when the spacecraft (M67-1) in the Spacecraft Assembly Facility becomes available, all sequences should be tested first by the Spacecraft Assembly Facility spacecraft.

(4) The capability of the spacecraft and our confidence in it should not be construed as a license to exercise all modes of operation without regard to their value to the primary mission objectives.

(5) No command will be approved that has not undergone a thorough analysis as to need and consequences.

(6) Command operations in support of failure analysis are discouraged unless this analysis is necessary to meet the primary objectives. Operations of this type must answer the question of whether this affects what we will do at the planet.

4. Critical operations. The *Mariner* Venus 67 mission was made up of a combination of three critical periods, each period being followed by a cruise phase or noncritical period. These three criticals periods were launch, midcourse maneuver, and encounter.

During the low-activity (cruise) period, the Venus operations controller assumed the coordination and control of the operations. The Venus operations controller position ensured that proper data acquisition, transmission, processing, and distribution were accomplished for mission monitoring. This position monitored the data, and notified appropriate personnel when established limits of subsystems aboard the spacecraft were violated.

The three high-activity periods (launch, midcourse maneuver, and encounter) created a much greater level of activity and personnel participation. These three periods of high activity demanded the greatest effort on the part of all mission elements to allow the quick response that was mandatory to resolve any nonstandard conditions that might appear either aboard the spacecraft or within the earth-based Mission Operations System. During a high-activity period, an orderly resolution of any nonstandard condition must be anticipated, and a planned reaction must be available. This calls for many hours of precritical phase planning.

Special procedures were established in the areas of command, data processing, and operations. A nominal sequence of events was established for each critical phase of operation. A spacecraft flow diagram was developed to provide a direction for corrective action, should certain nonstandard conditions come into existence.

The operations team, the analysis teams (FPAC, SPAC, and SSAC), project, DSN, DSIF, and other supporting agencies had to be staffed to allow for changing of personnel when activity extended over long periods. Special personnel were required to maintain communications facilities, to maintain access control to areas involved in analysis and control, and to operate dual-computer systems. Special personnel were also required in the complementary analysis team areas for real-time backup.

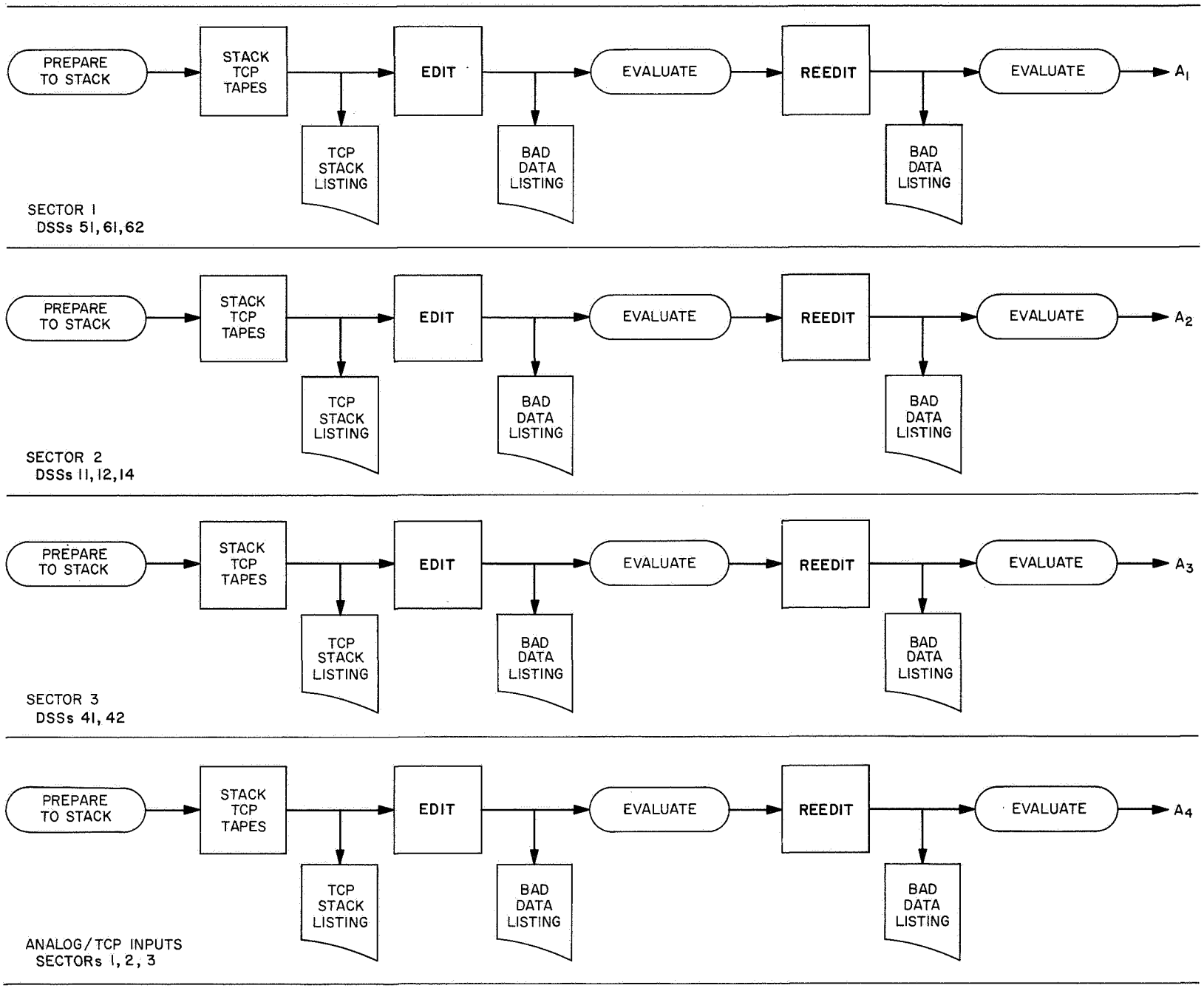


Fig. IV-35. 7094 master data library processing telemetry

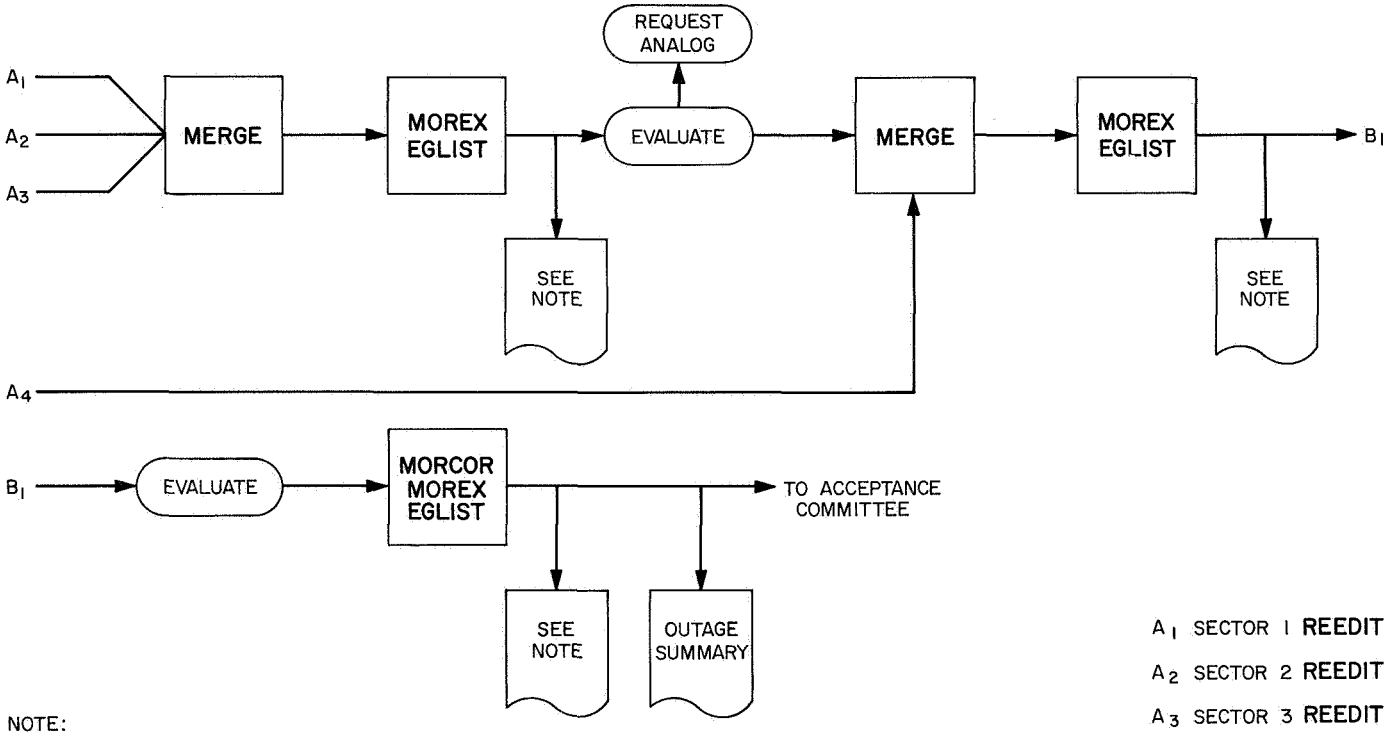


Fig. IV-35 (contd)

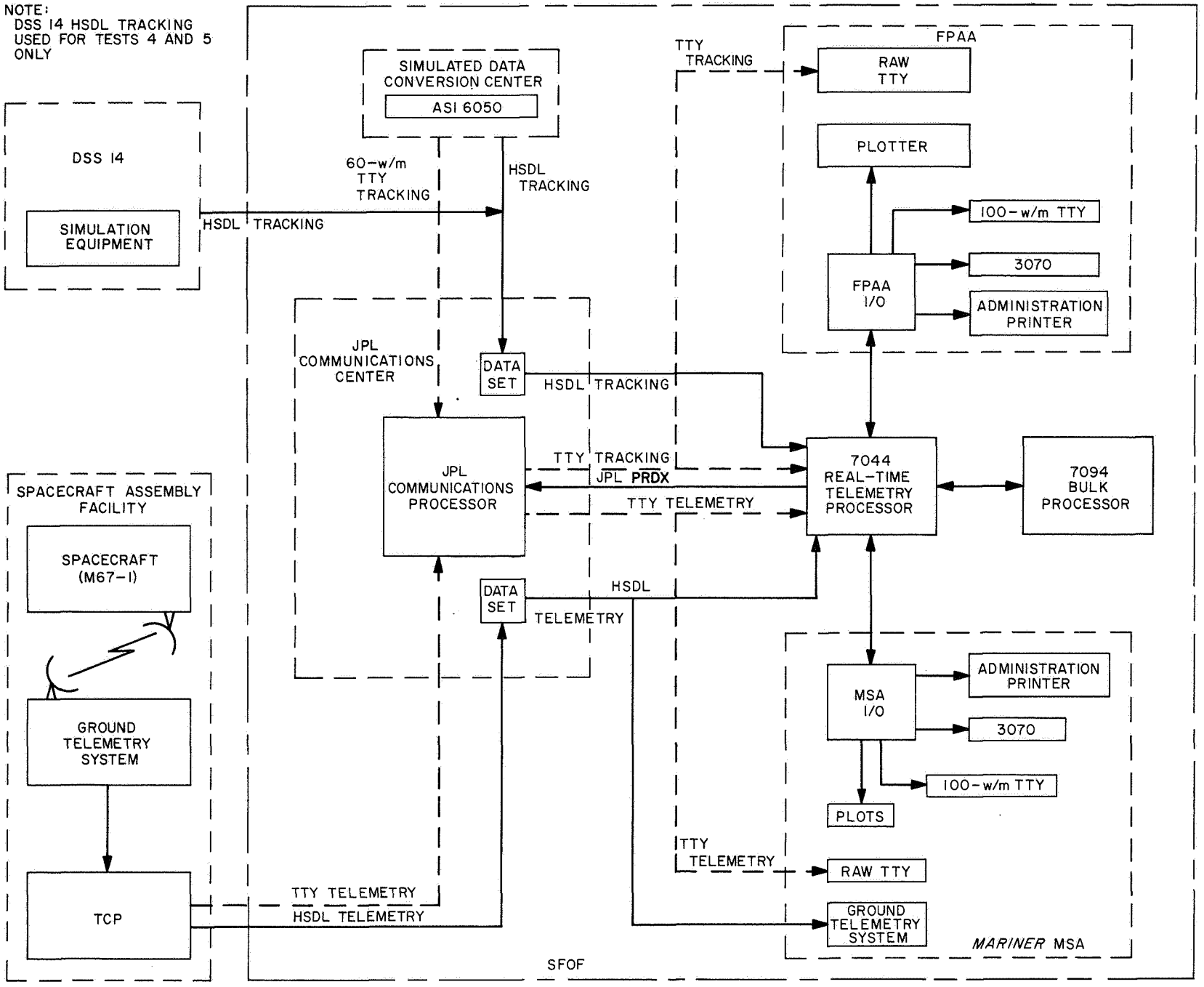


Fig. IV-36. Test configuration

Table IV-10. *Mariner V* flight chronology

Day	Date	Time, GMT	Event
165	Jun 14	05:58:00	CC&S inhibit release
		05:59:59	CC&S clear release
		06:01:00.176	Liftoff
		06:03:08.8	Mark 1 (booster cutoff)
		06:03:11.75	Mark 2 (booster jettison)
		06:05:41.90	Mark 3 (start of *Agena* auxiliary timer)
		06:05:56.84	Mark 4 (sustainer cutoff)
		06:06:08.57	Mark 5 (start of *Agena* standard timer)
		06:06:17.93	Mark 6 (vernier cutoff)
		06:06:20.24	Mark 7 (shroud ejection)
		06:06:22.28	Mark 8 (*Atlas/Agena* separation)
		06:07:21.80	Mark 9 (first *Agena* ignition)
		06:09:45.36	Mark 10 (first *Agena* cutoff)
		06:09:45.36	In parking orbit
		06:20:18	Out of earth's shadow
		06:23:01.2	Mark 11 (second *Agena* ignition)
		06:24:35.50	Mark 12 (second *Agena* cutoff)
		06:27:16.9	Pyrotechnics arming switch caused deck reset on three data encoder decks
		06:27:16.9	Mark 13 (*Agena*/spacecraft separation)
		06:27:17.57	Science on (observed on earth)
		06:27:20.1	Mark 14 (start of *Agena* yaw maneuver)
		06:27:28.9	Mark 15 (end of *Agena* yaw maneuver)
		06:29:42	Tape recorder off (observed on earth)
		06:29:42	CC&S relay hold off (observed on earth)
		06:29:42	RF power up (observed on earth)
		06:30:11.6 ±4.9	Separation-initiated timer deployed solar panels
		06:30:19.01	Solar panels and sunshade deployed
		06:32:16.9	Mark 16 (*Agena* posigrade maneuver)
		06:43:25.4 ±4.9	Acquired sun; start of magnetometer calibration roll
		06:53:56.6	CC&S L-1, solar panels and sunshade deployed
		06:57:56.0	CC&S L-2 turned on attitude control subsystem
		22:38:00.5	CC&S L-3 turned on Canopus sensor and initiated roll search about spacecraft Z axis
		22:49:01	Canopus sensor acquired earth (center of null)
		22:50:00	Gyros off
166	15	00:30:00	DC-V21 (roll override) transmitted
		00:30:38.2	DC-V21 received at spacecraft
		00:30:40.2 ±4.9	DC-V21 observed on earth
		00:34:00	DC-V21 transmitted
		00:34:38.2	DC-V21 received at spacecraft
		00:34:39.6 ±4.9	DC-V21 observed on earth
		01:09:12.6 ±0.7	Canopus acquired
		01:12:26.4 ±6.2	Gyros off
		21:58:07	CC&S CY-1 No. 1
169	18	02:43:00	Roll transient (yaw valve fired concurrently)
		16:38:08	CC&S CY-1 No. 2
170	19	03:00	Roll transient (yaw limit cycle reversed direction); midcourse maneuver
		20:18:00	QC-V1-1 (pitch turn +55.267 deg, duration 304 s) transmitted
		20:18:40.7	QC-V1-1 received at spacecraft
		20:18:44.4 ±6.3	QC-V1-1 observed on earth
		20:23:00	QC-V1-2 (roll turn +70.946 deg, duration 380 s) transmitted
		20:23:40.7	QC-V1-2 received at spacecraft
		20:23:45.2 ±6.3	QC-V1-2 observed on earth
		20:28:00	QC-V1-3 (motor burn 16.127 m/s, duration 17.66 s) transmitted
		20:28:40.7	QC-V1-3 received at spacecraft
		20:28:44.1	QC-V1-3 observed on earth
		20:38:00	DC-V29 (arm first prop maneuver) transmitted
		20:38:40.7	DC-V29 received at spacecraft

Table IV-10 (contd)

Day	Date	Time, GMT	Event
170	19	20:38:52.5 ±6.3	DC-V29 observed on earth
		20:48:00	DC-V14 (remove maneuver inhibit; remove prop inhibit) transmitted
		20:48:40.7	DC-V14 received at spacecraft
		20:48:44.7 ±6.3	DC-V14 observed on earth
		21:23:57	DC-V27 (initiate midcourse maneuver) transmitted
		21:24:39.7	DC-V27 received at spacecraft
		21:24:46 ±4.2	DC-V27 observed on earth
		21:24:46 ±4.2	Data encoder to mode 1
		21:24:46	Gyros on (observed on earth)
		22:24:10.9	Pitch turn start
		22:28:57	Solar panel 4A7 power turned off because of shading
		22:28:57	Battery sharing
		22:29:14.8	Pitch turn stop (+55.18 deg, duration 304 s)
		22:46:10.8	Roll turn start
		22:47:47	Solar panel 4A7 back in sun and providing power
		22:47:51	Solar panel 4A5 started shading
		22:52:31.1	Roll turn stop (+70.93 deg, duration 380 s)
		23:08:11.3	Motor burn start
		23:08:28	Motor burn stop (15.392 m/s, duration 17.66 s)
		23:14:10.9	Data encoder to mode 2
		23:14:10.9	Start sun reacquisition
		23:17:16	Confirmed battery charging
		23:21:24.2 ±5.3	Sun acquired
		23:32:19.2 ±5.7	Canopus acquired
		23:33:15	DC-V21 (roll override) transmitted
		23:33:55.7	DC-V21 received at spacecraft
		23:34:06	DC-V21 observed on earth
171	20	00:23:58.4 ±5.7	Canopus acquired
		00:25:00	DC-V21 transmitted
		00:25:42	DC-V21 received at spacecraft
		00:25:52.4 ±5.4	DC-V21 observed on earth
		00:43:12	Maneuver counter overflow
		01:16:54.2 ±5.7	Canopus acquired
		01:17:50	DC-V21 transmitted
		01:18:31.8	DC-V21 received at spacecraft
		01:18:35 ±5	DC-V21 observed on earth
		02:06:15 ±5.7	Canopus acquired
		02:09:49 ±5	Gyros off
		02:19:00	QC-V1-1 (minimum pitch turn) transmitted
		02:19:42	QC-V1-1 received at spacecraft
		02:20:13	QC-V1-1 observed on earth
		02:24:00	QC-V1-2 (minimum roll turn) transmitted
		02:24:42	QC-V1-2 received at spacecraft
		02:25:16	QC-V1-2 observed on earth
		02:29:00	QC-V1-3 (minimum motor burn) transmitted
		02:29:42	QC-V1-3 received at spacecraft
		02:30:1	QC-V1-3 observed on earth
		02:39:0	DC-V9 (switch ranging) transmitted
		02:39:42	DC-V9 received at spacecraft
		02:39:54	DC-V9 (ranging receiver on) observed on earth
		10:20	Roll transient
172	21	11:18:14	CC&S CY-1 No. 3 (ranging receiver off)
		19:25:00	DC-V9 transmitted
		19:25:49	DC-V9 received at spacecraft
		19:25:54	DC-V9 (ranging receiver on) observed on earth
174	23	21:08:20	Canopus sensor "dust particle"
175	24	05:58:26.8	CC&S CY-1 No. 4 (turn ranging receiver off)

Table IV-10 (contd)

Day	Date	Time, GMT	Event
176	Jun 25	03:08:00	DC-V9 transmitted
		03:08:47	DC-V9 received at spacecraft
		03:09:03	DC-V9 (ranging receiver on) observed on earth
177	26	—	Solar storm (proton)
		23:45:00	DC-V9 transmitted
		23:45:49	DC-V9 received at spacecraft
		23:46:04	DC-V9 (ranging receiver off) observed on earth
178	27	—	Solar storm (electron)
		00:28:00	DC-V7 (switch power amplifier) transmitted
		00:28:49	DC-V7 received at spacecraft
		00:29:05	DC-V7 observed on earth
		00:38:37.4	CC&S CY-1 No. 5
		00:58:00	DC-V28 (switch battery charger off) transmitted
		00:58:49	DC-V28 received at spacecraft
		00:59:05	DC-V28 observed on earth
		00:59:05	Data encoder deck skip
		01:18:00	DC-V9 transmitted
		01:18:49	DC-V9 received at spacecraft
		01:19:05	DC-V9 (ranging receiver on) observed on earth
179	28	19:18:34.9	CC&S CY-1 No. 6 (ranging receiver off)
181	30	19:45:00	DC-V9 (switch ranging) transmitted
		19:45:52	DC-V9 received at spacecraft
		19:46:15	DC-V9 (ranging receiver on) observed on earth
183	Jul 2	13:58:45	CC&S CY-1 No. 7 (ranging receiver off)
186	5	08:38:43	CC&S CY-1 No. 8
187	6	00:30:00	DC-V9 transmitted
		00:30:54	DC-V9 received at spacecraft
		00:31:12	DC-V9 (ranging receiver on) observed on earth
189	8	03:18:53	CC&S CY-1 No. 9 (ranging receiver off)
		19:30:00	DC-V9 (switch ranging) transmitted
		19:30:59	DC-V9 received at spacecraft
		19:31:16	DC-V9 (ranging receiver on) observed on earth
191	10	21:59:09	CC&S CY-1 No. 10 (ranging receiver off)
192	11	—	Solar storm (proton)
193	12	—	Solar storm (proton)
194	13	16:39:07	CC&S CY-1 No. 11
197	16	11:19:04 (predicted)	CC&S CY-1 No. 12 (no tracking)
200	19	05:59:28	CC&S CY-1 No. 13
203	22	00:39:20	CC&S CY-1 No. 14
		01:35:00	DC-V9 (switch ranging receiver on) transmitted
		01:36:10	DC-V9 received at spacecraft
		01:36:52	DC-V9 (ranging receiver on) observed on earth
205	24	19:19:21.4	CC&S MT-6 (switch to 8⅓ bits/s)
		19:19:21.4	CC&S CY-1 No. 15 (switch ranging receiver off)
208	27	13:59:57.0	CC&S CY-1 No. 16
		16:40:00	DC-V9 (switch ranging receiver on) transmitted
		16:41:16	DC-V9 received at spacecraft
		16:41:39	DC-V9 observed on earth
211	30	08:40:20.4	CC&S CY-1 No. 17 (switch ranging receiver off)
213	Aug 1	—	Solar storm (electron)
		09:04:17	Roll transient
214	2	—	Solar storm (proton)
		03:19:40.9	CC&S CY-1 No. 18

Table IV-10 (contd)

Day	Date	Time, GMT	Event
216	Aug 4	21:59:46	CC&S CY-1 No. 19 (not tracking)
219	7	16:40:03.3	CC&S CY-1 No. 20
221	9	07:15	Roll transient
222	10	—	Solar storm (proton and electron)
		11:20:14.8	CC&S CY-1 No. 21
223	11	—	Solar storm (proton)
225	13	06:00:26.6	CC&S CY-1 No. 22
		11:11:00	Roll transient
226	14	18:32:41	Roll transient
228	16	00:40:38.8	CC&S CY-1 No. 23
229 to 237	17 to 25	—	Pi-Scorpii in UV-photometer field of view
230	18	19:20:20	CC&S CY-1 No. 24 (not tracking)
233	21	14:01:03.5	CC&S CY-1 No. 25
234	22	07:40	Roll transient (yaw valve fired concurrently)
		14:14	Roll transient
236	24	08:41:32.8	MT-1 (update Canopus sensor cone angle)
239 to 245	Aug 27 to Sep 2	—	Tau-Scorpii in UV-photometer field of view
239	Aug 27	08:41:32.8	CC&S CY-1 No. 26
		03:21:17.2	CC&S CY-1 No. 27
241	29	22:01:43.4	CC&S CY-1 No. 28
244	Sep 1	16:40:07	CC&S CY-1 No. 29
247	4	11:21:21.4	CC&S CY-1 No. 30
250	7	06:01:36.3	CC&S CY-1 No. 31
253	10	00:41:51.5	MT-2 (update Canopus sensor cone angle)
		00:41:51.5	CC&S CY-1 No. 32
255	12	19:22:07.1	CC&S CY-1 No. 33
258	15	14:02:23.1	CC&S CY-1 No. 34
261	18	—	Solar storm (proton and electron)
		08:42:39	CC&S CY-1 No. 35
262	19	—	Solar storm (proton and electron)
263	20	—	Solar storm (proton and electron)
264	21	—	Solar storm (proton and electron)
		03:22:56.4	CC&S CY-1 No. 36
266	23	22:03:01.7	CC&S CY-1 No. 37
269	26	16:42:43	CC&S CY-1 No. 38
		16:42:43	MT-3 (update Canopus sensor cone angle)
272	29	11:22:57	CC&S CY-1 No. 39
274	Oct 1	16:43:33.8	MT-5 (switch spacecraft transmitter to high-gain antenna)
275	2	06:03:17.3	CC&S CY-1 No. 40
		07:28	Roll transient
		14:36	Roll transient
		16:38	Roll transient
277	4	05:00	CC&S CY-1 No. 41
		22:17	Roll transient
		23:55:00	DC-V9 (turn on ranging receiver) transmitted
278	5	23:59:02	DC-V9 received at spacecraft

Table IV-10 (contd)

Day	Date	Time, GMT	Event
279	Oct 6	00:01:52	DC-V9 observed on earth
		14:17	Roll transient (caused large rate increase in yaw limit cycle)
280	7	19:23:39 (predicted)	CC&S CY-1 No. 42 (bad data) (turn ranging receiver off)
282	9	22:00:00	DC-V9 (turn on ranging receiver) transmitted
		22:04:18	DC-V9 received at spacecraft
		22:07:24	DC-V9 observed on earth
283	10	13:50:00	DC-V9 (turn off ranging receiver) transmitted
		13:54:23	DC-V9 received at spacecraft
		13:57:29	DC-V9 observed on earth
		14:04:14.4	MT-4 (update Canopus sensor cone angle)
		14:04:14.4	CC&S CY-1 No. 43
		14:25:00	DC-V15 (Canopus gate inhibit override) transmitted to condition spacecraft for encounter
		14:29:23	DC-V15 received at spacecraft
		14:30:00	DC-V9 (turn on ranging receiver) transmitted
		14:32:69	DC-V15 observed on earth
		14:34:23	DC-V9 received at spacecraft
		14:37:31	DC-V9 observed on earth
285	12	20:40	Roll transient (caused large rate increase in yaw limit cycle)
286	13	08:44:33.9	CC&S CY-1 No. 44 (turn ranging receiver off)
		11:46	Roll transient
		12:42:00	DC-V9 (turn on ranging receiver) transmitted
		12:46:35	DC-V9 received at spacecraft
		12:52:00	DC-V9 observed on earth
287	14	09:49	Roll transient
289	16	01:31	Roll transient
		03:24:53.8	CC&S CY-1 No. 45 (ranging receiver off)
		16:10:00	DC-V9 (turn on ranging receiver) transmitted
		16:14:53	DC-V9 received at spacecraft
		16:19:09	DC-V9 observed on earth
		16:19:09	DC-V9 observed on earth
291	18	22:05:13.9	CC&S CY-1 No. 46 (ranging receiver off)
			ENCOUNTER
292	19	02:49:00	DC-V25 (begin encounter sequence; tape recorder on) transmitted
		02:54:02	DC-V25 received at spacecraft
		02:58:25	DC-V25 observed on earth
		03:11:39.3	Terminator sensor on (observed on earth)
		04:45:05.8	MT-7 (begin encounter sequence)
		08:50:00	DC-V9 (turn on ranging receiver) transmitted
		08:54:02	DC-V9 received at spacecraft
		08:59:38.8	DC-V9 observed on earth
		10:50:00	DC-V24 (switch to data mode 3) transmitted
		10:55:02	DC-V24 received at spacecraft
		10:57:29	DC-V24 observed on earth
		11:25:03.6	MT-8 (begin data automation system encounter mode)
		15:01:43	DC-V16 (start encounter backup clock) transmitted
		15:05:45	DC-V16 received at spacecraft
		15:11:00	Clock A enable
		15:11:36	DC-V16 observed on earth
		16:33:57 $\pm$25	Planet sensor output in science frame 98
		16:34:29	Recorder motor on (begin Venus data record, track No. 1)
		16:37:59 $\pm$25	Planet sensor output terminated as far limb of Venus passed out of field of view of sensor
		16:40:00	DC-V9 (turn off ranging receiver) transmitted
		16:44:02	DC-V9 received at spacecraft
		16:46:46	Begin Venus data record, track No. 2
		16:49:17	DC-V9 observed on earth

Table IV-10 (contd)

Day	Date	Time, GMT	Event
292	Oct 19	16:56:00	Plasma changes indicating magnetopause
		17:01:00	Plasma changes indicating magnetopause
		17:12:00	Plasma changes indicating magnetopause
		17:14:57 ±25	Planet sensor output in science frames 148–152 for near limb of planet
		17:18:09 ±25	Planet sensor output termination (science frame 153)
		17:34:55.8	Closest approach to Venus (4094 km)
		17:38:09	Enter S-band occultation (closed-loop receiver)
		17:38:10	Enter DFR occultation (49.8 MHz)
		17:39:00	Enter DFR occultation (423.3 MHz)
		17:42:05	Enter S-band occultation (open-loop receiver)
		17:46:49	Terminator sensor output (science frame 185) (antenna pointing angle change) event
		to	(from tape data)
		17:46:51.4	
		17:59:59	Exit S-band occultation
		18:00:31	Exit DFR occultation (423.3 MHz)
		18:00:51	Exit DFR occultation (49.8 MHz)
		to	
		18:01:11	
		18:03:13	DFR in solid lock
		18:19:10	Data automation system antenna pointing angle change backup command
		18:34:18	End of Venus data record, track No. 2
		18:41:51	End of tape (science frame 251); end of Venus track No. 1
		18:48:18	Data mode 2 science and engineering data
		19:00:00	DC-V9 (turn on ranging receiver) transmitted
		19:04:02	DC-V9 received of spacecraft
		19:09:30	DC-V9 observed on earth
		20:40:12	Roll transient
293	20	00:40:28	Roll transient
		—	Venus data playback
		07:25:23.4	MT-9 mode 4 (begin Venus data playback, track No. 1)
		07:26:12	Mode 1 engineering data
		07:44:33	Mode 4 data playback of test pattern, track No. 1
		08:00:36	Mode 1 engineering data
		08:04:50	Roll transient
		08:15:38	Switch to data mode 4 (playback of old test data)
		08:17:52	Start of Venus encounter data playback, track No. 1
294	21	01:13:01	End of tape, mode 1 (switch to track No. 2)
		01:14:28	Mode 4 data playback (all ones)
		01:14:35	Mode 1 engineering data
		01:32:59	Mode 4 data playback of test pattern, track No. 2
		01:49:03	Mode 1 engineering data
		03:58:08	Mode 4 Venus data playback, track No. 2
		16:55:58	CC&S CY-1 No. 47 mode 4 data (turn ranging receiver off)
		18:18:29.7	Mode 1 engineering data
		18:45:00	DC-V9 (turn on ranging receiver) transmitted
		18:50:09	DC-V9 received at spacecraft
		18:54:44	DC-V9 observed on earth
		19:18:17	End of tape, mode 4 (Venus data second playback, track No. 1)
		19:19:54	Mode 1 engineering data
		19:38:08	Mode 4 Venus data playback of test pattern, track No. 1
		19:54:14	Data mode 1 engineering data
		20:09:32	Data mode 4 playback of old test data
		20:11:45	Data mode 4 Venus data second playback, track No. 1
295	22	13:06:52	End of tape, mode 1 (switch to track No. 2)
		13:08:20	Mode 4 data playback (all ones)
		13:26:03	Mode 4 data playback of test pattern, track No. 2

Table IV-10 (contd)

Day	Date	Time, GMT	Event
295	Oct 22	13:42:06	Mode 1 engineering data
		15:51:29	Mode 4 Venus data second playback, track No. 2
296	23	06:11:50	Mode 1 engineering data
		07:11:39	End of tape, mode 4 (Venus data playback, track No. 1)
		07:13:13	Mode 1 engineering data
		07:31:31	Mode 4 data playback of test pattern, track No. 1
		07:47:31	Mode 1 engineering data
		07:55:00	DC-V2 (switch to mode 2 engineering and science data) transmitted
		08:00:16	DC-V2 received at spacecraft
		08:02:54	Mode 4 playback of old test data, track No. 1
		08:04:54	DC-V2 observed on earth (stopped playback 13 s before start of track No. 1 Venus encounter data)
		08:25:00	DC-V28 (turn off tape recorder and switch battery charger on) transmitted
		08:30:16	DC-V28 received at spacecraft
		08:35:27	DC-V28 observed on earth
297	24	11:25:48.9	CC&S CY-1 No. 48 (turn ranging receiver off)
			SWITCH BIT RATES
298	25	16:30:00	DC-V5 (switch to 33⅓ bits/s rate) transmitted
		16:35:23	DC-V5 received at spacecraft
		16:39:32	DC-V5 observed on earth
		20:35:00	DC-V5 (switch to 8⅓ bits/s rate) transmitted
		20:40:23	DC-V5 received at spacecraft
		20:44:33	DC-V5 observed on earth
299	26	20:55:00	DC-V19 (return attitude control subsystem to normal optical control) transmitted
		21:00:26	DC-V19 received at spacecraft
		21:05:56	DC-V19 observed on earth
		21:12:30	DC-V28 (turn off battery charger) transmitted
		21:17:56	DC-V28 received at spacecraft
		21:23:51	DC-V28 observed on earth
		21:23:51.4	Deck resets (low CH 305–300) (low–low CH 415–400)
300	27	06:05:17 (predicted)	CC&S CY-1 No. 49 (not tracking)
302	29	11:11:18	Roll transient
303	30	00:45:06.3	CC&S CY-1 No. 50
305	Nov 1	19:25:44 (predicted)	CC&S CY-1 No. 51 (not tracking)
308	4	14:06:07.7	CC&S CY-1 No. 52
		16:35:00	DC-V9 (turn on ranging receiver) transmitted
		16:40:58	DC-V9 received at spacecraft
		16:45:46	DC-V9 observed on earth
311	7	08:46:26.2	CC&S CY-1 No. 53 (turn ranging receiver off)
		—	Spacecraft rolled three times for UV-photometer calibration
		09:15:00	DC-V26 (battery charger to boost mode; turn off science) transmitted
		09:20:00	DC-V25 (science on; tape recorder on) transmitted
		09:21:10	DC-V26 received at spacecraft
		09:26:10	DC-V25 received at spacecraft
		09:26:47	DC-V26 observed on earth
		09:31:51	DC-V25 observed on earth (mode 3)
		10:13:00	DC-V16 (start data automation system clock A) transmitted
		10:18:10	DC-V16 received at spacecraft
		10:24:46.8	DC-V16 observed on earth
		10:30:00	DC-V2 (switch to mode 2 science and engineering data) transmitted
		10:36:10	DC-V2 received at spacecraft
		10:42:09	DC-V2 observed on earth
		12:16:10	DC-V21 (roll override) transmitted
		12:17:10	DC-V12 (transmit lo–receive lo) transmitted
		12:22:20	DC-V21 received at spacecraft

Table IV-10 (contd)

Day	Date	Time, GMT	Event
311	Nov 7	12:23:10	DC-V12 received at spacecraft (not accepted by spacecraft)
		12:25:48	Begin data record, track No. 1
		12:27:54	DC-V21 (start of roll) observed on earth
		12:29:00	DC-V12 observed on earth (not accepted by spacecraft)
		13:12:46	DC-V21 (roll override) transmitted
		13:13:00	Canopus acquired
		13:19:10	DC-V21 received at spacecraft
		13:20:00	DC-V12 (transmit lo–receive lo) transmitted
		13:24:30	DC-V21 (start of roll) observed on earth
		13:25:00	DC-V12 (transmit lo–receive lo) transmitted
		13:26:10	DC-V12 received at spacecraft
		13:31:10	DC-V12 received at spacecraft
		13:32:00	DC-V12 observed on earth
		13:32:08	Data automation system antenna pointing angle change backup
		13:37:00	DC-V12 observed on earth
		14:02:00	DC-V21 (roll override) transmitted
		14:08:00	DC-V21 (roll override) transmitted
		14:08:10	DC-V21 received at spacecraft
		14:11:25	Canopus acquired
		14:14:00	DC-V21 observed on earth
		14:14:10	DC-V21 received at spacecraft
		14:20:00	DC-V21 observed on earth
		14:25:54	Stop record, track No. 2
		14:33:30	End of tape (end of record sequence)
		14:39:20	Stop record, track No. 1
		15:12:45	Canopus acquired
		15:15:00	DC-V10 (transmit hi–receive lo) transmitted
		15:21:10	DC-V10 received at spacecraft
		15:26:07	DC-V10 observed on earth
312	8	21:00:00	DC-V4 (mode 4 begin data playback) transmitted
		21:06:13	DC-V4 received at spacecraft
		21:11:59	DC-V4 (mode 4 begin data playback, track No. 1) observed on earth
		21:13:23	Mode 1 engineering data
		21:31:44	Mode 4 (data playback of test pattern)
		21:47:41	Mode 1 engineering data
		22:03:08	Mode 4 data playback, track No. 1
		22:06:41	Begin data playback of UV-photometer calibration
313	9	15:00:04	End of tape, mode 1 (switch to data playback, track No. 2)
		15:01:32	Mode 4 data playback (all ones)
		15:01:39	Mode 1 engineering data
		15:19:15	Mode 4 (data playback of test pattern, track No. 2)
		15:35:16	Mode 1 engineering data
		17:45:54	Mode 4 data playback of track No. 2
		19:45:00	DC-V2 (switch to mode 2 science and engineering data) transmitted
		19:51:17	DC-V2 received at spacecraft
		19:57:07	DC-V2 (mode 2 science and engineering data) observed on earth
314	10	03:26:25 (predicted)	CC&S CY-1 No. 54 (not tracking)
		05:00:00	DC-V4 (mode 4 begin data playback) transmitted
		05:06:22	DC-V4 received at spacecraft
		05:12:25	DC-V4 (mode 4 remainder of track No. 2 data) observed on earth
		17:21:17	Mode 1 engineering data
		18:19:08	End of tape, mode 4 (switch to data playback of track No. 1)
		18:20:40	Mode 1 engineering data
		18:39:01	Mode 4 (data playback of test pattern, track No. 1)
		18:55:03	Mode 1 engineering data
		18:58:10	DC-V2 (switch to mode 2 science and engineering data) transmitted
		19:04:32	DC-V2 received at spacecraft

Table IV-10 (contd)

Day	Date	Time, GMT	Event
314	Nov 10	19:10:24	DC-V2 (mode 2 science and engineering data) observed on earth
		19:15:00	DC-V28 (tape recorder off; battery charger on) transmitted
		19:21:22	DC-V28 received at spacecraft
		19:27:46	DC-V28 observed on earth
		19:30:00	DC-V28 (battery charger off) transmitted
		19:36:22	DC-V28 received at spacecraft
		19:42:46	DC-V28 observed on earth
		19:42:53	Deck resets (low CH 208–200) (low–low CH 415–401)
		19:45:00	DC-V9 (ranging receiver on) transmitted
		19:51:22	DC-V9 received at spacecraft
		19:58:00	DC-V9 observed on earth
316	12	22:06:39 (predicted)	CC&S CY-1 No. 55 (turn ranging receiver off) (not tracking)
319	15	16:46:58.7 (predicted)	CC&S CY-1 No. 56
322	Nov 18	11:27:43.8	CC&S CY-1 No. 57
		—	UV-photometer pointing exercise
323	19	13:00:00	QC-V1-1 (17.18-deg pitch) transmitted
		13:05:00	QC-V1-2 (1800-s roll) transmitted
		13:07:19	QC-V1-1 received at spacecraft
		13:14:16.9	QC-V1-1 observed on earth
		13:12:19	QC-V1-2 received at spacecraft
		13:18:28	QC-V1-2 observed on earth
		13:25:00	DC-V14 (remove maneuver inhibit) transmitted
		13:30:00	DC-V26 (science off; battery charger to boost mode) transmitted
		13:32:19	DC-V14 received at spacecraft
		13:35:00	DC-V25 (science on; begin encounter sequence; switch to data mode 3) transmitted
		13:37:19	DC-V26 received at spacecraft
		13:38:39.4	DC-V14 observed on earth
		13:42:19	DC-V25 received at spacecraft
		13:43:41.8	DC-V26 observed on earth
		13:48:30	DC-V25 observed on earth (data mode 3)
		13:50:12	DC-V16 (start clock A) transmitted
		13:57:31	DC-V16 received at spacecraft
		14:03:55.7	DC-V16 observed on earth
		14:06:00	DC-V2 (switch to mode 2 science and engineering data) transmitted
		14:13:19	DC-V2 received at spacecraft
		14:19:34	DC-V2 observed on earth (data mode 2)
		14:21:13	Tape recorder on (first verification)
		14:25:00	DC-V29 (arm first propulsion maneuver) transmitted
		14:32:19	DC-V29 received at spacecraft
		14:39:07.6	DC-V29 observed on earth
		14:53:15	DC-V27 (initiate midcourse maneuver; switch to mode 1) transmitted
		15:00:34	DC-V27 received at spacecraft
		15:05:00	DC-V2 (switch to mode 2 science and engineering data) transmitted
		15:06:49	DC-V27 observed on earth (mode 1)
		15:14:08	DC-V2 received at spacecraft
		15:18:30	DC-V2 observed on earth (mode 2)
		15:51:00	DC-V12 (transmit lo–receive lo) transmitted
		15:58:19	DC-V12 received at spacecraft
		16:04:48.7	DC-V12 observed on earth
		16:04:54	Start tape in science frame 145
		16:05:30	Begin track No. 1 record
		16:06:17.0	Start ccw pitch turn
		(Not in data)	Stop ccw pitch turn
		16:17:37	Begin track No. 2 record (not observed on earth)
		(Not in data)	Start roll turn (+313 deg)
		(Not in data)	Stop roll; start sun reacquisition

Table IV-10 (contd)

Day	Date	Time, GMT	Event
323	Nov 19	17:11:17	Data automation system antenna pointing angle change backup
		17:41:30	Station locked on telemetry sideband
		17:41:30	Acquisition of Canopus
		18:05:36	End track No. 2 record
		18:12:39	End of tape
		18:15:00	DC-V10 (transmit hi–receive lo) transmitted
		18:18:43	End track No. 1 record
		18:22:19	DC-V10 received at spacecraft
		18:25:49	CC&S maneuver counter overflow
		18:28:49	DC-V10 observed on earth
		18:40:00	DC-V13 (maneuver command inhibit) transmitted; station dropped lock on sideband
		18:47:19	DC-V13 received at spacecraft
		18:50:00	DC-V26 (turn off science; battery charger to boost mode) transmitted
		18:53:38.9	DC-V13 observed on earth
		18:55:00	DC-V2 (switch to mode 2, science on) transmitted
		18:57:19	DC-V26 received at spacecraft
		19:02:19	DC-V2 received at spacecraft
		19:03:45.63	DC-V26 observed on earth
		19:08:47	DC-V2 observed on earth
		19:20:00	QC-V1-1 (minimum) transmitted
		19:25:00	QC-V1-2 (minimum) transmitted
		19:27:19	QC-V1-1 received at spacecraft
		19:30:00	QC-V1-3 (minimum) transmitted
		19:32:19	QC-V1-2 received at spacecraft
		19:33:58.3	QC-V1-1 observed on earth
		19:37:19	QC-V1-3 received at spacecraft
		19:39:08.7	QC-V1-2 observed on earth
		19:44:03.13	QC-V1-3 observed on earth
		19:45:00	DC-V11 (transmit hi–receive hi) transmitted
		19:53:19	DC-V11 received at spacecraft
		19:59:11.2	DC-V11 observed on earth
		22:00:00	DC-V4 (mode 4 begin data playback, track No. 1) transmitted
		22:07:19	DC-V4 received at spacecraft
		22:13:33	DC-V4 (mode 4 begin data playback, track No. 1) observed on earth
		22:14:58	Mode 1 engineering data
		22:32:00	Mode 4 data playback of test pattern, track No. 1
		22:48:00	Mode 1 engineering data
		23:04:41	Mode 4 data playback, track No. 1
324	20	16:01:45	End of tape, mode 1 switch to track No. 2
		16:21:08	Mode 4 data playback of test pattern, track No. 2
		16:37:08	Mode 1 engineering data
		16:58:10	DC-V2 (switch to mode 2 science and engineering data) transmitted
		17:05:33	DC-V2 received at spacecraft
		17:11:52	DC-V2 observed on earth (data mode 2)
		17:20:00	DC-V28 (turn on battery charger, turn off tape, 2.4 kHz) transmitted
		17:27:23	DC-V28 received at spacecraft
		17:30:00	DC-V28 (turn off battery charger) transmitted
		17:33:42	DC-V28 observed on earth
		17:35:00	DC-V16 (start clock A) transmitted
		17:37:23	DC-V28 received at spacecraft
		17:42:23	DC-V16 received at spacecraft
		17:43:47	DC-V28 observed on earth
		17:48:49	DC-V16 observed on earth
		17:49:25	All decks skipped
		19:50:39	Data automation system clock A decode for start track No. 1 record
		20:02:30	Data automation system clock A decode for start track No. 2 record

Table IV-10 (contd)

Day	Date	Time, GMT	Event
324	Nov 20	20:56:10	Data automation system clock A decode for antenna pointing angle change backup
		21:49:56	Data automation system clock A decode for stop track No. 2 record
		21:57:32	Data automation system clock A decode for end of tape
		22:03:22	Data automation system clock A decode for stop track No. 1 record
325	21	06:07:24 (predicted)	CC&S CY-1 No. 58 (not tracking)
			CONDITION SPACECRAFT FOR LONG-TERM CRUISE
		15:51:00	DC-V9 (turn on ranging receiver) transmitted
		15:58:28	DC-V9 received at spacecraft
		16:05:20.0	DC-V9 observed on earth
		18:35:00	DC-V15 (Canopus gate inhibit override) transmitted
		18:40:00	DC-V10 (transmit hi–receive lo) transmitted
		18:42:28	DC-V15 received at spacecraft
		18:45:00	DC-V9 (ranging receiver off) transmitted
		18:47:28	DC-V10 received at spacecraft
		18:49:09	DC-V15 observed on earth
		18:52:28	DC-V9 received at spacecraft
		18:54:11	DC-V10 observed on earth
		18:59:05	DC-V9 observed on earth
		19:18:05	DC-V12 (transmit lo–receive lo) transmitted
		19:25:43	DC-V12 received at spacecraft
		19:31:59	DC-V12 observed on earth
338	Dec 1	—	Project defined end of mission (Phase I)
	4	20:00:00	Last data observed (signal strength, 170 dBmW)

V. Organization and Function of SPAC

A. Organization of SPAC

In organizing the spacecraft performance analysis and command (SPAC) group for the *Mariner* Venus 67 mission, a great effort was made to take advantage of past experience in conducting SPAC flight operations. The general organization philosophy for the *Mariner* Venus 67 SPAC is, therefore, an outgrowth of the *Mariner* Mars 1964 SPAC organization. Only those aspects of the organization that changed the basic differences between the two missions, or those aspects that were deemed inefficient during the *Mariner* Mars 1964 operations, were modified. Many aspects of the organization were, in fact, identical in nature and function.

B. SPAC Operations

1. SPAC responsibility and function. The responsibility of the *Mariner* Venus 67 SPAC group was to monitor and analyze spacecraft performance, and to make recommendations for courses of action that would enhance the probability of achieving the mission objectives. This group was one of three analysis groups within the Space Flight Operations (SFO) organization established to support the *Mariner* Venus 67 project. The other analysis groups were the space science analysis and command (SSAC) and flight-path analysis and command (FPAC) groups. These groups were responsible for the analysis of science data and the analysis of the flight path (trajectory), respectively, and for making recommendations for ground commands to enhance mission success from their points of view. The directors of the analysis groups, in addition to the directors of the mission support groups, such as the data processing system (DPS) and the Deep Space Network (DSN), reported to the Space Flight Operations Director (SFOD).

In analyzing the spacecraft data, SPAC continually attempted to evaluate the actual performance against the anticipated performance based upon the design. Extensive effort was applied to explain every unexpected condition observed. Frequently the cause was an incomplete understanding of the spacecraft in a space environment.

Under guidelines established by the SSAC and the project office, SPAC also attempted to maximize the recovery of scientific data. The responsibility of the SPAC group relative to the attainment of scientific data was to assure the acquisition of the planet-oriented data; then, wherever possible within engineering constraints, to assure the acquisition of the maximum amount of interplanetary data.

The SPAC group developed a mission operations plan to fulfill its responsibilities. SPAC planning efforts were instrumental in development of the overall SFO sequence of events for the various mission phases.

2. *Organization.* The *Mariner* Venus 67 SPAC organization had as its nucleus the SPAC division representatives, the SPAC director, and the assistant SPAC director. SPAC division representatives were members of the following technical divisions at JPL: Division 32, Space Sciences; Division 33, Telecommunications; Division 34, Guidance and Control; Division 35, Engineering Mechanics; and Division 38, Propulsion. The SPAC director and assistant director represented Division 29, Project Engineering. In this manner, knowledge of the spacecraft was available in the SPAC organization from each of the broad disciplines that contributed to the design. This was the nucleus of the SPAC organization, and was responsible for implementing the goals of the group. These goals can be summarized as follows: Define facility, computer, and staffing requirements; adequately staff the various positions; effect training of SPAC personnel through procedure generation and test participation; analyze flight data; and recommend actions to be taken during the mission.

Detailed knowledge of the major subsystems aboard the spacecraft was acquired by the SPAC organization through subsystem representatives (usually the cognizant engineer or his alternate). Responsibilities of each representative included knowledge relative to the design, fabrication, test history, and capabilities of his subsystem in flight. In addition, the subsystem representative was responsible for achieving the detailed analysis of his hardware in flight, analyzing real-time telemetry, advising his division representative and the SPAC director of the performance of his subsystem, and providing information on the status of this subsystem during any discussion of action to be taken in case of a nonstandard spacecraft condition.

With the subsystem representatives supporting the SPAC nucleus, the nonstaff portion of the SPAC organization was essentially complete. This organization provided the SPAC director with only a small group to be managed directly by him. It also provided the desirable feature of making each subsystem representative responsible to a member of his own division. The SPAC line organization is shown in Fig. V-1.

During actual flight operations, especially the long-duration critical phases, some modification was necessary in the organization of the *Mariner* Venus 67 SPAC. For these operations, SPAC personnel were organized in a functional manner rather than by individual (as described above). During planning phases, the division representative, for example, is an individual charged with the responsibilities of that position. No alternate may act in his behalf unless duly authorized by the project office, SPAC, and the division in question. This is necessary because his duties involve commitments and recommendations that are binding on both the project and on his division. During an operation, however, two facts serve to void this necessity for individual responsibility: (1) It is not possible to require individual responsibility and extended full-time support simultaneously from the same person, and (2) all commitments and recommendations that require participation by this individual will have been previously made; the responsibility for those occurring during the operation rests with the SPAC director, the SFOD, and the project office. As a result, the operational organization of the *Mariner* Venus 67 SPAC permits the position of division representative to become a functional responsibility; therefore, any qualified person may serve in that capacity.

Early in the mission, it was attempted to treat the position of SPAC director in the same manner. The SPAC director, however, is still required to be individually accountable during a flight operation because he is the only spacecraft representative active in flight operations who is recognized directly by the SFOD and the project office. Thus, although an alternate could be appointed, neither full responsibility nor authority could be transferred. To reduce the burden upon the SPAC director, his duties were classified as to individual or functional responsibility. Those that were individual in nature were reserved for the SPAC director; the functional responsibilities were assigned to the assistant SPAC director position, which could be manned by any qualified member of the SPAC director's staff.

Another modification to the organizational structure of SPAC during flight operations was the elimination of the line-structure requirement that all interfacing between the SPAC direction team and the individual subsystem representatives be carried out via the appropriate

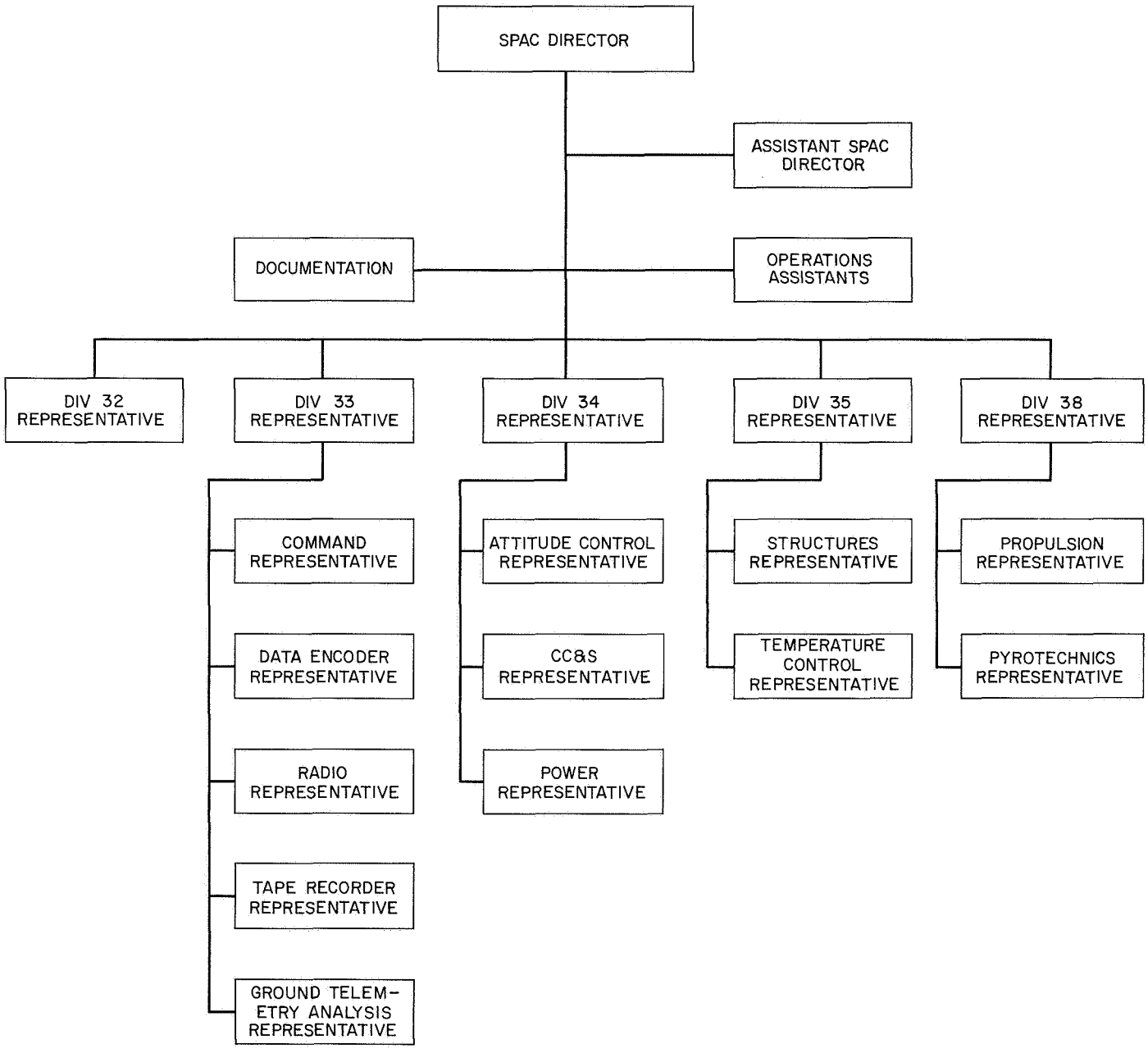


Fig. V-1. SPAC line organization

division representative. Before launch or during routine transactions of SPAC business, the direct insertion of the division representative is necessary in order to guarantee proper coordination of SPAC effort by that division. During an operation, however, this places upon the operation the unreasonable burden of maintaining an additional level in the organization. To avoid this, the subsystem representatives reported directly to the SPAC director, with all reports or recommendations being subject to the division representative's concurrence.

One staff function was performed for the SPAC director by individuals on loan from the organization of the SFOD. These individuals were called operations assistants, and aided in the integration of the mission-oriented SPAC group into the basically mission-independent spacecraft performance analysis area. They also aided in verification and checkout of computer programs to be used by SPAC. Subsequently, the operations assistants provided the SPAC interface with the facility and the computers during the critical (high-activity) phases of the mission. During the cruise phase, these individuals reverted back to the SFOD organization. Their function was then to serve as mission operations controllers during the 24-h/day tracking and data-acquisition activities of the cruise phase. During any of the critical phases of the mission, including encounter, the operations assistants were used to augment the activities required of the SFO organization.

Additional line support was available to the SPAC division representatives through specialized support from individuals within their divisions who were uniquely aware of various assemblies of the spacecraft or who had a special analytical ability or management responsibility. During critical phases of the mission, these individuals were not located in the spacecraft performance analysis area or the *Mariner* Venus 67 mission support area (MSA), but had access to the data within their own complementary analysis team areas, and could contact their division representatives by telephone, as required. They could be summoned into the operations area for consultation by their division representatives or by the SPAC director, as the need arose.

The SFOD requested periodic formal reports on spacecraft performance from the SPAC director. To achieve this objective, it was necessary for the *Mariner* Venus 67 SPAC to acquire a documentation engineer. With his assistance, the SPAC director was able to publish informal weekly reports (to keep appropriate personnel informed during the long cruise) on spacecraft performance, and also to maintain an operations log.

The organization of SPAC just before and immediately after launch was augmented by a group called SPAC JR at the Air Force Eastern Test Range (AFETR). SPAC JR consisted of personnel who were directly involved with the preparations of the spacecraft for launch, but were not members of the launch team. After launch, the launch team also joined this group. In order to use this existing talent at AFETR, SPAC JR was formed under the direction of the spacecraft system engineer. The main responsibility of SPAC JR was to support, in an advisory capacity, the effort of the test director before liftoff and that of the SPAC director after liftoff, this support to continue for Canopus acquisition and also for the midcourse maneuver. A block diagram of the SPAC–SPAC JR interface is shown in Fig. V-2.

3. ***Operations philosophy.*** The operations philosophy of the *Mariner* Venus 67 SPAC group was to maintain 24-h/day coverage by all of the SPAC representatives during the critical phases of the mission, such as launch, Canopus acquisition, midcourse maneuver, and encounter, and also for most situations requiring ground-command action. The basis for this philosophy was the recognition that (1) any major imminent change of state of the spacecraft should be preceded by an interval of extensive data examination before commitment to such action, and (2) any recent change of the spacecraft should be monitored to verify that all expected results are observed, and to ensure against an unexpected effect going unobserved.

A notable exception to the full SPAC coverage requirement stated above was the support requirement agreed upon by the project office and the SPAC director for the transmission of DC-V9 (ranging on) commands during cruise. This agreement was arrived at after a trial period that proved the command to have limited and clearly discernible effects upon the spacecraft. The agreement stated that SPAC support required for the DC-V9 command could be limited to cognizant areas that were involved in transmission of the command and in analysis of the effects of the command.

In the early phases of the mission (until L+2 days), SPAC manning for the interval between critical phases was provided only by division representatives (or their equivalent) and a member of the SPAC director's staff. After L+2 days, the SPAC effort was reduced to daily reviews of the data, followed by daily meetings of the SPAC director with the division representatives. Continuous monitoring of the data was accomplished by an

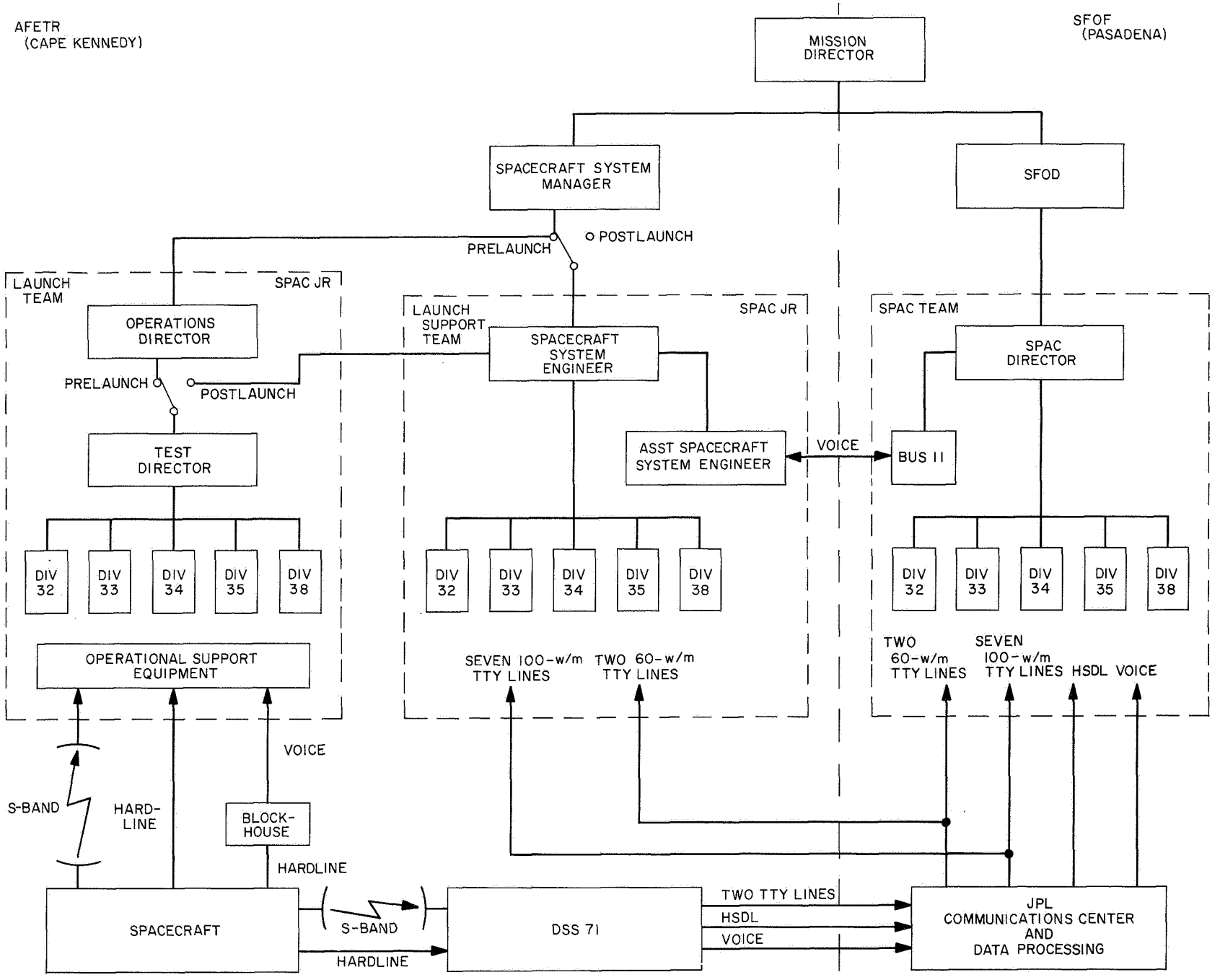


Fig. V-2. SPAC-SPAC JR interface

alarm program in the 7044 computer under the supervision of the Venus operations controller. Any violation of alarm limits previously read into the computer would cause the Venus operations controller to be alerted. He would, in turn, notify the SPAC director and the appropriate division or subsystem representatives, who would take whatever action was warranted.

Frequently, in situations where an unexpected condition existed, some action could be taken on the ground to provide better understanding of the condition of the spacecraft, or else there was an obvious need for the transmission of a ground command. More frequently, however, the unexpected condition was only the result of bad data or, perhaps, of some unknown condition. One aspect of the SPAC function was to ascertain the exact cause of an unexpected condition before any overt action was taken. The prevailing philosophy was that no intentional perturbation to the spacecraft would be initiated on the ground unless such action was clearly warranted and justified.

On previous missions, this had been interpreted as precluding the transmission of any ground command unless it was a corrective action for a particular problem. The nature of the *Mariner* Mars 1964 and *Mariner* Venus 67 missions, however, was such that an extension of the basic philosophy was evolved during the mission. Ground commands were used to preempt automatic features aboard the spacecraft, and to exercise a backup to an automatic function before the need for such a command was demonstrated. The necessity for this change in philosophy resulted from the intricacies of the spacecraft logic and from recognition of the appreciable one-way transmission time of signals between the spacecraft and earth at encounter. Before a ground command to correct an unexpected condition aboard the spacecraft at encounter could reach the spacecraft, the condition requiring the corrective command had existed for at least 9 min. If that much time was consumed before a backup command could be effective, its utility might be so marginal as to make it useless.

4. SPAC interfaces. To complete its task successfully, the SPAC group needed numerous interactions with other elements of the SFO organization. Those interfaces are described herein to provide an understanding of the broad scope of effort involved in a spacecraft performance analysis activity.

a. Facility. One of the major interfaces was with the Space Flight Operations Facility (SFOF), which housed all of the SFO activity at JPL during the *Mariner* Venus 67 mission. One segment was the MSA, which housed the SPAC team for the entire mission. To use the MSA properly, it was necessary for SPAC to define its equipment needs, including telephones, desks, data display devices, and communication-network requirements. After defining the equipment needs, it was necessary to derive a layout for the various items of equipment. It was essential that the staff have convenient access to various equipment, as required. The final MSA room arrangement is shown in Fig. V-3.

The MSA was completed and occupied by the *Mariner* Venus 67 project in February 1967. It provided an interference-free location where *Mariner* personnel could work, meet, and eventually test and execute the encounter sequence when the spacecraft passed the planet on October 19, 1967. The MSA also housed SSAC, the Venus operations controller, and the SFOD.

Several shortcomings inherent in the initial SPAC MSA were recognized and, in most cases, corrected. The noise level generated by the operation of the TTY machines was uncomfortable. This irritation was reduced by placing sponge-rubber pads beneath each machine, but the problem was never entirely alleviated. The space between desks (4 ft) was insufficient. A minimum of 5 ft would be desirable to remove the congestion that occurred during scheduled exercises. In most cases, it was difficult to pass behind a seated member without disturbing him, or snagging clothing on the TTY paper dispensers, or knocking objects off of the facing desk. The TTY paper dispensers were not part of the original plan; they were added later to keep the paper from piling up on the floor. Flashing lights were added to the telephones so that one could tell at a glance which of the many phones was ringing.

The 3070 printer displayed formatted spacecraft data for easy readability. Although the 3070 display lent itself readily to real-time data needs, it was very difficult to retrieve data several hours old. Unrolling and rewinding the output spools of paper were clumsy and time-consuming operations. The 3070 printing process produced a gritty carbon residue that tended to be messy. Also, after extended hours of operation, the 3070 gave off an obnoxious odor.

It was noted on many occasions that the response from the support chief was sluggish. Waiting 15 min or more for headsets, TTY paper, or TV monitor repair was not uncommon. Exercises were delayed until headsets were made available. A solution to this problem

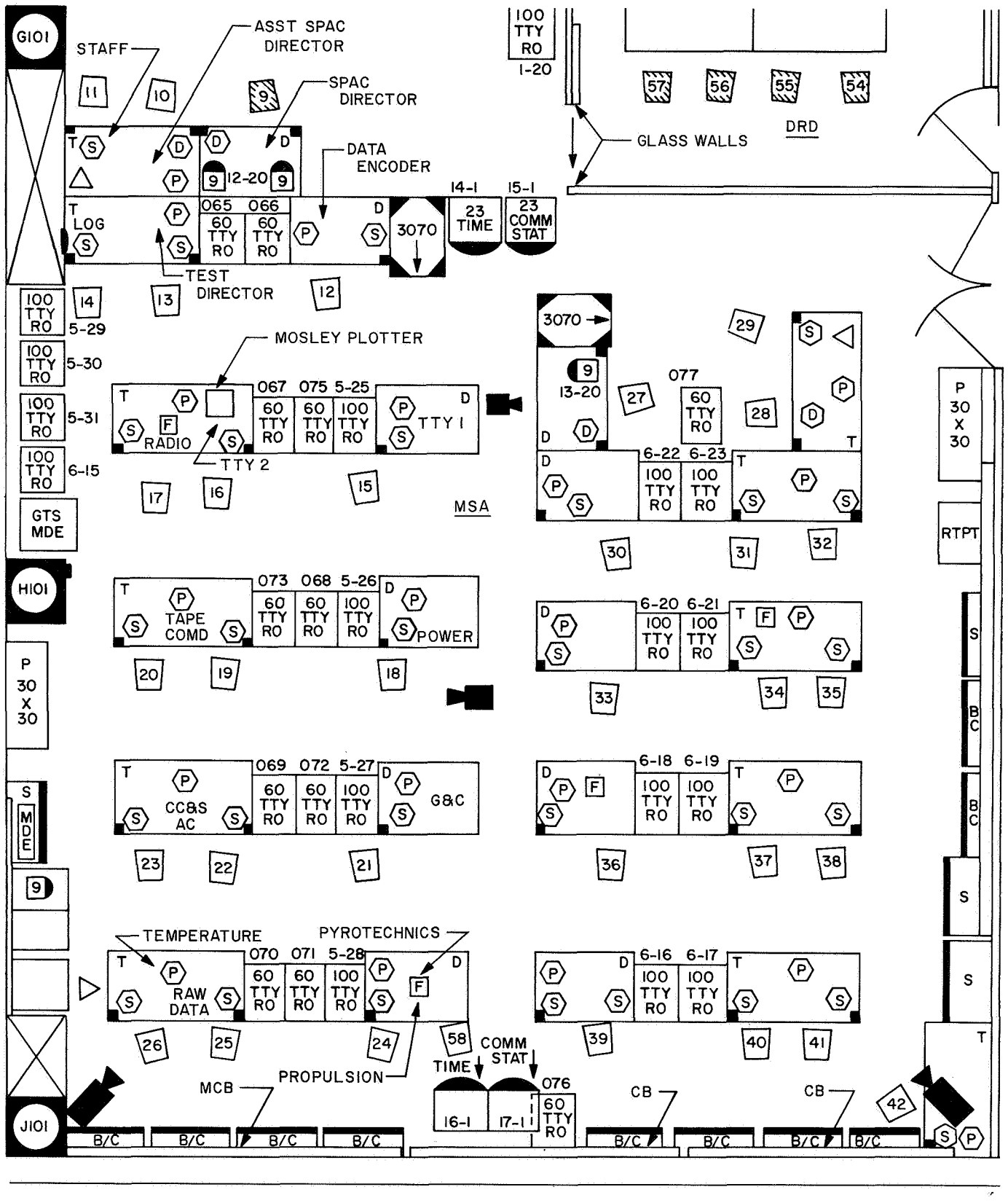


Fig. V-3. SPAC layout

would be to assign each SPAC member a headset for the duration of the mission.

b. Data processing system. The SPAC/DPS interface was one of the most important and frequently used interfaces throughout the *Mariner* Venus 67 mission. In spite of its relative importance, however, this has always been, and remains, one of the weakest interfaces.

The function of the DPS for SPAC was to perform various operations on spacecraft data in real and nonreal time in order to make the spacecraft data available to SPAC in an easily recognizable and useful form. The operations involved in performing these functions were buffering, computing, editing, formatting, and routing. For the *Mariner* Venus 67 mission, these functions were performed by the 7044 computer at the SFOF and by the telemetry and command processor (TCP) at the Deep Space Instrumentation Facility (DSIF). The interface between the DPS and SPAC should have been limited, therefore, to a bilateral specification of the SPAC data processing requirements and the request for certain unforeseen special data processing requirements arising during the conduct of the mission.

As in the past, the data processing requirements for SPAC were arrived at unilaterally by SPAC personnel who were generally unfamiliar with the organization and the capabilities of the DPS. There was, therefore, no *a priori* knowledge as to whether or not the DPS could efficiently meet SPAC requirements. The requests were accepted, and certain dates for DPS progress reports and deliveries were established. During the implementation of the SPAC data processing requirements, the periodic DPS progress reports made it increasingly clear that the established delivery dates would not be met. By far the major contributor to the schedule slips experienced by the DPS were those associated with the 7044 redesign. The 7044 redesign program was completed 3 mo behind schedule. It was a mission-independent program; therefore, no ready response was made to project requests. The 7044 redesign program, however, was germane to the *Mariner* Venus 67 data processing programs, and its schedule slips directly affected, and indeed were responsible for corresponding schedule slips of the mission-dependent programs. As a consequence of these schedule slips, many of the SPAC activities were adversely affected (see Subsection C-6).

In an attempt to salvage as much of the DPS capability as possible, the SPAC data processing requirements were assigned priorities by the SPAC director. The highest priorities were assigned to real-time, data-number SPAC formats. Through the exemplary efforts of various members of the DPS, these real-time formats were made available for launch, and were continuously improved upon throughout the mission. The price paid for the availability of the real-time programs, however, was the forfeiture of engineering-unit formats and the relatively poor response associated with the nonreal-time formats.

In retrospect, to eliminate many of the difficulties encountered during the *Mariner* Venus 67 mission, the following improvements should be considered for future missions:

(1) The generation of SPAC data processing requirements should be accomplished bilaterally between SPAC and the DPS with the aid of a DPS representative assigned to SPAC.

(2) The constraints imposed by mission-independent programs should be minimized.

(3) The project office should be able to influence the DPS in the DSN to a much greater extent than was possible for the *Mariner* Venus 67 mission.

(4) DPS capabilities should be demonstrated well in advance of SPAC tests.

Adherence to the above recommendations may not alleviate all of the problems historically associated with the SPAC/DPS interface, but will improve the status quo by at least an order of magnitude.

c. Deep Space Instrumentation Facility. The necessary interaction between the DSIF and SPAC was handled by the SPAC director and the telecommunications division representative (or their alternates). During critical operations, the DSIF project engineer was accessible to SPAC only through the SFOD. Because all telemetry was received by the DSIF stations, which also transmitted all commands, it is natural that much information about the DSIF stations at any particular point in the mission was of interest to SPAC.

The primary interface activities involved: (1) determination of a two-way tracking schedule in conjunction with the FPAC group, (2) discussion regarding the use of the 210-ft antenna at the Goldstone Mars Deep Space Station (DSS 14), and (3) determination of the procedures involved in sending commands and receiving spacecraft telemetry signals. Periodically, it was necessary to request from the DSIF such information as station

time, transmitter frequency, ground-received signal level, or a readout of some telemetry channel directly from the telemetry processing equipment at the station. When problems occurred in the communications lines bringing telemetry data into the SFOF, it was necessary to request the DSIF to monitor various telemetry channels, and report by voice when and if these channels changed in value. This permitted rapid action on the part of personnel in Pasadena, even if they were unable to view the telemetry that was being received at the station at that particular moment.

An example of the special functions that the DSIF was requested to perform is monitoring of the analog recorders at the station to fix the time when frequency transients were noted on the downlink signal. One type of frequency transient occurred when the spacecraft cyclic command occurred while the spacecraft receiver was in a one-way lock condition. The SPAC requirement for precise timing of the transients was based upon a need for accurate information about the spacecraft central computer and sequencer (CC&S) count rate.

The DSIF received-signal level was displayed during the mission in the *Mariner* MSA on an analog recorder and as digital data in a 100-w/m TTY. This requirement was established after detailed investigations into the implementation of the spacecraft roll inertial control mode indicated that the high-gain antenna pointing error was the only measurable roll-attitude indicator. This capability to monitor received-signal level permitted the telecommunications analyst in SPAC to gain some knowledge about the signal-level changes as a function of time.

d. Analysis areas. The interfaces with the other two analysis areas (SSAC and FPAC) were very important to the successful accomplishment of its responsibilities by SPAC. The SSAC group was able to assist SPAC in the interpretation of the scientific mission objectives so that proper determination of the mission plan could be effected. SPAC felt a responsibility to implement the desired goals of the scientific community whenever these could be accomplished without detrimental effect upon the final accomplishment of a successful encounter sequence.

Evaluation of the science data by the science-cognizant engineers and scientists provided the SPAC group with an indication of the environment that the spacecraft was observing, and also provided useful inputs to SPAC relative to the occurrence of various events.

Some of the state changes observed aboard the *Mariner V* spacecraft were evidenced in both the science and engineering telemetry. Correlation of the times of these occurrences in both telemetry types permitted more concrete verification and analysis of these changes. The interface between SPAC and the SSAC was effected by the SPAC director and the SPAC science representative, each of whom had contact with the SSAC director. Additionally, the SPAC science representative was in direct communication with the science subsystem cognizant engineers, who were located in the SSAC area. Later in the mission operations, direct communication of an informal nature between the SPAC director and SSAC personnel was found to be more convenient under certain circumstances.

The FPAC group provided SPAC with trajectory information, including the geometry of the spacecraft relative to the sun, earth, and other celestial objects during the mission, with special support being given during launch, midcourse maneuver, and encounter. This information permitted detailed and knowledgeable interpretation of the performance of the spacecraft as far as both the telemetry and the radio signals observed on earth were concerned. An important function of the FPAC group was the prediction of the frequency for transmisson to the spacecraft. This was necessary because of the continually changing doppler effect upon the radio signal. The availability of such information to SPAC permitted better analysis of the radio signals, as well as rapid lockup of both the uplink and downlink signals.

e. Venus encounter preparation working group. The Venus encounter preparation working group (VEPWG) greatly influenced operations within SPAC for the encounter portion of the mission. The VEPWG was one of several groups established by the *Mariner* project office in July 1967 to support SFO in preparations for the remainder of the *Mariner* Venus 67 mission. Basic responsibilities of VEPWG were to augment the SFO organization by studying the potential encounter phase at greater length, and to make recommendations to this organization and the *Mariner* project office as to the strategy that should be employed to maximize the probability of mission success. The major outputs of VEPWG were the following recommendations:

(1) Encounter in the DC-V15 attitude control (AC) roll mode.

(2) Preempt MT-7 with DC-V25.

(3) Preempt MT-8 with DC-V24.

(4) Enter S-band occultation in the one-way (noncoherent) tracking mode.

In addition, VEPWG generated the encounter-sequence flow diagram and sequence of events. The chairman of VEPWG was the SPAC director, and his committee was composed of experimenters, technical division representatives, SPAC division representatives, and representatives from DSIF, DSN, FPAC, SSAC, and DPS.

In the preparation for encounter, hidden facets of the spacecraft design and operation were uncovered and/or rediscovered to a much greater extent than had been anticipated. The acquisition of detailed knowledge relative to the spacecraft design and predicted performance, based upon testing, was very useful in the evolution of the encounter sequence plan. This plan was thoroughly tested before encounter with a series of tests conducted with the flight-support spacecraft.

5. SPAC data output. The *Mariner V* spacecraft data for SPAC were supplied by the following five sources: 7044 computer, 7094 computer, TCP teletype data, ground telemetry system (GTS) decommutator and Franklin printer, and green-box/brush-recorder data.

The 7044 computer provided three outputs that were used by SPAC. The first was the Stromberg–Carlson 3070 electrostatic printer. The second consisted of selected telemetry measurements sent to TTY machines that were modified to operate at a rate of 100 w/m. The third output of the 7044 was a plot of the telemetry data on a Milgo 30 × 30-in. plotter. This latter device had the capability of printing and displaying a total of 24 engineering channels. The plotter was broken down into 12 subfields, with a maximum of four channels per subfield.

In addition to several special programs, the 7094 computer provided three data outputs that were used by SPAC: (1) The engineering data decommutation program (**ENG. DECOM.**), which listed all of the data from each engineering channel, and decommutated and identified the lower deck positions and data. These data were distributed to SPAC personnel every week. (2) The systems suppressed data program (**SSDM**), which was used to reduce the printout of nonchanging engineering telemetry channels. This program was used for only a short time at the beginning of the mission. Its termination was based upon a survey showing that the suppressed data package was always larger than **ENG. DECOM.** with all data. (3) Output from the engineering telemetry plot program (**EDPLOT**). With the **EDPLOT** program, selected telemetry channels could be plotted to desired time scales, providing SPAC personnel with a graphic display of engineering telemetry data for each channel. The output from this program was reduced to the continuously changing channels of AC positions and ground-station automatic gain control (AGC) because of the short time scale over which the data were plotted.

A third source of data (the most important for real-time support) was TTY data. The prime TTY data source was the high-speed TTY machine (100 w/m). Data for the TTY line were formatted in the TCP at the tracking station, and then transmitted over the high-speed data line (HSDL) directly to the SFOF 7044 computer, which converted and formatted the data for the 100-w/m TTY machines. If required, the 7044 could also process the 8⅓ bits/s TTY data. This format, which came through the communications processor (CP) computers from the TCP at the stations, printed out only the engineering channels that the user at each position was interested in evaluating.

The second SPAC TTY data source was two 60-w/m TTY lines that were connected from the TCP computer at the station through the CP computers. Each TTY line could handle 30 bits/s of data. Because the spacecraft data rate could be as high as 33⅓ bits/s, two TTY machines were necessary to handle the data flow rate for the first month. The TTY machines were modified to print out data in data number (DN). The format for the 60-w/m TTY was so designed that the engineering sync word (127) for each high-rate deck would appear at the front of each line of TTY data. To indicate a DN greater than 100, a bar was placed under the first digit of a two-digit number, reading from left to right. To indicate low-rate deck channel numbers, the last two digits of each low deck channel number were placed on the right side of the TTY printout. Medium deck position and science frame count were also indicated to help facilitate data reading. All data, both engineering and science, were sent to Pasadena to ensure that all possibilities were considered in evaluating anomalous conditions.

The third type of TTY data used was called raw-data backup. The raw-data backup was transmitted over the same 60-w/m TTY as was used for the raw data. The difference in formatting was as follows: The raw-data backup had none of the low deck position indicators, and the word sync (127) could appear anywhere in the printout, whereas raw data had the sync word at the start of each TTY line. The SPAC team relied primarily on the high-speed data and the raw data for real-time engineering decisions.

The fourth data output available to the SPAC team was a GTS decommutator and a Franklin printer, which were located in the SPAC area. This output device was identical to that used at the System Test Complex during spacecraft system tests. The output of the Franklin printer was used primarily during periods when the raw TTY and 7044 high-speed TTY lines were down.

The green box was a special display source and hardwire computer employed within SPAC. The green box consisted of data-conversion equipment driven by either the HSDL or the 60-w/m TTY lines at 8⅓ bits/s. This equipment was developed and used by the guidance and control analysts to provide a rapid analog display of important telemetry channels. Some other important functions that the green box performed are as follows:

(1) Operated the station AGC plotter for telecommunication in the SPAC area; also, plotted station AGC on the brush recorder.

(2) Operated the real-time data translator (RTDT), which presented science data in octal form.

(3) Had octal counters that showed the number of events in channels 115 and 116.

(4) Had a red light indicator that monitored performance of the high-speed TTY line (light indicated whether data were continuous or intermittent).

(5) Contained a switch that could be initiated to change data beginning received in data bar back to normal data.

(6) Provided an interface with the incoming data for the GTS decommutator and Franklin printer.

(7) Provided signals to the Sanborn recorder that plotted telemetry channels aiding in Canopus acquisition.

This technique of displaying digital telemetry data to satisfy unique requirements proved to be worthwhile throughout the mission, particularly in the early phase, at the time of Canopus acquisition, and during the midcourse maneuver. The green box proved to be a vital source of data in its support of SPAC requirements.

Each of the outputs available to the SPAC team was intended to fulfill a specific purpose. The 3070 printer output was used continuously throughout the mission by the SPAC director and the mission operations controller to assess the status of the spacecraft, and by the telemetry subsystem analysts to verify the state of their subsystems. These printers had the desirable capability of printing all telemetry channels. Not all SPAC personnel had ready access to a 3070 printer, however, because only two were available. Subsystem data analysts used the output of the high-speed teleprinters, driven by the 7044 computer, as their prime data source throughout the mission. The outputs of these devices were specially formatted, with only telemetry channels of interest displayed to each analyst. The Milgo plotter output was used by the AC engineer to analyze the performance of the spacecraft control system in its limit-cycle operation.

The **ENG. DECOM.** program output was intended to provide a complete nonreal-time record of spacecraft engineering data in a reasonably compact form, thus supplying each SPAC analyst with a reference library of telemetry data. The **SSDM** program was intended to supplement **ENG. DECOM.**, but in a compressed form very similar to a nonreal-time alarm record. **SSDM** was of little value; therefore, it was terminated early in the mission. The **EDPLOT** output was to provide a graphical equivalent to **ENG. DECOM.** for selected measurements.

All data generated during the *Mariner* Venus 67 mission were stored by an organization of the SFOF called document control. Having all of these data on file provided the SPAC representatives with a means of obtaining and reviewing any segment of the mission.

A master data library (MDL) of engineering telemetry data has been generated to compile all of the best data recorded at the DSIF stations on magnetic tape. The MDL provides an accurate and reliable record of all mission data. The output of the MDL, as far as engineering telemetry is concerned, is in two forms. The first is a microfilm of an engineering lister, which is essentially a high-deck, decommutated listing of all engineering channels in their decimal-value format; i.e., without engineering conversion. The second form is **ENG. DECOM.** stored on magnetic tape.

C. Performance Evaluation

1. Performance parameters. It should be noted at the outset that no direct method is available to evaluate the SPAC group. The *Mariner* Venus 67 SPAC was chartered to monitor the spacecraft to determine from the telemetry the state of the spacecraft, and to recommend to the SFOD and the project office any action necessary to effect the achievement of the mission objectives. Because

SPAC performed these functions, and the mission objectives were achieved, the SPAC activity must be considered successful. The charter, however, allows such a broad spectrum of action that mission success is a very gross indicator of SPAC performance.

If the spacecraft is designed to perform its mission with no support from SPAC, and it does, then the SPAC group supporting that spacecraft is more successful than one heavily supporting a spacecraft that failed. Obviously, if the failure can be traced to an act of either commission or omission by SPAC, then the SPAC group was at fault; in all other cases, no absolute criterion exists for measuring the effectiveness of SPAC.

The true evaluation of the *Mariner* Venus 67 SPAC is further complicated by the fact that SPAC recognized the difficulty involved in responding to spacecraft anomalies with effective corrective action, especially at planetary-encounter distances, with the associated 9-min communications turn-around time. The primary effort, therefore, was directed towards the implementation of an operations plan that would prevent anomalous preemption of an automatic spacecraft function; as a result, operation of those automatic functions was never fully verified. Thus, no after-the-fact information is available to verify that the action of SPAC was required. Any evaluation of SPAC performance must rest solely on an assessment of the quality of the analyses that led to the adoption of preemption as a flight procedure.

To the SPAC personnel themselves, the best indication of the performance of SPAC was found in the high degree of preparedness for the critical phases of the mission demonstrated during SPAC anomaly tests (see Subsection C-6, below). A very large number of possible failure modes had been investigated and provided for, either through preventive action or the adoption of a plan for corrective action.

SPAC testing showed that the capability to react was high. Telemetry predictions allowed almost immediate recognition of failure modes; exchange of information was quick and complete; and nonstandard procedures were well understood. During actual mission operations, the SPAC representatives performed their duties with the efficiency and dispatch of a highly professional team.

As with any undertaking of this magnitude, a number of areas stand out as primary contributors to success, whereas others demonstrate considerable room for improvement. These latter areas are discussed in the paragraphs that follow.

2. *Facilities.* In general, the facilities provided for the *Mariner* Venus 67 mission operations were quite satisfactory. Two deficiencies, however, are worthy of special attention: (1) the DPS schedule slip that manifested itself in modified test schedules and the modification of the planned primary display devices for SPAC, and (2) the somewhat cramped and noisy quarters provided for SPAC operations.

During the initial planning phase of the *Mariner* Venus 67 SPAC data-display system, the prime real-time display devices were to be the 100-w/m TTY machines. These were to display 7044-processed, high-speed data for each of the SPAC members. The data were to have been of two general types, engineering units and DNs, specially formatted to the specific requirements of each SPAC member. Because of the 7044 redesign, however, it soon became apparent that the software design was behind schedule.

In an attempt to lighten the software load, the various SPAC formats were reevaluated by the SPAC director, and format priorities were established. The intent was to supply as much of the requested data processing capability as possible in the time remaining until launch. Because SPAC members were by that time well acquainted with the raw-data and raw-data-backup formats provided by the TCP (and used during numerous SPAC tests), first priority was given to DN formats, with lower priorities being given to engineering-unit formats. In addition to establishing a priority for various formats, the SPAC director requested the distribution of 60-w/m TTY machines throughout SPAC in case the 7044-processed data experienced further delays.

The SPAC area was, therefore, capable of operating completely independently of processed high-speed data. In a further effort to protect SPAC from possible data processing equipment failures, a Division 34 analog-to-digital converter (A/DC), the green box, was used in conjunction with the HSDL to drive the Division 33 GTS and the Division 32 RTDT (see Subsection C-6, below). The green box was to be the last source of data should both the CPs and the 7044 be malfunctioning. As conservative as this approach may seem, it proved to be fortunate during numerous operations when the green box was the only source of real-time data to SPAC. During the high-bit-rate portion of the flight, when the 60-w/m TTYs were lagging and the 7044 was not available, the green box again proved its usefulness when it was the only source of real-time spacecraft telemetry data.

The nonreal-time, telemetry data processing requirements for SPAC were the **ENG. DECOM.**, **EDPLOT**, and **SSDM** programs. Of these, **ENG. DECOM.** was by far the most useful. Its only deficiency was the fact that it was seldom available within the 24-h desirable period. **ENG. DECOM.** did, however, prove to be useful for nonreal-time data analysis. It was generally felt that the two latter formats, **EDPLOT** and **SSDM**, did not warrant the expense and effort required for their generation. **EDPLOT**, although it fulfilled a necessary function for Divisions 33 and 34, was found to be too cumbersome and expensive. For future missions, it is recommended that either a simpler computer method be employed or that this function be performed by hand plots. **SSDM** never fulfilled its data-compression function because its output was generally longer than the unsuppressed data.

The 7044-processed formats were found to be extremely useful for SPAC during the *Mariner* Venus 67 operation, and should be retained for future missions. These were the 100-w/m TTY formats, the alarm formats, and the latest available data formats. They permitted the automatic monitoring of the spacecraft during noncritical portions of the mission, thereby alleviating the necessity of full-time SPAC support for extended periods.

To avoid repetition of the difficulties experienced with the DPS on the *Mariner* Venus 67 and *Mariner* Mars 1964 missions, the following recommendations for future missions may prove to be helpful:

(1) SPAC should be assigned a permanent Division 31 representative for data processing.

(2) SPAC data processing requirements should be clearly stated in language understandable by the data processing support organization.

(3) SPAC data processing requirements should be made known to the support group early in the mission (approximately 15 mo before launch).

(4) The project office should be capable of exercising more influence on the DPS (mission-independent program requirements should be kept to a minimum).

(5) The DPS should demonstrate its ability to fully support SPAC operations 6 mo before launch.

Because of the unavailability of SPAC facilities in SFOF, the early phases of SPAC testing were conducted in the Spacecraft Assembly Facility (SAF) at the northwest corner of the high bay at JPL. This area, although physically small, fulfilled its intended function of checking out the TCP, and permitted the SPAC members to become familiar with the raw-data and raw-data-backup formats, as well as gaining a better understanding of the spacecraft itself.

In February 1967, the SPAC test operations were moved to the SFOF MSA (see Subsection C-6, below). This facility was so arranged as to house SPAC, SSAC, and the Venus operation controllers in one large, irregularly shaped room. Although the physical proximity of these three groups was desirable from a communications standpoint, the allocated space for these functions proved to be quite small. Because of this general lack of sufficient working area, the space allocated to SPAC members was restricted to half of a 3- by 5-ft table in the best case (during noncritical periods) and to a chair, without a working area, in the worst case (during critical periods).

For future missions, it is suggested that more space be allocated to SPAC operations, and that an attempt be made to design a facility with acoustically absorbent characteristics.

In summary, the facilities available to the SPAC group were adequate for the most part. The physical layout was cramped, but acceptable. The data processing facilities were generally adequate for real-time telemetry, although certainly not optimum. Computer outages proved to be a continuous problem throughout the cruise phase of the mission, although performance during the critical phases was generally quite good. Nonreal-time data processing never came up to expectations. Computer program development suffered significantly from the following: (1) lack of a firm schedule commitment, (2) lack of a clear definition of responsibility, and (3) lack of project control over the DPS. In the future, special requirements could be satisfied outside of the SFO system with the use of *Mariner*-peculiar equipment, when necessary.

3. *Organization.*

a. Internal organization of SPAC. Review of the SPAC organization revealed that basically it was adequate to accomplish its required tasks. The SPAC organization was fashioned along the lines of the *Mariner* Venus 67 project, with division representatives reporting to the SPAC director and subsystem representatives reporting to the division representatives. By bringing the influence of the SPAC division representatives to bear within their own divisions, the SPAC director had an effective means of implementing SPAC policies among all members of

the organization. This technique proved to be effective in achieving various tasks desired of the subsystem representatives.

Three noticeable deficiencies should be corrected for future missions. First, there was no full-time SPAC DPS representative. The requirement for such an individual was recognized during the *Mariner* Mars 1964 mission, but was never fully implemented. As a result, personnel who were not thoroughly familiar with many facets of the 7044/7094 computer system in the SFOF were forced to participate in the resolution of many computer-interface problems. With insufficient time to learn the computer system adequately, the SPAC personnel were not very helpful in resolving computer problems.

In retrospect, having the proper personnel responsible to the user side of this interface would have eased the problem experienced in checking out the computer programs. Another function of the data-handling representative would be to resolve any difficulties in the distribution of data or in the establishment of computer program operational requirements, working in conjunction with data processing and SPAC personnel. In the future, a plan should be worked out to provide such an individual, who would be influential in the DPS organization. The experience gained on this project indicates that the dollar savings possible through the use of a DPS representative would certainly justify his presence.

The second area that can be noted as a deficiency in the SPAC organization is the relationship between the SPAC director and the Division 32 science representatives and engineers, who report through him to the SPAC. It is suggested that future projects provide science-instrument engineers to be part of SPAC, reporting to the SPAC director through the Division 32 representative, as is the case with other technical divisions.

Informally, the SSAC directors on the *Mariner* Mars 1964 and *Mariner* Venus 67 projects have allowed the SPAC director to have nearly this type of interface with the Division 32 representative and instrument-cognizant engineers, as this requirement became clearer during each mission. This informal working arrangement had only minor problems in the past because of the good working arrangement of all concerned individuals. However, recognizing this need in the organization removes personalities from organizational consideration. This arrangement will also enhance direct communication, as required, between the instrument-cognizant engineers and other subsystem engineers on the *Mariner* SPAC. As was learned during the *Mariner* operations, frequent opportunities occur for exchange of information between the SPAC director and the science engineers and engineers from other spacecraft subsystems. This fact was not sufficiently acknowledged in the organization of SPAC and SSAC.

In actual practice, it was also confirmed that the science-analysis area can effectively be divided into operational personnel (instrument-cognizant engineers) and scientific data-analysis individuals. The latter are generally the cognizant scientists and associated investigators. A special interface was established with the scientific investigators who were located in another area. This interface was handled by the SSAC director and his alternate.

The experience of both the *Mariner* Mars 1964 and *Mariner* Venus 67 missions reinforced the necessity for a documentation engineer. Initially, this need was not sufficiently fulfilled, which was unfortunate (particularly on a mission of such long duration) because ability to document progress on a continuing basis is most important. Keeping of accurate records and logs is a prerequisite to good documentation. SPAC efforts in this respect were not of the desired quality (mostly in regard to timeliness). There is a great need for an individual on the SPAC director's staff whose sole responsibility would be SPAC documentation on a continuous and project-to-project basis.

From an operational point of view, the necessity for adequate procedures cannot be minimized. The documentation engineer should be able to provide the assistance required in having the procedures published. Another benefit of the documentation engineer's participation in the SPAC effort would be dissemination of spacecraft performance information on a weekly basis. This effort would serve to keep project personnel informed throughout the mission, including individuals who were reassigned to other projects after the spacecraft launch and initial flight operations. These weekly reports would solve one of the big potential problems of a mission of many months' duration; i.e., a sense of participation in flight operations for personnel who participated heavily in the prelaunch phase.

As a result of the *Mariner* Venus 67 SPAC experiences, it is recommended that, in the future, key positions in the project organization be staffed to include one qualified individual whose prime purpose is to provide full-time documentation support. This individual must be a

qualified and experienced technical writer, and a member of the SPAC director's staff. He should provide documentation support to the early SPAC testing, SPAC meetings, procedure meetings, and encounter-preparation meetings. The writing of the meeting minutes, test results, and preparation of procedures will better enable the keeping of an accurate operations log and the documentation of SPAC and spacecraft performance. His function will also free the engineers to do more planning by reducing their documentation time.

The daily Mission Operations System (MOS) meeting, although demanding, proved to be quite helpful in the dissemination of project status and other information. The documentation requirements of a daily report, a weekly report, and a final report were felt to be somewhat repetitive, but each fulfills a required need.

4. Preparation and planning. SPAC preparation and planning were done by the SPAC director with the aid of the division representatives. Most of the SPAC division representatives were spacecraft-design oriented, and were required to phase out of these activities to allow more time for flight-operations-oriented activities. Special meetings were held by the SPAC director with the division representatives to discuss such topics as data-display requirements, data processing requirements, SPAC organization, and SPAC testing requirements. These activities were complementary in regard to the establishment of the configuration of the *Mariner* MSA, checkout of (and familiarization with) the computer programs, and the generation of operations procedures for SPAC. These meetings also provided a sounding board for all aspects of the SPAC effort. The results of these meetings were instrumental in the success of the *Mariner* Venus 67 SPAC preparations.

After launch and the reorientation of mission operations into the more routine cruise phase, a series of daily (except weekend) SPAC meetings was initiated. The principal purpose of this series of meetings was reviewing spacecraft performance of the preceding day in order to provide feedback to the SFOD and the project office as to the progress of the mission. From the viewpoint of the SPAC direction team, the daily-meeting technique was extremely effective in providing total SPAC performance coverage.

As a result, these meetings provided much insight into the operation of the spacecraft by essentially dividing the discussion of spacecraft performance into smaller, more easily assimilated segments. Had the meetings been held less frequently, certain aspects of spacecraft performance might have been inadvertently ignored in the conduct of routine business. Ample opportunity was available to the participants to mention and discuss some of the finer points of spacecraft performance and operation because, on many days, there was only minimum reporting to be done. The overall education and training of the SPAC group members was enhanced through the exchange of information among them in specialized areas of operation.

Finally, it was the constant interaction between the SPAC director and SPAC division representatives that resulted in the ability of SPAC to take the lead in the generation of the mission operations plans that were developed and executed during the flight.

Operational procedures to be used during the critical phases of the mission were generated by the SPAC group before the respective phases occurred. Preparation of these procedures required considerable reflection upon what should be done in a great variety of situations. The very act of putting on paper the various plans that could be followed greatly increased the preparedness of the SPAC group for unexpected conditions. Without having considered in advance as many conditions as possible, it is questionable that all necessary considerations concerning any particular action would have been forthcoming when that condition actually occurred in flight. The procedures were highly complementary to mission operations. It is recognized, however, that a greater benefit accrued from generating the operational procedures than from having the procedures on hand at the beginning of the mission phases.

The philosophy of SPAC followed the project guidelines of sending as few spacecraft commands from the ground as possible. Each command that was transmitted was thoroughly justified; its effect upon the spacecraft was analyzed; the effect of failure modes that could be induced was analyzed; and, after all this analysis, the recommendation was made and permission was granted by the project office for the command to be transmitted. This rigorous review of anticipated action demanded individual mental and written justification of the intended operations the better to understand and explain some of the ramifications of the suggested action. In effect, if commands could not be justified, they were not sent. This philosophy is endorsed and recommended very highly for future mission operations.

One of the most significant assets to the *Mariner* Venus 67 SPAC in preparation for critical phases of the mission was the test program (see Subsection C-6, below). During

initial testing, the test objectives were to check out the DPS, the facility, and the analysis area in general. Whenever possible, live spacecraft data from either the *Mariner V* flight spacecraft (M67-2) or the flight-support spacecraft (M67-1) were used.

Because the spacecraft design calls for the successful completion of the mission without SPAC support, it follows that the primary function of the SPAC group must be to anticipate, diagnose, and correct anomalies. Nominal simulated spacecraft telemetry cannot adequately accommodate this function.

5. Operations. The participation of the SPAC group in flight operations went very smoothly. The primary reason for this was the realization that, during a critical operation, spacecraft-performance analysis is a full-time task, with no possible allowance for the presentation, discussion, decision, or recommendation of corrective actions. This meant that as many decisions as possible had to be anticipated so that SPAC response during the operation would be automatic. Recognition of a certain set of spacecraft events or parameters would thus lead directly to a recommendation of a specific course of action. In this manner, the major decisions by SPAC were made in advance (after thorough investigation, lengthy discussion, and careful review) rather than during the operation. The pressure of time and the necessity for correct action during the operation would, of course, severely limit the capability to give careful consideration to all pertinent aspects of the problem.

Two noteworthy problems were encountered by SPAC in flight operations: (1) Effort was required to adapt the SPAC organization to make it compatible with 24-h operations support, and (2) some difficulty was experienced in coordinating spacecraft-performance-analysis activities with SPAC recommendation and decision activities that could not be handled in advance.

Initially, little notice was taken of the fact that certain of the responsibilities of the members of the SPAC group were assignable, whereas others lay with specific individuals rather than positions in the SPAC structure. As a result, the early SPAC organization concept called for qualified alternates to replace the primary SPAC members in the less critical portions of any given mission phase. Not until after some anomaly tests had been performed was it realized that certain nonassignable responsibilities must be borne by the division representatives and the SPAC director, on a 24-h basis, regardless of any presupposition to the contrary. The nonassignable duties were specifically separated from the assignable ones by the division representatives. Therefore, in order to commit his division to support a specific operations phase, the division representative must necessarily have completed his nonassignable tasks. He may then be replaced in the operation by any alternate qualified to perform the same level of analysis without jeopardizing the coordination effort of the SPAC activities of that division.

The SPAC director's position presents a different problem. Many of his nonassignable responsibilities only begin as the effort shifts from preparation to operation. At the same time, the flight operation also brings with it a wealth of routine tasks involving the internal coordination of the SPAC group and the coordination of SPAC activities with the SFO groups external to it. In order for the SPAC director to do his job adequately (i.e., pursuing the analysis of spacecraft data and resolving potential problems), he had to be as free as possible from the routine operational problems and constraints imposed by the remainder of the SFOF and some of the mission operations. The routine features of the SFO organization were turned over to the operations assistants (Bus I, II, and III) for each of the major SPAC interfaces.

Observation of previous JPL project operations indicated that considerable emphasis was placed upon the SPAC director's participation in routine discussions with other members of the SFO organization, and upon his provision of liaison between SPAC and other elements of the SFOF. The *Mariner* Venus 67 SPAC maintained that an operations assistant, with sufficient training, could satisfy these requirements, freeing the SPAC director to concentrate on the analysis of the spacecraft. This did, however, create the problem of the director interfacing with the operations assistants. This particular interface required a good deal of effort. By the time of launch, however, it was felt that the operations assistant was an integral part of the organization, and his presence greatly aided the total SPAC operations capability.

During certain critical phases of the mission, conditions existed that required the SPAC director to be available to the SFOD and the project manager for extended periods of consultation and discussion. This was because he was the only official spacecraft representative during the flight-operations phase of the project. To meet this requirement, it was decided that the assignable tasks involved with the routine direction of the SPAC group should pass to the position of the assistant SPAC director, which could be occupied by any

of the SPAC director's staff. This concept of a SPAC direction team was employed throughout the mission. Inclusion of a communications network for the project manager, project staff, and each of the area directors reduced the number of times the SPAC director had to be absent from the SPAC team.

6. *SPAC testing.*

a. SPAC testing objectives. The two primary functions of SPAC are: (1) to evaluate the status and performance of the flight spacecraft from liftoff to end of mission, and (2) when and if required, to recommend to project courses of action involving the flight spacecraft that would enhance the probability of accomplishing the mission objectives. These two functions, although separately stated, are to a great degree dependent upon one another, and are highly complex in nature.

For SPAC to accomplish the above-stated functions successfully, the following nine conditions had to be met:

(1) Real-time spacecraft data must be available for SPAC analysis.

(2) The data must be routed, displayed, and formulated in a convenient and meaningful manner.

(3) Each discipline required to analyze the total behavior of the spacecraft must have access to appropriate portions (at least) of the spacecraft data.

(4) All of the disciplines must be organized (as SPAC) and directed (by the SPAC director) to achieve a specific goal.

(5) Free visual and audio communications must exist within and between the disciplines involved and the SPAC director.

(6) The personnel representing the various disciplines must be capable of analyzing and assessing the behavior of their corresponding spacecraft subsystems.

(7) The SPAC director, aided by the subsystem representatives, must be capable of determining the effect of specific behavior (nominal or anomalous) of one or more subsystems upon the entire spacecraft.

(8) A method must be available for potentially changing the status of the spacecraft.

(9) There must be free communication among various members of the project organization, other area directors, and the SPAC director.

The objective of SPAC testing was to ensure that all of the above nine requirements were met before SPAC was called upon to fulfill its obligation.

To obtain a better understanding of the general testing philosophy used, a brief description of the method of accomplishment of each of the above nine requirements is presented below.

Spacecraft data availability. Perhaps the most vital requirement of those cited above is the availability of spacecraft data; without these data, the analysis of spacecraft behavior would be impossible. Special attention was thus given to both the availability and integrity of real-time data.

Figure V-4 is a functional block diagram of the general methods used to ensure the reliable availability of real-time spacecraft data to SPAC. Aboard the spacecraft, transducers in the various subsystems send digital and analog data to the data encoder (DE). The analog data are converted to 7-bit binary words, and (along with the digital data) are sequentially sampled at various rates and modulated with a pseudo-noise code. The composite telemetry signal is then transmitted to the radio subsystem, where it is mixed with a stable RF source and multiplied to S-band frequency in the exciter. This low-level, S-band composite telemetry signal is next amplified by either of the two power amplifiers in the spacecraft, and finally transmitted to earth via the high- or low-gain antenna.

At the Deep Space Station (DSS), the S-band composite telemetry signal is received by the DSS 85- or 210-ft antenna. The signal is then amplified by the receiver, and demodulated. The demodulator transmits bit sync, word sync, and serial binary data to the TCP; the TCP, in turn, decommutates, identifies, and formats the data. At the output of the TCP, the spacecraft data are handled in two functionally redundant ways, via the HSDL and via the two 30-bits/s TTY lines. The TTY lines run directly to the SFOF through the CPs, where they drive 60-w/m TTY machines for SPAC personnel. After being processed by the telemetry processing station (TPS), the data on the HSDL are routed to the 7044 input/output (I/O) processor, which converts and formats the data for the 100-w/m TTY, the 30 × 30 Milgo plotter, and the 3070 high-speed printer in SPAC. The data on the HSDL are also used by the Division 34 green box to display data for Division 34 SPAC representatives, to drive the GTS and provide station AGC (SAGC) for Division 33 to SPAC representatives, and to drive the

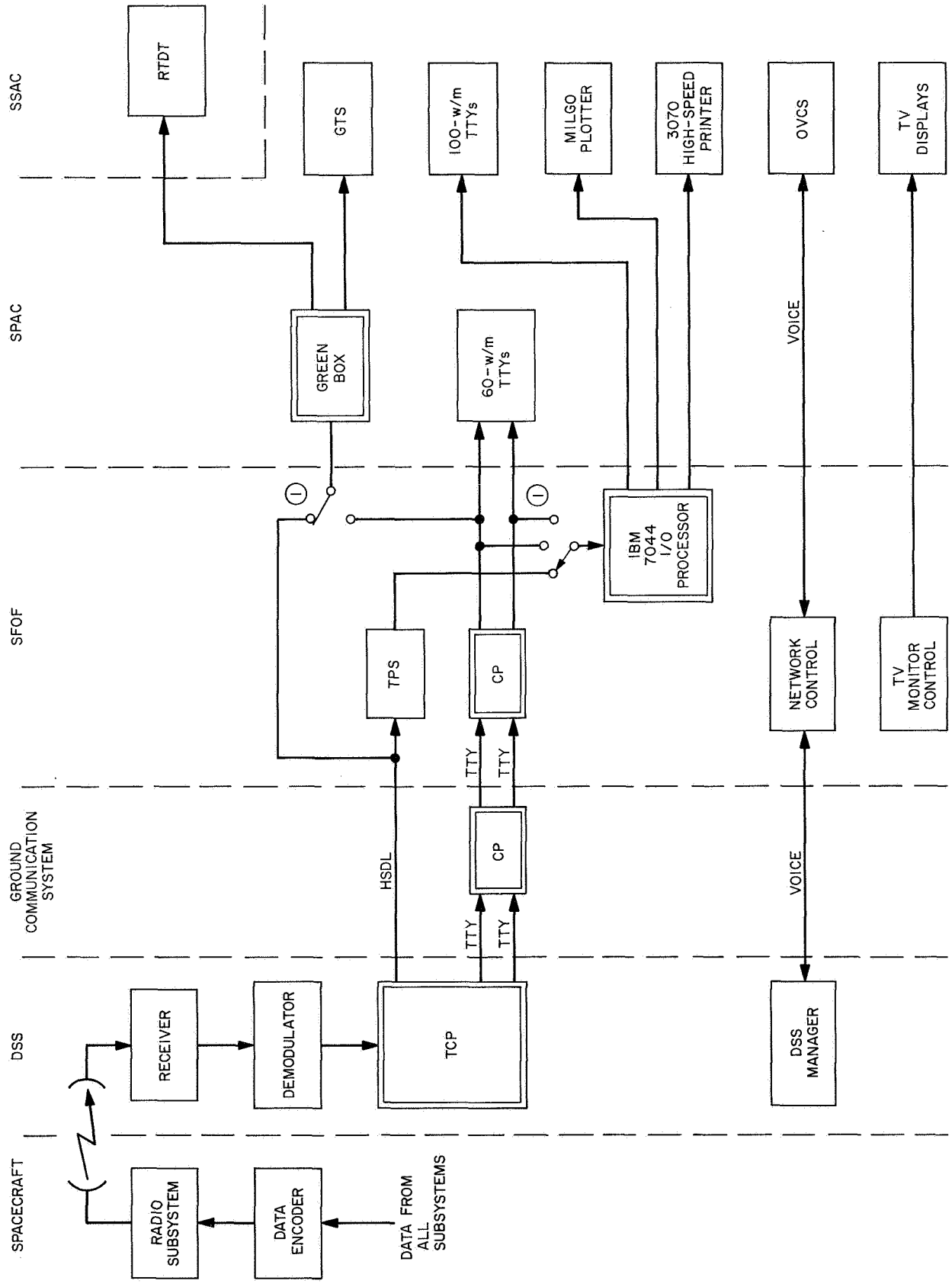


Fig. V-4. Spacecraft to SPAC real-time data transmission

RTDT for the SSAC. The capability also exists to select TTY lines as inputs to the 7044 in lieu of only the HSDL.

Of primary concern during SPAC testing were those items of equipment that were new for the *Mariner* Venus 67 project. These included the TCP, CP, 7044 redesign, and the green box (outlined in Fig. V-4). The intent was to pay particular attention to the TCP during the early testing phases because it was in series with both the high-speed data and the TTY data.[1] Another area that was to receive special attention was the presence of SAGC in the high-speed data.

Data display and formatting. There were two basic categories of SPAC formats for the *Mariner* Venus 67 project: (1) those associated with the 30-bits/s TTY lines and (2) those associated with the HSDL.[2]

The formats associated with the 30-bits/s TTY lines were designated as backup-data formats for the mission, and were called the raw-data format and the raw-data-backup format. Either of these formats could be displayed in special decimal form on the 60-w/m TTY machines for use by each SPAC representative. Because these data were the least complicated and required the least amount of data processing, they were to be made available to SPAC at the earliest time; therefore, they received a great deal of attention during the early phase of SPAC testing.

The formats associated with the HSDL were characterized by the fact that they required special data processing by the 7044 redesign software. Because there were many SPAC formats in this category, the testing philosophy was to place a priority on these formats, based upon their usefulness to SPAC, and proceed to test the formats sequentially. This led to a testing technique that was generally on the order of increasing data processing complexity.

Distribution of SPAC data. The basic objective of the distribution of SPAC data was the reliable availability to each SPAC representative of data that were considered necessary for the performance of in-depth subsystem analysis. As a consequence of this objective, a philosophy was adopted that required the presence of two functionally redundant data sources for each SPAC member. These sources were: (1) the 30-bits/s TTY data and (2) the high-speed (processed) data.

The 30-bits/s data appeared on 60-w/m TTY lines that were identical in format at all SPAC stations. Thus, this type of output was easily tested by carefully scrutinizing any of the many 60-w/m TTYs in the SPAC area.[3] The high-speed (processed) data, on the other hand, appeared on a number of devices and in a great variety of formats. It was necessary, therefore, to rely upon the SPAC members using these high-speed-data output devices for comments concerning the state of readiness and utility of these formats. This process of testing introduced an additional interface between the user and the agency responsible for correcting the data output. Because of the lower priority and greater complexity of mechanization and testing of these formats, it was natural that they be tested following the availability of the raw-data formats. The distribution of data and personnel within SPAC is shown in Fig. V-3.

Organization and direction. The SPAC organization is shown in Fig. V-5. It should be noted that the organization of SPAC is hybrid in nature. As shown by solid lines in Fig. V-5, the SPAC organization is that of a classical vertical organization, thereby ensuring the clear division of responsibility and authority at the price of degraded communications and slow response times. To alleviate these two major disadvantages, a horizontal communications system was employed (indicated by shaded areas in Fig. V-5), which enabled each SPAC member to listen to or speak with any other SPAC member. The combined vertical and horizontal organization thus afforded a highly responsive and functionally organized combined effort.

To test the effectiveness of the SPAC organization, a sequence of progressively more complicated SPAC tests was planned, from a relatively straightforward systems test to highly sophisticated induced-anomaly tests.

Intra-SPAC communication. The internal communications of SPAC are discussed above, and illustrated in Figs. V-3 and V-5. The testing philosophy employed to determine the efficiency of internal communications was the same as that described for SPAC organization and direction.

Subsystem analysis and evaluation. Detailed knowledge of the major subsystems aboard the spacecraft was brought into the SPAC organization through subsystem representatives, usually the cognizant engineer or his alternate. Responsibilities of each representative included

[1]In case of a TCP failure, data for SPAC would have been made available via voice reports from the DSS.

[2]During the later part of SPAC preparation, the capability of using the TTY data for 7044 data processing was also available.

[3]At the high bit rate (33⅓ bits/s), two 60-w/m TTYs were required to transmit all of the spacecraft data to SPAC.

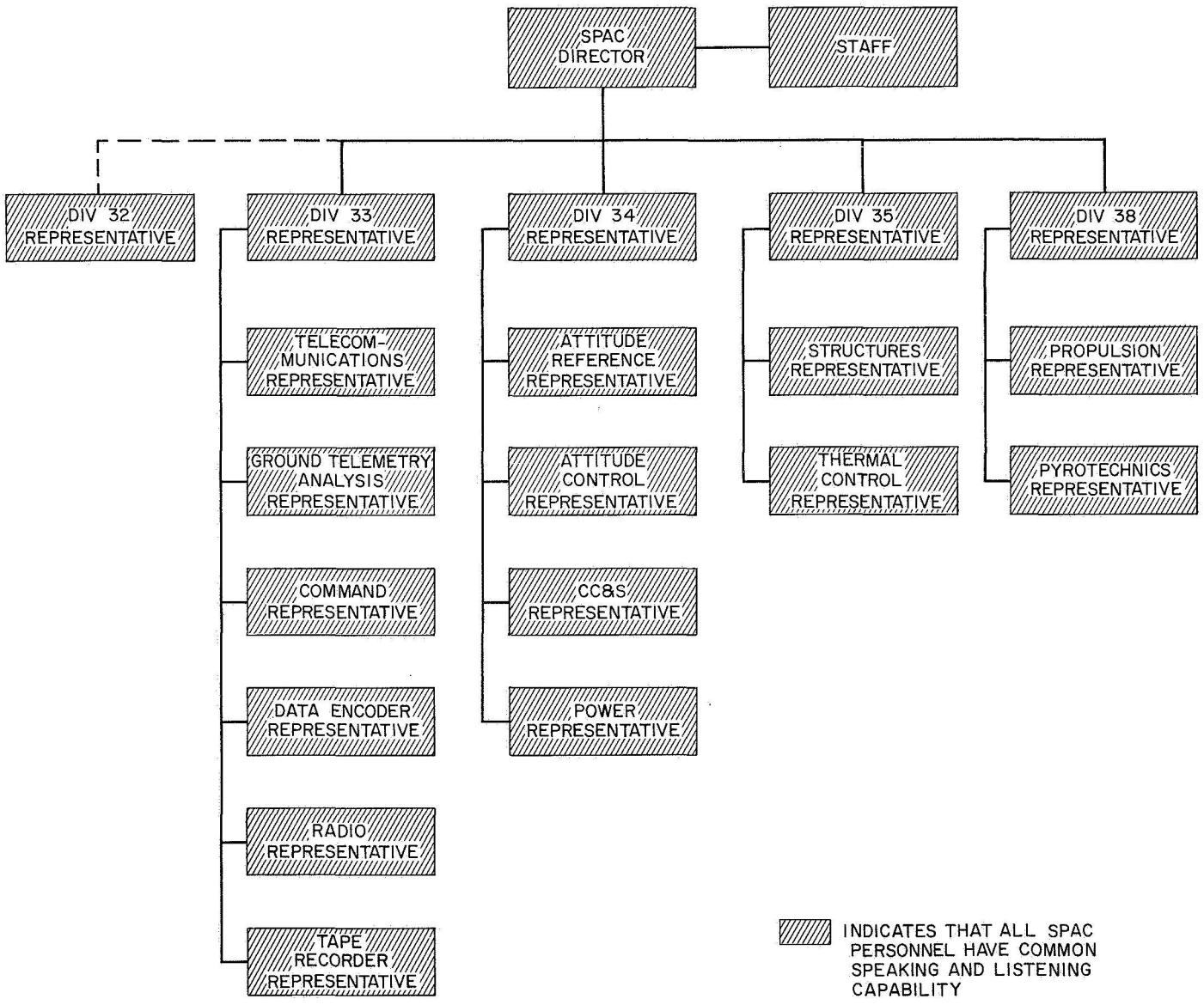


Fig. V-5. Internal SPAC organization and communications

knowledge relative to the design, fabrication, test history, and capabilities of his subsystem in flight. In addition, the subsystem representative was responsible for analyzing in detail his hardware in flight, analyzing real-time telemetry, advising his division representative and the SPAC director of the performance of his subsystem, and providing information on the status of his subsystem during any discussion of action to be taken in case of a nonstandard spacecraft condition. To aid the subsystem and division representatives in fulfilling their responsibilities, special analysis areas were set up for each division. These CAT areas consisted of personnel who, in the opinion of the division representatives, could significantly contribute (from a management and/or technical standpoint) to the analysis of spacecraft behavior during critical or nonstandard portions of the mission.

The philosophy employed in the testing of subsystem analysis and evaluation consisted of subjecting the SPAC members to progressively more sophisticated tests with either the *Mariner V* flight-support spacecraft (M67-1), the *Mariner V* flight spacecraft (M67-2) (before launch), or the *Mariner IV* flight spacecraft (MC-3) as a data source. The operating conditions of these tests would resemble, to as great a degree as possible, the actual conditions expected during mission operations.

Evaluation of overall spacecraft behavior. Before any recommendation to change the status of the spacecraft could be made, the overall behavior of the entire spacecraft had to be determined based upon the input of each SPAC member. This process was normally carried out in the SPAC area for nominal flight sequences, and in the decision–revision–decision (DRD) conference room, in the presence of appropriate personnel, during potentially anomalous or nonstandard spacecraft conditions. The general spacecraft condition having thus been determined, a SPAC recommendation would be agreed upon and made to project representatives by the SPAC director. This recommendation would be to either accept or change the status of the flight spacecraft.

The philosophy of testing employed to determine the effectiveness of performing the above task was to induce spacecraft anomalies (without the knowledge of SPAC) into the test spacecraft, and then to evaluate the response time and accuracy of SPAC in responding to these anomalies.

Changing the status of the spacecraft. A decision to change the status of the spacecraft having been arrived at, a method had to be available to effect this change. The method most frequently used was via ground command. There were 29 direct commands and one quantitative command available for changing the spacecraft status via ground command. A detailed description of these commands is provided in Table V-1. These commands, along with the applications of an uplink S-band signal and command modulation, were the sole means of controlling the status of the flight spacecraft. The judicious application of these methods was included in the SPAC recommendation.

As with many of the previous cases discussed, the philosophy of testing the efficiency with which SPAC made use of the above methods was to subject SPAC to progressively more sophisticated induced-anomaly tests. These tests were then evaluated, and corrections were made to any existing deficiencies.

SPAC interface communications. Because SPAC was only authorized to make recommendations for corrective action, and because in many cases other than SPAC information was needed for a project decision, a comprehensive method of communications between SPAC, project representatives, and other area directors was necessary. This communication was effected through the use of inter-area voice networks, inter-area TV monitors, and freedom of access (for selected personnel) to each of the MSAs for personal communication.

The effectiveness of these methods of communication was continuously assessed during the numerous SPAC tests.

b. SPAC test schedule. The schedule for SPAC testing is shown in Fig. V-6. The testing schedule was divided into 18 different types of tests generally representing the state of SPAC readiness to support various phases of the *Mariner* Venus 67 mission operations. Figure V-6 shows each of the 18 types of tests subdivided horizontally into two halves. The upper half of a particular item represents the planned schedule for the test in question; the lower half represents the actual achieved test during SPAC testing.

In all cases except two, at least as many tests were performed as planned, and completed within a relatively short time of the planned date. That there were any time variations at all can mostly be attributed to the fact that SPAC test operations were very closely tied to the spacecraft testing schedule. The latter, in turn, was dependent upon day-to-day progress, with only major objectives tied down to specific dates.

Table V-1. Direct and quantitative commands

No.	Name	Effect
DC-V1	Command TLM mode 1	Transfers data encoder to mode 1 operation (all engineering words) as soon as transfer is acceptable to data-encoder transfer logic.
DC-V2	Command TLM mode 2; turn on science	Transfers data encoder to mode 2 operation (20 engineering words, 40 science words) as soon as transfer is acceptable to data-encoder transfer logic; applies 2.4-kHz power to science instruments.
DC-V3	Track change command	Switches tape-recorder data tracks (playback only).
DC-V4	Command TLM mode 4	Transfers data encoder to mode 4/1 operation (recorded data or real-time engineering data) as soon as transfer is acceptable to data-encoder transfer logic. (If recorded data are available from tape recorder, recorded data are telemetered; if no recorded data are present at end of tapes, mode 1 engineering data are telemetered.) Stops tape-recorder mode if in operation.
DC-V5	Command switch data rate	Transfers data encoder from one bit rate to other (data encoder can operate at either 8⅓ or 33⅓ bits/s).
DC-V6	Command switch A/DC–PNG	Transfers data encoder from one A/DC–PNG to other (data encoder has two A/DC–PNGs, A and B).
DC-V7	Switch power amplifier	Transfers radio from one power amplifier to other; radio subsystem has two power amplifiers, A (traveling-wave tube) and B (cavity).
DC-V8	Switch exciters	Changes radio from one exciter to other (radio subsystem has two exciters, A and B).
DC-V9	Switch ranging	Turns spacecraft radio ranging receiver either on or off.
DC-V10	Transmit high–receive low	Causes radio subsystem circulator switches to be so conditioned that spacecraft transmits via high-gain antenna and receives via low-gain antenna.
DC-V11	Transmit high–receive high	Causes radio subsystem circulator switches to be so conditioned that spacecraft transmits and receives via high-gain antenna.
DC-V12	Transmit low–receive low	Causes radio subsystem circulator switches to be so conditioned that spacecraft transmits and receives via low-gain antenna.
DC-V13	Maneuver command inhibit; inhibit prop command (turn on Canopus sensor and AC)	Removes AC excitation power from CC&S control lines so that AC functions controlled by CC&S are disabled; also prevents pyrotechnics control circuits from firing motor start and stop squibs.
DC-V14	Remove maneuver inhibit; remove prop inhibit (resets DC-V13)	Reverses state of all relays acted upon by DC-V13; therefore, resets DC-V13, and reverts AC and pyrotechnics subsystems to CC&S control.
DC-V15	Canopus gate inhibit override	Causes Canopus-sensor roll-error signal to be applied to roll gas jet electronics at all times, regardless of whether or not roll-acquisition logic is satisfied; prevents roll-search signal from being applied to roll channel, and roll-acquisition logic violations from turning on gyros.
DC-V16	Start encounter backup clock	Toggles DAS timer A; used to issue backup commands for encounter sequence.
DC-V17	Cycle Canopus cone angle	Causes a step change in Canopus-sensor cone angle by changing voltage on deflection plates of image dissector of Canopus sensor.
DC-V18	Gyros on—inertial control (second-roll positive increment)	Turns on gyros (in inertial mode) and Canopus-sensor sun shade, and turns off Canopus sensor; also turns on turn-command generator and conditions AC circuits for commanded roll turns. (Each successive DC-V18 causes positive roll rotation of 2.25 deg.)
DC-V19	Gyros off—normal control	Serves as reset for DC-V15, DC-V18, and DC-V20.

Table V-1 (contd)

No.	Name	Effect
DC-V20	Remove roll control	Turns off Canopus sensor and turns on Canopus-sensor sun shade; inhibits roll-acquisition logic from turning on gyros.
DC-V21	Roll override—negative increment	Simulates a Canopus-acquisition logic violation, turns on gyros, and applies a negative roll-search signal to roll gas jet electronics, thereby causing spacecraft to roll search ccw to acquire a new target. (Each successive DC-V21 will cause spacecraft to roll turn 2.25 deg if preceded by a DC-V18.)
DC-V22	Antenna pointing angle change	Commands pyrotechnics to activate a pin-puller that allows antenna to change position for optimizing S-band occultation experiment.
DC-V23	Arm second prop maneuver	Sets relays in pyrotechnics subsystem so that CC&S commands M-6 and M-7 are routed to squibs allotted to second motor burn.
DC-V24	Begin DAS encounter mode (switch to data mode 3; planet-sensor power on; switch plasma probe to mode 3)	Begins DAS encounter mode; enables DAS timer B (toggle); switches to data mode 3; turns planet-sensor power on; switches plasma probe to encounter format.
DC-V25	Science on/overload inhibit override	Begins encounter sequence; applies power to terminator sensor and tape recorder; enables battery-charger boost mode, and removes booster-regulator overload inhibit.
DC-V26	Turn off science (battery charger to boost mode)	Removes 2.4-kHz power from all science loads (tape-recorder 2.4-kHz power remains on); enables battery-charger boost mode.
DC-V27	Initiate midcourse maneuver	Starts midcourse-maneuver sequence by issuing CC&S command M-1 (turn on gyros), applying power to maneuver clock, and removing maneuver clamp and a flip-flop reset signal from CC&S maneuver circuits.
DC-V28	Switch battery charger (tape-recorder electronics off)	Transfers battery charger from charge mode to boost-enable mode or vice versa; turns off 2.4-kHz power to tape recorder.
DC-V29	Arm first prop maneuver	Sets relays in pyrotechnics subsystem so that CC&S commands M-6 and M-7 are routed to squibs allotted to first motor burn.
QC-V1	Maneuver command bits to CC&S	See below.
QC-V1-1	(Pitch-turn duration)	Sets pitch-turn polarity and preloads CC&S pitch shift register so that, at a counting rate of 1 pulse/s, register will fill in interval required for AC subsystem to pitch-turn spacecraft amount required for a given midcourse maneuver.
QC-V1-2	(Roll-turn duration)	Sets roll-turn polarity and preloads CC&S roll shift register so that, at a counting rate of 1 pulse/s, register will fill in interval required for AC subsystem to roll-turn spacecraft amount required for a given midcourse maneuver.
QC-V1-3	(Motor-burn duration)	Preloads CC&S velocity shift register so that, at a counting rate of 20 pulses/s, register will fill in interval required for midcourse motor to burn so that spacecraft obtains required velocity change for a given midcourse maneuver.

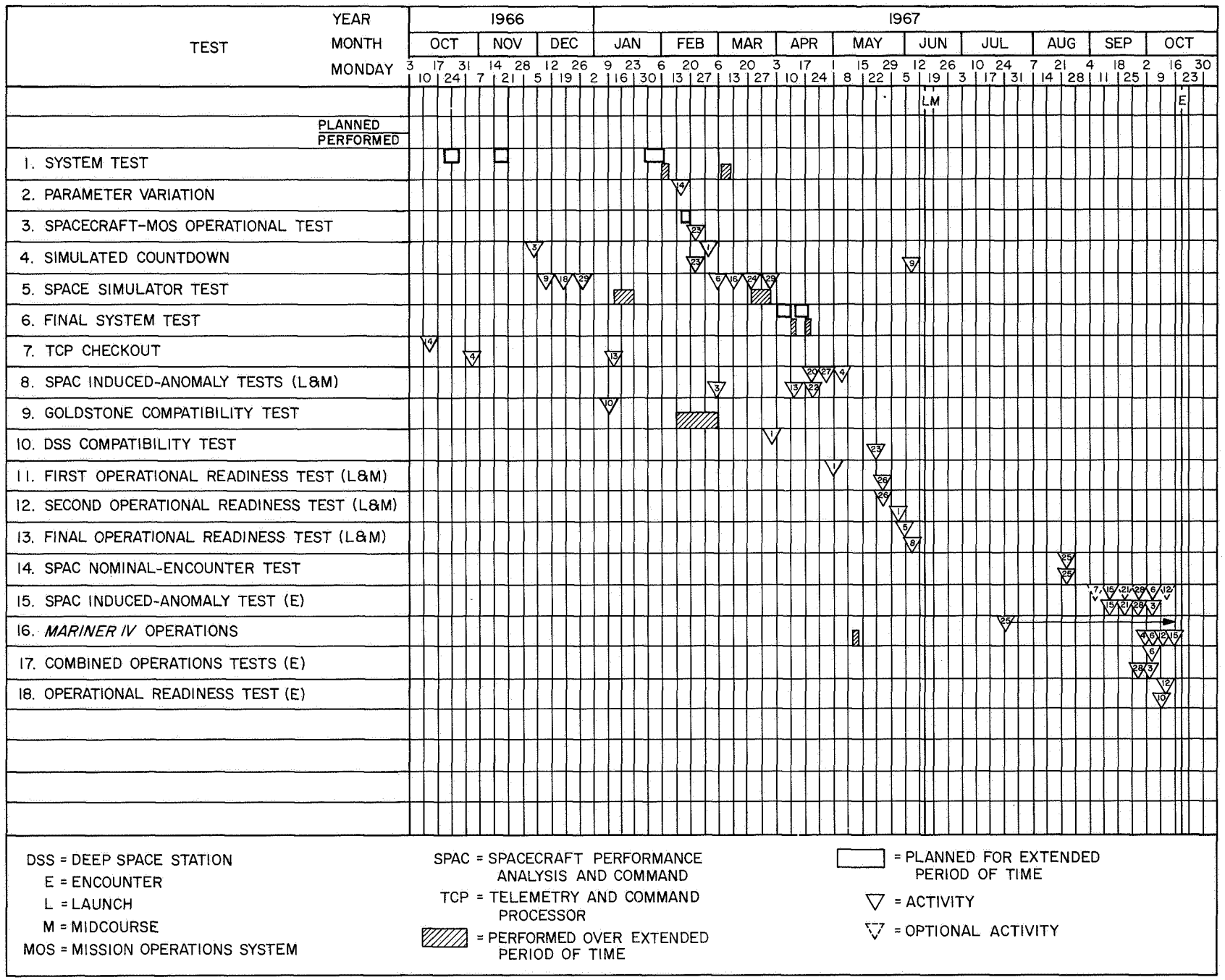


Fig. V-6. SPAC testing summary

The two exceptional cases (more tests planned than actually performed) were the system tests and the parameter-variation test. The early system tests were not supported because of the unavailability of TCP support. The parameter-variation test was omitted because of the general software lag. It was felt that the time available for the parameter-variation test could be more efficiently used by applying it to software generation in an effort to decrease the schedule slip.

The only other major deviations in the SPAC testing schedule were associated with the performance of the space simulator tests. The initial plan was to perform these tests so as to simulate mission operational conditions. Each critical phase of the mission was to be performed on a separate day, with both real-time and nonreal-time data made available to SPAC for analysis. This plan, however, had to be abandoned because the MOS software was not available for support. The tests were, therefore, conducted over a shorter period of time consistent with spacecraft testing requirements.

c. SPAC testing summary. A brief synopsis of the SPAC testing performed for the *Mariner* Venus 67 mission is presented in Table V-2. Some of the more significant results for each of the nine SPAC requirements discussed in Subsection C-6-a are described below.

Spacecraft data availability. During the planning phase of SPAC testing, it was expected that one of the potentially dangerous areas in SPAC operations would involve the availability of spacecraft data, mainly because of the use of new equipment and the 7044 redesign. These expectations were borne out by actual experience.

During early phases of SPAC testing, it became apparent that TCP software development was behind schedule and not sufficiently advanced to support some of the early SPAC tests. As a consequence, some of the later tests had to be either modified or canceled. Once operating, however, the TCP was found to be a useful and reliable device.

The CP, another new device, was consistently plagued by a variety of problems that, during the middle phases of SPAC testing, seriously affected the validity of the tests. On numerous occasions, the CP had to be wired around to make the test possible because the CP and the green box were the only sources of data for SPAC (the 7044 redesigned software was behind schedule, and so was not available). Even well into the *Mariner* Venus 67 mission, the CP experienced numerous outages that severely hampered SPAC mission operations and testing.

The 7044 redesign, another new item in the data stream for the *Mariner* Venus 67 mission, also slipped commitment schedules, thus requiring a sequential testing program based upon a format-priority system. As a consequence, much of the SPAC testing was conducted with raw data and green-box data exclusively. Most 7044 formats were available by the time of launch, however, thus providing two redundant data paths for SPAC mission support.

As a consequence of the many schedule slips associated with new equipment, SPAC became thoroughly competent in the use and interpretation of the raw-data and raw-data-backup formats, thereby negating the requirement for engineering-unit formats. More comprehensive insight into the problems associated with TCP, CP, and 7044 support during testing may be obtained by referring to Table V-2. It should be noted that, without the consistently excellent performance of the green box, many of the scheduled SPAC tests could not have been completed satisfactorily.

Data display and formatting. The formats and the display of SPAC data were generally satisfactory, with the exceptions noted above. One display device that was not as beneficial as expected was the 3070 high-speed printer. The main disadvantage of this device was that, because of its construction, the data as printed were not immediately visible to an operator, thereby necessitating the use of a "more real-time" device. The 3070 printer was useful, however, when a latest-available-data format was requested. This format, incidentally, proved to be most beneficial, and was used consistently throughout mission operations and SPAC testing.

Distribution of data. Because processed data were not available on the dates scheduled, the SPAC area was reconfigured to permit the installation of more 60-w/m TTYs, thus allowing raw-data analysis by every SPAC member. In addition to the new 60-w/m TTYs, a TV–TTY monitor was added for viewing by the SPAC director.

With the above exceptions, data distributions remained essentially stable, and were considered satisfactory.

Organization and direction. The organization of SPAC proved to be generally satisfactory, with a few notable exceptions.

Table V-2. SPAC testing summary

Test No.	Type	Data source	Start time	End time	Duration	Objectives	Results
1	TCP–SPAC interface	M67-1	Nov 4, 09:00 LMT[a]	Nov 4, 11:26 LMT	2 h, 26 min	1. TCP interface checkout 2. TCP raw data checkout 3. SAF–SPAC facility checkout 4. TTY format familiarization	1. TCP interface operative 2. Raw data format available 3. Deck position indication not available 4. *R* and *D* indications not available 5. Requested minor facility changes
2	Space simulator	M67-1	Jan 13, 18:25 LMT	Jan 13, 22:53 LMT	4 h, 28 min	1. TCP format checkout 2. SPAC–spacecraft familiarization 3. To support spacecraft testing and analyze environmental behavior	1. TCP *R* and *D* indications available 2. Deck position indication available but sync incorrect 3. Continued SPAC–spacecraft SPAC–format familiarization
3	Space simulator	M67-1	Jan 15, 18:25 LMT	Jan 15, 22:03 LMT	3 h, 38 min	1. TCP format checkout 2. SPAC–spacecraft familiarization 3. To support spacecraft testing and analyze environmental behavior	1. TCP *R* and *D* indications available 2. Deck position indication available but sync incorrect 3. Continued SPAC–spacecraft and SPAC–format familiarization 4. Raw-data-backup format operational
4	Space simulator	M67-1	Jan 16, 08:49 LMT	Jan 16, 11:49 LMT	3 h, 00 min	1. TCP format checkout 2. SPAC–spacecraft familiarization 3. To support spacecraft testing and analyze environmental behavior	1. TCP *R* and *D* indications functioning satisfactorily 2. Deck position indication available but sync incorrect 3. Continued SPAC–spacecraft and SPAC–format familiarization 4. SAGC calibration curves not available
5	Space simulator	M67-1	Jan 18, 17:02 LMT	Jan 19, 02:16 LMT	9 h, 14 min	1. TCP format checkout 2. SPAC–spacecraft familiarization 3. SPAC–TCP format familiarization 4. Check out SAGC 5. To support spacecraft testing and analyze environmental behavior	1. TCP *R* and *D* indications intermittent 2. Deck position indication available but sync incorrect 3. Continued SPAC–spacecraft and SPAC–TCP format familiarization 4. Experienced difficulty in synchronizing TCP–ETL[b]–SPAC clocks
6	Space simulator	M67-1	Jan 23, 08:54 LMT	Jan 23, 12:56 LMT	4 h, 02 min	1. TCP format checkout 2. SPAC–spacecraft familiarization 3. SPAC–TCP format familiarization 4. Check out SAGC 5. To support spacecraft testing and analyze environmental testing	1. TCP *R* and *D* indications intermittent 2. Deck position indication available but sync incorrect 3. Experienced difficulty in synchronizing TCP–ETL–SPAC clocks

[a]LMT = local mean time.

[b]ETL = Environmental Test Laboratory.

Table V-2 (contd)

Test No.	Type	Data source	Start time	End time	Duration	Objectives	Results
7	System test	M67-2	Feb 6, 11:45 LMT	Feb 6, 15:17 LMT	3 h, 32 min	1. TCP format checkout 2. SPAC–spacecraft familiarization 3. SPAC–TCP deck position indicators 4. Check out TCP deck position indicators 5. Check out *R* and *D* indicators 6. To support spacecraft testing and analyze system test behavior	1. *R* and *D* indications operational 2. Experienced four TCP outages (due to memory-parity error indications)
8	System test	M67-2	Feb 7, 08:12 LMT	Feb 7, 14:55 LMT	6 h, 43 min	1. TCP format checkout 2. SPAC–spacecraft familiarization 3. SPAC–TCP format familiarization 4. Check out TCP deck position indicators 5. Check out *R* and *D* indicators 6. To support spacecraft testing and analyze system test behavior	1. *R* and *D* indications satisfactory with new program 2. Raw data and raw data backup operational with new program 3. Experienced minor TCP down times
9	Simulated precountdown	M67-2	Feb 23, 09:08 LMT	Feb 23, 16:31 LMT	7 h, 23 min	1. Check out SFOF–SPAC facility 2. Check out 100-w/m operation 3. Check out 7044 formats 4. Check out CP operation 5. Check out 30 × 30 plotters 6. Check out 3070 printers 7. SPAC–SFOF familiarization and communications checkout 8. Check out Div 34 D/AC[c] 9. To support system testing	1. Requested minor changes in facility 2. 100-w/m formats inoperative 3. CP overflowing and lagging behind 4. SPAC–AO2 network inoperative 5. 30 × 30 plotters inoperative 6. 3070 printers have incorrect format 7. Div 34 D/AC operational 8. SAGC operational
10	Spacecraft–AFETR–MOS anomaly test (launch through Canopus acquisition)	M67-2	Mar 3, 08:30 LMT	Mar 3, 15:55 LMT	7 h, 25 min	1. Check out SPAC anomaly-detection capability 2. Determine response time of SPAC and effectiveness of recommendations 3. Check out sequence-flow diagrams 4. Final TCP checkout 5. 7044 committed for support	1. Minor facility anomalies 2. 7044 formats not operational to date 3. CP consistently troublesome 4. TTY–TV monitor requested for SPAC director 5. TCP program acceptable 6. Early CC&S relay holdoff diagnosed correctly 7. Early double CY-1; insufficient data for diagnosis 8. Inadvertent DC-V20 diagnosed correctly 9. A/DC–PNG[d] failure diagnosed correctly

[c]D/AC = digital-to-analog converter.

[d]PNG = pseudo-noise generator.

Table V-2 (contd)

Test No.	Type	Data source	Start time	End time	Duration	Objectives	Results
10 (contd)							10. Cavity failure diagnosed partially 11. False Canopus lock diagnosed correctly
11	System test	M67-2	Mar 7, 08:30 LMT	Mar 7, 18:07 LMT	9 h, 37 min	1. Check out SPAC anomaly-detection capability 2. Determine response time of SPAC and effectiveness of recommendations 3. Check out sequence-flow diagrams 4. Final TCP checkout 5. 7044 committed for support 6. To support spacecraft testing and analyze system test behavior	1. Minor facility anomalies 2. 7044 formats not operational to date 3. CP consistently troublesome 4. TTY–TV monitor requested for SPAC director
12	System test	M67-2	Mar 8, 13:44 LMT	Mar 8, 15:37 LMT	1 h, 53 min	1. SPAC–SFOF familiarization 2. SPAC–spacecraft familiarization 3. Continued checkout of SFOF support 4. To support spacecraft testing and analyze system test behavior	1. 100-w/m formats improved 2. CP bypassed because of time lags 3. 3070 printing engineering format 4. SPAC–AO2 network inoperative 5. 30 × 30 plotters printing *Mariner IV* formats
13	System test	M67-2	Mar 9, 12:16 LMT	Mar 9, 17:06 LMT	4 h, 50 min	1. SPAC–SFOF familiarization 2. SPAC–spacecraft familiarization 3. Continued checkout of SFOF support 4. To support spacecraft testing and analyze system test behavior	1. CP intermittent 2. 100-w/m TTYs lagging 38 min
14	System test	M67-2	Mar 10, 19:00 LMT	Mar 10, 21:00 LMT	2 h, 00 min	1. SPAC–SFOF familiarization 2. SPAC–spacecraft familiarization 3. Continued checkout of SFOF support 4. To support spacecraft testing and analyze system test behavior	Engineering-unit format not available to date
15	Space simulator	M67-2	Mar 22, 09:34 LMT	Mar 22, 12:32 LMT	2 h, 58 min	1. SPAC exposure to M67-2 in space environment 2. Expose new SPAC members to SPAC operations 3. Continue analyzing 7044 output formats 4. Improve interface with remainder of MOS 5. To support spacecraft testing and analyze environmental behavior	1. 100-w/m TTYs performing satisfactorily 2. 30 × 30 plotter formats inoperative 3. 7044 engineering formats inoperative 4. CP operation intermittent
16	Space simulator	M67-2	Mar 23, 15:42 LMT	Mar 23, 19:46 LMT	4 h, 04 min	1. SPAC exposure to M67-2 in space environment	1. 100-w/m TTYs performing satisfactorily

Table V-2 (contd)

Test No.	Type	Data source	Start time	End time	Duration	Objectives	Results
16 (contd)						2. Expose new SPAC members to SPAC operations 3. Continue analyzing 7044 output formats 4. Improve interface with remainder of MOS 5. To support spacecraft testing and analyze environmental behavior	2. 30 × 30 plotter formats 3. 7044 engineering formats inoperative 4. CP completely inoperative; required to bypass
17	Space simulator	M67-2	Mar 24, 13:00 LMT	Mar 24, 15:39 LMT	2 h, 39 min	1. SPAC exposure to M67-2 2. Expose new SPAC members to SPAC operations 3. Continue analyzing 7044 output formats 4. Improve interface with remainder of MOS 5. To support spacecraft testing and analyze environmental behavior	1. 100-w/m TTYs performing 2. 30 × 30 plotter formats inoperative 3. 7044 engineering format inoperative 4. CP intermittent 5. 7044 intermittent 6. CP printing old data
18	Space simulator	M67-2	Mar 27, 08:26 LMT	Mar 27, 15:41 LMT	7 h, 15 min	1. SPAC exposure to M67-2 in space environment 2. Expose new SPAC members to SPAC operations 3. Continue analyzing 7044 output formats 4. Improve interface with remainder of MOS 5. To support spacecraft testing and analyze environmental behavior	7044 inoperative; SPAC operating on 60-w/m TTY only
19	Space simulator	M67-2	Mar 31, 08:20 LMT	Mar 31, 11:16 LMT	2 h, 56 min	1. SPAC exposure to M67-2 in space environment 2. Expose new SPAC members to SPAC operations 3. Continue analyzing 7044 output formats 4. Improve interface with remainder of MOS 5. To support spacecraft testing and analyze environmental behavior	1. BUS network inoperative 2. SPAC–ETL interface intermittent 3. CP unable to respond to deck skips
20	System test	M67-1	Apr 10, 08:45 LMT	Apr 10, 17:00 LMT	8 h, 15 min	1. Continue analysis of 7044 formats 2. Continue analysis of CP operation 3. Check out 30 × 30 plotter format 4. Provide SPAC–M67-1 familiarization	1. CP intermittent 2. 7044 is operating 3. Engineering-unit format not available to date 4. 100-w/m data lagging 4–5 min

Table V-2 (contd)

Test No.	Type	Data source	Start time	End time	Duration	Objectives	Results
20 (contd)						5. To support spacecraft testing and analyze system test behavior	5. Green box/GTS–RTDT interface operative
21	System test	M67-1	Apr 11, 08:18 LMT	Apr 11, 16:07 LMT	7 h, 49 min	1. Continue analysis of 7044 formats 2. Continue analysis of CP operation 3. Check out 30 × 30 plotter format 4. Provide SPAC–M67-1 familiarization 5. To support spacecraft testing and analyze system test behavior	1. 7044 intermittent 2. 100-w/m data lagging 10–30 min 3. 30 × 30 plotter formats inoperative
22	MOS anomaly test No. 2	M67-1	Apr 13, 08:24 LMT	Apr 13, 17:00 LMT	8 h, 36 min	1. To expose SPAC and portions of MOS to a normal launch through Canopus-acquisition sequence 2. To expose SPAC and portions of MOS to an anomalous midcourse maneuver	1. TCP intermittent 2. Poor SPAC–BUS network communication 3. Extra counter 1 event; analyzed correctly 4. Earth acquisition; analyzed correctly 5. Loss of data; not analyzed correctly 6. QC-VI-1 not verified; correctly analyzed 7. Gyros not on for midcourse maneuver; insufficient time for analysis
23	System test	M67-2	Apr 17 02:30 LMT	Apr 17, 15:10 LMT	12 h, 40 min	1. Final facility checkout before combined operations test 2. Final checkout for 7044 3. Final checkout of CP operation before ORT[e] 4. To support spacecraft testing and analyze system test behavior	1. CP intermittent, affecting TCP 2. 100-w/m formats acceptable with exception of engineering units 3. 30 × 30 plotter formats not available 4. Facility satisfactory
24	System test	M67-2	Apr 18, 08:15 LMT	Apr 18, 11:36 LMT	3 h, 21 min	1. Final facility checkout before combined operations test 2. Final checkout for 7044 3. Final checkout of CP operation before ORT 4. To support spacecraft testing and analyze system test behavior	1. CP intermittent, affecting TCP 2. 100-w/m formats acceptable with exception of engineering units 3. 30 × 30 plotter formats not available 4. Facility satisfactory
25	*Mariner IV* command exercise	*Mariner IV*	May 11, 13:00 LMT	May 11, 22:30 LMT	9 h, 30 min	1. To demonstrate ability of SPAC to command a flight spacecraft 2. To transmit a minimum QC-1-1 command	1. SPAC demonstrated ability to carry out a command exercise 2. A QC-1-1 and a DC-13 were transmitted to spacecraft

[e]ORT = operational readiness tests.

Table V-2 (contd)

Test No.	Type	Data source	Start time	End time	Duration	Objectives	Results
25 (contd)						3. To transmit a DC-13 command 4. To familiarize SPAC with flight operations	3. SPAC received training in interpretation of high 6.4 error data
26	*Mariner IV* Canopus cone angle update exercises	*Mariner IV*	May 12, 08:30 LMT	May 12, 14:00 LMT	5 h, 30 min	1. To demonstrate ability of SPAC to command a flight spacecraft 2. To transmit a DC-15 command 3. To transmit seven DC-17 commands 4. To acquire Canopus 5. To familiarize SPAC with flight operations	1. SPAC demonstrated ability to carry out a command exercise 2. A DC-15 and seven DC-17 commands were transmitted to spacecraft 3. Canopus was not acquired 4. SPAC received training in interpretation of high 6.4 error data
27	MOS anomaly test No. 3	M67-1	May 22, 12:30 GMT	May 22, 21:30 GMT	9 h, 00 min	1. To continue midcourse maneuver anomaly test of Apr 13, 1967 (Test No. 22) 2. To expose SPAC and other portions of MOS to launch and initial-acquisition anomalies	1. SPAC JR receiving intermittent data 2. DAS[f] anomaly; analyzed correctly 3. Autopilot power-increase analysis partially correct 4. Early PSO[g]; analyzed incorrectly 5. Clock B malfunctioning; analyzed incorrectly 6. Magnetometer malfunction; analysis incomplete
28	Combined operations test	Taped data	May 23, 06:11 LMT	May 23, 13:27 LMT	7 h, 16 min	To expose entire MOS to a simulated launch, midcourse maneuver, and encounter sequence to prepare MOS to support these activities	1. Interfaces between DSS, track, FPAC, SSAC, SPAC, SPAC JR, and *Mariner* project were exercised 2. Minor interface procedural problems were noted and corrected
29	Combined operations test	Taped data	May 26, 01:30 LMT	May 26, 17:15 LMT	15 h, 45 min	Continuation of test conducted on May 23 (Test No. 28)	1. Interfaces between DSS, track, FPAC, SSAC, SPAC, SPAC JR, and *Mariner* project were exercised 2. Minor interface precedent problems were noted and corrected
30	Operational test	Taped data	Jun 1, 06:16 LMT	Jun 1, 10:58 LMT	4 h, 42 min	To expose MOS to prelaunch, launch-acquisition, and midcourse-maneuver sequence for familiarization	1. Experienced minor interface difficulties 2. 7044 was intermittent

[f]DAS = data automation system.

[g]PSO = planet sensor output.

Table V-2 (contd)

Test No.	Type	Data source	Start time	End time	Duration	Objectives	Results
31	MOS operational readiness test and *Mariner IV* data acquisition	Taped data	Jun 8, 06:00 LMT	Jun 8, 17:00 LMT	11 h, 00 min	1. To demonstrate ability of MOS to support launch, acquisition, and maneuver sequences 2. To demonstrate capability of supporting two flight operations	1. Engineering-unit formats available, but with incorrect parameters 2. All facility functions proved satisfactory for launch support 3. All data processing functions, with exception of engineering-unit formats, proved satisfactory for launch and maneuver 4. All personnel functions and interfaces proved satisfactory for launch and maneuver
32	Simulated launch	M67-2	Jun 9, 22:54 GMT	Jun 10, 03:17 GMT	4 h, 23 min	1. To expose SPAC to a final simulated launch 2. To check out all major and minor interface and facility anomalies 3. To familiarize SPAC with countdown procedure and launch status of spacecraft	1. All facility functions proved satisfactory for launch support 2. All data processing functions, with exception of engineering-unit formats, proved satisfactory for launch and maneuver 3. All personnel functions and interfaces proved satisfactory for launch and maneuver
33	Nominal encounter test	M67-1	Aug 25, 08:30 LMT	Aug 25, 18:00 LMT	9 h, 30 min	1. To expose SPAC personnel to proposed encounter sequence using GMT 2. To familiarize SPAC with encounter formats 3. To check out operational procedures for encounter	1. Encounter sequence was in process of change by VEPWG 2. Difficulty was encountered in updating mission clock and obtaining synchronism with SAF 3. Test was difficult to follow because of compression of 23-h encounter into 9 h of test time
34	Encounter anomaly test	M67-1	Sep 15, 08:30 LMT	Sep 15, 17:30 LMT	9 h, 00 min	To expose MOS to an anomalous encounter sequence to train personnel involved to detect, analyze, and successfully correct possible flight malfunctions	1. Clock stepping and synchronization improved, but still difficult to follow 2. TWT[h] failure; analyzed correctly 3. Possible power-on reset analyzed correctly 4. Improper command accepted; analyzed correctly 5. Clock B malfunction; analyzed incorrectly 6. CP malfunctioned

[h]TWT = traveling-wave tube.

Table V-2 (contd)

Test No.	Type	Data source	Start time	End time	Duration	Objectives	Results
35	Encounter anomaly test	M67-1	Sep 21, 08:30 LMT	Sep 21, 17:30 LMT	9 h, 00 min	To expose MOS to an anomalous encounter sequence to train personnel involved to detect, analyze, and successfully correct possible flight malfunctions	1. Requested SAGC voice reports 2. DFR[I] status-bit anomaly; analyzed correctly 3. Dust particles; analyzed correctly 4. Mode 2 encounter; analyzed correctly 5. Clock B malfunction; analyzed incorrectly 6. Clock B malfunction rerun; analyzed incorrectly 7. MT-3 position; analyzed incorrectly 8. TRD[J] failure; analyzed correctly
36	Encounter anomaly test	M67-1	Sep 28, 08:30 LMT	Sep 28, 15:30 LMT	7 h, 00 min	1. To expose MOS to an anomalous encounter sequence to train personnel involved to direct, analyze, and successfully correct possible flight malfunctions 2. Continuation of test conducted on Sep 21 (Test No. 35)	1. TRD failure; analyzed correctly 2. Clock A postencounter enabled; analyzed correctly 3. Tape recorder losing pressure; analyzed correctly 4. Slow TRD response time 5. Slow mode 4 data analysis
37	Encounter anomaly test	M67-1	Oct 3, 08:30 LMT	Oct 3, 18:30 LMT	10 h, 00 min	1. To expose MOS to an anomalous encounter sequence to train personnel involved to direct, analyze, and successfully correct possible flight malfunctions 2. Test started with DC-V25	1. Plasma probe high-voltage failure; analyzed correctly 2. Command decoder failure; analyzed correctly 3. Analog data failure; analyzed correctly 4. TRD anomaly; analyzed correctly 5. Tape recorder anomaly; analyzed correctly 6. BUS–ACE interface anomaly
38	*Mariner IV* Canopus acquisition	*Mariner IV*	Oct 4, 17:00 GMT	Oct 4, 23:40 GMT	6 h, 40 min	1. To provide SPAC personnel with operational experience on a flight spacecraft 2. To acquire Canopus as a preliminary step for pointing high-gain antenna at earth 3. To clock out CC&S maneuver clock	1. Transmitted five DC-17 commands 2. Transmitted DC-19 3. Transmitted DC-21 4. Transmitted DC-15 5. Canopus was acquired 6. SPAC performance during exercise was satisfactory 7. Transmitted DC-29 8. Transmitted DC-13 9. Transmitted QC-1-1 10. Transmitted DC-27

[I]DFR = dual-frequency receiver.
[J]TRD = trapped radiation detector.

Table V-2 (contd)

Test No.	Type	Data source	Start time	End time	Duration	Objectives	Results
39	*Mariner IV* high-gain antenna exercise	*Mariner IV*	Oct 6, 16:30 GMT	Oct 7, 16:00 GMT	23 h, 30 min	1. To point high-gain antenna at earth to obtain improved communications capability 2. To provide SPAC with flight experience for *Mariner V* encounter sequence with inertial roll control mode 3. To demonstrate ability of SPAC to function over extended periods	1. SPAC supported operations for 23 h, 30 min 2. SPAC successfully pointed high-gain antenna at earth, and switched transmit-high/receive-high 3. SPAC successfully mapped high-gain antenna pattern using DC-18(21) mode 4. SPAC successfully performed a spacecraft maneuver without a motor burn
40	Encounter readiness test	M67-1	Oct 10, 19:30 GMT	Oct 11, 08:30 GMT	13 h, 00 min	To expose SPAC and other areas of MOS to a real-time encounter sequence and demonstrate ability of MOS to support encounter operation	1. Experienced difficulty with CP and 7044 2. APAC[k] occurred before entering occultation
41	*Mariner IV* high-gain antenna adjustment	*Mariner IV*	Oct 12, 19:30 GMT	Oct 12, 23:00 GMT	3 h, 30 min	To improve pointing angle of high-gain antenna	High-gain antenna position was successfully adjusted
42	*Mariner IV* high-gain antenna adjustment	*Mariner IV*	Oct 15, 16:15 GMT	Oct 15, 18:15 GMT	2 h, 00 min	To improve pointing angle of high-gain antenna	High-gain antenna position was successfully adjusted

[k]APAC = *antenna pointing angle change.*

Perhaps one of the most significant weaknesses of the SPAC function was the relationship of SSAC to SPAC. In trying to assess overall spacecraft status, it is of the utmost importance to determine the exact status of all spacecraft subsystems. This determination was made difficult by the autonomous organization of SSAC. During SPAC induced-anomaly testing, it became obvious that the science subsystems were an integral part of the spacecraft and had profound interactions with other subsystems. These interactions could best be understood and analyzed when SPAC and SSAC acted as one unit. The organization (see Fig. V-5) presented serious communications and scheduling problems. To minimize these problems, SPAC and SSAC operated informally as one group on one communications network.

Another notable exception was the SPAC–SPAC JR relationship. This was found to be weak from a communications standpoint during the early SPAC–SPAC JR tests, and had to be strengthened as a result of test experience.

Finally, a minor weak point in the organization was found early in the testing period, when it became obvious that communications between the director's staff and SPAC members were too frequent and tended to be conflicting. This problem was rapidly recognized and alleviated by clarification of network procedures.

Intra-SPAC communications. Communications within SPAC were generally satisfactory, with the exception of the SPAC–SPAC JR interface noted above. A slight difficulty was experienced during induced-anomaly tests that would have been minimized somewhat with the availability of another SPAC network for brief discussions between appropriate SPAC members in the analysis of detailed subsystem behavior. The congestion was felt to be minor, however, and could generally be circumvented by the use of an adjacent conference room (DRD).

Analysis and evaluation of subsystems and spacecraft behavior and status. The same type of test (the induced-anomaly test) was used to evaluate and analyze subsystems, evaluate the overall behavior of the spacecraft, and analyze factors affecting the status of the spacecraft. This test was found to be the most effective.

In the induced-anomaly test, SPAC was in essence faced with a specific phase of the mission that was designed to be highly anomalous. The task of SPAC was to analyze the induced failure correctly and as rapidly as possible; then appropriately to change the status of the spacecraft via ground commands in order to maximize the probability of accomplishing the stated mission (or to effect partial mission success).

It was generally noted that the level of competence in performing each of the above SPAC functions increased directly with the number of tests that were made. Furthermore, it became apparent that most of the SFO facility problems that were finally corrected became obvious during the induced-anomaly tests. The changes that were brought about as a result of these tests are too numerous to be included here. The more significant ones, however, are noted in Table V-2 and in the minutes of the *Mariner* Venus 67 project meetings.

SPAC interface communications. During the early phases of SPAC testing, numerous minor problems concerning inter-area communications were detected. Most of these problems were alleviated by the assignment of networks to individuals, and by the clarification of network procedures. Some of the more serious problems were those encountered during testing that would not have presented difficulty during actual mission operations. Communications were generally inadequate at the test complex, both in SAF and in the Environmental Test Laboratory (ETL). These problems were never fully reconciled, mainly because of manpower limitations and the fact that they were problems that did not affect mission operations.

D. Planning Philosophy

A significant portion of the *Mariner* Venus 67 SPAC activity was devoted to preparation for the various phases of the mission. The objectives of this preparation were as follows: (1) to establish an acceptable plan for each phase of the mission, (2) to develop a nominal sequence of events and a set of criteria by which the performance of the spacecraft could be evaluated, (3) to establish the courses of action to be followed in case of nonstandard performance of the spacecraft, and (4) to develop in SPAC personnel and procedures the level of proficiency required to carry out the flight-operations responsibilities of the SPAC.

All of this activity was specifically directed towards developing the ability of SPAC to react correctly to any sequence of events, standard or nonstandard, in an actual mission.

Past experience has shown that the nature of the mission and the complexity of both the spacecraft and

the ground equipment precluded the successful execution of any course of action that had not been detailed and agreed upon in advance by all concerned parties. This was especially true in the SPAC area, where the personnel responsible for proposing and evaluating detailed alternative courses of action were the same as those responsible for evaluating spacecraft performance. During a critical phase of the flight operation, these two activities were mutually exclusive. If the SPAC members concerned themselves with evaluating the state of the spacecraft, they could not simultaneously generate a recommended and effective course of action. If they devoted their attention to formulating and evaluating a plan of action, little or no information on the state of the spacecraft would be obtained. Obviously, for a satisfactory SPAC operation, both complete knowledge of the current state of the spacecraft and an effective, well-understood plan of action are required.

As a corollary to this, even if the state of the spacecraft could be monitored effectively without the full-time support of the SPAC members, it was practically impossible spontaneously to generate a good emergency procedure in response to an unanticipated anomaly aboard the spacecraft. "Unanticipated" implies that the source or sources of the problem were unknown. If a failure existed, its impact upon the mission was not understood, and exact response of the spacecraft to any given set of ground actions was, at best, uncertain. Coupled with this were the facts that time was usually critical, and that all of the possible ground actions carried with them disadvantages as well as advantages, each of which had to be weighed and evaluated.

The following three principles underlay the *Mariner* Venus 67 SPAC planning philosophy:

(1) The performance of the spacecraft at each step in any sequence of events must be understood and verifiable, and each possible failure mode, its symptoms and its consequences, must be anticipated.

(2) For each possible failure mode, a plan for corrective action must be generated before the fact and agreed upon by the SPAC personnel. For probable or extremely time-critical failure modes, the plan for corrective action should be agreed upon in principle by all parties concerned in the flight operations, including the project manager, so that reaction time would be minimized. Given the proper SPAC preparation for any phase of the flight operation, any anomalous indication in the telemetry would be immediately recognizable, and the possible failure modes that would yield that particular anomaly would be cataloged, along with the recommended corrective action. The SPAC director, the SFOD, and the project manager should be thoroughly cognizant of the implications of both the anomaly and the action required to correct or circumvent it, so that the decision required to take corrective action is a simple approval or disapproval rather than a complex procedure of proposing, explaining, and evaluating. To a great degree, this function was achieved by categorizing certain failure modes into classes. Class I included nonstandard operations of the launch vehicle, the spacecraft, or the MOS that have been anticipated and for which corrective action has been planned. This class was broken into category IA, which, by prior agreement with the project manager, required no detailed real-time interface with the project manager for implementing corrective action; and category IB, whose operations required a detailed interface with the project manager prior to their execution. Class II nonstandard operations comprised situations wherein a nonstandard event occurred for which no specific corrective action had been planned but for which such action was possible. If such events occurred, the action taken was to be decided at the time of occurrence. Class III nonstandard operations were those for which no corrective action was possible. If such events occurred, the action taken was to be decided at the time of occurrence.

(3) No positive action is to be taken without a positive reason. The *Mariner V* spacecraft design is sufficiently complex that improper ground command action may place the spacecraft in a state from which recovery is not possible. Whenever a command is inserted into the spacecraft, there is the possibility that either the initial state of the spacecraft or the effect of the command is not completely understood, with the result that irreparable damage may be done to the mission. This risk must be outweighed by the value attached to ground action before any perturbation to the spacecraft is warranted.

The first activity in SPAC planning for any particular portion of the mission was the recommendation of a mission plan. For the standard phases of the mission, such as launch, midcourse maneuver, or encounter, a mission plan already existed in the form of the CC&S programmed sequence of events. This was in line, of

course, with the *Mariner V* design philosophy, which dictated that the spacecraft must be able to perform a nominal mission (except for the midcourse correction) without any ground-based intervention or support. It was also true, however, that the spacecraft was able to complete all of the mission objectives without the CC&S, relying solely upon ground commands. In fact, because the CC&S sequence of events was necessarily designed into the spacecraft long before launch, the response of the spacecraft to its environment during flight may have rendered the prelaunch nominal sequence less than optimum. In this case, the probability of achieving mission success might have been enhanced considerably by augmenting or preempting the CC&S events with ground commands.

It was the responsibility of SPAC either to generate a plan for each phase of the mission or, if a CC&S nominal plan existed, to review all possible alternatives, and then recommend the optimum plan. For certain phases of the mission, this task encompassed so much work that a separate ad hoc committee had to be formed to perform mission planning and evaluation. For the *Mariner V* encounter phase, the VEPWG was formed. The chairman of this committee was the SPAC director; its members were appropriate representatives of SPAC, SSAC, FPAC, DSN, and the *Mariner* project office.

To establish a mission plan, many alternative courses of action were examined in the light of the mission objectives as stated by the *Mariner* project office. Any proposed command action from the ground was evaluated by the SPAC group to determine undesirable side effects or possible failure modes the command might induce. If possible, quantitative analyses were made so that the relative desirability of alternate plans could be assessed.

This type of reasoning led to the adoption of a mission plan for encounter that was a slightly modified version of the nominal sequence programmed into the spacecraft before launch (see Section V-G). Perhaps the most significant aspect of this modification to the encounter plan was that the preemption of the nominal programmed CC&S plan by ground commands did not indicate that the nominal plan was deficient in any way. The programmed plan was developed to provide nominal mission capability to the spacecraft in case the spacecraft was denied any support from the ground. If this had occurred, the programmed plan would have done the job admirably. The actual plan was designed to make the most efficient use of the full capabilities of the entire DSN–spacecraft complex (which, of course, is the whole point of flight operations planning).

In the development of the mission plan, then, attention was not limited to the spacecraft alone, but was given to all of the areas and activities within this DSN–spacecraft complex. Many of the possible ground-command sequences that, when performed correctly, were the most attractive from a spacecraft point of view were discarded simply because ground-based operational difficulties precluded the guarantee of a sufficiently high probability of correct performance.

After a recommended plan for each phase of the mission had been formulated, it was presented, along with a discussion of its advantages and disadvantages, to the SFOD and the *Mariner* project office. Final responsibility for all *Mariner* mission plans rested with the *Mariner* project manager, who issued the approved plan and coordinated any activities required for its implementation.

The approval by the project office of a particular plan of attack initiated another activity of the *Mariner* Venus 67 SPAC group—the establishment of a nominal sequence of events for that plan. The sequence of events was a detailed chronology of all spacecraft changes of state that would occur during the execution of a particular mission plan. The SPAC members were especially oriented towards telemetry because nearly all of the information available concerning the state of the spacecraft was furnished by telemetry. Consequently, the effort to establish the sequence of events led directly to the tabulation of nominal telemetry values.

The sequence of events and its associated telemetry table provided SPAC with all of the tools required both to predict and to verify all changes of state of the spacecraft. Not only did this allow immediate recognition of a nonstandard occurrence aboard the spacecraft, but it also provided SPAC analysts with the primary diagnostic instrument for determining the cause of any deviation from normal performance.

Once the nominal sequence of events had been established, an effort was initiated to anticipate possible failure modes and appropriate corrective actions. One very important aspect of this activity during the *Mariner* Venus 67 mission was the generation of a series of sequence-flow diagrams. These depicted the large number of alternate paths that were possible, either by

option or because of failure, at any point in the sequence once the sequence had been initiated. This particular activity required much thought on the part of SPAC personnel in the area of nonstandard sequence plans. An important part of nonstandard sequence planning was the increased understanding gained by SPAC of the corrective capability within the spacecraft design.

Nonstandard sequence plans were submitted to the project office for approval and classification before the actual flight operation in order to provide the ability to take action in a timely fashion whenever a nonstandard condition arose.

The final test of any plan, of course, is how well it works when it is implemented. To verify that the mission plan, the sequence of events, and the alternate plans were adequate, SPAC conducted a series of tests (often in conjunction with general SFO tests). A large number of the tests conducted after *Mariner V* launch used the flight-support spacecraft as the data source rather than simulated data or available test tapes. So that the SPAC group could be put to the most severe test of its proficiency, and so that SPAC procedures could be best validated, the test director was allowed to induce or simulate spacecraft malfunctions at his discretion. The SPAC and SSAC operations personnel were then responsible for determining the corrective action required for successful completion of the test objectives. These tests proved to be most helpful in establishing the level of proficiency required for SPAC operations.

The planning philosophy, as stated in the preceding paragraphs, proved its validity during mission operations. The diligent application of this philosophy to the preparation for each of the mission phases provided SPAC with sufficiently firm guidelines to make possible the successful execution of the mission. This planning allowed for the establishment of a set of criteria by which certain actions would be taken. These criteria were approved and understood by the *Mariner* Venus 67 SPAC director, the SFOD, and the project manager, thereby guaranteeing a maximum of information flow and maximum ability to react.

E. Launch Planning

The launch phase of the mission, along with the midcourse maneuver and encounter, was one of the three critical phases of the *Mariner* Venus 67 mission. Of the three, the launch phase was perhaps the most demanding, as a large number of important events occurred within a relatively short time, and any one of these events, if anomalous, could have seriously affected or even prematurely terminated the mission. Seven main events were associated with the launch phase of the mission:

(1) Countdown and liftoff.
(2) Nose-fairing ejection.
(3) Spacecraft injection.
(4) Spacecraft–*Agena* separation.
(5) Sun acquisition.
(6) Magnetometer calibration.
(7) Canopus acquisition.

Of these seven major events, the first five were expected to occur within the first hour after liftoff. The critical nature of the launch phase stemmed from this rapid succession of highly consequential events. The primary objective of SPAC planning for the launch phase was, therefore, to ensure that: (1) six of the seven events (spacecraft injection is monitored by boost-vehicle and FPAC personnel) could be accurately monitored during mission operations, and (2) contingency plans were adequate and could be successfully implemented as required. The ability of SPAC to implement various contingency plans associated with the launch phase of the mission is discussed in Subsection C-6, above, under the heading of *SPAC testing*. The generation of the contingency plans, and their associated underlying philosophies, are discussed in the paragraphs that follow.

Recognizing the possible occurrence of a large number of different anomalies during the launch phase, and the importance of rapid reaction to these possible anomalies, the *Mariner* Venus 67 project manager initiated a system of anomaly classification that would reduce MOS reaction time as a function of effect on the *Mariner* Venus 67 mission. Possible anomalies were grouped into three classes.

Class I included nonstandard operations of the launch vehicle, the spacecraft, or the MOS that had been anticipated and for which corrective action had been planned. This class was divided into two categories: Category IA, which, by prior agreement with the project manager, required no detailed real-time interface with the project manager for implementing corrective action; and category IB, which required a detailed interface with the project manager before the execution of corrective action.

Class II nonstandard operations were situations wherein a nonstandard event occurred for which no specific

corrective action had been planned, but for which such action was possible. If such events occurred, the action to be taken would be decided at the time of occurrence.

Class III nonstandard operations were those for which no corrective action was possible. If such events occurred, the action to be taken would be decided at the time of occurrence.

In preparing SPAC for support of the launch phase, the above three classifications were used in conjunction with detailed sequence-flow diagrams to arrive at a comprehensive contingency plan for six of the seven subphases associated with launch. The general aspects of the contingency plans for each of these six launch subphases are discussed below.

1. Countdown and liftoff. Operational participation during the countdown and liftoff phase of the mission was limited to: (1) monitoring the activities of the launch team at AFETR in order to be aware of the initial launch status of the spacecraft, (2) monitoring the response of the spacecraft during countdown in an effort to support the launch team, and (3) effecting the smooth transfer of spacecraft operational control from the launch team at AFETR to the operations team at SFOF. It immediately became apparent that, to accomplish these objectives, a critical requirement for a comprehensive communications system between the launch team and SPAC at SFOF would have to be fulfilled. This was accomplished by the incorporation of a direct voice and TTY interface between SPAC JR and SPAC. (The SPAC–SPAC JR data and communications interface relationship is shown in Fig. V-2.)

SPAC planning for this phase of the mission was, therefore, largely concerned with ensuring that an adequate communications capability existed between the groups involved, and that SPAC was prepared to assist the launch team in analyzing the prelaunch behavior of the spacecraft (see Subsection C-6, above).

To effect a smooth transfer of mission operations control from the launch team to SFOF, full SPAC monitoring of the launch phase of the mission was planned to begin approximately 2 h before liftoff (with all of the countdown data), and continue through Canopus acquisition.

2. Nose-fairing ejection. Following the catastrophic failure of *Mariner III* in 1964, caused by an anomalous nose-fairing ejection, considerable effort was devoted to contingency planning for a possible similar anomaly aboard *Mariner V*. In the event of the nose fairing being partially ejected, the basic plan was to perform a midcourse maneuver motor burn of predetermined duration in an attempt to force spacecraft–nose-fairing separation. The duration of the motor burn would be arrived at by considering a number of specific conditions during flight.

Analysis of the possible failure modes revealed two primary shroud-ejection failure modes: (1) The nose-fairing skin and the motor thrust axis are perpendicular to each other; (2) they are at an angle of approximately 95.2 deg to each other. Only 2–3 s, respectively, were the times needed to burn through the fairing skin for these two modes. Once the motor exhaust penetrated the nose-fairing skin, the rocket motor would exert 50 lbf along the thrust axis of the motor. Depending upon the specific spin rates associated with the failure (which were to be obtained from the spacecraft telemetry), a motor burn time could then be calculated that would not exceed a maximum spin rate of approximately 4.5 rad/s, which was the maximum spin rate to allow reacquisition in 5 h, before AC gas and battery depletion.

3. Spacecraft injection. The injection of the spacecraft into a heliocentric orbit was accomplished with the second burn of the *Agena*. During this phase of the mission, the role of SPAC was passive, being confined to the careful monitoring of the spacecraft status.

4. Spacecraft–Agena separation. The spacecraft–*Agena* separation phase was the first phase of the flight during which the spacecraft underwent numerous automatic state changes. During this phase, three mechanical devices were activated; these, in turn, initiated nine different spacecraft functions, as shown in Table V-3. The main function of SPAC during the separation phase was to verify that each of the events had taken place or, in case any of the events had not taken place, to recommend such action as was necessary to accomplish the desired effect. Included in Table V-3 are the primary spacecraft indicators used by SPAC to confirm the successful accomplishment of each of the expected events. A discussion of each of the major functions is presented below.

a. Solar-panel deployment. Spacecraft telemetry permitted SPAC to determine the following conditions relative to solar-panel deployment:

(1) Whether the pyrotechnic subsystem had been armed by the pyrotechnic arming switch or the separation-initiated timer.

(2) Which of the pyrotechnic subsystems (or both) issued a solar-panel-deployment command.

Table V-3. Spacecraft–*Agena* separation functions

Time of activation	Mechanical device	Function	Primary SPAC indicator	Time of activation	Mechanical device	Function	Primary SPAC indicator
S[a]	Pyrotechnic-arming switch					10-kV inhibit off	
S + 0		*Agena* amplifier off		S + 0		RF power up	SAGC, power, radio, telemetry
S + 0		AC on	AC telemetry	S + 0		Science on	Telemetry, power
S + 0		Pyrotechnics armed	Event registers	S + 0–1 min		Tape recorder launch mode off	Power
S	Separation connector			S	Separation-initiated timer		
S + 0		CC&S relay hold off	Power, CC&S L-1, etc.	S + 30 s		Pyrotechnics armed	Event registers
S + 0		Plasma probe	Science telemetry	S + 3 min		Deploy solar panels	Event registers, power, AC

[a]S = separation.

(3) Which of the solar panels was deployed to within 20 deg of the full-open condition.

Because of the nature of the solar-panel-deployment mechanism, the latter condition inferred that a solar panel was completely deployed. It was also possible to observe whether or not the CC&S launch counter generated the first of its commands (CC&S L-1) to back up the initiation of solar-panel deployment. This particular function could be inhibited if the CC&S relay-holding current was not properly removed at separation. This feature was so mechanized that the holding current was definitely removed whenever the gyro power was turned off. If the solar panels had been observed to be in their launch position, and if the CC&S command had not been issued, the gyros would have been turned off by ground command. Following gyro turnoff, the CC&S would be permitted to issue the solar-panel-deployment command at some future time predictable from knowledge of the CC&S counting sequence.

After issuance of the CC&S L-1 command for solar-panel deployment, the gyros would be reenergized by the transmission of DC-V19 to effect sun acquisition; however, if the gyros were turned on in the future, it would be impossible for the CC&S to generate any of its internal commands from the launch counter or from the master timer (end counter). A midcourse maneuver would not be possible under the conditions of a relay-hold failure.

Should as many as two solar panels fail to deploy, a partial mission success could still be achieved by turning the battery charger and/or the gyros and/or the science subsystem off until more power was available at shorter heliocentric ranges.

The deployment of the solar panels also initiated the deployment of the sun shade. Failure of the sun shade to deploy would not seriously affect the spacecraft mission. It would, however, increase the temperature of the spacecraft bus; therefore, reevaluation of mission procedures would be required.

b. Science subsystem turn-on. Verification of science subsystem turn-on was obtained from observation of the spacecraft telemetry format, and from noting the change informat of each data frame from ⅔ zeros and ⅓ engineering data. It was only after the application of power to the science instruments and the data-automation subsystem that data were transmitted to the DE for subsequent transmission to earth. Analysis of science telemetry permitted verification of the fact that all science instruments were on and that the plasma probe 10-kV inhibit had been removed.

An alternate means of verifying science instrument turn-on was to analyze the power subsystem telemetry. If the science instruments and the DAS had not been automatically turned on at separation, ground command DC-V2 could have turned on the science subsystem through an alternate set of relay contacts. If DC-V2 also failed to turn on the science subsystem, and if a failure

of the main booster regulator had occurred, the science subsystem would have been turned on following gyro turnoff.

c. Increase of transmitted RF power. Before separation, RF power transmitted from the spacecraft was maintained at approximately 1 W by a relay-holding circuit passing through the spacecraft-separation connector. This circuit was to be opened upon spacecraft separation, powered by the power subsystem maneuver booster that was required to activate the gyros. If automatic RF power-up did not occur, it was possible to attain increased transmitted power from the spacecraft whenever the gyros were off. Conceivably, the entire mission could have been attained even in that degraded mode of operation; however, telemetry during the midcourse maneuver might have been degraded. The occurrence of RF power-up could easily be verified by monitoring the received signal level at the DSIF stations, in addition to the spacecraft telemetry, which would indicate the transmitted power.

d. Turnoff of tape recorder launch mode. The tape recorder subsystem record motor was energized during the launch phase to maintain tension on the Mylar tape to preclude its spilling off the reel during the vibration of the launch phase. The mechanization for turning off this launch mode was to sense the first end-of-tape (EOT) signal generated by the tape recorder subsystem after separation, and, upon this signal, opening the relay connecting the record motor with the power supply. Failure of this particular logic could be overridden by automatic or commanded turnoff of the gyros.

Because approximately 30 tape passes/h occur in the launch mode, concern was expressed regarding the extensive periods during which the launch mode should be operative. If the launch mode did not turn off shortly after separation, ground command DC-V15 would be transmitted to turn off the gyro power supply (and consequently the launch mode). Upon subsequent energizing of the gyros by DC-V19, the tape recorder launch-mode logic would be locked out. A constraint upon the use of the DC-V15 command in this condition is that, whenever the gyros are off, the spacecraft roll rate cannot be controlled, and a valid magnetometer-calibration roll sequence is not possible. Consequently, a choice had to be made between two alternatives: (1) to turn the gyros off immediately, preventing additional tape passes from accumulating at the price of sacrificing some of the most important magnetometer calibration time, or (2) to delay turning the gyros off for several hours in order to achieve magnetometer calibration at the price of accumulating an additional 30 passes/h on the tape recorder. The SPAC recommendation would have been to turn the tape recorder launch mode off immediately. The decision as to which alternative to take was a Class IB decision, and would have been made by the project manager in real time.

e. Removal of CC&S relay hold. The function of the CC&S relay-holding current was to prevent inadvertent actuation of relays within the CC&S during the launch phase, and consequent inadvertent initiation of portions of the mission sequence at inappropriate times. The relay-holding current was normally removed upon spacecraft separation, and also when the gyro power was turned off. Failure to release the relay-holding current prevented commands from being issued by the CC&S. Review of the spacecraft power subsystem telemetry readings verified that the holding current had indeed been released.

The exact time that the gyros should be turned off to provide a backup to the automatic spacecraft function of releasing the holding current would be a function of spacecraft requirements at that particular time. If sun acquisition were initiated, and the solar panels had been deployed, the relay-holding current could be permitted to remain on until the magnetometer-calibration rolls had been completed. However, if the backup capability provided by the CC&S launch commands were necessary, the gyros would be turned off as soon as possible to permit the spacecraft backup commands to be issued. The CC&S commands, L-1 and L-2, are normally issued before launch (L+60 min).

5. Sun acquisition. Sun acquisition commenced as soon as the AC switching amplifiers and sun sensors were turned on. The occurrence of the pyro-arming event in the telemetry, as mentioned above, implied that the pyrotechnic-arming switch had been activated and that the AC should have been turned on. If the telemetry indicated that the rates about the control axes were not decreasing, however, or that the sun sensors were not generating error signals, this function had probably not been accomplished. The primary corrective action would be to transmit DC-V13 to the spacecraft. This command would remove the 26 V from a relay, and supply power to the sun sensors and switching amplifiers.

A further backup function was also available as a command from the CC&S launch counter (CC&S L-2). This command was subject to the same failure mode

described above for solar-panel deployment. In this condition, the gyros would be maintained in the off mode by ground command long enough to permit the CC&S to generate this backup AC turn-on command if it became necessary. Following the CC&S command, the spacecraft would reacquire the sun in the derived-rate mode.

Acquisition of the sun by the spacecraft was completely automatic. No ground commands were available to aid in sun acquisition once the electronics had been turned on and the procedure had been initiated.

6. Magnetometer roll calibration. To increase the value of the magnetometer experiment, the spacecraft was designed to roll at a fixed rate for approximately 16 h following the sun-gate until the start of Canopus acquisition. The purpose was to obtain an in-flight calibration of the magnetic field of the spacecraft as observed by the magnetometer sensor. This calibration was possible because the observed magnetometer signals near earth would have rotating components caused by the external environment (the geomagnetic field) and fixed components caused by the spacecraft environment. Knowledge of the geomagnetic field of the earth permitted the determination of the spacecraft-induced magnetic field at the magnetometer sensor.

If the magnetometer-calibration sequence had not started as expected, consideration would have been given to transmitting a DC-V21 in an attempt to reset the AC roll-inhibit logic.

SPAC monitored the progress of the magnetometer-calibration phase of the mission by observing the AC gyro telemetry channels, the earth-sensor output, and the magnetometer response.

7. Canopus acquisition. The final phase of the launch operations was celestial roll-reference acquisition by the spacecraft. This phase was automatically initiated by the CC&S L-3 command at L+997 min. The spacecraft continued to roll in the ccw direction until an object of at least half the brightness of Canopus moved into the field of view (FOV) of the Canopus sensor. The roll-search sequence was then terminated, the gyros automatically turned off, and the cruise phase of the flight initiated.

The SPAC contingency plans for this phase of the mission included the major anomalies described below.

a. CC&S L-3 not available. If the L-3 command from the CC&S was not available to initiate Canopus acquisition, the Canopus sensor could be turned on by the transmission of DC-V13. This command would remove the 26-V excitation from a relay in the AC subsystem, thus turning Canopus sensor power on and producing a search rate for the AC roll axis. A midcourse maneuver in this mode is possible by ending DC-V27 before transmitting DC-V14.

b. Inertial roll control. An alternate means of obtaining roll stability was by use of the DC-V18 command, which places the spacecraft roll axis under inertial control by the gyros. This mode of operation is completely independent of the Canopus sensor, and could have been used throughout the mission. If the Canopus sensor were inoperative, the midcourse maneuver would be performed in this mode by use of the earth sensor as a roll reference.

c. Roll drift. Another alternative existed if a Canopus-sensor failure had occurred. It was possible to allow the spacecraft to continue in its heliocentric orbit independent of a roll reference. This mode could have been accomplished by the transmission of either DC-V15 or DC-V20. Both commands would turn the gyros off, and allow the spacecraft to perform the interplanetary cruise. This mode would have to be dropped by October 1, when communication on the high-gain antenna was required. Further and more detailed contingency plans were generated for such abnormal events as incorrect roll rate, failure of the gyros to turn off, etc.

One of the anticipated delays in the Canopus-acquisition sequence during flight operations was the possible acquisition of earth by the Canopus sensor. If this occurred, the accepted plan was to transmit one or more DC-V21 commands. These commands would override the Canopus sensor acquisition logic by rotating the spacecraft roll axis approximately 2.25 deg ccw per command, and reinitiate roll search.

F. Trajectory-Correction Maneuver Planning

The trajectory-correction maneuver is perhaps the most demanding phase of the *Mariner* Venus 67 mission insofar as SPAC is concerned. Normally, the accuracy of injection of the spacecraft is such that a trajectory-correction maneuver is required for a successful mission; no automatic provision can be made for this maneuver in the design, however, because the correction parameters must necessarily be furnished from the ground after

launch. Thus, the burden of performing the correction falls upon the SFO organization, and upon FPAC and SPAC in particular. All inputs must be transmitted to the spacecraft by means of ground command. During all portions of the sequence, the performance must be monitored carefully because at best a nonstandard midcourse maneuver means an unacceptable planetary miss distance; in the worst case, it may result in a total spacecraft failure.

The nominal midcourse maneuver was planned to occur 2–10 days after launch. The possibility existed, however, that the trajectory of the spacecraft, as determined by the launch vehicle, could have been outside the expected tolerances, thus necessitating a very early midcourse maneuver. In the maneuver planning, therefore, SPAC had to consider the performance of both a nominal midcourse maneuver and a very early maneuver (on the order of 5 h after launch).

The successful performance of a midcourse maneuver may conveniently be divided into two main phases: (1) The planning phase and (2) the execution phase. The planning phase, in turn, consists of two subphases: (a) The aiming-point selection subphase and (b) the maneuver-turns generation subphase. The execution phase consists of: (a) Command generation, (b) command transmission, (c) spacecraft maneuver execution, and (d) celestial reference reacquisition. SPAC planning for each of these major phases and subphases is discussed below.

1. *Midcourse maneuver planning phase.*

a. Aiming-point selection. In selecting the aiming point for the midcourse maneuver, it was necessary to have exact knowledge of criteria that define a progressively more desirable aiming-point location from the standpoint of a scientific experiment. This information was made available by SSAC, and is presented in Fig. V-7. The center of the graph represents the planet Venus in the $\mathbf{R} \cdot \mathbf{T}$[4] plane, with an impact circle at a radius of approximately 21,200 km. To avoid impacting the planet, the aiming point had to be selected outside of this circle. The V_{TOT} lines represent the total science-experiment value as a function of location in the aiming plane. It may be seen that, for a given radial line, V_{TOT} increases with increased proximity to the impact circle. Thus, the science requirements localize the selection of the aiming point to an area within approximately 285–360 deg, and 21,200–40,000 km, in the aiming plane.

The general area in the aiming plane having been selected, it was necessary to include some of the additional geometric and spacecraft constraints for the selection of the final aiming point. These constraints are shown roughly in Fig. V-8.

The Canopus-sensor constraint required that the Canopus–spacecraft–Venus angle be large enough to prevent Venus straylight from entering the FOV of the Canopus sensor and possibly causing the loss of roll-reference acquisition (for preliminary study, the angle used was 36 deg).

The sun-occultation constraint stated that the sun–spacecraft–Venus angle had to be greater than 0 deg at

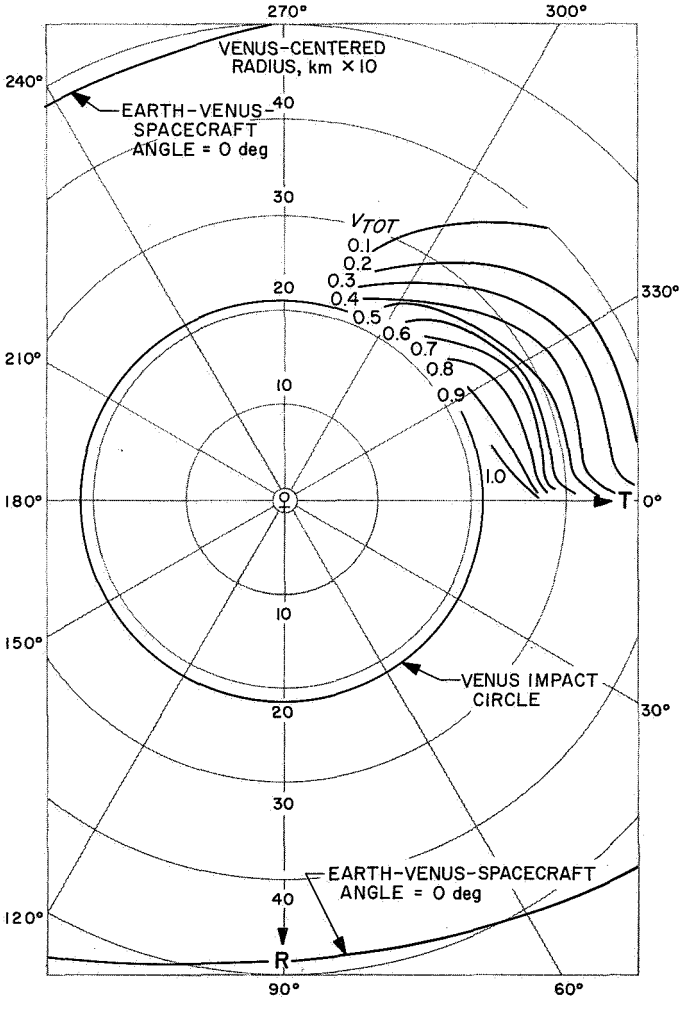


Fig. V-7. Science-experiment value function vs aiming-plane coordinates

[4]The vector **T** passes through the center of the planet parallel to the ecliptic plane and perpendicular to the spacecraft incoming asymptote **S**. The vector **R** is **S** × **T**.

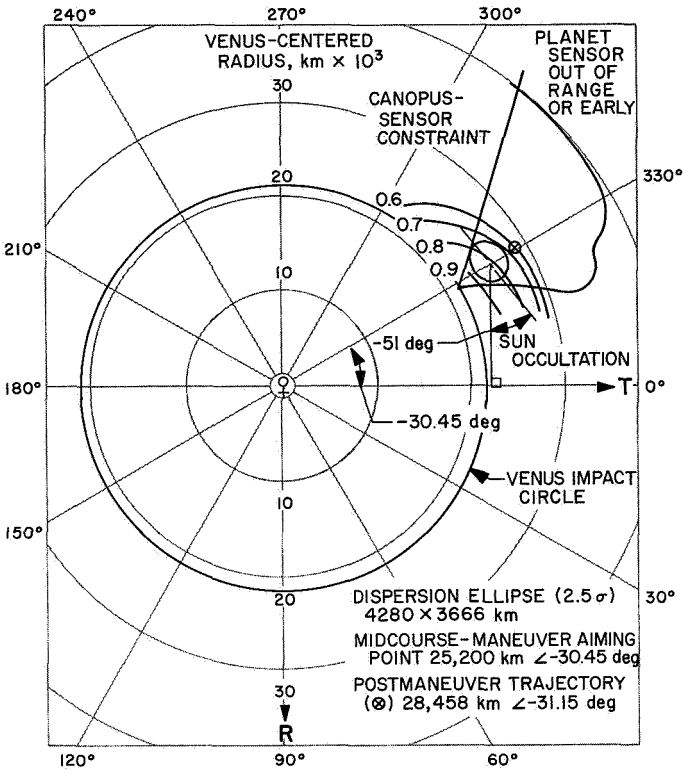


Fig. V-8. Midcourse maneuver final aiming point

all times. This constraint prevented the loss of sun acquisition, and supplied the spacecraft with solar power during the Venus encounter.

The planet-sensor constraint provided a planet-sensor output (PSO) within 12 min of the desired optimum time during the encounter sequence.

The final aiming point could now be chosen from the area within the above constraint boundaries by placing the center of a 2.58 (99.0%) maneuver ellipse[5] on the highest science-experiment value line with the ellipse tangent[6] to the constraint regions. The final aiming point thus chosen was a point at 25,200 km, −30.45 deg. For the sake of completeness, Fig. V-8 also shows the achieved maneuver at 28,458 km, −31.15 deg.

[5]The 1 δ maneuver ellipse used had a semi-minor axis of 733 km and a semi-major axis of 856 km, with the semi-major axis at an angle of −51 deg from **R**. These parameters were derived 4 days after launch; subsequent derivations did not change these values significantly.

[6]In Fig. V-8, a 2.50 δ ellipse is shown for convenience.

2. Midcourse maneuver execution phase. After a specific aiming point had been arrived at by the process described above, and after careful verification that none of the constraints was violated, the final phase of the maneuver planning was to convert the aiming-point parameters into spacecraft maneuver turn and motor-burn commands, then to transmit these commands to the spacecraft, and finally to initiate the midcourse maneuver at the appropriate time using a DC-V27 command.[7]

Conversion of the aiming-point parameters into spacecraft commands was performed by first comparing the pre-midcourse trajectory to the desired aiming point, then drawing a vector from the premidcourse trajectory point to the aiming point. This vector defined the magnitude and direction, in the **R** • **T** plane, of the required velocity-change vector ($\Delta\mathbf{V}$). This vector, modified by the desired arrival-time correction of 14:06:41, led to the computation of the $\Delta\mathbf{V}$ at the spacecraft for a prescribed point in the trajectory. Knowing the direction of the desired $\Delta\mathbf{V}$ at the spacecraft, the spacecraft turns in pitch and roll were computed in order to point the rocket motor exhaust nozzle in the $-\Delta\mathbf{V}$ direction. The turn commands were generated by computing the number of degrees, which knowledge of the exact behavior of the gyros at the flight temperature made possible. The burn duration was arrived at by use of the buring time estimation calculation (**BUTEC**) program, which takes into consideration detailed motor-burn phenomena, such as start-and-stop transients, steady-state responses, temperature effects, etc. The detailed sequence used to execute the midcourse maneuver is shown in Table V-4.

In the computation of the final maneuver parameters, certain turn constraints had to be taken into consideration in order to prevent damage to certain spacecraft components or the occurrence of other undesirable effects. The maneuver-turn constraints used for the generation of the *Mariner V* maneuver commands are listed in Table V-5 and shown in Figs. V-9 and V-10, along with the actual earth and sun maneuver loci.

[7]The specific spacecraft parameters used for the *Mariner* Venus 67 midcourse maneuver were:

$|\Delta\mathbf{V}|$ = 16.127 m/s = 17.66-s burn
QC-V1-3 = 6-302-3-0253-1

Pitch turn = +55.267 deg = 304-s turn (positive polarity)
QC-V1-1 = 6-303-2-6561-1

Roll turn = +70.946 deg = +380-s turn (positive polarity)
QC-V1-2 = 6-300-1-2035-1

Table V-4. *Mariner V* planned midcourse sequence of events, including UV-photometer rolls

Function	Ground time, GMT	Spacecraft time, GMT
Zero static phase error	Day 170 19:00	
Apply command modulation	19:18	
Normalize command	19:38	
QC-VI-1 (6-303-2-6561-1)	20:18	
QC-VI-2 (6-300-1-2035-1)	20:23	
QC-VI-3 (6-302-3-0253-1)	20:28	
DC-V29 (6120)	20:38	
DC-V14 (6240)	20:48	
DC-V27 (6470)	21:23:57	21:24:39
Pitch turn start		22:24:06
Pitch turn stop		22:28:10
Roll turn start		22:46:06
Roll turn stop		22:52:26
Motor burn start		23:08:06
Motor burn stop		23:08:23.6
Start reacquisition		23:14:06
Sun reacquired		Approx 23:19
Canopus reacquired		Approx 23:29
DC-V21 (1) (6720)	Approx 23:38	
Canopus reacquired	Day 171	Approx 00:25
DC-V21 (2) (6720)	Approx 00:26	
Maneuver counter overflow		00:43:06
Canopus reacquired		Approx 01:17
DC-V21 (3) (6720)	Approx 01:20	
Canopus reacquired		Approx 02:10
Gyros off		Approx 02:17
Minimum QC-VI-1 (6-303-2-5777-1)	02:19	
Minimum QC-VI-2 (6-300-1-5777-1)	02:24	
Minimum QC-VI-3 (6-302-3-5777-1) DC-V9 (6632)	02:29	

Table V-5. SPAC midcourse maneuver turn constraints

Division	Constraint
32	The UV-photometer pointing vector and the spacecraft–sun vector must intersect at an angle greater than 5 deg to prevent damage to the UV photometer.
33	1. The spacecraft Z axis–earth angle must be between 90 and 180 deg to maintain downlink communications. 2. The pitch or roll turns must not end in the high-gain antenna interferometer region (prior to APAC, an ellipse with center at 110.7 deg cone, 107.4 deg clock, major-axis slope as shown in Fig. V-10, semi-minor axis = 7.5 deg, semi-major axis = 15 deg; after APAC, centered at 96.4 deg cone, 96.5 deg clock, slope as shown in Fig. V-9).
34	1. The pitch turn must be smaller than 237.6 deg to prevent automatic motor-burn inhibit. 2. The roll turn must be small enough to allow time for the transmission of DC-V13, if required. 3. If the terminator sensor should be activiated, the angles subtended by the sun–earth–spacecraft vectors and the terminator–sensor boresight axis must be greater than 20 deg (the boresight of the terminator sensor is at 110 deg clock). 4. To prevent Canopus-sensor shutter activation, the spacecraft–sun vector should not pass within an area described by 0 ±25 deg clock, 90 ±33 deg cone.
35	None for expected heliocentric distances.[a]
38	The first maneuver motor-burn time must be shorter than 102.36 s.

[a]Pitch-turn temperature constraints become necessary at heliocentric distances smaller than 145×10^6 km.

3. Maneuver-inhibit planning. The design of the *Mariner V* spacecraft included a capability for termination of the midcourse maneuver before rocket-motor ignition by use of a ground command (DC-V13) if an anomaly were to jeopardize the successful execution of the maneuver. When an abort was required, the DC-V13 command caused the AC and pyrotechnics subsystems to disregard the maneuver commands issued by the CC&S. After a DC-V13 command, the CC&S continued counting and issuing its event register and timing telemetry signals to the DE until its maneuver clock was completely counted out and reset itself.

Barring gross failure, a terminated sequence had no real effect because the maneuver could be rescheduled and performed successfully regardless of the number of previous aborts. Thus, the operations philosophy for the midcourse correction phase was determined by the abort capability inherent in the spacecraft design. Based upon knowledge of the design, ground-test experience, and previous mission flight experience, it was fully expected that the maneuver would be executed successfully without deviation from the predetermined plan. An anomaly noted during the maneuver sequence had a potentially harmful effect; therefore, it was required that the maneuver be terminated and that the anomaly be evaluated to determine what corrective action, if any, should be taken.

Consideration was also given to ensure that the spacecraft entered the midcourse-maneuver sequence in the proper state. Subsystem and system testing before launch had demonstrated the possibility of logic-state changes aboard the spacecraft because of electrical-transient effects or shock and vibration effects upon relays. It was determined, therefore, that reliance upon nonverifiable,

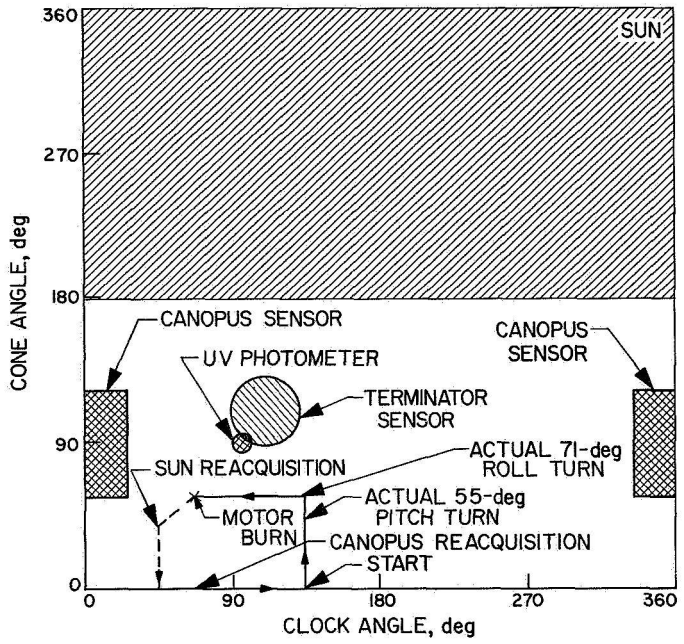


Fig. V-9. Sun constraint regions

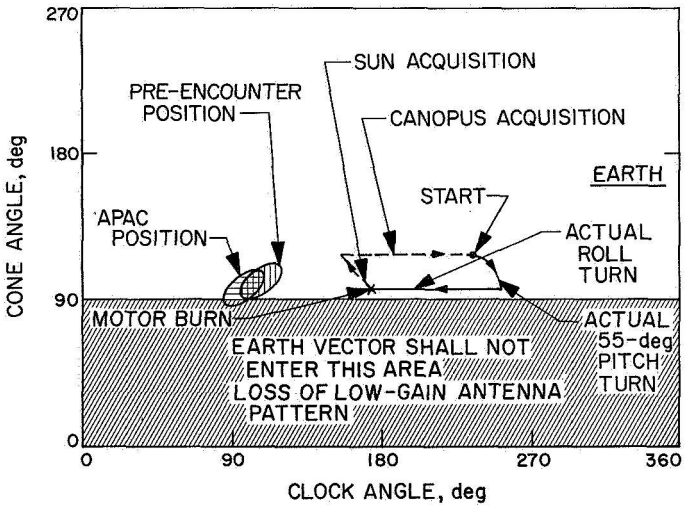


Fig. V-10. Earth constraint regions

present logic states was unnecessary. Thus, following the precedent set during the *Mariner IV* maneuver, two direct commands were added to the midcourse-maneuver sequence to ensure that the spacecraft would be in the proper state to perform the midcourse maneuver.

The first command, DC-V29, set the relays in each independent half of the pyrotechnics subsystem, arming the first set of motor-burn, start-and-stop squibs. The desirability of this is obvious if the results are considered. For example, it would be disastrous if a maneuver were to be performed on the first-burn stop squibs but with the second-burn start squibs. This is a distinct possibility if relay contacts are subject to movement as a result of shock during boost.

It was also thought advisable to ensure the arming of the midcourse maneuver by transmission of DC-V14 (the command to revoke DC-V13). Both commands were ultimately adopted as a part of the normal midcourse-command sequence, as shown in Table V-4.

Table V-6. SPAC criteria for use of DC-V13

Division	Criteria
29	1. Loss of real-time spacecraft data for a period considered long enough to prevent monitoring of the critical phases of the maneuver 2. Loss of communications within SPAC for a period long enough to prevent clear understanding of the state of the spacecraft 3 Loss of communications with DSS for an extended period or at frequent and unpredictable intervals during the maneuver 4. Malfunctioning of the on-line read–write–verify (RWV) at a critical time during the maneuver, necessitating transmission of a DC-V13 immediately after the standby RWV acquires command lock
33	1. Abnormal RF behavior that jeopardizes the ability to analyze spacecraft performance 2. Unexpected deck skips 3. Loss of telemetry data or inability to decommutate the data-encoder output 4. Improper event-register readings 5. Failure to switch data modes at appropriate times 6. RF signal-strength variations that do not agree with programmed spacecraft turns
34	1. Failure of gyros to turn on 2. Abnormal gyro behavior 3. Loss of Canopus before start of the spacecraft turns 4. Pitch or roll turn does not start 5. Pitch or roll turn has incorrect polarity 6. Pitch or roll turn does not stop 7. Pitch or roll turn does not have proper duration 8. Spacecraft does not start celestial-reference reacquisition 9. Power measurements are not as expected 10. CC&S timing of events is not within 1 DN of expected value
35	None
38	1. Fuel pressure not between 150 and 400 psia 2. Oxidizer pressure not between 300 and 450 psia 3. Fuel temperature not between 40 and 125°F 4. N_2 pressure not within tolerance at 800 psia (for 16 m/s)

In the process of midcourse-maneuver preparations, a list of criteria for the transmission of DC-V13 was generated, as shown in Table V-6. This list was compiled by the SPAC director, with inputs from the supporting divisions, and was approved by the SFOD and the project manager. Each division listed in Table V-6 was responsible to the SPAC director for ascertaining that its criteria were satisfied.

G. Encounter Planning

1. Description. The encounter sequence evolved as a joint effort of SPAC and VEPWG. The basic planning guideline was to establish an encounter sequence that would maximize the probability of mission success.

A description of the encounter-related ground commands is given for reference in Table V-7. These commands would be available for both primary and backup roles in the encounter sequence.

a. Initial conditions. The *Mariner V* spacecraft configuration prior to DC-V25, which is the start of the active encounter phase, is presented in Table V-8. Here the spacecraft would be in the cruise state, with the exception of the roll-control mode. The AC subsystem would be commanded from the normal roll-control mode to the DC-V15 mode approximately 10 days before encounter. No other pre-encounter conditioning was envisioned.

b. Encounter alternatives. Several alternatives that would have changed the spacecraft configuration at the start of (or during) the encounter phase are discussed herein. Each alternative spacecraft mode had to be carefully examined to ascertain whether the mission value obtained outweighed the risk involved.

Receive via high-gain antenna. During the final part of the cruise mode, the spacecraft received commands via the low-gain antenna and transmitted data to earth via the high-gain antenna. The capability both to receive commands and transmit data via the spacecraft high-gain antenna would be available using ground command DC-V11. The advantages and disadvantages of receiving on the high-gain antenna during the encounter phase are presented in Table V-9.

Careful analysis by the telecommunications group showed that the interferometer pattern would reinforce the uplink signal at encounter. This information, added to nominal telecommunication subsystem performance, gave SPAC a high degree of confidence that command capability would exist at encounter by means of the low-gain antenna, using a DSIF 10-kHz transmitter, as long as Canopus was acquired.

The time gained in reacquiring two-way lock at exit occultation using the high-gain antenna would be only a few seconds. This gain was judged to be of low value compared to the disadvantages of receiving via the high-gain antenna.

Table V-7. Ground commands related to the encounter sequence

Command	Function
DC-V2	(1) Can be used to turn science 2.4-kHz power on. DAS encounter logic is reset at power on. (2) Can be used to switch DE from data mode 1, 3, or 4 to data mode 2.
DC-V4	(1) Can be used to switch DE from data mode 1, 2, or 3 to data mode 4. (2) Backup to MT-9. (3) Can be used to stop tape-record mode.
DC-V5	Data-rate toggle command. Can be used to fast-count DAS clock A at 33⅓ bits/s if clock is running late. Resume normal count rate at 8⅓ bits/s by sending second DC-V5.
DC-V9	Ranging toggle command. Used to turn ranging channel on or off.
DC-V16	(1) Sets up DAS frame counter (clock A) to serve as backup source for clock B. Also provides toggle capability for enabling/disabling clock A outputs. (2) Resets frame count to zero.
DC-V22	Backup for switching high-gain antenna to position 2. Could not be used before encounter without jeopardizing enter-occulation data.
DC-V24	(1) Can be used to switch DE to mode 3. (2) Serves as a toggle function for enabling/disabling DAS clock B. (3) Backup for MT-8.
DC-V25	(1) Can be used to turn tape recorder 2.4-kHz power on. (2) Turns science power on. (3) Energizes terminator sensor. (4) Turns battery charger off. (5) Backup to MT-7. (6) Overrides gyros-on/main-booster-failed logic.
DC-V26	(1) Turns science power off. Can be used with DC-V2 or DC-V25 to reset DAS encounter logic via power-on-reset function. (2) Turns battery charger off.
DC-V28	(1) Provides only means of turning tape recorder 2.4-kHz power off. (2) Can be used to toggle battery charger on or off.

Table V-8. Spacecraft configuration before DC-V25

Subsystem	Status
Radio	Exciter B Power amplifier A (TWT) Transmit via high-gain antenna Receive via low-gain antenna High-gain antenna in position 1 Ranging off
Command	In lock
Power	Main booster on Maneuver booster off Battery charger off Boost mode enabled Science override off 620 W available from solar panels
Central computer and sequencer	L-1, L-2, and L-3 set MT-1, MT-2, MT-3, MT-4, MT-5, and MT-6 set MT-7, MT-8, and MT-9 have not occurred
Data encoder	Data mode 2 Data rate at 8⅓ bits/s Analog-to-digital converter–PNG B
Attitude control	Gyros off Canopus gate logic overridden by DC-V15 Canopus sensor cone angle at MT-4 position Planet sensor excitation off Terminator sensor excitation off
Pyrotechnics	All pyro devices except APAC squibs and second motor-burn squibs expended
Post-injection propulsion	Second motor-burn capability unarmed
Tape recorder	2.4-kHz off
Data automation	2.4-kHz power on Clock B not counting Clock A encounter outputs inhibited
Trapped radiation detector	Returning useful data
Plasma probe	High-voltage inhibit off Returning useful data Cruise mode data format
Magnetometer	Returning useful data
UV photometer	Normal calibration sequence Returning useful data
Dual-frequency receiver	Stanford transmitter off Returning useful housekeeping data

Laboratory tests and flight tests showed that ranging and command modulation could be applied simultaneously in the receive low-gain mode without adverse effects upon the command subsystem. The restriction to be placed upon this mode of operation was that total uplink-carrier suppression could not exceed 10 dB.

Table V-9. Receive via high-gain antenna

Advantages	Disadvantages
Higher signal level for receiving commands.	May lose command lock temporarily at switchover.
Eliminates interferometer pattern.	If roll control lost while receiving on the high-gain antenna, command capability could be lost for a maximum of 133 h.
Increases tracking rate capability for spacecraft receiver.	DC-V11 mode has not been previously tried in flight.
Obtains faster reacquisition of two-way lock upon emerging from occultation.	
Could have ranging and commanding capability simultaneously.	

Nominal carrier suppression caused by command modulation alone would be 3.2 dB.

Results of the decision to remain in the receive low-gain antenna mode became more evident once DC-V15 was chosen as the encounter roll-control mode. Receiving via the high-gain antenna in the DC-V15 mode was not a compatible choice. If roll control were lost, and uplink lock could not be obtained, it could take as long as 133 h (2 cyclics) before onboard logic would switch the radio subsystem back to the receive low-gain mode, and allow receipt of ground commands. This duration could be catastrophic, considering that the science data of highest interest would occur in a period estimated to be less than 2 h. The receive low-gain mode was used successfully during encounter with *Mariner IV*.

Alternate methods of roll control. The available modes of roll control at encounter were the normal mode, the DC-V18 mode, and the DC-V15 mode. In the normal mode, gyros would come on, and the spacecraft would start a ccw roll search if Canopus acquisition were lost. In the DC-V18 mode, the gyros would be turned on, the Canopus sensor turned off, and the roll axis placed on inertial control. If the AC subsystem were in the DC-V15 mode, the gyros would be inhibited from coming on if Canopus or sun acquisition were lost and the Canopus sensor low-brightness gate were disabled. The advantages and disadvantages of each roll control mode are listed in Table V-10.

Three items that could affect the AC subsystem at encounter were Venus straylight, dust particles, and APAC. The predicted trajectory aiming point was away

Table V-10. Roll-control modes for encounter

Roll mode	Advantages	Disadvantages
Normal (roll axis on optical control)	If Canopus acquisition were lost in cw direction, spacecraft would search back into Canopus immediately. Predicted roll motion caused by APAC was in cw direction No ground commands would be required to stay in this mode No problems have been experienced in this mode since launch Roll-position telemetry is available	If Canopus acquisition were lost in ccw direction, spacecraft will search away from Canopus at 7 deg/min. In worst case, loss of enter or exit occultation would occur during reacquisition
DC-V18 (roll axis on gyro control)	Eliminates straylight and dust-particle problems because Canopus sensor is off Prevents potential damage to Canopus sensor because bright objects such as Venus could not be acquired with sensor off	Gyros have been dormant since midcourse maneuver. A small chance that a malfunction could jeopardize mission Loss of roll-position telemetry in this mode. SPAC would have to use received signal strength to estimate and correct antenna clock because of gyro drift. Uncertainty in this method may degrade return of certain science data No in-flight experience in this mode with *Mariner V* More chances for human error because of type of coverage required during inertial mode
DC-V15	Spacecraft will not go into roll search if Canopus acquisition is lost, enhancing chances of obtaining occultation data Preventing gyros from coming on assures that DC-V25 can be used without danger Roll-position telemetry available This mode was used successfully for approximately 3 yr on *Mariner IV*	If Canopus acquisition is lost after closest approach in ccw direction, straylight from Venus may provide an error signal that would roll spacecraft towards Venus If DC-V15 cannot be reset and Canopus acquisition is lost, reacquisition of Canopus would be unlikely. This problem is in realm of double failures

from the Canopus sensor straylight-constraint area. Thus, straylight from Venus did not appear to be a problem; however, should Canopus acquisition be lost and the spacecraft start a roll search, Venus could be acquired. The critical period was calculated to be the first hour following encounter, when the limb of the planet was within the Canopus FOV during search. Acquiring Venus would degrade the Canopus sensor.

The occurrence of APAC was recognized as a possible source of dust particles. If one of these particles moved slowly enough through the Canopus sensor FOV, Canopus acquisition would be lost. To lose Canopus acquisition, the particle must be moving on the order of 0.5 deg/s in clock angle, and remain in the FOV long enough to roll the spacecraft beyond the FOV of the sensor. Canopus acquisition could be maintained as long as the star remained within about ± 3.5 deg of the boresite axis of the sensor. The probability of losing Canopus acquisition because of a dust particle was thought to be very small.

An analysis of the APAC effect upon spacecraft attitude was conducted by the AC group. The results indicated that the transient imparted upon the spacecraft as the high-gain antenna changed position was within the dynamic control range of the AC subsystem. There appeared to be no danger of losing celestial references. The predicted time for all position transients to settle back within the control deadband was 3–4 min.

The chances of mission success appeared to be enhanced by having the DC-V15 mode in effect, preventing the spacecraft from entering roll search during the period when stable roll orientation would be vital, especially as the risk associated with using DC-V15 would be nominal. For these reasons, DC-V15 was the recommended roll-control mode for encounter. Sending this command 10 days before encounter would allow sufficient time to gain operational experience in the DC-V15 mode.

One-way vs two-way entry. The ground transmitter was to be turned off approximately 1 h before *Mariner V* entered occultation. This would place the spacecraft in a one-way (noncoherent) tracking mode. In the noncoherent mode, the downlink carrier signal would be generated by an auxiliary oscillator (AO) in the spacecraft radio–exciter module. The radio receiver voltage-controlled oscillator (VCO) would supply the downlink carrier signal in the two-way (coherent) tracking configuration.

The principal disadvantages of entering occultation in the two-way mode would be as follows:

(1) Loss of uplink lock would degrade the results of the occultation experiment. During switchover from

VCO to AO, the VCO would become free-running and be driven by noise for about 20 s. Data derived from the downlink carrier during this interval would be meaningless.

(2) After switchover, the AO frequency would be changing rapidly during the initial stages of the temperature-warmup transient. Analysis of the data obtained during this interval would be extremely difficult.

(3) In the two-way tracking mode, the spacecraft downlink carrier frequency would be a direct multiple of the uplink carrier frequency; therefore, the effects of the Venusian atmosphere would enter twice. As a result of the frequency deviation in the downlink carrier, frequency would be doubled, necessitating a twofold increase in the receiver bandwidth required to track the signal.

(4) The closed-loop receivers would lose lock earlier for the same signal strength because of the doubled frequency rate. The ability to capture the surface ray for denser atmospheres would decrease.

The advantages of remaining in the two-way configuration as the spacecraft entered occultation were as follows:

(1) Greater precision of upper-atmosphere measurements could be attained because the VCO frequency is more stable than that of the AO.

(2) Ambiguous interpretation of small frequency variations in the lower-atmosphere measurements would be eliminated.

(3) Command capability could be maintained for the maximum period.

The principal investigator for the S-band occultation experiment felt that the advantages of switching to the one-way tracking configuration outweighed the advantages of remaining in the two-way configuration.

Exciter switch. The spacecraft design included two identical exciters for block redundancy in the radio subsystem, with only one exciter energized at any given time. A proposal was made to use DC-V8 to switch to exciter A in order to examine its characteristics as a potential exciter for entering occultation. Until this time, the spacecraft had retained the launch exciter (exciter B). The risk associated with this exercise appeared to be low, in that a double failure was required (exciter A inoperative and logic not available to switch back to exciter B). The gain from this exercise, which would be a possible refinement of upper-atmosphere measurements, was considered low. The decision made by the project manager was to switch exciters only if a substantial degradation in exciter B occurred.

2. *Encounter sequence development.*

a. Encounter sequence initiation. Two methods were available for initiating the encounter sequence: Ground command DC-V25 or CC&S command MT-7. After detailed study, DC-V25 was chosen as the best method of initiating the encounter sequence, and MT-7 served as the backup command.

The primary function of DC-V25 would be to activate encounter-related hardware normally dormant during the cruise phase of the mission; namely, the tape recorder and the terminator sensor. At the same time, excitation would be applied to the DAS APAC-command circuit. Also, special logic in the power subsystem protecting the maneuver booster would be disabled. In the absence of DC-V25, this logic would turn the science 2.4-kHz power off if the gyros came on during a main-booster failure.

The nominal spacecraft events for DC-V25 sent before MT-7, and for DC-V25 sent after MT-7, are listed for comparison in Table V-11. The decision to send DC-V25 before MT-7 was supported by the arguments presented below.

Confidence that the DC-V25 override function had actually occurred would be increased. The DE counter 4 event (the sole telemetry change for DC-V25 sent after MT-7) would indicate only that a 9-bit command was received at the spacecraft, of which the first three bits were correct. There would be no assurance that the remaining six bits used to decode the command were proper. A command having a fictitious address, or one

Table V-11. Effects of DC-V25

Command sequence	Spacecraft event
DC-V25 before MT-7	Tape recorder 2.4-kHz power on. Terminator sensor excitation on. Arm DAS APAC circuit. Override gyros-on/failed-main-booster logic (not seen in telemetry). Counter 4 event.
DC-V25 after MT-7	Override gyros-on/failed-main-booster logic (not seen in telemetry). Counter 4 event.

that was legitimate but had no effect on the state of the spacecraft, would give the same indication. By sending DC-V25 before MT-7, several power readings would change as a result of turning the tape recorder on. This additional information would show that the command subsystem had correctly received and decoded DC-V25. This knowledge would eliminate a major portion of the command subsystem as a series element in establishing a confidence factor that the DC-V25 override function was, indeed, in effect. Absolute certainty that the override function was activated was not possible because of telemetry limitations.

The knowledge attained by observing the results of DC-V25 could contribute strongly to future SPAC action. The additional reaction time gained would be about 2½ h.

Additional time would be available for conducting the AO test immediately after MT-7 was sent.

The logic in 4A8, which turns science power off if the gyros come on with the main booster failed, provides protection against over-stressing the maneuver booster. This logic could be overridden beforehand only by DC-V25—a fact that could be an argument for not sending DC-V25 at all.

A special test, which involved failing the main booster with DC-V15 and DC-V25 in effect, was conducted by the test team, who used the flight-support spacecraft (M67-1). The results were: (1) DC-V25 remained in effect; (2) DC-V15 was removed; (3) the DAS logic was reset to the cruise state, and the frame counter was reset to zero; (4) the tape recorder issued an EOT command; and (5) Canopus lock was lost, causing a roll search to be initiated. The test was repeated four times, with the same results. These results demonstrated a single failure mode in which gyros come on with the main booster failed. In this mode, the maneuver booster becomes subject to overstress because of the loads it must carry. At this point, failure of the maneuver booster would be catastrophic to the mission.

To reduce the chances of overstressing the maneuver booster, a special set of ground rules was established for transmitting DC-V25. The power subsystem personnel felt that DC-V25 could safely be transmitted under the following conditions: (1) Bay 8 temperature was less than 100°F, (2) the primary system voltage was higher than 40 V, and (3) the total load to be supported by the maneuver booster if the main booster failed did not exceed 155 W. The predictions for encounter were that Bay 8 temperature would be about 85°F, the power switch and logic voltage would be higher than 43 V, and the maximum possible load for the maneuver booster would be 145 W. The latter figure included gyros on, science power on, and all gas jets firing. Based upon these encounter predictions, it appeared that DC-V25 could safely be used.

Having DC-V25 in effect would prevent loss of scientific data in the following way: If a failure occurred in the 4A8 logic that produced a false gyros-on/failed-main-booster indication, science power would be turned off. If this failure occurred in close proximity to the planet, scientific returns for this mission could be greatly reduced.

b. Auxiliary oscillator test. The radio mode chosen for entering occultation was the noncoherent mode (AUX OSC). For this mode, it was highly desirable to check the characteristics of the auxiliary oscillator shortly before committing it to the sequence. If the AO was found to be unacceptable, the backup unit would be commanded on by DC-V8. Factors related to selecting a time in the encounter sequence to conduct the AUX OSC test are described below.

The total test period could extend beyond 2 h. The average AUX OSC warmup time was about 1 h. This information was obtained by conducting AUX OSC warmup tests once a week for several consecutive weeks before encounter. At the end of the warmup period, if AO performance was questionable, a DC-V8 would be sent to switch oscillators. An additional hour to test the backup unit would then be required. As the backup unit had not been used in flight, its stability characteristics could be worse than those of the AO. In this case, another DC-V8 would be sent to switch back to the original configuration. For each DC-V8, time would be required to go two-way and to lock up the command subsystem.

The nature of the AUX OSC test required that it be conducted in a continuous manner until completed.

If an emergency situation requiring ground-command action occurred during the AUX OSC test, reaction time would be lost in locking up the command loop.

The time chosen to make a last check of the AO before committing it to encounter was approximately 13 h before closest approach. This placed the start of the test 4 h before the next scheduled command (DC-V9) and immediately following verification of MT-7. At this time, the encounter sequence would be relatively inactive, and

emergency-command situations were rather unlikely. Also, there would be ample time to switch to the backup oscillator, if necessary.

c. Near-planet ranging. Ranging during the first 6 million miles of the mission was accomplished from any of the assigned tracking stations, using standard DSIF equipment. Ranging beyond that distance required special DSIF equipment available only at DSS 14. Thus, near-Venus ranging would be constrained to the DSS 14 encounter pass, which lasted about 11 h, with encounter nearly centered in the pass.

For optimum ranging return, it was desirable to range over as much of the DSS 14 pass as possible. The data of highest value for the celestial mechanics experiment would occur just before *Mariner V* entered occultation and immediately following exit occultation. These data would contribute significantly to a better determination of the astronomical unit, the mass of the planet, and the earth–Venus ephemeris.

Decisions related to integrating ranging into the encounter sequence were: (1) The time that DC-V9 should be transmitted to turn on the ranging channel; (2) the time to apply ranging modulation; (3) whether commands should be sent with ranging modulation present; and (4) whether ranging would degrade command-subsystem performance. These decisions had to be made before committing ranging to the encounter sequence.

The first step in the ranging procedure would be to turn on the ranging electronics. This function could be accomplished only by ground command DC-V9, which was a toggle-type command; i.e., if it were sent a second time, it would turn ranging off.

During system testing, it was found that the spacecraft receiver was adversely affected when ranging was turned on by DC-V9 at low signal levels (uplink). As a result, the command subsystem dropped lock. This potential operational problem led SPAC to conduct in-flight DC-V9 tests after the midcourse maneuver. For these tests, uplink signal strength was reduced to the predicted encounter level, and DC-V9 was then sent to turn ranging on. The results showed the command subsystem to be dropping lock. This information indicated the importance of not having the command subsystem enter into the false-lock state following DC-V9, as, in this state, the command subsystem could not process commands. This meant that enough time would have to be allowed between DC-V9 and the next command to remedy false lock if it occurred. After verifying false lock, the required action would be to turn command modulation off for several minutes, and then reapply it. The expected lockup time for the command loop at encounter was 6–12 min plus the two-way light time. An absolute minimum of 30 min would be needed between DC-V9 and the next command to ensure sufficient reaction time to false lock. The recommended DC-V9 time to turn ranging on was 08:50:00 GMT, which placed the command about 2 h before both the next command (DC-V24) and the DSS 14 rise.

At the request of VEPWG, laboratory tests were conducted to determine the effect of both command and ranging modulation on simultaneously upon command-subsystem performance. Based upon these test results and other considerations, the following criteria related to ranging and commanding were established:

(1) Total uplink carrier suppression could not exceed 10.0 dBmW. As command modulation added 3.2-dBmW carrier suppression, this allowed 6.8 dBmW for ranging modulation.

(2) Commands would not be sent with ranging modulation on. The amount of ranging data lost because of this constraint was not enough to offset potential problems related to losing command lock.

The time selected for applying ranging modulation was 12:44:00 GMT, which allowed 1 h in which to complete the scheduled two-way station transfer (DSS 62 to DSS 14), to verify spacecraft static phase error (SPE), and to lock up the command loop. Ranging modulation would be turned off for DC-V16 and DC-V9 per criterion (2), above. Ranging modulation would remain off following DC-V9 until after encounter because the spacecraft would enter occultation in the one-way tracking mode. After exit occultation, and after the ranging electronics were turned back on by DC-V9, ranging modulation would be reapplied as soon as possible. With this approach, another 2½ h of ranging could be obtained after exit occultation and before the DSS 14 pass ended.

An investigation of potential ranging failure modes that would be catastrophic to the mission revealed the following: If one of the decoupling filter capacitors in the 9.56-MHz isolation amplifier short-circuited to ground, a +14-V power supply would be reduced, making the radio receiver inoperative. This would abort further command and two-way tracking capability for the remainder of the mission. Because of the ranging success during the cruise phase, and also because the tendency

for this type of filter capacitor to fail is very slight (based upon *Mariner IV* flight experience), this failure mode was thought to be of low probability. All other failure modes resulting in adverse effects upon the mission would require double or triple failures.

d. Science subsystem conditioning. Two methods would be available to condition the science subsystem for the encounter phase: Ground command DC-V24 or CC&S command MT-8. Because of the advantages to be gained, DC-V24 was selected as the prime command, with MT-8 as the backup mode.

The expected spacecraft events for DC-V24 sent before MT-8, and for DC-V24 sent after MT-8, are listed in Table V-12.

The decision to preempt MT-8 was twofold: (1) Verification of DC-V24, if it came after MT-8, would not be possible in real time. Data encoder event-channel readings were not displayed in data mode 3; therefore, the counter 4 event would not be available in the telemetry. The DAS status bit assigned jointly to MT-8 and DC-V24 would already be *set* by MT-8, and would not change state for the first DC-V24. The remaining spacecraft functions available from DC-V24 would have already occurred as a result of MT-8. (2) The DC-V24 command served as a toggle function for enabling and disabling clock B. In the enabled state, clock B would begin counting upon receipt of the PSO. In the alternate state, clock B would be prohibited from starting upon receipt of PSO, or would be stopped if PSO had occurred. The latter function would be used, for example, if PSO occurred early, or if a failure caused clock B to count faster than normal. The clock B disable function was activated when an even number of DC-V24 commands were received by the spacecraft. By initiating the data mode 3 period with DC-V24, the spacecraft logic would then be set up for a faster or slower response for clock B inhibit because only one more DC-V24 would be required, as opposed to two for the MT-8 approach. Knowing the exact state of the DC-V24 toggle logic would be of paramount value in making operational decisions involving clock B. Specifically, verification of the first DC-V24 would be essential. As pointed out above, such verification would be available only if DC-V24 were sent before MT-8.

The recommended transmission time for DC-V24 was 10:50:00 GMT (about 27 min before MT-8).

e. Initiation of encounter backup clock. The data-storage sequence could be controlled by outputs from either clock A or clock B located in the DAS. Two clocks were provided for redundancy. Clock B, which was dormant during the cruise phase of the mission, would start counting upon occurrence of the PSO; clock A, which in reality was the frame counter during cruise, required ground command DC-V16. Command DC-V16 would reset the frame counter to zero and simultaneously enable the encounter output logic of the timer. The fixed outputs of clock A and clock B, with corresponding frame numbers are listed in Table V-13.

Table V-12. Effects of DC-V24

Command sequence	Spacecraft event
DC-V24 before MT-8	Data encoder switches to data mode 3. Excitation applied to planet sensor. Plasma probe switches to mode 3 format. Remove inhibit from clock B and set up toggle logic. Set up clock A for DC-V16. Counter 4 event (not seen in data). DAS status bit 17 changes state.
DC-V24 after MT-8	Counter 4 event (not seen in data). Set up clock B toggle logic (not seen in data).

Table V-13. Outputs from DAS encounter clocks

Clock function	Clock A frames from DC-V16	Clock B frames from planet sensor output
Issue "start tape" signals	145	1[a]
Begin track 1 data	145	1[a]
Inhibit UV-photometer calibrate sequence	145	1[a]
Begin track 2 data	160	16
Antenna pointing angle change	224	—
Stop track 2 data	288	144
Stop sending "start tape" signals	288	144
Switch to data mode 2	304	160
Remove plasma probe mode 3	304	160
Inhibit clock A outputs	304	160
Remove planet sensor excitation	304	160
Remove UV-photometer calibrate inhibit	304	160
Issue "stop tape" signal	304	160
Stop clock B	304	160
Stop track 1 data	304	160

[a]These functions are initiated by PSO, not by clock B.

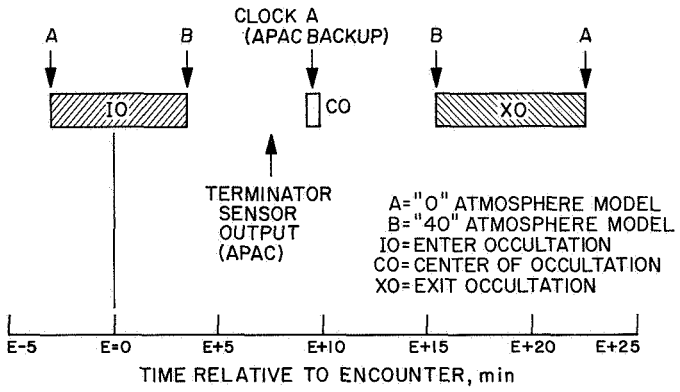


Fig. V-11. Occultation time dispersions

An item to be resolved by VEPWG was to establish the criteria for selecting the DC-V16 transmission time. As can be seen from Table V-12, clock A outputs fall into two categories: Clock B backups and the APAC backup. Factoring clock A outputs in this manner reveals two different criteria for choosing a DC-V16 transmission time; namely, DC-V16 could be sent to have the clock A backup functions coincide with or occur at a desired offset relative to the clock B functions, or the APAC backup could occur at a unique time relative to the center of occultation.

It was decided to transmit DC-V16 so that the clock A APAC function would occur at the center of the occultation dispersion block, as shown in Fig. V-11. The terminator sensor would remain the primary command source for APAC, and would occur about 2 min earlier. If the terminator sensor failed to give an output, clock A would then provide the APAC command at a time that maximized the chances of obtaining both the enter and exit surface rays. Based upon available trajectory information and the APAC constraint, DC-V16 would be transmitted approximately 3 h before encounter. This time would also establish clock A as a backup for clock B, with clock A lagging 5 to 10 min. This lag would allow a successful clock A record session if clock B failed.

Several weeks before encounter, a DFR measurement was requested. This was to occur at a unique time before encounter. Specifically, science word 21 was requested to occur in an even-numbered frame as close to (but no later than) 195 s before closest approach. The attempt would be to capture the last reading of the DFR modulation-phase signal just before the DFR dropped lock. This measurement enters the DC-V16 discussion because DC-V16 resets the frame counter to zero and establishes the time that the even-numbered frames will occur relative to encounter. A review of the DAS logic confirmed that, at most, the DFR constraint would shift DC-V16 transmission time by one frame (50.4 s). That this would, in turn, shift the DAS APAC command by a similar amount was felt to be of insignificant impact. Upon this basis, the final criteria agreed upon for establishing the DC-V16 transmission time were twofold:

(1) Clock A was to issue the APAC backup command within 50.4 s (one frame) of the center of occultation time predicted by the FPAC director.

(2) Word 21 in the real-time science frame would occur in an even-numbered frame as close as possible (but no later than) E−3.25 min.

Calculation of the DC-V16 transmission time deserved special attention as it established a time-critical, ground-command situation, as well as being a real-time computation. Upon this basis, algorithms were developed independently by SPAC and SSAC personnel for computing the DC-V16 transmission time. These algorithms were cross-checked many times, then tested in a simulated SPAC encounter test. The result showed that the algorithms could be manipulated swiftly and with a high degree of confidence.

A subtle point related to DAS mechanization was brought to light in developing the algorithms for DC-V16. The total time for clock A to count out a given output, such as the APAC command, could vary from 0 to 50.4 s, depending upon the time that DC-V16 arrived at the spacecraft relative to the science-gate pulse. The DAS increments the frame count at each science-gate pulse that is received from the data encoder. Upon receipt of DC-V16, the frame counter is zeroed, then advanced to a one-count (F/C = 1) at the next science-gate pulse. The length of the first frame can be from 0 to 50.4 s, depending upon where DC-V16 arrived with respect to the science-gate pulse. All remaining frames would be normal. The ambiguity in clock A count time was eliminated by using the telemetry to the science-gate times on the spacecraft. The arrival time of DC-V16 at the spacecraft was calculated by adding one-way light time and read–write–verify delay to the transmission time. Comparing the arrival time with the predicted science-gate times, the time of F/C−1 could be established within 1 s. Using F/C−1 as the reference point instead of F/C−0 would give 1-s resolution of the predicted clock A APAC time.

f. Planet acquisition. Acquisition of the planet would occur when the limb of Venus intersected the FOV of the planet sensor. This trajectory-dependent relationship

would be the reference point for initiating the data-storage sequence. The predicted time for the PSO was 68 min before encounter. The uncertainty associated with this time during the early encounter-planning stage was ±6 min.

The PSO uncertainty would decrease as the spacecraft neared the planet because the trajectory would become more accurately known from the additional tracking and ranging data. On the day of encounter, the PSO uncertainty would be about ±1 min, of which only a few seconds would be because of trajectory uncertainty. The primary contributors at that time would be uncertainty as to the brightness of the planet, the threshold of the planet sensor, and the AC limit cycle of the spacecraft.

Normal spacecraft response for the PSO was as follows:

(1) Clock B would start counting out the record sequence.

(2) DAS would begin issuing "start tape" signals to the tape recorder on 50.4-s centers.

(3) The tape recorder would begin recording data on track 1.

(4) The UV-photometer calibrate signal from DAS would be inhibited.

The latter three functions were not decodes of clock B; therefore, they could occur independently of clock B starting. Clock A would provide the backup mode for PSO. In the absence of PSO, clock A would start the tape recorder, inhibit the UV-photometer calibrate signal, and issue all of the commands normally available from clock B. Clock A would not start clock B. Under normal conditions, clock A would be counting in its encounter mode 2 h before the occurrence of PSO. This would allow sufficient time to justify complete confidence that the first clock A decode would be available at the expected time.

The nominal record pattern for both track 1 and track 2 would be as shown in Fig. V-12. The tape recorder would begin recording data on track 1 upon receipt of the DAS "start tape" command triggered by PSO. Clock B would initiate the recordings of track 2 data 12.6 min later. The track 2 record interval, which was 107.5 min, would be terminated by clock B. The track 1 record interval would end at the EOT command, and would be 127 min long. The DAS status bits would be available for acknowledging the presence or absence of both track 1 and track 2 data. Clock A would back up both the clock B and EOT functions.

A discussion of problems associated with an early PSO and the required corrective action is given in Subsection G-4-a, below.

g. Occultation. Based upon the computed trajectory, the spacecraft would drop RF lock within several minutes of closest approach, the exact time depending upon the atmospheric characteristics of Venus. The predicted occultation period ranged from 11 min for a 40-atm model to 35 min for a 0-atm model. The estimated enter- and exit-occultation times for several model atmospheres

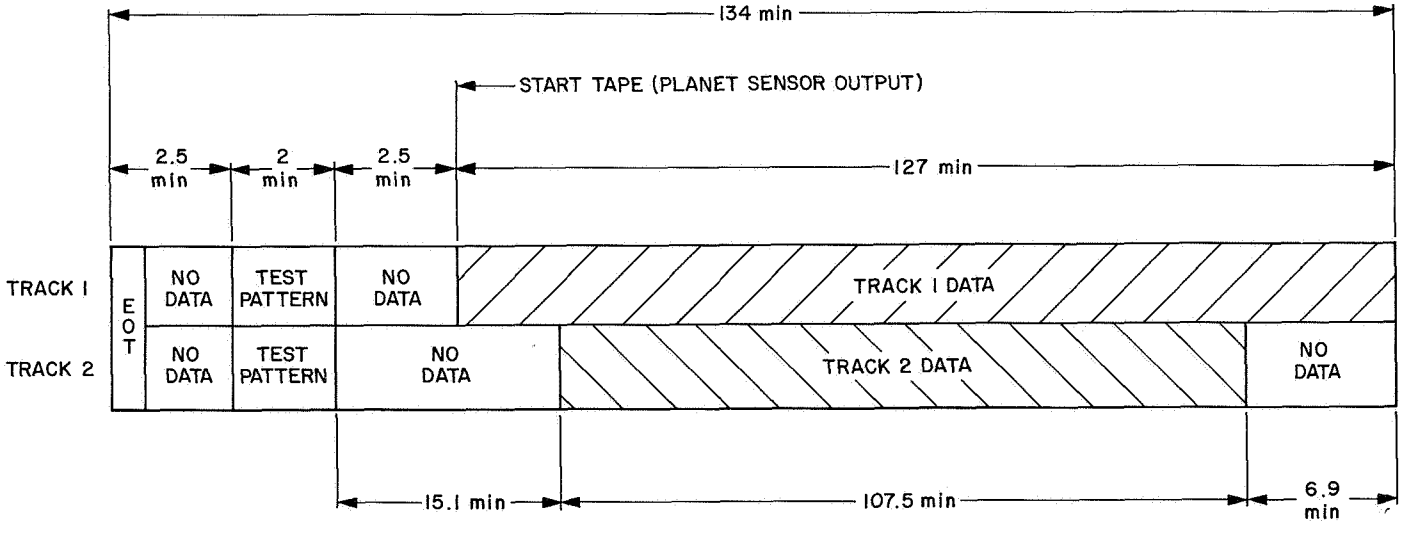


Fig. V-12. Nominal *Mariner V* record pattern

of Venus are listed in Table V-14. It was thought that the surface ray could not be captured for atmosphere models beyond 40 atm.

As the spacecraft entered and exited the occultation region, the S-band spacecraft-to-earth radio signal passed through the atmosphere and ionosphere of Venus. The change in amplitude, phase, and frequency of this signal will provide information from which a better model of the Venusian atmosphere and ionosphere can be constructed.

The spacecraft would enter occultation in one-way lock for the reasons discussed in Subsection G-1-b, above. When *Mariner V* emerged from occultation, two-way lock would be established just before the spacecraft entered the ionosphere. The two-way configuration would provide more accurate tracking data for determining ionospheric information on the sunlit side of Venus, and would also minimize SPAC response time if a command were needed. The two-way lock condition would be maintained until the start of the AUX OSC test scheduled approximately 4 h later.

All four Goldstone stations would be scheduled to support the S-band occultation experiment. The proposed configuration for entering occultation would have DSS 14 as the prime station for both open-loop and closed-loop data by DSS 11 and DSS 12.

The tracking configuration for retrieving the exit-occultation data would be different. Receiver 1 at DSS 11 and DSS 12 would be tuned to the predicted one-way frequency, and would lock up as quickly as possible upon reappearance of the downlink signal. Tuning would be accomplished while the spacecraft was occulted. At the same time, receiver 2 at both stations would be tuned to the predicted two-way frequency for the planned time of two-way acquisition. Also, the DSS 12 transmitter would be turned on in this interval, with the ground transmitter VCO set for the predicted best-lock frequency existing at E+1370 s. In this manner, the spacecraft would be illuminated when it emerged from behind the planet, but would not acquire the uplink signal until it swept into the best-lock frequency at E+1370 s. The DSS 12 transmitter would remain on until the time at which the transfer to DSS 14 would be made. The two-way station transfer was scheduled for 18:17:00 GMT. Before this time, DSS 14 would be in a one-way backup mode, and would be supplying 1-s resolution-doppler data to SFOF via the HSDL.

Table V-14. Predicted occultation times

Model atmosphere	Enter occultation	Exit occultation
0 atm	E−3 min	E+22 min 40 s
30 atm[a]	E+1 min	E+18 min
35 atm[a]	E+2.67 min	E+16 min
40 atm[a]	E+3.5 min	E+15.5 min

[a]These atmosphere models were used for planning. It was recognized that, as the amount of the gases in the actual atmosphere changed from the model, the occultation times could change drastically.

The recommended station configuration would ensure reliable retrieval of the maximum amount of S-band occultation data. In particular, the stations would be in their desired mode before the spacecraft exited occultation. No station adjustments that would change transmitter or receiver characteristics would be necessary. Such adjustments could introduce ambiguity into the data, and (in the worst case) data would be lost. The one-way mode would be maintained while the spacecraft passed through the critical atmosphere region. The two-way mode would be established after this region had been traversed, and in time to capture the ionosphere data. The required change from the one-way to the two-way mode would be at E+1370 s.

h. Record sequence termination. The encounter data-storage sequence would terminate about 1 h after closest approach. The sequence would be terminated by either the EOT foil passing over the EOT sensor or by the "stop tape" signal issued by the DAS. For a nominal sequence, the EOT signal would stop the record sequence 127 min after PSO. Otherwise, clock B would serve as the backup, and issue a "stop tape" command 134.5 min after PSO. For a clock A encounter, the DAS "stop tape" command could come 254.5 min after DC-V16. The clock A and clock B "stop tape" commands were exclusively "ORed" together in the DAS before being sent to the tape recorder.

Not to stop recording at the end of the record sequence would be a failure of serious consequence. Running the tape past the record heads a second time, while in the record mode, would result in a loss of critical data. If data were still being received by the data-track record drivers, re-recording of results and encounter data would be replaced by after-the-fact data. If no data were present at the record-driver inputs, the tape would be erased.

If the tape did not stop, the procedure to follow would be to send a DC-V4 followed by a DC-V2. The DC-V4

command would serve as a backup to the "stop tape" function by placing the tape recorder in its playback mode; the DC-V2 would then command the spacecraft to data mode 2, cancelling out the playback mode. The tape recorder would not return to the record mode following DC-V2. The record-playback relay in the tape recorder would remain in the playback state established by DC-V4.

The scheduled time for applying command modulation, following exit occultation, was 18:41:00 GMT. Round-trip plus command-lockup time would take 21 min in the worst case. Two command-correlation periods of 6 min each was assumed to be the worst case for command-lockup time. Round-trip time was taken as 9 min. At worst case, a command would reach the spacecraft at 19:06:30 GMT. The EOT signal would be due at 13:33:30 GMT. This time relationship would allow the erasure of 33 min of tape if the tape recorder had to be stopped by ground command. The leader at the beginning of the tape was 7 min long on track 1 and 19.6 min long on track 2 (Fig. V-12). In worst case, 26 min of track 1 data and 13.4 min of track 2 data would be lost. Also, the test pattern appearing in the leader would be lost. It was judged that only a small amount (if any) of significant data would be lost for this worst-case termination of the tape recorder sequence.

Additional functions occurring upon termination of the record sequence were the following:

(1) Switch to data mode 2.

(2) Remove planet-sensor excitation.

(3) Remove UV-photometer inhibit.

(4) Remove plasma probe mode 3.

(5) Stop clock B.

(6) Inhibit clock A encounter decodes.

These commands, available from both clock A and clock B, would return the subsystems to their cruise mode. The clock outputs were exclusively "ORed" together in the DAS before being sent to the subsystems.

At the end of the record sequence, if the data encoder failed to switch to data mode 2, the recommended procedure would be to send DC-V2 twice. The second DC-V2 command would be sent only to increase the chances of the command being received. For a normal spacecraft response, the first DC-V2 would change the data mode, and the second DC-V2 would have no effect other than producing a counter 4 event.

i. Playback. Approximately 14 h after encounter, the CC&S would issue the MT-9 command, which automatically switches the data encoder to data mode 4/1. The tape recorder would start playing back the stored data, one track at a time. The data encoder would remain in data mode 4 as long as the tape recorder was reconstructing bit sync from the tape. This would indicate that the tape was so positioned that stored encounter data could be read out by the playback heads. Otherwise, the data encoder would switch to data mode 1, and process only real-time engineering data while the tape playback continued.

The expected time and data-mode profile for playback is given in Fig. V-13. Both data-track combinations are given because either sequence is possible, depending upon the state of the data-track-select logic at turn-on. If track 1 was played back first, the initial 85 s of playback time would be in data mode 4, and would correspond to the last 10.6 s of recorded data on track 1. This peculiarity would occur because of the location of the playback head with respect to the record head. If playback started on track 2, no data would be present because track 2 data ends about 7 min before EOT. In this case, the data encoder would be switched to data mode 1 by the mode 4/1 logic. No real advantage could be found in playing back one track before the other. The capability to switch data tracks was provided by use of DC-V3; otherwise, the EOT signal switched data tracks at the end of each track playback. This EOT function occurred only if the tape recorder remained in its playback mode.

The total time required to play back both data tracks would be 35 h, 50 min $\pm$15 min. The uncertainty results from tape-recorder playback speed fluctuation during the "no data" periods. With data present on the tape, reconstructed bit sync would be compared to the data-encoder bit sync. The phase difference between these signals would then be used to control the VCO supplying the reference frequency for the playback motor. This forms a phase-lock loop for controlling playback speed, which is nominally 0.01 in./s. During the "no data" portion of playback, the phase-lock loop speed control would not exist. Laboratory test data showed that, in this configuration, the tape ran slower (0.0095 $\pm$0.0005 in./s).

The total cumulative "no data" period on track 2 was longer than that on track 1. For this reason, the playback time associated with each track would not be equal, track 2 requiring about 12 min longer than track 1.

It was not planned to initiate playback before the transmission of MT-9 if all spacecraft conditions appeared

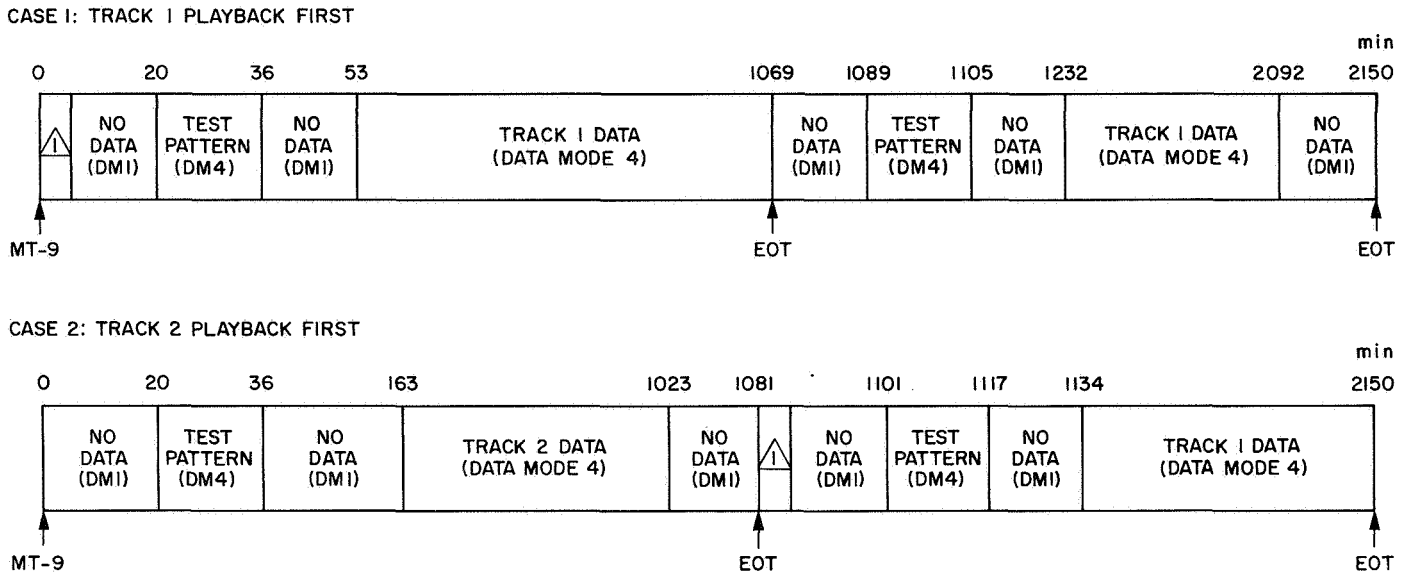


Fig. V-13. Nominal *Mariner V* playback times

normal. An early playback would be possible by preempting MT-9 with ground command DC-V4. As no strong arguments existed for playing back the encounter data earlier than MT-9, DC-V4 became the backup mode.

The desired tracking configuration during playback was the one-way (noncoherent) mode. The chances of losing data in the one-way mode are less than in the two-way (coherent) mode. In the two-way mode, a transient at the ground transmitter causing the uplink signal to malfunction would cause the spacecraft momentarily to shift the downlink frequency. If this frequency shift were too rapid, the ground receiver could not track it, and would drop lock. Telemetry would be lost until the receiver reacquired downlink lock. Also, the ground receiver could drop back at the time of the initial ground transmitter malfunction, and again data would be lost.

The project scientist requested that the encounter data be played back twice. On this basis, the decision was made to track the spacecraft in the two-way mode for at least the first playback. If the quality of the data turned out to be poor, the second playback would then be performed in the one-way mode. The advantage of using the two-way mode during the first playback was that additional ranging and two-way doppler data could be obtained near the planet. The entire DSS 14 pass, which started about 17 h after closest approach, would be available for ranging. These data would aid in determining more accurately the mass of Venus, the earth–Venus ephemeris, and the astronomical unit. The two-way doppler would provide much better resolution for redetermining the spacecraft trajectory.

A choice existed as to whether the tape recorder 2.4-kHz power should be turned off or left on upon termination of playback. Leaving tape-recorder power on would require fewer commands for the anticipated post-encounter UV-photometer exercises. The tape-recorder personnel favored turning the power off, as this instrument was not designed to remain on for long periods, and had not been subjected to prolonged life testing. Upon this basis, the recommended procedure for terminating playback was to transmit DC-V2, DC-V28, and again DC-V28. The DC-V2 command would inhibit further playback by placing the tape recorder in its "standby" mode. Also, the data encoder would be placed in the cruise mode (data mode 2). The first DC-V28 command would turn the tape recorder 2.4-kHz power off and turn the battery charger on. The second DC-V28 command would turn the battery charger off at a time designated by the power-cognizant engineer.

j. Planned encounter sequence chronology. The encounter sequence that was ultimately recommended and adopted by SPAC is given in chronological order in Table V-15.

Table V-15. Planned encounter sequence chronology

Event	Predicted time (earth-observed), GMT	Event	Predicted time (earth-observed), GMT
DSS 41 (Woomera) rise	291:18:06:14	Transmit DC-V9	292:16:40:00
Backup DSS 51 (Johannesburg) rise	292:01:48:00	Command modulation off (DSS 41)	16:41:30
Apply command modulation (DSS 41)	02:00:00	Transmitter off (DSS 14)	16:42:00
Transmit DC-V25	02:49:00	Start track 2 data (clock B)	16:44:29
DSS 62 (Cebreros) rise	02:50:11	Verify one-way RF signal	16:51:00
Transmit backup DC-V25 (if required)	03:14:00	Enter occultation	17:36:14
Command modulation off (DSS 41)	03:39:00	Encounter (Venus closest approach)	17:38:49
Nominal two-way station transfer (DSS 41 to DSS 62)	03:49:00	Terminator sensor output	17:46:06
		DAS clock A APAC command	17:48:08
Apply command modulation (DSS 62)	04:14:00	Center of occultation	17:48:50
Backup DSS 42 (Tidbinbilla) set	04:26:00	Transmitter on at closest approach + 17 min 24 s (DSS 12)[a]	17:51:44
MT-7 observed (register 2 event)	04:44:39		
Command modulation off (DSS 62)	04:49:00	Exit occultation	17:53:47
Transmitter off (DSS 62); start AUX OSC test	04:50:00	Backup DSS 42 rise	18:02:16
DSS 41 set	05:34:37	DSS 41 rise	18:05:00
Transmitter on (DSS 62); end AUX OSC test	05:49:00	Nominal two-way station transfer (DSS 12 to DSS 14)	18:17:00
FPAC exciter evaluation	06:10:00		
Apply command modulation (DSS 62)	06:18:00	Stop track 2 data (clock B)	18:31:59
Transmit DC-V9	08:50:00	EOT	18:37:59
Stanford rise	10:43:35	Apply command modulation (DSS 14)	18:41:00
DSS 12 (Echo) rise	10:43:53	Data encoder to mode 2 (clock B)	18:45:25
Transmit DC-V24	10:50:00	Transmit DC-V9	19:10:00
DSS 14 (Mars 210-ft antenna) rise	10:51:15	Ranging modulation on	19:29:00
Backup DSS 11 (Pioneer) rise	11:09:04	Ranging modulation off	21:48:00
MT-8	11:24:41	Command modulation off	21:49:00
Command modulation off (DSS 62)	11:30:00	Transmitter off (DSS 14); start postencounter AUX OSC test	21:50:00
Nominal two-way station transfer (DSS 62 to DSS 14)	11:47:00		
		DSS 14 set	22:38:14
Apply command modulation (DSS 14)	12:17:00	DSS 12 set	22:45:28
Apply ranging modulation	12:44:00	Backup DSS 11 set	22:45:39
Backup DSS 51 set	12:50:25	Transmitter on (DSS 41); end AUX OSC test	22:50:00
Latest trajectory data (E — 4 h)	13:30:00	AUX OSC test evaluation from FPAC	23:10:00
Ranging modulation off	14:20:00	Stanford set	23:38:13
Transmit DC-V16	14:30:54	Backup DSS 51 rise	293:01:47:02
Apply ranging modulation	14:50:00	DSS 62 rise	02:50:43
Latest trajectory data (E — 2 h)	15:39:00	Nominal two-way station transfer (DSS 41 to DSS 62)	04:17:00
DSS 62 set	15:39:00		
Ranging modulation off	16:30:00	Backup DSS 42 set	04:26:19
Planet sensor output observed; begin track 1 recording	16:30:59	DSS 41 set	05:35:00
		Apply command modulation (DSS 62)	06:00:00
Verify ranging modulation off	16:39:00	MT-9 observed	07:24:48

[a]Ground transmitter VCO set for X_A of closest approach +1370 s (see Fig. V-14).

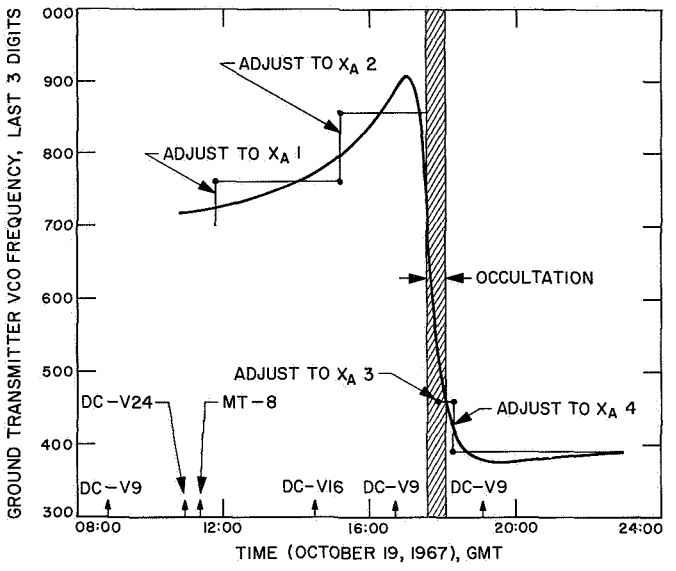


Fig. V-14. Expected doppler shift at encounter

3. ***Operational considerations.*** The planning for the encounter phase also considered the ground-transmitter operational characteristics to be established for prime designation, configuration, usage, and transmission frequency and procedures.

a. DSIF transmitter frequency. At the beginning of the encounter phase, the DSIF transmitter VCO frequencies would be so chosen that one frequency would be satisfactory for an extended period. In the spacecraft, the static phase error (SPE) would not be maintained at a zero offset. Procedurally, a transmitter VCO frequency would be initially chosen so that the spacecraft SPE telemetry channel would indicate a positive error of approximately 30 Hz. In time, the SPE would decrease, and eventually would assume a negative value. The correct setting for the DSIF transmitter VCO frequency would be available from the tracking data analyst.

Studies indicated that the doppler shifts at closest approach would be quite large, and could not be accommodated without adjusting SPE. The tracking site during this time would be Goldstone. The predicted doppler-shift effects are shown in Fig. V-14.

The solid curve in Fig. V-14 is the ground-transmitter VCO frequency required to give a continuous best-lock frequency at *Mariner V* as the spacecraft was accelerated, then decelerated, by the planet. A zero SPE would be maintained only if the ground-transmitter VCO frequency was continuously updated to fit this curve. This operation was not desirable because of the possibility of dropping uplink lock. Instead, it was recommended that the SPE be updated at four discrete times, as shown on the figure.

It should be noted that three of the recommended SPE updates occur just before sending a ground command. This assured solid radio-lock conditions for the command periods.

b. Ground-command transmission procedures. The practice of normalizing the ground-command subsystem frequency (8 f_s) after locking up the command loop would not be used at encounter. (As used here, "normalizing" refers to adjusting the ground-command frequency to the setting that would drive the spacecraft command subsystem to its preferred best-lock operating frequency.) Instead, the ground-command frequency would be chosen to provide an offset from the normalized frequency. The intent was to maximize the probability of regaining command lock in minimum time if a transient from the ground transmitter should cause a loss of lock. It was judged that the ability of the spacecraft successfully to receive commands was insignificantly affected by this practice.

c. Use of Goldstone stations during encounter. The 20-kW transmitter at DSS 14 would be the prime transmitter up to enter-occultation time. The 10-kW transmitter at DSS 12 would serve as the backup transmitter. The 10-kW transmitter at DSS 11 would also be available in case of an emergency. Following exit occultation, DSS 12 would become the prime transmitting station after going two-way at E+1370 s. A two-way station transfer at 18:17:00 GMT would establish DSS 14 as prime once again for the remainder of the pass.

The ground-receiver configuration used during the Goldstone encounter pass is illustrated in Fig. V-15. Three ground telemetry subsystems and two TCPs would be available. The TCP at DSS 12 could receive input from either of the two interchangeable ground telemetry subsystems located at that station. The data from DSS 14 would be routed to DSS 12, making two data sources available for the DSS 12 ground telemetry subsystem. DSS 12 would be the prime station for processing spacecraft telemetry because of its redundant hardware and data source. DSS 11 would serve as the backup station.

The prime ground receiver was located at DSS 14. This station used a 210-ft antenna, giving it a 9- to 10-dBmW advantage over the other Goldstone stations, which use

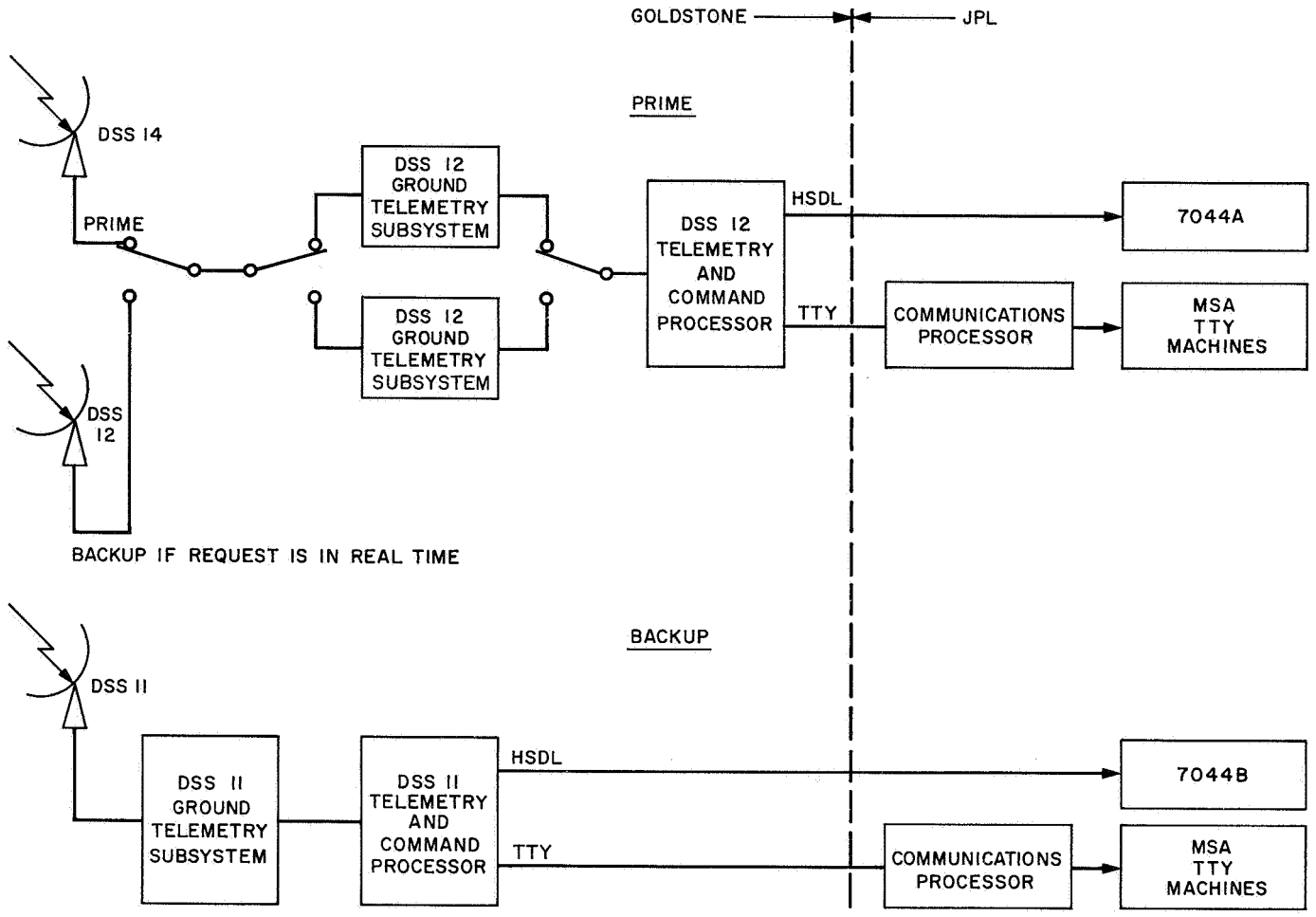


Fig. V-15. Receiver configuration during Goldstone encounter pass

85-ft antennas. In addition, DSS 14 had the capability to supply station AGC over the HSDL. This feature could be extremely useful if the spacecraft started rolling unexpectedly. DSS 14 could be used with or without the diplexer in the "listen only" mode. Eliminating the diplexer would decrease the received signal loss by approximately 1.4 dBmW. The time required to switch from the "listen only" mode to the diplexer mode would be done electrically, and would take only a fraction of a second. This switch sometimes caused the ground telemetry subsystem demodulator to drop lock for a short time.

4. Contingency plans. One of the primary aims of SPAC and VEPWG was to determine nonstandard events that might arise during the encounter phase. The associated ground action required to remedy an anomalous situation could then be formulated well in advance. The response time to such a condition would then be reduced to the time required to perform the recommended action. Valuable time would not be wasted in real-time analysis of an unexpected event. A list of nonstandard events and the recommended responses to them is given in Table V-16. A portion of the encounter decision diagram developed by SPAC is shown in Fig. V-16. A discussion is included herein for anomalies not mentioned earlier.

a. Early PSO. The planet sensor could give an early output under any of the following conditions: A component failure in the sensor, a particle in the FOV of the sensor, or reflected or direct light into the sensor during a loss of spacecraft attitude.

The primary purpose of the PSO was to provide the spacecraft with an automatic means of initiating the DAS encounter sequence. This function would have no effect upon the spacecraft unless preceded by an MT-8 or an odd number of DC-V24 commands. In the recommended encounter plan, DC-V24 would preempt MT-8. The region for an early PSO, therefore, was limited to the region between DC-V24 and the desired PSO time.

Table V-16. Emergency action summary

Single failure or problem	Indication	Action
Tape recorder remains off when DC-V25 is transmitted	Power telemetry channels 203, 205, and 227	Send DC-V25 again. If no response, send DC-V28 followed by DC-V25. If that does not work, wait for MT-7. If still no response, data storage capability is lost.
Terminator sensor not energized when DC-V25 is transmitted.	Telemetry channel 306	Send DC-V25 again. If still no action, wait for MT-7. If no response, depend solely on clock A for APAC command during occultation. A late backup would be DC-V22.
Data encoder does not switch to data mode 3 when DC-V24 is transmitted.	Telemetry remains in data mode 2 format	Send DC-V24 twice. If no response, wait for MT-8. If still no action, use data mode 2 for encounter.
Planet sensor not energized when DC-V24 is transmitted.	DAS status bit 291	Wait for MT-8. If still no response, then either clock B will noi be available for controlling record sequence or status bit is wrong. Clock A would control encounter sequence if clock B is not available.
Clock B not enabled when DC-V24 is transmitted.	DAS status bit 17	Same as above.
Plasma probe does not switch to mode 3 format	DAS status bit 315 plasma probe data	Wait for MT-8. By this time, plasma-probe data can be used to determine validity of status bit. If no response follows MT-8, encounter with plasma probe in mode 2.
DC-V16 acknowledgment	DAS status bits 18 and 281 and science frame count	If both status bits remain unchanged, and frame count does not reset to zero, assume that command was not received. Reverify command-lock conditions, and transmit another DC-V16. If still no response, assume that clock A is not available for controlling record sequence and issuing APAC backup. If frame count is reset to zero, assume status bit or bits to be in error. Take no further action.
Frame count set to wrong number when DC-V16 is transmitted	Frame count in telemetry	Inhibit clock A by sending DC-V16 (especially if APAC will occur early.). If frame count resets properly with DC-V16, use of clock A could be reconsidered.
PSO does not occur	Clock B frame count and DAS status bit 19	No action possible; record sequence becomes dependent on clock A.
UV-photometer calibration not inhibited at PSO	DAS status bit 401, UV-photometer real-time data	Take no action. Lose every eighth word of UV-photometer data.
Tape recorder does not switch to record mode at PSO	DAS status bit 26	Wait for clock A backup command. If status bit still does not change, either status bit is not working or record mode is lost.
No track 1 data indication at PSO	DAS status bit 313	Wait for clock A backup. If problem is not corrected, record capability is lost or status bit is in error.
No track 2 data indication	DAS status bit 314	Same as above.
Plasma probe remains in mode 3 following encounter	Plasma probe data format	Take no action. A DAS power-on reset would only reissue PP mode 3 command because MT-8 is in effect.

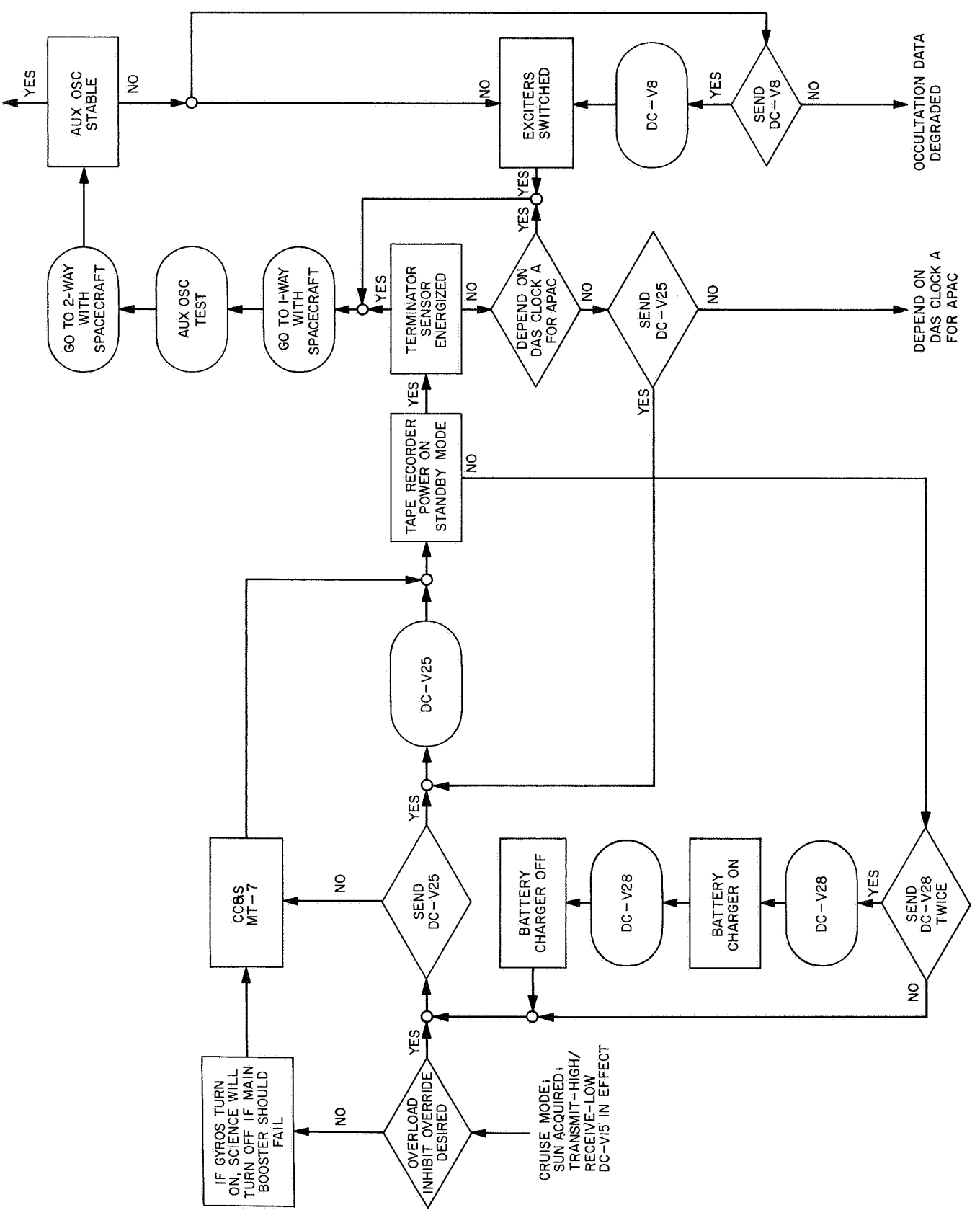


Fig. V-16. Encounter decision diagram

Before the command was sent, DC-V24 PSO would have no effect. After the desired PSO time, PSO would be late, and so would fall into a different category. The early PSO region was about 6 h in duration.

The specific functions initiated by the DAS upon receipt of PSO are described below.

Start clock B. This function starts clock B counting in such a way that the count is incremented once every 50.4 s. The clock issues encounter commands at fixed known intervals. The first command, which starts the recording of DFR data on track 2, would occur at PSO + 13.44 min. Knowing that the two-way light time is approximately 9 min, it is doubtful that ground action could be initiated in time to stop this command if PSO were early. The next clock B command comes at PSO + 121 min. There would be sufficient time to initiate ground action before this command was transmitted.

Start tape. The "start tape" command is issued every 50.4 s to assure that the tape recorder is switched from the standby mode to the record mode. This function is issued independently of clock B starting, and is discontinued by clock B at PSO + 121 min or by clock A at frame 288.

Track 1 data sync. The DAS begins serially shifting track 1 data and bit sync, at 66⅔ bits/s, to the tape recorder. This function is not controlled by clock B.

Inhibit UV-photometer calibrate. The DAS inhibits the UV photometer from entering its calibrate mode. This function is independent of clock B starting.

The above functions indicate that an early PSO would initiate a premature data-storage sequence controlled by clock B. The science data recorded on both tracks of the tape recorder could be of low value compared to the desired data, depending upon how early PSO arrived. Ambiguity could be introduced into the UV-photometer data based upon the calibrate mode of the instrument being inhibited earlier than planned.

The following reaction modes were considered as responses to an early PSO:

The first mode would turn the tape recorder off with DC-V28, then back on at the desired time with DC-V25. The "start tape" commands from PSO would still be occurring, which would cause the tape to start running. Clock B would be inhibited by DC-V24. Otherwise, clock B would count out to the end of its sequence, then issue a "stop clock B" command and an "inhibit clock A decodes" command. These commands would prevent further DAS clock control of the encounter sequence unless a DAS "power-on-reset" command was executed.

The second mode would remove the effects of PSO completely by resetting the DAS encounter logic to the cruise state with a "power-on-reset" command. This would be accomplished by turning the science power off and then back on with a DC-V26 followed by a DC-V25. The desired encounter sequence would then be controlled by clock A.

The third mode would disable clock B with DC-V24, and let the tape recorder run. A partial removal of PSO would be in effect, as "start tape" commands would continue to be issued, the UV-photometer calibrate mode would remain inhibited, and the tape would be recording track 1 data. Clock A would then become the controlling clock for stopping the record sequence and returning the spacecraft to its cruise state after encounter.

A disadvantage of the first approach is that the tape recorder might not have come back on. In the second approach, a power transient at turn-on might cause a failure in the DAS power converter or in the encounter logic section. No flight data were available for resetting the DAS logic after operating in a space environment for over 4 mo.

Another disadvantage would be that clock B becomes permanently disabled because its sole starting means, PSO, had occurred. The remaining encounter sequence becomes completely dependent upon clock A, which is started by a critically timed DC-V16 command. The second method would not work if the failed state gave PSO continuously and MT-8 had occurred.

The third approach seemed to be the most reasonable in that it eliminated the risks, however small or large, associated with the first two modes. A minimum amount of spacecraft electronics would be disturbed with this approach. Also, a minimum number of ground commands would be required.

Two of the guidelines used to establish the tape length required for the encounter data-storage period were: (1) UV-photometer data were to be recorded from E−45 to E+45 min, and (2) DFR data were to be recorded from 10 min before *Mariner V* entered occultation until 10 min after the spacecraft exited from occultation. The UV-photometer data would be recorded on track 1; DFR data would appear on both tracks.

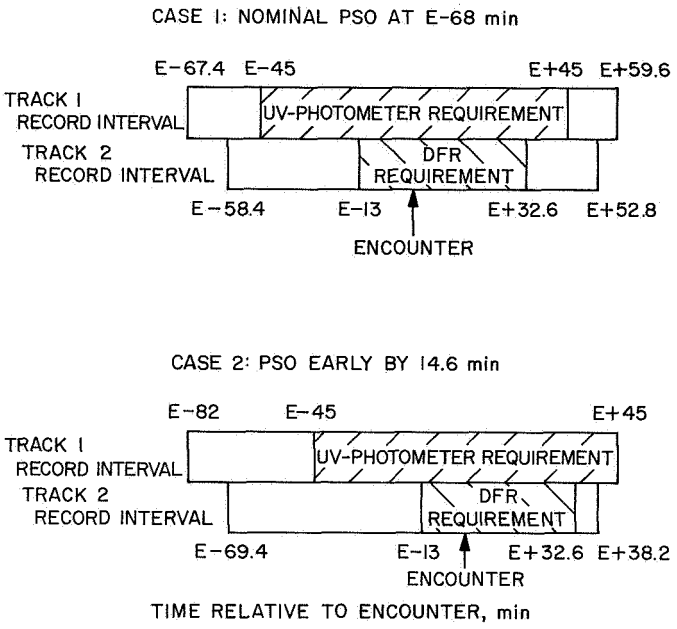


Fig. V-17. Data storage relative to encounter

The record period covered on each data track, relative to encounter for a nominal PSO, is shown as Case 1 in Fig. V-17. The shaded portions show the desired record intervals of DFR and UV-photometer data. A O-atm model of Venus was assumed for the DFR interval. The track 1 and track 2 record intervals easily capture the desired data for a nominal PSO. For an early PSO, the outer track 1 and track 2 rectangles shift to the left with reference to the stationary shaded areas. That is, the recording sequence begins and ends earlier with respect to encounter. Desired UV-photometer data are lost for a PSO occurring earlier than 14.6 min from nominal.

The record intervals for PSO early by exactly 14.6 min are shown as Case 2 in Fig. V-17. The end of the track 1 record interval is coincident with the edge of the desired UV-photometer data period. The inference is that a satisfactory record sequence can be obtained as long as PSO comes no earlier than 14.6 min.

The recommended action for an early PSO was two-fold. If PSO was early by 14.6 min or less, no action would be required. An acceptable clock B record sequence was achievable, as discussed above.

For a PSO early by more than 14.6 min, the recommended action would be to send a DC-V24 before clock B reached frame 144. Clock B would then be disabled before it removed the "start tape" command. Also, clock B would be prevented from disabling itself at frame 160 and inhibiting further clock A outputs. The remaining DAS encounter commands would be issued by clock A. The tape would stop recording when it reached the EOT foil 127 min after PSO. The EOT logic would then be overridden by the PSO-triggered start tape function being issued every frame, and the tape would restart. This restart condition would prevail until E+63.4 min, when clock A would inhibit further "start tape" commands. The record sequence would then be terminated by either the EOT foil or the clock A "stop tape" command (whichever came first after E+63.4 min. The time relationships of the clock A outputs and the PSO-initiated "start tape" commands are shown in Fig. V-18 for a PSO early by 5 h.

The total number of tape passes to be expected if the tape recorder continued to run following an early PSO is plotted in Fig. V-19. The effective period of an early PSO starts at DC-V24, which occurs approximately 5.7 h before nominal PSO. This corresponds to the vertical line on the right side of the figure. The nominal PSO time is E−68 min, and is the zero reference point on the abscissa. The first tape pass, determined by the EOT foil position at the end of the launch phase, would be 127 min. Each pass thereafter would be 134 min. As an example, if PSO occurs 3 h early, the number of tape passes read from the figure is about 2.5. This means that the tape would stop at the desired encounter time midway in the third pass. The total time that the tape recorder remained in the record mode would be 328 min $(127 + 134 + 0.5 \times 134)$.

In the "no action" region of Fig. V-19, clock B is allowed to continue controlling the record sequence just as if PSO were nominal. The EOT sensor would stop the tape after completing one pass. In the "send DC-V24" region, the tape would continually recycle until stopped by clock A or by an EOT. The interval of constant slope corresponds to those cases of early PSO for which the tape is stopped by clock A. The flat portions of the curve represent cases of early PSO for which the EOT sensor stops the tape. The latter condition exists when an EOT occurs between the stop "start tape" and the "stop tape" commands issued by clock A. This interval, which is from E+63.4 to E+76.9 min, is shown in Fig. V-18.

b. Enigmatic loss of radio signal during encounter. A sudden loss of the RF downlink signal would probably be caused by either a radio subsystem failure or a loss of spacecraft attitude. Losing sun–Canopus orientation could occur from an AC subsystem failure or from an

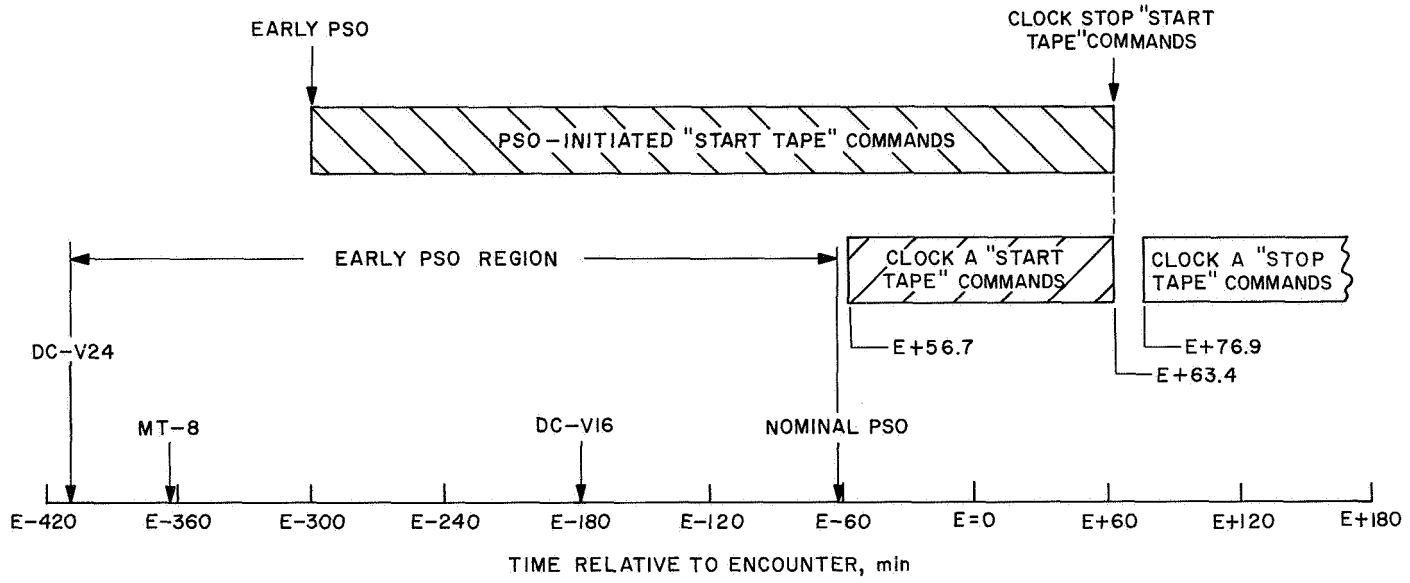


Fig. V-18. Early planet sensor output timing diagram

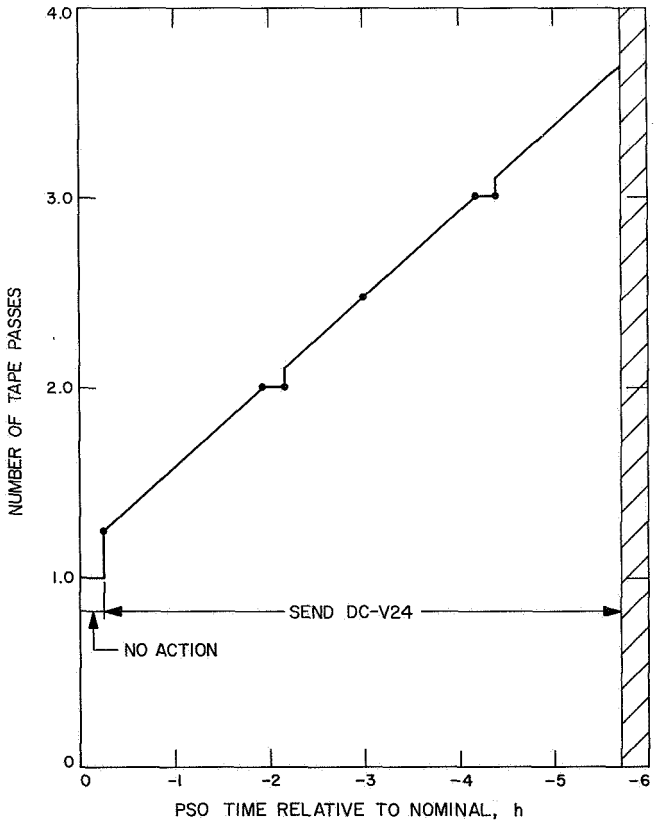


Fig. V-19. Number of tape passes for early planet sensor output

external phenomenon (dust particle, meteorite, etc.). The probability was very small that both the radio and AC subsystems would experience a failure at the same time. During encounter planning, all engineering subsystems had operated successfully for over 2000 h.

A procedure was developed to guide SPAC reaction in case of an unexpected loss of downlink signal. The procedure presented several alternate routes to follow because the problem could be induced by either spacecraft radio or spacecraft attitude. The mode of action to be selected would be based upon information conveyed by the SAGC signal and/or the telemetry available up to the time of the anomaly. If the spacecraft were in data mode 3, little (if any) information would be provided by the telemetry. A failed radio amplifier, exciter, or power supply would tend to cause immediate loss of RF. In this case, the information available for pinpointing the problem would be very scant unless a period of degradation, observable in the data, occurred beforehand.

More information would be available in a case of the spacecraft rolling far enough in the high-gain antenna pattern to drop the strength of the downlink signal below receiver RF threshold at the tracking station. The time to roll to this threshold position can be calculated if the spacecraft angular acceleration in roll and the appropriate high-gain antenna information are known. For a torque developed by continuous-roll jet firing, the maximum acceleration would be about 0.5 mrad/s^2. Downlink threshold would be exceeded if the spacecraft rolled more than 6.0 deg ccw or 12.0 deg cw. Using classical physics, it would take 20 s to roll 6.0 deg. During this period, SAGC would drop in a known pattern. Changes

in certain high-deck telemetry channels, such as Canopus intensity (CH 108) and roll position (CH 114), would exist if the spacecraft were in data mode 2 and the telemetry were sampled at the right time. Verification that the spacecraft had rolled into the downlink blackout area because of an attitude-induced problem would then be possible.

The criterion chosen for SPAC was to assume that a radio problem existed if SAGC fell below threshold in less than 8 s. Otherwise, the problem was assumed to be AC-related.

The radio-induced problem could not be uniquely defined from the SAGC signal. The problem could only be categorized as such by an abrupt drop below threshold. It remained to establish the radio subassembly that had failed and whether the failure was an open- or short-circuit condition.

If the SAGC signal dropped off in less than 8 s, and either the communciations converter input current (CH 204) or the 2.4-kHz output current (CH 227) changed, it was assumed that the radio power amplifier was not driving the spacecraft transmitter. The required action was to transmit DC-V7, which would switch the cavity amplifier on line. If the traveling-wave tube had failed, this procedure would correct the problem; the RF signal would then reappear after two-way light time following the transmission of DC-V7.

If telemetry channels 204 and 227 held constant or were not available in the above condition, the procedure would then become more complex. A DC-V8, a DC-V7, a DC-V8, and a DC-V7 would be sent, in that order, with each DC-V7 being sent 2 min after the previous DC-V8. The second DC-V8 would be sent 5 min after the first DC-V7. The total command sequence, starting with the first DC-V8, would take 9 min. If the radio exciter had failed, the first DC-V8 would switch the backup exciter on line in place of the failed unit. After two-way light time, the RF signal would reappear for 7 min until the second DC-V8 placed the failed exciter back on line. If the failure was in the power amplifier (traveling-wave tube), the first DC-V7 would switch to the cavity amplifier, and the RF signal would appear for 7 min until the failed unit was switched back on line by the second DC-V7. Upon completion of this command sequence, the spacecraft would be back in its original failed state, and SPAC would know whether the problem was induced by a failed exciter or power amplifier. Another DC-V7 or DC-V8 would then be sent to correct the problem.

If the problem was not corrected after the above sequence had been performed, it would then be assumed that the command subsystem had dropped lock and reacquired on an RF sideband. The procedure was then to drop command modulation, wait 1 min and tune the ground transmitter to the best-lock frequency. After tuning had been completed, the procedure was to reapply command modulation, and wait 12 min for command to lock up in the blind. The DC-V8, DC-V7, DC-V8, and DC-V7 sequence was then again repeated.

If SAGC decreased steadily for more than 8 s and RF threshold had not been reached, it was assumed that an AC problem existed. A very slowly dropping signal (on the order of 4–5 deg/h maximum) would be characteristic of a Canopus-sensor failure resulting in a zero-roll error signal. In the DC-V15 mode, the spacecraft, assuming that it was perfectly balanced, would continue to move at the limit-cycle roll rate existing at the time of the failure. The SPAC response would be to send a DC-V18, which would place the spacecraft in the inertial roll-control mode, and stop the roll. Downlink capability would be reacquired or maintained if the DC-V18 was followed by additional DC-V18 or DC-V21 commands, as needed, to point the high-gain antenna back at earth.

If the Canopus sensor were tracking a dust particle, the spacecraft could move 6 deg max in 20 s. If this motion were in the ccw direction, earth would appear to move out of the high-gain antenna pattern far enough to lose downlink lock. Also, command lock would probably be lost because of the interferometer effect upon the uplink during the roll. The uplink signal strength required for reliable command lock was -140 dBmW. Using the 85-ft antenna at 10 kW would give about -141 dBmW (excluding any interferometer effects). Thus, the 210-ft antenna at 10 kW would be required to send commands; the objects acquirable by the Canopus sensor would be earth at 101 deg clock and Venus at 85–185 deg clock. The corrective action to be taken would be to relock the command loop, wait 12 min for command to lock up, and send DC-V19 to remove DC-V15, allowing the spacecraft to go into roll search.

After two-way time plus 17 min (time to roll from earth to Canopus) had elapsed, the procedure would be to send DC-V2 if the spacecraft were in data mode 3 or 4 and if the signal did not appear. This would provide engineering information to speed up Canopus acquisition if the signal appeared following the next step, which would be to send DC-V12. This command would switch the spacecraft to transmit via the low-gain antenna, which

would provide threshold telemetry capability if the 210-ft antenna were receiving and the digital demodulation technique were being used. A DC-V21 command would then be transmitted to override the Canopus-acquisition logic if an object other than Canopus were acquired. If telemetry became available, a sequence generated by the AC personnel to point the high-gain antenna at earth would then be followed. A DC-V10 command would be used to return the spacecraft to the proper mode to transmit via the high-gain antenna following Canopus acquisition. The spacecraft would be returned to data mode 3 by the transmission of DC-V24. A second DC-V24 command would be necessary to reestablish the DAS clock B enable logic. Otherwise, clock B would not start counting at the time of PSO.

H. Postencounter Planning

1. Description. Planning for the postencounter phase of the *Mariner* Venus 67 mission consisted of determining, evaluating, and selecting activities that would enhance the return of scientific and engineering data from *Mariner V* before the communications threshold with the spacecraft was reached. The activities under consideration were those needed to calibrate instruments, prolong communications with the spacecraft during 1967, enhance the possibility of reacquisition of the spacecraft in 1968, and gain further knowledge concerning the behavior of *Mariner V* in the space environment for a prolonged period.

The basic ground rules used to make decisions relative to the postencounter activities were that the accepted activity had to perform one of the following: (1) Enhance data already received, (2) enable the spacecraft to return a maximum amount of deep-space data during 1967, or (3) enhance the possibility of reacquiring the spacecraft in late 1968. Special spacecraft tests that did not jeopardize the successful achievement of the above objectives were also permissible. The final decisions as to the activities that were to be conducted rested with the project manager.

2. Operations. Operational aspects of the postencounter phase are described in the paragraphs that follow.

a. UV-photometer bit-rate change. Accepting the ground rule that any operation performed on the spacecraft should enhance the understanding of existing data, the switch of data rates to aid in UV-photometer calibration was proposed. Upon transmission of MT-6 *Mariner V* switched from the 33⅓ to the 8⅓ bits/s data rate. After the bit-rate switch, it was observed that the UV-photometer tube C had a substantial increase in data number (DN). The data-rate-change test was designed to confirm whether or not the increase in DN was an instrument-oriented phenomenon. This test would also afford cognizant personnel a second opportunity to observe the DN-increase phenomenon, and to compare the actual DN increase with the predicted values.

In making the decision to execute the data-rate change, the advantages and risks of transmitting the proposed commands had to be evaluated. The risk involved was a very remote possibility that the spacecraft would not switch back to the 8⅓ bits/s rate after operating at 33⅓ bits/s. If *Mariner V* could not be returned to the 8⅓ bits/s data rate, the spacecraft telemetry threshold would occur approximately 2 wk sooner than expected for the low bit rate. If the test were successful, a more thorough understanding of the UV photometer would be obtained, thus permitting a more meaningful interpretation of the data. Because the risk to the spacecraft would be relatively small, project approval was given to transmit two DC-V5 (command switch data rates) commands. Both commands, the first to switch the spacecraft data rate to 33⅓ bits/s and the second to return the spacecraft to the 8⅓ bits/s data rate, were transmitted on October 25, 1967 (day 298).

b. Second set of three spacecraft rolls conducted to enhance understanding of UV-photometer data. Planning for a second set of three *Mariner V* spacecraft rolls was predicated upon results obtained from the first set of three spacecraft rolls conducted immediately after the midcourse maneuver on days 170 and 171, 1967. The first set of spacecraft rolls was to be conducted to verify and corroborate the unexpectedly high data obtained from the UV photometer during the magnetometer-roll calibration (after spacecraft–*Agena* separation). The magnetometer-roll calibration was to be conducted in the extended upper atmosphere of the earth, whereas the first set of spacecraft rolls was conducted outside of the external influence of the earth. Because of an unexplainable shift in the average DN reading of the UV photometer during the midcourse maneuver, it was not possible to correlate the data obtained from the magnetometer-roll calibration with data from the first set of rolls conducted immediately after the midcourse maneuver.

Upon request from the principal UV-photometer experimenter, it was decided that, as one of the postencounter operations, a second set of three spacecraft rolls would be performed to enhance understanding of the UV-photometer data. It was estimated that at approximately 12:00 GMT on day 311, the spacecraft would be at

180 deg in celestial longitude from the position where the first three spacecraft rolls were performed. A spacecraft roll maneuver at this time would allow the UV photometer to observe approximately the same region of the sky as was observed during the first spacecraft rolls.

The second set of spacecraft rolls would have to be performed at a data rate of 8⅓ bits/s because of the increased transmission range. To determine a scaling factor, and the influence that a data-rate change of 33⅓ bits/s might have on the UV photometer, it was decided to perform a data-rate switching test just before the second set of spacecraft rolls, on day 298 at approximately 16:00 GMT.

In preparing the *Mariner V* tracking schedule, it was discovered that *Surveyor* tracking priority would limit the tracking period available to *Mariner V* to 6 h on day 311 (DSSs 62, 11, 12, and 14 tracking). Playback of the UV-photometer data would take place on days 312, 313, and 314.

To prepare the spacecraft for the roll maneuver, a DC-V26 command was to be transmitted to the spacecraft to turn the science subsystem off. A DC-V25 command was then to be transmitted to turn the science and tape-recorder subsystems on, placing the spacecraft in mode 3. This sequence of commands was used to initiate a power-on reset in the science DAS, which would be necessary to condition the science and tape-recorder subsystems for a record sequence. A DC-V16 command was then to be transmitted to reset the science frame count and to start the science-record sequence.

To determine the exact region of the galaxy that the UV photometer would be scanning during the rolls, it would be necessary to transmit DC-V2 and place the spacecraft in mode 2, allowing the spacecraft to transmit engineering and science data during the rolls. The engineering data would be used to determine where the spacecraft was pointing as a function of time during the rolls.

To receive spacecraft data continually during the rolls, it was necessary to command the spacecraft to transmit data over the low-gain antenna. To minimize the transition in signal strength when switching antennas, it was decided to transmit a DC-V21, which would start the first spacecraft roll, and then time a DC-V12 to switch antennas when the signal strength of the high-gain antennas would be the same. This crossover time was predicted to occur approximately 1 min after the roll turn had started. Because of the difficulty in estimating the time of completion of one spacecraft roll, two DC-V21 commands would be sent 6 min apart.

The first DC-V21 would be timed to reach the spacecraft just after the minimum predicted time of Canopus acquisition; the second DC-V21 would be timed to reach the spacecraft 6 min after the first. This second DC-V21 time was chosen to correspond to one correlation of the command loop. The function of the DC-V21 was to override the Canopus sensor, and cause the spacecraft to continue on into the next roll. Upon completion of the three rolls and Canopus acquisition, a DC-V10 was to be transmitted to switch the spacecraft back to transmitting on the high-gain antenna and receiving on the low-gain antenna.

Because of tracking priorities, no further commands were to be sent to the spacecraft until the next day (312), at which time a DC-V4 was to be transmitted to begin the playback sequence. The spacecraft was to play back data continually through days 312 and 313; then, because of tracking priorities, the playback sequence would be terminated for an 8-h period. A DC-V4 command was to be transmitted to place the spacecraft in mode 2, with the tape positioned as before encounter, for the next record exercise. Two DC-V28 commands were then to be transmitted to turn the tape recorder and battery charger off. At this point, the UV-photometer roll exercise would be completed, and the spacecraft would be in the cruise mode.

c. UV-photometer MT-6 exercise. The CC&S issued the MT-6 command on July 24, 1967, and switched the spacecraft data rate from 33⅓ to 8⅓ bits/s. The celestial longitude of the spacecraft at that time was 300 deg. Following the data-rate change, the UV-photometer tube-C reading started drifting gradually from a reading of 36 DN; by the middle of November, the reading had dropped to about 24 DN. The cause of the drift was not clear. It could have been an actual change in the interstellar hydrogen density or a change in the sensitivity of the instrument at the lower data rate. After encounter, it was desirable to point the UV photometer at the same region of the sky that it had observed on July 24. If the tube-C reading again indicated about 36 DN, then the observed phenomena would be real rather than hardware-induced. This information would enhance the value of the post-MT-6 UV-photometer data, particularly the encounter data.

At 37 days after encounter (November 25, 1967), the spacecraft would be at a celestial longitude of 120 deg. At this time, the spacecraft would have traveled exactly 180 deg in longitude, and thus would be diametrically opposite (in the ecliptic plane) to its MT-6 position. A

pure spacecraft roll at this point would allow the UV photometer once again to observe the point in the celestial hemisphere that it observed at MT-6. The outlook for telecommunication capability for November 25, however, was bleak. *Mariner V* would be near a null in the interferometer pattern. The spacecraft limit cycle could move the antenna into the null, which would cause the command subsystem to drop lock. Also, it appeared very likely that the spacecraft would roll through two nulls for a 360-deg roll. Telemetry return via the 210-ft antenna was doubtful. An earlier date for performing the UV-photometer MT-6 exercise was necessary.

A study of the spacecraft/celestial-space geometry showed that the desired UV-photometer exercise would be performed earlier by first pitching, then rolling the spacecraft. This capability would be available using the spacecraft midcourse-maneuver sequence without a motor burn. The proper date on which to perform the exercise became earlier for increasingly negative pitch angles.

A constraint of ± 20 deg was placed on the allowable spacecraft pitch angle. As the spacecraft was pitched off the sunline, normally shaded surfaces and ancillary equipment became exposed to the sun. Items of particular concern for pitch angles greater than 15 deg were the magnetometer, the louver assemblies, and the trapped-radiation detector. For certain roll attitudes, the magnetometer would become sunlit, and could exceed its upper temperature limit of 149°F. The louver assemblies would be exposed to untested solar-intensity levels, with possibly detrimental results. The trapped-radiation detector X-ray tube would approach its upper temperature limit of 122°F if bay 4 remained sunlit for any length of time.

The date selected by SPAC for performing the UV-photometer MT-6 exercise was November 19, 1967. Telemetry capability, during the playback period of the recorded UV-photometer data on track 1, would be good to marginal. The turns required would be a -17.2-deg pitch and a $+173.2$-deg roll. For this maneuver, the UV-photometer tube C would be pointed at its MT-6 position from the other side of the sun. At the nominal turn rate of 0.18 deg/s, the pitch turn would take 1.5 min and the roll turn about 15.5 min. This particular "aimed" position could be inertially held for 12.5 min. During this interval the UV-photometer data could be stored by the tape recorder as the spacecraft limit-cycled the instrument in the region of interest.

The procedure requested by the UV-photometer personnel was to roll the spacecraft so that the UV-photometer tube C would view the region of interest by sweeping through it once rather than stopping and limit-cycling on the region. This plan would produce the desired information needed to determine the state of the instrument. In addition, further mapping of the celestial heavens would be possible as the spacecraft continued to roll past the MT-6 region. A study of the maneuver geometry showed that, for a maximum spacecraft roll, the UV photometer would also sweep through the Milky Way (near the Crux constellation) in a southerly direction. During sun–Canopus reacquisition, which followed the maneuver, the UV photometer would again sweep through the Milky Way in a northerly direction and on a different trace. A maximum roll following the -17.2-deg pitch turn was desired.

The maximum roll duration available in the CC&S maneuver sequence was normally 22 min. However, if a rocket-motor burn was not required, the roll period could be extended to 28 min. That is, the spacecraft could roll from M+82 to M+110 min. At M+110 min, the roll-turn relay in 5A6 would be reset, inhibiting further torquing current to the roll gyro. The maximum roll angle would be 314 deg for the predicted roll-turn rate of 0.1866 deg/s. The QC-V1-2 command recommended for the exercise was for a 30-min roll, assuring that the spacecraft would roll for the maximum 28 min. The roll would be terminated by the CC&S M+110 command rather than by the normal roll-register-overflow signal.

The UV-photometer MT-6 exercise would require an encounter sequence to record the UV-photometer data plus a maneuver sequence to pitch and roll. The supporting command sequence recommended by SPAC is given in Table V-17. The appropriate quantitative commands would be sent to establish the CC&S pitch and roll registers. A DC-V14 command would be required to remove the maneuver inhibit in effect. A DAS power-on-reset command would then reset the DAS encounter logic to the cruise state. The DAS was the sole command source for starting the tape recorder. The "start-tape" command would be available from either clock A or PSO at encounter. Following encounter and a power-on-reset command, the DC-V14 command was available only from clock A (clock B needed PSO, and PSO needed a light stimulus). The DC-V26/DC-V25 combination would establish a power-on-reset mode. The DC-V26 command turned science power off, and DC-V25 turned it back on; also, DC-V25 turned the tape-recorder power on. Since MT-8 was set and would remain set for the remainder of the mission, the DAS would issue a switch-to-mode 3 command whenever the DAS power was turned on by DC-V25.

Table V-17. Proposed sequence for UV-photometer MT-6 exercise

Command	Transmit time, GMT	Verify time, GMT	Event	Command	Transmit time, GMT	Verify time, GMT	Event
QC-V1-1	13:00:00	13:13:30	Load roll turn	M-5	—	16:28:30	Start roll turn
QC-V1-2	13:05:00	13:18:30	Load pitch turn	M-6 inhibited	—	16:50:30	Start burn (inhibited)
DC-V14	13:25:00	13:38:30	Remove DC-V13	M-7	—	16:50:31	Stop burn
DC-V26	13:30:00	13:43:30	Science off	M-1, 2, 3, 5 reset	—	16:56:30	Stop roll/start sun reacquisition
DC-V25	13:35:00	13:48:30	Science and tape recorder on, data mode 3	Sun gate	—	16:59:30	Start Canopus search
DC-V16[a]	13:51:00	14:04:30	F/C = 0, enable clock A	Roll search complete	—	17:41:30	Acquire Canopus
DC-V2	14:06:00	14:19:30	Data mode 2	Clock A	—	18:05:36	End track 2 recording
DC-V29	14:25:00	14:38:00	Arm first burn	End of tape	—	18:12:30	End track 1 recording
DC-V27[a]	14:53:00	15:06:30	Start maneuver sequence, data mode 1	Clock A	—	18:18:12	End encounter sequence
DC-V2	15:05:00	15:18:30	Data mode 2	DC-V10	18:05:00	18:18:30	Transmit high–receive low
DC-V12	15:51:00	16:04:30	Transmit low–receive low	DC-V13	18:10:00	18:23:30	Apply maneuver inhibit
Clock A	—	16:05:30	Begin track 1 recording			18:25:30	Maneuver counter overflow
M-4	—	16:06:30	Start pitch turn	DC-V26	18:20:00	18:33:30	Science off
M-4 reset	—	16:08:03	Stop pitch turn	DC-V2	18:25:00	18:38:30	Science on, override off
Clock A	—	16:18:06	Begin track 2 recording	QC-V1-1	18:45:00	18:58:30	Load minimum pitch
				QC-V1-2	18:50:00	19:03:30	Load minimum roll
				QC-V1-3	18:55:00	19:08:30	Load minimum burn

[a]Time-critical command.

The data encoder would respond to this command, and switch to data mode 3. Clock A began counting out its encounter commands upon receipt of DC-V16. The DC-V16 command would be so timed that the clock A "start-tape" command occurred 1 min before the pitch turn start. This timing would allow the tape recorder to record UV-photometer data throughout both the pitch–roll maneuver and the sun–Canopus reacquisition period. EOT would occur at M+186 min, and the clock A encounter sequence would terminate at M+192 min. The maneuver counter overflow, which terminated the maneuver sequence, would occur at M+199 min. The used maneuver registers were set for a maximum count-out duration at this time.

A DC-V2 command would be sent following the verification of DC-V16 to switch back to data mode 2. A DC-V29 command would then be sent to assure that the steering relay in the gyro was still in the "first-burn" already-used position. Under normal conditions, this relay would already be in the proper condition, as would the CC&S motor-burn-command inhibit, because pitching or rolling during the burn interval would have inhibited the CC&S motor-burn relay. The DC-V27, a critically timed command, would start the maneuver sequence. AC personnel would supply the DC-V27 transmission time so as to start the pitch maneuver 1 min after the tape recording started. Another DC-V2 would be sent to remove the data mode 1 state established by the CC&S response to DC-V27. In data mode 2, both engineering and science subsystems could be monitored before committing to the maneuver at M+60 min. Also, UV-photometer data would be obtained for reference before the turn began. Special digital demodulation equipment would be available in data mode 2, extending the telemetry-threshold capability. The digital demodulation equipment at the tracking stations were not to process the data mode 1 format. At 2 min before the pitch turn began, DC-V12 would switch the radio subsystem from the receive-low–transmit-high to the receive-low–transmit-low mode. It was hoped that this antenna mode change would allow real-time telemetry during the exercise.

Upon completion of the encounter and maneuver sequences, a DC-V10 would be sent to return the antenna to its transmit-high mode. A DC-V13 command would inhibit further maneuvers. Minimum QC commands for pitch, roll, and motor burn would be sent at the end of the sequence to provide a safety margin in case a failure-induced maneuver should occur in the future.

A special test was conducted at SAF on November 13, 1967, in support of the UV-photometer MT-6 exercise. Essentially, the purpose of the test was to run through the proposed command sequence given in Table V-17, using the flight-support spacecraft (M67-1). A simultaneous spacecraft encounter and midcourse-maneuver sequence had not previously been tested.

An anomaly occurred during the midcourse-maneuver–encounter sequence test. The DAS frame count jumped backwards in count about 16 min after the completion of the pitch turn. No spacecraft functions coincided with this time; the tape recorder was recording both track 1 and track 2 data, and the data encoder was in data mode 2 at 8⅓ bits/s. As a result of the change in frame count, the clock A encounter outputs were issued 56 frames late.

The investigation of the anomaly that followed was threefold. First, the tape-recorder data were investigated for possible clues as to the cause of the anomaly. Second, the test facility monitoring equipment was examined in the hope of finding a facility malfunction. Third, the sequence was repeated twice.

The results of the investigation were as follows: (1) all science and engineering tape data, with the exception of frame count, were normal; (2) no test facility or operational support equipment malfunctions were noted; and (3) the anomaly did not recur in the repeated tests. On the basis of the latter result, it was concluded that the problem was not spacecraft-induced; therefore, the combined encounter–midcourse-maneuver sequence could be safely used for the UV-photometer MT-6 postencounter exercise.

d. Spacecraft receiver SPE test. The receiver SPE test was designed to measure the SPE of the spacecraft receiver over a wider-than-normal operating range. This would be accomplished by observing how far the uplink carrier frequency could be varied from the best-lock point before the spacecraft receiver dropped uplink lock. The information obtained would be used to evaluate the operation of the spacecraft receiver phase-lock loop, including the phase detector and the VCO. This information would also be compared with similar laboratory data to determine whether there had been any degradation in the spacecraft receiver since launch.

The test would be conducted at a spacecraft-received signal level of −128 dBmW, and would begin at the best-lock frequency. The station transmitter VCO would be varied each minute at a 4-Hz rate. At fixed-frequency increments (±100, ±150, ±200 Hz, etc.), tuning would be stopped for approximately 10 min at each increment to obtain a stable data point. A plot of SPE vs frequency could then be drawn from the acquired data, and compared with the prelaunch plot.

e. Spacecraft receiver threshold test. This test was designed to measure, within the limits of the spacecraft telemetry system, the signal level of the receiver carrier-tracking threshold. In addition, data were gathered to plot a curve of receiver AGC vs uplink signal level. The information obtained was used to determine overall receiver performance, and to check for any significant degradation to the radio subsystem during the *Mariner* Venus 67 mission.

The test was to begin by establishing two-way lock with the spacecraft, then adjusting the ground-transmitter frequency so that the doppler effect would shift the frequency to the best-lock point when threshold was reached. The station transmitter power was then to be reduced to 1 kW. With a 100-kHz signal phase-modulating the transmitter, the carrier was then to be suppressed in 1-dB increments to threshold.

A second set of threshold tests was to be conducted with the station transmitter by offsetting the VCO best-lock frequency by +50, +100, −50, and −100 Hz, and conducting the threshold test at each offset.

f. Command-lock threshold tests. These tests were designed to measure, within the ability of the telemetry system of the spacecraft, the command-subsystem threshold level. In addition, the tests were to evaluate both receiver and command subsystem performance. Any degradation to the receiver noise figure or the signal-to-noise ratio of the detected command signal would be discovered during these tests.

After spacecraft receiver and command lock had been obtained, the station transmitter output was to be reduced. By phase-modulating the transmitter with a 100-kHz signal, the uplink signal would be suppressed in 1-dB increments until a point was reached where the command subsystem was in and out of lock for equivalent intervals. At this point, it would be marginally possible to send and act upon a command if the command reached the spacecraft when the command subsystem was in lock.

g. Mission termination—Phase I. The primary purpose of the final exercise of the postencounter phase of the mission on November 21, 1967, was to prepare *Mariner V* for long-term cruise, and to optimize its condition for reacquisition of telemetry data in late 1968. In addition, a final exercise of the planetary-ranging subsystem was to be performed.

The ranging exercise was to be initiated in an attempt to obtain final ranging information from the spacecraft

before the telemetry threshold was reached. A DC-V9 (ranging receiver on/off) command was to be transmitted to the spacecraft to turn on the ranging channel in the spacecraft radio subsystem. After telemetry verified that the ranging channel was on, ranging modulation was to be applied to the uplink carrier.

The first step in conditioning *Mariner V* for long-term cruise (Table V-18) was to be the transmission of a DC-V15 (Canopus gate inhibit override) command. With the DC-V15 command in effect, the spacecraft would not go into roll search when Canopus acquisition was lost. This command opens the line to the gyro switch control, preventing the gyros from turning on after roll-reference acquisition is lost. In addition, the sensor would acquire (as a roll reference) any object in its FOV that is of sufficient brightness to generate a roll-error signal.

This AC mode was preferable to the DC-V19 (gyros off–normal cruise) mode for the following three reasons: (1) Cruising in the DC-V15 mode will eliminate the possibility of the gyros operating near perihelion. A gyros-on condition would result in an additional 56 W being dissipated in the spacecraft. The associated rise in temperature would have a detrimental effect upon the ability of the *Mariner V* spacecraft to survive perihelion temperatures. (2) It is possible to lose the roll reference and not have an acquirable object in the Canopus sensor FOV for several days during segments of the spacecraft orbit. During these periods, if the spacecraft were in the DC-V19 mode, the gyros would go on, a roll search would be initiated, and the search would continue until an acquirable object came into the FOV. With the DC-V15 command in effect, the possibility of operating in a roll-search mode for extended periods is eliminated. (3) Each time the roll reference is lost, fewer spacecraft components will be exercised in the DC-V15 mode.

The next step in planning the long-term cruise conditioning of *Mariner V* was the transmission of the DC-V10 (transmit-high–receive-low) command. In this mode, the radio-subsystem personnel will be able to obtain final data points for their telecommunication performance margin curves. A DC-V9 command was then planned to turn off the ranging channel in the spacecraft radio subsystem.

The final command to be planned during Phase I was a DC-V12 (transmit-low–receive-low) command, which was to transfer the complete spacecraft radio subsystem to the omni antenna. The transfer had a dual purpose: (1) To put *Mariner V* in the best condition to act as a planetary beacon, and (2) to put *Mariner V* in the optimum condition for reacquisition of telemetry data in late 1968. Transmission of the DC-V12 command was to be defined as the end of mission for the active portion of the *Mariner* Venus 67 Phase I effort.

Table V-18. Phase I — conditioning for long-term cruise plan

Command	Sequence
DC-V9	Turns on ranging channel in spacecraft radio subsystem.
DC-V15	Prevents spacecraft from going into roll search when roll-reference acquisition is lost.
DC-V10	Switches spacecraft transmitter to high-gain antenna and receiver to low-gain antenna (was high–high).
DC-V9	Turns off ranging channel in spacecraft radio subsystem.
DC-V12	Switches both spacecraft transmitter and receiver to low-gain antenna.

VI. Spacecraft Performance

A. *Mariner V* Description

The *Mariner V* spacecraft, which was designed for the *Mariner* Mars 1964 flyby mission, was subsequently converted for use on the *Mariner* Venus 67 mission.

The *Mariner V* design (Figs. VI-1 and VI-2) was a modification of the *Mariner IV* spacecraft; the redesign objectives were to enable the spacecraft to fly by Venus and to accommodate a complement of scientific instruments appropriate to the mission. The Venus flight plan included the following steps:

(1) Launch by an *Atlas/Agena.*

(2) Establishment of a cruise mode.

(3) Performance of a trajectory-correction maneuver early in flight, if necessary.

(4) Gathering of interplanetary data.

(5) Start of planetary encounter sequence and gathering of data regarding Venus.

(6) Playback of data acquired during Venus encounter.

The spacecraft, fully stabilized in attitude, used the sun and the star Canopus as references. Cold-gas jets pointed the spacecraft in all three axes. Gyroscopes were available for initial sun and Canopus acquisition, and for inertial yaw and pitch control during trajectory corrections; inertial roll control could also be achieved if required.

The *Mariner V* power subsystem used photovoltaic cells arranged on four panels. This subsystem had a body-fixed orientation for cruise operations and a rechargeable battery for launch, trajectory-correction maneuvers, and use as a temporary backup. Power-conversion equipment delivered regulated, 2.4-kHz square-wave, 400-Hz step-square-wave, and unregulated dc electricity for distribution to the spacecraft subsystems. A central computer and sequencer (CC&S) provided synchronizing signals for frequency stabilization, and performed the sequencing of onboard switching.

The spacecraft guidance subsystem permitted variable orientation for trajectory-correction maneuvers; the post-injection propulsion subsystem (PIPS) was capable of executing two of these corrections.

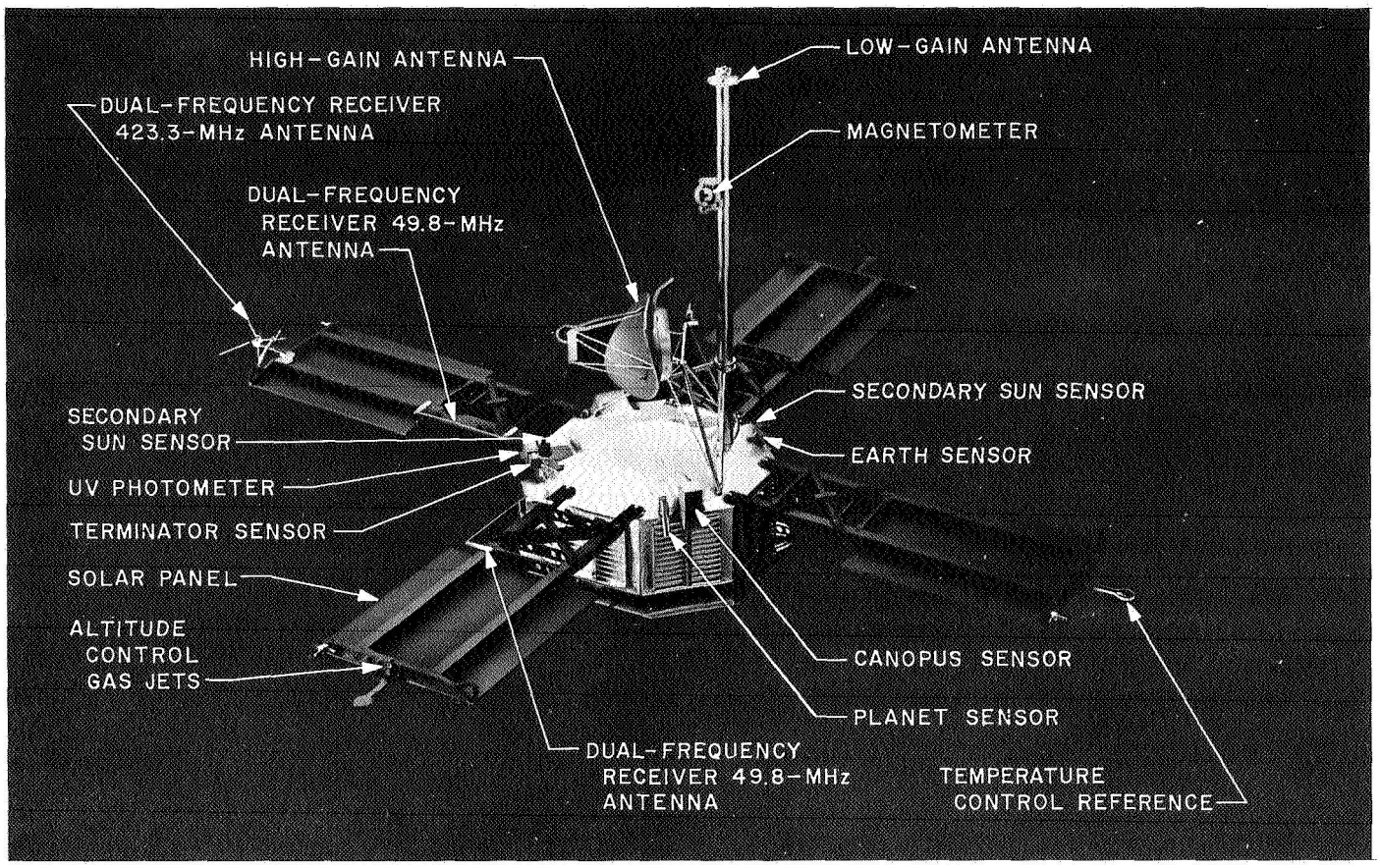


Fig. VI-1. *Mariner V* spacecraft configuration (top view)

A two-way, S-band radio subsystem transmitted telemetry to earth, commands to the spacecraft, and angle-tracking doppler and ranging information for orbit determination. The subsystem included a low-gain antenna and a two-position, high-gain antenna, either of which could be used to transmit or receive. Switching between antennas was performed by automatic onboard failure-mode logic or by ground command.

The command subsystem detected and decoded incoming command messages, and transmitted them to the various onboard equipment.

Two types of commands were used: (1) direct commands that resulted in direct action by the receiving subsystem, and (2) quantitative commands that were transferred to the CC&S, and stored for later use in trajectory-correction maneuvers. A data encoder (DE) subsystem formatted, sequenced, and (when needed) provided analog-to-digital conversion of the telemetry data.

A data automation subsystem (DAS) furnished control and synchronization; performed necessary data conversions and encoding functions; and buffered the science data, transmitting them to the DE at the various appropriate rates and times.

B. *Mariner* Spacecraft Conversion From Mars to Venus

Converting *Mariner IV* spacecraft to accommodate the *Mariner* Venus 67 mission required changing a spacecraft designed to fly away from the sun into one required to fly towards the sun. The solar-panel celled surfaces were rotated 180 deg so that they would face the sun, and the radio antennas were reoriented so that they would face the earth.

The increase in solar energy available to a spacecraft flying towards the sun permitted a reduction in the total solar-panel area required for power conversion. *Mariner IV* required 70.4 ft², whereas *Mariner V* required 43.6 ft². Because solar-panel temperatures increase as a spacecraft approaches the sun, there is a decrease in solar-cell

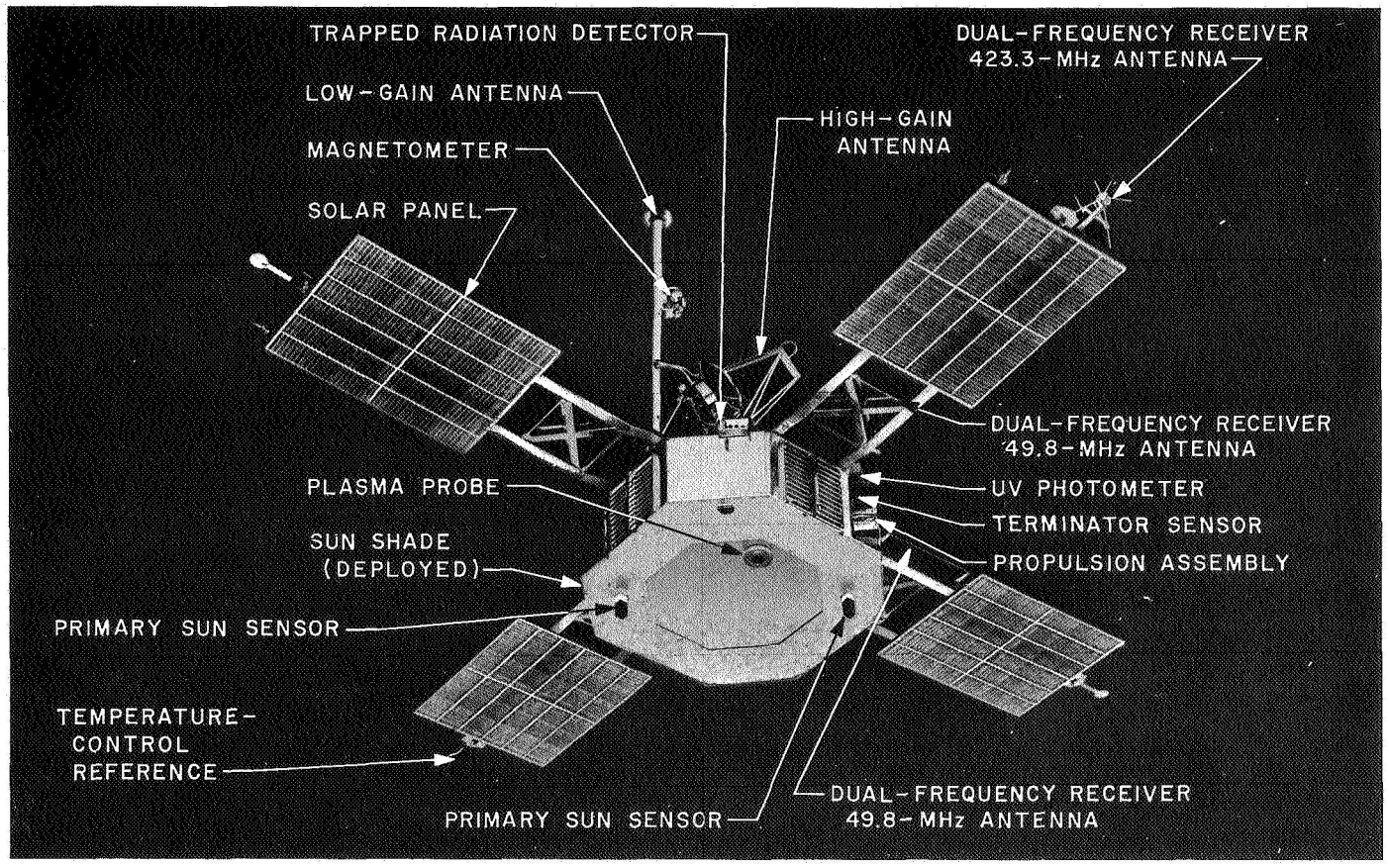


Fig. VI-2. *Mariner V* spacecraft configuration (bottom view)

output voltages. As a result, the series–parallel arrangement of the solar cells had to be reorganized to prevent solar-panel output voltage from dropping below the 33-V battery voltage. Because the power subsystem diode-isolates the solar panels and the battery, the reorganization of the cells was required to prevent battery power drain.

The thermal-control design philosophy of isolating the spacecraft octagon (bus) from solar-heat inputs was integrally related to the solar-panel design. The reduced solar-panel area permitted removal of approximately 2 ft of solar-panel substrate nearest the bus; therefore, less solar energy absorbed by the panels was reradiated onto the surfaces of the electronic compartments. In the interest of economy, overall dimensions of the solar panels were maintained, and existing handling frames and attitude-gas system plumbing were used. A thermal shield isolated the bus from solar heat and prevented the electronic compartments from exceeding temperature limits. The sun shade, which was approximately 2½ in. away from the spacecraft on the sun side when deployed, and extended approximately 4½ in. past the edges of the octagon, resulted in a decrease of 30°F in the average bus temperatures at Venus.

Sun-sensor voltages also had to be reduced from 16 to 12 V so that thermal inputs and electrical power dissipation would not cause the sensors to exceed thermal operational limits.

Although the *Mariner* Venus 67 mission required thermal shielding over most of the spacecraft, certain elements required additional heat because the spacecraft was inverted, relative to the sun, for the flight to Venus. Some spacecraft appendages that were on the sun side during the *Mariner* Mars 1964 mission were on the shaded side for the *Mariner* Venus 67 mission. For example, heaters had to be installed on the magnetometer, which was located on the mast of the omni-antenna facing earth; approximately 3 W of raw dc power was used to heat the magnetometer.

The trajectory of *Mariner V*, as it relates to communication distance, spacecraft–earth and spacecraft–Canopus angles, and the scientific objectives, required several

engineering changes to the *Mariner IV* spacecraft and a modified flight sequence. The spacecraft CC&S had to be reprogrammed to change telemetry data rates, to transfer from the low-gain omni-antenna to the high-gain directional antenna, and to update the Canopus sensor cone angle at times dictated by the *Mariner* Venus 67 mission trajectory. Also, the CC&S had to be programmed to issue the necessary commands to carry out the encounter sequence developed for the *Mariner* Venus 67 mission.

The scientific objectives of the mission required the spacecraft to fly as close to the planet as possible, but not to be captured by it. Capture would have violated the planetary-quarantine constraint placed upon the mission. As a result of the requirement to fly close to the planet (the *Mariner V* planned miss distance was 2460 mi), and because of the albedo of the planet, a special light hood had to be designed for the Canopus sensor to prevent planetary straylight from interfering with the sensor lock on the star Canopus during encounter.

A data-mode switch (to all science data) was required 6 h before closest approach for the *Mariner* Venus 67 mission (as compared to 1 h for the *Mariner* Mars 1964 mission) to maximize the data accumulated as the spacecraft passed through the magnetopause of the planet. For the *Mariner* Mars 1964 mission, 1 h of no engineering data was the acceptable risk. Six hours of operation without radio-subsystem or command-subsystem performance data was judged to be detrimental to the reliability with which a command could be transmitted to the *Mariner V* spacecraft if an emergency developed during the encounter sequence. Therefore, the *Mariner V* data encoder was modified to gate-in radio and command data during this period of high scientific interest.

Science instruments for the *Mariner* Venus 67 mission consisted of a plasma probe, a magnetometer, and a trapped radiation detector (TRD), all of which had flown on *Mariner IV*, and a UV photometer that had previously been developed as an encounter instrument for *Mariner IV*. A new instrument, added for the *Mariner* Venus 67 mission, was a VHF/UHF dual-frequency receiver (DFR). Dispersive doppler and differential group path lengths were measured by the DFR to determine interplanetary electron density and to aid in deriving profiles of the ionosphere and neutral atmosphere of Venus.

The UV photometer was converted from its role as an encounter instrument for the *Mariner* Mars 1964 mission to a cruise-and-encounter instrument for the *Mariner* Venus 67 mission. The conversion allowed a density determination to be made among the three sources of atomic hydrogen: solar, planetary, and galactic. This conversion consisted primarily of redesigning the timing circuits and logic so that the instrument operated at the early cruise rate of 33⅓ bits/s.

For the Venus encounter, the stepping sequence of the plasma probe was changed so that the sequence consisted of simultaneously sampling all three segments of its three-element sensing devices instead of alternating samples of the individual elements in the sequence, as was done during cruise.

The reduction of the data rate to the tape recorder (10,700 bits/s for the TV data for *Mariner IV* to 66⅔ bits/s for the science instruments of *Mariner V*), along with the increase in the required record time for the *Mariner* Venus 67 mission (2 h for the *Mariner* Venus 67 mission vs 25 min for the *Mariner* Mars 1964 mission), required reduction of the tape-recorder speed. The tape recorder was redesigned so that the motor could also be used for recording (rather than only during playback, as on the *Mariner* Mars 1964 mission). As was the case for *Mariner IV*, the *Mariner V* playback motor was driven at a speed of 0.08 in./s for recording, and was phase-lock-loop controlled, using sync pulses for a playback speed of 0.01 in./s.

The different scientific payload and tape-recording sequences required a new DAS. The DAS controls the readout and sequencing of each of the scientific instruments, which means that it has to be optimized for each payload. The type of circuits used for the *Mariner IV* DAS were not easily available, and standard components consumed too large a packaging volume. The DAS was built mainly of integrated circuits. These were primarily new, low-power-consuming, integrated circuits that did not require power subsystem redesign.

Like *Mariner IV*, the *Mariner V* spacecraft used the S-band transponder to perform an occultation experiment; however, unlike its predecessor, *Mariner V* optimized the S-band occultation experiment by positioning the antenna for maximum gain of an RF signal that traveled through an atmosphere at the start of occultation. The antenna was then switched to a second position to optimize the pointing angle of the antenna for a signal emerging from an atmosphere at the end of occultation. It was necessary to compensate for the refractive atmospheric effects on the RF signals that traveled through the atmosphere of the planets so that the

atmosphere of Venus, which was expected to be dense, could be explored. If the radio signals had been strong enough to be tracked all the way to the surface of the planet, they could also have been used to determine the diameter and depth of the Venusian atmosphere.

Many other minor changes were made to the *Mariner IV* design to make it completely compatible with the *Mariner* Venus 67 mission. The earth-sensor field of view (FOV) was modified to allow a roll-reference backup to the Canopus sensor for the first 20 days. The solar-panel launch-mode stowing mechanism became a tip-latching mechanism because the old solar-panel quarter-point mechanism was in the path of the second position of the high-gain antenna. The terminator sensor and planet sensor had to be attached to the spacecraft with the correct geometry to produce their outputs at the correct time in the encounter sequence. *Mariner IV* absorptivity standards were replaced with an upgraded thermal-control-reference experiment.

C. *Mariner V* Performance

Mariner V was launched from the Air Force Eastern Test Range (AFETR) on June 14, 1967 (day 165 of the year). It was the only spacecraft scheduled by NASA for the 1967 Venus opportunity.

From launch until the nominal end of mission on November 21, 1967, the performance of the spacecraft was excellent. The interplanetary-cruise portion of the mission produced a large amount of useful scientific and engineering data; during the planetary-encounter phase, all primary mission objectives were successfully met.

On November 21, 1967, *Mariner V* was still performing in an excellent manner. At that time, the combination of high-gain-antenna pointing and earth–spacecraft range exceeded the limits required for obtaining useful telemetry data; as a result, the spacecraft transmitter was commanded to switch from the high-gain to the low-gain antenna. This command was designed to enable the reacquisition of telemetry data if the spacecraft were still operating. Analysis of spacecraft performance indicated the distinct possibility that data from the spacecraft might continue to be received in the last quarter of 1968.

The nominal flight sequence of events for *Mariner V* was designed to be totally automatic, requiring no action from the ground for a normal flight (except for the trajectory-correction maneuver and turning on of the ranging receiver). Such a design relieved the mission from any dependence upon the ground-to-spacecraft communication link (uplink), provided that the CC&S operated correctly. The ground-command function would be necessary to the success of the mission only if the CC&S were to fail. This was the cornerstone of the functional–redundancy philosophy employed in the *Mariner* V design that provided for independent and physically different means of performing all critical functions. When both means are available, as was the case in the *Mariner* Venus 67 mission, a strict reliance upon the onboard functional branch may lead to a flight sequence that is less than optimum. This proved to be true in a number of cases during the flight, with the result that the nominal sequence was preempted or modified at times when it was advantageous to do so. The nominal flight sequence adopted for *Mariner V* prior to launch is presented in Table VI-1; the major departures from the nominal sequence of events are presented in Table VI-2.

Table VI-3 presents a chronological sequence of events during the *Mariner* Venus 67 mission, starting with liftoff and concluding with the transfer of the spacecraft transmitter to the low-gain antenna on November 21, 1967.

Although spacecraft performance was generally excellent, the *Mariner* Venus 67 mission was not without incident. A summary of problems and unexpected performance characteristics that were encountered during the mission is presented in Table VI-4. A Problem Failure Report (PFR) was initiated for each problem that could have endangered the *Mariner* Venus 67 mission.

These problems and performance characteristics were primarily concerned with individual subsystems, and are described in detail in Subsections D through I. During the flight, many of them had a pronounced effect upon the systems aspect of the flight operation, and resulted in some modification to the flight-operations philosophy. The material in the paragraphs that follow is presented to provide some insight into the *Mariner* Venus 67 mission from an overall systems point of view.

1. Launch to Canopus acquisition. Launch was accomplished on June 14, 1967, at 06:01:00.176 GMT after a flawless countdown (one hold was called in the countdown to allow better down-range telemetry coverage than the nominal opening of the window). Both the *Atlas* and the *Agena* launch vehicles performed well, injecting the spacecraft on a trajectory well within launch tolerances.

Table VI-1. Flight sequence adopted before launch

Event	Time	Source	Destination	Comments
1. Verify number of encounter update pulses to be inserted at T−7 min (event 3)	T−15 min	LCE[a]	CC&S	Number of pulses inserted determines time from launch to CC&S MT-7, which varies with trajectory flight time
2. Switch to internal power	T−7 min	LCE	Power	
3. Clear counters and insert encounter update pulses	T−7 min	LCE	CC&S	
4. Release LCE relay hold	T−5 min	LCE	CC&S	
5. Tape recorder to launch mode	T−4 min	LCE	Tape recorder	Monitor DE channel 221; maneuver B/R[b] output current to determine whether tape recorder is in launch mode
6. Release CC&S real-time inhibit	T−3 min	LCE	CC&S	
7. Clear relay release	Event 6+119 s	CC&S	LCE	
8. Liftoff	T = 0	—	—	Provided event 7 occurs within tolerance relative to event 6
9. Shroud separation	T+317 s (approx)	Agena timer	Agena pyrotechnics	S-band signal level increases
10. Spacecraft injection	I (T+19.1 to T+35.2 min)	Agena D	—	Injection is completion of Agena second burn
11. Spacecraft separation	S = I+2.6 min	Agena D timer	Agena pyrotechnics	Spacecraft V-band released
a. RF power-up and turn on science	—	Separation connector	Power	Backup to RF power-up is gyros off; backup to science on is DC-V2
b. Remove relay hold and enable CC&S	—	Separation connector	CC&S	
c. End tape-recorder launch mode	S = 0 to S + 114 s	Separation connector	Tape recorder	This signal is "NANDed" with first end of tape (EOT) signal after separation and switches tape-recorder launch motor off; gyro power off at spacecraft acquisition is a backup to tape-recorder launch motor off
d. Remove plasma probe 10-kV inhibit	—	Separation connector	Plasma probe	This will allow plasma probe to supply 10 kV to its sensor
e. Arm pyrotechnics	—	Pyrotechnics arming switch	Pyrotechnics	This switch is wired in parallel with separation-initiated timer for redundancy
f. Agena isolation amplifier turned off	—	Pyrotechnics arming switch	DE	Event in DE register 3
g. Turn on AC[c] subsystem	—	Pyrotechnics arming switch	AC	Initiate sun acquisition
h. Separation-initiated timer activated	—	Separation	Pyrotechnics, DE	
(1) Arm pyrotechnics	S+30 ±20 s	Separation-initiated timer	Pyrotechnics	Backup to event 11e
(2) Pyrotechnics-armed indication	S+180 ±80 s	Separation-initiated timer	DE	Event in DE register 3 if event in step step 11f has not occurred
(3) Deploy solar panels and sun shade	S+190 ±80 s	Separation-initiated timer	Pyrotechnics	

[a]LCE = launch complex equipment.
[b]B/R = booster-regulator.
[c]AC = attitude control.

Table VI-1 (contd)

Event	Time	Source	Destination	Comments
12. Deploy solar panels and sun shade	T+53 min	CC&S L-1	Pyrotechnics	Backup event 11h(3)
13. Turn on AC subsystem	T+57 min	CC&S L-2	AC	Backup to event 11g (backup: DC-V13)
14. Sun acquisition complete; begin to calibrate magnetometer roll rate	Event 11h or 13+0 to 20 min	Sun gate	AC	If DC-V13 was used to turn on AC, Canopus acquisition will begin at event 14
15. Start magnetometer calibration	T+4 hr	—	—	Begin calibration after spacecraft has passed 8 earth radii
16. Turn on Canopus sensor and initiate roll search about spacecraft Z axis	T+997 min	CC&S L-3	AC	Backup: DV-V13. Inhibit magnetometer-calibration roll signal
17. Canopus acquisition complete	Event 16+0 to 16+60 min	—	—	This is at 0.1 deg/s
18. Begin trajectory-correction maneuver	T+2 to T+10 days	—	—	
a. Load pitch-turn duration and polarity	—	Command QC-V1-1	CC&S	
b. Load roll-turn duration and polarity	—	Command QC-V1-2	CC&S	
c. Load motor-burn duration	—	Command QC-V1-3	CC&S	
d. Arm first propulsion maneuver	M−10 min	Command DC-V29	Pyrotechnics	This will ensure that propulsion transfer relays are in proper state for first maneuver
e. Remove propulsion inhibit	M−5 min	Command DC-V14	Pyrotechnics	This will ensure that pyrotechnic relays are not inhibited
f. Initiate maneuver sequence	M	Command DC-V27	CC&S	
g. Maneuver sequence start	M=0			
(1) Turn on gyros for warmup		CC&S M-1	AC	
(2) Switch to data mode 1		AC	DE	Backup: DC-V1
h. Begin maneuver	M+59 to M+60 min			
(1) Spacecraft to inertial control (all axes); autopilot on; Canopus sensor off		CC&S M-2	AC	
(2) Set turn polarity		CC&S M-3 or M-3	AC	M-3 positive turns, M-3 negative turns
(3) Start pitch turn		CC&S M-4	AC	
i. Stop pitch turn	Event 18h+1 to 1319 s (1-s resolution)	CC&S M-4	AC	Magnitude inserted by QC-V1-1 before maneuver start (1000 s = 180-deg turn)
Reset turn polarity		CC&S M-3	AC	
j. Start roll turn	Event 18h+22 min	CC&S M-5	AC	
Set turn polarity		CC&S M-3 or M-3	AC	See comments on event 18h(2)
k. Stop roll turn	Event 18j+1 to 1319 s (1-s resolution)	CC&S M-5	AC	Magnitude inserted by QC-V1-2 prior to maneuver start (1000 s = 180-deg turn)
Reset turn polarity		CC&S M-3	AC	
l. Ignite midcourse motor	Event 18h+44 min	CC&S M-6	Pyrotechnics	Relay pulsed
m. Stop midcourse motor	Event 18l+0.060 to 102.34 s (0.040- to 0.080-s resolution)	CC&S M-7	Pyrotechnics	Relay pulsed; magnitude inserted by QC-V1-3 before maneuver start

Table VI-1 (contd)

Event	Time	Source	Destination	Comments
19. Commence automatic reacquisition of references	Event 18h+50 min	CC&S M-1 and M-2	AC	If L-3 has failed to operate in event 16, Canopus sensor will be turned off by this signal; this condition can be corrected by sending DC-V13
Switch to data mode 2		AC	DE	Backup: DC-V2
20. Sun acquisition complete	Event 19+0 to 20 min	—	—	
21. Canopus acquisition complete	Event 20+0 to 60 min	—	—	
22. Turn off maneuver counter	Event 18f+199 min	CC&S	CC&S	Internal function to CC&S that permits subsequent maneuver to be executed
23. Maneuver sequence inhibit	Event 22+10 min	—	—	Loading minimum turns and motor-burn times into CC&S maneuver clock prevents possibility of maximum-duration maneuver events occurring if CC&S maneuver clock was actuated as a result of certain possible component failures
a. Load minimum pitch-turn duration		Command QC-V1-1	CC&S	
b. Load minimum roll-turn duration		Command QC-V1-2	CC&S	
c. Load minimum motor-burn duration		Command QC-V1-3	CC&S	
24. Transfer to TWT[d] amplifier	T+10 days (nominal)	Command DC-V7	Radio	This transfers radio power amplifier from low-power cavity amplifier used during launch to higher power TWT amplifier
25. Second maneuver sequence Repeat steps 18–23 if a second maneuver is required	—	—	—	
26. Switch bit rate to 8⅓ bits/s	E−87.0 days	CC&S MT-6	DE	Backup: DC-V5
27. Set Canopus sensor cone angle No. 1	E−56.4 days	CC&S MT-1	AC	Backup: DC-V17
28. Set Canopus sensor cone angle No. 2	E−39.7 days	CC&S MT-2	AC	Backup: DC-V17
29. Set Canopus sensor cone angle No. 3	E−23.0 days	CC&S MT-3	AC	Backup: DC-V17
30. Transmit via high-gain antenna—receive via low-gain antenna	E−18.5 days	CC&S MT-5	Radio	Backup: DC-V10
31. Set Canopus sensor cone angle No. 4	E−9.2 days	CC&S MT-4	AC	Backup: DC-V17
32. Turn off ranging	E−19⅓ h	CC&S CY-1	Radio	CC&S CY-1 turns ranging receiver off; S-band occultation constraints preclude ranging turn-on during occultation period; backup: DC-V9
33. Begin encounter sequence	E−12⅔ h (nominal)	CC&S MT-7	Power	Backup: DC-V25
a. Tape recorder power on		MT-7	Power	Tape recorder receives power; however, recording sequence is inhibited
b. Energize terminator sensor		MT-7	Pyrotechnics	
c. Battery charger to boost mode		MT-7	Power	

[d]TWT = traveling-wave tube.

Table VI-1 (contd)

Event	Time	Source	Destination	Comments
34. Begin DAS encounter mode	E−6 h (nominal)	CC&S MT-8	DAS	Backup: DC-V24
a. Switch to data mode 3	—	DAS	DE	With data mode 3, a faster sample rate for science data is established for real-time transmission by eliminating engineering frame from data format; no data are stored at this time
b. Planet-sensor power on	—	DAS	Planet sensor	
c. Switch plasma probe to encounter format	—	DAS	Plasma probe	
d. Remove inhibit from timer B	—	DAS	Timer B	
35. Initiate DAS timer A	E−3 h, 8 min (approx)	Command DC-V16	DAS	DC-V16 is transmitted at a time so that outputs from timer A occur to serve as backups to critical encounter events
36. Acquisition of planet (PSO)[e]	E−60 ±12 min	Planet sensor	DAS	
a. Start timer B	—	Planet sensor	DAS	MT-8 or DC-V24 must have occurred
b. Start tape recorder	E−59 min, 10 s	DAS	Tape recorder	Tape recorder requires approx 0.25 s to reach record speed
c. Begin track 1 recording	E−59 min, 10 s	DAS	Tape recorder	Data to track 1 preceded by 80 zeros
d. Begin UV-photometer high data rate	—	DAS	DAS	
e. Inhibit UV-photometer calibrate signal	—	DAS	UV photometer	Inhibit removed by timer A or B
f. Issue backup	Receipt of DC-V16+121 min (approx)	Timer A	DAS	Backup for PSO event
37. Begin track 2 recording	Event 36 (PSO) +13.45 min	DAS (timer B)	Tape recorder	Begins high-data-rate sampling and storage of DFR data; 80 zeros precede data
Issue backup	Receipt of DC-V16+ 2 h, 13 min (approx)	DAS (timer A)	Tape recorder	
38. Enter occultation	E−5 min (nominal estimate)	Trajectory	—	During period preceding occultation, RF signal transmitted from earth-based transmitters will be refracted through atmosphere of planet
39. Closest approach	E = 0	—	—	
40. Antenna pointing angle change	E+8 min (approx)	Terminator sensor	Pyrotechnics	Pyrotechnics activates a pin-puller that allows antenna to change position for optimizing S-band occultation experiment; for command backup, see event 45
Issue backup	Receipt of DC-V16 + 3 h, 8 min (approx), E+15 min (approx)	DAS (timer A)	Pyrotechnics	Timer output serves as backup to terminator sensor
41. Exit occultation	E+21 min (nominal estimate)	Trajectory	—	Spacecraft RF signal emerges from behind planet
42. Stop recording on track 2	Event 37+107.5 min	DAS (timer B)	Tape recorder	Terminate storage of dual-frequency radio propagation data
Issue backup	Receipt of DC-V16 + 4 h, 2 min (approx)	DAS (timer A)	Tape recorder	An output of timer A serves as a backup for this event from timer B

[e]PSO = planet sensor output.

Table VI-1 (contd)

Event	Time	Source	Destination	Comments
43. EOT[f] in tape recorder	E+1 h, 10 ±3 min	Tape recorder (EOT foil)	Tape recorder DAS	This stops record motor and thereby terminates data-storage sequence
44. Switch to data mode 2	E+1 h, 14 min	DAS (timer B)	DE	Backup: DC-V2
a. Start sending "stop tape" commands	—	DAS (timer B)	Tape recorder	Backup to event 43; "stop tape" commands issued every 50.4 s from this point
b. Planet sensor off	—	DAS (timer B)	Planet sensor	
c. Release UV-photometer calibrate inhibit	—	DAS (timer B)	UV photometer	
d. Switch plasma probe to cruise format	—	DAS	Plasma probe	
e. Issue backup	Receipt of DC-V16 +4 h, 15 min (approx)	Timer A	DAS	Timer A serves as a backup for event 44
f. Inhibit encounter outputs of timers A and B	—	DAS	Timers A and B	
45. Transmit DC-V22	As soon as possible after exit occultation (if necessary)	Command	Pyrotechnics	Because of high doppler rates that exist during encounter, successful command transmission could not be assumed until some time after encounter
46. Transmit DC-V9	As soon as possible after two-way lock is established	Command	Radio	Turns on ranging receiver
47. Switch to data mode 4	E+14 h	CC&S MT-9	DE	Backup: DC-V4
Begin stored-data playback	—	DE	Tape recorder	
48. Switch tape-recorder data tracks	E+32.2 h	EOT foil	Tape recorder	Backup: DC-V3
49. Turn off ranging	E+1 day (23.33 h)	CC&S CY-1	Radio	Backup: DC-V9
50. End of first data playback	E+2 days (2.4 h)	Tape recorder	—	Data playback consists of approx 1 h of real-time engineering data followed by 17 h of science data on track 1, and approx 2 h of real-time engineering data followed by 14 h of science data followed by 1 h of real-time engineering data on track 2 (no assurance existed as to which track tape recorder would select to begin playback)
51. Start of second data playback	E+2 days (2.4 h)	EOT foil	Tape recorder	Second playback was an optional operation
52. Transmit DC-V9	E+2 days (2.9 h)	Command	Radio	Turn on ranging receiver assuming no second data playback
53. Switch tape-recorder data tracks	E+2 days (20.6 h)	EOT foil	Tape recorder	Backup: DC-V3
54. End of second data playback	E+3 days (14.8 h)	Tape recorder	—	
55. Switch to data mode 2	E+3 days (14.8 h) (approx)	Command DC-V2	DE	If only one playback of stored data is performed, this command would be transmitted after first playback sequence is terminated
56. Transmit DC-V9 commands	At appropriate Goldstone rise times	Command	Radio	Exercise ranging subsystem as long as capability lasts

[f]EOT = end of tape.

Table VI-2. Major deviations from nominal flight sequence

No.	Deviation	No.	Deviation
1	The spacecraft was rolled three times following the midcourse maneuver to allow the UV photometer to scan for atomic hydrogen in the extended atmosphere of the earth and as a calibration of the instrument.	6	A bit-rate change exercise was performed for UV-photometer calibration and signal-level change monitoring.
2	Lunar ranging was turned on after the midcourse maneuver to obtain an independent data source for orbit redetermination.	7	The spacecraft was rolled three times to allow the UV photometer a calibration at 8⅓ bits/s when the spacecraft had completed 180 deg of a revolution, in the heliocentric orbit, from No. 1, above. The dual-frequency radio propagation experiment also wanted these data for comparison with the earth-based measurements of antenna patterns.
3	The battery charger was turned off when the battery was fully charged.		
4	The planetary encounter sequence was modified by ground command to provide maximum in backup capability for all critical functions.	8	An encounter exercise and midcourse pointing exercise were combined to allow a calibration of the UV photometer by repointing the sensor at the point in celestial space it had been observing at the time of the CC&S MT-6 event.
5	Planetary ranging was obtained as close to the planet before encounter as possible for celestial mechanics and orbit determination.	9	The spacecraft was conditioned for the long-term cruise.

Table VI-3. *Mariner V* sequence of events

Date, 1967	Time, GMT	Event
Jun 14	06:01:00	Liftoff
	06:27:17	RF power up, science on, plasma-probe high voltage on, CC&S relay-hold off, *Agena* channel F telemetry off, pyrotechnics armed, SIT[a] started, AC on, and tape recorder launch mode off
	06:30:19	Solar panels and deployable sun shade deployed
	06:43:25	Sun acquisition complete; beginning of magnetometer-calibrate roll
	06:53:57	CC&S L-1 event (deploy solar panels and deployable sun shade); no action (preempted by SIT)
	06:57:56	CC&S L-2 event (turn on AC); no action (preempted by PAS[b])
	22:38:00	CC&S L-3 event (turn on Canopus sensor); spacecraft into roll search
Jun 15	01:12:26	Gyroscopes off; spacecraft had acquired Canopus after two roll-override commands (DC-V21)
Jun 19	21:23:57	Trajectory-correction maneuver initiated (DC-V27)
	23:08:11	Start motor burn
	23:32:19	Sun and Canopus reacquired after trajectory-correction maneuver
Jun 20	02:09:49	Gyroscopes off upon completion of three rolls for UV photometer
	02:30:18	Last of minimum turn and motor-burn-duration commands observed
	02:39:00	Ranging receiver turned on (DC-V9 No. 1)
Jun 27	00:28:00	DC-V7 (switch power amplifiers) transmitted; TWT into 90-s warmup, then standard mode at 40.2-dBmW output
	00:59:05	Battery charger off; boost mode enabled
Jul 24	19:19:21	CC&S MT-6 (switch bit rates) transferred telemetry to 8⅓ bits/s
Aug 24	08:41:33	CC&S MT-1 (Canopus sensor cone-angle update) switched sensor cone angle from 79.7 to 84.5 deg
Sep 10	00:41:52	CC&S MT-2 (Canopus sensor cone-angle update) switched sensor cone angle from 84.5 to 90.0 deg
Sep 26	16:42:43	CC&S MT-3 (Canopus sensor cone-angle update) switched sensor cone angle from 90.0 to 95.2 deg
Oct 1	16:43:08	CC&S MT-5 (transfer spacecraft transmitter to high-gain antenna)
Oct 10	14:04:14	CC&S MT-4 (Canopus sensor cone-angle update) switched sensor cone angle from 95.2 to 100.3 deg
	14:25:00	DC-V15 (Canopus-gate-inhibit override) transmitted

[a]SIT = separation-initiated timer.
[b]PAS = pyrotechnics arming switch.

Table VI-3 (contd)

Date, 1967	Time, GMT	Event
Oct 19	02:49:00	DC-V25 (begin encounter sequence; tape recorder on) transmitted; tape recorder on, terminator sensor excitation on, and science-overload-inhibit override on
	04:45:06	CC&S MT-7 (begin encounter sequence; tape recorder on); no action (preempted by DC-V25)
	08:50:00	DC-V9 (turn on ranging receiver No. 16) transmitted
	10:50:00	DC-V24 (begin DAS encounter mode) transmitted; DE switched to data mode 3, DAS clock B enabled, planet sensor excitation on, and plasma probe to mode 3
	11:25:04	CC&S MT-8 (begin DAS encounter mode); no action (preempted by DC-V24)
	15:01:43	DC-V16 (start encounter backup clock) transmitted; DAS clock A enabled, and science frame count reset to zero
	16:33:57	Planet sensor output, start DAS timer B, start tape-recorder record motor, begin track 1 recording, and inhibit UV-photometer calibrate signal
	16:40:00	DC-V9 (turn off ranging receiver No. 2 by command) transmitted
	17:46:51	Terminator sensor output and APAC
	18:41:51	*Tape recorder EOT and tape-recorder record motor off*
	18:48:18	Switch to data mode 2, DAS clock B inhibit outputs of timers A and B, planet sensor off, release UV-photometer calibration inhibit, and switch plasma probe to cruise format
	19:00:00	*DC-V9 (turn on ranging receiver No. 17) transmitted*
Oct 20	07:25:23	CC&S MT-9, start of Venus recorded data playback; data encoder transferred to data mode 4
Oct 21	18:45:00	DC-V9 (turn on ranging receiver No. 18) transmitted (CC&S CY-1 No. 47 had turned it off)
Oct 23	07:55:00	DC-V2 (data encoder transferred to data mode 2, tape recorder to standby mode) transmitted; a later DC-V28 turned on battery charger
Oct 25	20:35:00	DC-V5 (switch back to 8⅓ bits/s) transmitted; earlier DC-V5 switched to 33⅓ bits/s
Oct 26	20:55:00	DC-V19 (return AC to normal mode) transmitted; DC-V28 turned off battery charger
Nov 7	09:15:00	DC-V26 (turn science off) transmitted; subsequent commands turned science on; data mode 3, tape recorder on, started DAS clock A counting; switched to data mode 2; started record sequence; rolled spacecraft; acquired Canopus; rolled spacecraft; switched to transmit low-gain antenna; acquired Canopus; rolled spacecraft; EOT stopped record sequence; acquired Canopus; switched to transmit high-gain antenna (this ended recording of three-roll UV-photometer calibration data)
Nov 8	21:00:00	DC-V4 (mode 4 begin data playback) transmitted; subsequent commands switched tape recorder to standby mode and restarted playback
Nov 10	18:58:10	DC-V2 (transfer data encoder to data mode 2, and tape recorder to standby mode) transmitted; subsequent commands turned tape recorder off, battery charger on, and battery charger off
Nov 19	13:00:00	QC-V1-1 (−17.18-deg pitch) transmitted; subsequent commands to point UV photometer at CC&S MT-6 point in celestial space set up roll magnitude; removed maneuver inhibit; turned science off; turned science on; data mode 3, tape recorder on, started DAS clock A counting; switched to data mode 2; armed first burn; initiated midcourse-maneuver sequence; gyros on, data mode 1; switched to data mode 2; switched to transmit low-gain antenna; started record sequence; pitched; rolled; reacquired sun; acquired Canopus; EOT stopped record sequence; switched to transmit high-gain antenna
	18:40:00	DC-V13 (maneuver command inhibit) transmitted; subsequent commands removed science on/overload-inhibit override; turned science off; turned science on; minimum pitch; minimum roll; minimum burn duration; transmit and receive on high-gain antenna
	22:00:00	DC-V4 (start tape playback) transmitted
Nov 20	16:58:10	DC-V2 (transfer data encoder to data mode 2, tape recorder to standby mode) transmitted; subsequent commands turned tape recorder off; battery charger on; battery charger off; started DAS clock A counting to restore plasma-probe mode 2 format
Nov 21	19:18:05	DC-V12 (switch receiver and transmitter to low-gain antenna) transmitted; previous commands turned on ranging for twenty-first time; established Canopus gate inhibit override mode; turned off ranging for third time by command; switched receiver to low-gain antenna
Dec 1	—	Project end of *Mariner* Venus 67 mission—Phase I
Dec 4	20:00:00	Last tracking of *Mariner V* at −170.0-dBmW signal level

Table VI-4. Spacecraft problems and minor anomalies during mission

No.	Problem
1	UV-photometer tube-C reading had a step function decrease in average reading following trajectory-correction maneuver
2	UV-photometer calibrates and drift checks changed frame count on which they occurred following trajectory-correction maneuver
3	Trajectory-correction maneuver change in velocity was smaller than predicted
4	UV-photometer tube-C reading increased significantly more than expected at the switch in data-encoder bit rate (CC&S MT-6) to 8⅓ bits/s
5	CC&S produced two event-register indications when master-timer events and cyclic events occurred concurrently
6	SAGC[a] and data-subcarrier SNR[b] increased at switch in data-encoder bit rate from 33⅓ to 8⅓ bits/s

No.	Minor anomaly
1	Data-encoder deck skip upon arming of pyrotechnics
2	Sun sensors acquired earth-straylight false null
3	Canopus sensor acquired earth straylight during Canopus search
4	Open-circuit voltage of standard solar cell higher than predicted
5	Ranging receiver turn-on was observable by small current and temperature increases
6	Many small roll transients observed
7	Battery charger off produced a data-encoder deck skip and a DAS status-bit change in step
8	UV-photometer temperature increased above predicted value after switch to 8⅓ bits/s
9	White TCRs[c] degraded (darkened) faster than predicted; black TCR degraded (bleached) faster than predicted
10	UV photometer had a slight error in pointing angle
11	PIPS[d] propellant decomposition caused a slight pressure increase
12	Transmission of DC-V9 caused command subsystem to drop lock
13	Earth sensor observed Venus straylight, which had not been predicted
14	Tape-recorder subsystem dropped a few bits during playback
15	Solar panels degraded because of radiation damage
16	UV photometer tube-C data were much higher than predicted when spacecraft was pitched and rolled to point in celestial sphere where CC&S MT-6 had occurred
17	Planet sensor observed both first and second limb of Venus
18	APAC[e] squib had shorted combustion products that produced an event at APAC backup

[a]SAGC = station automatic gain control.
[b]SNR = signal-to-noise ratio.
[c]TCR = temperature-control reference.
[d]PIPS = postinjection propulsion system.
[e]APAC = antenna pointing angle change.

The Deep Space Station (DSS) at Cape Kennedy (DSS 71) tracked the spacecraft until L+7 min. At the nominal time for shroud ejection, the received carrier power from the spacecraft increased, indicating shroud ejection. After DSS 71 set, the *Agena* channel F (98-kHz) spacecraft telemetry was sent from Antigua by a submarine cable to DSS 71, and was processed in real time until L+12 min. Ascension (DSS 72) transmitted data from L+22 min, 14 s until L+26 min in real time to the Space Flight Operations Facility (SFOF). During that period, spacecraft telemetry confirmed that the solar panels were reacting to sunlight. At L+28 min, 45 s, Johannesburg (DSS 51) acquired demodulator lock, and data were continuously available after that time.

When DSS 51 acquired the spacecraft, the data-encoder event channels had changed from a reading of 0614 to 2735 (octal), indicating that all separation functions had occurred normally; i.e., pyrotechnics were armed, pyrotechnic current flowed in A and B channels, and all four solar panels were deployed. Other telemetry measurements indicated that the sun shade was deployed, science was on, radio power was switched to the high-power mode, the tape-recorder launch motor was off, the CC&S relay hold was off, and the spacecraft was starting to acquire the sun. A data-encoder deck skip (probably associated with the arming of pyrotechnics upon spacecraft separation) occurred. Deck skips with this event had been experienced during the system testing; therefore, this one was considered normal.

The sun sensors that were activated by the pyrotechnics arming switch (PAS) upon spacecraft separation initially had saturated outputs. The spacecraft was driven cw in pitch and ccw in yaw to acquire the sun. Earthlight on the secondary sun sensors biased the electrical null at least 78 mrad (4.5 deg) off the spacecraft–sun line. The attitude-control (AC) subsystem acquired the false null in yaw at 06:33:50 GMT, and began to limit-cycle about it. The sun-gate FOV was a cone of approximately 5.1 deg. Fortunately, the location of the false null was such that points of its limit cycle placed the sun in the sun-gate FOV.

The AC subsystem acquired the sun-gate event at 06:44:23 GMT, indicating that the pitch axis was also less than 5.1 deg. The sun-gate event terminated the power to the secondary sun sensors, which removed the false null and allowed the sun to be acquired. This placed the spacecraft into a programmed roll at 12.4 deg/min to furnish calibration data for the magnetometer.

At 06:53:56.6 GMT, telemetry showed an event in register 2, indicating that the CC&S L-1 event had occurred on time. The solar panels had been deployed by the separation-initiated timer (SIT), so there were no other changes at that time. No events occurred in registers 1 and 3, which indicated that no short circuits existed in the combustion products from the SIT solar-panel pin-puller squib firings. The CC&S LT-2 event occurred normally at 06:57:56.0 GMT, backing up the already completed PAS function of turning on the AC sun sensors and acquisition logic.

The roll for the magnetometer calibration was a spin of -3.6 mrad/s, which was within the resolution of the telemetry and the roll-rate deadband and about the nominal spin rate of -3.5 mrad/s. There were 33 complete rolls during the calibration period. The magnetometer, TRD, and plasma probe each observed the magnetopause and shockwave of the earth, and gave the expected indications.

Mariner IV had an earth detector that shared a telemetry channel with the roll gyro. When the gyros were on, however, only the roll-gyro output was available. It was recognized that, for the *Mariner* Venus 67 mission, the earth sensor could be used as a backup for the Canopus sensor to perform the trajectory-correction maneuver. This backup capability required that the earth sensor have its own high-rate telemetry channel so that its output could be read out while the gyros were on. This also provided the capability for the earth sensor to view the earth during each roll of the magnetometer calibration. The data provided on the apparent motion of the earth and its size allowed an accurate prediction of the spacecraft spin rate. This rate was extrapolated to the CC&S L-3 event to determine where in the celestial sphere the Canopus sensor would be pointing at turn-on. A prediction of the objects that might be acquired by the Canopus sensor was thus allowed.

On June 14, 1967, at 22:38:00.5 GMT, the CC&S L-3 event was observed in the data. The Canopus-sensor telemetry confirmed that it was powered, and the spacecraft went into a normal roll search. Before launch, it was recognized that the Canopus sensor might be able to acquire straylight from the earth. Modeling of the terrestrial straylight was very difficult, and was felt to be an order-of-magnitude indication only; the cone angle of the earth at acquisition was 111 deg, or 30 deg outside of the Canopus-sensor FOV, and the effective Canopus ratio of earth was approximately 2.5×10^6 times Canopus. As predicted, the straylight from the earth was able to enter the sensor FOV, and permit acquisition of earth straylight at 22:49:01 GMT. The predicted earth brightness was 0.75 times that of Canopus, and the maximum straylight brightness detected was 2.5 times that of Canopus, indicating that the prediction technique was good.

It was recognized that the spacecraft could remain acquired to earth straylight for several days until the brightness fell below the Canopus-sensor dropout gate. The spacecraft would then automatically search to Canopus and acquire it. No advantage was apparent in following that plan, whereas there was an advantage in acquiring Canopus early. The major advantage was to establish the pretrajectory correction cruise phase as early as possible. This argument centered on the level of personnel coverage required to monitor spacecraft performance. However, if the spacecraft were left alone, the exact time of the roll search to Canopus could not be predicted, and many spacecraft performance analysis and command (SPAC) members would be required to monitor the data.

It was decided to proceed with the Canopus acquisition via ground command from DSS 11. The first roll-override command (DC-V21) was transmitted to the spacecraft and verified in the telemetry at 00:31:07 GMT on June 15, 1967. The gyros turned on, and the spacecraft went into a normal roll search off the first stable null of the earth. In an effort to prevent the gyros from turning off if a reacquisition were accomplished on the second stable null of the earth, a second DC-V21 was sent 4 min after the first. The second DC-V21 caused the spacecraft to roll off the terrestrial straylight second stable null, and to search until acquisition of lunar straylight was achieved. On the basis of the brightness of the earth straylight, the acquisition of the lunar straylight was predicted. The lunar straylight apparently did not have a stable null, and a limit cycle was not established; the sensor moved off of the lunar straylight in the ccw search direction, indicating a low gate dropout of 0:22–0.19 $\times$ Canopus. The maximum observed lunar straylight was 1.6 $\times$ Canopus. The spacecraft acquired Canopus at 01:09:02 GMT, which established the logic for gyro turn-off some 200 s later. This completely normal sequence was the initiation of the pretrajectory-correction cruise phase of the mission.

2. Pretrajectory-correction cruise. This portion of the early flight was mainly without incident, except that the temperature-control references did not follow the preflight predictions. The white samples had an increase in absorptance (darkening) that was larger than anticipated, and the black sample began bleaching at a faster rate than expected. These changes had no effect upon the mission, but supplied information that could be used for the temperature control of future spacecraft. All spacecraft temperatures were within 2°F of their predictions, and all external equipment showed larger deviations, but all were well within tolerances.

Although the open-circuit voltage of the standard solar cell had the predicted output, the short-circuit current of the standard cell was approximately 4% above the predicted preflight values. An investigation revealed that the current-sampling resistors used during the 80,000-ft balloon calibration were not those used for the *Mariner V* flight subsystem. The short-circuit current for the standard solar cell was recalibrated on the basis of this information, and a new prediction was generated.

The spacecraft continued to function in a very nominal manner. SPAC had completed the trajectory-correction maneuver planning, testing, and selection of the aiming point in concert with other project elements. To redetermine the spacecraft orbital parameters quickly and accurately, it was recommended that the trajectory-correction maneuver be performed as early as possible. A thorough evaluation of the available information indicated that the optimum date for the first trajectory-correction attempt would be June 19, 1967, during the DSS 11 pass, with June 20 and 21 as alternatives.

3. Trajectory-correction maneuver.

a. Midcourse maneuver. The trajectory-correction maneuver (M) was initiated at 21:24:46 GMT on June 19, 1967, and was successfully completed. Canopus acquisition was maintained until the inertial-control mode was established at M+60 min. Telemetry during the maneuver sequence verified that all turns were correct, and that the PIPS motor burn appeared to be normal.

The CC&S was programmed for a 304-s pitch turn that had a 55.267-deg magnitude. The pitch turn accomplished was a positive 55.18-deg turn from trajectory information, which was a 0.2-σ turn in terms of standard deviations. The CC&S was programmed for a 380-s roll turn that had a 70.946-deg magnitude. The roll turn accomplished was a positive 70.93-deg turn from trajectory information, which was a 0.04-σ turn in terms of standard deviations. The CC&S was programmed for a 17.651-s burn time, which is equivalent to 16.127 m/s in spacecraft velocity. The thrust chamber pressure telemetry was 1 or 2 DN (1.5%) below the burning time estimation calculation (**BUTEC**) predictions, but well within tolerance.

That the autopilot maintained the thrust-vector orientation of the spacecraft during the motor burn was inferred by the postmidcourse analysis of the pitch and roll turns. The analysis of the AC subsystem indicated large deflections of the jet vanes during the motor burn. The trajectory analysis indicated that a 15.392-m/s change in velocity occurred as a result of the motor burn, which was 4.5% (approximately 6 σ) less than the desired motor burn. This moved the aiming point from $\mathbf{B} \cdot \mathbf{T}$ of 81,483 to 24,278 km; $\mathbf{B} \cdot \mathbf{R}$ of 65,340 to −14,855 km; and time of arrival from 03:53 to 17:59 GMT on October 19, 1967.

The analysis of this problem is described separately in Section VII of this report. The trajectory-correction maneuver, although not optimum, did not violate any engineering constraints, and provided a Venus miss distance of 2480 mi, which satisfied all of the science requirements and removed the necessity of performing a second trajectory maneuver.

b. Battery sharing. The magnitude of the pitch turn (55.18 deg) was great enough to cause the deployed sun shade to shade the first few solar cells on the end of solar panel 4A7. This effectively cut off the current flow in each of the solar cells shaded. The solar cells were in three sections on each panel, arranged in series–parallel combinations to produce the desired current and voltage. When the current flow from solar panel 4A7 was inhibited, the spacecraft went into a battery-share mode. When the spacecraft performed the 70.93-deg roll turn, solar panel 4A7 again became sunlit, and current began to flow. The end of solar panel 4A5 became partially shaded, so some sections did not produce current. The maneuver required a total of 2.33 A-h to be drained from the battery, which exceeded the predicted amount for unshaded, conducting solar panels.

The geometry of the sun shade in the deployed position, the solar-panel celled surface, and the pitch turn was such that the end of the panel was certain to be shaded. It was thought that the cells would not conduct when shaded, and thus perform as if they were open-circuited, requiring additional battery drain. This was not a problem, as 53.17 A-h battery capacity remained.

c. Bay 2 primary sun-sensor temperature. During the trajectory-correction maneuver, the bay 2 primary sun sensor reached a maximum temperature of about 98°F, which was 12°F lower than predicted. These data were of considerable interest because the primary sun sensors represented a key factor in determining the pitch constraint of a possible second midcourse maneuver near Venus encounter. The difference between the predicted and actual ΔT was almost wholly attributed to a less-severe "soakback" from the motor burn than had been expected. Most of the increase in temperature was attributed to solar heating, which agreed very well with predictions. The thermal analysis that constrained the pitch angle for near-sun maneuvers considered only that heat factor; consequently, the constraints generated before launch appeared to be realistic.

d. Ultraviolet-photometer three-roll exercise. The start of sun reacquisition after the maneuver also switched the data encoder back to data mode 2. During the maneuver, science was on, but not read out, to allow more engineering data. The reacquisition of the sun was completed at 23:21:18.99 GMT after a normal sequence of slightly over 7 min. Canopus was reacquired at 23:32:27 GMT after a completely normal roll-search sequence. This reacquisition process also allowed the UV photometer to view an additional segment of the celestial sphere.

The UV photometer observed the earth and its upper atmosphere following spacecraft separation, as had been predicted. The instrument also observed atomic hydrogen in the extended upper atmosphere and a lesser amount in the anti-earth direction during the magnetometer calibration. These facts, plus the UV-photometer C-tube rest state of approximately 20 DN, which was slightly higher than predicted, caused the experimenter to request that the spacecraft be rolled following the midcourse maneuver.

The decision to roll the spacecraft three times after the midcourse maneuver was successfully completed was based upon the potential scientific value to be gained and the fact that no spacecraft function was required that had not been successfully performed in this flight.

The sequence was as follows: As soon as Canopus was acquired, command DC-V21 was sent to override Canopus acquisition and to put the spacecraft into the normal ccw roll search. The first DC-V21 was observed in the data at 23:34:07 GMT. Each of the roll overrides was accomplished before the gyros turned off to reduce the power transients induced into the spacecraft. Each of the three rolls in the roll-search mode was completely normal, and Canopus was reacquired for the last time before Venus encounter at 02:06:20 GMT on June 20, 1967. The gyros turned off approximately 200 s later preparatory to the cruise state following the trajectory-correction maneuver. These rolls allowed the UV photometer to *see*, during each roll, some stars that were ultraviolet sources; data were also obtained that showed the northern galactic hemisphere to contain a higher concentration of atomic hydrogen than does the southern galactic hemisphere.

e. Ultraviolet-photometer anomalies. Prior to the trajectory-correction maneuver, the UV-photometer calibrate occurred on frame numbers divisible by 16, and the drift checks on frame numbers divisible by 16 with a remainder of 8. Following this maneuver, the calibrate occurred on frame numbers divisible by 16 with a remainder of 7, and the drift check occurred on frame numbers divisible by 16 with a remainder of 15. The analysis of this problem is described in Section VII of this report.

The UV-photometer C-tube reading dropped from an average of 22 DN before the trajectory-correction maneuver to an average of 6 DN approximately 14 frames after the maneuver. The steady-state value of the reading remained an average of 6 DN after the rolls until the CC&S MT-6 event in July, when it increased to approximately 38 DN. The analysis of this problem is described in Section VII of this report.

During the three rolls for the UV photometer, each of the three tubes observed stars that were slightly outside of the UV-photometer FOV. An analysis was undertaken to understand where the three tubes were physically pointing. The error was found to be not sufficiently large to compromise the Venus-encounter data. This anomaly is discussed further in Subsection C-4 and Section VII of this report.

4. Interplanetary cruise. Following the reestablishment of cruise-mode operations after the trajectory corrections, the spacecraft entered the interplanetary-cruise phase of the mission. This phase continued until the start of the planetary-encounter phase on October 19, 1967. Included in the cruise phase were the following flight-operation sequences that modified the cruise configuration to some extent:

(1) The insertion of the maneuver minimum-turn and burn-duration commands as protection against a failure-induced, inadvertent trajectory-correction maneuver while the spacecraft was not being monitored.

(2) The turning on and off of the spacecraft ranging receiver.

(3) The switching of the spacecraft transmitter from the triode-cavity power amplifier to the traveling-wave tube (TWT) power amplifier to maximize the probability of mission success.

(4) The turning off of the battery charger when the battery was fully charged.

(5) The DC-V15 roll-control mode command to make the loss of the roll reference less likely.

The interplanetary-cruise portion of the mission included the execution of six CC&S master-timer (MT) commands and the occurrence of some minor anomalies.

a. Minimum-maneuver commands. The minimum-maneuver commands were transmitted to the spacecraft following the CC&S maneuver-counter-overflow event (the first time that new values could be stored in the CC&S after the start of the trajectory-correction maneuver). The minimum-pitch-turn command (the first to be sent) was observed in the data at 02:20:13 GMT on June 20, 1967. The three commands were transmitted on 5-min centers, and all produced the expected results. This series of commands was included at this point in the sequence to prevent the possibility of a maximum-duration maneuver occurring if the CC&S maneuver clock were activated as a result of certain possible component failures. This sequence was required because the Deep Space Network (DSN) could not track *Mariner V* continuously, as many other programs were being supported concurrently. The pitch turn was of most concern because of the decreasing heliocentric distance as the spacecraft neared Venus. This constraint on pitch turn became increasingly critical until November 19, 1967. The maximum pitch turn that was not a potential thermal risk to the spacecraft was ± 20 deg.

b. Ranging. The first time that *Mariner V* used the turn-around ranging capability was on June 20, 1967. At 02:39:00 GMT, a DC-V9 command was transmitted to activate the spacecraft ranging receiver to provide an additional independent data source for orbit redetermination after the maneuver. Ranging and doppler data could be used to determine whether a second trajectory-correction maneuver would be required. Using these data, it was determined that the second midcourse maneuver would not be required after 5 days of data had been acquired.

Additional considerations associated with the turning on of ranging for the first time were as follows: A spacecraft operating completely normally was required, and there was no known command action before the next CC&S cyclic. Concern about ranging was associated with a spacecraft-ranging problem discovered shortly before the launch of *Mariner IV*. All known sources of this problem (ranging receiver on induced RF self-lock) were designed out of the *Mariner V* spacecraft; for additional reliability, a ranging receiver turn-off function was added to the CC&S cyclic, which occurred every 66⅔ h.

Ranging-receiver performance was excellent throughout the mission, permitting use of ranging whenever the signal was above threshold, ranging time was available at the stations, and the need existed for orbit-determination or celestial-mechanics data.

When a DC-V9 command was transmitted to turn on the ranging receiver, many small indications showed that the command had been acted upon. An additional 0.7 W of 2.4-kHz power was required when the ranging receiver was on. The changes were not observed each time because the resolutions of the power channels were typically 1 W for channel 227 (2.4-kHz output amperes), 3.8 W for channel 203 (dual-booster input amperes), 1.8 W for channel 225 (solar panel 4A7 amperes), and 2.1 W for channel 205 (main-booster output amperes). The 0.7 W of additional power also caused the temperatures of the following to change by 1 DN part of the time: bays 4–8, Canopus sensor, tape recorder, and auxiliary oscillator (AO). The voltage-controlled oscillator (VCO) temperature increased by 1 or 2 DN each time. When the ranging receiver was switched off, all of the readings returned to their preranging levels.

All of these changes were normal. They were not observed during the testing phase because of the small magnitude of the changes that required complete steady-state conditions before making the change of state.

At 23:45:00 GMT on June 26, 1967, a DC-V9 command was transmitted, and the ranging receiver was turned off. This toggle capability of DC-V9 was checked to ensure that emergency-command action could be taken to correct any future failure or problem in any subsystem.

The Mark I (lunar) ranging system did not reach threshold until July 7, 1967. At that time, the geocentric range was in excess of 6×10^6 km. This was an uplink, received signal level of approximately -120 dBmW, which was much better than originally predicted.

c. Roll transient. At 21:08:20 GMT on June 23, 1967, a roll transient was observed. The Canopus sensor observed a bright object, and tracked it for several seconds. Optical control of the roll axis was not lost, and it took 11.5 min for the roll-limit cycle to return to normal. *Mariner IV* had many roll transients during its flight, necessitating an in-flight operational mode change. A *Mariner V* design change was made to remove the roll override associated with Canopus intensity, which was too high. The change proved to be very effective; more than 20 roll transients were observed in the *Mariner V* data, and none caused a loss of roll control.

Several models were proposed to explain the transients; the one that appeared to best fit the data in all cases attributed the transients to dust particles illuminated by the sun. This theory accounted for the large error signals observed, which could not be explained in terms of normal spacecraft motion. One of the hypotheses offered to explain the roll transients was that micrometeoroids impinging on the spacecraft either knocked loose dust held to the spacecraft electrostatically or produced spalling (possibly of thermal-control paint), and that these secondary particles passing through the view of the Canopus sensor were responsible for the sensor brightness readings.

d. Power amplifier switching by command. Early in the *Mariner V* flight, a formal recommendation was made to SPAC by telecommunications personnel to switch the radio to the TWT amplifier via ground-command action. This action represented the implementation of a radio flight plan formulated before launch. The recommendation was approved by SPAC, the Space Flight Operations Director (SFOD), and the project manager. Command action (DC-V7) was initiated on June 27, 1967, at 00:28:00 GMT, and the transfer from the cavity amplifier to the TWT amplifier was successfully completed.

This decision, which was based upon an evaluation of the characteristics of the two different amplifiers, was based upon the following considerations: The TWT had a predicted lifetime far in excess of the minimum *Mariner* Venus 67 mission requirements, and its known failure modes led to immediate, catastrophic failure. The cavity amplifier, however, was known to show definite aging effects that limited its useful lifetime to approximately twice the length of the *Mariner* Venus 67 Mission.

It was necessary to use the cavity amplifier for launch because the TWT did not have the low-power mode required for the launch phase; if the cavity amplifier were employed throughout the flight, however, it was probable that aging would degrade its performance approximately 2 dB by Venus encounter. This would have amounted to approximately 4 dB less capability, compared to the TWT, for obtaining RF occultation data. Consequently, operation of both the cavity amplifier and the TWT would be required for a successful mission. However, if the TWT were employed from some early point in the flight, it would be capable of serving for the entire mission (barring catastrophic failure). In case of TWT failure at some later time, the cavity amplifier would be available, undegraded by excessive use, for the balance of the flight. Thus, the mission could be successfully completed if either the TWT or a combination of the TWT and cavity amplifier were capable of operation. The additional backup capability afforded by the latter mode of operation led to its adoption for the flight.

Another factor contributed to the decision to transfer to the TWT by ground command: The spacecraft was designed with the capability to automatically transfer to the TWT by ground command from one power amplifier to the other if the amplifier output were to drop below a fixed point. Because the most likely failure mode of the TWT was catastrophic failure, automatic switching to the cavity amplifier would occur in case of such a failure. However, the most likely failure mode of the cavity amplifier was gradual degradation; therefore, if command capability were lost, the spacecraft could reach a state in which the cavity amplifier output was highly degraded, and yet not degraded enough to cause automatic switching to the TWT.

After the switch had been made from the cavity to the TWT amplifier, and the battery charger had been turned off, the low-gain-antenna mast temperature rose 11°F because of increased RF losses with higher TWT output. This effect had been observed in the simulator tests, and was not unexpected. If losses were uniform in the waveguide, about 0.5-W dissipation would account for this temperature rise. The magnetometer temperature also rose 4°F, indicating better-than-expected coupling with the low-gain antenna mast.

e. Battery charger turn-off. On June 27, 1967, at 00:58:00 GMT, the battery charger was turned off. The battery charger had returned 5.64 A-h to the battery since the maneuver, and it was fully charged with a capacity of 58.8 A-h. In an effort to demonstrate long-term battery storage in space, it was decided to keep the *Mariner V* battery fully charged during the flight

and not to trickle-charge it. The battery performance data could then be compared with those from *Mariner IV* to determine the better storage technique.

The battery-charger-off power transient produced a data-encoder deck skip and a malfunction in the DAS-read UV-status bit. The status bit normally alternates one, zero, one, zero, etc. Following the DC-V28 command, the bit remained a zero two frames in a row, thus changing the sequence. This behavior had no effect on any of the science instruments. Both of these events had occurred during system testing, and were not considered abnormal.

f. Central computer and sequencer master timer events. Six CC&S MT events occurred during the interplanetary-cruise phase of the *Mariner* Venus 67 mission. Although all of the commands issued by the CC&S were correctly transferred to the appropriate spacecraft subsystems, several anomalous indications accompanied the first command.

The first MT command issued was the bit-rate switch event (MT-6), which occurred on July 24, 1967, at 19:19:21 GMT. The data encoder responded normally, switching from a rate of 33⅓ to 8⅓ bits/s.

The data encoder responded to the MT-6 event by properly switching to 8⅓ bits/s and producing two events in register 2 because the CC&S cyclic (CY-1) No. 15 occurred at the same time. The investigation that followed revealed that the CC&S was so mechanized that, whenever a cyclic and an MT event occurred simultaneously, the cyclic relay was set 20 ms before the MT relay. The secondary set of relay contacts is capacitively coupled to the event-register circuit, with a time constant less than 20 ms. Two events were generated 20 ms apart. The data encoder can respond to events that are approximately 4 ms apart; therefore, this condition was normal.

The UV-photometer tube-C readings changed from an average of 6 to an average of 38 DN following MT-6. The predicted reading after MT-6 had been 20 DN. The investigation that followed indicated that the triggering voltage was at a steady-state level when the data were sampled at 8⅓ bits/s. This same voltage was in the transient stage and still increasing when the reading was sampled at 33⅓ bits/s. Because of these results, it was desirable to perform two tests in the postencounter phase. A detailed discussion of this problem is contained in Section VII of this report.

The ground-received automatic gain control (AGC) from the spacecraft increased from −147.6 to −146.6 dBmW, as observed by DSS 14 (the Goldstone Mars site, 210-ft antenna) at MT-6. At the same time, DSS 11 (the Goldstone Pioneer site, 85-ft antenna), which was concurrently tracking the spacecraft, reported an increase from −152.28 to −151.5 dBmW. The spacecraft ranging receiver was turned off by CC&S CY-1 No. 15, which would typically produce an increase of 0.7 dBmW. The signal-to-noise ratio (SNR) estimator had been set up at DSS 11 to monitor the MT-6 event. The SNR increased 6 dB, as was expected in the bit-rate change. The data-subcarrier SNR was observed to increase about 0.5–1 dB with respect to the carrier. It was impossible to tell whether this was because of the bit-rate change or noise-modulation removal because of ranging receiver turn-off. A bit-rate change was planned for inclusion in 1968 during the extended mission to answer this question. A test to resolve this problem was attempted with the ranging receiver off after Venus encounter. The station AGC (SAGC) did not appear to change within the station resolution, and it became apparent during later data evaluation that the SNR estimator was not set up correctly; these latter data were thus invalidated.

The UV-photometer temperature increased 2°F more than predicted following the bit-rate change. This unexpected temperature rise could be attributed to an increase in internal power dissipation of approximately 0.5 W within the instrument. Investigation indicated that this condition was normal. The duty cycle of the high-voltage power supply located in the sensor changed, leaving the high-voltage power supply on for a longer period at 8⅓ bits/s than at 33⅓ bits/s, and resulting in an average power-consumption increase of approximately 0.5 W in the instrument. This was not observed during testing because a steady-state condition must be reached before the bit-rate change and after it. Three days were required to establish that this was a real effect in flight.

The first Canopus-sensor cone-angle update (MT-1) was issued by the CC&S on August 24, 1967, at 08:41:33 GMT (as observed on earth). The event was normal in every respect in so far as the data were concerned, and telemetry subsequently verified that the cone angle had changed from the preset position of 79.68 deg to the MT-1 position of 84.45 deg (CC&S CY-1 No. 26 occurred concurrently, and produced the other expected event).

The second Canopus-sensor cone-angle update (MT-2) was observed in the telemetry data on September 10 at 00:41:52 GMT (CC&S CY-1 No. 32 occurred concurrently, and produced the other expected event). The

event was normal in every respect, and telemetry subsequently verified that the cone angle had changed to 90.04 deg.

The third Canopus-sensor cone-angle update (MT-3) was received in the data on September 26, 1967, at 16:42:43 GMT (CC&S CY-1 No. 38 occurred concurrently, and produced the other expected event). All data indicated a cone-angle update to 95.19 deg, which was normal in every respect.

The fifth CC&S MT command issued was the transmitter switch to the high-gain antenna (MT-5), which occurred on October 1, 1967, at 16:43:08 GMT. The SAGC changed from a reading of −165.4 to −156.8 dBmW following MT-5. This was well within the predicted signal-level change for the antenna–earth cone and clock angles. All of the expected changes were verified in the data. The removal of all RF losses from the low-gain antenna mast caused the antenna to drop 19°F in temperature. The magnetometer sensor also decreased significantly (7°F), indicating that the conductive coupling between the sensor and mast was quite good.

The fourth Canopus-sensor cone-angle update from 95.19 to 100.26 deg by a CC&S command (MT-4) occurred at 14:04:14 GMT on October 10, 1967. The event was normal in every respect (CC&S CY-1 No. 43 occurred concurrently, and produced the expected event).

g. Temperature-control references. The temperature-control reference (TCR) performance proved that independence from net absorbed solar thermal energy must be used for planetary spacecraft thermal design.

The S13-M white TCR went off scale on July 23, 1967, only 39 days after launch. The apparent solar absorptance had changed from 0.20 to 0.326 in a period that had been predicted to be from 60 to 100 days. These data indicate that more laboratory testing is required. The 0.12 change in absorptance in 900 h compares to two separate laboratory tests of 1200 and 1500 h wherein the results were 0.06 and 0.02, respectively. This rapid degradation was on a treated white paint that was formulated to improve stability for application in spacecraft design.

The S-13 white TCR went off scale on August 1, 1967, which was 32 days earlier than predicted from laboratory tests. The white paint on the TCR (the type used on the spacecraft for thermal control) was used, even though degradation was known to be relatively high, because it was the best characterized white paint available (S13-M was flown to AFETR for the S12-M TCR). The degradation rate was quite rapid for the first 4 days, after which the rate approached that of the S13-M sample. The solar absorptance of S-13 became a fairly constant 0.07 higher than the S13-M sample (on July 20, S-13 was 0.388, compared to S13-M of 0.319). This clearly shows that S13-M is a better white paint that, unfortunately, nevertheless degrades.

Thermal shades and shields were used on the *Mariner V* spacecraft for protection against direct-sunlight degradation of the white paint. The black TCR used Cat-A-Lac black paint, and went off scale on October 27, 1967, 22 days after the nominal expected time. Bleaching of approximately 4% of the black TCR had occurred by the time it went off scale. This black paint was used widely on the spacecraft where high absorptivity is required.

h. Thermal deviations. The thermal predictions were within tolerances for all measurements where the material properties did not change from those predicted. The lower thermal-shield temperature increased faster than expected because of degradation (darkening) of the Teflon outer layer; the effect upon the bus temperatures was negligible. The increased temperature did not represent a threat to the shield materials, which have a failure limit of 300°F compared to a predicted perihelion temperature of 249°F. Higher temperature on the lower thermal shield did, however, affect the plasma-probe and sun-sensor temperatures.

The primary sun-sensor temperatures had increased 19°F more than predicted by October 2, 1967. This increase was not considered a problem for encounter, but the extrapolation of these data to perihelion produced a prediction of 175°F for the bay 6 primary sun sensor. Although this estimate was conservative (high), it caused some concern because the upper type-approval (TA) level was 167°F, and a prolonged life test at 175°F was the only one run. The upper failure limit was thought to be over 200°F. (Indium solder melts at 230°F).

Nearly 20% of the increased temperature was thought to be caused by the darkening of the lower thermal shield, which increased the infrared input to the sides of the assembly and pedestal. The balance of the temperature rise was probably caused by a shifting of the solar shade towards the bus and by the reflectance properties of the Teflon. These would cause additional heat input to the sides of the pedestal and sensor assembly. Other possible causes could be flaking paint, transducer detachment, simulation inaccuracies, or a reduction in

conduction coupling. Of these possibilities, only the flaking paint is probable, as the same effects occurred on the plasma probe.

The plasma-probe temperature was 16°F above the predicted level by October 2, 1967. This was not a problem at encounter, but caused some concern at perihelion where the temperature was 293°F (at the transducer location). The critical component at high temperature is the high-voltage grid ring, which melts at 347°F. The grid ring probably was about 20°F warmer than the transducer at perihelion, providing a reasonable margin. The deviation from prediction was apparently caused by degradation (darkening) of the lower thermal shield and degradation of the S-13 white paint on the sides of the plasma probe. These effects increased the input of radiated infrared and reflected solar energy from the shield.

i. Ultraviolet-photometer pointing. The UV photometer observed the star Pi-Scorpii on August 22 and 23, 1967. Tube C peaked at approximately 120 DN, and tubes A and B each peaked at approximately 60 DN. The readings of each tube and the AC position were combined to determine the direction in which the tubes were pointing. The results were: 89.6 ±0.2 deg cone and 95.7 ±0.2 deg clock for tube B; 90.2 ±0.2 deg cone and 95.5 ±0.2 deg clock for tube A; 90.5 ±0.2 deg cone and 95.7 ±0.2 deg clock for tube C. These compared to 90.0 ±0.2 deg cone and 95.5 ±0.2 deg clock required for each tube.

The UV photometer observed the star Tau-Scorpii on August 29–31, 1967. Tube C peaked at approximately 160 DN, and tubes A and B peaked at approximately 90 DN. As expected, all tubes responded to the AC limit-cycling during the observation, and these data were used to refine the exact UV-photometer pointing angles. The results were: 89.4 ±0.2 deg cone and 95.8 ±0.2 deg clock for tube B; 90.3 ±0.2 deg cone and 95.7 ±0.2 deg clock for tube A; and 90.3 ±0.2 deg cone and 95.8 ±0.2 deg clock for tube C.

The tolerance between the sun sensors and the UV-photometer mounting pad was measured before launch as 6 s of arc. The allowable tolerance for the UV-photometer mounting pad was ±0.5, but was actually much better. The tolerance between the boresight of the tubes and the UV-photometer mounting pad was not measured, but was specified at ±0.2 deg in accordance with other measurements.

This minor pointing error has no effect upon the encounter data because the error was small and AC data were not telemetered during encounter. The reason for the small pointing error has not been determined.

j. Expected deviations. Many minor *Mariner IV* anomalies were not considered serious enough to require modification of the *Mariner V* design. These minor anomalies are briefly listed below to document that the *Mariner V* spacecraft performed as designed.

Frequency shift at CY-1. The *Mariner V* spacecraft-transmitted frequency increased by about 5 Hz at S-band frequency during the CC&S CY-1s. To achieve this effect, the station had to be in one-way RF lock with the spacecraft at the cyclic, and two-way RF lock had to be acquired during the previous 66⅔ h. The shift was produced by a slight loading of the AO supply voltage by logic circuits (whose state was controlled by the CC&S CY-1), which occurred every 66⅔ h. This effect was used to determine the CC&S timing more exactly. The accurate timing capability was used before the trajectory-correction maneuver to obtain desired telemetry during certain specific portions of the maneuver.

Postinjection propulsion system propellant decomposition. On August 22, 1967, an increase of 4 psi in the PIPS propellant-tank pressure was observed in the data. This change in pressure occurred earlier than predicted upon the basis of increasing temperature alone. The pressure increase was caused by an incompatibility between the propellant-tank butyl-rubber bladder and the hydrazine fuel, or (more literally) from propellant decomposition. This situation was noted during the *Mariner IV* flight, and was not a problem because the total change in pressure by the end of the mission amounted to only 16 psi.

Auxiliary-oscillator stability. The stability of the AO was very important to the mission because most of the Venus atmospheric data could only be obtained with the S-band occultation experiment going into and emerging from occultation in RF one-way lock. The AO was the frequency source of the RF signal when the spacecraft was in one-way RF lock with the receiving antenna on earth. Plots of both the AO frequency shift during warmup and the AO frequency stability were made at various times during the mission. This AO information enabled the S-band occultation experimenters to gain confidence in the repeatability of the warmup transient and the stability of the AO frequency. In general, the plots followed a predictable pattern, although occasionally an unexplained small deviation (on the order of ±3 Hz at S-band in most cases) occurred.

The most notable deviation occurred on July 23, 1967, between 02:44:00 and 03:34:00 GMT, when a change of 15 Hz at S-band took place. No correlation between spacecraft activity or DSN station operation could be made. Checks of the AO frequency after the deviation verified that the AO continued to operate very well, and that all deviations were well within stability-specification limits. Few (if any) correlations could be made between spacecraft or ground activity and the deviations from the normal warmup transients.

In future spacecraft designs, where the AO may be required for an experimental frequency source, the AO should be energized at all times, and be designed with temperature compensation built in. The present AO varies at a rate of approximately 350 Hz at S-band for each degree Fahrenheit of change.

k. Telecommunications grayout. Before launch, telecommunications predicted that a period (grayout) would exist when the spacecraft antenna sum of the negative tolerance (−158.5 dBmW) would not have the required gain to telemeter data that could be demodulated after they were received by a standard 85-ft Deep Space Instrumentation Facility (DSIF) antenna. It was also predicted that a period (blackout) would exist when the antenna nominal tolerance (−164.5 dBmW) would not have the required gain to telemeter data that could be demodulated after being received by a standard 85-ft DSIF antenna. The predicted grayout period was approximately September 5–29, and the blackout was September 23–28, if the switch to high-gain was commanded on the first day possible. The CC&S MT-5 command was chosen for October 1, 1967, which ensured a good signal after the switch to the high-gain antenna. During the planning phase, the blackout period required that the 210-ft antenna be used to receive telemetry.

Spacecraft performance followed the nominal predictions quite closely. After September 20, all stations reported signal levels less than −164.5 dBmW, for the greater part of each pass, until the switch on October 1. Useful data continued to be received after September 20. There were several reasons for this, none of which could be assured during the design phase. The DSN improved its performance on the 85-ft antennas approximately 1.4 dB by using a receive-only feed that reduced system-noise temperature. Two stations (DSS 12 and DSS 51) made modifications so that a 3-Hz loop bandwidth was used instead of the standard 12-Hz loop bandwidth. These two improvements yielded increased signal levels of approximately 3 db.

An additional aid was the introduction of a digital demodulation technique (**DDT**) computer program in half of the telemetry and command processor (TCP) computers at DSS 12 and DSS 51. This **DDT** program replaced the standard demodulator, and enabled the system to maintain telemetry lock at a lower signal level.

The AC limit-cycle motion also produced large differences in signal level during part of the grayout period. This was caused by two separate antenna phenomena: (1) The interferometer effect caused by the earth being aligned with the first side lobe of the high-gain directional antenna while the spacecraft was transmitting via the low-gain antenna caused a maximum of ±2.5-dB difference in the received signal strength; because this pattern was not large in terms of degrees, the AC limit-cycle motion caused the antenna to change pointing directions, which varied the size of the interferometer effect. (2) After the switch to transmitting via the high-gain antenna, the AC limit-cycle motion caused large variations in signal strength because the earth was just coming into the antenna pattern in cone and clock angles. Small angle changes produced large signal-level changes.

l. Cruise flight-testing for encounter. A few questions were raised in the design and planning of the encounter sequence that required flight testing. Each of these sequences was first tested under laboratory conditions, where large numbers of tests could be performed to obtain statistical results. After successful completion of the laboratory testing, a series of tests was performed on the flight-support spacecraft. These tests proved that the results did not change when the tests were performed in the total spacecraft environment. At this point, a presentation of successful test results was made to the project manager to show the advantages of each of the sequences during encounter. The project manager approved four of the five suggested changes, and these four were tried on the flight spacecraft well in advance of Venus encounter, thus to provide recovery time if any unforeseen development occurred.

The first test was conducted on July 22, 1967, with the transmission of DC-V9 to activate the ranging receiver. The test objective was to demonstrate that, with the spacecraft received carrier power reduced to the lowest expected uplink signal (−136 dBmW for this test), activation of the ranging receiver would cause a momentary drop of RF lock. (This happens because the ranging receiver uses the same power supply as the RF receiver; when ranging is turned on, the RF receiver VCO reacts to the voltage change by producing a frequency transient. When the RF receiver momentarily drops lock, it causes

the command subsystem to drop command lock as it did in this case.) The command was normalized for this test so that it was unable to reacquire lock itself. The test provided several useful items of information. The most important of these was the possibility that, when the RF lock was dropped, it might lock up on the command sideband, requiring turn-off of command modulation to regain RF lock. This possibility did not occur during this or any of the flight tests; however, if it had, command would have been reapplied with an offset frequency to regain lock. In this test, it would have been necessary to offset the frequency to regain lock if that had been desired.

On July 27, another DC-V9 was transmitted to activate the ranging receiver. This command was sent at a strong signal level (−123 dBmW), and produced a momentary command out-of-lock indication. The command was out of lock for such a short time that lock was reacquired even though command was normalized. Because relock with command normalized could not be assured, tests were then run with a non-normalized command subsystem.

It was recognized that sending commands with a non-normalized command subsystem provided a time saving of approximately 20 min at encounter (approximately 5 min to verify command lock, 1 min to change frequency, 9 min for two-way transmission, and 5 min to verify that solid command lock was still present). The first command to be sent without normalizing the command subsystem was a DC-V9 at 23:55:00 GMT on October 5. All subsequent commands were successfully received by the spacecraft, using this method. For the same reasons, this method of sending commands was used successfully during the *Mariner IV* encounter with Mars.

It was recognized that, if the ground-transmitted frequency could be updated with command modulation on and command in lock, SPAC could react to any problem more quickly. The previous method was to remove the command modulation, adjust the ground-transmitted frequency so that the spacecraft static phase error (SPE) stayed near zero (would go through zero) during the next period, then reapply command modulation and reacquire command lock. The first test of varying the SPE with command in lock was performed on October 14, 1967. The successful completion of the test allowed this sequence to be included in the encounter planning. The tuning rate of 3 cycles/min at the VCO was established as the safe rate at which to tune the ground transmitter. As an added safety measure, the tuning was done at the times established with the old sequence so that, if a problem occurred, there would be recovery time before the next critical event.

The last approved test was the application of ranging modulation while command modulation was applied and command was in lock. This test, successfully performed at 13:27 GMT on October 6, was desired to increase the total time during which ranging data could be gathered before encounter, and to allow ranging closer to the point of entering occultation. The latter capability allowed a potential increase in astronomical-unit (AU) resolution from 40 to 7 km. One change was made in the amount of suppression for ranging modulation when used with command modulation. When applying ranging modulation, 9 dBmW of suppression was usually used; however, this, totaled with command-modulation suppression (3.2 dBmW), exceeded 10 dB and approached the nonlinear operating range of the radio subsystem. Tests indicated that 6 dBmW of suppression for the ranging modulation allowed all subsystems to operate normally when command modulation was on. This value was used in all flight tests and in the actual operations.

The last test discussed, but declined by the project manager, was ranging during the transmission of commands. This capability would have provided additional ranging time by not requiring the removal of ranging modulation at least 10 min before any command action, then reapplying ranging modulation and reacquiring ranging lock. This capability was not granted on the basis that unknown interaction might exist that could not be planned for and could potentially abort encounter, whereas the added ranging capability would not significantly increase the value of the mission.

m. Planetary ranging. The spacecraft ranging receiver functioned independently of both the lunar-ranging and the planetary-ranging subsystems. The lunar- and planetary-ranging subsystems were both used during the Mark I (lunar) capability period to ensure that the new experimental planetary-ranging subsystem was functioning properly. After the Mark I ranging subsystem reached threshold on July 7, the planetary-ranging subsystem was used until it reached threshold for the low-gain antenna on July 30, 1967. This produced ranging data to a geocentric range in excess of 12×10^6 km at an uplink signal strength of approximately −123 dBmW.

After the MT-5 event that switched the transmitter to the high-gain antenna, the planetary-ranging capability was again used on October 10, 1967, and data were gathered through Venus encounter. The ranging receiver

was commanded on for the last time at 19:58 GMT on November 10, 1967, when ranging data were acquired. This was at a geocentric range in excess of 104×10^6 km. Planetary ranging was tried unsuccessfully on the last day of *Mariner V* operations (November 21, 1967). Three separate attempts to lock up the range code, each of 30-min duration, were unsuccessful; the ranging receiver was then turned off in preparation for long-term cruise.

n. Establishing encounter initial conditions (DC-V15). The only action required to establish the initial conditions for encounter was a modification of the AC logic. The DC-V15 command was transmitted at 14:25:00 GMT on October 10, 1967. This command (Canopus gate inhibit override) removed the low-brightness gate, and prevented the gyros from coming on if Canopus or sun acquisition were lost. The normal AC mode that had been used until then had performed very well. This mode was preferred while the spacecraft could not be tracked continuously because, if Canopus acquisition had been lost, the gyros-on event would have recorded that fact even while the spacecraft was not being tracked. *Mariner V* had been subjected to many roll transients, indicating that, under normal conditions, the normal mode functioned well. During encounter, however, the APAC would occur. The APAC event could possibly dislodge from the spacecraft particles that might pass in front of the Canopus sensor FOV. If the particle were moving slowly enough, and remained in the FOV long enough, it would have been possible for the spacecraft to track the particle and lose Canopus acquistion. In the normal mode, the spacecraft would go into the ccw roll-search mode as soon as the particle moved out of the FOV. The search rate was 7 deg/min, which meant that all outgoing occultation data would be lost if the particle were on the ccw side of Canopus. With DC-V15 in effect, the Canopus sensor would acquire another object when the particle left the FOV. It was considered unlikely that the spacecraft would track a particle more than a few degrees from Canopus; therefore, some useful occultation data should be possibly independent of roll direction. The DC-V15 produced the expected event in the data encoder when it was received. The command was sent on October 10, 1967, to provide a rather long operational experience base before encounter operations began. The AC performance was as expected during the time up to encounter, which reduced the total concern for encounter operations.

5. Planetary encounter. The basic design of the *Mariner V* spacecraft provided for a completely automatic planetary-encounter sequence without any ground action required. Because the ground-command option was available, however, there were a number of possible backups to the onboard functions; in addition, there were a number of alternate modes that might have been superior to the normal mode of operation.

To provide the best possible sequence of events for encounter, the Venus encounter planning working group (VEPWG) was formed in July 1967. The VEPWG was to operate in parallel with SPAC to investigate all spacecraft encounter-related operations and modes, and to recommend to the *Mariner* Venus 67 project manager a detailed sequence of events for encounter. The VEPWG was composed of appropriate SPAC, flight-path analysis and command (FPAC), space science analysis and command (SSAC), DSIF, DSN, SFOD, and S-band occultation experiment representatives, with the *Mariner V* SPAC director as chairman. Also formed was the occultation working group for the purpose of recommending the configuration of the SFOF, the DSIF stations, and the spacecraft, during occultation of the spacecraft by Venus, to provide the most meaningful occultation data.

The objectives of the VEPWG were as follows:

(1) Develop an encounter sequence that provides the maximum assurance of obtaining useful experimental instrument and occultation data.

(2) Determine the operational mode that provides the greatest assurance of maintaining atitude stabilization throughout encounter, thereby assuring real-time planetary field and particles data and occultation data.

(3) Provide for full use of backup methods for all critical functions.

(4) Select appropriate alternate modes for any operations that are both functionally critical and time-critical.

A recommended encounter sequence of events (Fig. VI-3) was formulated by the SPAC director on the basis of the VEPWG findings, and was approved by the *Mariner* Venus 67 project manager.

A problem in the *Mariner* Venus 67 encounter operations was transmission delay between earth and the spacecraft, although the problem was not as severe as it had been for the *Mariner* Mars 1964 encounter. Approximately 4.5 min were required from data transmission at the spacecraft until data presentation in SPAC; more than 4.5 min were required from command initiation at a DSN station until command execution at the spacecraft. Therefore, immediate response to anomalous indications

CRUISE PHASE	DC-V25	MT-7	ONE-WAY RF LOCK	TWO-WAY RF LOCK	DC-V9	DC-V24	MT-8	RANGING MODULATION ON	RANGING MODULATION OFF	DC-V16	RANGING MODULATION ON	RANGING MODULATION OFF	DC-V9	PLANET SENSOR OUTPUT
DATA AUTOMATION SUBSYSTEM ON						DAS CLOCKS A AND B ENABLED				DAS CLOCK A STARTS COUNTING				DAS CLOCK B STARTS COUNTING
UV PHOTOMETER ON														INHIBIT ULTRAVIOLET CALIBRATE
PLASMA-PROBE CRUISE FORMAT						PLASMA-PROBE MODE 3								
TOTAL SPACECRAFT POWER DEMAND (177 W)	TOTAL SPACECRAFT POWER DEMAND (184 W)				TOTAL SPACECRAFT POWER DEMAND (185 W)								TOTAL SPACECRAFT POWER DEMAND (184 W)	TOTAL SPACECRAFT POWER DEMAND (188 W)
DUAL-FREQUENCY RECEIVER ON								STANFORD TRANSMITTER ON, START OF PASS						
RANGING RECEIVER OFF					RANGING RECEIVER ON			TURN-AROUND RANGING FUNCTIONING	RANGING RECEIVER ON		TURN-AROUND RANGING FUNCTIONING	RANGING RECEIVER ON	RANGING RECEIVER OFF	
TAPE RECORDER 2.4-kHz POWER OFF	TAPE RECORDER 2.4-kHz POWER ON													
TERMINATOR SENSOR OFF	TERMINATOR SENSOR ENERGIZED													
PLANET SENSOR OFF						PLANET SENSOR ENERGIZED								PLANET SENSOR OUTPUT
DATA MODE 2						DATA MODE 3								
HIGH-GAIN ANTENNA PRE-ENCOUNTER POSITION														
TAPE RECORD MOTOR OFF	TAPE RECORD MOTOR STANDBY MODE													TAPE STARTS RECORDING TRACK I DATA
VCO (TWO-WAY RF LOCK)			AUXILIARY OSCILLATOR	VCO										
CRUISE PHASE ESTABLISHED AFTER THE SWITCH TO THE TRAVELING-WAVE TUBE ON JUNE 26, 1967 (PDT)	PREEMPTS MT-7; VERIFIES DC-V25 CAPABILITY IF NEEDED IN RECYCLE; PROVIDES CAPABILITY FOR SCIENCE TO BE ON WHEN GYROS ARE ON IF THE MAIN BOOSTER REGULATOR FAILED	BACKUP TO DC-V25; EXCEPT DOES NOT PROVIDE CAPABILITY FOR SCIENCE TO BE ON WHEN GYROS ARE ON IF THE MAIN BOOSTER REGULATOR FAILS	PROVIDES LAST AUXILIARY OSCILLATOR STABILITY CHECK BEFORE ENTERING OCCULTATION (AUXILIARY OSCILLATOR USED FOR ENTER-OCCULATION S-BAND EXPERIMENT)	END OF AUXILIARY OSCILLATOR STABILITY CHECK; NEED TWO-WAY CAPABILITY FOR COMMANDS, TWO-WAY DOPPLER, AND RANGING	SWITCH THE RANGING RECEIVER ON; THIS PROVIDES CAPABILITY TO TAKE PLANETARY-RANGING DATA	PREEMPTS MT-8; VERIFIES DC-V24 CAPABILITY IF NEEDED TO STOP DAS CLOCK B DURING A MALFUNCTION (DC-V24 IS A TOGGLE FUNCTION)	BACKUP TO DC-V24; EXCEPT IT IS NOT A TOGGLE FUNCTION	PROVIDES PLANETARY-RANGING DATA BEFORE CLOSEST APPROACH	TURN OFF RANGING MODULATION FOR TRANSMISSION OF DC-V16	TRANSMIT TIME SELECTED TO PROVIDE APAC BACKUP AT CENTER OF OCCULTATION AND DFR DATA NEAR ENCOUNTER; THE DAS CLOCK A OUTPUTS BACK UP CLOCK B OUTPUTS	PROVIDES PLANETARY-RANGING DATA BEFORE CLOSEST APPROACH	TURN OFF RANGING MODULATION FOR TRANSMISSION OF DC-V9	SWITCH RANGING RECEIVER OFF; INCREASED DOWNLINK SIGNAL ~0.7dBmW	ISSUED WHEN PLANE SENSOR "SEES" PLANET; STARTS DAS SENDING "START TAPE" COMMANDS; INHIBIT ULTRAVIOLET CALIBRATE, START DAS CLOCK B, WHIC STARTS SENDING TRACK I DATA TO TAPE; DAS CLOCK A BACKUP PROVIDED

(2)

F LOCK	ENTER OCCULTATION	TERMINATOR SENSOR OUTPUT	EXIT OCCULTATION	PLANET SENSOR OUTPUT +121 min	END-OF-TAPE	PLANET SENSOR OUTPUT +134 min	DC-V9	RANGING MODULATION ON	RANGING MODULATION OFF	ONE-WAY RF LOCK	TWO-WAY RF LOCK	MT-9	MT-9 +20 min	MT-9 +36 min	MT-9 +53 min
				DAS CLOCK B STOPS TRACK 2 DATA		DAS CLOCKS A AND B INHIBITED									
						ULTRAVIOLET CALIBRATE INHIBIT REMOVED									
						PLASMA PROBE CRUISE FORMAT									
					TOTAL SPACECRAFT POWER DEMAND (184 W)		TOTAL SPACECRAFT POWER DEMAND (185 W)					TOTAL SPACECRAFT POWER DEMAND (188 W)			
	STANFORD UPLINK SIGNAL CANNOT BE DETECTED		STANFORD UPLINK SIGNAL CAN BE DETECTED						STANFORD TRANSMITTER OFF, END OF PASS						
							RANGING RECEIVER ON	TURN-AROUND RANGING FUNCTIONING	RANGING RECEIVER ON						
		TERMINATOR SENSOR OUTPUT	TERMINATOR SENSOR ENERGIZED												
						PLANET SENSOR OFF									
						DATA MODE 2						DATA MODE 4/I RECORDED DATA (RT ENG DATA)	DATA MODE 4/I RECORDED DATA (DATA MODE 4)	DATA MODE 4/I RECORDED DATA (RT ENG DATA)	DATA MODE 4/I RECORDED DATA (VENUS DATA)
		HIGH-GAIN ANTENNA PAST ENCOUNTER POSITION													
				TAPE STOPS RECORDING TRACK 2 DATA	TAPE RECORD MOTOR OFF										
RY LATOR			VOLTAGE-CONTROLLED OSCILLATOR							AUXILIARY OSCILLATOR	VOLTAGE-CONTROLLED OSCILLATOR				
OR ENTER TION; S TY TO GET IN A ERE DROPPING	THE SPACECRAFT-TRANSMITTED SIGNAL CAN NO LONGER BE DETECTED ON EARTH DUE TO VENUS AND ITS ATMOSPHERE	ISSUED WHEN TERMINATOR SENSOR "SEES" PLANET; SIGNAL SENT TO PYROTECHNICS, WHICH FIRES SQUIBS, HIGH-GAIN ANTENNA POINTING ANGLE CHANGES	THE SPACECRAFT-TRANSMITTED SIGNAL CAN BE DETECTED ON EARTH AGAIN. THE UPLINK SIGNAL WILL BE ACQUIRED, PROVIDING IONOSPHERE DATA ALSO; DAS CLOCK A PROVIDES A BACKUP	DAS CLOCK B STOPS SENDING TRACK 2 DATA TO TAPE AND "START TAPE" COMMANDS STOP; DAS CLOCK A PROVIDES A BACKUP	RECORDING STOPS AT EOT; PREVENTS RECORDING INTO MODE-I AND TEST-PATTERN PERIODS	BACKUP LOGIC IN DAS TO STOP TAPE; SWITCHES DE TO DATA MODE 2 AND RE-ESTABLISHES CRUISE SCIENCE MODE; DAS CLOCK A PROVIDES A BACKUP TO CLOCK B	SWITCH RANGING RECEIVER ON; THIS PROVIDES CAPABILITY TO TAKE PLANETARY-RANGING DATA	PROVIDES PLANETARY-RANGING DATA AFTER CLOSEST APPROACH	END OF DSS 14 TRACKING CAPABILITY	TO CHECK OUT EXCITER WARM-UP CURVE AFTER ENCOUNTER	TWO-WAY LOCK FOR APPLICATION OF COMMAND MODULATION FOR POSSIBLE BACKUP TO MT-9	ENERGIZES PLAYBACK MOTOR IN TAPE RECORDER; INITIAL DATA WILL BE MODE 4 FOR APPROXIMATELY 2 min FOLLOWED BY 18 min OF MODE I DATA (RT=REAL TIME)	TAPE TEST PATTERN OF DATA MODE 4 PROVIDES A CHECK OF PLAYBACK SYSTEM AND WHICH TRACK WILL BE PLAYED BACK FIRST	REAL-TIME ENGINEERING DATA FOR FINAL EVALUATING BEFORE MODE 4 STARTS	VENUS ENCOUNTER DATA PLAYBACK STARTS FROM TRACK I

Fig. VI-3. Nominal *Mariner* Venus 67 encounter sequence matrix

in the data could reduce the effective reaction time in an emergency to only about 9 min. Because most of the commands to be transmitted during the planetary encounter were time-critical or functionally critical, it was most important to prevent accidental losses of command lock, and (in case any occurred) to provide for minimum-time reacquisition of the command loop.

a. Planetary acquisition and record sequence. The encounter sequence was initiated with the transmission of DC-V25 from DSS 41 at 02:49:00 GMT on October 19, 1967. The time was selected to permit the start of the encounter sequence before the CC&S MT-7 event. A station transfer was required just before MT-7; therefore, DC-V25 had to be sent approximately an hour earlier than would have been required otherwise. This DC-V25 time also fulfilled another criterion: There had to be sufficient time before a possible APAC (for a failed DAS clock A decode-enable switch) event so that corrective action could be taken. The tape recoder starting the record sequence early would have been the indicator, and the corrective action would have been to turn off science to reset the DAS frame count.

The DC-V25 was observed in the data at 02:58:25 GMT; spacecraft response was normal; the tape recorder subsytem 2.4-kHz power was turned on; the terminator sensor was energized; and power levels and temperature increased as predicted. These indications meant that the science-on/overload-inhibit override was probably on, as desired. The backup DC-V25 was not required.

A normal, two-way RF transfer was made from DSS 41 to DSS 62 at 03:49:02 GMT. The nominal magnetometer calibration occurred at the normal 58-h interval at 04:11:00 GMT. Command modulation was reapplied, and was in lock at 04:28:09 GMT. This established a spacecraft status that could respond to anomalies if any occurred at the CC&S MT-7 event.

The CC&S MT-7 event was observed in the telemetry at 04:45:05.8 GMT; inasmuch as it had been preempted by DC-V25, however, it had no effect upon spacecraft performance.

The DSS 62 transmitter was turned off at 04:50:00 GMT, and one-way RF lock was established at 04:59:29 GMT to perform the last test of AO stability and warm-up characteristics before committing the spacecraft to enter occultation. The received signal was highly stable, and increased in frequency as predicted. The test was terminated by turning on the DSS 62 ground transmitter, which switched the frequency reference for the exciter to the VCO for two-way RF lock at 05:58:13 GMT.

Command modulation was applied and command in-lock was established at 06:30:07 GMT to prepare for DC-V9 to turn on the ranging receiver. The spacecraft was operating normally, so DC-V9 was transmitted at 08:50:00 GMT. The ground receiver dropped lock at 08:59:28, and reacquired it at 08:59:30 GMT, with approximately 1-dBmW decrease in signal level. The spacecraft command subsytem was out of lock until 09:01:49 GMT, when the spacecraft returned to normal with ranging on. Each of these events was normal; the DC-V9 command was sent at that time for the following reasons: (1) To recover from this kind of event, and to return to normal before DC-V24 was required; (2) to allow confirmation that ranging was on in data mode 2; and (3) to have the ranging receiver on before DSS 14 rise to maximize the ranging time available (planetary-ranging equipment was available only at DSS 14).

The command to begin the DAS encounter mode (DC-V24) was transmitted at 10:50:00 GMT. The switch to data mode 3 occurred at 10:57:29 GMT, along with the DAS status bits indicating that DAS clock B was enabled, the plasma probe had gone to mode 3, and the planet-sensor excitation was on. The DC-V24 command was sent before the CC&S MT-8 event to set up the DAS logic so that only one DC-V24 would be required to inhibit DAS clock B if it malfunctioned. Sending DC-V24 before MT-8 also provided evidence that the command functioned.

The CC&S MT-8 event occurred at 11:25:03 GMT as a change in DAS status bit 16. Since DC-V24 had preempted MT-8, this was the only change. The plasma probe completed a cycle before it actually switched to the new mode. Consequently, the DC-V24 command set up the plasma-probe mode 3 logic, but the instrument did not go to mode 3 operation until 11:28:00 GMT.

The operation and performance of the spacecraft was completely normal up to this point; therefore, command modulation was removed at 11:31:00 GMT to allow two-way RF transfer from DSS 62 to DSS 14. The two-way transfer was completed at 11:47:00 GMT, and command was in lock at 12:30:19 GMT. The time to acquire command in-lock is a variable, and for planning purposes 12 min had been used. In this case, approximately 4 min were required, so the application of ranging modulation was moved up from 12:44:00 GMT to maximize ranging time. The planetary-ranging modulation was applied at 12:35:00, and was in lock at 12:48:35 GMT. Ranging modulation was turned off at 14:20:00 GMT in preparation for the transmission of DC-V16.

The DC-V16 command (start encounter backup clock) was a timed command. Two criteria were used for selecting the transmission time: (1) It was desired to select a time based upon the latest available trajectory data (E−4 h) so that DAS clock A would provide APAC backup at the center of occultation. This was an attempt to obtain potentially the most data for any atmosphere. (2) It was desired to obtain a DFR modulation phase-measurement (DAS word 21) in an even-numbered DAS frame as close as possible to (but no later than) 195 s before closest approach. This would be the most useful single item of DFR data that could be obtained in real time.

The transmission time for DC-V16 was selected as 14:31:43 GMT, which would provide the DFR measurement in frame 208. The read–write–verify (RWV) was set up in the automatically timed start mode, which was the mode used for all prior commands. The initiation of the automatic mode at 14:31:00 started as expected; however, at 14:31:03 GMT (40 s early), the RWV tape reader began to read the tape. It took 27 s before the RWV began to transmit the command; therefore, no command bits were sent because the command modulation was removed before the command left the RWV. The onboard spacecraft system continued to operate well, which meant that the primary function would complete encounter in a nominal manner.

While DSS 14 transferred to the backup RWV and re-established command lock, a trade-off analysis was made. Three courses of action were available: (1) To do nothing and assume that the primary system would function flawlessly, providing all real-time as well as recorded data. (2) To send DC-V16 as soon as possible, and allow DAS clock A to back up the tape-record functions. The backup APAC function would be late; therefore, it had to be timed to occur after exit occultation to ensure that APAC would not take place while the reduced upper-atmosphere exit-occultation data were being acquired. (3) To send DC-V16 quickly, followed by DC-V5, which would cause the bit rate to switch to 33⅓ bits/s; then, at the proper time, send DC-V5 again to switch back to 8⅓ bits/s, thus increasing the frame-counting rate for a specified length of time. If all of this went well, the spacecraft would have been back to normal, as if nothing abnormal had occurred. On the other hand, if the operations went badly, all encounter data might be lost. This would occur if the DAS did not supply valid data to the tape recorder at 33⅓ bits/s (not a required spacecraft mode) and APAC occurred early (before Venus) so that the second DC-V5 could not be transmitted.

The second possibility was the only one that seemed reasonable, as it was not yet known why the RWV had started early. There seemed to be little risk in simply sending DC-V16, and it provided most of the required backup capability. The command subsystem was in lock at 14:49:06, and DC-V16 was transmitted at 15:01:43 GMT. The DC-V16 command was sent this time in the RWV manual mode. The expected reaction to DC-V16 was observed in the data at 15:11:36 GMT. The DAS reset the frame count to zero, and set two status bits, the DC-V16 bit and the clock A decode-enable bit. It was later determined that the malfunction was caused by a bent pin in a cable connector between the frequency and timing subsystem and the RWV. The bent pin was in the 10-s digit complement in the 4 (4,2,1) position; therefore, at 03 and 43 s, the OR gate was satisfied to initiate this command in the automatic mode. The manual mode does not use the timing function, and so it bypassed the problem.

The station began to tune the ground transmitter VCO at 15:15:18, and completed tuning by 15:45:43 GMT. Ranging modulation was applied at 15:47:00, and was in lock at 16:00:24 GMT. Ranging modulation was removed at 16:30:00 GMT in preparation for the record mode.

The planet sensor output (PSO) was provided at 16:34:22 GMT. This inhibited UV-photometer calibrates, caused the DAS to begin issuing "start tape" commands every 50.4 s, and caused the track 1 data record to start. The far limb of Venus passed out of the planet sensor FOV at 16:38:24 GMT. This behavior was completely normal in function and time of occurrence. The planet sensor started DAS clock B, which in turn started the tape-recorder record mode, and was the primary method (as discussed in the DC-V16 problem description).

The DC-V9 command to turn off the spacecraft ranging receiver was transmitted at 16:40:00 GMT. This command increased the spacecraft-received signal strength by 0.7 dBmW, providing the capability to go slightly deeper into the atmosphere during occultation. The spacecraft was performing in a very nominal manner, so command modulation was removed at 16:41:30 GMT, and the ground transmitter was turned off 30 s later. This prepared the spacecraft for the desired one-way RF mode to enter occultation.

The tape recorder started recording data on tape track 2 at 16:46:46 GMT. The normal onboard command to start this record sequence came from DAS clock B. Data recorded on track 2 are DFR data plus a few

housekeeping bits. The AO began warmup at 16:50:52 GMT for the occultation experiment.

A second PSO occurred at 17:15:02 GMT. This was not expected in that it had been overlooked. One minute was required to verify from the planet sensor 1620 program output in hand that this would have been expected at this time if it had been looked for. During the design phase, in fact, this second limb had been considered for triggering the record sequence, but the limb was too close to the planet for the desired record time, and the plan was discarded. The planet sensor stopped providing a near-limb output at 17:18:34 GMT. This PSO had no effect on the spacecraft because the first PSO had started DAS clock B.

b. Occultation. The spacecraft S-band RF signal was lost on the closed-loop receiver at DSS 14 (Mars site, 210-ft antenna, Goldstone) at 17:39:08 GMT on October 19, 1967, as *Mariner V* entered the earth-occultation region of Venus. Four Goldstone S-band stations were tracking the spacecraft during the occultation experiment: DSS 14 was prime because of the extra capability afforded by the 210-ft antenna; DSS 13 was the primary backup because of its lower system-noise temperature; and DSS 11 and DSS 12 provided additional backup. All stations were able to acquire usable data. The open-loop receiver at DSS 14 was able to maintain lock until 17:42:05 GMT, providing additional data.

The terminator sensor provided its output, which caused APAC to occur in the data, at 17:46:51.4 GMT. These data were actually the recorded data, as was determined during the playback. The 17.6-deg APAC for the S-band high gain produced a decrease of approximately 2–3 dBmW in ground-received signal strength.

The closest approach to Venus occurred at 17:34:55.841 GMT (at the spacecraft). The altitude above the Venusian surface was 4094 km, using a Venus radius of 6056 km. On earth, this event took place during the occultation, and was derived from the FPAC trajectory data. The orbit was nearly as predicted. For planning purposes 3 mo earlier, the closest-approach time of 17.34 $\pm$2 min GMT had been used. The orbit-determination program output at E$-$6 h produced a closest-approach time of 17:34:56 GMT; at E$-$4 h, the value was not directly predicted, but was observed indirectly by predicting the times when PSO, terminator sensor output (TSO), and enter- and exit-occultation should occur, as well as by predicting spacecraft frequency changes caused by the doppler effect. All were very nominal for this encounter.

The spacecraft S-band and RF system began exit occultation, which allowed the DSS 14 receiver to acquire lock at 17:59:59 GMT. The received signal strength was 3 dBmW lower than before occultation, giving an early indication of a successful APAC. The predicted time for exit occultation, based upon the entire occultation time, was accurate to approximately 1 min. The DAS real-time data confirmed the APAC event after the demodulator acquired lock. All spacecraft data indicated a completely normal encounter.

The DSS 12 transmitter had been turned on at 17:52:00 GMT, with a transmitter frequency for closest approach plus 1370 s at the spacecraft (17:57:45 GMT). This frequency was chosen to acquire all of the denser atmospheric data in one-way lock and the ionospheric data in two-way lock. This would prevent the possibility of acquiring two-way lock and losing it again before a solid two-way lock could be established. The attenuation effects of the Venusian atmosphere and the doppler effects caused by the mass of Venus combined to prevent the spacecraft best-lock frequency from reaching the transmitter frequency. After the atmospheric effects had diminished to zero, the doppler effects of Venus had reduced the best-lock frequency so that the best-lock frequency went away from the uplink signal.

When the ground receiver did not acquire two-way lock at 18:02:11 GMT as had been predicted, many questions were raised. The unknown nature of the Venus effects made it uncertain whether the frequency had been too low and would acquire soon or had been missed for some other reason. It soon became apparent that two-way lockup had been missed as previously described. So that none of the one-way RF data that were being acquired would be lost, it was decided to reduce the DSS 14 acquisition frequency to the expected value, and go to two-way lock at the time of the scheduled DSS 14 takeover from DSS 12. In retrospect, since the atmosphere and doppler effects are now known, the spacecraft would have acquired lock if the prediction had been based on a frequency for 13 s later. The loss of data as a result of not going to two-way lock at the desired time consisted of a reduction of resolution in the upper-atmospheric data and the loss of some celestial-mechanics data that would have provided information for the determination of higher-order terms in the Venus gravity equations.

The DFR consisted of two receivers aboard the spacecraft; consequently, the times reported in this document are for the earth-observed effects of the spacecraft.

The DFR had been receiving a signal from the Stanford transmitter since station rise. The 49.8-MHz signal had been acquired at 11:05:42, and the 423.3-MHz signal at 11:09:04 GMT. The 49.8-MHz signal dropped lock because of earth occultation at 17:38:10, and the 423.3-MHz signal lost lock at 17:39:00 GMT. At exit occultation, the 423.3-MHz signal was reacquired at 18:00:31, and the 49.8-MHz signal acquired solid lock at 18:03:13 GMT. There was also a short period, from 18:00:51 to 18:01:11 GMT, when the 49.8-MHz signal was obtained. The DFR performed very much as had been predicted for occultation. The Stanford ground antenna used is a 150-ft, parabolic, steerable antenna using transmitter powers of 350 kW at the lower, and 30 kW at the higher, frequency.

c. Completion of record sequence. The DSS 14 transmitter was turned on at 18:17:00 GMT. Two-way RF lock was re-established at 18:19:00 GMT. The DSS 14 station was used for two reasons: (1) DSS 14 was the only station that had the capability of planetary ranging, and (2) the extra uplink capability of this station could be used for commanding the spacecraft even if it lost roll control. It was important to acquire two-way lock early after occultation to obtain two-way doppler data. These data were needed for orbit determination (for flight use as well as for the celestial-mechanics experiment).

The APAC backup command was given by DAS clock A at 18:19:10 GMT, as expected. The terminator sensor had performed the APAC function during occultation, so only the DAS status bit changed at that time. After the data encoder switched back to data mode 2, an extra event was found, which indicated that a path to ground existed through the squib-combustion products. This type of event first occurred on *Mariner II*, and occurs roughly 25% of the time.

The commands to end track 2 data and to stop sensing "start tape" commands were given by DAS clock B at 18:34:18 GMT. The tape recorder turned the record motor off at 18:41:51 GMT, when the EOT foil passed over the record heads. Clock B also stopped the record sequence at 18:47:45 GMT, removed plasma-probe mode 3, and switched the data encoder to data mode 2. Each of these events occurred on schedule, and the spacecraft continued to perform in an excellent manner.

The command subsystem was in lock at 18:51:03 GMT, allowing the ranging-receiver-on command (DC-V9) to be transmitted at 19:00:00 GMT (10 min earlier than scheduled). "Ranging modulation on" was observed in the data at 19:25:17 GMT. The ranging code was locked up within the next 40 min, and remained in lock until after ranging modulation was removed at 21:48:00 GMT because of station (DSS 14) set.

d. Postencounter–preplayback cruise. The earth sensor was receiving straylight from Venus when the switch to data mode 2 took place. The Venus clock and cone angles were such that the straylight continued to be observed by the earth sensor until data mode 4 started again at 20:09:32 GMT on October 21, 1967, during the second playback.

The temperature effects of the encounter with Venus were evident when the spacecraft switched back to data mode 2. The high-gain antenna registered an increase in temperature of 34°F from −151°F; the temperature later decreased to −130°F. The difference between the latter value and the peak was attributed to the thermal input from Venus. This behavior was as predicted. The APAC event reduced the radiative coupling between the high-gain antenna and the upper thermal shield, and increased the coupling between the high-gain antenna and the solar panels, resulting in a temperature decrease of 12°F for the upper thermal shield and an increase of 21°F for the high-gain antenna. The magnetometer was 14°F warmer (18°F) and the low-gain antenna was 23°F warmer (−60°F) at the time of first data after encounter. The magnetometer temperature returned to pre-encounter levels, and the low-gain antenna temperature increased 4°F because of the effects described above. The spacecraft bus performed as expected; temperatures increased 1–2°F because of the effects of Venus.

The DSS 14 transmitter was turned off on time. This produced an out-of-lock condition at 21:59:03 GMT because of the spacecraft switching from the VCO to the AO (RF one-way mode). The stability of the AO remained normal, and produced the expected warmup curve. This was a postcalibration test for the S-band occultation experiment. The AO test ended at 23:00:41 GMT, when two-way RF lock was re-established with DSS 41 as predicted. The Stanford station was set at 23:10:00 GMT, completing the real-time, near-Venus DFR data.

The second roll transient in the near-Venus environment was observed in the AC data at 00:40:28 GMT on October 20, 1967. This roll transient showed that the roll-position readout had been approaching the cw limit-cycle edge at about 3 μrad/s, and suddenly went to

the ccw limit-cycle edge at approximately 170 μrad/s. A normal limit-cycle reversal is 14 μrad/s for both valves firing once. The roll motion was back to normal within 10 min. Two other roll transients in the near-Venus environment, at 20:20:12 GMT on October 19 and at 08:04:50 GMT on October 20, were less dynamic.

The two-way RF handover from DSS 41 to DSS 62 went smoothly at 04:19:00 GMT on October 20. Command modulation was applied, and command was in lock at 06:16:21 GMT for any malfunction that might occur at the beginning of the Venus-recorded data playback. The spacecraft had performed exactly as planned throughout the entire Venus-encounter sequence.

6. Playback. The tape-recorder playback was initiated by the CC&S MT-9 event at 07:25:23.4 GMT on October 20, as observed in the data. The switch to data mode 4/1 was confirmed by approximately 50 s of mode 4 data. These were the last Venus data recorded on track 1. The track 1 recording continued until the EOT stopped the tape-record motor. Track 2 recording was commanded off approximately 7 min before EOT, so no data were near the EOT foil on track 2. The data mode 1 data (engineering) that started at 07:26:12 GMT indicated that all subsystems were performing properly. The CC&S MT-9 event was registered, and turn-on of the tape-recorder playback motor was observed in the power readings.

The track 1/data mode 4 test pattern began at 07:44:33 GMT, exactly as the readout of these data occurred in the prelaunch tests. This demonstrated the tape-recorder playback capability and the proper functioning of the tape-recorder/data-encoder interface. The track 1 test pattern ended at 08:00:36 GMT, and switched the data-encoder 4/1 logic back to data mode 1. The engineering data were normal, so command modulation was removed, and command went out of lock at 08:15:04 GMT.

The switch to data mode 4 at 08:15:38 GMT started the playback of some old test data. The tape did not always stop in exactly the same place at the end of the launch because of temperature effects on the launch motor, bearings, and tape. The launch mode ended on the tape where the record run-up started. This was as expected, and the Venus-data playback started at 08:17:52 GMT. All of the recorded data appeared very normal. Every eighth bit was an encounter, real-time bit. These were compared with the data received on earth in real time while the record sequence was occurring. These bits also filled in the data gap caused by the earth occultation.

Two-way and three-way doppler data and ranging data were desired during the playback phase to redetermine the spacecraft orbit, and also to provide a larger data base for the celestial-mechanics experiment. Very few cases of dropping two-way lock had occurred during the cruise phase; therefore, the decision was made to risk a few minutes of data outage to obtain these data. The condition was added that one-way lock would be used if uplink data anomalies occurred frequently. As it happened, only one data anomaly occurred, and it was during the second playback. When the spacecraft came up over DSS 14, the ranging code was locked up by 12:23:34 GMT; ranging was continued until 21:39:00 GMT, when ranging modulation was removed.

The track 1 Venus-data playback ended at 01:13:01 GMT on October 21, 1967, when the EOT foil switched the playback heads to track 2. Command modulation was applied just before EOT in case the switch to track 2 did not take place. The mode 1 data at the beginning of the tape ended when the track 2 test pattern started at 01:32:59 GMT. The test pattern was unchanged from the prelaunch test readouts. The test pattern ended, and the 4/1 logic switched back to data mode 1 at 01:49:03 GMT. All subsystems were performing normally, so command modulation was removed.

The first playback of the track 2 Venus data started at 03:58:08 GMT. This playback went very smoothly until 16:44:58 GMT, when CC&S CY-1 No. 47 turned off the spacecraft ranging receiver. This produced a small receiver anomaly at DSS 12; the data were obtained by using the predemodulator tapes at both DSS 12 and DSS 11. The track 2 playback ended at 18:18:29.7 GMT when the switch to data mode 1 took place.

Command modulation was applied so that DC-V9 could be sent to turn on the ranging receiver, and also in case the switch to track 1 did not occur after EOT. The DC-V9 was observed in the data at 18:54:44 GMT. All indications were normal for the ranging-receiver-on mode. The EOT occurred at 19:18:17 GMT, which switched the tape back to track 1 and a very normal second playback. This second playback was necessary to ensure the recovery of any data missing from the first transmission, and to provide duplication of the remainder of the data for purposes of comparison.

Four bits were missing from the first playback, and five different bits were missing from the second playback. The dropped bits were a known playback phenomenon that occurred when tape-recorder-playback phase lock was dropped momentarily and the motor ran faster to

relock up and "squeezed" out one bit. This gave a bit-error rate of 0.45×10^{-5} for this type of problem, which is a factor of 2 better than the specification for the total of 2×10^6 bits. Spot checks of the data from both transmissions confirmed that the data were repeatable. It was planned, therefore, to return the spacecraft to the cruise mode after the end of the second playback.

It was known that the tape recorder would be required in at least one UV-photometer experiment in the future. This meant that, in order to have the mode 1 data for spacecraft evaluations between tracks, the tape had to be positioned as it had been before the Venus encounter. This was accomplished after the start of the third playback on track 1. The playback could be terminated and cruise mode restored by the transmission of DC-V2, which would inhibit the playback motor and switch to data mode 2. The DC-V2 command was transmitted at 07:55:00 GMT, and was observed at 08:04:54 GMT. Data mode 2 indicated that all of the science instruments were functioning correctly. The 2.4-kHz power to the tape-recorder electronics was turned off to protect the spacecraft from any possible failure in the tape-recorder subsystem while its energizing was not required. The DC-V28 command, which turned off the tape-recorder 2.4-kHz electronics, and turned the battery charger on or off, was transmitted at 08:25:00 GMT, and was observed at 08:35:27 GMT. Telemetry verified that the tape-recorder 2.4-kHz power was turned off, and that the battery charger was turned on. The battery charger was charging at a 15-mA rate, and was left on to completely charge the battery. This was an effort to put the battery in the mode (fully charged) that was least likely to degrade during the warm period around perihelion. All science instruments and engineering subsystems were now back to a cruise condition, thereby ending the playback sequence.

7. *Postencounter cruise.* The spacecraft continued to perform well throughout the final month of Phase I of the *Mariner* Venus 67 mission. This phase consisted mainly of operations to obtain additional calibration data for the UV photometer, communication subsystem performance tests, and conditioning for long-term heliocentric cruise.

a. Bit-rate-change test. The results of the CC&S MT-6 event in July produced an interest in switching bit rates after encounter. The signal level in the transmit high-gain antenna mode was such that, on October 25, a switch to 33⅓ bits/s was commanded. The results of the DC-V5 command were observed in the data at 16:39:32 GMT, when the data encoder switched to 33⅓ bits/s. The UV photometer tube C had been reading a DN of 28 previously; this changed to about 4.5 DN after DC-V5 had been transmitted. This was the predicted value based upon the change in values that took place at CC&S MT-6.

The data encoder was switched back to 8⅓ bits/s at 20:44:33 GMT (as observed on earth) as a result of another DC-V5. The UV-photometer tube C retraced its change in DN, indicating that, for this level of signal, a conversion from 33⅓ to 8⅓ bits/s could be made with a fair amount of confidence. The SAGC and the SNR estimator were also monitored closely because of the signal-level changes associated with the CC&S MT-6 when the ranging receiver was turned off upon switching from 33⅓ to 8⅓ bits/s. Ranging was off before this bit-rate-change test was started. The SAGC did not appear to change within the station resolution. It was discovered later, during the evaluation of the data, that the SNR estimator was not set up correctly, so that the data were worthless. A bit-rate change will have to be tried in 1968 during the extended mission to answer this question.

The command DC-V5 had been transmitted at 17:07:00 GMT in an attempt to switch back to 8⅓ bits/s. The DSS 12 RWV, which was in command lock, dropped ground sync during the sixth transmitted bit, producing an error indication. The RWV operator was instructed to drop command modulation, which was completed before the ninth bit was transmitted. This prevented a command from being decoded by the spacecraft. The backup RWV would not go into mode 2 verify when it was brought on line; therefore, operations were stopped at DSS 12 for equipment repair. The command was transmitted by DSS 41, as explained above. The following day, DSS 12 again had RWV problems, and the scheduled commands were sent from DSS 41.

b. Postencounter cruise conditioning. The AC subsystem had been commanded to the DC-V15 mode before encounter. At this time, the tracking stations could no longer be committed to 24-h coverage of *Mariner V.* This necessitated returning the spacecraft to the normal mode so that, if roll control were lost, the spacecraft would automatically search to Canopus. This would also provide a gyros-on event that would be stored and provide data for the nontracked periods. The DC-V19 to restore the normal AC mode was seen in the data at 21:05:56 GMT on October 26.

After approximately 84 h of charging, the battery was fully charged with 60 A-h capacity, which was an increase of 1.2 A-h during the charging period. The DC-V28 that turned off the battery charger was observed on earth at 21:23:51 GMT. A data-encoder deck skip of the low and low-low decks took place as a result of the battery-charger-off transient. Deck skips associated with this function were very common during the test phase, and were considered normal.

c. Three spacecraft rolls for UV photometer. The UV-photometer-cognizant scientist and the project scientist requested that the spacecraft be rolled three times on November 7, 1967. At this time, the spacecraft had completed 180 deg of a revolution in the heliocentric orbit from the point at which the three rolls following the midcourse maneuver had been performed. A roll at that point would expose the UV photometer to the same space and stars, but in the opposite order from the earlier rolls. This roll would be performed with the data encoder at 8⅓ bits/s, whereas it had been at 33⅓ bits/s during the former exercise. This would provide an additional calibration of the UV photometer that could be used for evaluation of the 33⅓ bits/s data. The project manager approved the exercise on the basis that the value to be gained appeared to be worth the very small risk.

On November 7, 1967, the exercise was initiated by transmitting DC-V26 at 09:15:00 GMT to cause a power-on reset of the DAS logic circuits when DC-V25 was sent. The completion of the encounter sequence had set up the DAS logic so that another record sequence could not be performed unless a power-on reset were performed. The DC-V26 was observed in the data at 09:26:47 GMT, when all science was off. The DC-V25 was observed in the data at 09:31:51 GMT. At that time, the science came back on, the tape-recorder 2.4-kHz electronics were energized, and the data encoder switched to data mode 3. The UV photometer was reading the same values as it had before DC-V26, indicating that its performance was repeatable. All other subsystems were performing as expected. The DC-V16 command was transmitted to the spacecraft to start DAS clock A, which controlled the tape-record sequence that was needed to obtain the UV-photometer and DFR data recorded during the active exercise. The DC-V16 was observed on earth at 10:24:46.8 GMT, when the science frame count reset to zero, the DC-V16 DAS-status bit was set, and the clock A-decodes-status bit was set. It was desired to watch the exercise in data mode 2 so that the AC motion could be used for determining the direction in which the spacecraft was pointing as a function of time. The results of the DC-V2 were observed in the data at 10:42:09 GMT. The tape recorder turn-on had produced an event-register reading that was now observed in data mode 2 (this had frequently occurred in testing, and so was not surprising).

The DFR acquired lock with the Stanford transmitter at 11:24:59 GMT. A station transfer was completed from DSS 62 to DSS 14, and command was back in lock at approximately 12:02 GMT. *Mariner V* was tracked by DSS 14 for only 4 h, starting at 11:25 GMT, because DSS 14 was required for a *Surveyor* landing backup. The DSS 14 site was required for *Mariner V* to command and receive signals while the spacecraft was rolling.

The tape recorder started recording data on track 1 at 12:25:48 GMT as a result of the DAS clock A output. At 12:27:54 GMT, the spacecraft began to roll in the Canopus search as a result of the first DC-V21. The spacecraft had rolled into the first deep null in the high-gain antenna pattern by the time DC-V12 was received at the spacecraft. As a result, the spacecraft dropped lock and the command was not received, causing loss of real-time data for that period. These data were later recovered by processing the predemodulation tape with the 7094 **DDT** program.

When the spacecraft signal was again seen in the real-time data, the second DC-V21 was transmitted. The spacecraft reacquired Canopus at 13:13:00 GMT, completing the first full roll. The second DC-V21, which started the second roll, was observed in the data at 13:24:30 GMT. Two DC-V12s were sent to the spacecraft 4 min apart to switch the spacecraft transmitter to the low-gain antenna. The first DC-V12 arrived at the spacecraft after it had rolled away from the interferometer pattern and command was back in lock. The spacecraft switched to transmitting via the low-gain antenna at 13:32:00 GMT, and data were available in real time. Canopus was acquired at 14:11:25 GMT, completing the second roll.

Two DC-V21s were sent 6 min apart before Canopus was acquired to start the third roll search. The first DC-V21 (third in the sequence) started the roll, and was observed at 14:14:00 GMT. The EOT stopped the record mode approximately one-third of the way through this third roll, at 14:33:30 GMT. Canopus was acquired at 15:12:45, completing the third roll and the exercise.

The spacecraft was commanded to transmit via the high-gain antenna to restore communication with the standard DSIF 85-ft antenna. The signal strength increased from −166 to −140 dBmW, at 15:26:07 GMT

when DC-V10 was observed. The spacecraft was now ready to play back the recorded data, but *Mariner V* was not scheduled to be tracked until the following day.

The playback of the recorded three-roll exercise began with the transmission of DC-V4 at 21:00:00 GMT on November 8, 1967. The start of playback was observed on earth at 21:11:59 GMT. Track 1 data were played back to supply much finer detail on the UV-photometer observations. These data consisted of two readings every 2.4 s, compared to three readings every 50.4 s for the real-time data. The EOT switched to track 2, and the analog DFR data started playback. These data were played back to acquire an in-flight calibration of the DFR antenna patterns. Again, the DSIF antennas were committed to other spacecraft; therefore, a DC-V2 was transmitted to stop the playback until the following day. The tape recorder went to the standby mode, and the data encoder went to data mode 2, at 19:57:07 GMT.

Playback was resumed at 05:12:25 GMT on November 9, when DC-V4 was observed in the data. Tape track 2 completed its playback, and the EOT switched back to track 1. The tape playback was again stopped by DC-V2 at 19:10:24 GMT, when the tape was positioned as it had been before encounter in preparation for future record sequences. The DC-V28 command was then transmitted to turn off the tape-recorder 2.4-kHz electronics, as described earlier. This command also turned on the battery charger, which indicated normal performance. A second DC-V28 was transmitted to turn off the battery charger, and was observed in the data at 19:42:53 GMT, returning the spacecraft to its normal cruise condition. The ranging receiver was turned on approximately 15 min later by DC-V9. This established the mode that allowed ranging to be performed on the following day. This was the last time that ranging was successfully accomplished.

The UV-photometer data thus obtained indicated that the tube-C background level was approximately 20 DN at the start of the roll, and increased in a cyclic manner 8 DN. The data from the three rolls were in very close agreement, and indicated that the northern galactic hemisphere contains more hydrogen than does the southern. This result had been observed at 33⅓ bits/s, but the change was only 2 DN with a 6-DN background level because of the different scale factor. Detailed analysis the data by the cognizant scientist is continuing.

The DFR data obtained from the playback enabled the cognizant scientist to compare the antenna pattern with earth-based measurements. The antenna pattern at 423.3 MHz was the same, and the 49.8-MHz pattern was similar. The latter had slight deviations caused by fluctuations in the ionosphere of the earth and the propagation path. The cone angle at which the roll was performed was not the encounter cone angle, but it nevertheless provided a calibration of the earth-based measurements.

d. Communications tests. A series of tests of the communications subsystems was proposed to the project office by the radio- and command-subsystems cognizant engineers. These tests would be conducted exactly as a series of tests had been at the end of Phase I of the *Mariner* Mars 1964 mission, and as laboratory tests had been made of the *Mariner V* equipment. The results of these tests would then be compared with the laboratory results to determine whether any degradation had taken place in the space environment. These tests were approved by the project manager on the basis that they were similar enough to normal operations that they would not be a risk to the spacecraft, and would provide additional performance data.

The test series was started on November 13, when the first half of the SPE test was performed. The ground-transmitter VCO frequency was slowly varied at 4 Hz from the best-lock frequency with a spacecraft-received signal level of −128 dBmW. The tuning was stopped every 50 Hz to obtain stable readings. The transmitter VCO was forced to +625 Hz without dropping lock, and to −491 Hz on another day, when a too-rapid change in frequency caused a drop in lock. It was concluded that the receiver characteristics of the VCO and detector were unchanged because the static-phase-error curve matched the prelaunch test curve.

The AGC threshold test was performed on November 14. Two-way lock was established with the spacecraft, and the station transmitter power was reduced to 1 kW. With a 100-kHz signal phase-modulating the transmitter, the carrier was suppressed in 1-dB increments to threshold. The RF threshold was measured to be about −151 dBmW at the best-lock frequency. This test was repeated with ±50 and ±100 Hz offset to the station transmitter VCO. The receiver AGC curve and threshold were unchanged from the prelaunch values.

The command-lock threshold test was performed on November 16. Two-way lock and command lock were established, and transmitter power was reduced until the spacecraft-received power was about −138 dBmW. Then the carrier was suppressed in 1-dB increments, as in the AGC threshold test, with phase-modulation of the 100-kHz signal. The command threshold, which was defined as the point at which the common subsystem was in and

out of lock for equivalent intervals, was found to be −146 dBmW. This was the same level that was measured before launch at 8⅓ bits/s, and indicated that the receiver noise value and the SNR of the command output of the receiver had not degraded.

e. Solar-panel radiation degradation. The solar panels appeared to have degraded approximately 12.5% by the end of the mission. This degradation was approximately linear during the mission because there were no large solar flares to cause degradation as there had been for *Mariner IV*. The basis for the degradation was the standard cell readings, which were assumed to be an accurate indication of the panels. The short-circuit current of the I_{sc} –V_{oc} transducer cell had decreased 8% from the predicted value. The open-circuit voltage had decreased 5.5%. Maximum power was then calculated by drawing the new current-vs-voltage curve. The open-circuit voltage changed about 1% for each 2°C temperature difference; therefore, an error in prediction of temperature could affect the results significantly. This amount of degradation would not affect spacecraft performance because the spacecraft would always be inside the Venus orbit, where the solar-panel capability greatly exceeds the requirement (the solar panels were sized for the near-earth condition). The P-on-N type of solar cells used for *Mariner V* were known to degrade significantly because of radiation, so this result was not unexpected.

f. Pointing UV photometer at MT-6 point in celestial space. The UV-photometer tube-C reading had gradually reduced from an average reading of 36 DN after the CC&S MT-6 event in July 1967. This reading was approximately 24 DN by the middle of November. It was not clear whether this indicated a real change in the hydrogen density or a change in the sensitivity of the instrument. During the roll exercises, indications were that the northern galactic hemisphere had a higher reading than the southern. These readings tended to agree with the performance, but the rolls were at a celestial longitude of 267.5 deg. The CC&S MT-6 event occurred at a celestial longitude of 300 deg, so it was desired to roll the spacecraft at that point. The spacecraft would have reached that point on November 25, which would be after the telecommunication threshold had been reached. The data were obtainable earlier by pitching to the intersecting plane, then rolling to the CC&S MT-6 point in space.

This exercise required performing an encounter sequence (to record the data on the tape) and a midcourse-maneuver sequence (to pitch and roll) simultaneously, and had been performed successfully on the spare spacecraft in the Spacecraft Assembly Facility. Consequently, the project manager approved the exercise for the in-flight spacecraft.

The exercise started on November 19, 1967, with the transmission of QC-V1-1 at 13:00:00 GMT. This was the required pitch turn of −17.18 deg to place the spacecraft roll axis perpendicular to the intersecting plane. The QC-V1-2 command was an 1800-s roll, which exceeded the spacecraft capability and allowed the spacecraft to roll approximately +313 deg. (At +173 deg, the UV photometer was pointed at the CC&S MT-6 point.) This roll inhibited the motor-burn relays, and stopped only when the maneuver relays were reset. A DC-V14 was transmitted to ensure that the inhibit on the CC&S–AC interface was removed so that the turns could be performed.

The power-on reset of the DAS logic was required to set up the record logic. The DC-V26 command turned off all science. The DC-V25 command turned the science back on, turned on the tape-recorder 2.4-kHz electronics, and switched the data encoder to data mode 3. The DC-V16, which was observed in the data at 14:03:55.7 GMT, started DAS clock A. During this exercise, engineering and science data were desired whenever possible; therefore, DC-V2 was sent to switch to data mode 2. The extra precaution of sending DC-V29 was taken to ensure that the first-burn (already-fired) squibs were those on line. The DC-V27 was transmitted so that the record sequence would start approximately 1 min before the start of the pitch turn. The DC-V27 turned on the gyros, and switched the data encoder to data mode 1. A DC-V2 switched the data encoder back to data mode 2. The DC-V12 command was transmitted to switch the transmitter to the low-gain antenna. This allowed data to be observed in real time while Canopus was still acquired, and the received signal to be recorded at DSS 14 after the turns had started. This recorded signal was later processed with the 7094 **DDT** program, and some data were recovered.

The tape-recorder record motor was turned on by DAS clock A, and track 1 data began to be recorded. The −17.18-deg pitch turn started approximately 1 min later. The real-time data were lost shortly after the pitch turn was completed (after 95 s), and the spacecraft held its inertial position until the roll turn started. The positive roll (cw) turn of 1680 s was completed when the spacecraft reacquired the sun. The search for Canopus in the ccw direction was then started. This traced out approximately another 313 deg of a longitude line for the UV photometer.

The spacecraft should have completed the reacquisition of Canopus, but no RF signal was acquired. An RF signal was observed later, but data could not be demodulated. The switch back to spacecraft transmission via the high-gain antenna was commanded, providing a signal level of −154.4 dBmW, which was about 7.5 dBmW lower than expected. All high- and medium-deck telemetry channels were checked for spacecraft performance. When it was determined that all were normal, the station was asked to drop the downlink lock and reacquire it. This corrected the problem by dropping the sideband lock.

The preplayback cruise state was then established. The inhibit-maneuver command (DC-V13) was reestablished as protection against an accidental "start maneuver" command. The science-overload-inhibit override was removed by turning science off with a DC-V26 and turning science back on with a DC-V2. This reestablished the safety factor of allowing the science or gyros an exclusive circuit to function if the main-booster regulator were to fail. This became more important as the spacecraft neared perihelion and tracking was impossible even though the DC-V15 in effect should have kept the gyros off. The three minimum QC-V1s (pitch, roll, and motor burn) were transmitted to provide a margin of safety if a failure-induced maneuver should be performed. The transmit-high- and receive-high-gain antenna mode was commanded on so that the spacecraft could be commanded by the standard 85-ft antennas during the recorded data playback. The spacecraft was performing in a nominal manner; therefore, command modulation was turned off, at 20:00:00 GMT, and DSS 14 tracking was released.

The start of playback (DC-V4) was commanded by DSS 41 at 22:00:00 GMT on November 19. The track 1 playback was normal, and the EOT switched to track 2 playback. There was more interest in real-time science data than in the track 2 recorded data. The command to stop the playback (DC-V2) and to switch to data mode 2 was observed in the data at 17:11:52 GMT on November 20. The tape stopped on track 2 just beyond the point on track 1 where the data were recorded. This set up the tape for future record sequences in the extended mission. The tape-recorder 2.4-kHz power was commanded off with DC-V28. This command also turned on the battery charger, and a second DC-V28 was transmitted to turn it off again.

The plasma probe had been in mode 3 format since science had been turned off and back on. This was because CC&S MT-8 was still set, so that each time science was turned on, it reacted to MT-8. A DC-V16 command was transmitted to allow DAS clock A to count out an encounter. This reestablished the postencounter science cruise mode 2, when the encounter sequence was clocked out. No other conditions changed because the tape-recorder 2.4-kHz power was off during this sequence.

The playback of the UV-photometer tube C recorded data around the CC&S MT-6 point had a value of 90 DN. The average value at the time of MT-6 was 36 DN, which indicated that some other phenomenon was occurring during this exercise. The 90-DN output was not an isolated sample, but was approximately 30 deg wide. There could be several reasons for this; the two most likely are described below.

Natural phenomena, such as a narrow stream of hydrogen extending into the ecliptic plane and stopping, would allow the hydrogen to be observed while the instrument scanned across the ecliptic plane, but not to be observed when it scanned away from the sun in the ecliptic plane. The extended mission would confirm this possibility by rolling the spacecraft until the entire celestial sphere has been mapped for ultraviolet sources to a high degree of accuracy.

Reflection off the spacecraft into the sensor appears to be a more likely explanation. The thermal can that protects the propulsion motor extends approximately 2 in. beyond the ultraviolet sensor, but many degrees off axis. The sunlight might be reflected off the top edge of the can into the ultraviolet sensor, and the FOV limiters could be reflecting into the sensors. Reflection is not normally a problem because the sensor is at 90-deg cone angle. The −17.18-deg pitch turn decreased the sun–spacecraft–ultraviolet-sensor angle during the roll, making it suspect. The only sensor that observed this large increase was tube C, which has the largest FOV (2¼ deg) and the largest spectral response (1050–1900 Å); also, of course, it was the only one that contained the atomic hydrogen 1216-Å wavelength. Tests will be performed to determine the susceptibility of the UV photometer to straylight at 1216 Å.

g. Conditioning for long-term cruise. The start of spacecraft conditioning for the long-term cruise was at the end of the UV-photometer exercise, as previously explained. Only two commands were required to set up the long-term cruise, but it was decided to obtain a small amount of additional data by sending three other commands.

The exercise began at 15:51:00 GMT on November 21, 1967, when DSS 14 sent a DC-V9 command to turn the

ranging receiver on. The turn-on was observed in the data 14 min, 20 s later. Ranging modulation was turned on to obtain a range fix on the spacecraft before the long-term cruise began. Three separate attempts of 30 min each were made to lock up the range code. They were all unsuccessful because the ranging threshold had been slightly exceeded, which was caused by the pointing geometry of the antenna and the range being in excess of 118×10^6 km.

One of the commands required to establish the long-term cruise mode was the DC-V15. The Canopus-gate-inhibit override was observed in the data at 18:49:09 GMT. This command was sent to keep the gyros off when Canopus acquisition was lost. If the command were not sent, there would be days when no stars of the required brightness would fall within the Canopus-sensor acquisition level; therefore, the roll search would continue until a star satisfied the logic. The gyros would be on for rather long periods, increasing the internal bus temperature. This temperature increase plus the switching transients associated with turning the gyros on and off was not desirable when the acquisition of a definite object was not required.

It was accepted that Canopus acquisition would be lost in late December 1967, when the star Canopus moved out of the MT-4 Canopus-sensor FOV. The heliocentric orbit would be quite fast later (less than 200 days), which would require Canopus cone-angle updates frequently (even one was impossible after this time because the *Mariner V* antennas pointed away from earth until late July 1968).

The spacecraft was next commanded to transmit on the high-gain antenna and receive on the low-gain antenna. This configuration provided a few data samples for interferometer pattern mapping. The ranging receiver was commanded off, leaving only one command required to set up the long-term cruise.

The DC-V12 command to transmit and receive on the low-gain antenna was observed in the data at 19:31:59 GMT, when the ground-receiver AGC dropped from −149.2 to −159.0 dBmW. This established the long-term-cruise mode by setting up the spacecraft to transmit data to earth so that they could be received in late July 1968. The spacecraft was capable of receiving an uplink signal slightly earlier.

A record-only pass was performed with DSS 14 on December 4 between 16:02:00 and 20:00:00 GMT at a signal level of −170.0 dBmW. This indicated that the spacecraft was still functioning as designed. At that time, *Mariner V* had been in space for 173 days, 14 h. The spacecraft had performed Phase I of the mission in an excellent manner; it had transmitted more than 210 million bits of data to earth, and had successfully responded to 96 ground commands.

D. Science Instrument Performance

1. Data automation subsystem. The primary functions of the DAS were to sequence instrument data, code and format data, perform analog-to-digital conversion, and to transmit these data by two parallel channels to the digital tape recorder and by one channel to the flight telemetry system.

A block diagram of the encounter portion of the DAS is shown in Fig. VI-4. The formats for real-time and recorded data are shown in Figs. VI-5 and VI-6. The encounter-oriented inputs and outputs are incorporated in Table VI-5.

At the end of the midcourse maneuver (23:14:26 GMT, July 24, 1967), the DAS had operated for 136.8 h and produced 39,082 frames of science data. Since the midcourse maneuver, the DAS has functioned without a single anomaly. In more than 3200 h of operation since the midcourse maneuver of the *Mariner* Venus 67 mission, more than 192 million bits of data have been processed by the DAS. One flip-flop had changed state more than 5×10^{12} times.

Forty days after launch, the communication range was great enough for the performance margin of the DSIF to be reduced to almost zero at the high data rate; therefore, the data rate was changed with the MT-6 command from 33⅓ to 8⅓ bits/s. A cruise condition was maintained until ground command DC-V25 started the encounter sequence (backed up by MT-7). This command turned on tape-recorder power and energized the terminator sensor.

The next command, DC-V24, switched the DAS and the data encoder to mode 3, and enabled the DAS-generated encounter functions. Switching from mode 2 to 3 expanded the telemetry format from 280 to 405 bits of science, and allowed the DAS SSAC analysis team to observe several status bits not previously seen.

At 14:31:43 GMT (3 h 42 min after DC-V24), ground command DC-V16 was scheduled to be sent to start backup clock A so that it would issue the same commands as clock B, but delayed 12 min. This command was sent 30 min late because of a ground-station problem.

Because of this delay, it was necessary for the next spacecraft function, PSO, to perform properly, and for the terminator sensor to work properly, so that APAC would occur on time (Fig. VI-7). The APAC had to occur during occultation so that the S-band occultation experiment could be performed during exit occultation. The alternative to allowing functions to proceed normally from that point was sending DC-V5, which would have changed the data rate to 33⅓ bits/s. This would, in effect, make up for the 30 min of lost time. However, if the data rate could not be changed back to 8⅓ bits/s, the entire encounter-recorded data would have been lost because of the logic mechanization of the DAS. The DC-V5 command was not sent.

The planet sensor started the $02^h07^m41^s$ recording sequence on time. The PSO caused the primary clock (clock B) to begin counting, and also started the recording sequence. The end of the encounter period occurred after all of the recorded data had been played back twice, and sufficient time had elapsed for verification that the science subsystem was operating correctly in mode 2.

On October 26, the data rate was changed from 8⅓ to 33⅓ bits/s and back again to correlate the first data-rate change with a UV-photometer anomaly at that time. On November 7, 1967, the spacecraft was rolled three times for the primary purpose of allowing the UV photometer to observe and map the same region of the sky as it had during the postmidcourse roll maneuver. Data were recorded and played back. A similar exercise was performed on November 19, 1967.

During a DAS-controlled recording sequence, the UV photometer observed the same region of the sky as it had during MT-6 (the initial data-rate change). The differences between the November 19 and October 26 exercises are the spacecraft maneuvers and the recording sequence in the former, and only a data-rate change in the latter.

The DAS performed nominally during all of the above described operations.

On November 21, 1967, the spacecraft was set up for long-term cruise.

2. Helium-magnetometer performance. The magnetometer performed as expected throughout the mission. No anomalous behavior was noted during the cruise, encounter, or postencounter phases of *Mariner V* operation. Instrument calibration was unchanged, and the periodic in-flight calibration functioned properly throughout the flight.

3. Trapped radiation detector performance. The performance of the TRD was normal from the time of science turn-on, and remained normal throughout the mission. No anomalies were observed in the data. However, the counting rates appeared low as the spacecraft traversed the Van Allen belts. This was discovered to be a computer problem in handling the overflow bit in the data. Raw data were checked, and found to agree with expected values.

At no time after leaving the Van Allen belts did any of the detectors saturate. The TRD counting rates remained unchanged when the telemetry bit rate was changed from 33⅓ to 8⅓ bits/s.

The TRD performance verified that the design limits of the instrument and the DAS were adequate.

Several solar flares were observed during the cruise phase of the mission. Notable flares occurred on the days listed below, along with the type of event associated with each flare:

Time	Event
Day 177	Proton
Day 178	Electron
Day 192	Proton
Day 193	Proton
Day 213	Electron
Day 214	Proton
Day 222	Proton and electron
Day 233	Proton
Day 261	Proton and electron
Day 262	Proton and electron
Day 263	Proton and electron
Day 264	Proton and electron
Day 280	Minor event
Day 282	Minor event

In addition to these electron and proton events, several hundred solar X-ray events were observed. No increase above interplanetary background rates of energetic particles with energies above 45 keV was noted in the vicinity of the planet Venus.

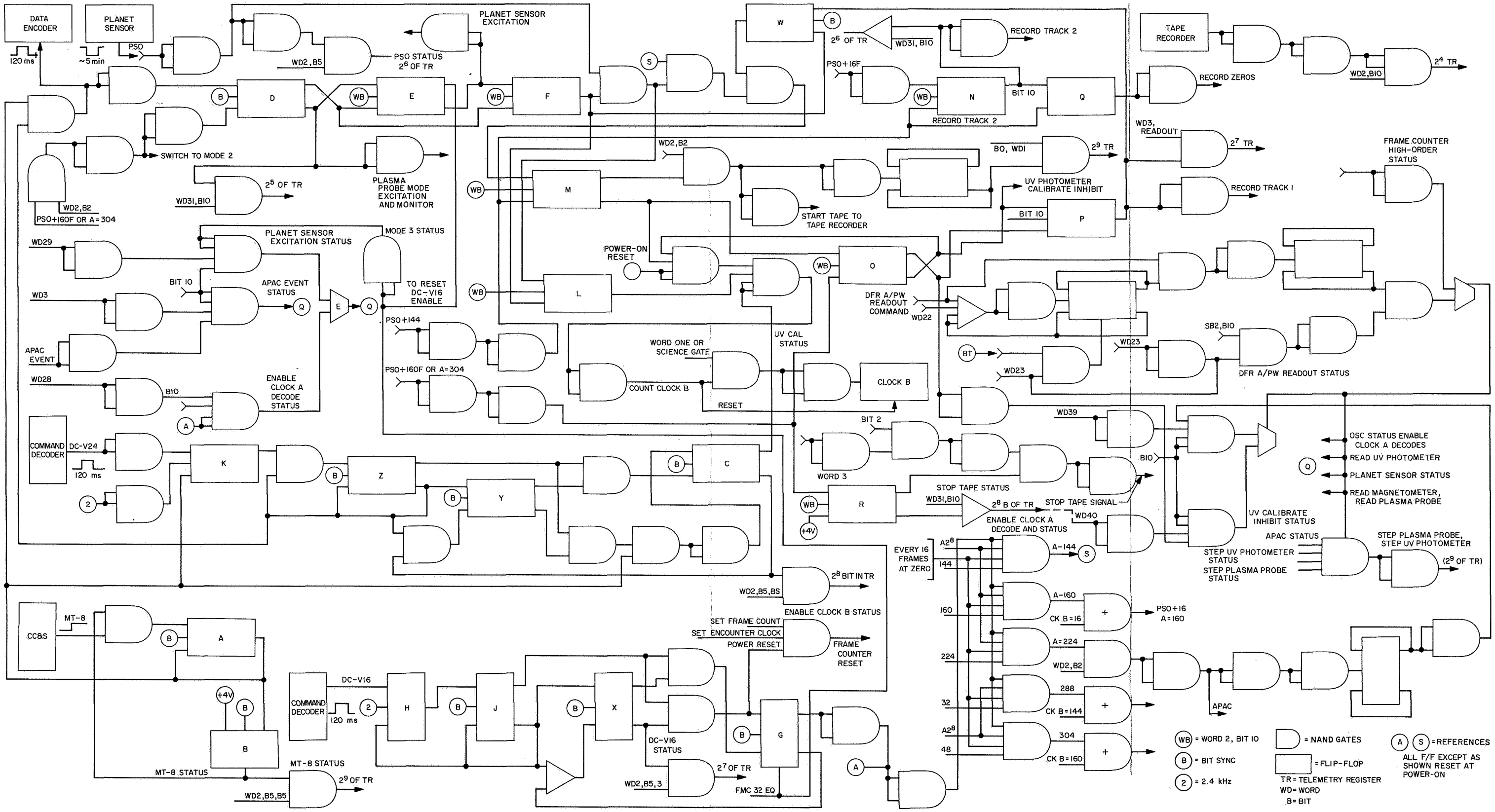


Fig. VI-4. *Mariner* Venus 67 encounter logic diagram

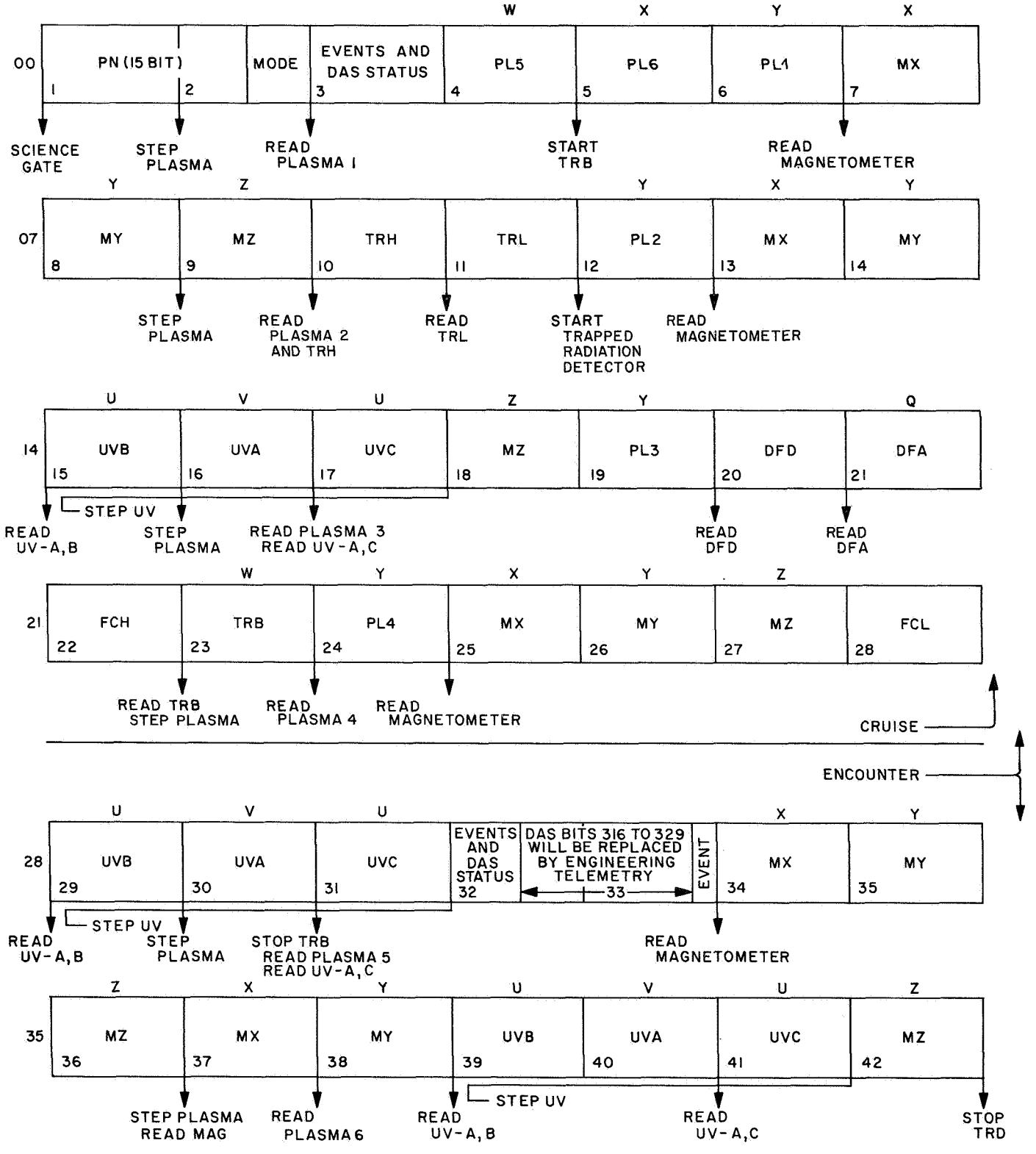
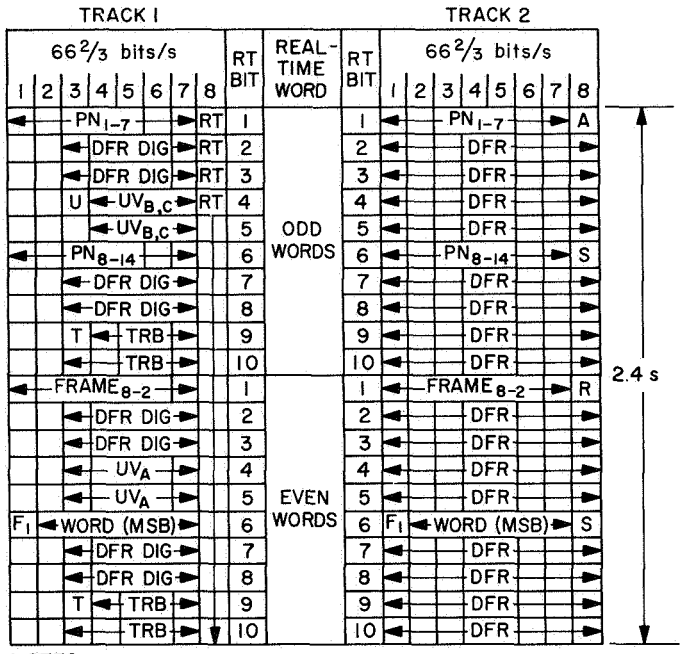


Fig. VI-5. Data automation subsystem real-time data format

Table VI-5. Data automation subsystem real-time word description

Abbreviation	Data format word	Description
PN	1, 2	Fifteen-bit pseudo-noise sequence used to identify beginning of each real-time data frame. Sequence is: 000011101100101
TRB	23	Readout of B-channel count of TRD[a] data accumulated in 10-bit W-register
TRH	10	Ten high-order bits (bits 11–20) of T-counter assigned to TRD
TRL	11	Ten low-order bits (bits 1–10) of T-counter assigned to TRD
UVA	16, 30, 40	Three sets of A/PW[b] data from UV photometer
UVB	15, 29, 30	
UVC	17, 31, 41	
DFA	21	A/PW data from DFR
DFD	20	Binary whole-word digital data from DFR
FCH	22	Nine high-order bits (bits 11–19) of frame counter. Clock B is substituted in this word on alternate frames
FCL	28	Ten low-order bits (bits 1–10) of frame counter
MX	7, 13, 25, 34, 37	A/PW data from helium-magnetometer X-axis
MY	8, 14, 26, 35, 38	A/PW data from helium-magnetometer Y-axis
MZ	9, 18, 27, 36, 42	A/PW data from helium-magnetometer Z-axis
PL1	6	Six sets of A/PW data from plasma probe
PL2	12	
PL3	19	
PL4	24	
PL5	4	
PL6	5	

[a]TRD = trapped radiation detector.
[b]A/PW = analog-to-pulse width.

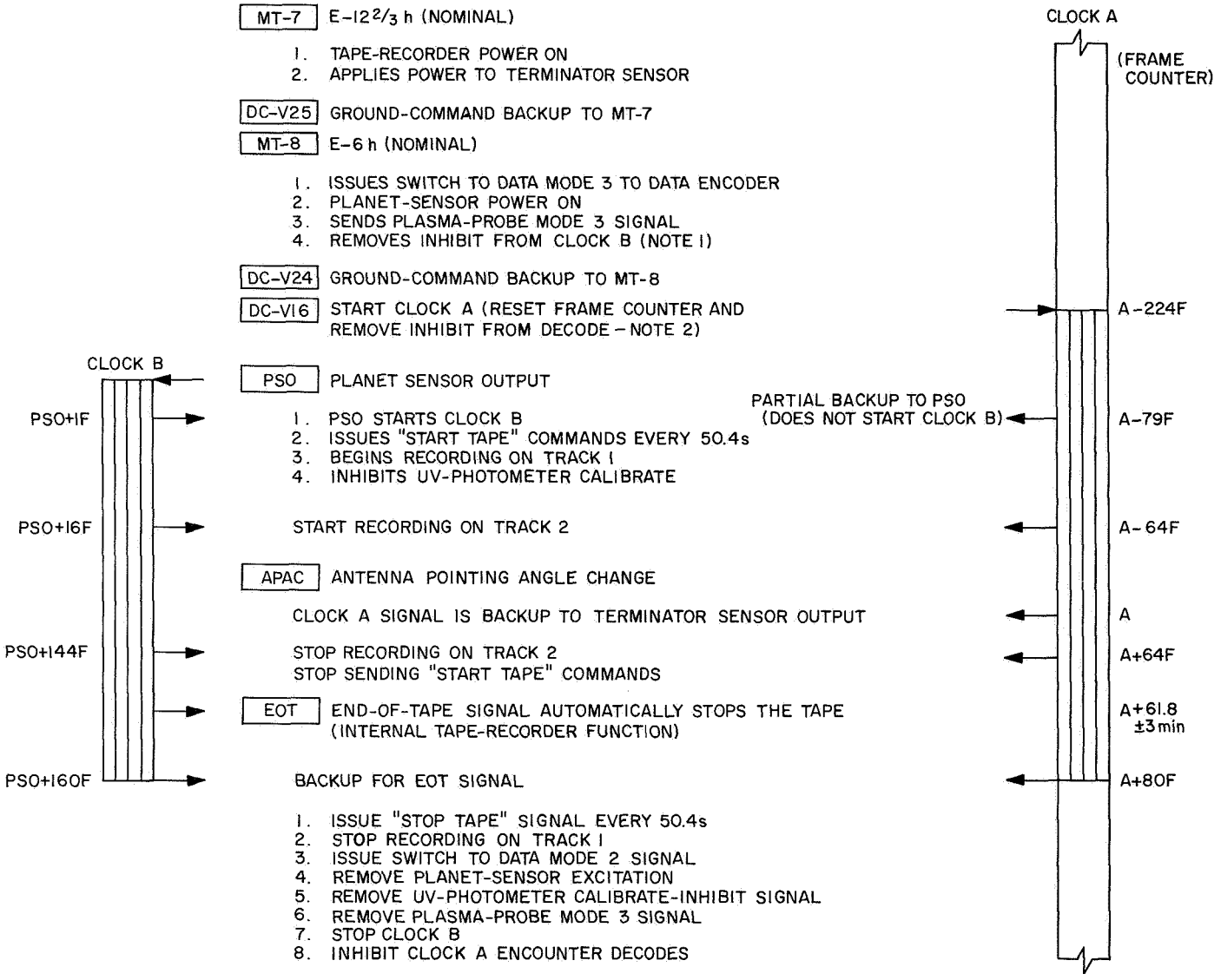


NOTES:
1. DATA FOR DFR, UV PHOTOMETER, AND TRB ARE RECORDED MSB FIRST, LSB LAST.
2. ABBREVIATIONS USED:

PN_{1-7} = BITS 1-7 OF 15-BIT PN SEQUENCE (0000111)
PN_{8-14} = BITS 8-14 OF 15-BIT PN SEQUENCE (0110010)
$FRAME_{8-2}$ = FRAME COUNTER, LEAST SIGNIFICANT BITS 8-2
F_1 = FRAME COUNTER, LEAST SIGNIFICANT BIT 1
TRB = TRAPPED RADIATION DETECTOR, DATA B
DFR DIG = DFR DIGITAL DATA
DFR = DFR ANALOG DATA
UV_A = UV PHOTOMETER, DATA A
$UV_{B,C}$ = UV PHOTOMETER, DATA B OR C
RT = REAL-TIME DATA
WORD (MSB) = COARSE WORD COUNT:
S = APAC STATUS BIT
A = "1" IF DFR-A IS NEXT RECORDED WORD
U = "1" IF $UV_{B,C}$ IS UV_C
T = "1" IF TRB IS TRB:
"0" IF TRB IS PL-5
BLANK SPACES = ONES ON TRACK 1
R: = STATE CHANGE INDICATES LAST 8 DFR ANALOG WORDS WERE ACDE BCDE, AND THAT NEXT 664 WORDS ARE IN BCDE SEQUENCE

RT WORDS	WORD (MSB)
1-7	100000
8-14	010000
15-21	001000
22-28	000100
29-35	000010
36-45	000001

Fig. VI-6. Data automation subsystem stored-data format



NOTES: 1. CLOCK B MAY BE INHIBITED BY ISSUING AN EVEN NUMBER OF DC-V24 COMMANDS
2. CLOCK A FRAME COUNT MAY BE RESET BY DC-V16 AT ANY TIME
3. CLOCK B MAY BE RESET BY POWER-ON RESET
4. ABOVE DAS EVENTS ARE MONITORED AND DISPLAYED IN REAL TIME
F = FRAMES

Fig. VI-7. *Mariner* Venus 67 encounter sequence and data automation subsystem events

4. Plasma-probe performance. The plasma probe operated perfectly during the flight of *Mariner V*. All planned events occurred as expected, and no anomalous events were noted. In particular, no abnormal collector currents were measured at the steps corresponding to the highest modulator grid voltage. This shows that no high-voltage problem was present in the system, and confirms the prelaunch belief that the high-voltage-related anomaly observed during testing was the result of environmental conditions. It further indicates that the concern over the outgassing properties of the materials in the high-voltage cable was unnecessary.

A discussion of the significant spacecraft events that caused changes in plasma-probe status is presented below.

a. Launch. The plasma probe was turned on, along with the rest of the science, at 06:27 GMT on day 165. Processed real-time data were erratic during this period, so the first plasma-probe calibrate sequence was observed at 06:40 GMT on day 165. At this time, it was confirmed that the high-voltage inhibit had been removed by the separation connector, and that the instrument was operating in a normal manner. If data processing had been perfect, this could have been observed at 06:30 GMT on day 165. The first indication of actual plasma measurements occurred at 09:44 GMT on day 165 as the spacecraft entered the magnetosphere.

b. Data-rate change. At 19:22 GMT on day 205, the data rate was reduced from 33⅓ to 8⅓ bits/s. As expected, this caused a reduction in value of all plasma-probe measurements by 3 or 4 DN. This reduction is caused by the discharge characteristic of the sample-and-hold circuits within the instrument; the plasma probe is calibrated for both conditions.

c. Encounter. The first plasma-probe status change during the encounter sequence occurred when the DAS was switched to mode 3 at 10:57 GMT on day 292. At this time, the instrument was near the beginning of its 24-frame mode 2 sequence, which it completed before switching to mode 3. Proper mode 3 operation was confirmed at 11:28 GMT on day 292. The instrument performed properly during encounter, yielding valuable scientific information. Switching back to mode 2 was accomplished successfully at 19:10 GMT on day 292.

5. Ultraviolet-photometer performance. The UV photometer is basically an optical instrument designed to measure atomic hydrogen and oxygen resonance radiation in interplanetary space and in the outer atmosphere of Venus. The performance, events, and operations of the UV photometer from postmidcourse maneuver through the end of the mission are discussed in the paragraphs that follow.

At 19:19:21.42 GMT on day 205, the MT-6 event occurred at the spacecraft, changing the data rate from 33⅓ to 8⅓ bits/s. After MT-6, the UV photometer showed the following changes:

(1) Drift check changed from 2, 0, and 2 (for tubes B, A, and C, respectively) to 1, 1, and 1.

(2) The calibrate changed from 259, 250, and 259 (for tubes B, A, and C, respectively) to 258, 250, and 258.

(3) Tube-C readings changed from approximately 7 to approximately 36 DN.

(4) Tubes B and A showed negligible change.

Items 1, 2, and 4 are considered normal. Analysis of data recorded in the JPL space simulator indicates that similar phenomena occurred in the tube-C readings at data-rate changes (item 3).

On day 298, the spacecraft data encoder was commanded to switch from a data rate of 8⅓ to 33⅓ bits/s, and back to 8⅓ bits/s. In this case, tube C changed from a reading of 25 to 4 DN, then back to 25 DN. This behavior is similar to that observed at MT-6 on day 205.

During the three rolls after the midcourse maneuver, it was observed that the photomultipliers were not aligned precisely. The centers of the FOV of each tube should have been the same. The roll rate was such that the Canopus-sensor output maps of the roll arc through the celestial sphere were able to define positions only to within 5 deg. These Canopus-sensor output maps permit the determination of the UV-photometer pointing vector position in ecliptic latitude during a roll maneuver.

Examination of the predicted UV-photometer viewing track across the celestial sphere showed that the nominal track would pass very close to two bright, ultraviolet-emitting stars in the constellation Scorpius. These stars are Pi-Scorpii (seen first) and Tau-Scorpii (seen about 1 wk later). During the period in which the UV-photometer viewing track crossed near these stars, the normal oscillations of the spacecraft in its AC deadband allowed the UV-photometer pointing vector to move about the celestial sphere near the stars. Contour plots of the ultraviolet intensity were made from the flight data. Each reading was assigned a point in space as if the UV photometer were pointing out from its nominal

position of 90-deg cone and 95.5-deg clock (spacecraft coordinates). The result of this comparison is the plot shown in Fig. VI-8. The position of the real star is set at 0-deg lon, 0-deg lat. The apparent position of the star Tau-Scorpii found by each tube is shown in the boxes marked A, B, and C. The coordinates show the error in the real pointing position in degress of ecliptic longitude and latitude.

The analysis for both Tau-Scorpii and Pi-Scorpii agree to within the ±0.2-deg estimated error of the method used. The resulting correction to spacecraft coordinates is as follows:

Pointing direction	Tube		
	A	B	C
Cone angle, deg	90.3	89.4	90.3
Clock angle, deg	95.7	95.8	95.8

As one of the postencounter operations to enhance the understanding of the UV-photometer output, a series of rolls was performed on day 311. At this time, the UV photometer was pointing 180 deg from the location it viewed during the time of the midcourse maneuver on day 170. The roll maneuver allowed the UV-photometer pointing vector to sweep across the celestial sphere approximately in the same arc as that followed by the UV photometer in the postmidcourse-maneuver rolls.

The roll sequence was recorded and played back from the spacecraft tape recorder after the final Canopus acquisition. The data were plotted, and showed several interesting characteristics. Because the postmidcourse-maneuver rolls were performed at 33⅓ bits/s and the postencounter rolls at 8⅓ bits/s, there is a slight difference in the mesh size and, therefore, in the details of the output map. Assuming a nearly identical roll rate for each operation, the map produced postencounter has only three data points compared to four data points for the same length of arc in the postmidcourse-maneuver rolls.

The general background level of tube C was approximately 6 DN during the postmidcourse-maneuver rolls. Any cyclic behavior of the baseline is very difficult to see because the analog-to-digital conversion is accurate only to ±1 DN, which represents more than a 15% change at this signal level. This would mask any but the most prominent features. This was not the case with the postencounter roll maneuver. The tube-C background level was about 20 DN at the start of the rolls, and the observed cyclic changes of 8 DN are both easily seen and reproducible.

It appears possible that there may be a large anisotropy in the amount and direction of Lyman-alpha emission being scanned by the UV photometer. The other statement, which seems accurate, is that a detailed comparison of the two sets of rolls cannot be made without great difficulty. Insufficient AC information, coupled with the nonlinearity of the response of the instrument at the two data rates, practically obscures all of the common quantitative aspects of the data.

An opportunity existed during the flight sequence to check the long-term behavior of the UV photometer. On day 323, a pitch-and-roll maneuver was performed. This permitted the UV photometer to scan back from almost the other side of the sun to the portion of space that was observed when MT-6 occurred. If no strange effects appear because of the sun being closer, then the UV photometer should have received the same signal it received at the time of the MT-6 event. The entire pitch–roll sequence was recorded on the spacecraft tape recorder, and the playback data were plotted. The point of the MT-6 event was found, assuming a uniform roll rate throughout the 310-deg roll.

The data showed a broad band (about 30 deg wide) of Lyman-alpha emission in the vicinity of the MT-6 position. The readings were approximately 90 DN. This feature is so large in angular size that it does not seem possible that it could be associated with any celestial object. Because the spacecraft pitched off the normal sun line (which meant that the UV-photometer pointing vector was no longer perpendicular to the sun–spacecraft line), solar reflections into the instrument were thought to be possible.

A complete analysis of the parts of the spacecraft that might have reflected light back toward the UV photometer has not been made at this time, however, it does

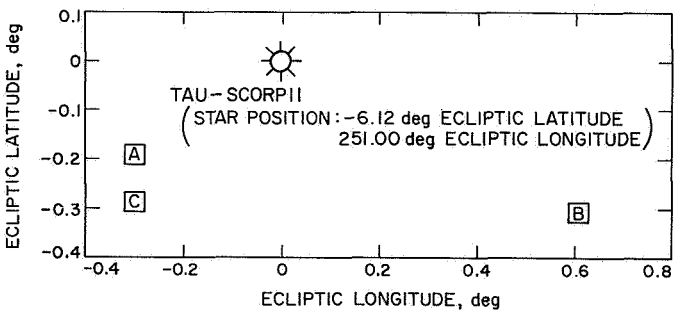


Fig. VI-8. Pointing directions of UV-photometer tubes A, B, and C (apparent position of Tau-Scorpii as seen by each tube)

not appear possible for this to be the cause of the emission seen. One possibility that has not been examined carefully is the presence of a cloud of gas from the AC subsystem that performed the pitch-and-roll maneuver. If sunlit, this could have reflected light into the UV photometer if the instrument scanned in that direction.

6. Dual-frequency receiver flight performance. During the interplanetary cruise, the DFR measured the integrated electron density along the propagation path from the Stanford ground transmitter to the spacecraft. Similar instruments aboard *Pioneer* spacecraft made it possible to study radio-propagation effects of widely separated points in space. The antenna pattern of the Stanford transmitter and the positions of the spacecraft permitted simultaneous operation of both spacecraft on the 49.8-MHz channel. Each operating day, as the spacecraft rose above the horizon, the DFR locked onto the signals and returned its scientific data without fault. More than 625 h of data were obtained.

The DFR performed within its design requirements throughout the mission. On day 242, the carrier-difference readout became zero, and the 49.8-MHz VCO reading was lower than it had been previously. This condition was traced to a maladjustment at the ground station. The behavior of the DFR carrier-difference readout was subsequently investigated for various transmitter conditions, and was found to be normal. The modulation phase as a function of phase angle agreed with the preflight calibration. The carrier amplitudes were compared with the calculated values. Near earth, the agreement was excellent; however, the 49.8-MHz amplitude was lower than calculated for ranges greater than 1×10^6 km.

Because the *Pioneer* instruments showed similar effects, and because of the extensive radio-interference testing of *Mariner V*, the possible space phenomena that could cause the lower signal are being investigated. The VCO readings obtained when the Stanford transmitter was not sending are an indication of the stability of the phase-locked-loop circuits. The drift from the rest-frequency position is negligible.

On day 311, the spacecraft was rolled three times. The DFR antenna pattern obtained by this maneuver is shown in Fig. VI-9. The 423.3-MHz pattern is the same as that measured on earth. The 49.8-MHz pattern, although obscured by fluctuations in the ionosphere and propagation path, is similar to the earth-based measurements. The main antenna beam extends from clock angles of 50–120 deg, and has minimums at 150-, 315-, and 10-deg clock angles.

During the encounter with Venus, the DFR performed as planned. There was about 20 dB of dynamic range for the signal-amplitude measurement. The VCOs remained near the rest frequency during occultation so that the phase-lock loops could reacquire the signal without delay. Along with the other spacecraft subsystems, the DFR operated with no evidence of anomalous behavior.

E. Telecommunications System Performance

1. Description. The telecommunications system for the *Mariner* Venus 67 mission consisted of both onboard spacecraft equipment and equipment located at the ground stations of the DSIF. This equipment provided the capabilities for telemetering spacecraft data to earth; commanding the spacecraft from earth; tracking the spacecraft RF carrier in both one- and two-way lock; and ranging with the spacecraft, using the Mark II ranging system close to earth and the research and development (R&D) planetary code near encounter.

Mariner V used a telecommunications system that was identical to the *Mariner IV* system except for changes made to meet the requirements of the *Mariner* Venus 67 mission and modifications to improve and update the equipment. Handling of telemetry data on the ground was modified considerably from the *Mariner* Mars 1964 mission to take advantage of increased ground-station capabilities. Details of these modifications are described in Subsections E-1-b and E-2.

a. Analysis. Techniques used for predicting telecommunications performance for *Mariner V* were identical to those for *Mariner IV* except that additional capability

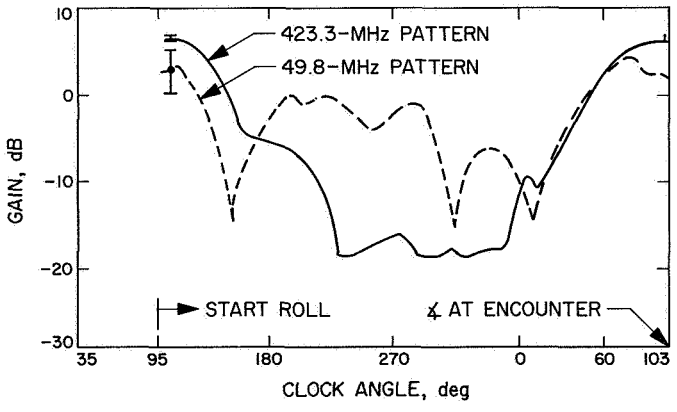


Fig. VI-9. Dual-frequency receiver antenna gain, day 311

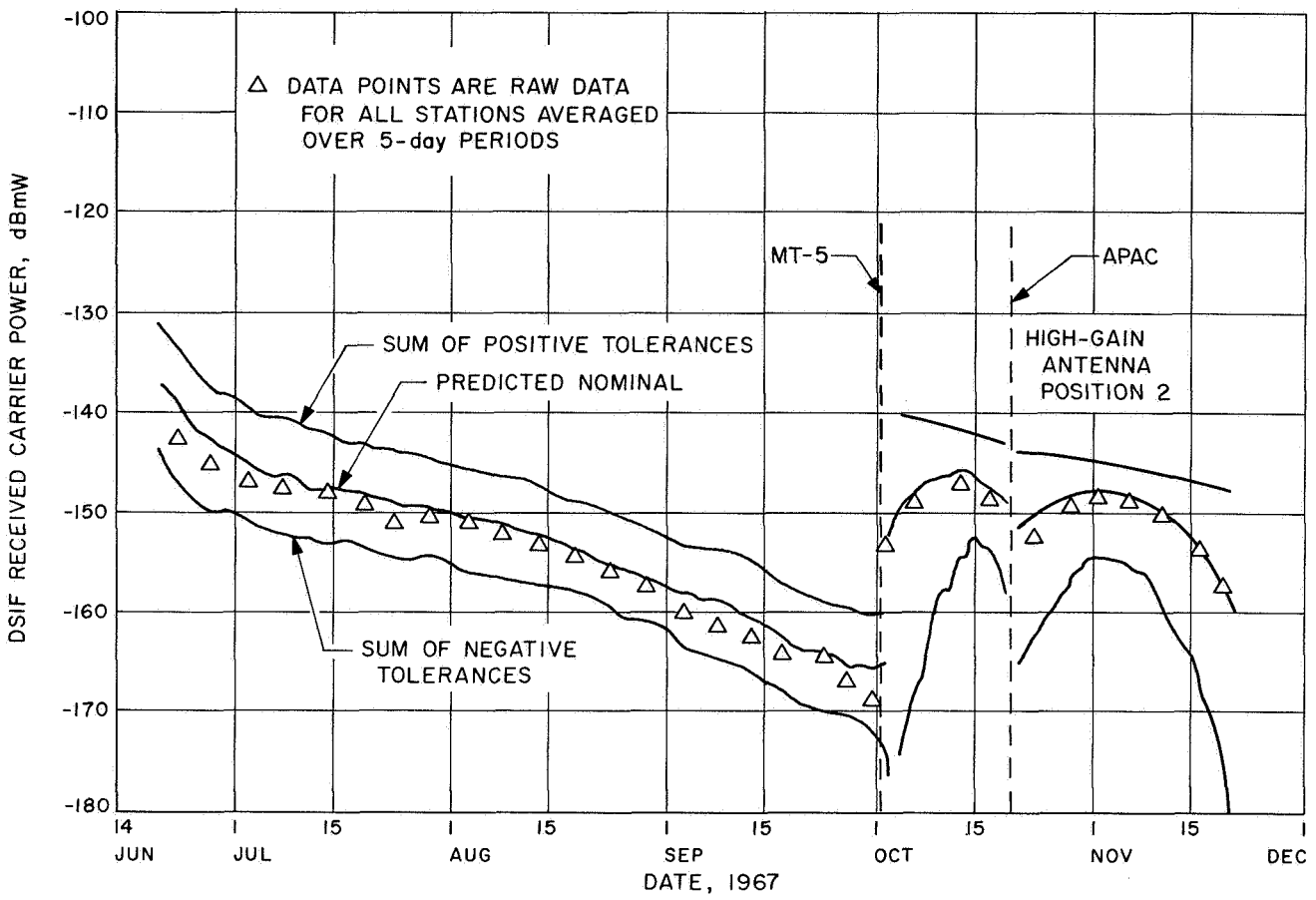


Fig. VI-10. Telecommunications performance analysis, downlink, 85-ft antenna

was provided to analytically generate a high-gain antenna pattern pointed at any spacecraft-to-earth look angle by computer. This capability was known as the analytical digital antenna pattern program (**ADAP**), and was used during the premission design phase to optimize antenna pointing for telemetery and occultation coverage. Because *Mariner V* had two high-gain antenna positions instead of one, as had *Mariner IV*, this capability was doubly useful in reducing manual calculations involved in the antenna-pointing analysis.

Along with these antenna patterns, a tape of trajectory parameters, and communications system parameter inputs, the communications prediction program (**CPPM**) was used to generate plots of predicted signal levels and performance margins for both the uplink and downlink channels. A problem that had been observed during the *Mariner* Mars 1964 mission was repeated for *Mariner V* in that the formats of the trajectory tapes were constantly changed to increase their information content. This resulted in about a 3-wk delay in finishing the first run of the *Mariner V* communications predictions while the **CPPM** program was modified to accept the latest trajectory-tape format.

Received-signal-level data from spacecraft and ground-station AGC compared favorably with the predictions. The average deviaton from nominal was about −2 to −3 dB, and was well within the negative tolerances assigned (Figs. VI-10 and VI-11). Because the deviations are averaged over several stations for several days, any large variations between stations and station passes are averaged out. These large variations ranged from as low as 5–6 dB below nominal to (in some cases) as high as 2–3 dB above nominal. The larger variations between stations and passes of one station tended to diminish in both frequency of occurrence and amplitude as the mission progressed. The reason for this phenomenon is not clearly understood, but it is possible that improved techniques for monitoring received and transmitted signals at DSN stations were responsible.

Variations of 2–3 dB from nominal, as observed in the *Mariner* Venus 67 mission, compare to variations of

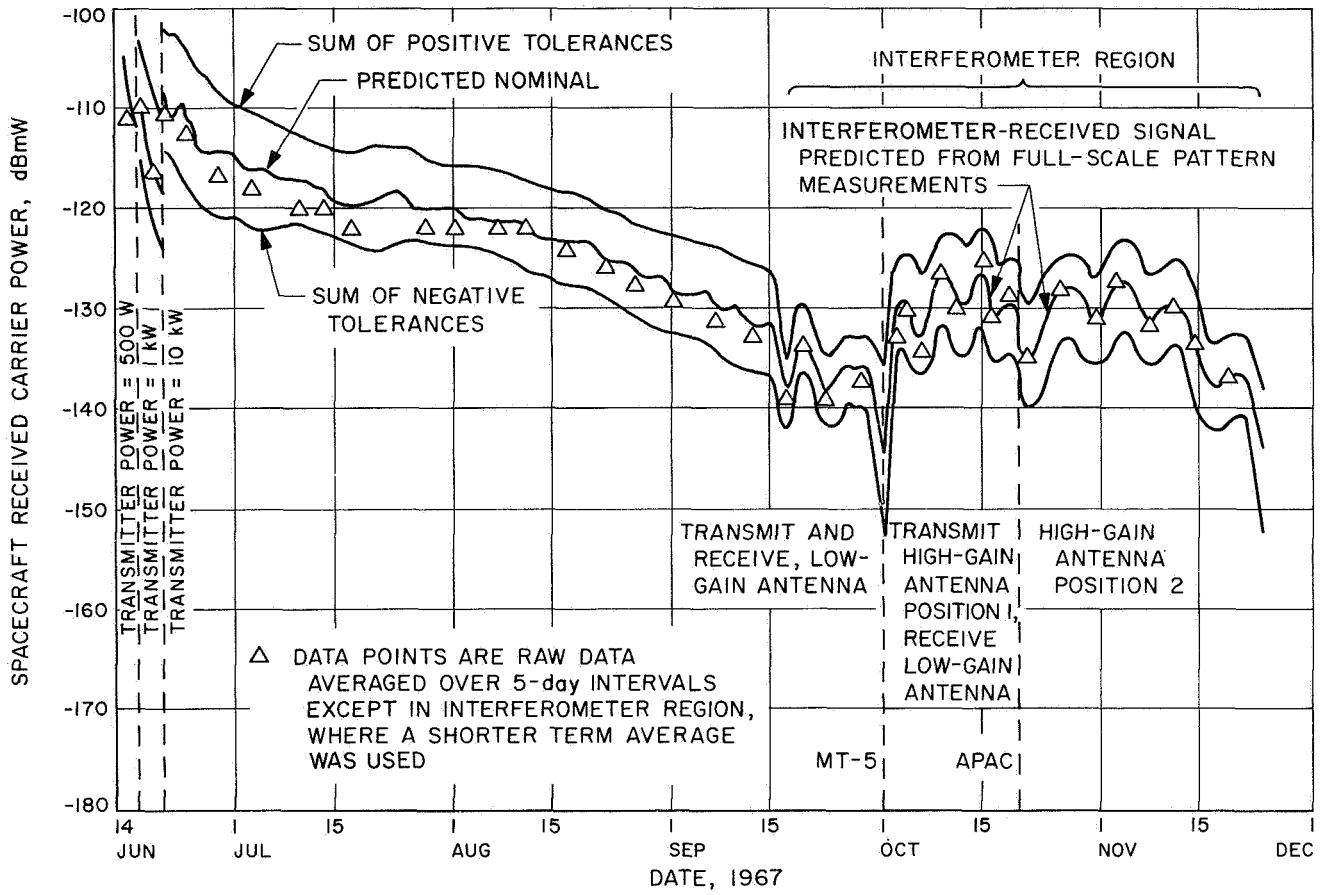


Fig. VI-11. Telecommunications performance analysis, uplink, 85-ft antenna

1–2 dB observed during the *Mariner* Mars 1964 mission. The closeness of the *Mariner* Mars 1964 mission numbers was achieved only after an extensive analysis of station calibration errors applicable to the mission. This detailed an analysis was not performed for the *Mariner* Venus 67 mission.

A major difference between the two missions was the amount of time devoted to tracking the spacecraft. During the *Mariner* Mars 1964 mission, there was practically no competition from other spacecraft projects for DSN station tracking time; as a result, *Mariner IV* was tracked nearly continuously (sometimes by more than one station). This resulted in a great deal of data with which to compare station performance, calibrations, etc., and more time was available to evaluate differences between stations. Thus, the overall level of performance analysis for the *Mariner* Mars 1964 mission was higher than for the *Mariner* Venus 67 mission.

This difference was noted very clearly in the analysis of the uplink-antenna interferometer patterns for the *Mariner* Venus 67 mission as compared to those for the *Mariner* Mars 1964 mission. With nearly continuous tracking, *Mariner* Mars 1964 mission engineers were able to plot the interferometer effect through all nulls and peaks, and to predict the future nulls and peaks very accurately. In contrast, the sporadic tracking of *Mariner V* led to instances in which only one data point on each side of an interferometer peak or null would be observed. Coupled with station-to-station variations in uplink-signal level and AC limit cycles, this situation made it very difficult accurately to predict future peaks and nulls.

b. Data handling. A major change in the ground-data-handling configuration for *Mariner V* that was closely monitored by the telecommunications group was the use of the DSIF TCP to replace the *Mariner* IV decommutator, TTY encoder, and high-speed data line (HSDL) formatter. Use of the TCP appeared to be desirable; but, as it had not been previously demonstrated on the *Mariner* Mars 1964 mission, there was some concern.

While the TCP programs were being written and the interface hardware with the *Mariner V* demodulators

was being developed, a TCP computer (actually only half of a complete TCP configuration) was installed adjacent to the system test complex in the Spacecraft Assembly Facility. This computer was used to monitor spacecraft-system testing until the spacecraft was shipped to AFETR. During this period, the TCP was subjected to careful scrutiny by SPAC and all personnel concerned with its operation. By the time of launch, enough confidence in the TCP had been developed to justify its use as the prime ground-data-handling mode for *Mariner V*. Performance of the TCP during the mission was excellent.

c. Telecommunications SPAC. The telecommunications SPAC team was headed by a Division 33 SPAC representative and supported by a representative from each of the following areas: radio, data encoder, tape recorder, command, antennas, and ground telemetry. Team members were assigned before performance of the first system test on *Mariner V*. Each representative was required to have knowledge of the design, fabrication, test history, and flight performance of his subsystem. Each SPAC member was responsible for analyzing his hardware in flight, analyzing real-time telemetry, and advising the division representative or SPAC director as to the status of his hardware. During periods of high activity, it was not possible for one individual to cover a 24-h period. For this reason, at least two individuals were assigned to each required representative position.

Planning for the *Mariner* Venus 67 mission SPAC team started in the spring of 1966, with a series of meetings to discuss data-format requirements, SPAC operating procedures, and facilities requirements. The Division 33 telecommunications representative furnished inputs to these SPAC planning meetings based upon experience of the *Mariner* Mars 1964 mission and inputs from telecommunications subsystem engineers.

Telecommunications SPAC support for the *Mariner* Venus 67 mission started on November 4, 1966. The SPAC group supported all of the major spacecraft tests to acquire as much knowledge as possible of spacecraft functions. Early SPAC training was encouraged to familiarize members with computer-formatted data, spacecraft-system operation, and SPAC operations. Several mission-operations tests were conducted in which simulated failures were induced. The SPAC personnel were expected to identify, analyze, and recommend corrective action for all induced failures. In addition to failure-mode testing, SPAC participated in simulated precountdown and countdown tests conducted both in the Spacecraft Assembly Facility and at AFETR. Correspondingly, several pre-encounter practices were held to familiarize personnel with encounter procedures and encounter failure-mode testing.

d. Operations.

Launch and midcourse maneuver. The telecommunications SPAC team supported launch operations starting with a simulated precountdown on L−1 day (June 12, 1967). Full SPAC support was required on a 24-h/day basis until L+45 h. SPAC representatives alternated 10-h shifts during this period. From L+45 h to the midcourse maneuver (M−6 h), one SPAC member from each division was required on a 24-h basis except during normal working hours, when all SPAC representatives were required on station. From M−6 h to M+5 h, all members were required. After M+5 h, one representative from each subsystem was on call, at all times, until encounter activities commenced.

Cruise phase. During the period from the midcourse maneuver to encounter, a representative from each subsystem would review data from the previous day during the morning of normal work days (Monday morning data would also cover the weekend). From these data, a daily report would be written that summarized the activities of each subsystem, listed all command activity and mission operations, and compared current telemetry data to data from the previous day.

During the cruise phase, also, many exercises and tests were conducted that were not planned before launch. An example would be the tests run to evaluate the UV-photometer calibration. These exercises were supported on an as-needed basis, and planning for them was on a real-time basis. Planning for SPAC for future missions should allow a few extra personnel during cruise to provide coverage for these contingencies.

Encounter. Full SPAC support for encounter started at E−18 h and continued until E+48 h. This period covered events from terminator sensor excitation turn-on (DC-V25) to completion of the first playback of encounter data stored by the tape-recorder subsystem. Minimal telecommunications support (tape-recorder representative) was required for the second playback of stored encounter data, which was completed on October 23, 1967.

SPAC logs. For the *Mariner* Venus 67 mission, a log keeper was assigned to maintain a central log of the SPAC operation, including significant events from all subsystems. This arrangement proved to be unsatisfactory

because the logkeeper was not sufficiently familiar with the details of the spacecraft to enable him independently to choose important items to log, and the subsystem engineers were too busy during mission operations to provide him with inputs.

During SPAC operations, maintaining an adequate, detailed, written log by each subsystem-cognizant engineer is desirable, but can cause attention to be diverted from incoming data. Also, compiling several separate logs into a daily summary requires too much of the engineer's time.

An idea suggested for future use is to have a dictaphone on the SPAC director's desk, and one for each division, to record events as they occur. This would require a specific, well-defined input format, including name of the person contributing, time of event (GMT), subsystem name, and event description, so that all information could be in the same format for the typist. These items could be typed in four columns as a rough log to be maintained intact. Each engineer could quickly edit a copy of his rough log; the secretary could then excerpt the desired inputs, and generate a daily summary sheet. This would be more detailed and less time-consuming than the present method.

Ground station data. For the *Mariner* Venus 67 mission, a digital display of ground-station telemetry was implemented in lieu of the analog system used for the *Mariner* Mars 1964 mission. The digital system processed station AGC in the TCP, and sent it to SFOF over the HSDLs. It was then processed by the 7044 computer, and displayed in the SPAC area on the telecommunications 100-w/m printer format. Digital display proved to be a more stable and reliable source of station-received signal-level information than did the analog system used for the *Mariner* Mars 1964 mission.

Ground-received signal level was used to estimate spacecraft clock angle during roll maneuvers, and to verify spacecraft turn polarities during the midcourse maneuver. It was also used to compare station-received signal levels to predictions in real time, but post-tracking station reports were used as the final data for these comparisons.

In addition to ground-station AGC, real-time information on ground-transmitter and receiver frequencies in some readable form could have been used by the telecommunications and radio subsystem analysts. These data would have been useful during the exit-occultation phase, when the ground station was attempting to acquire the spacecraft two-way; they also would have been useful for keeping a real-time record of spacecraft frequencies as they varied with temperature and age during the mission. Maintaining an up-to-date record of spacecraft frequencies was necessary to ensure RF acquisitions in minimum time throughout the mission. *Mariner V* frequency data were not readily available in real time, but the advent of the DSN monitor system should make these data available on future missions.

e. Telecommunications complementary analysis team. The telecommunications complementary analysis team (TCAT) was the Division 33 portion of the *Mariner* Venus 67 mission complementary analysis team organization. TCAT was implemented to use the resources of detailed spacecraft design knowledge possessed by personnel not assigned to flight operations in SPAC. Real-time data were displayed in the TCAT area in parallel with telecommunications SPAC displays. This provided the capability for a prompt analysis by the most knowledgeable personnel of any subsystem anomaly that could occur during flight. TCAT also served as advisors to the SPAC team during critical phases of operation.

f. Venus encounter preparation working group. The VEPWG, which was assembled shortly after launch, and met weekly until encounter, was established by the SPAC director to study the encounter phase and to recommend any strategy that should be employed to ensure mission success. Two telecommunications representatives attended all meetings of the VEPWG, and they were supported in analysis of encounter problems by the entire SPAC team. The following were some of the items investigated by the telecommunications members of the VEPWG:

(1) Temperature variations of bays 5 and 6 effect on frequency measurements.

(2) Radio lockup times after occultation.

(3) Low-gain antenna interferometer pattern effects expected during encounter.

(4) Uplink and downlink communications performance margins at encounter.

(5) Action required if tape recorder did not start on time.

(6) Consequences of downlink frequency changing rapidly near Venus.

(7) Determination of X_A frequency for possible two-way enter-occultation.

The final outputs of the VEPWG were an encounter-sequence plan and a set of flow charts covering actions to be taken for a nominal encounter sequence. Another set of flow charts depicted possible abnormal encounter sequences and the appropriate actions to be taken should they occur.

2. *Mission-related hardware.* Mission-related hardware (MRH) for the *Mariner* Venus 67 mission consisted of the ground telemetry subsystem (GTS) and ground command subsystem (GCS). The units used for the *Mariner* Mars 1964 mission were refurbished, then transferred to the DSN, and deployed to ground stations supporting the *Mariner* Venus 67 mission.

A philosophy different from that for the *Mariner* Mars 1964 mission was adopted for the *Mariner* Venus 67 mission for processing the demodulated telemetry data stream at the ground stations. The incoming spacecraft data stream was both demodulated and decommutated in the MRH during the *Mariner* Mars 1964 mission. The decommutated data stream was then passed through an electromechanical TTY/encoder combination, and formatted for transmission from the DSN stations to JPL.

For the *Mariner* Venus 67 mission, TCP computers were available at the DSIF stations, and were used to perform both decommutation and formatting functions. The *Mariner IV* type of hardware decommutators were maintained with the GTS equipment as a backup at the stations, but the TCP was used as the prime telemetry processor. Part of the GTS refurbishment between the two missions consisted of installing an interface drawer to make the output of the hardware demodulator compatible with the TCP input requirements. The TCP was used very successfully by the *Mariner* Venus 67 project, and proved to be more reliable and flexible than the TTY/encoder combination used for the *Mariner* Mars 1964 mission.

After deployment of the MRH to the DSIF stations supporting the *Mariner* Venus 67 mission, the DSN was responsible for maintenance and operations of the MRH. As a part of this responsibility, the DSN installed engineering change requirements (ECRs) for any modifications that were designed after the units had been shipped to the stations. The DSN also maintained a trouble- and failure-reporting system designed to keep both the project and the DSN advised of failure trends and problems with the MRH units.

a. Mission-related hardware ECRs implemented by DSIF stations.

Read–write–verify. After arrival of the RWVs at the DSIF stations, it was decided to incorporate three more ECRs. The ECRs, which were the results of problems that were observed after shipment to the stations, are detailed in Table VI-6.

Considerable effort was required to incorporate ECR 8839 without jeopardizing the mission. The several hundred transistors were procured on a rush basis and had been screened by a contractor. This ECR was incorporated on the assumption that no RWV at any station

Table VI-6. Mission-related hardware ECRs (RWV)

ECR No.	Function
8839	During the refurbishment of the RWVs, two power supplies were found to be inoperative because the series-regulator transistors (2N1544) had failed. After shipment of the RWVs to the stations, three more power supplies failed. The series regulator in the −18-V line was at fault in all cases. An investigation by the parts analysis group indicated that the leakage and beta of the transistors were extremely sensitive to elevated temperatures. The parts analysis group suggested that replacement of the transistors with new units should be sufficient to correct the failure tendency because the manufacturing methods used on this type of device had been improved since these units were originally fabricated.
8841	Called for the removal of one bulb from each of the IN PROCESS and READY displays. Repeated failures of the lamp-driver transistor indicated that the unit was being overrated. Calculations and measurements showed that the units were operating within specifications for steady-state conditions. When the indicators were switched on, however, the transient current could reach a maximum of 4½ times the rated maximum if all bulbs were installed. Eliminating the redundant bulbs reduced the maximum switched current to about twice the rated value of the transistor. This was known before releasing the RWVs to the DSN; consequently, the units were shipped with the correct number of bulbs. ECR 8841 was written to alert the stations not to replace the apparently missing bulbs, and to add this information to the RWV documentation.
8855	This ECR, which was simultaneously submitted by DSS 11 and DSS 42, called for use of the power switch associated with the tape-punch unit to control the tape reader as well. This would allow both the tape reader and tape punch to be placed in a standby mode, thus minimizing mechanical wear on both units instead of only the tape punch. This modification was installed in a typical RWV, serial number (SN) 109, and was found to be too difficult for a field modification before encounter. As a result, SN 109 is the only unit with this modification.

would be "down" at any time because of its incorporation. Also, only screened parts were used for the modification, and all board changes were made at the Goldstone repair depot. This was accomplished by using spare cards and boards from power supplies that were on hand at Goldstone and JPL. Sufficient boards were in existence so that five power supplies or spares complements at the various stations could be replaced at a time. The replaced cards were then returned to Goldstone, modified, and sent to another DSS, where the same process was repeated. A flow diagram was prepared to schedule the shipments of power-supply boards between the Goldstone repair depot and the stations. Since the incorporation of this ECR, there have been no known failures of this type.

Ground telemetry subsystem. The ECRs that were incorporated at the stations following the arrival of the GTS units are detailed in Table VI-7.

b. Mission-related hardware TFRs from DSIF stations. Failures in the RWV and GTS units were documented by the DSN in the form of DSIF trouble and failure reports (TFRs). This discussion covers the time from receipt of the units at the stations until the end of the mission. The failure types range from those occurring during preventive maintenance to those occurring during spacecraft tracking. No attempt will be made here to discuss specific failures. In general, the failure trends were similar to those observed during the refurbishment program.

From the project viewpoint, the TFR forms used by the stations did not contain enough detail to describe many of the failures that occurred. This may have been because of misinterpretation of the data required by the operator filling out the form. In addition, many cases occurred for which it was difficult to determine the serial-number unit in which the failure had occurred.

Table VI-7. Mission-related hardware ECRs (GTS)

ECR No.	Function
8827	It was discovered that a possibility existed of burning out a solenoid in the Franklin printer because of a nut working loose. The two ribbon-reversing solenoids are joined together by a metal bar, each joined to the bar by a screw and a hex nut. This ECR called for replacing the screw with a longer one and a self-locking nut.
8853,8854, 8857, 8858	These ECRs were required to incorporate the **DDT** program into the GTS.

In general, the TFR system did not work out as satisfactorily as the PFR system used by the project, and it is felt that further emphasis should be placed upon this area.

During the 10-mo period from prelaunch until the end of the mission, 162 RWV failures were reported from 10 Deep Space Stations that used 11 RWVs, an average of 15 failures per RWV.

For the same 10-mo period, 190 GTS failures were reported from 9 Deep Space Stations that used 8 GTS units, or an average of 24 failures per GTS.

c. Digital demodulation technique. Prediction of telecommunication performance for the *Mariner* Venus 67 mission showed that a 2-wk period would occur when the received-signal level would be below threshold at the standard 85-ft Deep Space Stations with MRH demodulators. During this period, spacecraft telemetry data would be available only from DSS 14, and scheduling difficulties would not permit the mission continuous use of DSS 14.

It was decided to try to develop an experimental digital computer program for the TCP that would synchronize on the data-bit stream itself, and not be dependent upon the telemetry sync subcarrier. This technique had been previously demonstrated on an SDS-930. It was desired to adapt the technique to an SDS-920 (one-half of a TCP), and use the other half of the TCP for the decommutation and formatting program.

Development of the **DDT** program for the TCP was begun only a few months before it would be needed, and it was thus necessary to expedite its development. For 3–4 mo, TCP programmers and MRH engineers worked together, without a detailed request for programming, designing the program and its interface with the stations. The program was completed and operational by the middle of September 1967, and was used to support both *Mariner IV* and *Mariner V* tracking.

The program was not completely analyzed theoretically in the beginning, and engineering judgment was used to determine some of the parameters necessary for program operation. Further analysis has provided a better theoretical base for these parameters. The disadvantage of the **DDT** program, as it was implemented for the *Mariner* Venus 67 mission, was that it would operate only in spacecraft mode 2 at 8⅓ bits/s.

Operations with the **DDT** verified its usefulness as a data-gathering tool. Its use, in conjunction with some R&D improvements to the receivers at DSS 51, made it possible to receive usable telemetry about 5 dB below the point at which the MRH demodulator would normally drop lock.

The bit-error rate of the telemetry data near the useful limit of the **DDT** was higher than the 1/200 associated with the MRH demodulator threshold. This was to be expected, as the **DDT** useful limit was at a lower SNR than that of the MRH demodulator threshold. As a rough estimate, it was found that useful data could be obtained at bit-error rates approaching 1/25.

The ECR modifications that were made to the *Mariner* Venus 67 mission GTS to incorporate the **DDT** are described in Table VI-8.

d. Recommendations. Recommendations for the MRH are contained in Volume I of this report. Field operations during the *Mariner* Venus 67 mission confirmed these recommendations. (For example, it took as much as 6 mo or more for the project to be notified of the incorporation of ECRs; this was in spite of memoranda, TTY exchanges, and telephone calls requesting notification.)

To facilitate hardware configuration control in future projects, it is recommended that a positive and timely reporting system be incorporated and enforced to confirm the incorporation of ECR modifications.

3. Radio subsystem performance. During the *Mariner V* flight, the operation of the radio subsystem (RSS), as indicated by telemetry, was as predicted, but with several minor discrepancies that require explanation.

Table VI-8. Ground telemetry system ECRs to incorporate DDT

ECR No.	Function
8853	Added interface circuits between the TCP and the GTS BEC[a] to make their logic families compatible.
8854	Added a connector to the *Mariner V* encoder simulator so that required data could be sent to BEC.
8857	Added circuits to provide the necessary filtering, amplification, and AC coupling of the receiver output signal to drive the beta TCP computer properly.
8858	Written to provide for the cable necessary to carry the composite signal from the GTS to the computer analog-to-digital converter.

[a]BEC = bit-error checker.

Notably predictable during the flight were various RSS supply voltages that were characterized by their stability. These were: channel 109 (power switch and logic volts), channel 301 (exciter −25-V monitor), and channel 302 (exciter −15-V monitor).

The operation of the TWT amplifier was also as expected and highly stable, as shown by its telemetered parameters. The only item of interest was the current variations that were apparent on telemetry channel 300 (cathode/helix current), shown in Appendix C, Fig. C-34; this phenomenon is a known characteristic of TWT amplifiers under these conditions. Aside from this phenomenon, the TWT helix current showed a decrease of only 1 DN for the length of the flight, with an occasional ±1-DN short-term excursion (1 DN is equivalent to 0.15 mA).

The stability of the TWT RF power output was also observed in the antenna-drive channels: channel 213 (high-gain antenna drive) (see Fig. C-17) and channel 214 (low-gain antenna drive) (see Fig. C-18). Channel 213 showed only 1-DN change during its entire active operation (RSS in transmit high-gain antenna mode); this might be attributable to either a TWT power-output change or a change in the reflected power from the low-gain antenna caused by an impedance change with temperature (see channel 431). Channel 214 also exhibited only a 1-DN change during its TWT operation (RSS in transmit low-gain antenna mode). The only other change to these two channels occurred on day 263; this was a simultaneous increase of 1 DN on channel 214 and a decrease of 1 DN on channel 213. The change was attributed to a change in impedance match outboard of the power amplifiers (antenna temperature changes), and was probably not caused by any TWT variation. (On these channels, 1 DN is equivalent to about 0.16 dB in power.)

Channels 300, 213, and 214 also monitored the cavity amplifier while it was in operation during the launch phase and for the first 10 days of the flight. During this time, channel 214 was steady, which was to be expected because the spacecraft was transmitting on the low-gain antenna. The first change came immediately after the amplifier was switched to full power by the *Agena*-separation event. The amplifier warmup curve at first appeared anomalous compared to Spacecraft Assembly Facility testing data. By comparing this flight warmup with the data obtained in space-chamber testing, however, it was determined that the flight warmup was normal in a vacuum environment, the temperature gradients being different from those encountered in atmospheric environmental testing.

The second apparent power-output change came during the midcourse maneuver when both channels 300 and 213 dropped 1 DN each (0.65 mA and 0.11 dB, respectively). This change was attributed to the temperature change caused by orienting the spacecraft for the maneuver. After the midcourse maneuver, the cavity amplifier returned to normal operation.

Radio-subsystem temperature channel 404 (bay 5 temperature), channel 405 (bay 6 temperature), channel 418 (AO No. 2 temperature), and channel 424 (VCO temperature) were also highly stable, and their changes during the flight were quite predictable (see Figs. C-40, C-41, C-55, and C-57). All of these channels followed the same general pattern: an initial decrease in temperature for the first flight day or two, then no changes until the midcourse maneuver caused a sharp upward transient. This was followed by a return to the same premaneuver temperature-stable point. The entire RSS increased in temperature when the TWT amplifier was switched on because the TWT dissipated approximately 29 W more than did the cavity amplifier. After this, the RSS temperature showed a long-term gentle slope upward as the spacecraft–sun distance decreased. Superimposed on this gradual increase were +1-DN short-term excursions on channel 424 as the RSS VCO was switched on automatically by RSS acquisition of two-way RF lock. In addition, both channels 404 and 405 showed +1- to +3-DN excursions caused by encounter and tape-recorder-on conditions.

Channel 210 (spacecraft-receiver local-oscillator drive) showed a total change of 2 DN during the flight. The first DN change occurred when the TWT amplifier was switched on, and the second change occurred about two-thirds of the way to encounter. In addition, a 1-DN transient occurred during the midcourse maneuver. These were all increasing changes. Comparison of these three changes in channel 210 with the telemetry temperature channels shows that, when bay 5 temperature increased, so did local oscillator drive. This was normal and expected receiver operation.

Channel 229 (exciter RF power output) was unchanged during the entire flight.

Channels 111 and 215 (spacecraft-receiver AGC coarse and fine, respectively) are functions of ground-transmitter power, spacecraft–earth range, and antenna mode (both ground and spacecraft); these, of course, varied in accordance with the above conditions. Their operation was normal.

Channel 106 (spacecraft-receiver SPE) is dependent upon whether the receiver is in uplink lock and how far the received signal is off best-lock frequency. This channel also showed proper performance for the flight.

The *Mariner V* RSS normal operation was characterized by a number of secondary interactions; that is, changes in one area of the subsystem affected the operation of other areas (sometimes seemingly unrelated areas).

The significant variations of this type were all of the temperature-interaction variety. For example, an increase in temperature caused a decrease in cavity-amplifier cathode current and a subsequent, corresponding decrease in spacecraft RF power output. An example of this condition was the RSS temperature increase that occurred during the midcourse maneuver. This was, of course, caused by the unusual spacecraft attitude with respect to the sun.

Spacecraft-receiver local-oscillator drive showed a slight positive temperature coefficient. This led to the small increase in local-oscillator drive over the duration of the flight. However, this increase had no effect upon receiver performance. In particular, the receiver threshold showed no change at the end of the mission, compared with preflight measurements.

Most notable of the temperature-sensitive RSS parameters are the auxiliary oscillator and best-lock frequencies. Both of these frequencies exhibit a negative temperature coefficient. Before the flight, these curves were quite well defined experimentally to aid in flight operation. Another auxiliary oscillator characteristic that it was necessary to define was the warmup curve of frequency vs time. Some data were obtained in preflight testing (notably in the space simulator), but the best data were taken during flight under true space conditions.

Another thermal interaction was caused by change in radio mode. Turning on the ranging channel caused an increased power dissipation and resultant heating in the area of the VCO module. This caused a small change in the best-lock frequency, and could be observed as a 1-DN change in channel 424.

In addition to the heating interactions, there were several transient operational characteristics. The execution of a DC-V9 command to switch ranging on or off caused a small frequency anomaly in the VCO. This was caused by a current transient within a common power supply. This generally caused a momentary loss of command lock, and, in some cases, a loss of RF lock.

The CC&S CY-1 pulses, which occurred every 66⅔ h, generally affected the RSS only if ranging were on, in which case the CY-1 pulse turned ranging off, with the result mentioned above.

a. In-flight postencounter radio subsystem test. After encounter, several special tests were performed to determine whether the basic electrical parameters of the transponder had changed during the flight.

The ground transmitter was so adjusted in frequency that the spacecraft VCO frequency was pulled to +625 and −491 Hz while monitoring telemetered SPE. The voltage sensitivity and center frequency of the VCO showed no change from the prelaunch data.

The uplink power to the spacecraft was decreased to spacecraft-receiver threshold while offsetting the VCO best-lock frequencies: 0, ±50, and ±100 Hz, respectively. When these data were compared with preflight data, it was determined that no receiver threshold degradation had occurred during flight.

Command-lock threshold was also measured, and was found to agree with preflight data. This indicated that the receiver noise figure had not deteriorated.

b. Conclusions and recommendations. The usefulness of telemetry channel 215 (AGC fine) was significantly less for this flight than it might have been if the range had been shifted upward 10 dB. The present range for this channel is from −131 to −151 dBmW. Usefulness would have been improved if the range had been shifted upward to −121 through −141 dBmW, as the greater portion of the flight was in this signal-strength range. Also, below −140 dBmW, the fine AGC is so noisy that it becomes practically useless at the present sample rate.

Telecommunications personnel of the SPAC team would be better informed and, therefore, of more operational usefulness if both the ground-transmitter and ground-receiver VCO frequencies were displayed in the SPAC area. These frequencies should be displayed with the doppler residuals removed; i.e., as the spacecraft would observe them, since all of the preflight RSS data were collected statically.

More extensive use of on-line instrumentation computers during preflight calibration testing would save hundreds of man-hours in data reduction. This is particularly applicable during tests involving frequency predictions, frequency stability, and ranging delay times.

4. Interferometer performance. As is discussed in Volume I of this report, the uplink interferometer was used to extend the reception range of the RSS when operating in the normal encounter radio mode (transmit on high-gain antenna and receive on low-gain antenna). The nominal low-gain received signal, without the interferometer effect, was predicted to reach command threshold at encounter with the DSS 85-ft antennas transmitting at 10 kW. To ensure command reception near encounter, it would have been necessary to enter encounter in the less desirable receive-high-gain mode or to redesign the low-gain antenna.

Encountering in the receive-high-gain antenna mode was considered too risky because a DC-V15 (Canopus-gate override) might be used by AC during planetary flyby. This would keep the spacecraft from going into roll search if the Canopus sensor started to track a dust particle (which could be dislodged at APAC) far enough to lose Canopus lock during this critical period. Without a DC-V15, the spacecraft would go on inertial control and into roll search, which could result in loss of occultation data. With a DC-V15 in effect, the gyros would be inhibited even if Canopus reference were lost; consequently, the RSS would not receive a switch-to-low-gain antenna signal from the CC&S subsystem. This would result in a loss of both uplink and downlink communications if the spacecraft had rolled far enough to point the high-gain antenna beam away from the earth. Also, if the spacecraft tried to reacquire Canopus the long way around, it could burn out the Canopus sensor if the bright limb of the planet entered its FOV. As a result, the mission was constrained to use a DC-V15, and to receive uplink commands via the low-gain antenna.

Use of the interferometer, which is activated by the high-gain-antenna received signal combining with the normal low-gain-antenna received signal through a leakage path, precluded the necessity of a low-gain-antenna redesign.

Analysis showed (see Volume I) that the isolation between the high- and low-gain antennas had to be reduced to 9.5 ±1.5 dB to assure uplink communications with worse-case phasing at or near encounter. During the flight, the exact phasing between the two received signals was indeterminate until the earth vector entered the interferometer region. At that time, after the location of a null and the peak to minimum amplitude was established, a realistic interferometer antenna pattern could be predicted and measured on the full-scale spacecraft antenna range. This was accomplished between October 9 and 11, 1967.

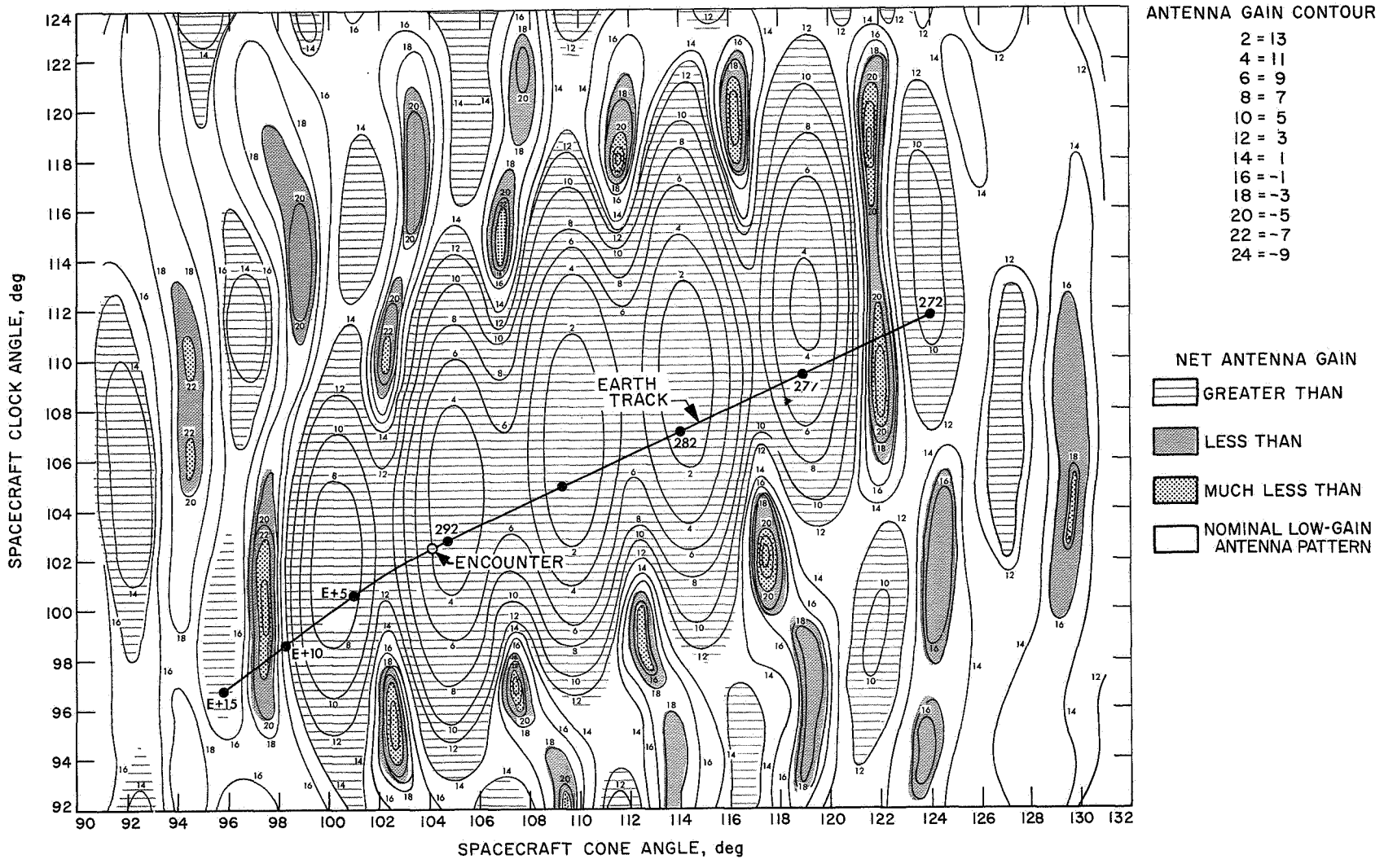


Fig. VI-12. Interferometer antenna pattern, high-gain antenna in position No. 1

From these measurements, three-dimensional contour plots of the interferometer pattern for both positions of the high-gain antenna (pre- and postencounter) were generated. These patterns are shown in Figs. VI-12 and VI-13, respectively. It could also be determined that the actual effective isolation between the antennas was 8.0 dB instead of the designed 9.5 dB. The effect of this was to increase the received signal strength in the interferometer region to the worst-case high prelaunch prediction. The change in isolation was probably caused by differences in antenna impedances on earth at room temperature and in space at cold temperatures.

The actual and predicted interferometer received-signal strength for the 32 days before and after encounter, along with the positive and negative tolerance limits, are shown in Fig. VI-14. The plotted postencounter received-signal data points follow the predicted curve more closely than the pre-encounter points because the actual spacecraft attitude, in its 3-axis limit cycle, was accounted for. The pre-encounter points were determined by averaging a large number of samples without regard for limit-cycle position. The APAC failure-mode, received-signal predictions, along with a plot of the nominal low-gain antenna received signal without the interferometer, are shown in Fig. VI-15.

5. Flight command subsystem performance. Ground commands were used to acquire Canopus, perform a midcourse maneuver, switch power amplifiers, initiate and back up encounter, perform several in-flight tests, and condition the spacecraft for postencounter cruise. During this period, the command subsystem performed as designed, and no anomalies attributable to command-subsystem malfunction were observed. Ground stations transmitted 96 commands to the spacecraft from launch on June 14, 1967, through conditioning of the spacecraft for long-term cruise on November 21, 1967.

One command transmitted from the ground was not processed by the command subsystem. This was a DC-V12 command transmitted on November 7, 1967, during a postencounter maneuver sequence. The spacecraft was in a roll-search mode, near an antenna-pattern null, when the command was received. The spacecraft receiver momentarily dropped uplink RF lock, causing the command subsystem to drop lock, and inhibiting the processing of the DC-V12. This is proper command-subsystem operation.

After encounter, a series of tests was run to verify that the command subsystem had not degraded during the mission. From these tests, it was ascertained that the command-subsystem lock-up point and threshold had not degraded since launch. It was determined that the command subsystem would maintain a marginal lock status down to a spacecraft-received carrier power of −146 dBmW, which is comparable to prelaunch data. This result is in agreement with the results of similar tests performed with the *Mariner IV* spacecraft in 1964 and 1967.

6. Data encoder performance. The *Mariner V* data encoder received data from both engineering and science subsystems, coded them, added synchronization data, and transmitted the data to earth. Data from launch, midcourse-maneuver, cruise, encounter, and post-encounter operations were transmitted to earth with no data-encoder anomalies.

As expected, spacecraft power transients resulted in several deck skips and resets, but these are well-characterized phenomena for which a fix was proposed during the design phase of the mission. The fix was judged not to be necessary to mission success; therefore, it was not implemented. Data encoder deck-skip phenomena were observed six times during the mission. The first occurred at *Agena*–spacecraft separation, and the other five when the battery charger was turned off. Both of these conditions are recognized sources of spacecraft power transients that have resulted in deck skips during spacecraft systems tests. Unlike *Mariner IV*, *Mariner V* did not experience deck skips when the spacecraft passed through the Van Allen belt soon after launch.

The *Mariner V* spacecraft was launched with the data encoder on A/DC and pseudo-noise generator (PNG) combination B, and this was used throughout the mission. Power was not applied to A/DC–PNG combination A during the flight. At launch, the telemetry bit rate was 33⅓ bits/s, and there was sufficient ground-received signal to support this rate until E−87 days. CC&S command MT-6 was then used to switch the bit rate to 8⅓ bits/s, at which it remained for the rest of the mission (except for some tests run to check calibration of the UV photometer).

7. Tape-recorder subsystem performance. The tape-recorder subsystem (TRS) was first operated in launch mode as the spacecraft was launched. At *Agena* separation, a signal was sent to the TRS to shut off the launch motor at the next EOT. The tape stopped in the proper position for Venus encounter. The TRS was placed in cruise mode, with 283 tape passes (16 at launch), 224.3 h on the new electronics, and 690.3 h on the 1964 electronics. In the cruise mode, TRS power was off.

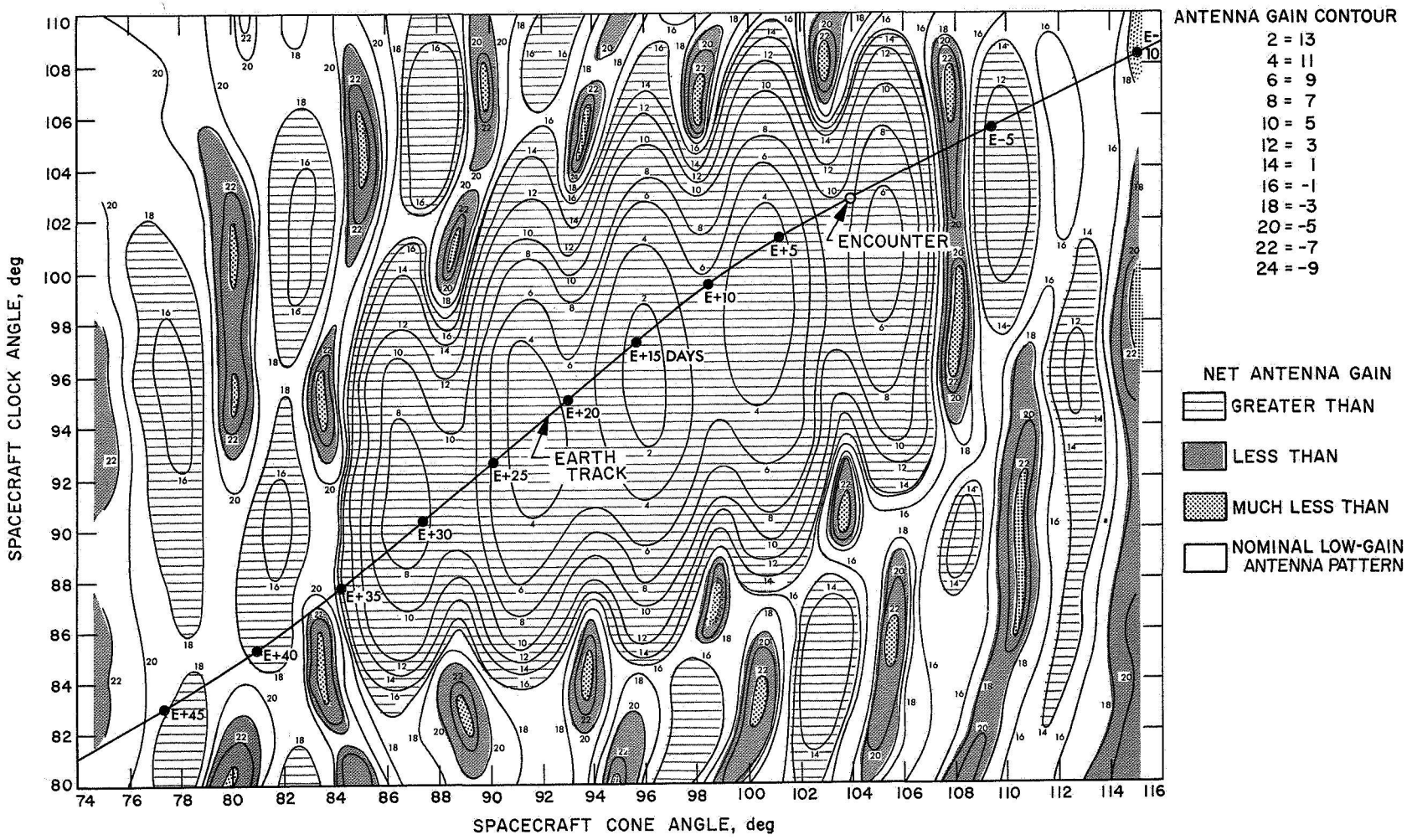


Fig. VI-13. Interferometer antenna pattern, high-gain antenna in position No. 2

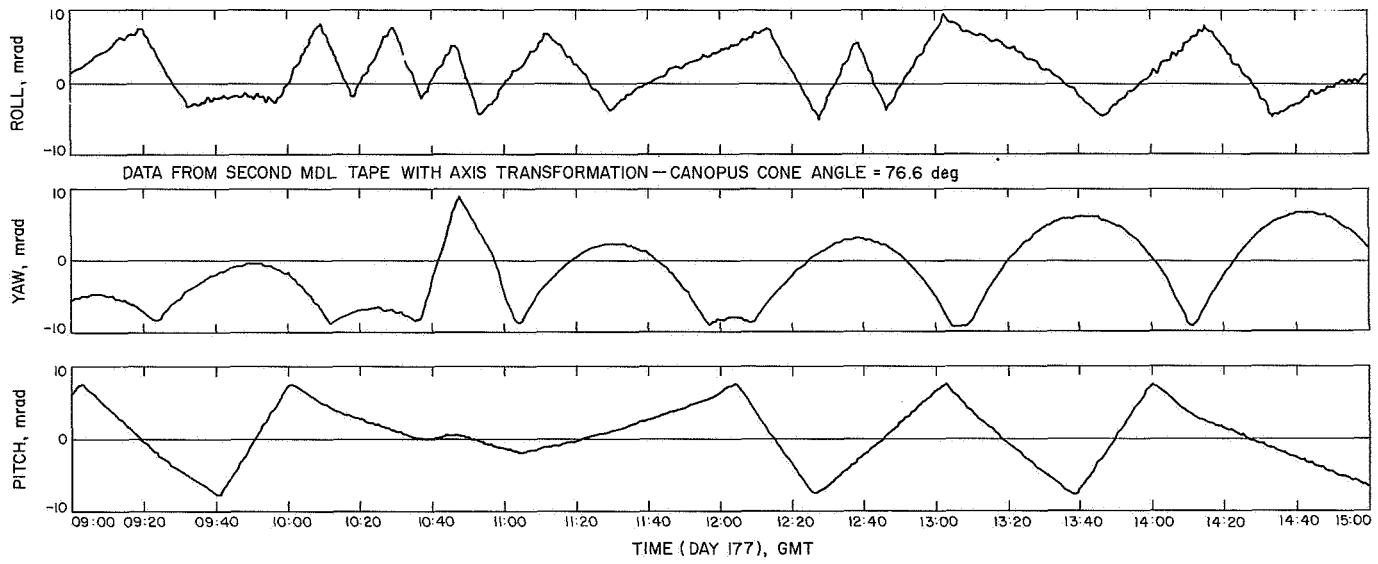


Fig. VI-14. Uplink received signal strength in interferometer region

a. Encounter phase. On October 19, 1967, the TRS was turned on by a DC-V25 command in preparation for the Venus encounter. A counter 3 event occurred at this time; this was the predicted EOT pulse that occurs in this subsystem at power turn-on. Telemetry channel 227 (2.7-kHz inverter output current) increased from 62 to 65–66 DN, indicating that the TRS was in the standby mode.

At PSO, the record motor was turned on, and it ran until stopped by the EOT signal 2 h, 7 min later. The science status bits for record motor on, track 1 data, track 2 data, stop record signals, and start record signals indicated normal operation. The times at which these events occurred are listed in Table VI-9.

b. Postencounter phase. On October 20, 1967, a DC-V4 command was sent to start playback. The TRS began playback on track 1, and the encounter data were played back twice to assure that all data were recovered. Playback performance was normal, with playback times very close to those predicted. A chart of the predicted playback times is shown in Fig. VI-16.

The TRS dropped lock several times during playback, but this was expected on the basis of bit-error tests that were performed before launch. Typically, one bit of data is dropped during a loss of lock because the motor runs faster during this time and the data bits are "squeezed." An illustration of this function is provided in Fig. VI-17. The actual bit-error rate of this playback will not be known unless a bit-by-bit analysis of the data is made. Bit-error tests on this subsystem at JPL produced one error in 0.64×10^5 bits. There were both loss-of-lock and single-bit errors, with single-bit errors predominating.

The tape positions as EOT occurs (the record head drive is inhibited and the record motor stopped) and after the tape has come to rest are shown in Figs. VI-18 and VI-19. The distance indicated as record-motor rundown cannot normally be recorded when the tape recorder is aboard the spacecraft and an EOT signal stops the tape because of this rundown time. This segment of the tape is recorded during bench tests by inhibiting the EOT sensor so that it does not sense an EOT. An all-ones code was recorded on this portion of the tape as a result of a flutter test performed before the TRS was placed aboard the spacecraft.

At the beginning of track 1 data, the starting points of several old record sequences were seen because the tape does not stop at exactly the same spot each time as it slows down from launch-mode speed. The total tape distance on which these sequences were seen was approximately 1.2 in. This was expected; the large number of tape passes at launch should have loosened up the tape pack so that it would slow down farther than it had when in the Spacecraft Assembly Facility, where the tape was normally positioned with only one tape pass.

At the end of the second playback, the TRS switched to track 1, and began the third playback. A DC-V2 was so timed that the playback was stopped just as track 1 encounter data were reached. This left the tape positioned as it had been before encounter. The TRS was then turned off by a DC-V28 command.

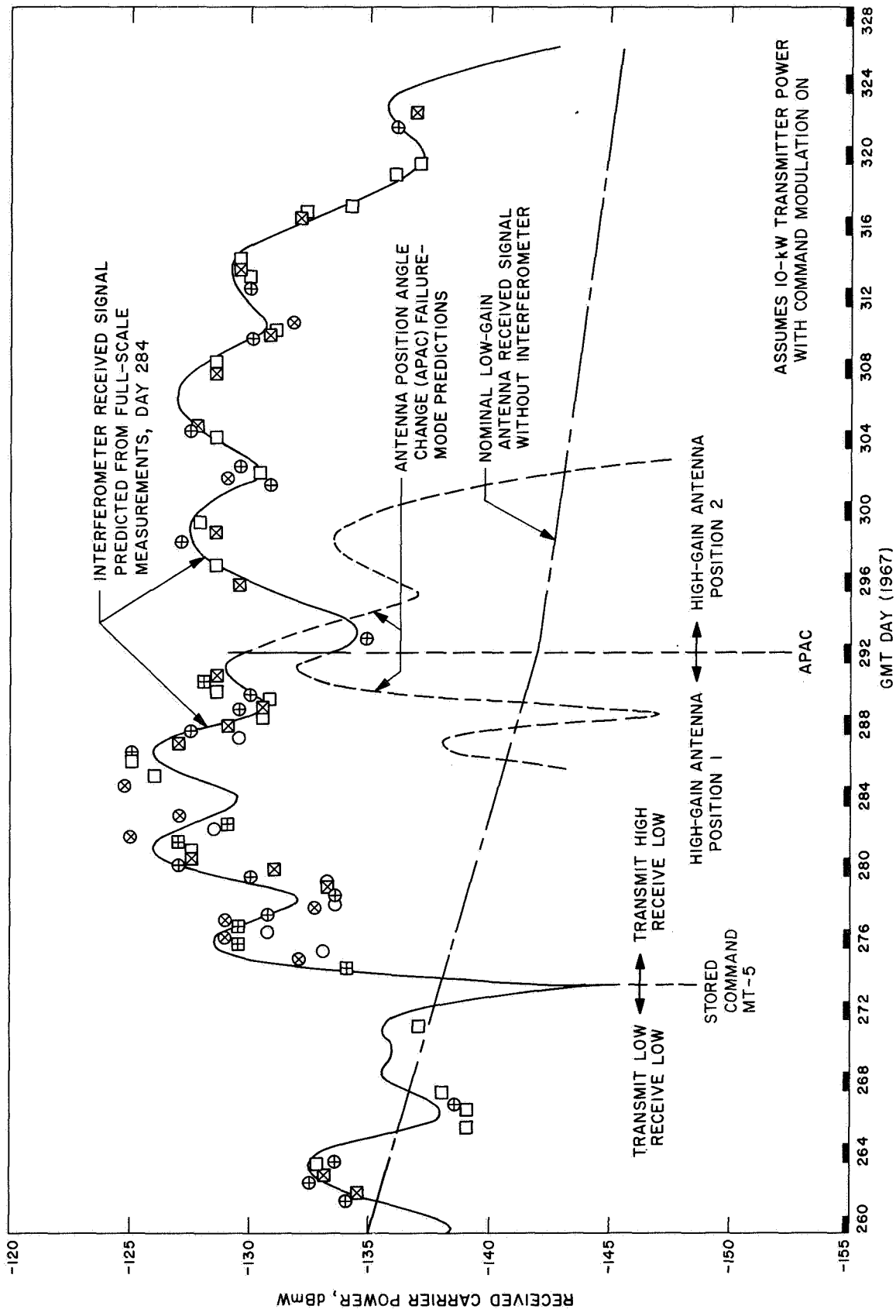


Fig. VI-15. Uplink recevied signal strength in interferometer region (low-gain antenna used)

Table VI-9. Log of *Mariner* Venus 67 mission tape recorder subsystem operations

Command	Day (1967)	Earth-observed time, GMT	Event/comment
Venus encounter			
DC-V25	292	02:58:25	TRS power on; counter 3 event from EOT; channel 227, 65–66 DN
DC-V24	292	10:50:00	Switch to mode 3
		16:33:57 ±25	Planet sensor output
		16:34:29	Record motor on, track 1 data
		16:46:46	Track 2 data start
		18:34:18	Track 2 data stop; stop and start-record signals
		18:41:51	End of tape
		18:47:45	Switch to mode 2
	293	07:24:46	MT-9; start playback in mode 4
		07:26:12	Switch to mode 1
		07:44:33	Switch to mode 4; begin track 1 test pattern
		08:00:36	Switch to mode 1
		08:15:39	Switch to mode 4; beginning of several old record sequences
		08:17:52	Begin track 1 Venus encounter data
	294	01:13:01	EOT No. 1; switch to mode 1; counter 3 event
		01:14:28	Switch to mode 4; all ones
		01:14:35	Switch to mode 1
		01:32:59	Switch to mode 4; begin track 2 test pattern
		01:49:03	Switch to mode 1
		03:58:08	Switch to mode 4; begin track 2 Venus encounter data
		18:18:29	Switch to mode 1
		19:18:17	EOT No. 2; counter 3 event; switch to mode 4; begin second playback
		19:19:54	Switch to mode 1
		19:38:08	Switch to mode 4; begin track 1 test pattern
		19:54:14	Switch to mode 1
		20:09:32	Switch to mode 4; beginning of several old record sequences
		20:11:45	Begin track 1 Venus encounter data
	295	13:06:52	EOT No. 3; switch to mode 1; counter 3 event
		13:08:20	Switch to mode 4; all ones
		13:08:28	Switch to mode 1
		13:26:03	Switch to mode 4; begin track 2 test pattern
		13:42:06	Switch to mode 1
		15:51:29	Switch to mode 4; begin track 2 Venus encounter data
	296	06:11:50	Switch to mode 1
		07:11:39	EOT No. 4; switch to mode 4; begin third playback; counter 3 event
		07:13:13	Switch to mode 1
		07:31:31	Switch to mode 4; begin track 1 test pattern
		07:47:31	Switch to mode 1
		08:02:54	Switch to mode 4; beginning of several old record sequences
DC-V2	296	08:04:54	Switch to mode 2; stop playback 13 s before start of track 1 Venus encounter data
DC-V28	296	08:35:27	TRS power off; channel 227, 61 DN
First UV-photometer calibration sequence			
DC-V26	311	09:26:47	Science off
DC-V25	311	09:31:51	TRS and science on; counter 3 event
DC-V16	311	10:24:46	Start DAS clock A
DC-V2	311	10:42:09	Switch to mode 2; channel 227, 66 DN
		12:25:48	Start recording
		14:33:30	EOT; counter 3 event
DC-V4	312	21:11:59	Start playback in mode 4
		21:13:23	Switch to mode 1
		21:31:44	Switch to mode 4; begin track 1 test pattern
		21:47:41	Switch to mode 1; channel 227, 68 DN
		22:03:08	Switch to mode 4; beginning of old record sequences
		22:06:41	Start of UV-photometer calibration data
	313	15:00:04	EOT; switch to mode 1; counter 3 event
		15:01:32	Switch to mode 4; all ones
		15:01:39	Switch to mode 1
		15:19:15	Switch to mode 4; begin track 2 test pattern
		15:35:16	Switch to mode 1
		17:45:54	Switch to mode 4; begin track 2 UV-photometer calibration data
DC-V2	313	19:57:07	Switch to mode 2; stop playback
DC-V4	314	05:12:25	Start playback in track 2
		17:21:17	Switch to mode 1
		18:19:08	EOT; counter 3 event
		18:20:42	Switch to mode 1
		18:39:01	Switch to mode 4; begin track 1 leader data
		18:55:03	Switch to mode 1

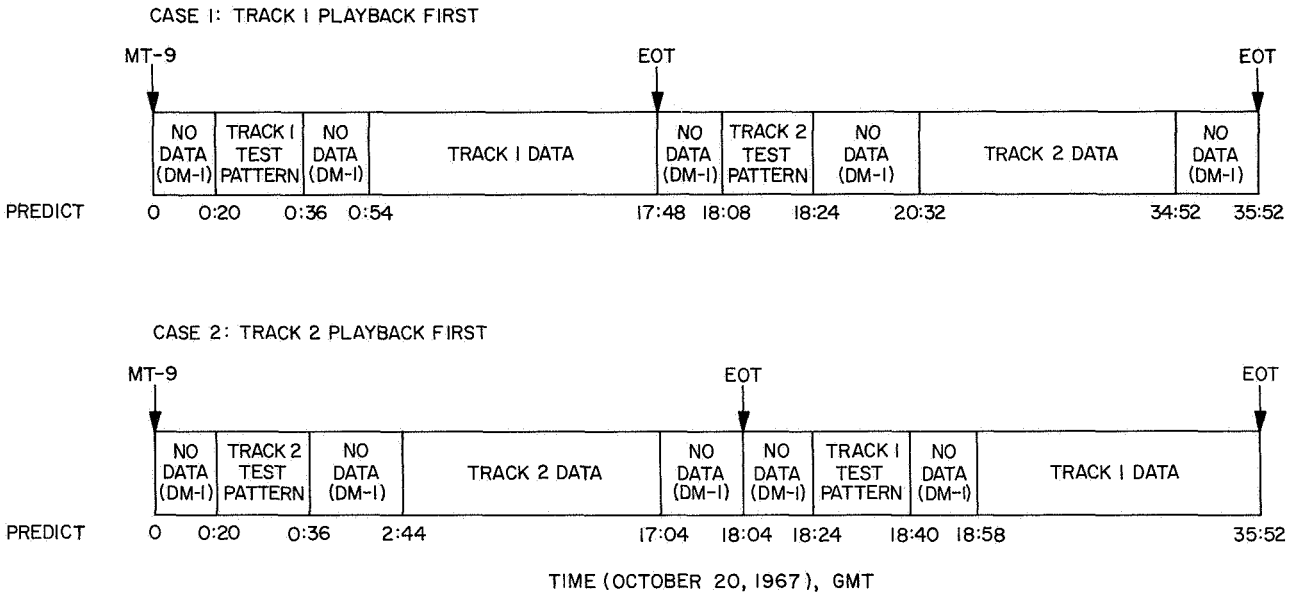


Fig. VI-16. *Mariner V* playback times

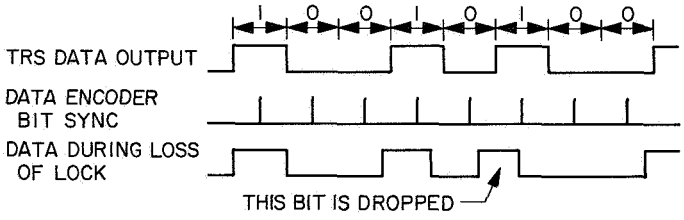


Fig. VI-17. How a bit is dropped during loss of lock

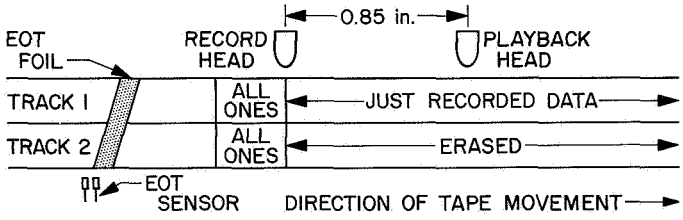


Fig. VI-18. Tape position after playback-motor rundown

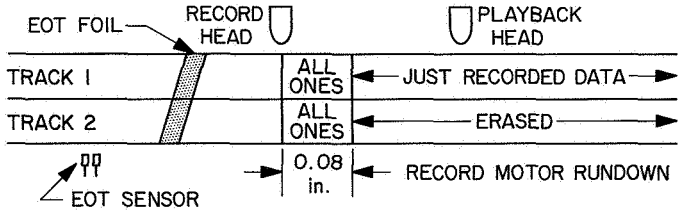


Fig. VI-19. Tape position after record-motor rundown

On November 7, 1967, a second encounter sequence was performed while the spacecraft was rolling. The purpose of this exercise was UV-photometer calibration. A counter 3 event was observed when the TRS was turned on by a DC-V25. Science was reset by a DC-V26 and a DC-V25. Clock A was started by a DC-V16, which began the encounter sequence. The record sequence was normal, and was performed with the data encoder in mode 2.

A DC-V4 command started playback on track 1. Playback was stopped on track 2 by a DC-V2, and resumed the next day by a DC-V4 because of no DSN coverage during that time. Playback continued into track 1, and a DC-V2 stopped playback just as track 1 UV-photometer data were reached, leaving the tape positioned as before. The TRS was turned off by a DC-V28 command.

On November 19, 1967, a second UV-photometer exercise was performed in the same manner as the first. A DC-V25 turned on the TRS in the standby mode. A counter 3 event occurred at this time. Science was reset by a DC-V26 and a DC-V25, and the encounter sequence was run by science clock A starting a DC-V16. The data encoder was in mode 2 during this test.

A DC-V4 started playback on track 1. Playback continued through track 1 and into track 2. A DC-V2 stopped the playback in the mode 1 portion of the track 2 leader data. Track 2 was not played back. The tape was then positioned about 2 min of record time past the start of track 1 data. If another record sequence had been started

from this point, the record time to EOT would be about 125 min. The TRS was turned off by a DC-V25 command.

c. Temperature and pressure profiles. At launch, telemetry channel 304 (tape-recorder pressure) was 66 DN, or 20.56 psia. This pressure increased with an increase in temperature until it stabilized at 68 DN, or 21.18 psia, on day 203 and has since remained at this value.

From launch on day 165 until day 178, channel 436 (tape-recorder temperature) varied from 54 to 60°F. On day 178, the TWT amplifier was switched on, and the temperature increased to 62°F. From this point, the temperature slowly increased to 66.8°F at Venus encounter. When the TRS was turned on, the temperature rose to 68.8°F, increased to 72.7°F during the record sequence, and was 71.7°F during playback.

At the first UV-photometer calibration sequence, the temperature increased from 66.8 to 68.8°F with TRS power on, and increased to 72.7°F during the record and playback sequences.

At the second UV-photometer calibration sequence, the temperature was 68.8°F before the TRS was turned on; available data indicated the temperature to be 71.7°F during playback.

These temperature changes were expected. In general, the temperature should rise about 2°F when the TRS is turned on, and 2–3°F when it is in a record or playback mode. The last data available, on day 325, indicated that the temperature had stabilized at 68.8°F.

The *Mariner V* TRS performance was excellent. A normal Venus encounter record and playback sequence was performed. The TRS dropped lock several times during this playback, but this was within the performance criteria for the subsystem. A bit-error rate is not known at present, and is pending a complete comparison of the two playbacks.

During the two UV-photometer calibration sequences, the TRS performed normally. It appeared that the drop of lock during playback of the first calibration sequence did not occur as often as the Venus encounter data playback. However, as with the encounter data, a bit-by-bit reconstruction of the data would be necessary to evaluate the bit-error rate.

The tape-recorder temperature and pressure were as expected, with readings of 21.18 psia and 68.8°F on day 325.

The tape was positioned just past the start of track 1 data. A record sequence starting from this position would run 125 min to the end of the tape.

8. Dual-frequency receiver antenna subsystem performance. On day 311 of the *Mariner* Venus 67 mission (November 7, 1967), the spacecraft was rolled three times. Data on the DFR antenna pattern were obtained from the SNR data received at the spacecraft and telemetered to earth. This subsection presents these results, and compares them with performance requirements and predictions.

a. Performance predictions. Two Stanford specifications of interest were as follows:

(1) Gain in the direction of earth at encounter relative to linear isotropic:
   (a) 49.8-MHz antenna ≥ 0 dB.
   (b) 423.3-MHz antenna $\geq +4$ dB.

(2) The primary pattern coverage requirement for each antenna is the minimum gain at encounter specified above. The antenna pattern should contain no rapid variations or nulls within the envelope of expected look angles to earth predicted for the period from L+1 mo to encounter.

The gains predicted by JPL (in the direction of earth at encounter relative to linear isotropic) for the 49.8- and 423.3-MHz antennas were +0.5 and +6.5 dB, respectively, referenced at the antenna terminals. For each antenna, a broad main beam in the direction of earth at encounter was predicted, with no nulls in the direction of the required look angles.

The data provided to Stanford were based upon measurements with 1:8.5, 1:5, and full-scale model spacecraft. Circularly polarized illumination was desired because the Stanford illuminator was to be circular during the actual mission. The final iteration of 423.3-MHz antenna data furnished to Stanford by JPL consisted of a full-sphere-coverage contour plot recorded at 423.3 MHz with circularly polarized illumination. For the 49.8-MHz antenna, a circularly polarized illuminator was used with the scaled models. At full scale, a circularly polarized, 49.8-MHz antenna was not available, and linearly polarized illumination was used. Only limited coverage over the sphere surrounding the spacecraft could be obtained with linear illumination because of polarization loss at certain angular orientations. Therefore, the full-sphere-coverage contour plot for the 49.8-MHz antenna, which was furnished to Stanford by JPL, was that of the 1:8.5 scale model. The gain predicted by the scaled model measurements was 2 dB higher than that predicted by the full-scale data.

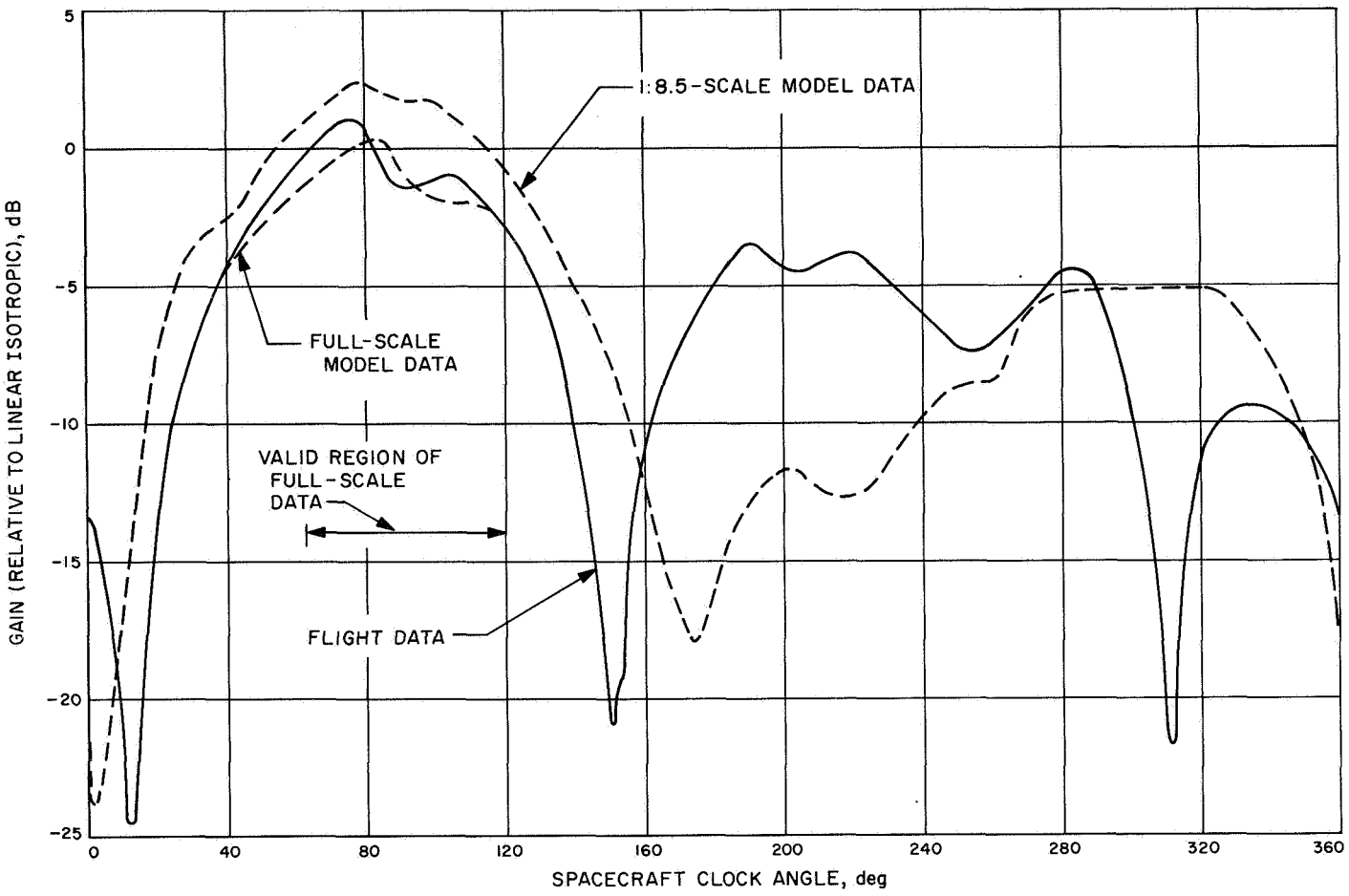


Fig. VI-20. DFR 49.8-MHz antenna patterns from flight data and predicted performance

b. Flight results. On day 311, the spacecraft was rolled three times. The SNR data received at the spacecraft by each antenna from earth-based transmission were included as telemetry data, and transmitted to earth. The results are included in the form of pattern data in Figs. VI-20 and VI-21 for the 49.8- and 423.3-MHz antennas, respectively. The patterns recorded on the JPL range for each antenna are included for comparison. The gain reference point in each case is at the antenna terminals.

49.8-MHz antenna. The JPL-predicted 49.8-MHz antenna performance shown in Fig. VI-20 includes that from both the 1:8.5-scale model, full-sphere contour plot and the full-scale patterns recorded with linearly polarized illumination. The full-scale data are not plotted over the full 360 deg because of polarization-loss discrepancies. It is difficult to assess the accuracy of the JPL-predicted 49.8-MHz antenna performance based upon the flight data because scientific analysis has not been completed.

The received-signal strength is determined as a function of received SNRs. The SNRs may be degraded by cosmic noise. This would result in an apparent dip in the antenna pattern. Consequently, complete scientific analysis of the cosmic-noise effects is necessary to obtain an accurate determination of the pattern level.

The predicted gain and pattern data based upon the full-scale measurements were within ± 1 dB of the flight data in the region plotted. These results are especially good when the difficulty of making accurate pattern measurements at 49.8 MHz is considered.

423.3-MHz antenna. The JPL-predicted 423.3-MHz antenna performance shown in Fig. VI-21 is from the full-sphere contour plot, which was taken from full-scale patterns recorded with circularly polarized illumination. It may be seen that the predicted performance is in excellent agreement with the flight data, and is within ± 0.5 dB over most of the main lobe.

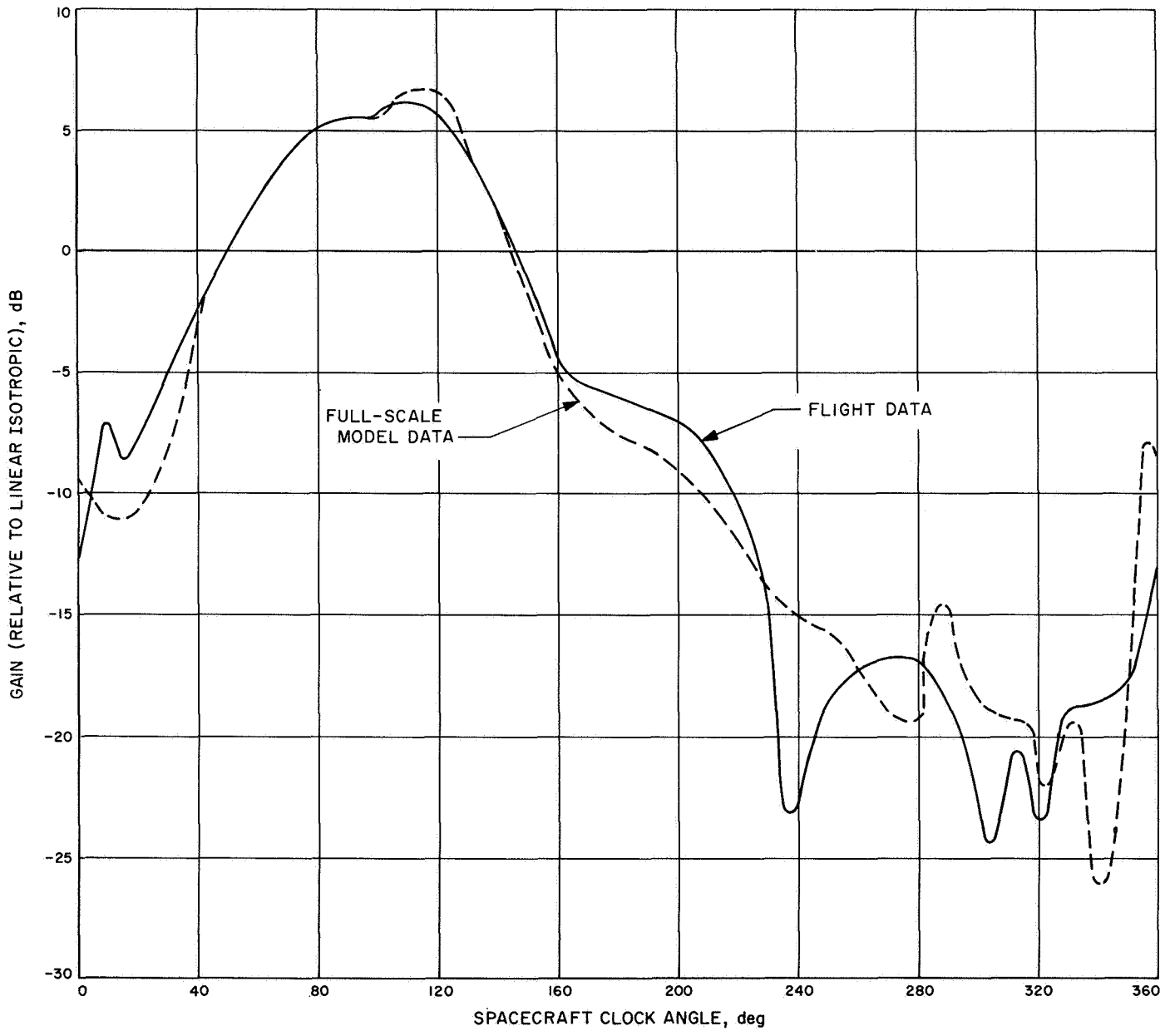


Fig. VI-21. DFR 423.3-MHz antenna patterns from flight data and predicted performance

F. Guidance and Control Subsystem Performance

1. Introduction. The spacecraft control subsystems for the *Mariner* Venus 67 mission consisted of the AC subsystem; the autopilot; and the earth, planet, and terminator sensors. The AC subsystem oriented the spacecraft to a set of celestial references (the sun and the star Canopus), and maintained that orientation throughout the cruise and encounter phases of the mission. In addition, the AC subsystem had the capability to rotate the spacecraft about two axes to some new position for the midcourse maneuver, and, upon termination of the midcourse-maneuver sequence, to return to the sun–Canopus orientation. If a noncatastrophic disturbance caused the AC to lose these references, the subsystem had the capability to reacquire them. Finally, spacecraft attitude about one axis could be inertially referenced and controlled by ground command.

The autopilot controlled spacecraft attitude during the motor-burn portion of the midcourse-maneuver sequence by deflecting the motor-thrust vector. The spacecraft position and rate were inertially referenced during the entire midcourse-maneuver sequence, and appropriate commands from the autopilot aligned the motor-thrust vector with the spacecraft center-of-mass to maintain spacecraft stability and maneuver accuracy.

The function of the earth sensor was to provide a backup reference for the midcourse maneuver. In case of failure of the Canopus sensor (which referenced spacecraft position to Canopus), the earth sensor could be used to reference spacecraft position to the earth. The planet sensor was designed to detect the lighted limb of Venus as *Mariner V* approached the planet, and then to send a signal to the DAS to initiate the science encounter sequence.

The function of the terminator sensor was to detect the terminator of the planet when the spacecraft was occulted by the planet, and then to send a signal to the pyrotechnics subsystem to initiate the high-gain APAC.

2. Description.

a. Attitude control. The AC subsystem is functionally composed of the control electronics package, gyro control assembly (GCA), sun sensors, sun gate, Canopus sensor, and gas system. The three spacecraft gyros in the GCA are turned on before launch to maximize their chances of surviving the launch environment and to minimize the possibility of a spin-motor bearing race being brinelled. The gyros are thus able to provide spacecraft rate data during the *Atlas* and *Agena* thrusting periods and at spacecraft–*Agena* separation. Upon separation, the PAS turns on the AC subsystem.

The sun-acquisition process begins immediately, with the cruise and acquisition sun sensors supplying position-error signals and the gyros providing rate limiting. Jet valves at the ends of the solar panels torque the spacecraft by expelling nitrogen gas, and the spacecraft turns to face the solar panels towards the sun. In this position, the spacecraft positive roll axis points at the sun.

When the roll axis is within a cone of approximately 5 deg half-angle centered on the spacecraft–sun line, the sun gate is enabled, and the acquisition sun sensors are deenergized. Position-error signals are then generated by the cruise sun sensors, and the spacecraft roll axis is maintained on the sun line to within ± 0.5 deg. The sun gate event also initiates a controlled turn at a nearly constant rate of -3.5 mrad/s (12.1 deg/min ccw) about the roll axis. This is the magnetometer-calibrate roll spin.

At CC&S event L-3, 997 min after launch, the Canopus sensor is turned on, and the roll rate is reduced to the search rate of -2.0 mrad/s (6.88 deg/min ccw), beginning the star-acquisition process. When a light source of sufficient intensity falls within the FOV of the Canopus sensor, the sensor enables the Canopus-gate logic circuits in the control electronics. If the position-error signal generated by the sensor fulfills the acquisition logic, that signal is switched into the roll-control circuits, and the signal generating the search rate is removed. If the object in view is not Canopus, the roll search can be reinitiated by ground command, and the acquisition process can be repeated indefinitely until Canopus is acquired.

Approximately 205 s after a celestial object is acquired in this manner, the spacecraft gyros are automatically turned off. The spacecraft is now stabilized in position with the sun and Canopus (or some other object) as references.

Rate stabilization is achieved in the following manner: When the spacecraft angular deviation (as measured by the sun or Canopus sensor) exceeds ± 0.5 deg about the pitch and yaw axes (two orthogonal axes normal to the roll axis), or ± 0.25 deg about the roll axis, the error signal generated by the sensor is processed by the control electronics to energize two gas-jet valves for 20 ms. These valves produce a couple (acting on one axis through the spacecraft CG) that tends to reduce the error signal. Ideally, only one 20-ms impulse is needed to reduce the error to within the given limits (the deadband), but the process is repeated if necessary.

To control spacecraft rate, a signal proportional to the length of time a jet valve has been on is reapplied to

the control electronics, and summed with the position-error signal. Thus, two jet valves will be fired when the deadband is exceeded. If the spacecraft rate is too high, however, a single firing will not be enough to return the spacecraft to within the deadband, and the valves will be fired again. The error signal from the sensor is reduced by an amount proportional to the time the valves have been on, and the spacecraft rate is reduced by the torquing action of the gas thrust.

This process continues until (1) the spacecraft rate has reached zero or reversed direction or (2) the feedback signal reaches a preset clamp level. If the spacecraft rate is zero and the valves are not firing, the decay of the feedback signal will cause the valves to fire, reducing the error signal. If the spacecraft rate has reversed direction, the error from the sensor will be reduced as a function of the change in position of the spacecraft, and the valves will not be fired. If the feedback signal has reached its clamp level, the valves will continue to fire until the spacecraft rate is reversed and the error signal is within the deadband. This derived-rate feedback thus limits spacecraft rates in the steady state, and permits the spacecraft gyros to be turned off, establishing the cruise mode of operation of the AC subsystem.

During the midcourse-maneuver sequence, the spacecraft is repositioned to point the PIPS thrust vector in some arbitrary, ground-determined direction. This is accomplished by turning on the gyros, placing them in the inertial (rate-plus-position) mode, and turning off all sensors. Spacecraft rate and position are then controlled by the gyros, and a turn at a constant rate for a commanded duration is performed about the pitch and roll axes (in that order). The turn is produced by introducing a constant-error signal into the gyro control loop. To null the error, the spacecraft is turned at a constant rate by firing gas-jet valves to accelerate the spacecraft to a rate at which the rate-signal-minus-error signal is within the rate-plus-position deadband. The duration of the error signal is determined by ground command; when the signal is removed, the spacecraft decelerates until the rate-plus-position mode is again within the deadband. In this manner, the spacecraft can be repositioned to any desired orientation.

Upon termination of the maneuver sequence, the sun-acquisition process described above is initiated. When the sun is acquired (i.e., when the sun-gate event occurs), the star-acquisition process is initiated. Cruise-mode operation is again established when Canopus is acquired, and the gyros are turned off.

If the Canopus sensor loses acquisition of Canopus, the gyros are turned on, and the star-acquisition process is repeated. If the sun sensors or sun gate lose sun acquisition, the gyros are turned on, and the sun-acquisition process is repeated, followed by the star-acquisition process. If the disturbance was noncatastrophic, these processes will be normal, and cruise mode will be reestablished. By ground command, it is possible to prevent the gyros from being turned on upon a loss of acquisition. In this mode, sun acquisition using derived rate is possible because the acquisition sun sensors have a 4π sr FOV, and provide an error signal regardless of spacecraft orientation. However, the Canopus sensor has a limited FOV, and acquisition of a given star may not be possible.

If the Canopus sensor should fail or be unable to function properly, an alternative mode of roll control is available. The spacecraft gyros are turned on by ground command, with the roll gyro placed in the inertial (rate-plus-position) mode and the pitch and yaw gyros placed in the rate-only mode. In this roll-inertial-control mode, spacecraft position in pitch and yaw is controlled by the sun sensors; spacecraft rate in pitch and yaw is controlled by derived-rate and pitch-and-yaw-rate gyros; and spacecraft rate and position in roll are controlled by the roll gyro. Spacecraft position in roll can also be controlled by ground command in the form of 2.25-deg cw or ccw incremental turns, each 2.25-deg turn requiring a command. This mode requires careful surveillance of the spacecraft, as a typical gyro drift rate requires one command per day to update the position of the spacecraft.

b. Autopilot. The spacecraft autopilot is functionally composed of the autopilot electronics (physically located within the control electronics), the GCA, and the thrust-vector-control assembly, the latter of which, in turn, is composesd of four jet-vane actuators (JVAs) and a mounting ring. The autopilot is turned on at the start of the pitch turn in the midcourse-maneuver sequence, but has no effect on spacecraft attitude until the PIPS motor is ignited. If the motor thrust vector does not pass through the spacecraft center of mass (c.m.), a torque is generated on the spacecraft, and the spacecraft begins to turn. The gyros generate error signals, which are processed by the autopilot electronics, transforming them into appropriate vane-rotation commands to the JVAs. The jet vanes are located in the exhaust stream of the PIPS, and vane rotations deflect the net thrust vector so that it tends to pass through the c.m. In this manner, the autopilot maintains spacecraft stability and thrust-vector pointing accuracy.

Error signals are received by the autopilot electronics from the GCA that are referenced to the spacecraft pitch,

yaw, and roll (*X*, *Y*, and Z) axes. The autopilot is referenced to the **a–b–c** coordinate system, where **a** is the direction of the undeflected thrust vector, **b** is normal to **a** and parallel to the *X–Y* plane, and **c** completes the right-hand coordinate system. Because the undeflected thrust vector points out of bay 2 of the spacecraft, the projection of the **a** axis on the *X–Y* plane forms an angle with the *X* axis of 45 deg; because PIPS can be tilted in its mounting frame to minimize the offset of the spacecraft c.m. from the undeflected thust vector, the angle between the **a** axis and the Z axis is 88.5 deg.

Corrective torques about the **a** axis are produced by rotation of all four jet vanes in the same sense; torques about the **b** axis are produced by rotation of the vanes mounted in the **a–b** plane; and torques about the **c** axis are produced by rotation of the vanes lying in the **a–c** plane. The autopilot electronics must then transform the *X–Y–Z* referenced gyro outputs to appropriate commands in the **a–b–c** system. This is accomplished by each of the three gyros feeding each of the four JVA amplifier inputs through a scaling resistor. These 12 resistors, plus an additional roll-scaling resistor and three differential-input balancing resistors, form the autopilot resistor-mix matrix. The mix matrix can be adjusted to compensate for changes in the spacecraft dynamical properties, PIPS tilt angle, and known CG offsets by removal and replacement of resistors.

c. Earth sensor. The function of the earth sensor was to provide an independent and backup roll reference for the midcourse maneuver. If the Canopus sensor should fail or function improperly, the earth could be used as a roll reference by placing it in the FOV of the sensor and maintaining the spacecraft position with the roll-inertial-control mode.

Earth could be acquired in two ways: (1) placing the spacecraft in the roll-inertial-control mode and incrementally stepping the spacecraft in roll by ground command until earth had been acquired; or (2) placing the spacecraft in the roll-search mode until earth appeared in the FOV of the sensor, and then commanding the roll-inertial-control mode.

The *Mariner V* earth sensor was a modification of the *Mariner IV* earth detector. The earth detector was so located on the *Mariner IV* spacecraft that, when Canopus was acquired by the Canopus sensor, earth would appear in the FOV of the earth detector, verifying that Canopus was the star acquired. Flight operations experience with the star-acquisition process showed that this aid was not necessary; therefore, for *Mariner V*, the sensor was relocated on the spacecraft, and its FOV was modified from 26 deg in clock and 83 deg in cone to 3 deg in clock and 50 deg in cone. This narrow-clock-angle FOV helps to define the position of the earth in spacecraft roll, whereas the cone-angle FOV permits the use of earth as a reference for the range of launch dates. The earth sensor provides a usable output up to 20 days after launch.

d. Planet sensor. The planet sensor was a newly designed instrument, based upon the *Mariner IV* narrow-angle Mars gate. The function of the planet sensor was to sense the lighted limb of Venus when the spacecraft was 60 $\pm$26 min from closest approach to the planet, and to provide a PSO signal to the DAS at that time. This signal would be used to initiate the science encounter sequence (start DAS clock B, begin tape recording on track 1, inhibit the UV-photometer calibrate sequence).

The planet appears as a crescent as the spacecraft approaches it from above the planet orbital plane, and the planet sensor is so mounted on the spacecraft that its FOV sweeps over the near horn of the crescent. To maximize the total amount of light entering the 4.55 $\times$ 1.55-deg rectangular FOV, the major axis of the FOV is rotated 41.4 deg cw from the sensor vertical (the vertical is perpendicular to the mounting plane), so that the major axis is more nearly aligned with the horn. The sensor is mounted on the spacecraft at a look-angle of 0 deg clock and 24.9 deg cone, necessitating a high straylight rejection factor to avoid a PSO from sunlight when the instrument is energized by the DAS at CC&S event MT-8.

e. Terminator sensor. The terminator sensor is a modified *Mariner IV* narrow-angle Mars gate, whose function is to sense the terminator of Venus during the time that the spacecraft is radio-occulted by the planet. When energized at CC&S event MT-7, the terminator sensor draws excitation power from the pyrotechnics subsystem, and supplies a signal to that subsystem at TSO. This signal is used to trigger the pyrotechnics circuit that fires the high-gain APAC squibs.

As the spacecraft approaches midoccultation, the planet appears gibbous, with the terminator at a cone angle greater than 90 deg. To maximize the distinction between the lighted and dark areas on either side of the terminator, the look angle of the sensor was chosen so that the FOV sweeps across the central portion of the planet. The FOV is 1.5 deg in clock and 2.5 deg in cone, centered on look angles of 110 deg in clock and 110 deg in cone.

3. Flight performance.

a. Launch. The spacecraft gyros were turned on when spacecraft power was turned on at 01:07:30 GMT on June 14, 1967. Gyro-heading data taken at about 04:00 GMT agreed with the data from the previous day, and were about 1.7% off the heading circle generated by the gyro calibrations at AFETR.

The heading circle and on-pad heading data are shown in Fig. VI-22. The azimuth of the $+X$ axis is determined by the point on the circle defined by the on-pad heading data; this agrees closely with the reported Canopus-sensor azimuth (the sensor is 45 deg ccw of the $+X$ axis).

The countdown proceeded without incident until liftoff, but some gyro activity (typically, ± 0.3 mrad/s) occurred before launch, indicating launch vehicle sway, probably from winds. Launch occurred at 06:01:00.176 GMT. The gyro activity from launch to the start of sun acquisition is shown in Fig. VI-23; the event numbers are keyed to the events listed in Table VI-10. An expanded plot of the gyro telemetry received upon spacecraft–*Agena* separation is provided in Fig. VI-24. A prediction of separation rates had been made by the Lockheed Missiles and Space Company, and a comparison of the predicted and best estimates of the actual rates is given in Table VI-11.

b. Sun acquisition. The sun-acquisition process began upon spacecraft–*Agena* separation, at 06:27:16.2 GMT, when the PAS turned on the AC subsystem. The initial acquisition rates were $+4.92 \pm 0.15$ mrad/s in pitch and -4.84 ± 0.15 mrad/s in yaw. The SIT event occurred at 06:30:11.6 ± 4.9 GMT, 175.4 ± 4.9 s after separation. The four events with solar panels deployed were recorded by 06:30:19.2 GMT, and the acquisition rates decreased to $+3.46 \pm 0.15$ mrad/s in pitch and -3.02 ± 0.15 mrad/s in yaw. (Although conservation of angular momentum considerations would indicate that the angular velocity should increase when the panels deploy, as the moment of inertia about both the pitch and yaw axes decreases, the moment arm for the pitch and yaw gas jets increased from about 1 to 8 ft at deployment, and acted to decrease the acquisition rate.)

Table VI-10. *Mariner V* launch events[a]

No.	Event[b]	Time, GMT	Gyro activity
1	Launch	06:01:00.176	—
2	*Atlas* roll maneuver	06:01:02–06:01:15.2	ccw roll maneuver
3	*Atlas* pitch maneuver	06:01:15.2–06:03:08.6	ccw pitch and yaw maneuver
4	BECO and booster separation	06:03:09–12	ccw pitch and yaw, cw roll transient
5	SECO	06:05:57	—
6	VECO and shroud separation	06:06:18–20	ccw pitch and yaw transient
7	*Agena* first-burn ignition	06:07:22	cw yaw and roll transient
8	*Agena* first-burn cutoff	06:09:45	—
9	*Agena* second-burn ignition	06:23:01.2	ccw pitch and roll, cw yaw transient
10	Injection	06:24:25.6	No data
11	*Agena* second-burn cutoff	06:24:35.5	No data
12	*Agena*-spacecraft separation: PAS, AC on	06:27:16.2	cw pitch, ccw yaw and roll transient, sun acquisition begins
13	SIT: solar panels deploy	06:30:11.6 ± 4.9	Acquisition rates decrease

[a]Shown in Fig. VI-23.
[b]BECO = booster engine cutoff; SECO = sustainer engine cutoff; VECO = vernier engine cutoff; PAS = pyrotechnics arming switch; AC = attitude control; and SIT = separation-initiated timer.

Table VI-11. Spacecraft–*Agena* separation data

Predicted	Pitch, deg/s	Yaw, deg/s	Roll, deg/s	Vector sum, deg/s
Zero residual (*Agena*) rate	0.23	0.91	—	0.94
3σ (0.14 deg/s) residual rate	0.33	1.04	—	1.07
Actual (best estimate)	0.43	−0.99	−0.23	1.10

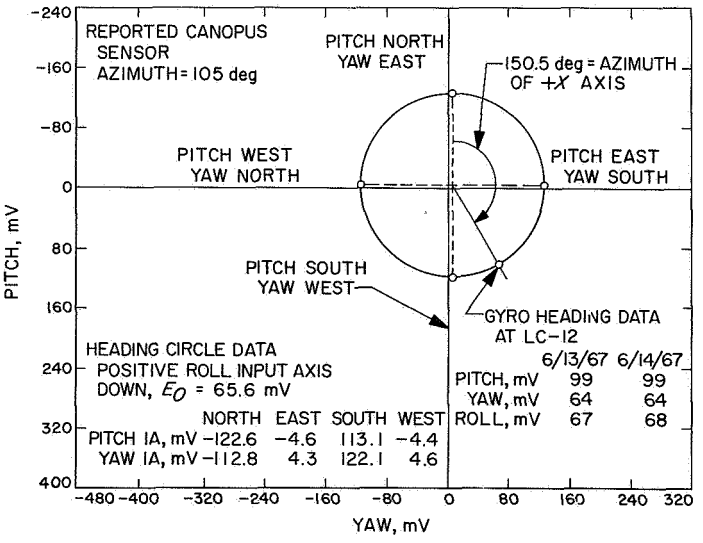


Fig. VI-22. Flight spacecraft (M67-2) gyro headings (AFETR)

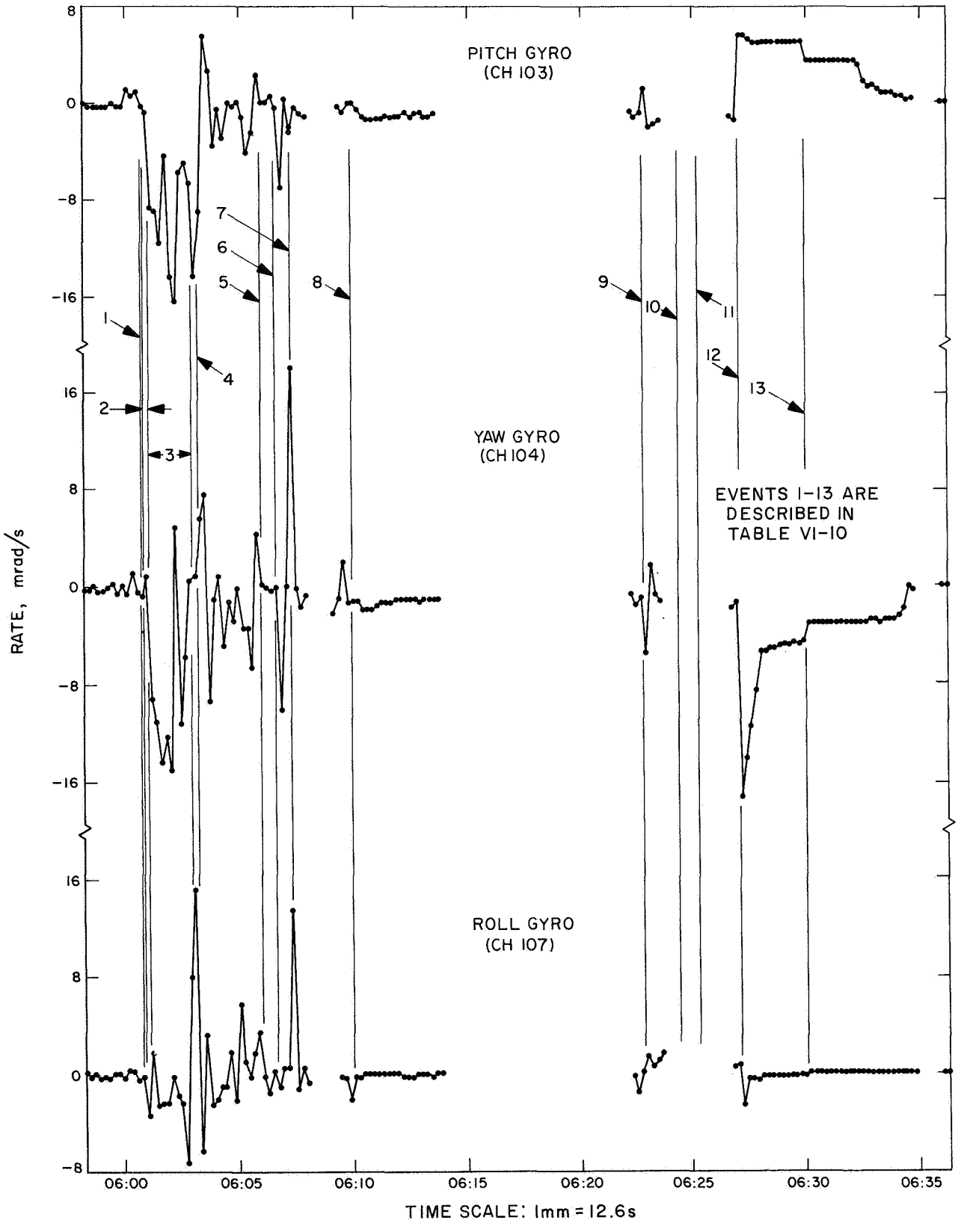


Fig. VI-23. *Mariner V* gyro activity (launch to start of sun acquisition)

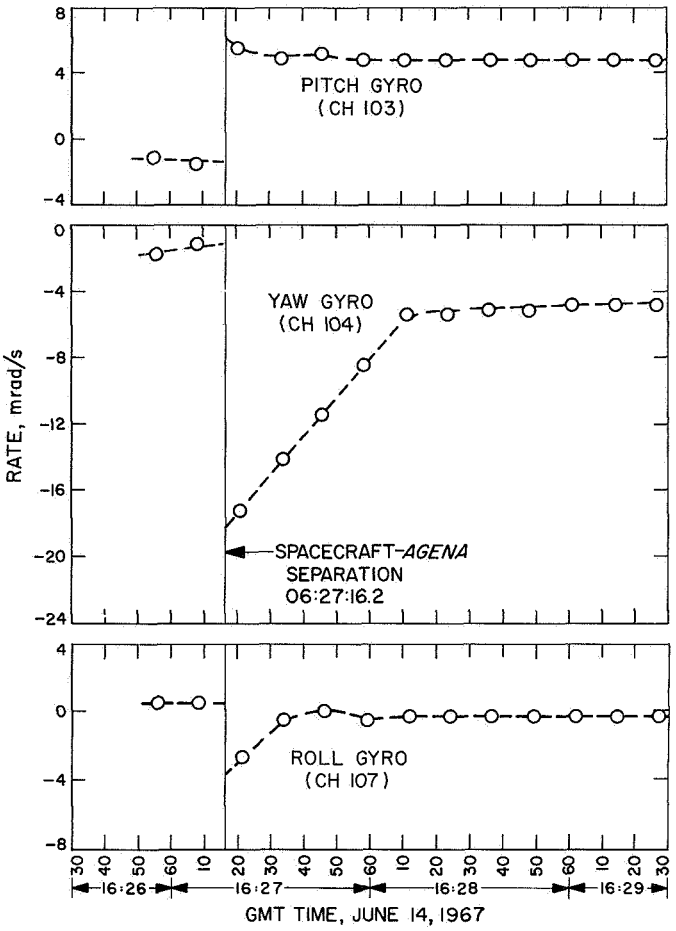


Fig. VI-24. *Mariner V* spacecraft–*Agena* separation, June 14, 1967

The sun sensors were activated at PAS (06:27:16.2 GMT), and initially showed saturated outputs. The spacecraft was driven cw in pitch and ccw in yaw to acquire the sun, but earthlight on the secondary sun sensors biased the electrical null at least 78 mrad (4.5 deg) off the spacecraft–sun line.

The geometry of the acquisition is shown in Fig. VI-25. The false null had to be acquired in both pitch and yaw to trigger the sun gate. It should be noted that Fig. VI-25 depicts the observer as if he were aboard the spacecraft; therefore, the sun–spacecraft and false-null–spacecraft vectors are represented as points in a plane containing the sun. It should also be noted that, for convenience, the sun-gate FOV is shown centered on the sun instead of about the spacecraft $+Z$ axis.

The sun-gate event occurred at 06:43:25.4 $\pm$4.9 GMT. Fortunately, the location of the false null was such that all of the points of a normal limit cycle within the deadband placed the sun in the sun-gate FOV. The sun-gate event, therefore, in removing the power to the secondary sun sensors, also removed the false null.

c. Magnetometer calibration. The sun-gate event initiated the magnetometer calibration in which the spacecraft, sun-acquired in the X and Y axes, spins ccw about the Z axis at a constant rate. The specified spin rate is -3.5 mrad/s, plus or minus the roll-rate deadband of 0.37 mrad/s. It was expected that the actual rate would be near the upper edge of the deadband, that is, between -3.5 and -3.87 mrad/s. The rate determined from the roll-gyro telemetry was initially -3.45 $\pm$0.13 mrad/s, but within a few minutes the telemetry settled at -3.72 $\pm$0.13 mrad/s.

An independent measure of roll rate was available from the earth sensor. The earth sensor would view the planet during each roll for a length of time that was a function of the spacecraft roll rate, the brightness of the earth, and the relative earth–spacecraft motion. Once a model of the response of the sensor to the earth is defined, the spacecraft roll rate can then be determined very accurately.

A plot of rate vs time for the magnetometer-calibration period is shown in Fig. VI-26. The exponential increase in the rate corresponds closely to the exponential decrease in bay 7 temperature during this period. The change in rate is probably caused more by temperature effects in the control electronics than in the GCA (or in the gyros themselves) because a similar change at similar temperatures only changes a typical commanded turn rate by 0.001 mrad/s (approximately 0.03%).

During the roll spin, after the initial acquisition transient, the pitch- and yaw-axis motions were sinusoidal with a period of about 35 min and an amplitude in pitch of $+7.2$ to -4.9 mrad and in yaw of -8.5 to $+9.3$ mrad.

d. Canopus acquisition. The magnetometer calibration was terminated by CC&S event L-3 at 22:38:00.5 $\pm$0.7 GMT, after 33 revolutions. The Canopus sensor was turned on for the first time at a spacecraft clock angle of approximately 312 deg (as determined from the earth-sensor output).

Earth acquisition occurred at 22:46:30.6 $\pm$5.6 GMT, when the roll-error signal from the Canopus sensor was switched into the roll-control channel. The decision was made to continue the roll search by sending two DC-V21 roll-override commands.

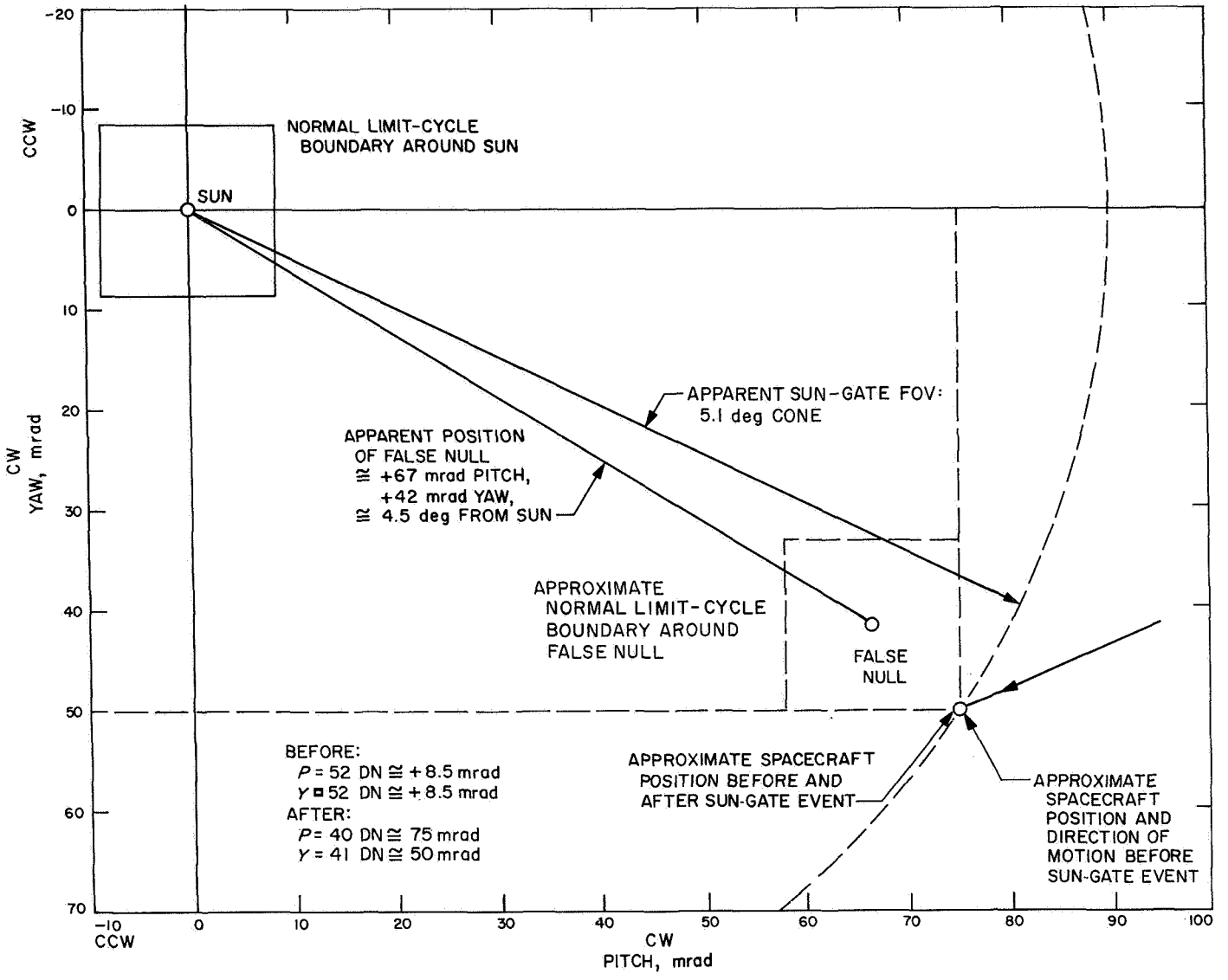


Fig. VI-25. Geometry of false null at initial sun acquisition

The first DC-V21 was sent to the spacecraft, and received in the data at 00:30:40.2 ±4.9 GMT on June 15, 1967; the second command was received in the data at 00:34:39.6 ±4.9 GMT. The second command reinitiated the roll search, as planned.

Search continued until 01:09:12.6 ±0.7 GMT, when Canopus was acquired.

The spacecraft gyros turned off at 01:12:26.4 ±6.2 GMT, 193.8 ±6.9 s after the sensor assumed roll-position control of the spacecraft.

Star acquisitions are treated separately, and in more detail, below.

e. Earth cruise. Attitude-control performance throughout the earth-cruise phase of the mission was normal. The operating parameters of the AC subsystem are summarized in Table VI-12. Two roll transients were noted in nonreal-time data analysis, but neither caused more than a momentary disturbance in the limit cycles.

Attitude-control gas usage through the midcourse maneuver was negligible. The calculated N_2 gas weight in each half of the subsystem is shown in Fig. VI-27.

The transients at launch and at the midcourse maneuver were caused primarily by thermal effects as the temperature of the gas vessels reached equilibrium. The resolution

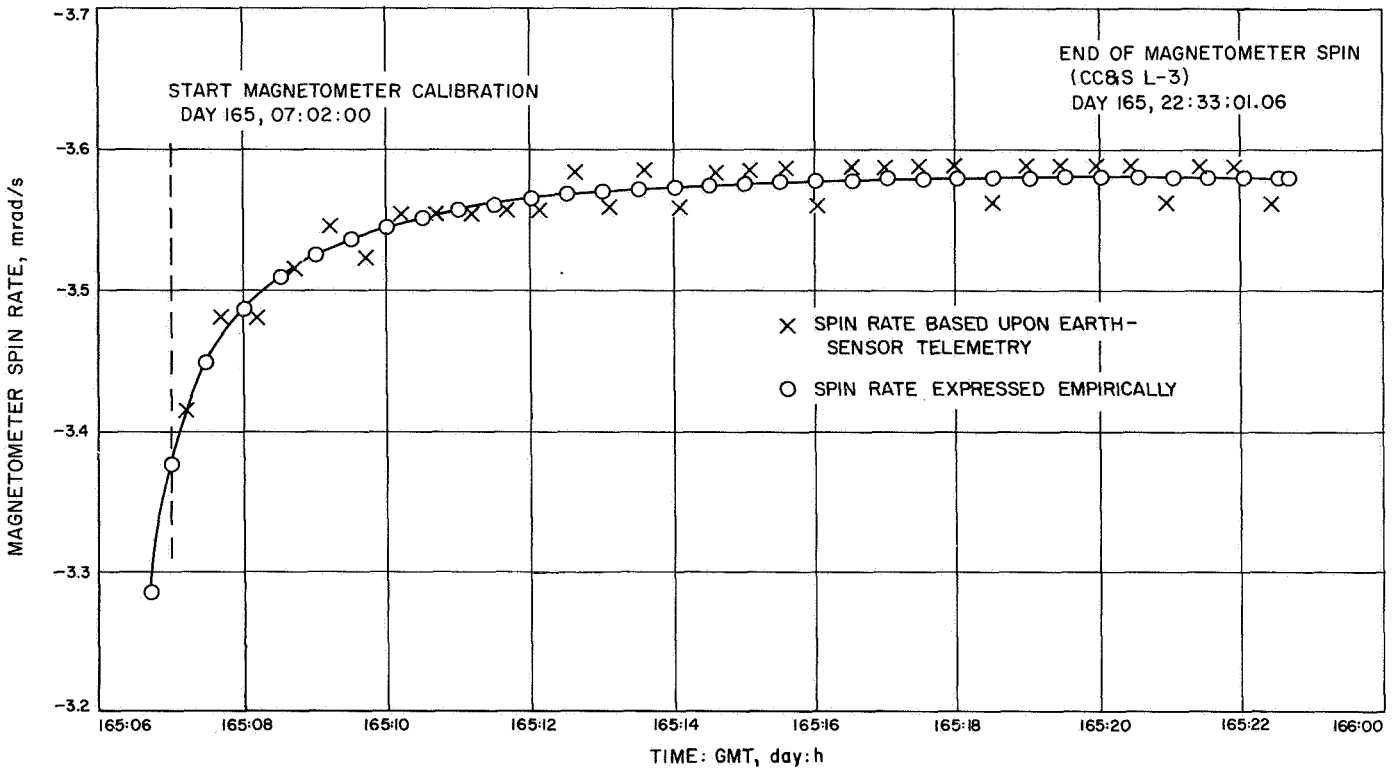


Fig. VI-26. Spacecraft spin rate from earth-sensor data

of gas weight was 0.006 lb/DN in temperature, but a change in temperature could cause a change in the telemetered pressure DN, and that resolution was 0.015 lb/DN.

f. Midcourse maneuver. The midcourse-maneuver sequence was initiated on June 19, 1967, with the transmission of QC-V1-1 (pitch-turn duration) to the spacecraft. The commanded turn rates for the pitch and roll turns were predicted about 1 day in advance of the midcourse maneuver by obtaining an estimate from the thermal-control analysts of bay 7 temperature at the start of the pitch turn.

Table VI-12. Attitude-control subsystem cruise operating parameters

Axis	Pitch	Yaw	Roll
Deadband	7.6 ±0.1	8.4 ±0.05	6.3 ±0.4
Size, mrad	−7.9 ±0.1	−8.69 ±0.16	−3.0 ±0.5
Minimum rate increment, mrad/s	17.8 ±0.4 −18.8 ±0.7	18.1 ±0.4 −18.4 ±0.5	18.1 ±1.7 −16.8 ±1.5
External torque, dyne-cm (typical)	−1 to 2	−8.5	—

The average gyro-case temperature during the turn was calculated from the data shown in Fig. VI-28, and the average turn rate during the pitch turn was finally obtained from the data shown in Fig. VI-29.

The effects on bay 7 of heating caused by the post-pitch-turn orientation were estimated by the thermal-control analysis to be small; therefore, the roll-turn rate was calculated in the same manner as the pitch-turn rate was calculated.

These turn rates determined the pitch- and roll-turn-duration quantitative commands that would achieve the desired turns. The opportunity existed to make a vernier correction to the engine-burn-duration quantitative command to account for the effects of jet-vane drag in the exhaust stream; however, premaneuver autopilot simulations indicated this correction to be negligible.

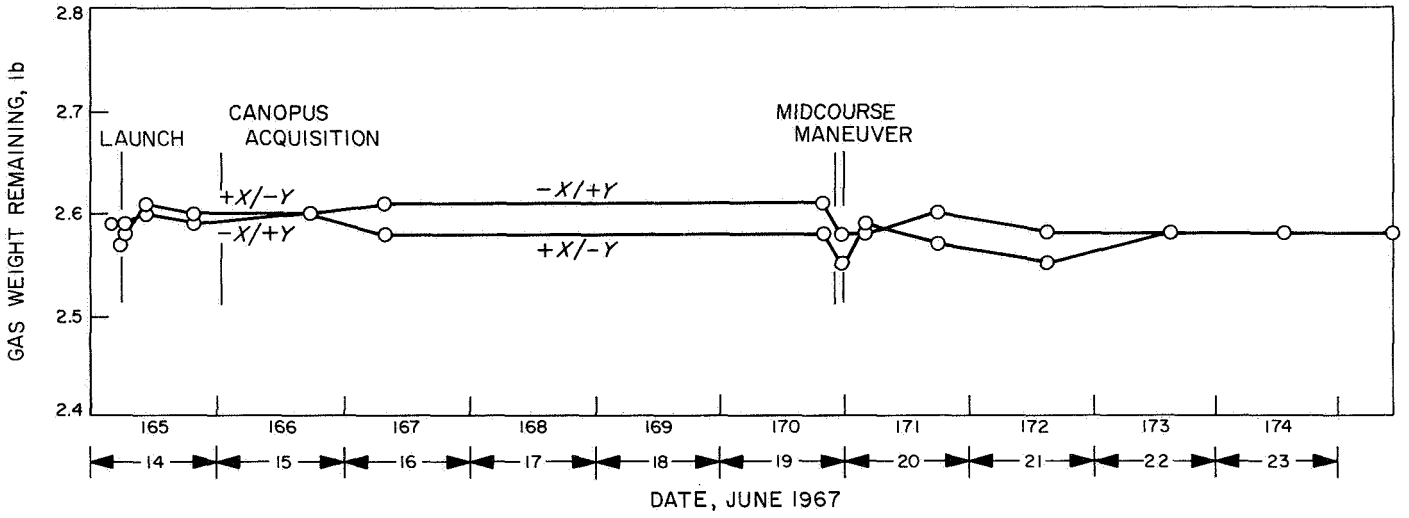


Fig. VI-27. Attitude-control gas weight from launch through midcourse maneuver

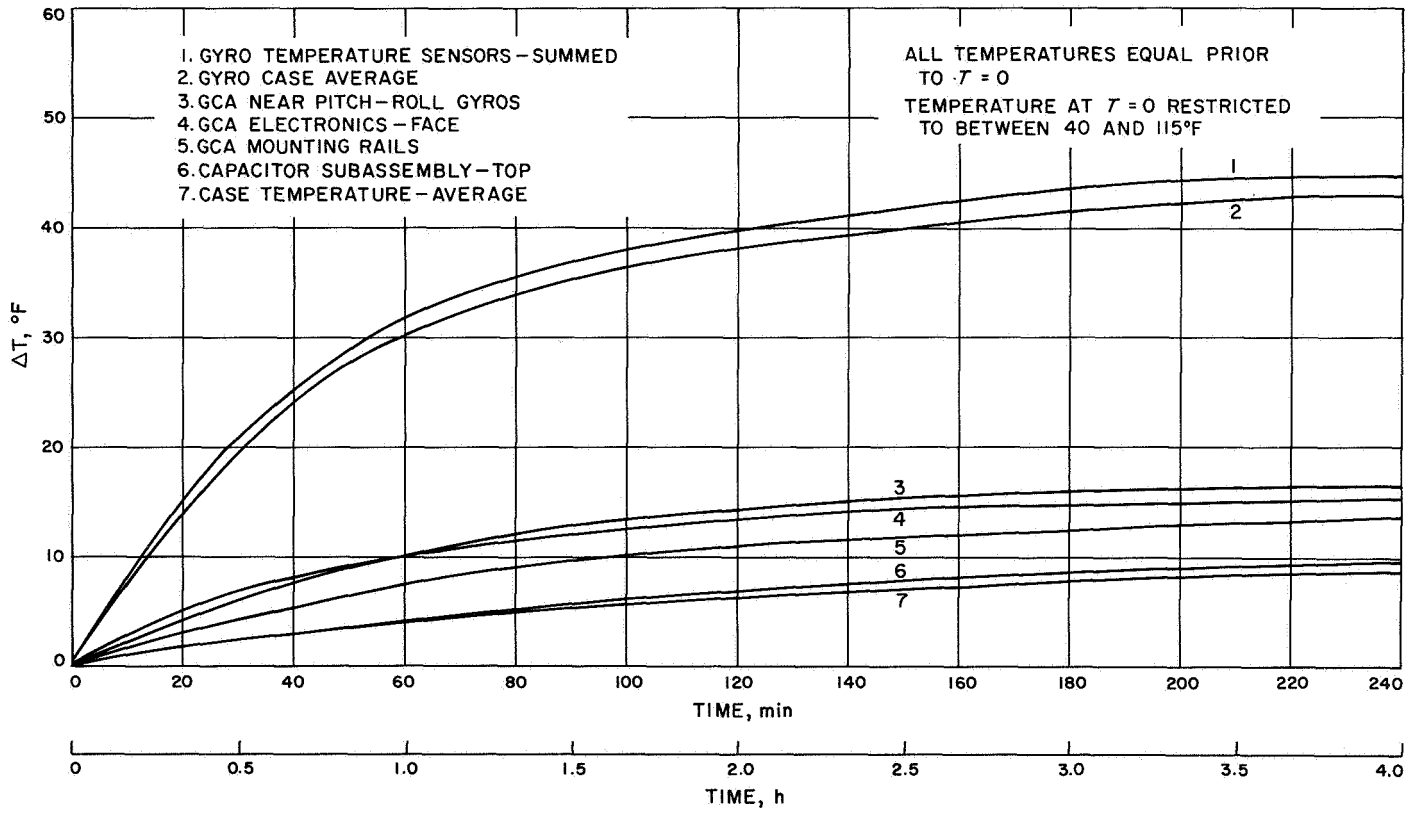


Fig. VI-28. "Best-estimate" temperatures in vacuum after GCA turn-on

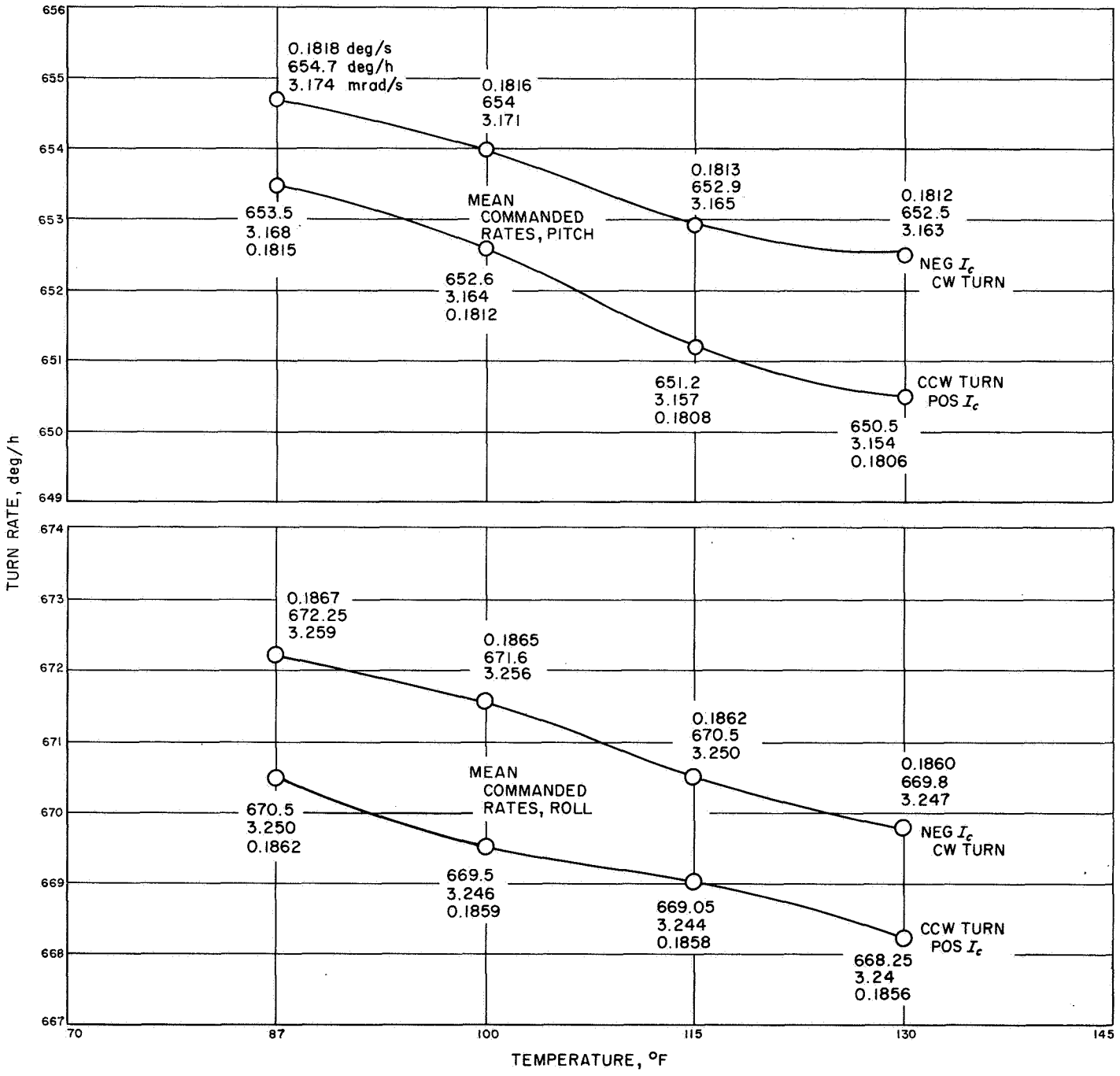


Fig. VI-29. *Mariner V* gyro-commanded turn rates

Table VI-13. Midcourse maneuver performance sequence

Event	Time observed in data, GMT	Description	Event	Time observed in data, GMT	Description
QC-V1-1 received	170:20:18:55.42 ±6.3	304-s duration pitch-turn command	CC&S M-6; start motor burn	23:08:11.3 ±0.2	—
QC-V1-2 received	20:23:45.23 ±6.3	380-s duration roll-turn command	CC&S M-7; stop motor burn	23:08:28.0 ±1.6	—
QC-V1-3 received	20:28:37.64 ±6.3	17.66-s duration motor-burn command	CC&S M-1; M-2 reset; begin sun acquisition	23:14:10.9 ±0.3	Gyros to rate mode
DC-V29 received	20:38:52.45 ±6.3	Arm-first-burn-engine-squibs command	Sun-gate event; initiate roll search	23:21:24.2 ±5.3	Sun acquired
			Canopus acquisition	23:32:19.2 ±5.7	—
DC-V14 received	20:48:44.66 ±6.3	Remove maneuver-inhibit command	DC-V21 No. 1 received	23:34:06.4 ±0.6	Initiate first post-maneuver roll search
DC-V27 received; CC&S M-1; gyros on; mode 1 data	21:24:46.03 ±0.42	*Initiate midcourse-maneuver command*	Canopus acquisition	171:00:23:58.4 ±5.7	—
CC&S M-2, M-3, and M-4; pitch turn start	22:24:10.87 ±0.00	Gyros to rate + position mode; start cw pitch turn	DC-V21 No. 2 received	00:25:52.4 ±5.4	Initiate second post-maneuver roll search
			Canopus acquisition	01:16:54.2 ±5.7	—
CC&S M-4 reset; stop pitch turn	22:29:14.8 ±0.42	—	DC-V21 No. 3 received	01:18:35.1 ±5.2	*Initiate third post-maneuver roll search*
CC&S M-5 and M-3; start roll turn	22:46:10.8 ±0.42	Start cw roll turn			
			Canopus acquisition	02:06:15.2 ±5.7	—
CC&S M-5 reset; stop roll turn	22:52:31.1 ±0.2	—	Gyros off	02:09:48.9 ±5.2	—

Table VI-14. Postmaneuver analysis, midcourse maneuver performance

Parameter	Required[a]	Commanded[a]	Achieved[a]	Standard deviation, σ
Pitch turn (rate = 0.1818 deg/s)	55.3503	55.267	55.18	0.2
Roll turn (rate = 0.1867 deg/s)	71.0248	70.946	70.93	0.04
Velocity increment	16.127 m/s	16.135 m/s	15.412 m/s	6
Motor burn	17.651 s	17.66 s	17.66 s	—

[a] In deg except as noted.

After the reacquisition of Canopus terminated the midcourse-maneuver sequence, three roll searches were performed to provide additional data to aid in the evaluation of the performance of the UV photometer. Table VI-13 summarizes the sequence of operations from the beginning of the midcourse maneuver to the final reacquisition of Canopus.

Postmaneuver analysis. At the time of the midcourse maneuver, a preliminary indication that the velocity increment was smaller than desired was obtained from the doppler tracking data. It was determined from postmaneuver orbit-determination analysis that the velocity increment was, in fact, less than commanded by 4.65%, but that the commanded turns were quite accurate. Table VI-14 lists the significant midcourse-maneuver parameters.

A detailed analysis of the trajectory-correction anomaly is presented in Section VII-C of this report.

g. Interplanetary cruise. From the standpoint of attitude control, the interplanetary-cruise phase of the mission

was uneventful. Eighteen roll transients were observed in nonreal-time data analysis during the period of June 20–October 18, 1967. Figure VI-30 shows the roll-limit-cycle action during three typical roll transients. An unusually violent transient, coupled with a large transient on the Canopus-intensity channel, is shown in Fig. VI-31.

None of these transients caused more than a momentary disruption in the operation of the AC subsystem, thus verifying the adequacy of the solution to the roll-transient problem for *Mariner V*.

On day 236, event MT-1 (the first update of the cone-angle FOV of the Canopus sensors) occurred. The telemetered response of the Canopus sensors is compared with the response predicted by the star identification program (**SIPM**), for the duration of the mission, in Subsection C-3 (the center of the cone-angle FOV is compared with the actual cone angle of Canopus). It is evident that the sensor performed well, the average difference between the telemetered intensity reading and the **SIPM**-predicted reading being on the order of 25 mV. Cone-angle updates MT-1, MT-2, MT-3, and MT-4 occurred without incident.

The cruise parameters of the AC subsystem did not change significantly from those listed in Table VI-13, with one exception. The external torque in pitch seemed to increase from approximately 1 dyne-cm (listed) to approximately +5 dyne-cm. A representative plot of the pitch-, yaw-, and roll-limit cycles during cruise is shown in Fig. VI-32.

h. Planetary encounter. Preparations for planetary encounter began on October 10, 1967, with the transmittal of a DC-V15 command to the spacecraft. The effect of this command was to prevent the spacecraft gyros from coming on in case acquisition of the sun or Canopus were lost, and to remove the lower brightness restriction on the object in view of the Canopus sensor. The purpose of the command was to prevent the spacecraft from going into an automatic roll search during the encounter sequence; e.g., if dust particles in the direction of Venus should cause the Canopus sensor to track away from Canopus, this mode of operation would allow the sensor to establish roll control on any object in its FOV. If such an event had occurred, the scientific value of encounter would be degraded, but probably not nullified (as it would have been by a roll search).

At 02:49 GMT on October 19, 1967, a DC-V25 command was transmitted to the spacecraft to preempt CC&S MT-7 and begin the encounter sequence. The terminator sensor was turned on at this time, and the first indication of terminator-sensor excitation was received at 03:11:39 GMT. At 10:50 GMT, a DC-V24 was transmitted to preempt CC&S MT-8 and begin the DAS encounter sequence, switching the data from mode 2 (science plus engineering) to mode 3 (science only), and energizing the planet sensor.

From this time through the encounter sequence, no data on the AC subsystem itself were available; therefore, it was not possible to determine the attitude of the spacecraft at any time during the planetary encounter.

A backup ground command was available to supplement the PSO initiation of the encounter sequence; because of difficulties at the transmitting site, however, the command was transmitted approximately 30 min after the optimum time. The prime responsibility for initiation of the encounter sequence approximately 60 min before closest approach, therefore, rested upon the planet sensor. The PSO occurred in the data (science frame 28) at 16:33:57 GMT, 66 min before the predicted closest approach and within 1 min of the predicted PSO time. A more detailed discussion of planet-sensor timing appears in Subsection F-3-i, below.

The spacecraft entered occultation at 17:38:09 and exited occultation at 17:59:59 GMT. No data were available during this period, but when the spacecraft exited occultation, it was determined that the pointing angle of the high-gain antenna had changed to the post-APAC position, indicating that the terminator sensor had fulfilled its function as planned.

The time of TSO was fixed from the data playback at 17:42:25 GMT, approximately 8 min after closest approach. More detailed information on the terminator sensor also appears in Subsection F-3-i.

Engineering data again became available when the telemetry was automatically switched to data mode 2 at 18:48:18 GMT. At this time, the condition of the AC was normal, indicating that acquisition of the sun and Canopus had been maintained, and that the AC subsystem had performed normally during encounter.

i. Sensor orientation and timing for encounter. Orientation of the planet sensor and terminator sensor, star identification, midcourse-maneuver acquisition, postmidcourse-maneuver rolls, star orientation, postencounter rolls, and postencounter maneuver turns, as well as timing for encounter, are described in the paragraphs that follow.

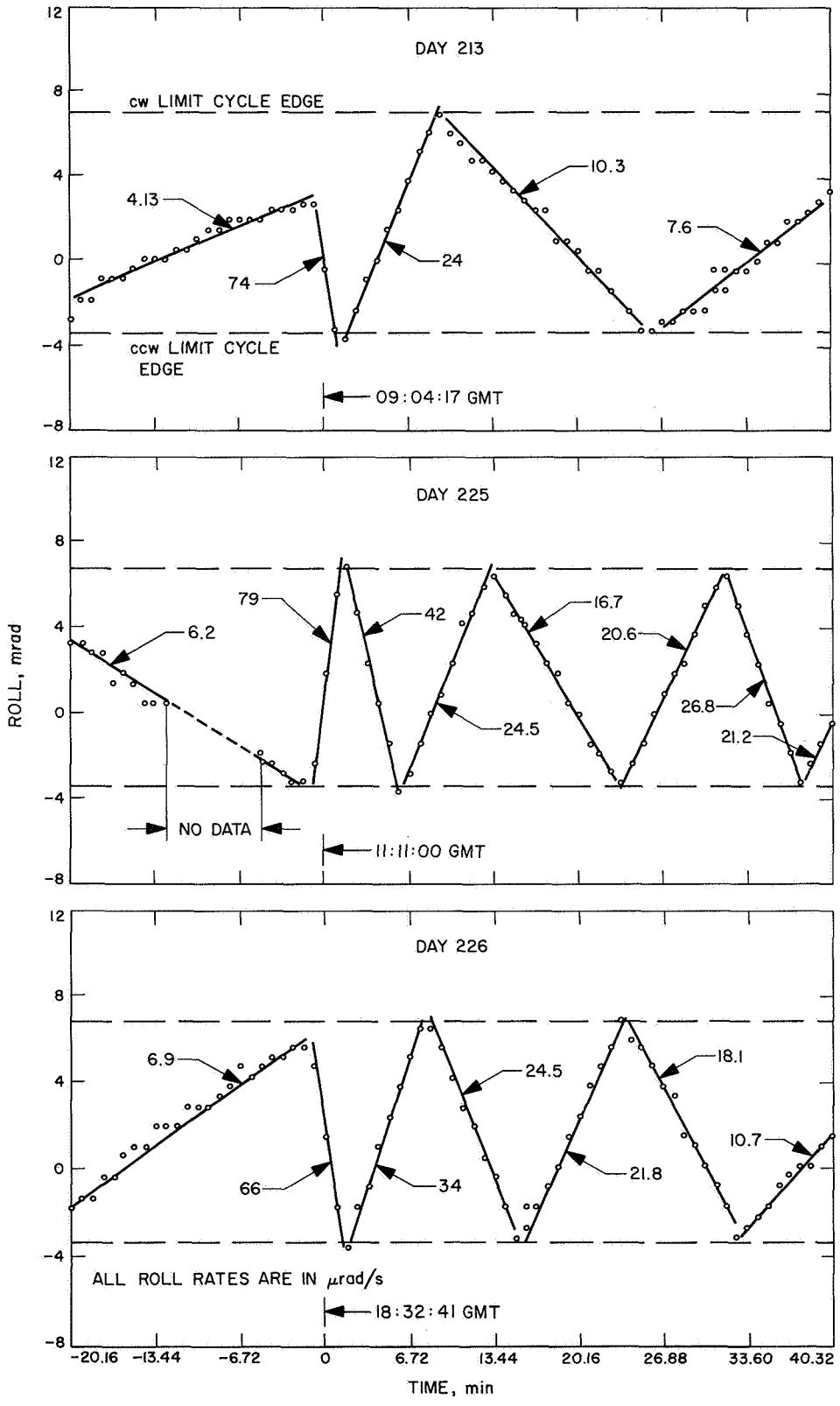


Fig. VI-30. Representative *Mariner V* roll transients

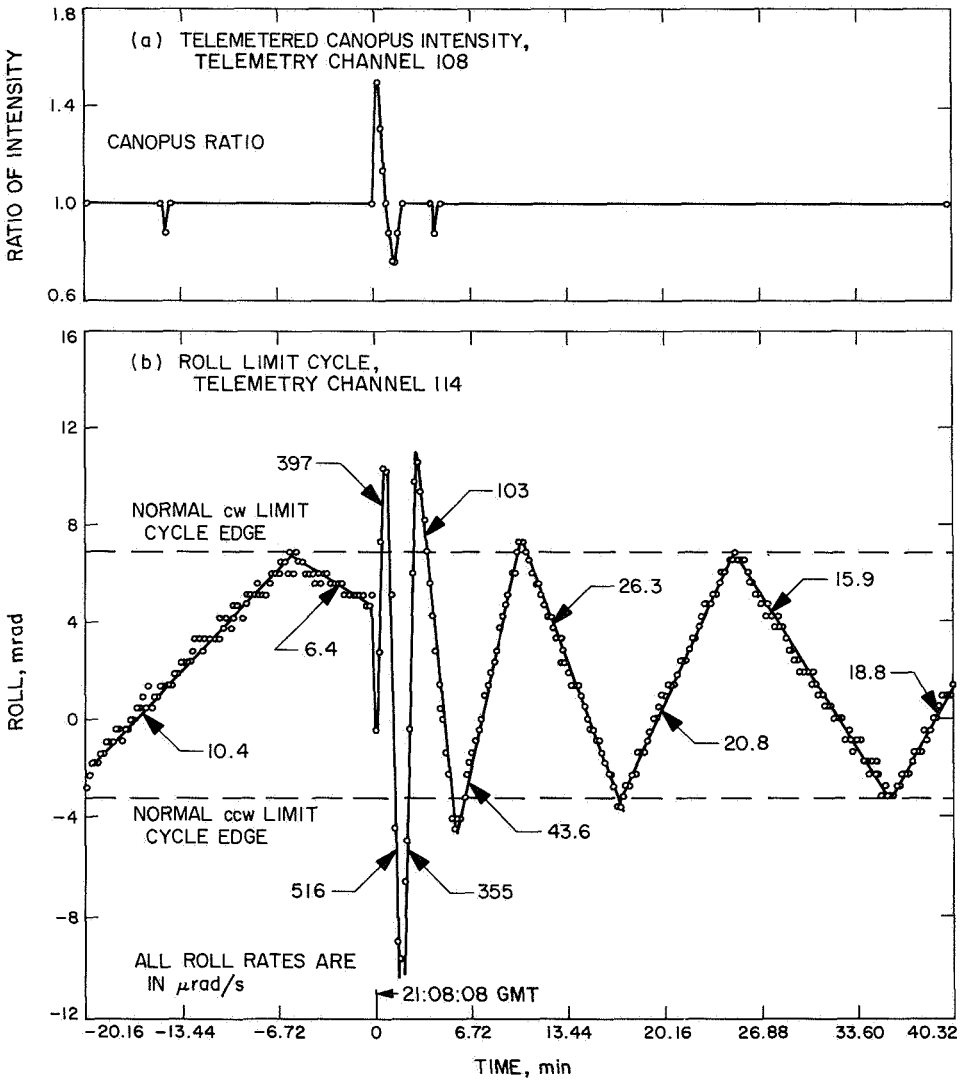


Fig. VI-31. Roll transient, June 23, 1967

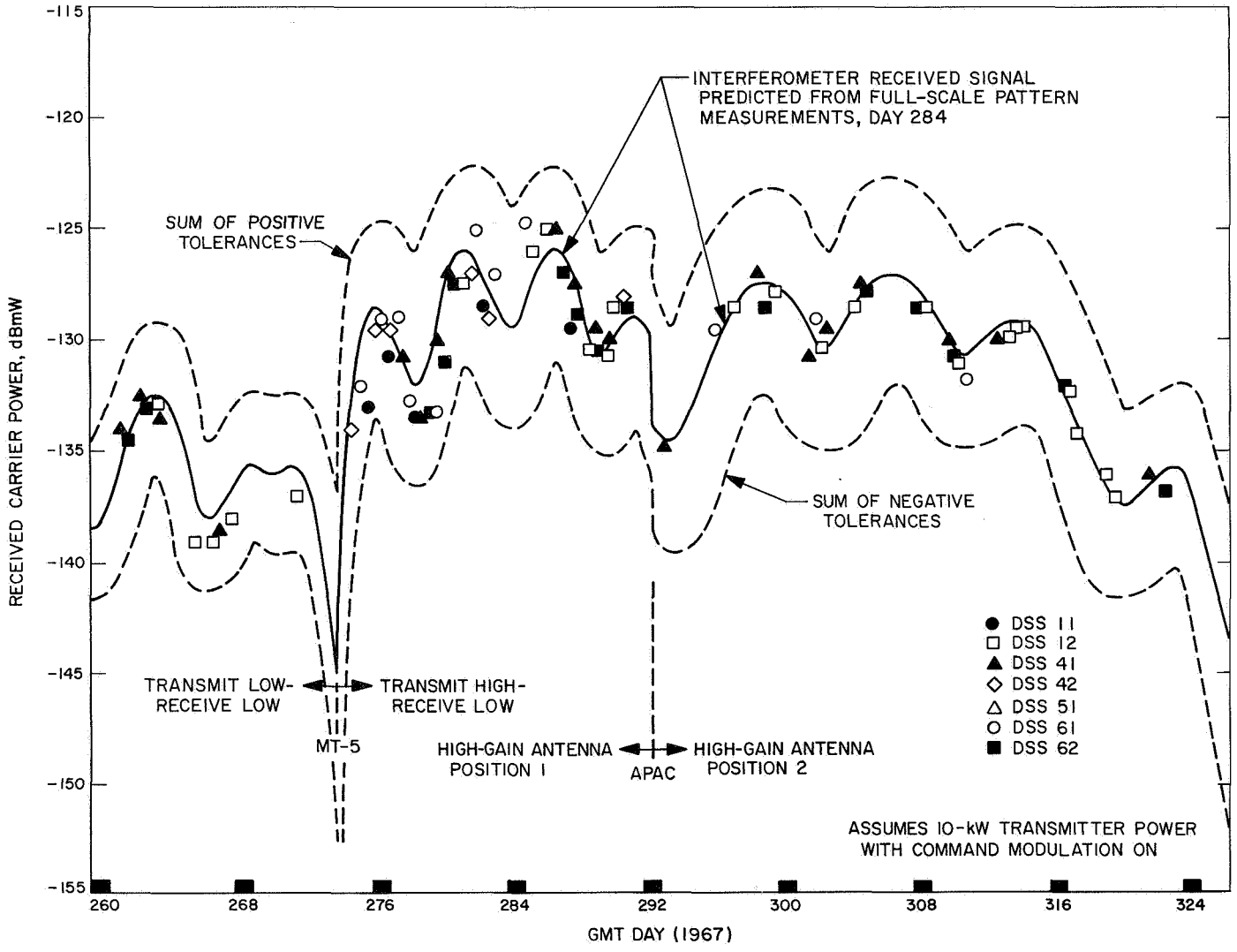


Fig. VI-32. *Mariner V* attitude data

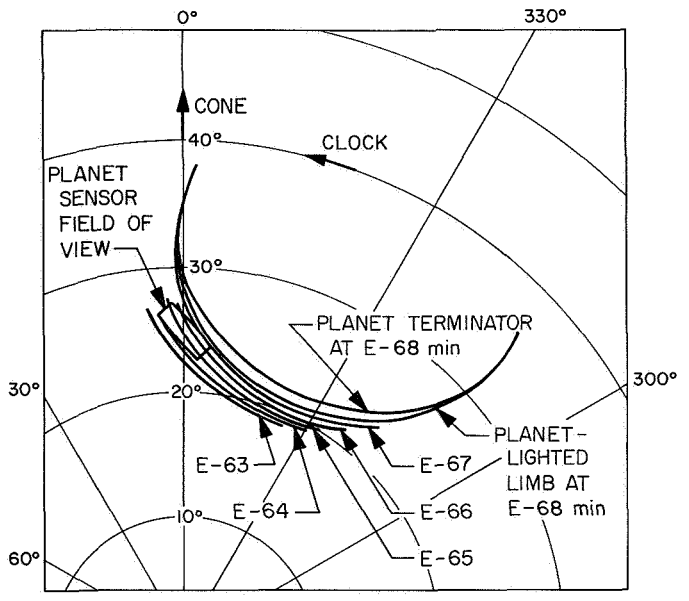


Fig. VI-33. Venus-lighted limb geometry at planet sensor output

Planet sensor. The planet sensor was used for onboard initiation of the encounter sequence. Its fixed orientation had been designed to observe a horn of the lighted limb of the planet at 60 ±12 min before encounter for all trajectories being considered. After launch, an exact estimate of the time of PSO was required for encounter-planning purposes.

A computer program that had been developed during the design phase of the *Mariner V* spacecraft was again used. This program calculates the cone and clock angles of the limb and terminator of the planet as a functon of time along a conic trajectory. Figure VI-33 shows the clock and cone geometry as the planet limb enters the FOV of the sensor.

Another previously developed computer program was used to calculate the brightness of the limb of the planet when it entered the FOV of the sensor. This program was required for an estimate of the length of time the planet sensor would stay on. To satisfy logic within the science DAS, the sensor would have to be on for 50.4 s in the worst case. Figure VI-34 shows one of the plots generated by this program. The contours are lines of constant brightness (luminance) in foot-lamberts.

Using the postmidcourse-maneuver estimate of the Venus-encounter orbit and these programs, the time of PSO turn-on was estimated as 67 ±0.5 min before encounter; the time of PSO turn-off was estimated as 63 ±0.5 min. Based upon an orbit 1 wk before encounter, these estimates were revised to 66.5 ±0.5 and 62.5 ±0.5 min, respectively. These estimates did not include the possible deviation in time caused by the position of the spacecraft within its limit-cycle deadbands. It was estimated that the position could shift the PSO on and off times by approximately ±0.5 min. However, the shift could not be determined at encounter because no engineering data were available.

The planet sensor performed as expected on the day of encounter. The PSO turn-on was observed in the data at 16:33:22 and PSO turn-off at 16:38:24 GMT on October 19, 1967. Based upon the postencounter trajectory, these times correspond to 66 and 61 min before encounter, respectively. As a sidelight, a second PSO turn-on was observed in the data 17:15:22 and turn-off at 17:19:34 GMT or 22 and 19.8 min before encounter, respectively.

No prediction of the second PSO had been made; however, the PSO was quickly explained as the sensor viewing the other horn of the limb of the planet. Figure VI-35 shows the approximate geometry for the two PSOs. As expected, the second PSO had no effect upon the DAS logic. Postencounter analysis showed that the second PSO occurred very close to the nominal time.

Terminator sensor. The terminator sensor was designed to initiate the high-gain APAC as close as possible to the midoccultation point. Figure VI-36 shows the approximate encounter geometry and the region of terminator sensor turn-on times for all trajectory variations. As part of encounter planning, an exact estimate of the time of TSO was made after the midcourse maneuver.

Based upon the postmidcourse-maneuver determination of the orbit and a previously developed computer program, TSO was estimated to occur 7.5 min after closest approach to Venus. Figure VI-37 is a plot of the computer-program output, and shows the lighted limb of the planet in spacecraft clock and cone coordinates 7 and 8 min after encounter. The time was approximately 2 min before the estimated time of the center of occultation, which was within the design tolerance.

No data were available at the time TSO occurred, as the spacecraft was behind the planet. However, after the spacecraft emerged from behind the planet, verification of APAC indicated that TSO had occurred. Later information, taken from the spacecraft playback of the

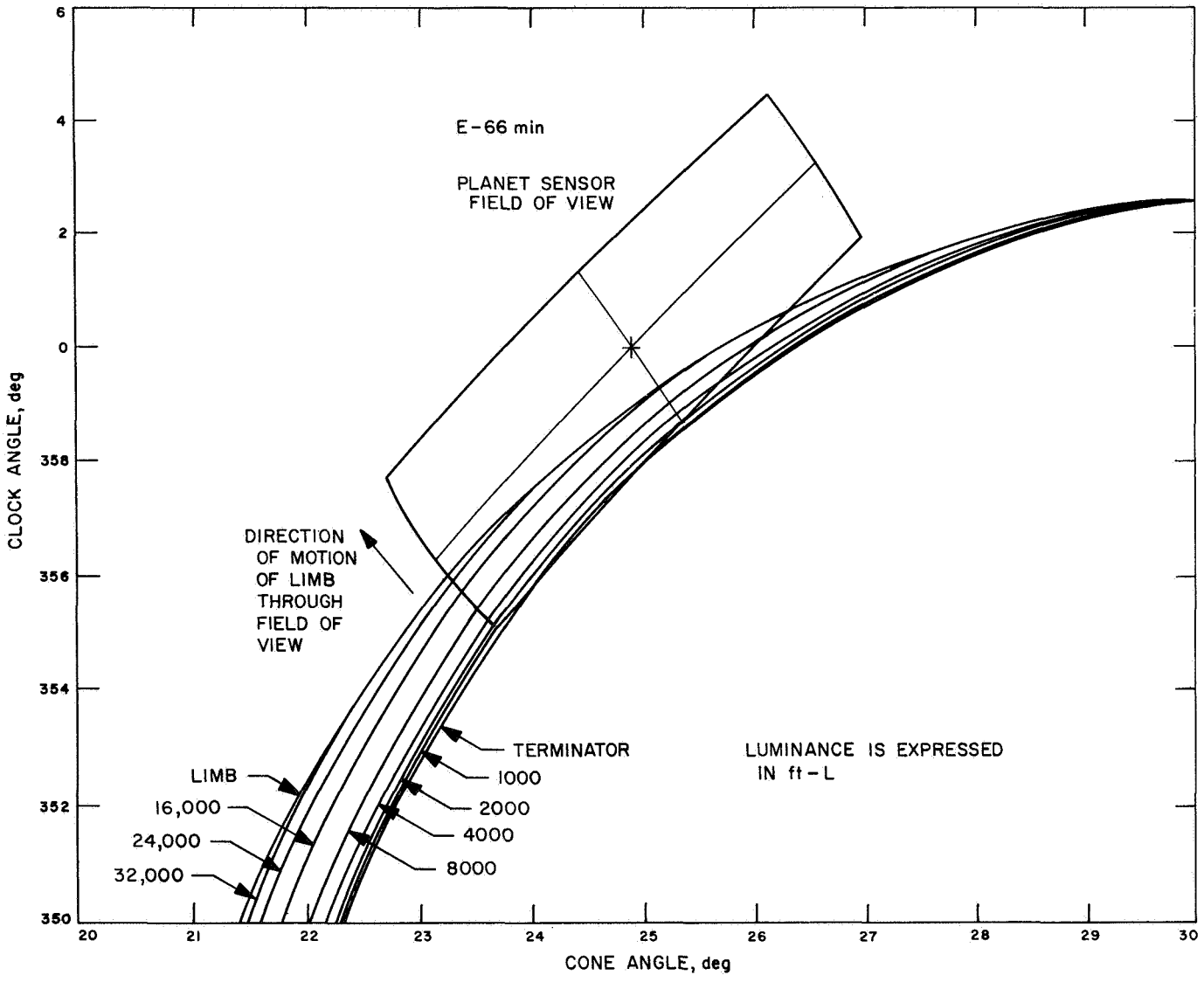


Fig. VI-34. Contours of constant luminance for Venus encounter

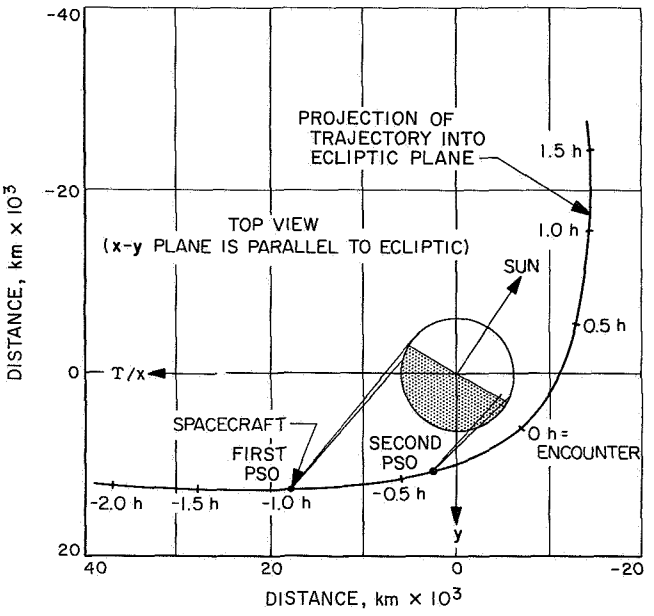


Fig. VI-35. Planet sensor—approximate encounter orientation

science data recorded through encounter, indicated that TSO had occurred at 17:42:25 GMT on October 19, 1967. This corresponds to 7.5 min after closest approach.

Star identification. The **SIPM** program was developed and effectively used to identify celestial objects and to determine the objects that could be acquired by the Canopus sensor during roll search. The program also furnished orientation and geometry information for other scientific experiments.

Roll search was initiated at 22:38:00 GMT on June 14, 1967, by the CC&S. Estimates based upon earth-sensor outputs during the spin mode that was used to calibrate the helium magnetometer showed that the Canopus sensor was at a clock angle of 311 deg when roll search began.

After the spacecraft was rolled 73 deg, reflected light caused by the earth was acquired at 22:48:08 GMT. Figure VI-38 shows the *a priori* brightness map made by **SIPM** and the telemetered brightness for this acquisition. Tests made on the Canopus sensor before launch indicated that two portions of this reflected light were acquirable.

A direct command (DC-V21) was initiated at 00:30:00 GMT on June 15, 1967, to cause the spacecraft to begin searching a second time. The acquired reflected light was lost, and the *Mariner V* spacecraft rolled another 11 deg towards Canopus. Another portion of the reflected earthlight was then acquired, as shown in Fig. VI-39. Because the second acquisition had been anticipated, a second DC-V21 had been planned, and the command was initiated 4 min after the first command.

The second DC-V21 caused the spacecraft to begin searching a third time. After rolling 99 deg, *Mariner V* attempted to acquire reflected light caused by the moon. However, after the spacecraft had rolled 11 deg without being able to find a stable null in the Canopus-sensor roll-error signal, the reflected light passed out of the FOV of the sensor, and the spacecraft again began searching in the roll mode. No further interruptions in the search occurred, and Canopus was acquired at 01:09:44 GMT after a total roll of 311 deg. Figure VI-39 shows the *a priori* and telemetered brightness for this portion of initial Canopus acquisition.

From the attempted acquisition of the moon, it was possible to observe the value of the drop-out voltage of the Canopus-sensor low gate fairly accurately (1.133 $\pm$0.024 V). This value was found to agree quite well with the preflight value of 1.138 V.

Midcourse-maneuver acquisition. The second acquisition of Canopus occurred at 23:32:59 GMT on June 19, 1967. This was the first acquisition after the midcourse maneuver.

Roll search was automatically initiated as *Mariner V* was completing its postmidcourse-maneuver reacquisition of the sun at 23:21:19 GMT. **SIPM** brightness maps for this time had predicted that only Canopus could be acquired. After an uneventful roll of 73 deg, the reacquisition of Canopus was completed.

Postmidcourse-maneuver rolls. To obtain additional scientific and engineering information during the early portion of the flight, it was decided to command *Mariner V* to perform three 360-deg rolls after the midcourse maneuver. These rolls were performed by commanding the spacecraft to deacquire Canopus and begin a roll search. Because **SIPM** had indicated that Canopus was the only source of light that would be acquired at this time, it was expected that *Mariner V* would search 360 deg and acquire Canopus.

The first direct command (DC-V21) was initiated at 23:33:15 GMT on June 19, 1967. *Mariner V* lost Canopus acquisition, and began a roll search. Canopus was acquired at 00:24:32 GMT on June 20, 1967, after a 360-deg

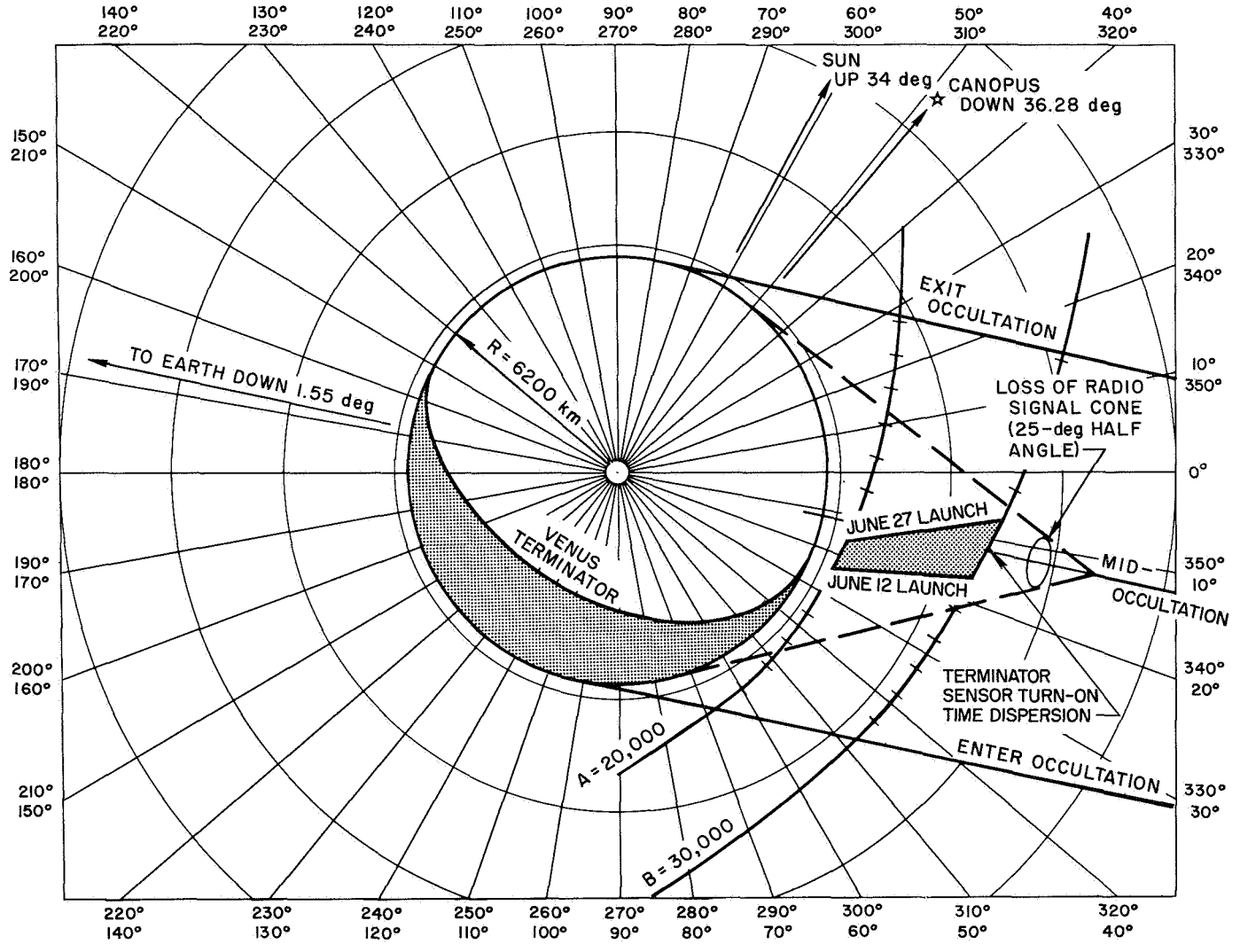


Fig. VI-36. Terminator sensor—approximate encounter geometry

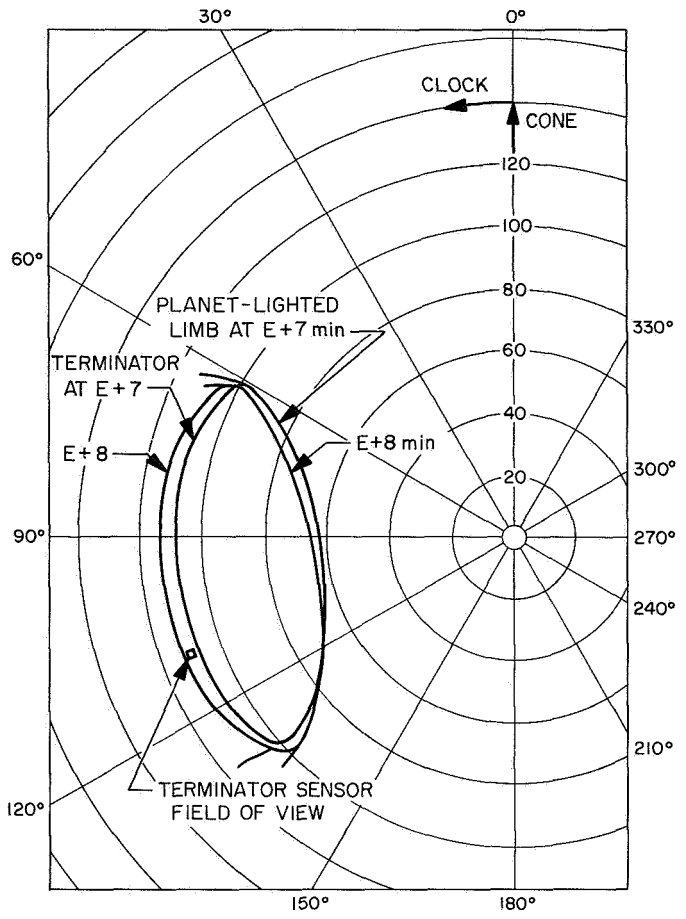


Fig. VI-37. Venus-lighted limb geometry at terminator sensor output

roll search that lasted 50 min, 37 s. As expected, no other celestial sources of light were acquired.

The second DC-V21 was initiated at 00:25:00 GMT on June 20, 1967. After a 360-deg roll search, which lasted 51 min, 41 s, Canopus was acquired at 01:17:27 GMT.

The third DC-V21 was initiated at 01:17:50 GMT. The 360-deg search lasted 48 min, 19 s, and Canopus was acquired at 02:06:48 GMT.

Star orientation. In addition to predicting the stars that would be acquirable during roll search, **SIPM** was used to determine spacecraft orientation with respect to various stars for scientific purposes, including the UV-photometer experiment. Figure VI-40 shows a plot from **SIPM** output of the position of two stars that passed close to the UV-photometer FOV during cruise. Similar uses of **SIPM** occurred frequently during the flight.

Postencounter rolls. A decision was made to command *Mariner V* to execute three complete rolls, early in November 1967, to obtain additional scientific and engineering data. This time was chosen because the *Mariner V* spacecraft was approximately 180 deg in celestial longitude from its location at the time of the three rolls following the midcourse maneuver. As a result, the UV photometer would scan the same part of the sky as it had during the previous rolls. In addition, according to **SIPM**, only three direct commands would be required because Canopus was the only celestial source of light that the Canopus sensor would acquire.

The first of the three DC-V21 commands was initiated at 12:22:10 GMT on November 7, the second at 13:18:27 GMT on November 7, and the third at 14:08:01 GMT on November 17. In all three cases, *Mariner V* lost Canopus acquisition and initiated a roll search. In each case, the spacecraft rolled 360 deg and acquired Canopus. A null in the Canopus-sensor roll-error signal (acquisition) occurred, for each of the three commands, as follows: the first at 13:08:24 GMT, the second at 14:06:22 GMT, and the third at 15:06:51 GMT.

Postencounter maneuver turns. On November 19, 1967, *Mariner V* was commanded to perform a −17.2-deg pitch turn and a 173.2-deg roll turn so that additional information could be obtained from the UV photometer. *A priori* **SIPM** maps had indicated that only Canopus could be acquired at this time. After these turns were performed, Canopus was reacquired at approximately 17:45:34 GMT.

From its launch on June 14, 1967, until 40 days after Venus encounter, *Mariner V* had acquired Canopus a total of nine times.

j. Postencounter cruise. Some roll transients were observed in the days immediately following encounter; Fig. VI-41 depicts the first three observed. Because there were only about 4 h of engineering or engineering and science data for the 4 days following encounter, it is probable that many more transients occurred than the three recorded.

The spacecraft was returned to normal optical control on October 26 with the transmission of a DC-V12 command that revoked the DC-V15 earlier transmitted for encounter purposes. Twelve days later, on November 7, three roll searches were performed to gather data to aid

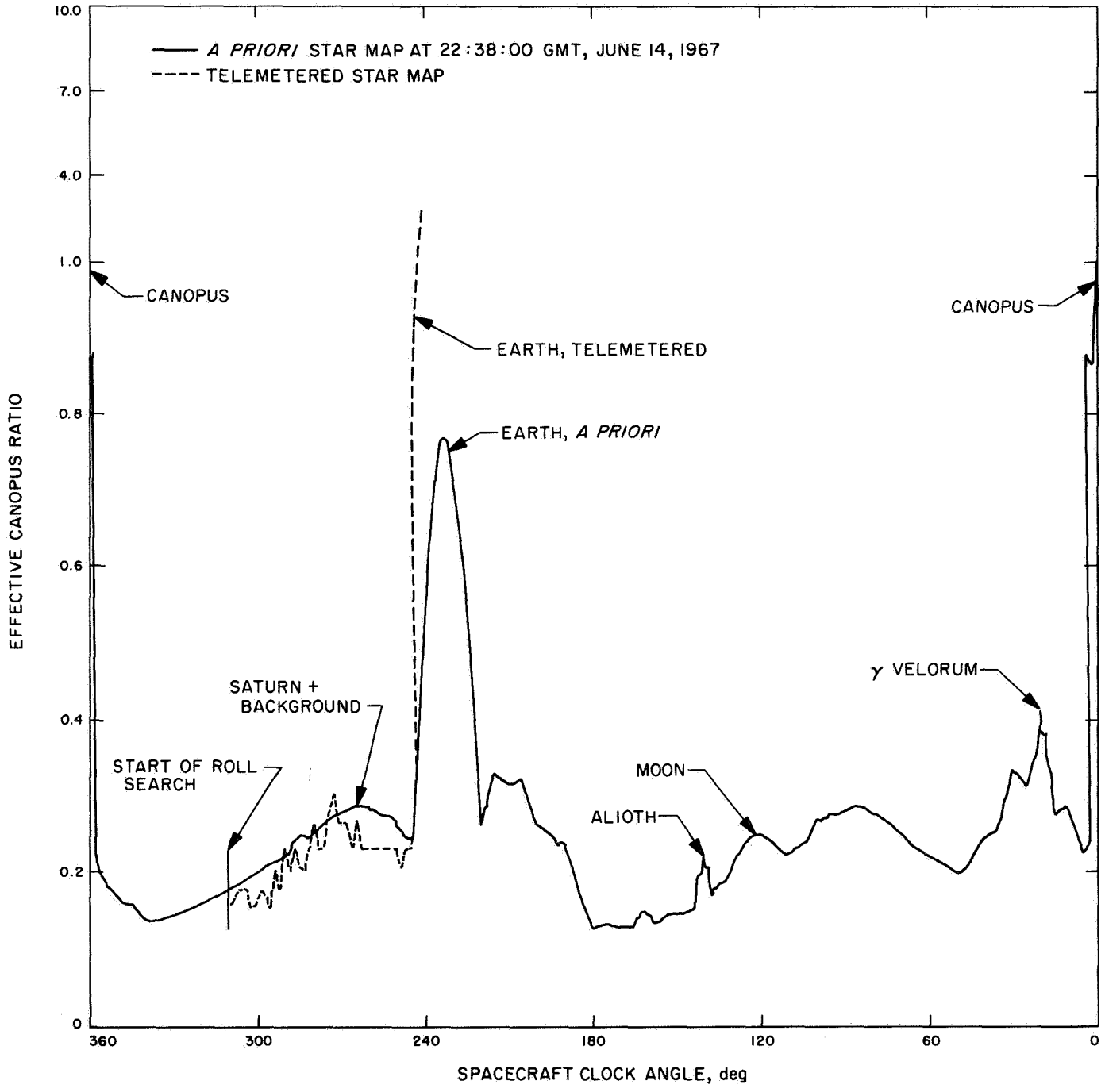


Fig. VI-38. *A priori* and telemetered star maps (roll search start to earth acquisition)

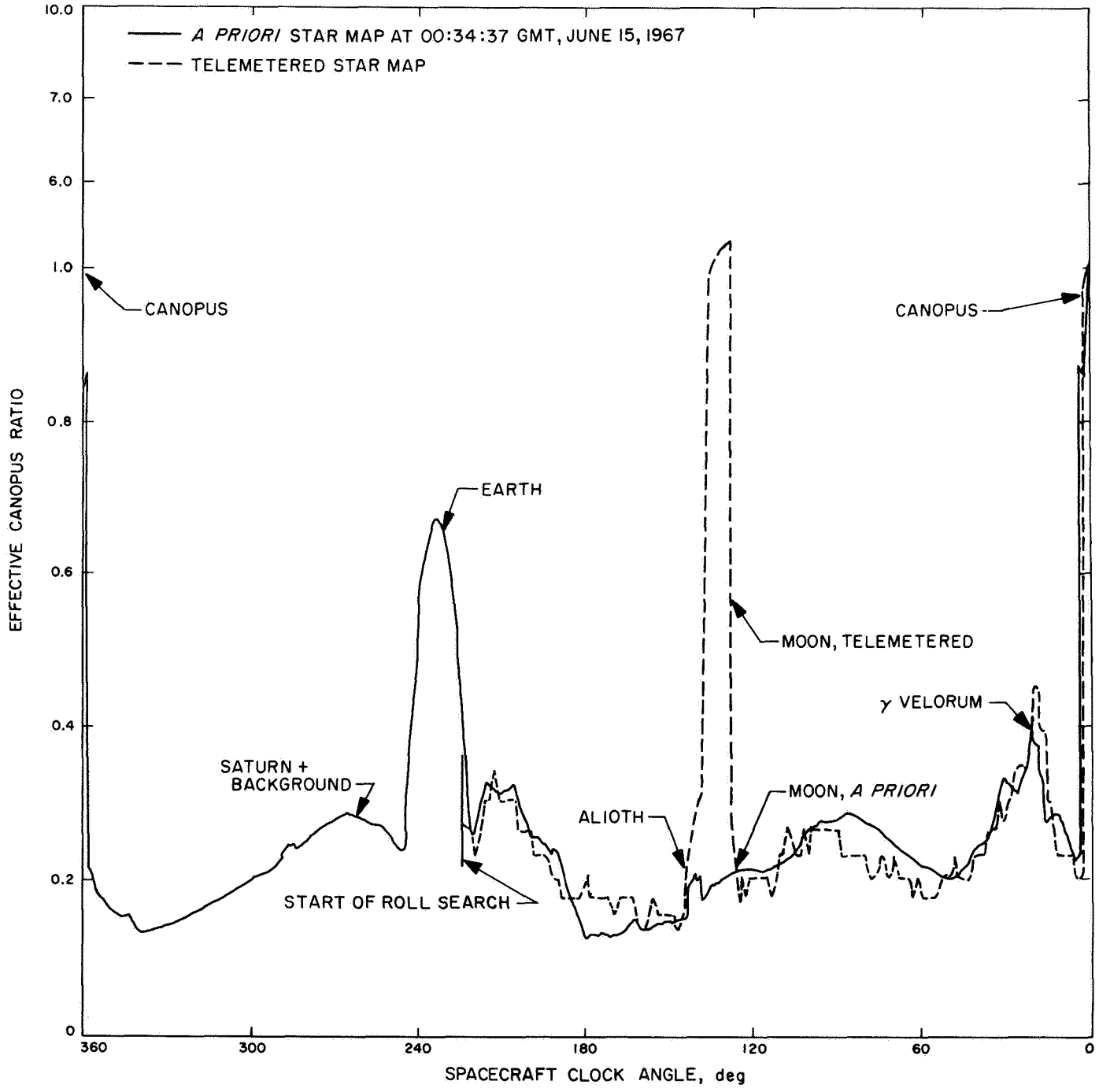


Fig. VI-39. *A priori* and telemetered star maps (earth acquisition to Canopus acquisition)

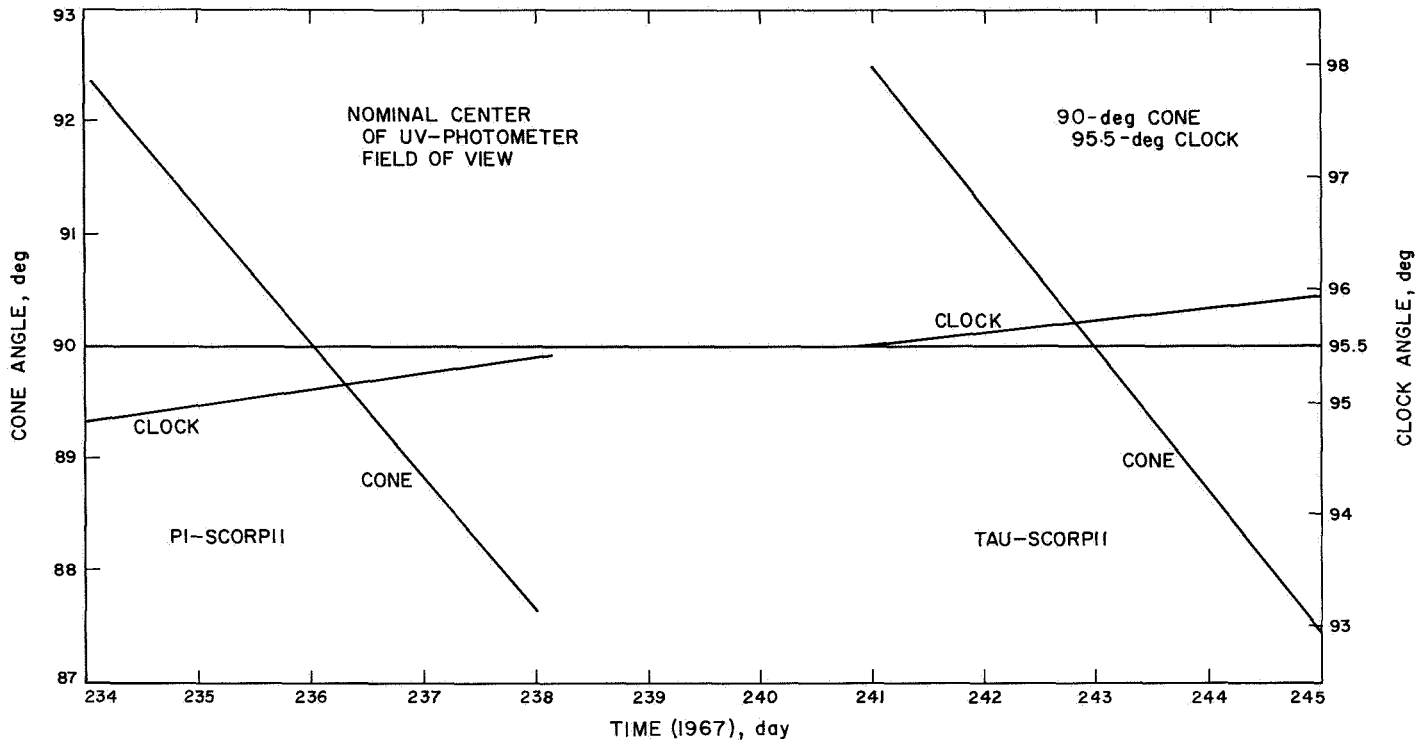


Fig. VI-40. Stars near UV-photometer field of view

in the analysis of the performance of the UV photometer; 12 days after that, a second midcourse-maneuver sequence (without a motor burn) was performed for the same purpose.

Because communication with the spacecraft during the roll searches was not possible, the data were stored on tape and played back later. The AC subsystem performed normally during these exercises. The acquisition of Canopus after each roll, and the acquisition of the sun and Canopus after the maneuver sequence, were normal and uneventful.

The *Mariner V* mission-length gas-weight history is illustrated in Fig. VI-42. Total gas consumption during the mission was 0.41 lb, an average of 0.00246 lb/day. At this rate, the *Mariner V* AC gas will be depleted in October 1973.

The spacecraft was conditioned for long-term cruise on November 21, 1967, by transmitting a DC-V15 and a DC-V12. These commands inhibited the gyros from coming on if sun or Canopus acquisition should be lost, allowed the Canopus sensor to establish roll control about any object in its FOV, and switched the spacecraft transmitter from the high- to the low-gain antenna. Because cone-angle updates to the Canopus sensor are not automatic, it was estimated that Canopus would disappear from the FOV on or about December 19, 1967. Roll control from that time on would be dependent upon whatever star appeared in the FOV of the sensor.

4. Recommendations.

a. Roll-transient problem. Because the flight of *Mariner V* showed that the roll transients were not peculiar to *Mariner IV*, some type of transient-rejection mechanism should be included in future AC subsystems. The solution used for *Mariner V* is not adequate if an extremely bright object (such as the earth, the moon, or a planet) could appear in or near the FOV of the sensor. The trajectories for *Mariner V* were such that this solution was feasible, as the cone angle of the earth was always greater than 110 deg and, therefore, outside of the cone-angle FOV.

b. Midcourse-maneuver anomaly. The type of nonsystematic failure that probably occurred in the *Mariner V* autopilot cannot be designed out of the system or detected in advance. However, the JVA mounting ring should be increased in diameter to minimize the side forces generated by vane rotation in the exhaust stream. Ideally, the ring should be eliminated to prevent the side forces, but the present design of the PIPS and actuators requires some mounting surface for the actuators.

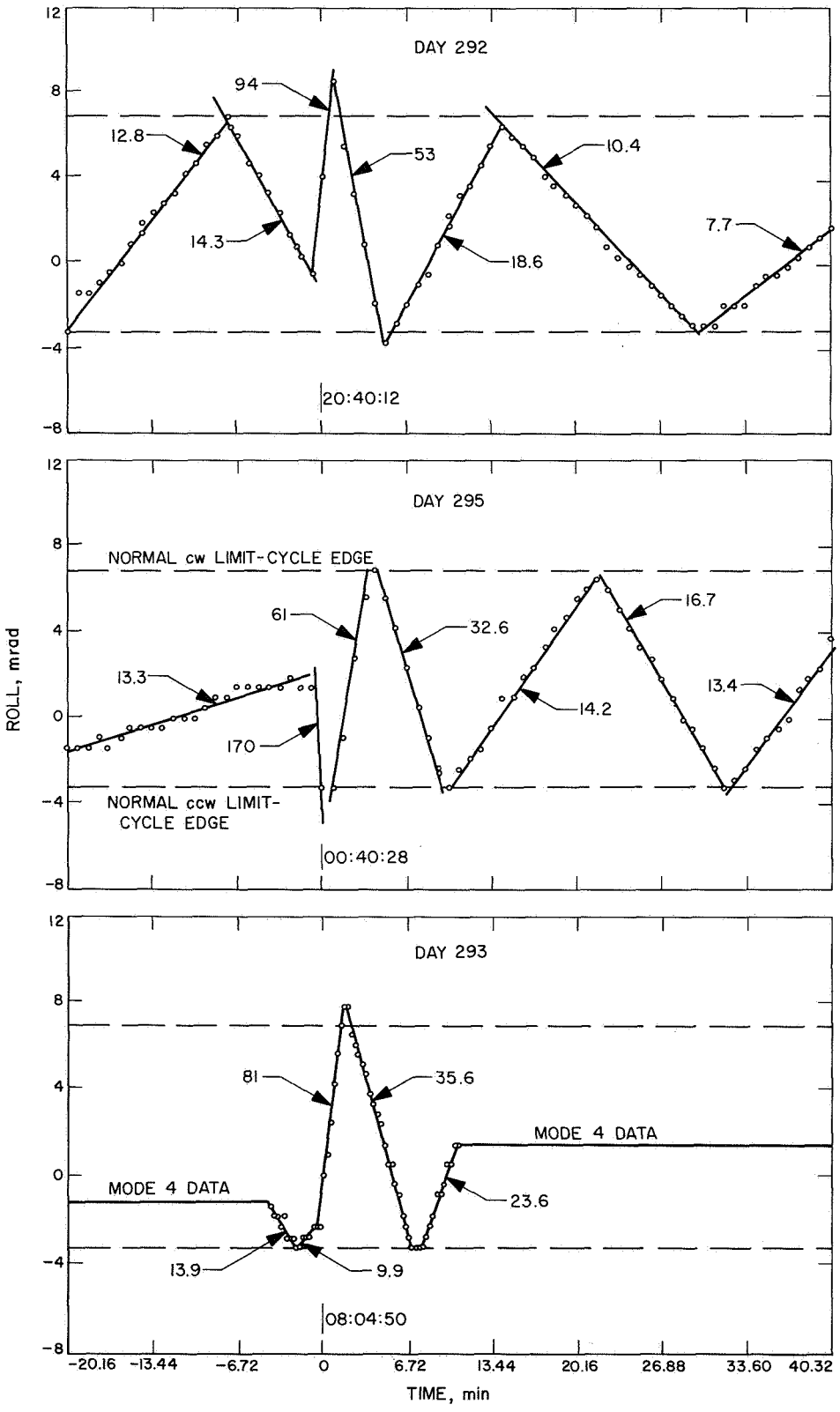


Fig. VI-41. Postencounter roll transients

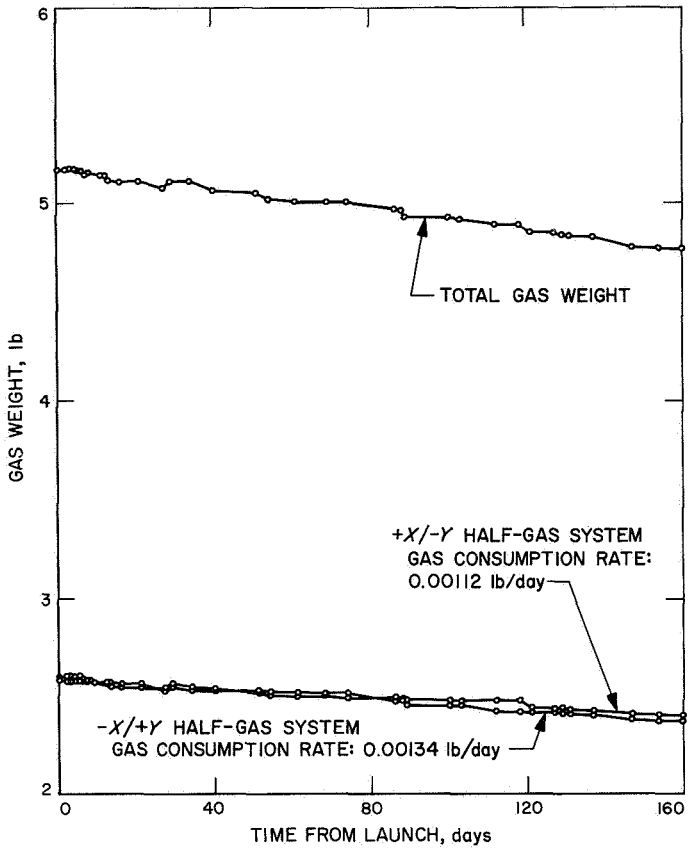


Fig. VI-42. Gas-weight history, June 14–November 21, 1967

c. Telemetry resolution. Currently, resolution of the gyro telemetry channels is approximately 0.3 mrad/s in pitch and yaw, and 0.27 mrad/s in roll. The sun-sensor resolution (on the fine sensor channels) is 0.24–0.30 mrad in pitch and yaw, and 0.46 mrad in roll. Canopus-intensity resolution is 0.23 mV, or about 0.12 × Canopus in Canopus ratio. These ranges of resolution are usable, but it would be desirable to have greater resolution for all of these functions. In each case, the resolution available is a consequence of buffering the voltages feeding the data encoder so that no more than ±1.5 or +3 V are applied to the data encoder when the function being monitored is at saturation level.

To obtain greater resolution, the telemetry buffer could be adjusted for the desired resolution when the function being monitored is behaving normally, and a diode clamp or other limiting network could be used to prevent overdriving the data encoder. Alternatively, the data encoder could be modified to operate linearly in the ±1.5 or 0–3-V range, and to clamp signal levels outside of that range.

d. Additional telemetry. Analysis of the autopilot performance during the midcourse maneuver was seriously hampered by lack of data. The only data available were the gyro outputs, whose data rate was slow compared to the autopilot response. Data-compression techniques could be used for purposes of autopilot performance analysis during the midcourse maneuver.

These techniques would be a natural extension of the present practice of switching to data mode 1 (all engineering telemetry) during the midcourse maneuver, and would involve telemetering the four JVA feedback-potentiometer voltages on four high-rate channels (currently, four high-rate channels are unused during the midcourse maneuver: coarse pitch and yaw sun sensors, roll position, and Canopus intensity).

To obtain a higher data rate, the three gyro outputs and the four JVA-position outputs (feedback-potentiometer telemetry) could each be telemetered on two channels instead of only one. This additional switching could be initiated at CC&S event M-6 (motor-burn start) and terminated at CC&S event M-7 (motor-burn stop) to provide the maximum data available on autopilot performance during the thrusting period with the present telemetry plan.

e. All-axes inertial control. Although the possibility is remote, failure of a cruise sun sensor could result in termination of the mission. If redundant cruise sun sensors are not installed on future spacecraft, the only other method of maintaining AC is to place the spacecraft gyros in the rate-plus-position mode, and complete the mission under inertial control. This was not possible for *Mariner V*; only the roll axis could be indefinitely left under inertial control. The spacecraft was in a 3-axis, rate-plus-position mode only during the midcourse maneuver, from M-2 to M-2 reset, and could not be again placed in inertial control until the CC&S had clocked out the maneuver sequence (at M+199 min), a DC-V27 had been sent, and the CC&S clocked out at M-2 (at M+60, or 60 min after receipt of the DC-V27).

A command or a sequence to place the spacecraft in all-axes inertial AC should be developed as a failure-mode backup. For *Mariner V*, such a mode would have added the capability of pointing the various science instruments (e.g., the UV photometer) in any desired direction to aid in the evaluation of their performance.

5. Power subsystem flight performance. The overall performance of the *Mariner* Venus 67 mission power

subsystem during the cruise and encounter of *Mariner V* followed expected characteristics. Variations from the expected data occurred in the outputs of the I_{sc} and I_{scr} experimental solar cells and in solar-panel temperature, but no failures were noted.

The battery was used twice during the mission: for launch and for the midcourse maneuver. The initial battery use started with the transfer to internal power at L−7 min, and continued until the sun was acquired about 30 min after liftoff. The battery was then recharged until the time of the midcourse maneuver, when the pitch turn caused a shading of one solar panel and sharing between the solar panels and battery. The battery was used for an additional 46 min at this time. When the sun was reacquired after completion of the midcourse maneuver, the battery resumed charging. The battery charger was turned off 13 days after launch.

The solar panels provided power for the spacecraft from sun orientation after spacecraft–*Agena* separation until the midcourse maneuver, and thence throughout the remainder of the mission. Sharing of the solar panels and battery occurred during the midcourse maneuver, as described above. Panel capability was estimated to be 405 W near earth, and 615 W near Venus.

The power-conditioning equipment functioned as programmed throughout the mission. The power subsystem responded to and executed each command as expected.

6. Solar-panel flight performance. After the successful launch and separation of *Mariner* V, early telemetry data of the solar-panel characteristics indicated that the panels were performing well. Two deviations from predicted data were noted, however: (1) The solar-panel substrate temperature (Appendix C, Fig. C-45) after L+5 days was approximately 7°C cooler than had been estimated. (2) The outputs of the I_{sc} and I_{scr} cells (Figs. C-20 and C-21) were approximately 3% higher than expected. Although these data were considered to be within the limits of prediction capability and the resolution of the telemetry system, a detailed study was initiated to re-evaluate the preflight solar-panel analysis.

The study of the 7°C temperature differential revealed that the original temperature predictions had been based upon an assumed power usage from the solar panels that was somewhat lower than actually experienced. The spacecraft power requirements were well known from system test data.

However, the operating point of the zener diodes (and consequently the power that they dissipated) was higher than had been predicted. During the near-earth portion of the flight, the operating voltage of the zener shunts was such that nearly all of the solar-panel power not being used by the spacecraft was being dissipated. Because of the poor thermal path between the panel spars on which the diodes are mounted and the panel substrate, the power dissipated by the diodes did not contribute significantly to the substrate temperature. It was determined that the additional power being drawn from the panels, together with the lack of substrate reheating by the zener diodes, accounted for the observed 7°C temperature differential.

The substrate temperature prediction was recalculated, taking these factors into account, and the data followed this new prediction closely for the remainder of the flight (Fig. C-49). The actual spar temperature was plotted using measured space-simulator values for the predicted spar temperature with and without zener-diode dissipation (Fig. C-50). As the plotted data show, the spar temperature was higher than predicted after 5 days.

Preliminary analysis of the I_{sc}–I_{scr} anomaly indicated that a calibration problem existed. A review of the original calibration curves and the transfer to the telemetry calibration revealed no discrepancies. It is theorized that the difference between the calibration resistors used on the balloon flight and those used on *Mariner V* was the cause of the 3% higher-than-expected value. Further studies have failed to resolve this anomaly.

The telemetry outputs of the I_{sc}–V_{oc} transducer showed a continuous and significant degradation during the flight (Fig. C-10), but the solar-panel performance appeared to be nominal. The ability to resolve degradation to the panels is restricted, however, because of the zener diode limiting the panel voltage early in the flight, and the operation was well down on the I–V curve close to open-circuit voltage later in the mission.

The rate of degradation observed in the I_{sc}–I_{scr} cells did not appear to be a function of the spacecraft heliocentric distance, nor was it the type of degradation associated with radiation damage by solar flares. Spacecraft instrumentation detected no significant high-energy proton flux. Other possible sources of this degradation are heat, ultraviolet radiation, and low-energy proton degradation on unprotected portions of the solar cells. Studies at JPL have indicated that both the short-circuit current (Figs. C-22–C-25) and open-circuit voltage of

cells can degrade as a function of time at elevated temperature. However, the results of these studies did not indicate that degradation of this magnitude should be expected.

Upon the basis of the I_{sc}–V_{oc} transducer data, it must be concluded that the panels had degraded, perhaps as much as 17%, by the end of the mission. Transducer data taken at face value indicate that approximately 10% of this degradation may be caused by particle radiation, whereas the remainder could be caused by other space conditions (primarily heat and ultraviolet rays). Other interpretations of these data are possible, including load-resistance changes on the transducers, low-energy proton degradation on the unprotected portions of the cells, and different rates of heat degradation for irradiated and nonirradiated cells.

7. Power-conditioning equipment flight performance. The power-conditioning equipment functioned exactly as designed throughout the *Mariner* Venus 67 mission. All voltages and currents telemetered were as predicted during launch, midcourse maneuver, cruise, and encounter.

Loading of the inverters and booster regulators (Figs. C-30–C-32) was in accordance with the data obtained during spacecraft system testing; the main-inverter output voltage (Fig. C-14) was maintained between 50.12 and 50.48 V. A value of 50.30 V was obtained at launch, prior to star acquisition, and then again during encounter and the tape playback. The lowest value (50.12 V) occurred during the midcourse maneuver.

The power-distribution subassembly responded properly to all spacecraft and ground commands, starting with spacecraft–*Agena* separation when cruise science was turned on and RF power up. The DC-V28 battery-charger on–off toggle command was used several times during the mission. At encounter, the DC-V25 command was verified, and later the DC-V26 and DC-V2 commands were used.

Plots of the power switch and logic voltage, and the primary currents from the sources and to the power subsystem, are shown in Figs. C-13 and C-26, respectively.

8. Battery flight performance. Use of the *Mariner V* battery started 7 min before liftoff, when the spacecraft was transferred to internal power. To maintain as automatic a spacecraft as possible, the battery charger was on during launch. The battery then supplied all spacecraft power until the sun was acquired after spacecraft–*Agena* separation some 37 min later. The battery started charging after sun acquisition.

The battery was again used 5½ days later, when the pitch turn of the midcourse maneuver caused sharing between the solar panels and the battery. The battery supplied a portion of spacecraft power for 46 min until the sun was reacquired after the motor burn.

The battery charger, which had been left on since launch, again started charging at sun reacquisition. The battery was allowed to recharge until June 27, 1967, or 13 days after launch and 7½ days after the midcourse maneuver. The battery-terminal voltage at this time was 33.45 V, and an estimated 58.8 A-h capacity was available.

Within a few hours after battery-charger turn-off, the battery-terminal voltage dropped to 33.4 V, which is normal for the *Mariner V* silver-zinc battery. The terminal voltage remained stable at the 33.4-V level through the remainder of the cruise, encounter, and tape-playback periods.

The battery was not used again after the midcourse maneuver. However, as part of the effort to determine the condition of the battery, the battery charger was turned on after the second tape playback for an additional 84 h of charging. At turn-on of the battery, the terminal voltage rose to 34.45 V and the charge rate was 10 mA, exactly the same as the voltage and current at charger turn-off after the midcourse maneuver. The additional charging provided as estimated 1.2 A-h, bringing the total battery capacity to about 60.0 A-h. A curve of battery-terminal voltage is shown in Fig. C-15.

No anomalies were observed in the battery telemetry during any of the discharge, charge, or stand periods. The battery apparently was in good condition when the spacecraft was set up for long-term cruise on November 21, 1967.

9. Central computer and sequencer flight performance. The flight performance of the CC&S during Phase I of the mission was completely normal. All CC&S commands were issued at the expected times. Table VI-15 lists the sequenced commands and Table VI-16 lists the cyclic commands. Figure VI-43 provides a graphic summary of case 7 temperature and accumulated CC&S clock error vs time after launch. Figure VI-44 is a daily and weekend clock-error average during Phase I. The limits of

Table VI-15. *Mariner V* CC&S sequenced events

Event	Time, GMT		Event	Time, GMT	
Inhibit release	165:05:58:00		Motor stop	170:23:08:28.0 ±1.6	(17 s)
Clear release	165:05:59:59		Reacquire	170:23:14:10.9 ±0.3	
L-1	165:06:53:56.6 ±6.3		Counter overflow	171:00:43:06.4 ±6.3	
L-2	165:06:57:56.0 ±6.3				
L-3	165:22:38:00.5 ±0.5		MT-6	205:19:19:21.4	
			MT-1	236:08:41:07.6 ±25.2	
Midcourse maneuver			MT-2	253:00:41:26.3 ±25.2	
DC-V27 received	170:21:24:46.0 ±0.4		MT-3	Bad data	
Pitch start	170:22:24:10.9		MT-5	274:16:43:08.6 ±25.2	
Pitch stop	170:22:29:14.8 ±0.4	(304 s)	MT-4	283:14:03:49.2 ±25.2	
Roll start	170:22:46:10.8 ±0.4		MT-7	292:04:44:40.6 ±25.2	
Roll stop	170:22:52:31.1 ±0.2	(380 s)	MT-8	292:11:24:38.4 ±25.2	
Motor start	170:23:08:11.3 ±0.2		MT-9	293:07:24:58.2 ±25.2	

Table VI-16. *Mariner V* CC&S cyclic events

Cyclic No.	Time, GMT	Cyclic No.	Time, GMT	Cyclic No.	Time, GMT	Cyclic No.	Time, GMT
1	166:21:58:01.3 ±6.3	16	208:13:59:31.8 ±25.2	31	250:06:01:11.1 ±25.2	46	291:22:04:48.7 ±25.2
2	169:16:38:07.5 ±0.5	17	211:08:39:55.2 ±25.2	32	253:00:41:26.3 ±25.2	47	Mode 4
3	172:11:18:13.5 ±0.5	18	214:03:19:15.7 ±25.2	33	255:19:21:41.9 ±25.2	48	297:11:25:23.7 ±25.2
4	175:05:58:20.5 ±6.3	19	Bad data	34	258:14:01:57.9 ±25.2	49	No data
5	178:00:38:31.1 ±6.3	20	219:16:39:38.1 ±25.2	35	261:08:42:14 ±25.2	50	303:00:45:06.3 ±25.2
6	180:19:18:28.6 ±6.3	21	222:11:19:49.6 ±25.2	36	264:03:22:31.2 ±25.2	51	No data
7	183:13:58:39.0 ±6.3	22	225:06:00:01.4 ±25.2	37	266:22:02:36.5 ±25.2	52	308:14:05:42.5 ±25.2
8	186:08:38:36.7 ±6.3	23	228:00:40:13.4 ±25.2	38	Bad data	53	311:08:46:01.0 ±25.2
9	189:03:18:47.1 ±6.3	24	No data	39	Bad data	54	No data
10	191:21:58:57.4 ±6.3	25	233:14:00:38.3 ±25.2	40	275:06:02:52.1 ±25.2	55	No data
11	194:16:38:55.2 ±6.3	26	236:08:41:07.6 ±25.2	41	278:00:42:58.2 ±25.2	56	319:16:46:58.7 ±25.2
12	No data	27	239:03:20:52.0 ±25.2	42	Bad data	57	322:11:27:18.6 ±25.2
13	200:05:59:16.0 ±6.3	28	241:22:01:18.2 ±25.2	43	283:14:03:49.2 ±25.2	58	No data
14	203:00:39:13.9 ±6.3	29	244:16:40:41.8 ±25.2	44	286:08:44:08.7 ±25.2	59	No data
15	205:19:19:21.4	30	247:11:20:56.2 ±25.2	45	289:03:24:28.6 ±25.2		

the lines on the graph represent calculation-error limits. The weekends have a 3-day average, and thus have tighter limits. The lines drawn connecting these weekend limits enclose an area that is a good approximation of the CC&S clock error vs day of year. The clock error is steadily decreasing, which is consistent with increasing spacecraft temperature. Figure VI-44 shows, in effect, the slope of the clock error in Fig. VI-43 for any given time.

G. Engineering Mechanics

This subsection includes descriptions of the four engineering-mechanics subsystems and a discussion of their performance from launch to mission termination.

1. Structure subsystem.

a. Description. The structure subsystem consisted of the structural elements that enabled the many items composing a functional spacecraft to withstand the boost and midcourse-maneuver environment, and to maintain geometric relationships and alignments from initial assembly to mission completion. Hardware elements composing the subsystem were as follows:

(1) The octagon structure provided structural support for the seven electronic assemblies and the PIPS, which occupied bay 8; for the AC gas-system pressure vessels, celestial sensors, most scientific instruments, solar panels, antennas, cabling, and thermal shields. The octagon structure also included the spacecraft–*Agena* adapter-attachment provisions.

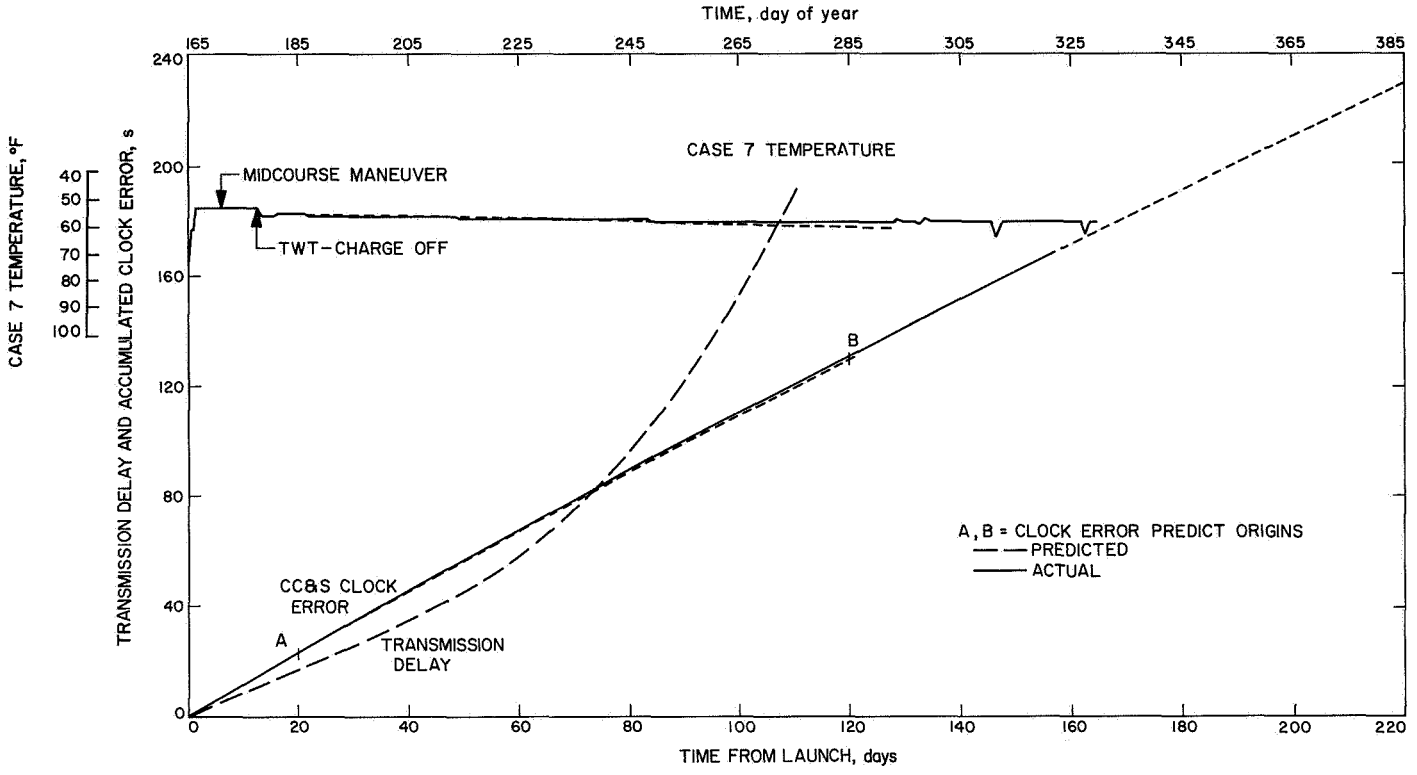


Fig. VI-43. Case 7 temperature and CC&S clock error

(2) The superstructure supported the high-gain antenna and APAC mechanism above the octagonal structure.

(3) The high-gain antenna structure consisted of the elliptical honeycomb parabolic antenna reflector, the antenna feed truss, and the backing structure required to attach the antenna to the superstructure.

(4) The low-gain antenna structure consisted of a tubular RF waveguide and ground plane. The tube structure contained attachment points for the magnetometer sensor, cabling, and low-gain antenna support dampers.

(5) Each of the four solar-panel structures provided approximately 10.6 ft² of area for the solar cells and attachment provisions for solar-panel wiring, AC gas plumbing, 423- and 49.5-MHz DFR antennas and associated cabling, solar-panel tip dampers, panel-latch pin-pullers, and pyrotechnics cables.

(6) The structure-subsystem electronic subchassis and assembly harnesses were mounted in the electronic-assembly chassis in six of the seven electronic bays.

(7) The PIPS support structure mounted the PIPS to the octagon structure. It contained provisions for positioning the PIPS thrust axis through the measured spacecraft CG.

b. Performance. Because all of the structural items were passive after launch, and because it was difficult to obtain dynamic or loading information, no direct telemetry was transmitted concerning the performance of the structure subsystem. The in-flight performance of these items can only be deduced from other spacecraft telemetry. For example, the successful execution of the midcourse maneuver indicates that the PIPS support structure adequately aligned the PIPS thrust axis through the spacecraft CG.

All information received during the flight indicated that the structure-subsystem elements performed as designed.

2. *Mechanical-devices subsystem.*

a. Description. Mechanical devices included items associated with the latching, structural damping, and nonservoed actuations of the various spacecraft elements. The following devices were included in the subsystem.

(1) Eight concentric-tube viscous dampers were mounted at the tips of the solar panels to minimize the dynamic environment and to restrain them until deployment.

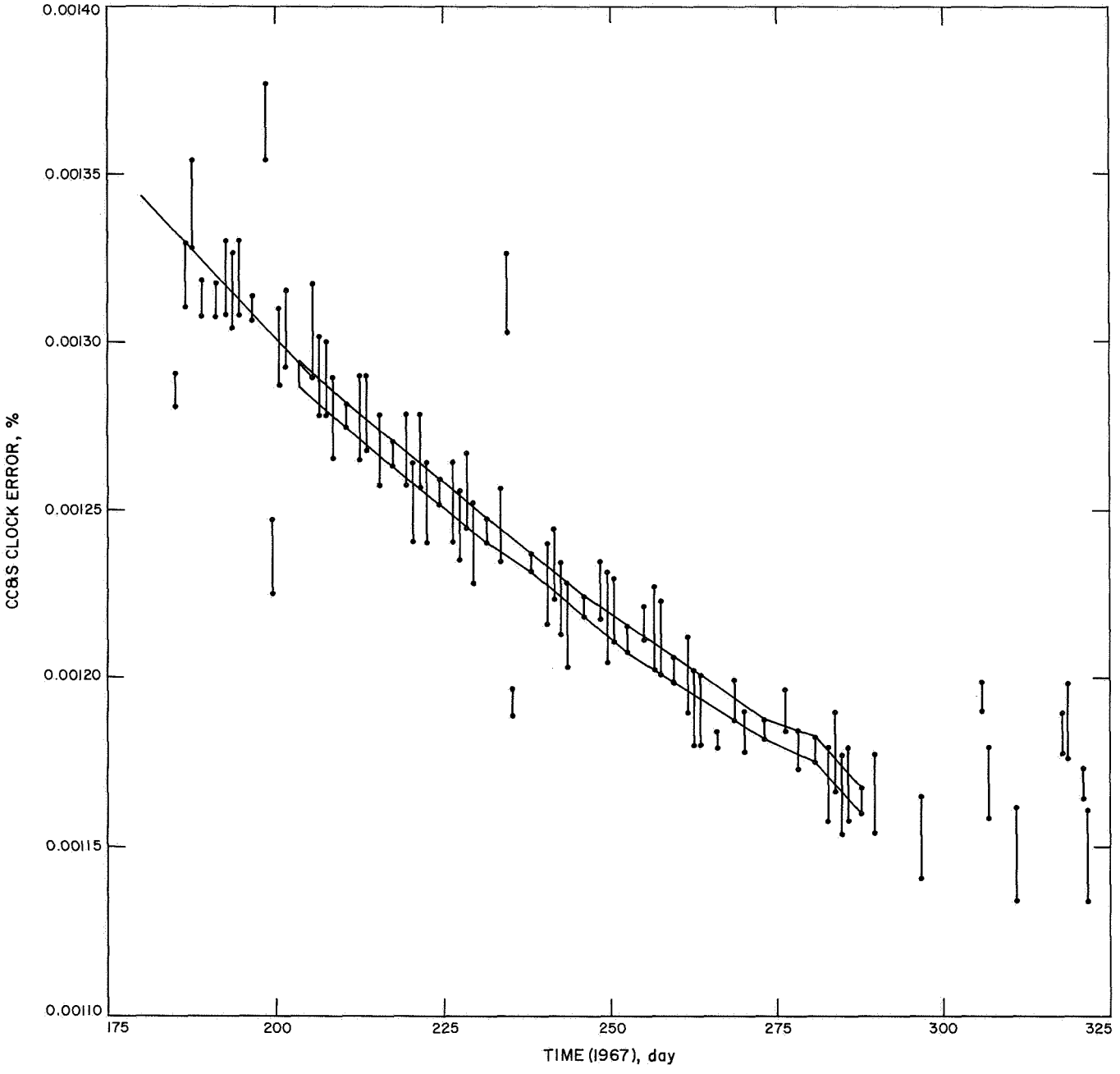


Fig. VI-44. Daily CC&S clock error

(2) Two orthogonally mounted concentric-tube viscous dampers supported and aligned the low-gain antenna and minimized its dynamic environment.

(3) Solar-panel-deployment springs provided the torque to deploy the panels after the pyrotechnic pin-puller latches were released. Switches were provided to telemeter panel deployment at a point approximately 20 deg from the fully open position.

(4) Cruise dampers and latches decelerated the solar panels upon opening, latched the panels in the desired extended position, and minimized the dynamic interactions between the solar panels and autopilot during the firing of the PIPS.

(5) The APAC deployment mechanism consisted of two clock springs, low-friction bearings, and a pyrotechnic latch that, upon release, allowed the high-gain antenna to rotate from one fixed position to another at encounter. A switch was provided near the second antenna position to telemeter antenna deployment.

(6) The PAS was composed of several microswitches that, when actuated at spacecraft separation, armed the pyrotechnic control assembly, turned off the *Agena* isolation amplifier in the data encoder, and turned on the AC subsystem.

(7) The SIT provided time-delayed microswitch closing as a backup to the PAS by redundantly arming the pyrotechnic control assembly 30 ±20 s after separation. It also provided the signal to the pyrotechnic control assembly (160 ±80 s after the arming signal) to fire the squibs in the solar-panel pin-pullers.

b. Performance. As in the case of the structure subsystem, the in-flight performance of many of the elements in the mechanical-devices subsystem can only be deduced from other flight information because of the absence of direct performance measurements. All information recovered during the flight indicated that the solar-panel boost dampers, low-gain antenna support dampers, and cruise dampers and latches performed as designed.

Direct information was received about the performance of the following mechanical devices:

(1) Pyrotechnics arming switch.

(2) Separation-initiated timer.

(3) Solar-panel deployment springs and switches.

(4) APAC deployment mechanism.

Telemetry indicated that the PAS activated nominally upon spacecraft separation at 06:27:17 GMT. This was deduced from science turn-on information.

The SIT squib-firing-current event occurred between 06:30:07 and 06.30:12 GMT, based upon solar-panel event channel telemetry and an assumed maximum panel-deployment time of 7 s. The corresponding SIT actuation time after separation was 172 ±2 s, which, in turn, corresponded to a SIT temperature of 74 ±4°F (Fig. VI-45). This temperature range agrees reasonably well with the nominal value of 80°F. It is concluded, therefore, that SIT performance was nominal.

Telemetry from the solar-panel-deployment switches, through the data-encoder event counters, indicated that each of the four panels was released by the pyrotechnic pin-pullers, and was deployed to within 20 deg of fully open, by the panel-deployment springs. Temperature, attitude-control, and power measurements later confirmed full panel deployment.

The microswitch-closure telemetered information through the science data that the APAC deployment mechanism had successfully deployed the high-gain antenna. There was no indication that the antenna-deployment velocity was not within design limits.

3. Cabling subsystem.

a. Description. The cabling subsystem provided all separable electrical interconnections (and some soldered connections) between subassemblies, assemblies, subsystems, and all peripheral items with electrical interfaces. Cabling was categorized by the following three areas:

(1) System (ring) harnesses.

(2) Assembly harnesses.

(3) Peripheral harnesses.

An upper-ring signal- and power-harness assembly and lower-ring harness assembly interconnected the equipment in the eight bays of the spacecraft.

Assembly harnesses interconnected the subassemblies within each electronic assembly into a functional subsystem, and connected these subsystems to the ring harnesses and operational-support equipment during checkout.

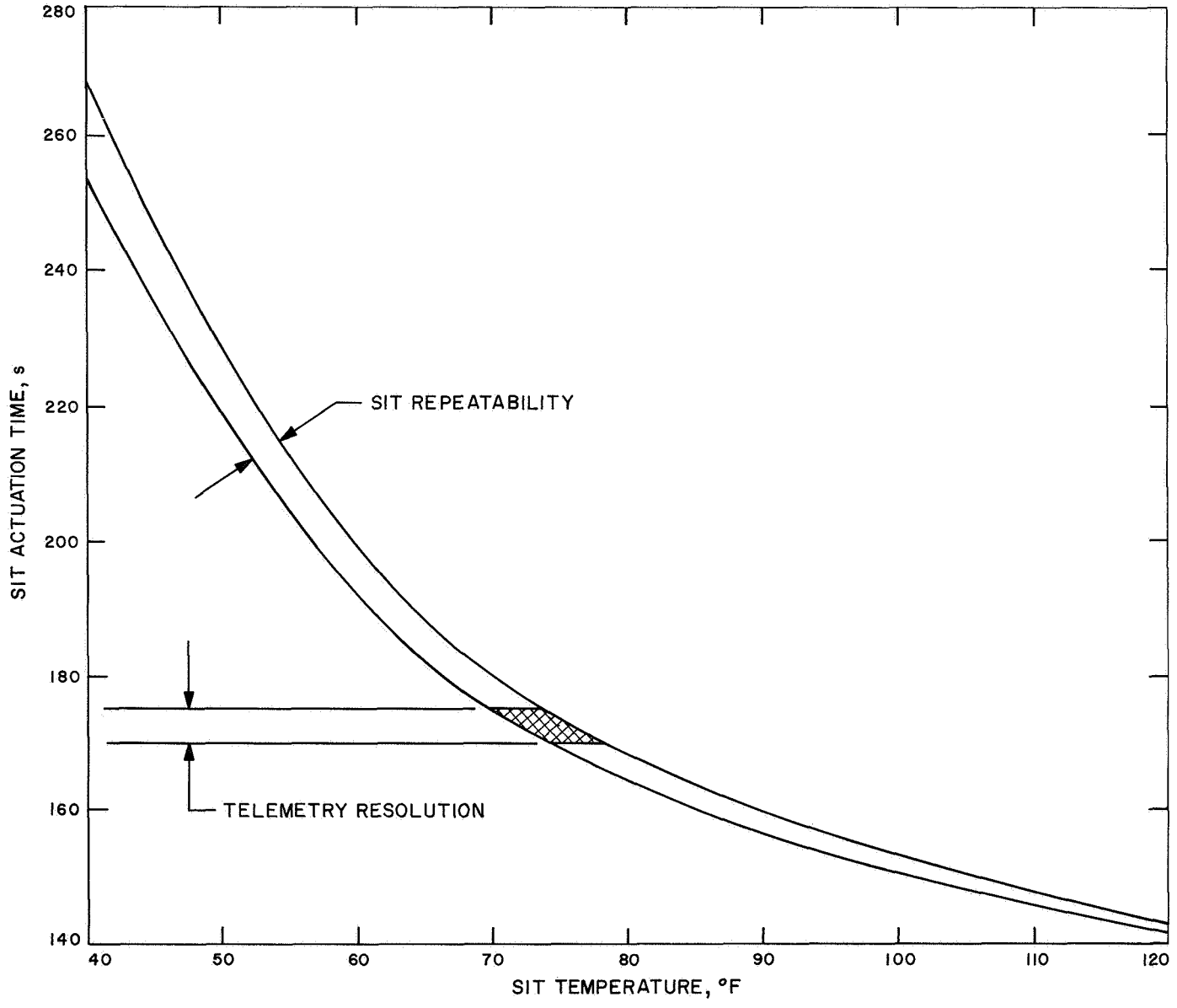


Fig. VI-45. Separation-initiated timer temperature

Peripheral harnesses connected the various spacecraft items located around the extremities of the spacecraft with the appropriate ring or assembly harnesses.

b. Performance. As was the case with the structure subsystem, and much of the mechanical-devices subsystem, the in-flight performance of the cabling-subsystem hardware could only be inferred from the behavior of the other flight subsystems. The successful completion of the mission, with no anomalies that could be traced to cabling, indicates that the cabling-subsystem hardware performed successfully.

4. Temperature-control subsystem. The thermal design of the *Mariner V* spacecraft was similar in concept to that of preceding *Mariner* missions, which include *Mariner II* and *Mariner IV*. The *Mariner II* design was marginal; Venus-encounter temperatures ranged from 120 to 150°F for most electronics. The spacecraft failure 3 wk after encounter was caused, at least in part, by overheating. The *Mariner IV* design was considerably more successful; spacecraft temperatures remained within tolerance for more than 3 yr in space. However, significant changes to this design were required to complete a Venus mission successfully.

The flight spacecraft for the *Mariner* Venus 67 mission was to be the reworked flight spare from the *Mariner* Mars 1964 project. Changes within the bus being relatively minor, little modification to the internal thermal design was required. The important thermal differences between the 1964 and 1967 missions were boundary-condition changes.

Because of antenna-pointing requirements, *Mariner V* was flown "upside-down" relative to the sun as compared with *Mariner IV*. The second significant boundary-condition change was caused by the greatly increased solar intensity to which *Mariner V* was exposed: 126 W/ft² at launch, 248 W/ft² at encounter, and 386 W/ft² at perihelion (Fig. VI-46). The critical thermal problems of the *Mariner V* spacecraft were caused by the need to control the external heat balance so that acceptably cool spacecraft temperatures would result.

The design approach for the temperature-control subsystem used both test and analysis; there was perhaps more emphasis upon space-simulator tests and less emphasis upon analysis than is usual. Early in the program, a fairly coarse (80-node) computer model was generated. Based upon this model and *Mariner* Mars 1964 project experience, a preliminary design was derived. The design was verified, and modified as necessary, during space-simulator testing of a full-scale temperature-control model.

Spacecraft temperature response to various input parameters was also obtained during these tests. The computer model was revised upon the basis of these results for use in the prediction of flight temperatures for situations that could not be simulated: launch, midcourse-maneuver, and encounter transients. Space-simulator testing of the flight spacecraft provided additional cruise-temperature data, which (after correction for known test errors) formed the basis for flight predictions. Minor modifications to the thermal design were made during these tests to provide final adjustments in temperature.

The *Mariner* Venus 67 mission philosophy was, thus, to use test data whenever possible for both design purposes and flight predictions. This was possible because of the nature of the *Mariner* flyby missions, which facilitated duplication of flight conditions in a space simulator. Because of scientific and long-range communications requirements, these spacecraft were three-axes stabilized.

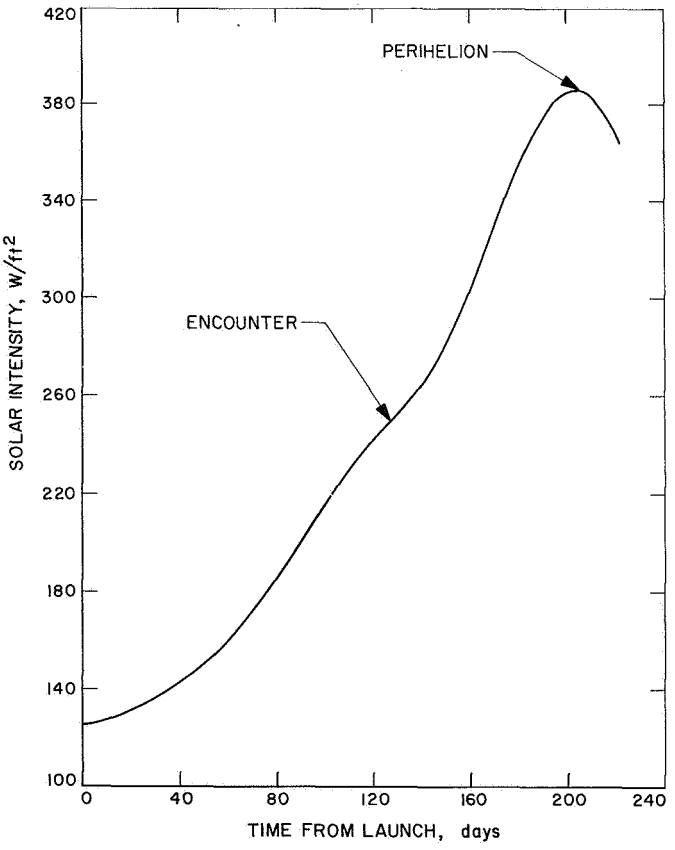


Fig. VI-46. Solar intensity

The interplanetary trajectories take the spacecraft beyond the thermal influence of the earth about an hour after launch, and encounter geometries are such that the spacecraft is only mildly affected by the planetary encounter. Hence, most of the spacecraft flight is spent in a quasi-equilibrium condition, with solar heating the only significant external heat input.

Furthermore, in the *Mariner V* design, every effort was made to minimize the influence of solar heating on most of the spacecraft. Thus, the spacecraft had relatively simple boundary conditions, and was insensitive to solar spectrum and intensity. These factors combined to make the *Mariner* space-simulator tests both straightforward and generally accurate. The "one-shot" nature of the *Mariner* Venus 67 mission demanded the utmost in reliability, and this design approach was considered the most conservative available.

a. Subsystem hardware description. The temperature-control subsystem consisted of mechanical hardware used to maintain the spacecraft-element temperatures within specified bounds. This equipment consisted of the following:

(1) Louvers.

(2) Thermal blankets.

(3) Deployable sun shade.

(4) Fixed shields.

(5) Temperature-control references.

Emittance-control louvers were located on six of the eight bay faces to minimize temperature excursions caused by changes in the heat load within the spacecraft octagonal compartment.

The thermal blankets were multilayer, metallized-plastic radiation shields that were fitted over the top and bottom of the spacecraft to minimize heat rejection or acceptance along the roll axis.

A sun shade, deployed at solar-panel extension, was provided on the sunlit side of the spacecraft. This shade prevented direct solar irradiation of the booster-interface components mounted on the sunlit side of the spacecraft and items (such as louvers) that extended outboard of the bay faces.

The fixed shields were thin-gage, polished-aluminum structures that were mounted on various areas of the bay faces to limit the fixed heat-rejection area of the octagonal compartment. Separate shades and shields provided local thermal protection for critical items mounted outside the bus compartment.

The TCRs were painted-fiberglass, paddle-like structures mounted at the tips of three solar panels. The measured TCR temperatures helped to correlate flight and space-simulator data, and also improved understanding of the optical properties of typical surface-paint coatings used for temperature control.

b. Temperature-control results—cruise. Table VI-17 describes the flight-temperature instrumentation and lists telemetry channels by which temperature data were transmitted. Significant flight data and preflight predictions are listed in Table VI-18. Cruise temperatures as a function of flight time are shown in Appendix C (Figs. C-36–C-72). Nominal temperatures (postlaunch predictions) are also shown for comparison. A discussion of the results obtained from individual telemetry channels is provided below.

Bus measurements. An estimate of the error sources in the JPL 10-ft space-simulator test setup indicated that test temperatures were about 2°F high for earth modes and 3°F high for Venus modes. Therefore, the test data for the flight spacecraft were corrected by these amounts, yielding the flight predictions shown in Table VI-18.

In the worst case, the uncertainty in these predictions was ±10°F, but the probable error was believed to be within ±5°F. Actually, the average bus temperature was 1–2°F above prediction for most of the flight. The maximum deviation for any measurement was 4°F. As the flight data were about midway between prediction and simulator data, it might appear that the simulator data were overcorrected. However, from data received after encounter, this is not believed to be the case.

The prelaunch predictions described above were revised after launch upon the basis of near-earth data to obtain the best possible predictions for the remainder of the flight.

A comparison of flight data with these predictions shows that typical bus temperatures were slightly higher than these nominal levels until after encounter, when the actual temperatures tended to be somewhat lower than nominal. The distortion in the curve shape is probably caused by an inaccurate representation of louver behavior. Possibly the assumed emittance–temperature

Table VI-17. Locations of temperature transducers

Channel	Location	Channel	Location
401	Bay 1 electronics chassis (power and pyrotechnics control)	428	Battery (bay 8)
421	Bay 2 shear web (postinjection propulsion system)	419	High-gain antenna reflector
217	PIPS propellant tank (bay 2)	431	Low-gain antenna mast at magnetometer
408	PIPS N_2 gas bottle	439	Magnetometer sensor
402	Bay 3 electronics chassis (science and data automation system)	434	Upper thermal shield, exterior
437	UV-photometer sensor	430	Primary sun sensor (bay 2)
423	Bay 4 electronics chassis (data encoder and command)	435	Lower thermal shield, exterior
438	Trapped radiation detector	422	Plasma probe
404	Bay 5 electronics chassis (receiver and tape recorder)	406	+X roll/yaw jet assembly (4A1 solar panel)
424	Voltage-controlled oscillator (bay 5)	425	−Y pitch jet assembly (4A7 solar panel)
436	Tape recorder (bay 5)	433	−X roll/yaw jet assembly (4A5 solar panel)
405	Bay 6 electronics chassis (transmitter)	403	$I_{sc} - V_{oc}$ transducer (4A5 solar panel)
414	Auxiliary oscillator 1 (bay 6)	427	Spar near zener diode (4A5 solar panel)
418	Auxiliary oscillator 2 (bay 6)	409	4A1 solar panel (+X axis)
426	Bay 7 electronics chassis (attitude control and central computer and sequencer)	429	4A5 solar panel (−X axis)
218	+X/−Y attitude-control N_2 gas bottle	412	Temperature-control reference (S-13 white), 4A1 solar panel
219	−X/+Y attitude-control N_2 gas bottle	432	Temperature-control reference (S-13M white), 4A5 solar panel
407	Power regulator (bay 8 hot spot)	413	Temperature-control reference (Cat-A-Lac black), 4A7 solar panel
410	*Canopus* sensor		

function was wrong, or else bearing friction slightly retarded the opening of the blades as the temperature rose.

In any case, by the time telemetry was lost in late November 1967, the bus temperatures were almost exactly at the levels expected before launch, which tends to verify the assessment of space-simulator conditions. In view of the size of the test errors, the agreement of flight data with preflight estimates is remarkable.

Thermal effects of ranging had not been evaluated before launch. During the flight, it was found that a temperature rise of about 1°F could be expected in bays 4 through 8 when the ranging receiver was turned on.

UV photometer. The temperature–time history of this instrument throughout the flight was as expected, except for a 2–3°F temperature increase after MT-6 (33⅓–8⅓ bits/s). This increase resulted from a power change of about 0.5 W; the change was normal, but its effect had been overlooked in preflight testing.

Upper thermal shield—shaded side of spacecraft. This measurement was primarily intended to compare the flight environment to space-simulator conditions, and also to allow some evaluation of shield performance. Using flight data, the heat loss from the bus was computed to be nearly constant at 0.78 W/ft², and the effective emittance of the shield was 0.02. These values must be regarded as upper limits, as part of the heat loss at the transducer was caused by heat conduction down the leads.

A significant result of these calculations is the derivation of space-simulator heat inputs to the upper shield. The external heat input (radiation from shield minus input from bus) was calculated to be 1.3 W/ft² at earth intensity, which is about double the amount expected from previous evaluations of stray radiation. The increase was undoubtedly caused by the presence of the spacecraft and associated hardware in the simulator.

High-gain antenna. The temperature prediction for the high-gain antenna, based upon analysis, proved to be about 25°F low. Considering the low temperatures involved, such a discrepancy is not surprising. During the flight, the temperature varied in sun-dependent fashion because the heat input was primarily by radiation from the solar panels. The position change (APAC) at encounter reduced the radiative coupling between the high-gain antenna and the upper thermal shields, and increased the coupling between the high-gain antenna and the solar panels. These changes lowered the upper thermal shield temperature 12°F, and raised

Table VI-18. Telemetered flight temperatures

Telemetry channel	Location	Pre-Canopus acquisition,[a] °F		Earth cruise,[b] °F		Venus cruise,[c] °F	
		Predicted	Actual	Predicted	Actual	Predicted	Actual
401	Bay 1	72	74	68	68	65	67
421	Bay 2	50	53	45	47	55	57
402	Bay 3	62	64	57	59	67	69
422	Plasma probe	105	105	105	105	196	214
403	I_{sc}–V_{oc} transducer	127	104	127	104	239	226
423	Bay 4	59	63	54	56	68	70
404	Bay 5	58	60	52	53	66	68
424	Voltage-controlled oscillator	64	66	59	59	74	76
405	Bay 6	62	63	57	57	72	75
425	−Y pitch jet assembly	−30	−15	−30	−12	52	53
406	+X roll and yaw jet assembly	−30	−25	−30	−25	52	44
426	Bay 7	63	63	54	54	60	60
407	Bay 8	91	95	86	85	83	83
427	Solar panel 5 spar	43	85	43	93	140	132
408	Postinjection propulsion system N_2 tank	57	60	51	52	60	62
428	Battery	71	71	64	62	65	65
409	Solar panel 4A1	127	119	127	119	239	240
429	Solar panel 4A5	127	116	127	118	239	239
410	Canopus sensor	64	65	59	57	61	61
430	Primary sun sensor	52	54	47	49	78	101
431	Low-gain antenna mast	−105	−90	−105	−90	−95	−83
412	Temperature-control reference S-13	Off scale	Off scale	−25	−29	Off scale	Off scale
432	Temperature-control reference S-13M	−55	−52	−55	−48	Off scale	Off scale
413	Temperature-control reference black	149	140	149	138	Off scale	Off scale
433	−X roll and yaw jet assembly	−30	−25	−30	−24	52	46
414	Auxiliary oscillator 1	68	70	62	62	73	74
434	Upper thermal shield	−192	−194	−192	−197	−142	−170
435	Lower thermal shield	45	35	45	37	132	167
436	Tape recorder	58	61	52	54	66	68
437	UV photometer	52	54	47	46	59	60
418	Auxiliary oscillator 2	68	67	62	62	75	75
438	Trapped radiation detector	48	52	43	45	56	58
419	High-gain antenna	−220	−195	−220	−197	−175	−151
439	Magnetometer	−16	7	−16	7	−25	5
217	Propellant tank	61	65	55	56	64	66
218	+X/−Y N_2 tank	65	68	58	59	65	66
219	−X/+Y N_2 tank	61	64	56	57	67	69

[a]Cavity amplifier on; battery charger on; gyros on.
[b]Cavity amplifier on; battery charger on; gyros off.
[c]Traveling-wave tube on; battery charger off; gyros off.

the high-gain antenna temperature 21°F. These seemingly dramatic changes were actually caused by very small changes in energy inputs, as explained below.

Low-gain antenna mast. Low-temperature spacecraft components are very sensitive to extraneous heat inputs in space-simulator tests because small changes in heat input cause large temperature changes. A change in heat flux that produces a 10°F ΔT at 70°F will produce a 32°F ΔT at −100°F. For this reason (and others), the heavily corrected space-simulator data that yield temperature predictions for these items have sizable uncertainties, perhaps ±30°F. The agreement between predicted and flight data for the low-gain antenna mast is, therefore, fairly good.

The mast (waveguide) temperature proved to be sensitive to RF losses. The temperature increased 11°F when the TWT amplifier replaced the cavity amplifier, and the temperature dropped 19°F when the switch to the high-gain antenna occurred. About 4°F of the first temperature change was caused by the temperature change in bay 6. The remaining ΔT was the result of power-loss changes in the waveguide.

Magnetometer. The thermal behavior of the helium-magnetometer sensor during the flight was anomalous. The actual flight temperatures of the sensor were 7°F at earth and 5°F at Venus (23 and 30°F higher than predicted).

Because the predictions were based upon data from flight-spacecraft space-simulator tests, it is likely that the discrepancy was caused by an inaccurate assessment of the differences between the chamber and space. Two corrections were applied to space-simulator magnetometer temperatures: (1) a negative correction of 10°F to account for the effective chamber sink temperature, and (2) a positive correction of 0°F at earth and 5°F at Venus to account for the fact that the spacecraft was tested with shortened ("stubby") solar panels because of chamber size limitations.

Even if the sink-temperature correction were reduced to zero, a worst-case analysis of the solar-panel effect would not explain the discrepancy between flight and predicted temperatures.

Except for the initial temperature offset at earth, the thermal behavior of the sensor during the remainder of the mission was normal. Early in the flight, it was thought that the sensor was too responsive to changes in the mast temperature, which would indicate a significant change in the conductive coupling between the mast and the sensor. However, a review of test data revealed that the flight behavior was normal, but this had not been apparent during tests because of nonsteady-state conditions.

Although the temperature control of the magnetometer was anomalous, the performance of the instrument was in no way affected because it was designed to operate over a range of −30 to +150°F.

Lower thermal shield—sunlit side of spacecraft. In the absence of any change in radiative properties, this temperature should have been very nearly proportional to the fourth root of the solar intensity. A small correction is necessary to account for the fact that the transducer temperature really was somewhere between the temperature of the first and second layers of the shield rather than exactly at the temperature of the first (Teflon) layer.

This effect caused a maximum decrease of 4 or 5°F in the measured earth-to-Venus temperature rise, as compared to that computed for an idealized adiabatic flat plate; it was neglected in the postlaunch prediction. The temperature rise in flight exceeded both simulator results and postlaunch predictions (see Table VI-18 and Fig. VI-47); this was caused by darkening of the Teflon outer-shield layer. Neglecting the relatively small correction discussed above, the increase in absorptance α during the flight was as shown in Fig. VI-48. The initial absorptance α_0 was 0.13.

The 10°F difference in temperature between flight and the simulator test for near-earth solar intensity was probably caused by an infrared heat input in the simulator rather than by any overall intensity discrepancy.

Plasma probe. Near earth, the flight temperature was the same as the corresponding simulator temperature. At encounter, the plasma-probe temperature had risen 18°F above prediction. This temperature rise was no doubt the result of: (1) increased infrared radiant heating on the white sides of the instrument caused by the degradation of the lower shield, and (2) increased reflected solar heating caused by a darkening of the white paint on the sides of the plasma probe.

Primary sun sensor. When temperature stabilization was reached after launch, the primary sun-sensor temperature was very close to prediction (about 2°F warm).

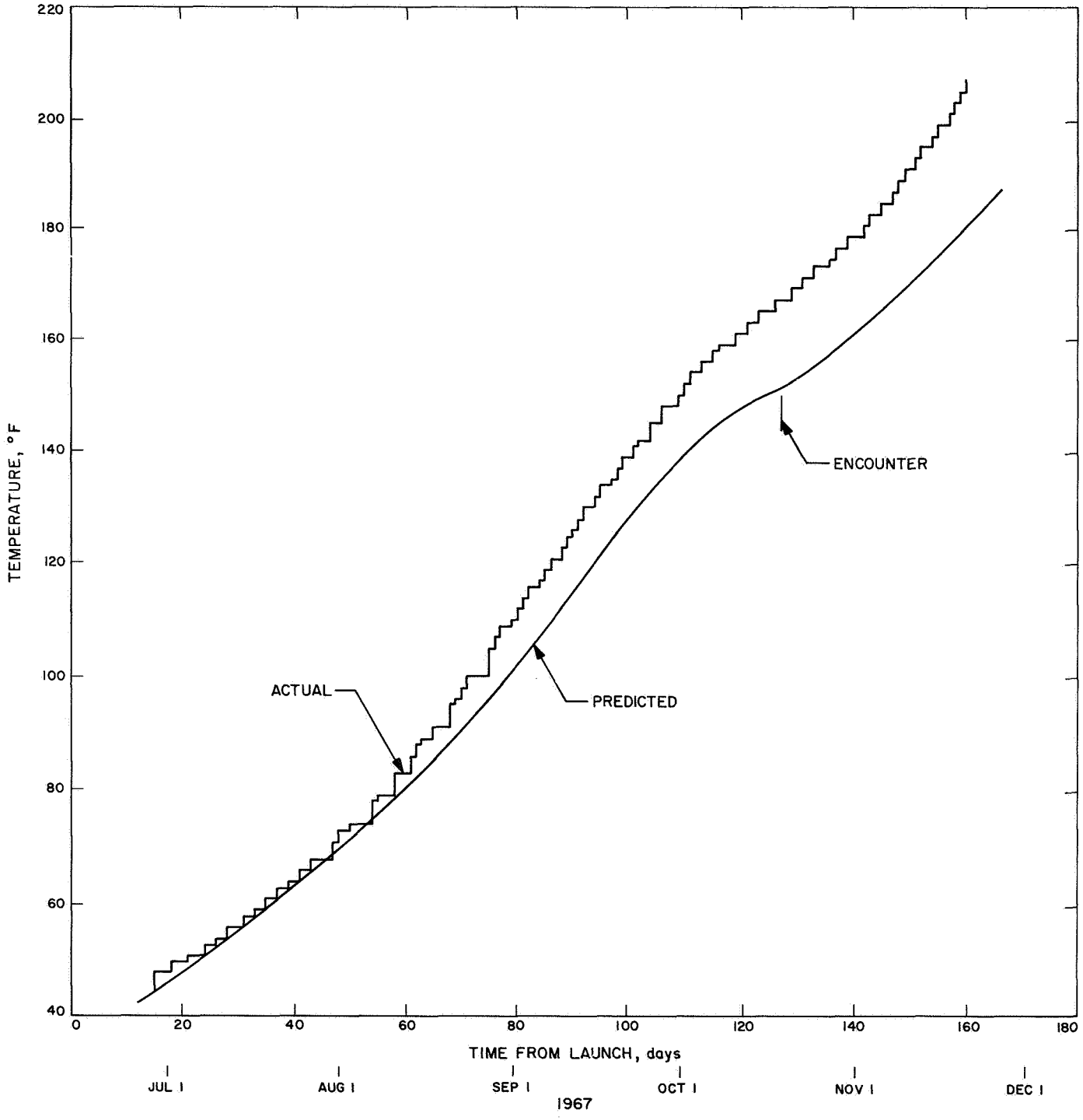


Fig. VI-47. Battery-charger temperature

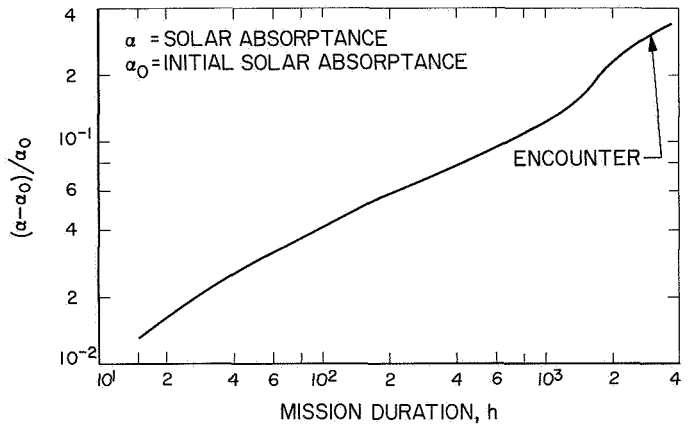


Fig. VI-48. Increase in solar absorptance

As the flight progressed, the temperature increased more rapidly than expected. At encounter, the deviation from prediction reached 23°F; after encounter, the sensor temperature continued to rise abnormally.

Data had been obtained during thermal control model testing to evaluate the effect of increasing the heat input to the primary sun-sensor assemblies. From these data, it was deduced that an incremental heat input of 3.2 W at Venus would produce the 23°F discrepancy observed. About 0.7 W of this total was caused by the darkening of the lower thermal shield, which increased the infrared input to the sides of the assembly and pedestal. The darkening of the white paint on the sides of the pedestal no doubt also contributed to an increased reflective solar input. The remaining input, something less than 2.5 W, probably resulted from one or more of the following effects:

(1) Increase in diffuse component of shield and shade reflectance.

(2) Shift in shade position.

(3) Decrease in conduction coupling to bus.

Other possible causes, considered less likely, are flaking paint, transducer detachment, or space-simulator test inaccuracies. By the process of elimination, it seems most probable that optical changes in the Teflon and/or some shifting of the shade position increased the heat input to the sides of the pedestal and sensor assembly.

Attitude-control gas-jet assemblies (Figs. C-58–C-60). The temperature predictions for these assemblies were made on the basis of type-approval test results in the JPL 10-ft space simulator. Agreement with flight data was reasonably good.

Solar panels (Figs. C-46–C-50). Flight predictions were made upon the basis of *Mariner IV* flight data, corrected for the electrical energy withdrawn from the panels and dissipated by the spacecraft. No account was taken of the energy dissipated in the zener diodes. Near earth, where the diodes dissipated about 230 W, the effect was to lower the panel temperatures 8–10°F and raise the spar temperature 40°F. At Venus, when panel voltage dropped to the point where the zener diodes were no longer firing, the panels and the spar were very near nominal temperatures. The temperature of the solar-cell output transducer (I_{sc}–V_{oc}) was monitored to assist in interpreting the data from this cell. Its temperature was cooler than the panel average because of its location in an area of relatively low solar absorptance near the panel edge.

c. Temperature-control results—launch, midcourse-maneuver, and encounter transients. Very little temperature change was observed in the bus during ascent and parking orbit. Temperatures at sun acquisition were on the cool side of nominal (1 or 2°F), but within expected tolerances. Cooling of external items occurred during boost because of gas expansion under the shroud; then further cooling occurred while the spacecraft was in the shadow of the earth. Limited data were received during this period; therefore, detailed analysis of the transient is not possible. All data obtained were normal.

The midcourse maneuver (pitch, 55 deg; roll, 71 deg; burn, 15 s) resulted in a moderately severe temperature transient. The effects were most pronounced in bay 2 and adjacent bays. The temperature-vs-time history for locations most influenced by solar heating and subsequent motor-heat soakback is shown in Figs. VI-49–VI-53. These data agreed reasonably well with analytical predictions.

Temperature data were not obtained at encounter during the period of maximum planetary heating of the spacecraft. The temperature decay observed beginning 1 h after closest approach was consistent with predictions. The average increase in the bus was approximately 1°F; temperature increases ranging up to 34°F (high gain) were observed on external items. Bus cruise temperatures decreased slightly (1 or 2°F) after encounter. This decrease can be attributed in part to ranging turn-off on October 19, and partially to minor louver hysteresis effects associated with encounter and postencounter heating transients and with APAC jarring.

d. Conclusions and recommendations. The performance of all hardware within the temperature-control subsystem was successful. With minor exceptions, the

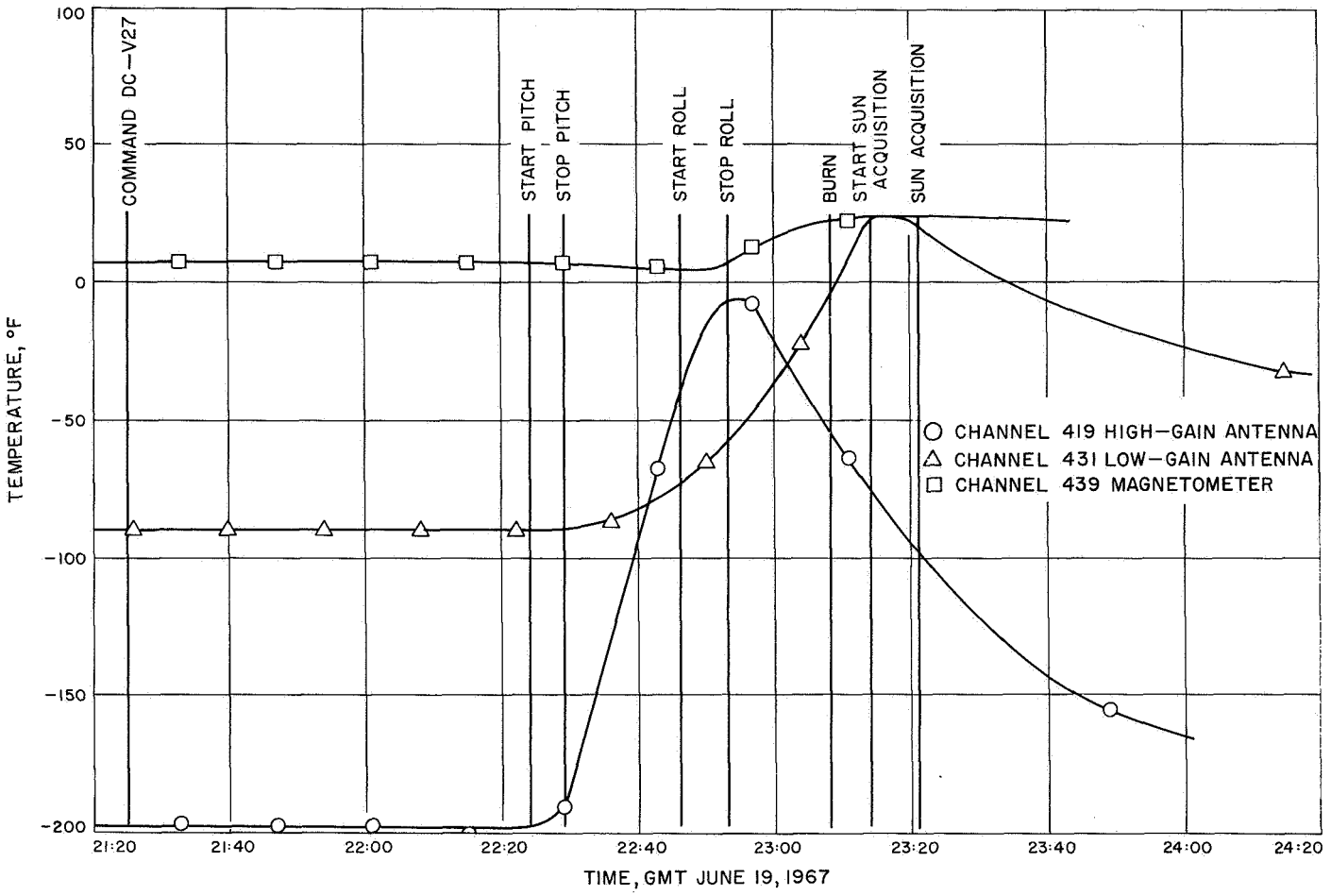


Fig. VI-49. Temperature vs time, midcourse maneuver (high- and low-gain antennas and magnetometer)

louvers, shields, and sun shade faithfully reproduced prelaunch test behavior in flight. The darkening of the lower thermal shield and possibly a minor shift in position of the sun shade caused some temperature increases in sunlit items, but the vital function of heat protection for the bus was unimpaired. Louver performance was nominal; the observed effect of bearing friction (about 1°F) is mainly of interest in defining the ultimate limit of temperature predictability.

The *Mariner V* spacecraft thermal design proved to be effective in flight. The techniques used to isolate the spacecraft from solar heating were sufficient both for the primary mission to Venus and for the secondary mission through perihelion, where the solar intensity was three times that at earth. The average bus-temperature increase in transit from earth to Venus was an order of magnitude smaller than that for *Mariner II* (1962). All temperatures remained within operating limits during the primary mission (launch to E+10 days). With the exception of those for the primary sun sensors and the plasma probe, all temperatures were expected to remain within operating limits through perihelion.

The techniques developed for solar isolation should prove to be useful on future Venus and Mercury missions. However, uncertainty as to materials degradation in flight and the inherent difficulties of space simulation continue to be factors that must be taken into account in thermal design.

The basic approach to spacecraft temperature control employed for this project proved to be valid. This approach, which is typical of *Mariner* missions, contained the following elements:

(1) Exhaustive space-simulator testing of a temperature-control model and all flight spacecraft.

(2) Design for insensitivity to solar intensity and space-simulator limitations.

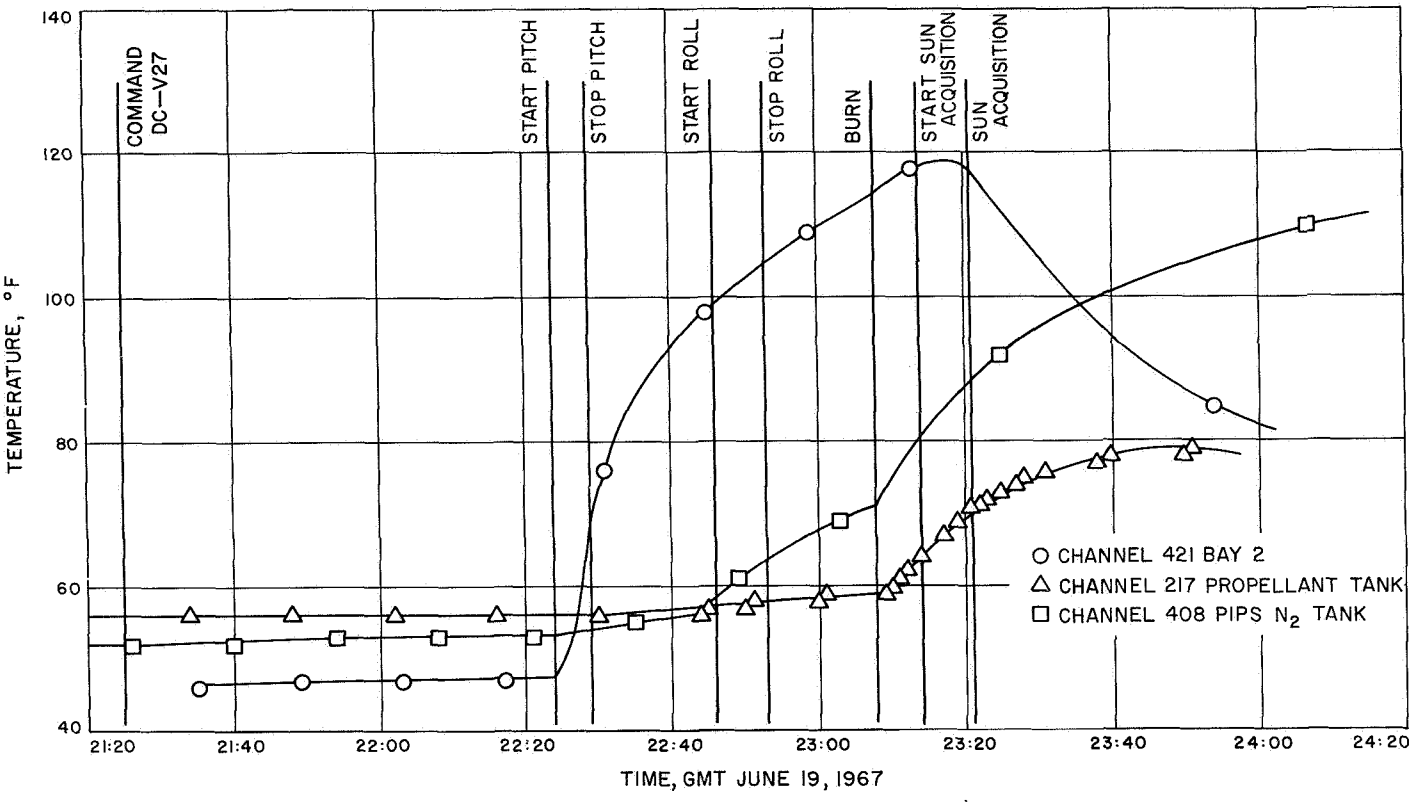


Fig. VI-50. Temperature vs time, midcourse maneuver (bay 2, propellant tank, and PIPS N_2 tank)

(3) Early design inputs to spacecraft configuration.

(4) Employment of a project-oriented temperature-control group.

e. Temperature-control reference results. The purpose of the *Mariner V* TCR was to measure in space the net solar thermal energy absorbed by typical spacecraft temperature-control surfaces for correlation with solar thermal-simulation and laboratory measurements of thermal radiative properties. In addition, changes of absorbed energy in space in temperature-control coatings could be determined for correlation with laboratory materials testing.

The coatings slected for use on the TCR assemblies were as follows:

(1) Cat-A-Lac flat black epoxy,* a widely used spacecraft black coating that was one of the test surfaces for the *Mariner IV* absorptivity standard. Its reflectance does not vary with wavelength, so it is insensitive to spectral discrepancies between the sun and a solar simulator.

(2) S-13 white, a widely used spacecraft white coating that was known to degrade, but not as extensively as the TCR results have indicated. This white was used on the TCR because it is of general engineering interest and because it was used elsewhere aboard *Mariner V*.

(3) S-13M (modified) white, an experimental white coating that was undergoing development at the time of the *Mariner V* launch. Laboratory results indicated that it is substantially more stable than S-13, and of interest primarily for use on future spacecraft.

Each TCR measured the resistance of a calibrated platinum element, and thus measured the temperature of a flat plate normal to the sun and radiating from both sides. From this temperature, after making suitable corrections for conduction losses, the product $S\alpha_s/\epsilon$ was computed, where S is solar intensity, α is absorptance, ϵ is emittance. The net quantity $S\alpha/\epsilon$ is of interest for spacecraft temperature control, particularly in the case of the black, which is of significant interest for simulation testing of future spacecraft.

*Finch Paint and Chemical Co., Torrance, Calif.

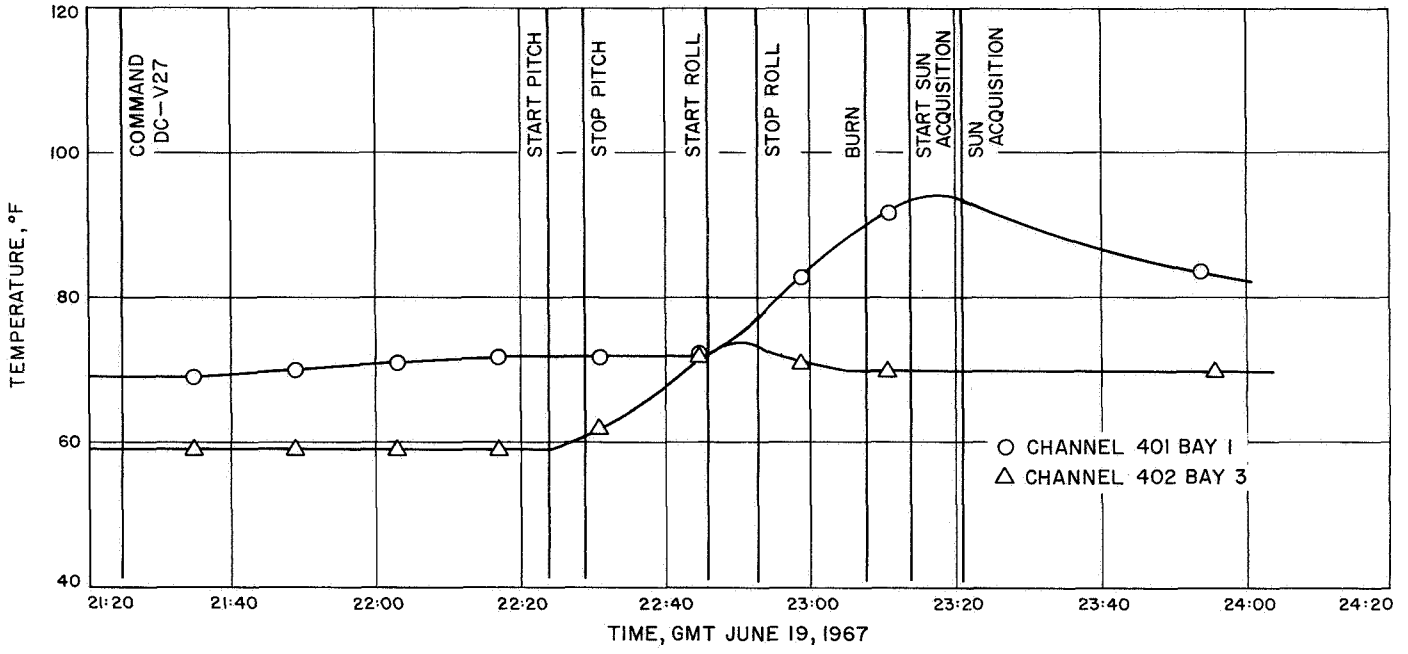


Fig. VI-51. Temperature vs time, midcourse maneuver (bays 1 and 3)

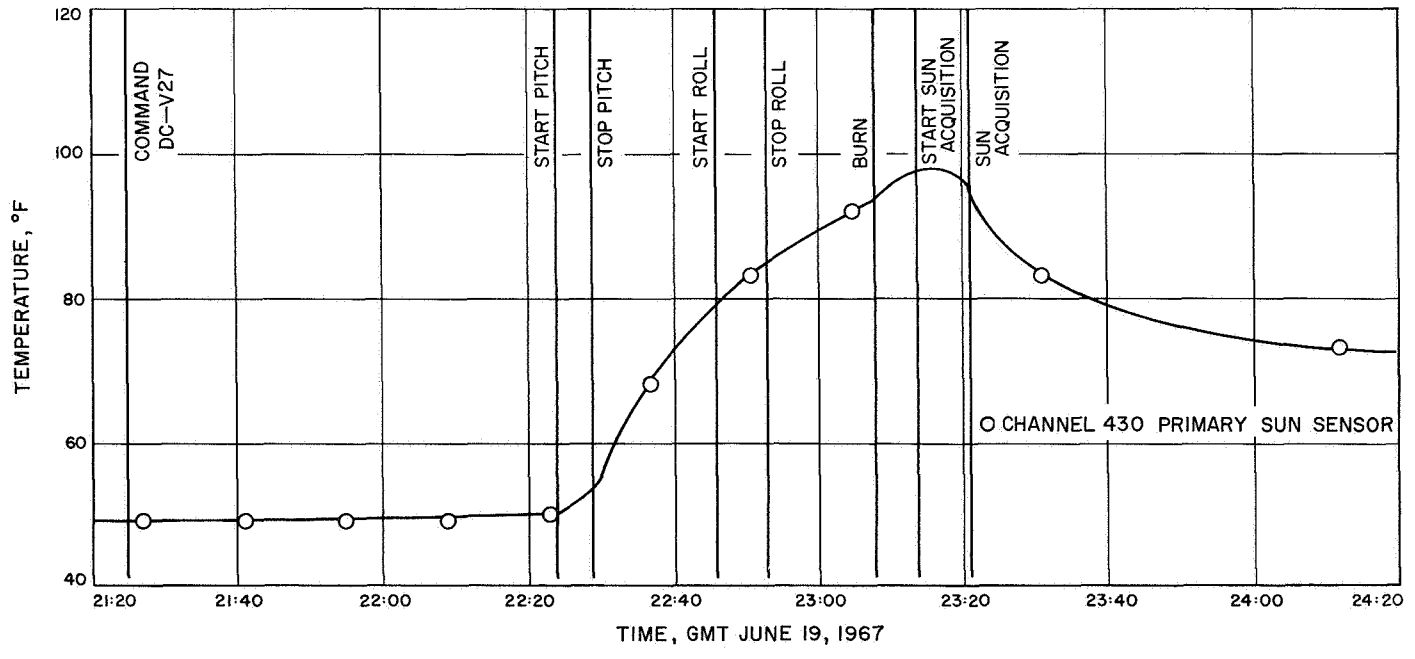


Fig. VI-52. Temperature vs time, midcourse maneuver (primary sun sensor)

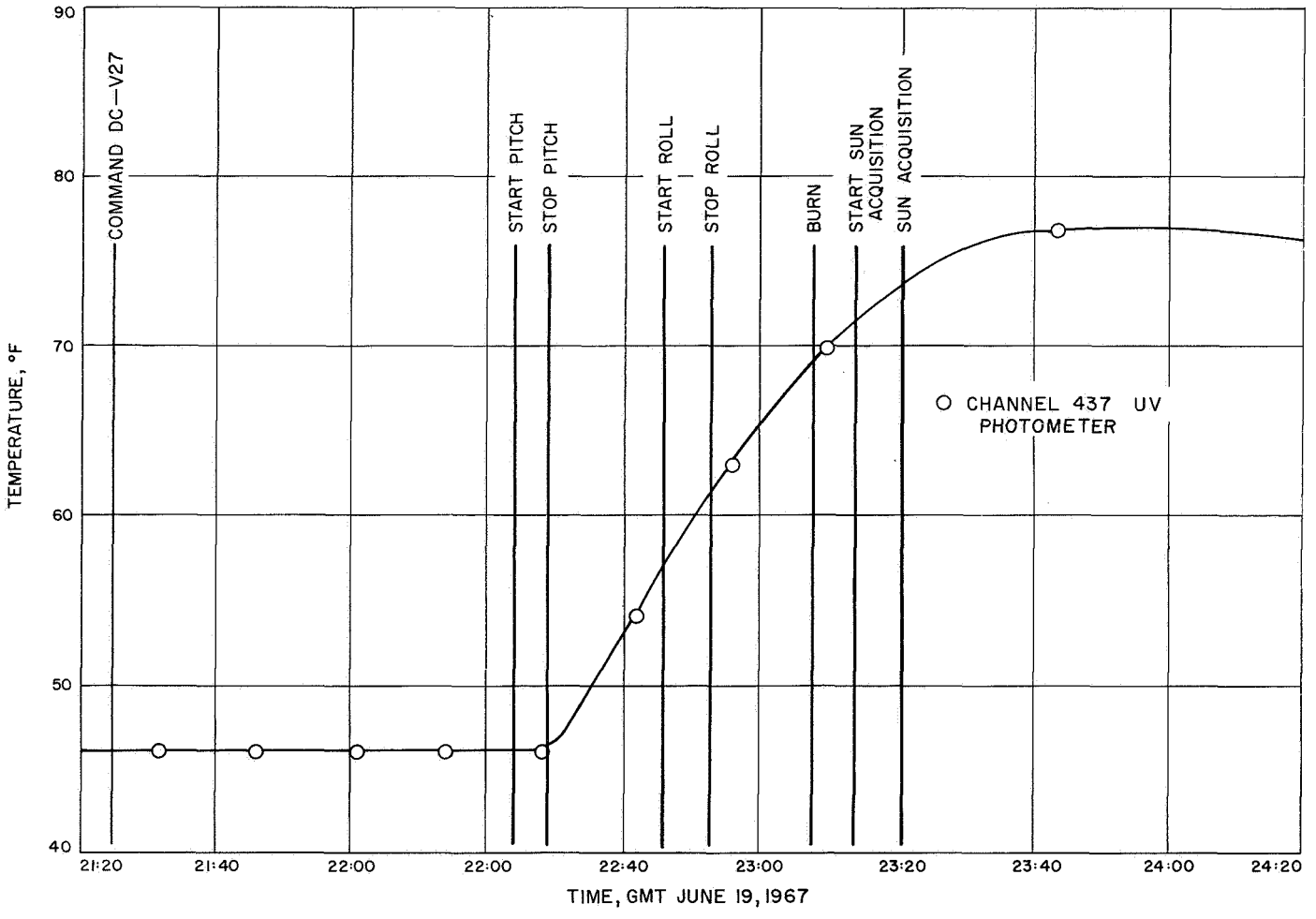


Fig. VI-53. Temperature vs time, midcourse maneuver (UV photometer)

Postlaunch performance. Results from the TCR during the early portion of the *Mariner* Venus 67 mission verified equipment design, implementation, and sensitivity. The first data were obtained approximately 0.5 h after sun acquisition. All values were within predicted tolerances (including channel 412, S-13 coated, which was off scale below −30°F). A subsequent decrease in DN value of the black TCR (413) and the S-13M white TCR (432) over the following 3 h indicated a decreasing thermal input from the earth early in the mission. The resultant lower equilibrium temperatures, apparently beyond earth influence, were still within predicted tolerances.

Cruise performance. The in-flight temperature measurements of the black, S-13 white, and S-13M white TCRs are given in Figs. VI-54 and VI-55. Prelaunch temperature predictions are included for the black coating. At the time of sensor design, good data were not expected early in the mission; therefore, the temperature range for the S-13 coating was biased upward to come on scale at a solar absorptance of approximately 0.25 to allow for the anticipated initial rapid degradation. The S-13 coating was expected to degrade and be on scale within 10–15 h after launch. This did not occur until L+30 h, indicating either a lower initial solar absorptance or a slower initial degradation rate. On the basis of earth input computed from early temperatures for the black and the modified white coatings, the absorptance for the first data can be shown to be equal to or less than 0.23.

Early mission data for the S-13M coating clearly show that degradation started at a consistent rate early in the mission. By interpolation of flight results, degradation rates can be resolved with greater precision than is possible in the laboratory.

Results of degradation of both white coatings are shown in Fig. VI-56. The end of the curve indicates that no further data were obtained because the temperature had reached the upper limit of the sensor range. These curves show apparent solar absorptance vs mission duration, assuming a constant emittance of 0.86 and a solar intensity of 0.878 W/in.^{2} at 1 AU. (This value was indicated by early results from the black TCR.)

The observed bleaching (more than 4%) of the Cat-A-Lac black sample was totally unexpected, and is significantly larger than anything observed in the laboratory. Simulation testing indicated a change of about 1% in solar absorptance for equivalent exposure.

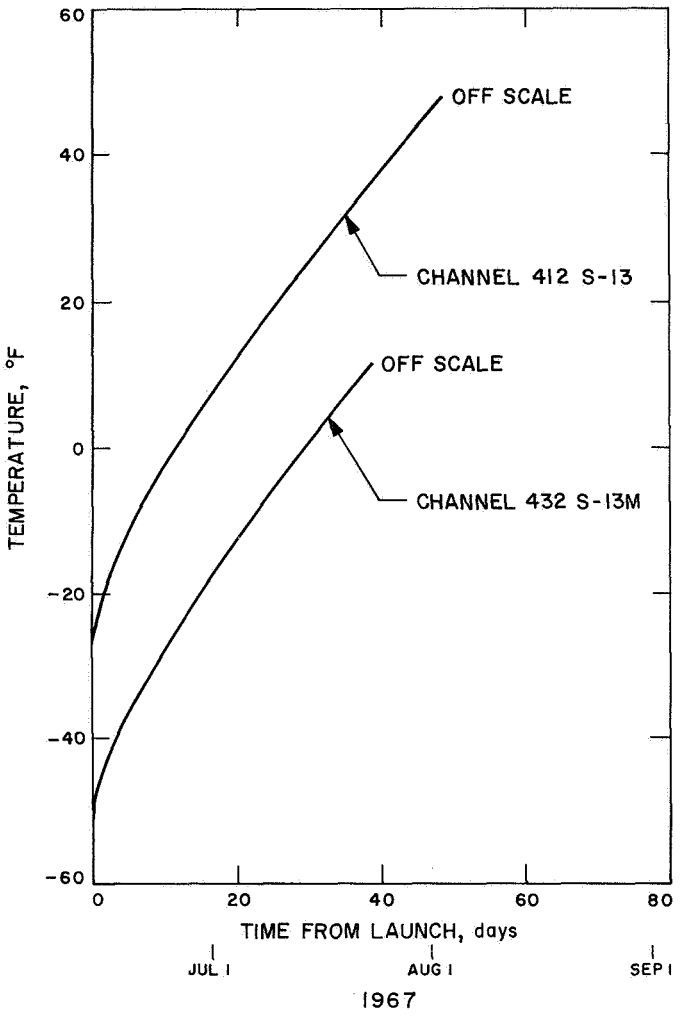


Fig. VI-54. In-flight temperatures of S-13 and S-13M white coatings

Change in apparent absorptance/emittance α/ϵ during the mission is shown in Fig. VI-57.

Conclusions and observations. Results from the black TCR during the early portion of the *Mariner* Venus 67 mission appeared to confirm the recently published value for solar intensity of 1.95 cal/cm^2 min. Definitive verification of this value was impossible, however, in view of the observed degradation and uncertainties in surface properties, conduction effects, and data-encoder and spacecraft telemetry. Nonetheless, a comparison of flight results to those obtained from the cone radiometer will make it possible to adjust the JPL 10-ft simulator to a one-sun level for future testing independent of the absolute value of solar intensity.

Initial values from the black TCR (413) and the S-13M white TCR (432) showed reasonable agreement with

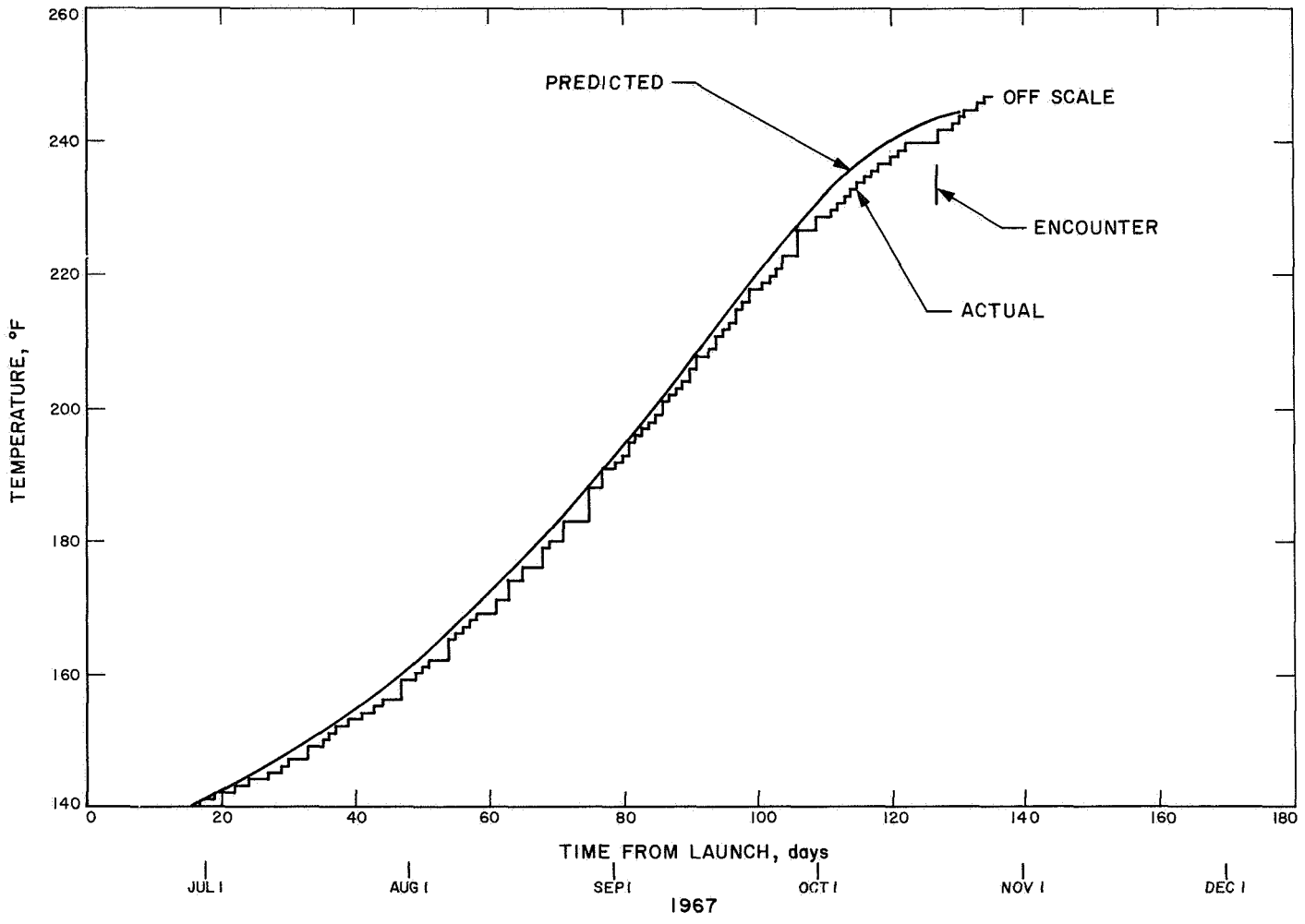


Fig. VI-55. Predicted and actual temperatures of black coating

measured surface properties. The black TCR was somewhat colder (about 3°F) following launch, after apparent earth input had decreased to insignificance, indicating a lower α/ϵ than that measured in the laboratory. However, assuming the cone radiometer to be accurate, comparison of flight data to results in the space simulator indicated that this discrepancy was caused by solar intensity rather than by surface properties. This tends to confirm the recently published values of the solar intensity as well as the measured surface properties. The S-13M white TCR

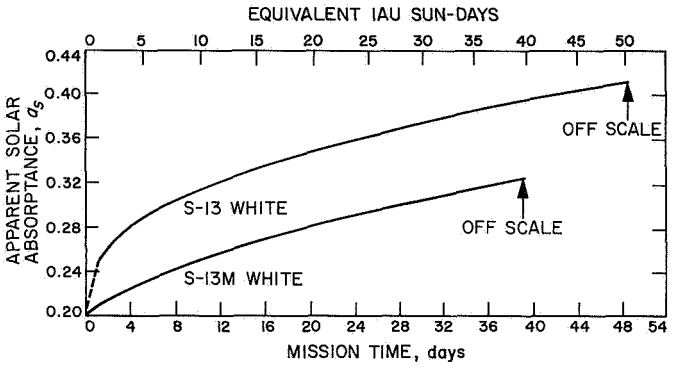


Fig. VI-56. Degradation of S-13 and S-13M white coatings

(432) indicated an initial $\alpha/\epsilon = 0.23$, compared to laboratory measurements of $\alpha = 0.18$, $\epsilon = 0.86$, or $\alpha/\epsilon = 0.21$. This 10% difference was well within the uncertainties in surface-property determinations.

Considering uncertainties in measurements, solar intensity, and spectral distribution, as well as telemetry, there was good agreement between laboratory measurements of radiative properties and the results obtained in space.

The TCR results have raised serious questions about the stability of temperature-control coatings in space, and about laboratory testing of these coatings. In space, the changes of the white TCR coatings permitted more precise resolution of changes in solar absorptance than is possible in the laboratory. However, discrepancies between data obtained by laboratory simulation and those in space show disagreements by factors of 1½–10, depending upon the laboratory results that are used.

It has long been recognized that deficiencies exist in laboratory testing, and that disagreement has occurred among investigators as to anticipated performance in space; but it is clear from the TCR results that very little good simulation testing has been done to date.

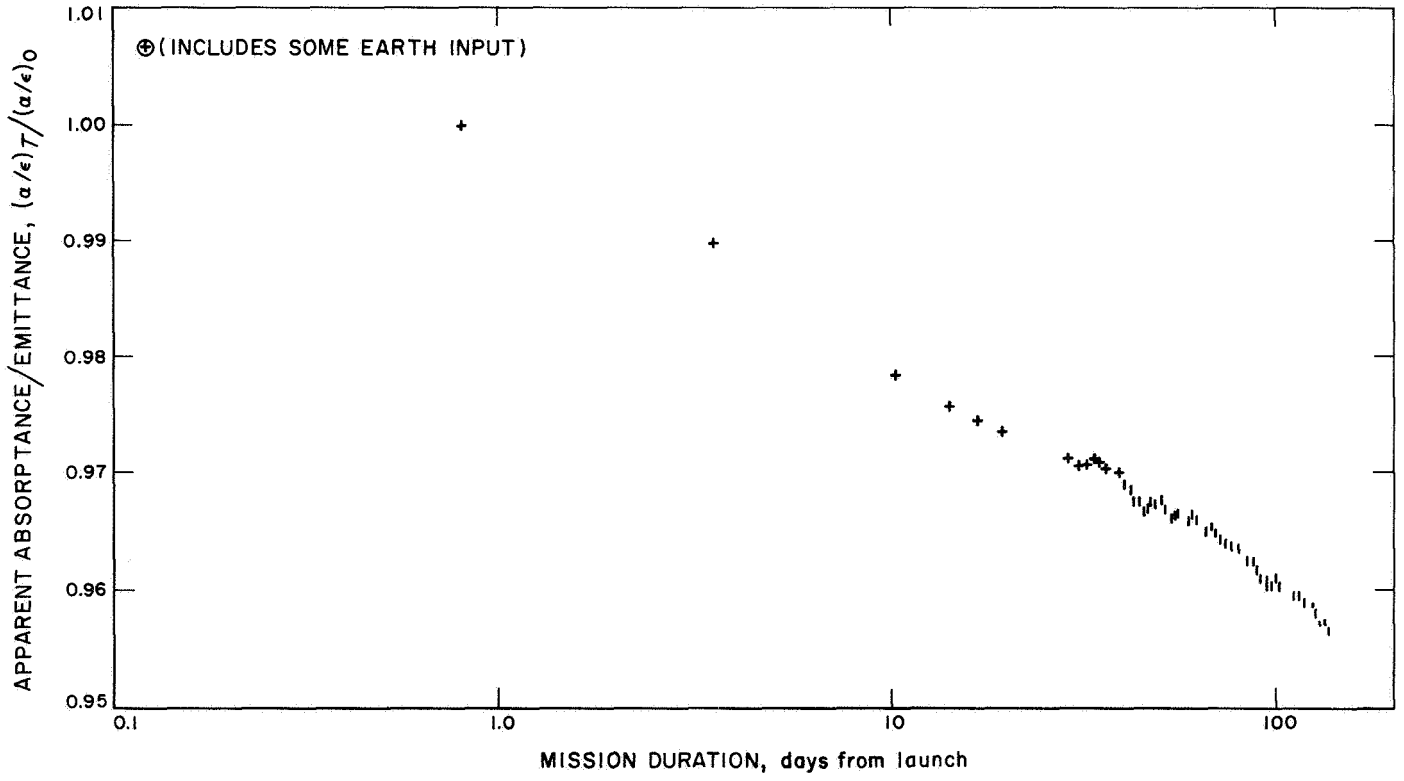


Fig. VI-57. Change in apparent absorptance/emittance during mission

Recommendations. The *Mariner V* vehicle provided almost ideal conditions for a measurement of this type. The instrumentation performed as expected, but the "stability" of the coatings was substantially less than anticipated from laboratory simulation. Recommendations are as follows:

(1) In view of the results on coating performance, it would have been advantageous to increase the range, thereby sacrificing resolution for all three channels. This decrease in resolution would have yielded data on the white coatings over a longer period of time, and perhaps could have indicated some equilibrium in degradation.

(2) The addition of a precision-switching thermometer (similar to those used for the *Mariner IV* absorptivity standard), in conjunction with a precision-resistance thermometer, could have provided a temperature-calibration point to eliminate uncertainties of the data encoder, and, in addition, would have increased the total measurable range.

(3) A significant increase in TCR accuracy could have been achieved by reducing the assembly thickness, increasing the through-thermal conductance, or by measuring the true average temperature. The schedule did not permit these refinements.

(4) The poor correlation between laboratory testing and performance in space indicates the need for improved simulation testing as well as for additional flight experiments of this type.

(5) Experiments to permit separate measurement of S, α_s, and ϵ would be desirable for spacecraft temperature control, and would provide a correlation for improved laboratory measurement of radiative properties (α_s and ϵ).

H. Propulsion Subsystem Performance

1. Propulsion subsystem.

a. Trajectory-correction maneuver. The *Mariner V* midcourse maneuver was performed on June 19, 1967. The desired spacecraft velocity increment of 16.127 m/s resulted in a predicted motor-burn duration of 17.651 s. This prediction was made using the burning-time estimation calculation (**BUTEC**) link to the midcourse-maneuver program. As a result of this prediction, the closest CC&S timer interval of 17.66 s was actually used for coding the QC-V1-3 burn-duration command for transmission to the spacecraft.

Performance of the propulsion subsystem during motor burn appeared nominal, except for a slightly lower thrust-chamber pressure than had been predicted. Fuel-tank pressure was as predicted (302–306 vs the predicted 304 psia). The oxidizer-start-cartridge pressure change during oxidizer expulsion was 28 psi, which was within the expected tolerance.

Because of the relatively short burn time required, only four chamber-pressure telemetry readings were returned from spacecraft motor operation. These averaged about 1.5% below the predicted values (see Fig. VII-3). Although these telemetry data were within the nominal assigned tolerance, the large velocity error of 4.5% associated with the *Mariner V* maneuver (as indicated by tracking data) prompted a critical reevaluation of transducer and data-encoder capabilities.

Results of this review indicated that the potentiometer pressure transducers used aboard *Mariner V* can introduce an uncertainty of as much as 1.5% of the indicated pressure because of mechanical friction and hysteresis inherent in the transducer design. As a result, a precise assessment of motor performance is not possible from the chamber-pressure measurement.

On the basis of the limited data, therefore, the propulsion subsystem probably performed nominally, although steady-state thrust could have been 0–3% lower than predicted. There were no indications in the motor performance data of thrust or transient errors as large as 4.5% of the delivered impulse, as was indicated by the tracking data.

b. Cruise. The pressure vessels incorporated in the propulsion subsystem (i.e., propellant tank, nitrogen tank, and oxidizer-start cartridge) remained leak-tight throughout the mission. As was the case with the *Mariner IV* propulsion subsystem, slow propellant decomposition produced a gradual increase in propellant-tank pressure throughout the mission. This pressure increase was in addition to that predicted because of increasing temperatures as the spacecraft approached the sun. The rate of pressure rise caused by decomposition was nearly identical to that of *Mariner IV* (0.1 psi/day at 65°F). Decomposition at the temperatures experienced by *Mariner V* was sufficiently slow to constitute no threat to the mission.

The limitations of the potentiometer pressure transducer were apparent when pressures were monitored during cruise. As with the chamber pressure transducer, hysteresis and poor repeatability, together with the limited resolution of the data encoder, resulted in uncertainties of as much as 3% in pressure readings under some circumstances. Cruise telemetry readings of propellant-tank, nitrogen-tank, and oxidizer-start-cartridge pressures are shown in Figs. C-6, C-7, and C-9, respectively.

c. Recommendations. The increasing emphasis on performance analysis during planetary missions suggests several areas in which instrumentation performance and data return could be enhanced:

(1) A high-data-rate maneuver telemetry mode that returns several samples per second of propulsion and other related parameters is required for adequate analysis of propulsion-subsystem performance. Higher resolution in telemetry data than is possible with the current 7-bit engineering word is also required.

(2) The potentiometer-type pressure transducer should be replaced with a strain-gage or solid-state transducer to provide less hysteresis and better repeatability.

(3) Continuing research is required to isolate the mechanisms producing propellant decomposition during long-term storage in space. Although it was not a problem during the earth–Venus phase of the *Mariner V* mission, longer storage times and/or higher propellant temperatures can produce pressure increases much higher than have been observed to date.

2. Pyrotechnics subsystem.

a. Flight performance. Operation of the pyrotechnics subsystem was normal throughout the *Mariner V* mission. The subsystem was armed by the PAS at *Agena*–spacecraft separation. The solar-panel pin-puller squibs were fired when commanded by the SIT. The propulsion subsystem start and stop squibs were fired by the CC&S, with no evidence of abnormal operation.

Excitation was supplied to the terminator sensor following receipt by the spacecraft of the DCV-25 command during the encounter sequence. Telemetry data indicated that the expected excitation voltage was applied to the sensor. The APAC was successfully accomplished as the terminator of the planet passed through the FOV of the terminator sensor.

b. Recommendations. A means of determining capacitor charge condition would be useful in monitoring the status of the pryotechnics subsystem before squib-firing events.

I. Reliability Spacecraft Program Results

1. Basic areas of reliability concern. *Mariner V* has proven itself to be an extremely reliable in-flight spacecraft. This may not appear to be remarkable in view of the high order of reliability that was demonstrated by its predecessor, *Mariner IV*, during its flight to Mars in 1964. However, the modification of an already-built *Mariner IV* type of bus and science payload, together with the development of new bus and science subsystems for the *Mariner* Venus 67 mission, presented a variety of reliability problems.

These problem areas were intensified by resource (schedule, manpower, and financial) constraints inherent in the *Mariner* Venus 67 project from its inception. Some of the major reliability problems involving electronic piece parts, environmental and system test constraints, new (to JPL) development hardware, and PFRs are discussed in the paragraphs that follow.

2. Electronic piece parts. Much of the basic bus hardware used for *Mariner V* was spare hardware from the *Mariner* Mars 1964 project. Most of the electronic parts incorporated in these subsystems were manufactured in 1962 or early 1963, and had been subjected to many hours of subsystem operation as part of the *Mariner IV* subsystem functional and environmental test effort.

These parts were analyzed for wearout or partial wearout and known unreliability because of either a previous failure history or a known manufacturing fault. Much of the effort to effectively solve such part problems within the resource constraints was undertaken as part of a suspect parts team investigation, which is described in Section IV-M of Volume I of this report.

Another critical electronic-parts problem area was the procurement and screening effort necessary to obtain parts to build new subsystems, to replace unreliable parts, and to provide spares. These tasks were accomplished through an all-out coordinated effort on the part of the technical division project representatives, parts specialists, and parts acquisition and reliability personnel.

The *Mariner* Venus 67 project was the first *Mariner* project that had certain types of electronic parts showing the failure mechanism of wearout. Eight parts were

classified as wearout failures after reliability analysis. All were failures detected before launch.

Six of the wearout failures were adjustable capacitors in the radio subsystem. These capacitors had to be constantly adjusted for calibration purposes, and the inside bushing threads eventually wore to such a degree that the capacitors could not be adjusted to the required accuracy. All of the worn capacitors were in hardware originally fabricated for *Mariner IV*, and most had been exposed to almost 2000 h of operation (and hundreds of adjustments) before wearout.

All but one of these failures were on nonflight hardware. The remaining two wearout failures were tubes used in the science-payload hardware. One of these failures was a Geiger–Mueller tube that failed after several thousand hours of use on the trapped radiation detector TA unit. The other tube-wearout failure was a phototube on the UV-photometer proof-test model. Both of these tubes had operating lifetimes that exceeded their specification limits, and both were on nonflight hardware. No wearout failures were detected aboard *Mariner V* after launch through the end of Phase I of the mission.

A total of 16 relevant electronic-part failures occurred on *Mariner* Venus 67 mission hardware before launch. No relevant failures were detected aboard the *Mariner V* spacecraft after launch through the end of Phase I of the mission. [A relevant failure is defined as a random failure occurring after power turn-on during module, subsystem, or system testing, or during flight. Excluded are failures caused by human error and failures induced by operational-support equipment. Also excluded are failures caused by design errors, mishandling, screening rejections, and faulty workmanship; also, early-life failures (those during the first 10 h of power-on). A relevant failure is the type of failure that would have the highest probability of occurrence during the flight of a well-designed spacecraft, if any failure would occur.]

The 16 relevant failures included those of six capacitors, one crystal, two diodes, one gyro, two integrated circuits, one relay, one transducer, one transformer, and one transistor.

The large number of capacitor failures in relation to the other part failures can be attributed to the failure of certain tantalum wet-slug capacitors having a rubber hermetic seal and process that was state-of-the-art when the capacitors were manufactured before the start of the *Mariner* Mars 1964 project. This seal/process combination eventually cracked and leaked the electrolytic after repeated thermal–vacuum environmental tests.

Failure of these capacitors is a good example of one of the known reliability risks assumed by the *Mariner* Venus 67 project. This type of capacitor was considered highly reliable (in fact, one of the best available in its class) when it was manufactured in 1962. Since then, however, the manufacturer has improved the internal construction of the device and provided a Teflon seal, with a subsequent improvement of reliability.

A further discussion of relevant failures on the *Mariner* Venus 67 project will be found in Ref. 27.

3. ***Environmental and system test constraints.*** The *Mariner* Venus 67 project had to assume certain reliability risks in environmental testing. Because there was only a flight system and a flight spare, the flight spare had to double as a proof-test model during certain system functional testing. Also, the proof-test model could not be used as a TA system test bed because TA environmental test levels are not intended for use on flight hardware.

In some cases, *Mariner* Mars 1964 TA units were available for subsystem TA testing. However, a ground rule of the project was that subsystem designs qualified during the *Mariner* Mars 1964 project and not undergoing major design changes for the *Mariner* Venus 67 project would not have to be requalified, not through the full retype-approval cycle at least.

All major new development, or new-to-JPL hardware (e.g., the DAS and DFR), required a TA unit for design qualification at the subsystem level. Because of delivery difficulties with TA hardware for these two subsystems, the TA testing was done late in the project, when any major design deficiencies uncovered by the TA level of environments would be extremely difficult to correct in time to meet the launch window. Fortunately, TA testing uncovered no major design difficulties for these subsystems.

The spare flight spacecraft (M67-1) proved to be an efficient test bed for exposing problems that were avoided when the flight spacecraft (M67-2) was subjected to environmental and functional testing. The efficiency of this method was attributed in part to the use of a single test team for both spacecraft during system testing at the

Spacecraft Assembly Facility and AFETR, as opposed to the normal approach of using one test team per spacecraft. This technique proved to be very effective, especially from a human-factors–training aspect.

Another interesting result of system testing was the discovery and elimination of systematic design defects inherent in the *Mariner* Mars 1964 mission hardware. All of the hardware involved had been subjected to comprehensive TA environmental testing (during the *Mariner* Mars 1964 project) for design qualification; however, it appears that design defects of a systematic nature still remained. These defects were found during system functional and flight-acceptance testing on the flight vehicle and the flight spare before the launch of *Mariner V*.

Further studies in this area are being made by JPL systems engineers and a study contractor, but initial results indicate that subsystem and system qualification testing of TA hardware is not enough to fully qualify design. Although such testing eliminates many design deficiencies, it appears that environmental testing of the actual flight hardware is required to provide full confidence in the adequacy of the flight-hardware design.

4. New development hardware. The science payload aboard *Mariner V* had one subsystem, the DAS, that was of an entirely new design from that of *Mariner IV*, and another subsystem, the DFR, with which JPL had had no experience. Most of the DFR hardware was identical with that of an instrument flown successfully in the *Pioneer* spacecraft series; nevertheless, it was not known how well the DFR would interface with the existing *Mariner* Venus 67 system hardware.

The DAS had to be designed, fabricated, and tested on a very tight schedule, and had to meet strict size and weight requirements. Consequently, the decision was made to design the DAS using integrated circuits (ICs) and multilayer laminates, both state-of-the-art devices with relation to JPL subsystem–system environmental testing and deep-space, long-life missions. To verify process and manufacturing controls of the laminates and ICs, a parallel evaluation test program was initiated. Also, in an attempt to improve IC yields and reliability, JPL quality assurance microscopically inspected the ICs at the manufacturer's facility prior to the normal electrical screening cycle.

Some of the reliability problems encountered (and subsequently resolved) during the DAS design-through-test phases were: (1) lids coming off of the IC flatpacks because of improper lid-bonding temperatures; (2) status-bit toggling caused by system noise; (3) ICs that appeared not to operate properly in the hardware after satisfactory checkout; (4) crystal interference with the DFR; and (5) a large lot of pulse transformers that had passed screening, but contained unsoldered internal leads that eventually led to part failures and a subsequent major retrofit effort.

The DFR presented a different set of problems. The flight and qualification units were, for the most part, of a firm, proven design, having flown successfully in the *Pioneer* program. However, the differences in environmental test requirements of the two projects were enough to cause some hardware difficulties during TA testing. But the major problem encountered with the DFR was system noise associated with integrating the DFR into the spacecraft. The DFR was designed to measure dispersive doppler radio frequencies at 423.3 and 49.8 MHz during planetary-occultation entry and exit. The *Mariner IV* spacecraft was not designed for insensitivity to electromagnetic interference at these frequencies, and RF noise was generated in the 49.8-MHz band. The following steps were taken to solve this noise-interference problem: (1) replacing certain diodes in the power subsystem; (2) changing the frequency of the DAS master oscillator crystal; (3) installing ferrite beads at the DAS connectors for all wires in the science instruments case harness; (4) wrapping the DAS interconnect harness with aluminized mylar; and (5) adding bandpass and low-pass filters to the DFR input circuits. The spacecraft then successfully passed electromagnetic-interference testing, and caused no problems to the DFR during the flight.

A breakdown of the electronic parts composing the *Mariner V* spacecraft is shown in Table VI-19. Of the 25,268 electronic parts listed, 594 were ICs (566 ICs in the DAS and 28 ICs in the DFR). A total of 19,812 equivalent discrete parts would be required to replace the ICs. Therefore, *Mariner V* had the equivalent of 44,486 discrete parts (25,268 − 594 + 19,812). This is actually in excess of 5000 parts more than the electronic-parts count of 39,220 for *Mariner IV*, which was composed entirely of discrete parts (except for a few low-complexity ICs in the scan-platform system).

5. Problem failure report summary. One of the reliability goals of the *Mariner* Venus 67 project was to improve the PFR system over that of the *Mariner* Mars 1964 project. Fewer PFRs were written for *Mariner*

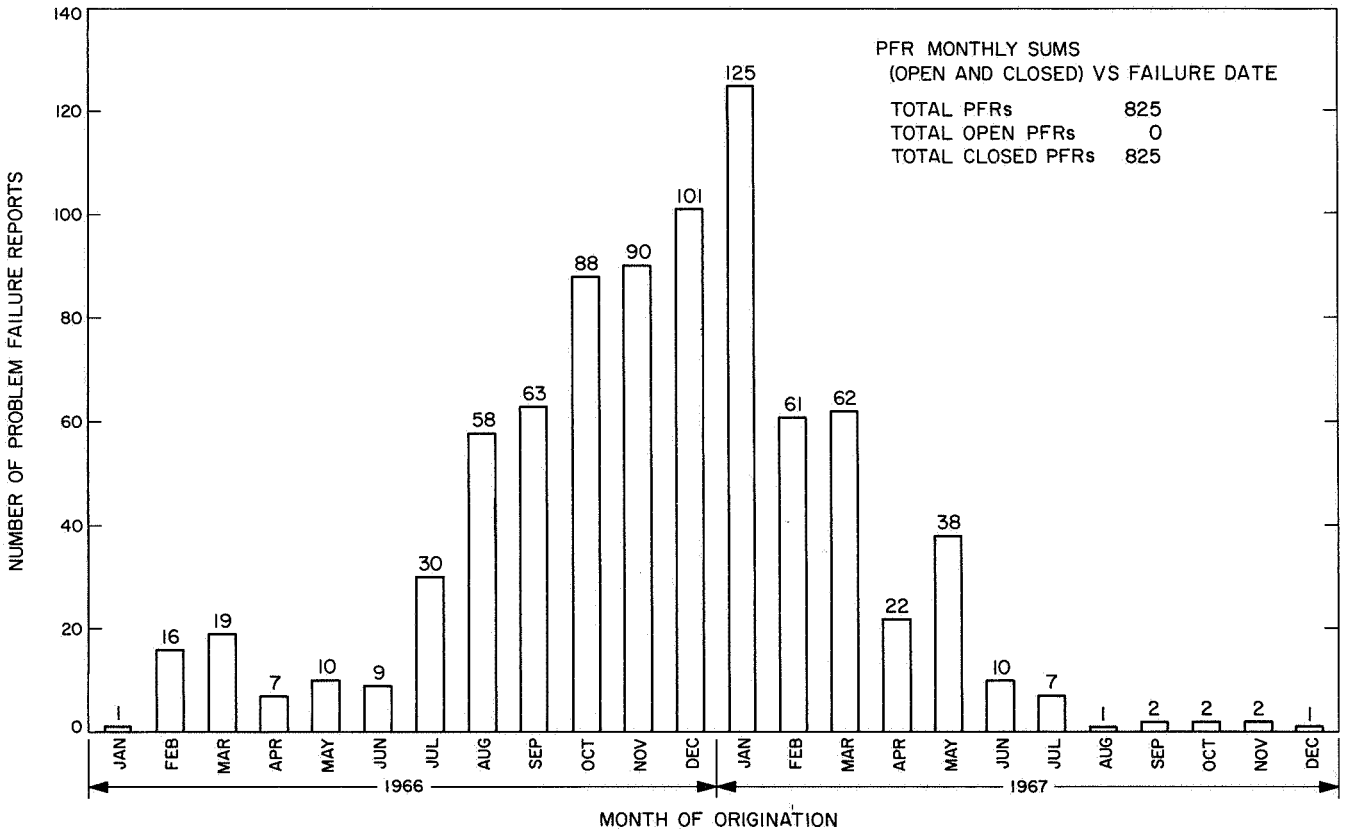


Fig. VI-58. Histogram of problem failure report activity vs time

Venus 67 than for *Mariner* Mars 1964 (825 vs 1500) because of less hardware, a shorter schedule, and a much greater quantity of proven hardware. However, the *Mariner* Venus 67 PFR quality was higher, and acceptance of PFRs as an invaluable aid in technical and managerial corrective action was more pronounced than in the *Mariner* Mars 1964 project.

A brief description of the means used to implement the PFR system in the project is presented in Section IV-M of Volume I of this report. A histogram of PFR activity plotted against time is shown in Fig. VI-58. Before launch, 817 PFRs were written on flight and ground-support equipment; eight PFRs were written on the flight spacecraft during Phase I of the mission.

Table VI-19. Summary of *Mariner V* parts count by subsystem

Subsystem	Reference designator	Capacitors	Diodes	Resistors	Transistors	Other[a]	Total[b]
Radio	(02)	594	203	658	122	197	1774
Command	(03)	406	791	1030	338	50	2615
Power	(04)	145	293	395	134	97	1064
Central computer and sequencer	(05)	257	728	1059	266	260	2570
Data encoder	(06)	1465	1464	3416	1055	185	7585
Attitude control	(07)	227	291	523	119	101	1261
Pyrotechnics	(08)	42	48	114	4	32	240
Wiring	(09)	0	0	0	0	0	0
Thermal	(11)	0	0	0	0	3	3
Mechanical	(12)	6	4	6	0	13	29
Tape recorder	(16)	232	331	686	197	33	1479
Data automation subsystem	(20)	144	89	261	62	617[c]	1173
Trapped radiation detector	(25)	94	38	206	61	18	417
Plasma probe	(32)	162	425	684	211	12	1494
Magnetometer	(33)	212	83	597	153	6	1051
UV photometer	(34)	203	148	665	155	52	1223
Dual-frequency receiver	(35)	405	111	481	150	143[d]	1290
Total subsystem parts		4594	5047	10,781	3027	1819	25,268

[a]"Other" includes inductors, relays, transformers, microcircuits, cores, silicon-controlled rectifiers and switches, crystals, thermistors, sensitors, fuses, and tubes.
[b]Total does not include 518 connectors.
[c]There were 566 microcircuits in the data automation system.
[d]There were 28 microcircuits in the dual-frequency receiver.

VII. Flight Support Testing

A. Postlaunch Test Operations

Postlaunch test operations consisted of five procedures, which are discussed in the following paragraphs; major Spacecraft Assembly Facility (SAF) electrical operations are summarized in Table VII-1.

1. Support at Air Force Eastern Test Range. This support at the Air Force Eastern Test Range included the following: (1) The spare (M67-1) spacecraft was turned on and conditioned to the same status as the flight (M67-2) spacecraft; i.e., cruise mode. (2) The maneuver commands were then transmitted to the spare spacecraft

Table VII-1. *Mariner V* (M67-1) Spacecraft Assembly Facility electrical operations

Date, 1967	Operation
Jul 3	Verification of all spacecraft and OSE[a] functions
Jul 13	SPAC[b] support testing of procedure for using inertial mode to acquire star Spica to calibrate UV photometer
Jul 18	Verification of all STCDS[c] functions and data modes
Jul 27	Evaluation test of UV photometer and planet sensor output signal interface with data automation subsystem
Aug 10	Verification of STCDS telemetry and science data program
Aug 24	Investigation of prototype Canopus sensor problem
Aug 25	SPAC support testing of encounter procedure
Sep 9	Investigation of UV-photometer problem
Sep 11	Investigation of UV-photometer problem
Sep 15	SPAC support testing of encounter procedure
Sep 21	SPAC support testing of encounter procedure
Sep 25	Special test of main booster-regulator failure mode
Sep 26	Preparation for SPAC support testing
Sep 28	SPAC support testing of encounter procedure
Oct 2	SPAC support testing of encounter procedure
Oct 3	SPAC support testing of encounter procedure
Oct 4	SPAC support testing of encounter procedure
Oct 5	SPAC support testing of encounter procedure
Oct 6	Special tests of UV photometer
Oct 10	SPAC encounter support testing
Oct 12	SPAC encounter support testing
Oct 19	SPAC real-time *Mariner* V encounter support
Oct 25	Special battery-charger tests
Oct 26	UV-photometer problem investigation
Nov 13	Special SPAC test to verify procedure for midcourse maneuver and recording sequence used for in-flight calibration of *Mariner* V UV photometer
Nov 17	Rerun of special SPAC midcourse maneuver and recording sequence
Nov 20	Special UV-photometer test
Nov 27	Special electromagnetic-interference test
Nov 28	Special electromagnetic-interference test
Dec 15	Pre-storage system verification test

[a]OSE = operational support equipment.
[b]SPAC = spacecraft performance analysis and command.
[c]STCDS = System Test Complex Data System.

prior to transmission to the flight spacecraft to verify coding and responses. (3) A "junior" spacecraft performance analysis and command (SPAC) team (SPAC JR) monitored the flight spacecraft operation for a week subsequent to launch. This provided a backup to the JPL SPAC.

2. Return of the spare spacecraft to JPL. The spare spacecraft returned to JPL was functionally tested (system-verification test MV67 300) without incident. However, one failure occurred in the central computer and sequencer (CC&S) operational support equipment (OSE). A terminal in the blockhouse power supply was broken and, as a result, the power supply was intermittent.

3. Spacecraft performance analysis and command encounter tests and special tests. During this period, the following tests were performed:

a. Science UV-photometer tests. Many tests were performed on the spare spacecraft science subsystem to investigate the UV-photometer problem (shift in quiescent reading), which occurred on the flight spacecraft science subsystem.

b. Mission Operations System test. This test was performed to verify the readiness of Space Flight Operations Facility (SFOF) personnel for encounter. Included were normal encounter and cruise tests, and the same tests repeated with simulated failures.

c. SPAC anomaly tests. Several tests were performed to simulate possible spacecraft malfunctions. Some of these tests were as follows:

(1) Simulated failure of main booster-regulator (B/R). For this test, a special switch was installed in the input to the main B/R to provide a realistic simulation of main B/R failure and resulting transfer to maneuver B/R. Photographs of spacecraft transients on B/R input current and voltage were taken during the changeover from main to maneuver B/R. Results of this test appeared to be the same as if the spacecraft external power had been turned off and then on again.

(2) Failed command tests. With failures introduced in the command decoder hardware, a series of RF commands were sent to the spacecraft and procedures for recovering from each situation were devised.

(3) The effects of spacecraft battery-charger current limits on the spacecraft system. The battery was removed from the spacecraft and a variable-load box was connected across the battery charger. The load was varied and the effect on the spacecraft system due to noise generated by the charger was observed by all OSE personnel. Various anomalies occurred as a result of the noise, such as loss of science bit sync and engineering transverse magnetic bit sync. Charger current was increased to a maximum of 0.84 A. Previous charger analysis revealed a theoretical upper limit of 0.60 A.

d. Electromagnetic-interference tests. These tests were performed to measure noise levels and turn-on transients between various spacecraft returns and on several supply voltages. A report on this test is being written.

4. Standby during flight spacecraft encounter. The spare spacecraft was operated in the same modes as the flight spacecraft during encounter so that possible problems during encounter could be duplicated and investigated. No flight spacecraft problems occurred.

5. Preparation for storage of the spare spacecraft. After all encounter and postencounter tests were complete, the spare spacecraft was disassembled, cleaned, and reassembled. After this, a system-verification test (MV67 300) was performed to verify spacecraft operation before placing the spare spacecraft in storage.

B. Occultation Ground Equipment Description and Configuration

A device was built that was capable of testing all facets of the data collection and reduction techniques by simulating the anticipated signal characteristics. Basically, this simulator consisted of a signal source of which the frequency and amplitude could be varied in a programmed manner. Specifically, the components included a voltage-controlled oscillator (VCO), retuned to operate at 19 MHz, that functioned as a basic signal source. This was followed by an X3 multiplier, an amplifier, and a step recovery diode-type spectrum generator. The desired component of 2295 MHz was selected by a filter and the initial signal level set by a variable attenuator. The final component in this string was a voltage-controlled attenuator (VCA). A block diagram of the simulator is shown in Fig. VII-1.

Voltage functions required to drive the VCO and VCA were obtained from nonlinear voltage dividers in the form of two ganged, multiple-tap potentiometers driven

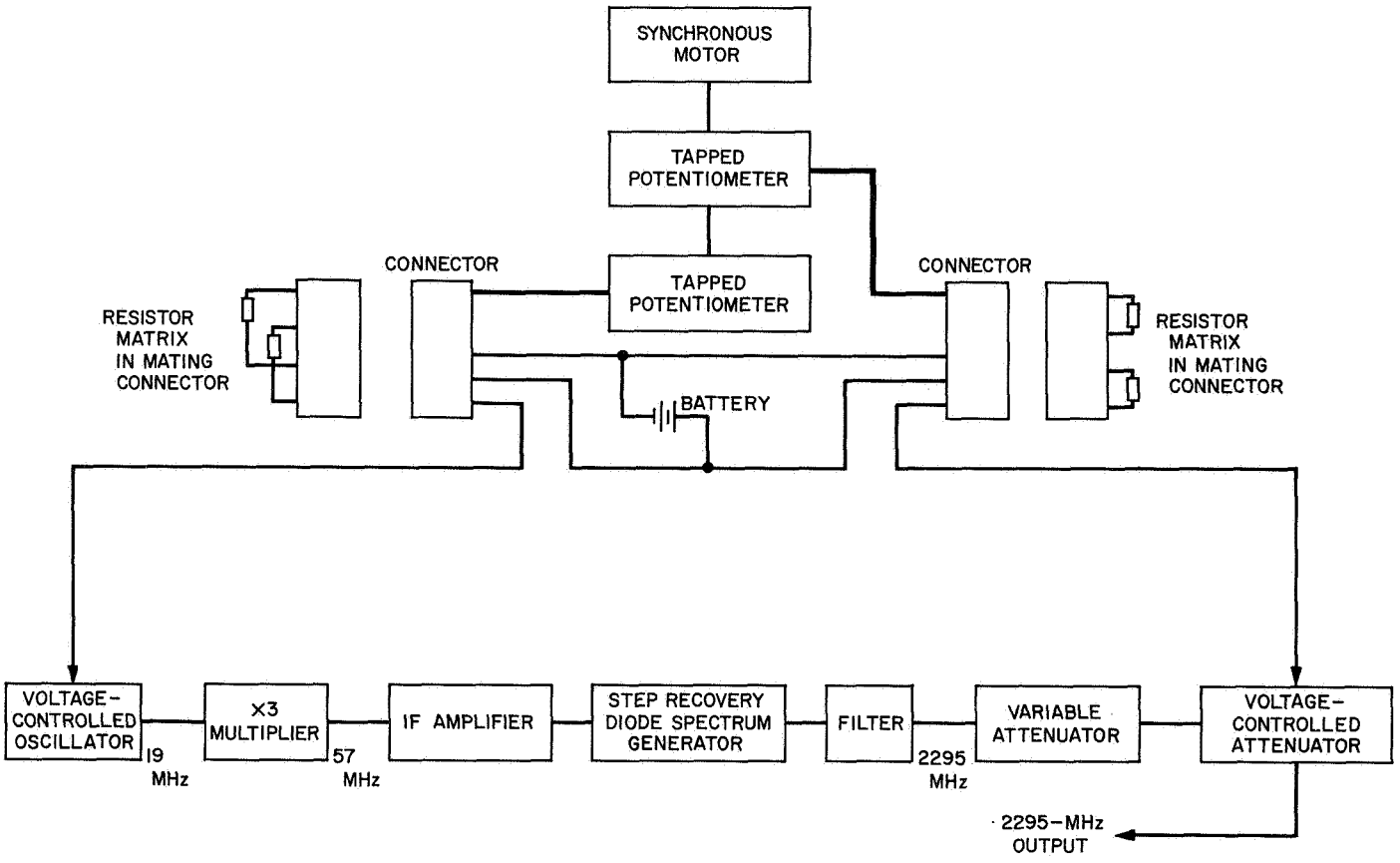


Fig. VII-1. Occultation simulator block diagram

by a synchronous motor. The taps of the potentiometers were wired to connectors and a resistor matrix was soldered into the mating portion of the connector. The use of different connectors with different resistor matrixes permitted the generation of any desired voltage function. Use of different speed motors permitted a variation in duration of atmospheric effects.

The output signal, which was at S-band, was fed into the traveling-wave maser (TWM) input at Deep Space Stations (DSS) 13 and 14. This permitted checking the receiver operation to obtain an idea of when loss of lock would occur, and also provided some operator training. In addition, the signal was recorded by the open-loop receiving system and reduced by the proposed data-reduction technique to prove its suitability.

C. Trajectory-Correction Maneuver Anomaly

1. Introduction. The trajectory-correction (midcourse) maneuver of *Mariner V* was anomalous in that the velocity increment achieved was 95.4% of that commanded. The first indication of an incorrect midcourse maneuver was revealed by the real-time doppler tracking data, which showed a frequency shift of 12.6 Hz instead of the expected 13.6 Hz. Postmaneuver trajectory analysis confirmed the anomaly, and determined the maneuver results presented in Table VII-2. An immediate analysis of the performance of the autopilot, propulsion, and pyrotechnics subsystems was undertaken in an effort to uncover the cause of the anomaly.

2. Propulsion subsystem. The propulsion subsystem investigation consisted of three major efforts. Those efforts were: analyze the received telemetry data, review the preflight calibration data, and recompute the values for the burning time estimation calculation (**BUTEC**) program input.

a. Telemetry data analysis. Because the propulsion telemetry data rates and spacecraft instrumentation accuracy and resolution were designed to identify gross performance only, it must be emphasized that subtle

deviations from predicted performance were very difficult to detect. Propulsion parameters did not provide any definitive information on timing or duration of the motor burn. Estimates of the CC&S event times were used to analyze the data.

The sequence of telemetry events during motor burn is shown in Fig. VII-2. The only telemetry data indicating thrust chamber performance during the firing were those from channel 117 (thrust chamber pressure). The four data points obtained during this firing are shown plotted along with the expected value in Fig. VII-3. Using the comparison of the expected value, the average chamber pressure of these four points was approximately 1.5% below the prediction. This corresponded to 1–2 data numbers, and was within the acceptable tolerance of the instrumentation for this particular measurement.

During steady-state thrusting (i.e., several seconds after completion of oxidizer injection), the chamber pressure was directly proportional to thrust. To a first approximation, a 1.5% loss in steady-state chamber pressure, if real, would be reflected in a 1.5% loss in steady-state thrust and, therefore, in delivered impulse (the time integral of thrust). It should also be noted that the chamber pressure itself was not a steady pressure. Fluctuations during firing resulted from small localized movement of the hydrazine decomposition zone within the catalyst bed and from resonance within the chamber cavity. Because the data-encoder sample time was quite short, it cannot

Table VII-2. Midcourse maneuver performance parameters

Parameter	Required[a]	Commanded[a]	Achieved[a]	Standard deviation, σ
Pitch turn (rate = 0.1818 deg/s)	55.3503	55.267	55.18	0.2
Roll turn (rate = 0.1867 deg/s)	71.0248	70.946	70.93	0.04
Velocity increment	16.127 m/s	16.135 m/s	15.412 m/s	6.0
Motor burn	17.651 s	17.66 s	17.66 s	—

[a]In deg except as noted.

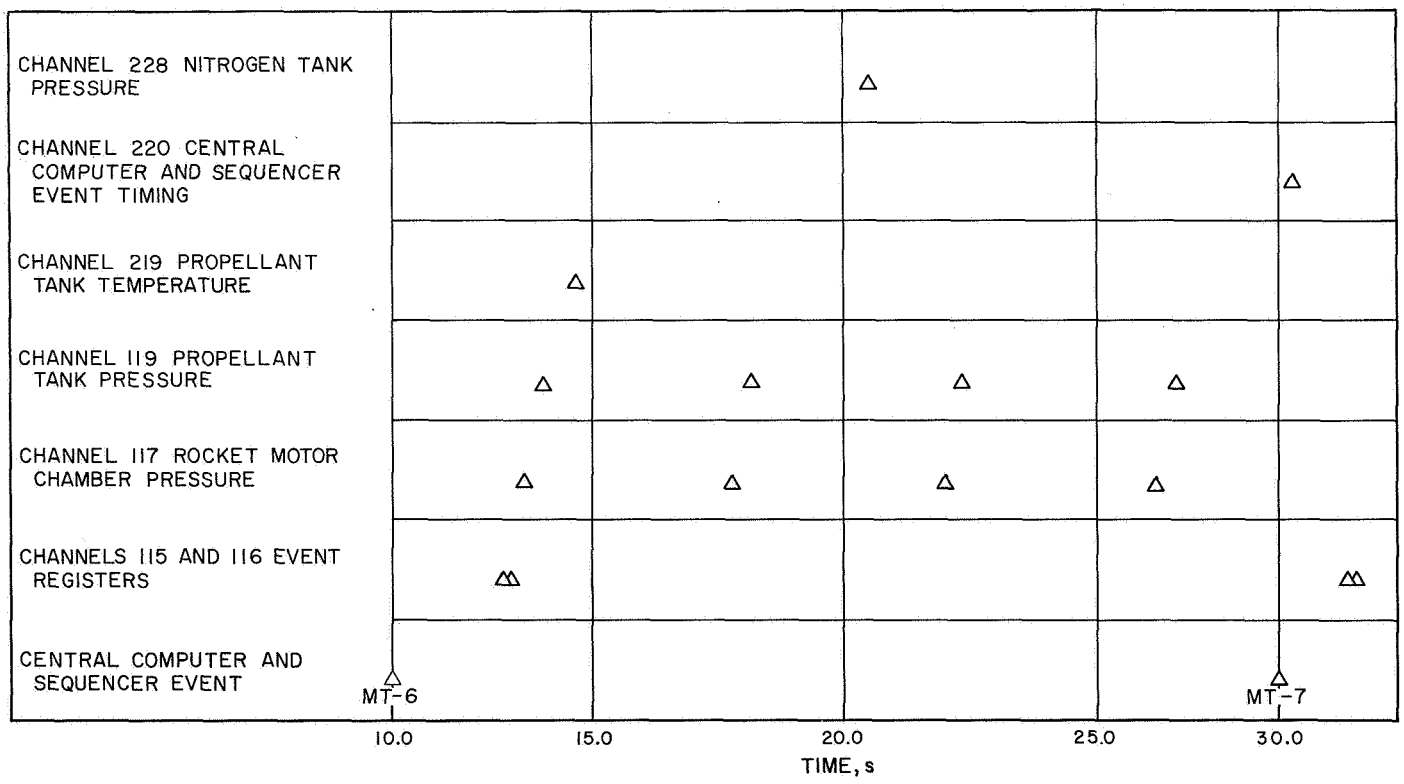


Fig. VII-2. Maneuver telemetry sequence of events from 23:08:10 ±0.1 GMT on day 170

be stated with assurance that the four samples obtained represent the average pressure in the chamber at a given time. Because these were the best data obtained for this measurement during firing, they are inconclusive; however, they did not indicate more than a 1.5% chamber-pressure degradation.

Telemetry data from the propellant-tank transducer during firing are shown in Fig. VII-4. Because this transducer, unlike the chamber-pressure transducer, was calibrated through the data encoder, the telemetered pressure readings are believed to be accurate. As shown in Fig. VII-4, agreement with the predicted value is very close. These data imply that the regulator was working properly 3 s after the start of motor firing. The regulator controls the flow of high-pressure nitrogen into the propellant tank and maintains the propellant tank at a constant pressure. There is a possibility that the regulator may have stuck in the closed position at motor ignition, and then recovered within 3 s. Such a performance is remotely possible, but if such a malfunction had occurred, the maximum impulse lost would have been approximately 2%.

In-flight performance of the oxidizer-start cartridge was reviewed to determine, again within limits of the telemetered data, whether the engine-start transient could have been degraded as a result of a problem with the oxidizer feed system. The loaded oxidizer volume was determined from measurements of oxidizer-loaded weight as measured at AFETR during filling. This volume was assumed to be evenly divided between the two oxidizer bellows (bellows volume was not measured directly). The volume of the start-cartridge nitrogen cavity was also calculated. From these volumes, a pressure change of 31 psi was predicted for expelling the oxidizer contained in one bellows. Telemetry data show a change of 28 psi, which compared quite favorably with the predicted pressure change considering the accuracy of the calculation and the fact that telemetry resolution is 4 psi on that channel.

Test experience with this type of motor indicates that, if the start transient is degraded substantially, as would be the case if a smaller than normal amount of oxidizer is injected or if injection is too slow, the chamber pressure during the first 5–10 s of the burn is noticeably lowered. Both the telemetered chamber pressure and the start-cartridge pressure change indicate that a normal start was obtained. Again, subtle degradations cannot be identified from the telemetry.

Midcourse-maneuver nitrogen-tank pressure data provided little insight into propulsion-subsystem performance. (Predictions of nitrogen usage during propellant expulsion are notoriously difficult to make.)

During propellant expulsion, the nitrogen gas works on itself, and the gas temperature drops. Assuming

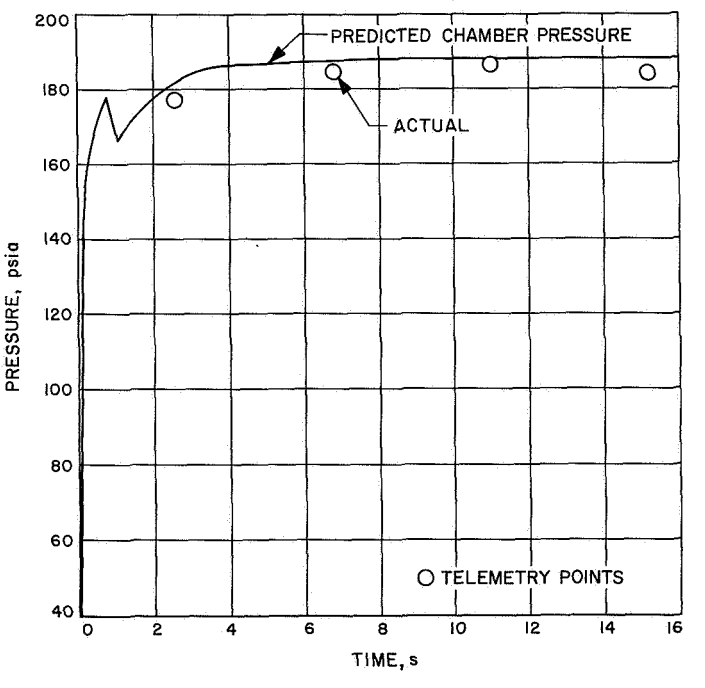


Fig. VII-3. Chamber pressure telemetry data points

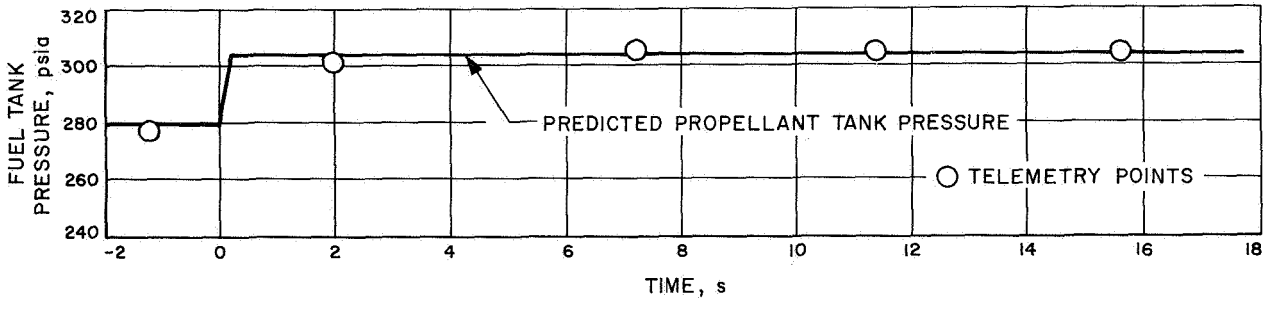


Fig. VII-4. Propellant tank pressure telemetry data points

the gas is initially in equilibrium with its container, heat is then transferred into the gas as it cools. The mechanism for heat transfer is primarily natural convection within the tank. However, the difference in g level between testing on earth (1 g) and the maneuver in space (at about 0.1 g) produces a substantial difference in heat-transfer rates. It is for this reason that the maneuver was timed to obtain a channel-228 reading during motor firing.

Analysis of the nitrogen-tank pressure data with the aim of calculating the amount of propellant actually pumped was completed, but results are inconclusive. The best that can be said is that *approximately* the correct amount of propellant was pumped, but the calculations are only accurate to approximately ±10%.

These areas of the propulsion subsystem are the areas that would be involved in an error of this type. Other areas of the propulsion subsystem have been investigated (i.e., squib valves, filters, and propellant-feed subsystem), but there is no way to determine whether subtle malfunctions of these components actually occurred.

b. Preflight calibration data. A careful check was made of all data used in the **BUTEC** prediction of the motor flight performance. Each step in the propulsion-subsystem calibration process was reviewed. Several questions arose during this review concerning instrumentation accuracies and method or technique, but the maximum deviation that could be attributed to this source would be 1%.

c. Burning time estimation calculation rerun. The **BUTEC** program was checked for completeness and accuracy. A new output was generated using the same input values used for the flight maneuver. In addition, a computer run was made with the propellant temperature actual value at the time of firing rather than the maneuver estimate used for the premaneuver prediction. This calculation resulted in an estimated change of only 0.005 s in firing time, which is a value too small to be seen in the resolution of this system. This review revealed no errors in the **BUTEC** inputs or method of calculation.

3. Pyrotechnics subsystem. The pyrotechnics subsystem telemetry data are limited to event-register changes in registers 1 and 3. The possibility of a squib or pyro-unit malfunction changing the firing duration is considered remote. All squibs have dual bridgewires, with separate energy-storage units firing two sets of squib bridgewires. Both units apparently discharged at motor ignition and motor shut-off, as events were recorded each time in registers 1 and 3. Telemetered data on the propulsion subsystem indicate that all valves functioned. A squib hang-fire or delayed capacitor discharge is considered most unlikely.

4. Autopilot analysis. Prelaunch and premaneuver analyses of the performance of the *Mariner IV* autopilot had been expanded for the *Mariner* Venus 67 mission by simulation of the autopilot with a six-degree-of-freedom program using DSL/90 simulation language on the 7094 computer. As an extension of the autopilot program used on the *Mariner* Mars 1964 project, the six-degree-of-freedom simulation was able to handle the effects of solar-panel dynamics, the actual thrust-time profile of the *Mariner V* motor, known coupling between axes, and was, in general, a more sophisticated model of the autopilot.

Several studies of the autopilot, with emphasis placed on the selection of solar-panel cruise dampers, center-of-gravity offsets, and autopilot mix-matrix resistors, had been accomplished during the system-tesing phase. A simulation had even been made of autopilot performance with two solar panels undeployed on the assumption that a deployment failure could be corrected by firing the midcourse-maneuver motor for a short period of time (the autopilot was stable, according to the simulation, even in this configuration).

The only data available on autopilot performance during the actual maneuver were gyro rate-plus-position output telemetry; there is no telemetry on jet vane position. In addition, the data rate during the maneuver provided a gyro output only once every 4.2 s. Finally, the quantized nature of the telemetry word permitted a resolution of the gyro output to only 0.57 ±0.29 V in pitch and yaw and 0.47 ±0.24 V in roll. The most appropriate manner in which to analyze autopilot performance during a maneuver is then to provide the simulation with the initial conditions observed in the telemetry, and attempt to duplicate the gyro outputs observed during the maneuver by varying certain parameters in the simulation, such as center-of-gravity offsets, engine thrust-time profile, solar-panel dynamics, jet vane actuator (JVA) stiction characteristics, autopilot mix-matirix resistors, and others. When this normal analysis procedure failed to duplicate, or even approximate, the observed gyro telemetry readings, it became obvious that either an autopilot failure had occurred or simulation was incomplete.

A steady-state transformation of the initial conditions and of the four pitch, yaw, and roll gyro outputs observed during the burn into jet-vane deflection angles resulted in the jet-vane deflection shown in Fig. VII-5. The jet-vane drag in the exhaust stream determined from these

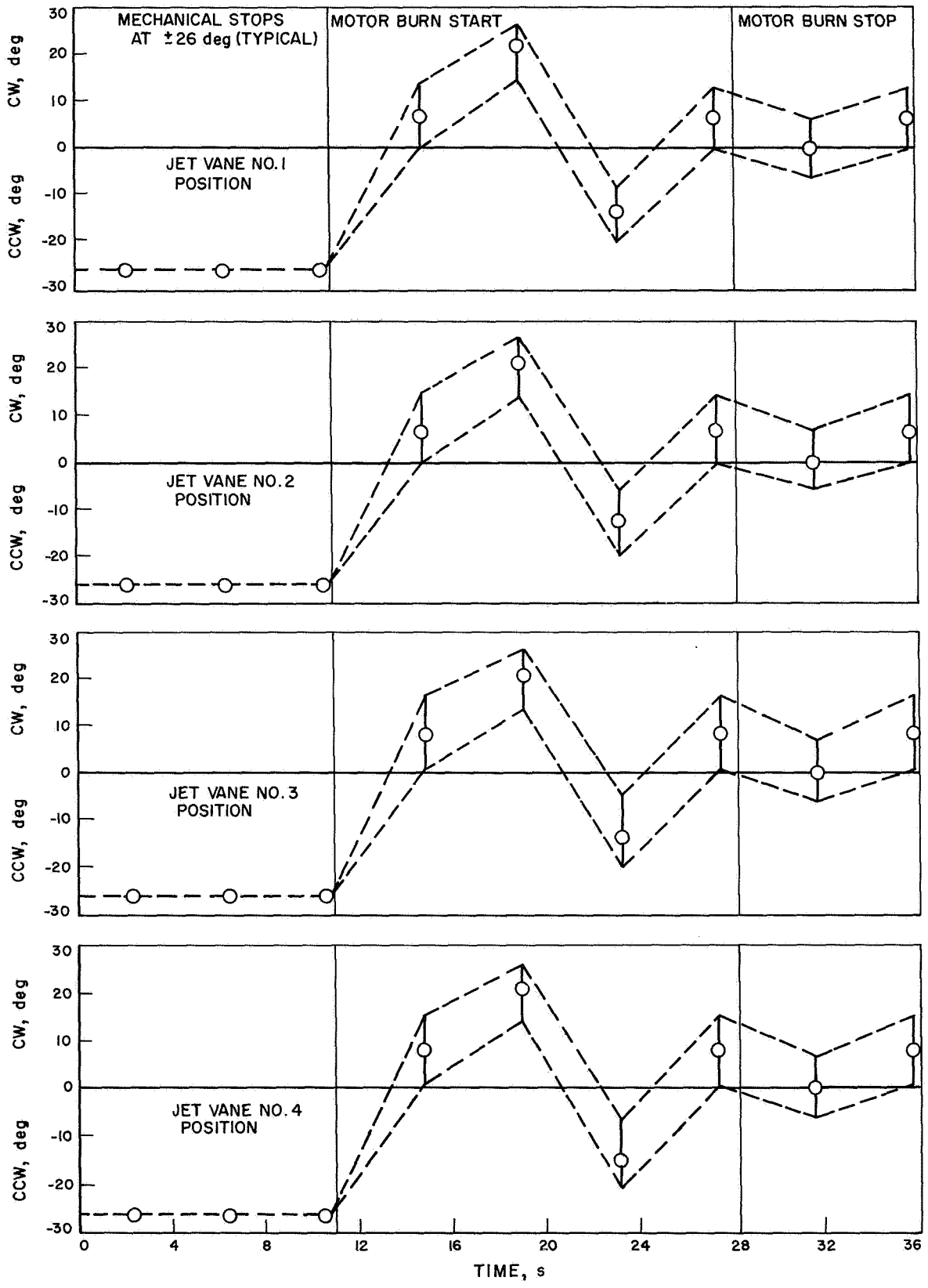


Fig. VII-5. Jet vane positions during midcourse maneuver No. 1

Table VII-3. Jet-vane interaction test summary

Test No.	Date, 1967	ETS[a] test No.	Purpose of test	Results of test
1	Aug 24	DD-249	Evaluation of actuator stiction model and testing method using flight (M67-2) actuators	Verified stiction model, low stiction level of flight actuators, and coincidence of vane center-of-pressure with axis of rotation (vane aerodynamic neutrality)
2	Oct 6	DD-252	Evaluation of aerodynamic interaction between vanes using new six-component firing test stand	Six-component stand (measuring three-axes forces and moments) disclosed side force generation as a function of vane rotation
3	Oct 18	DD-254	Repeat of DD-252 using smaller *Ranger* vanes to determine if side forces were caused by vane interaction	Disclosed that lift, drag, and side forces scaled with vane area
4	Dec 8	DD-256	Repeat of DD-252 using two modified *Mariner* vanes (thermal shield removed) to determine if side force was generated on thermal shield	Disclosed that side force was not generated by aerodynamic shock force at thermal shield; side forces were the same as DD-252
5	Dec 13	DD-257	Test with a single unmodified *Mariner* vane to determine if side forces were caused by vane-to-vane interaction	Disclosed that side forces were due to interaction between vane-to-actuator mounting ring and not from vane-to-vane interaction
6	Dec 21	DD-258	Test with a 1-in. larger diameter ring and modified *Mariner* vanes	Side forces were reduced by a factor of three

[a]ETS = Edwards Test Station.

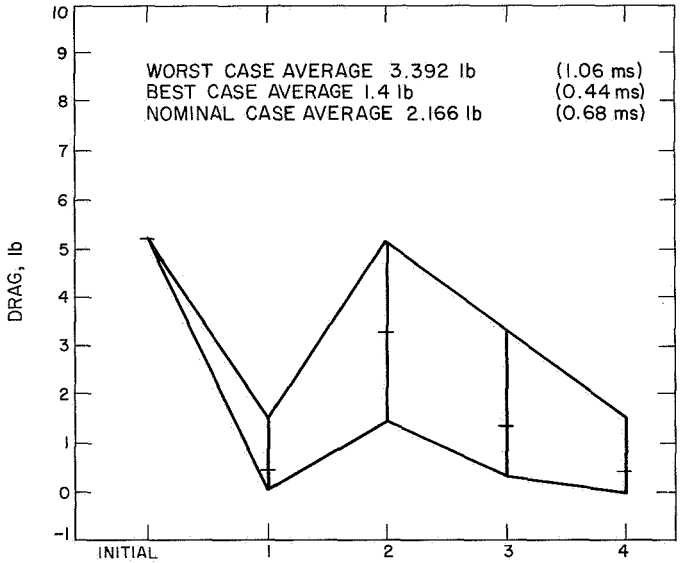


Fig. VII-6. Jet vane drag

angles is shown in Fig. VII-6. Both figures are approximations of actual performance because of the nature of the data and the use of steady-state analysis in a dynamic system; however, several conclusions can be drawn from them.

First, the velocity decrements associated with the drag forces shown in Fig. VII-6 bracket the observed velocity decrement. The average decrement, 0.68 m/s, was close to the observed decrement, 0.735 m/s.

Second, the behavior of the vanes demonstrated that the autopilot was atypical. All four vanes rotating in the same direction, with the same amplitude, was indicative of a spacecraft rotation about the motor thrust axis. There was no case where the simulation predicted this motion.

Third, data presented in Table VII-2 show that the autopilot obviously maintained spacecraft stability and pointing accuracy during the maneuver; therefore, no gross failure occurred. The net effect of the anomaly was on the thrust-vector magnitude only, with a negligible effect on its direction.

The six-degree-of-freedom autopilot simulation was next reexamined for accuracy and completeness. Data on the performance of the gyros, solar-panel and spacecraft dynamics, autopilot-electronics characteristics, JVAs, and the program were reevaluated. Based on this reevaluation, it was decided that more data were required on the JVA stiction model and on the interaction between the vanes in the rocket exhaust stream. Accordingly, a series of firings of a *Mariner* motor at Edwards Test Station, with the actuators mounted and instrumented, was scheduled to provide data on stiction and vane interaction during motor firing in a vacuum environment. Table VII-3 summarizes the firings.

The first firing was conducted on August 24, 1967, to provide data on the stiction model of the actuators under the conditions of thermal shock and heating encountered

during an actual firing. The vanes were programmed through a series of deflections, once before the firing and four times during the firing. Oscillographic records of input to the actuator torquer, torquer current, and vane position before and during the firing were then compared to determine the stiction level. The results on these flight (M67-2) actuators were that the stiction level was very low and the specified 0.6-oz-in. static friction was easily met.

The second firing was delayed until construction of a six-component test stand, designed expressly for this program, was completed.

To provide a test stand with 6 deg of freedom for the purpose of measuring side forces during the motor firing with deflected jet vanes, the test stand used for axial thrust measurement was modified. This modification consisted of mounting additional structure to the original stand to provide for load-cell mounting in the lateral orthogonal axes (Fig. VII-7).

Because the difficulty of building a successful six-component test stand at JPL was well known, this modification emphasized a simple design geometry; the minimum disturbance of the axial thrust measurement (for reference only) was secondary to obtaining good data from the lateral load cells.

The details of stand construction are shown in Figs. VII-8 and VII-9. The technique of prefabricating a welded structure and then bolting it to the original stand mount was used to minimize the permanent configuration change of the original stand. All machined surfaces were held to close tolerances to reduce the assembed out-of-tolerance alignment. Because the test stand was of rigid construction for the cell mounts and rocket-motor mount, relative motion across the moving interface was taken up by flexure rods connecting the load cells to the motor ring mount.

The test stand was installed in the test facility and aligned by mechanical measurement. No special effort was made to hold this lateral-axis alignment to better than 5 deg of true position because off-center alignments of this magnitude or less could be compensated for in the computer side-force analysis program. The test-stand assembly included a final mechanical calibration of the load cells and a wrapping of insulation material around each load cell to reduce convective heating of the load cells during the motor firing.

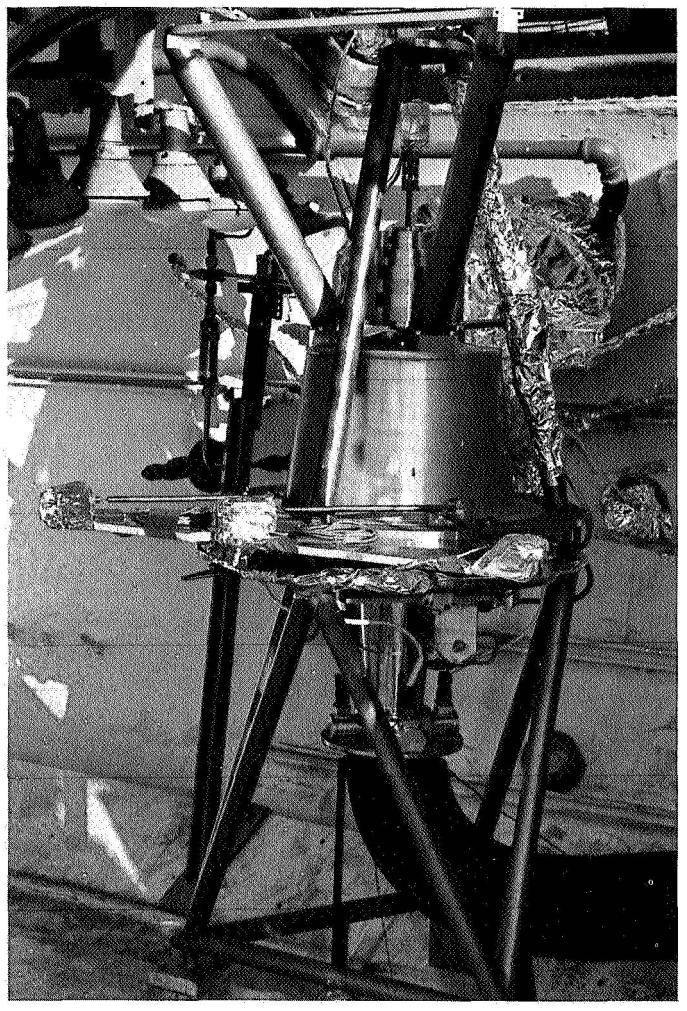


Fig. VII-7. Six-component test stand

The input signals to the JVAs were designed to reduce the high-frequency components, which might cause the test stand to ring. A computer simulation was made assuming 10-Hz resonant frequencies for all stand axes. The results of this simulation indicated that stand resonances would not be excited to any great extent.

A checkout test was performed on this stand using a live motor and near-vacuum environment. There were no JVAs present on this test, but the results showed a very low noise level on the lateral load-cell outputs. Since the transient and steady-state performance of the actuators, not the motor itself (i.e., not motor-start transient), were of prime interest, these levels were deemed low enough to resolve the suspected lateral forces in the range of the dynamic resolution of the subsystem.

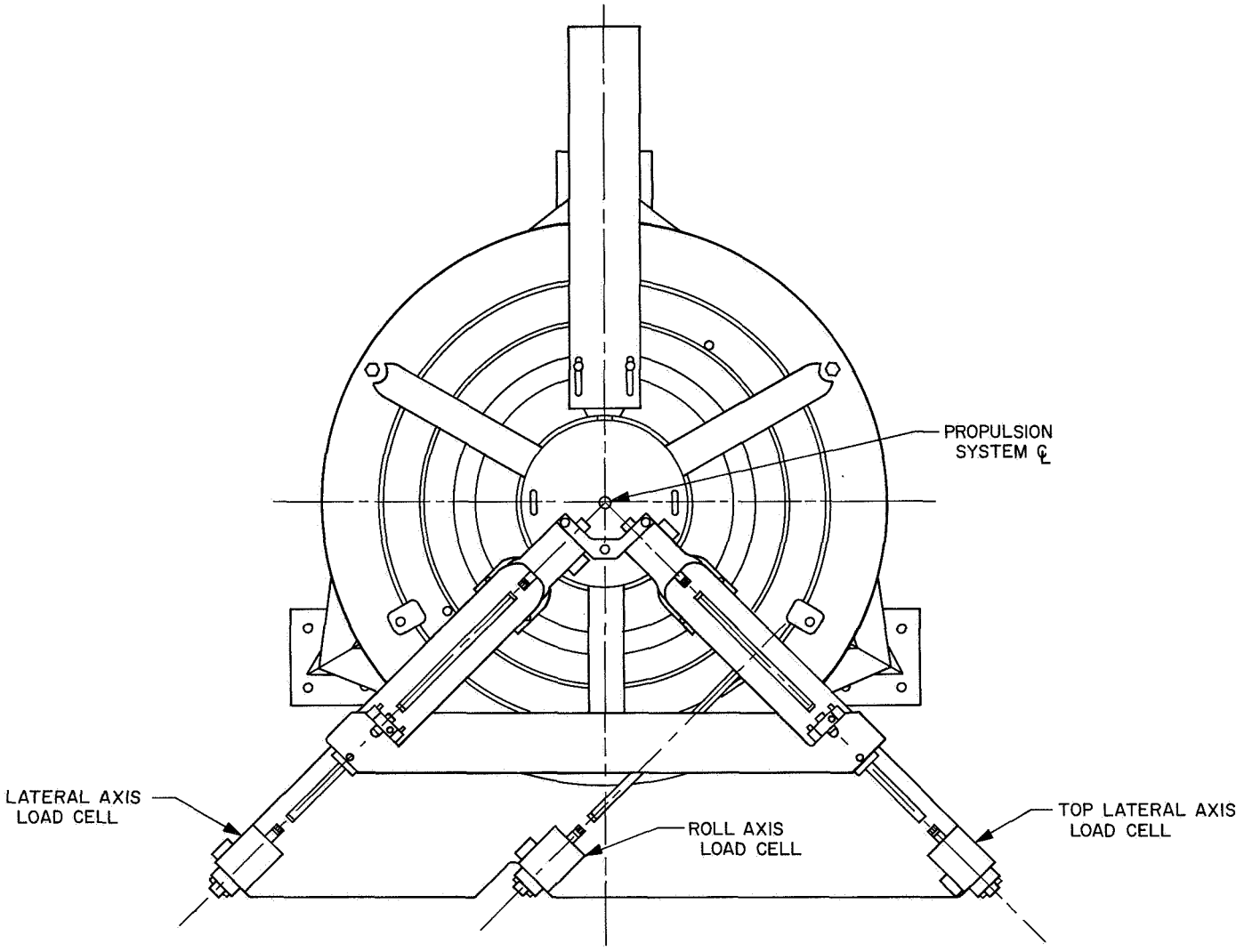


Fig. VII-8. Six-component test stand, top view

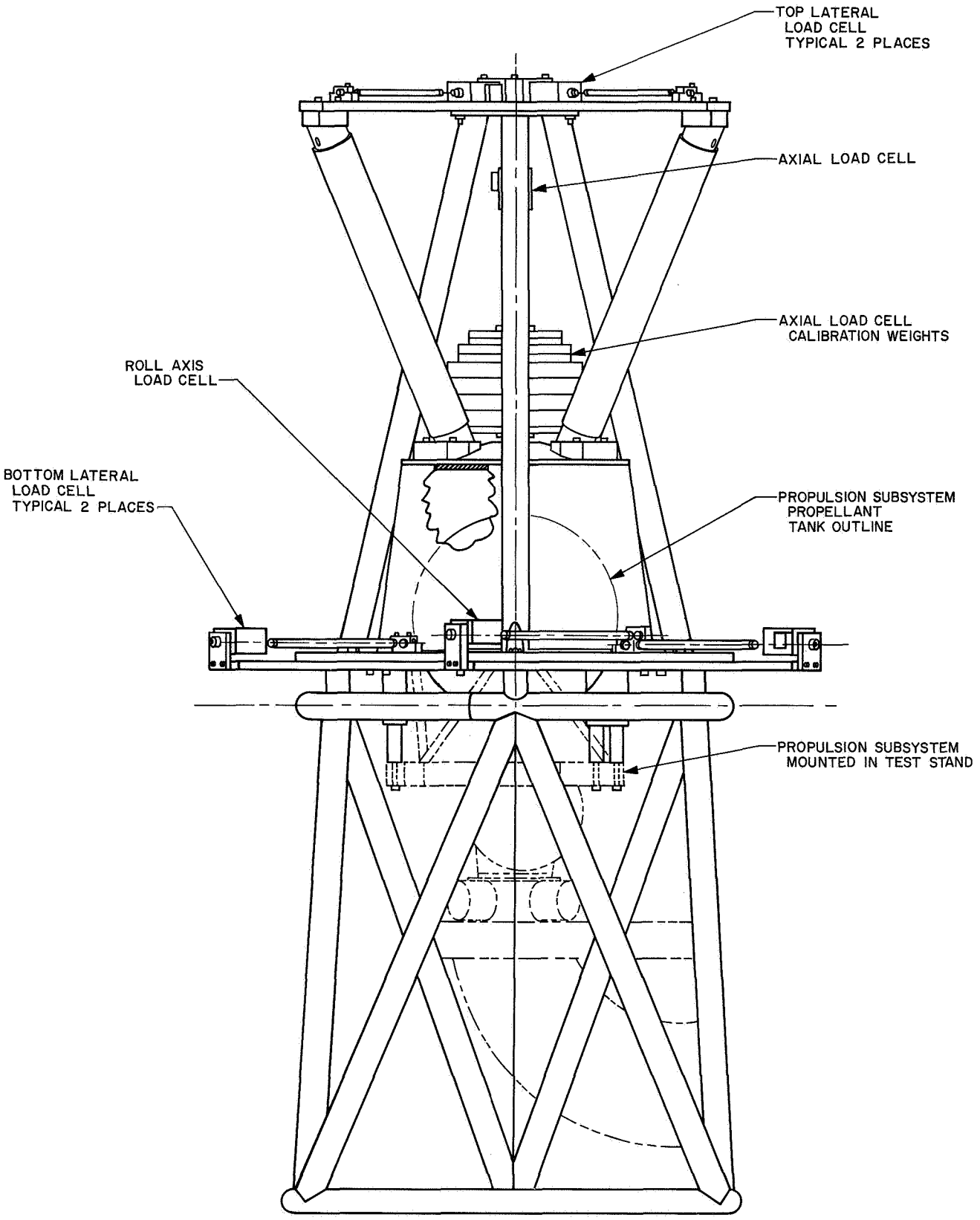


Fig. VII-9. Six-component test stand, side view

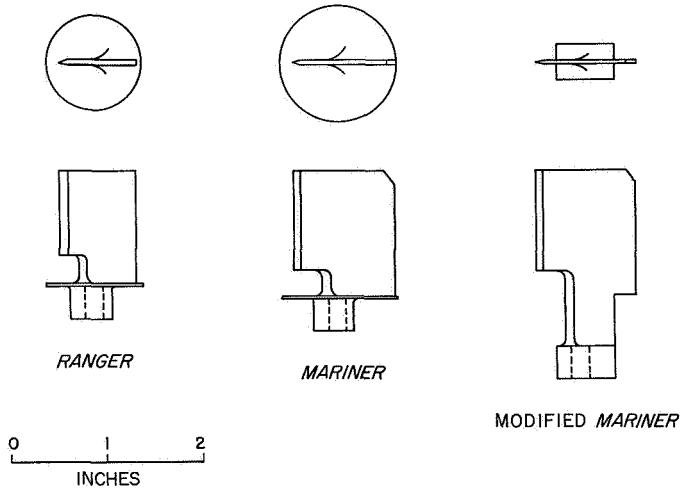


Fig. VII-10. Jet vanes (full scale)

This second test was designed to measure any interaction between vanes in the rocket exhaust. The vanes were again programmed through a series of deflections, forces, and moments generated as a result of vane deflection, and were measured along with vane positions. This test disclosed that extraneous forces were being generated proportional to the square of vane-deflection angle. These forces were normal to the lift force produced by the vane and along the axis of rotation of the vane in the outboard direction (i.e., toward the outside of the motor). These forces had been theoretically predicted, but until the development of the six-component stand, there was no method of verifying their existence. Because the jet vanes for *Mariner V* were scaled-up versions of the *Ranger* jet vanes (Fig. VII-10 shows a comparison of the vanes), a third test was scheduled to determine whether the scaling up had produced vane-to-vane interaction in the rocket

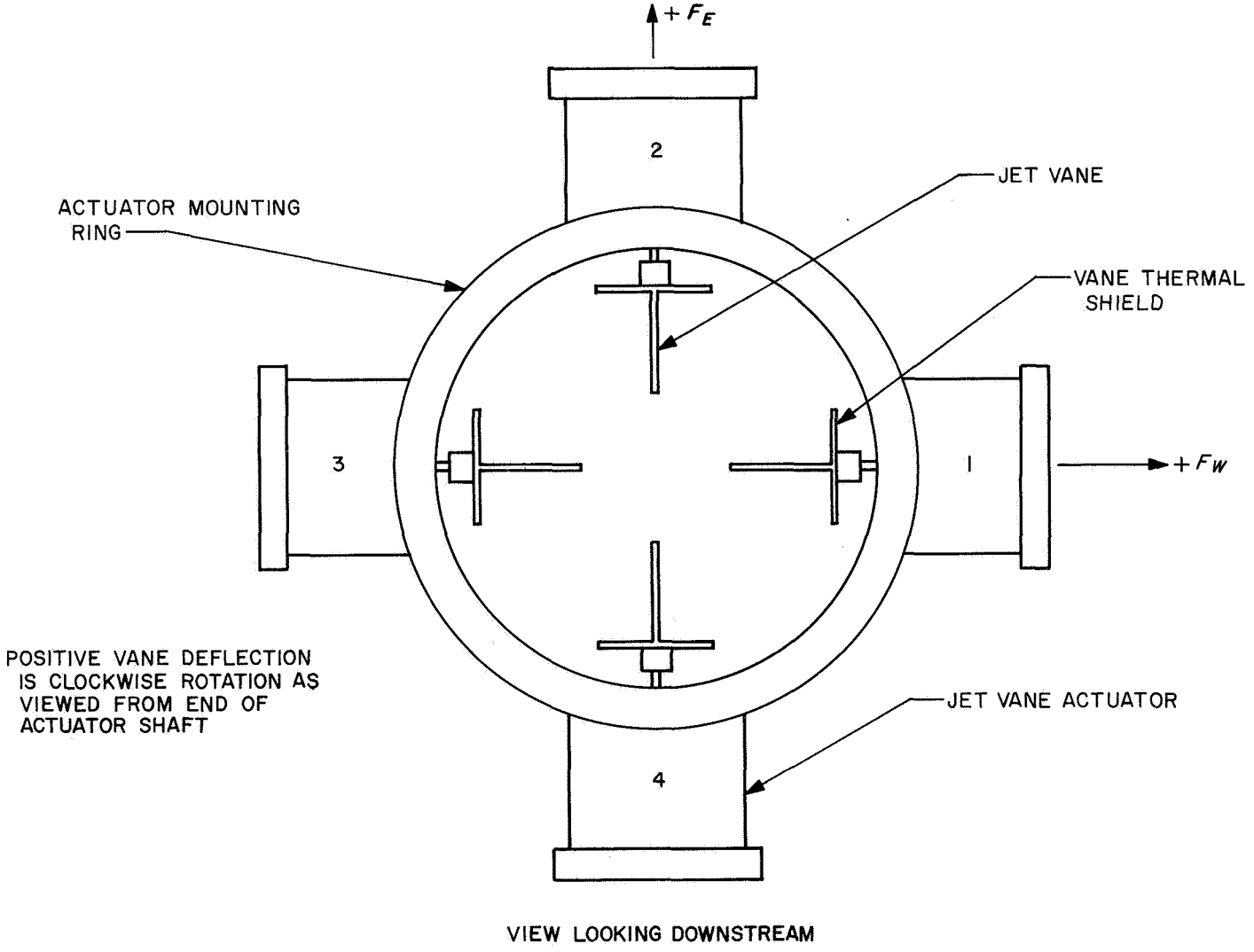


Fig. VII-11. Sign conventions for vane-produced forces

exhaust. The results of this test were similar to those of the previous test, and are shown in Figs. VII-11–VII-13. Figure VII-11 shows the jet-vane positions and force-measurement conventions. Normally, rotation of vanes 1 and 3 should produce F_E forces; vanes 2 and 4 produce F_W forces. Figure VII-12 shows the actual forces produced, and Fig. VII-13 shows the transfer characteristics derived from the test. The only difference in results from tests 2 and 3 was caused by the area difference between *Mariner* and *Ranger* jet vanes: the lift, drag, and side forces generated as a function of deflection angle scaled directly with vane area.

The next test used two modified *Mariner* vanes (see Fig. VII-10). The thermal shield was removed from the vane in an effort to reduce the area available for side-force generation. An important consideration in eliminating these shields was *hot spot* generation on the actuator shaft and vane mounting surfaces, but the test results showed that these areas were actually cooler during the firing because of the less turbulent flow. The side forces were not materially reduced by the elimination of the shield, however.

The fifth test used a single, unmodified *Mariner* vane to determine whether the side forces were a result of vane-to-vane interaction or vane-to-ring interaction. Test results were the same as those of the second test, proving that the side forces were being generated on the ring as a result of an aerodynamic shock wave generated at the edge of the vane. The final test in the series used the two modified *Mariner* vanes and a 1-in. larger diameter ring to determine whether the larger ring would reduce the side forces. The results showed that the forces were reduced to approximately one-third of the original value.

Figures VII-14–VII-16 show the *Mariner* thrust-vector control assembly before and after modification. Figures VII-14 and VII-15 show the thrust-vector control assembly looking downstream, in the direction of the exhaust.

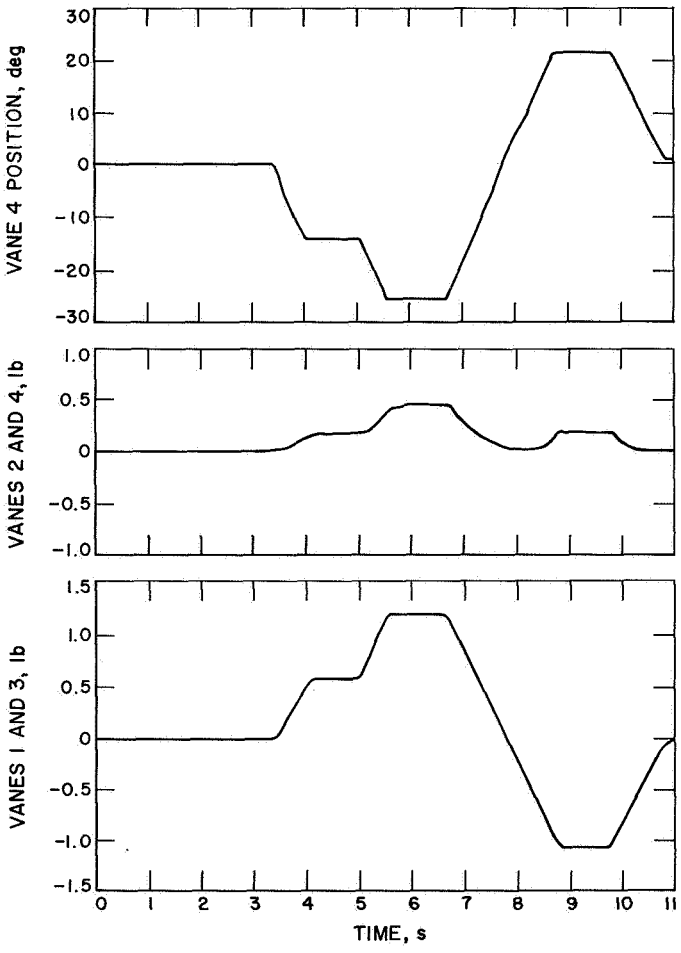


Fig. VII-12. Autopilot interaction test of *Ranger* jet vanes

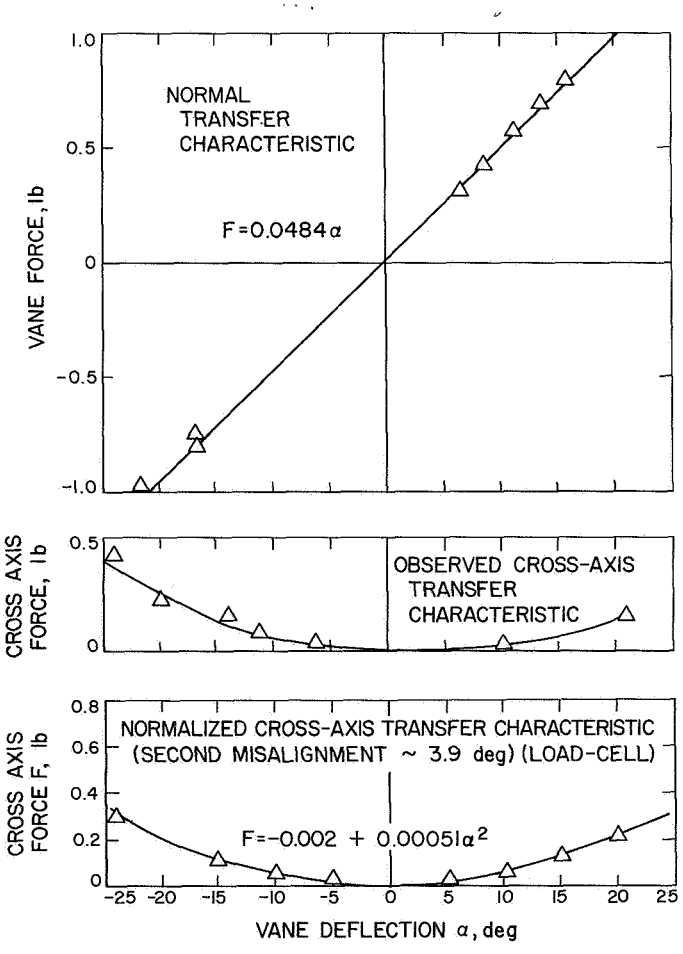


Fig. VII-13. Transfer characteristics of *Ranger* jet vanes

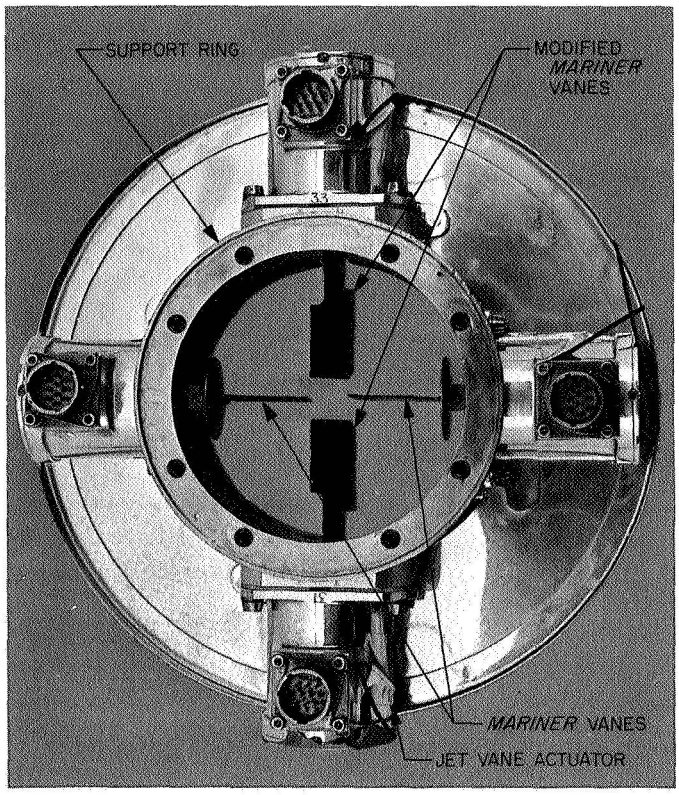


Fig. VII-14. *Mariner V* thrust vector control assembly

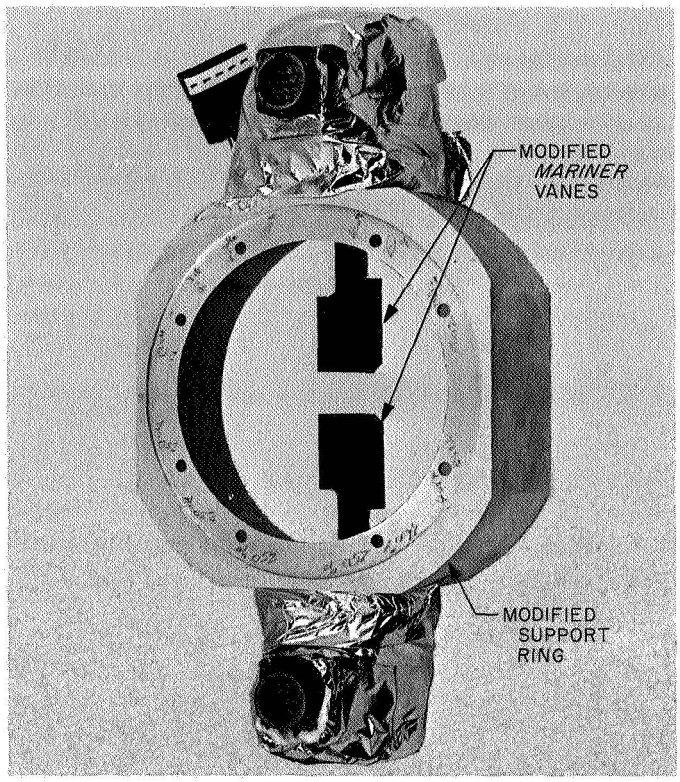


Fig. VII-15. Modified *Mariner V* thrust vector control assembly (only two actuators mounted)

Figure VII-16 shows the larger ring, looking into the exhaust.

When the effects of the side forces were included in the autopilot simulation, the observed gyro telemetry during the midcourse maneuver still could not be duplicated. Failure-mode simulations were made with such obvious failures as a failed mix-matrix resistor, open JVA winding or feedback potentiometer, closed-loop gain degradation, and others, but no solutions resulted in the apparent slow oscillation about the motor axis experienced by the *Mariner V* autopilot. A simulation of the first and second midcourse maneuvers of the *Mariner IV* spacecraft was performed, with results closely approximating the telemetered data, verifying that the autopilot program and simulation were basically correct.

5. Conclusions and recommendations. The following conclusions can be drawn from the investigations, analyses, and tests described:

(1) The midcourse maneuver was anomalous, as evidenced by trajectory analysis, because the commanded velocity increment was not achieved within the allotted error distribution.

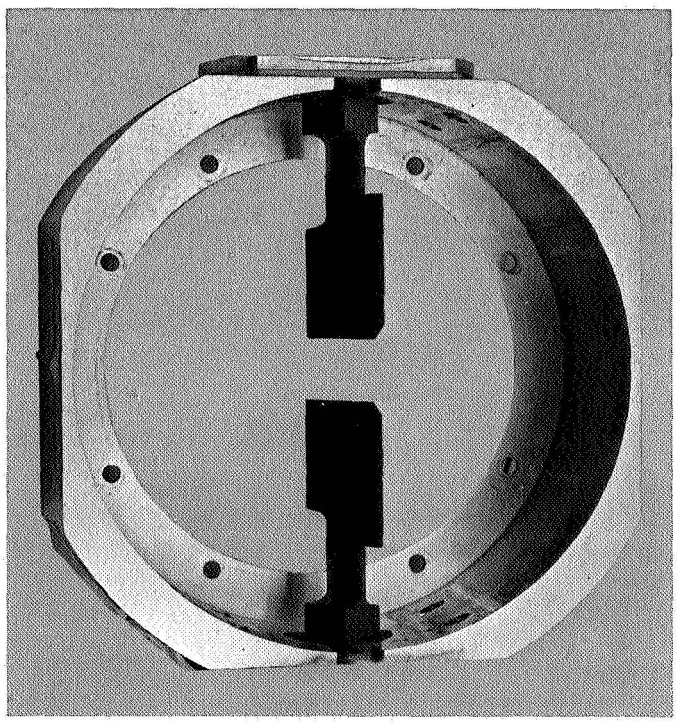


Fig. VII-16. Modified *Mariner V* thrust vector control assembly (view looking up engine nozzle)

(2) The postinjection propulsion subsystem (PIPS) performed substantially as predicted, as verified by data obtained from telemetry and analysis of subsystem performance.

(3) The pyrotechnics subsystem performed without anomaly, as evidenced by received telemetry data and propulsion subsystem performance.

(4) The autopilot performed its functions of maintaining spacecraft stability and pointing accuracy, as verified by postmaneuver trajectory analysis.

(5) An unexpected drag force, produced by excessive deflection of the jet vanes in the PIPS exhaust stream, reduced the magnitude of the thrust vector and thus the commanded velocity increment, creating the anomaly.

(6) The causes of the excessive vane deflections were a combination appreciable side forces, produced by large vane deflections, and an unspecified failure in the autopilot control loop that prevented adequate compensation within the loop for these side forces; thus, an oscillatory condition was allowed to exist.

(7) The side forces can be materially reduced by increasing the diameter of the JVA mounting ring.

(8) The thermal shields on the jet vanes are not necessary for thermal protection of the actuator shaft and vane mounting areas, and, in fact, are undesirable.

The following recommendations are made on the basis of the investigations, analyses, and tests described, including recommendations that would materially improve the capability of analyzing the in-flight performance of the autopilot:

(1) Enlarge the diameter of the JVA mounting ring by a minimum of 1 in. to reduce the magnitude of the side forces generated by jet-vane deflection.

(2) Eliminate the thermal shields from the jet vanes to allow the actuator shaft to operate at a lower temperature during the motor burn.

(3) Provide telemetry of the jet-vane position during the motor-burn portion of the maneuver.

(4) Increase the resolution of the gyro-output telemetry to a minimum of 0.10 $\pm$0.05 V during the motor-burn portion of the maneuver.

(5) Increase the data rate of gyro and jet-vane-position outputs to a minimum of one sample every 2.1 s during the motor-burn portion of the maneuver.

Appendix A

Project Organization and Management

A. Structure

Key function and responsibility assignments for accomplishing mission activities during flight and encounter of *Mariner V* spacecraft were essentially the same as those discussed at length in the companion volume of this report. The organization was adjusted to give greater emphasis to flight analysis and operations activities. Many individuals who formerly had a development role were reassigned to support the flight phase. Significantly, an information function was added to keep the public adequately informed of this phase of the mission. The interface with the public information offices grew in proportion to the mission's success. The basic relationships among major supporting elements are diagrammed in Figs. A-1 and A-2.

In the area of temporary and special organizations, most noteworthy was the Encounter Planning Working Group, organized after the maneuver activities with a large representation of spacecraft performance analysis and command (SPAC), and occultation personnel. The group met regularly to analyze all facets of encounter until an optimum plan and sequence were evolved and alternates were understood. Contingency planning for nonstandard modes of operation was stressed.

B. Implementation

A similar management structure and approach were used for this phase of the mission as were applied to the flight phases of the *Mariner* Mars 1964 mission. Methods and techniques for direction and control of the effort were refined and improved from those of the earlier mission. The flight of the *Mariner V* spacecraft had few deviations from the standard events and sequences that were developed before launch. As a result, the mission was controlled and monitored easily. Also, there were few changes in the ground configuration and capability. Changes consisted primarily of refining computer programs and convenience items for operating personnel.

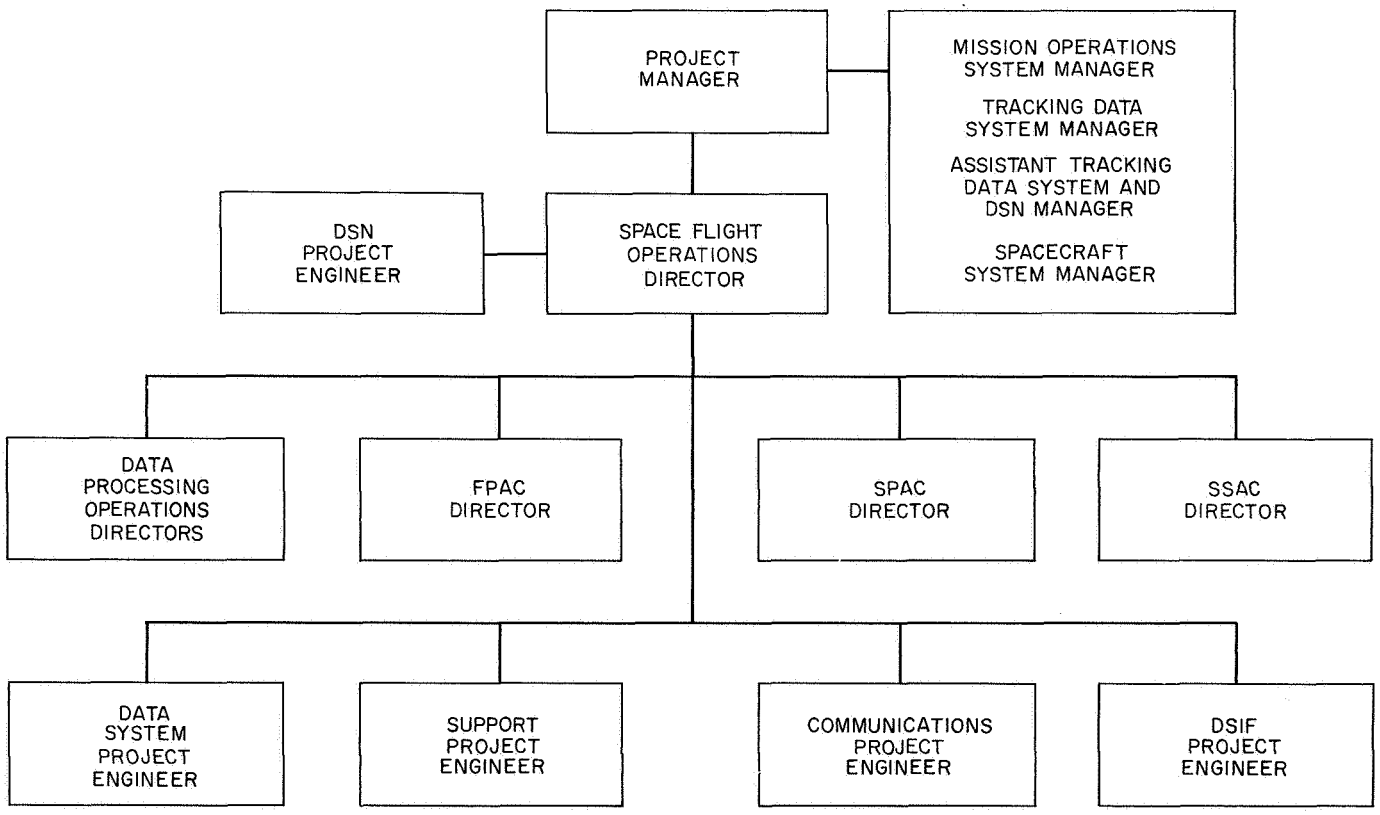


Fig. A-1. Key elements of the *Mariner V* Space Flight Operations organization (conventional structure)

The project exploited the companion *Mariner* Mars 1964 mission to the fullest extent practical, gaining experience and perfecting procedures applicable to the *Mariner V* spacecraft. The generation of test plans was required for all similar special sequences and investigations. The criteria for evaluating these plans were the protection of encounter and minimum jeopardy to the spacecraft.

Four notable situations deviated from the ideal mission. Two of these were flight anomalies and resulted in intensive investigations. These are the UV instrument performance and the midcourse results, which are discussed in Section VI. The third area was the availability, late in the mission, of a technique to attempt recording of bistatic radio reflections from the surface of the planet. The attendant modification of the 210-ft antenna at Goldstone was made on a carefully controlled schedule, structured to protect the prime encounter station for the flyby events. The fourth item was caused by the heavy loading of the Deep Space Network (DSN) during 1967 with other missions. As a result, project personnel had to avoid possible confusion with other flight operations and had to maintain clear priorities.

Another area of possible difficulty resulted from the two flights being handled simultaneously by one group of people. Nevertheless, no degradation occurred to either mission. The problem and failure reporting system used during pre-launch activities was applied again to record and to alleviate exceptions to nominal flight performance. Although the problem list (P-list) system was available to flag troubles, it was not needed.

C. Status Reporting

The absolute irrevocability of flight events imposed even more stringent demands on the precision and thoroughness of scheduling than did the pre-liftoff events; e.g., encounter necessitated more exact timetable adherence than did countdown. Obviously, encounter could not be postponed two days, as the launch was.

The success of the mission shows that the design and execution of the schedules were effective. The schedules are shown graphically in Figs. A-3 and A-4. The obvious exception is the master data library generation which clearly is not a series element in real-time actions.

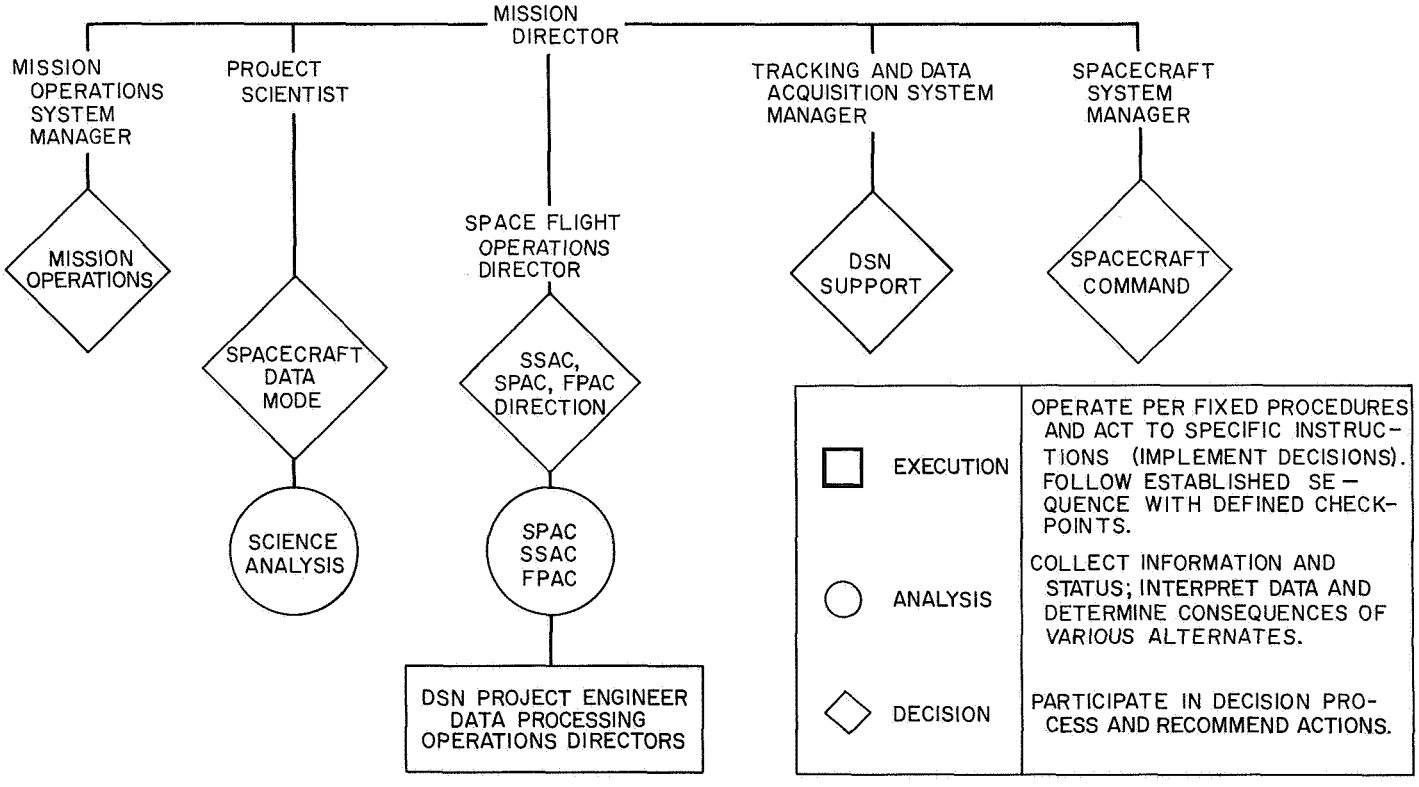
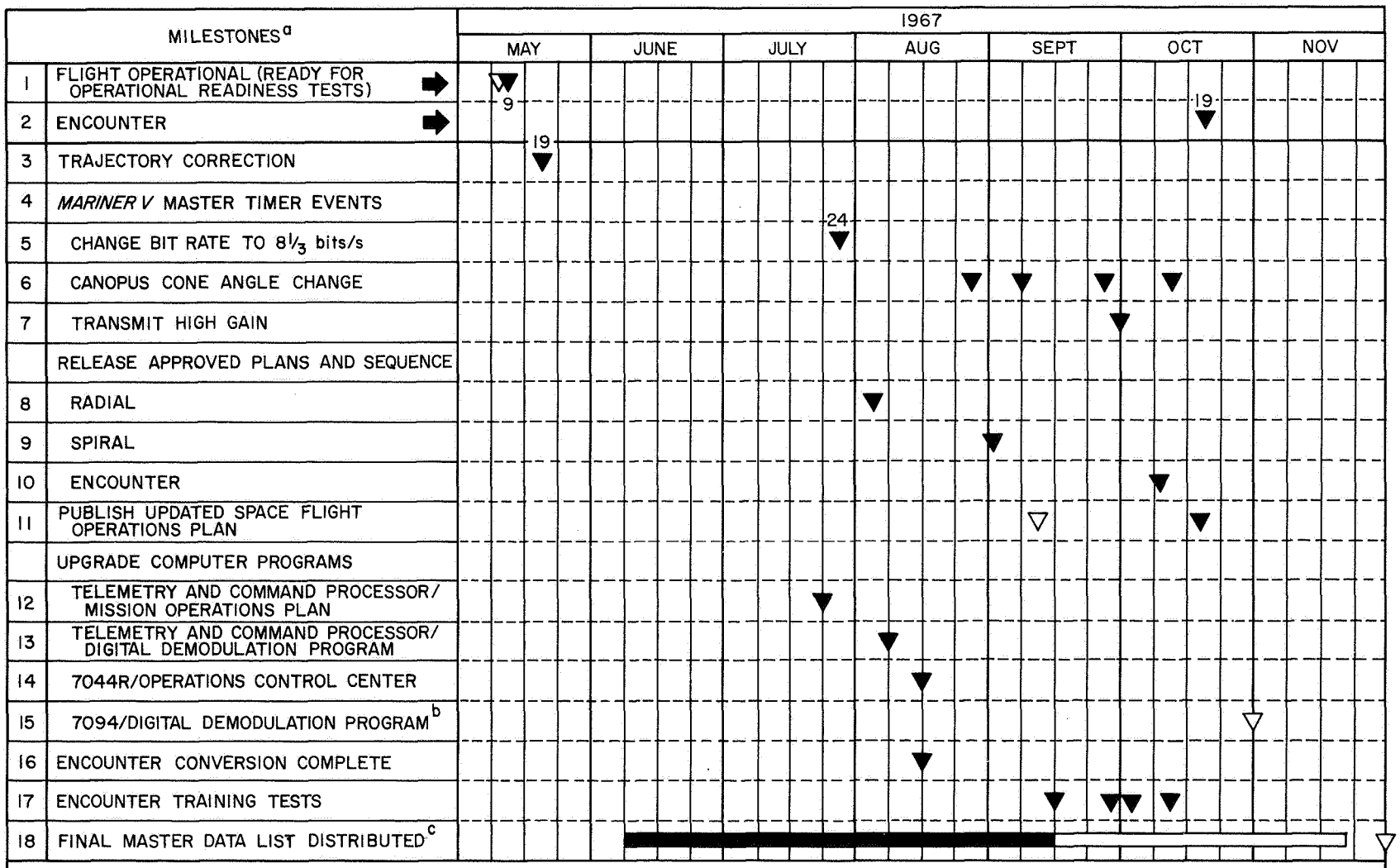


Fig. A-2. Space Flight Operations functional arrangement

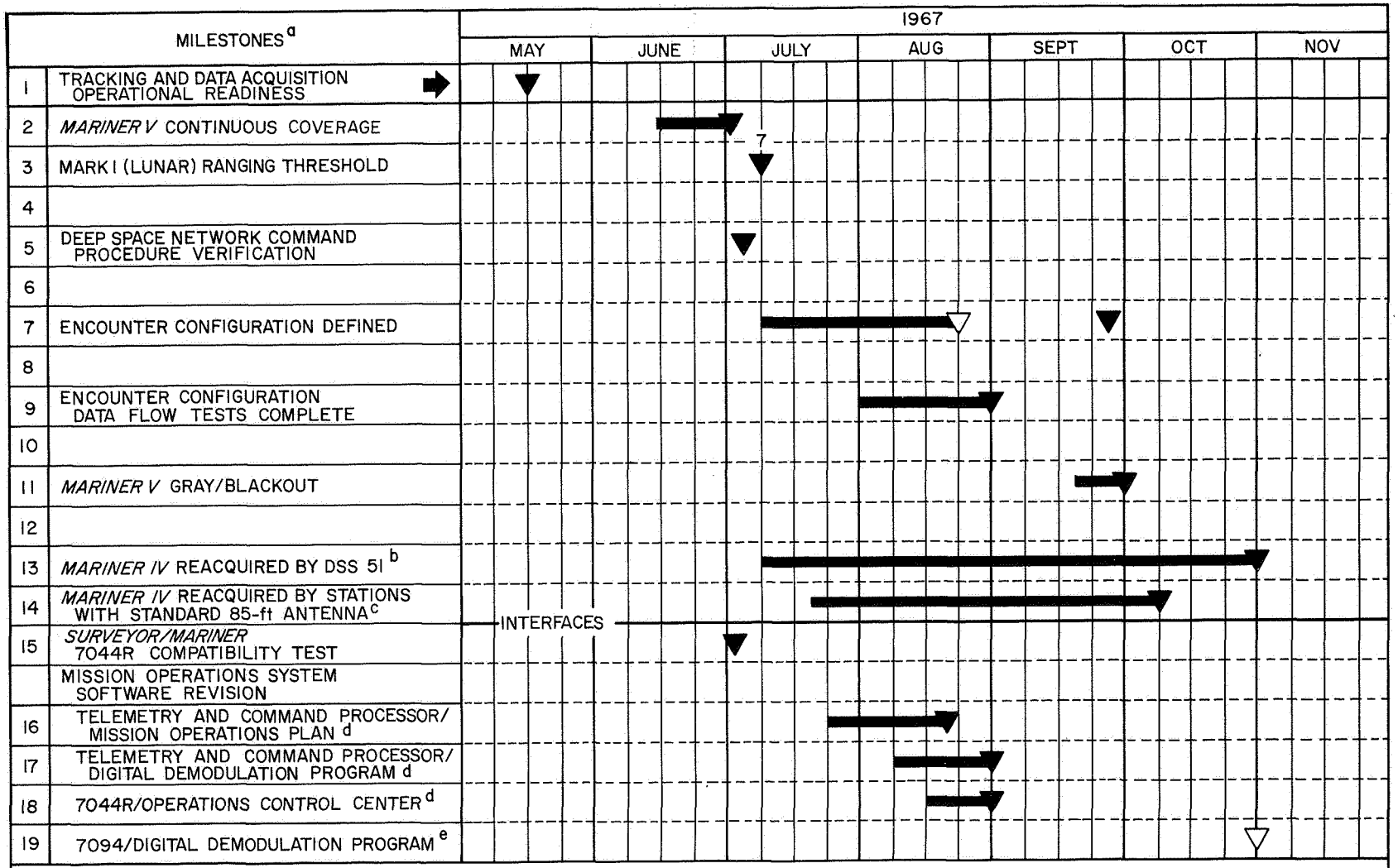


[a] STATUS AS OF JANUARY 17, 1968.

[b] TO BE PRODUCED ON A BEST-EFFORTS BASIS.

[c] MASTER DATA LIST COMPLETION SCHEDULE BASED UPON INITIAL END OF MISSION DEFINITION, i.e., EARLIER OF ENCOUNTER PLUS TWO PLAYBACKS, OR 10 DAYS.

Fig. A-3. *Mariner* Venus 67 project—Mission Operations System schedule



	MILESTONES[a]
1	TRACKING AND DATA ACQUISITION OPERATIONAL READINESS
2	*MARINER V* CONTINUOUS COVERAGE
3	MARK I (LUNAR) RANGING THRESHOLD
4	
5	DEEP SPACE NETWORK COMMAND PROCEDURE VERIFICATION
6	
7	ENCOUNTER CONFIGURATION DEFINED
8	
9	ENCOUNTER CONFIGURATION DATA FLOW TESTS COMPLETE
10	
11	*MARINER V* GRAY/BLACKOUT
12	
13	*MARINER IV* REACQUIRED BY DSS 51[b]
14	*MARINER IV* REACQUIRED BY STATIONS WITH STANDARD 85-ft ANTENNA[c]
15	*SURVEYOR/MARINER* 7044R COMPATIBILITY TEST
	MISSION OPERATIONS SYSTEM SOFTWARE REVISION
16	TELEMETRY AND COMMAND PROCESSOR/ MISSION OPERATIONS PLAN[d]
17	TELEMETRY AND COMMAND PROCESSOR/ DIGITAL DEMODULATION PROGRAM[d]
18	7044R/OPERATIONS CONTROL CENTER[d]
19	7094/DIGITAL DEMODULATION PROGRAM[e]

[a] STATUS AS OF JANUARY 17, 1968.

[b] INCLUDES ABOUT 1 mo OF DEGRADED DATA AT EACH END OF PERIOD.

[c] STANDARD 85-ft COVERAGE EXTENDED INDEFINITELY BY PLACING SPACECRAFT ON ROLL INERTIAL CONTROL.

[d] TESTING AND OPERATIONAL USE.

[e] TO BE PRODUCED ON A BEST-EFFORTS BASIS.

Fig. A-4. *Mariner* Venus 67 project—tracking and data system schedule

Test critiques and reviews were effective techniques used to ensure that problems were receiving proper attention. These techniques were stressed during reviews of this phase of the project internally and by laboratory management, and NASA Headquarters, as shown in Table A-1.

Unless superseded by more important reviews, weekly meetings of the project representatives were held. In addition, daily flight operations briefings were conducted. Unusual spacecraft or science activities were discussed in these sessions. The briefings were documented in daily technical bulletins, which were distributed to JPL management and to NASA Headquarters. Summary flash sheets were issued weekly to keep all JPL personnel informed of developments on both missions.

D. Documentation

The pattern of documentation for this mission closely parallels the approach used for *Mariner* Mars 1964. Two distinct levels were used. The first and critical group included the material needed in real time by operating personnel for conduct of flight activities. At the same time, comparable information was released to keep management and the public informed. These publications contained simple illustrations to depict the time sensitivity and functioning of the complex world-wide system employed during critical mission phases. Hence, these publications were not as exact and complete as the working-level documents.

Table A-1. Major review sessions

Date 1967	Subject	Location
Aug 3 to 4	Midmission review	NASA Hq
Oct 4	Encounter readiness	JPL
Dec 13 to 14	Postencounter review	NASA Hq

Appendix B

Encounter Sequence and Command Descriptions

A. Encounter Summary

Encounter operations started with the transmission of direct command DC-V25 at 02:49:00 GMT, October 19, 1967, and continued through completion of the second playback, which occurred on October 23, 1967, at approximately 07:04:48 GMT.

1. Commands. Table B-1 lists all of the commands, the function of each command, and the octal value of each command.

2. Two-way transmission times. Figure B-1 is a graph of the two-way transmission times vs flight time during the period of time bracketing encounter.

3. Nominal sequence of events. Table B-2 presents the sequence of events of the *Mariner* Venus 67 mission for the encounter phase on October 12, 1967. This sequence of events included all major events compiled by the spacecraft performance analysis and command teams, the Deep Space Network, and the Mission Operations System.

The sequence started with those activities required prior to encounter for checking out and verifying those systems required for encounter. The sequence terminated following completion of the second playback.

Table B-1. *Mariner V* command list

Name	Description	Octal
DC-V1	Command telemetry mode 1	6030
DC-V2	Command telemetry mode 2 (turn on science)	6332
DC-V3	Track change command	6530
DC-V4	Command telemetry mode 4	6350
DC-V5	Command switch data rate	6050
DC-V6	Command switch A/DC–PNG[a]	6060
DC-V7	Switch power amplifiers	6110
DC-V8	Switch exciters	6652
DC-V9	Switch ranging	6632
DC-V10	Transmit high–receive low	6600
DC-V11	Transmit high–receive high	6560
DC-V12	Transmit low–receive low	6550
DC-V13	Maneuver command inhibit. Inhibit propulsion command (turn on Canopus sensor and attitude control)	6270
DC-V14	Remove maneuver inhibit. Remove propulsion inhibit (resets DC-V13)	6240
DC-V15	Canopus gate inhibit override	6140
DC-V16	Start encounter backup clock	6500
DC-V17	Cycle Canopus cone angle	6210
DC-V18	Gyros on—inertial control (second DC-V18—roll positive increment)	6440
DC-V19	Gyros off—normal control (resets DC-V15, DC-V18, and DC-V20)	6420
DC-V20	Remove roll control	6740
DC-V21	Roll override—negative increment	6720
DC-V22	Antenna pointing angle change	6710
DC-V23	Arm second propulsion maneuver	6170
DC-V24	Begin DAS[b] encounter mode (switch to data mode 3) (planet sensor power on) (switch plasma probe to mode 3)	6410
DC-V25	Science on, overload inhibit override—begin encounter sequence (tape recorder power on) (energize terminator sensor) (battery charger to boost mode)	6220
DC-V26	Turn off science (battery charger to boost mode)	6360
DC-V27	Initiate midcourse maneuver	6470
DC-V28	Switch battery charger (tape recorder electronics off)	6662
DC-V29	Arm first propulsion maneuver	6120
QC-V1	Maneuver command bits to CC&S[c]	
QC-V1-1	(Pitch turn duration)	6303-2
QC-V1-2	(Roll turn duration)	6300-1
QC-V1-3	(Motor burn duration)	6302-3

[a]A/DC = Analog-to-digital converter; PNG = pseudonoise generator.

Table B-1 (contd)

[b]DAS = Data automation system.
[c]CC&S = Central computer and sequencer.

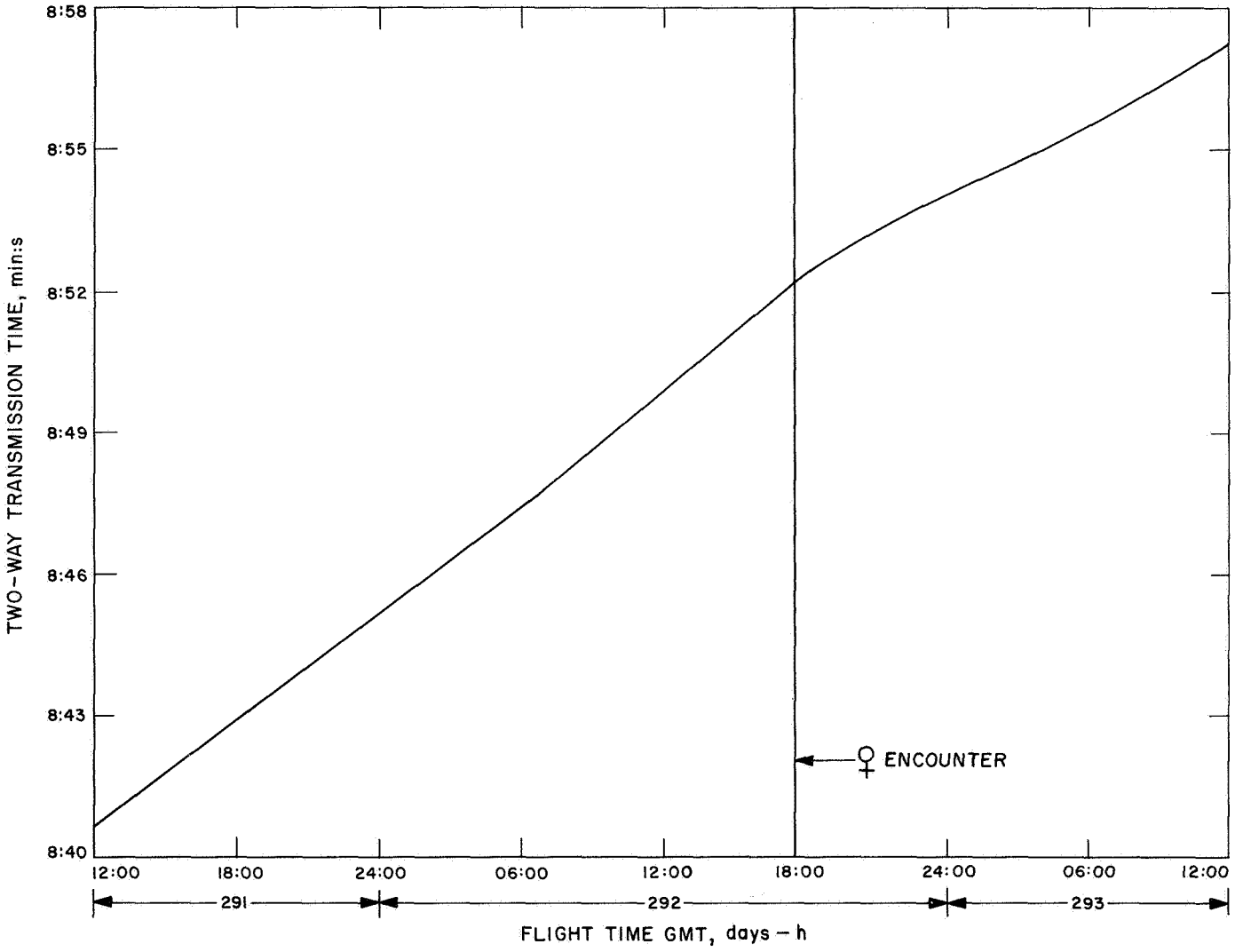


Fig. B-1. Two-way transmission time vs flight time

Table B-2. Sequence of events for *Mariner* Venus 67 encounter

ITEM	TIME	STA.	REPORT BY-TO	NET	EVENT	CHECK WHEN COMPLETE	LINE
1.0.	E- 14D	SUPT			.1. TECHNICAL AREA ASSISTANTS CHECK SUPPLIES AND ORDER THOSE THAT WILL BE REQUIRED IN SUPPORT OF ENCOUNTER		1.
							2.
							3.
							4.
1.1.		COMM			.1. ORDER NECESSARY PAPER, TAPE, RIBBONS, AND AUDIO RECORDING TAPE.		5.
							6.
							7.
					.2. NOTIFY PT+T, JPL PBX, WESTERN UNION MICROWAVE REGARDING PERSONNEL SUPPORT FOR ENCOUNTER COVERAGE.		8.
							9.
							10.
							11.
1.2.		MAR CH.			.1. ADVISE SUPPORT CHIEF OF ACCESS CONTROL REQUIREMENTS		12.
							13.
							14.
2.0.	E- 13D	SUPT			.1. PUBLISH IOM TO SECTION 713 SPECIFYING DATES AND TIMES OF STANDBY GENERATOR COVERAGE		15.
							16.
							17.
					.2. PUBLISH IOM TO EMPLOYEE SERVICE DEFINING CAFETERIA SUPPORT REQ'D.		18.
							19.
							20.
					.3. PUBLISH IOM TO SECURITY REQUESTING GUARDS FOR ACCESS CONTROL IN THE SFOF		21.
							22.
							23.
					.4. ARRANGE FOR SPECIAL TRANSPORTATION.(IF REQ'D)		24.
							25.
3.0.	E- 10D	COMM			.1. REQUEST SPECIAL COVERAGE FROM NNSG/GSFC		26.
					.2. PREPARE FOR PLANT CHECKOUT		27.
							28.
4.0.	E- 9D	COMM			.1. BEGIN PLANT CHECKOUT, ALL MARINER SYSTEMS		29.
							30.
4.1.		MAR CH.			.1. SUBMIT DISPLAY REQUIREMENTS TO DSM P.E.		31.
							32.
5.0.	E- 8D	COMM			.1. RUN SYSTEM TESTS- GTS MICROWAVE,AND DSS HSD		33.
							34.
5.0.	E- 7D	MAR CH.			.1. SUBMIT ACCESS LIST FOR ALL MISSION DEPENDENT PERSONNEL TO SUPPORT		35.
							36.
							37.
6.1.		SFOF MGR			.1. PUBLISH SFOF FREEZE DATES AND HOURS		38.
							39.

Table B-2 (contd)

ITEM	TIME	STA.	REPORT BY-TO	NET	EVENT	CHECK WHEN COMPLETE	LINE
6.2.		DSIF MGR			.1. PUBLISH DSIF FREEZE DATES AND HOURS		40. 41.
6.3.		COMM			.1. RECEIVE NNSG/GSFC CONFIRMATION OF COMMUNICATION CIRCUITS AND SPECIAL COVERAGE .2. CONFIRM MICROWAVE AND PT+T SPECIAL COVERAGE		42. 43. 44. 45.
7.0.	E- 6D	COMM			.1. PLANT CHECKOUT COMPLETE		46. 47.
7.1.		DSIF			.1. REPORT DSIF STATUS AT DSN STATUS MEETING		48. 49.
7.2.		COMM			.1. REPORT COMM STATUS AT DSN STATUS MEETING .2. TWX ENCOUNTER CIRCUIT SCHEDULE TO SUPPORTING DSS .3. PLANT FREEZE		50. 51. 52. 53. 54. 55. 56.
7.3.		DPS			.1. REPORT DPS STATUS AT DSN STATUS MEETING		57. 58.
7.4.		SUPT			.1. REPORT FACILITY STATUS AT DSN STATUS MEETING .2. CHECK DISPLAY FOR CORRECT INFORMATION .3. REAL TIME DATA DISTRIBUTION IS IN EFFECT PER SOP NO. MV72-403		59. 60. 61. 62. 63. 64. 65.
7.5.		DSN			.1. REPORT DSN STATUS AT PROJECT STATUS MEETING		66. 67.
8.0.	289D 3H13M25S	DSS-61			.1. DSS-61 AOS		68. 69. 70.
9.0.	289D 3H30M	TRACK	TKCH 62.	DSS-62	.1. REQUEST STATION TO TURN ON TRANSMITTER AND REPORT XMTR ON TIME TO MAR CHIEF		71. 72. 73.
9.1.		MAR CH.			.1. PREPARE DC-V9 COMMAND MESSAGE AND DELIVER TO TRACK CHIEF.		74. 75. 76.

Table B-2 (contd)

ITEM	TIME	STA.	REPORT BY-TO	NET	EVENT	CHECK WHEN COMPLETE	LINE
10.0.	289D 3H40M	SPAC	BC ACE5.	VAL-PRIME	.1. VERIFY TWO-WAY RF LOCK		77.
							78.
11.0.	289D 3H42M	MAR CH. TR CH DSS-62.		FAC-PRIME	.1. BEGIN COMMAND READINESS PROCEDURES		79. 80. 81. 82.
11.1.		SPAC	BC ACE5.	VAL-PRIME	.1. REQUEST S/C SPE TO BE ADJUSTED (IF REQUIRED)		83. 84. 85.
12.0.	289D 3H43M	SPAC	BC ACE5.	VAL-PRIME	.1. PROVIDE RWV BF VALUE		86. 87.
13.0.	289D 3H52M	ACE-5	ACE5 BC.	VAL-PRIME	.1. REPORT COMMAND MOD ON TIME		88. 89.
14.0.	289D 4H 2M	SPAC	BC ACE5.	VAL-PRIME	.1. REPORT COMMAND STATUS		90. 91.
15.0.	289D 4H20M	SPAC	BC ACE5.	VAL-PRIME	.1. REPORT S/C READY FOR COMMAND		92. 93.
15.1.		MAR CH. TRACK DSS-62.		MAR COMMAND	.1. PERFORM DCV COMMAND PROCEDURE		94. 95. 96. 97.
16.0.	289D 4H38M	SPAC	BC ACE5.	VAL-PRIME	.1. REPORT SPACECRAFT STATUS FOR COMMAND		98. 99.
17.0.	289D 4H40M	DSS-62.			.1. TRANSMIT DC-V9		100. 101.
18.0.	289D 4H42M	ACE-5	ACE5 BC.	VAL-PRIME	.1. REPORT COMMAND INITIATE AND COMPLETION TIMES		102. 103.
19.0.	289D 4H52M	SPAC	BC ACE5.	VAL-PRIME	.1. REPORT SPACECRAFT STATUS		104. 105.
					.2. REQUEST REMOVAL OF COMMAND MODULATION GIVE TIME		106. 107. 108.
20.0.	289D 4H53M	MAR CH.	MRCH TKCH.	MAR COMMAND	.1. REMOVE COMMAND MODULATION AT .....Z.		109. 110. 111.

Table B-2 (contd)

ITEM	TIME	STA.	REPORT BY-TO	NET	EVENT	CHECK WHEN COMPLETE	LINE
21.0.	289D 4H56M	ACE-5	ACE5 BC.	VAL-PRIME	.1. REPORT REMOVAL OF COMMAND MODULATION. GIVE TIME		112. 113. 114.
22.0.	289D11H34M	SUPT			.1. CHECK ALL FIRST FLOOR DISPLAYS INCORPORATING DDU FOR CORRECT OPERATION		115. 116. 117.
					.2. CHECKOUT AND VERIFY THE OPERATION OF A. EIDOPHOR PROJECTOR B. MISSION EVENTS PROJECTOR C. TELEPROMPTER PROJECTORS		118. 119. 120. 121. 122.
					.3. RECEIVE STANDBY ELECTRICIANS NAME AND WORK SCHEDULE		123. 124. 125.
					.4. CHECK MISSION TIME FOR CORRECT INDICATIONS		126. 127.
23.0.	289D14H34M	COMM			.1. COMMENCE GO, NO/GO TESTS ON ALL EQUIPTMENT		128. 129.
23.1.	289D17H34M	FPAC			.1. RUN TDPX, ODGX, ODPM. GENERATE CURRENT BEST ORBIT.		130. 131. 132.
24.0.	290D 0H34M	COMM			.1. COMPLETE GO, NO/GO TESTS ON ALL EQUIPMENT.		133. 134.
25.0.	290D 4H	DPS			.1. START DPS/FSD SYSTEM DIAGNOSTICS		135. 136.
26.0.	290D14H	DPS			.1. COMPLETE DPS/FSD SYSTEM DIAGNOSTICS		137. 138.
					.2. START IBM P.M.		139. 140.
					.3. START TPS P.M.		141. 142.
					.4. START I/O P.M.		143. 144.
26.1.	290D17H34M	FPAC			.1. RUN PRDX FOR DSS-41, 62, 14, 12 FROM E-24H TO E+24H.		145. 146. 147.
					.2. RUN PRDX FOR DSS-42, 61, 11, 14 FROM E-24H TO E+24H.		148. 149. 150.

Table B-2 (contd)

ITEM	TIME	STA.	REPORT BY-TO	NET	EVENT	CHECK WHEN COMPLETE	LINE
27.0.	291D	DPS			.1. IBM P.M. COMPLETE		151.
							152.
					.2. TPS P.M. COMPLETE		153.
							154.
					.3. I/O P.M. COMPLETE		155.
							156.
					.4. START FINAL DPS/FSD SYSTEM DIAGNOSTICS		157.
							158.
28.0.	291D 1H49M 3S	DSS-51			.1. DSS-51 AOS		159.
							160.
29.0.	291D 3H12M47S	DSS-61			.1. DSS-61 AOS		161.
							162.
30.0.	291D 4H26M17S	DSS-42			.1. DSS-42 LOS		163.
							164.
31.0.	291D 5H34M51S	DSS-41			.1. DSS-41 LOS		165.
							166.
31.1.		FPAC			.1. RUN TDPX, ODGX, ODPM TO GENERATE CURRENT BEST ORBIT.		167. 168. 169.
32.0.	291D 6H	DPS			.1. DPS SYSTEM CHECKOUT COMPLETE		170.
							171.
33.0.	291D10H44M36S	DSS-12			.1. DSS-12 AOS		172.
							173.
34.0.	291D12H50M37S	DSS-51			.1. DSS-51 LOS		174.
							175.
35.0.	291D11H 9M16S	DSS-11			.1. DSS-11 AOS		176.
							177.
36.0.	291D15H 6M 8S	DSS-61			.1. DSS-61 LOS		178.
							179.
37.0.	291D17H34M	SUPT			.1. ADVISE ALL PERSONNEL THAT ACCESS CONTROL IS NOW IN EFFECT (VIA SFOF PAGE AND ENTER ON SFOF STATUS PHONE 354-6211)		180. 181. 182. 183.
38.0.	291D18H 3M 5S	DSS-42			.1. DSS-42 AOS.		184.
							185.

Table B-2 (contd)

ITEM	TIME	STA.	REPORT BY-TO	NET	EVENT	CHECK WHEN COMPLETE	LINE
39.0.	291D18H 6M14S.	DSS-41.			.1. DSS-41 AOS.		186.
		..					187.
40.0.	291D18H10M	.DSS-41.			.1. TRANSFER TWO-WAY LOCK FROM DSS-11 TO DSS-41		188.
		..					189.
41.0.	291D18H13M	.TRACK			.1. ADJUST GND XMTR VCO FOR TRACK SYN FREQ.		190.
		..					191.
42.0.	291D18H22M	.TRACK			.1. REPORT DSS-41 IN TWO-WAY WITH THE S/C		192.
		..					193.
43.0.	291D21H24M	.SUPT			.1. FACILITY WILL BE SWITCHED TO GENERATOR POWER IN TEN MINUTES		194.
							195.
							196.
44.0.	291D21H34M	.SUPT			.1. FACILITY SWITCHED TO GENERATOR POWER (E-20H)		197.
							198.
45.0.	291D22H 4M37S.	S/C			.1. RANGING TURNED OFF BY CY1-46 (E-19.5H)		199.
							200.
46.0.	291D22H45M58S.	DSS-11.			.1. GOLDSTONE LOS		201.
		12.					202.
		14.					203.
		..					204.
47.0.	291D23H30M	.DPS					205.
							206.
							207.
							208.
					.1. THE DPS TO BE COMPLETELY CHECKED OUT BY THIS TIME TO FULFILL THE MARINER PROJECT REQUIREMENT OF DUAL MODE II AT THIS TIME.		209.
							210.
							211.
							212.
							213.
							214.
							215.
							216.
48.0.	292D 0H45M	.OPS			.1. ALL SPAC/SSAC PERSONNEL ON STATION IN THE SFOF FOR ENCOUNTER.(FPAC PARTIALLY STAFFED)		217.
		TEAM.	ACE5.				218.
		.FPAC					219.
		.SPAC					220.
		.SSAC					221.
		.DACON					222.

Table B-2 (contd)

ITEM	TIME	STA.	REPORT BY-TO		NET	EVENT	CHECK WHEN COMPLETE	LINE.
49.0.	292D 1H20M	MAR CH.				1. BEGIN COMMAND READINESS PROCEDURES.		223.
		TK CH						224.
		DSS 41.						225.
								226.
49.1.		SPAC	BC	ACE5.	VAL-PRIME	1. REQUEST S/C SPE TO BE ADJUSTED (IF REQ'D)		227.
								228.
50.0.	292D 1H48M	DSS-51.				1. DSS-51 AOS		229.
								230.
51.0.	292D 1H50M	SPAC	BC	ACE5.	VAL PRIME	1. PROVIDE RWV 8F VALUE.		231.
								232.
52.0.	292D 2H	DSS-41.	TKCH	41.	DSS-41	1. TURN ON COMMAND MOD.		233.
								234.
53.0.	982D 2H 1M	ACE-5	ACE5	BC.	VAL-PRIME	1. REPORT COMMAND MOD. TURN ON TIME.		235.
								236.
54.0.	292D 2H 2M	MAR CH.				1. PREPARE DC-V25 COMMAND MESSAGE AND DELIVER TO TK CH.		237.
								238.
								239.
55.0.	292D 2H18M	SPAC	BC	ACE5.	VAL PRIME	1. VERIFY COMMAND IN LOCK.		240.
								241.
55.1.		MAR CH.	TKCH	MRCH.	MAR	1. PERFORM DC-V COMMAND PROCEDURE		242.
		TRACK			COMMAND			243.
		RWV DP.						244.
								245.
56.0.	292D 2H44M	SPAC	BC	ACE5.	VAL PRIME	1. REPORT S/C READY FOR COMMAND.		246.
								247.
57.0.	292D 2H47M	SPAC	BC	ACE5.	VAL-PRIME	1. REPORT SPACECRAFT STATUS FOR COMMAND.		248.
								249.
58.0.	292D 2H49M	DSS-41.				1. TRANSMIT DC-V25.		250.
								251.
58.1.	292D 2H50M11S	DSS-62.				1. DSS-62 AOS.		252.
								253.
59.0.	292D 2H50M36S	DSS-62.				1. DSS-62 AOS		254.
								255.
60.0.	292D 2H51M	ACE-5	ACE5	BC.	VAL-PRIME	1. REPORT INITIATE AND COMPLETION TIMES.		256.
								257.

Table B-2 (contd)

ITEM	TIME	STA.	REPORT BY-TO	NET	EVENT	CHECK WHEN COMPLETE	LINE
61.0.	292D 2H57M47S.				1. DC-V25 SEEN IN DATA.		258.
					BEGIN ENCOUNTER SEQUENCE		259.
					TAPE RECORDER ON STANDBY MODE		260.
					TERMINATOR SENSOR ENERGIZED		261.
					REGISTER 4 EVENT (POSSIBLE REGISTER 3		262.
					EVENT-EOT)		263.
							264.
62.0.	292D 3H 4M	SPAC	BC ACE5.	VAL-PRIME	1. REPORT S/C STATUS AS THE RESULT OF DC-V25.		265.
							266.
63.0.	292D 3H12M32S.	DSS-61.			1. DSS-61 AOS		267.
							268.
64.0.	292D 3H14M	RWV OP.	RWV TC.	DSS-41	1. TRANSMIT BACKUP DC-V25 (IF REQUIRED)		269.
							270.
65.0.	292D 3H22M47S.				1. BACKUP DC-V25 SEEN IN DATA.		271.
							272.
66.0.	292D 3H24M	SPAC	BC ACE5.	VAL-PRIME	1. REPORT RESULTS OF BACKUP DC-V25 (IF SENT)		273.
							274.
67.0.	292D 3H39M	DSS-41.			1. TURN OFF COMMAND MOD.		275.
							276.
67.1.		ACE-5	ACE5 BC.	VAL-PRIME	1. REPORT COMMAND MOD. OFF TIME		277.
							278.
68.0.	292D 3H40M	DSS-62.			1. ADJUST GND. XMTR VCO TO XA OF 2 WAY HANDOVER		279.
							280.
69.0.	292D 3H49M	DSS-41.			1. NOMINAL TWO-WAY STATION XFER (DSS-41 TO		281.
		DSS-62.			DSS-62)		282.
							283.
70.0.	292D 3H51M	DSS-62.			1. ADJUST GND. XMTR VCO FOR TRACK SYN FREQ.		284.
							285.
71.0.	292D 3H57M				1. PERFORM COMMAND READINESS PROCEDURES		286.
							287.
72.0.	292D 4H10M	SPAC			1. VERIFY PROPER SPE		288.
							289.
73.0.	292D 4H14M	DSS-62.	62 TKCH.		1. APPLY COMMAND MOD.		290.
							291.

Table B-2 (contd)

ITEM	TIME	STA.	REPORT BY-TO	NET	EVENT	CHECK WHEN COMPLETE	LINE
74.0.	292D 4H15M	ACE-5	ACE5 BC.	VAL-PRIME	.1. REPORT TIME OF COMMAND MOD. ON		292.
							293.
75.0.	292D 4H26M 2S	DSS-42.			.1. DSS-42 LOS		294.
							295.
76.0.	292D 4H30M	SPAC	BC ACE5.	VAL-PRIME	.1. VERIFY COMMAND IN LOCK		296.
							297.
76.1.					.1. PERFORM DCV COMMAND PROCEDURE		298.
							299.
77.0.	292D 4H44M39S	S/C			.1. MT-7 EVENT SEEN IN DATA (REGISTER 2 EVENT)		300. 301. 302.
78.0.	292D 4H45M	SPAC	BC ACE5.	VAL-PRIME	.1. REPORT MT-7 EVENT		303.
							304.
79.0.	292D 4H49M	DSS-62.	62 TKCH.	DSS-62	.1. REMOVE COMMAND MOD.		305.
							306.
80.0.	292D 4H50M	DSS-62.	62 TKCH.	DSS-62	.1. TRANSMITTER OFF.		307.
							308.
80.1.		ACE-5	ACE5 BC.	VAL-PRIME	.1. REPORT COMMAND MOD. OFF TIME		309.
							310.
80.2.		FPAC			.1. START AUX OSC WARM UP		311.
							312.
81.0.	292D 4H51M	ACE-5	ACE5 BC.	VAL-PRIME	.1. REPORT TRANSMITTER OFF TIME		313.
							314.
82.0.	292D 4H55M	DSS-62.	TKCH 62.	DSS-62	.1. START TDH SAMPLES 60 SEC/10 SEC. SEND 10 SEC FORMAT 15		315. 316. 317.
83.0.	292D 4H58M47S	SPAC	BC ACE5.	VAL-PRIME	.1. VERIFY 1-WAY RF SIGNAL		318.
							319.
84.0.	292D 5H34M	FPAC			.1. RUN TDPX (PRIME STRING)		320.
							321.
					.2. FPAC 50 PER CENT STAFFED		322.
							323.
85.0.	292D 5H34M37S	DSS-41.			.1. DSS-41 LOS		324.
							325.

Table B-2 (contd)

ITEM	TIME	STA.	REPORT BY-TO	NET	EVENT	CHECK WHEN COMPLETE	LINE
86.0.	292D 5H44M	FPAC			1. RUN ODGX (PRIME STRING)		326.
							327.
87.0.	292D 5H49M	DSS-62	62 TKCH	DSS-62	1. TRANSMITTER ON. REPORT TIME		328.
							329.
88.0.	292D 5H50M	ACE-5	ACE5 BC	VAL-PRIME	1. REPORT TRANSMITTER ON TIME.		330.
							331.
89.0.	292D 5H54M	FPAC			1. RUN ODPM (PRIME STRING)		332.
							333.
90.0.	292D 5H57M47S	SPAC	BC	ACE5 VAL-PRIME	1. REPORT 2-WAY STATUS (END AUX OSC TEST)		334.
							335.
91.0.	292D 6H	DSS-62			1. ADJUST GND XMTR VCO TO TRACK SYN FREQ.		336.
							337.
92.0.	292D 6H	DSS-62	TKCH 62	DSS-62	1. START TDH SAMPLES AT 30 SEC/30 SEC. SEND		338.
					30 SEC. FORMAT 15		339.
							340.
93.0.	292D 6H	MAR CH.			1. BEGIN COMMAND READINESS PROCEDURES.		341.
		TK CH					342.
		DSS-62.					343.
							344.
							345.
94.0.	292D 6H 1M	SPAC	BC	ACE5 VAL-PRIME	1. REPORT XFER TO VCO AT .....Z		346.
							347.
95.0.	292D 6H 4M	FPAC			1. RUN TDPX (BACKUP STRING)		348.
							349.
96.0.	292D 6H10M	FPAC	FC BC	VAL-PRIME	1. FPAC EXCITER EVALUATION , REPORT RESULTS		350.
							351.
97.0.	292D 6H13M	SPAC	BC	ACE5 VAL-PRIME	1. PROVIDE RWV 8FS VALUE.		352.
							353.
98.0.	292D 6H14M	FPAC			1. RUN ODGX (BACKUP STRING)		354.
							355.
99.0.	292D 6H18M	DSS-61.			1. APPLY COMMAND MODULATION		356.
							357.
100.0.	292D 6H19M	ACE-5	ACE5 BC	VAL-PRIME	1. REPORT TIME OF COMMAND MODULATION ON		358.
							359.

Table B-2 (contd)

ITEM	TIME	STA.	REPORT BY-TO	NET	EVENT	CHECK WHEN COMPLETE	LINE
101.0.	292D 6H24M	FPAC			1. RUN ODPM (BACKUP STRING)		360.
							361.
102.0.	292D 6H39M	SPAC	BC ACE5.	VAL-PRIME	1. VERIFY COMMAND IN LOCK.		362.
							363.
103.0.	292D 7H 4M	FPAC			1. RUN FLYM (PRIME STRING)		364.
							365.
104.0.	292D 7H34M	FPAC			1. RUN TJ3M (BACKUP STRING)		366.
							367.
					2. RUN TDPX (PRIME STRING)		368.
							369.
					3. FPAC COMPLETELY STAFFED FOR ENCOUNTER.		370.
							371.
105.0.	292D 7H44M	FPAC			1. RUN ODGX (PRIME STRING)		372.
							373.
106.0.	292D 7H54M	FPAC			1. RUN ODPM (PRIME STRING)		374.
							375.
107.0.	292D 7H56M	MAR CH.			1. PREPARE DC-V9 COMMAND MESSAGE AND DELIVER		376.
		..			TO TRACK CHIEF.		377.
							378.
108.0.	292D 8H 4M	FPAC			1. RUN TDPX (BACK UP STRING).		379.
							380.
109.0.	292D 8H14M	FPAC			1. RUN ODGX (BACK UP STRING).		381.
							382.
110.0.	292D 8H22M	MAR CH.	TKCH MRCH.	MAR	1. PERFORM DC-V COMMAND PROCEDURE		383.
		TRACK		COMMAND			384.
		RWV OP.					385.
		..					386.
110.1.	292D 8H24M	FPAC			1. RUN ODPM (BACK UP STRING).		387.
							388.
111.0.	292D 8H38M	SPAC	BC ACE5.	VAL-PRIME	1. REPORT S/C READY FOR COMMANDS.		389.
							390.
112.0.	292D 8H40M	SPAC	BC ACE5.	VAL-PRIME	1. REPORT COMMAND STATUS AND REQUEST THE		391.
					XMISSION OF DC-V9 AT 0850.		392.
							393.
113.0.	292D 8H47M	SPAC	BC ACE5.	VAL-PRIME	1. REPORT COMMAND STATUS.		394.
							395.

Table B-2 (contd)

ITEM	TIME	STA.	REPORT BY-TO	NET	EVENT	CHECK WHEN COMPLETE	LINE
114.0.	292D 8H50M	DSS-62			.1. TRANSMIT DC-V9		396.
							397.
115.0.	292D 8H52M	ACE-5	ACE5 BC.	VAL-PRIME	.1. REPORT INITIATION AND COMPLETION TIMES		398.
							399.
116.0.	292D 8H58M49S.	SPAC	BC ACE5.	VAL-PRIME	.1. REPORT RANGING RECEIVER ON		400.
							401.
117.0.	292D 9H 4M	FPAC			.1. RUN PRDX FOR DSS-14, 12, 13, 41 FROM E-7H TO E+5H (PRIME STRING).		402.
							403.
							404.
118.0.	292D 9H34M	FPAC			.1. RUN PRDX FOR DSS-14, 11, 42 FROM E-7H TO E+5H.(BACKUP STRING)		405.
							406.
							407.
					.2. RUN TDPX (PRIME STRING).		408.
							409.
118.1.		FPAC			.1. RUN ODGX (PRIME STRING).		410.
							411.
119.0.	292D 9H40M	DACON			.1. XMIT MODE II PREDICTS TO DSS-12,13,14,41		412.
							413.
120.0.	292D 9H52M	MAR CH.			.1. PREPARE DC-V24 COMMAND MESSAGE AND DELIVER TO TRACK CHIEF.		414.
							415.
							416.
121.0.	292D 9H54M	FPAC			.1. RUN ODPM (PRIME STRING).		417.
							418.
122.0.	292D10H 4M	FPAC			.1. RUN TDPX (BACK UP STRING).		419.
							420.
123.0.	292D10H14M	FPAC			.1. RUN ODGX (BACK UP STRING).		421.
							422.
123.1.		MAR CH. TRACK RWV OP.	TKCH MRCH.	MAR COMMAND	.1. PERFORM DC-V COMMAND PROCEDURE		423. 424. 425. 426.
124.0.	292D10H24M	FPAC			.1. RUN ODPM (BACK UP STRING).		427.
							428.
125.0.	292D10H30M				.1. XMIT MODE II PREDICTS TO DSS-11,42		429.
							430.

Table B-2 (contd)

ITEM	TIME	STA.	REPORT BY-TO	NET	EVENT	CHECK WHEN COMPLETE	LINE
126.0.	292D10H32M	SPAC	BC ACE5	VAL-PRIME	1. REPORT SPAC STATUS AND REQUEST TRANSMISSION OF DC-V24 AT 1050 00Z		431. 432. 433.
127.0.	292D10H43M35S	STAN			1. STANFORD AOS.		434. 435.
128.0.	=+292D10H43M53S	DSS-12			1. DSS-12 AOS		436. 437.
129.0.	292D10H46M	SPAC	BC AC55	VAL-PRIME	1. REPORT S/C STATUS		438. 439.
130.0.	292D10H47M	VOPS	VOPS BC	VAL-PRIME	1. REPORT TIME OF DSS-12 AOS		440. 441.
131.0.	292D10H50M	DSS-62			1. TRANSMIT DC-V24		442. 443.
132.0.	292D10H51M15S	DSS-14			1. DSS-14 AOS		444. 445.
133.0.	292D10H52M	ACE-5	ACE5 BC	VAL-PRIME	1. REPORT INITIATION AND COMPLETION TIME OF CMD		446. 447.
134.0.	292D10H58M	ACE-5	ACE5 DCN	VAL-PRIME	1. PREPARE FOR MODE 3 DATA AT 1058 50Z.		448. 449.
135.0.	292D10H58M50S				1. DC-V24 SEEN IN DATA A. SWITCH TO DATA MODE 3 B. PLANET SENSOR EXCITATION ON C. PLASMA PROBE MODE 3 D. CLOCK B ENABLED E. REGISTER 4 EVENT (NOT SEEN IN DATA)		450. 451. 452. 453. 454. 455. 456.
136.0.	292D10H58M50S	12,51 61,62	ACE5 TKCH	FAC-PRIME	1. REQUEST ALL DSS TO CHANGE TCP FOR MODE 3 DATA		457. 458. 459.
137.0.	292D11H 2M	SPAC	BC ACE5	VAL-PRIME	1. REPORT DC-V24 STATUS		460. 461.
137.1.	292D11H 4M	FPAC			1. RUN FLYM (PRIME STRING).		462. 463.
138.0.	292D11H 9M 4S	DSS-11			1. DSS-11 AOS		464. 465.

Table B-2 (contd)

ITEM	TIME	STA.	REPORT BY-TO		NET	EVENT	CHECK WHEN COMPLETE	LINE
139.0.	292D11H21M	SPAC	BC	ACE5.	VAL-PRIME	1. REQUEST REMOVAL OF COMMAND MOD AT 1130Z		466.
								467.
140.0.	292D11H24M41S	S/C				1. MT-8 OBSERVED		468.
								469.
141.0.	292D11H26M	SPAC	BC	ACE5.	VAL-PRIME	1. REPORT MT-8 EVENT		470.
								471.
						2. REPORT SPAC READY FOR STATION XFER AT 1147Z		472.
								473.
142.0.	292D11H30M	ACE-5	ACE5	BC.	VAL-PRIME	1. REPORT REMOVAL OF COMMAND MODULATION		474.
								475.
143.0.	292D11H31M	DSS-14.				1. ADJUST GND XMTR VCO TO XA OF TWO-WAY HANDOVER.		476.
								477.
144.0.	292D11H32M	ACE-5	ACE5	BC.	VAL-PRIME	1. REPORT START OF STATION XFER.		478.
								479.
145.0.	292D11H34M	FPAC				1. RUN TJ3M (PRIME STRING).		480.
								481.
						2. RUN FLYM (BACK UP STRING).		482.
								483.
						3. ACTIVATE HSDL FROM DSS-14 TO SFOF		484.
								485.
146.0.	292D11H47M	DSS-62.				1. NOMINAL TWO-WAY TRANSFER FROM DSS-62 TO		486.
		DSS-14.				DSS-14. GND XMTR VCO SET TO 22.039763 MHZ		487.
								488.
147.0.	292D11H49M					1. ADJUST GND. XMTR VCO TO XA OF 22.039765 MHZ.		489.
								490.
148.0.	292D11H50M	ACE-5	ACE5	BC.	VAL-PRIME	1. REPORT TIME OF COMPLETION OF STATION XFER		491.
								492.
149.0.	292D12H13M	SPAC	BC	ACE5.	VAL-PRIME	1. PROVIDE RWV 8F VALUE, SPE STATUS AND TIME FOR		493.
						APPLICATION OF COMMAND MODULATION.		494.
								495.
150.0.	292D12H17M	DSS-14.				1. APPLY COMMAND MODULATION		496.
								497.
151.0.	292D12H18M	ACE-5	ACE5	BC.	VAL-PRIME	1. REPORT TIME OF APPLICATION OF COMMAND MOD.		498.
								499.
152.0.	292D12H29M	SPAC	BC	ACE5.	VAL-PRIME	1. REPORT COMMAND MOD. SEEN AT THE S/C		500.
								501.

Table B-2 (contd)

ITEM	TIME	STA.	REPORT BY-TO	NET	EVENT	CHECK WHEN COMPLETE	LINE
153.0.	292D12H34M	FPAC			.1. RUN TDPX (PRIME STRING).		502.
							503.
					.2. RUN TDPX (BACK UP STRING).		504.
							505.
154.0.	292D12H38M	SPAC	BC ACE5.	VAL-PRIME	.1. REPORT COMMAND IN LOCK. REQUEST APPLICATION		506.
					OF RANGING MOD AT 1244Z		507.
							508.
155.0.	292D12H44M	DSS-14			.1. APPLY RANGING MODULATION		509.
		..					510.
156.0.	292D12H44M	FPAC			.1. RUN ODGX (PRIME STRING).		511.
							512.
					.2. RUN ODGX (BACK UP STRING).		513.
							514.
157.0.	292D12H45M	ACE-5	ACE5 BC.	VAL-PRIME	.1. REPORT TIME OF RANGING MOD. ON		515.
							516.
158.0.	292D12H50M	DSS-14			.1. START TDH SAMPLES 30 SEC/10 SEC. SEND 10 SEC		517.
					FORMAT 06		518.
							519.
159.0.	292D12H50M25S	DSS-51			.1. DSS-51 LOS		520.
		..					521.
160.0.	292D12H54M	FPAC			.1. RUN ODPM (PRIME STRING).		522.
							523.
					.2. RUN ODPM (BACK UP STRING).		524.
							525.
161.0.	292D13H 6M	SPAC	BC ACE5.	VAL-PRIME	.1. VERIFY RANGING IN LOCK.		526.
							527.
162.0.	292D13H21M	MAR CH.			.1. BEGIN COMMAND READINESS PROCEDURES		528.
		TRACK					529.
		DSS-14.					530.
		..					531.
163.0.	292D13H22M	MAR CH.			.1. PREPARE DC-V16/DC-V9 COMMAND MESSAGE AND		532.
		..			DELIVER TO TRACK CHIEF.		533.
							534.
164.0.	292D13H30M	FPAC			.1. LATEST TRAJECTORY DATA (E-4 HRS.)		535.
							536.

Table B-2 (contd)

ITEM	TIME	STA.	REPORT BY-TO	NET	EVENT	CHECK WHEN COMPLETE	LINE
165.0.	292D13H34M	FPAC			1. RUN FLYM (PRIME STRING)		537.
							538.
					2. RUN FLYM (BACKUP STRING)		539.
							540.
166.0.	292D14H 4M	FPAC			1. RUN TJ3M (PRIME STRING)		541.
							542.
					2. RUN TDPX (BACKUP STRING)		543.
							544.
166.1.		MAR CH. TRACK . RWV OP. ..			1. PERFORM DCV COMMAND PROCEDURE		545. 546. 547. 548.
167.0.	292D14H 5M	SPAC	BC ACE5.	VAL-PRIME	1. REPORT SPAC STATUS AND REQUEST REMOVAL OF RANGING MOD. AT 1420Z		549. 550. 551.
168.0.	292D14H12M	SPAC	BC ACE5.	VAL-PRIME	1. REPORT SPAC STATUS AND REQUEST XMISSION OF DC-V16 AT 1432 25Z		552. 553. 554.
169.0.	292D14H14M	FPAC			1. RUN ODGX (BACKUP STRING)		555. 556.
169.1.		FPAC	FC BC.	VAL-PRIME	1. RECOMMEND BEST TIME TO TRANSMIT DC-V16		557. 558.
170.0.	292D14H20M	..			1. RANGING MODULATION OFF.		559. 560.
171.0.	292D14H21M	ACE-5	ACE5 BC.	VAL-PRIME	1. REPORT TIME OF RANGING MOD. OFF		561. 562.
172.0.	292D14H24M	FPAC			1. RUN ODPM (BACKUP STRING)		563. 564.
173.0.	292D14H27M	SPAC	BC ACE5.	VAL-PRIME	1. REPORT SPAC STATUS FOR XMISSION OF DC-V16 AT .....Z		565. 566. 567. 568.
174.0.	292D14H28M47S	SPAC	BC ACE5.	VAL-PRIME	1. VERIFY RANGING MOD. OFF		569. 570.
175.0.	292D14H30M	DSS-12 ..	TKCH 12.	DSS-12 DSS-14	1. START TDH SAMPLES 30 SEC/10 SEC. SEND 10 SEC FORMAT 07		571. 572. 573.

Table B-2 (contd)

ITEM	TIME	STA.	REPORT BY-TO		NET	EVENT	CHECK WHEN COMPLETE	LINE
176.0.	292D14H32M25S					.1. TRANSMIT DC-V16		574.
								575.
177.0.	292D14H34M	ACE-5	ACE5	BC.	VAL-PRIME	.1. REPORT COMMAND INITIATE AND COMPLETION TIME		576.
								577.
178.0.	292D14H41M	SPAC	BC	ACE5.	VAL-PRIME	.1. REPORT S/C STATUS (AFTER DC-V16)		578.
								579.
179.0.	292D14H41M16S					.. DC-V16 SEEN IN DATA		580.
						A. FRAME COUNT RESET TO ZERO		581.
						B. CLOCK A DECODES ENABLED		582.
						C. REGISTER 4 EVENT (NOT SEEN IN DATA)		583.
						D. DC-V16 DAS STATUS BIT 281 SET		584.
								585.
180.0.	292D14H43M	SPAC	BC	ACE5.	VAL-PRIME	.1. REPORT THE STATUS OF DC-V16 AND REQUEST APPLICATION OF Ranging MODULATION.		586.
								587.
								588.
181.0.	292D14H50M					.1. RANGING MOD. ON.		589.
		SPAC	BC	ACE5.	VAL-PRIME			590.
182.0.	292D14H59M	SPAC	BC	ACE5.	VAL-PRIME	.1. VERIFY RANGING MOD ON.		591.
								592.
183.0.	292D15H 4M	FPAC				.1. RUN PRDX FOR DSS-12,13,14 FROM E- 25M TO E+ 55M (PRIME STRING)		593.
								594.
								595.
184.0.	292D15H 4M47S	DSS-61				.1. DSS-61 LOS		596.
								597.
185.0.	292D15H 5M	VOPS	VOPS	BC.	VAL-PRIME	.1. REPORT DSS-61 LOS.		598.
								599.
186.0.	292D15H10M	DSS-14	TKCH	14.	DSS-14	.1. ADJUST GND. XMTR VCO FREQ. TO 22.039856		600.
								601.
187.0.	292D15H12M	ACE-5	ACE5	BC.	VAL-PRIME	.1. REPORT TIME SPE ADJUSTMENT STARTED		602.
								603.
								604.
								605.
188.0.	292D15H15M	ACE-5	ACE5	BC.	VAL-PRIME	.1. REPORT RANGING RECEIVER IN LOCK		606.
								607.

Table B-2 (contd)

ITEM	TIME	STA.	REPORT BY-TO	NET	EVENT	CHECK WHEN COMPLETE	LINE
189.0.	292D15H17M	ACE-5	ACE5 BC.	VAL-PRIME	.1. REPORT TIME SPE ADJUSTMENT COMPLETE		608.
							609.
190.0.	292D15H24M	FPAC			.1. RUN PRDX FOR SPECIAL OCCULTATION (PRIME STRING)		610.
							611.
							612.
191.0.	292D15H30M	DACON			.1. XMIT MODE II PREDICTS TO DSS-12,13,14		613.
							614.
192.0.	292D15H30M	ACE-5	ACE5 BC.	VAL-PRIME	.1. REPORT STATUS OF SPE		615.
							616.
193.0.	292D15H39M	FPAC			.1. LATEST TRAJECTORY DATA (E-2H)		617.
							618.
194.0.	292D15H39M	FPAC			.1. RUN PRDX FOR SPECIAL OCCULTATION (BACKUP STRING)		619.
							620.
							621.
194.1.		FPAC	FC BC.	VAL-PRIME	.1. LATEST TRAJECTORY DATA (E-2 HRS)		622.
							623.
195.0.	292D15H39M33S	DSS 62.			1. DSS 62 LOS.		624.
							625.
196.0.	292D15H42M	VOPS	VOPS BC.	VAL-PRIME	.1. REPORT TIME OF DSS-62 LOS		626.
							627.
197.0.	292D15H43M	DSS-14	14 TK.	DSS-14	.1. TUNNING COMPLETE.		628.
							629.
198.0.	292D15H48M	MAR CH TRACK RWV OP.	TKCH MRCH.	MAR COMMAND	.1. PERFORM DC-V COMMAND PROCEDURE		630.
							631.
							632.
							633.
199.0.	292D15H51M	DSS-14	14 TKCH.	DSS-14	.1. REPORT COMPLETION OF FREQUENCY CHANGE.		634.
							635.
200.0.	292D15H52M	SPAC	BC ACE5.	VAL-PRIME	1. VERIFY SPE		636.
							637.
200.1.		DACON	DACN ACE5.	VAL-PRIME	1. REPORT PREDICTS AVAILABLE FOR TRANSMISSION.		638.
							639.
					2. XMIT PREDICTS UPON APPROVAL.		640.
							641.

Table B-2 (contd)

ITEM	TIME	STA.	REPORT BY-TO	NET	EVENT	CHECK WHEN COMPLETE	LINE
201.0.	292D16H 4M	FPAC			1. RUN TDPX (PRIME STRING)		642.
							643.
202.0.	292D16H14M	FPAC			1. RUN ODGX (PRIME STRING)		644.
							645.
					2. RUN TDPX (BACKUP STRING)		646.
							647.
203.0.	292D16H23M	SPAC	BC ACE5.	VAL-PRIME	1. REPORT SPAC STATUS AND REQUEST THE REMOVAL		648.
					OF COMMAND MODULATION.		649.
							650.
204.0.	292D16H24M	FPAC			1. RUN ODPM (PRIME STRING)		651.
							652.
					2. RUN ODGX (BACKUP STRING)		653.
							654.
205.0.	292D16H30M	DSS-14			1. RANGING MODULATION OFF		655.
							656.
205.1.		SPAC	BC ACE5.	VAL-PRIME	1. REPORT SPAC STATUS AND REQUEST TRANSMISSION		657.
					OF DC-V9 AT 1640Z		658.
							659.
206.0.	292D16H32M	ACE-5	ACE5 BC.	VAL-PRIME	1. REPORT TIME OF RANGING MOD. OFF		660.
							661.
207.0.	292D16H32M25S	SPAC	BC ACE5.	VAL-PRIME	1. REPORT PSO EVENT--START CLOCK B		662.
					TIME HAS A TOLERANCE OF +50 SEC -0 SEC		663.
					A. INHIBIT UV CALIBRATE		664.
					B. DAS-START TAPES		665.
					C. TRACK 1 DATA RECORD START		666.
							667.
208.0.	292D16H34M	FPAC			1. RUN ODPM (BACKUP STRING)		668.
							669.
209.0.	292D16H39M	SPAC	BC ACE5.	VAL-PRIME	1. VERIFY RANGING MOD. OFF		670.
							671.
210.0.	292D16H40M				1. TRANSMIT DC-V9 (RANGING RECEIVER OFF)		672.
							673.

Table B-2 (contd)

ITEM	TIME	STA.	REPORT BY-TO	NET	EVENT	CHECK WHEN COMPLETE	LINE
211.0.	292D16H41M	DSS-14.			1. REMOVE COMMAND MOD. REPORT TIME.		674.
							675.
							676.
							677.
							678.
							679.
					NOTE. IF PSO OCCURS DURING THE EARLY PORTION OF ITS TOLERANCE PERIOD, THE COMMAND MOD. OFF TIME AND TRANSMITTER OFF TIME CAN OCCUR EARILIER THAN INDICATED. THIS WILL BE A REAL TIME MODIFICATION TO THE SOE.		680.
							681.
							682.
							683.
							684.
							685.
							686.
							687.
							688.
							689.
							690.
212.0.	292D16H42M	ACE-5	ACE5 BC.	VAL-PRIME	1. XMTR OFF. REPORT TIME.		691.
							692.
					2. REPORT DC-V9 XMISSION TIME		693.
							694.
213.0.	292D16H45M	ACE-5	ACE5 BC.	VAL-PRIME	1. REPORT COMMAND MODULATION OFF		695.
							696.
214.0.	292D16H45M49S.				1. TRACK 2 DATA RECORD START		697.
							698.
215.0.	292D16H48M	SPAC	BC ACE5.	VAL-PRIME	1. REPORT TRACK NUMBER 2 STATUS		699.
							700.
216.0.	292D16H51M	SPAC	BC ACE5.	VAL-PRIME	1. VERIFY ONE-WAY RF SIGNAL.		701.
							702.
216.1.		11,12, 14 SFOF			1. START DATA MONITOR PLOT (10 SEC DATA)		703.
							704.
							705.
							706.
217.0.	292D16H57M	DSS-12. DSS-14.	12. 14.	292 16. VAL-PRIME	57 00 FPAC FC BC 1. REPORT EXCITER STATUS		707. 708.
							709.
218.0.	292D17H	DSS-11.	TKCH 11.	DSS-11 DSS-12 DSS-14	1. START TDH SAMPLES 10 SEC/1 SEC. SEND 10 SEC FORMAT 07		710. 711. 712.
							713.

Table B-2 (contd)

ITEM	TIME	STA.	REPORT BY-TO	NET	EVENT	CHECK WHEN COMPLETE	LINE.
219.0.	292D17H15M	DSS-14			1. BEGIN 1-SEC DATA VIA HSDL		714.
							715.
220.0.	292D17H18M	FPAC			1. REMOVE BIAS,INITIALIZE SCALES FOR ENTRY PLOT		716.
							717.
221.0.	292D17H20M	DSS-11			1. CHANGE PAPER TAPE ON 1 SEC PUNCH, RESUME		718.
		DSS-12			1 SEC SAMPLES		719.
							720.
222.0.	292D17H24M41S	11,12,			1. START OPEN LOOP RECORDERS.		721.
		13,14					722.
					2. START DIS TAPE RECORDER		723.
							724.
223.0.	292D17H25M	DSS-14			1. CHANGE PAPER TAPE ON 1 SEC. PUNCH, RESUME		725.
					1 SEC SAMPLES		726.
							727.
224.0.	292D17H26M41S	FPAC			1. START ENTRY PLOT		728.
							729.
225.0.	292D17H35M20S	S/C			1. CLOSEST APPROACH TO VENUS (E).(AT S/C)		730.
					TIME HAS A TOLERANCE OF PLUS OR MINUS 2 MIN.		731.
							732.
226.0.	292D17H37M11S	11,12,			1. OCCULTATION OBSERVED (NO ATMOSPHERE)		733.
		13,14					734.
							735.
226.1.		ACE-5	ACE5	BC. VAL-PRIME	1. REPORT LOSS OF RF SIGNAL		736.
							737.
227.0.	292D17H38M10S	S/C			1. LOSS OF RF SIGNAL (DFR)		738.
							739.
228.0.	292D17H39M47S	S/C			1. E(CLOSEST APPROACH) EARTH OBSERVED		740.
							741.
229.0.	292D17H40M	DSS-12			1. TRANSMITTER ON. (SET GND XMTR VCO FOR XA FOR		742.
					TIME OF CLOSEST APPROACH PLUS 1370 SEC.)		743.
							744.
230.0.	292D17H41M29S	S/C			1. LOSS OF RF SIGNAL (30 ATM)		745.
							746.
231.0.	292D17H43M	ACE-5	ACE5	BC. VAL-PRIME	1. REPORT XMTR ON TIME		747.
							748.

Table B-2 (contd)

ITEM	TIME	STA.	REPORT BY-TO	NET	EVENT	CHECK WHEN COMPLETE	LINE
232.0.	292D17H44M45S.	S/C			1. CENTER OF OCCULTATION		749.
							750.
233.0.	292D17H45M 1S.	S/C			1. ENTER OCCULTATION (40 ATMOSPHERE MODEL)		751.
							752.
233.1.		11,12,			1. REPORT RECEIVER OUT-OF-LOCK TIMES TO TRACK		753.
		13,14			CHIEF		754.
							755.
233.2.		11,12,			1. STOP AND RELOAD ALL TDH PUNCHES		756.
		14					757.
							758.
234.0.	292D17H45M	13,14			1. STOP OPEN LOOP RECORDERS AND REPLACE TAPES.		759.
							760.
234.1.		FPAC			1. STUDY ENTRY PLOT.		761.
							762.
					2. RESET SCALES		763.
							764.
					3. CHANGE PAPER FOR EXIT PLOT.		765.
							766.
235.0.	292D17H47M	OCCUL	OCLT FC.	PPAA-3	1. REPORT EXIT BIAS AND TIME OF SIGNAL		767.
					REAPPEARANCE.		768.
							769.
236.0.	292D17H47M21S.				1. TERMINATOR SENSOR APAC (NO DATA).		770.
							771.
237.0.	292D17H48M	FPAC	FC TKCH.	FAC-PRIME	1. REPORT EXIT FREQ. PREDICTION (INCL. BIAS)		772.
					AND TIME OF SIGNAL REAPPEARANCE.		773.
							774.
238.0.	292D17H48M 5S.				1. DAS CLOCK A APAC.(NO DATA)		775.
							776.
239.0.	292D17H49M	TRACK	TKCH 11.		1. REPORT ONE-WAY,TWO-WAY RECEIVER FREQUENCIES		777.
			12.				778.
			14.				779.
							780.
239.1.		11			1. SET RECEIVER 1 TO BIASED ONE-WAY FREQUENCY		781.
		12					782.
		14			2. SET RECEIVER 2 TO TWO-WAY FREQUENCY AT		783.
					18 02 16		784.
							785.

Table B-2 (contd)

ITEM	TIME	STA.	REPORT BY-TO	NET	EVENT	CHECK WHEN COMPLETE	LINE
240.0.	292D17H49M11S.				.1. CENTER OCCULTATION (EARTH OBSERVED)		786.
							787.
241.0.	292D17H50M	.13,14			.1. START OPEN LOOP RECORDERS		788.
		..					789.
241.1.		.11,12,			.1. START TDH SAMPLES 10 SEC/1 SEC, SEND 10 SEC		790.
		.14			FORMAT 07		791.
		..					792.
241.2.		.FPAC			.1. START EXIT PLOT		793.
							794.
241.3.		.11,12,			.1. START PAPER TAPE PUNCHES AT 1/SEC RATE		795.
		.14					796.
		..			.2. START DIS RECORDER		797.
							798.
242.0.	292D17H52M	.SPAC	.BC	ACE5. VAL-PRIME	.1. REPORT ONE-WAY RF LOCK (MAX. ATMOSPHERE).		799.
							800.
243.0.	292D17H53M18S.	S/C			. 1. EXIT OCCULTATION (40 ATMOSPHERE).		801.
							802.
243.1.		.DSS-11.	11 TKCH.		.1. REPORT RECEIVER-IN-LOCK TIMES		803.
		.DSS-12.	12				804.
		.DSS-13.	13				805.
		.DSS-14.	14				806.
		..					807.
244.0.	292D17H55M	.ACE-5	.ACE5 BC.	VAL-PRIME	.1. REPORT TIMES RF SIGNAL ACQUIRED		808.
							809.
245.0.	292D17H57M35S.	.DSS-11.			.1. RF SIGNAL RECEIVED (30 ATM)		810.
		.DSS-12.					811.
		.DSS-14.					812.
		..					813.
246.0.	292D18H 2M16S.	.DSS-42.			.1. DSS-42 AOS.(START TDH SAMPLES 10 SEC/1SEC.		814.
		..			SEND 10 SEC., FORMAT 07		815.
							816.
247.0.	292D18H 2M40S.	.DSS-11.			.1. RF SIGNAL RECEIVED (ND ATM)		817.
		.DSS-12.					818.
		.DSS-14.			.2. LOSS OF ONE-WAY LOCK ON REC. 1, ACQUIRE TWO-		819.
		..			WAY WITH REC. 2 (AT 11,12) AND REC. 1 AT 14.		820.
					REPORT LOSS AND ACQ. TIMES		821.
							822.

Table B-2 (contd)

ITEM	TIME	STA.	REPORT BY-TO	NET	EVENT	CHECK WHEN COMPLETE	LINE
248.0.	292D18H 3M	VOPS	VOPS BC.	VAL-PRIME	1. REPORT TIME OF DSS-42 AOS		823. 824.
249.0.	292D18H 4M36S	S/C			1. RF SIGNAL RECEIVED (DFR)		825. 826.
250.0.	292D18H 5M	MAR CH.			1. PREPARE DC-V9 COMMAND MESSAGE AND DELIVER TO TRACK.		827. 828. 829.
250.1.		DSS 41.			1. DSS 41 AOS.(START TDH SAMPLES 10 SEC/1 SEC SEND 10 SEC., FORMAT 07)		830. 831. 832.
251.0.	292D18H 6M	VOPS	VOPS BC.	VAL-PRIME	1. REPORT TIME OF DSS-41 AOS		833. 834.
252.0.	292D18H 8M	SPAC	BC ACE5.	VAL-PRIME	1. REPORT SPAC STATUS AND REQUEST STATION XFER AT 1817Z		835. 836. 837.
253.0.	292D18H10M	DSS-11. DSS-12.			1. CHANGE PAPER ON 1 SEC PUNCH, RESUME 1 SEC SAMPLES.		838. 839. 840.
254.0.	292D18H11M58S	11,12, 13,14			1. STOP OPEN LOOP RECORDERS, PAPER TAPES, AND D.I.S. REC.		841. 842. 843.
					2. STOP EXIT PLOT.		844. 845.
255.0.	292D18H15M	DSS-14.			1. CHANGE PAPER ON 1 SEC PUNCH, RESUME 1 SEC SAMPLE		846. 847. 848.
256.0.	292D18H17M	12,14			1. NOMINAL 2-WAY STATION TRANSFER (DSS-12 TO DSS-14)		849. 850. 851.
257.0.	292D18H19M	DSS-14.			1. ADJUST GND. XMTR VCO TO VALUE PROVIDED BY SPAC		852. 853. 854.
258.0.	292D18H25M	ACE-5	ACE5 BC.	VAL-PRIME	1. REPORT START AND COMPLETION OF STATION XFER		855. 856.
259.0.	292D18H28M	DSS-12.	TKCH 12.	DSS-12	1. START CHANGING GND XMTR VCO FREQ TO 22.039392		857. 858. 859.

Table B-2 (contd)

ITEM	TIME	STA.	REPORT BY-TO	NET	EVENT	CHECK WHEN COMPLETE	LINE
260.0.	292D18H28M	MAR CH.			1. START COMMAND READINESS PROCEDURES.		860.
		TK CH					861.
		DSS 14.					862.
		..					863.
261.0.	292D18H30M	DSS-14.			1. START TDH SAMPLES 30 SEC/10 SEC. SEND 10 SEC		864.
		..			FORMAT 06		865.
							866.
262.0.	292D18H30M	DSS-11.			1. START TDH SAMPLES 60 SEC/60 SEC., SEND 60 SEC.		867.
		DSS-12.			FORMAT 15		868.
		DSS-42.					869.
		..					870.
263.0.	292D18H33M	SPAC	BC	ACE5. VAL-PRIME	1. END OF TRACK 2 RECORD		871.
							872.
264.0.	292D18H34M	DSS 14.	14	TKCH. DSS-14	1. REPORT 2-WAY STATUS		873.
		..					874.
264.1.		SPAC	BC	ACE5. VAL-PRIME	1. VERIFY XA (SPE)		875.
							876.
265.0.	292D18H36M	SPAC	BC	ACE5. VAL-PRIME	1. REPORT TRACK 2 STATUS AND SPE STATUS.		877.
							878.
266.0.	292D18H38M	SPAC	BC	ACE5. VAL-PRIME	1. REQUEST APPLICATION OF COMMAND MODULATION.		879.
							880.
267.0.	292D18H39M	11,12,			1. STOP TAKING 1 SEC/10 SEC DOPPLER AND START		881.
		14			TAKING 10 SEC/60 SEC DOPPLER		882.
		..					883.
268.0.	292D18H39M30S	SPAC	BC	ACE5. VAL-PRIME	1. PROVIDE RWV 8FS VALUE.		884.
							885.
269.0.	292D18H40M15S				1. END OF TAPE, PSO TAPE START (NOT SEEN IN		886.
					DATA)		887.
							888.
270.0.	292D18H41M	DSS 14.			1. APPLY COMMAND MOD.		889.
		..					890.
271.0.	292D18H42M	ACE 5	ACE5	BC. VAL-PRIME	1. REPORT TIME OF COMMAND MOD ON.		891.
							892.
272.0.	292D18H43M	MAR CH.	MRCH	TKCH. MAR COMMAND	1. REQUEST TCP TRANSFER TO DATA MODE 2.		893.
							894.
							895.

Table B-2 (contd)

ITEM	TIME	STA.	REPORT BY-TO	NET	EVENT	CHECK WHEN COMPLETE	LINE
273.0	292D18H44M	SPAC	BC ACE5	VAL-PRIME	1. REPORT S/C STATUS.		896.
							897.
274.0	292D18H45M	ACE-5	ACE5 DCN	VAL-PRIME	1. PREPARE FOR MODE 2 DATA AT 184529.		898.
							899.
275.0	292D18H45M29S	SPAC	BC ACE5	VAL-PRIME	1. D/E TO MODE 2 DATA.		900.
					A. UV CALIBRATE INHIBIT REMOVED		901.
					B. PLASMA PROBE MODE 3 REMOVED		902.
					C. EOT BACKUP (CLOCK B)		903.
					D. REG. 1 EVENT (APAC)		904.
					E. REG. 2 EVENT (MT-8)		905.
					F. REG. 3 EVENTS (APAC AND REC. EOT)		906.
					G. REG. 4 EVENTS (DC-V24,DC-V16,AND DC-V9)		907.
							908.
276.0	292D18H55M	SPAC	BC ACE5	VAL-PRIME	1. VERIFY COMMAND IN LOCK.		909.
							910.
					2. REPORT SPAC STATUS AND REQUEST TRANSMISSION		911.
					OF DC-V9.		912.
							913.
277.0	292D19H 5M	FPAC			1. RUN TDPX (PRIME STRING)		914.
							915.
278.0	292D19H 8M	SPAC	BC ACE5	VAL-PRIME	1. REPORT S/C STATUS.		916.
							917.
279.0	292D19H10M	DSS-14			1. TRANSMIT DC-V9.		918.
							919.
280.0	292D19H12M	ACE 5	ACE5 BC	VAL-PRIME	1. REPORT COMMAND INITIATE AND COMPLETION		920.
					TIMES.		921.
							922.
281.0	292D19H15M	FPAC			1. RUN ODGX (PRIME STRING)		923.
							924.
282.0	292D19H19M51S	SPAC	BC ACE5	VAL-PRIME	1. REPORT DC-V9 STATUS.		925.
							926.
283.0	292D19H25M	FPAC			1. RUN ODPM (PRIME STRING)		927.
							928.
					2. RUN TDPX (BACKUP STRING)		929.
							930.
284.0	292D19H26M	DSS 14	14 TC	DSS-14	1. COMMAND MOD REMOVED (ONLY IF LOCKED ON		931.
					SIDEBAND).		932.
							933.

Table B-2 (contd)

ITEM	TIME	STA.	REPORT BY-TO	NET	EVENT	CHECK WHEN COMPLETE	LINE
285.0.	292D19H27M	DSS 14			1. ADJUST GND XMTR VCO.		934.
							935.
286.0.	292D19H29M	DSS 14			1. APPLY RANGING MODULATION.		936.
							937.
287.0.	292D19H35M	FPAC			1. RUN ODGX (BACKUP STRING)		938.
							939.
288.0.	292D19H45M	FPAC			1. RUN ODPM (BACKUP STRING)		940.
							941.
289.0.	292D19H52M	DSS 14	14 TC.	DSS-14	1. REPORT RANGING CODE LOCKED UP.		942.
							943.
290.0.	292D19H54M	ACE 5	ACE5 BC.	VAL-PRIME	1. REPORT TIME RANGING IN LOCK.		944.
							945.
291.0.	292D20H	FPAC	ALL ACE5.	VAL-PRIME	1. REPORT SFO STATUS.		946.
		SPAC					947.
		SSAC					948.
		DACON					949.
292.0.	292D20H35M	FPAC			1. RUN PRDX FOR DSS-12,14,41,62 FROM E+ 4.5H TO E+ 8 DAYS (PRIME STRING)		950.
							951.
							952.
293.0.	292D21H25M	SPAC	BC ACE5.	VAL-PRIME	1. REQUEST REMOVAL OF RANGING MODULATION.		953.
							954.
294.0.	292D21H48M	DSS-14			1. TURN RANGING MOD OFF.		955.
							956.
295.0.	292D21H49M	..			1. COMMAND MOD. OFF.		957.
							958.
296.0.	292D21H50M	..			1. XMTR OFF (DSS-14).		959.
							960.
297.0.	292D21H55M	DSS 14			1. START TDH SAMPLES 60 SEC/60 SEC,SEND 60 SEC, FORMAT 15.		961.
							962.
							963.
298.0.	292D21H55M	DSS 41			1. START TDH SAMPLES 60 SEC/10 SEC, SEND 10 SEC, FORMAT 15.		964.
							965.
							966.
299.0.	292D21H58M53S.		SPAC BC.		1. VERIFY ONE WA●.		967.
							968.

Table B-2 (contd)

ITEM	TIME	STA.	REPORT BY-TO	NET	EVENT	CHECK WHEN COMPLETE	LINE
299.1.		DSS-14.			.1. START AUX OSC TEST.		969.
							970.
300.0.	DELETE						971.
							972.
							973.
							974.
301.0.	292D22H36M	SPAC	BC ACE5.	VAL-PRIME	.1. REPORT SPAC STATUS AND REQUEST DSS-41 XMTR ON AT 2250Z.		975. 976. 977.
302.0.	292D22H38M14S.	DSS 14.			1. DSS 14 LOS.		978.
							979.
303.0.	292D22H40M	VOPS	VOPS BC.	VAL-PRIME	.1. REPORT TIME OF DSS-14 LOS.		980. 981.
304.0.	292D22H45M28S.	DSS 12.			1. DSS 12 LOS.		982.
							983.
305.0.	292D22H45M39S.	DSS 11.			.1. DSS 11 LOS.		984.
							985.
306.0.	292D22H50M	DSS 41.			SEND 60 SEC, FORMAT 15). .1. 41 XMTR ON (START TDH SAMPLES 60 SEC/60 SEC,		986. 987. 988.
307.0.	292D22H52M	ACE 5	ACE5 BC.	VAL-PRIME	.1. REPORT XMTR ON TIME.		989. 990.
308.0.	292D22H58M53S.	SPAC	BC ACE5.	VAL-PRIME	.1. VERIFY 2-WAY RF LOCK (DSS-41). (END AUX OSC TEST)		991. 992. 993.
309.0.	292D23H 1M	DSS 41.			.1. ADJUST GND XMTR VCO TO TRACK SYN FREQ.		994. 995.
310.0.	292D23H10M	FPAC			.1. AUX OSC EVALUATION		996. 997.
311.0.	292D23H20M	DSS-41.			.1. VERIFY SPE.		998. 999.
312.0.	DELETE						1000. 1001. 1002.

Table B-2 (contd)

ITEM	TIME	STA.	REPORT BY-TO		NET	EVENT	CHECK WHEN COMPLETE	LINE
313.0.	292D23H38M13S.	STAN				1. STANFORD LOS.		1003.
								1004.
314.0.	292D23H40M	VOPS	VOPS	BC.	VAL-PRIME	1. REPORT TIME OF STANFORD LOS.		1005.
								1006.
314.1.	DELETE							1007.
								1008.
								1009.
315.0.	293D 1H47M 2S.	DSS 51.				1. DSS 51 AOS.		1010.
								1011.
316.0.	293D 2H50M43S.	DSS 62.				1. DSS 62 AOS.		1012.
								1013.
317.0.	293D 3H12M50S.	DSS 61.				1. DSS 61 AOS.		1014.
								1015.
318.0.	293D 3H35M	FPAC				1. RUN PRDX FOR DSS-11,42,61 FROM E+ 15H TO E+ 8 DAYS		1016. 1017. 1018.
319.0.	293D 4H19M	DSS-62.				1. ADJUST GND XMTR VCO TO XA FOR 2 WAY HANDOVER.		1019. 1020. 1021.
320.0.	293D 4H17M	41/62				1. NOMINAL 2-WAY TRANSFER (DSS-41 TO DSS-62)		1022.
								1023.
321.0.	293D 4H19M	DSS-62.				1. GND XMTR VCO SET TO TRACK SYN FREQ.		1024.
								1025.
322.0.	293D 4H26M19S.	DSS 42.				1. DSS 42 LOS.		1026.
								1027.
323.0.	293D 5H35M	DSS 41.				1. DSS 41 LOS.		1028.
								1029.
324.0.	293D 5H36M					1. BEGIN COMMAND READINESS PROCEDURES.		1030.
								1031.
324.1.	293D 5H40M	SPAC	BC		ACE5. VAL PRIME	1. PROVIDE RWV8FS.		1032.
								1033.
325.0.	293D 5H51M	SPAC	BC		ACE5. VAL-PRIME	1. REQUEST THE APPLICATION OF COMMAND MOD AT 0600Z.		1034. 1035.
								1036.

Table B-2 (contd)

ITEM	TIME	STA.	REPORT BY-TO	NET	EVENT	CHECK WHEN COMPLETE	LINE
326.0.	293D 6H	DSS-62			.1. APPLY COMMAND MODULATION		.1037. .1038.
327.0.	293D 6H 1M	ACE 5	ACE5 BC.	VAL-PRIME	.1. REPORT TIME COMMAND MOD APPLIED.		.1039. .1040.
328.0.	293D 6H14M	SPAC	BC ACE5.	VAL-PRIME	.1. VERIFY COMMAND LOCK		.1041. .1042.
328.1.		MAR CH. TRACK RWV OP.	TKCH MRCH.	MAR COMMAND	.1. PERFORM DC-V COMMAND PROCEDURES		.1043. .1044. .1045. .1046.
329.0.	293D 6H37M	SPAC	BC ACE5.	VAL-PRIME	.1. REPORT SPAC STATUS.		.1047. .1048.
330.0.	293D 7H23M	MAR CH.	MRCH TKCH.	MAR COMMAND	.1. CHANGE TCP FOR MODE 1 DATA AT 072448.		.1049. .1050. .1051.
330.1.		ACE 5	ACE5 DACN.	VAL-PRIME	.1. PREPARE FOR MODE 1 DATA.		.1052. .1053.
331.0.	293D 7H24M48S.	SPAC	BC ACE5.	VAL-PRIME	.1. REPORT MT-9 EVENT. BEGIN 1ST NO DATA PERIOD (DATA MODE 1).		.1054. .1055. .1056.
331.1.	074400	MAR CH.	MRCH TKCH.	MAR COMMAND	.1. CHANGE TCP FOR MODE 4 DATA.		.1057. .1058. .1059.
331.2.	074400	ACE 5	ACE5 DACN.	VAL-PRIME	.1. PREPARE FOR MODE 4 DATA.		.1060. .1061. .1062. .1063. .1064. .1065. .1066. .1067. .1068. .1069.
332.0.	293D 7H45M	SPAC	BC ACE5.	VAL-PRIME	.1. REPORT TRACK 1 TEST PATTERN (DATA MODE 4).		.1070. .1071.
333.0.	293D 8H	MAR CH.	MRCH TKCH.	MAR COMMAND	.1. CHANGE TCP FOR DATA MODE 1 AT 080100.		.1072. .1073. .1074.

*****TRACK 1 PLAYBACK FIRST*****

Table B-2 (contd)

ITEM	TIME	STA.	REPORT BY-TO	NET	EVENT	CHECK WHEN COMPLETE	LINE
333.1.		ACE 5	ACE5 DACN.	VAL-PRIME	.1. PREPARE FOR MODE 1 DATA.		.1075. .1076.
334.0.	293D 8H 1M	SPAC	BC ACE5.	VAL-PRIME	.1. REPORT 2ND 'NO DATA' PERIOD (DATA MODE 1).		.1077. .1078.
335.0.	293D 8H 5M	DSS-62	62 TC.	DSS-62	.1. REMOVE COMMAND MOD. REPORT TIME.		.1079. .1080.
335.1.	293D 8H10M	DSS-62	62 TC.	DSS-62	.1. TRANSMITTER OFF. REPORT TIME.		.1081. .1082.
336.0.	293D 8H15M	MAR CH.	MRCH TKCH.	MAR COMMAND	.1. CHANGE TCP FOR MODE 4 DATA AT 081748.		.1083. .1084. .1085.
336.1.		ACE 5	ACE5 DACN.	VAL-PRIME	.1. PREPARE FOR MODE 4 DATA.		.1086. .1087.
337.0.	293D 8H17M48S.	SPAC	BC ACE5.	VAL-PRIME	.1. REPORT TRACK 1 DATA (MODE 4).		.1088. .1089.
337.1.	293D10H43M31S.	DSS-12.			.1. DSS-12 AOS.		.1090. .1091.
337.2.	293D10H51M51S.	DSS-14.			.1. DSS-14 AOS.		.1092. .1093.
337.3.	293D11H 9M38S.	DSS-11.			.1. DSS-11 AOS.		.1094. .1095.
337.4.	293D15H 3M15S.				.1. DSS-61 LOS.		.1096. .1097.
337.5.	293D15H38M 4S.	DSS-62.			.1. DSS-62 LOS.		.1098. .1099.
337.6.	293D18H-0M13S.	DSS-42.			.1. DSS-42 AOS.		.1100. .1101.
337.7.	293D18H 3M46S.	DSS-41.			.1. DSS-41 AOS.		.1102. .1103.
337.8.	293D22H36M59S.	DSS-14.			.1. DSS-14 LOS.		.1104. .1105.
337.9.	293D22H45M12S.	DSS-12.			.1. DSS-12 LOS.		.1106. .1107.

Table B-2 (contd)

ITEM	TIME	STA.	REPORT BY-TO	NET	EVENT	CHECK WHEN COMPLETE	LINE
338.0.	294D 1H10M	MAR CH.	MRCH TKCH.	MAR COMMAND	1. CHANGE TCP FOR MODE 1 DATA AT 011348.		1108. 1109. 1110.
338.1.		ACE 5	ACE5 DACN.	VAL-PRIME	1. PREPARE FOR MODE 1 DATA.		1111. 1112.
339.0.	294D 1H13M48S.	SPAC	BC ACE5.	VAL-PRIME	1. REPORT EOT/CHANGE TRACK. BEGIN 3RD 'NO DATA' PERIOD (DATA MODE 1).		1113. 1114. 1115.
340.0.	294D 1H32M	MAR CH.	MRCH TKCH.	MAR COMMAND	1. CHANGE TCP FOR MODE 4 DATA AT 01 33 48.		1116. 1117. 1118.
340.1.		ACE 5	ACE5 DACN.	VAL-PRIME	1. PREPARE FOR MODE 4 DATA.		1119. 1120.
341.0.	294D 1H33M48S.	SPAC	BC ACE5.	VAL-PRIME	1. REPORT TRACK 2 TEST PATTERN (DATA MODE 4).		1121. 1122.
342.0.	294D 1H49M48S.	SPAC	BC ACE5.	VAL-PRIME	1. REPORT 4TH 'NO DATA' PERIOD (DATA MODE 1).		1123. 1124.
342.1.	294D 2H51M32S.	DSS-62.			1. DSS-62 AOS.		1125. 1126.
342.2.	294D 3H13M22S.	DSS-61.			1. DSS-61 AOS.		1127. 1128.
343.0.	294D 3H56M48S.	SPAC	BC ACE5.	VAL-PRIME	1. REPORT TRACK 2 DATA (DATA MODE 4).		1129. 1130.
343.1.	294D 4H26M47S.	DSS-42.			1. DSS-42 LOS.		1131. 1132.
343.2.	294D 5H35M33S.	DSS-11.			1. DSS-41 LOS.		1133. 1134.
343.3.	294D10H43M10S.	DSS-12.			1. DSS-12 AOS.		1135. 1136.
343.4.	294D10H52M28S.	DSS-14.			1. DSS-14 AOS.		1137. 1138.
343.5.	294D11H10M11S.	DSS-11.			1. DSS-11 AOS.		1139. 1140.

Table B-2 (contd)

ITEM	TIME	STA.	REPORT BY-TO	NET	EVENT	CHECK WHEN COMPLETE	LINE
344.0.	294D18H15M	MAR CH.	MRCH TKCH.	MAR COMMAND	1. CHANGE TCP FOR MODE 1 DATA AT 181648.		1141. 1142. 1143.
344.1.		ACE 5	ACE5 DACN.	VAL-PRIME	1. PREPARE FOR MODE 1 DATA.		1144. 1145.
345.0.	294D18H16M48S.	SPAC	BC ACE5.	VAL-PRIME	1. REPORT 5TH 'NO DATA' PERIOD (DATA MODE 1).		1146. 1147.
346.0.	294D19H14M48S.	SPAC	BC ACE5.	VAL-PRIME	1. REPORT EOT/END OF FIRST PLAYBACK. BEGIN FIRST NO DATA PERIOD, TRACK 1 (DATA MODE 1).		1148. 1149. 1150.
347.0.	294D19H33M	MAR CH.	MRCH TKCH.	MAR COMMAND	1. CHANGE TCP FOR MODE 4 DATA AT 193448.		1151. 1152. 1153.
347.1.		ACE 5	ACE5 DACN.	VAL-PRIME	1. PREPARE FOR MODE 4 DATA.		1154. 1155.
348.0.	294D19H34M48S.	SPAC	BC ACE5.	VAL-PRIME	1. REPORT TRACK 2 TEST PATTERN (DATA MODE 4).		1156. 1157.
349.0.	294D19H49M	MAR CH.	MRCH TKCH.	MAR COMMAND	1. CHANGE TCP FOR MODE 1 DATA AT 195048.		1158. 1159. 1160.
349.1.		ACE 5	ACE5 DACN.	VAL-PRIME	1. PREPARE FOR MODE 1 DATA.		1161. 1162.
350.0.	294D19H50M48S.	SPAC	BC ACE5.	VAL-PRIME	1. REPORT SECOND NO DATA PERIOD (DATA MODE 1).		1163. 1164.
351.0.	294D21H56M	MAR CH.	MRCH TKCH.	MAR COMMAND	1. CHANGE TCP FOR MODE 4 DATA AT 215748.		1165. 1166. 1167.
351.1.		ACE 5	ACE5 DACN.	VAL-PRIME	1. PREPARE FOR MODE 4 DATA.		1168. 1169.
352.0.	294D21H57M48S.	SPAC	BC ACE5.	VAL-PRIME	1. REPORT TRACK 2 DATA (MODE 4).		1170. 1171.
353.0.	294D22H35M45S.	DSS-14.			1. DSS-14 LOS.		1172. 1173.
354.0.	294D22H44M56S.	DSS-12.			1. DSS-12 LOS.		1174. 1175.

Table B-2 (contd)

ITEM	TIME	STA.	REPORT BY-TO	NET	EVENT	CHECK WHEN COMPLETE	LINE.
355.0.	294D22H45M 6S.	DSS-11.			.1. DSS-11 LOS.		.1176. .1177.
356.0.-=	295D 1H45M11S.	DSS-51.			.1. DSS-51 AOS.		.1178. .1179.
357.0.	295D 2H52M21S.	DSS-62.			.1. DSS-62 AOS.		.1180. .1181.
358.0.	295D 3H13M54S.	DSS-61.			.1. DSS-61 AOS.		.1182. .1183.
359.0.	295D 4H27M16S.	DSS-42.			.1. DSS-42 LOS.		.1184. .1185.
360.0.	295D 5H36M 7S.	DSS-41.			.1. DSS-41 LOS.		.1186. .1187.
361.0.	295D10H42M51S.	DSS-12.			.1. DSS-12 AOS.		.1188. .1189.
362.0.	295D10H53M 6S.	DSS-14.			.1. DSS-14 AOS.		.1190. .1191.
363.0.	295D11H10M45S.	DSS-11.			.1. DSS-11 AOS.		.1192. .1193.
364.0.	295D12H52M 1S.	DSS-51.			.1. DSS-51 LOS.		.1194. .1195.
365.0.	295D13H14M	.MAR CH.	.MRCH TKCH.	MAR COMMAND	.1. CHANGE TCP FOR MODE 1 DATA AT 131548.		.1196. .1197. .1198.
365.1.		.ACE 5	.ACE5 DACN.	VAL-PRIME	.1. PREPARE FOR MODE 1 DATA.		.1199. .1200.
366.0.	295D13H15M48S.	.SPAC	.BC ACE5.	VAL-PRIME	.1. REPORT EOT/CHANGE TRACK (DATA MODE 1).		.1201. .1202.
367.0.	295D13H35M48S.	.SPAC	.BC ACE5.	VAL-PRIME	.1. REPORT TRACK 1 TEST PATTERN (DATA MODE 1).		.1203. .1204.
368.0.	295D13H50M	.MAR CH.	.MRCH TKCH.	MAR COMMAND	.1. CHANGE TCP FOR MODE 4 DATA AT 135148.		.1205. .1206. .1207.
368.1.		.ACE 5	.ACE5 DACN.	VAL-PRIME	.1. PREPARE FOR MODE 4 DATA.		.1208. .1209.

Table B-2 (contd)

ITEM	TIME	STA.	REPORT BY-TO	NET	EVENT	CHECK WHEN COMPLETE	LINE
369.0.	295D13H51M48S.	SPAC	BC ACE5.	VAL-PRIME	.1. REPORT FOURTH NO DATA PERIOD (DATA MODE 4).		.1210.
							.1211.
370.0.	295D15H-0M21S.	DSS-61.			.1. DSS-61 LOS.		.1212.
							.1213.
371.0.	295D15H35M14S.	DSS-62.			.1. DSS-62 LOS.		.1214.
							.1215.
372.0.	295D17H57M24S.	DSS-42.			.1. DSS-42 AOS.		.1216.
							.1217.
373.0.	295D18H 1M24S.	DSS-41.			.1. DSS-41 AOS.		.1218.
							.1219.
374.0.	295D22H34M33S.	DSS-14.			.1. DSS-14 LOS.		.1220.
							.1221.
375.0.	295D22H44M42S.	DSS-12.			.1. DSS-12 LOS.		.1222.
							.1223.
376.0.	295D22H44M44S.	DSS-11.			.1. DSS-11 LOS.		.1224.
							.1225.
377.0.	296D 1H44M17S.	DSS-51.			.1. DSS-51 AOS.		.1226.
							.1227.
378.0.	296D 2H53M14S.	DSS-62.			.1. DSS-62 AOS.		.1228.
							.1229.
379.0.	296D 3H14M30S.	DSS-61.			.1. DSS-61 AOS.		.1230.
							.1231.
380.0.	296D 4H27M48S.	DSS-42.			.1. DSS-42 LOS.		.1232.
							.1233.
381.0.	296D 5H36M43S.	DSS-41.			.1. DSS-41 LOS.		.1234.
							.1235.
382.0.	.2960D 7H 4M48S.	SPAC	BC ACE5.	VAL-PRIME	.1. REPORT EOT/END OF SECOND PLAYBACK.		.1236.
							.1237.
							.1238.
							.1239.
							.1240.
							.1241.
							.1242.

Table B-2 (contd)

ITEM	TIME	STA.	REPORT BY-TO	NET	EVENT	CHECK WHEN COMPLETE	LINE
383.0.							1243.
							1244.
							1245.
					*****TRACK 2 PLAYBACK FIRST*****		1246.
							1247.
							1248.
							1249.
384.0.	293D 7H43M	MAR CH.	MRCH TKCH.	MAR COMMAND	.1. CHANGE TCP FOR MODE 4 DATA AT 074448.		1250.
							1251.
							1252.
384.1.		ACE 5	ACE5 DACN.	VAL-PRIME	.1. PREPARE FOR MODE 4 DATA.		1253.
							1254.
385.0.	293D 7H44M48S.	SPAC	BC ACE5.	VAL-PRIME	.1. REPORT TRACK 2 TEST PATTERN (DATA MODE 4).		1255.
							1256.
386.0.	293D 8H	MAR CH.	MRCH TKCH.	MAR COMMAND	.1. CHANGE TCP FOR MODE 1 DATA AT 080048.		1257.
							1258.
							1259.
386.1.		ACE 5	ACE5 DACN.	VAL-PRIME	.1. PREPARE FOR MODE 1 DATA.		1260.
							1261.
387.0.	293D 8H-0M48S.	SPAC	BC ACE5.	VAL-PRIME	.1. REPORT 2ND 'NO DATA' PERIOD (DATA MODE 1).		1262.
							1263.
388.0.	293D 8H 5M	DSS-62.	62 TC.	DSS-62	.1. REMOVE COMMAND MOD. REPORT TIME.		1264.
							1265.
388.1.	293D 8H10M	DSS-62.	62 TC.	DSS-62	.1. TRANSMITTER OFF. REPORT TIME.		1266.
							1267.
389.0.	293D10H 6M	MAR CH.	MRCH TKCH.	MAR COMMAND	.1. CHANGE TCP FOR MODE 4 DATA AT 100748.		1268.
							1269.
							1270.
389.1.		ACE 5	ACE5 DACN.	VAL-PRIME	.1. PREPARE FOR MODE 4 DATA.		1271.
							1272.
390.0.	293D10H 7M48S.	SPAC	BC ACE5.	VAL-PRIME	.1. REPORT TRACK 2 DATA (DATA MODE 4).		1273.
							1274.
390.1.	293D10H43M31S.	DSS-12.			.1. DSS-12 AOS.		1275.
							1276.
390.2.	293D10H51M51S.	DSS-14.			.1. DSS-14 AOS.		1277.
							1278.

Table B-2 (contd)

ITEM	TIME	STA.	REPORT BY-TO	NET	EVENT	CHECK WHEN COMPLETE	LINE
390.3.	293D11H 9M38S.	DSS-11.			.1. DSS-11 AOS.		.1279.
							.1280.
390.4.	293D15H38M 4S.	DSS-62.			.1. DSS-62 LOS.		.1281.
							.1282.
390.5.	293D18H-0M13S.	DSS-42.			.1. DSS-42 AOS.		.1283.
							.1284.
390.6.	293D18H 3M46S.	DSS-41.			.1. DSS-41 AOS.		.1285.
							.1286.
390.7.	293D22H36M59S.	DSS-14.			.1. DSS-14 LOS.		.1287.
							.1288.
391.0.	294D 0H26M	.MAR CH.	MRCH TKCH.	MAR COMMAND	.1. CHANGE TCP FOR MODE 1 DATA AT 002748.		.1289.
							.1290.
							.1291.
391.1.		.ACE 5	.ACE5 DACN.	VAL-PRIME	.1. PREPARE FOR MODE 1 DATA.		.1292.
							.1293.
392.0.	294D-0H27M48S.	SPAC	.BC ACE5.	VAL-PRIME	.1. REPORT 3RD 'NO DATA' PERIOD (DATA MODE 1).		.1294.
							.1295.
393.0.	294D 1H25M48S.	SPAC	.BC ACE5.	VAL-PRIME	.1. REPORT EOT/CHANGE TRACK (DATA MODE 1).		.1296.
							.1297.
394.0.	294D 1H44M	.MAR CH.	MRCH TKCH.	MAR COMMAND	.1. CHANGE TCP FOR MODE 4 DATA AT 014548.		.1298.
							.1299.
							.1300.
394.1.		.ACE 5	.ACE5 DACN.	VAL-PRIME	.1. PREPARE FOR MODE 4 DATA.		.1301.
							.1302.
395.0.	294D 1H45M48S.	SPAC	.BC ACE5.	VAL-PRIME	.1. REPORT TRACK 1 TEST PATTERN (DATA MODE 4).		.1303.
							.1304.
396.0.	294D 2H	.MAR CH.	MRCH TKCH.	MAR COMMAND	.1. CHANGE TCP FOR MODE 1 DATA AT 020148.		.1305.
							.1306.
							.1307.
396.1.		.ACE 5	.ACE5 DACN.	VAL-PRIME	.1. PREPARE FOR MODE 1 DATA.		.1308.
							.1309.
397.0.	294D 2H 1M48S.	SPAC	.BC ACE5.	VAL-PRIME	.1. REPORT 4TH 'NO DATA' PERIOD (DATA MODE 1).		.1310.
							.1311.

Table B-2 (contd)

ITEM	TIME	STA.	REPORT BY-TO	NET	EVENT	CHECK WHEN COMPLETE	LINE
397.1.	294D 2H51M32S.	DSS-62.			.1. DSS-62 AOS.		.1312. .1313.
398.0.	294D 2H17M	MAR CH.	MRCH TKCH.	MAR COMMAND	.1. CHANGE TCP FOR MODE 4 DATA AT 021848.		.1314. .1315. .1316.
398.1.		ACE 5	ACE5 DACN.	VAL-PRIME	.1. PREPARE FOR MODE 4 DATA.		.1317. .1318.
399.0.	294D 2H18M48S.	SPAC	BC ACE5.	VAL-PRIME	.1. REPORT TRACK 1 DATA (DATA MODE 4).		.1319. .1320.
399.1.	294D 4H26M47S.	DSS-42.			.1. DSS-42 LOS.		.1321. .1322.
399.2.	294D10H52M28S.	DSS-14.			.1. DSS-14 AOS.		.1323. .1324.
400.0.	294D19H13M	MAR CH.	MRCH TKCH.	MAR COMMAND	.1. CHANGE TCP FOR MODE 1 DATA AT 191448.		.1325. .1326. .1327.
400.1.		ACE 5	ACE5 DACN.	VAL-PRIME	.1. PREPARE FOR MODE 1 DATA.		.1328. .1329.
401.0.	294D19H14M48S.	SPAC	BC ACE5.	VAL-PRIME	.1. REPORT EOT/END OF FIRST PLAYBACK. BEGIN FIRST NO DATA PERIOD, TRACK 2 (DATA MODE 1).		.1330. .1331. .1332.
402.0.	294D19H33M	MAR CH.	MRCH TKCH.	MAR COMMAND	.1. CHANGE TCP FOR MODE 4 DATA AT 193448.		.1333. .1334. .1335.
402.1.		ACE 5	ACE5 DACN.	VAL-PRIME	.1. PREPARE FOR MODE 4 DATA.		.1336. .1337.
403.0.	294D19H34M48S.	SPAC	BC ACE5.	VAL-PRIME	.1. REPORT TRACK 1 TEST PATTERN (DATA MODE 4).		.1338. .1339.
404.0.	294D19H49M	MAR CH.	MRCH TKCH.	MAR COMMAND	.1. CHANGE TCP FOR MODE 1 DATA AT 195048.		.1340. .1341. .1342.
404.1.		ACE 5	ACE5 DACN.	VAL-PRIME	.1. PREPARE FOR MODE 1 DATA.		.1343. .1344.
405.0.	294D19H50M48S.	SPAC	BC ACE5.	VAL-PRIME	.1. REPORT SECOND NO DATA PERIOD (DATA MODE 1).		.1345. .1346.

Table B-2 (contd)

ITEM	TIME	STA.	REPORT BY-TO	NET	EVENT	CHECK WHEN COMPLETE	LINE.
406.0.	294D20H 6M	MAR CH.	MRCH TKCH.	MAR COMMAND	.1. CHANGE TCP FOR MODE 4 DATA AT 200748.		.1347. .1348. .1349.
406.1.		ACE 5	ACE5 DACN.	VAL-PRIME	.1. PREPARE FOR MODE 4 DATA.		.1350. .1351.
407.0.	294D20H 7M48S.	SPAC	BC ACE5.	VAL-PRIME	.1. REPORT TRACK 1 DATA (MODE 4).		.1352. .1353.
408.0.	294D22H35M45S.	DSS-14.			.1. DSS-14 LOS.		.1354. .1355.
409.0.	294D22H44M56S.	DSS-12.			.1. DSS-12 LOS.		.1356. .1357.
410.0.	294D22H45M 6S.	DSS-11.			.1. DSS-11 LOS.		.1358. .1359.
411.0.	295D 1H45M11S.	DSS-51.			.1. DSS-51 AOS.		.1360. .1361.
412.0.	295D 2H52M21S.	DSS-62.			.1. DSS-62 AOS.		.1362. .1363.
413.0.	295D 3H13M54S.	DSS-61.			.1. DSS-61 AOS.		.1364. .1365.
414.0.	295D 4H27M16S.	DSS-42.			.1. DSS-42 LOS.		.1366. .1367.
415.0.	295D 5H36M 7S.	DSS-41.			.1. DSS-41 LOS.		.1368. .1369.
416.0.	295D10H42M51S.	DSS-12.			.1. DSS-12 AOS.		.1370. .1371.
417.0.	295D10H53M 6S.	DSS-14.			.1. DSS-14 AOS.		.1372. .1373.
418.0.	295D11H10M45S.	DSS-11.			.1. DSS-11 AOS.		.1374. .1375.
419.0.	295D12H16M	MAR CH.	MRCH TKCH.	MAR COMMAND	.1. CHANGE TCP FOR MODE 1 DATA AT 121748.		.1376. .1377. .1378.
419.1.		ACE 5	ACE5 DACN.	VAL-PRIME	.1. PREPARE FOR MODE 1 DATA.		.1379. .1380.

Table B-2 (contd)

ITEM	TIME	STA.	REPORT BY-TO	NET	EVENT	CHECK WHEN COMPLETE	LINE
420.0.	295D12H17M48S.	SPAC	BC ACE5.	VAL-PRIME	.1. REPORT THIRD NO DATA PERIOD (DATA MODE 1).		.1381. .1382.
421.0.	295D14H 7M	MAR CH.	MRCH TKCH.	MAR COMMAND	.1. CHANGE TCP FOR MODE 4 DATA AT 140848.		.1383. .1384. .1385.
421.1.		ACE 5	ACE5 DACN.	VAL-PRIME	.1. PREPARE FOR MODE 4 DATA.		.1386. .1387.
422.0.	295D14H 8M48S.	SPAC	BC ACE5.	VAL-PRIME	.1. REPORT TRACK 1 DATA (DATA MODE 4).		.1388. .1389.
423.0.	295D12H52M 1S.	DSS-51.			.1. DSS-51 LOS.		.1390. .1391.
424.0.	295D13H 2M	MAR CH.	MRCH TKCH.	MAR COMMAND	.1. CHANGE TCP FOR MODE 1 DATA AT 130348.		.1392. .1393. .1394.
424.1.		ACE 5	ACE5 DACN.	VAL-PRIME	.1. PREPARE FOR MODE 1 DATA.		.1395. .1396.
425.0.	295D13H 3M48S.	SPAC	BC ACE5.	VAL-PRIME	.1. REPORT EOT/CHANGE TRACK. BEGIN THIRD DATA PERIOD (DATA MODE 1).		.1397. .1398. .1399.
426.0.	295D13H22M	MAR CH.	MRCH TKCH.	MAR COMMAND	.1. CHANGE TCP FOR MODE 4 DATA AT 132348.		.1400. .1401. .1402.
426.1.		ACE 5	ACE5 DACN.	VAL-PRIME	.1. PREPARE FOR MODE 4 DATA.		.1403. .1404.
427.0.	295D13H23M48S.	SPAC	BC ACE5.	VAL-PRIME	.1. REPORT TRACK 2 TEST PATTERN (DATA MODE 4).		.1405. .1406.
428.0.	295D13H38M	MAR CH.	MRCH TKCH.	MAR COMMAND	.1. CHANGE TCP FOR MODE 1 DATA AT 133948.		.1407. .1408. .1409.
428.1.		ACE 5	ACE5 DACN.	VAL-PRIME	.1. PREPARE FOR MODE 1 DATA.		.1410. .1411.
429.0.	295D13H39M48S.	SPAC	BC ACE5.	VAL-PRIME	.1. REPORT FOURTH NO DATA PERIOD (DATA MODE 1).		.1412. .1413.
430.0.	295D15H-0M21S.	DSS-61.			.1. DSS-61 LOS.		.1414. .1415.

Table B-2 (contd)

ITEM	TIME	STA.	REPORT BY-TO	NET	EVENT	CHECK WHEN COMPLETE	LINE
431.0.	295D15H35M14S.	DSS-62.			.1. DSS-62 LOS.		.1416.
							.1417.
432.0.	295D15H45M	.MAR CH.	MRCH TKCH.	MAR COMMAND	.1. CHANGE TCP FOR MODE 4 DATA AT 154648.		.1418. .1419. .1420.
432.1.		.ACE 5	.ACE5 DACN.	VAL-PRIME	.1. PREPARE FOR MODE 4 DATA.		.1421. .1422.
433.0.	295D15H46M48S.	.SPAC	.BC ACE5.	VAL-PRIME	.1. REPORT TRACK 2 DATA (DATA MODE 4).		.1423. .1424.
434.0.	295D17H57M24S.	.DSS-42.			.1. DSS-42 AOS.		.1425. .1426.
435.0.	295D18H 1M24S.	.DSS-41.			.1. DSS-41 AOS.		.1427. .1428.
436.0.	295D22H34M33S.	.DSS-14.			.1. DSS-14 LOS.		.1429. .1430.
437.0.	295D22H44M42S.	.DSS-12.			.1. DSS-12 LOS.		.1431. .1432.
438.0.	295D22H44M44S.	.DSS-11.			.1. DSS-11 LOS.		.1433. .1434.
439.0.	296D 1H44M17S.	.DSS-51.			.1. DSS-51 AOS.		.1435. .1436.
440.0.	296D 2H53M14S.	.DSS-62.			.1. DSS-62 AOS.		.1437. .1438.
441.0.	296D 3H14M30S.	.DSS-61.			.1. DSS-61 AOS.		.1439. .1440.
442.0.	296D 4H27M48S.	.DSS-42.			.1. DSS-42 LOS.		.1441. .1442.
443.0.	296D 5H36M43S.	.DSS-41.			.1. DSS-41 LOS.		.1443. .1444.
444.0.	296D 6H 5M	.MAR CH.	MRCH TKCH.	MAR COMMAND	.1. CHANGE TCP FOR MODE 1 DATA AT 060648.		.1445. .1446. .1447.
444.1.		.ACE 5	.ACE5 DACN.	VAL-PRIME	.1. PREPARE FOR MODE 1 DATA.		.1448. .1449.

Table B-2 (contd)

ITEM	TIME	STA.	REPORT BY-TO	NET	EVENT	CHECK WHEN COMPLETE	LINE
445.0.	296D 6H 6M48S.	SPAC	BC	ACE5. VAL-PRIME	1. REPORT FIFTH NO DATA PERIOD (DATA MODE 1).		1450.
							1451.
446.0.	296D 7H 4M48S.	SPAC	BC	ACE5. VAL-PRIME	1. REPORT EOT/END OF SECOND PLAYBACK.		1452.
							1453.
							1454.
							1455.
							1456.
							1457.
							1458.

Appendix C

Telemetry Data Curves

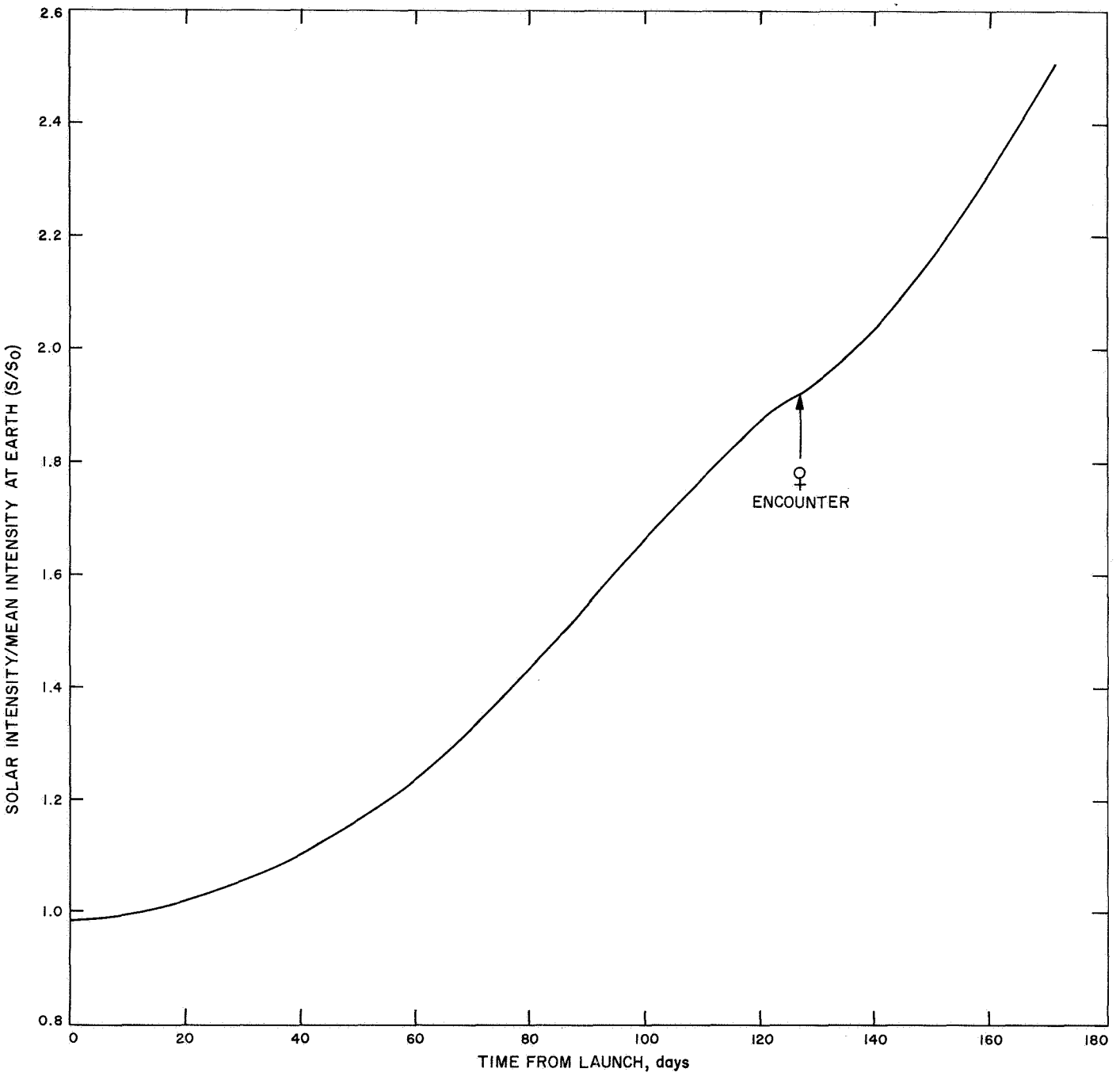


Fig. C-1. Solar intensity

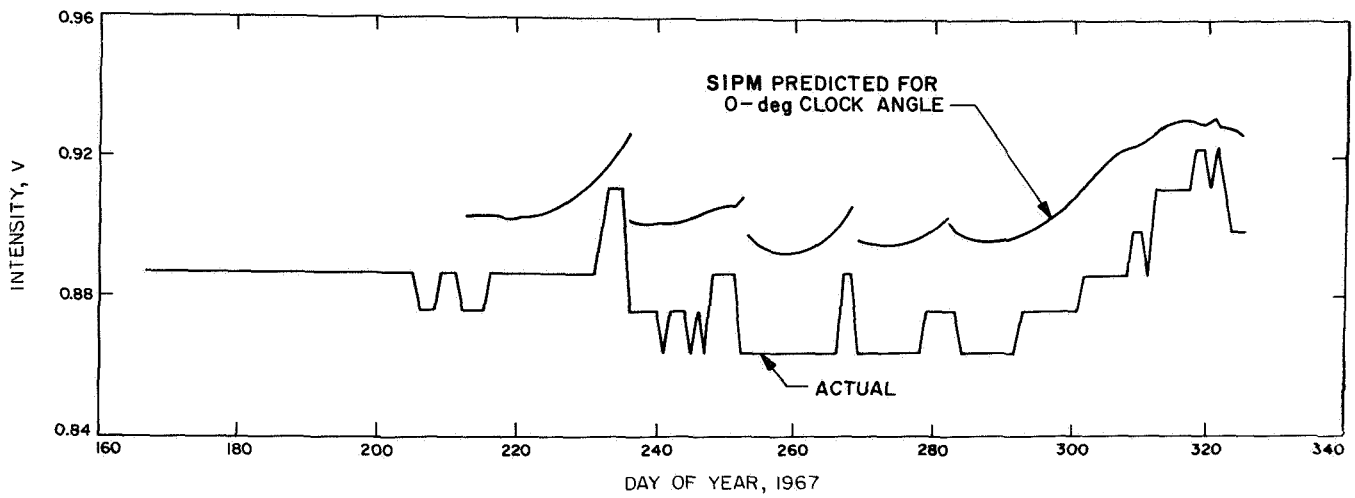


Fig. C-2. Canopus sensor intensity, channel 108

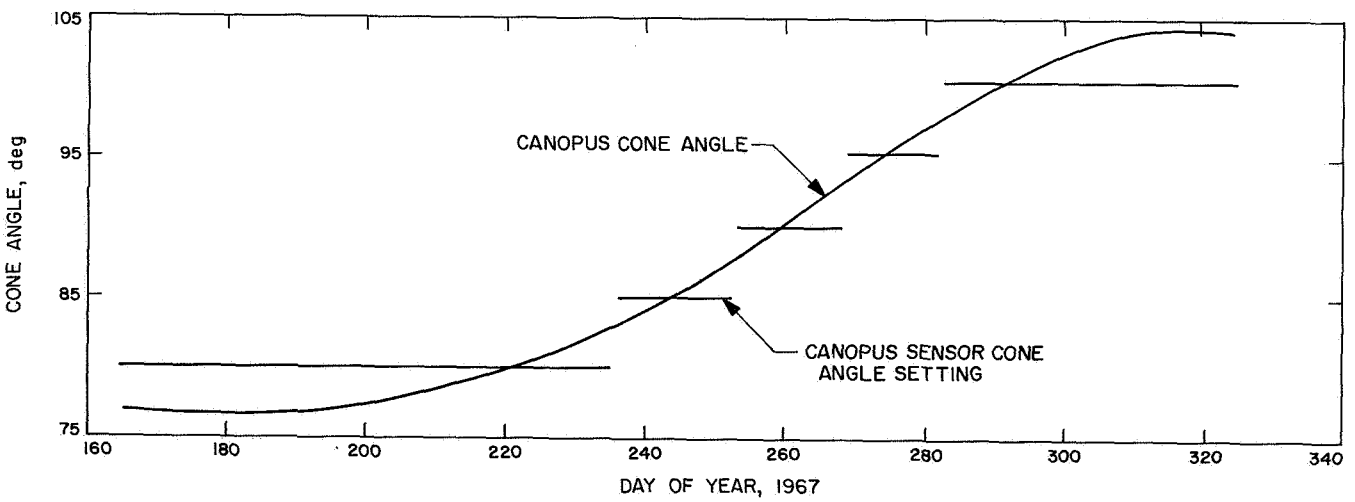


Fig. C-3. Canopus sensor cone angle, channel 303

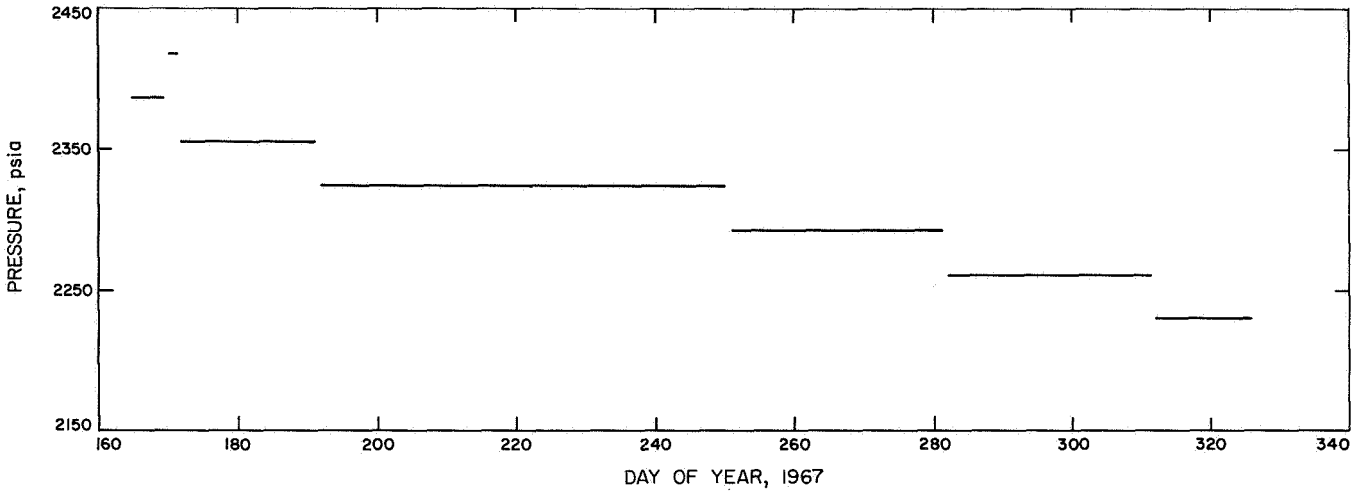


Fig. C-4. Nitrogen gas (+X/−Y) pressure, channel 208

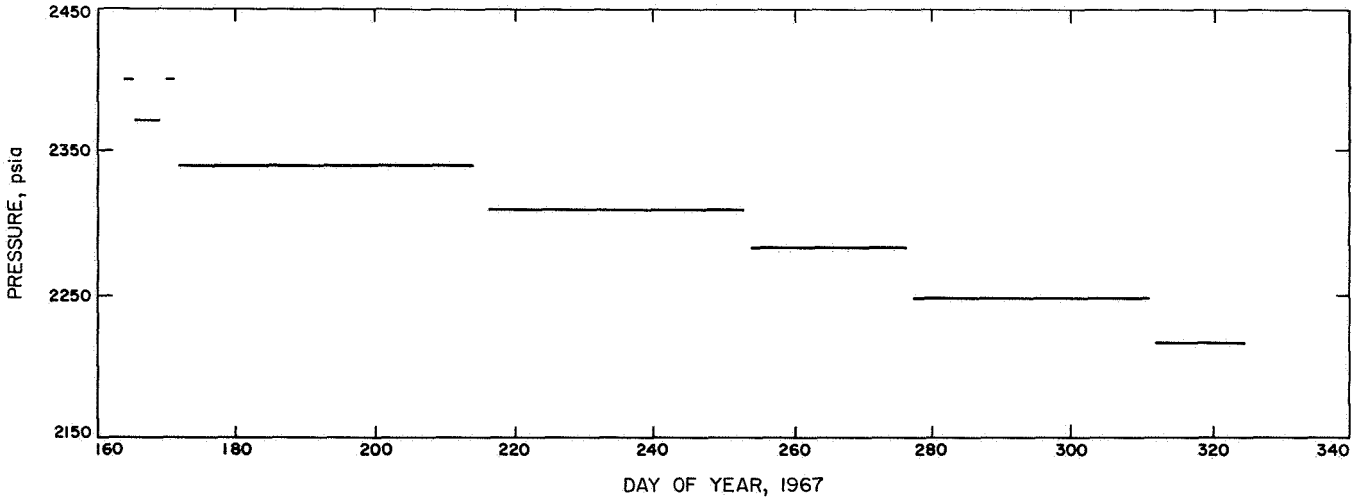


Fig. C-5. Nitrogen gas (−X/+Y) pressure, channel 209

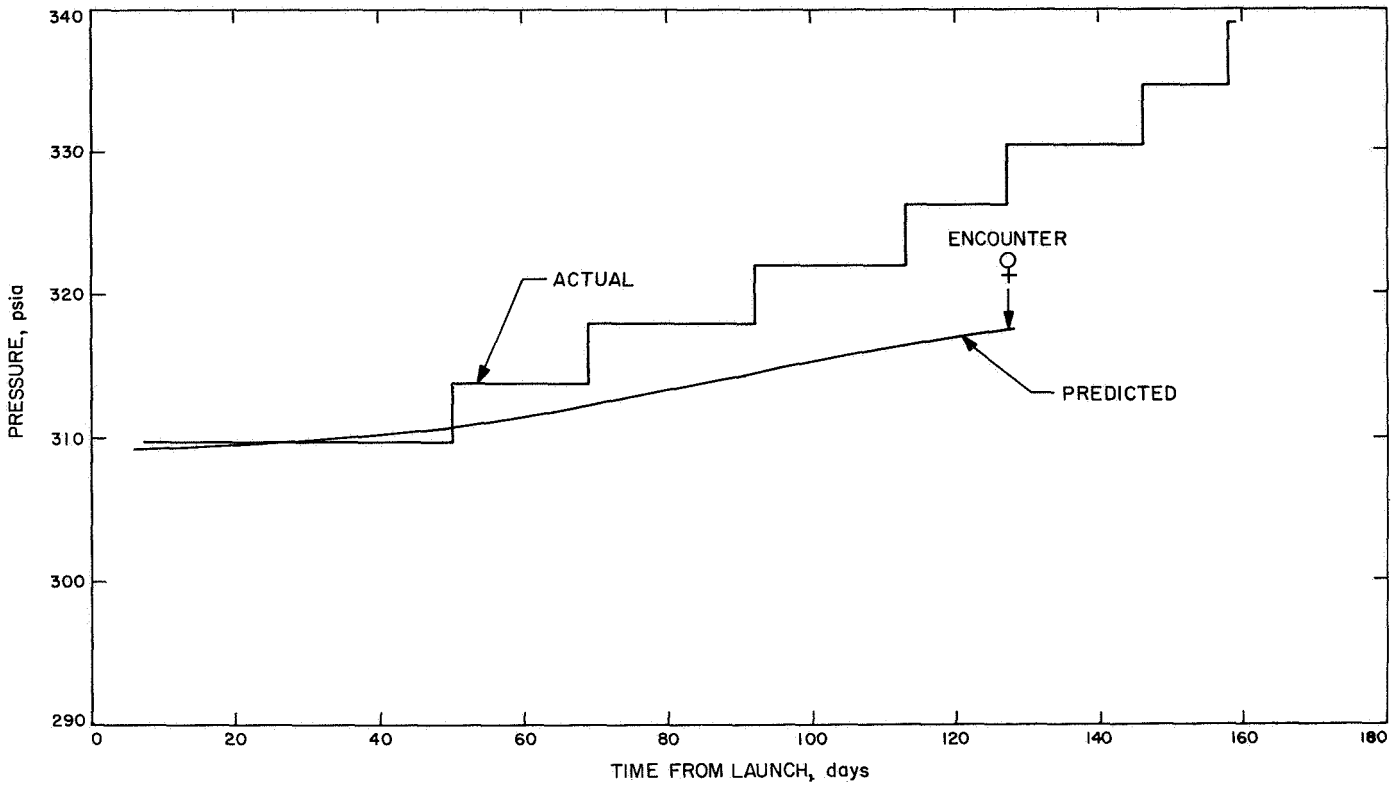


Fig. C-6. Propellant tank pressure (postmaneuver), channel 119

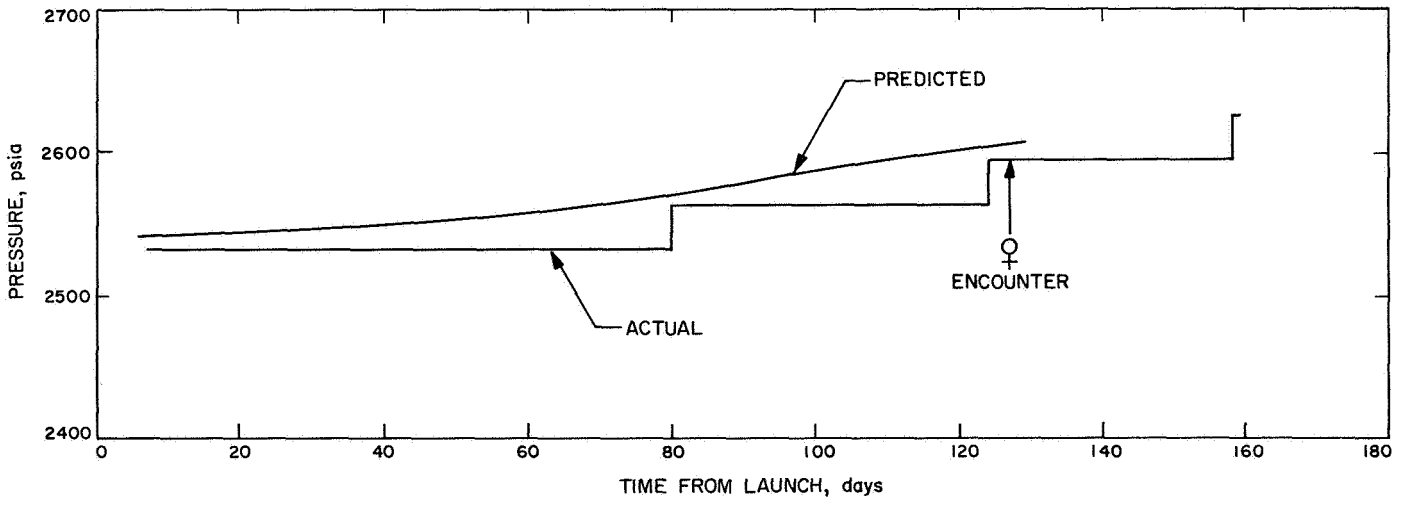


Fig. C-7. Nitrogen tank pressure (postmaneuver), channel 228

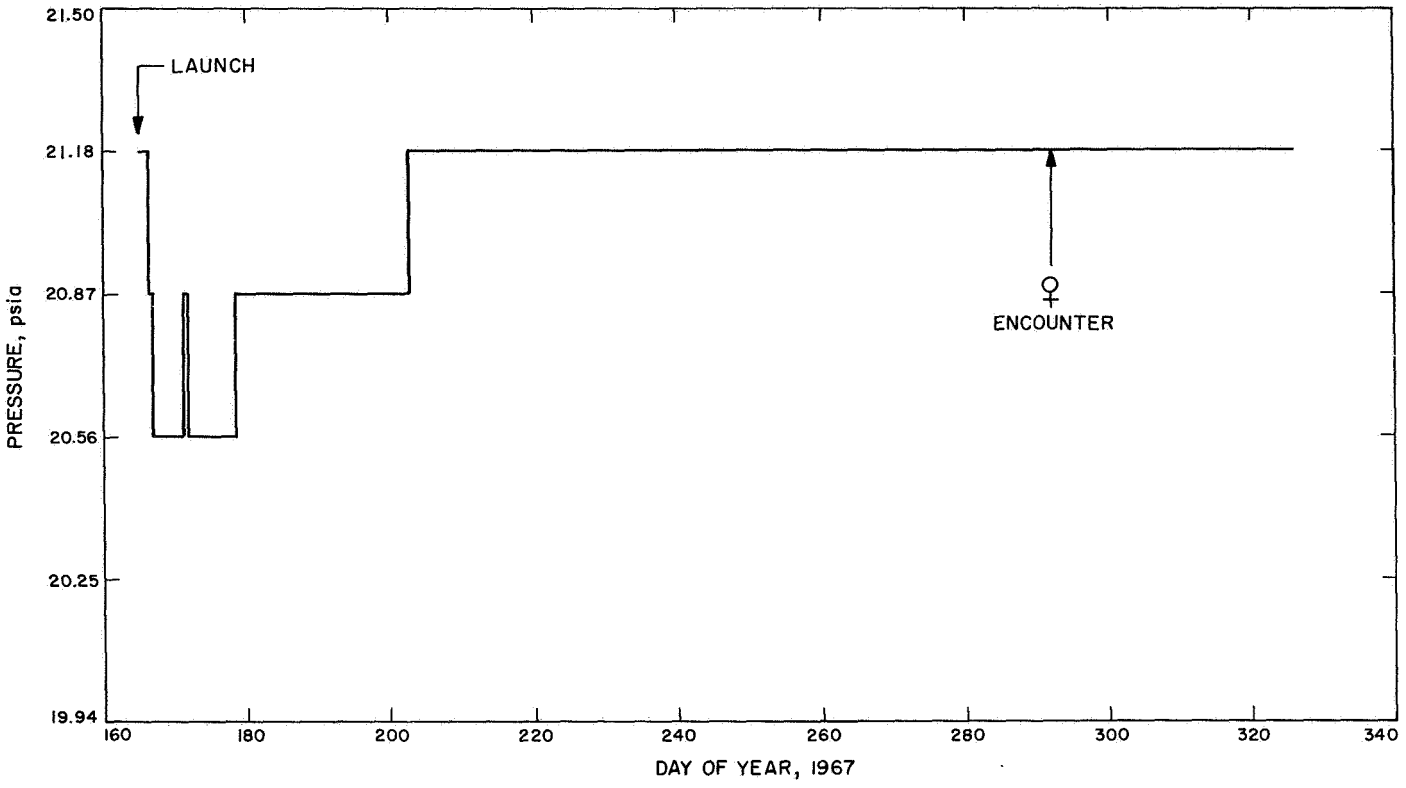


Fig. C-8. Tape recorder pressure, channel 304

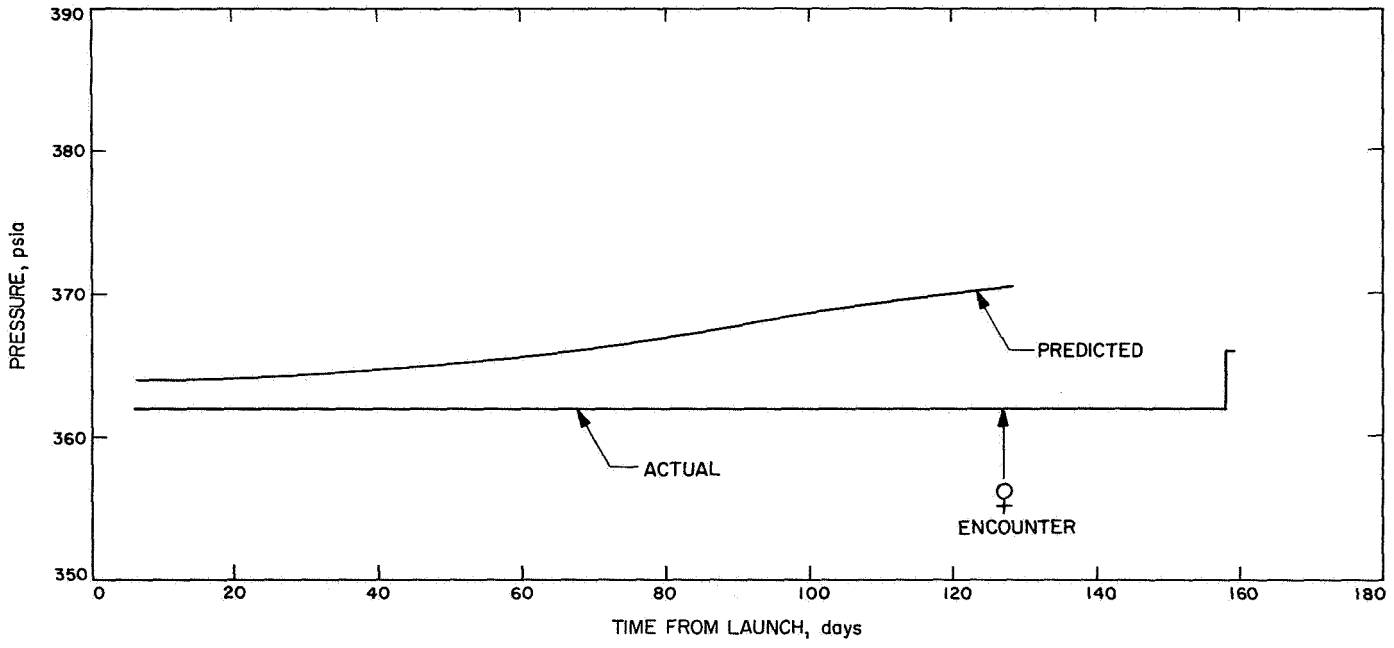


Fig. C-9. Oxidizer pressure, channel 305

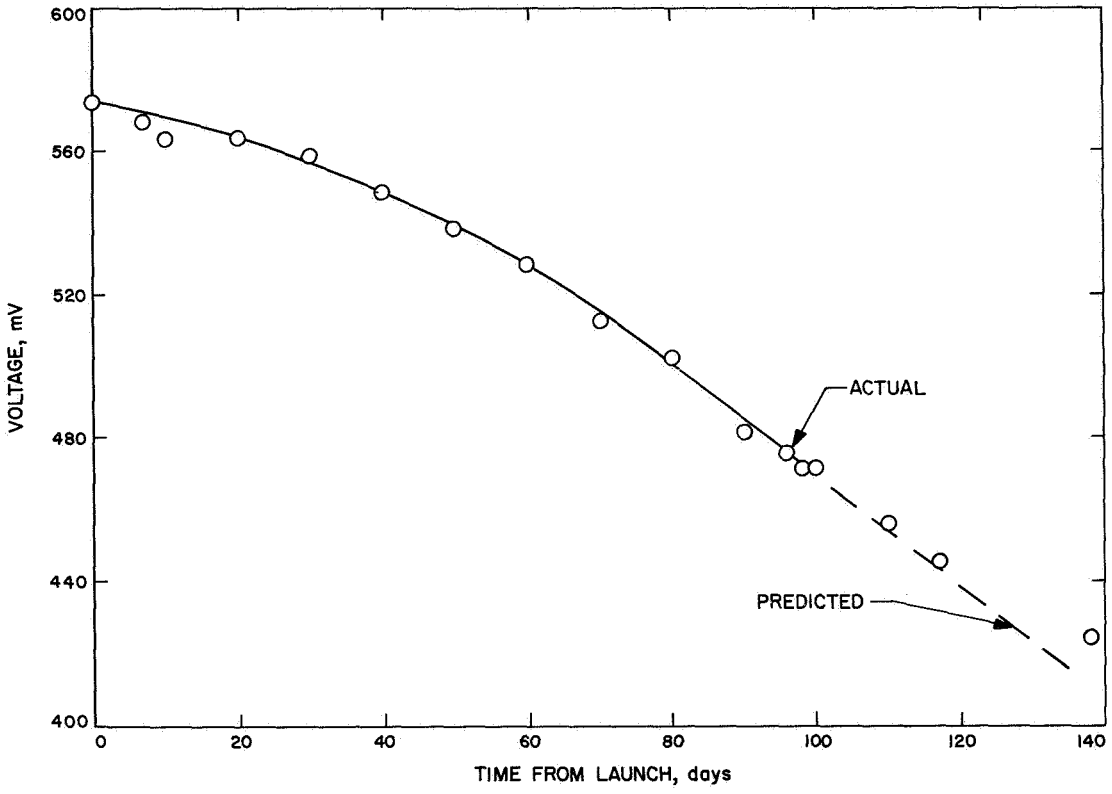


Fig. C-10. Solar panel 4A5 V_{OC} cell output, channel 417

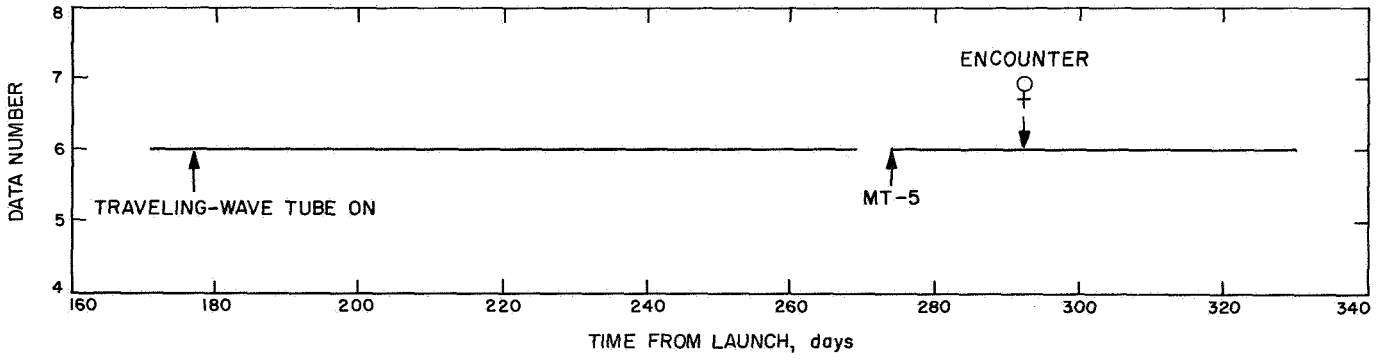


Fig. C-11. Exciter No. 1 (−25) voltage (data number), channel 301

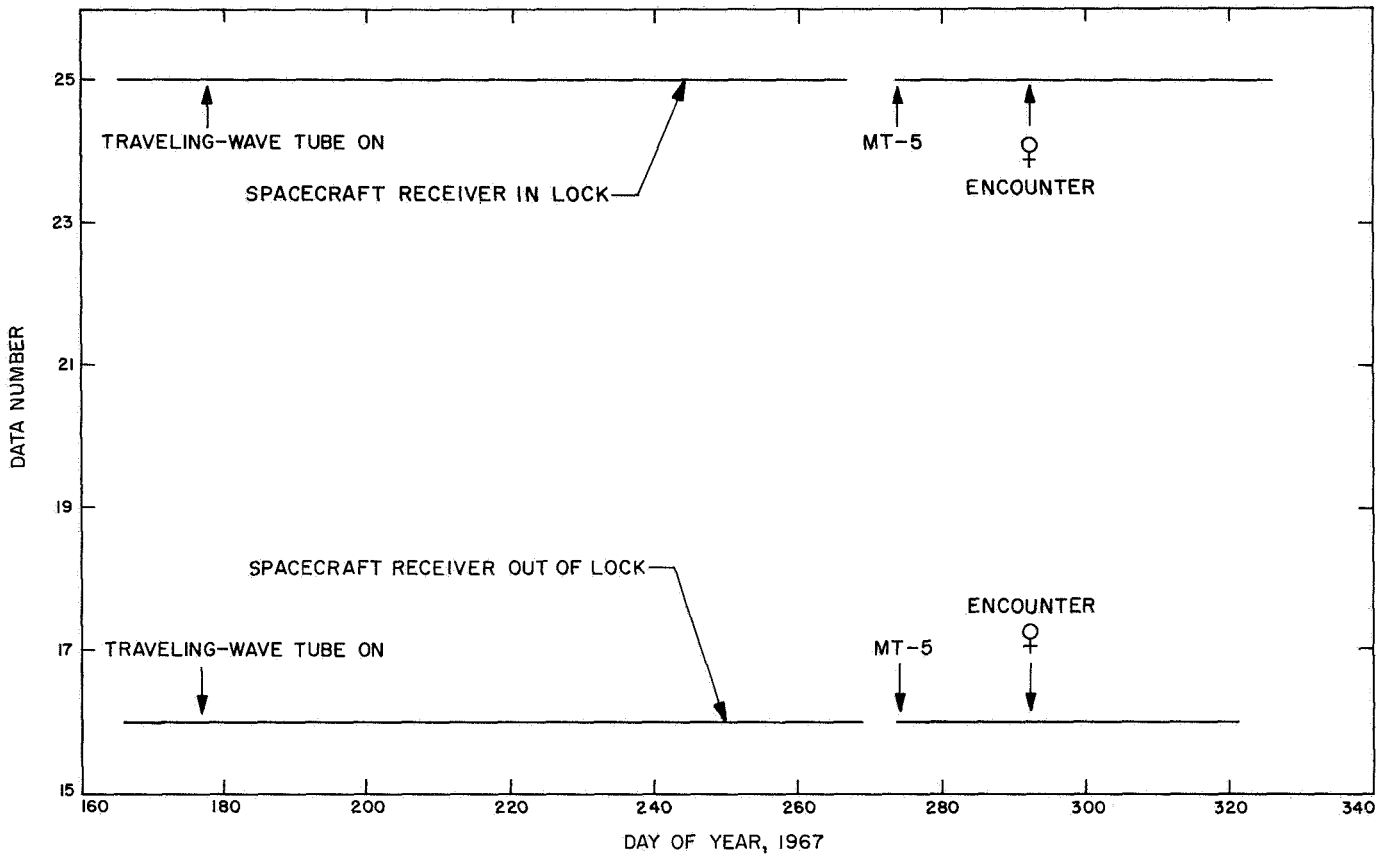


Fig. C-12. Exciter No. 2 (−15) voltage (data number), channel 302

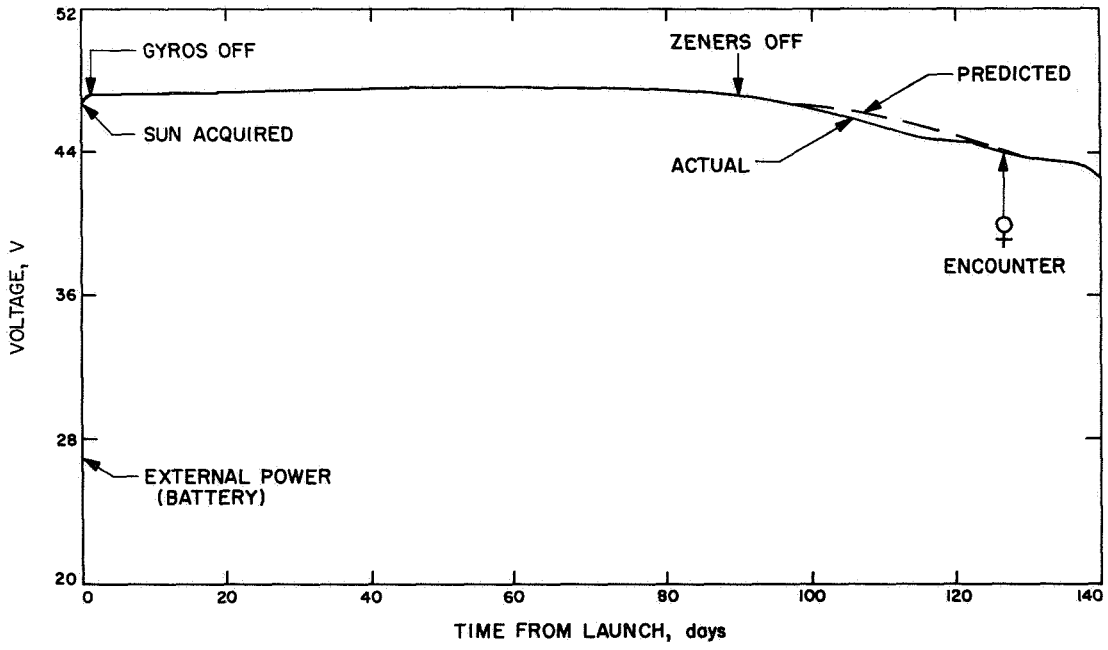


Fig. C-13. Power switching and logic voltage, channel 109

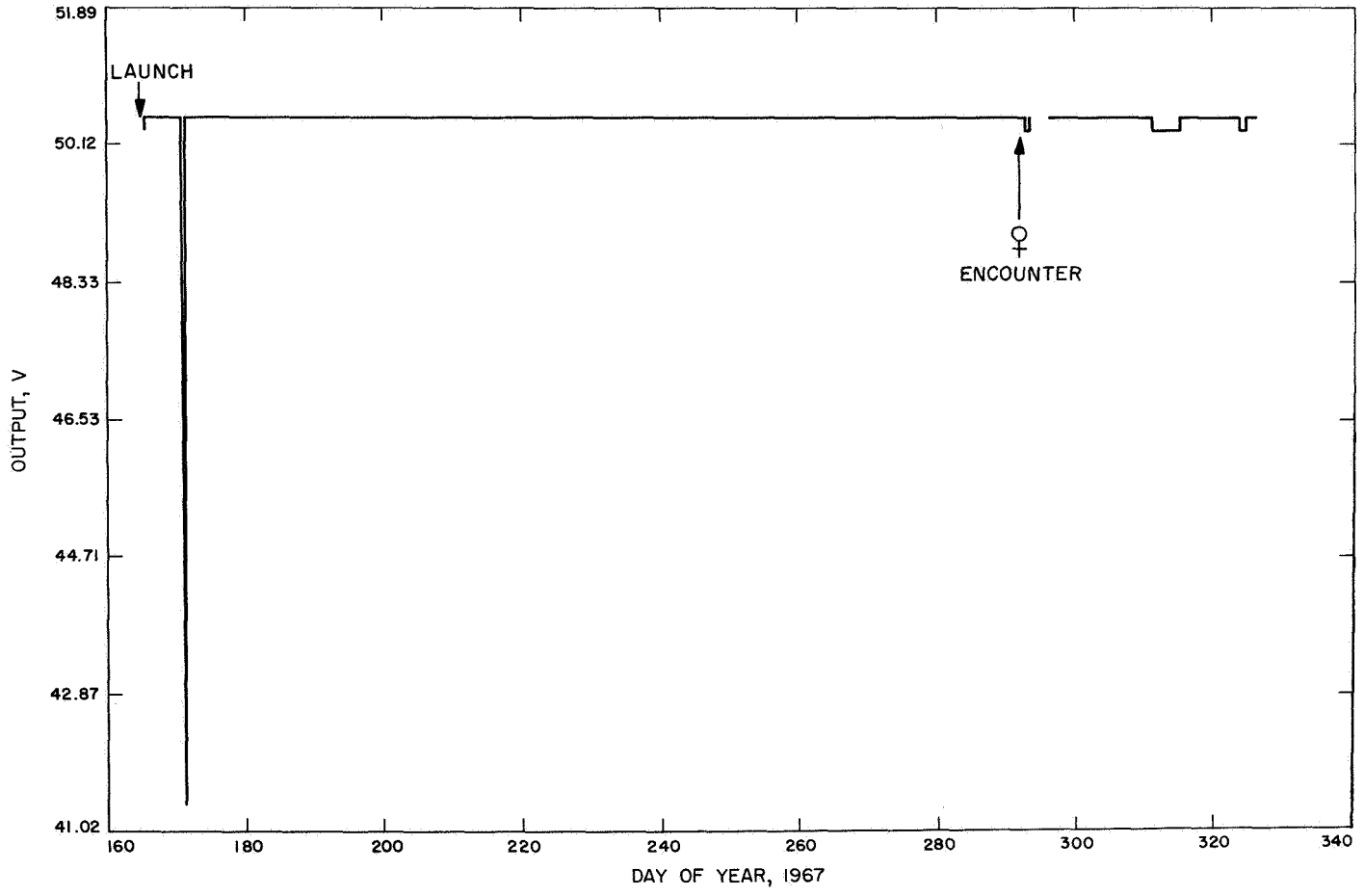


Fig. C-14. 2400-Hz inverter output voltage, channel 207

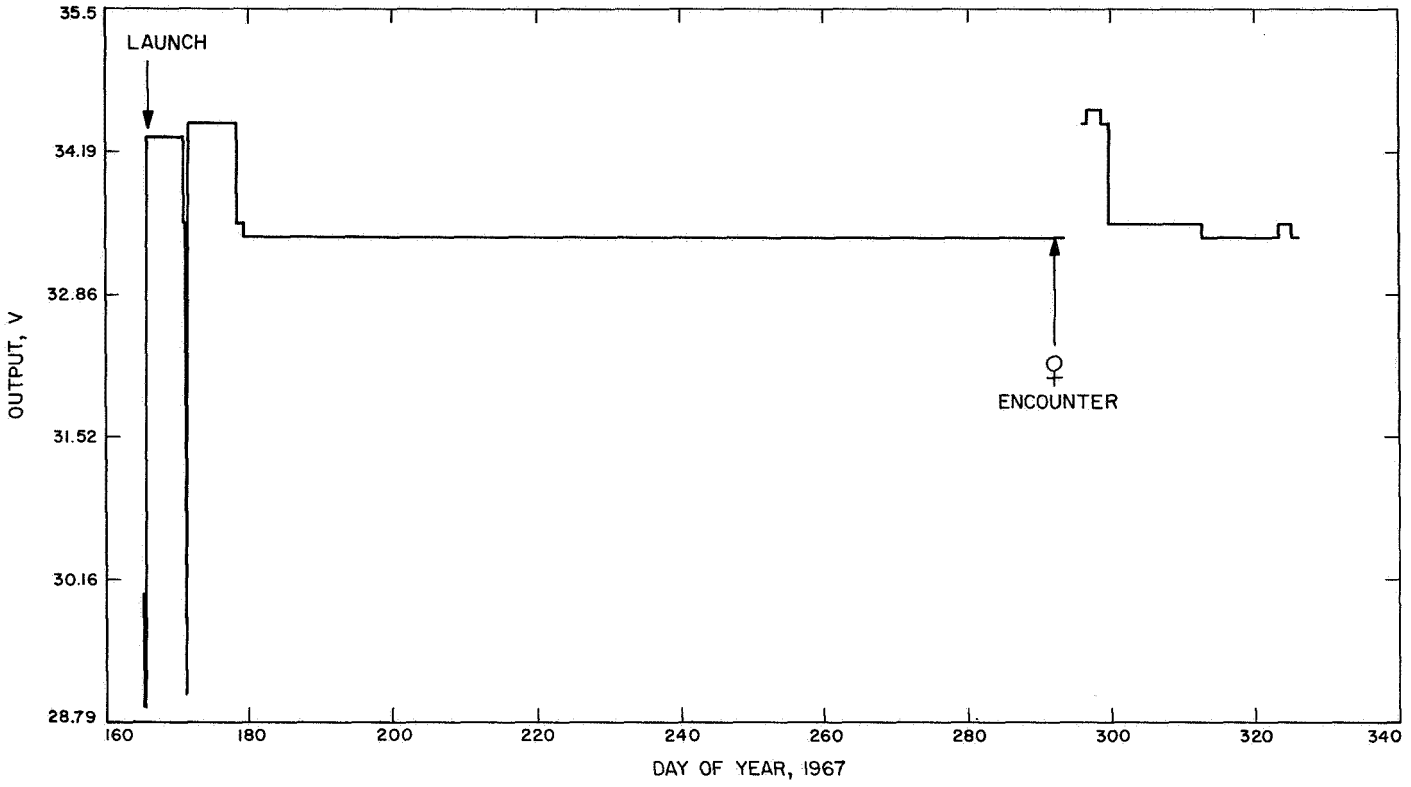


Fig. C-15. Battery voltage, channel 206

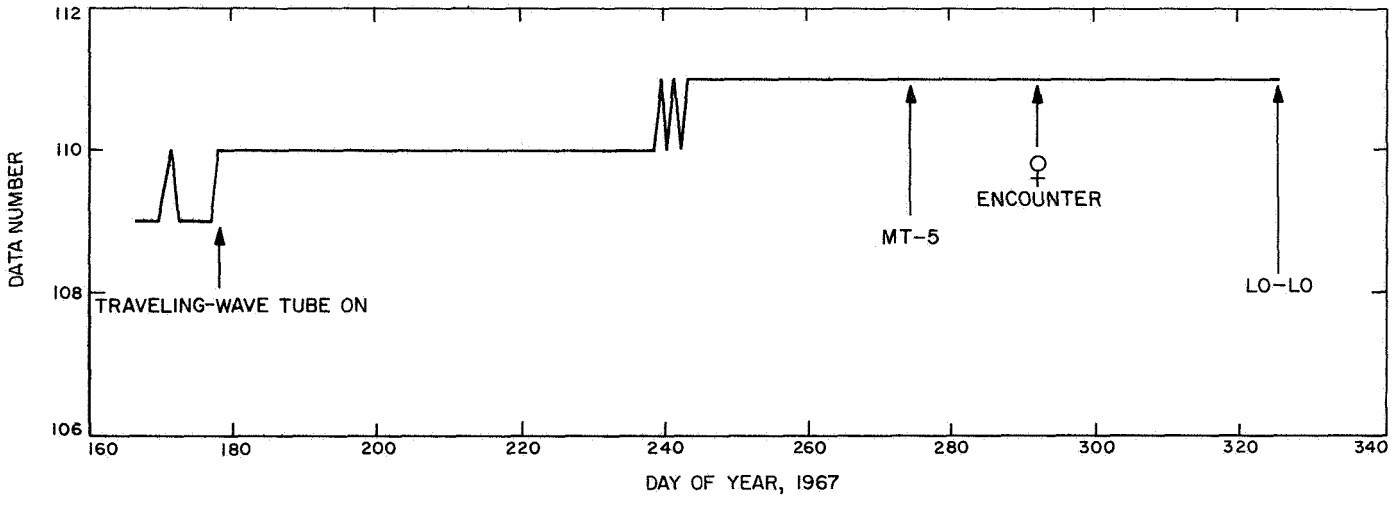


Fig. C-16. Spacecraft receiver low-drive (data number), channel 210

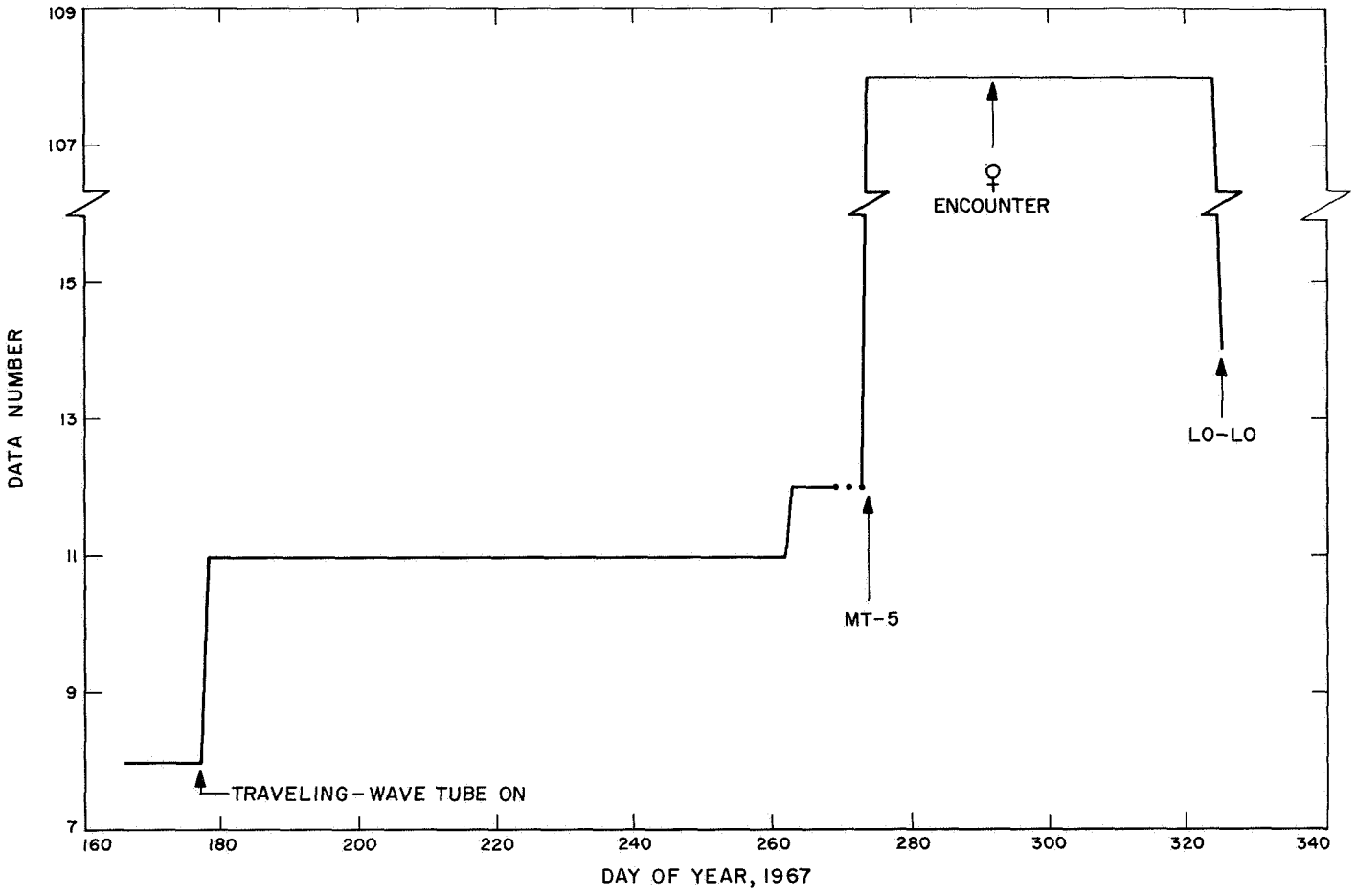


Fig. C-17. High-gain antenna drive (data number), channel 213

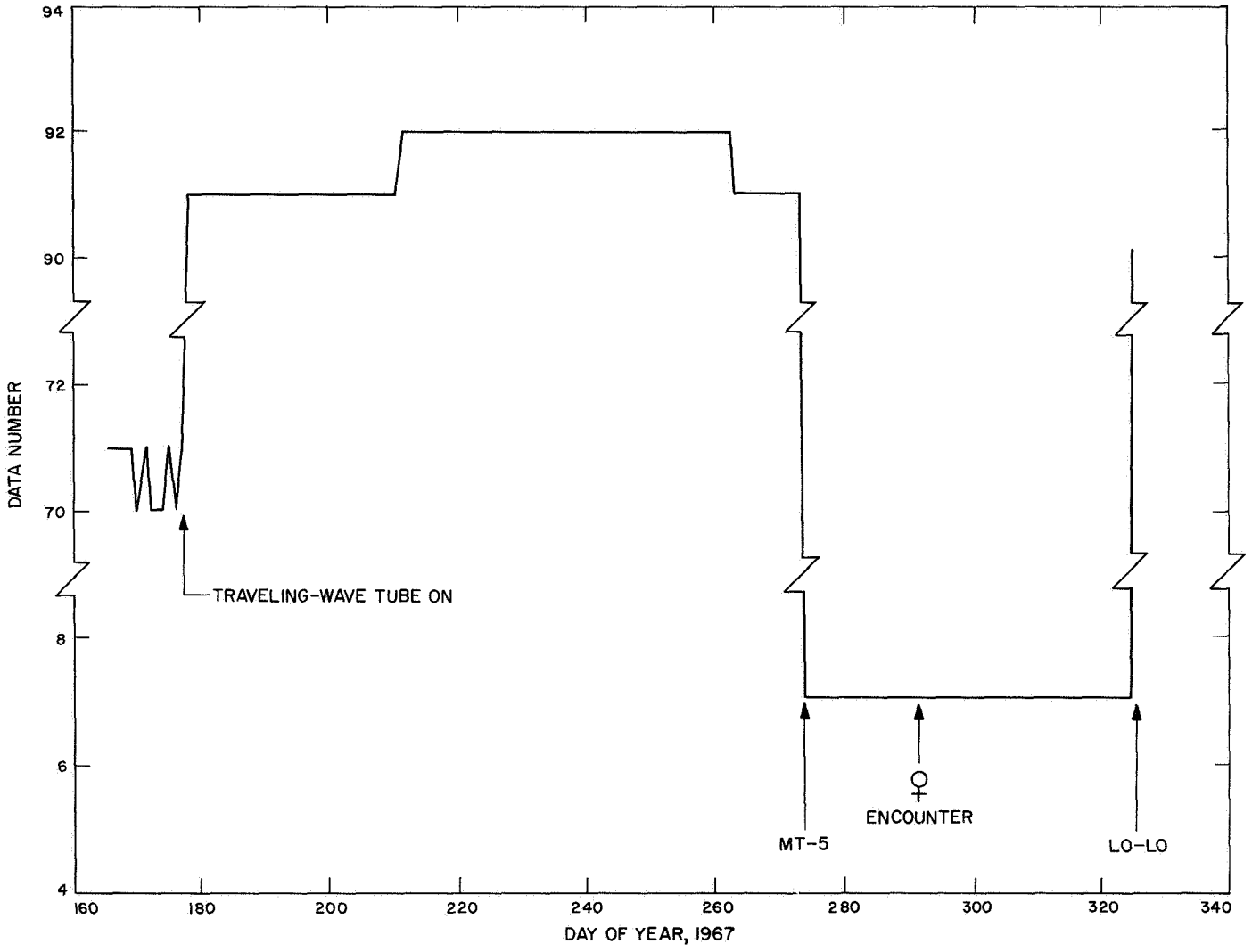


Fig. C-18. Low-gain antenna drive (data number), channel 214

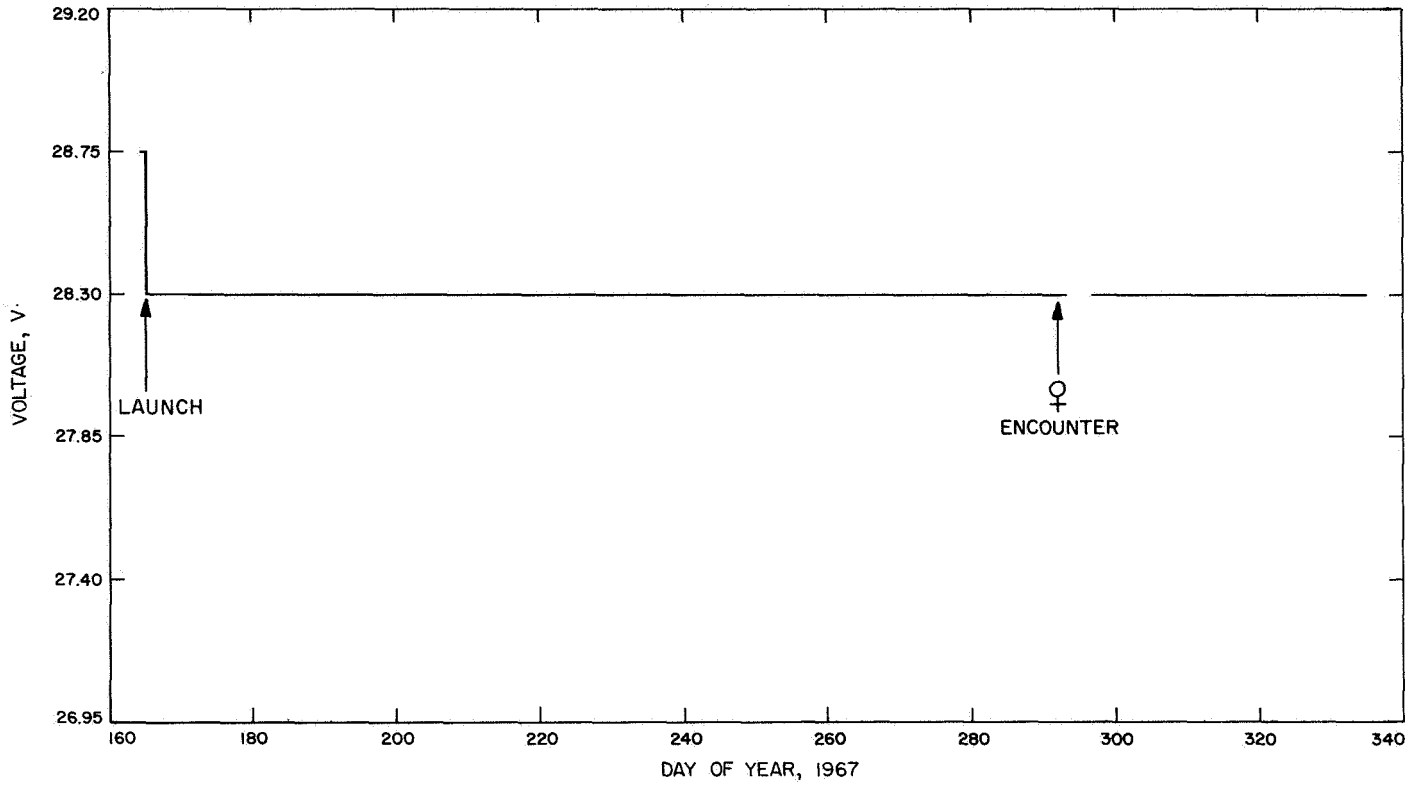


Fig. C-19. *Central computer and sequencer* 28-V monitor, channel 309

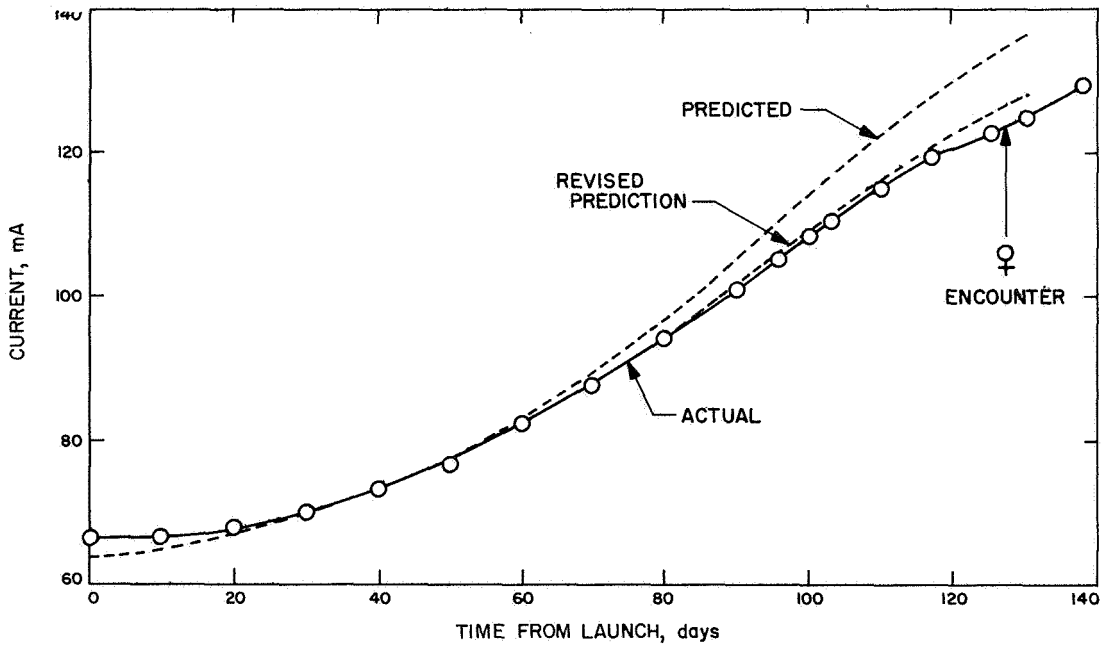


Fig. C-20. Solar panel 4A5 I_{SC} cell output, channel 415

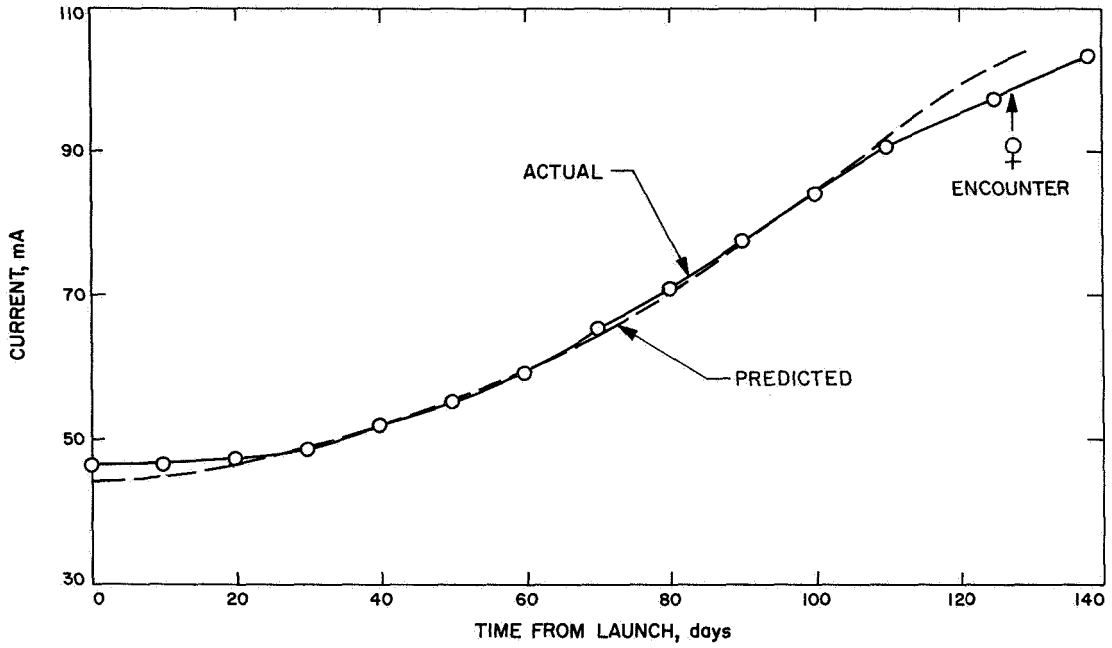


Fig. C-21. Solar panel 4A5 I_{SCR} cell output, channel 416

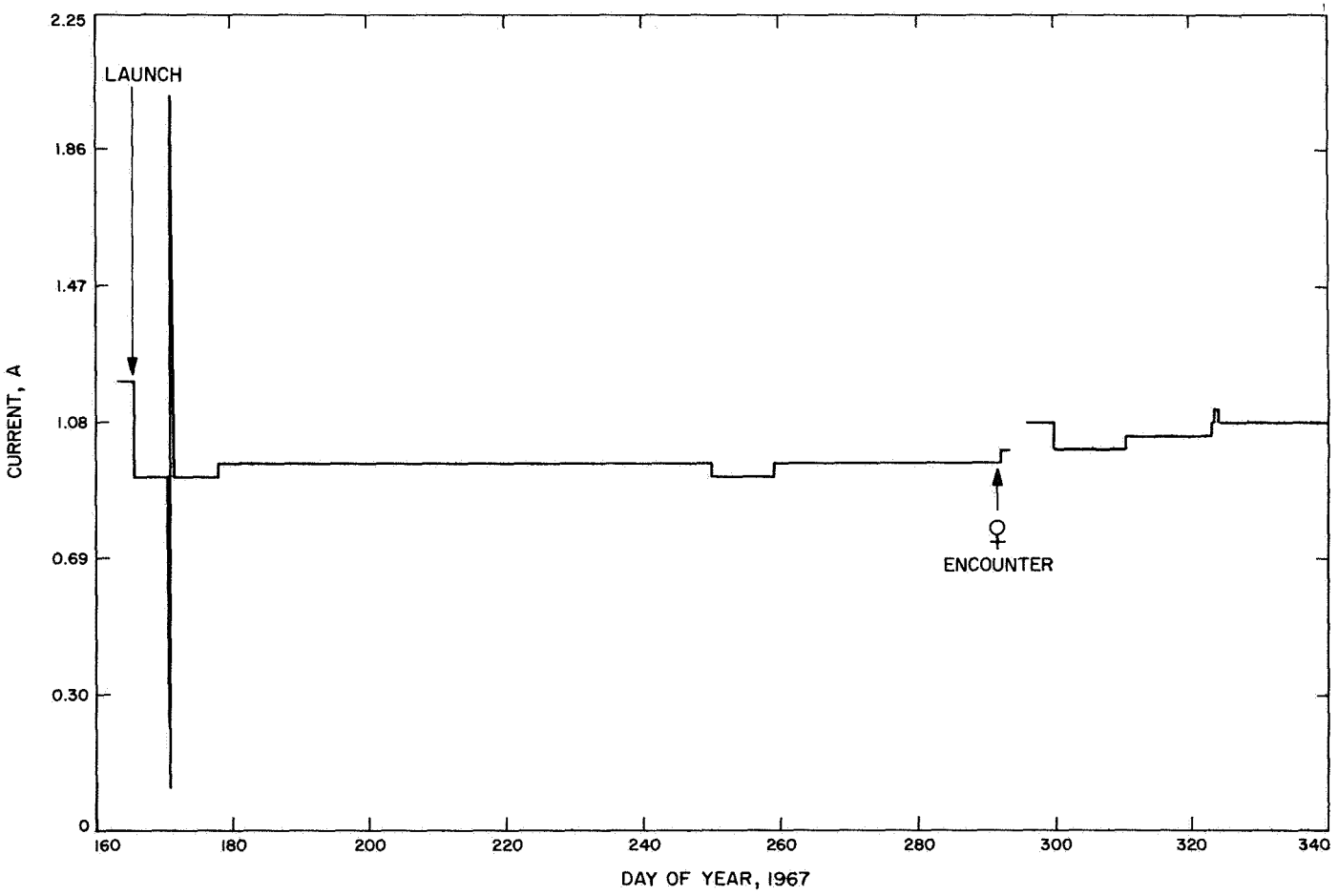


Fig. C-22. Solar panel 4A1 current, channel 222

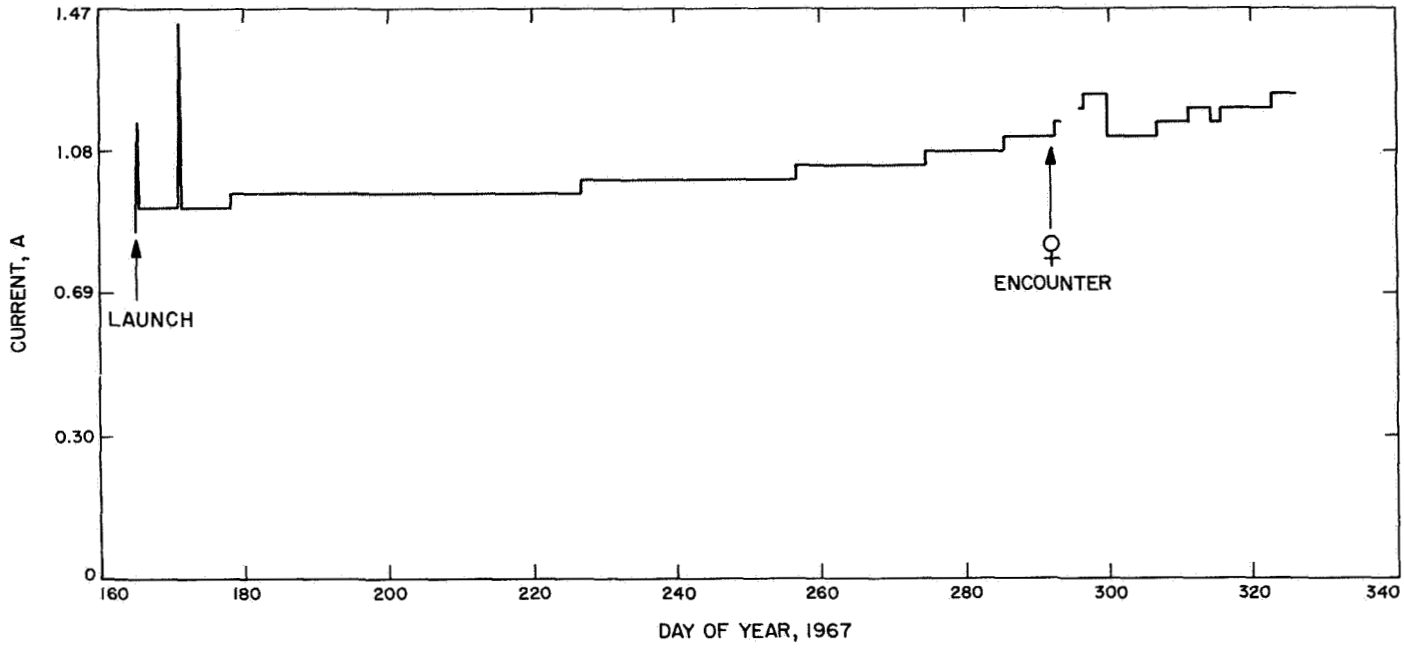


Fig. C-23. Solar panel 4A3 current, channel 224

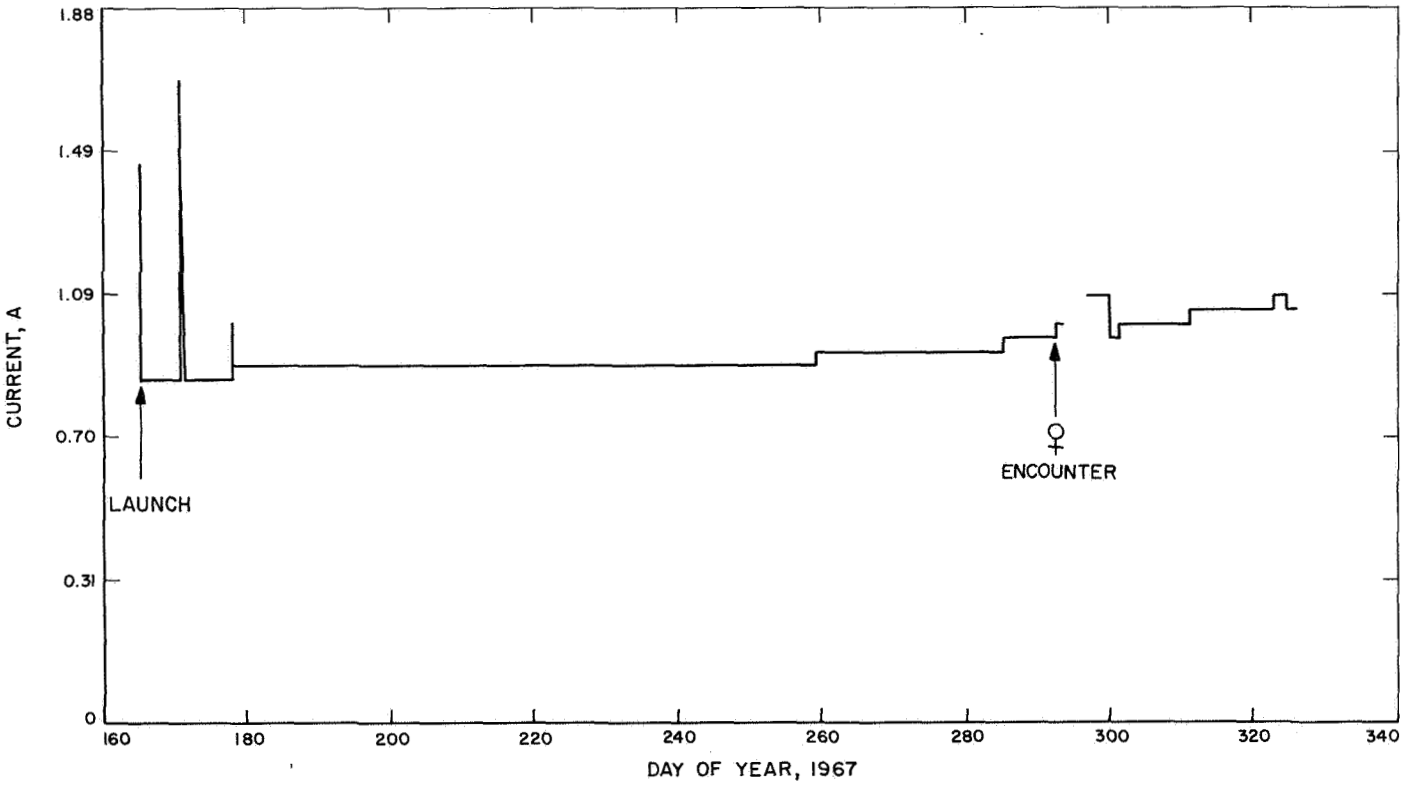


Fig. C-24. Solar panel 4A5 current, channel 223

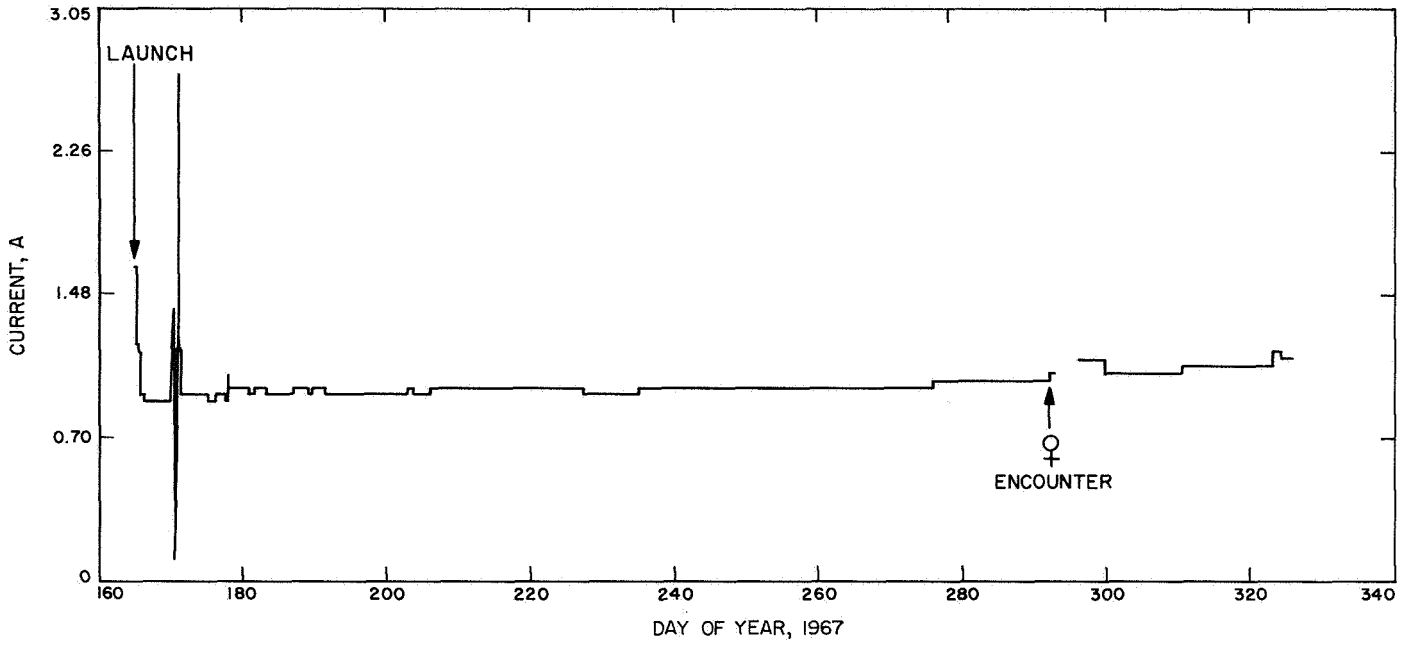


Fig. C-25. Solar panel 4A7 current, channel 225

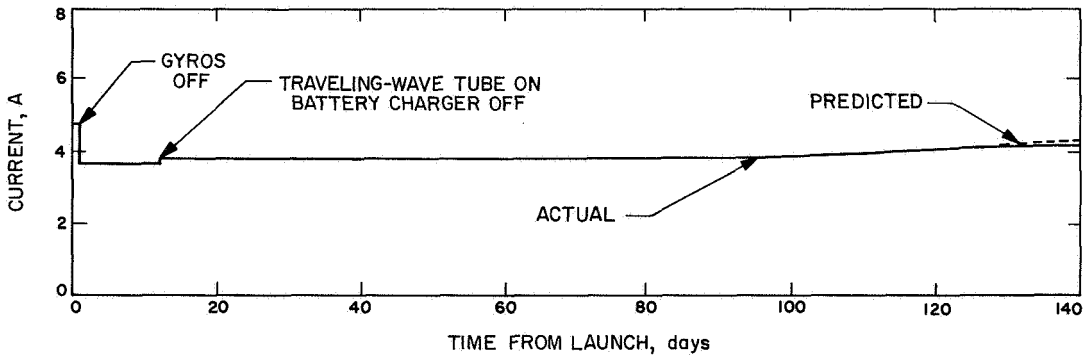


Fig. C-26. Total current of solar panels 4A1, 4A3, 4A5, and 4A7, channels 222, 223, 224, and 225, respectively

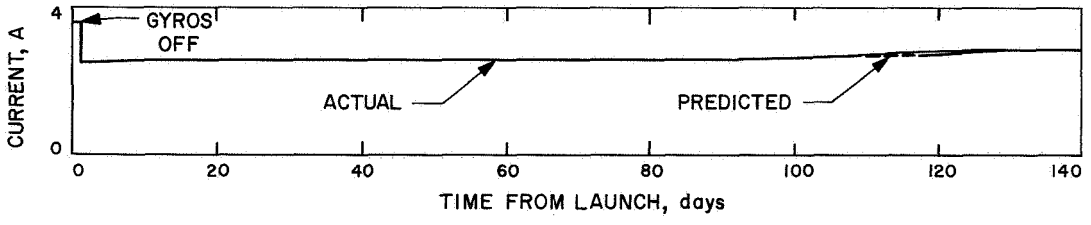


Fig. C-27. Dual booster-regulator input current, channel 203

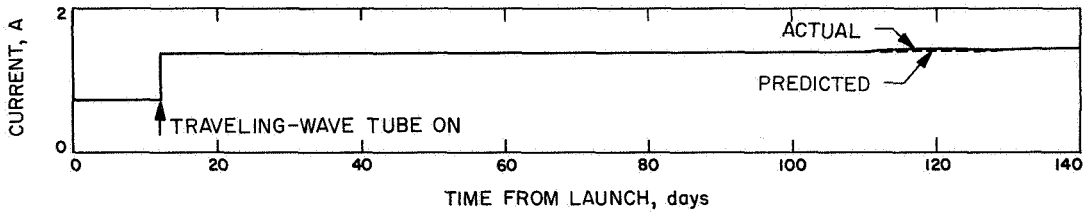


Fig. C-28. Communications converter and magnetic heater current, channel 204

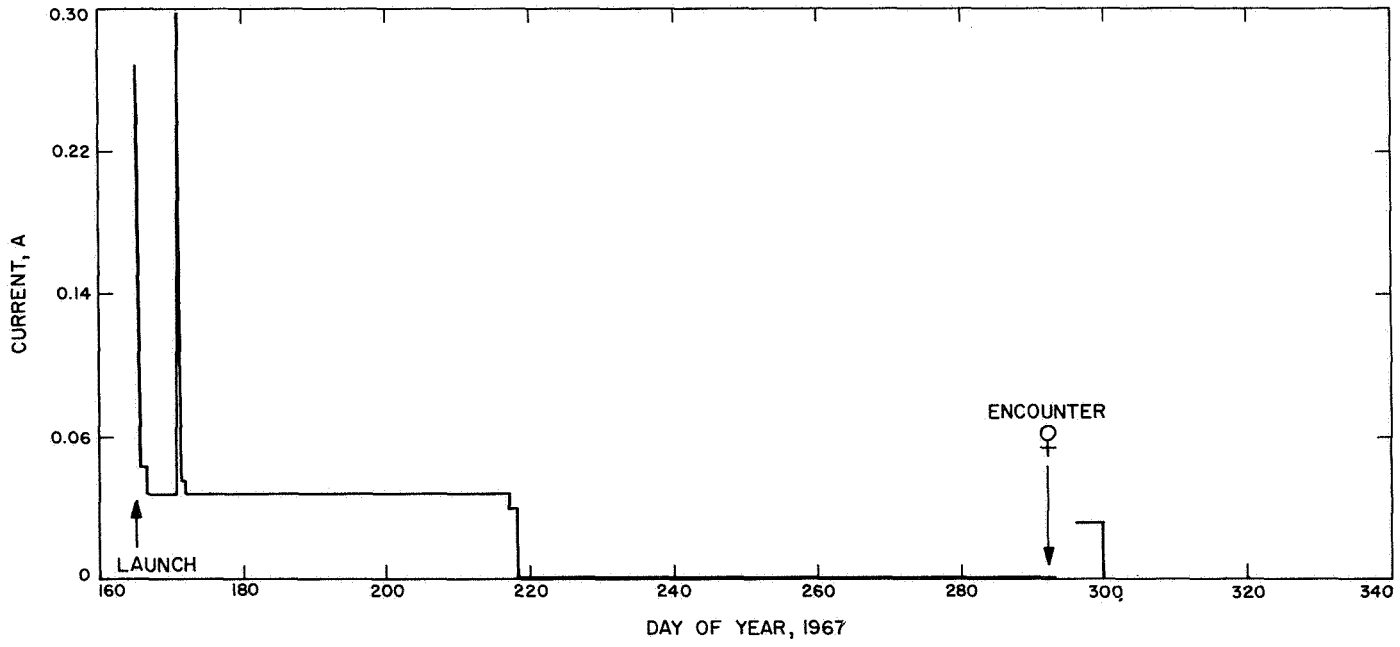


Fig. C-29. Battery charger current, channel 216

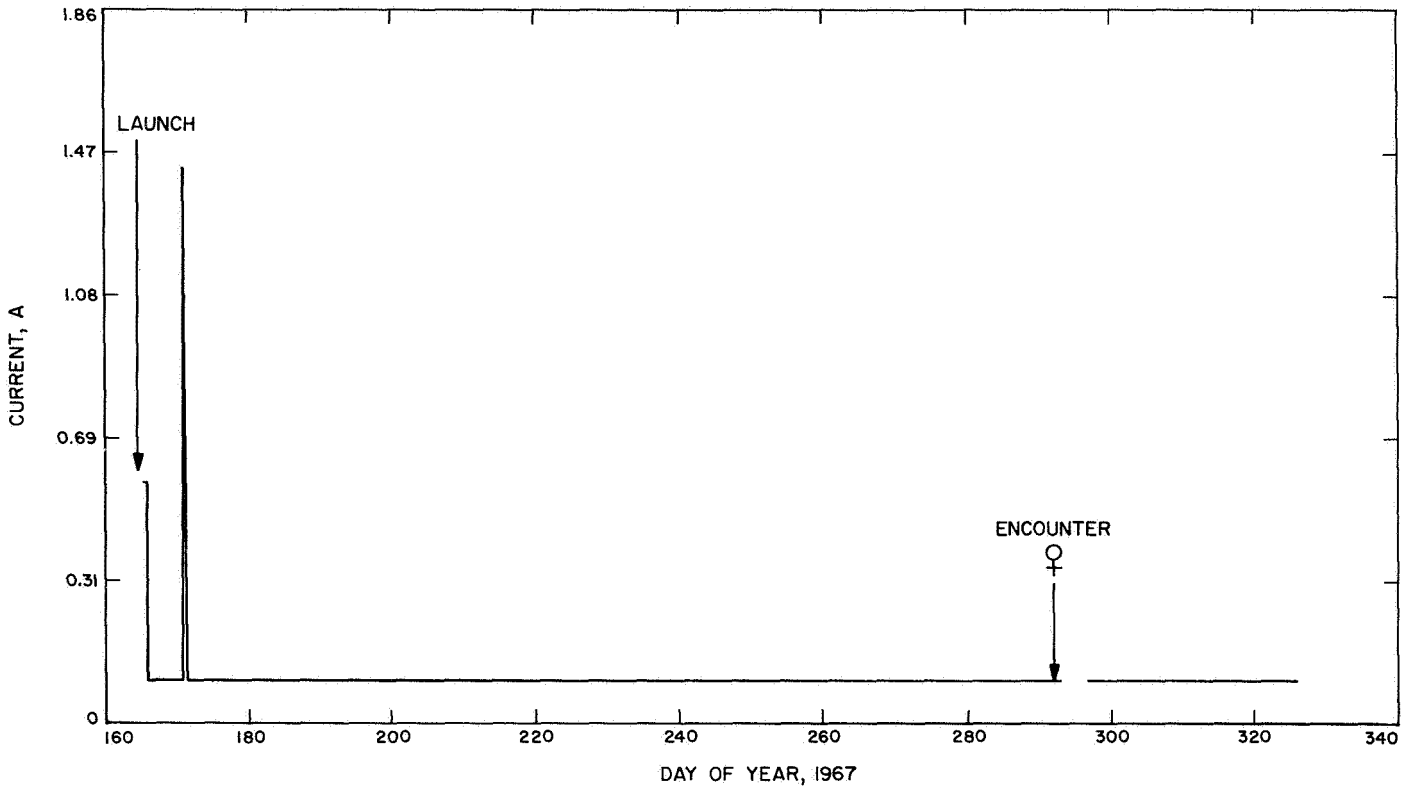


Fig. C-30. Maneuver booster-regulator output current, channel 221

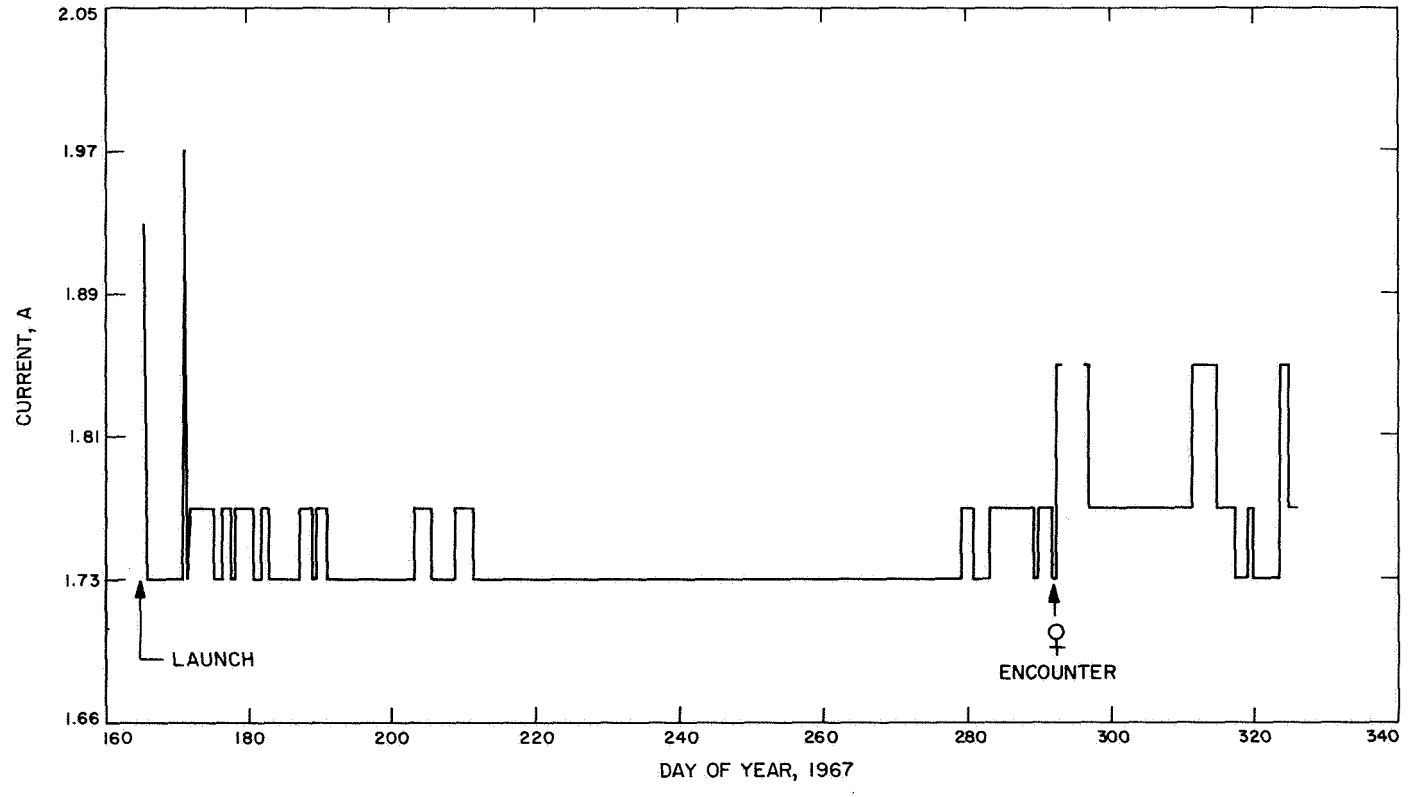


Fig. C-31. Main booster-regulator output current, channel 205

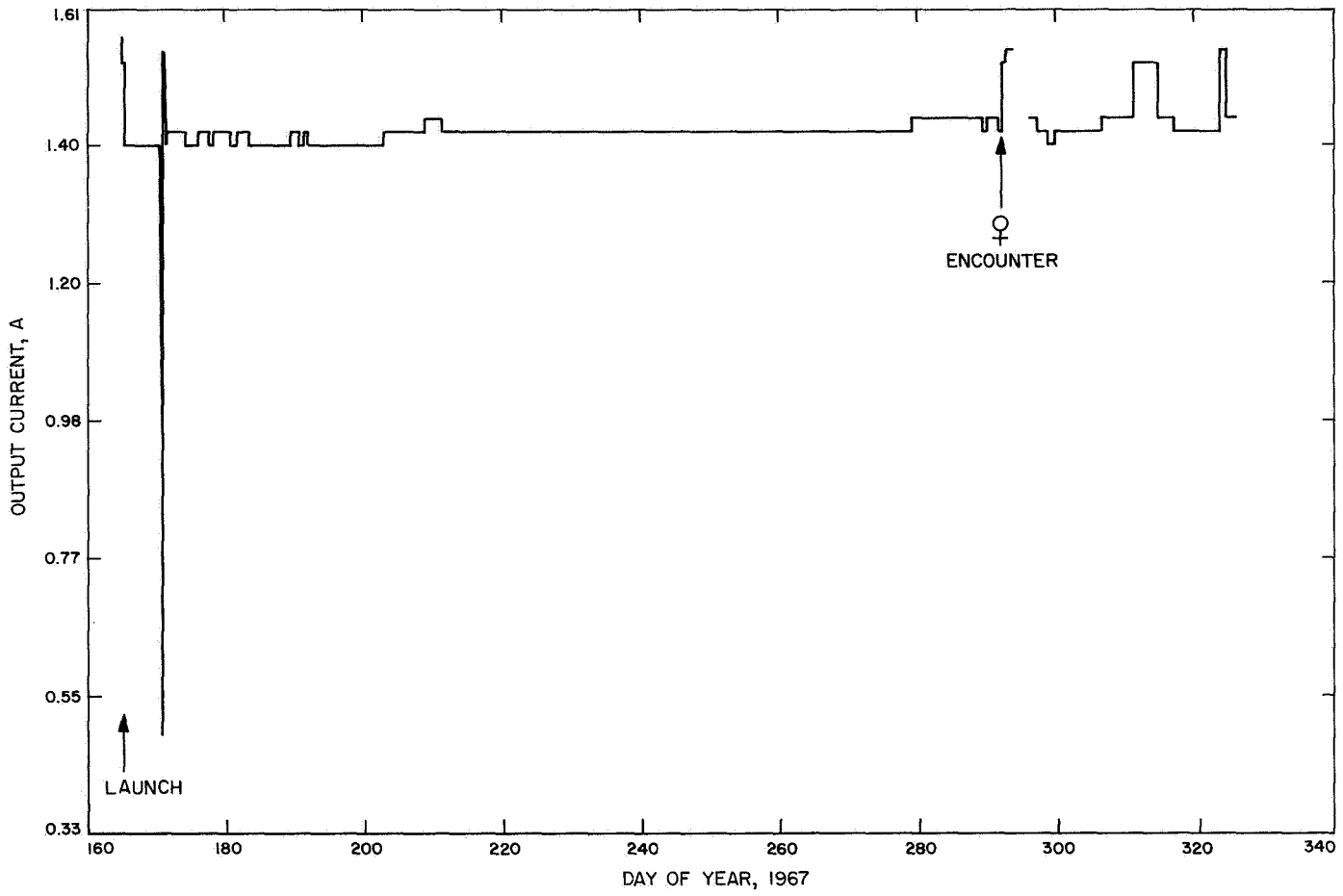


Fig. C-32. 2400-Hz inverter output current, channel 227

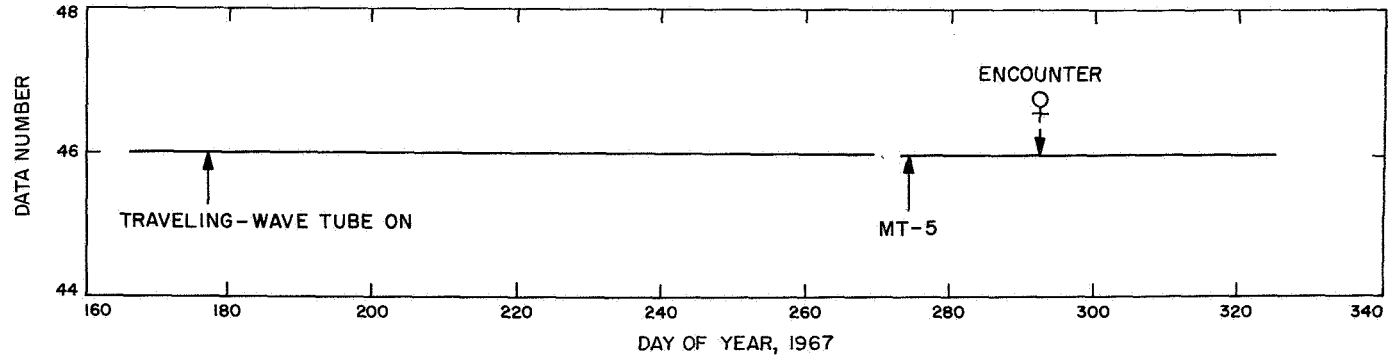


Fig. C-33. External RF power output (data number), channel 229

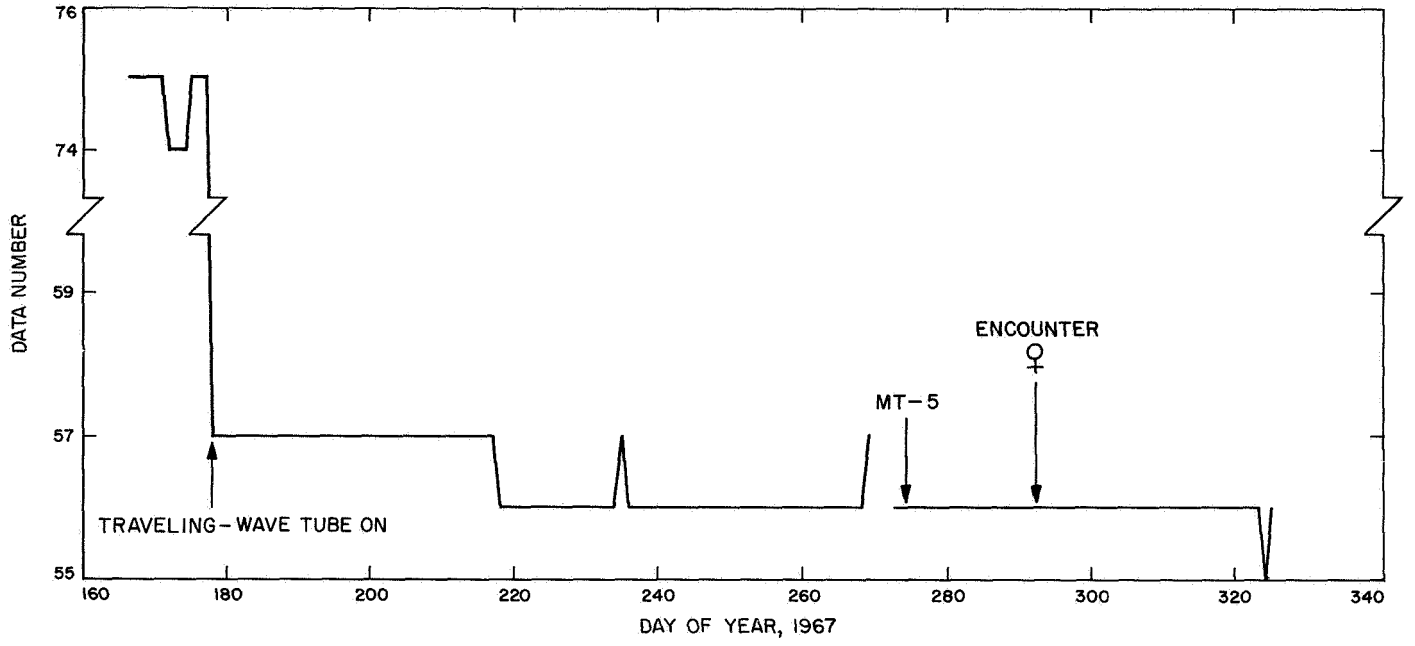


Fig. C-34. Traveling-wave tube cathode/helix current (data number), channel 300

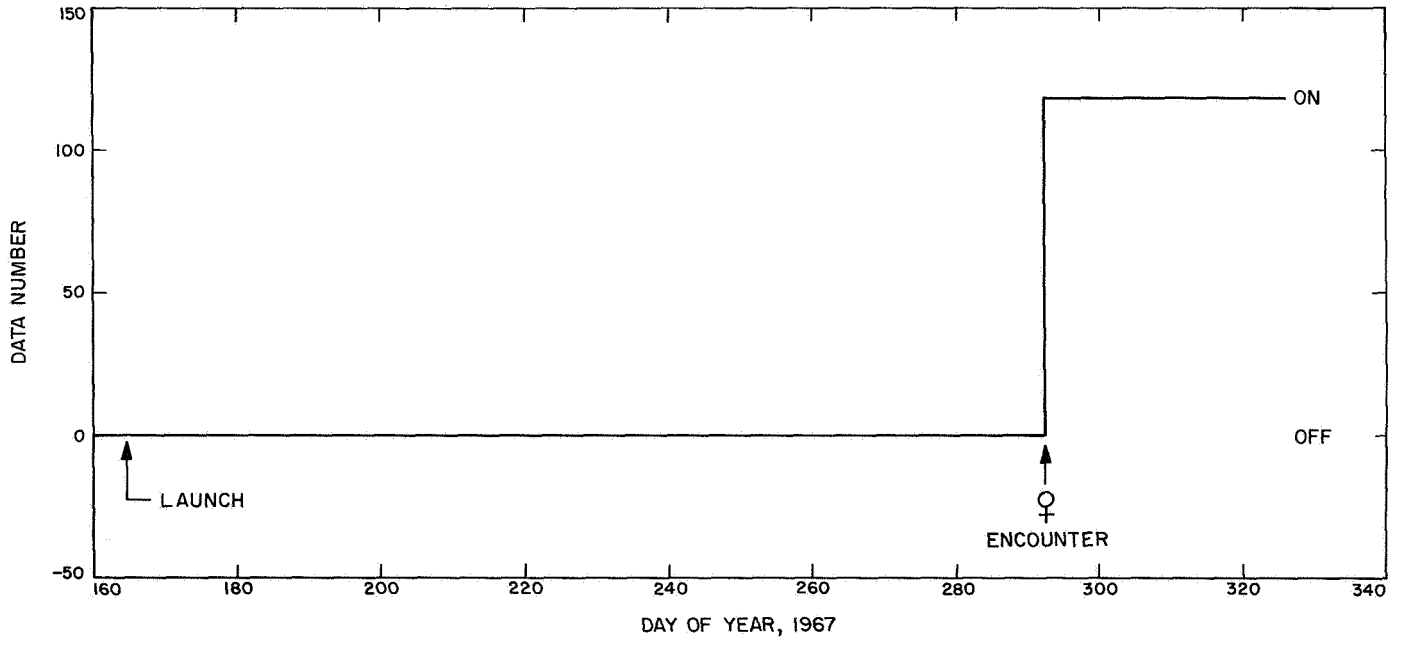


Fig. C-35. Terminator sensor excitation (data number), channel 306

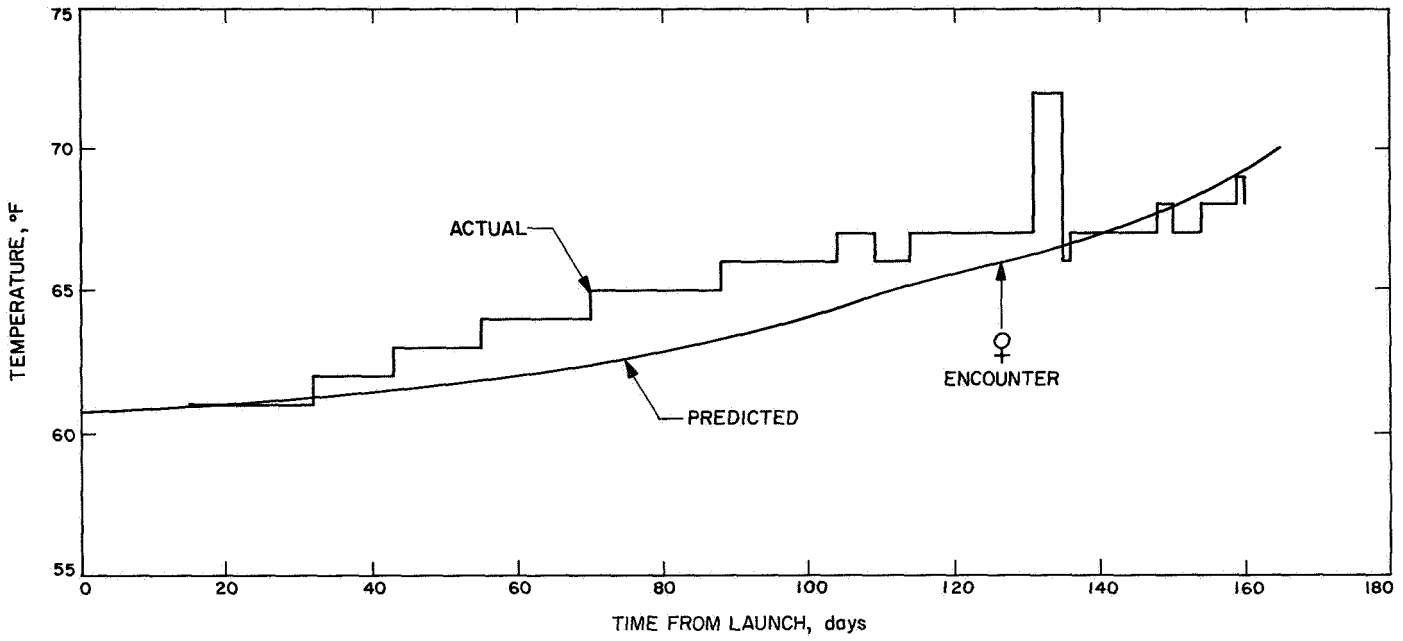


Fig. C-36. Bay 1 temperature, channel 401

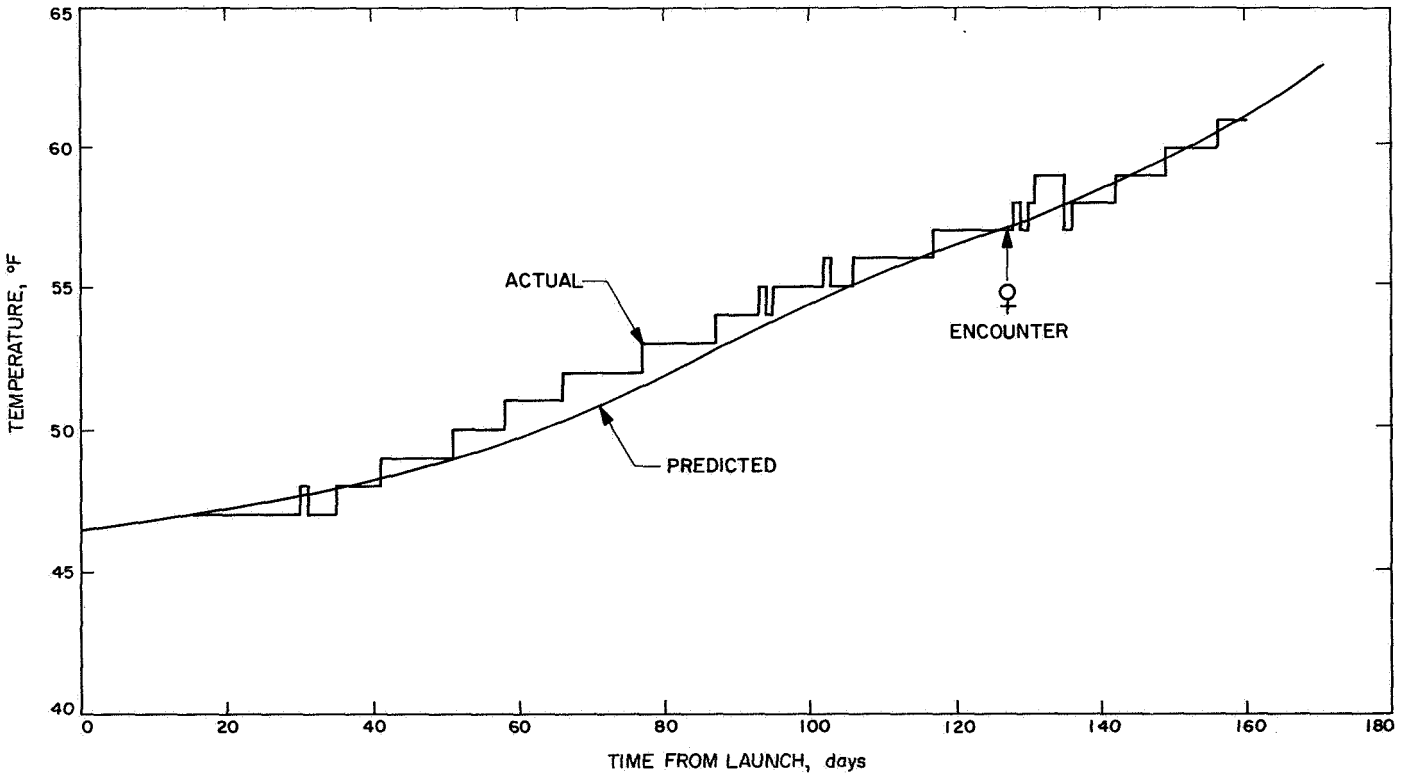


Fig. C-37. Bay 2 temperature, channel 421

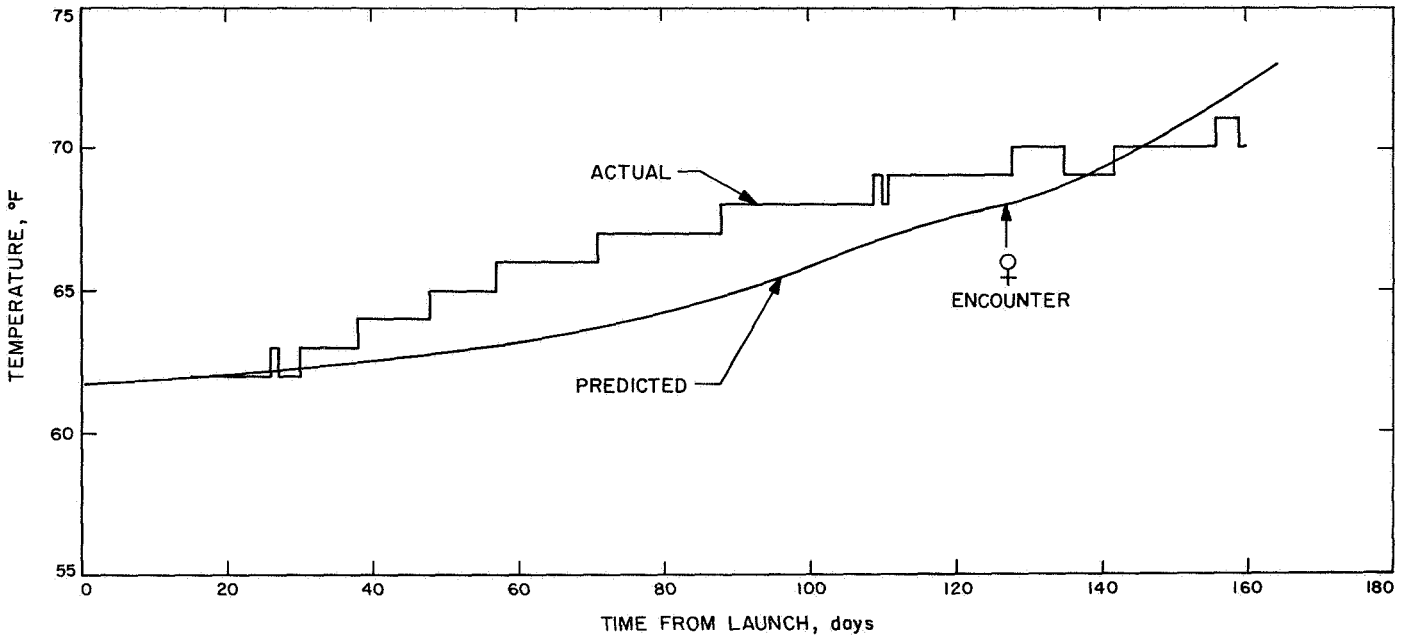


Fig. C-38. Bay 3 temperature, channel 402

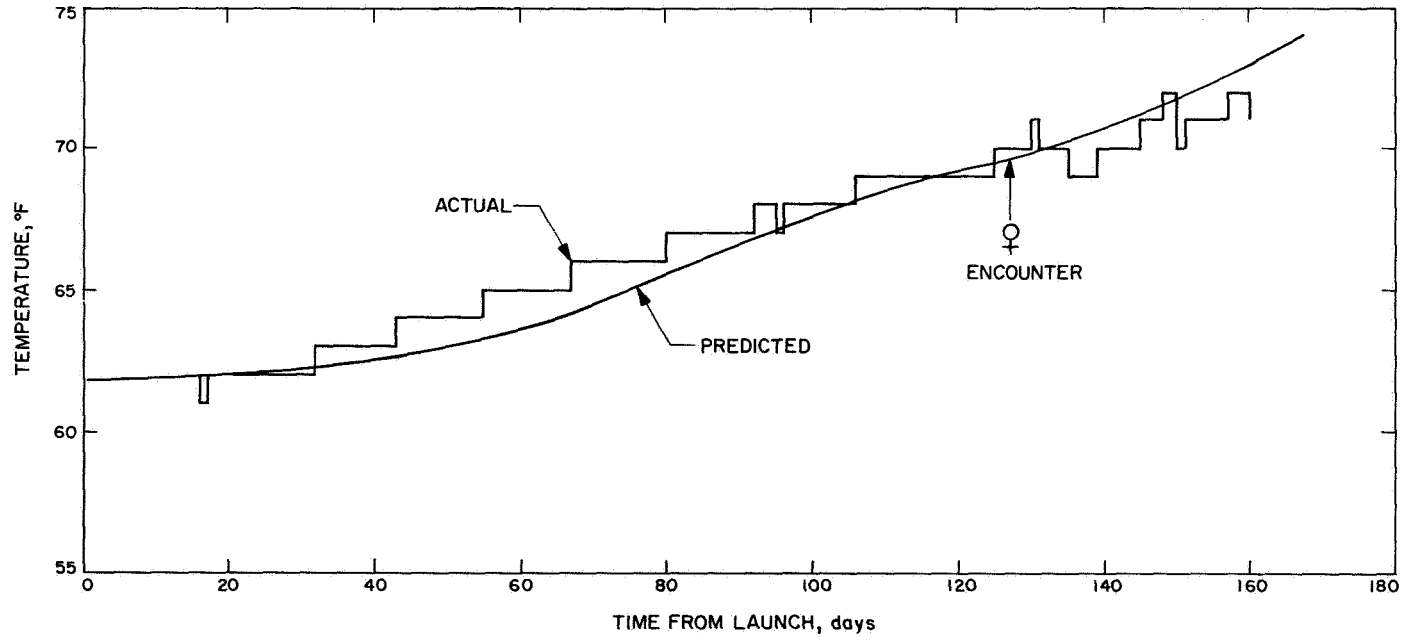


Fig. C-39. Bay 4 temperature, channel 423

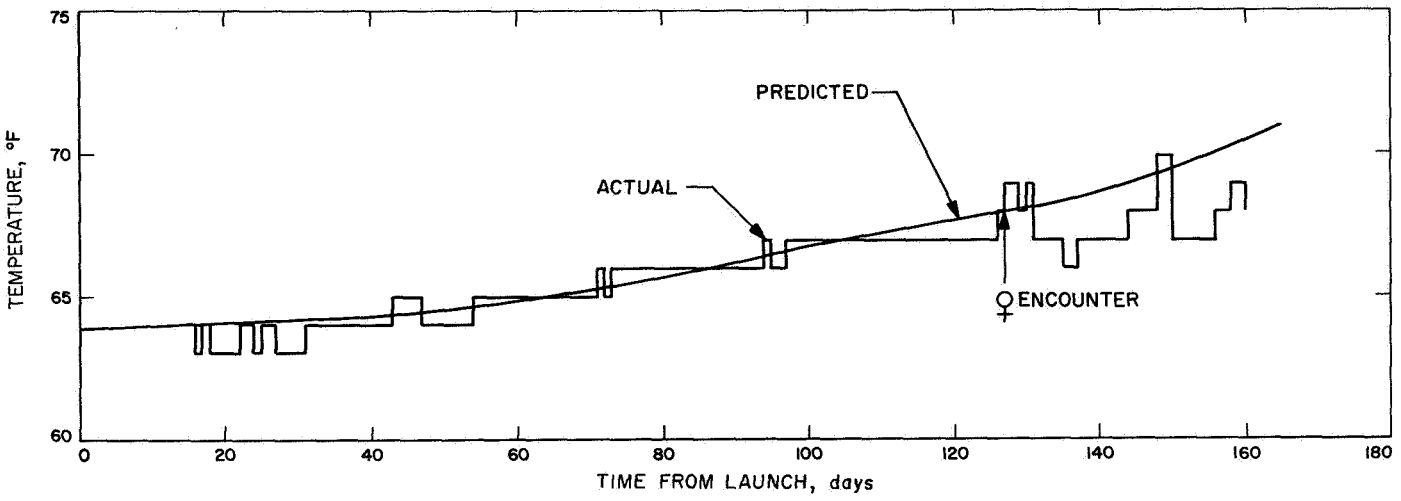


Fig. C-40. Bay 5 temperature, channel 404

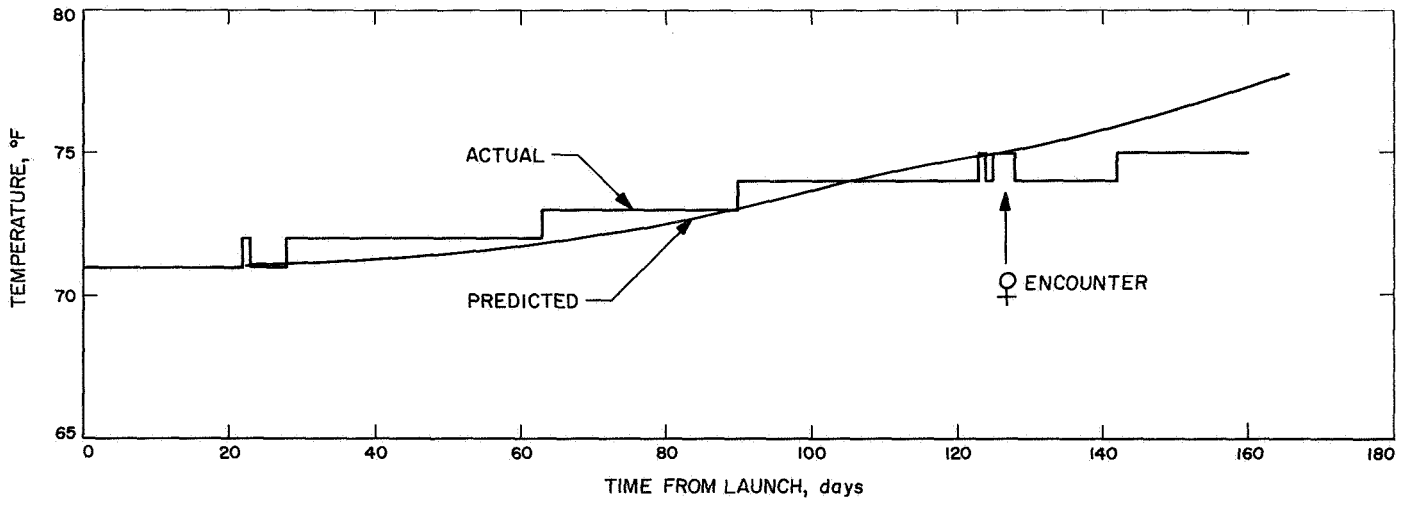


Fig. C-41. Bay 6 temperature, channel 405

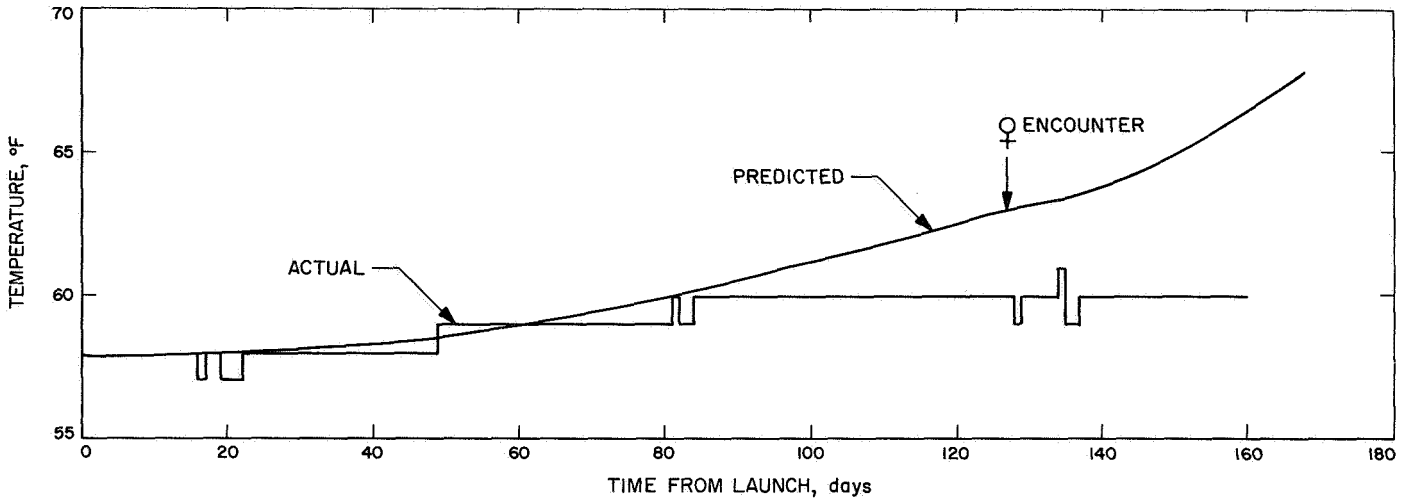


Fig. C-42. Bay 7 temperature, channel 426

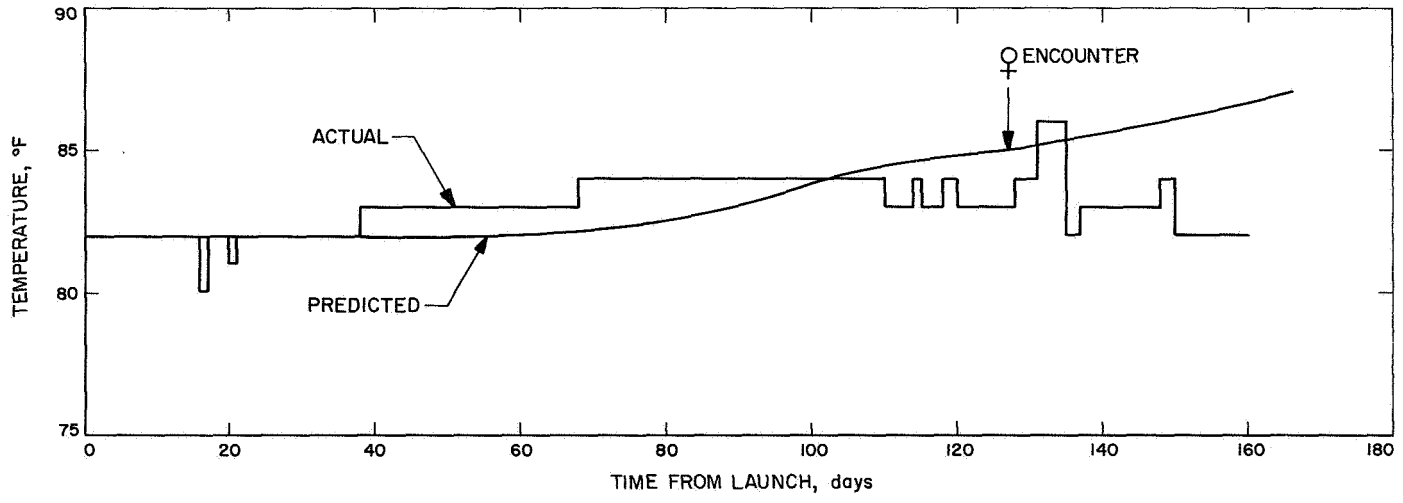


Fig. C-43. Bay 8 temperature, channel 407

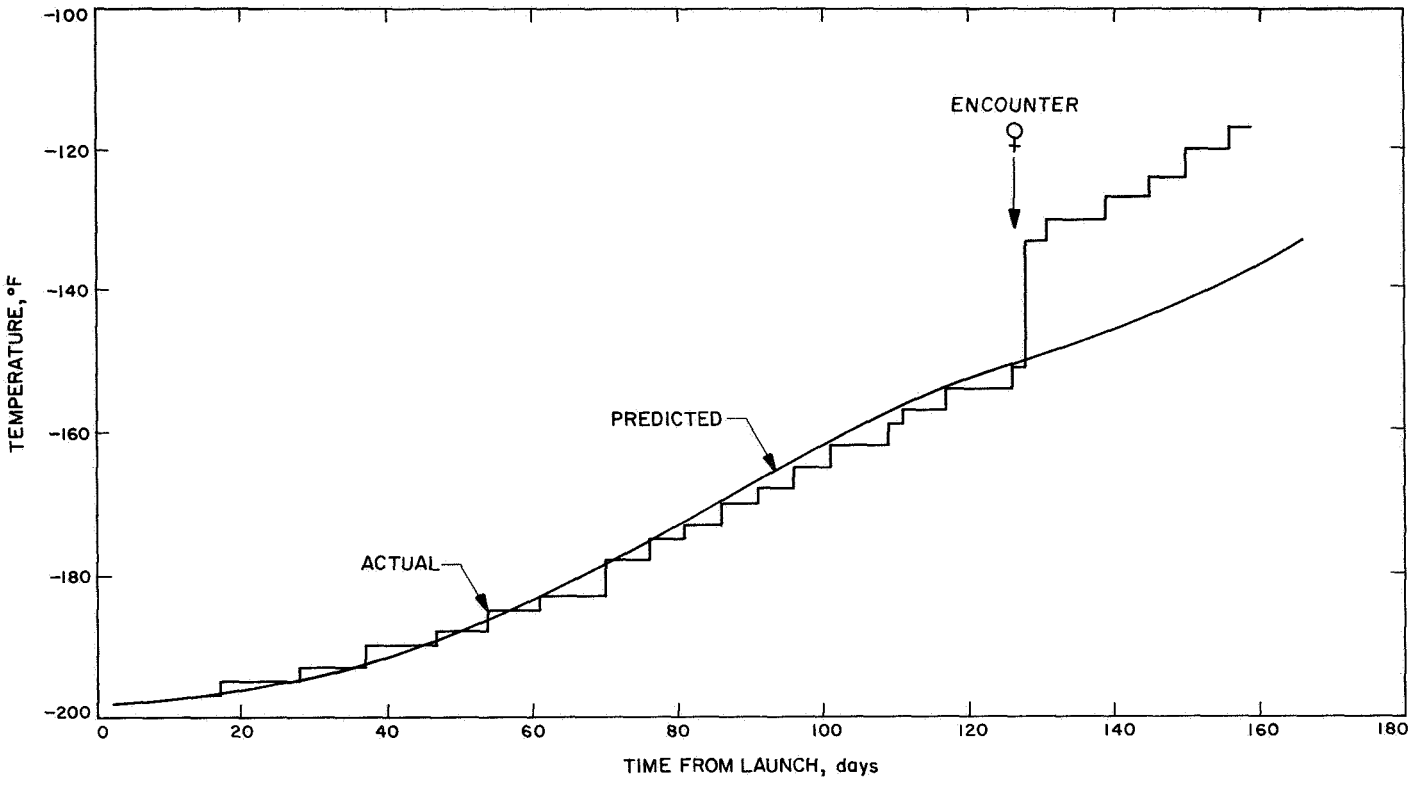


Fig. C-44. High-gain antenna temperature, channel 419

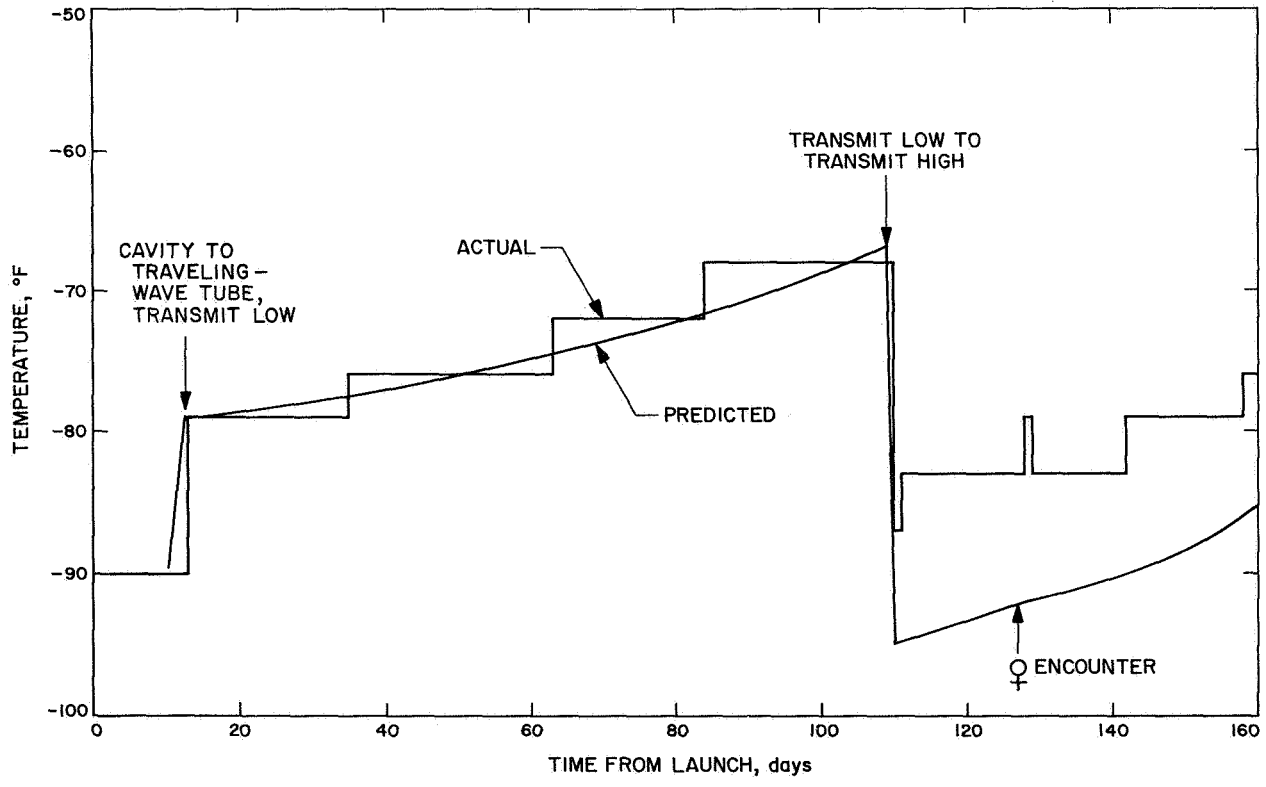


Fig. C-45. Low-gain antenna temperature, channel 432

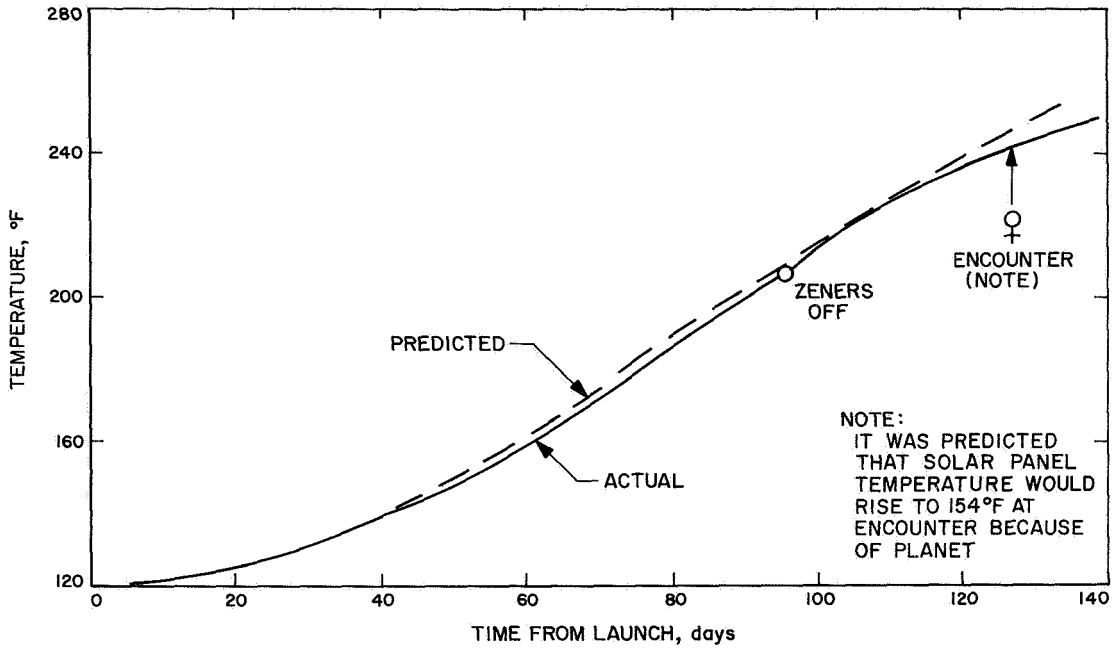


Fig. C-46. Solar panel 4A1 and 4A5 substrate temperature, channels 409 and 429

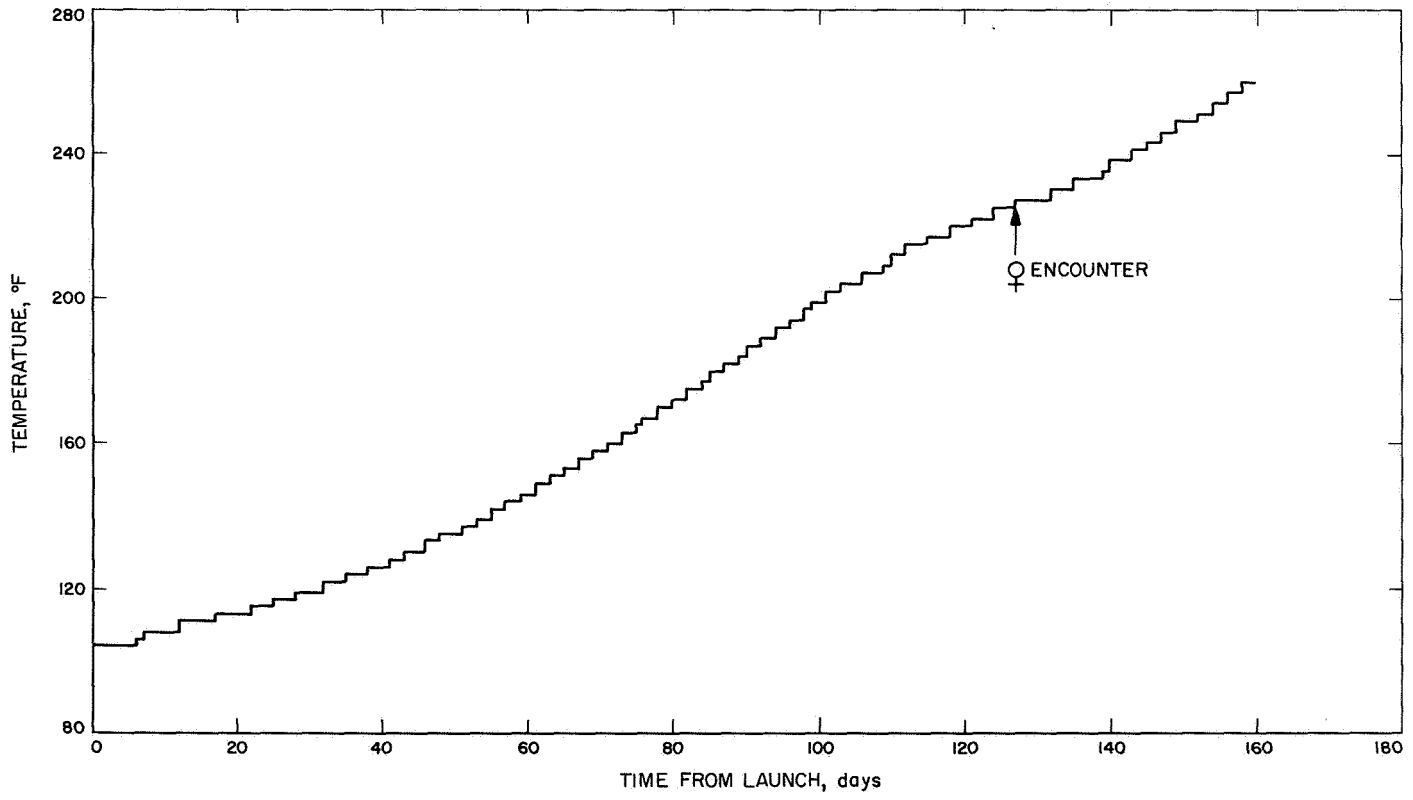


Fig. C-47. Solar cell (I_{SC} — V_{OC}) temperature, channel 403

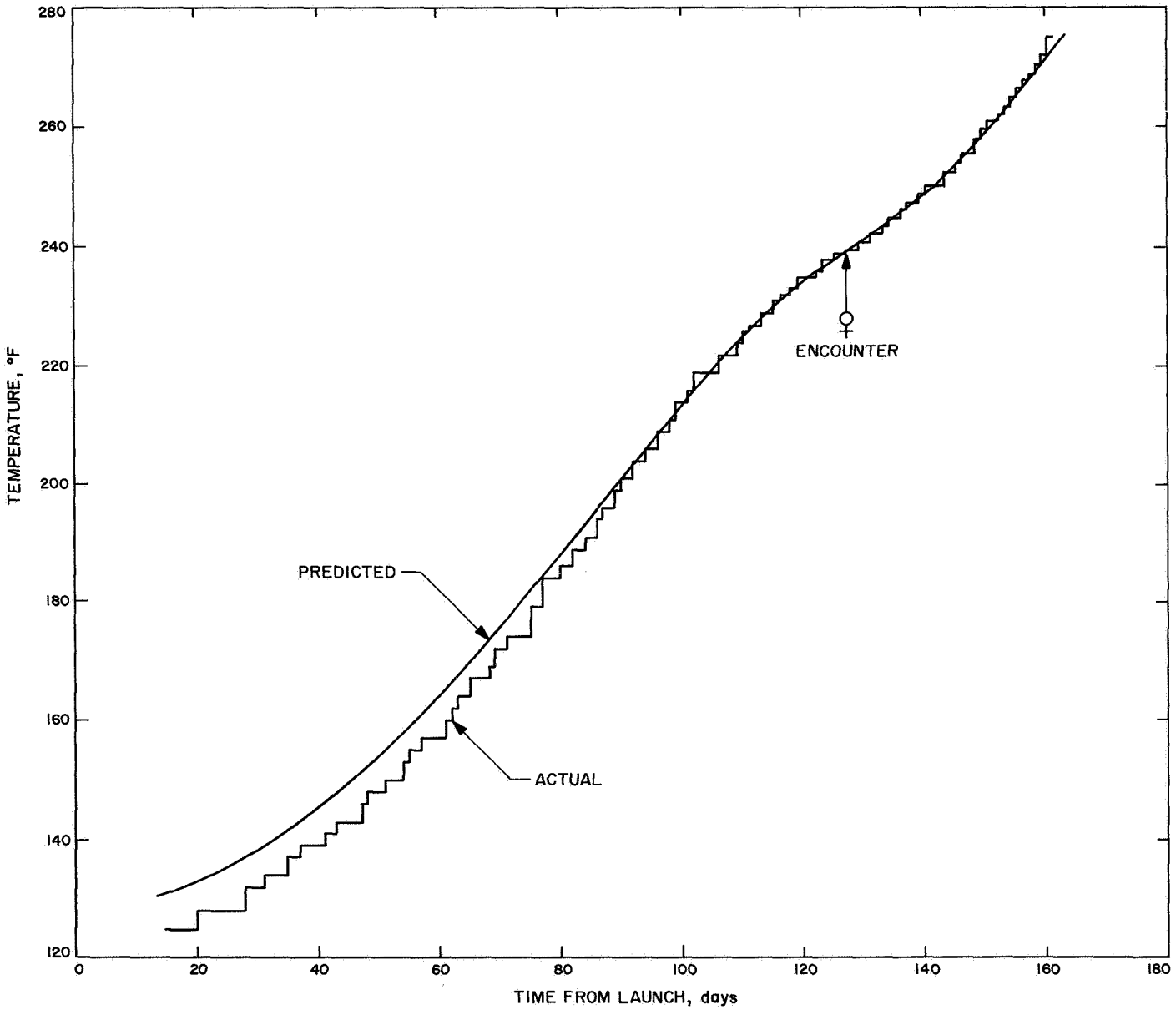


Fig. C-48. Solar panel temperature, channels 409 and 429

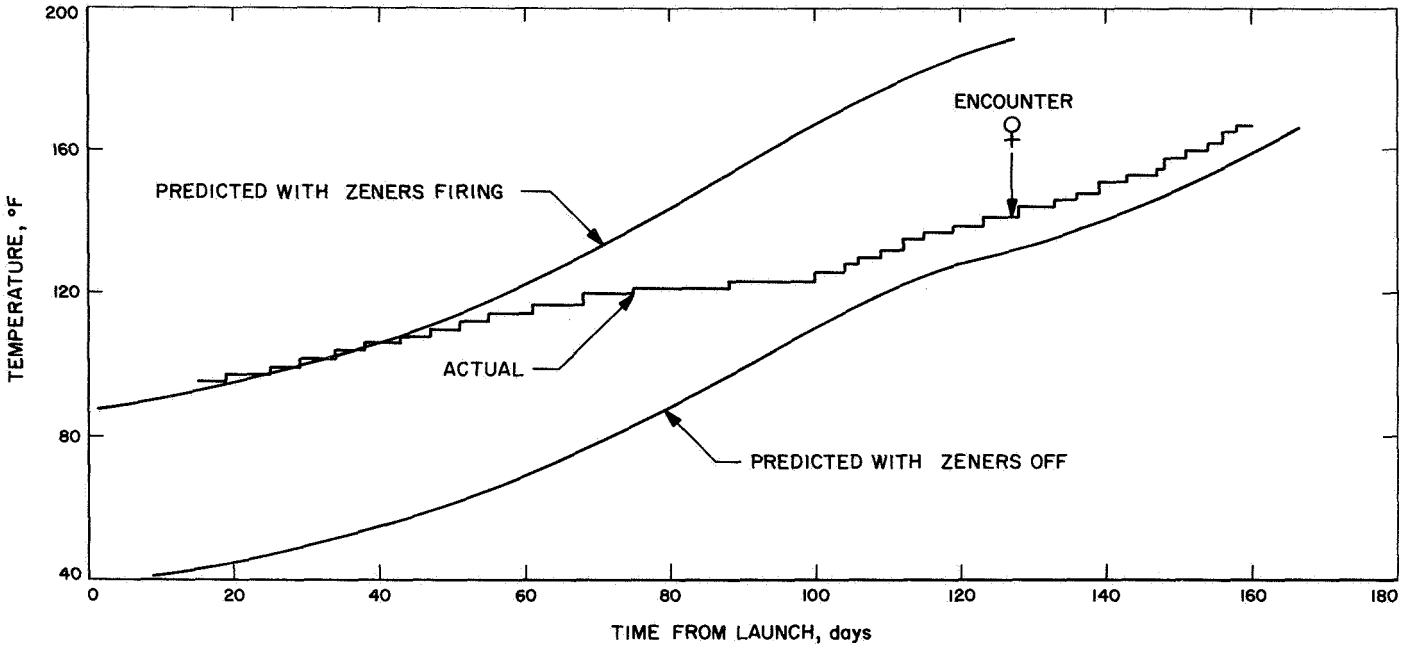


Fig. C-49. Solar panel spar temperature, channel 427

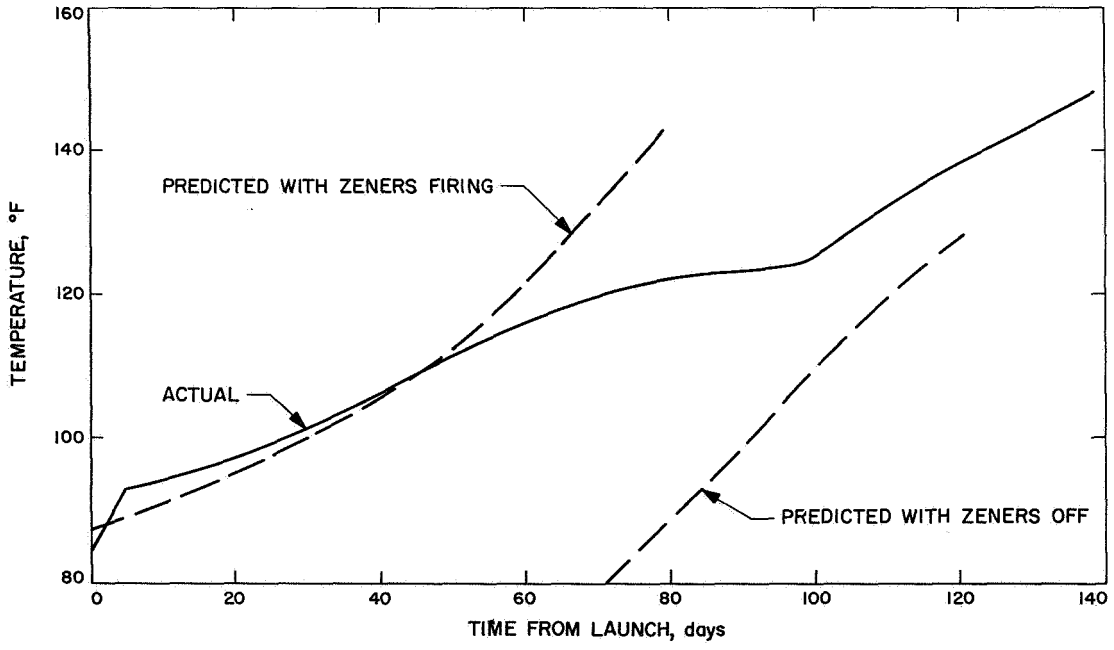


Fig. C-50. Solar panel 4A5 spar zener temperature, channel 427

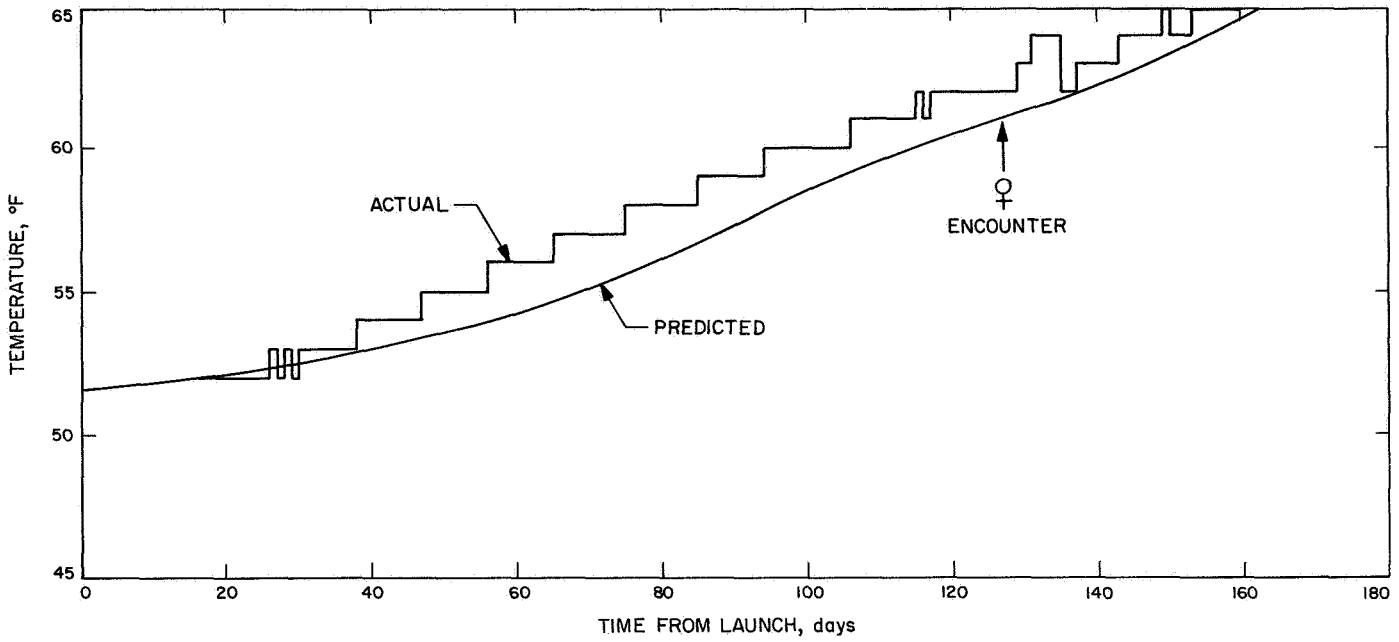


Fig. C-51. Postinjection propulsion system nitrogen temperature, channel 408

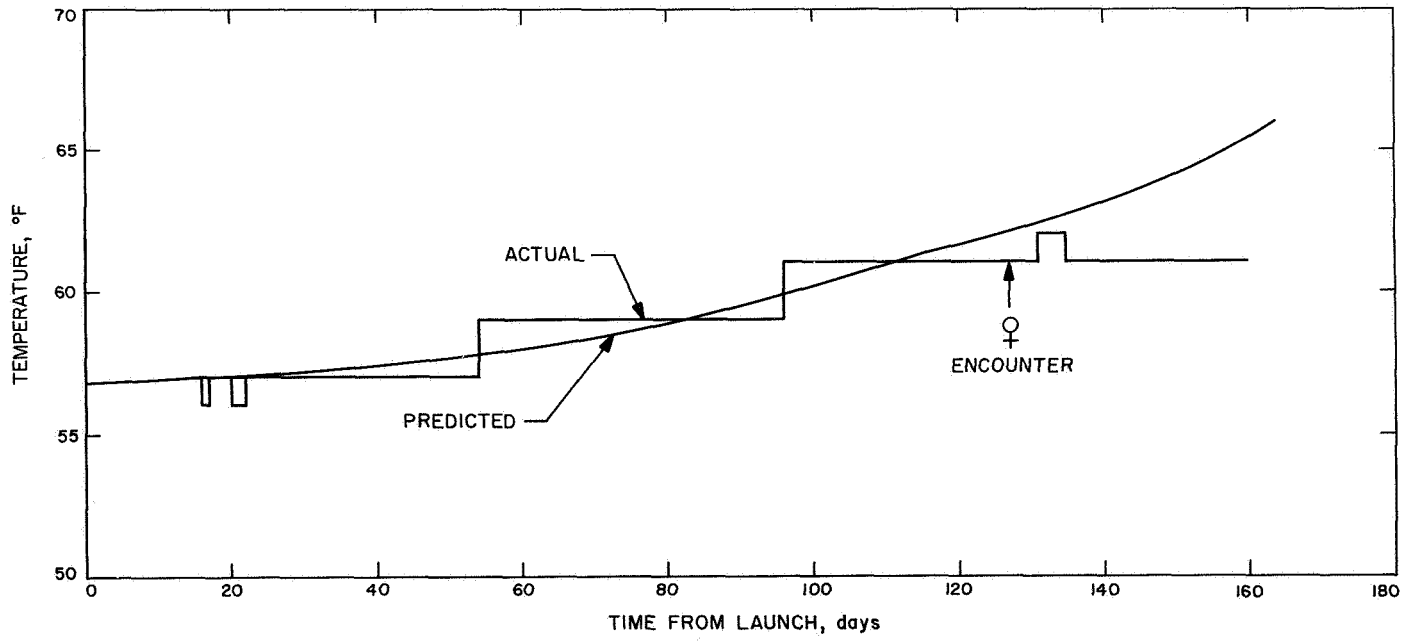


Fig. C-52. Canopus tracking temperature, channel 410

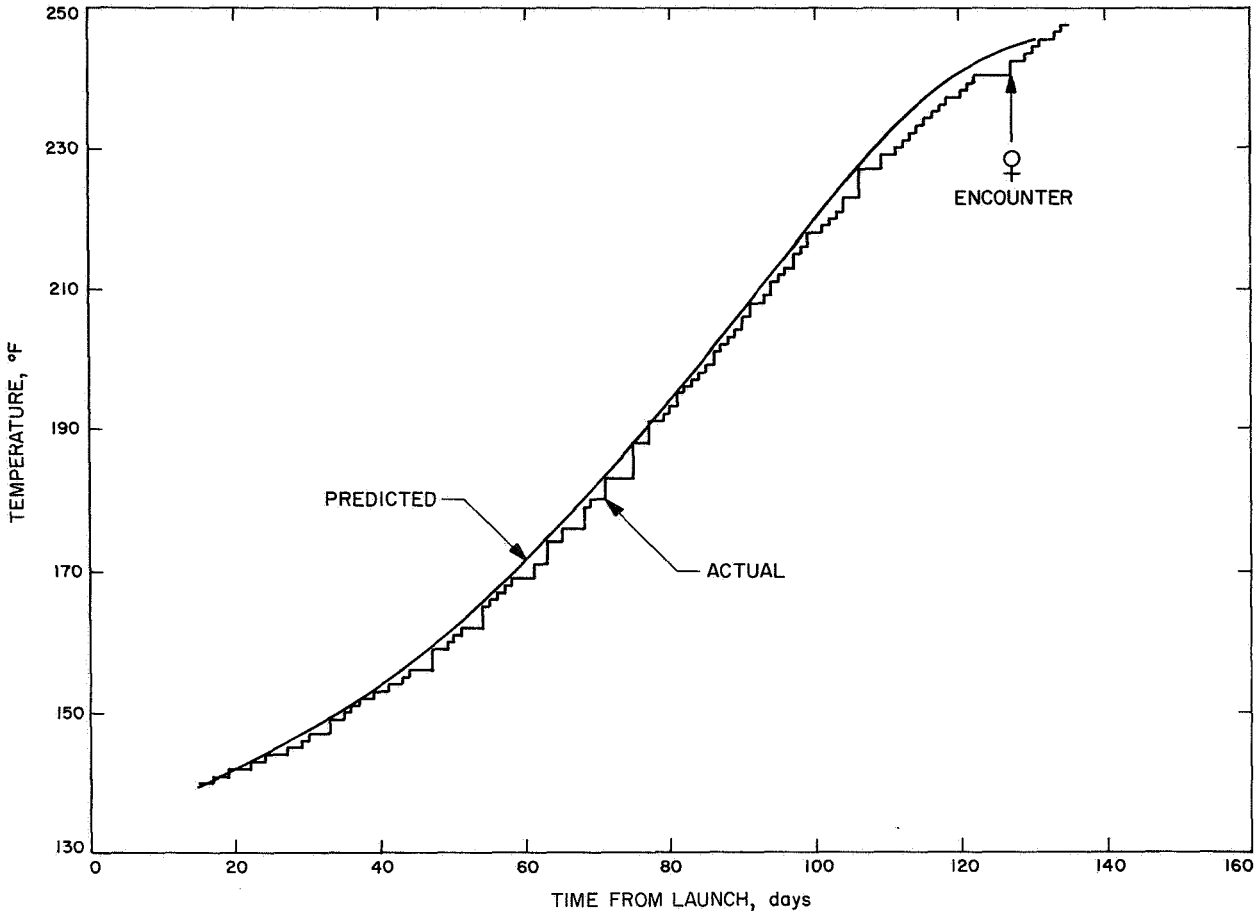


Fig. C-53. Black temperature control reference temperature, channel 413

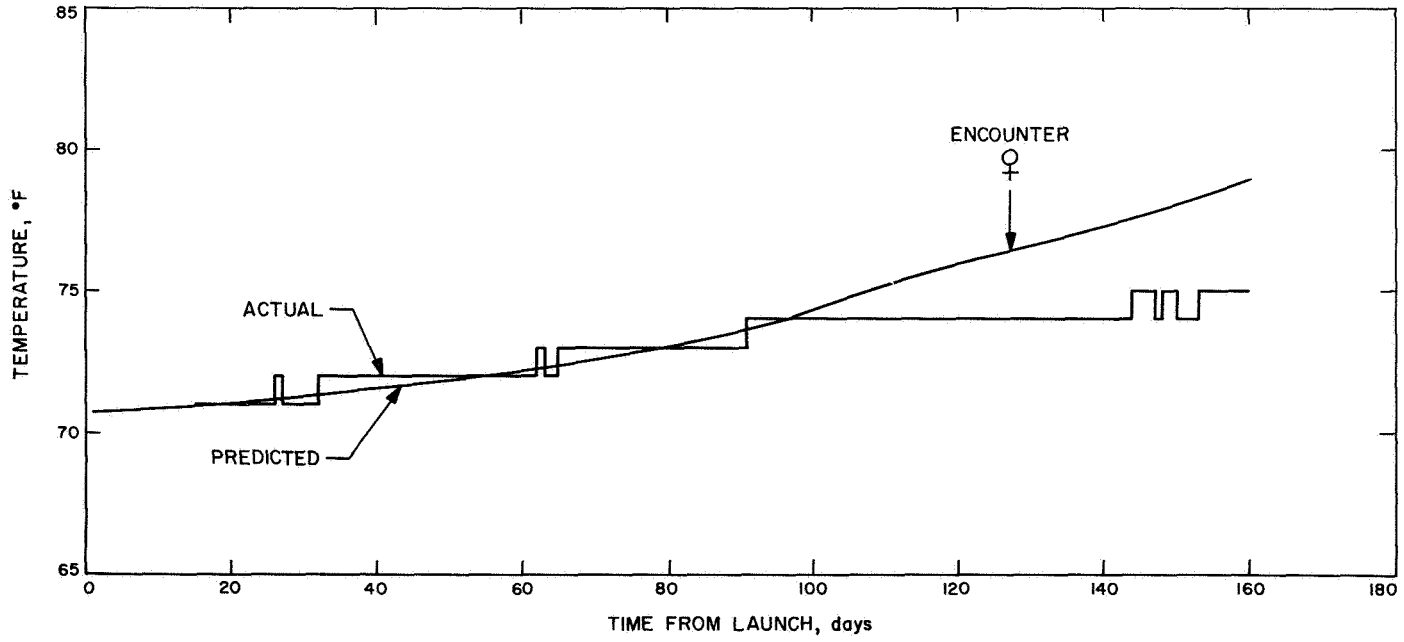


Fig. C-54. Auxiliary oscillator No. 1 temperature, channel 414

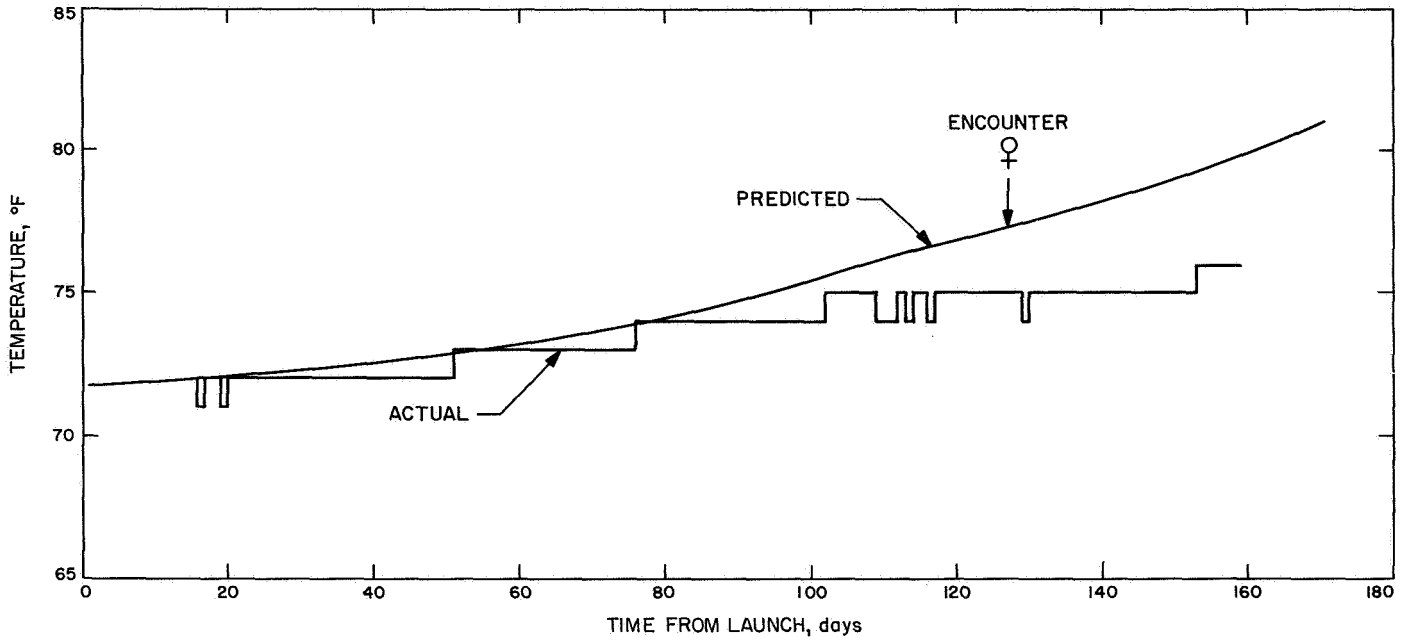


Fig. C-55. Auxiliary oscillator No. 2 temperature, channel 418

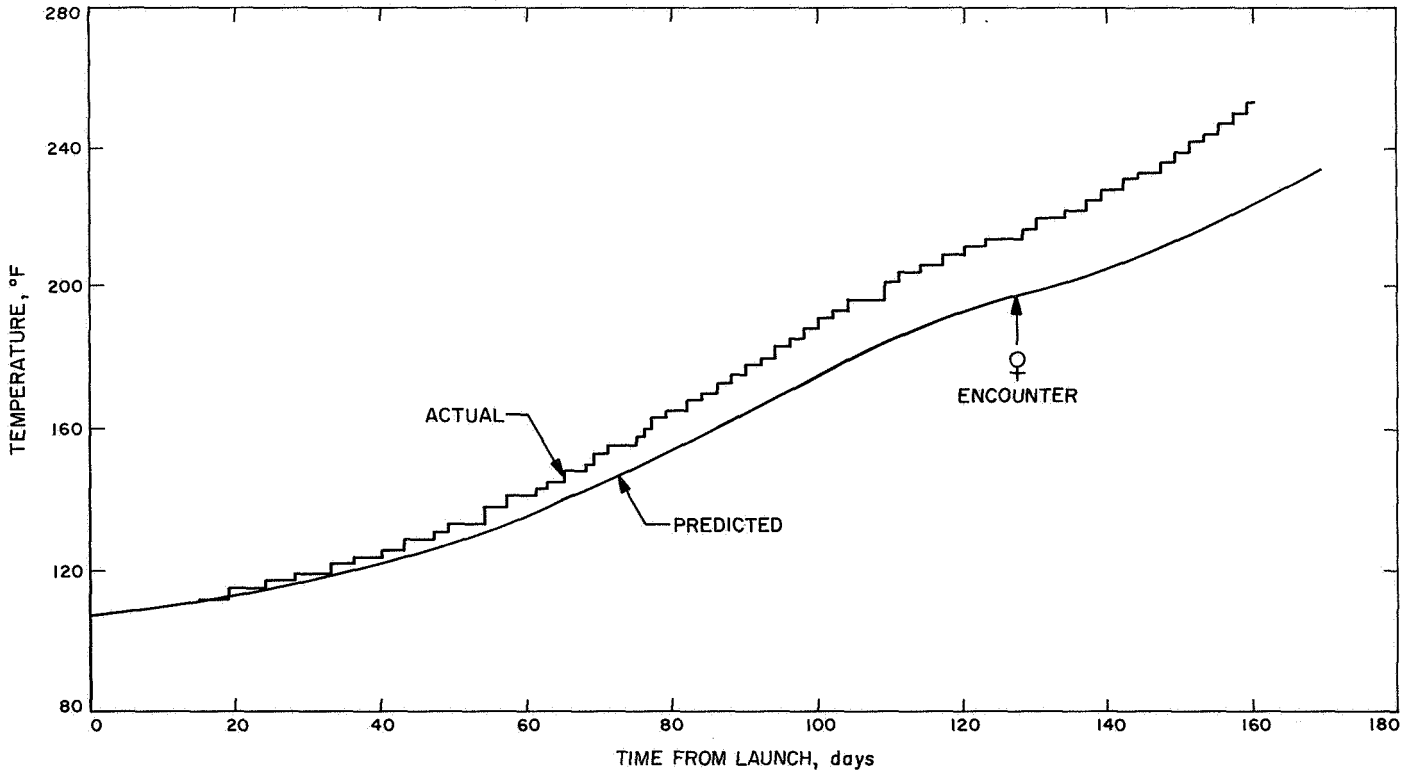


Fig. C-56. Plasma probe temperature, channel 422

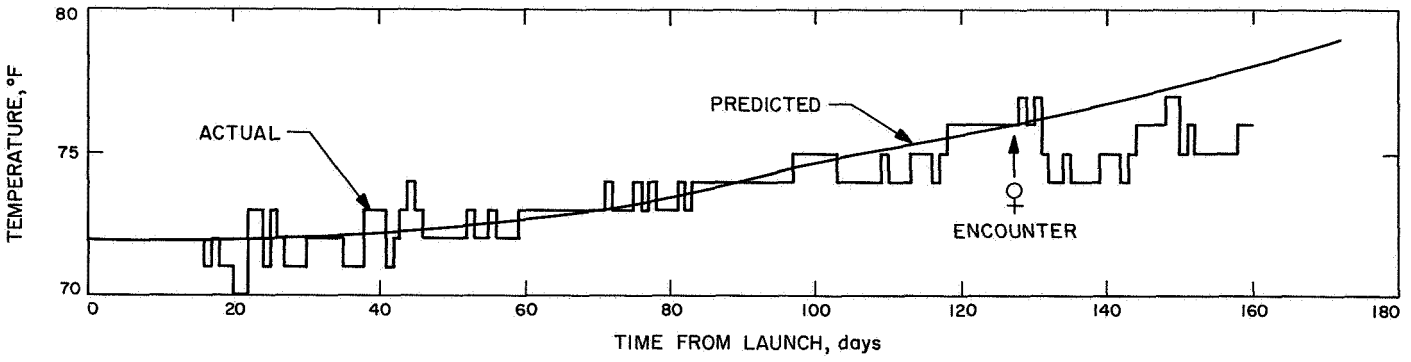


Fig. C-57. Voltage-controlled oscillator temperature, channel 424

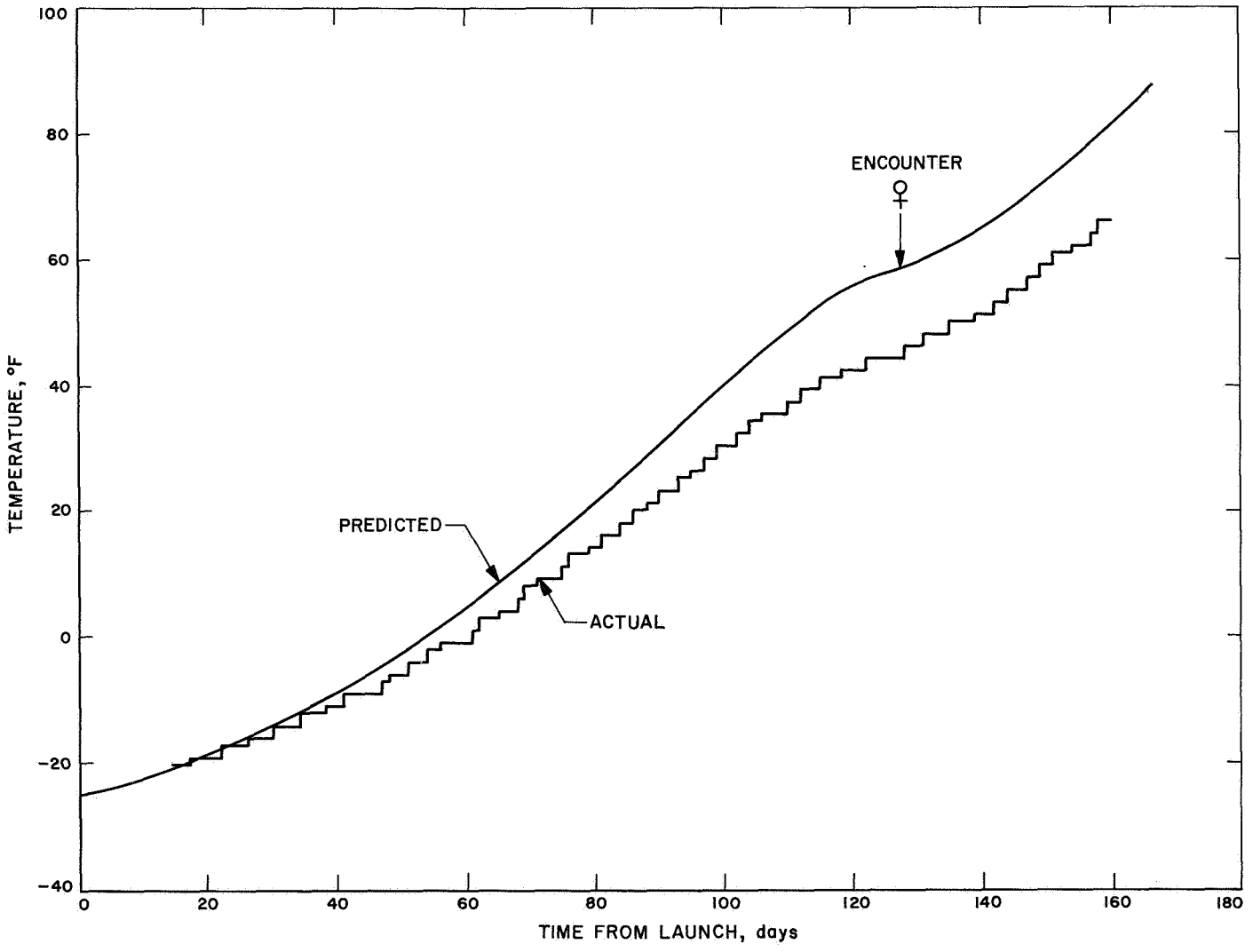


Fig. C-58. Roll and yaw (+X) jet temperature, channel 406

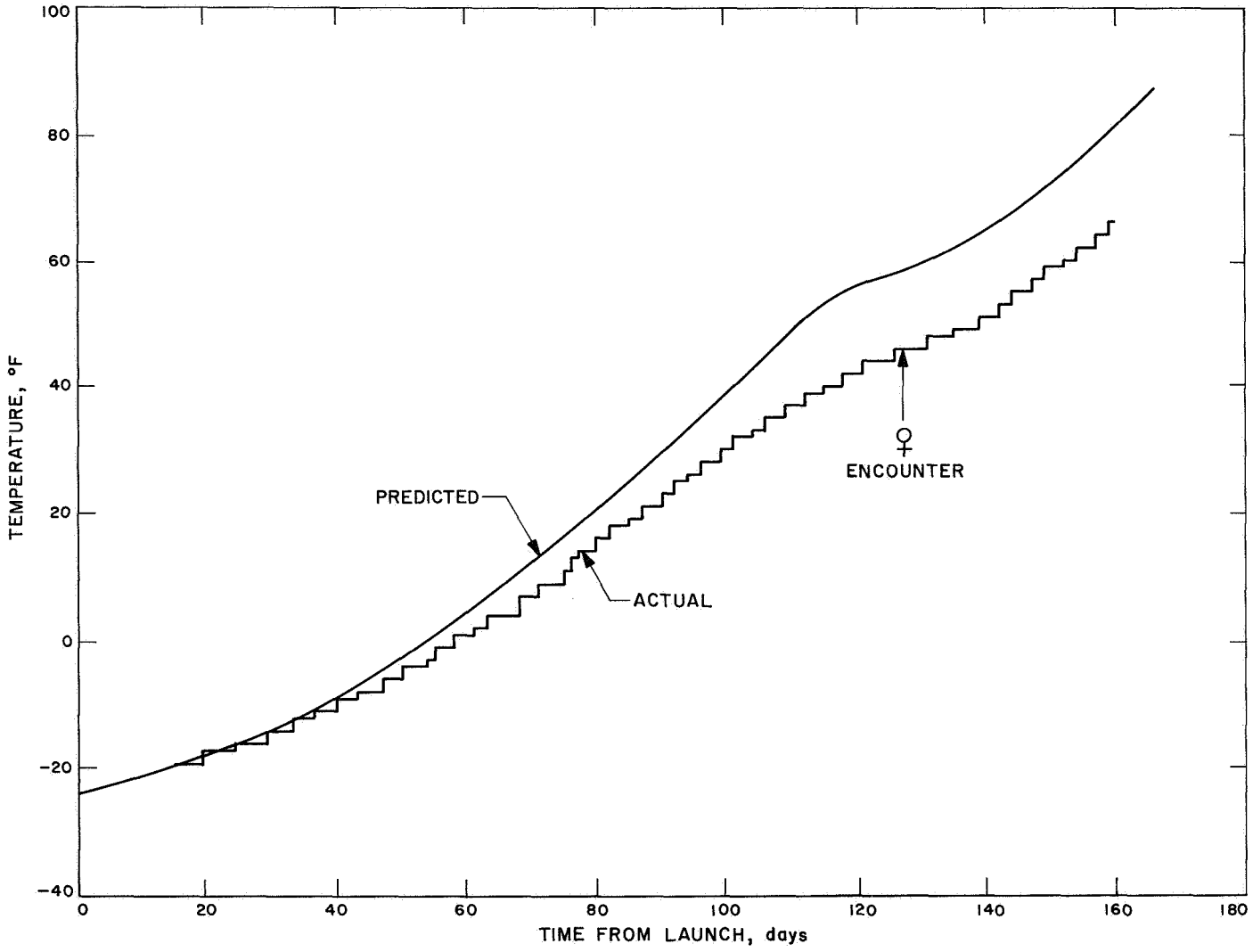


Fig. C-59. Roll and yaw (−X) jet temperature, channel 433

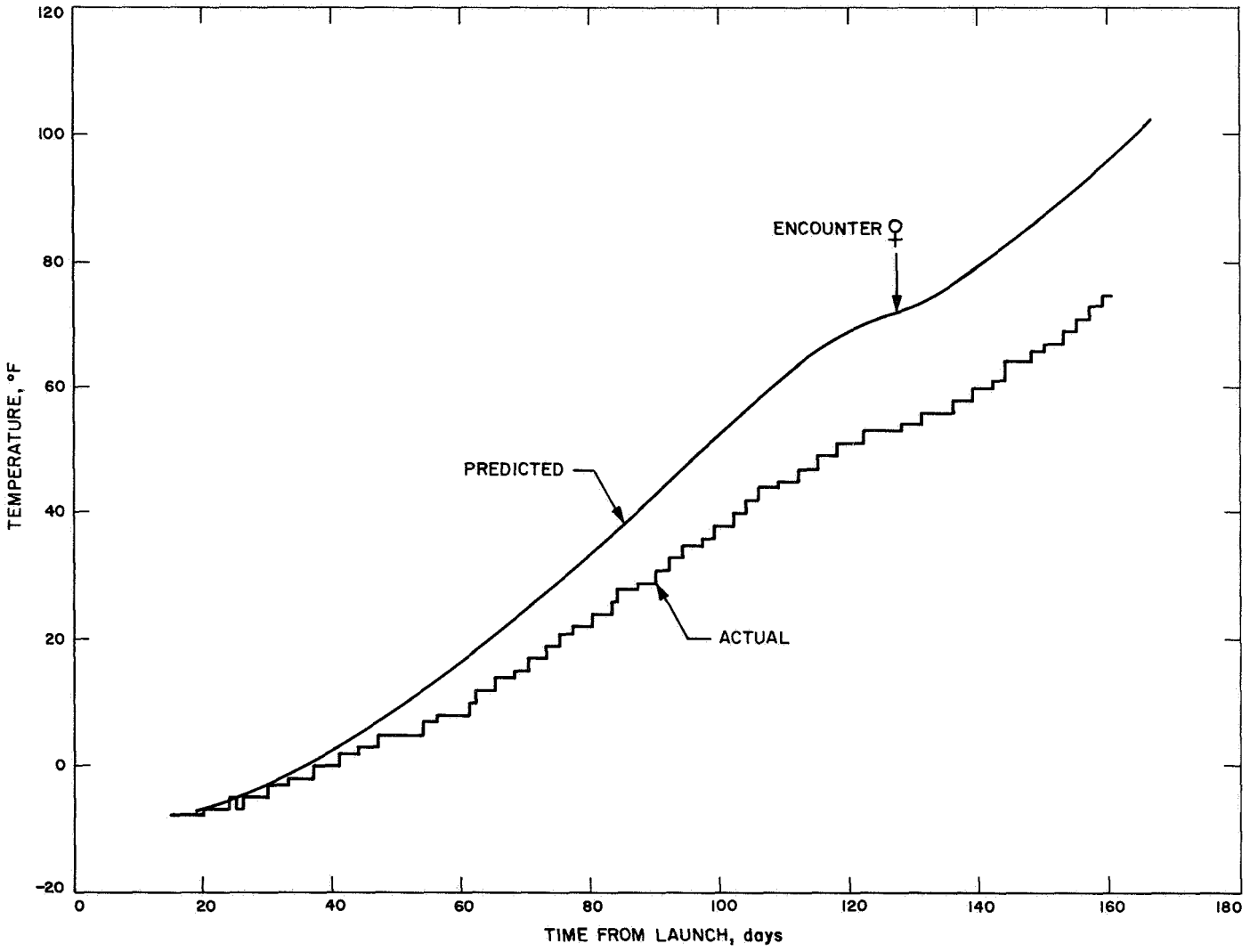


Fig. C-60. Attitude control (−Y) jet temperature, channel 425

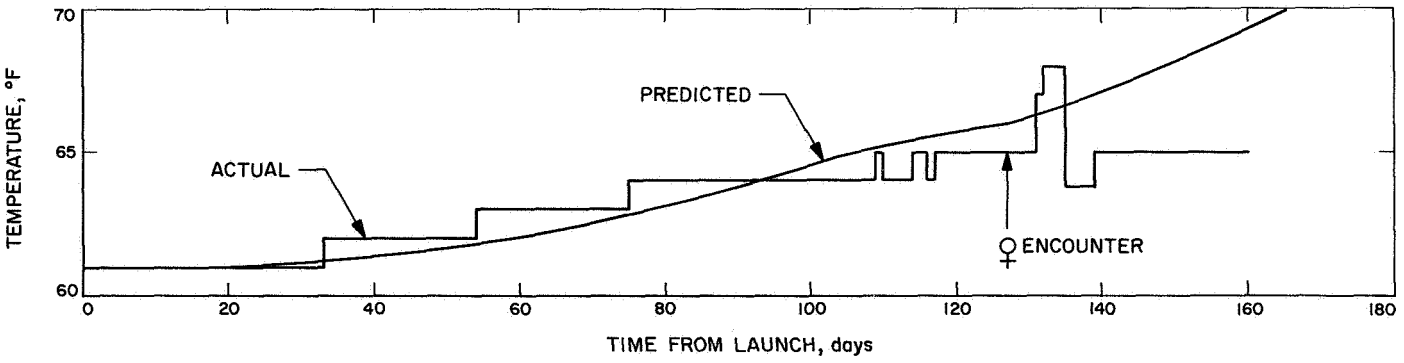


Fig. C-61. Battery temperature, channel 428

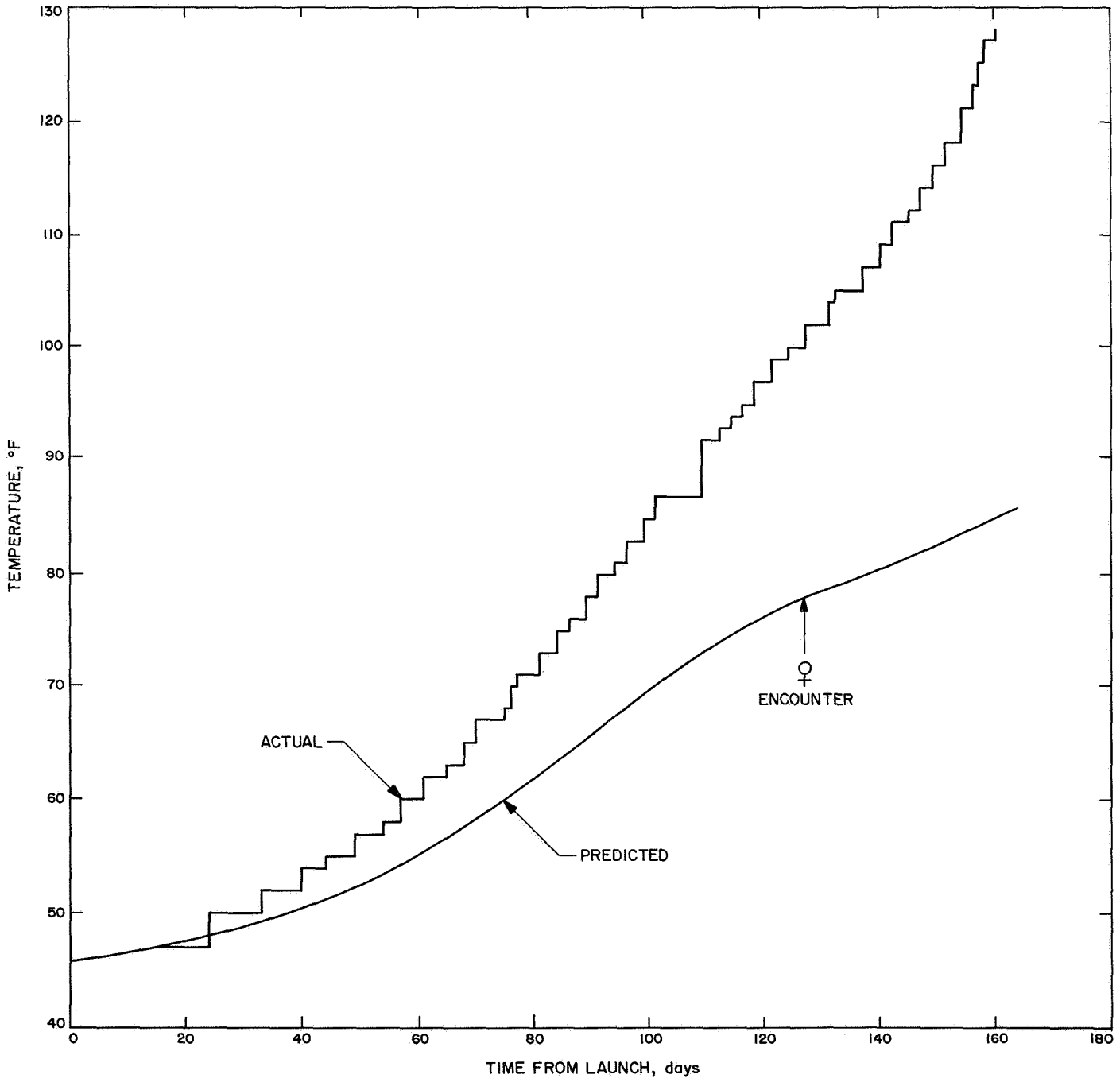


Fig. C-62. Primary sun sensor temperature, channel 430

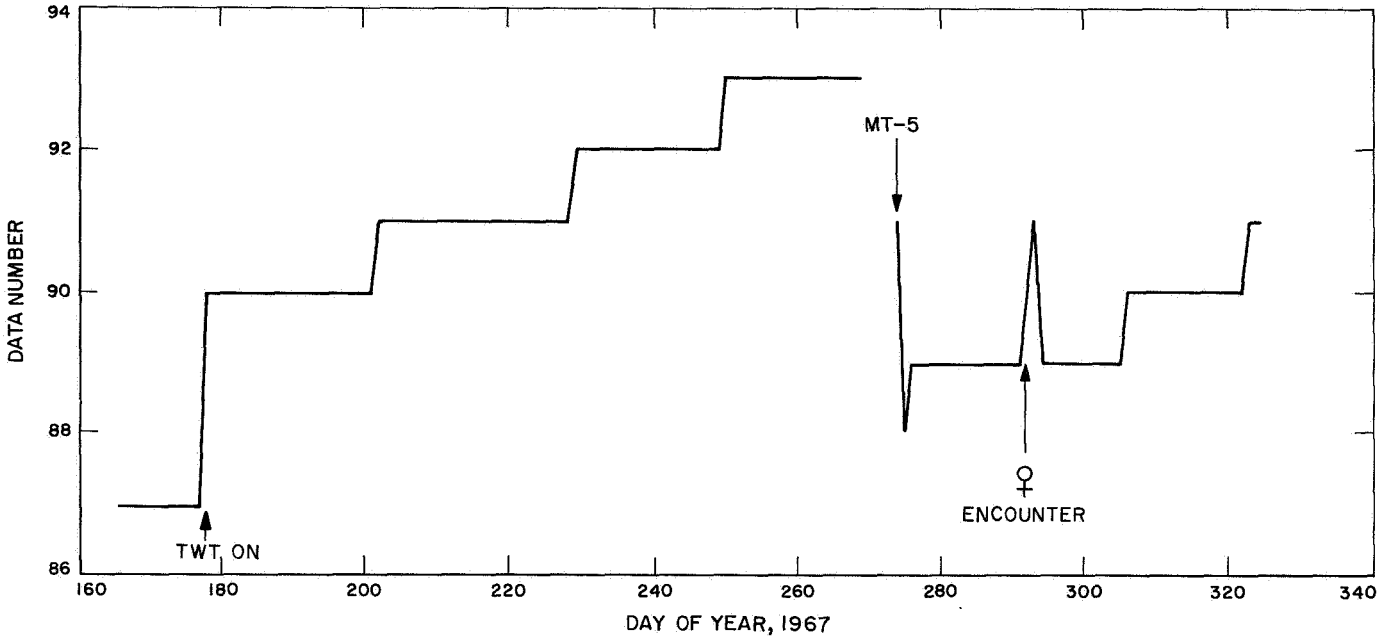


Fig. C-63. Omni-antenna mast temperature (data number), channel 431

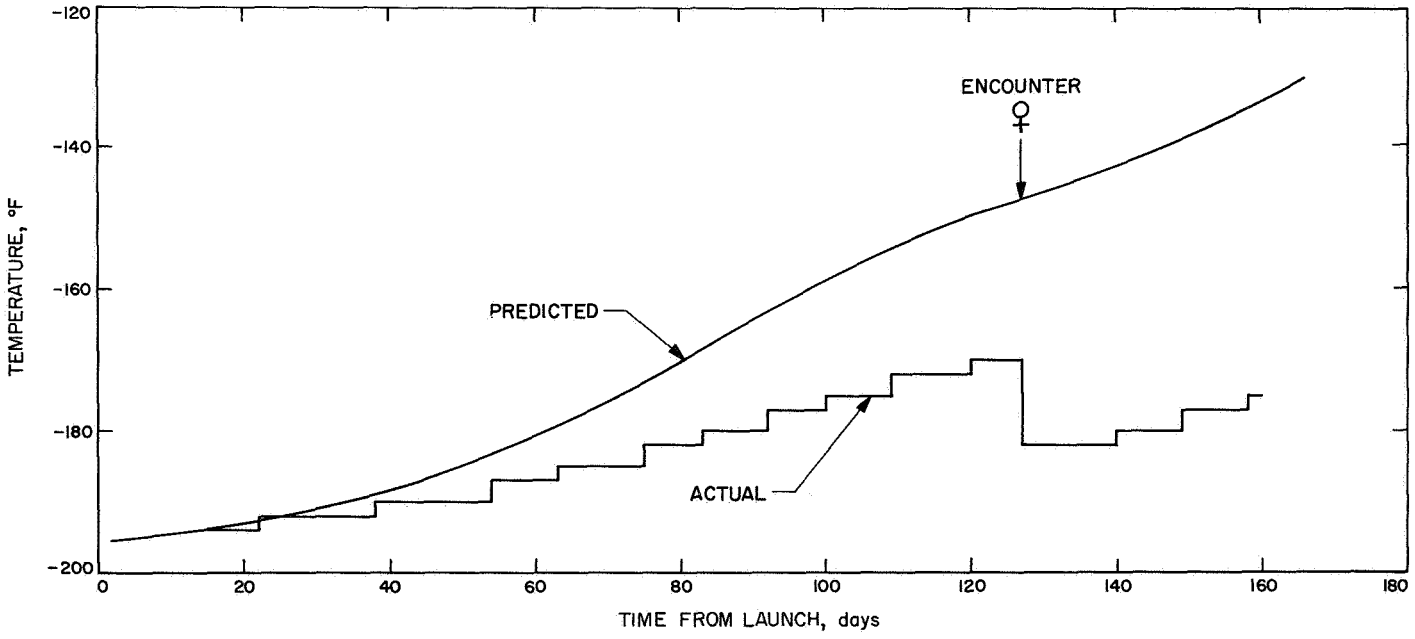


Fig. C-64. Upper shield temperature, channel 434

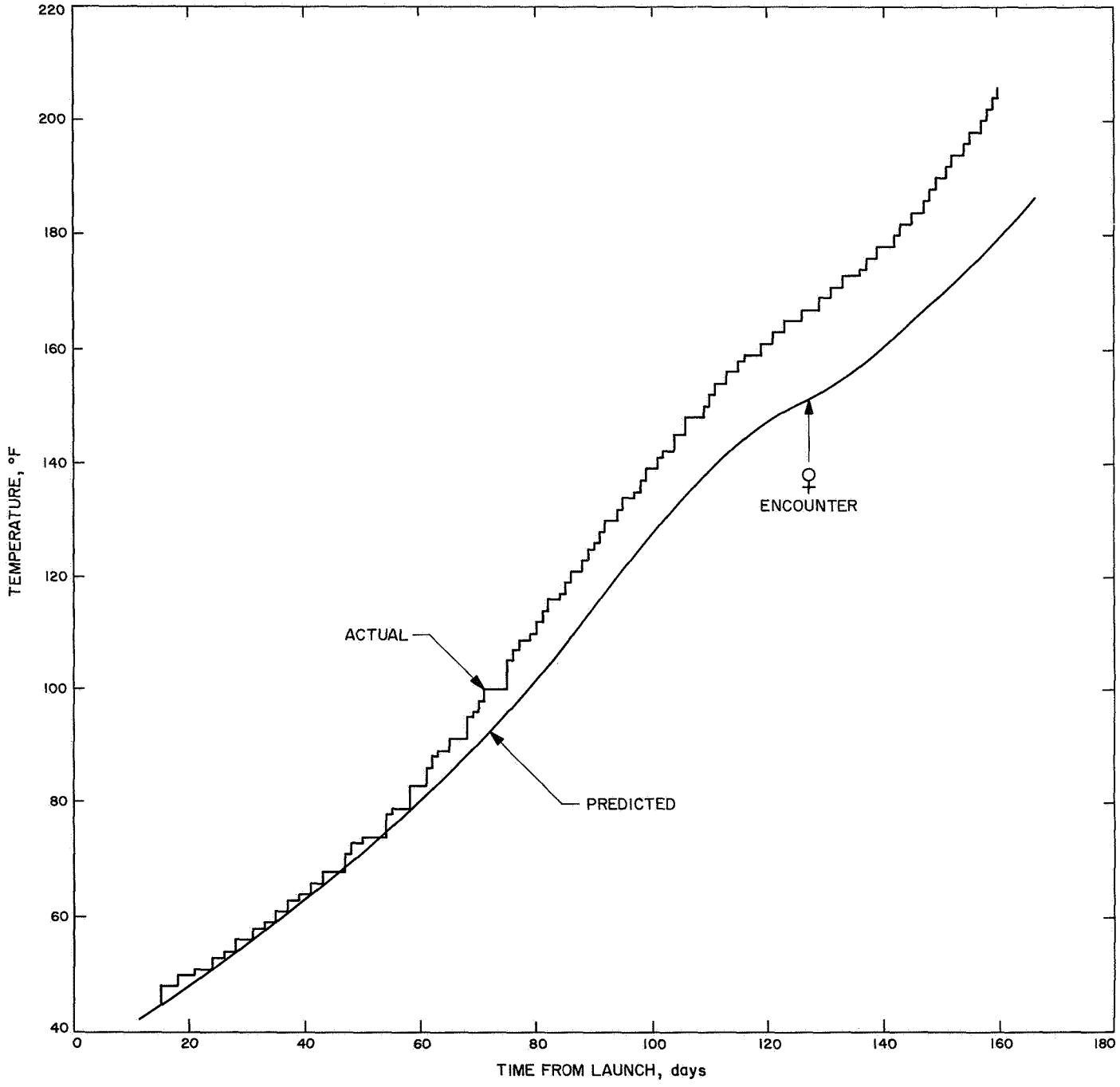


Fig. C-65. Lower shield temperature, channel 435

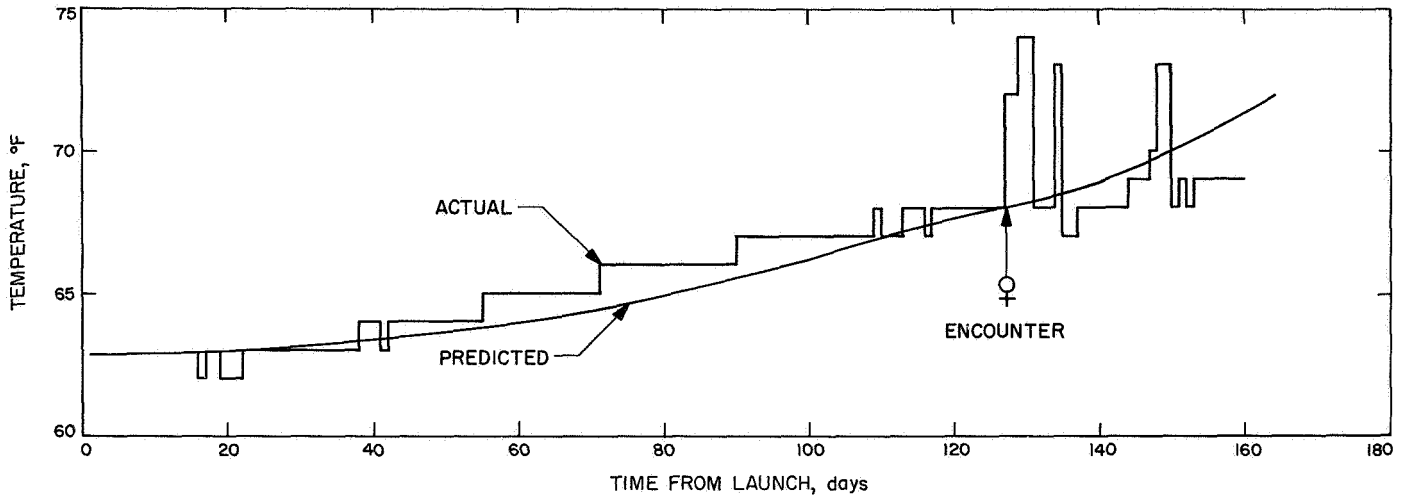


Fig. C-66. Tape recorder temperature, channel 436

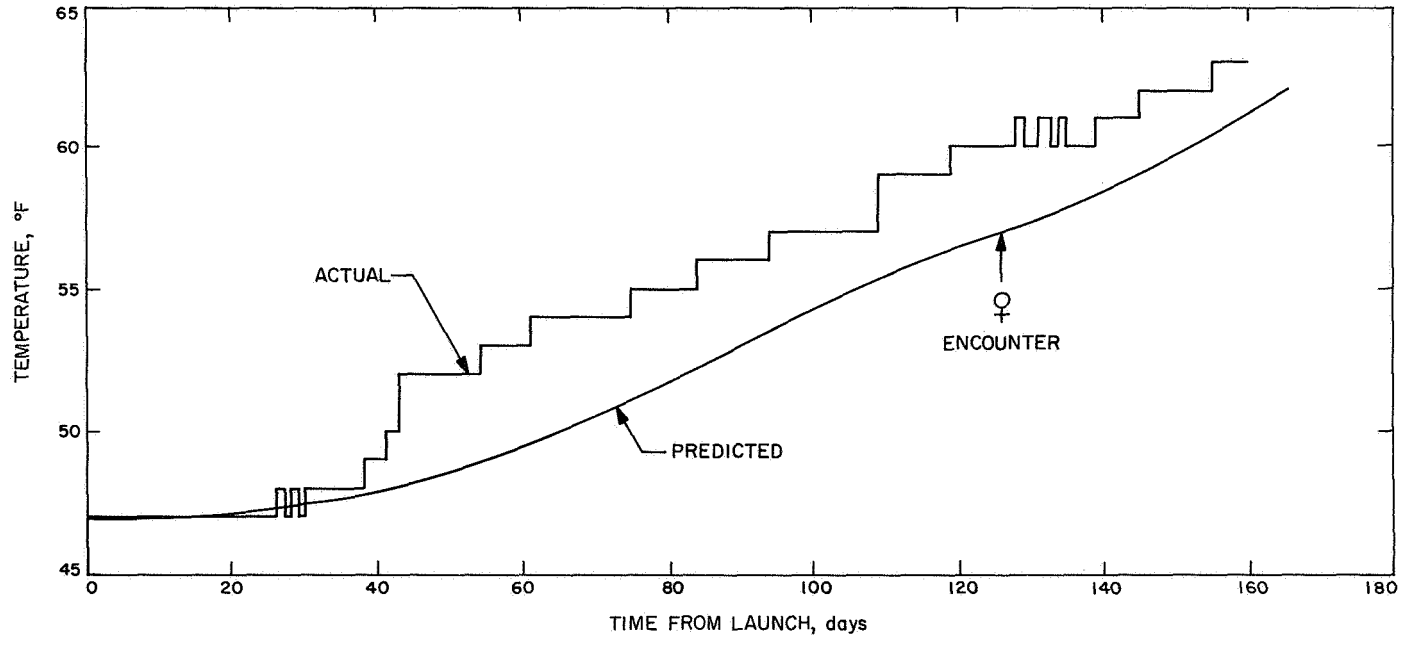


Fig. C-67. Ultraviolet photometer temperature, channel 437

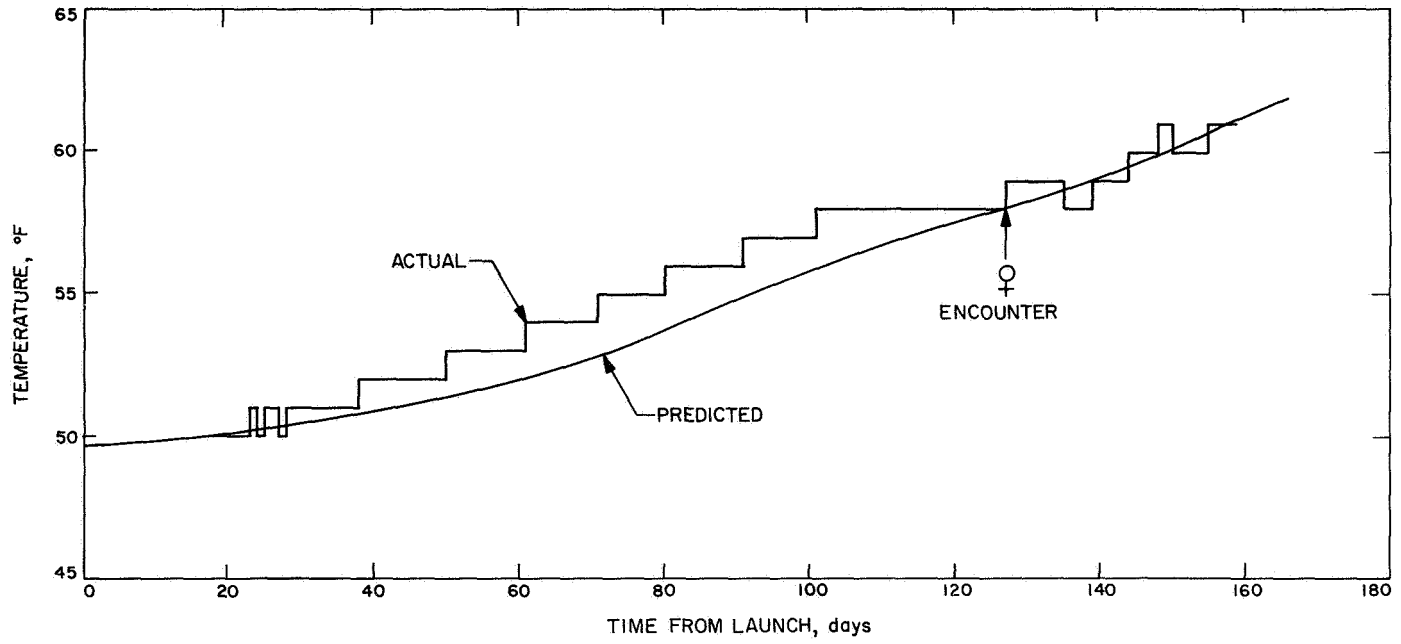


Fig. C-68. Trapped radiation detector temperature, channel 438

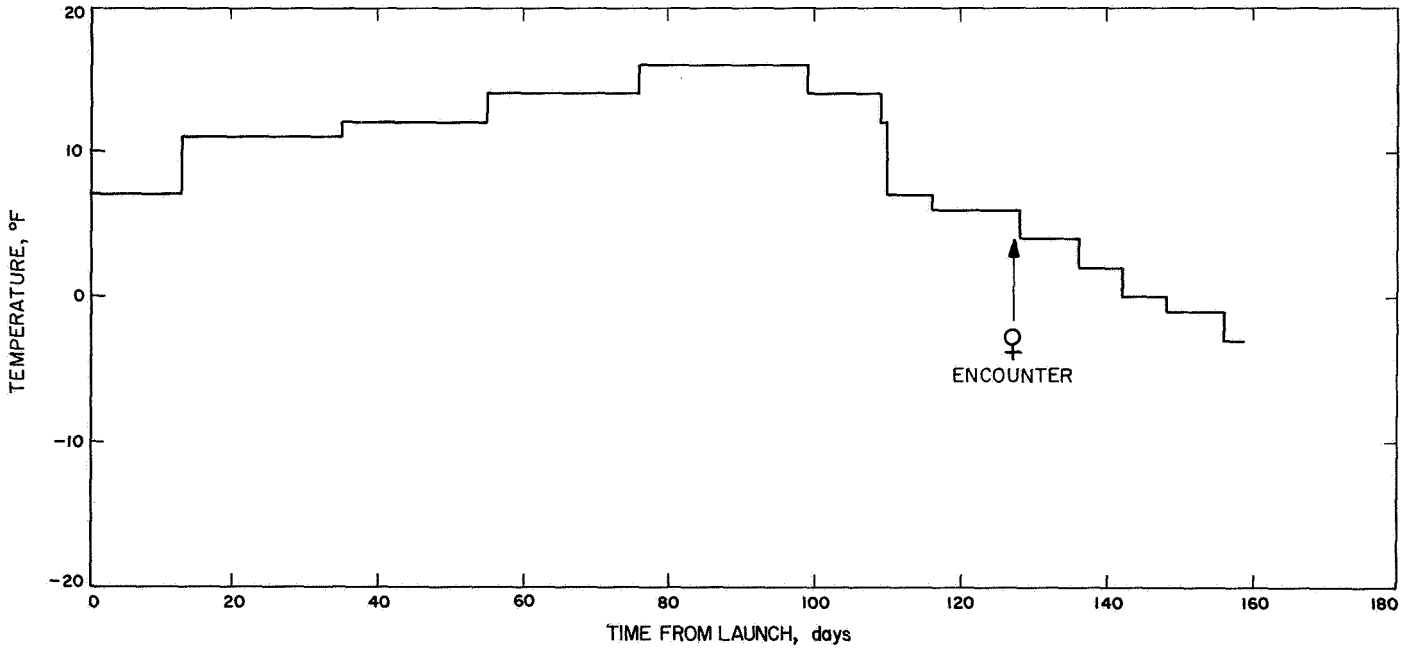


Fig. C-69. Magnetometer temperature, channel 439

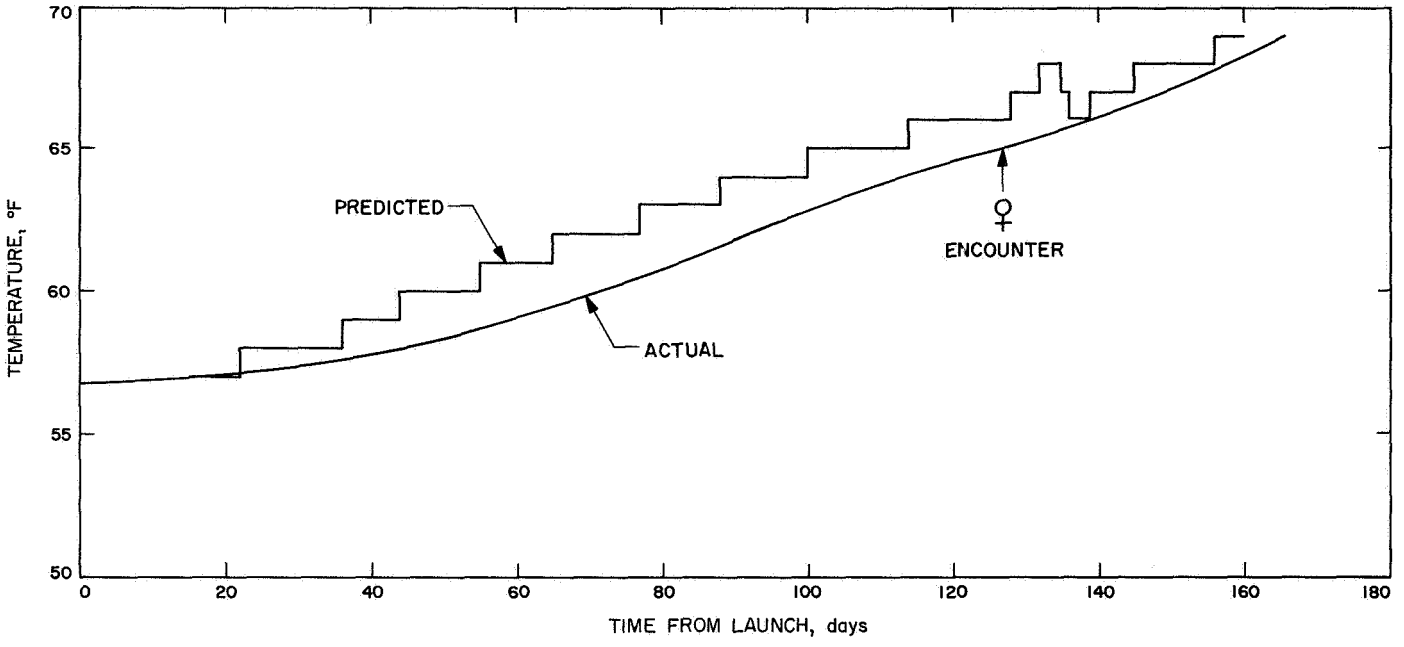


Fig. C-70. Propulsion fuel temperature, channel 217

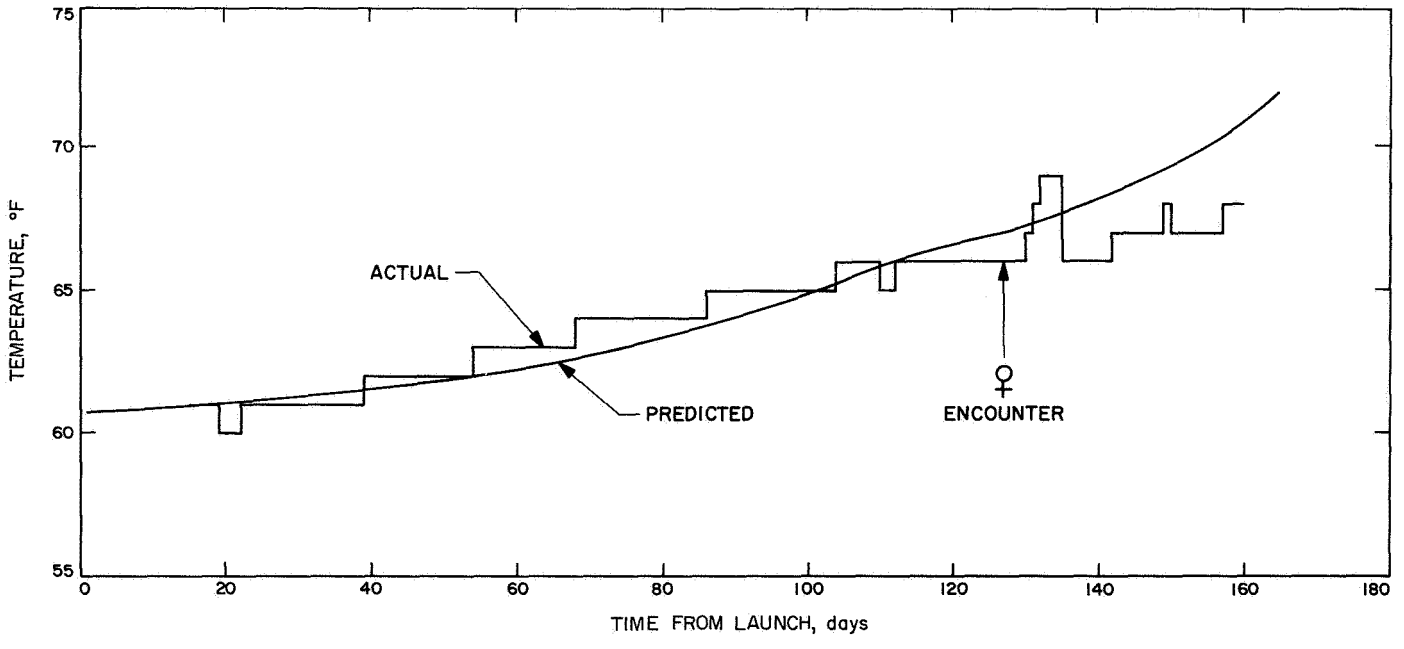


Fig. C-71. Nitrogen tank (+X/−Y) temperature, channel 218

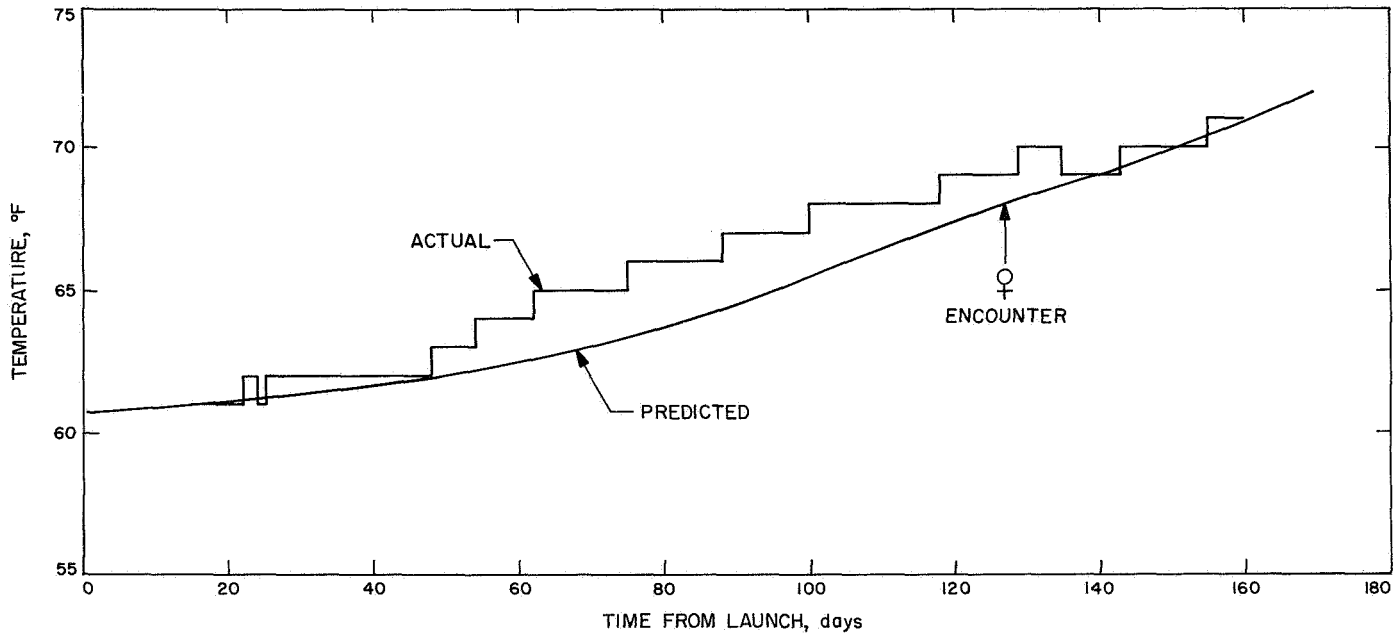


Fig. C-72. Nitrogen tank (−X/+Y) temperature, channel 219

Glossary

AAS	advanced antenna system
AC	attitude control
A/DC	analog-to-digital converter
AFETR	Air Force Eastern Test Range
AGC	automatic gain control
AO	auxiliary oscillator
APAC	antenna pointing angle change
ASE	aphrodiocentric–solar–ecliptic (coordinates)
AU	astronomical unit
AUX OSC	auxiliary oscillator test mode
BEC	bit-error checker
BECO	booster engine cutoff
B/R	booster-regulator
BUSS	SPAC analysis control network
CAT	complementary analysis team
CC&S	central computer and sequencer
CG	center of gravity
c.m.	center of mass
CP	communications processor
D/AC	digital-to-analog converter
DAS	data automation subsystem
DE	data encoder
DFR	dual-frequency receiver
DN	data number
DPS	data processing system
DRD	decision–revision–decision (conference room)
DSIF	Deep Space Instrumentation Facility
DSN	Deep Space Network
DSS	Deep Space Station
E	encounter (+ time)
ECR	engineering change requirement
EMI	electromagnetic interference
EOT	end of tape
ETL	Environmental Test Laboratory
FDX	full duplex
FOV	field of view
FPAA	flight-path analysis area
FPAC	flight-path analysis and command
GCA	gyro control assembly
GCS	ground command subsystem
GSDS	Goldstone duplicate standard
GTS	ground telemetry system
HSDL	high-speed data line
IBSYS	International Business Machines System
IC	integrated circuit
I/O	input/output
JVA	jet vane actuator
L	launch (+ time)
L&M	launch and midcourse
LCE	launch complex equipment
LMT	local mean time
M	maneuver (+ time)
MDL	master data library
MOS	Mission Operations System
MRH	mission-related hardware
MSA	mission support area
MT	master timer
NASCOM	NASA Communications Network
ORT	operational readiness tests
OSE	operational support equipment

Glossary (contd)

PAS	pyrotechnics arming switch
PFR	problem failure report
PIPS	postinjection propulsion system
PNG	pseudo-noise generator
PRS	planetary ranging subsystem
PSO	planet sensor output
PTM	proof-test model
R&D	research and development
RIS	Range Instrumentation Ship
RSS	radio subsystem
RT	real time
RTDT	real-time data translator
RU	range unit
RWV	read–write–verify
S	separation (+ time)
SAF	Spacecraft Assembly Facility
SAGC	station automatic gain control
SDA	systems data analysis
SECO	sustainer engine cutoff
SFO	Space Flight Operations
SFOD	Space Flight Operations Director
SFOF	Space Flight Operations Facility
SIRD	support instrumentation requirements document
SIT	separation-initiated timer
SN	serial number
SNR	signal-to-noise ratio
SPAC	spacecraft performance analysis and command
SPACE	SSAC analysis control network
SPAC JR	auxiliary SPAC group
SPE	static phase error
SSAC	space science analysis and command
STCDS	System Test Complex Data System
TA	type approval
TCAT	telecommunications complementary analysis team
TCD	telemetry and command data
TCP	telemetry and command processor
TCR	temperature control reference
TCVA	thrust vector control assembly
TDH	tracking data handling
TFR	trouble and failure report
TM	transverse magnetic; telemetry (on figures only)
TPS	telemetry processing station
TRD	trapped radiation detector
TRS	tape recorder subsystem
TSO	terminator sensor output
TWM	traveling-wave maser
TWT	traveling-wave tube
VCA	voltage-controlled attenuator
VCO	voltage-controlled oscillator
VECO	vernier engine cutoff
VEPWG	Venus encounter preparation working group

Computer Programs

ADAP	analytical digital antenna pointing
AGCM	automatic gain control calibration
ATTREF	attitude reference
BUTEC	burning time estimation calculation
CPPM	communication prediction
DDT	digital demodulation technique
EDIT	MDL software
EDPLOT	engineering data plotting
EGLIST	engineering lister
ENG. DECOM.	engineering data decommutation
MC1M	midcourse maneuver
MERGE	MDL software
MORCOR	corrector
MOREX	extractor

Glossary (contd)

ODGX orbit data generator

ODPM orbit determination

POWM trajectory computation

PRDX predicts

REEDIT MDL software

RSID residual

SIPM star identification

SPODP single precision orbit determination program

SSDM systems suppressed data

SSPM suppression

TDPX tracking data processor

TJIM trajectory computation

References

1. Smith, E. J., et al., "Magnetic Measurements Near Venus," *J. Geophys. Res.*, Vol. 70, p. 1571, Apr. 1, 1965; Neugebauer, M., and Snyder, C. W., "Solar Wind Measurements Near Venus," *Ibid.*, p. 1587.

2. Coleman, P. J., Jr., et al., "Measurements of Magnetic Fields in the Vicinity of the Magnetosphere and in Interplanetary Space: Preliminary Results From Mariner IV," in *Space Research-COSTAR: Volume VI*, pp. 907–930. Edited by R. J. Smith-Rose. North Holland Publishing Co., Amsterdam, 1966.

3. Davis, L., Jr., and Smith, E. J., paper in preparation.

4. Siscoe, G. L., et al., "Magnetic Fluctuations in the Magnetosheath: Mariner IV," *J. Geophys. Res.*, Vol. 72, No. 1, pp. 1–18, Jan. 1, 1967.

5. Lazarus, A. J., et al., "Initial Results From the Mariner IV Solar Plasma Experiment," in *Space Research-COSTAR: Volume VII*, pp. 1296–1305. Edited by R. J. Smith-Rose. North Holland Publishing Co., Amsterdam, 1967.

6. Behannon, K. W., *Mapping of the Earth's Bow Shock and Magnetic Tail by Explorer XXXIII*, Report X-612-67-344. NASA–Goddard Space Flight Center, Greenbelt, Md., July 1967.

7. Eshleman, V. R., "Radar Astronomy," *Science*, Vol. 158, No. 3801, pp. 585–597, Nov. 3, 1967.

8. Wolfe, J. H., et al., "The Compositional Anisotropic and Non-Radial Flow Characteristics of the Solar Wind," *J. Geophys. Res.*, Vol. 71, p. 3329, Dec. 1, 1966; Hundausen, A. J., et al., "Vela Satellite Observations of Solar Wind Ions," *J. Geophys. Res.*, Vol. 72, p. 1979, Apr. 1, 1967.

9. Lyon, E. F., Bridge, H. W., and Binsack, J. H., "Explorer XXXV Plasma Measurements in the Vicinity of the Moon," *J. Geophys. Res.*, Vol. 72, p. 6113, Dec. 1, 1967.

10. Colburn, D. S., et al., "Diamagnetic Solar-Wind Cavity Discovered Behind Moon," *Science*, Vol. 158, No. 3804, pp. 1040–1042, Nov. 24, 1967; Ness, N. F., et al., "Early Results From the Magnetic Field Experiment on Lunar Explorer XXXV," *J. Geophys. Res.*, Vol. 72, No. 23, pp. 5769–5778, Dec. 1, 1967.

11. Kliore, A. J., et. al., "Occultation Experiment: Results of the First Direct Measurement of Mars's Atmosphere and Ionosphere," *Science*, Vol. 149, p. 3689, Sept. 10, 1965.

12. Kliore, A. J., et al., "A Radio Occultation Experiment to Probe the Atmosphere of Venus," *J. Spacecraft Rockets*, Vol. 4, No. 10, pp. 1339–1346, Oct. 1967.

13. Levy, G., Otoshi, T., and Seidel, B., "Ground Instrumentation for Mariner IV Occultation Experiment," *IEEE Trans. Inst. Meas.*, Vol. IM-6, No. 2, pp. 1339–1346, June 1967.

14. Fjeldbo, G., and Eshleman, V. R., "The Bistate Radar-Occultation Method for the Study of Planetary Atmospheres," *J. Geophys. Res.*, Vol. 70, No. 13, pp. 3217–3225, July 1, 1965.

15. Ash, M. E., Shapiro, I. I., and Smith, W. B., "Astronomical Constants and Planetary Ephemerides Deduced From Radar and Optical Observations," *Astron. J.*, Vol. 72, No. 3, pp. 338–350, Apr. 1967.

References (contd)

16. Fjeldbo, G., and Eshleman, V. R., *The Atmosphere of Mars Analyzed by Integral Inversion of the Mariner IV Occultation Data,* Final Report SU-SEL-67-109, Contract NGR-05-020-065, Stanford University Radioscience Laboratory, Stanford, Calif., Nov. 1967. (Also available as NASA-CR-92718, N68-16732.)

17. Barth, C., et al., "Ultraviolet Emissions Observed Near Venus From Mariner V," *Science,* Vol. 158, p. 3908, Dec. 29, 1967.

18. Fjeldbo, G., et al., "The Two-Frequency Bistate Radar Occultation Method for the Study of Planetary Ionospheres," *J. Geophys. Res.,* Vol. 70, p. 3701, Aug. 1, 1965.

19. Gold, T., "The Magnetosphere of the Moon," in *The Solar Wind,* pp. 381–389. Edited by R. J. Mackin, Jr., and M. Neugebauer. Pergamon Press, New York, 1966.

20. Dessler, A. J., "Ionizing Plasma Flux in the Martian Upper Atmosphere," in *Atmospheres of Venus and Mars,* pp. 241–250. Edited by J. C. Brandt and M. B. McElroy. Gordon and Breach, London, 1967.

21. Axford, W. I., "The Interaction of the Solar Wind With Comets," *Planetary Space Sci.,* Vol. 12, No. 719, 1964.

22. Smith, E. J., et al., "Magnetic Field Measurements Near Mars," *Science,* Vol. 149, p. 1241, Sept. 10, 1965; Kliore, A. J., et al., "Occultation Experiment Results of the First Direct Measurement of Mars Atmosphere and Ionosphere," *Science,* Vol. 149, pp. 1243–1248, Sept. 10, 1965.

23. Gordon, H. J., *Functional Design of Mariner Midcourse Maneuver Operation Program,* Technical Report 32-1139, Appendix A. Jet Propulsion Laboratory, Pasadena, Calif., July 15, 1967.

24. Vegos, C. J., and Trask, D. W., "Ranger Combined Analysis, Part II: Determination of the Masses of the Earth and Moon From Radio Tracking Data," in *The Deep Space Network,* Space Programs Summary 37-44, Vol. III, pp. 11–28. Jet Propulsion Laboratory, Pasadena, Calif., Mar. 31, 1967.

25. Anderson, J. D., *Determination of the Masses of the Moon and Venus and the Astronomical Unit From Radio Tracking Data of the Mariner II Spacecraft,* Technical Report 32-816. Jet Propulsion Laboratory, Pasadena, Calif., July 1, 1967.

26. Null, G. W., *The Mariner IV Flight Path and Its Determination From Radio Tracking Data,* Technical Report 32-1108. Jet Propulsion Laboratory, Pasadena, Calif., Aug. 1, 1967.

27. Wright, F. H., *Failure Rate Analysis Based on Mariner Venus 1967 Spacecraft Data,* Technical Report 32-1266. Jet Propulsion Laboratory, Pasadena, Calif. (to be published).